VOLUME 28 / NUMBER 2
JANUARY 23, 1990
ACC. NOS. N90-10828 TO N90-11691

STAR

AN ABSTRACT JOURNAL

Scientific and Technical Aerospace Reports

PRODUCED BY THE
SCIENTIFIC AND TECHNICAL
INFORMATION
DIVISION

NASA

NATIONAL AERONAUTICS AND SPACE ADMINISTRATION

WHAT YOU CAN DO FOR *STAR*

All users of this abstract service are urged to forward reports to be considered for announcement in *STAR*. This will aid NASA in its efforts to provide the fullest possible coverage of all scientific and technical publications that might support aeronautics and space research and development. If you have prepared relevant reports (other than those that you will transmit to NASA, DOD, or DOE through the usual contract- or grant-reporting channels), please send them for consideration to the NASA Scientific and Technical Information Facility, P.O. Box 8757, BWI Airport, MD 21240.

Reprints of journal articles, book chapters, and conference papers are also welcome. These will be considered for announcement in *STAR's* companion journal, *International Aerospace Abstracts*.

You may specify a particular source to be included in a report announcement if you wish; otherwise the report will be placed on public sale at the National Technical Information Service. Copyrighted publications will be announced but not distributed or sold.

PURCHASE OF *STAR*

The semimonthly issues are available to registered users on annual subscription from the NASA Scientific and Technical Information Facility, ATTN: Registration Services, P.O. Box 8757, BWI Airport, MD 21240. *STAR* is publicly available on annual subscription from the Superintendent of Documents, U.S. Government Printing Office, Washington, DC 20402.

PUBLISHED BY:

UNITED STATES GOVERNMENT
NATIONAL AERONAUTICS AND SPACE ADMINISTRATION
SCIENTIFIC AND TECHNICAL INFORMATION DIVISION
Scientific and Technical Aerospace Reports, Volume 28, is prepared by the NASA Scientific and Technical Information Facility operated for the National Aeronautics and Space Administration by RMS Associates.

The Administrator of the National Aeronautics and Space Administration has determined that the publication of this periodical is necessary in the transaction of the public business required by law of this agency. Use of funds for printing this periodical has been approved by the Director of the Office of Management and Budget through March 22, 1991.

US ISSN 0036-8741

Scientific and Technical Aerospace Reports (STAR) is issued twice a month and contains abstracts and indexes of meeting papers, conference proceedings, and unlimited distribution reports that have been added to the NASA Scientific and Technical Information Database during the preceding period. These citations may also be accessed online via NASA/RECON or via AIAA's Aerospace Database (File 108) through Dialog Information Services, Inc.

STAR subject coverage includes all aerospace-related areas that will help NASA achieve its mission. Material is gathered from all over the world and includes significant input from many countries under exchange and access agreements.

Consult the indexes at the back of this volume to help zero in on what you are looking for. These include:

Subject Index
Personal Author Index
Corporate Source Index
Contract Number Index
Report/Accession Number Index

STAR's companion abstract journal *International Aerospace Abstracts* should be used if you are looking for references to periodicals, books, and published meeting papers or conference proceedings.

Questions and comments should be addressed to:

NASA Scientific and Technical Information Facility
User Services
P.O. Box 8757
BWI Airport, MD 21240
301-621-0150

VOLUME 28 NUMBER 2 / JANUARY 23, 1990

TABLE OF CONTENTS

AERONAUTICS

Includes aeronautics (general); aerodynamics; air transportation and safety; aircraft communications and navigation; aircraft design, testing and performance; aircraft instrumentation; aircraft propulsion and power; aircraft stability and control; and research and support facilities (air).

For related information see also *Astronautics.*

01 AERONAUTICS (GENERAL) 145

02 AERODYNAMICS 145

Includes aerodynamics of bodies, combinations, wings, rotors, and control surfaces; and internal flow in ducts and turbomachinery.

For related information see also *34 Fluid Mechanics and Heat Transfer.*

03 AIR TRANSPORTATION AND SAFETY 147

Includes passenger and cargo air transport operations; and aircraft accidents.

For related information see also *16 Space Transportation* and *85 Urban Technology and Transportation.*

04 AIRCRAFT COMMUNICATIONS AND NAVIGATION 148

Includes digital and voice communication with aircraft; air navigation systems (satellite and ground based); and air traffic control.

For related information see also *17 Space Communications, Spacecraft Communications, Command and Tracking* and *32 Communications and Radar.*

05 AIRCRAFT DESIGN, TESTING AND PERFORMANCE 151

Includes aircraft simulation technology.

For related information see also *18 Spacecraft Design, Testing and Performance* and *39 Structural Mechanics.* For land transportation vehicles see *85 Urban Technology and Transportation.*

06 AIRCRAFT INSTRUMENTATION 155

Includes cockpit and cabin display devices; and flight instruments.

For related information see also *19 Spacecraft Instrumentation* and *35 Instrumentation and Photography.*

07 AIRCRAFT PROPULSION AND POWER 156

Includes prime propulsion systems and systems components, e.g., gas turbine engines and compressors; and onboard auxiliary power plants for aircraft.

For related information see also *20 Spacecraft Propulsion and Power, 28 Propellants and Fuels,* and *44 Energy Production and Conversion.*

08 AIRCRAFT STABILITY AND CONTROL 156

Includes aircraft handling qualities; piloting; flight controls; and autopilots.

For related information see also *05 Aircraft Design, Testing and Performance.*

09 RESEARCH AND SUPPORT FACILITIES (AIR) 157

Includes airports, hangars and runways; aircraft repair and overhaul facilities; wind tunnels; shock tubes; and aircraft engine test stands.

For related information see also *14 Ground Support Systems and Facilities (Space).*

ASTRONAUTICS

Includes astronautics (general); astrodynamics; ground support systems and facilities (space); launch vehicles and space vehicles; space transportation; space communications, spacecraft communications, command and tracking; spacecraft design, testing and performance; spacecraft instrumentation; and spacecraft propulsion and power.

For related information see also *Aeronautics.*

12 ASTRONAUTICS (GENERAL) 158

For extraterrestrial exploration see *91 Lunar and Planetary Exploration.*

13 ASTRODYNAMICS N.A.

Includes powered and free-flight trajectories; and orbital and launching dynamics.

14 GROUND SUPPORT SYSTEMS AND FACILITIES (SPACE) 159

Includes launch complexes, research and production facilities; ground support equipment, e.g., mobile transporters; and simulators.

For related information see also *09 Research and Support Facilities (Air).*

15 LAUNCH VEHICLES AND SPACE VEHICLES 160

Includes boosters; operating problems of launch/space vehicle systems; and reusable vehicles.

For related information see also *20 Spacecraft Propulsion and Power.*

16 SPACE TRANSPORTATION 161

Includes passenger and cargo space transportation, e.g., shuttle operations; and space rescue techniques.

For related information see also *03 Air Transportation and Safety* and *18 Spacecraft Design, Testing and Performance.* For space suits see *54 Man/System Technology and Life Support.*

17 SPACE COMMUNICATIONS, SPACECRAFT COMMUNICATIONS, COMMAND AND TRACKING N.A.

Includes telemetry; space communications networks; astronavigation and guidance; and radio blackout.

For related information see also *04 Aircraft Communications and Navigation* and *32 Communications and Radar.*

18 SPACECRAFT DESIGN, TESTING AND PERFORMANCE 175

Includes satellites; space platforms; space stations; spacecraft systems and components such as thermal and environmental controls; and attitude controls.

For life support systems see *54 Man/System Technology and Life Support.* For related information see also *05 Aircraft Design, Testing and Performance, 39 Structural Mechanics,* and *16 Space Transportation.*

19 SPACECRAFT INSTRUMENTATION N.A.

For related information see also *06 Aircraft Instrumentation* and *35 Instrumentation and Photography.*

20 SPACECRAFT PROPULSION AND POWER 189

Includes main propulsion systems and components, e.g. rocket engines; and spacecraft auxiliary power sources.

For related information see also *07 Aircraft Propulsion and Power, 28 Propellants and Fuels, 44 Energy Production and Conversion,* and *15 Launch Vehicles and Space Vehicles.*

CHEMISTRY AND MATERIALS

Includes chemistry and materials (general); composite materials; inorganic and physical chemistry; metallic materials; nonmetallic materials; propellants and fuels; and materials processing.

23 CHEMISTRY AND MATERIALS (GENERAL) N.A.

24 COMPOSITE MATERIALS 190

Includes physical, chemical, and mechanical properties of laminates and other composite materials.

For ceramic materials see *27 Nonmetallic Materials.*

25 INORGANIC AND PHYSICAL CHEMISTRY 192

Includes chemical analysis, e.g., chromatography; combustion theory; electrochemistry; and photochemistry.

For related information see also *77 Thermodynamics and Statistical Physics.*

26 METALLIC MATERIALS 197

Includes physical, chemical, and mechanical properties of metals, e.g., corrosion; and metallurgy.

27 NONMETALLIC MATERIALS 199

Includes physical, chemical, and mechanical properties of plastics, elastomers, lubricants, polymers, textiles, adhesives, and ceramic materials.

For composite materials see *24 Composite Materials.*

28 PROPELLANTS AND FUELS 203

Includes rocket propellants, igniters and oxidizers; their storage and handling procedures; and aircraft fuels.

For related information see also *07 Aircraft Propulsion and Power, 20 Spacecraft Propulsion and Power,* and *44 Energy Production and Conversion.*

29 MATERIALS PROCESSING 209

Includes space-based development of products and processes for commercial application.

For biological materials see *55 Space Biology.*

ENGINEERING

Includes engineering (general); communications and radar; electronics and electrical engineering; fluid mechanics and heat transfer; instrumentation and photography; lasers and masers; mechanical engineering; quality assurance and reliability; and structural mechanics.

For related information see also *Physics.*

31 ENGINEERING (GENERAL) 209

Includes vacuum technology; control engineering; display engineering; cryogenics; and fire prevention.

32 COMMUNICATIONS AND RADAR 211

Includes radar; land and global communications; communications theory; and optical communications.

For related information see also *04 Aircraft Communications and Navigation* and *17 Space Communications, Spacecraft Communications, Command and Tracking.* For search and rescue see *03 Air Transportation and Safety,* and *16 Space Transportation.*

33 ELECTRONICS AND ELECTRICAL ENGINEERING 215

Includes test equipment and maintainability; components, e.g., tunnel diodes and transistors; microminiaturization; and integrated circuitry.

For related information see also *60 Computer Operations and Hardware* and *76 Solid-State Physics.*

34 FLUID MECHANICS AND HEAT TRANSFER 218

Includes boundary layers; hydrodynamics; fluidics; mass transfer and ablation cooling.

For related information see also *02 Aerodynamics* and *77 Thermodynamics and Statistical Physics.*

35 INSTRUMENTATION AND PHOTOGRAPHY 222

Includes remote sensors; measuring instruments and gauges; detectors; cameras and photographic supplies; and holography.

For aerial photography see *43 Earth Resources and Remote Sensing.* For related information see also *06 Aircraft Instrumentation* and *19 Spacecraft Instrumentation.*

36 LASERS AND MASERS 226

Includes parametric amplifiers.

For related information see also *76 Solid-State Physics.*

37 MECHANICAL ENGINEERING 228

Includes auxiliary systems (nonpower); machine elements and processes; and mechanical equipment.

38 QUALITY ASSURANCE AND RELIABILITY 231

Includes product sampling procedures and techniques; and quality control.

39 STRUCTURAL MECHANICS 231

Includes structural element design and weight analysis; fatigue; and thermal stress.

For applications see *05 Aircraft Design, Testing and Performance* and *18 Spacecraft Design, Testing and Performance.*

GEOSCIENCES

Includes geosciences (general); earth resources and remote sensing; energy production and conversion; environment pollution; geophysics; meteorology and climatology; and oceanography.

For related information see also *Space Sciences.*

42 GEOSCIENCES (GENERAL) **N.A.**

43 EARTH RESOURCES AND REMOTE SENSING **235**

Includes remote sensing of earth resources by aircraft and spacecraft; photogrammetry; and aerial photography.

For instrumentation see *35 Instrumentation and Photography.*

44 ENERGY PRODUCTION AND CONVERSION **236**

Includes specific energy conversion systems, e.g., fuel cells; global sources of energy; geophysical conversion; and windpower.

For related information see also *07 Aircraft Propulsion and Power, 20 Spacecraft Propulsion and Power,* and *28 Propellants and Fuels.*

45 ENVIRONMENT POLLUTION **237**

Includes atmospheric, noise, thermal, and water pollution.

46 GEOPHYSICS **239**

Includes aeronomy; upper and lower atmosphere studies; ionospheric and magnetospheric physics; and geomagnetism.

For space radiation see *93 Space Radiation.*

47 METEOROLOGY AND CLIMATOLOGY **250**

Includes weather forecasting and modification.

48 OCEANOGRAPHY **253**

Includes biological, dynamic, and physical oceanography; and marine resources.

For related information see also *43 Earth Resources and Remote Sensing.*

LIFE SCIENCES

Includes life sciences (general); aerospace medicine; behavioral sciences; man/system technology and life support; and space biology.

51 LIFE SCIENCES (GENERAL) **254**

52 AEROSPACE MEDICINE **254**

Includes physiological factors; biological effects of radiation; and effects of weightlessness on man and animals.

53 BEHAVIORAL SCIENCES **254**

Includes psychological factors; individual and group behavior; crew training and evaluation; and psychiatric research.

54 MAN/SYSTEM TECHNOLOGY AND LIFE SUPPORT **255**

Includes human engineering; biotechnology; and space suits and protective clothing.

For related information see also *16 Space Transportation.*

55 SPACE BIOLOGY **N.A.**

Includes exobiology; planetary biology; and extraterrestrial life.

MATHEMATICAL AND COMPUTER SCIENCES

Includes mathematical and computer sciences (general); computer operations and hardware; computer programming and software; computer systems; cybernetics; numerical analysis; statistics and probability; systems analysis; and theoretical mathematics.

59 MATHEMATICAL AND COMPUTER SCIENCES (GENERAL) **N.A.**

60 COMPUTER OPERATIONS AND HARDWARE **256**

Includes hardware for computer graphics, firmware, and data processing.

For components see *33 Electronics and Electrical Engineering.*

61 COMPUTER PROGRAMMING AND SOFTWARE **257**

Includes computer programs, routines, algorithms, and specific applications, e.g., CAD/CAM.

62 COMPUTER SYSTEMS **260**

Includes computer networks and special application computer systems.

63 CYBERNETICS **261**

Includes feedback and control theory, artificial intelligence, robotics and expert systems.

For related information see also *54 Man/System Technology and Life Support.*

64 NUMERICAL ANALYSIS **263**

Includes iteration, difference equations, and numerical approximation.

65 STATISTICS AND PROBABILITY **268**

Includes data sampling and smoothing; Monte Carlo method; and stochastic processes.

66 SYSTEMS ANALYSIS **269**

Includes mathematical modeling; network analysis; and operations research.

67 THEORETICAL MATHEMATICS **269**

Includes topology and number theory.

PHYSICS

Includes physics (general); acoustics; atomic and molecular physics; nuclear and high-energy physics; optics; plasma physics; solid-state physics; and thermodynamics and statistical physics.

For related information see also *Engineering.*

70 PHYSICS (GENERAL) **270**

For precision time and time interval (PTTI) see *35 Instrumentation and Photography;* for geophysics, astrophysics or solar physics see *46 Geophysics, 90 Astrophysics,* or *92 Solar Physics.*

71 ACOUSTICS 271
Includes sound generation, transmission, and attenuation.
For noise pollution see *45 Environment Pollution.*

72 ATOMIC AND MOLECULAR PHYSICS 272
Includes atomic structure, electron properties, and molecular spectra.

73 NUCLEAR AND HIGH-ENERGY PHYSICS 273
Includes elementary and nuclear particles; and reactor theory.
For space radiation see *93 Space Radiation.*

74 OPTICS 273
Includes light phenomena and optical devices.
For lasers see *36 Lasers and Masers.*

75 PLASMA PHYSICS 276
Includes magnetohydrodynamics and plasma fusion.
For ionospheric plasmas see *46 Geophysics.* For space plasmas see *90 Astrophysics.*

76 SOLID-STATE PHYSICS 280
Includes superconductivity.
For related information see also *33 Electronics and Electrical Engineering* and *36 Lasers and Masers.*

77 THERMODYNAMICS AND STATISTICAL PHYSICS 286
Includes quantum mechanics; theoretical physics; and Bose and Fermi statistics.
For related information see also *25 Inorganic and Physical Chemistry* and *34 Fluid Mechanics and Heat Transfer.*

SOCIAL SCIENCES

Includes social sciences (general); administration and management; documentation and information science; economics and cost analysis; law, political science, and space policy; and urban technology and transportation.

80 SOCIAL SCIENCES (GENERAL) 287
Includes educational matters.

81 ADMINISTRATION AND MANAGEMENT 287
Includes management planning and research.

82 DOCUMENTATION AND INFORMATION SCIENCE 288
Includes information management; information storage and retrieval technology; technical writing; graphic arts; and micrography.
For computer documentation see *61 Computer Programming and Software.*

83 ECONOMICS AND COST ANALYSIS 289
Includes cost effectiveness studies.

84 LAW, POLITICAL SCIENCE AND SPACE POLICY N.A.
Includes NASA appropriation hearings; aviation law; space law and policy; international law; international cooperation; and patent policy.

85 URBAN TECHNOLOGY AND TRANSPORTATION 289
Includes applications of space technology to urban problems; technology transfer; technology assessment; and surface and mass transportation.
For related information see *03 Air Transportation and Safety, 16 Space Transportation,* and *44 Energy Production and Conversion.*

SPACE SCIENCES

Includes space sciences (general); astronomy; astrophysics; lunar and planetary exploration; solar physics; and space radiation.
For related information see also *Geosciences.*

88 SPACE SCIENCES (GENERAL) N.A.

89 ASTRONOMY 290
Includes radio, gamma-ray, and infrared astronomy; and astrometry.

90 ASTROPHYSICS 291
Includes cosmology; celestial mechanics; space plasmas; and interstellar and interplanetary gases and dust.
For related information see also *75 Plasma Physics.*

91 LUNAR AND PLANETARY EXPLORATION 295
Includes planetology; and manned and unmanned flights.
For spacecraft design or space stations see *18 Spacecraft Design, Testing and Performance.*

92 SOLAR PHYSICS 296
Includes solar activity, solar flares, solar radiation and sunspots.
For related information see *93 Space Radiation.*

93 SPACE RADIATION 297
Includes cosmic radiation; and inner and outer earth's radiation belts.
For biological effects of radiation see *52 Aerospace Medicine.* For theory see *73 Nuclear and High-Energy Physics.*

GENERAL

Includes aeronautical, astronautical, and space science related histories, biographies, and pertinent reports too broad for categorization; histories or broad overviews of NASA programs.

99 GENERAL 297

Note: N.A. means that no abstracts were assigned to this category for this issue.

SUBJECT INDEX I-1
PERSONAL AUTHOR INDEX I-55
CORPORATE SOURCE INDEX I-63
CONTRACT NUMBER INDEX I-75
REPORT/ACCESSION NUMBER INDEX I-77
APPENDIX—ABOUT STAR A-1

TYPICAL CITATION AND ABSTRACT

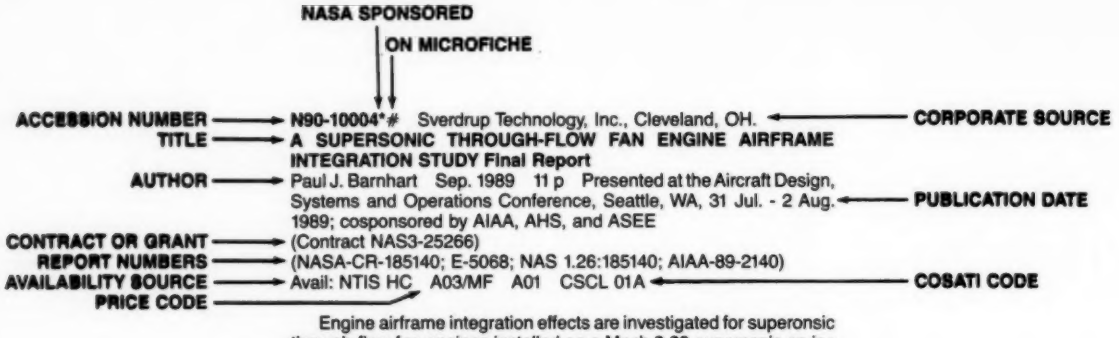
NASA SPONSORED
ON MICROFICHE
ACCESSION NUMBER
TITLE
AUTHOR
CONTRACT OR GRANT
REPORT NUMBERS
AVAILABILITY SOURCE
PRICE CODE
CORPORATE SOURCE
PUBLICATION DATE
COSATI CODE
N90-10004*# Sverdrup Technology, Inc., Cleveland, OH.
A SUPERSONIC THROUGH-FLOW FAN ENGINE AIRFRAME INTEGRATION STUDY Final Report
Paul J. Barnhart Sep. 1989 11 p Presented at the Aircraft Design, Systems and Operations Conference, Seattle, WA, 31 Jul. - 2 Aug. 1989; cosponsored by AIAA, AHS, and ASEE
(Contract NAS3-25266)
(NASA-CR-185140; E-5068; NAS 1.26:185140; AIAA-89-2140)
Avail: NTIS HC A03/MF A01 CSCL 01A

Engine airframe integration effects are investigated for superonsic through-flow fan engines installed on a Mach 3.20 supersonic cruise vehicle. Six different supersonic through-flow fan engine installations covering the effects of engine size, nacelle contour, nacelle placement, and approximate bypass plume effects are presented. The different supersonic through-flow fan installations are compared with a conventional turbine bypass engine configuration on the same basic airframe. The supersonic through-flow fan engine integrations are shown to be comparable to the turbine bypass engine configuration on the basis of installed nacelle wave drag. The supersonic through-flow fan engine airframe integrated vehicles have superior aerodynamic performance on the basis of maximum lift-to-drag ratio than the turbine bypass engine installation over the entire operating Mach number range from 1.10 to 3.20. When approximate bypass plume modeling is included, the supersonic through-flow fan engine configuration shows even larger improvements over the turbine bypass engine configuration. Author

VOLUME 28 NUMBER 2 / JANUARY 23, 1990

Scientific and Technical Aerospace Reports

A Semimonthly Publication of the National Aeronautics and Space Administration

01 AERONAUTICS (GENERAL)

N90-10828*# National Aeronautics and Space Administration. Ames Research Center, Moffett Field, CA.
TRANSFER FUNCTIONS FOR NONLINEAR SYSTEMS VIA FOURIER-BOREL TRANSFORMS
Sumer Can (Santa Clara Univ., CA.) and Aynur Unal Feb. 1988 30 p Prepared in cooperation with Army Aviation Systems Command, Moffett Field, CA
(NASA-TM-100034; USAAVSCOM-TR-87-A-6; A-88002; NAS 1.15:100034) Avail: NTIS HC A03/MF A01 CSCL 01B

An analytical functional can be expressed as a sum of some nonlinear functional expansions which we shall call Fliess's generalized expansions. These nonlinear functional expansions are analogous to Fourier series or integral expansions of response functions of linear systems. The shuffle product which is the characteristic of the noncommutative algebra introduced plays a very significant role in this approach. Moreover what makes this approach more attractive is the possibility of doing all of the noncommutative algebra on a computer in any of the currently available symbolic programming languages such as Macsyma, Reduce, PL1, and Lisp. Nonlinear functional expansions for the solution of nonlinear ordinary differential equations can be summarized by the newly introduced Laplace-Borel transforms. Some properties of these transforms are obtained by the second author earlier. Some further properties will be given in this paper for the first time. The main theorem of the paper gives the transform of the response of the nonlinear system as a Cauchy product of its transfer function which is introduced for the first time here and the transform of the input function of the system together with memory effects. Applications of this new transfer-function approach are given using nonlinear electronic circuits. Two categories of applications are presented, namely, analysis of circuits, and synthesis of circuits. We would like to remind the reader that various other examples can be given from other nonlinear dynamical systems; for example nonlinear aerodynamics, nonlinear flight mechanics in which cases these two classes of problems can be called either direct problems or inverse problems. Author

02 AERODYNAMICS

Includes aerodynamics of bodies, combinations, wings, rotors, and control surfaces; and internal flow in ducts and turbomachinery.

For related information see also *34 Fluid Mechanics and Heat Transfer.*

N90-10829*# National Aeronautics and Space Administration. Langley Research Center, Hampton, VA.
MEASUREMENTS OF PRESSURES ON THE TAIL AND AFT FUSELAGE OF AN AIRPLANE MODEL DURING ROTARY MOTIONS AT SPIN ATTITUDES
James S. Bowman, Jr., Randy S. Hultberg, and Colin A. Martin (Aeronautical Research Labs., Melbourne, Australia) Washington Nov. 1989 85 p
(NASA-TP-2939; L-16570; NAS 1.60:2939) Avail: NTIS HC A05/MF A01 CSCL 01A

An investigation was conducted in the Langley Spin Tunnel to measure the pressures on the surface of the horizontal and vertical tail and the aft fuselage of an aircraft model. The pressures were measured on a model of a proposed Australian Primary Trainer airplane configuration while the model was rotating at spinning attitudes. The test results indicate that the presence of the horizontal tail adversely modifies the surface pressure on the vertical tail. The presence of the wing also adversely modifies the pressures on the horizontal and vertical tails. Author

N90-10830*# National Aeronautics and Space Administration. Langley Research Center, Hampton, VA.
LOW-SPEED, HIGH-LIFT AERODYNAMIC CHARACTERISTICS OF SLENDER, HYPERSONIC ACCELERATOR-TYPE CONFIGURATIONS
Gregory M. Gatlin Washington Nov. 1989 46 p
(NASA-TP-2945; L-16537; NAS 1.60:2945) Avail: NTIS HC A03/MF A01 CSCL 01A

Two investigations were conducted in the Langley 14 by 22 Foot Subsonic Tunnel to determine the low-speed aerodynamic characteristics of a generic hypersonic accelerator-type configuration. The model was a delta wing configuration incorporating a conical forebody, a simulated wrap-around engine package, and a truncated conical aftbody. Six-component force and moment data were obtained over a range of attack from -4 to 30 degrees and for a sideslip range of + or - 20 degrees. In addition to tests of the basic configuration, component build-up tests were conducted; and the effects of power, forebody nose geometry, canard surfaces, fuselage strakes, and engines on the lower surface alone were also determined. Control power available from deflections of wing flaps and aftbody flaps was also investigated and found to be significantly increased during power-on conditions. Large yawing moments resulted from asymmetric flow fields exhibited by the forebody as revealed by both surface pressure data and flow visualization. Increasing nose bluntness reduced the yawing-moment asymmetry, and the addition of a canard eliminated the yawing-moment asymmetry. Author

N90-10831 Illinois Univ. at Urbana-Champaign, Savoy.
NUMERICAL SIMULATION OF LEADING-EDGE VORTEX ROLLUP AND BURSTING Ph.D. Thesis
Steven Allan Brandt 1988 117 p
Avail: Univ. Microfilms Order No. DA8908627

Vortex aerodynamics has played an important role in the development of high performance aircraft in recent years. Although computer codes which solve the 3-D Euler equations have been used extensively to study vortex flows they dont include physical viscosity effects associated with vortex flows. The Euler solvers do, however, contain numerical viscosity. As a result, viscosity effects in the Euler solutions such as vortex core size, vortex burst location, leading edge separation, and vortex rollup often do not agree quantitatively with results of physical experiments. Models are defined for these physical viscosity effects which can be coupled with an Euler solver to improve modeling of vortex physics. A vortex core model is derived from the steady, incompressible Navier-Stokes equations written in cylindrical coordinates. The core model is coupled with an Euler solver and tested on a variety of delta wings over a range of angles of attack. The resulting surface pressure distributions and vortex burst locations are shown to be much closer to wind tunnel data and results from Navier-Stokes

solutions than results from Euler codes alone. A second model is defined for viscosity effects in the viscous shear layer near the rounded leading edge of a highly swept wing based on an analogy to the boundary layer on a flat plate. The model is incorporated into an Euler code through the surface boundary condition and source terms in the boundary cells. The modified code is tested on several highly swept wings with rounded leading edges. Results are also shown to be in closer agreement with wind tunnel data for the same wing geometry than results from an unmodified Euler code. Dissert. Abstr.

N90-10832 Arizona State Univ., Tempe.
LOW-REYNOLDS-NUMBER MODELING OF COMPLEX FLOWS WITH AND WITHOUT DENSITY VARIATION Ph.D. Thesis
Geun Jong Yoo 1988 216 p
Avail: Univ. Microfilms Order No. DA8907748

Design of modern combustors and gas turbines require detailed analysis of near-wall flow because complex effects due to geometry, external forces and boundary conditions play dominant roles in the development of the wall boundary layers. Analysis of the near-wall flow behavior reveals the importance of viscous effects and forms the basis of a modified model to calculate the entire flow field including the near-wall region. Based on a near-wall flow analysis, a low Reynolds number full Reynolds stress model was developed and tested against fully developed flow. The model is further applied to calculate complex turbulant flows, such as developing pipe flow with uniform wall transpiration, rotating boundary layers, axisymmetric sudden expansion flows with and without rotation and flows with variable density effects. Different closures used to model turbulent diffusion, redistribution and dissipation rates of the Reynolds stress equations are also investigated in this study. Comparison of the calculated results with measurements show that the low Reynolds number model displays an excellent ability to predict the different types of complex effects. However, it is found that further modifications are necessary in order to better predict the normal components of the Reynolds stresses and the mass fluxes. Dissert. Abstr.

N90-10833*# Institute for Computer Applications in Science and Engineering, Hampton, VA.
LINEAR INSTABILITY OF SUPERSONIC PLANE WAKES Final Report
D. T. Papageorgiou (City Coll. of the City Univ. of New York, NY.) Sep. 1989 48 p Submitted for publication
(Contract NAS1-18605)
(NASA-CR-181911; ICASE-89-66; NAS 1.26:181911) Avail: NTIS HC A03/MF A01 CSCL 01A

In this paper we present a theoretical and numerical study of the growth of linear disturbances in the high-Reynolds-number and laminar compressible wake behind a flat plate which is aligned with a uniform stream. No ad hoc assumptions are made as to the nature of the undisturbed flow (in contrast to previous investigations) but instead the theory is developed rationally by use of proper wake-profiles which satisfy the steady equations of motion. The initial growth of near wake perturbation is governed by the compressible Rayleigh equation which is studied analytically for long- and short-waves. These solutions emphasize the asymptotic structures involved and provide a rational basis for a nonlinear development. The evolution of arbitrary wavelength perturbations is addressed numerically and spatial stability solutions are presented that account for the relative importance of the different physical mechanisms present, such as three-dimensionality, increasing Mach numbers enough (subsonic) Mach numbers, there exists a region of absolute instability very close to the trailing-edge with the majority of the wake being convectively unstable. At higher Mach numbers (but still not large-hypersonic) the absolute instability region seems to disappear and the maximum available growth-rates decrease considerably. Three-dimensional perturbations provide the highest spatial growth-rates. Author

N90-10834*# Old Dominion Univ., Norfolk, VA. Dept. of Mechanical Engineering and Mechanics.
AN EXPERIMENTAL INVESTIGATION OF THE AERODYNAMIC CHARACTERISTICS OF SLANTED BASE OGIVE CYLINDERS USING MAGNETIC SUSPENSION TECHNOLOGY
Charles W. Alcorn and Colin Britcher Nov. 1988 90 p
(Grant NAG1-716)
(NASA-CR-181708; NAS 1.26:181708) Avail: NTIS HC A05/MF A01 CSCL 01A

An experimental investigation is reported on slanted base ogive cylinders at zero incidence. The Mach number range is 0.05 to 0.3. All flow disturbances associated with wind tunnel supports are eliminated in this investigation by magnetically suspending the wind tunnel models. The sudden and drastic changes in the lift, pitching moment, and drag for a slight change in base slant angle are reported. Flow visualization with liquid crystals and oil is used to observe base flow patterns, which are responsible for the sudden changes in aerodynamic characteristics. Hysteretic effects in base flow pattern changes are present in this investigation and are reported. The effect of a wire support attachment on the 0 deg slanted base model is studied. Computational drag and transition location results using VSAERO and SANDRAG are presented and compared with experimental results. Base pressure measurements over the slanted bases are made with an onboard pressure transducer using remote data telemetry. Author

N90-10835*# Scientific Research Associates, Inc., Glastonbury, CT.
USER'S MANUAL FOR PEPSIG NASA TIP VORTEX VERSION
Tommy M. Tsai, Frederick J. deJong, and Ralph Levy Aug. 1988 59 p
(Contract NAS3-24881)
(NASA-CR-182178; NAS 1.26:182178; R88-900064-F) Avail: NTIS HC A04/MF A01 CSCL 01A

The tip vortex flowfield plays a significant role in the performance of advanced aircraft propellers. The flowfield in the tip region is complex, three-dimensional and viscous with large secondary velocities. A computer code was developed to predict the tip vortex flowfield of advanced aircraft propellers. This document is the user's manual. The analysis and a series of test cases are presented in NASA-CR-182179. Author

N90-10836*# Scientific Research Associates, Inc., Glastonbury, CT.
COMPUTATION OF THE TIP VORTEX FLOWFIELD FOR ADVANCED AIRCRAFT PROPELLERS
Tommy M. Tsai, Frederick J. deJong, and Ralph Levy Aug. 1988 62 p
(Contract NAS3-24881)
(NASA-CR-182179; NAS 1.26:182179; R88-900064-F) Avail: NTIS HC A04/MF A01 CSCL 01A

The tip vortex flowfield plays a significant role in the performance of advanced aircraft propellers. The flowfield in the tip region is complex, three-dimensional and viscous with large secondary velocities. An analysis is presented using an approximate set of equations which contains the physics required by the tip vortex flowfield, but which does not require the resources of the full Navier-Stokes equations. A computer code was developed to predict the tip vortex flowfield of advanced aircraft propellers. A grid generation package was developed to allow specification of a variety of advanced aircraft propeller shapes. Calculations of the tip vortex generation on an SR3 type blade at high Reynolds numbers were made using this code and a parametric study was performed to show the effect of tip thickness on tip vortex intensity. In addition, calculations of the tip vortex generation on a NACA 0012 type blade were made, including the flowfield downstream of the blade trailing edge. Comparison of flowfield calculations with experimental data from an F4 blade was made. A user's manual was also prepared for the computer code (NASA CR-182178). Author

N90-10837 Purdue Univ., West Lafayette, IN.
FREQUENCY DOMAIN AERODYNAMIC ANALYSIS OF INTERACTING ROTATING SYSTEMS Ph.D. Thesis
Jinsoo Cho 1988 135 p
Avail: Univ. Microfilms Order No. DA8911891

A multiple harmonic, frequency domain panel method based on linear compressible aerodynamic theory is developed for the aerodynamic analysis of interacting rotating systems. Each stage of the iteration involves the solution of an isolated propeller or wing problem, the interaction being done through the Fourier transform of the induced velocity field. The method was validated by comparing the predicted velocity field about an isolated propeller with detailed laser Doppler velocimeter measurements. The unsteady aerodynamic coupling between a propeller and a wing is analyzed. The mean loads are compared with the measured data and comparisons were made between the fluctuating loads predicted by the present method and a quasi-steady vortex lattice scheme. Also a counter rotating propeller system was investigated. The mean performance parameters are compared with measured data, and the predicted velocity field with detailed laser Doppler velocimeter measurements. Comparisons were also made between the fluctuating loads predicted by the present method and a time domain panel method. Dissert. Abstr.

N90-10838 Tennessee Univ., Knoxville.
A SCALAR/VECTOR POTENTIAL SOLUTION FOR AERODYNAMIC COEFFICIENTS IN WIND SHEAR Ph.D. Thesis
Jyh-Chyang Alex Wang 1988 227 p
Avail: Univ. Microfilms Order No. DA8911769

A recent innovation in aerodynamic calculation techniques is a formulation for the velocity field based on scalar and vector potentials. This technique is presented and implemented into the panel method such that it is able to solve not only irrotational flow but also rotational flow. The application of interest is to two-dimensional airfoils moving into a nonuniform approach flow. Comparisons with theoretical and numerical results are included. Furthermore, the variations of lift and moment coefficients of quasi-steady simulated flight of an airfoil through JAWS wind shear are also studied. Although the present study does demonstrate the hazard of microbursts, the indicated wind shear effects on aerodynamic coefficients are not as great as expected. The present method only indicates the decrease of the effective angle of attack as an important factor. However, in a wind field with intense downdrafts, viscous effects and flow separation should also be crucial. Although the present inviscid model has shown great advantages as a preliminary study of the wind shear effects on aerodynamic coefficients, it cannot predict viscous effects and flow separation phenomena. Therefore, further investigation is recommended to implement viscous effects. For potential flow calculations, comparable accuracy to that obtainable from higher-order panel methods can be achieved by the present formulation using the same number of control points. The present conceptual split of the onset flow into two components, V sub 0 sub n normal and V sub 0 sub t tangential to the zero lift line, is new. The proper vorticity distribution can be determined from - V sub 0 sub n x n directly without imposing an artificial vorticity distributor. This split also supplies a numerically superior form for the Neumann-type lower-order formulation. Author

N90-10839# Los Alamos National Lab., NM. Computing and Communications Div.
A PARALLEL NUMERICAL SIMULATION FOR SUPERSONIC FLOWS USING ZONAL OVERLAPPED GRIDS AND LOCAL TIME STEPS FOR COMMON AND DISTRIBUTED MEMORY MULTIPROCESSORS
N. R. Patel, W. B. Sturek (Ballistic Research Labs., Aberdeen Proving Ground, MD.), and Robert Hiromoto 1989 17 p Presented at the Conference on Applications of Supercomputers in Engineering, Southampton, England, 5-7 Sep. 1989
(Contract W-7405-eng-36)
(DE89-015252; LA-UR-89-2429; CONF-890941-1) Avail: NTIS HC A03/MF A01

Parallel Navier-Stokes codes are developed to solve both two-dimensional and three-dimensional flow fields in and around ramjet and nose tip configurations. A multi-zone overlapped grid technique is used to extend an explicit finite-difference method to more complicated geometries. Parallel implementations are developed for execution on both distributed and common-memory multiprocessor architectures. For the steady-state solutions, the use of the local time-step method has the inherent advantage of reducing the communications overhead commonly incurred by parallel implementations. Computational results of the codes are given for a series of test problems. The parallel partitioning of computational zones is also discussed. DOE

N90-10840*# Eloret Corp., Sunnyvale, CA.
PARTICLE KINETIC SIMULATION OF HIGH ALTITUDE HYPERVELOCITY FLIGHT Semiannual Report, 1 Jan. 1989 - 30 Jun. 1989
Iain D. Boyd 2 Nov. 1989 24 p
(Contract NCC2-582)
(NASA-CR-186003; NAS 1.26:186003) Avail: NTIS HC A03/MF A01 CSCL 01A

A new model for simulating the transfer of energy between the translational and rotational modes was derived for a homogeneous gas of diatomic molecules. The model was developed specifically for use in discrete particle simulation methods where molecular motion and inter-molecular collisions are treated at the molecular level. In such methods it is normal to assume a constant rotational collision number for the entire flowfield. The new model differs in that a temperature dependence is introduced which has been predicted by theory and observed in experiment. The new model is applied to the relaxation of rotational temperature, and is found to produce significant differences in comparison with the model normally employed at both high and low temperatures. Calculations have also been performed for a Mach 7 normal shock wave. Large differences in the solutions are again observed, with the new model offering an improved correspondence to the available experimental data. Author

03 AIR TRANSPORTATION AND SAFETY

Includes passenger and cargo air transport operations; and aircraft accidents.

For related information see also *16 Space Transportation* and *85 Urban Technology and Transportation.*

N90-10841*# National Aeronautics and Space Administration. Ames Research Center, Moffett Field, CA.
DESIGN OF A FINAL APPROACH SPACING TOOL FOR TRACON AIR TRAFFIC CONTROL
Thomas J. Davis, Heinz Erzberger, and Hugh Bergeron Sep. 1989 27 p Prepared in cooperation with NASA. Langley Research Center, Hampton, VA
(NASA-TM-102229; A-89235; NAS 1.15:102229) Avail: NTIS HC A03/MF A01 CSCL 01C

This paper describes an automation tool that assists air traffic controllers in the Terminal Radar Approach Control (TRACON) Facilities in providing safe and efficient sequencing and spacing of arrival traffic. The automation tool, referred to as the Final Approach Spacing Tool (FAST), allows the controller to interactively choose various levels of automation and advisory information ranging from predicted time errors to speed and heading advisories for controlling time error. FAST also uses a timeline to display current scheduling and sequencing information for all aircraft in the TRACON airspace. FAST combines accurate predictive algorithms and state-of-the-art mouse and graphical interface technology to present advisory information to the controller. Furthermore, FAST exchanges various types of traffic information and communicates with automation tools being developed for the Air Route Traffic Control Center. Thus it is part of an integrated traffic management system for arrival traffic at major terminal areas. Author

N90-10842# National Oceanic and Atmospheric Administration, Boulder, CO. Wave Propagation Lab.
REMOTE SENSING TECHNIQUES OF THE WAVE PROPAGATION LABORATORY FOR THE MEASUREMENT OF SUPERCOOLED LIQUID WATER: APPLICATIONS TO AIRCRAFT ICING
E. R. Westwater and R. A. Kropfli May 1989 35 p
(PB89-208102; NOAA-TM-ERL-WPL-163) Avail: NTIS HC A03/MF A01 CSCL 01C

The technical memorandum reviews the processes causing aircraft icing, describes promising new remote sensing instruments and methodologies, and suggests how these can be applied to help solve the aircraft icing problem. Author

N90-10843# Questek, Inc., Centerport, NY.
SEE AND AVOID/COCKPIT VISIBILITY
Walton Graham Oct. 1989 25 p
(DOT/FAA/CT-TN89/18) Avail: NTIS HC A03/MF A01

This study was conducted in response to the Federal Aviation Administration's (FAA) Office of Aviation Safety and the recommendations of the Interagency Near Midair Collision (NMAC) Working Group, dated July 21, 1986, which suggested a review of see and avoid effectiveness, conspicuity enhancement, and their relationship to cockpit visibility. This report summarizes the salient facts in these areas, based on a review of the literature, and assesses the potential for significant reduction of collision risk. The study was conducted by Walton Graham, Questek, Incorporated, who was previously involved in numerous FAA see and avoid, pilot warning instrument/collision risk studies and analyses of the near midair collision data. Author

N90-10844# Oak Ridge National Lab., TN. Computing and Telecommunications Div.
A PRELIMINARY SENSITIVITY ANALYSIS OF THE GENERALIZED ESCAPE SYSTEM SIMULATION (GESS) COMPUTER PROGRAM
Jonas T. Holdeman, Gunar E. Liepins, Brian D. Murphy, Sang Y. Ohr, Thomas J. Sworski, and Gordon E. Warner Jun. 1989 17 p
(Contract DE-AC05-84OR-21400)
(DE89-016891; ORNL/CSD/TM-250) Avail: NTIS HC A03/MF A01

The Generalized Escape System Simulation (GESS) program is a computerized mathematical model for dynamically simulating the performance of existing or developmental aircraft ejection seat systems. The program generates trajectory predictions with 6 degrees of freedom for the aircraft, seat/occupant, occupant alone, and seat alone systems by calculating the forces and torques imposed on these elements by seat catapults, rails, rockets, stabilization and recovery systems included in most escape system configurations. User options are provided to simulate the performance of all conventional escape system designs under most environmental conditions and aircraft attitudes or trajectories. The concept of sensitivity analysis is discussed, as is the usefulness of GESS for retrospective studies, whereby one attempts to determine the aircraft configuration at ejection from the ejection outcome. A very limited and preliminary sensitivity analysis was done with GESS to study the way the performance of the ejection system changes with certain user-specified options or parameters. A more complete analysis would study correlations, where simultaneous correlated variations of several parameters might affect performance to an extent not predictable from the individual sensitivities. Uncertainty analysis is discussed. Even with this limited analysis, a difficulty with some simulations involving a rolling aircraft was discovered; the code produces inconsistent trajectories. One explanation is that the integration routine is not able to deal with the stiff differential equations involved. Another possible explanation is that the coding of the coordinate transformations is faulty when large angles are involved. DOE

N90-10845# General Accounting Office, Washington, DC. National Security and International Affairs Div.
TEST AND EVALUATION: REDUCING RISKS TO MILITARY AIRCRAFT FROM BIRD COLLISIONS. REPORT TO THE CHAIRMAN, LEGISLATION, AND NATIONAL SECURITY SUBCOMMITTEE, COMMITTEE ON GOVERMENT OPERATIONS, HOUSE OF REPRESENTATIVES
13 Jul. 1989 29 p
(AD-A210670; GAO/NSIAD-89-127) Avail: NTIS HC A03/MF A01 CSCL 01/3

This report responds to a request concerning military aircraft testing against bird collisions and development of nonflammable hydraulic fluid. We specifically reviewed: (1) the extent of bird collision damage to military aircraft, (2) the specifications for testing engines against bird collisions, (3) the relationship between engine contractors and the government during tests to identify risks from bird collisions, and (4) the development and use of nonflammable hydraulic fluid to reduce risks from fires. We also reviewed some nontesting measures to reduce the risk to military aircraft, such as bird avoidance efforts and the redesign of aircraft transparencies to withstand bird collisions. GRA

04 AIRCRAFT COMMUNICATIONS AND NAVIGATION

Includes digital and voice communication with aircraft; air navigation systems (satellite and ground based); and air traffic control.

For related information see also *17 Space Communications, Spacecraft Communications, Command and Tracking* and *Communications and Radar.*

N90-10846# Department of Defense, Washington, DC.
FEDERAL RADIONAVIGATION PLAN, 1988 Final Report, Jan. 1987 - Dec. 1988
1988 177 p Prepared in cooperation with DOT, Washington, DC
(PB89-163075; DOD-4650.4; DOT-TSC-RSPA-88-4) Avail: NTIS HC A09/MF A01 CSCL 17G

The Federal Radionavigation Plan (FRP) delineates policies and plans for radionavigation services provided by the U.S. Government to ensure efficient use of resources and full protection of national interests. Developed jointly by the U.S. Departments of Defense and Transportation, the FRP sets forth the Federal interagency approach to the implementation and operation of radionavigation systems. The FRP is updated biennally. The fifth edition describes respective areas of authority and responsibility, and provides a management structure by which the individual operating agencies will define and meet requirements in a cost-effective manner. Moreover, the edition contains the current policy on the radionaviagation systems mix. The constantly changing radionavigation user profile and rapid advancements in systems technology, combined with delays in the U.S. space program, require that the FRP remain as dynamic as the issues it addresses. GRA

N90-10847# Advisory Group for Aerospace Research and Development, Neuilly-Sur-Seine (France). Guidance and Control Panel.
KALMAN FILTER INTEGRATION OF MODERN GUIDANCE AND NAVIGATION SYSTEMS
Jun. 1989 181 p In ENGLISH and FRENCH Lecture series held in Delft, Netherlands, 26-27 Jun. 1989, in Neubiberg, Fed. Republic of Germany, 29-30 Jun. 1989, and in London, England, 3-4 Jul. 1989
(AGARD-LS-166; ISBN-92-835-0514-X) Copyright Avail: NTIS HC A09/MF A01

The integration of modern guidance and navigation systems is usually performed with a suboptimal implementation of the Kalman filter. The most difficult problem is how to develop that suboptimal implementation when considering system modeling, algorithm design, and real hardware nonlinearities. This lecture series brings

together a group of speakers with outstanding practical experience in the design of integrated systems, providing the audience with the principles, insights, and mechanisms of real, current-day system synthesis approaches, and giving the overall background necessary for synthesizing future practical guidance and navigation systems. Two of the lectures deal with the synthesis of solutions to tracking problems. The remainder of the lectures deal with the integrations of avionics systems. For individual titles, see N90-10848 through N90-10854.

N90-10848# Norwegian Defence Research Establishment, Kjeller.
DESIGN OF A KALMAN FILTER FOR TRANSFER ALIGNMENT
Oddvar Hallingstad *In* AGARD, Kalman Filter Integration of Modern Guidance and Navigation Systems, Jun. 1989 14 p (For primary document see N90-10847 02-04)
Copyright Avail: NTIS HC A09/MF A01

The design philosophy used in the development of the alignment subsystem of the inertial midcourse navigation system for the air launched Penguin antiship missile adopted for the F-16 fighter aircraft is described. The desired performance was achieved through a three level Kalman filter (KF) design process. On the first level it was assumed that the system is linear and then the KF was designed. On the second level the design of the preprocessor which makes the linear assumptions on level one valid, was presented. The last level deals with the field testing of the missile navigation system which is the final test of the validity of the design procedure. Author

N90-10849# Messerschmitt-Boelkow-Blohm G.m.b.H., Munich (Germany, F.R.).
DEVELOPMENT OF THE INTEGRATED ALL-WEATHER NAVIGATION SYSTEM FOR TORNADO
Frank Hupke and Florian Schwegler *In* AGARD, Kalman Filter Integration of Modern Guidance and Navigation Systems Jun. 1989 15 p (For primary document see N90-10847 02-04)
Copyright Avail: NTIS HC A09/MF A01

The integrated navigation system for the Tornado weapon system was now in service for almost 10 years. A detailed presentation will be given on the following topics: primary development approach, problems encountered in development and solutions, side developments that were not implemented for various reasons, methods used for optimization, and modifications of the filter as revisions of the Tornado navigation system were performed. Author

N90-10850# Ferranti Defence Systems Ltd., Edinburgh (Scotland). Dept. of Navigation Systems.
A HIGH PERFORMANCE AIRBORNE INS/GPS INTEGRATED NAVIGATION SYSTEM
David I. Callender *In* AGARD, Kalman Filter Integration of Modern Guidance and Navigation Systems Jun. 1989 15 p (For primary document see N90-10847 02-04)
Copyright Avail: NTIS HC A09/MF A01

The system architecture and the trade-offs that drive its evolution are examined for a practical high-performance Integrated System designed for a number of current requirements. The system incorporates a 4 gimbal inertial navigator of inherently high stand-alone performance, integrated with a state-of-the-art 5 channel F-code GPS receiver. The system partitioning and interfacing are configured to optimize system accuracy during potentially lengthy periods when a full GPS solution may be unavailable, while providing satisfactory integrity under reversionary conditions. The main Kalman Filter takes pseudo-range and range rate measurements from the GPS rather than position and velocity and in the primary navigation mode models INS and GPS error parameters. The Kalman Filter in the GPS receiver operates independently to provide the desired reversionary capability. The system architecture, both in hardware and software, allows a high degree of inherent flexibility which is required to tailor the Integrated Navigation System to a wide variety of specific applications. Author

N90-10851# Defence Research Establishment, Ottawa (Ontario). Electromagnetics Section.
THE DEVELOPMENT OF MISSION-SPECIFIC ADVANCED INERTIALLY-BASED AVIONICS SYSTEM
D. F. Liang and D. J. DiFilippo *In* AGARD, Kalman Filter Integration of Modern Guidance and Navigation Systems Jun. 1989 25 p (For primary document see N90-10847 02-04)
Copyright Avail: NTIS HC A09/MF A01

The Defence Research Establishment Ottawa (DREO) was involved in the development of several mission-specific airborne inertially based multi-sensor integrated avionics systems. More specifically, DREO has successfully completed the Phase 2 development and flight trial evaluation of an airborne Synthetic Aperture Radar Motion Compensation System (SARMCS). To achieve high resolution, high contrast and low geometric distortion in synthetic aperture radar imagery, it is necessary to apply accurate motion compensation to the radar returns. The hardware configuration consists of a ring laser gyro inertial navigation system, a Doppler radar, a baroaltimeter and a specially designed strapped-down Motion Compensation Inertial Measurement Subsystem (MCIMS). The Department of National Defence is also undertaking a program to develop and flight test a Helicopter Integrated Navigation System (HINS) which can satisfy the operational requirements of Canadian New Shipborne Aircraft (NSA). The roles of this maritime helicopter include search and rescue, Anti-Surface Surveillance and Targeting (ASST), Anti-Submarine Warfare (ASW), and Anti-Ship Missile Defence (ASMD). The development of appropriate Kalman filters to integrate the selected avionics configurations is described. Design objectives, configuration definition, simulation analysis and some flight test data are presented. Author

N90-10852# Defence Research Establishment, Ottawa (Ontario). Electromagnetics Section.
DEVELOPMENT OF A MARINE INTEGRATED NAVIGATION SYSTEM
D. F. Liang and J. C. McMillan *In* AGARD, Kalman Filter Integration of Modern Guidance and Navigation Systems Jun. 1989 23 p (For primary document see N90-10847 02-04)
Copyright Avail: NTIS HC A09/MF A01

Startling advances in electronics and computer technologies over the last two decades have significantly altered the scope of military operations, weapon systems and some of the required supporting services. The increased range, speed and accuracy of modern weapon systems impose stringent accuracy and reliability requirements upon the navigation systems of military platforms. Over the last few years, DREO was involved in the development of a microprocessor-based Marine Integrated Navigation System (MINS). The present version of the MINS can work with a variety of types and brands of navigation sensors such as Omega, Transit, GPS, Loran C, speedlog and gyrocompass as well as operator-entered position or sextant measurements. It has been successfully tested on both Canadian and U.S. Navy vessels and it is due to be installed on almost all of Her Majesty's Canadian ships in 1988. The application of Kalman filter design to optimally and synergistically combine the diverse types of navigation sensor information is described. Technical problems, design objectives and some design features unique to this application are highlighted. Results of sea trial evaluations are compared to simulation results. Integrated system design guidelines and road maps derived from the Canadian experience are also presented. Author

N90-10853# Air Force Inst. of Tech., Wright-Patterson AFB, OH. Dept. of Electrical and Computer Engineering.
ADAPTIVE TRACKING OF MANEUVERING TARGETS BASED ON IR IMAGE DATA **c74**
Peter S. Maybeck *In* AGARD, Kalman Filter Integration of Modern Guidance and Navigation Systems Jun. 1989 18 p (For primary document see N90-10847 02-04)
Copyright Avail: NTIS HC A09/MF A01

The capability of tracking dynamic targets from forward looking infrared (FLIR) measurements was improved substantially by replacing standard correlation trackers with adaptive extended

Kalman filters or enhanced correlator/Kalman filter combinations. A tracker able to handle multiple hot-spot targets, in which digital and/or optical signal processing is employed on the FLIR data to identify the underlying target shape is investigated. Furthermore, multiple model adaptive filtering is investigated as a means of changing the field-of-view as well as the tracker bandwidth when target acceleration can vary over a wide range. Enhancements are developed and analyzed: (1) allowing some of the elemental filters within the adaptive algorithm to have rectangular fields-of-view and to be tuned for target dynamics that are harsher in one direction than others; (2) considering both Gauss-Markov acceleration models and constant turn-rate models for target dynamics; and (3) devising an initial target acquisition algorithm to remove important biases in the estimated target template to be used within the tracker. The performance potential of such a tracking algorithm is shown to be substantial. Author

N90-10854# Centre d'Etudes et de Recherches, Toulouse (France).
PASSIVE TRAJECTOGRAPHY BY AZIMUTH: IMPROVEMENT OF ESTIMATION QUALITY [TRAJECTOGRAPHIE PASSIVE PAR AZIMUT: AMELIORATION DE LA QUALITE D'ESTIMATION]
Pierre Vacher, Michel Gauvrit, Guy MaynarddeLavalette, and Philippe Mennecier (CAPCA, Le Pradet, France) *In* AGARD, Kalman Filter Integration of Modern Guidance and Navigation Systems Jun. 1989 30 p In FRENCH (For primary document see N90-10847 02-04)
Copyright Avail: NTIS HC A09/MF A01

Many of the difficulties are described for target tracking such as nonlinearities and maneuvers when using bearings-only tracking whose characteristic feature is poorness of information in terms of observability. Investigations are described for recursive and global algorithms as well as leg by leg estimation techniques. Conditioning of the computations, the implementation of the algorithms, and the accuracy of the estimators are presented. Author

N90-10855# Computer Resource Management, Inc., Vienna, VA.
GROUND AND OBSTACLE AVOIDANCE (GOA) CONCEPT OF OPERATIONS
William Trent, Rodney Kuhn, and Thomas Pickerell Jun. 1989 39 p
(Contract DTFA01-88-Y-10173)
(DOT/FAA/DS-89/08) Avail: NTIS HC A03/MF A01

A requirement for the National Airspace System (NAS) is to provide for detecting the need for and assisting in ground and obstacle avoidance activities, as identified in the NAS System Requirement Specification, NAS-SR-1000. A concept is presented of operations for ground and obstacle avoidance. Ground and obstacle avoidance assistance capabilities are described and the relationships are shown between subsystems, facilities, information, and operators/users. A common perspective is provided for personnel involved in ground and obstacle avoidance activities, assist in determining whether the ground and obstacle avoidance activities meet formal requirements, and support coordination among the organizations involved. Author

N90-10856# Federal Aviation Administration, Atlantic City, NJ.
HELICOPTER VISUAL SEGMENT APPROACH LIGHTING SYSTEM (HALS) Test Report
Barry R. Billmann and Scott Shollenberger Jun. 1989 318 p
(Contract FAA-T0701-U)
(ACD-330; DOT/FAA/CT-TN89/21) Avail: NTIS HC A14/MF A02

A test designed to obtain pilot performance subjective pilot data on the Helicopter Visual Segment Approach Lighting System (HALS) is reported. Results identify the performance measures which correlate with the pilot's ability to visually acquire a HALS equipped heliport. Conclusions state that HALS can support existing minima to heliports. Pilots reported unacceptable Cooper-Harper ratings for rate of closure and workload without HALS. Author

N90-10857 Virginia Polytechnic Inst. and State Univ., Blacksburg.
OPTIMAL AND ON-BOARD NEAR-OPTIMAL MIDCOURSE GUIDANCE Ph.D. Thesis
Shevach Katzir 1988 143 p
Avail: Univ. Microfilms Order No. DA8911055

Optimal midcourse guidance is examined for an air-to-air missile featuring boost-coast-sustain propulsion. A vertical plane, point-mass model is studied with load factor as a control variable. Time-range-energy optimal trajectories are computed, open-loop, via the usual necessary conditions and a multiple-shooting algorithm. A requirement on terminal velocity magnitude is examined for its effect on firing range. Next, a study of the optimal midcourse guidance problem with reduced-order models is presented. The models under study, in addition to the point-mass model, are: (1) Singularly perturbed model with gamma as fast variable; (2) Point mass model with approximation of the induced-drag; and (3) Energy model. One of the major results is that the reduced-order models are not accurate enough to approximate the optimal trajectories and so are of limited use as reference trajectories in an on-board scheme. Thus, optimal trajectories, computed by using the point-mass model, are selected as the reference trajectories for a closed-loop guidance scheme. Finally, an approach to on-board real-time calculations for an optimal guidance approximation is derived. Extremal fields and neighboring extremal theory ideas are used together with pre-calculated Euler solutions to construct a closed-loop guidance algorithm. The method is applied to the midcourse guidance of an air-to-air missile and was found to perform quite well. Dissert. Abstr.

N90-10858 Nottingham Univ. (England).
HIGH ACCURACY COORDINATE DETERMINATION USING THE GLOBAL POSITIONING SYSTEM Ph.D. Thesis
Clive delaFuente 1988 339 p
Avail: Univ. Microfilms Order No. BRD-85419

The Global Positioning System (GPS) is a space based navigation system. Using the signals emitted from NAVSTAR satellites it will soon be possible for a user to obtain an instantaneous position fix, anywhere on the Earth, 24 hours a day, without regard to weather conditions. Indeed, even if the user is travelling at very high velocities above the Earth's surface this will still be possible. The accuracies attainable using these signals are sufficient for navigational purposes, but not for geodesy. However, by taking measurements on the carrier wave (onto which the navigational signals are modulated) it is possible to perform relative positioning to a much higher degree of accuracy. Typical values for this interferometric analysis are around the 1 part per million level. However for this to be achieved an observation time of over 40 minutes is required. The theories are reviewed which are behind GPS and details the algorithms required to analyse GPS data. The formation is described of a package of programs for the processing of GPS observations both in the navigational and the interferometric mode of operation. The package was designed so that it is highly flexible, having the capability to input data from several different types of GPS receiver. In interferometric mode it is then possible to combine the observations for each receiver in a single network analysis. In order to validate the software several field trials were undertaken and the data processed. The results from these tests are presented, along with a discussion of the factors which have influenced them. Other topics which are considered include the error sources which contaminate the carrier phase data and a technique for cutting down the observation time from many minutes to several seconds. Dissert. Abstr.

N90-10859# Mayflower Communications Co., Inc., Reading, MA.
STS-GPS (SPACE TRANSPORTATION SYSTEM - GLOBAL POSITIONING SYSTEM) TRACKING EXPERIMENT FOR GRAVITATION ESTIMATION: FEASIBILITY STUDY Final Report, 25 Jul. 1986 - 25 Oct. 1988
Triveni N. Upadhyay, George Priovolos, Wallace E. VanderVelde,

and Harley Rhodehamel Feb. 1989 161 p
(Contract F19628-86-C-0136)
(AD-A211265; MCCI-TR-89-861002; AFGL-TR-89-0035) Avail: NTIS HC A08/MF A01 CSCL 08/5

The report summarizes the results of a feasibility study to estimate the gravitation parameters using GPS and IMU measurements onboard the Space Shuttle. The primary objective of the study was to determine the feasibility of estimating perturbations in the gravity vector at the Shuttle altitude to an accuracy of 1 mgal or better (1-sigma) in each axis. A detailed error analysis of the effect of measurement errors on the Shuttle acceleration estimation accuracy was carried out which resulted in the identification of critical errors. Techniques to mitigate the effect of these critical errors were developed. A survey of available hardware to demonstrate the experiment on the Shuttle in 1990 to 1991 was undertaken and candidate instruments (e.g., GPS receiver, IMU, processor, tape recorder) to support the experiment objectives were identified. Integration of the experiment instrumentation system on the shuttle as a mission kit was carried out. The results of the error analysis, hardware selection and Shuttle integration analysis clearly established the feasibility of the proposed Air Force experiment to map the gravity field in regions where data availability is generally limited. The Air Force STS-GPS Tracking experiment is a low-cost alternative to obtain the gravitation data in restricted areas. GRA

05 AIRCRAFT DESIGN, TESTING AND PERFORMANCE

Includes aircraft simulation technology.

For related information see also *18 Spacecraft Design, Testing and Performance* and *39 Structural Mechanics*.For land transportation vehicles see *85 Urban Technology and Transportation*.

N90-10860# Advisory Group for Aerospace Research and Development, Neuilly-Sur-Seine (France). Flight Mechanics Panel.

FLIGHT TEST TECHNIQUES

Jul. 1989 419 p In ENGLISH and FRENCH Symposium held at Edwards AFB, CA, 17-20 Oct. 1988
(AGARD-CP-452; ISBN-92-835-0509-3) Copyright Avail: NTIS HC A18/MF A03

It is important that the flight test community meet regularly so that techniques for flight test, instrumentation and data analysis can be disseminated to ensure safe, efficient, and timely testing. The number of systems submitted for airborne trials and testing is increasing. The major development and test challenge common to most aircraft is that of avionic/software subsystems development and integration. Systems and applications include programmable signal process radars, integrated flight, fire and propulsion systems, multifunction pilot displays, and other on-board software-intensive systems. The focus was on the means of reducing the overall cost of test and development within defence program. Ground based simulation offers the potential for saving many test flying hours in the area of system integration. It is an indispensable tool for system failure analysis for sophisticated avionics of all types. For individual titles, see N90-10861 through N90-10887.

N90-10861# Naval Air Test Center, Patuxent River, MD. Advanced Tactical Aircraft Program.

US NAVY PRINCIPAL SITE TESTING CONCEPT AND THE F-18

Joe L. Dunn *In* AGARD, Flight Test Techniques Jul. 1989 4 p (For primary document see N90-10860 02-05)
Copyright Avail: NTIS HC A18/MF A03

In 1975, a decision was made to conduct the F-18 Full Scale Development (FSD) Program at a primary Navy location, the U.S. Naval Air Test Center (NAVAIRTESTCEN). Previous FSD programs had utilized multiple test locations which resulted in significant program duplication from a facilities, logistics, and test data viewpoint. The principal site concept provides for a primary Navy location where all test assets are co-located. These assets include developmental aircraft, contractor and Navy test personnel, maintenance personnel, and all test equipment. The success of the F-18 principal site testing program paved the way for the AV-8B and LAMPS MK 3 programs at the NAVAIRTESTCEN. The principal site concept has had excellent benefits for the U.S. Navy in terms of improved test aircraft utilization, better visibility into the contractor's test program, elimination of redundant testing by utilizing a common data base, and improved utilization of government test facilities. From the Navy's T and E community viewpoint, it is preferable to conduct the programs at a Navy test activity. Due to program funding constraints, this may not always be possible. With the F-14D and A-6F upgrade programs, the testing is being conducted at the contractor's facility as opposed to a Navy facility. In this case, the Navy has established a Navy Test Team on-site and is participating actively with the contractor during the FSD programs. The impact of the principal site testing concept will be examined from the prospective of both the Navy and the contractor in terms of impact on the individual organizations. Author

N90-10862# Deutsche Forschungs- und Versuchsanstalt fuer Luft- und Raumfahrt, Brunswick (Germany, F.R.). Inst. for Flight Mechanics.

ATTAS FLIGHT TESTING EXPERIENCES

H.-H. Lange, D. Rohlf, A. Zach, and H.-L. Meyer *In* AGARD, Flight Test Techniques Jul. 1989 14 p (For primary document see N90-10860 02-05)
Copyright Avail: NTIS HC A18/MF A03

An overview of recent development and flight test experiences of the DFVLR's flight test vehicle Advanced Technologies Testing Aircraft System (ATTAS) equipped with a digital fly-by-wire/light flight control system is presented. System design, multiprocessor communication management, parallel data processing, redundancy management as well as software development and validation are summarized. Further, the role of ground based system simulation for development and testing, flight test procedures and interesting flight test results are dealt with in several examples. Author

N90-10863# I.A.M. Rinaldo Piaggio, Finale Ligure (Italy).

P-180 AVANTI: PROJECT AND FLIGHT TEST PROGRAM COMPREHENSIVE OVERVIEW

R. dePompeis and E. Traini *In* AGARD, Flight Test Techniques Jul. 1989 28 p (For primary document see N90-10860 02-05)
Copyright Avail: NTIS HC A18/MF A03

Among the turboprops in advanced flight testing phase, the Piaggio P-180 AVANTI possesses exciting features. Very unconventional shape, characterized by 3 lifting surfaces, pusher props, mid-wing very rearback mounted, is coupled with outstanding speed and range performances. The project and flight test programs planning has required much care for the peculiar characteristic of the aircraft. Areas of extensive in-flight investigation were: flutter expansion; stability and control at high angle of attack; laminar flow investigation; flap system tuning; and propeller stress. The focus is on the P-180 project and flight test programs presenting the project concepts and the test results achieved to date. The flight test program, actually in the certification phase, has achieved more than 600 flight hours and RAI/FAA initial certification is expected for mid 1989. Author

N90-10864# Airbus Industrie, Blagnac (France). Dept. Essais en Vol.

A320 FLIGHT TESTS: PARTICULARITIES AND INNOVATIONS [ESSAIS EN VOL A320]

Gerard Guyot *In* AGARD, Flight Test Techniques Jul. 1989 5 p In FRENCH (For primary document see N90-10860 02-05)
Copyright Avail: NTIS HC A18/MF A03

The general architecture of the electronic flight control system for the A320 Airbus is described and the functions of the SPATIAL system are outlined. Protection against electromagnetic radiation is addressed and related ground and flight tests are briefly described. Author

N90-10865# British Aerospace Public Ltd. Co., Preston (England). Military Aircraft Div.
THE EXPERIMENTAL AIRCRAFT FLIGHT TEST PROGRAMME
R. A. Hartley *In* AGARD, Flight Test Techniques Jul. 1989 11 p (For primary document see N90-10860 02-05)
Copyright Avail: NTIS HC A18/MF A03

The Experimental Aircraft Program has grown out of the studies carried out over the last decade to investigate the needs for the next generation of fighter. These studies resulted in the definition of a large number of new technologies for which it was recognized that there would be significant benefits to be gained by their integration into a demonstrator aircraft. The objectives and progress of the flying program are described for this demonstrator and how it has lead on to the European Fighter Aircraft. Author

N90-10866*# National Aeronautics and Space Administration. Ames Research Center, Moffett Field, CA.
REAL-TIME FLIGHT TEST ANALYSIS AND DISPLAY TECHNIQUES FOR THE X-29A AIRCRAFT
John W. Hicks and Kevin L. Petersen *In* AGARD, Flight Test Techniques Jul. 1989 17 p (For primary document see N90-10860 02-05)
Copyright Avail: NTIS HC A18/MF A03 CSCL 01C

The X-29A advanced technology demonstrator flight envelope expansion program and the subsequent flight research phase gave impetus to the development of several innovative real-time analysis and display techniques. These new techniques produced significant improvements in flight test productivity, flight research capabilities, and flight safety. These techniques include real-time measurement and display of in-flight structural loads, dynamic structural mode frequency and damping, flight control system dynamic stability and control response, aeroperformance drag polars, and aircraft specific excess power. Several of these analysis techniques also provided for direct comparisons of flight-measured results with analytical predictions. The aeroperformance technique was made possible by the concurrent development of a new simplified in-flight net thrust computation method. To achieve these levels of on-line flight test analysis, integration of ground and airborne systems was required. The capability of NASA Ames Research Center, Dryden Flight Research Facility's Western Aeronautical Test Range was a key factor to enable implementation of these methods. Author

N90-10867# Avions Marcel Dassault-Breguet Aviation, Istres (France).
FLIGHT TEST TECHNIQUES ADOPTED BY AVIONS MARCEL DASSAULT-BREGUET AVIATION
Jean Costard *In* AGARD, Flight Test Techniques Jul. 1989 35 p In FRENCH and ENGLISH (For primary document see N90-10860 02-05)
Copyright Avail: NTIS HC A18/MF A03

The ever-increasing complexity of aircraft and systems entailed, in parallel, a very substantial increase in development tests, and consequently a rise of cost. Avions Marcel Dassault-Breguet Aviation (AMD-BA) have adopted techniques enabling to reduce the number of flight tests for the benefit of less expensive ground tests: flights must be saved for demonstation with the aim of qualification. These techniques allowed to keep in control of data acquisition rates while preserving reasonable means of computation and facilitating analysis. Author

N90-10868# Deutsche Forschungs- und Versuchsanstalt fuer Luft- und Raumfahrt, Brunswick (Germany, F.R.). Inst. fuer Flugmechanik.
GRATE: A NEW FLIGHT TEST TOOL FOR FLYING QUALITIES EVALUATION
R. Koehler, E. Buchacker, and D. J. Biezad (Air Force Inst. of Tech., Wright-Patterson AFB, OH.) *In* AGARD, Flight Test Techniques Jul. 1989 18 p (For primary document see N90-10860 02-05)
Copyright Avail: NTIS HC A18/MF A03

A flight test tool was worked out by DFVLR for flying quality evaluations of ground attack tracking phases. This Ground Attack Technique (GRATE) was proven in test flights of the German Federal Armed Forces Engineering Center for Aircraft and was integrated in the Large Amplitude Multimode Aerospace Research Simulator (LAMARS) of Air Force Wright Aeronautical Laboratories (AFWAL) in Dayton. The German/U.S. cooperation was supported by the Memorandum of Understanding (MoU) Flight Control Concepts. A description of the flight test method and of the pilot's role and ratings is given. Head-up-display films evaluated to determine a so called align-time and a circular error probability (CEP). The influence of different test conditions on the mission parameters were investigated. The results of the numerical analysis and the pilot ratings were compared. The determined gradients show the sensitivity of a pilot rating to the mission parameters. In this context a configuration with slight PIO-tendencies is discussed. Simulator tests have shown that the technique is an effective tool for unmasking aircraft handling problems. The effects caused by different turbulence levels on pilot ratings were found to be small in comparison to conventional methods. Author

N90-10869# Aeritalia S.p.A., Caselle Torinese (Italy). Combat Aircraft Group.
IN FLIGHT RELIGHT TESTS ON AM-X SINGLE ENGINE FLY-BY-WIRE AIRCRAFT
G. Menso and G. Gamalero *In* AGARD, Flight Test Techniques Jul. 1989 17 p (For primary document see N90-10860 02-05)
Copyright Avail: NTIS HC A18/MF A03

The in-flight relight evaluation of a single engine aircraft could be considered one of the more interesting aspects of flight testing. When the engine is intentionally shut down in flight to attempt the relight, possibility of an unsuccessful one must always be taken into account and therefore a flame out landing must be contemplated, otherwise the aircraft is lost. This event may be particularly serious on a fly-by-wire aircraft on which the loss of the engine and all its driven accessories will make control very difficult if not impossible. Therefore, the planning and the execution of this kind of test not only concerns the propulsion aspects, but involves all the aircraft, because full evaluation (both theoretic and flight test) of aircraft and systems performance and reliability in engine out condition must be carried out in advance of the actual relight tests. Besides the relight evaluation must be carried out as early as possible on the program to allow safe performing of those tests that may cause a flame out. All the activities carried out by AERITALIA Flight Test Department in connection with relight tests of AM-X are described and may therefore be looked upon as a reference for smooth test planning and execution. Author

N90-10870# Technische Univ., Brunswick (Germany, F.R.). Inst. for Flight Guidance and Control.
FLIGHT TEST RESULTS OF A COMPLEX PRECISE DIGITAL FLIGHT CONTROL SYSTEM
Gunther Schaenzer *In* AGARD, Flight Test Techniques Jul. 1989 9 p (For primary document see N90-10860 02-05)
Copyright Avail: NTIS HC A18/MF A03

The presented flight control systems consist of an open loop control system and a more conventional state vector feed back closed system. The open loop actuator control includes a quasistationary aircraft model and a full state command model. For the flight tests of this control system, the minimization of the state vector error was the basic target. To improve the flight test quality, an onboard real time wind and turbulence measurement system has been used. The flexible flight test instrumentation including sensors and computers will be described and some typical flight test results will be demonstrated. Author

N90-10871# Office National d'Etudes et de Recherches Aerospatiales, Toulouse (France). Dept. Automatique.
ANALYSIS OF FLUTTER TESTS WITH THE USE OF A TELEMETRY SYSTEM [ANALYSE DES ESSAIS DE FLOTTEMENT A L'AIDE D'UN SYSTEME DE TELEMESURE]
Alain Bucharles, Gerald Lignon, and Henri Cassan (Aerospatiale, Toulouse, France) *In* AGARD, Flight Test Techniques Jul. 1989 10 p In FRENCH (For primary document see N90-10860

02-05)
Copyright Avail: NTIS HC A18/MF A03
The principles and procedures of in-flight flutter testing are discussed with particular emphasis given to the use of telemetry. Data processing and analysis techniques are described. Application of such in-flight testing methods to the A320 Airbus is discussed. Author

N90-10872# Air Force Flight Test Center, Edwards AFB, CA.
THE AIR FORCE FLIGHT TEST CENTER FLIGHT TEST SAFETY PROGRAM
Kelly J. Adams and Mark R. Crawford *In* AGARD, Flight Test Techniques Jul. 1989 10 p (For primary document see N90-10860 02-05)
Copyright Avail: NTIS HC A18/MF A03
The success of the AFFTC flight test safety program is based on: (1) careful attention to the safety planning aspects of testing by each program manager, with thorough review of any applicable formal safety analyses, investigation of more experienced personnel in the subject of test and review of past programs of similar nature for successful and faulty safety planning; (2) management review of the safety aspects, endorsement and approval of every new and modified test program; (3) the establishment of a staff system safety division which facilitates an independent review of every new and modified test program; (4) flexibility in the safety documentation when programmatic changes occur; (5) attention to test disciplines of control room procedures, conduct and communication; and (6) the presence of a Unit System Safety Officer at each project to review the safety documentation for completeness and accuracy. Author

N90-10873# Aeronautica Macchi S.p.A., Varese (Italy). Technical Dept.
RESULTS AND PRACTICAL EXPERIENCE USING PARAMETER IDENTIFICATION TECHNIQUES ON THE AM-X PROGRAM AT AERMACCHI
M. Lucchesini, P. Maestrelli, L. Manfriani, and P. Chimetto *In* AGARD, Flight Test Techniques Jul. 1989 16 p (For primary document see N90-10860 02-05)
Copyright Avail: NTIS HC A18/MF A03
The results and the practical experience gained by introducing the parameter identification technique in AM-X flight test analysis at Aermacchi are presented. Taking into account the Company's requirement, preference was given to a well known and established program that could guarantee excellent cost effectiveness. The Iliff-Maine code used (MMLE3 program) during the flight test program is shown to be robust enough to provide useable results rapidly in almost any conditions. Aerodynamic derivatives were evaluated using linear and parabolic models over a wide range of Mach numbers, altitudes and angles of incidence. Both longitudinal results and an analysis of a lateral departure are presented. Author

N90-10874# Centre d'Essais en Vol, Bretigny-sur-Orge (France).
LESSONS LEARNED FROM THE INTEGRATION OF FLIGHT SYSTEMS [LES ENSEIGNEMENTS DE L'INTEGRATION DES SYSTEMES EMBARQUES]
Jacques Tresset *In* AGARD, Flight Test Techniques Jul. 1989 9 p In FRENCH (For primary document see N90-10860 02-05)
Copyright Avail: NTIS HC A18/MF A03
Suggestions for minimizing overall costs and delays of flight tests related to the integration of aircraft flight systems are presented. Experiences with the ACT Rafale program are discussed. Author

N90-10875# Messerschmitt-Boelkow-Blohm G.m.b.H., Munich (Germany, F.R.). Military Aircraft Div.
FLIGHT TESTING OF THE TORNADO TERRAIN FOLLOWING SYSTEM
Thomas Fleck *In* AGARD, Flight Test Techniques Jul. 1989 12 p (For primary document see N90-10860 02-05)
Copyright Avail: NTIS HC A18/MF A03
The flight test activities on the assessment of the Tornado Terrain Following System are reviewed. Extensive hardware and pilot in the loop simulation, a stepwise approach to the lowest height and proceeding from VMC to IMC kept the risk at a minimum level. For a demonstration of system performance a method of comparing simulation was applied that considers avionic parameters, aerodynamic parameters, and flight control data. Special emphasis was placed on system integrity and flight safety, including human factors of the aircrew. Today, after having absolved more than 200 successful test flights and rectified a considerable number of problems, the system was adopted by the services and is a substantial part of the low level missions. Author

N90-10876# Royal Aerospace Establishment, Farnborough (England).
EVALUATION OF STORE CARRIAGE (AND RELEASE) ENVIRONMENT USING FLIGHT INSTRUMENTED STORES
H. A. Torode, P. J. Driffill, and D. Charles (Cranfield Inst. of Tech., Bedford, England) *In* AGARD, Flight Test Techniques Jul. 1989 19 p (For primary document see N90-10860 02-05)
Copyright Avail: NTIS HC A18/MF A03
The approach adopted by Attack Weapons Department, Royal Aerospace Establishment, Farnborough, in conjunction with Cranfield Institute of Technology for obtaining experimental data pertinent to the carriage and release of conventional free fall weapons is described. To this end a series of instrumented, flight cleared stores were developed for various data gathering exercises, and results from several of the flight experiments completed to date, are discussed. In addition some future developments are presented. Author

N90-10877# Aerospace Engineering Test Establishment, Cold Lake (Alberta).
CF 18 480 GALLON EXTERNAL FUEL TANK STORES CLEARANCE PROGRAM
Douglas N. Kobayashi and Mirko B. Zgela *In* AGARD, Flight Test Techniques Jul. 1989 15 p (For primary document see N90-10860 02-05)
Copyright Avail: NTIS HC A18/MF A03
The Canadian Government has embarked on a program with Canadian industry to manufacture a composite 480 gallon external fuel tank (EFT) designed for the CF-18 aircraft by McDonnell Aircraft Company (McAir). Prior to commencing the production phase of the program, the Aerospace Engineering Test Establishment (AETE) of the Canadian Forces (CF) was tasked to support McAir in the flight test certification of the 480 EFT on the inboard wing stations of the CF-18. The main objective was to provide a proof of concept flight demonstration as well as establish an operational flight envelope for the carriage and jettison of the 480 EFT with and without adjacent stores. The certification process involved a progressive series of analyses, laboratory tests, wind tunnel tests, ground tests and flight tests. As the CF flight test authority, AETE was responsible for conducting all flight testing activities including flutter, active oscillation control (AOC), structural mode interactions (SMI), stability and control, structural carriage loads, separation/jettison, and dynamic response testing. An overview is presented of the the joint CF-18 480 EFT stores clearance program and its main emphasis is in describing the analyses and tests performed during the ground vibration testing, flutter, AOC, SMI and carriage loads phases. The aircraft instrumentation and the qualification/ground tests performed on the tanks prior to the beginning of flight test activities are briefly discussed. Test results and the technical problems encountered during the program are also presented. Author

N90-10878*# National Aeronautics and Space Administration. Ames Research Center, Moffett Field, CA.
FLOW VISUALIZATION TECHNIQUES FOR FLIGHT RESEARCH
David F. Fisher and Robert R. Meyer, Jr. *In* AGARD, Flight

Test Techniques Jul. 1989 32 p (For primary document see N90-10860 02-05)
Copyright Avail: NTIS HC A18/MF A03 CSCL 01C

In-flight flow visualization techniques used at the Dryden Flight Research Facility of NASA Ames Research Center (Ames-Dryden) and its predecessor organizations are described. Results from flight tests which visualized surface flows using flow cones, tufts, oil flows, liquid crystals, sublimating chemicals, and emitted fluids were obtained. Off-surface flow visualization of vortical flow was obtained from natural condensation and two methods using smoke generator systems. Recent results from flight tests at NASA Langley Research Center using a propylene glycol smoker and an infrared imager are also included. Results from photo-chase aircraft, onboard and postflight photography are presented. Author

N90-10879# Air Force Wright Aeronautical Labs., Wright-Patterson AFB, OH. Survivability Enhancement Branch.
AIRCRAFT LIVE FIRE TESTING
R. W. Lauzze and M. D. Waddell *In* AGARD, Flight Test Techniques Jul. 1989 10 p (For primary document see N90-10860 02-05)
Copyright Avail: NTIS HC A18/MF A03

Testing military systems in peacetime to determine their ability to successfully operate in a combat environment was done for years. Some of the tough lessons learned on the battlefield and in the skies during wartime can be examined in the laboratory to help assure that new systems do not incorporate the shortcomings of those of the past. Live Fire Testing (LFT) of aircraft, that is, actual ballistic testing of full scale aircraft/aircraft subsystems, can be performed to evaluate their ability to resist or tolerate battle damage. This testing, combined with analytical tools, can assist the designer in assuring that the aircraft incorporates optimum protection for the system and crew at minimum weight. Events such as a fuel or hydraulic fire in flight, hydraulic ram damage due to a tumbling projectile in a fuel tank, or synergistic effects such as bleed air enhancing a dry bay fire are extremely difficult to analyze. Live fire testing allows evaluation of these and other effects and allows a check of vulnerability analyses that were performed. It also provides an effective tool for evaluation of Aircraft Battle Damage Repair (ABDR) techniques. Author

N90-10880# Aeritalia S.p.A., Caselle Torinese (Italy). Flight Test Dept.
FLIGHT TESTING A NEWLY-DESIGNED STAND-OFF WEAPON DISPENSER
G. Ferretti and P. Duranti *In* AGARD, Flight Test Techniques Jul. 1989 18 p (For primary document see N90-10860 02-05)
Copyright Avail: NTIS HC A18/MF A03

Skyshark is a newly-designed Stand-off Weapon Dispenser recently developed by AERITALIA and SNIA-BPD. These Italian companies formed in 1986 a joint venture named CASMU, which in Italian stands for Multi-Usage Stand-off Armament Consortium. Designed specifically for being launched by AM-X and Tornado aircraft, the Skyshark will be easily integrated with most of the modern attack aircraft. Released at a distance from the target variable with speed/altitude conditions this new weapon, capable of following a pre-defined path, will operate independently thanks to a proper inertial navigation system coupled to a pre-programmed computer for stabilization and maneuvering. Once reached the target, a dedicated armament system will come into action dispensing submunitions that can, as the case requires, be selected amongst various combinations and timed for the attack. Five of the planned six demonstration launches were performed so far with satisfactory results, allowing to acquire significant data about aerodynamics, flight-control and armament systems characteristics. The flight test activities carried out during the demonstration phase, aimed at proving the correctness of the general concept are presented. The most interesting peculiarities related to test-flying such unusual flying machine and the experiences acquired are described. Author

N90-10881# Identification Friend, Foe, or Neutral Joint Test Force, Kirtland AFB, NM.
IDENTIFICATION FRIEND, FOE OR NEUTRAL JOINT TEST **c32**
James E. Haile *In* AGARD, Flight Test Techniques Jul. 1989 12 p (For primary document see N90-10860 02-05)
Copyright Avail: NTIS HC A18/MF A03

The Identification Friend, Foe, or Neutral (IFFN) Joint Test Force (JTF) located at Kirtland AFB, NM, has developed a testbed that is composed of high fidelity, real time man-in-the-loop simulators designed to replicate the NATO Central Region Integrated Air Defense System. The purpose of the test is to assess the ability of this air defense system to correctly identify and engage enemy aircraft. The testbed represents the largest real time command and control (C2) simulation which consists of 57 medium and high fidelity tactical consoles and over a million lines of code. The OSD-sponsored testbed development and test is scheduled to run through July 1989. After this the testbed will beome the Theater Air Command and Control Simulation Facility (TACCSF) operated by the USAF Tactical Air Warfare Center (TAWC). The facility will be used by both Army and Air Force commands to resolve joint operational issues and support test and evaluation of the NATO Air Command and Control System (ACCS). Author

N90-10882# Army War Coll., Carlisle Barracks, PA. Military History Inst.
FLIGHT TESTING AND FLIGHT RESEARCH: FROM THE AGE OF THE TOWER JUMPER TO THE AGE OF THE ASTRONAUT
Richard P. Hallion *In* AGARD, Flight Test Techniques Jul. 1989 13 p (For primary document see N90-10860 02-05)
Copyright Avail: NTIS HC A18/MF A03

Since the beginning of flight, aerospace vehicle design has depended upon data gathered from the performance of actual flight vehicles. This flight testing and flight research process has led to today's air-and-space-craft, and points the way for future flight. Within this process, the flight test planner, test pilot, and flight test engineer occupy positions of critical importance. A review of the history of flight testing and flight research indicates that both were traditionally characterized by a professional approach emphasizing the derivation and utilization of methodologies to best enable investigators to acquire a maximum amount of information as quickly as is consistent with safety. As the technological sophistication of aircraft systems has increased, so, too, has the necessity for improving, modifying, and adding to the capabilities of the flight testing and flight research process. This pattern may be expected to hold true for the subsequent development of future advanced aerospace vehicle systems. Author

N90-10883# Naval Air Test Center, Patuxent River, MD.
AIR COMBAT ENVIRONMENT TEST AND EVALUATION FACILITY (ACETEF) **c09**
R. R. Smullen and S. D. Harris *In* AGARD, Flight Test Techniques Jul. 1989 3 p (For primary document see N90-10860 02-05)
Copyright Avail: NTIS HC A18/MF A03

Recent combat experience has brought to light a critical need to assess the mission effectiveness of Naval aviation weapons systems and vehicles against a myriad of new threats. Flight testing is the primary source of data on the effectiveness of our aircraft and weapons, but flight testing is costly, and limited to only a few of the most crucial questions. Flight testing is also inherently a public event; it can be observed with impunity. Hence, flight testing is patently unsatisfactory for dealing with some issues related to national security interests. Senior decision-makers in the Department of Defense (DOD) require objective, quantitative assessments of the effectiveness of the weapons and people against literally thousands of possible combinations of threat and contingency planning conditions. A revolutionary approach is needed to obtain the requisite data. The Naval Air Test Center (NAVAIRTESTCEN) has begun to develop an innovative system, known as the Air Combat Environment Test and Evaluation Facility (ACETEF), to meet this need. Author

N90-10884# National Aerospace Lab., Amsterdam (Netherlands).
FLIGHT TESTING IN THE NETHERLANDS: AN OVERVIEW
J. T. M. vanDoorn and R. L. vanderVelde *In* AGARD, Flight Test Techniques Jul. 1989 25 p (For primary document see N90-10860 02-05)
Copyright Avail: NTIS HC A18/MF A03

An overview is given for the flight test activities and capabilities in The Netherlands. A general description of the flight test programs of the last decades with civil and military aircraft, helicopters and research aircraft are given. Some of the highlights of the more recent programs are presented, i.e., the type certification of the Fokker 50 and Fokker 100 civil transport aircraft, evaluation and certification trials with the military F16 fighter aircraft, helicopter-ship compatibility testing and the determination of the mathematical model of the Cessna Citation 500 for a Phase 2 flight simulator. Furthermore a short description is given of the flight test instrumentation and flight test techniques that have become available in The Netherlands during the last decade. Author

N90-10885# Lisbon Univ. (Portugal). Inst. Superior Tecnico.
ON THE DEVELOPMENT OF A BASIC FLIGHT TEST CAPABILITY AND SOME RELATED RESEARCH PROJECTS
L. M. B. C. Campos, A. A. Fonseca, and H. F. Ramos *In* AGARD, Flight Test Techniques Jul. 1989 26 p (For primary document see N90-10860 02-05)
Copyright Avail: NTIS HC A18/MF A03

The development of a basic flight test capability in Portugal, through the cooperation between the Portuguese Air Force (FAP) and Lisbon Technical University (UTL), with support from The National Aerospace Laboratory (NLR) in The Netherlands and Braunschweig Technical University (TU-BS) in Germany, under the AGARD support program for the NATO Southern Flank Nations is described. After indicating in the introduction the motivations for this program, the National Flight Test Facility (LNEV) is described. Indicating the forms of program management used in the development of the instrumentation system, the first research projects which the facility will be used, are outlined, mentioning in passing application programs, and concentrating on two projects of fundamental rsearch on flight in perturbed atmospheres and linear stability. In conclusion, some of the benefits of the program are mentioned. Author

N90-10886# Aerodata Flugmesstechnik G.m.b.H., Brunswick (Germany, F.R.).
REALTIME PROCESSING AND DISPLAY **c09**
A. Redeker *In* AGARD, Flight Test Techniques Jul. 1989 7 p (For primary document see N90-10860 02-05)
Copyright Avail: NTIS HC A18/MF A03

Concept and realization of a data system for airborne research and development applications are presented. Aspects of hardware architecture and software organization are discussed. The system is used for prototype testing and certification and is also layed out for the operation of research aircraft, where sensor configurations and measuring instruments are varying from one experiment to another. All system users have access to a pool of common sensor- and software resources. Special hard- and software interfaces were defined for a simple integration of individual sensor signals and computation algorithms. The system performs realtime processing, recording, and on-line monitoring of sensor data. It is the aim of the system design to enable the operator to perform quick error detection as well as to optimize the flight conditions for an experiment. Examples for flight-mechanical and meteorological system applications are given. Author

N90-10887# British Aerospace Public Ltd. Co., Preston (England). Flight Test Instrumentation Data Processing Dept.
FLIGHT TEST INSTRUMENTATION AND DATA PROCESSING AT BRITISH AEROSPACE, WARTON, U.K. **c09**
Roger E. Porter and Michael F. Armour *In* AGARD, Flight Test Techniques Jul. 1989 16 p (For primary document see N90-10860 02-05)
Copyright Avail: NTIS HC A18/MF A03

British Aerospace Warton was engaged in the development and testing of a wide range of military fighter aircraft including Jaguar, Tornado and the E.A.P. During the next decade Warton will be a major flight test center for the European Fighter Aircraft (EFA). An overview is given of the instrumentation and data processing facilities in current use, planned development for the next 10 years covering the proposed instrumentation system for EFA. It describes the ground station, computing hardware, specialized analysis capability, onboard equipment, the extensive use of telemetry for real time processing and intermaneuvre analysis in real time. Also included are the facilities for integration of airborne data aquisition systems, together with procurement, automated calibration, and design and development. Author

N90-10888# Aeronautical Research Labs., Melbourne (Australia).
THE SPINNING OF AIRCRAFT: A DISCUSSION OF SPIN PREDICTION TECHNIQUES INCLUDING A CHRONOLOGICAL BIBLIOGRAPHY
Colin A. Martin Aug. 1988 45 p
(ARL-AERO-R-177; AR-005-530) Avail: NTIS HC A03/MF A01

Aircraft spinning is an important area of design for general aviation and military aircraft, and has been so, since the early days of aviation. In many of the major aeronautical laboratories in the world, aircraft spinning has been the subject of intensive periods of research. However, the resulting design criteria are still only adequate for predicting gross trends in aircraft spin behavior. To enable flight testing to proceed with confidence and to minimize modifications during flight development, most major aircraft development programs include extensive scale-model spin testing. Here, the development of these techniques and their application for spin prediction are discussed. Author

N90-10889*# National Aeronautics and Space Administration. Langley Research Center, Hampton, VA.
INTEGRATED MULTIDISCIPLINARY DESIGN OPTIMIZATION OF ROTORCRAFT
Howard M. Adelman and Wayne R. Mantay (Army Aviation Systems Command, Hampton, VA.) Jul. 1989 13 p Presented at the AIAA/AHS/ASEE 1989 Aircraft Design and Operations Meeting, Seattle, WA, 31 Jul. - 2 Aug. 1989 Previously announced in IAA as A89-49478
(NASA-TM-101642; NAS 1.15:101642; AVSCOM-TM-89-B-008)
Avail: NTIS HC A03/MF A01 CSCL 01C

The NASA/Army research plan for developing the logic elements for helicopter rotor design optimization by integrating appropriate disciplines and accounting for important interactions among the disciplines is discussed. The optimization formulation is described in terms of the objective function, design variables, and constraints. The analysis aspects are discussed, and an initial effort at defining the interdisciplinary coupling is summarized. Results are presented on the achievements made in the rotor dynamic optimization for vibration reduction, rotor structural optimization for minimum weight, and integrated aerodynamic load/dynamics optimization for minimum vibration and weight. IAA

06 AIRCRAFT INSTRUMENTATION

Includes cockpit and cabin display devices; and flight instruments.

For related information see also *19 Spacecraft Instrumentation* and *35 Instrumentation and Photography.*

N90-10890# National Aerospace Lab., Tokyo (Japan). Instrumentation and Control Div.
STUDY FOR OPTIMIZATION OF REDUNDANT VANE-TYPE FLOW-DIRECTION SENSING SYSTEMS AND NUMERICAL ANALYSIS FOR DESIGN OF THE SYSTEMS
Takeo Kimura, Minoru Takizawa, and Tadao Uchida Apr. 1987

43 p In JAPANESE; ENGLISH summary
(NAL-TM-571; ISSN-0452-2982; JTN-88-80066) Avail: NTIS HC A03/MF A01

In a previous investigation, it was shown that the determinant of a covariance matrix should be recognized as a reasonable criterion for comparing the quality of observation systems. The determinant criterion was applied to find the optimum observation systems for two-dimensional vector sensing in cases where the observation errors were not correlated with each other. The errors were normally distributed with zero means and equal variances. In the present investigation, it is explained that the vane-type flow-direction sensing systems are approximately equal to the two-dimensional vector sensing systems mentioned above from the view-point of evaluation analysis for the observation systems. The optimum orientations of the redundant vane-type systems are shown. Furthermore the general properties of the orientations are clarified. Last, numerical experiments of error propagation are exercised to show how much influence the measurement and misalignment errors have on the final solutions. NASDA

07 AIRCRAFT PROPULSION AND POWER

Includes prime propulsion systems and systems components, e.g., gas turbine engines and compressors; and onboard auxilliary power plants for aircraft.

For related information see also *20 Spacecraft Propulsion and Power, 28 Propellants and Fuels,* and *44 Energy Production and Conversion.*

N90-10891*# National Aeronautics and Space Administration. Lewis Research Center, Cleveland, OH.
ADVANCED TECHNOLOGIES IMPACT ON COMPRESSOR DESIGN AND DEVELOPMENT: A PERSPECTIVE
Calvin L. Ball Sep. 1989 18 p Presented at Aerotech '89, Anaheim, CA, 25-28 Sep. 1989; sponsored by SAE
(NASA-TM-102341; E-5039; NAS 1.15:102341) Avail: NTIS HC A03/MF A01 CSCL 21E

A historical perspective of the impact of advanced technologies on compression system design and development for aircraft gas turbine applications is presented. A bright view of the future is projected in which further advancements in compression system technologies will be made. These advancements will have a significant impact on the ability to meet the ever-more-demanding requirements being imposed on the propulsion system for advanced aircraft. Examples are presented of advanced compression system concepts now being studied. The status and potential impact of transitioning from an empirically derived design system to a computationally oriented system are highlighted. A current NASA Lewis Research Center program to enhance this transitioning is described. Author

N90-10892# Los Alamos National Lab., NM.
CRITICAL REACTION RATES IN HYPERSONIC COMBUSTION CHEMISTRY
Richard C. Oldenborg, David M. Harradine, Gary W. Loge, John L. Lyman, Garry L. Schott, and Kenneth R. Winn 1989 7 p Presented at the 1989 American Chemical Society National Meeting, Miami Beach, FL, 10-15 Sep. 1989
(Contract W-7405-eng-36)
(DE89-014278; LA-UR-89-2170; CONF-890902-12) Avail: NTIS HC A02/MF A01

High Mach number flight requires that the scramjet propulsion system operate at a relatively low static inlet pressure and a high inlet temperature. These two constraints can lead to extremely high temperatures in the combustor, yielding high densities of radical species and correspondingly poor chemical combustion efficiency. As the temperature drops in the nozzle expansion, recombination of these excess radicals can produce more product species, higher heat yield, and potentially more thrust. The extent to which the chemical efficiency can be enhanced in the nozzle expansion depends directly on the rate of the radical recombination reactions. A comprehensive assessment of the important chemical processes and an experimental validation of the critical rate parameters is therefore required if accurate predictions of scramjet performance are to be obtained. This report covers the identification of critical reactions, and the critical reaction rates in hypersonic combustion chemistry. DOE

N90-10893# Pennsylvania State Univ., University Park. Dept. of Mechanical Engineering.
ANALYTICAL STUDY OF MISTUNING/FRICTION/AERODYNAMICS INTERACTION IN A BLADED DISK ASSEMBLY Final Report, May 1987 - Jan. 1989
Alok Sinha and Shing Chen 6 Feb. 1989 80 p
(Grant AF-AFOSR-0142-87; AF Proj. 2302)
(AD-A211139; AFOSR-89-1059TR) Avail: NTIS HC A05/MF A01 CSCL 20/11

An analytical technique is shown to be valid for the computation of the statistics of a blade's vibratory amplitude when the distributions of modal parameters of a mistuned bladed disk assembly are non-Gaussian. The results from the analytical technique are compared with those from numerical simulations for triangular and uniform distributions. It was found that the probability density function of the amplitude is insensitive to the types of mistuning distributions. Next, an analytical technique was developed to efficiently compute the probability density function of the maximum amplitude on a mistuned bladed disk assembly. This technique uses the direct Taylor series expansion in terms of the perturbation in an amplitude as a function of perturbations in modal stiffnesses. The validity of the techniques has been corroborated by comparison with the results from numerical simulations. Lastly, the statistics of the forced response of a structurally and aerodynamically coupled bladed disk assembly were computed efficiently by the analytical technique. The results from the analytical technique agree well with those from numerical simulations. The effects of the following parameters on the statistics of the maximum amplitude were studied: the aerodynamic couplings among blades, the fluid density and the cascade stagger angle. GRA

08 AIRCRAFT STABILITY AND CONTROL

Includes aircraft handling qualities; piloting; flight controls; and autopilots.

For related information see also *05 Aircraft Design, Testing and Performance.*

N90-10894 Bristol Univ. (England).
THE ACTIVE CONTROL OF AN UNSTABLE CANARD AIRCRAFT Ph.D. Thesis
David A. Cowling 1988 216 p
Avail: Univ. Microfilms Order No. BRDX85245

The design of control systems which utilize the independence of a canard aircraft's 2 pitch control surfaces is investigated. Eigenstructure assignment is used to calculate the gains for simple feedback structures. To cater for the multiloop designs, robustness and system sensitivity measures and objectives are formulated in terms of the minimum values of the return difference and inverse return difference matrices. An optimization scheme is developed which links this analysis with the eigenstructure assignment design procedure. This method allows system eigenvalues to be fixed whilst the eigenvector assignment is used to optimize the robustness and sensitivity. Results indicate that even with the classical pitch rate demand system robustness can be improved and gains reduced, by the independent use of the control surfaces. Designs incorporating incidence feedback appear more robust and less sensitive to parameter changes than the pitch rate alone feedback, even though the performance is the same. Gust response analysis also suggests that the multiloop design has improved characteristics. Finally, the application of the methods is demonstrated on a gross maneuvering multimode system. Dissert. Abstr.

N90-10895 York Univ. (England).
AN ASSESSMENT OF ROBUSTNESS OF FLIGHT CONTROL SYSTEMS BASED ON VARIABLE STRUCTURE TECHNIQUES
Ph.D. Thesis
Sarah Katherine Spurgeon 1988 270 p
Avail: Univ. Microfilms Order No. BRDX84782

Variable Structure Control Systems (VSCS) have received considerable attention in recent years as a possible solution to the problem of controlling time-varying and uncertain systems. The aim of this research is to investigate the application of the theory of VSCS to the design of flight control systems. Chapter One presents all of the necessary aircraft background which is required to formulate the design procedures developed by this work. Chapter Two offers an introduction to the theory of VSCS. Robust control system design using eigenstructure assignment is the subject of Chapter Three; this work is central to the algorithmic VSCS design procedure which is shown to be most effective for the aircraft system. Chapter Four formulates a generalized design technique for VSCS and considers an assessment of the robustness of a VSCS scheme. Chapter Five presents an overview of the theory relating to variable structure model-following control laws. Having developed the necessary tools, the design of control laws for a number of different aircraft maneuvers is considered. Non-linear aircraft simulations are used throughout to assess the performance of the control schemes developed. Dissert Abstr.

09 RESEARCH AND SUPPORT FACILITIES (AIR)

Includes airports, hangars and runways; aircraft repair and overhaul facilities; wind tunnels; shock tubes; and aircraft engine test stands.

For related information see also *14 Ground Support Systems and Facilities (Space).*

N90-10896# Army Cold Regions Research and Engineering Lab., Hanover, NH.
DEFINITION OF RESEARCH NEEDS TO ADDRESS AIRPORT PAVEMENT DISTRESS IN COLD REGIONS
T. S. Vinson, R. L. Berg, I. Zomerman, and W. Haas May 1989 146 p
(Contract DTFA01-84-Z-02038)
(DOT/FAA/DS-89/13; CRREL-89-10) Avail: NTIS HC A07/MF A01

In early fall 1984, a questionnaire was sent to over 325 general aviation airports in cold regions. The results from over 200 responses were compiled and evaluated and over 20 airport managers contacted for additional details. Site visits were made to 36 airports to obtain additional information. The most common pavement problems identified were associated with nontraffic-related phenomena and include: (1) preexisting cracks reflecting through asphalt concrete overlays (in two years or less); (2) thermal cracking; and (3) longitudinal cracking (at a construction joint). Most of the airports experienced: (1) water pumping up through cracks and joints in the pavements during spring thaw; or (2) additional roughness due to differential frost heave in the winter and spring. Many pavement problems can be traced to the evolutionary history of general aviation airports and the lack of consideration for site drainage. Based on the recognition of these problems, several future research programs are identified.
Author

N90-10897# Federal Aviation Administration, Atlantic City, NJ.
HELIPORT SURFACE MANEUVERING TEST RESULTS
Technical Note, Oct. 1987 - Jan. 1988
Rosanne M. Weiss, Christopher J. Wolf, Scott L. Erlichman, John G. Morrow, and Walter E. Dickerson Jun. 1989 81 p
(Contract FAA-T0701-R)
(ACD-330; DOT/FAA/CT-TN88/30) Avail: NTIS HC A05/MF A01

During late fall 1987 and early spring 1988 flight tests were conducted at the Federal Aviation Administration (FAA) Technical Center's National Concepts Development and Demonstration Heliport. The purpose of these tests was to measure pilot perception of helicopter tip clearances for parking and taxiing maneuvers and to measure pilot performance during these maneuvers. Over 100 parking and taxiing maneuvers were conducted using a UH-1H helicopter. The parking procedures were conducted under head, tail, and crosswind conditions, both with and without an obstacle in place. The taxiing procedures were carried out with a centerline, with only side markings, and with no ground markings. A ground based laser tracker system was used to track the taxiing procedures. Pilot subjective data in reference to these maneuvers were collected via a post-flight questionnaire. Pilot interview were conducted at heliports across the country. These interviews gathered pilot views concerning rotor tip clearances for parking and hover taxiing maneuvers, ground markings for parking operations, and hover taxiing heights. The results of this activity are documented. The data collection and analysis methodology is described along with an objective as well as subjective issues. Statistical and graphical analysis of pilot performance and perception data and pilot subjective data are provided.
Author

N90-10898# National Aerospace Lab., Tokyo (Japan). Flight Research Div.
FLIGHT SIMULATOR EVALUATION OF A HEAD-DOWN DISPLAY
Keiji Tanaka and Hiroyasu Kawahara May 1987 19 p In JAPANESE; ENGLISH summary
(NAL-TM-573; ISSN-0452-2982; JTN-88-30068) Avail: NTIS HC A03/MF A01

A Head-Down Display (HDD) designed for the NAL (National Aerospace Laboratory) Quiet Short Take-Off and Landing (QSTOL) experimental aircraft ASUKA, was evaluated using the STOL Flight Simulator. The HDD employs a shadow-mask type color cathode ray tube (CRT), and utilizes the flexibility of computer graphics. The simulator evaluation of the HDD installed on the right instrument panel of the STOL simulator cockpit is described. In the experiment, performances of the following three types of approach and landing flights were compared: (1) flights with conventional instruments (left seat); (2) HDD without the STOL flight director (right seat); and (3) HDD with the flight director (right seat). The flight records as well as pilot comments indicated performance improvement with the aid of the STOL flight director, while no significant differences were observed between flight performances with conventional instruments and with HDD without the flight director. Suggestions to improve the display format, such as to provide better lateral and directional control cues, contributed to a modified display format which is to be evaluated as the next step of the HDD development program.
NASDA

N90-10899# National Aerospace Lab., Tokyo (Japan). STOL Aircraft Project Group.
FLIGHT SIMULATION TEST FACILITY: FUNCTION AND SPECIFICATION OF THE SIMULATOR COCKPIT SYSTEM
Hiroyasu Kawahara, Masanori Okabe, Akira Watanabe, Toshio Bando, and Kaoru Wakairo Nov. 1987 69 p In JAPANESE
(NAL-TM-577; ISSN-0452-2982; JTN-88-80069) Avail: NTIS HC A04/MF A01

Flight simulators for research and development are indispensable as design tools in the development phase of aircraft. The National Aerospace Laboratory (NAL) has used a flight simulator for tests and research regarding the development and revamping of various aircraft since 1963, improving its simulation accuracy and scale. The original simulator became old and was no longer able to meet the demands for higher simulation test accuracy or for large equipment to be simulated. For this reason, the NAL decided to install a flight simulation test facility fully utilizing the latest technology. The functions, configuration and performance of the simulated cockpit equipment manufactured in 1980 and 1981 are described.
NASDA

N90-10883# Naval Air Test Center, Patuxent River, MD.
AIR COMBAT ENVIRONMENT TEST AND EVALUATION FACILITY (ACETEF)
R. R. Smullen and S. D. Harris *In* AGARD, Flight Test Techniques Jul. 1989 3 p (For primary document see N90-10860 02-05)
Copyright Avail: NTIS HC A18/MF A03

N90-10886# Aerodata Flugmesstechnik G.m.b.H., Brunswick (Germany, F.R.).
REALTIME PROCESSING AND DISPLAY
A. Redeker *In* AGARD, Flight Test Techniques Jul. 1989 7 p (For primary document see N90-10860 02-05)
Copyright Avail: NTIS HC A18/MF A03

N90-10887# British Aerospace Public Ltd. Co., Preston (England). Flight Test Instrumentation Data Processing Dept.
FLIGHT TEST INSTRUMENTATION AND DATA PROCESSING AT BRITISH AEROSPACE, WARTON, U.K.
Roger E. Porter and Michael F. Armour *In* AGARD, Flight Test Techniques Jul. 1989 16 p (For primary document see N90-10860 02-05)
Copyright Avail: NTIS HC A18/MF A03

12 ASTRONAUTICS (GENERAL)

For extraterrestrial exploration see *91 Lunar and Planetary Exploration.*

N90-10900# Joint Publications Research Service, Arlington, VA.
JPRS REPORT: SCIENCE AND TECHNOLOGY. USSR: SPACE
28 Jun. 1989 103 p Transl. into ENGLISH from various Russian articles
(JPRS-USP-89-007) Avail: NTIS HC A06/MF A01

This Joint Publications Research Service (JPRS) publication contains articles on Soviet space research in the areas of: (1) manned mission highlights; (2) space sciences; (3) interplanetary sciences; (4) life sciences (in space); (5) space engineering; (6) space technology applications (on earth); and (7) Soviet space policy and administration. For individual titles, see N90-10901 through N90-10906.

N90-10901# Joint Publications Research Service, Arlington, VA.
PROJECT RADIOASTRON **c90**
V. V. Andreyanov *In its* JPRS Report: Science and Technology. USSR: Space 28 Jun. 1989 p 13-17 Transl. into ENGLISH from Zemlya i Vselennaya (Moscow, USSR), no. 1, Jan.-Feb. 1989 p 13-17 (For primary document see N90-10900 02-12)
Copyright Avail: NTIS HC A06/MF A01

The prospects of basic research in astrophysics are linked to the improvement of two telescope parameters - angular resolution and sensitivity. One technique that makes it possible to increase angular resolution by many orders of magnitude is radio interferometry. The use of this technique with the transport of one of the elements of the radio interferometer into space is planned in the international project Radioastron. The Radioastron interferometer consists of four large interrelated systems: a space-based radiotelescope, ground-based radiotelescopes, a radio communications system, and a data processing system. The Radioastron project is a long-term program for studying deep space. its final stage calls for the creation of a space-based aperture synthesis system consisting of several space-based radiotelescopes at various distances from the Earth, with periods of revolution ranging from 24 hours to a year, and operating in the millimeter range of radiowaves. Author

N90-10902# Joint Publications Research Service, Arlington, VA.
MEETING OF INTERCOSMOS SPACE PHYSICS GROUP **c90**
N. A. Frolova *In its* JPRS Report: Science and Technology. USSR: Space 28 Jun. 1989 p 17-19 Transl. into ENGLISH from Zemlya i Vselennaya (Moscow, USSR), no. 1, Jan.-Feb. 1989 p 46-48 (For primary document see N90-10900 02-12)
Copyright Avail: NTIS HC A06/MF A01

The 22nd meeting of scientists and specialists of Socialist countries in the Intercosmos program was held in April 1988, in Tbilisi. Taking part in the meeting were well-known Soviet scientists and major foreign specialists from Bulgaria, Hungary, GDR, Cuba, Mongolia, Poland, Rumania, and Czechoslovakia. The meeting focused on a plan for collaboration in space physics for the 1991 to 1995 period and up to the year 2000. The Mars-94 project, which is a component part of the program, Mars-2000, proposed by Soviet scientists, is discussed along with other proposed planetary projects. In the area of high energy astrophysics, a project involving a large orbital observatory (Spektr-Rentgen-Gamma) is being prepared for solving problems associated with cosmology, extragalactic astronomy, and stellar astronomy. It will be carried out through international cooperation with significant developments effected by socialist countries. Two other projects discussed include Radioastron which involves radiointerferometry, and Relikt-2 which will continue research that was begun aboard the unmanned Prognoz-9 station. In the area of solar terrestrial physics, instruments are being designed for the study of X-ray active formations in the solar atmosphere and processes that take place in solar plasma (the Koronas-1, F project, and the Neytron project). The study of cosmic plasma is called for in the Interbol project. Also, the Czech furnace Kristallizator-ChSk-1 is in operation aboard the Mir orbital station and the launch of another unit is expected. All 10 Intercosmos countries are taking part in the preparation of experiments involving space-based materials science. K.C.D.

N90-10903# Joint Publications Research Service, Arlington, VA.
SOVIET MARS PROGRAM
Yu. I. Zaytsev *In its* JPRS Report: Science and Technology. USSR: Space 28 Jun. 1989 p 32-41 Transl. into ENGLISH from Zemlya i Vselennaya (Moscow, USSR), no. 1, Jan.-Feb. 1989 p 19-26 (For primary document see N90-10900 02-12)
Copyright Avail: NTIS HC A06/MF A01

The feasibility of Mars missions is considered. The Soviet mission to Phobos, a satellite of Mars, is discussed. In the 1990's, the Soviet Mars program calls for global research of the surface and the atmosphere of Mars with artificial satellites, balloon probes, surface excursion vehicles, weather probes, and penetrator probes delivered to the surface, and a subsatellite that separates from the main craft. These systems are discussed along with the technology for delivering Martian soil samples to Earth. Possibilities for international cooperation on a Mars mission are also discussed. K.C.D.

N90-10904# Joint Publications Research Service, Arlington, VA.
LANDING TESTS FOR BURAN SHUTTLE WITH JET ENGINE-EQUIPPED MOCK-UP **c16**
Stepan Anastasovich Mikoyan *In its* JPRS Report: Science and Technology. USSR: Space 28 Jun. 1989 p 50 Transl. into ENGLISH from Sovetskaya Latviya (Riga, USSR), 27 Jan. 1989 p 3 (For primary document see N90-10900 02-12)
Copyright Avail: NTIS HC A06/MF A01

Problems of controlling unmanned flights of the reusable spaceship Buran and landing it in a gliding mode, without the use of engine thrust are discussed. Particular attention is devoted to the use of an operating mock-up of the Buran in rehearsing landings and training pilots. As compared with the Buran itself, this mock-up possesses features which ensure flight similar to that of a conventional airplane. The mock-up has four jet airplane engines which enable it to take off and climb to an altitude of 5 to 6 kilometers. It is equipped with a landing-gear retraction system and ejectable seats for two test-pilots. The mock-up is identical to the Buran in most other respects. The control systems of the two crafts are similar, which enabled the mock-up to make 16 landings in the automatic mode. Author

N90-10905# Joint Publications Research Service, Arlington, VA.
USSR AND INTERNATIONAL COOPERATION IN SPACE **c84**
S. A. Nikitin *In its* JPRS Report: Science and Technology. USSR: Space 28 Jun. 1989 p 64-69 Transl. into ENGLISH from Novoye v Zhizni, Nauke, Tekhnike: Seriya Kosmonavtika, Astronomiya (Moscow, USSR), No. 12, Dec. 1988 p 32-47 (For

primary document see N90-10900 02-12)
Copyright Avail: NTIS HC A06/MF A01

In 1988 cooperation was successfully pursued in the framework of the multilateral program Intercosmos with nine socialist countries (Bulgaria, Hungary, Vietnam, East Germany, the Republic of Cuba, Mongolia, Poland, Rumania, Czechoslovakia) and on a bilateral basis with Austria, Great Britain, India, the United States, Finland, France, West Germany, Switzerland, Sweden and other nations, as well as the European Space Agency. Joint projects in the Intercosmos program are being carried out in the area of space physics (including space materials science), space meteorology, communications, space biology and medicine, as well as remote sensing of the Earth for purposes of studying its natural resources. Joint projects in space on a bilaterial basis with the aforementioned countries have covered practically all main areas of cosmonautics. In 1988 the main events in the international cooperation of the USSR in space were: international experiments aboard the Mir orbital scientific research complex, flights of Soviet-Bulgarian and Soviet-Afghan international crews, the launching of two unmanned interplanetary Phobos vehicles, and the launching of the Indian satellite IRS-1A on a commericial basis. K.C.D.

N90-10906# Joint Publications Research Service, Arlington, VA.
SAGDEYEV DISCUSSES SPACE MISSIONS, POLICY, MARS PLANS
Roald Zinnurovich Sagdeyev *In its* JPRS Report: Science and Technology. USSR: Space 28 Jun. 1989 p 69-79 Transl. into ENGLISH from PRIRODA (Moscow, USSR), no. 1, Jan. 1989 p 33-46 (For primary document see N90-10900 02-12)
Copyright Avail: NTIS HC A06/MF A01

An indepth interview with Roald Zinnurovich Sagdeyev on space research by PRIRODA correspondent N. D. Morozovaya is presented. Sagdeyev, an academician, is a specialist in the field of plasma physics and space research, chairman of the Soviet Scientists' Peace Committee, hero of Socialist Labor, recipient of the Lenin and State prizes, member of the U.S. National Academy of Sciences, the Swedish Royal Academy, the Max Planck Society and a number of other academies. He headed up the USSR Academy of Sciences' Space Research Institute for more than 15 years. He shares his views on Soviet space missions, policies and Mars mission plans. K.C.D.

N90-10907*# National Aeronautics and Space Administration, Washington, DC.
SPACE STATION FREEDOM: A FOOTHOLD ON THE FUTURE
1989 48 p Original contains color illustrations
(NASA-NP-107/10-88; NAS 1.83:107/10-88) Avail: NTIS HC A03/MF A01 CSCL 22A

An overview of the Space Station Freedom is given. Its modules are discussed and illustrated along with its microgravity research facilities. These facilities include the advanced protein crystal growth facility, the containerless processing facility, a furnace facility, a combustion facility, and a fluid physics/dynamics facility. The topic of living in space is also addressed. K.C.D.

N90-10908# European Office of Aerospace Research and Development, London (England).
AERITALIA SPACE SYSTEMS GROUP, TURIN, ITALY
Vincent Donlan Feb. 1989 13 p
(EOARD-LR-89-041; AV-235-4376) Avail: NTIS HC A03/MF A01

Aeritalia has been involved in European space programs since the early 1960's. Space activities grew to the point that in 1984 Aeritalia established a separate Space Systems Group (SSG), located in Turin. Today, SSG is involved in dozens of projects, some of them jointly with NASA and U.S. aerospace companies. Here, several of the major projects, such as the Tethered Satellite system, HIPPARCOS, Columbus Pressurized Module, Italian Research Interim Stage, and others are briefly described. Author

13 ASTRODYNAMICS

Includes powered and free-flight trajectories; and orbital and launching dynamics.

No abstracts in this category.

14 GROUND SUPPORT SYSTEMS AND FACILITIES (SPACE)

Includes launch complexes, research and production facilities; ground support equipment, e.g., mobile transporters; and simulators.

For related information see also *09 Research and Support Facilities (Air).*

N90-10909*# National Aeronautics and Space Administration. Goddard Space Flight Center, Greenbelt, MD.
RESEARCH AND TEST FACILITIES FOR DEVELOPMENT OF TECHNOLOGIES AND EXPERIMENTS WITH COMMERCIAL APPLICATIONS
1989 72 p
(NASA-TM-101789; NAS 1.15:101789) Avail: NTIS HC A04/MF A01 CSCL 14B

One of NASA'S agency-wide goals is the commercial development of space. To further this goal NASA is implementing a policy whereby U.S. firms are encouraged to utilize NASA facilities to develop and test concepts having commercial potential. Goddard, in keeping with this policy, will make the facilities and capabilities described in this document available to private entities at a reduced cost and on a noninterference basis with internal NASA programs. Some of these facilities include: (1) the Vibration Test Facility; (2) the Battery Test Facility; (3) the Large Area Pulsed Solar Simulator Facility; (4) the High Voltage Testing Facility; (5) the Magnetic Field Component Test Facility; (6) the Spacecraft Magnetic Test Facility; (7) the High Capacity Centrifuge Facility; (8) the Acoustic Test Facility; (9) the Electromagnetic Interference Test Facility; (10) the Space Simulation Test Facility; (11) the Static/Dynamic Balance Facility; (12) the High Speed Centrifuge Facility; (13) the Optical Thin Film Deposition Facility; (14) the Gold Plating Facility; (15) the Paint Formulation and Application Laboratory; (16) the Propulsion Research Laboratory; (17) the Wallops Range Facility; (18) the Optical Instrument Assembly and Test Facility; (19) the Massively Parallel Processor Facility; (20) the X-Ray Diffraction and Scanning Auger Microscopy/Spectroscopy Laboratory; (21) the Parts Analysis Laboratory; (22) the Radiation Test Facility; (23) the Ainsworth Vacuum Balance Facility; (24) the Metallography Laboratory; (25) the Scanning Electron Microscope Laboratory; (26) the Organic Analysis Laboratory; (27) the Outgassing Test Facility; and (28) the Fatigue, Fracture Mechanics and Mechanical Testing Laboratory. K.C.D.

N90-10910# Ballistic Research Labs., Aberdeen Proving Ground, MD.
A THERMOCHEMICAL ANALYSIS OF PROPOSED WORKING FLUIDS FOR ELECTROTHERMAL GUNS Final Report, Oct. 1987 - Oct. 1988
Steven W. Bunte and William F. Oberle Jun. 1989 49 p Submitted for publication
(AD-A210661; BRL-TR-3000) Avail: NTIS HC A03/MF A01 CSCL 19/6

The thermochemical equilibrium code BLAKE has been used to calculate the thermochemical properties of a variety of mixtures for possible use as working fluids in an electrothermal (ET) gun. The mixtures studied included water, octane/hydrogen peroxide, titanium hydride/aluminum/water, and lithium borohydride/water. The relative merits of each of these mixtures will be discussed as well as possible applications. GRA

N90-10911*# Southwest Research Inst., San Antonio, TX.
ADVANCED MANNED SPACE FLIGHT SIMULATION AND TRAINING: AN INVESTIGATION OF SIMULATION HOST COMPUTER SYSTEM CONCEPTS Final Technical Report
Bruce C. Montag, Alfred M. Bishop, and Joe B. Redfield 10 Nov. 1989 53 p
(Grant NAG9-394; SwRI Proj. 05-3050)
(NASA-CR-185998; NAS 1.26:185998) Avail: NTIS HC A04/MF A01 CSCL 14B

The findings of a preliminary investigation by Southwest Research Institute (SwRI) in simulation host computer concepts is presented. It is designed to aid NASA in evaluating simulation technologies for use in spaceflight training. The focus of the investigation is on the next generation of space simulation systems that will be utilized in training personnel for Space Station Freedom operations. SwRI concludes that NASA should pursue a distributed simulation host computer system architecture for the Space Station Training Facility (SSTF) rather than a centralized mainframe based arrangement. A distributed system offers many advantages and is seen by SwRI as the only architecture that will allow NASA to achieve established functional goals and operational objectives over the life of the Space Station Freedom program. Several distributed, parallel computing systems are available today that offer real-time capabilities for time critical, man-in-the-loop simulation. These systems are flexible in terms of connectivity and configurability, and are easily scaled to meet increasing demands for more computing power. Author

N90-11041# Industrieanlagen-Betriebsgesellschaft m.b.H., Ottobrunn (Germany, F.R.).
DEVELOPMENT OF A THERMOACOUSTIC TEST FACILITY
G. Bayerdoerfer *In* ESA, Spacecraft Structures and Mechanical Testing Jan. 1989 p 407-412 (For primary document see N90-10986 02-18)
Copyright Avail: NTIS HC A99/MF E06

N90-11064# European Space Agency. European Space Research and Technology Center, ESTEC, Noordwijk (Netherlands).
THE ENVIRONMENTAL TEST CENTRE AT ESTEC (AN OVERVIEW)
E. Classen *In its* Spacecraft Structures and Mechanical Testing Jan. 1989 p 603-605 (For primary document see N90-10986 02-18)
Copyright Avail: NTIS HC A99/MF E06

N90-11065# European Space Agency. European Space Research and Technology Center, ESTEC, Noordwijk (Netherlands). Testing Div.
TWO YEARS EXPERIENCE WITH THE ESTEC MULTISHAKER SYSTEM
P. Bonnot *In its* Spacecraft Structures and Mechanical Testing Jan. 1989 p 607-612 (For primary document see N90-10986 02-18)
Copyright Avail: NTIS HC A99/MF E06

N90-11066# European Space Agency. European Space Research and Technology Center, ESTEC, Noordwijk (Netherlands). Testing Div.
NEW DATA HANDLING SYSTEM (MDH) FOR MECHANICAL TESTS AT ESTEC
C. Fransen *In its* Spacecraft Structures and Mechanical Testing Jan. 1989 p 613-617 (For primary document see N90-10986 02-18)
Copyright Avail: NTIS HC A99/MF E06

N90-11067# European Space Agency. European Space Research and Technology Center, ESTEC, Noordwijk (Netherlands).
THE LARGE EUROPEAN ACOUSTIC FACILITY AT ESTEC
W. E. Gruen and W. A. Shickle *In its* Spacecraft Structures and Mechanical Testing Jan. 1989 p 619-627 (For primary document see N90-10986 02-18)
Copyright Avail: NTIS HC A99/MF E06

N90-11068# Commissariat a l'Energie Atomique, Saclay (France).
TAMARIS: A NEW EUROPEAN FACILITY FOR LOW FREQUENCY MULTI-AXIS VIBRATION SIMULATION
P. Buland, C. Berriaud, and Ph. Jamet *In* ESA, Spacecraft Structures and Mechanical Testing Jan. 1989 p 631-634 (For primary document see N90-10986 02-18)
Copyright Avail: NTIS HC A99/MF E06

N90-11069# Ometron Ltd., London (England).
ADVANCES IN INSTRUMENTATION FOR EXPERIMENTAL STRESS AND VIBRATION ANALYSIS AND ITS APPLICATIONS
A. J. Barker and D. J. Berry *In* ESA, Spacecraft Structures and Mechanical Testing Jan. 1989 p 635-639 (For primary document see N90-10986 02-18)
Copyright Avail: NTIS HC A99/MF E06

N90-11070# Intespace, Toulouse (France).
A NEW EUROPEAN VIBRATION TEST FACILITY FOR ARIANE 4 CLASS SATELLITES
Jean-Claude Pasquet and J. F. Imbert *In* ESA, Spacecraft Structures and Mechanical Testing Jan. 1989 p 643-648 (For primary document see N90-10986 02-18)
Copyright Avail: NTIS HC A99/MF E06

15 LAUNCH VEHICLES AND SPACE VEHICLES

Includes boosters; operating problems of launch/space vehicle systems; and reusable vehicles.

For related information see also *20 Spacecraft Propulsion and Power.*

N90-10912*# National Aeronautics and Space Administration. Lewis Research Center, Cleveland, OH.
EVALUATION OF SUPERCRITICAL CRYOGEN STORAGE AND TRANSFER SYSTEMS FOR FUTURE NASA MISSIONS
Hugh Arif, John C. Aydelott, and David J. Chato 1989 10 p Prepared for presentation at the 28th Aerospace Sciences Meeting, Reno, NV, 8-11 Jan. 1990; sponsored by AIAA
(NASA-TM-102394; E-5144; NAS 1.15:102394; AIAA-90-0719)
Avail: NTIS HC A02/MF A01 CSCL 22B

Conceptual designs of Space Transportation Vehicles (STV), and their orbital servicing facilities, that utilize supercritical, single phase, cryogenic propellants were established and compared with conventional subcritical, two phase, STV concepts. The analytical study was motivated by the desire to avoid fluid management problems associated with the storage, acquisition and transfer of subcritical liquid oxygen and hydrogen propellants in the low gravity environment of space. Although feasible, the supercritical concepts suffer from STV weight penalties and propellant resupply system power requirements which make the concepts impractical. Author

N90-11015# Intespace, Toulouse (France).
DYNAMIC SUBSTRUCTURING FOR MODULAR ANALYSIS AND TESTING
A. Girard and L. P. Bugeat *In* ESA, Spacecraft Structures and Mechanical Testing Jan. 1989 p 213-218 (For primary document see N90-10986 02-18)
(Contract ESA-6819/86/NL/PH(SC))
Copyright Avail: NTIS HC A99/MF E06

N90-11045# Construcciones Aeronauticas S.A., Madrid (Spain). Space Div.
INDUCED SHOCK LOADS DURING THE SEPARATION OF THE ARIANE 5 VEB STRUCTURE
C. Huerta, V. GomezMolinero, E. Alarcon, S. GomezLera, and J. Molina (Polytechnical Univ. of Madrid, Spain) *In* ESA, Spacecraft

Structures and Mechanical Testing Jan. 1989 p 447-454 (For primary document see N90-10986 02-18)
Copyright Avail: NTIS HC A99/MF E06

N90-11048# Arianespace, Evry (France). Dept. Analyse de Mission.
FLIGHT-MECHANICAL ENVIRONMENT ON ARIANE LAUNCH VEHICLE PAYLOADS [ENVIRONNEMENT MECANIQUE EN VOL SUR LES CHARGES UTILES MISES EN ORBITE PAR LES LANCEURS ARIANES]
J. L. Caneilles *In* ESA, Spacecraft Structures and Mechanical Testing Jan. 1989 p 467-480 In FRENCH (For primary document see N90-10986 02-18)
Copyright Avail: NTIS HC A99/MF E06

N90-11057# European Space Agency. European Space Research and Technology Center, ESTEC, Noordwijk (Netherlands).
ARIANE 5 STRUCTURAL DESIGN AND DEVELOPMENT
A. L. GonzalezBlasquez *In its* Spacecraft Structures and Mechanical Testing Jan. 1989 p 543-546 (For primary document see N90-10986 02-18)
Copyright Avail: NTIS HC A99/MF E06

N90-11058# Avions Marcel Dassault-Breguet Aviation, Saint-Cloud (France).
THERMAL AND STRUCTURAL ANALYSIS OF HERMES
C. Petiau *In* ESA, Spacecraft Structures and Mechanical Testing Jan. 1989 p 547-556 Previously announced in IAA as A89-17756 (For primary document see N90-10986 02-18)
Copyright Avail: NTIS HC A99/MF E06

16 SPACE TRANSPORTATION

Includes passenger and cargo space transportation, e.g., shuttle operations; and space rescue techniques.

For related information see also *03 Air Transportation and Safety* and *18 Spacecraft Design, Testing and Performance.* For space suits see *54 Man/System Technology and Life Support.*

N90-10913*# McDonnell-Douglas Astronautics Co., Houston, TX. Space Transportation System Engineering and Operations Support.
INDEPENDENT ORBITER ASSESSMENT (IOA): ANALYSIS OF THE MANNED MANEUVERING UNIT
P. S. Bailey 21 Nov. 1986 175 p
(Contract NAS9-17650)
(NASA-CR-185565; NAS 1.26:185565; Rept-1.0-WP-VA86001-09)
Avail: NTIS HC A08/MF A01 CSCL 22B

Results of the Independent Orbiter Assessment (IOA) of the Failure Modes and Effects Analysis (FMEA) and Critical Items List (CIL) are presented. The IOA approach features a top-down analysis of the hardware to determine failure modes, criticality, and potential critical items (PCIs). To preserve indepedence, this analysis was accomplished without reliance upon the results contained within the NASA FMEA/CIL documentation. This report documents the independent analysis results corresponding to the Manned Maneuvering Unit (MMU) hardware. The MMU is a propulsive backpack, operated through separate hand controllers that input the pilot's translational and rotational maneuvering commands to the control electronics and then to the thrusters. The IOA analysis process utilized available MMU hardware drawings and schematics for defining hardware subsystems, assemblies, components, and hardware items. Final levels of detail were evaluated and analyzed for possible failure modes and effects. Criticality was assigned based upon the worst case severity of the effect for each identified failure mode. The IOA analysis of the MMU found that the majority of the PCIs identified are resultant from the loss of either the propulsion or control functions, or are resultant from inability to perform an immediate or future mission. The five most severe criticalities identified are all resultant from failures imposed on the MMU hand controllers which have no redundancy within the MMU. Author

N90-10914*# McDonnell-Douglas Astronautics Co., Houston, TX. Space Transportation System Engineering and Operations Support.
INDEPENDENT ORBITER ASSESSMENT (IOA): ASSESSMENT OF THE ELECTRICAL POWER GENERATION/FUEL CELL POWERPLANT SUBSYSTEM FMEA/CIL
K. L. Brown and P. J. Bertsch 20 Mar. 1987 119 p
(Contract NAS9-17650)
(NASA-CR-185562; NAS 1.26:185562; Rept-1.0-WP-VA86001-24)
Avail: NTIS HC A06/MF A01 CSCL 22B

Results of the Independent Orbiter Assessment (IOA) of the Failure Modes and Effects Analysis (FMEA) and Critical Items List (CIL) are presented. The IOA effort first completed an analysis of the Electrical Power Generation/Fuel Cell Powerplant (EPG/FCP) hardware, generating draft failure modes and potential critical items. To preserve independence, this analysis was accomplished without reliance upon the results contained within the NASA FMEA/CIL documentation. The IOA results were then compared to the proposed Post 51-L NASA FMEA/CIL baseline. A resolution of each discrepancy from the comparison was provided through additional analysis as required. This report documents the results of that comparison for the Orbiter EPG/FCP hardware. Author

N90-10915*# McDonnell-Douglas Astronautics Co., Houston, TX. Space Transportation System Engineering and Operations Support.
INDEPENDENT ORBITER ASSESSMENT (IOA): ANALYSIS OF THE ELECTRICAL POWER GENERATION/FUEL CELL POWERPLANT SUBSYSTEM
K. L. Brown and P. J. Bertsch 5 Dec. 1986 100 p
(Contract NAS9-17650)
(NASA-CR-185561; NAS 1.26:185561; Rept-1.0-WP-VA86001-10)
Avail: NTIS HC A05/MF A01 CSCL 22B

Results of the Independent Orbiter Assessment (IOA) of the Failure Modes and Effects Analysis (FMEA) and Critical Items List (CIL) are presented. The IOA approach features a top-down analysis of the hardware to determine failure modes, criticality, and potential critical items. To preserve independence, this analysis was accomplished without reliance upon the results contained within the NASA FMEA/CIL documentation. This report documents the independent analysis results corresponding to the Orbiter Electrical Power Generation (EPG)/Fuel Cell Powerplant (FCP) hardware. The EPG/FCP hardware is required for performing functions of electrical power generation and product water distribution in the Orbiter. Specifically, the EPG/FCP hardware consists of the following divisions: (1) Power Section Assembly (PSA); (2) Reactant Control Subsystem (RCS); (3) Thermal Control Subsystem (TCS); and (4) Water Removal Subsystem (WRS). The IOA analysis process utilized available EPG/FCP hardware drawings and schematics for defining hardware assemblies, components, and hardware items. Each level of hardware was evaluated and analyzed for possible failure modes and effects. Criticality was assigned based upon the severity of the effect for each failure mode. Author

N90-10916*# McDonnell-Douglas Astronautics Co., Houston, TX. Space Transportation System Engineering and Operations Support.
INDEPENDENT ORBITER ASSESSMENT (IOA): ANALYSIS OF THE RUDDER/SPEED BRAKE SUBSYSTEM
R. E. Wilson and J. R. Riccio 21 Nov. 1986 70 p
(Contract NAS9-17650)
(NASA-CR-185560; NAS 1.26:185560; Rept-1.0-WP-VA86001-04)
Avail: NTIS HC A04/MF A01 CSCL 22B

The results of the Independent Orbiter Assessment (IOA) of the Failure Modes and Effects Analysis (FMEA) and Critical Items List (CIL) are presented. The IOA approach features a top-down analysis of the hardware to determine failure modes, criticality, and potential critical items. To preserve independence, this analysis

was accomplished without reliance upon the results contained within the NASA FMEA/CIL documentation. The independent analysis results for the Orbiter Rudder/Speedbrake Actuation Mechanism is documented. The function of the Rudder/Speedbrake (RSB) is to provide directional control and to provide a means of energy control during entry. The system consists of two panels on a vertical hinge mounted on the aft part of the vertical stabilizer. These two panels move together to form a rudder but split apart to make a speedbrake. The Rudder/Speedbrake Actuation Mechanism consists of the following elements: (1) Power Drive Unit (PDU) which is composed of hydraulic valve module and a hydraulic motor-powered gearbox which contains differentials and mixer gears to provide PDU torque output; (2) four geared rotary actuators which apply the PDU generated torque to the rudder/speedbrake panels; and (3) ten torque shafts which join the PDU to the rotary actuators and interconnect the four rotary actuators. Each level of hardware was evaluated and analyzed for possible failures and causes. Criticality was assigned based upon the severity of the effect for each failure mode. Critical RSB failures which result in potential loss of vehicle control were mainly due to loss of hydraulic fluid, fluid contaminators, and mechanical failures in gears and shafts.

Author

N90-10917*# McDonnell-Douglas Astronautics Co., Houston, TX. Space Transportation System Engineering and Operations Support.

INDEPENDENT ORBITER ASSESSMENT (IOA): ASSESSMENT OF THE DATA PROCESSING SYSTEM FMEA/CIL

H. J. Lowery and W. A. Haufler 28 Nov. 1986 305 p

(Contract NAS9-17650)

(NASA-CR-185546; NAS 1.26:185546; Rept-1.0-WP-VA86001-08)

Avail: NTIS HC A14/MF A02 CSCL 22B

The results of the Independent Orbiter Assessment (IOA) of the Failure Modes and Effects Analysis (FMEA) and Critical Items List (CIL) are presented. The IOA effort first completed an analysis of the Data Processing System (DPS) hardware, generating draft failure modes and potential critical items. To preserve independence, this analysis was accomplished without reliance upon the results contained within the NASA FMEA/CIL documentation. The IOA results were then compared to the NASA FMEA/CIL baseline with proposed Post 51-L updates included. A resolution of each discrepancy from the comparison is provided through additional analysis as required. The results of that comparison is documented for the Orbiter DPS hardware.

Author

N90-10918*# McDonnell-Douglas Astronautics Co., Houston, TX. Space Transportation System Engineering and Operations Support.

INDEPENDENT ORBITER ASSESSMENT (IOA): ANALYSIS OF THE ELECTRICAL POWER GENERATION/POWER REACTANT STORAGE AND DISTRIBUTION SUBSYSTEM

S. M. Gotch 5 Dec. 1986 205 p

(Contract NAS9-17650)

(NASA-CR-185556; NAS 1.26:185556; Rept-1.0-WP-VA86001-11)

Avail: NTIS HC A10/MF A02 CSCL 22B

The results of the Independent Orbiter Assessment (IOA) of the Failure Modes and Effects Analysis (FMEA) and Critical Items List (CIL) are presented. The IOA approach features a top-down analysis of the hardware to determine failure modes, criticality, and potential critical items. To preserve independence, this analysis was accomplished without reliance upon the results contained within the NAA FMEA/CIL documentation. The independent analysis results corresponding to the Orbiter Electrical Power Generation (EPG)/Power Reactants Storage and Distribution (PRSD) System Hardware is documented. The EPG/PRSD hardware is required for performing critical functions of cryogenic hydrogen and oxygen storage and distribution to the Fuel Cell Powerplants (FCP) and Atmospheric Revitalization Pressure Control Subsystem (ARPCS). Specifically, the EPG/PRSD hardware consists of the following: Hydryogen (H2) tanks; Oxygen (O2) tanks; H2 Relief Valve/Filter Packages (HRVFP); O2 Relief Valve/Filter Packages (ORVFP); H2 Valve Modules (HVM); O2 Valve Modules (OVM); and O2 and H2 lines, components, and fittings. Author

N90-10919*# McDonnell-Douglas Astronautics Co., Houston, TX. Space Transportation System Engineering and Operations Support.

INDEPENDENT ORBITER ASSESSMENT (IOA): ANALYSIS OF THE ORBITAL MANEUVERING SYSTEM

C. D. Prust, D. J. Paul, and V. J. Burkemper 12 Jan. 1987 1023 p

(Contract NAS9-17650)

(NASA-CR-185554; NAS 1.26:185554; Rept-1.0-WP-VA86001-21)

Avail: NTIS HC A99/MF E09 CSCL 22B

The results of the Independent Orbiter Assessment (IOA) of the Failure Modes and Effects Analysis (FMEA) and Critical Items List (CIL) are presented. The IOA approach features a top-down analysis of the hardware to determine failure modes, criticality, and potential critical items. To preserve independence, this analysis was accomplished without reliance upon the results contained within the NASA FMEA/CIL documentation. The independent analysis results for the Orbital Maneuvering System (OMS) hardware are documented. The OMS provides the thrust to perform orbit insertion, orbit circularization, orbit transfer, rendezvous, and deorbit. The OMS is housed in two independent pods located one on each side of the tail and consists of the following subsystems: Helium Pressurization; Propellant Storage and Distribution; Orbital Maneuvering Engine; and Electrical Power Distribution and Control. The IOA analysis process utilized available OMS hardware drawings and schematics for defining hardware assemblies, components, and hardware items. Each level of hardware was evaluted and analyzed for possible failure modes and effects. Criticality was asigned based upon the severity of the effect for each failure mode.

Author

N90-10920*# McDonnell-Douglas Astronautics Co., Houston, TX. Space Transportation System Engineering and Operations Support.

INDEPENDENT ORBITER ASSESSMENT (IOA): ANALYSIS OF THE GUIDANCE, NAVIGATION, AND CONTROL SUBSYSTEM

W. H. Trahan, R. A. ODonnell, K. C. Pietz, and J. M. Hiott 19 Dec. 1986 179 p

(Contract NAS9-17650)

(NASA-CR-185555; NAS 1.26:185555; Rept-1.0-WP-VA86001-16)

Avail: NTIS HC A09/MF A01 CSCL 22B

The results of the Independent Orbiter Assessment (IOA) of the Failure Modes and Effects Analysis (FMEA) and Critical Items List (CIL) is presented. The IOA approach features a top-down analysis of the hardware to determine failure modes, criticality, and potential critical items. To preserve independence, this analysis was accomplished without reliance upon the results contained within the NASA FMEA/CIL documentation. The independent analysis results corresponding to the Orbiter Guidance, Navigation, and Control (GNC) Subsystem hardware are documented. The function of the GNC hardware is to respond to guidance, navigation, and control software commands to effect vehicle control and to provide sensor and controller data to GNC software. Some of the GNC hardware for which failure modes analysis was performed includes: hand controllers; Rudder Pedal Transducer Assembly (RPTA); Speed Brake Thrust Controller (SBTC); Inertial Measurement Unit (IMU); Star Tracker (ST); Crew Optical Alignment Site (COAS); Air Data Transducer Assembly (ADTA); Rate Gyro Assemblies; Accelerometer Assembly (AA); Aerosurface Servo Amplifier (ASA); and Ascent Thrust Vector Control (ATVC). The IOA analysis process utilized available GNC hardware drawings, workbooks, specifications, schematics, and systems briefs for defining hardware assemblies, components, and circuits. Each hardware item was evaluated and analyzed for possible failure modes and effects. Criticality was assigned based upon the severity of the effect for each failure mode.

Author

N90-10921*# McDonnell-Douglas Astronautics Co., Houston, TX. Space Transportation System Engineering and Operations Support.

INDEPENDENT ORBITER ASSESSMENT (IOA): ANALYSIS OF THE NOSE WHEEL STEERING SUBSYSTEM

Anthony Scott Mediavilla 21 Nov. 1986 117 p

(Contract NAS9-17650)

(NASA-CR-185548; NAS 1.26:185548; Rept-1.0-WP-VA86001-03)

Avail: NTIS HC A06/MF A01 CSCL 22B

The results of the Independent Orbiter Assessment (IOA) of the Failure Modes and Effects Analysis (FMEA) and Critical Items List (CIL) are presented. The IOA approach features a top-down analysis of the hardware to determine failure modes, criticality, and potential critical items. To preserve independence, this analysis was accomplished without reliance upon the results contained within the NASA FMEA/CIL documentation. The independent analysis results for the Orbiter Nose Wheel Steering (NWS) hardware are documented. The NWS hardware provides primary directional control for the Orbiter vehicle during landing rollout. Each level of hardware was evaluated and analyzed for possible failure modes and effects. Criticality was assigned based upon the severity of the effect for each failure mode. The original NWS design was envisioned as a backup system to differential braking for directional control of the Orbiter during landing rollout. No real effort was made to design the NWS system as fail operational. The brakes have much redundancy built into their design but the poor brake/tire performance has forced the NSTS to upgrade NWS to the primary mode of directional control during rollout. As a result, a large percentage of the NWS system components have become Potential Critical Items (PCI). Author

N90-10922*# McDonnell-Douglas Astronautics Co., Houston, TX. Space Transportation System Engineering and Operations Support.

INDEPENDENT ORBITER ASSESSMENT (IOA): FMEA/CIL INSTRUCTIONS AND GROUND RULES

S. T. Traves 14 Oct. 1986 73 p

(Contract NAS9-17650)

(NASA-CR-185551; NAS 1.26:185551; Rept-1.0-WP-VA86001-01)

Avail: NTIS HC A04/MF A01 CSCL 22B

The McDonnell Douglas Astronautics Company was selected to conduct an independent assessment of the Orbiter Failure Mode and Effects Analysis/Critical Items List (FMEA/CIL). Part of this effort involved an examination of the FMEA/CIL preparation instructions and ground rules. Assessment objectives were to identify omissions and ambiguities in the ground rules that may impede the identification of shuttle orbiter safety and mission critical items, and to ensure that ground rules allow these items to receive proper management visibility for risk assessment. Assessment objectives were followed during the performance of the assessment without being influenced by external considerations such as effects on budget, schedule, and documentation growth. Assessment personnel were employed who had a strong reliability background but no previous space shuttle FMEA/CIL experience to ensure an independent assessment would be achieved. The following observations were made: (1) not all essential items are in the CIL for management visibility; (2) ground rules omit FMEA/CIL coverage of items that perform critical functions; (3) essential items excluded from the CIL do not receive design justification; and (4) FMEAs/CILs are not updated in a timely manner. In addition to the above issues, a number of other issues were identified that correct FMEA/CIL preparation instruction omissions and clarify ambiguities. The assessment was successful in that many of the issues have significant safety implications. Author

N90-10923*# McDonnell-Douglas Astronautics Co., Houston, TX. Space Transportation System Engineering and Operations Support.

INDEPENDENT ORBITER ASSESSMENT (IOA): ASSESSMENT OF THE ELECTRICAL POWER GENERATION/POWER REACTANT STORAGE AND DISTRIBUTION SUBSYSTEM FMEA/CIL

B. E. Ames 22 Feb. 1988 239 p

(Contract NAS9-17650)

(NASA-CR-185545; NAS 1.26:185545; Rept-1.0-WP-VA88003-15)

Avail: NTIS HC A11/MF A02 CSCL 22B

The results of the Independent Orbiter Assessment (IOA) of the Failure Modes and Effects Analysis (FMEA) and Critical Items List (CIL) is presented. The IOA effort first completed an analysis of the Electrical Power Generation/Power Reactant Storage and Distribution (EPG/PRSD) subsystem hardware, generating draft failure modes and potential critical items. To preserve independence, this analysis was accomplished without reliance upon the results contained within the NASA FMEA/CIL documentation. The IOA results were then compared to the NASA FMEA/CIL baselines with proposed Post 51-L updates included. A resolution of each discrepancy from the comparison is provided through additional analysis as required. The results of that comparison are documented for the Orbiter EPG/PRSD hardware. The comparison produced agreement on all but 27 FMEAs and 9 CIL items. The discrepancy between the number of IOA findings and NASA FMEAs can be partially explained by the different approaches used by IOA and NASA to group failure modes together to form one FMEA. Also, several IOA items represented inner tank components and ground operations failure modes which were not in the NASA baseline. Author

N90-10924*# McDonnell-Douglas Astronautics Co., Houston, TX. Space Transportation System Engineering and Operations Support.

INDEPENDENT ORBITER ASSESSMENT (IOA): ANALYSIS OF THE DPS SUBSYSTEM

H. J. Lowery, W. A. Haufler, and K. C. Pietz 24 Oct. 1986 123 p

(Contract NAS9-17650)

(NASA-CR-185549; NAS 1.26:185549; Rept-1.0-WP-VA86001-02)

Avail: NTIS HC A06/MF A01 CSCL 22B

The results of the Independent Orbiter Assessment (IOA) of the Failure Modes and Effects Analysis/Critical Items List (FMEA/CIL) is presented. The IOA approach features a top-down analysis of the hardware to independently determine failure modes, criticality, and potential critical items. The independent analysis results corresponding to the Orbiter Data Processing System (DPS) hardware are documented. The DPS hardware is required for performing critical functions of data acquisition, data manipulation, data display, and data transfer throughout the Orbiter. Specifically, the DPS hardware consists of the following components: Multiplexer/Demultiplexer (MDM); General Purpose Computer (GPC); Multifunction CRT Display System (MCDS); Data Buses and Data Bus Couplers (DBC); Data Bus Isolation Amplifiers (DBIA); Mass Memory Unit (MMU); and Engine Interface Unit (EIU). The IOA analysis process utilized available DPS hardware drawings and schematics for defining hardware assemblies, components, and hardware items. Each level of hardware was evaluated and analyzed for possible failure modes and effects. Criticality was assigned based upon the severity of the effect for each failure mode. Due to the extensive redundancy built into the DPS the number of critical items are few. Those identified resulted from premature operation and erroneous output of the GPCs. Author

N90-10925*# McDonnell-Douglas Astronautics Co., Houston, TX. Space Transportation System Engineering and Operations Support.

INDEPENDENT ORBITER ASSESSMENT (IOA): ANALYSIS OF THE ATMOSPHERIC REVITALIZATION PRESSURE CONTROL SUBSYSTEM

M. J. Saiidi, R. E. Duffy, and T. D. McLaughlin 28 Nov. 1986 309 p

(Contract NAS9-17650)

(NASA-CR-185593; NAS 1.26:185593; Rept-1.0-WP-VA86001-12)

Avail: NTIS HC A14/MF A02 CSCL 22B

The results of the Independent Orbiter Assessment (IOA) of the Failure Modes and Effects Analysis/Critical Items List (FMEA/CIL) are presented. The IOA approach features a top-down analysis of the hardware to determine failure modes, criticality, and potential critical items. To preserve independence, this analysis

was accomplished without reliance upon the results contained within the NASA FMEA/CIL documentation. The independent analysis results corresponding to the Orbiter Atmospheric Revitalization and Pressure Control Subsystem (ARPCS) are documented. The ARPCS hardware was categorized into the following subdivisions: (1) Atmospheric Make-up and Control (including the Auxiliary Oxygen Assembly, Oxygen Assembly, and Nitrogen Assembly); and (2) Atmospheric Vent and Control (including the Positive Relief Vent Assembly, Negative Relief Vent Assembly, and Cabin Vent Assembly). The IOA analysis process utilized available ARPCS hardware drawings and schematics for defining hardware assemblies, components, and hardware items. Each level of hardware was evaluated and analyzed for possible failure modes and effects. Criticality was assigned based upon the severity of the effect for each failure mode. Author

N90-10926*# McDonnell-Douglas Astronautics Co., Houston, TX. Space Transportation System Engineering and Operations Support.

INDEPENDENT ORBITER ASSESSMENT (IOA): ANALYSIS OF THE REMOTE MANIPULATOR SYSTEM

F. Tangorra, R. F. Grasmeder, and A. D. Montgomery 12 Jan. 1987 618 p

(Contract NAS9-17650)

(NASA-CR-185585; NAS 1.26:185585; Rept-1.0-WP-VA86001-23)

Avail: NTIS HC A99/MF A04 CSCL 22B

The results of the Independent Orbiter Assessment (IOA) of the Failure Modes and Effects Analysis (FMEA) and Critical Items List (CIL) are presented. The IOA approach features a top-down analysis of the hardware to determine failure modes, criticality, and potential critical items (PCIs). To preserve independence, this analysis was accomplished without reliance upon the results contained within the NASA FMEA/CIL documentation. The independent analysis results for the Orbiter Remote Manipulator System (RMS) are documented. The RMS hardware and software are primarily required for deploying and/or retrieving up to five payloads during a single mission, capture and retrieve free-flying payloads, and for performing Manipulator Foot Restraint operations. Specifically, the RMS hardware consists of the following components: end effector; displays and controls; manipulator controller interface unit; arm based electronics; and the arm. The IOA analysis process utilized available RMS hardware drawings, schematics and documents for defining hardware assemblies, components and hardware items. Each level of hardware was evaluated and analyzed for possible failure modes and effects. Criticality was assigned based upon the severity of the effect for each failure mode. Of the 574 failure modes analyzed, 413 were determined to be PCIs. Author

N90-10927*# McDonnell-Douglas Astronautics Co., Houston, TX. Space Transportation System Engineering and Operations Support.

INDEPENDENT ORBITER ASSESSMENT (IOA): ANALYSIS OF THE ORBITER MAIN PROPULSION SYSTEM

W. J. McNicoll, M. McNeely, K. A. Holden, T. E. Emmons, and H. J. Lowery 16 Jan. 1987 747 p

(Contract NAS9-17650)

(NASA-CR-185584; NAS 1.26:185584; Rept-1.0-WP-VA86001-22)

Avail: NTIS HC A99/MF A04 CSCL 22B

The results of the Independent Orbiter Assessment (IOA) of the Failure Modes and Effects Analysis (FMEA) and Critical Items List (CIL) are presented. The IOA approach features a top-down analysis of the hardware to determine failure modes, criticality, and potential critical items (PCIs). To preserve independence, this analysis was accomplished without reliance upon the results contained within the NASA FMEA/CIL documentation. The independent analysis results for the Orbiter Main Propulsion System (MPS) hardware are documented. The Orbiter MPS consists of two subsystems: the Propellant Management Subsystem (PMS) and the Helium Subsystem. The PMS is a system of manifolds, distribution lines and valves by which the liquid propellants pass from the External Tank (ET) to the Space Shuttle Main Engines (SSMEs) and gaseous propellants pass from the SSMEs to the ET. The Helium Subsystem consists of a series of helium supply tanks and their associated regulators, check valves, distribution lines, and control valves. The Helium Subsystem supplies helium that is used within the SSMEs for inflight purges and provides pressure for actuation of SSME valves during emergency pneumatic shutdowns. The balance of the helium is used to provide pressure to operate the pneumatically actuated valves within the PMS. Each component was evaluated and analyzed for possible failure modes and effects. Criticalities were assigned based on the worst possible effect of each failure mode. Of the 690 failure modes analyzed, 349 were determined to be PCIs. Author

N90-10928*# McDonnell-Douglas Corp., Houston, TX. Space Transportation System Engineering and Operations Support.

INDEPENDENT ORBITER ASSESSMENT (IOA): ANALYSIS OF THE INSTRUMENTATION SUBSYSTEM

B. S. Howard 12 Dec. 1986 139 p

(Contract NAS9-17650)

(NASA-CR-185571; NAS 1.26:185571; Rept-1.0-WP-VA86001-17)

Avail: NTIS HC A07/MF A01 CSCL 22B

The results of the Independent Orbiter Assessment (IOA) of the Failure Modes and Effects Analysis (FMEA) and Critical Items List (CIL) are presented. The IOA approach features a top-down analysis of the hardware to determine failure modes, criticality, and potential critical items. To preserve independence, this analysis was accomplished without reliance upon the results contained within the NASA FMEA/CIL documentation. The independent analysis results for the Instrumentation Subsystem are documented. The Instrumentation Subsystem (SS) consists of transducers, signal conditioning equipment, pulse code modulation (PCM) encoding equipment, tape recorders, frequency division multiplexers, and timing equipment. For this analysis, the SS is broken into two major groupings: Operational Instrumentation (OI) equipment and Modular Auxiliary Data System (MADS) equipment. The OI equipment is required to acquire, condition, scale, digitize, interleave/multiplex, format, and distribute operational Orbiter and payload data and voice for display, recording, telemetry, and checkout. It also must provide accurate timing for time critical functions for crew and payload specialist use. The MADS provides additional instrumentation to measure and record selected pressure, temperature, strain, vibration, and event data for post-flight playback and analysis. MADS data is used to assess vehicle responses to the flight environment and to permit correlation of such data from flight to flight. The IOA analysis utilized available SS hardware drawings and schematics for identifying hardware assemblies and components and their interfaces. Criticality for each item was assigned on the basis of the worst-case effect of the failure modes identified. Author

N90-10929*# McDonnell-Douglas Corp., Houston, TX. Space Transportation System Engineering and Operations Support.

INDEPENDENT ORBITER ASSESSMENT (IOA): ANALYSIS OF THE ASCENT THRUST VECTOR CONTROL ACTUATOR SUBSYSTEM

R. E. Wilson and J. R. Riccio 21 Nov. 1986 59 p

(Contract NAS9-17650)

(NASA-CR-185579; NAS 1.26:185579; Rept-1.0-WP-VA86001-06)

Avail: NTIS HC A04/MF A01 CSCL 22B

The results of the Independent Orbiter Assessment (IOA) of the Failure Modes and Effects Analysis (FMEA) and Critical Items List (CIL) are presented. The IOA approach features a top-down analysis of the hardware to determine failure modes, criticality, and potential critical items. To preserve independence, this analysis was accomplished without reliance upon the results contained within the NASA FMEA/CIL documentation. The independent analysis results for the Ascent Thrust Vector Control (ATVC) Actuator hardware are documented. The function of the Ascent Thrust Vector Control Actuators (ATVC) is to gimbal the main engines to provide for attitude and flight path control during ascent. During first stage flight, the SRB nozzles provide nearly all the steering. After SRB separation, the Orbiter is steered by gimbaling of its main engines. There are six electrohydraulic servoactuators, one pitch and one yaw for each of the three main engines. Each

servoactuator is composed of four electrohydraulic servovalve assemblies, one second stage power spool valve assembly, one primary piston assembly and a switching valve. Each level of hardware was evaluated and analyzed for possible failure modes and effects. Criticality was assigned based upon the severity of the effect for each failure mode. Critical failures resulting in loss of ATVC were mainly due to loss of hydraulic fluid, fluid contamination and mechanical failures. Author

N90-10930*# McDonnell-Douglas Corp., Houston, TX. Space Transportation System Engineering and Operations Support.

INDEPENDENT ORBITER ASSESSMENT (IOA): ANALYSIS OF THE BODY FLAP SUBSYSTEM

R. E. Wilson and J. R. Riccio 21 Nov. 1986 68 p

(Contract NAS9-17650)

(NASA-CR-185574; NAS 1.26:185574; Rept-1.0-WP-VA86001-05)

Avail: NTIS HC A04/MF A01 CSCL 22B

The results of the Independent Orbiter Assessment (IOA) of the Failure Modes and Effects Analysis (FMEA) and Critical Items List (CIL) are presented. The IOA approach features a top-down analysis of the hardware to determine failure modes, criticality, and potential critical items (PCIs). To preserve independence, this analysis was accomplished without reliance upon the results contained within the NASA FMEA/CIL documentation. The independent analysis results for the Orbiter Body Flap (BF) subsystem hardware are documented. The BF is a large aerosurface located at the trailing edge of the lower aft fuselage of the Orbiter. The proper function of the BF is essential during the dynamic flight phases of ascent and entry. During the ascent phase of flight, the BF trails in a fixed position. For entry, the BF provides elevon load relief, trim control, and acts as a heat shield for the main engines. Specifically, the BF hardware comprises the following components: Power Drive Unit (PDU), rotary actuators, and torque tubes. The IOA analysis process utilized available BF hardware drawings and schematics for defining hardware assemblies, components, and hardware items. Each level of hardware was evaluated and analyzed for possible failure modes and effects. Criticality was assigned based upon the severity of the effect for each failure mode. Of the 35 failure modes analyzed, 19 were determined to be PCIs. Author

N90-10931*# McDonnell-Douglas Astronautics Co., Houston, TX.

INDEPENDENT ORBITER ASSESSMENT (IOA): ANALYSIS OF THE AUXILIARY POWER UNIT

J. E. Barnes 12 Dec. 1986 388 p

(Contract NAS9-17650)

(NASA-CR-185568; NAS 1.26:185568; Rept-1.0-WP-VA86001-14)

Avail: NTIS HC A17/MF A02 CSCL 22B

The results of the Independent Orbiter Assessment (IOA) of the Failure Modes and Effects Analysis (FMEA) and Critical Items List (CIL) are presented. The IOA approach features a top-down analysis of the hardware to determine failure modes, criticality, and potential critical items. To preserve independence, this analysis was accomplished without reliance upon the results contained within the NASA FMEA/CIL documentation. This report documents the independent analysis results corresponding to the Orbiter Auxiliary Power Unit (APU). The APUs are required to provide power to the Orbiter hydraulics systems during ascent and entry flight phases for aerosurface actuation, main engine gimballing, landing gear extension, and other vital functions. For analysis purposes, the APU system was broken down into ten functional subsystems. Each level of hardware was evaluated and analyzed for possible failure modes and effects. Criticality was assigned based upon the severity of the effect for each failure mode. A preponderance of 1/1 criticality items were related to failures that allowed the hydrazine fuel to escape into the Orbiter aft compartment, creating a severe fire hazard, and failures that caused loss of the gas generator injector cooling system. Author

N90-10932*# McDonnell-Douglas Astronautics Co., Houston, TX. Space Transportation System Engineering and Operations Support.

INDEPENDENT ORBITER ASSESSMENT (IOA): ANALYSIS OF THE BACKUP FLIGHT SYSTEM

E. E. Prust, R. W. Mielke, and L. W. Hinsdale 8 Dec. 1986 63 p

(Contract NAS9-17650)

(NASA-CR-185567; NAS 1.26:185567; Rept-1.0-WP-VA86001-18)

Avail: NTIS HC A04/MF A01 CSCL 22B

The results of the Independent Orbiter Assessment (IOA) of the Failure Modes and Effects Analysis (FMEA) and Critical Items List (CIL) are presented. The IOA approach features a top-down analysis of the hardware to determine failure modes, criticality, and potential critical items. To preserve independence, this analysis was accomplished without reliance upon the results contained within the NASA FMEA/CIL documentation. This report documents the analysis results corresponding to the Orbiter Backup Flight System (BFS) hardware. The BFS hardware consists of one General Purpose Computer (GPC) loaded with backup flight software and the components used to engage/disengage that unique GPC. Specifically, the BFS hardware includes the following: DDU (Display Driver Unit), BFC (Backup Flight Controller), GPC (General Purpose Computer), switches (engage, disengage, GPC, CRT), and circuit protectors (fuses, circuit breakers). The IOA analysis process utilized available BFS hardware drawings and schematics for defining hardware assemblies, components, and hardware items. Each level of hardware was evaluated and analyzed for possible failure modes and effects. Criticality was assigned based upon the severity of the effect for each failure mode. Of the failure modes analyzed, 19 could potentially result in a loss of life and/or loss of vehicle. Author

N90-10933*# McDonnell-Douglas Astronautics Co., Houston, TX.

INDEPENDENT ORBITER ASSESSMENT (IOA): ANALYSIS OF THE ELECTRICAL POWER DISTRIBUTION AND CONTROL/ELECTRICAL POWER GENERATION SUBSYSTEM

Jeff A. Patton 19 Dec. 1986 303 p

(Contract NAS9-17650)

(NASA-CR-185538; NAS 1.26:185538; Rept-1.0-WP-VA86001-19)

Avail: NTIS HC A14/MF A02 CSCL 22B

The results of the Independent Orbiter Assessment (IOA) of the Failure Modes and Effects Analysis (FMEA) and Critical Items List (CIL) are presented. The IOA approach features a top-down analysis of the hardware to determine failure modes, criticality, and potential critical items. To preserve independence, this analysis was accomplished without reliance upon the results contained within the NASA FMEA/CIL documentation. This report documents the independent analysis results corresponding to the Orbiter Electrical Power Distribution and Control (EPD and C)/Electrical Power Generation (EPG) hardware. The EPD and C/EPG hardware is required for performing critical functions of cryogenic reactant storage, electrical power generation and product water distribution in the Orbiter. Specifically, the EPD and C/EPG hardware consists of the following components: Power Section Assembly (PSA); Reactant Control Subsystem (RCS); Thermal Control Subsystem (TCS); Water Removal Subsystem (WRS); and Power Reactant Storage and Distribution System (PRSDS). The IOA analysis process utilized available EPD and C/EPG hardware drawings and schematics for defining hardware assemblies, components, and hardware items. Each level of hardware was evaluated and analyzed for possible failure modes and effects. Criticality was assigned based upon the severity of the effect for each failure mode. Author

N90-10934*# McDonnell-Douglas Astronautics Co., Houston, TX.

INDEPENDENT ORBITER ASSESSMENT (IOA): ANALYSIS OF THE HYDRAULICS/WATER SPRAY BOILER SUBSYSTEM

J. D. Duval, W. R. Davidson, and William E. Parkman 19 Dec. 1986 486 p

(Contract NAS9-17650)
(NASA-CR-185541; NAS 1.26:185541; Rept-1.0-WP-VA86001-20)
Avail: NTIS HC A21/MF A03 CSCL 22B

The results of the Independent Orbiter Assessment (IOA) of the Failure Modes and Effects Analysis (FMEA) and Critical Items List (CIL) are presented. The IOA approach features a top-down analysis of the hardware to determine failure modes, criticality, and potential critical items (PCIs). To preserve independence, this analysis was accomplished without reliance upon the results contained within the NASA FMEA/CIL documentation. This report documents the independent analysis results for the Orbiter Hydraulics/Water Spray Boiler Subsystem. The hydraulic system provides hydraulic power to gimbal the main engines, actuate the main engine propellant control valves, move the aerodynamic flight control surfaces, lower the landing gear, apply wheel brakes, steer the nosewheel, and dampen the external tank (ET) separation. Each hydraulic system has an associated water spray boiler which is used to cool the hydraulic fluid and APU lubricating oil. The IOA analysis process utilized available HYD/WSB hardware drawings, schematics and documents for defining hardware assemblies, components, and hardware items. Each level of hardware was evaluated and analyzed for possible failure modes and effects. Criticality was assigned based upon the severity of the effect for each failure mode. Of the 430 failure modes analyzed, 166 were determined to be PCIs. Author

N90-10935*# McDonnell-Douglas Corp., Houston, TX. Space Transportation System Engineering and Operations Support.
INDEPENDENT ORBITER ASSESSMENT (IOA): ANALYSIS OF THE ELEVON SUBSYSTEM
R. E. Wilson and J. R. Riccio 21 Nov. 1986 56 p
(Contract NAS9-17650)
(NASA-CR-185576; NAS 1.26:185576; Rept-1.0-WP-VA86001-07)
Avail: NTIS HC A04/MF A01 CSCL 22B

The results of the Independent Orbiter Assessment (IOA) of the Failure Modes and Effects Analysis (FMEA) and Critical Items List (CIL) are presented. The IOA approach features a top-down analysis of the hardware to determine failure modes, criticality, and potential critical items. To preserve independence, this analysis was accomplished without reliance upon the results contained within the NASA FMEA/CIL documentation. This report documents the independent analysis results for the Orbiter Elevon system hardware. The elevon actuators are located at the trailing edge of the wing surface. The proper function of the elevons is essential during the dynamic flight phases of ascent and entry. In the ascent phase of flight, the elevons are used for relieving high wing loads. For entry, the elevons are used to pitch and roll the vehicle. Specifically, the elevon system hardware comprises the following components: flow cutoff valve; switching valve; electro-hydraulic (EH) servoactuator; secondary delta pressure transducer; bypass valve; power valve; power valve check valve; primary actuator; primary delta pressure transducer; and primary actuator position transducer. Each level of hardware was evaluated and analyzed for possible failure modes and effects. Criticality was assigned based upon the severity of the effect for each failure mode. Of the 25 failure modes analyzed, 18 were determined to be PCIs.
Author

N90-10936*# McDonnell-Douglas Astronautics Co., Houston, TX. Space Transportation System Engineering and Operations Support.
INDEPENDENT ORBITER ASSESSMENT (IOA): ANALYSIS OF THE ELECTRICAL POWER DISTRIBUTION AND CONTROL/REMOTE MANIPULATOR SYSTEM SUBSYSTEM
W. W. Robinson 17 Feb. 1987 384 p
(Contract NAS9-17650)
(NASA-CR-185526; NAS 1.26:185526; Rept-1.0-WP-VA86001-26)
Avail: NTIS HC A17/MF A02 CSCL 22B

The results of the Independent Orbiter Assessment (IOA) of the Failure Modes and Effects Analysis (FMEA) and Critical Items List (CIL) are presented. The IOA approach features a top-down analysis of the Electrical Power Distribution and Control (EPD and C)/Remote Manipulator System (RMS) hardware to determine failure modes, criticality, and potential critical items. To preserve independence, this analysis was accomplished without reliance upon the results contained in the NASA FMEA/CIL documentation. This report documents the results of the independent analysis of the EPD and C/RMS (both port and starboard) hardware. The EPD and C/RMS subsystem hardware provides the electrical power and power control circuitry required to safely deploy, operate, control, and stow or guillotine and jettison two (one port and one starboard) RMSs. The EPD and C/RMS subsystem is subdivided into the four following functional divisions: Remote Manipulator Arm; Manipulator Deploy Control; Manipulator Latch Control; Manipulator Arm Shoulder Jettison; and Retention Arm Jettison. The IOA analysis process utilized available EPD and C/RMS hardware drawings and schematics for defining hardware assemblies, components, and hardware items. Each level of hardware was evaluated and analyzed for possible failure modes and effects. Criticality was assigned based on the severity of the effect for each failure mode. Author

N90-10937*# McDonnell-Douglas Astronautics Co., Houston, TX.
INDEPENDENT ORBITER ASSESSMENT (IOA): ANALYSIS OF THE EXTRAVEHICULAR MOBILITY UNIT
Gary G. Raffaelli 15 Dec. 1986 558 p
(Contract NAS9-17650)
(NASA-CR-185540; NAS 1.26:185540; Rept-1.0-WP-VA86001-15)
Avail: NTIS HC A24/MF A03 CSCL 22B

The results of the Independent Orbiter Assessment (IOA) of the Failure Modes and Effects Analysis (FMEA) and Critical Items List (CIL) are presented. The IOA approach features a top-down analysis of the hardware to determine failure modes, criticality, and potential critical items (PCIs). To preserve independence, this analysis was accomplished without reliance upon the results contained within the NASA FMEA/CIL documentation. This report documents the independent analysis results corresponding to the Extravehicular Mobility Unit (EMU) hardware. The EMU is an independent anthropomorphic system that provides environmental protection, mobility, life support, and communications for the Shuttle crewmember to perform Extravehicular Activity (EVA) in Earth orbit. Two EMUs are included on each baseline Orbiter mission, and consumables are provided for three two-man EVAs. The EMU consists of the Life Support System (LSS), Caution and Warning System (CWS), and the Space Suit Assembly (SSA). Each level of hardware was evaluated and analyzed for possible failure modes and effects. The majority of these PCIs are resultant from failures which cause loss of one or more primary functions: pressurization, oxygen delivery, environmental maintenance, and thermal maintenance. It should also be noted that the quantity of PCIs would significantly increase if the SOP were to be treated as an emergency system rather than as an unlike redundant element.
Author

N90-10938*# McDonnell-Douglas Astronautics Co., Houston, TX.
INDEPENDENT ORBITER ASSESSMENT (IOA): ANALYSIS OF THE REACTION CONTROL SYSTEM, VOLUME 1
V. J. Burkemper, W. A. Haufler, R. A. ODonnell, and D. J. Paul 19 Jan. 1987 790 p
(Contract NAS9-17650)
(NASA-CR-185532-Vol-1; NAS 1.26:185532-Vol-1; Rept-1.0-WP-VA86001-27-Vol-1) Avail: NTIS HC A99/MF E06 CSCL 22B

The results of the Independent Orbiter Assessment (IOA) of the Failure Modes and Effects Analysis (FMEA) and Critical Items List (CIL) are presented. The IOA approach features a top-down analysis of the hardware to determine failure modes, criticality, and potential critical items. To preserve independence, this analysis was accomplished without reliance upon the results contained within the NASA FMEA/CIL documentation. This report documents the independent analysis results for the Reaction Control System (RCS). The purpose of the RCS is to provide thrust in and about the X, Y, Z axes for External Tank (ET) separation; orbit insertion maneuvers; orbit translation maneuvers; on-orbit attitude control;

rendezvous; proximity operations (payload deploy and capture); deorbit maneuvers; and abort attitude control. The RCS is situated in three independent modules, one forward in the orbiter nose and one in each OMS/RCS pod. Each RCS module consists of the following subsystems: Helium Pressurization Subsystem; Propellant Storage and Distribution Subsystem; Thruster Subsystem; and Electrical Power Distribution and Control Subsystem. Of the failure modes analyzed, 307 could potentially result in a loss of life and/or loss of vehicle. Author

N90-10939*# McDonnell-Douglas Astronautics Co., Houston, TX.
INDEPENDENT ORBITER ASSESSMENT (IOA): ANALYSIS OF THE REACTION CONTROL SYSTEM, VOLUME 2
V. J. Burkemper, W. A. Haufler, R. A. ODonnell, and D. J. Paul 19 Jan. 1987 797 p
(Contract NAS9-17650)
(NASA-CR-185532-Vol-2; NAS 1.26:185532-Vol-2; Rept-1.0-WP-VA86001-27-Vol-2) Avail: NTIS HC A99/MF E06 CSCL 22B

The results of the Independent Orbiter Assessment (IOA) of the Failure Modes and Effects Analysis (FMEA) and Critical Items List (CIL) are presented. The IOA approach features a top-down analysis of the hardware to determine failure modes, criticality, and potential critical items. To preserve independence, this analysis was accomplished without reliance upon the results contained within the NASA FMEA/CIL documentation. This report documents the independent analysis results for the Reaction Control System (RCS). The RCS is situated in three independent modules, one forward in the orbiter nose and one in each OMS/RCS pod. Each RCS module consists of the following subsystems: Helium Pressurization Subsystem; Propellant Storage and Distribution Subsystem; Thruster Subsystem; and Electrical Power Distribution and Control Subsystem. Volume 2 continues the presentation of IOA analysis worksheets. Author

N90-10940*# McDonnell-Douglas Astronautics Co., Houston, TX.
INDEPENDENT ORBITER ASSESSMENT (IOA): ANALYSIS OF THE REACTION CONTROL SYSTEM, VOLUME 3
V. J. Burkemper, W. A. Haufler, R. A. ODonnell, and D. J. Paul 19 Jan. 1987 767 p
(Contract NAS9-17650)
(NASA-CR-185532-Vol-3; NAS 1.26:185532-Vol-3; Rept-1.0-WP-VA86001-27-Vol-3) Avail: NTIS HC A99/MF A04 CSCL 22B

The results of the Independent Orbiter Assessment (IOA) of the Failure Modes and Effects Analysis (FMEA) and Critical Items List (CIL) are presented. The IOA approach features a top-down analysis of the hardware to determine failure modes, criticality, and potential critical items. To preserve independence, this analysis was accomplished without reliance upon the results contained within the NASA FMEA/CIL documentation. This report documents the independent analysis results for the Reaction Control System (RCS). The RCS is situated in three independent modules, one forward in the orbiter nose and one in each OMS/RCS pod. Each RCS module consists of the following subsystems: Helium Pressurization Subsystem; Propellant Storage and Distribution Subsystem; Thruster Subsystem; and Electrical Power Distribution and Control Subsystem. Volume 3 continues the presentation of IOA analysis worksheets and the potential critical items list. Author

N90-10941*# McDonnell-Douglas Astronautics Co., Houston, TX. Space Transportation System Engineering and Operations Support.
INDEPENDENT ORBITER ASSESSMENT (IOA): ANALYSIS OF THE ELECTRICAL POWER DISTRIBUTION AND CONTROL SUBSYSTEM, VOLUME 1
K. R. Schmeckpeper 3 Apr. 1987 832 p
(Contract NAS9-17650)
(NASA-CR-185529-Vol-1; NAS 1.26:185529-Vol-1; Rept-1.0-WP-VA86001-28-Vol-1) Avail: NTIS HC A99/MF E06 CSCL 22B

The results of the Independent Orbiter Assessment (IOA) of the Failure Modes and Effects Analysis (FMEA) and Critical Items List (CIL) are presented. The IOA approach features a top-down analysis of the hardware to determine failure modes, criticality, and potential critical items. To preserve independence, this analysis was accomplished without reliance upon the results contained within the NASA FMEA/CIL documentation. This report documents the independent analysis results corresponding to the Orbiter Electrical Power Distribution and Control (EPD and C) hardware. The EPD and C hardware performs the functions of distributing, sensing, and controlling 28 volt DC power and of inverting, distributing, sensing, and controlling 117 volt 400 Hz AC power to all Orbiter subsystems from the three fuel cells in the Electrical Power Generation (EPG) subsystem. Each level of hardware was evaluated and analyzed for possible failure modes and effects. Criticality was assigned based upon the severity of the effect for each failure mode. Of the 1671 failure modes analyzed, 9 single failures were determined to result in loss of crew or vehicle. Three single failures unique to intact abort were determined to result in possible loss of the crew or vehicle. A possible loss of mission could result if any of 136 single failures occurred. Six of the criticality 1/1 failures are in two rotary and two pushbutton switches that control External Tank and Solid Rocket Booster separation. The other 6 criticality 1/1 failures are fuses, one each per Aft Power Control Assembly (APCA) 4, 5, and 6 and one each per Forward Power Control Assembly (FPCA) 1, 2, and 3, that supply power to certain Main Propulsion System (MPS) valves and Forward Reaction Control System (RCS) circuits. Author

N90-10942*# McDonnell-Douglas Astronautics Co., Houston, TX. Space Transportation System Engineering and Operations Support.
INDEPENDENT ORBITER ASSESSMENT (IOA): ANALYSIS OF THE ELECTRICAL POWER DISTRIBUTION AND CONTROL SUBSYSTEM, VOLUME 2
K. R. Schmeckpeper 3 Apr. 1987 884 p
(Contract NAS9-17650)
(NASA-CR-185529-Vol-2; NAS 1.26:185529-Vol-2; Rept-1.0-WP-VA86001-28-Vol-2) Avail: NTIS HC A99/MF E06 CSCL 22B

The results of the Independent Orbiter Assessment (IOA) of the Failure Modes and Effects Analysis (FMEA) and Critical Items List (CIL) are presented. The IOA approach features a top-down analysis of the hardware to determine failure modes, criticality, and potential critical items. To preserve independence, this analysis was accomplished without reliance upon the results contained within the NASA FMEA/CIL documentation. This report documents the independent analysis results corresponding to the Orbiter Electrical Power Distribution and Control (EPD and C) hardware. The EPD and C hardware performs the functions of distributing, sensing, and controlling 28 volt DC power and of inverting, distributing, sensing, and controlling 117 volt 400 Hz AC power to all Orbiter subsystems from the three fuel cells in the Electrical Power Generation (EPG) subsystem. Volume 2 continues the presentation of IOA analysis worksheets and contains the potential critical items list. Author

N90-10943*# McDonnell-Douglas Astronautics Co., Houston, TX. Space Transportation System Engineering and Operations Support.
INDEPENDENT ORBITER ASSESSMENT (IOA): ANALYSIS OF THE LANDING/DECELERATION SUBSYSTEM
J. M. Compton, H. G. Beaird, and W. D. Weissinger 19 Jan. 1987 298 p
(Contract NAS9-17650)
(NASA-CR-185569; NAS 1.26:185569; Rept-1.0-WP-VA86001-25) Avail: NTIS HC A13/MF A02 CSCL 22B

The results of the Independent Orbiter Assessment (IOA) of the Failure Modes and Effects Analysis (FMEA) and Critical Items List (CIL) are presented. The IOA approach features a top-down analysis of the hardware to determine failure modes, criticality,

and potential critical items. To preserve independence, this analysis was accomplished without reliance upon the results contained within the NASA FMEA/CIL documentation. This report documents the independent analysis results corresponding to the Orbiter Landing/Deceleration Subsystem hardware. The Landing/Deceleration Subsystem is utilized to allow the Orbiter to perform a safe landing, allowing for landing-gear deploy activities, steering and braking control throughout the landing rollout to wheel-stop, and to allow for ground-handling capability during the ground-processing phase of the flight cycle. Specifically, the Landing/Deceleration hardware consists of the following components: Nose Landing Gear (NLG); Main Landing Gear (MLG); Brake and Antiskid (B and AS) Electrical Power Distribution and Controls (EPD and C); Nose Wheel Steering (NWS); and Hydraulics Actuators. Each level of hardware was evaluated and analyzed for possible failure modes and effects. Criticality was assigned based upon the severity of the effect for each failure mode. Due to the lack of redundancy in the Landing/Deceleration Subsystems there is a high number of critical items. Author

N90-10944*# McDonnell-Douglas Astronautics Co., Houston, TX.
INDEPENDENT ORBITER ASSESSMENT (IOA): ANALYSIS OF THE MECHANICAL ACTUATION SUBSYSTEM
J. L. Bacher, A. D. Montgomery, M. W. Bradway, and W. T. Slaughter 30 Nov. 1987 770 p
(Contract NAS9-17650)
(NASA-CR-185525; Rept-1.0-WP-VA87001-03; NAS 1.26:185525)
Avail: NTIS HC A99/MF A04 CSCL 22B

The results of the Independent Orbiter Assessment (IOA) of the Failure Modes and Effects Analysis (FMEA) and Critical Items List (CIL) are presented. The IOA approach features a top-down analysis of the hardware to determine failure modes, criticality, and potential critical items. To preserve independence, this analysis was accomplished without reliance upon the results contained within the NASA FMEA/CIL documentation. This report documents the independent analysis results corresponding to the Orbiter Mechanical Actuation System (MAS) hardware. Specifically, the MAS hardware consists of the following components: Air Data Probe (ADP); Elevon Seal Panel (ESP); External Tank Umbilical (ETU); Ku-Band Deploy (KBD); Payload Bay Doors (PBD); Payload Bay Radiators (PBR); Personnel Hatches (PH); Vent Door Mechanism (VDM); and Startracker Door Mechanism (SDM). The IOA analysis process utilized available MAS hardware drawings and schematics for defining hardware assemblies, components, and hardware items. Each level of hardware was evaluated and analyzed for possible failure modes and effects. Criticality was assigned based upon the severity of the effect for each failure mode. Author

N90-10945*# McDonnell-Douglas Astronautics Co., Houston, TX. Space Transportation System Engineering and Operations Support.
INDEPENDENT ORBITER ASSESSMENT (IOA): ANALYSIS OF THE PYROTECHNICS SUBSYSTEM
W. W. Robinson 1 Jan. 1988 82 p
(Contract NAS9-17650)
(NASA-CR-185530; NAS 1.26:185530; Rept-1.0-WP-VA88005-01)
Avail: NTIS HC A05/MF A01 CSCL 22B

The results of the Independent Orbiter Assessment (IOA) of the Failure Modes and Effects Analysis (FMEA) and Critical Items List (CIL) are presented. The IOA approach features a top-down analysis of the hardware to determine failure modes, criticality, and potential critical items. To preserve independence, this analysis was accomplished without reliance upon the results contained within the NASA FMEA/CIL documentation. This report documents the independent analysis results corresponding to the Orbiter Pyrotechnics hardware. The IOA analysis process utilized available pyrotechnics hardware drawings and schematics for defining hardware assemblies, components, and hardware items. Each level of hardware was evaluated and analyzed for possible failure modes and effects. Criticality was assigned based upon the severity of the effect for each failure mode. Author

N90-10946*# McDonnell-Douglas Astronautics Co., Houston, TX. Space Transportation System Engineering and Operations Support.
INDEPENDENT ORBITER ASSESSMENT (IOA): ASSESSMENT OF THE PYROTECHNICS SUBSYSTEM
W. M. Robinson 5 Feb. 1988 90 p
(Contract NAS9-17650)
(NASA-CR-185531; NAS 1.26:185531; Rept-1.0-WP-VA88005-05)
Avail: NTIS HC A05/MF A01 CSCL 22B

The results of the Independent Orbiter Assessment (IOA) of the Failure Modes and Effects Analysis (FMEA) and Critical Items List (CIL) are presented. The IOA effort first completed an analysis of the Pyrotechnics (PYRO) hardware, generating draft failure modes and potential critical items. To preserve independence, this analysis was accomplished without reliance upon the results contained within the NASA FMEA/CIL documentation. The IOA results were then compared to the NASA FMEA/CIL baseline with proposed Post 51-L updates included. A resolution of each discrepancy from the comparison is provided through additional analysis as required. This report documents the results of that comparison for the Orbiter Pyrotechnics hardware. Author

N90-10947*# McDonnell-Douglas Astronautics Co., Houston, TX.
INDEPENDENT ORBITER ASSESSMENT (IOA): ASSESSMENT OF THE NOSE WHEEL STEERING SUBSYSTEM
Anthony Scott Mediavilla 11 Mar. 1988 139 p
(Contract NAS9-17650)
(NASA-CR-185533; NAS 1.26:185533; Rept-1.0-WP-VA88003-22)
Avail: NTIS HC A07/MF A01 CSCL 22B

The results of the Independent Orbiter Assessment (IOA) of the Failure Modes and Effects Analysis (FMEA) and Critical Items List (CIL) are presented. The IOA effort first completed an analysis of the Nose Wheel Steering (NWS) hardware, generating draft failure modes and potential critical items. To preserve independence, this analysis was accomplished without reliance upon the results contained within the NASA FMEA/CIL documentation. The IOA results were then compared to the proposed NASA post 51-L FMEA/CIL baseline. A resolution of each discrepancy from the comparison is provided through additional analysis as required. This report documents the results of that comparison for the Orbiter NWS hardware. Author

N90-10948*# McDonnell-Douglas Astronautics Co., Houston, TX. Engineering Services.
INDEPENDENT ORBITER ASSESSMENT (IOA): WEIBULL ANALYSIS REPORT
Gary G. Raffaelli 14 Dec. 1987 37 p
(Contract NAS9-17650)
(NASA-CR-185534; NAS 1.26:185534; Rept-1.0-WP-VA88003-01)
Avail: NTIS HC A03/MF A01 CSCL 22B

The Auxiliary Power Unit (APU) and Hydraulic Power Unit (HPU) Space Shuttle Subsystems were reviewed as candidates for demonstrating the Weibull analysis methodology. Three hardware components were identified as analysis candidates: the turbine wheel, the gearbox, and the gas generator. Detailed review of subsystem level wearout and failure history revealed the lack of actual component failure data. In addition, component wearout data were not readily available or would require a separate data accumulation effort by the vendor. Without adequate component history data being available, the Weibull analysis methodology application to the APU and HPU subsystem group was terminated. Author

N90-10949*# McDonnell-Douglas Astronautics Co., Houston, TX.
INDEPENDENT ORBITER ASSESSMENT (IOA): ASSESSMENT OF THE PURGE, VENT AND DRAIN SUBSYSTEM
M. C. Bynum, III 5 Feb. 1988 109 p
(Contract NAS9-17650)
(NASA-CR-185535; NAS 1.26:185535; Rept-1.0-WP-VA88005-02)
Avail: NTIS HC A06/MF A01 CSCL 22B

The results of the Independent Orbiter Assessment (IOA) of

the Failure Modes and Effects Analysis (FMEA) and Critical Items List (CIL) are presented. The IOA effort first completed an analysis of the Purge, Vent and Drain (PV and D) hardware, generating draft failure modes and potential critical items. To preserve independence, this analysis was accomplished without reliance upon the results contained within the NASA FMEA/CIL documentation. The IOA results were then compared to the NASA FMEA/CIL baseline with proposed Post 51-L updates included. A resolution of each discrepancy from the comparison is provided through additional analysis as required. This report documents the results of that comparison for the Orbiter PV and D hardware. The PV and D Subsystem controls the environment of unpressurized compartments and window cavities, senses hazardous gases, and purges Orbiter/ET disconnect. Author

N90-10950*# McDonnell-Douglas Astronautics Co., Houston, TX.
INDEPENDENT ORBITER ASSESSMENT (IOA): ASSESSMENT OF THE EXTRAVEHICULAR MOBILITY UNIT, VOLUME 1
Gary G. Raffaelli 10 Mar. 1988 546 p
(Contract NAS9-17650)
(NASA-CR-185536-Vol-1; NAS 1.26:185536-Vol-1;
Rept-1.0-WP-VA88003-41-Vol-1) Avail: NTIS HC A23/MF A03 CSCL 22B

The results of the Independent Orbiter Assessment (IOA) of the Failure Modes and Effects Analysis (FMEA) and Critical Items List (CIL) are presented. The IOA effort performed an independent analysis of the Extravehicular Mobility Unit (EMU) hardware and system, generating draft failure modes criticalities and potential critical items. To preserve independence, this analysis was accomplished without reliance upon the results contained within the NASA FMEA/CIL documentation. The IOA results were than compared to the most recent proposed Post 51-L NASA FMEA/CIL baseline. A resolution of each discrepancy from the comparison was provided through additional analysis as required. This report documents the results of that comparison for the Orbiter EMU hardware. Author

N90-10951*# McDonnell-Douglas Astronautics Co., Houston, TX.
INDEPENDENT ORBITER ASSESSMENT (IOA): ASSESSMENT OF THE EXTRAVEHICULAR MOBILITY UNIT, VOLUME 2
Gary G. Raffaelli 10 Mar. 1988 403 p
(Contract NAS9-17650)
(NASA-CR-185536-Vol-2; NAS 1.26:185536-Vol-2;
Rept-1.0-WP-VA88003-41-Vol-2) Avail: NTIS HC A18/MF A03 CSCL 22B

The results of the Independent Orbiter Assessment (IOA) of the Failure Modes and Effects Analysis (FMEA) and Critical Items List (CIL) are presented. The IOA effort performed an independent analysis of the Extravehicular Mobility Unit (EMU) hardware and system, generating draft failure modes criticalities and potential critical items. To preserve independence, this analysis was accomplished without reliance upon the results contained within the NASA FMEA/CIL documentation. The IOA results were then compared to the most recent proposed Post 51-L NASA FMEA/CIL baseline. A resolution of each discrepancy from the comparison was provided through additional analysis as required. This report documents the results of that comparison for the Orbiter EMU hardware. Volume 2 continues the presentation of IOA analysis worksheets and contains the potential critical items list and NASA FMEA to IOA worksheet cross references and recommendations. Author

N90-10952*# McDonnell-Douglas Astronautics Co., Houston, TX.
INDEPENDENT ORBITER ASSESSMENT (IOA): ASSESSMENT OF THE MECHANICAL ACTUATION SUBSYSTEM, VOLUME 1
M. W. Bradway and W. T. Slaughter 7 Mar. 1988 562 p
(Contract NAS9-17650)
(NASA-CR-185527-Vol-1; NAS 1.26:185527-Vol-1;
Rept-1.0-WP-VA88003-09-Vol-1) Avail: NTIS HC A24/MF A03 CSCL 22B

The results of the Independent Orbiter Assessment (IOA) of the Failure Modes and Effects Analysis (FMEA) and Critical Items List (CIL) are presented. The IOA approach features a top-down analysis of the hardware to determine draft failure modes, criticality, and potential critical items. To preserve independence, this analysis was accomplished without reliance upon the results contained within the NASA FMEA/CIL documentation. The IOA results were then compared to the proposed Post 51-L NASA FMEA/CIL baseline that was available. A resolution of each discrepancy from the comparison was provided through additional analysis as required. These discrepancies were flagged as issues, and recommendations were made based on the FMEA data available at the time. This report documents the results of that comparison for the Orbiter Mechanical Actuation System (MAS) hardware. Specifically, the MAS hardware consists of the following components: Air Data Probe (ADP); Elevon Seal Panel (ESP); External Tank Umbilical (ETU); Ku-Band Deploy (KBD); Payload Bay Doors (PBD); Payload Bay Radiators (PBR); Personnel Hatches (PH); Vent Door Mechanism (VDM); and Startracker Door Mechanism (SDM). Criticality was assigned based upon the severity of the effect for each failure mode. Author

N90-10953*# McDonnell-Douglas Astronautics Co., Houston, TX.
INDEPENDENT ORBITER ASSESSMENT (IOA): ASSESSMENT OF THE MECHANICAL ACTUATION SUBSYSTEM, VOLUME 2
M. W. Bradway and W. T. Slaughter 7 Mar. 1988 562 p
(Contract NAS9-17650)
(NASA-CR-185527-Vol-2; NAS 1.26:185527-Vol-2;
Rept-1.0-WP-VA88003-09-Vol-2) Avail: NTIS HC A24/MF A03 CSCL 22B

The results of the Independent Orbiter Assessment (IOA) of the Failure Modes and Effects Analysis (FMEA) and Critical Items List (CIL) are presented. The IOA approach features a top-down analysis of the hardware to determine draft failure modes, criticality, and potential critical items. To preserve independence, this analysis was accomplished without reliance upon the results contained within the NASA FMEA/CIL documentation. The IOA results were then compared to the proposed Post 51-L NASA FMEA/CIL baseline that was available. A resolution of each discrepancy from the comparison was provided through additional analysis as required. These discrepancies were flagged as issues, and recommendations were made based on the FMEA data available at the time. This report documents the results of that comparison for the Orbiter Mechanical Actuation System (MAS) hardware. Specifically, the MAS hardware consists of the following components: Air Data Probe (ADP); Elevon Seal Panel (ESP); External Tank Umbilical (ETU); Ku-Band Deploy (KBD); Payload Bay Doors (PBD); Payload Bay Radiators (PBR); Personnel Hatches (PH); Vent Door Mechanism (VDM); and Startracker Door Mechanism (SDM). Criticality was assigned based upon the severity of the effect for each failure mode. Volume 2 continues the presentation of IOA analysis worksheets and contains the potential critical items list, detailed analysis, and NASA FMEA/CIL to IOA worksheet cross reference and recommendations. Author

N90-10954*# McDonnell-Douglas Astronautics Co., Houston, TX. Space Transportation System Engineering and Operations Support.
INDEPENDENT ORBITER ASSESSMENT (IOA): CIL ISSUES RESOLUTION REPORT, VOLUME 1
Kenneth J. Urbanowicz, L. W. Hinsdale, and J. E. Barnes 16 Sep. 1988 949 p
(Contract NAS9-17650)
(NASA-CR-185524-Vol-1; NAS 1.26:185524-Vol-1;
Rept-1.0-WP-VA88003-48-Vol-1) Avail: NTIS HC A99/MF E06 CSCL 22B

The results of the Independent Orbiter Assessment (IOA) of the Failure Modes and Effects Analysis (FMEA) and Critical Items List (CIL) are presented. This report contains IOA assessment worksheets showing resolution of outstanding IOA CIL issues that were summarized in the IOA FMEA/CIL Assessment Interim Report, dated 9 March 1988. Each assessment worksheet has been

updated with CIL issue resolution and rationale. The NASA and Prime Contractor post 51-L FMEA/CIL documentation assessed is believed to be technically accurate and complete. No assessment issues remain that has safety implications. Volume 1 contain worksheets for the following sybsystems: Landing and Deceleration Subsystem; Purge, Vent and Drain Subsystem; Active Thermal Control and Life Support Systems; Crew Equipment Subsystem; Instrumentation Subsystem; Data Processing Subsystem; Atmospheric Revitalization Pressure Control Subsystem; Hydraulics and Water Spray Boiler Subsystem; and Mechanical Actuation Subsystem. Author

N90-10955*# McDonnell-Douglas Astronautics Co., Houston, TX. Space Transportation System Engineering and Operations Support.

INDEPENDENT ORBITER ASSESSMENT (IOA): CIL ISSUES RESOLUTION REPORT, VOLUME 2

16 Sep. 1988 924 p

(Contract NAS9-17650)

(NASA-CR-185524-Vol-2; NAS 1.26:185524-Vol-2) Avail: NTIS HC A99/MF E06 CSCL 22B

The results of the Independent Orbiter Assessment (IOA) of the Failure Modes And Effects Analysis (FMEA) and Critical Items List (CIL) are presented. This report contains IOA assessment worksheets showing resolution of outstanding IOA CIL issues that were summarized in the IOA FMEA/CIL Assessment Interim Report, dated 9 March 1988. Each assessment worksheet has been updated with CIL issue resolution and rationale. Volume 2 contains the worksheets for the following subsystems: Nose Wheel Steering Subsystem; Remote Manipulator Susbystem; Atmospheric Revitalization Subsystem; Extravehicular Mobility Unit Subsystem; Power Reactant Supply and Distribution Subsystem; Main Propulsion Subsystem; and Orbital Maneuvering Subsystem. Author

N90-10956*# McDonnell-Douglas Astronautics Co., Houston, TX. Space Transportation System Engineering and Operations Support.

INDEPENDENT ORBITER ASSESSMENT (IOA) CIL ISSUES RESOLUTION REPORT, VOLUME 3

16 Sep. 1988 928 p

(Contract NAS9-17650)

(NASA-CR-185524-Vol-3; NAS 1.26:185524-Vol-3) Avail: NTIS HC A99/MF E06 CSCL 22B

The results of the Independent Orbiter Assessment (IOA) of the Failure Modes and Effects Analysis (FMEA) and Critical Items List (CIL) are presented. This report contains IOA assessment worksheets showing resolution of outstanding IOA CIL issues that were summarized in the IOA FMEA/CIL Assessment Interim Report, dated 9 March 1988. Each assessment worksheet has been updated with CIL issue rsolution and rationale. Volume 3 contains the worksheets for the Reaction Control Subsystem and the Communications and Tracking Subsystem. Author

N90-10957*# McDonnell-Douglas Astronautics Co., Houston, TX. Space Transportation System Engineering and Operations Support.

INDEPENDENT ORBITER ASSESSMENT (IOA): ASSESSMENT OF THE ATMOSPHERIC REVITALIZATION PRESSURE CONTROL SUBSYSTEM FMEA/CIL

M. J. Saiidi 19 Feb. 1988 374 p

(Contract NAS9-17650)

(NASA-CR-185594; NAS 1.26:185594; Rept-1.0-WP-VA88003-09) Avail: NTIS HC A16/MF A02 CSCL 22B

The results of the Independent Orbiter Assessment (IOA) of the Failure Modes and Effects Analysis (FMEA) and Critical Items List (CIL) are presented. The IOA effort first completed an analysis of the atmospheric Revitalization Pressure Control Subsystem (ARPCS) hardware, generating draft failure modes and potential critical items. To preserve independence, this analysis was accomplished without reliance upon the results contained within the NASA FMEA/CIL documentation. The IOA results were then compared to the NASA FMEA/CIL proposed Post 51-L updates based upon the CCB/PRCB presentations and an informal criticality summary listing. A discussion of each discrepancy from the comparison is provided through additional analysis as required. These discrepancies were flagged as issues, and recommendations were made based on the FMEA data available at the time. This report documents the results of that comparison for the Orbiter ARPCS hardware. Author

N90-10958*# McDonnell-Douglas Astronautics Co., Houston, TX. Space Transportation System Engineering and Operations Support.

INDEPENDENT ORBITER ASSESSMENT (IOA): ANALYSIS OF THE CREW EQUIPMENT SUBSYSTEM

Susan Sinclair, L. Graham, Bill Richard, and H. Saxon 2 Nov. 1987 435 p

(Contract NAS9-17650)

(NASA-CR-185591; NAS 1.26:185591; Rept-1.0-WP-VA87001-01) Avail: NTIS HC A19/MF A03 CSCL 22B

The results of the Independent Orbiter Assessment (IOA) of the Failure Modes and Effects Analysis (FMEA) and Critical Items List (CIL) are presented. The IOA approach features a top-down analysis of the hardware to determine failure modes, criticality, and potential critical (PCIs) items. To preserve independence, this analysis was accomplished without reliance upon the results contained within the NASA FMEA/CIL documentation. The independent analysis results coresponding to the Orbiter crew equipment hardware are documented. The IOA analysis process utilized available crew equipment hardware drawings and schematics for defining hardware assemblies, components, and hardware items. Each level of hardware was evaluated and analyzed for possible failure modes and effects. Criticality was assigned based upon the severity of the effect for each failure mode. Of the 352 failure modes analyzed, 78 were determined to be PCIs. Author

N90-10959*# McDonnell-Douglas Astronautics Co., Houston, TX. Space Transportation System Engineering and Operations Support.

INDEPENDENT ORBITER ASSESSMENT (IOA): ASSESSMENT OF THE ASCENT THRUST VECTOR CONTROL ACTUATOR SUBSYSTEM FMEA/CIL

R. E. Wilson 5 Feb. 1988 67 p

(Contract NAS9-17650)

(NASA-CR-185590; NAS 1.26:185590; Rept-1.0-WP-VA88003-03) Avail: NTIS HC A04/MF A01 CSCL 22B

The results of the Independent Orbiter Assessment (IOA) of the Failure Modes and Effects Analysis (FMEA) and Critical Items List (CIL) are presented. The IOA effort first completed an analysis of the Ascent Thrust Vector Control Actuator (ATVD) hardware, generating draft failure modes and potential critical items. To preserve independence, this analysis was accomplished without reliance upon the results contained within the NASA FMEA/CIL documentation. The IOA results were then compared to the NASA FMEA/CIL baseline with proposed Post 51-L updates included. A resolution of each discrepancy from the comparison is provided through additional analysis as required. This report documents the results of that comparison for the Orbiter ATVC hardware. The IOA product for the ATVC actuator analysis consisted of 25 failure mode worksheets that resulted in 16 potential critical items being identified. Comparison was made to the NASA baseline which consisted of 21 FMEAs and 13 CIL items. This comparison produced agreement on all CIL items. Based on the Pre 51-L baseline, all non-CIL FMEAs were also in agreement. Author

N90-10960*# McDonnell-Douglas Astronautics Co., Houston, TX. Space Transportation System Engineering and Operations Support.

INDEPENDENT ORBITER ASSESSMENT (IOA): FMEA/CIL ASSESSMENT Final Report

L. W. Hinsdale, L. J. Swain, and J. E. Barnes 16 Sep. 1988 104 p

(Contract NAS9-17650)

(NASA-CR-185589; NAS 1.26:185589; Rept-1.0-WP-VA88003-47)
Avail: NTIS HC A06/MF A01 CSCL 22B

The McDonnell Douglas Astronautics Company (MDAC) was selected to perform an Independent Orbiter Assessment (IOA) of the Failure Modes and Effects Analysis (FMEA) and Critical Items List (CIL). Direction was given by the Orbiter and GFE Projects Office to perform the hardware analysis and assessment using the instructions and ground rules defined in NSTS 22206. The IOA analysis featured a top-down approach to determine hardware failure modes, criticality, and potential critical items. To preserve independence, the analysis was accomplished without reliance upon the results contained within the NASA and Prime Contractor FMEA/CIL documentation. The assessment process compared the independently derived failure modes and criticality assignments to the proposed NASA post 51-L FMEA/CIL documentation. When possible, assessment issues were discussed and resolved with the NASA subsystem managers. Unresolved issues were elevated to the Orbiter and GFE Projects Office manager, Configuration Control Board (CCB), or Program Requirements Control Board (PRCB) for further resolution. The most important Orbiter assessment finding was the previously unknown stuck autopilot push-button criticality 1/1 failure mode. The worst case effect could cause loss of crew/vehicle when the microwave landing system is not active. It is concluded that NASA and Prime Contractor Post 51-L FMEA/CIL documentation assessed by IOA is believed to be technically accurate and complete. All CIL issues were resolved. No FMEA issues remain that have safety implications. Consideration should be given, however, to upgrading NSTS 22206 with definitive ground rules which more clearly spell out the limits of redundancy. Author

N90-10961*# McDonnell-Douglas Astronautics Co., Houston, TX. Space Transportation System Engineering and Operations Support.

INDEPENDENT ORBITER ASSESSMENT (IOA): ASSESSMENT OF THE DISPLAYS AND CONTROLS SUBSYSTEM

W. H. Trahan and E. E. Prust 26 Dec. 1987 397 p
(Contract NAS9-17650)
(NASA-CR-185588; NAS 1.26:185588; Rept-1.0-WP-VA88005-04)
Avail: NTIS HC A17/MF A03 CSCL 22B

The results of the Independent Orbiter Assessment (IOA) of the Failure Modes and Effects Analysis (FMEA) and Critical Items Llist (CIL) are presented. The IOA effort first completed an analysis of the Displays and Control hardware, generating draft failure modes and potential critical items. To preserve independence, this analysis was accomplished without reliance upon the results contained within the NASA FMEA/CIL documentation. The IOA results were than compared to the NASA FMEA/CIL baseline with proposed Post 51-L updates included. A resolution of each discrepancy is provided through additional analysis as required. The results of that comparison for the Orbiter D and C hardware are documented. Author

N90-10962*# McDonnell-Douglas Astronautics Co., Houston, TX. Space Transportation System Engineering and Operations Support.

INDEPENDENT ORBITER ASSESSMENT (IOA): ASSESSMENT OF THE ORBITER EXPERIMENT (OEX) SUBSYSTEM

J. M. Compton 5 Feb. 1988 127 p
(Contract NAS9-17650)
(NASA-CR-185587; NAS 1.26:185587; Rept-1.0-WP-VA88005-03)
Avail: NTIS HC A07/MF A01 CSCL 22B

The results of the Independent Orbiter Assessment (IOA) of the Failure Modes and Effects Analysis (FMEA) and Critical Items List (CIL) are presented. The IOA effort first completed an analysis of the Orbiter Experiments (OEX) hardware, generating draft failure modes and potential critical items. To preserve independence, this analysis was accomplished without reliance upon the results contained within the NASA FMEA/CIL documentation. The IOA results were then compared to the NASA FMEA/CIL baseline with proposed Post 51-L updates included. A resolution of each discrepancy from the comparison is provided through additional analysis as required. The results of that comparison for the Orbiter OEX hardware are documented. The IOA product for the OEX analysis consisted of 82 failure mode worksheets that resulted in two potential critical items being identified. Author

N90-10963*# McDonnell-Douglas Astronautics Co., Houston, TX. Space Transportation System Engineering and Operations Support.

INDEPENDENT ORBITER ASSESSMENT (IOA): ANALYSIS OF THE ORBITER EXPERIMENT (OEX) SUBSYSTEM

J. M. Compton 21 Aug. 1987 119 p
(Contract NAS9-17650)
(NASA-CR-185586; NAS 1.26:185586; Rept-1.0-WP-VA87001-07)
Avail: NTIS HC A06/MF A01 CSCL 22B

The results of the Independent Orbiter Assessment (IOA) of the Failure Modes and Effects Analysis (FMEA) and Critical Items List (CIL) are presented. The IOA approach features a top-down analysis of the hardware to determine failure modes, criticality, and potential critical items. To preserve independence, this analysis was accomplished without reliance upon the results contained within the NASA FMEA/CIL documentation. This report documents the independent analysis results corresponding to the Orbiter Experiments hardware. Each level of hardware was evaluated and analyzed for possible failure modes and effects. Criticality was assigned based upon the severity of the effect for each failure mode. The Orbiter Experiments (OEX) Program consists of a multiple set of experiments for the purpose of gathering environmental and aerodynamic data to develop more accurate ground models for Shuttle performance and to facilitate the design of future spacecraft. This assessment only addresses currently manifested experiments and their support systems. Specifically this list consists of: Shuttle Entry Air Data System (SEADS); Shuttle Upper Atmosphere Mass Spectrometer (SUMS); Forward Fuselage Support System for OEX (FFSSO); Shuttle Infrared Laced Temperature Sensor (SILTS); Aerodynamic Coefficient Identification Package (ACIP); and Support System for OEX (SSO). There are only two potential critical items for the OEX, since the experiments only gather data for analysis post mission and are totally independent systems except for power. Failure of any experiment component usually only causes a loss of experiment data and in no way jeopardizes the crew or mission. Author

N90-10964*# McDonnell-Douglas Astronautics Co., Houston, TX. Space Transportation System Engineering and Operations Support.

INDEPENDENT ORBITER ASSESSMENT (IOA): ASSESSMENT OF THE REMOTE MANIPULATOR SYSTEM FMEA/CIL

F. Tangorra, R. F. Grasmeder, and A. D. Montgomery 26 Feb. 1988 968 p
(Contract NAS9-17650)
(NASA-CR-185592; NAS 1.26:185592; Rept-1.0-WP-VA88003-16)
Avail: NTIS HC A99/MF E06 CSCL 22B

The results of the Independent Orbiter Assessment (IOA) of the Failure Modes and Effects Analysis (FMEA) and Critical Items List (CIL) are presented. The IOA effort first completed an analysis of the Remote Manipulator System (RMS) hardware, generating draft failure modes and potential critical items. To preserve independence, this analysis was accomplished without reliance upon the results contained within the NASA FMEA/CIL documentation. The IOA results were than compared to the NASA FMEA/CIL baseline with proposed Post 51-L updates included. A resolution of each discrepancy from the comparison is provided through additional analysis as required. The results of that comparison for the Orbiter RMS hardware are documented. The IOA product for the RMS analysis consisted of 604 failure mode worksheets that resulted in 458 potential critical items being identified. Comparison was made to the NASA baseline which consisted of 45 FMEAs and 321 CIL items. This comparison produced agreement on all but 154 FMEAs which caused differences in 137 CIL items. Author

N90-10965*# McDonnell-Douglas Astronautics Co., Houston, TX. Space Transportation System Engineering and Operations Support.
INDEPENDENT ORBITER ASSESSMENT (IOA): ASSESSMENT OF THE EPD AND C/REMOTE MANIPULATOR SYSTEM FMEA/CIL
W. W. Robinson 4 Mar. 1988 471 p
(Contract NAS9-17650)
(NASA-CR-185583; NAS 1.26:185583; Rept-1.0-WP-VA88003-35)
Avail: NTIS HC A20/MF A03 CSCL 22B

The results of the Independent Orbiter Assessment (IOA) of the Failure Modes and Effects Analysis (FMEA) and Critical Items List (CIL) are presented. The IOA effort first completed an analysis of the Electrical Power Distribution and Control (EPD and C)/Remote Manipulator System (RMS) hardware, generating draft failure modes and potential critical items. To preserve independence, this analysis was accomplished without reliance upon the results contained within the NASA FMEA/CIL documentation. The IOA analysis of the EPD and C/RMS hardware initially generated 345 failure mode worksheets and identified 117 Potential Critical Items (PCIs) before starting the assessment process. These analysis results were compared to the proposed NASA Post 51-L baseline of 132 FMEAs and 66 CIL items. Author

N90-10966*# McDonnell-Douglas Corp., Houston, TX. Space Transportation System Engineering and Operations Support.
INDEPENDENT ORBITER ASSESSMENT (IOA): ASSESSMENT OF THE LANDING/DECELERATION (LDG/DEC) SUBSYSTEM FMEA/CIL
R. A. ODonnell and D. Weissinger 18 Mar. 1988 379 p
(Contract NAS9-17650)
(NASA-CR-185570; NAS 1.26:185570; Rept-1.0-WP-VA88003-43)
Avail: NTIS HC A17/MF A02 CSCL 22B

The results of the Independent Orbiter Assessment (IOA) of the Failure Modes and Effects Analysis (FMEA) and Critical Items List (CIL) are presented. The IOA effort first completed an analysis of the Landing/Deceleration (LDG/DEC) hardware, generating draft failure modes and potential critical items. To preserve independence, this analysis was accomplished without reliance upon the results contained within the NASA FMEA/CIL documentation. The IOA contained within the NASA FMEA/CIL documentation. The IOA results were then compared to the NASA FMEA/CIL baseline with proposed Post 51-L updates included. A resolution of each discrepancy from the comparison is provided through additional analysis as required. This report documents the results of that comparison for the Orbiter LDG/DEC hardware. The IOA product for the LDG/DEC analysis consisted of 259 failure mode worksheets that resulted in 124 potential critical items being identified. Comparison was made to the NASA baseline which consisted of 267 FMEA's and 120 CIL items. This comparison produced agreement on all but 75 FMEA's which caused differences in 51 CIL items. Author

N90-10967*# McDonnell-Douglas Astronautics Co., Houston, TX. Space Transportation System Engineering and Operations Support.
INDEPENDENT ORBITER ASSESSMENT (IOA): ANALYSIS OF THE COMMUNICATION AND TRACKING SUBSYSTEM
J. R. Gardner, W. M. Robinson, W. H. Trahan, E. S. Daley, and W. C. Long 31 Dec. 1987 1025 p
(Contract NAS9-17650)
(NASA-CR-185582; NAS 1.26:185582; Rept-1.0-WP-VA87001-09)
Avail: NTIS HC A99/MF E09 CSCL 22B

The results of the Independent Orbiter Assessment (IOA) of the Failure Modes and Effects Analysis (FMEA) and Critical Items List (CIL) are presented. The IOA approach features a top-down analysis of the hardware to determine failure modes, criticality, and potential critical items. To preserve independence, this analysis was accomplished without reliance upon the results contained within the NASA FMEA/CIL documentation. This report documents the independent analysis results corresponding to the Orbiter Communication and Tracking hardware. The IOA analysis process utilized available Communication and Tracking hardware drawings and schematics for defining hardware assemblies, components, and hardware items. Each level of hardware was evaluated and analyzed for possible failure modes and effects. Criticality was assigned based upon the severity of the effect for each failure mode. Author

N90-10968*# McDonnell-Douglas Corp., Houston, TX. Space Transportation System Engineering and Operations Support.
INDEPENDENT ORBITER ASSESSMENT (IOA): ASSESSMENT OF THE BODY FLAP SUBSYSTEM FMEA/CIL
R. E. Wilson 5 Feb. 1988 92 p
(Contract NAS9-17650)
(NASA-CR-185575; NAS 1.26:185575; Rept-1.0-WP-VA88003-04)
Avail: NTIS HC A05/MF A01 CSCL 22B

The results of the Independent Orbiter Assessment (IOA) of the Failure Modes and Effects Analysis (FMEA) and Critical Items List (CIL) are presented. The IOA effort first completed an analysis of the Body Flap (BF) hardware, generating draft failure modes and potential critical items. To preserve independence, this analysis was accomplished without reliance upon the results contained within the NASA FMEA/CIL documentation. The IOA results were then compared to the NASA FMEA/CIL baseline with proposed Post 51-L updates included. A resolution of each discrepancy from the comparison is provided through additional analysis as required. This report documents the results of that comparison for the Orbiter BF hardware. The IOA product for the BF analysis consisted of 43 failure mode worksheets that resulted in 19 potential critical items being identified. Comparison was made to the NASA baseline which consisted of 34 FMEAs and 15 CIL items. This comparison produced agreement on all CIL items. Based on the Pre 51-L baseline, all non-CIL FMEAs were also in agreement. Author

N90-10969*# McDonnell-Douglas Astronautics Co., Houston, TX. Space Transportation System Engineering and Operations Support.
INDEPENDENT ORBITER ASSESSMENT (IOA): ANALYSIS OF THE PURGE, VENT AND DRAIN SUBSYSTEM
M. C. Bynum, III 18 Nov. 1987 97 p
(Contract NAS9-17650)
(NASA-CR-185547; NAS 1.26:185547; Rept-1.0-WP-VA87001-04)
Avail: NTIS HC A05/MF A01 CSCL 22B

The results of the Independent Orbiter Assessment (IOA) of the Failure Modes and Effects Analysis (FMEA) and Critical Items List (CIL) are presented. The IOA approach features a top-down analysis of the hardware to determine failure modes, criticality, and potential critical items. To preserve independence, this analysis was accomplished without reliance upon the results contained within the NASA FMEA/CIL documentation. This report documents the independent analysis results corresponding to the Orbiter PV and D (Purge, Vent and Drain) Subsystem hardware. The PV and D Subsystem controls the environment of unpressurized compartments and window cavities, senses hazardous gases, and purges Orbiter/ET Disconnect. The subsystem is divided into six systems: Purge System (controls the environment of unpressurized structural compartments); Vent System (controls the pressure of unpressurized compartments); Drain System (removes water from unpressurized compartments); Hazardous Gas Detection System (HGDS) (monitors hazardous gas concentrations); Window Cavity Conditioning System (WCCS) (maintains clear windows and provides pressure control of the window cavities); and External Tank/Orbiter Disconnect Purge System (prevents cryo-pumping/icing of disconnect hardware). Each level of hardware was evaluated and analyzed for possible failure modes and effects. Criticality was assigned based upon the severity of the effect for each failure mode. Four of the sixty-two failure modes analyzed were determined as single failures which could result in the loss of crew or vehicle. A possible loss of mission could result if any of twelve single failures occurred. Two of the criticality 1/1 failures are in the Window Cavity Conditioning System (WCCS) outer window cavity, where leakage and/or restricted flow will cause failure to depressurize/repressurize the window cavity. Two criticality 1/1 failures represent leakage and/or restricted flow in

the Orbiter/ET disconnect purge network which prevent cryopumping/icing of disconnect hardware. Each level of hardware was evaluated and analyzed for possible failure modes and effects. Criticality was assigned based upon the severity of the effect for each failure mode. Author

N90-10970*# McDonnell-Douglas Corp., Houston, TX. Space Transportation System Engineering and Operations Support.
INDEPENDENT ORBITER ASSESSMENT (IOA): ASSESSMENT OF THE ELEVON ACTUATOR SUBSYSTEM FMEA/CIL
R. E. Wilson 5 Feb. 1988 60 p
(Contract NAS9-17650)
(NASA-CR-185578; NAS 1.26:185578; Rept-1.0-WP-VA88003-05)
Avail: NTIS HC A04/MF A01 CSCL 22B

The results of the Independent Orbiter Assessment (IOA) of the Failure Modes and Effects Analysis (FMEA) and Critical Items List (CIL) are presented. The IOA effort first completed an analysis of the Elevon Subsystem hardware, generating draft failure modes, and potential critical items. To preserve independence, this analysis was accomplished without reliance upon the results contained within the NASA FMEA/CIL documentation. The IOA results were then compared to the NASA FMEA/CIL baseline with proposed Post 51-L updates included. A resolution of each discrepancy from the comparison is provided through additional analysis as required. This report documents the results of that comparison for the Orbiter Elevon hardware. The IOA product for the Elevon analysis consisted of 25 failure mode worksheets that resulted in 17 potential critical items being identified. Comparison was made to the NASA FMEA/CIL, which consisted of 23 FMEAs and 13 CIL items. This comparison produced agreement on all CIL items. Based on the Pre 51-L baseline, all non-CIL FMEAs were also in agreement. Author

N90-10971*# McDonnell-Douglas Corp., Houston, TX. Space Transportation System Engineering and Operations Support.
INDEPENDENT ORBITER ASSESSMENT (IOA): ASSESSMENT OF THE CREW EQUIPMENT SUBSYSTEM
H. Saxon, Bill Richard, and S. K. Sinclair 12 Feb. 1988 591 p
(Contract NAS9-17650)
(NASA-CR-185577; NAS 1.26:185577; Rept-1.0-WP-VA88005-07)
Avail: NTIS HC A25/MF A04 CSCL 22B

The results of the Independent Orbiter Assessment (IOA) of the Failure Modes and Effects Analysis (FMEA) and Critical Items List (CIL) are presented. The IOA effort first completed an analysis of the Crew Equipment hardware, generating draft failure modes and potential critical items. To preserve independence, this analysis was accomplished without reliance upon the results contained within the NASA FMEA/CIL documentation. The IOA results were then compared to the NASA FMEA/CIL baseline with proposed Post 51-L updates included. A resolution of each discrepancy from the comparison is provided through additional analysis as required. This report documents the results of that comparison for the Orbiter Crew Equipment hardware. The IOA product for the Crew Equipment analysis consisted of 352 failure mode worksheets that resulted in 78 potential critical items being identified. Comparison was made to the NASA baseline which consisted of 351 FMEAs and 82 CIL items. Author

N90-10972*# McDonnell-Douglas Corp., Houston, TX. Space Transportation System Engineering and Operations Support.
INDEPENDENT ORBITER ASSESSMENT (IOA): ASSESSMENT OF INSTRUMENTAL SUBSYSTEM FMEA/CIL
J. R. Gardner and A. W. Addis 18 Feb. 1988 190 p
(Contract NAS9-17650)
(NASA-CR-185572; NAS 1.26:185572; Rept-1.0-WP-VA88003-07)
Avail: NTIS HC A09/MF A01 CSCL 22B

The McDonnell Douglas Astronautics Company (MDAC) was selected in June 1986 to perform an Independent Orbiter Assessment (IOA) of the Failure Modes and Effects Analysis (FMEA) and Critical Items List (CIL). The IOA effort first completed an analysis of the Instrumentation hardware, generating draft failure modes and potential critical items. To preserve independence, this analysis was accomplished without reliance upon the results contained within the NASA FMEA/CIL documentation. The IOA results were then compared to the NASA FMEA/CIL baseline. A resolution of each discrepancy from the comparison is provided through additional analysis as required. The results of that comparison for the Orbiter Instrumentation hardware are documented. The IOA product for Instrumentation analysis consisted of 107 failure mode worksheets that resulted in 22 critical items being identified. Comparison was made to the Pre 51-L NASA baseline with 14 Post 51-L FMEAs added, which consists of 96 FMEAs and 18 CIL items. This comparison produced agreement on all but 25 FMEAs which caused differences in 5 CIL items. Author

N90-10973*# McDonnell-Douglas Astronautics Co., Houston, TX. Space Transportation System Engineering and Operations Support.
INDEPENDENT ORBITER ASSESSMENT (IOA): ASSESSMENT OF THE BACKUP FLIGHT SYSTEM FMEA/CIL
E. E. Prust, J. J. Ewell, Jr., and L. W. Hinsdale 22 Feb. 1988 87 p
(Contract NAS9-17650)
(NASA-CR-185566; NAS 1.26:185566; Rept-1.0-WP-VA88003-17)
Avail: NTIS HC A05/MF A01 CSCL 22B

The results of the Independent Orbiter Assessment (IOA) of the Failure Modes and Effects Analysis (FMEA) and Critical Items List (CIL) are presented. The IOA effort first completed an analysis of the Backup Flight System (BFS) hardware, generating draft failure modes and Potential Critical Items. To preserve independence, this analysis was accomplished without reliance upon the results contained within the NASA FMEA/CIL documentation. The IOA results were then compared to the proposed NASA Post 51-L FMEA/CIL baseline. A resolution of each discrepancy from the comparison is provided through additional analysis as required. This report documents the results of that comparison for the Orbiter BFS hardware. The IOA product for the BFS analysis consisted of 29 failure mode worksheets that resulted in 21 Potential Critical Items (PCI) being identified. This product was originally compared with the proposed NASA BFS baseline and subsequently compared with the applicable Data Processing System (DPS), Electrical Power Distribution and Control (EPD and C), and Displays and Controls NASA CIL items. The comparisons determined if there were any results which had been found by the IOA but were not in the NASA baseline. The original assessment determined there were numerous failure modes and potential critical items in the IOA analysis that were not contained in the NASA BFS baseline. Conversely, the NASA baseline contained three FMEAs (IMU, ADTA, and Air Data Probe) for CIL items that were not identified in the IOA product. Author

N90-10974*# McDonnell-Douglas Astronautics Co., Houston, TX. Space Transportation System Engineering and Operations Support.
INDEPENDENT ORBITER ASSESSMENT (IOA): ASSESSMENT OF THE MANNED MANEUVERING UNIT
M. Huynh, R. E. Duffy, and M. J. Saiidi 12 Feb. 1988 326 p
(Contract NAS9-17650)
(NASA-CR-185564; NAS 1.26:185564; Rept-1.0-WP-VA88003-11)
Avail: NTIS HC A15/MF A02 CSCL 22B

The results of the Independent Orbiter Assessment (IOA) of the Failure Modes and Effects Analysis (FMEA) and Critical Items List (CIL) are presented. The IOA effort first completed an analysis of the Manned Maneuvering Unit (MMU) hardware, generating draft failure modes and potential critical items. To preserve independence, this analysis was accomplished without reliance upon the results contain within the NASA FMEA/CIL documentation. The IOA results were then compared to the proposed Martin Marietta FMEA/CIL Post 51-L updates. A discussion of each discrepancy from the comparison is provided through additional analysis as required. These discrepancies were flagged as issues, and recommendations were made based on the FMEA data available at the time. The results of this comparison for the Orbiter MMU hardware are documented. The IOA product for the MMU analysis consisted of 204 failure mode worksheets

that resulted in 95 potential critical items being identified. Comparison was made to the NASA baseline which consisted of 179 FMEAs and 110 CIL items. This comparison produced agreement on all 121 FMEAs which caused differences in 92 CIL items. Author

N90-10975*# McDonnell-Douglas Astronautics Co., Houston, TX. Space Transportation System Engineering and Operations Support.

INDEPENDENT ORBITER ASSESSMENT (IOA): ASSESSMENT OF THE RUDDER/SPEED BRAKE SUBSYSTEM FMEA/CIL

R. E. Wilson 5 Feb. 1988 99 p

(Contract NAS9-17650)

(NASA-CR-185558; NAS 1.26:185558; Rept-1.0-WP-VA88003-08) Avail: NTIS HC A05/MF A01 CSCL 22B

The results of the Independent Orbiter Assessment (IOA) of the Failure Modes and Effects Analysis (FMEA) and Critical Items List (CIL) are presented. The IOA effort first completed an analysis of the Rudder/Speed Brake (RSB) hardware, generating draft failure modes and potential critical items. To preserve independence, this analysis was accomplished without reliance upon the results contained within the NASA FMEA/CIL documentation. The IOA results were then compared to the NASA FMEA/CIL baseline along with the proposed Post 51-L CIL updates included. A resolution of each discrepancy from the comparison was provided through additional analysis as required. This report documents the results of that comparison for the Orbiter RSB hardware. The IOA product for the RSB analysis consisted of 38 failure mode worksheets that resulted in 27 potential critical items being identified. Comparison was made to the NASA baseline which consisted of 34 FMEAs and 18 CIL items. This comparison produced agreement on all CIL items. Based on the Pre 51-L baseline, all non-CIL FMEAs were also in agreement. Author

N90-10976*# McDonnell-Douglas Astronautics Co., Houston, TX. Space Transportation System Engineering and Operations Support.

INDEPENDENT ORBITER ASSESSMENT (IOA): ASSESSMENT OF THE AUXILIARY POWER UNIT

J. E. Barnes 19 Feb. 1988 452 p

(Contract NAS9-17650)

(NASA-CR-185580; NAS 1.26:185580; Rept-1.0-WP-VA88003-010) Avail: NTIS HC A20/MF A03 CSCL 22B

The results of the Independent Orbiter Assessment (IOA) of the Failure Modes and Effects Analysis (FMEA) and Critical Items List (CIL) are presented. The IOA effort first completed an analysis of the Auxiliary Power Unit (APU) hardware, generating draft failure modes and potential critical items. To preserve independence, this analysis was accomplished without reliance upon the results contained within the NASA FMEA/CIL documentation. The IOA results were then compared to the NASA FMEA/CIL baseline with proposed Post 51-L updates included. A resolution of each discrepancy from the comparison is provided through additional analysis as required. This report documents the results of that comparison for the Orbiter APU hardware. The IOA product for the APU analysis, covering both APU hardware and APU electrical components, consisted of 344 failure mode worksheets that resulted in 178 potential critical items being identified. A comparison was made of the IOA product to the NASA APU hardware FMEA/CIL baseline which consisted of 184 FMEAs and 57 CIL items. The comparison identified 72 discrepancies. Author

N90-10977*# McDonnell-Douglas Astronautics Co., Houston, TX. Space Transportation System Engineering and Operations Support.

INDEPENDENT ORBITER ASSESSMENT (IOA): ASSESSMENT OF THE LIFE SUPPORT AND AIRLOCK SUPPORT SYSTEMS, VOLUME 1

J. D. Arbet, R. E. Duffy, K. Barickman, and M. J. Saiidi 26 Feb. 1988 566 p

(Contract NAS9-17650)

(NASA-CR-185581-Vol-1; NAS 1.26:185581-Vol-1; Rept-1.0-WP-VA88003-19-Vol-1) Avail: NTIS HC A24/MF A03 CSCL 22B

The results of the Independent Orbiter Assessment (IOA) of the Failure Modes and Effects Analysis (FMEA) and Critical Items List (CIL) are presented. The IOA effort first completed an analysis of the Life Support and Airlock Support Systems (LSS and ALSS) hardware, generating draft failure modes and potential critical items. To preserve independence, this analysis was accomplished without reliance upon the results contained within the NASA FMEA/CIL documentation. The IOA results were then compared to the NASA FMEA/CIL baseline with proposed Post 51-L updates included. The discrepancies were flagged for potential future resolution. This report documents the results of that comparison for the Orbiter LSS and ALSS hardware. The IOA product for the LSS and ALSS analysis consisted of 511 failure mode worksheets that resulted in 140 potential critical items. Comparison was made to the NASA baseline which consisted of 456 FMEAs and 101 CIL items. The IOA analysis identified 39 failure modes, 6 of which were classified as CIL items, for components not covered by the NASA FMEAs. It was recommended that these failure modes be added to the NASA FMEA baseline. The overall assessment produced agreement on all but 301 FMEAs which caused differences in 111 CIL items. Author

N90-10978*# McDonnell-Douglas Astronautics Co., Houston, TX. Space Transportation System Engineering and Operations Support.

INDEPENDENT ORBITER ASSESSMENT (IOA): ASSESSMENT OF THE LIFE SUPPORT AND AIRLOCK SUPPORT SYSTEMS, VOLUME 2

K. Barickman 26 Feb. 1988 317 p

(Contract NAS9-17650)

(NASA-CR-185581-Vol-2; NAS 1.26:185581-Vol-2; Rept-1.0-WP-VA88003-19-Vol-2) Avail: NTIS HC A14/MF A02 CSCL 22B

The McDonnell Douglas Astronautics Company (MDAC) was selected in June 1986 to perform an Independent Orbiter Assessment (IOA) of the Failure Modes and Effects Analysis (FMEA) and Critical Items List (CIL). The IOA effort first completed an analysis of the Life Support and Airlock Support Systems (LSS and ALSS) hardware, generating draft failure modes and potential critical items. To preserve independence, this analysis was accomplished without reliance upon the results contained within the NASA FMEA/CIL documentation. The IOA results were then compared to the NASA FMEA/CIL baseline with proposed Post 51-L updates included. The discrepancies were flagged for potential future resolution. This report documents the results of that comparison for the Orbiter LSS and ALSS hardware. Volume 2 continues the presentation of IOA worksheets and contains the critical items list and NASA FMEA to IOA worksheet cross reference and recommendations. Author

N90-10979*# McDonnell-Douglas Corp., Houston, TX. Space Transportation System Engineering and Operations Support.

INDEPENDENT ORBITER ASSESSMENT (IOA): ASSESSMENT OF THE ACTIVE THERMAL CONTROL SYSTEM

S. K. Sinclair 12 Feb. 1988 510 p

(Contract NAS9-17650)

(NASA-CR-185573; NAS 1.26:185573; Rept-1.0-WP-VA88005-06) Avail: NTIS HC A22/MF A03 CSCL 22B

The results of the Independent Orbiter Assessment (IOA) of the Failure Modes and Effects Analysis (FMEA) and Critical Items List (CIL) are presented. The IOA effort first completed an analysis of the Active Thermal Control System (ATCS) hardware, generating draft failure modes and potential critical items. To preserve independence, this analysis was accomplished without reliance upon the results contained within the NASA FMEA/CIL documentation. The IOA results were then compared to the available NASA FMEA/CIL data. Discrepancies from the comparison were documented, and where enough information was available, recommendations for resolution of the discrepancies were made. This report documents the results of that comparison

for the Orbiter ATCS hardware. The IOA product for the ATCS independent analysis consisted of 310 failure mode worksheets that resulted in 101 potential critical items (PCI) being identified. A comparison was made to the available NASA data which consisted of 252 FMEAs and 109 CIL items. Author

N90-10980*# National Aeronautics and Space Administration. Marshall Space Flight Center, Huntsville, AL.
ATMOSPHERIC ENVIRONMENT FOR SPACE SHUTTLE (STS-29) LAUNCH
G. L. Jasper and G. W. Batts (Computer Sciences Corp., Huntsville, AL.) Jul. 1989 41 p
(NASA-TM-100376; NAS 1.15:100376) Avail: NTIS HC A03/MF A01 CSCL 22A

This report presents a summary of selected atmospheric conditions observed near Space Shuttle STS-29 launch time on March 13, 1989, at Kennedy Space Center, Florida. Values of ambient pressure, temperature, moisture, ground winds, visual observations (cloud), and winds aloft are included. The sequence of pre-launch Jimsphere-measured vertical wind profiles is given in this report. The final atmospheric tape, which consists of wind and thermodynamic parameters versus altitude, for STS-29 vehicle ascent has been constructed. The STS-29 ascent atmospheric data tape has been constructed by Marshall Space Flight Center's Earth Science and Applications Division to provide an internally consistent data set for use in post-flight performance assessments. Author

N90-10981*# National Aeronautics and Space Administration. Marshall Space Flight Center, Huntsville, AL.
ATMOSPHERIC ENVIRONMENT FOR SPACE SHUTTLE (STS-30) LAUNCH
G. L. Jasper and G. W. Batts (Computer Sciences Corp., Huntsville, AL.) Jul. 1989 41 p
(NASA-TM-100381; NAS 1.15:100381) Avail: NTIS HC A03/MF A01 CSCL 22A

This report presents a summary of selected atmospheric conditions observed near Space Shuttle STS-30 launch time on May 4, 1989, at Kennedy Space Center, Florida. Values of ambient pressure, temperature, moisture, ground winds, visual observations (cloud), and winds aloft are included. The sequence of pre-launch Jimsphere-measured vertical wind profiles is given in this report. The final atmospheric tape, which consists of wind and thermodynamic parameters versus altitude, for STS-30 vehicle ascent has been constructed. The STS-30 ascent atmospheric data tape has been constructed by Marshall Space Flight Center's Earth Science and Applications Division to provide an internally consistent data set for use in post-flight performance assessments. Author

N90-10982*# National Aeronautics and Space Administration, Washington, DC.
SHUTTLE ATLANTIS TO DEPLOY GALILEO PROBE TOWARD JUPITER
Oct. 1989 47 p
(NASA-TM-101888; NAS 1.15:101888;
NASA-News-Release-89-151; P89-10151) Avail: NASA Scientific and Technical Information Facility, PO Box 8757, BWI Airport, MD 21240

The objectives of Space Shuttle Mission STS-34 are described along with major flight activities, prelaunch and launch operations, trajectory sequence of events, and landing and post-landing operations. The primary objective of STS-34 is to deploy the Galileo planetary exploration spacecraft into low earth orbit. Following deployment, Galileo will be propelled on a trajectory, known as Venus-Earth-Earth Gravity Assist (VEEGA), by an inertial upper stage (IUS). The objectives of the Galileo mission are to study the chemical composition, state, and dynamics of the Jovian atmosphere and satellites, and investigate the structure and physical dynamics of the Jovian magnetosphere. Secondary STS-34 payloads include the Shuttle Solar Backscatter Ultraviolet (SSBUV) instrument; the Mesoscale Lightning Experiment (MLE); and various other payloads involving polymer morphology, the effects of microgravity on plant growth hormone, and the growth of ice crystals. M.G.

N90-10904# Joint Publications Research Service, Arlington, VA.
LANDING TESTS FOR BURAN SHUTTLE WITH JET ENGINE-EQUIPPED MOCK-UP
Stepan Anastasovich Mikoyan *In its* JPRS Report: Science and Technology. USSR: Space 28 Jun. 1989 p 50 Transl. into ENGLISH from Sovetskaya Latviya (Riga, USSR), 27 Jan. 1989 p 3 (For primary document see N90-10900 02-12)
Copyright Avail: NTIS HC A06/MF A01

N90-11043# Rockwell International Corp., Downey, CA. Space Transportation Systems Div.
AUTOMATED STRESS ANALYSIS OF SHUTTLE ORBITER THERMAL PROTECTION SYSTEM
J. Rowe, F. Alfonso, M. Jain, and B. A. Castillo *In* ESA, Spacecraft Structures and Mechanical Testing Jan. 1989 p 423-438 (For primary document see N90-10986 02-18)
Copyright Avail: NTIS HC A99/MF E06

17 SPACE COMM., SPACECRAFT COMM., COMMAND & TRACKING

Includes telemetry; space communications networks; astronavigation and guidance; and radio blackout.

For related information see also *04 Aircraft Communications and Navigation* and *32 Communications and Radar.*

No abstracts in this category.

18 SPACECRAFT DESIGN, TESTING AND PERFORMANCE

Includes satellites; space platforms; space stations; spacecraft systems and components such as thermal and environmental controls; and attitude controls.

For life support systems see *54 Man/System Technology and Life Support.* For related information see also *05 Aircraft Design, Testing and Performance, 39 Structural Mechanics,* and *16 Space Transportation.*

N90-10983*# General Dynamics Corp., San Diego, CA. Space Systems Div.
EVOLUTIONARY SPACE STATION FLUIDS MANAGEMENT STRATEGIES Final Report
Aug. 1989 167 p
(Contract NAS3-25354)
(NASA-CR-185137; NAS 1.26:185137; GDSS-CRAD-89-002)
Avail: NTIS HC A08/MF A01 CSCL 22/2

Results are summarized for an 11-month study to define fluid storage and handling strategies and requirements for various specific mission case studies and their associated design impacts on the Space Station. There are a variety of fluid users which require a variety of fluids and use rates. Also, the cryogenic propellants required for NASA's STV, Planetary, and Code Z missions are enormous. The storage methods must accommodate fluids ranging from a high pressure gas or supercritical state fluid to a sub-cooled liquid (and superfluid helium). These requirements begin in the year 1994, reach a maximum of nearly 1800 metric tons in the year 2004, and trail off to the year 2018, as currently planned. It is conceivable that the cryogenic propellant needs for the STV and/or Lunar mission models will be met by LTCSF LH2/LO2 tanksets attached to the SS truss structure. Concepts and corresponding transfer and delivery operations have been presented for STV propellant provisioning from the SS. A growth orbit maneuvering vehicle (OMV) and associated servicing capability

will be required to move tanksets from delivery launch vehicles to the SS or co-orbiting platforms. Also, appropriate changes to the software used for OMV operation are necessary to allow for the combined operation of the growth OMV. To support fluid management activities at the Space Station for the experimental payloads and propellant provisioning, there must be truss structure space allocated for fluid carriers and propellant tanksets, and substantial beam strengthening may be required. The Station must have two Mobile Remote Manipulator Systems (MRMS) and the growth OMV propellant handling operations for the STV at the SS. Propellant needs for the Planetary Initiatives and Code Z mission models will most likely be provided by co-orbiting propellant platform(s). Space Station impacts for Code Z mission fluid management activities will be minimal. Author

N90-10984# WEA, Cambridge, MA.
WAVE-MODE COORDINATE ANALYSIS OF L JUNCTION IN LSS Annual Report, 15 Jan. 1988 - 30 Mar. 1989
James H. Williams, Jr. and Derrick S. Webb 30 Mar. 1989 71 p
(Contract F49620-88-C-0036; AF Proj. 2302)
(AD-A211116; AFOSR-89-1063TR) Avail: NTIS HC A04/MF A01 CSCL 22/2

The propagation of structural disturbances through large space structures is of practical interest in the design and nondestructive evaluation of such large space systems. Many wave propagation analyses of large space structures must consider the reflection and transmission of waves at interconnecting junctions. Using the concepts of wave-mode coordinate analysis, a frequency domain study of wave propagation through an L lattice junction is conducted. Each lattice member is modeled as a combined longitudinal rod and Timoshenko beam. The joint in the assembly is modeled as a rigid mass of negligible geometric extent with mass rotary inertia. In order to determine the input wave-mode vector, the joint coupling matrix is applied to a point along a lattice member which is subjected to externally applied sinusoidal loads. The input wave-mode vector contains a mathematical description of the waves generated by the applied sinusoidal loads. The joint coupling matrix for the rigid joint with mass and rotary inertia is presented and used to obtain the scattering matrix of the L junction. The scattering matrix contains the reflection and transmission coefficients which the incoming waves will encounter as they enter the joint. Finally, the frequency response function of each Fourier transformed state variable of the transmitted waves is presented analytically. GRA

N90-10985# Systems Engineering Labs., Inc., Greenbelt, MD.
FREQUENCY DOMAIN DESIGN OF ROBUST CONTROLLERS FOR SPACE STRUCTURES Final Report, Sep. 1988 - Feb. 1989
William H. Bennett and C. LaVigna Aug. 1989 60 p
(Contract F33615-88-C-3215)
(AD-A211172; SEI-89-03-15-WB; WRDC-TR-89-3089) Avail: NTIS HC A04/MF A01 CSCL 12/1

The purpose of the Phase 1 effort was to investigate and demonstrate the feasibility of a new class of computational algorithms for the design of high performance control laws for flexible space structures based on frequency response modeling and to consider advanced techniques for the implementation of real time control for precision (wide bandwidth) applications. Typical applications requiring advanced realtime control of flexible space structure include vibration suppression and isolation of payload subsystems. Performance of vibration suppression and isolation systems are critical factors effecting achievable levels of performance for space based optical systems. In the Phase 1 effort, a prototype software code was developed for testing computational algorithms for spectral factorization, causal projection, and coprime factorization-critical steps in frequency domain design of precision control laws. GRA

N90-10986# European Space Agency, Paris (France).
SPACECRAFT STRUCTURES AND MECHANICAL TESTING
W. R. Burke, comp. Jan. 1989 753 p In ENGLISH and FRENCH International conference held in Noordwijk, Netherlands, 19-21 Oct. 1988; sponsored by ESA, CNES, and DFVLR
(ESA-SP-289; ISSN-0379-6546; ETN-89-95384) Copyright
Avail: NTIS HC A99/MF E06

Diverse aspects of spacecraft structure design and testing are discussed. Special attention is given to dynamic control, structural analysis tools, vibroacoustics, hardware development, thin walled structures, solar arrays, and composite materials. Structural technology issues for Ariane, Columbus, Hermes and the International Space Station are discussed. For individual titles, see N90-10987 through N90-11078.

N90-10987# Aerospatiale, Cannes (France).
EVALUATION OF TESTS AND DESIGN FACTORS
C. Vidal, T. deMollerat, and M. Klein (European Space Agency. European Space Research and Technology Center, ESTEC, Noordwijk, Netherlands) *In* ESA, Spacecraft Structures and Mechanical Testing Jan. 1989 p 3-14 Previously announced as N89-23889 (For primary document see N90-10986 02-18)
Copyright Avail: NTIS HC A99/MF E06

A method for the definition of the safety factors ensuring structural reliability is presented. The proposed procedure encompasses both theoretical reliability and practical aspects, combining design requirements, qualification, and acceptance tests. Design criteria in terms of reliability were defined based on previous spacecraft projects and then translated into structural design requirements that can be met in a practical design process. This was performed using a rational approach in terms of statistical variation coefficients of both strength and loads. A set of safety factors is proposed which is valid for unmanned spacecrafts up to 2000 kg. The methodology can easily be extended to larger masses. Complementary factors are defined for manned spacecraft applications. A computer implementation was developed in order to make the application of this methodology simpler and more efficient. ESA

N90-10988# Messerschmitt-Boelkow-Blohm G.m.b.H., Munich (Germany, F.R.). Space Communications and Propulsion Systems Div.
ENVIRONMENTAL TESTING: AN APPROACH TO MORE COST EFFICIENCY
E. D. Sach *In* ESA, Spacecraft Structures and Mechanical Testing Jan. 1989 p 15-19 (For primary document see N90-10986 02-18)
Copyright Avail: NTIS HC A99/MF E06

An environmental testing philosophy in which cost considerations play an important role is developed. Various environmental requirements are given different levels of importance depending on the type of structural part concerned. The need for verification of the basic analytical model and verification of the structure or its essential parts to the decisive design constraint in the structure considered is stressed. It is proposed that the reliability of analytical models, well substantiated by tests, allows one to avoid complicated load simulations thus decreasing testing costs. ESA

N90-10989*# National Aeronautics and Space Administration. Lyndon B. Johnson Space Center, Houston, TX.
STS PAYLOAD DESIGN LOAD EVOLUTION
David A. Hamilton and Donald C. Wade *In* ESA, Spacecraft Structures and Mechanical Testing Jan. 1989 p 21-26 (For primary document see N90-10986 02-18)
Copyright Avail: NTIS HC A99/MF E06 CSCL 22B

Payload development and design load requirements for the U.S. National Space Transportation System (STS) are discussed. The STS requires that all payloads be compatible with STS verification loads which are calculated approximately one year prior to launch. Payload design and all verification testing are completed prior to this final load cycle. Various approaches to preliminary design loads, load updates, and test load definitions and also to STS model and forcing functions revisions are presented. ESA

N90-10990# Fokker B.V., Amsterdam (Netherlands). Space and Systems Div.

QUALIFICATION BY SIMULATION: DREAM OR REALITY

M. P. Nieuwenhuizen *In* ESA, Spacecraft Structures and Mechanical Testing Jan. 1989 p 27-35 (For primary document see N90-10986 02-18)

Copyright Avail: NTIS HC A99/MF E06

The possibility of eliminating a number of development tests to be replaced by computerized simulations is presented. The cost reductions involved in using generic designs are discussed. The use of identical or similar hardware elements in subsequent programs is presented as another cost reduction technique. The need to test the validity of computerized simulations is stressed. It is concluded that qualification by simulation alone is still a dream even for a generic product. A Fokker solar array generic design effort is presented as an example of how certain development tests can be eliminated. ESA

N90-10991# Communications Research Centre, Ottawa (Ontario).

EXPERIMENTAL IDENTIFICATION OF MODAL MOMENTUM COEFFICIENTS AND MODAL IDENTITY PARAMETERS OF THE FLECS STRUCTURE

F. R. Vigneron, R. K. Singal, and Y. Soucy *In* ESA, Spacecraft Structures and Mechanical Testing Jan. 1989 p 39-45 Prepared in cooperation with DFVLR, Porz, Fed. Republic of Germany (For primary document see N90-10986 02-18)

Copyright Avail: NTIS HC A99/MF E06

The Flexible European Communications Satellite type Structure (FLECS), representative of a typical modular spacecraft in terms of mass properties and modal density, is used to identify modal momentum coefficients and modal identity parameters. The results of laboratory tests aimed at assessing the practicality of the procedure in the case of a complex structure are described. It is concluded that the procedure can be used but that there are pitfalls to be avoided. These pitfalls and ways of avoiding them are described. ESA

N90-10992# Deutsche Forschungs- und Versuchsanstalt fuer Luft- und Raumfahrt, Goettingen (Germany, F.R.). Inst. of Aeroelasticity.

UPDATING OF FINITE ELEMENT MODEL BY MEANS OF NORMAL MODE PARAMETERS **c39**

N. Niedbal, E. Klusowski, and W. Luber (Messerschmitt-Boelkow-Blohm G.m.b.H., Ottobrunn, Germany, F.R.) *In* ESA, Spacecraft Structures and Mechanical Testing Jan. 1989 p 47-53 (For primary document see N90-10986 02-18)

Copyright Avail: NTIS HC A99/MF E06

The updating procedure used in reconciling two data sets in order to create a realistic and reliable dynamic model is presented. The updated mass and stiffness values of a truss structure are outlined. The use of finite element analysis and modal survey tests in structural dynamic qualification and verification of aerospace structures is described. The need of a method for reconciling discrepancies between analytical and experimental normal mode parameters is stressed. ESA

N90-10993# Imperial Coll. of Science and Technology, London (England).

A REVIEW OF THE ERROR OF MATRIX METHOD (EMM) FOR STRUCTURAL DYNAMIC MODEL COMPARISON **c39**

D. J. Ewins, J. He, and N. Lieven *In* ESA, Spacecraft Structures and Mechanical Testing Jan. 1989 p 55-62 (For primary document see N90-10986 02-18)

Copyright Avail: NTIS HC A99/MF E06

The development of the Error Matrix Method (EMM) and some of the envisaged improvements of the method are discussed. Different model reduction methods as well as different graphic presentations of the results are called for. How the EMM method can be used in predicting vibration characteristics is described. The need for such methods in load prediction, stability analysis, system design, and structural coupling applications is discussed. ESA

N90-10994# Besancon Univ. (France). Lab. de Mecanique Appliquee.

PARAMETRIC IDENTIFICATION OF CONSERVATIVE SELF ADJOINT STRUCTURES **c39**

G. Lallement, J. Piranda, and R. Fillod *In* ESA, Spacecraft Structures and Mechanical Testing Jan. 1989 p 63-68 (For primary document see N90-10986 02-18)

Copyright Avail: NTIS HC A99/MF E06

The parametric correction of the symmetric mass and stiffness matrices representing the linear elastodynamic behavior of the associated conservative structure to a real dissipative structure are examined. The initial estimations of these matrices are considered to have been constructed by a finite element discretization. Their parametric correction is based on the minimization of the distance between the eigensolutions of the model to be corrected and the identified eigensolutions of the physical structure. ESA

N90-10995# Erno Raumfahrttechnik G.m.b.H. Bremen (Germany, F.R.).

OVERVIEW OF ACTUAL BUCKLING CALCULATION METHODS FOR SPACE VEHICLE STRUCTURES **c39**

W. Huessler and H. Oery (Technische Hochschule, Aachen, Germany, F.R.) *In* ESA, Spacecraft Structures and Mechanical Testing Jan. 1989 p 71-78 (For primary document see N90-10986 02-18)

Copyright Avail: NTIS HC A99/MF E06

The complexities involved in the buckling analysis of cylindrical shells is presented. The deficiencies of present methods of buckling calculations and of the design codes and specifications based on these calculations are described. The need for updating these methods and for the systematization and synthesis of available results is stressed. The so called lower bound design curves which do not differentiate between badly or well manufactured shells need to be revised in order to reach maximum cost and mass effectiveness in lightweight spacecraft structures. The need for design guidelines for some practical load combinations is stressed. ESA

N90-10996# Technische Univ., Brunswick (Germany, F.R.). Inst. fuer Flugzeugbau und Leichtbau.

THEORETICAL AND EXPERIMENTAL INVESTIGATION OF THIN-WALLED ALUMINUM PANELS UNDER CYCLIC SHEAR LOAD **c39**

P. Horst and H. Kossira *In* ESA, Spacecraft Structures and Mechanical Testing Jan. 1989 p 79-84 Sponsored by the Deutsche Forschungsgemeinschaft, Bonn, Fed. Republic of Germany (For primary document see N90-10986 02-18)

Copyright Avail: NTIS HC A99/MF E06

Experimental and theoretical results for thin walled aluminum plates under cyclic shear load are presented. The theoretical results are obtained using a finite element code taking into account geometric as well as material nonlinearities. A slightly modified two-surface model is used in order to achieve the special characteristics of the cold worked aluminum alloy 2024 T3. Experimental investigations are performed on a special device that exhibits nearly pure shear. Good agreement of experimental and theoretical results is demonstrated. ESA

N90-10997# Politecnico di Torino (Italy). Dept. of Aerospace Engineering.

A CONTRIBUTION TO THE STABILITY ANALYSIS OF LARGE SPACE STRUCTURES

E. Antona and M. DiSciuva *In* ESA, Spacecraft Structures and Mechanical Testing Jan. 1989 p 85-89 (For primary document see N90-10986 02-18)

Copyright Avail: NTIS HC A99/MF E06

A general perturbation approach for the solution of linear eigenvalue problems is presented. The problems addressed deal with the vibration of structures subject to stability limit phenomena.

A method for obtaining the critical stability modes from unloaded structure vibration modes is presented. A reiterative process is proposed and applied to some sample problems. A means of validating large space structures which are too large to be submitted to buckling tests on Earth is proposed. ESA

N90-10998# Politecnico di Torino (Italy). Dept. of Aerospace Engineering.
EQUILIBRIUM AND STABILITY IN COMPOSITE THIN SHELL **c39**
E. Antona and U. Icardi (Fiat Research Center, Orbassano, Turin, Italy) *In* ESA, Spacecraft Structures and Mechanical Testing Jan. 1989 p 91-97 (For primary document see N90-10986 02-18)
Copyright Avail: NTIS HC A99/MF E06

A way of carrying out theoretical stability analyses on imperfect multilayered composite shells is proposed. The evolution of metric and curvature coefficients over the course of increasing external loads is measured. Elastic displacements involved in the process are also taken into consideration. The analysis of the geometric evolution of load increases could be useful in finite element analysis. In order to test the proposal on a practical application, shells made by orthotropic laminae are considered. They are modeled by the Kirchoff-Love hypothesis and by the Von Karman-Tzien strain tensor. The imperfections are shape defects of a general kind. The behavioral equations are obtained taking only the fundamental term displacements into consideration. ESA

N90-10999# Ingemansson Anatrol A.B., Askim (Sweden).
VISCOELASTIC TUNED DAMPERS FOR CONTROL OF STRUCTURAL DYNAMICS **c39**
William G. Halvorsen *In* ESA, Spacecraft Structures and Mechanical Testing Jan. 1989 p 101-106 (For primary document see N90-10986 02-18)
Copyright Avail: NTIS HC A99/MF E06

The use of viscoelastic materials as the combined stiffness and damping element in the construction of tuned dampers is described. The variability of the dynamic mechanical properties of viscoelastic materials with environmental factors such as temperature, frequency, and dynamic strain amplitude lead to some difficulties in design and to possible instabilities in performance in certain applications. The effectiveness of tuned dampers is illustrated with an application for controlling low frequency fuselage response in a propeller aircraft. ESA

N90-11000# Dornier System G.m.b.H., Friedrichshafen (Germany, F.R.).
REDUCTION OF DYNAMIC RESPONSE OF SPACECRAFT STRUCTURES AND PAYLOADS
L. Kolsch and H. Baier *In* ESA, Spacecraft Structures and Mechanical Testing Jan. 1989 p 107-119 (For primary document see N90-10986 02-18)
Copyright Avail: NTIS HC A99/MF E06

Different techniques of vibration reduction in spacecraft structures are presented. The merits and disadvantages of each technique are outlined. Dynamic response minimization is best carried out by separation of excitation and eigenfrequencies. Where such a tuning is not possible, the resulting dynamic loads have to be diminished either by damping, absorption or isolation. These anti-vibration provisions can be translated into reality either by passive or active measures. Some of these anti-vibration techniques are outlined. The need for more research in the field of high and low frequency vibration reduction is emphasized. ESA

N90-11001*# Jet Propulsion Lab., California Inst. of Tech., Pasadena. Applied Technologies.
ADAPTIVE STRUCTURES TO MEET FUTURE REQUIREMENTS FOR LARGE PRECISION STRUCTURES **c39**
B. K. Wada, J. L. Fanson, J. A. Garba, and G.-S. Chen *In* ESA, Spacecraft Structures and Mechanical Testing Jan. 1989 p 121-126 (For primary document see N90-10986 02-18)
(Contract NAS7-918)
Copyright Avail: NTIS HC A99/MF E06 CSCL 20K

The role of adaptive structures in meeting the structural requirements for future NASA missions is described. Many of NASA's future missions require large precision truss type structures where prespecified locations on the structure must maintain micron level accuracies with respect to each other when subjected to manufacturing errors and static, thermal, and dynamic inputs. In many cases the incorporation of the adaptive structures concepts into the structural design to adjust the on-orbit structure will be the only feasible means to attain the desired accuracies. In order for the structures to be able to change structural characteristics on orbit they must be uncoupled and independent of the control system used to impart the required rigid body motion to the spacecraft. ESA

N90-11002# MATRA Espace, Toulouse (France). Dept. of Mechanical Engineering.
SYSTEM AND PERFORMANCE ANALYSIS OF A LOW DENSITY ACTIVELY CONTROLLED MIRROR FOR ASTRONOMIC OBSERVATION **c89**
B. Laviron and M. Duran *In* ESA, Spacecraft Structures and Mechanical Testing Jan. 1989 p 127-132 (For primary document see N90-10986 02-18)
Copyright Avail: NTIS HC A99/MF E06

The primary mirror of a large spaceborne telescope is described. The thin deformable glassy mirror is monitored in orbit by push-pull devices fixed on the rear face of the mirror. A presentation of the mirror characteristics is made followed by the description of the active control loop. The theoretical expression of the control algorithm is outlined. The performances are evaluated using finite element modeling techniques for the correction of thermoelastic distortion as well as residual defects after polishing. The theoretical simulation studies are to be correlated with ground test results on a reduced scale demonstration model. ESA

N90-11003# Rome Univ. (Italy). Dipt. Aerospaziale.
ANALYTIC SIGNALS IN THE DAMPING COEFFICIENT ESTIMATION **c64**
Alessandro Agenni and Luigi Balis Crema *In* ESA, Spacecraft Structures and Mechanical Testing Jan. 1989 p 133-139 Sponsored in part by the Italian Ministry of Public Education (For primary document see N90-10986 02-18)
(Grant CNR-85/01244/11)
Copyright Avail: NTIS HC A99/MF E06

The analysis of the complex signal formed by the impulse response of a structure and its Hilbert transform is presented. Numerical simulations on damping factor estimation with particular reference to low frequencies and damping are shown. The numerical results prove the effectiveness of the approach and the possibility of obtaining significant results even when relatively limited time windows are used and highly truncated signals are considered. The advantages of the damping factor estimation method over the half power method are presented. ESA

N90-11004# Liege Univ. (Belgium).
A SUPER ELEMENT FOR MULTIBODY DYNAMICS **c39**
A. Cardona and M. Geradin *In* ESA, Spacecraft Structures and Mechanical Testing Jan. 1989 p 143-148 (For primary document see N90-10986 02-18)
Copyright Avail: NTIS HC A99/MF E06

A superelement formulation capable of handling large finite rotations is developed. It is based on a small rotation and displacement hypothesis in a local frame to the superelement. A standard component mode approach is adopted together with a lumped mass inertia approximation. The resulting degrees of freedom of the formulation are the positions and orientations at the so-called boundary nodes of the superelement, plus a given number of internal mode amplitudes. The use of these formulations in the deployment of an antenna-like structure is presented as a test case. ESA

N90-11005# Aerospatiale, Cannes (France).
GEMMES: A NEW TOOL FOR DYNAMIC MODELING **c39**
C. Garnier and P. Rideau *In* ESA, Spacecraft Structures and Mechanical Testing Jan. 1989 p 149-154 Previously announced as N89-24078 (For primary document see N90-10986 02-18)
Copyright Avail: NTIS HC A99/MF E06

The new GEMMES software is presented as an alternative to currently used numerical simulation software. It computes the equations of the mechanical systems in a symbolic nonnumerical form. The GEMMES generated equations are just like hand written ones, but the use of a computer provides faultless and infinitely faster calculations. The final version of GEMMES will be capable of modeling whatever system may arise from assembling rigid and/or flexible bodies together. The present version thoroughly handles tree like systems. It allows for description of the geometry of the mechanical system and of its flexible constituents. It provides complete calculations of the dynamic equations, routines useful for results simplification, and a FORTRAN interface that automatically generates a simulator of the system. Computation of the equations of a closed loop system is much more complicated. ESA

N90-11006# Katholieke Univ. te Leuven (Belgium). Mechanische Konstruktie en Produktie.
EMPLOYMENT OF MODAL SURVEY METHODOLOGIES IN DYNAMIC ANALYSIS PROCEDURES **c39**
W. Heyen, T. Janter, and P. Sas *In* ESA, Spacecraft Structures and Mechanical Testing Jan. 1989 p 155-159 (For primary document see N90-10986 02-18)
Copyright Avail: NTIS HC A99/MF E06

The use of modal analysis techniques in the vibration analysis of dynamic behavior in mechanical structures is outlined. The principle of this approach is to describe the dynamics of a structure by its modal parameters (resonance frequencies and mode shape vectors). The modal parameters can be determined through experimental testing or analytical modeling. The modal parameters are very useful for trouble shooting, locating the sources of dynamic problems, in determining the most efficient modifications, or for updating analytical models in the design or redesign process. ESA

N90-11007# Intespace, Toulouse (France).
INTEGRATION OF ANALYTICAL AND TEST SOFTWARE FOR OPTIMAL STRUCTURAL DESIGN UNDER DYNAMIC LOADS **c39**
L. P. Bugeat, N. A. Roy, A. Girard, and J.-F. Imbert *In* ESA, Spacecraft Structures and Mechanical Testing Jan. 1989 p 161-166 (For primary document see N90-10986 02-18)
Copyright Avail: NTIS HC A99/MF E06

An approach which allows for efficient integration of dynamic analysis in design and qualification cycles is described. The three major categories of numerical tools: analysis, diagnosis, and optimization are considered. The organization of the software using a common analysis and test data base is presented. A brief description of software programs is given with two examples illustrating structural modification and sensitivity analysis. ESA

N90-11008# Construcciones Aeronauticas S.A., Madrid (Spain). Space Div.
EXPERIENCES USING A MAJOR FEM PACKAGE INTERACTIVELY FOR SPACECRAFT APPLICATIONS
J. SanchezCercos and V. GomezMolinero *In* ESA, Spacecraft Structures and Mechanical Testing Jan. 1989 p 167-172 (For primary document see N90-10986 02-18)
Copyright Avail: NTIS HC A99/MF E06

The advantages and disadvantages of the interactive execution mode compared with the batch mode in using an FEM (finite element models) package are described. These two approaches are compared for a variety of environments determined by the type of user and the class of calculation carried out. Results based on experiments in spacecraft structural design are presented. Present and future applications of the ASKAIN (ASKA Interactive) software program are discussed. These include using the interactive program to train inexperienced engineers as well as create new analytical procedures not directly related to the mother program. ESA

N90-11009# Aeronautical Research Inst. of Sweden, Bromma.
CALCULATION OF SOUND TRANSMISSION THROUGH A CYLINDRICAL SHELL USING ASKA ACOUSTICS **c71**
P. Goransson *In* ESA, Spacecraft Structures and Mechanical Testing Jan. 1989 p 175-180 (For primary document see N90-10986 02-18)
Copyright Avail: NTIS HC A99/MF E06

The transmission of an external acoustic field is calculated using a finite element model of an aluminum honeycomb cylindrical shell. The ASKA ACOUSTICS software program is used to analyze the results. From the eigenmodes of the coupled fluid structure system the frequency response is obtained for certain angles of incidence of the plane wave excitation. The noise reduction is calculated using the average of the acoustic pressure in the interior of the shell. The results of the analyses performed indicate that fluid-structure interaction is important in obtaining the reduction. This fact is accentuated by results obtained with helium in the interior. The predictions done with the finite element method are compared to measurements of similar configurations. The agreement is good for most frequencies. ESA

N90-11010# Centre National d'Etudes Spatiales, Toulouse (France).
ACOUSTIC RESPONSE ANALYSIS IN THE LOW FREQUENCY DOMAIN **c71**
F. Mercier, D. Gangloff, and A. Mamode *In* ESA, Spacecraft Structures and Mechanical Testing Jan. 1989 p 181-185 (For primary document see N90-10986 02-18)
Copyright Avail: NTIS HC A99/MF E06

The formulation of acoustic excitation responses in large light space structures based on modal superposition is presented. Loads are predicted as random acceleration or modal energy power. Acoustic analysis of several configurations of solar array and antenna reflectors is carried out. Modal parameters such as damping and added mass effects are assessed. The importance of such tests in calculating the dimensions of light satellite appendages is stressed. As such structures are good radiators the need for radiation correction to reach a stable energy balance is discussed. It is concluded that further study of intermodal coupling terms is needed. ESA

N90-11011# Texas Univ., Austin. Dept. of Aerospace Engineering and Engineering Mechanics.
USE OF LANCZOS VECTORS IN STRUCTURAL DYNAMICS **c39**
Roy R. Craig, Jr., Tzu-Jeng Su, and Hyoung M. Kim *In* ESA, Spacecraft Structures and Mechanical Testing Jan. 1989 p 187-192 (For primary document see N90-10986 02-18)
Copyright Avail: NTIS HC A99/MF E06

The use of Krylov vectors and Lanczos vectors for reduced order modeling in structural dynamics and control of flexible structures is illustrated. An unsymmetric block Lanczos method for systems with unsymmetric damping, Lanczos vectors and Krylov vectors for use in component synthesis, and control of flexible structures using reduced-order models based on Krylov vectors are discussed. New results obtained on the topic of control of flexible structures are given particular emphasis. ESA

N90-11012# Politecnico di Milano (Italy). Dipt. di Ingegneria Aerospaziale.
THERMOELASTIC BEHAVIOR OF LARGE SPACE STRUCTURES: MODELING AND CONTROL
F. Bernelli-Zazzera, A. Ercoli-Finzi, and P. Montegazza *In* ESA, Spacecraft Structures and Mechanical Testing Jan. 1989 p 195-200 (For primary document see N90-10986 02-18)
Copyright Avail: NTIS HC A99/MF E06

A method for the analysis and control of thermally induced vibrations of flexible structures is presented. The structure is represented by a double finite element model, one for the structural

displacements and one for the temperature distribution. Based on these two finite element models, the system is entirely described in terms of structural and thermal modal coordinates. The unstable coupling effects, which are shown to be present, are actively controlled by applying a digital suboptimal linear quadratic control technique to a reduced order modal model. ESA

N90-11013# Industrieanlagen-Betriebsgesellschaft m.b.H., Ottobrunn (Germany, F.R.).
NUMERICAL ANALYSIS OF NONLINEAR VISCOELASTIC STRUCTURES: APPLICATION TO ELASTOMERS AND RUBBER-LIKE MATERIALS **c39**
W. W. Jarzab, J. Bauer, and P. Foros *In* ESA, Spacecraft Structures and Mechanical Testing Jan. 1989 p 201-206 (For primary document see N90-10986 02-18)
Copyright Avail: NTIS HC A99/MF E06

The finite element code ANVS (advanced numerical viscoelastodynamical simulation) which permits the investigation of complex elastomer structures is described. Different kinds of mounts and shock absorbers are analyzed. The dynamic stiffness and the loss factor are nonlinear functions of the static preloading, the displacement amplitude and the frequency. The stress strain hysteresis characterizes the nonlinearities, the damping behavior response energy dissipation and the dynamical stiffness of the elastomer structure. Structural modifications lead to a reduction of dynamic stiffness and an improvement of damping. ESA

N90-11014# Rome Univ. (Italy). Dipt. Aerospaziale.
EVALUATION OF DISPERSIVE BEHAVIOR IN PERIODIC STRUCTURES BY DISCRETE FOURIER TRANSFORM **c39**
S. Sgubini and A. Agneni *In* ESA, Spacecraft Structures and Mechanical Testing Jan. 1989 p 207-212 Sponsored by the Italian Ministry of Public Education (For primary document see N90-10986 02-18)
Copyright Avail: NTIS HC A99/MF E06

A method for estimating the dispersion curves and the wave number versus angular frequency for periodic structures based on the Fourier transform algorithm is presented. These periodic structures present a nonlinear behavior, and have some frequency bands where the energy, given by the forcing system, is trapped in a few bays and the waves decrease their vibration amplitude as they move away from the section where the force is applied. An evaluation of the errors in wave number estimation is obtained by comparing the estimated values with the theoretical results for some structures with both longitudinal and transverse excitation. The application of this research to the modular design of large space structures is summarized. ESA

N90-11015# Intespace, Toulouse (France).
DYNAMIC SUBSTRUCTURING FOR MODULAR ANALYSIS AND TESTING **c15**
A. Girard and L. P. Bugeat *In* ESA, Spacecraft Structures and Mechanical Testing Jan. 1989 p 213-218 (For primary document see N90-10986 02-18)
(Contract ESA-6819/86/NL/PH(SC))
Copyright Avail: NTIS HC A99/MF E06

Basic substructuring processes required in the verification process of modular design concepts are compared. Special emphasis is given to transfer function coupling. The launch vehicle payload coupling is considered using the concept of equivalent forces currently used in the Ariane project, and the dynamic loads verification process of modular spacecraft is described, encompassing analysis and testing of components, launch vehicle and spacecraft mini-coupled analysis to derive the interface response, and recovery of spacecraft responses. Typical examples are given for illustration. ESA

N90-11016# Rome Univ. (Italy). Dipt. Aerospaziale.
NUMERICAL TREATMENT OF THE THERMO-STRUCTURAL-DYNAMIC PROBLEMS: THE INTERPOLATION TECHNIQUES **c39**
C. Arduini, G. Laneve, D. Mortari, and M. Parisse *In* ESA, Spacecraft Structures and Mechanical Testing Jan. 1989 p 219-224 (For primary document see N90-10986 02-18)
(Contract ESA-6819/86/NL/PH(SC))
Copyright Avail: NTIS HC A99/MF E06

Results of thermostructural interfacing research are presented. An interpolation technique used when transferring thermal data from a general thermal model to a thermostructural one is described. Results of simulated interpolations are shown. Accurate interpolations are concluded possible once the thermal problem was remodeled. ESA

N90-11017# Centre National d'Etudes Spatiales, Toulouse (France).
THE THIRD GENERATION RIGID SOLAR ARRAY GSR3 **c39**
A. Mamode, D. Gangloff, J. L. Bastard, and Ph. Auffray (Aerospatiale, Cannes, France) *In* ESA, Spacecraft Structures and Mechanical Testing Jan. 1989 p 227-232 (For primary document see N90-10986 02-18)
Copyright Avail: NTIS HC A99/MF E06

The design of a prototype solar array model featuring a new deployment mechanism is presented. The solar array is pre-flight tested using prediction tools. The structure of the solar panels and the hinge mechanism between panels is described. The GSR3 panels are concluded to be suitable for orbiting stations and retractable solar arrays. The GSR3 panels, which cover a wide range of specifications and have a modular design, can be used in a variety, of missions, thus lowering the costs of the individual missions. ESA

N90-11018# International Telecommunications Satellite Organization, Washington, DC.
ADVANCES IN DESIGN AND TESTING OF SPACECRAFT STRUCTURES
Brij N. Agrawal *In* ESA, Spacecraft Structures and Mechanical Testing Jan. 1989 p 233-237 (For primary document see N90-10986 02-18)
Copyright Avail: NTIS HC A99/MF E06

The results of Intelsat research and development projects in the area of spacecraft structural analysis, design and testing are summarized. These research projects show advances in the determination of the accuracy of predicted dynamic launch loads by coupled analysis, simpler methods to update launch loads, composite material analysis, prediction of acoustic response, improvements of design verification tests, and development of deployable offset reflectors. Further development work is required in some of these areas. ESA

N90-11019# Aerospatiale, Chatillon (France).
TELESCOPE STRUCTURE FOR CRYOGENIC APPLICATION **c89**
J. A. Massoni *In* ESA, Spacecraft Structures and Mechanical Testing Jan. 1989 p 239-245 In FRENCH; ENGLISH summary Previously announced as N89-23940 (For primary document see N90-10986 02-18)
Copyright Avail: NTIS HC A99/MF E06

The structure and development of the Infrared Space Observatory (ISO) satellite developed by Aerospatiale for the European Space Agency is outlined. The ISO satellite, scheduled for launch in April 1993, carries a 60 cm Ritchey-Chretien telescope designed to detect wavelengths between 2 and 200 nanometers. In order to maintain the kind of precision necessary, the optics are cooled to 4 k. The cryogenic system using liquid helium is described. The mechanical and optical techniques used in the project are outlined and the cryogenic test facilities used in developing the satellite, are described. ESA

N90-11020# National Space Development Agency, Tokyo (Japan).
DEVELOPMENT OF THE LARGE SPACECRAFT STRUCTURE
K. Nakamura, H. Mitsuma, A. Tsujihata, T. Katoh, T. Tsukashima, and F. Kuwao (Toshiba Corp., Kawasaki, Japan) *In* ESA, Spacecraft Structures and Mechanical Testing Jan. 1989 p 247-252 (For primary document see N90-10986 02-18)
Copyright Avail: NTIS HC A99/MF E06

The development work involved in designing the ETS-6 (engineering test satellite-6) satellite is described. The ETS-6 satellite is a two ton class geostationary spacecraft to be launched in the summer of 1992. Structural tests were carried out on a full-scale model. The results of these tests of structural design, analysis and construction technique are included. The feasibility of a large scale lightweight structure which meets the requirements of ETS-6 is confirmed. ESA

N90-11021# Construcciones Aeronauticas S.A., Madrid (Spain). Space Div.

THE SERVICE MODULE STRUCTURE OF THE IOS SPACECRAFT DEVELOPMENT AND QUALIFICATION PROGRAM

Francisco Gonzales *In* ESA, Spacecraft Structures and Mechanical Testing Jan. 1989 p 253-260 (For primary document see N90-10986 02-18)

Copyright Avail: NTIS HC A99/MF E06

The work carried out in establishing the structure of the ISO (infrared space observatory service module) is described. The contraints involved in designing the module are outlined including the necessity for low conductance with the payload module. This calls for the use of glass fiber in making the main structure struts near to the cryostat. The rest of the struts are made of carbon fiber composites. Analytical models used and the results obtained are presented. ESA

N90-11022# Industrieanlagen-Betriebsgesellschaft m.b.H., Ottobrunn (Germany, F.R.).

FLUID-STRUCTURE INTERACTION EFFECTS IN TANK STRUCTURES DUE TO SLOSHING AND HYDRODYNAMIC RAM: COUPLED LAGANGIAN-EULERIAN SIMULATIONS c34

W. W. Jarzab, R. Chwalinski, W. E. Pfrang, and G. Tokar *In* ESA, Spacecraft Structures and Mechanical Testing Jan. 1989 p 263-268 (For primary document see N90-10986 02-18)

Copyright Avail: NTIS HC A99/MF E06

Numerical simulation of hydrodynamic ram and of liquid sloshing with respect to large structural deformations is investigated. The effect of free surfaces is investigated using different partially filled tanks. The resultant structural loadings are discussed taking local loading, global loading, failure, and coupled response into consideration. The loading and unloading of structural members by shock waves, complex reflections, and cavitational effects are treated using coupled algorithms. ESA

N90-11023# Messerschmitt-Boelkow-Blohm G.m.b.H., Munich (Germany, F.R.). Space Communications and Propulsion Systems Div.

MODELING OF LIQUID SLOSHING EFFECTS IN MULTIBODY SYSTEMS c34

K. Ebert *In* ESA, Spacecraft Structures and Mechanical Testing Jan. 1989 p 269-275 (For primary document see N90-10986 02-18)

Copyright Avail: NTIS HC A99/MF E06

Two modeling methods for the sloshing dynamics of liquids in partially filled tanks in a spinning spacecraft are presented. A homogeneous vortex flow approximation and a boundary layer model are discussed. A modeling method which was used to implement liquid sloshing effects in a simulation program for multi body systems is discussed. Computer programs for the analysis of sloshing effects and an extended simulation program are applied to the Intelsat 6 spacecraft. ESA

N90-11024# Ingenieurgesellschaft fuer Technische Software G.m.b.H., Stuttgart (Germany, F.R.).

MODAL ANALYSIS OF FLUID-STRUCTURE SYSTEMS BY PARALLEL SUBSPACE ITERATION c34

H. Wandinger *In* ESA, Spacecraft Structures and Mechanical Testing Jan. 1989 p 277-282 (For primary document see N90-10986 02-18)

Copyright Avail: NTIS HC A99/MF E06

A method for the modal analysis of coupled fluid-structure systems is presented. For the fluid, a pressure formulation is adopted. The resulting unsymmetric eigenvalue problem is solved by special subspace iteration schemes using the original matrices of the uncoupled systems. Full advantage can thus be taken of a sparse population of these matrices. Singularities, i.e. rigid body modes of the solid structure and constant pressure modes of the fluid, are treated by means of decoupling transformations. This procedure enables the handling of singularity interaction effects as they occur e.g. in the case of floating structures. The method can be used to analyze coupled fluid-structure systems with compressible and incompressible fluids, including surface wave effects. Examples are given to illustrate the different classes of problems that can be solved as well as the applicability for the analysis of large problems. ESA

N90-11025*# Jet Propulsion Lab., California Inst. of Tech., Pasadena.

COMPARISON OF SINE DWELL AND BROADBAND METHODS FOR MODAL TESTING

Jay-Chung Chen *In* ESA, Spacecraft Structures and Mechanical Testing Jan. 1989 p 285-292 (For primary document see N90-10986 02-18)

Copyright Avail: NTIS HC A99/MF E06

The objectives of modal tests for large complex spacecraft structural systems are outlined. The comparison criteria for the modal test methods, namely, the broadband excitation and the sine dwell methods, are established. Using the Galileo spacecraft modal test and the Centaur G Prime upper stage vehicle modal test as examples, the relative advantage or disadvantage of each method is examined. The usefulness or shortcomings of the methods are given from a practical engineering viewpoint. ESA

N90-11026# Deutsche Forschungs- und Versuchsanstalt fuer Luft- und Raumfahrt, Goettingen (Germany, F.R.). Inst. of Aeroelasticity.

MODAL ANALYSIS OF SPACE STRUCTURES WITH THE IBRAHIM TIME DOMAIN METHOD

A. Schenk *In* ESA, Spacecraft Structures and Mechanical Testing Jan. 1989 p 293-299 (For primary document see N90-10986 02-18)

Copyright Avail: NTIS HC A99/MF E06

The use of the Ibrahim Time Domain (ITD) algorithm in extracting the structural modal parameters for the free vibration of test structures is described. The major advantage of this method is that no detailed information on excitation must be made available. The measurements are very short, covering only the free decay vibrations of conventional engineering structures, which usually last only a few seconds. To analyze operational vibration responses due to random excitation, ITD can be combined with the RDT (random decrement technique) method which prepares the free decay response such that ITD can be used. Other possible uses of the combined RDT and ITD methods are discussed. ESA

N90-11027# Communications Research Centre, Ottawa (Ontario).

COMPARISON OF PHASE RESONANCE, MODE SEPARATION, AND DRIVEN-BASE MODAL IDENTIFICATION METHODS APPLIED TO THE FLECS TEST STRUCTURE

R. K. Singal, F. R. Vigneron, T. Steele, A. Bertram, and M. Degener (Deutsche Forschungs- und Versuchsanstalt fuer Luft- und Raumfahrt, Goettingen, Germany, F.R.) *In* ESA, Spacecraft Structures and Mechanical Testing Jan. 1989 p 301-308 (For primary document see N90-10986 02-18)

Copyright Avail: NTIS HC A99/MF E06

The flexible ECS Structure (FLECS) was used to carry out validation tests of different dynamic identification methods. The methods tested are the phase resonance method with appropriated excitation, the mode separation method with excitation at locations on the structure with complex exponential and with ISSPA (identification of structural systems parameters), and a driven-base method with unidirectional base excitation. Since the structural damping level of FLECS is low compared to actual fully equipped satellite structures, the modal identification methods were also applied to a configuration of FLECS with supplemental

non-proportional viscous damping. For this purpose, dampers were manufactured and integrated into the FLECS structure. Results of the validation tests are given and the merits of the different dynamic identification methods compared. ESA

N90-11028# Old Dominion Univ., Norfolk, VA.
A DIRECT TWO RESPONSE APPROACH FOR UPDATING ANALYTICAL DYNAMIC MODELS OF STRUCTURES WITH EMPHASIS ON UNIQUENESS **c39**
S. R. Ibrahim, C. Stavrinidis, E. Fissette, and O. Brunner (European Space Agency. European Space Research and Technology Center, ESTEC, Noordwijk, Netherlands) *In* ESA, Spacecraft Structures and Mechanical Testing Jan. 1989 p 309-315 (For primary document see N90-10986 02-18)
Copyright Avail: NTIS HC A99/MF E06

An approach, based on utilizing only two sets of structural responses and the enforcement of the conditions for a solution is presented for the updating of finite element models. The responses required can be either any two identified normal modes, any two identified complex modes, or two forced harmonic response vectors in the neighborhood of any two natural frequencies of the structure under test. The mass, stiffness, and damping matrices are interactively and simultaneously corrected in a direct noniterative procedure. A uniqueness factor is automatically computed in the procedure to indicate the correctability of the finite element model under consideration. The number of measurement locations is assumed to be less than the number of degrees of freedom of the analytical model. Provisions for completing and smoothing the measured or identified responses are included to reduce the effects of measurement, noise and identification errors. Preliminary results on simple models are presented in support of the proposed technique. ESA

N90-11029# European Space Agency. European Space Research and Technology Center, ESTEC, Noordwijk (Netherlands). Structural Design Section.
REVIEW OF THE ESA FRACTURE CONTROL POLICY **c39**
T. K. Henriksen *In its* Spacecraft Structures and Mechanical Testing Jan. 1989 p 319-324 (For primary document see N90-10986 02-18)
Copyright Avail: NTIS HC A99/MF E06

The efforts of ESA in developing a unified approach to damage tolerance and fracture control research are outlined. Based on experience gained with Spacelab and Eureca, the ESA Fracture Control Board has defined a set of fracture control requirements applicable to all ESA space systems. The reasoning behind the fracture control requirements is discussed. Examples of applications of these requirements are given. The development of the second space telescope solar array is given as a specific example. ESA

N90-11030# Deutsche Forschungs- und Versuchsanstalt fuer Luft- und Raumfahrt, Stuttgart (Germany, F.R.). Inst. for Structures and Design.
LIQUID INFILTRATED C/SiC: AN ALTERNATIVE MATERIAL FOR HOT SPACE STRUCTURES **c24**
W. Krenkel and H. Hald *In* ESA, Spacecraft Structures and Mechanical Testing Jan. 1989 p 325-330 (For primary document see N90-10986 02-18)
Copyright Avail: NTIS HC A99/MF E06

The technology involved in creating liquid infiltrated C/SiC (a carbon fiber reinforced silicon carbon ceramic matrix composite) is described. It is presented as a means of cost and fabrication time reduction in producing fiber reinforced composites. The mechanical properties of preliminary material samples were evaluated. Bending, tension and shear tests were carried out with specimens at room temperature. Extreme thermal tests in oxidative atmospheres with simulated reentry conditions were performed in an arc heated plasma channel at temperatures up to 1800 C. These tests are described and the results included. ESA

N90-11031# Deutsche Forschungs- und Versuchsanstalt fuer Luft- und Raumfahrt, Cologne (Germany, F.R.). Inst. for Materials Research.
FATIGUE CRACK GROWTH RATES AS A FUNCTION OF DELTA K: VARIABILITY AND MATERIAL PROPERTY **c39**
G. Marci, D. E. Castro, and V. Bachmann *In* ESA, Spacecraft Structures and Mechanical Testing Jan. 1989 p 331-342 (For primary document see N90-10986 02-18)
Copyright Avail: NTIS HC A99/MF E06

Fatigue crack propagation threshold measurements as influenced by closure phenomena are described. The way in which individual material properties determine crack propagation is outlined. A material property threshold beyond which crack propagation occurs is established. The microstructural differences of aluminum alloys are shown to influence primarily via the closure effects. The microstructural differences have a substantial influence on long cracks but very little influence on short crack growth behavior. ESA

N90-11032# Aeritalia S.p.A., Turin (Italy). Space Systems Group.
MATERIAL PROPERTIES OF 2219-T851 ALUMINUM ALLOY PLASMA WELDED COMPARED TO TIG WELDING **c39**
Giorgio Banino and Edoardo Tacchino *In* ESA, Spacecraft Structures and Mechanical Testing Jan. 1989 p 343-348 (For primary document see N90-10986 02-18)
Copyright Avail: NTIS HC A99/MF E06

The Variable Polarity Plasma Arc (VPPA) technique, using the aluminum alloy 2219-T851 was tested. The tests were performed with two primary objectives. The first was to optimize the welding process and microstructure of the joint versus tensile properties. The second was a complete mechanical characterization of the joints by means of experimental activities concerned with fatigue, fracture mechanics, stress corrosion cracking and residual stresses. All the results were compared with the TIG (Inert Gas Tungsten arc welding) process used in the Spacelab program. The 2219-T851 alloy is the basic material used in making the Columbus pressurized modules. ESA

N90-11033# Rome Univ. (Italy). Dept. of Aerospace.
STUDY OF A GALLIUM ARSENIDE SOLAR CELL INTERCONNECTOR **c24**
R. S. Capitanio, M. Marchetti, and S. Tizzi *In* ESA, Spacecraft Structures and Mechanical Testing Jan. 1989 p 351-357 Sponsored by Fabrica Italiana Apparecchiature Radioelettriche S.p.A., Milan (For primary document see N90-10986 02-18)
Copyright Avail: NTIS HC A99/MF E06

Out-of-plane stress relief loop interconnectors and in-plane solutions are tested for a gallium arsenide solar cell. Stress distributions in interconnector loops are calculated using mathematical models and finite element methods. The importance of substrate choice is emphasized. Stresses induced in the interconnector loops by a carbon fiber composite sandwich are found to be substantially inferior (35 to 40 percent less) to those induced by an aluminum sandwich. A theoretical analysis of fatigue life is presented for the interconnector, which is subjected to up to 60,000 thermal cycles in a ten year lifetime in low earth orbit. ESA

N90-11034# Deutsche Forschungs- und Versuchsanstalt fuer Luft- und Raumfahrt, Brunswick (Germany, F.R.). Inst. fuer Strukturmechanik.
TRANSVERSE SHEAR STIFFNESS OF COMPOSITE AND SANDWICH FINITE ELEMENTS
K. Rohwer *In* ESA, Spacecraft Structures and Mechanical Testing Jan. 1989 p 363-368 (For primary document see N90-10986 02-18)
Copyright Avail: NTIS HC A99/MF E06

A technique for calculating transverse shear stiffness in composite and sandwich finite elements is proposed. Integrating the equilibrium conditions leads to shear stresses as functions of membrane force and bending moment derivatives, which can be replaced by transverse shear forces if cylindrical bending states

are assumed. These functions are used in the complementary energy density estimation to determine improved stiffnesses. For homogeneous materials they correspond with Reissner's correction factor of 5/6 as applied to shear modulus times thickness. Isotropic layers show correction factors between 0.45 and 1.0 depending on the layer thickness and modulus ratios. The proposed formulation covers orthotropic material as well as sandwich constructions. This technique makes different versions of layered and sandwich elements obsolete. ESA

N90-11035# Veritas Research A.S., Hovik (Norway).
NONLINEAR COLLAPSE SIMULATION OF ANISOTROPIC PLATES AND CORRUGATED PANELS **c39**
P. G. Bergan, R. O. Bjoerum, and M. K. Nygard *In* ESA, Spacecraft Structures and Mechanical Testing Jan. 1989 p 369-376 (For primary document see N90-10986 02-18)
Copyright Avail: NTIS HC A99/MF E06

Advances in nonlinear finite element analysis of anisotropic and corrugated plates and shells are described. Free formulation plate and shell elements with six freedoms per node are developed for this purpose. Efficient ways of establishing the ultimate carrying capacity of structures are discussed. The combined use of nonlinear simulation and linearized eigenvalue analysis is given particular attention. Two examples are presented: a buckling analysis of an anisotropic cylindrical panel with a circular hole and a collapse analysis of a corrugated panel. ESA

N90-11036# Deutsche Forschungs- und Versuchsanstalt fuer Luft- und Raumfahrt, Brunswick (Germany, F.R.). Inst. fuer Strukturmechanik.
ANALYSIS OF DELAMINATION GROWTH **c24**
H. Eggers *In* ESA, Spacecraft Structures and Mechanical Testing Jan. 1989 p 377-381 (For primary document see N90-10986 02-18)
Copyright Avail: NTIS HC A99/MF E06

A simplified method is developed, in which a delaminated specimen is modeled by two layers of coupled beam lattices. The approximation is based on the known solution for buckled beams and can be used to analyze plane specimens with and without prebuckled imperfections. Close to the crack front an approximate modified plane strain state exists. Based on this assumption the Energy Release Rates (ERRs) for a layered structure are determined via forces and moments of the beam lattice. Buckling of a beam element, transformation of crack tips, and energy release rates, are studied. ESA

N90-11037# Katholieke Univ. te Leuven (Belgium). Dept. of Metallurgy and Materials Science.
INFLUENCE OF THE FIBER/MATRIX INTERFACE ON DAMAGE DEVELOPMENT IN CFRP **c24**
J. Ivens, M. Wevers, I. Verpoest, and P. DeMeester *In* ESA, Spacecraft Structures and Mechanical Testing Jan. 1989 p 383-386 (For primary document see N90-10986 02-18)
Copyright Avail: NTIS HC A99/MF E06

Carbon fibers are surface treated in order to obtain the good interfacial properties needed for a good stress transfer between fiber and resin. A controlled oxidative surface treatment strongly improves the interfacial strength, depending on the treatment level. The influence of this surface treatment level on the damage development in a cross ply carbon epoxy laminate during monotonic tensile testing is investigated. The crack path is shown to be influenced by the interface strength. It is shown that the mechanical properties of a cross ply laminate improve by a low surface treatment level, while they decrease strongly for higher treatment levels. ESA

N90-11038# Dornier System G.m.b.H., Friedrichshafen (Germany, F.R.).
A HIGH PRECISION GRAVITY COMPENSATION SYSTEM FOR THE DEPLOYMENT TEST OF THE ERS-1 SAR ANTENNA
R. Sippel *In* ESA, Spacecraft Structures and Mechanical Testing Jan. 1989 p 389-394 (For primary document see N90-10986 02-18)
Copyright Avail: NTIS HC A99/MF E06

The gravity compensation system used for the deployment tests of a foldable 10 m by 1 m planar array antenna made of Carbon Fiber Reinforced Plastics (CFRP) used on the ERS-1 (environmental research satellite) is described. After the satellite is launched, the antenna will be deployed by means of an electric motor and spring drives. The complete deployment sequence was successfully tested under terrestrial conditions on the antenna engineering model. Limitations in the allowable latching shocks allowed only small driving forces which made the use of a high quality gravity compensation system necessary. The gravity compensation system used, maintains each antenna wing at one point with the help of two cranes which passively follow the antenna motion during deployment. The gravity induced driving forces were reduced to very small values without introducing significant additional friction. The manufactured system geometry, stiffness, and suspension force magnitude, were adjusted following problem oriented adjustment methods. ESA

N90-11039# Industrieanlagen-Betriebsgesellschaft m.b.H., Ottobrunn (Germany, F.R.).
TRANSIENT VIBRATION TESTING OF SPACECRAFT STRUCTURES. EXPERIENCE WITH MULTIAXIAL BASE MOTION AND COMBINED BASE MOTION AND POINT FORCE EXCITATION
K. Muehlbauer, U. Schildt, and W. Raasch *In* ESA, Spacecraft Structures and Mechanical Testing Jan. 1989 p 395-400 (For primary document see N90-10986 02-18)
Copyright Avail: NTIS HC A99/MF E06

Practical aspects of transient vibration testing were studied using both a multiaxis hydraulic and a uniaxial electrodynamic vibration test facility. The experimental investigations with the hydraulic system demonstrated that excitation in six degrees of freedom operates in principle but must be improved in its reproduction accuracy. Uniaxial transient vibration testing turned out to be feasible with the electrodynamic four shaker system available. An attempt was made to achieve more realistic test results by simulating the dominant translatory load by uniaxial base excitation and the secondary loading degrees of freedom by additionally applied point forces. The results show that this technique, although limited in its range of application, is able to produce more realistic structural loads than the uniaxial tests alone. ESA

N90-11040# Intespace, Toulouse (France).
TRANSIENT TESTS FOR SPACECRAFT STRUCTURES
L.-P. Bugeat, A. Girard, and J. Merlet *In* ESA, Spacecraft Structures and Mechanical Testing Jan. 1989 p 401-405 Sponsored by ESA, CNES, and Aerospatiale (For primary document see N90-10986 02-18)
Copyright Avail: NTIS HC A99/MF E06

The use of transient tests in the dynamic qualification of spacecraft structures is outined. The technique uses a combination of spacecraft dynamic mass identification tests and open loop transient tests based on an impedance coupling and an equivalent force formulation. A closed loop transient vibration test theoretical formulation is presented as well as a prototype implementation. A comparison of the two techniques, transient tests and sine vibration tests, is given. Accuracy, monitoring, and control are given special attention. The closed loop driving procedure gives better results than the open loop driving method. ESA

N90-11041# Industrieanlagen-Betriebsgesellschaft m.b.H., Ottobrunn (Germany, F.R.).
DEVELOPMENT OF A THERMOACOUSTIC TEST FACILITY **c14**
G. Bayerdoerfer *In* ESA, Spacecraft Structures and Mechanical Testing Jan. 1989 p 407-412 (For primary document see N90-10986 02-18)
Copyright Avail: NTIS HC A99/MF E06

The thermoacoustic test facility at the Industrieanlagen-Betriebsgesellschaft (IABG) at Ottobrunn (RFA)

is described. The facility consists of a progressive wave tube used to simulate dynamic pressure fluctuations with the help of acoustic noise generators plus a heating system installed in the progressive wave tube. IABG is investigating the possibility of using a flame heating system. Preliminary tests show that temperatures beyond 1000 C can be achieved using relatively simple techniques. The need for instruments capable of measuring the loading and response data under such high temperatures is stressed. ESA

N90-11042# Messerschmitt-Boelkow-Blohm G.m.b.H., Bremen (Germany, F.R.).
MULTI-AXIS TRANSIENT TESTING: EXPERIMENTAL INVESTIGATIONS
K. Eckhardt and G. Schmidt (Hochtemperatur Reaktorbau, Juelich, Germany, F.R.) *In* ESA, Spacecraft Structures and Mechanical Testing Jan. 1989 p 413-419 (For primary document see N90-10986 02-18)
Copyright Avail: NTIS HC A99/MF E06

The technique of using multi-axis transient testing in obtaining correct stress distributed loading of spacecraft structure hardware is outlined. Test results from a pilot facility, located at the Hochtemperatur Reaktorbau in Julich (Federal Republic of Germany) are presented. The goal of the research is to determine the limits of load capacity and define specific facility constraints, e.g. noise level, cross talk, input reproducibility, resonances, control mode selection, and safety measures. Results are compared with existing requirements for a facility capable of carrying out spacecraft transient testing. Areas requiring improvement are identified. ESA

N90-11043# Rockwell International Corp., Downey, CA. Space Transportation Systems Div.
AUTOMATED STRESS ANALYSIS OF SHUTTLE ORBITER THERMAL PROTECTION SYSTEM **c16**
J. Rowe, F. Alfonso, M. Jain, and B. A. Castillo *In* ESA, Spacecraft Structures and Mechanical Testing Jan. 1989 p 423-438 (For primary document see N90-10986 02-18)
Copyright Avail: NTIS HC A99/MF E06

The computerized methods used in carrying out stress analysis of the tiles used in the thermal protection system of the Space Shuttle are described. ASAT (automatic structural analysis of tiles) can be used for analyzing eighty percent of the tiles. Tiles of complex shape, which require an uneconomic modeling time under ASAT analysis, are individually analyzed with COMAND (computer organized manufacturing analysis and design). The capacity of these systems to receive , assemble, store, retrieve, and operate upon large amounts of data is described. ESA

N90-11044# Rome Univ. (Italy). Dipt. Aerospaziale.
STRUCTURAL PROBLEMS OF ACCURATE INFLATABLE SURFACES **c39**
C. Arduini and U. Ponzi *In* ESA, Spacecraft Structures and Mechanical Testing Jan. 1989 p 439-445 Sponsored by Contraves Italiana, Rome (For primary document see N90-10986 02-18)
Copyright Avail: NTIS HC A99/MF E06

A toroidal ring used as a stiffner in a large inflatable antenna is analyzed. Analytical and numerical methods are used in the analysis of the ring and numerical results are given. Particular attention is given to the pressure-induced shape modifications which may affect the surface accuracy of the structure. A perfect toroidal membrane is considered and possible practical approximations of the same shape proposed. ESA

N90-11045# Construcciones Aeronauticas S.A., Madrid (Spain). Space Div.
INDUCED SHOCK LOADS DURING THE SEPARATION OF THE ARIANE 5 VEB STRUCTURE **c15**
C. Huerta, V. GomezMolinero, E. Alarcon, S. GomezLera, and J. Molina (Polytechnical Univ. of Madrid, Spain) *In* ESA, Spacecraft Structures and Mechanical Testing Jan. 1989 p 447-454 (For primary document see N90-10986 02-18)
Copyright Avail: NTIS HC A99/MF E06

Tests used to simulate the separation of the lower stage of the Ariane Vehicle Equipment Bay (VEB) were carried out on a flat full scale model. Theoretical studies carried out prior to testing are described. Three different mathematical methods, finite element, component element, and wave propagation, were used. Comparison of the predicted theoretical results with the actual test results is planned. ESA

N90-11046# IKO Software Service G.m.b.H., Stuttgart (Germany, F.R.).
A NEW ASPECT FOR THE USE OF THIN WALLED BEAMS AS SHELL STIFFENERS OF SPACECRAFT STRUCTURES
Ferenc Kiss *In* ESA, Spacecraft Structures and Mechanical Testing Jan. 1989 p 455-460 (For primary document see N90-10986 02-18)
Copyright Avail: NTIS HC A99/MF E06

A consistent and compatible transformation for seven parameter Timoshenko beams is introduced. This transformation is applied to the new beam elements of the ASKA software program system. The comparison of the results obtained by different methods shows the validity of the solution and points to specific problems, where the effect in question plays an important role. One such problem is the modeling of a shell-like spacecraft structure by thin-walled beams eccentrically connected to the covering surface modeled by the shell. ESA

N90-11047# Rome Univ. (Italy). Dipt. Aerospaziale.
JOE: JORDAN OPTIMIZED EIGENSOLVER. A STEP TOWARD A NUMERICAL JORDAN FORM ANALYZER FOR CONTROL AND INTERACTIVE THERMO-STRUCTURAL-DYNAMIC APPLICATIONS **c39**
C. Arduini and D. Mortari *In* ESA, Spacecraft Structures and Machanical Testing Jan. 1989 p 461-465 (For primary document see N90-10986 02-18)
Copyright Avail: NTIS HC A99/MF E06

The JOE (Jordan Optimized Eigensolver) software program is described. It differs from other software programs of its kind in using screening criteria on eigenvector parallelism and eigenvalue coalescence once they are generated on a standard eigenanalyzer. The screening is dependent on user selected parameters allowing for a flexible search for successful decompositions. Results of test cases show success for matrices as large as 100 by 100 and multiple roots up to 16. The results of this technique are shown and possible improvements discussed. ESA

N90-11048# Arianespace, Evry (France). Dept. Analyse de Mission.
FLIGHT-MECHANICAL ENVIRONMENT ON ARIANE LAUNCH VEHICLE PAYLOADS [ENVIRONNEMENT MECANIQUE EN VOL SUR LES CHARGES UTILES MISES EN ORBITE PAR LES LANCEURS ARIANES] **c15**
J. L. Caneilles *In* ESA, Spacecraft Structures and Mechanical Testing Jan. 1989 p 467-480 In FRENCH (For primary document see N90-10986 02-18)
Copyright Avail: NTIS HC A99/MF E06

A summary of the in-flight mechanical environments of payloads on various Ariane launches is presented. The results obtained from the initial Ariane 4 launch are analyzed and compared to mathematical predictions. The low frequency domain is given priority in reviewing different, payload distribution possibilities. Satellite launching projects are analyzed in terms of load and stiffness limits. Dimensioning procedures are outlined. ESA

N90-11049# Centre National d'Etudes Spatiales, Toulouse (France).
MATHEMATICAL MODEL AND PREDICTIONS FOR STATIC AND DYNAMIC BEHAVIOR OF SOLAR ARRAY STRUCTURE **c39**
D. Gangloff, F. Mercier, N. Priou, and J. F. David (Aerospatiale, Les Mureaux, France) *In* ESA, Spacecraft Structures and Mechanical Testing Jan. 1989 p 483-489 (For primary document see N90-10986 02-18)
Copyright Avail: NTIS HC A99/MF E06

The technical requirements, mathematical models and test correlation analysis used in the qualification procedure of new solar array structures are described. These criteria are applied to the mathematical models devised to predict performance in the following areas: quasi-static loads, stiffness, sine vibration, and acoustic noise. The pre-flight qualification philosophy takes into account the need for greater electrical power and reduced payload volume, mass, and cost in designing future satellites and solar arrays. ESA

N90-11050# Mitsubishi Electric Corp., Tokyo (Japan).
TEST RESULTS ON CONCEPTUAL MODELS OF THE LARGE DEPLOYABLE ANTENNA FOR MOBILE COMMUNICATIONS SATELLITES **c39**
Yuichiro Baba, Yuji Tsutsumi, Akio Iso, and Kazuo Yamamoto *In* ESA, Spacecraft Structures and Mechanical Testing Jan. 1989 p 491-496 (For primary document see N90-10986 02-18)
Copyright Avail: NTIS HC A99/MF E06

A preliminary study of a large antenna reflector for mobile communications, functioning on a Geostationary Platform (GPF) is described. The use of the 800/900 MHz band and an aperture diameter of about 30 m are assumed. The partial and scale models of three new truss configurations are introduced. They are fabricated and tested to confirm the soundness of their structural concept and to study their practicality more concretely. The results of the tests are outlined. ESA

N90-11051# IKO Software Service G.m.b.H., Stuttgart (Germany, F.R.).
SPACE TELESCOPE SOLAR ARRAY: NONLINEAR TEST AND ANALYSIS EFFECTS **c39**
Ph. Deloo and M. Klein (European Space Agency. European Space Research and Technology Center, ESTEC, Noordwijk, Netherlands) *In* ESA, Spacecraft Structures and Mechanical Testing Jan. 1989 p 497-504 (For primary document see N90-10986 02-18)
Copyright Avail: NTIS HC A99/MF E06

A geometrical and material nonlinear model of a solar array boom of the space telescope is developed and its static behavior fitted to experimental data. The model is used to perform a nonlinear dynamic assessment of the real boom response to in-orbit loads. Allowable in-orbit loads are derived based on allowable bending moments computed from static test results. An accurate correlation of the model with the fully nonlinear system is achieved. ESA

N90-11052# Aerospatiale, Cannes (France).
ESA-D: AN INTEGRATED SOFTWARE FOR ANTENNA DESIGN AND ANALYSIS **c61**
L. Marro, J. P. Boisset, and K. Pontoppidan (TICRA A/S, Copenhagen, Denmark) *In* ESA, Spacecraft Structures and Mechanical Testing Jan. 1989 p 505-510 Previously announced as N89-23784 (For primary document see N90-10986 02-18)
(Contract ESTEC-6659/86/NL/PH)
Copyright Avail: NTIS HC A99/MF E06

The functional and architectural characteristics of the ESA-D software are described. This software allows full evaluation of the dimensional characteristics of satellite antenna reflectors in an integrated and interactive way. Such reflector profile requirements are fundamental design drivers for reflector design and manufacturing, and as such have to be thoroughly evaluated early in the design phase. Either rigid, unfurlable or inflatable types of reflectors can be processed using this software. ESA

N90-11053# Virginia Polytechnic Inst. and State Univ., Blacksburg. Materials Response Group.
THE USE OF DAMAGE CHARACTERIZATION FOR LIFE PREDICTION METHODOLOGIES **c38**
Kenneth L. Reifsnider *In* ESA, Spacecraft Structures and Mechanical Testing Jan. 1989 p 513-519 (For primary document see N90-10986 02-18)
(Contract N62269-85-C-2345; AF-AFOSR-0087-85)
Copyright Avail: NTIS HC A99/MF E06

An attempt to construct a life prediction methodology which can be used for space structures on the basis of the analysis of damage development in composite components is described. Special attention is given to the use of damage characterization methods and test techniques which provide the data necessary to construct a mechanistic representation which can be used to anticipate performance under combinations of conditions that are unfamiliar or difficult to reproduce in the laboratory. These modeling concepts have been successfully applied to the prediction of remaining tensile and compressive strength of laminates constructed from two different composite material systems. ESA

N90-11054# Centre National d'Etudes Spatiales, Toulouse (France).
DEVELOPMENT OF GRAPHITE-MAGNESIUM COMPOSITES FOR SPACE APPLICATIONS **c24**
Ph. Roy and J. F. Patin (Aerospatiale, Cannes, France) *In* ESA, Spacecraft Structures and Mechanical Testing Jan. 1989 p 521-527 (For primary document see N90-10986 02-18)
Copyright Avail: NTIS HC A99/MF E06

The work, technological approach, and logic involved in the development of metal matrix composites are described. Secondary structures of satellites, such as antenna reflectors and truss optical instrument supports, require a high structural stability to remain accurate. They must display low coefficients of thermal expansion, no sensitivity to radiation and moisture, no outgassing under vacuum environments, and better thermal and electrical conductivity. A magnesium matrix increases composite specific properties (stiffness and strength), due to its very low density. These characteristics make magnesium matrix composites very attractive for future spacecraft applications. ESA

N90-11055# Katholieke Univ. te Leuven (Belgium). Dept. of Metallurgy and Materials Engineering.
HYGROTHERMAL DEFORMATIONS OF COMPOSITE SHELLS **c39**
Lawrence E. Doxsee, Jr. *In* ESA, Spacecraft Structures and Mechanical Testing Jan. 1989 p 529-534 Sponsored in part by the Hughes Space and Communications Group and General Motors Research Labs. (For primary document see N90-10986 02-18)
Copyright Avail: NTIS HC A99/MF E06

A method developed for determining the deformations of laminated fiber-reinforced composite plates and shells subjected to changes in temperature and moisture concentration is described. The method consists of two parts: a two-dimensional shell theory which includes the effects of transverse shear and normal strains, and a displacement based finite element program for shells of revolution with axisymmetric temperature and moisture distributions. The shell theory and the finite element program were verified by obtaining solutions to a wide variety of problems using the finite element program and comparing these solutions to existing analytical solutions. Numerical examples demonstrate the importance of including transverse normal strains in the shell theory. ESA

N90-11056# Aerospatiale Aquitaine, Saint-Medard en Jalles (France).
SPACE ENVIRONMENT EFFECTS ON CARBON/EPOXY MATERIALS **c24**
P. Plotard and C. Durin (Departement d'Etudes et de Recherches en Technologie Spatiale, Toulouse, France) *In* ESA, Spacecraft Structures and Mechanical Testing Jan. 1989 p 535-540 In FRENCH; ENGLISH summary (For primary document see N90-10986 02-18)
Copyright Avail: NTIS HC A99/MF E06

Tests carried out on structural composite materials in a space environment simulation facility are described. A carbon/epoxy filamentous composite and a carbon/epoxy laminated composite were tested. The space environment simulation facility and the simulation methods are described. Results of X-ray analysis, of micro fissure generation and of induced ageing of the composites

are presented. It is concluded that such simulation tests are useful but do not take into account such parameters as ageing due to the presence of atomic oxygen in low orbit environments. ESA

N90-11057# European Space Agency. European Space Research and Technology Center, ESTEC, Noordwijk (Netherlands).
ARIANE 5 STRUCTURAL DESIGN AND DEVELOPMENT c15
A. L. GonzalezBlasquez *In its* Spacecraft Structures and Mechanical Testing Jan. 1989 p 543-546 (For primary document see N90-10986 02-18)
Copyright Avail: NTIS HC A99/MF E06

The structural design and the flight environments encountered by Ariane 5 are reviewed. An overview of the general configuration of the launcher with its functional parameters is presented. A description of the different structures of the boosters, the cryogenic stage and the upper composite is presented. The relevant flight events are detailed. The quasi-static and dynamic loads and the thermal and acoustic environments are discussed. The dimensioning guidelines are outlined and the development program tests described. ESA

N90-11058# Avions Marcel Dassault-Breguet Aviation, Saint-Cloud (France).
THERMAL AND STRUCTURAL ANALYSIS OF HERMES c15
C. Petiau *In* ESA, Spacecraft Structures and Mechanical Testing Jan. 1989 p 547-556 Previously announced in IAA as A89-17756 (For primary document see N90-10986 02-18)
Copyright Avail: NTIS HC A99/MF E06

The organization of the thermal and structural analysis of the Hermes project is described. A way to resolve the problem of connections between calculations performed by the different Hermes partners is outlined. The interactions between the general model of TPS (thermal protection system) used for global dimensioning of insulation, and refined thermal models giving accurate temperature map details of hot and cold structures, are described. The organization of the structural analysis is based on a finite element general model which supports preliminary design, loads and vibration analyses. Boundary conditions for refined subpart analyses, are cut to size, into the general model by super element techniques. This process involves the use by all partners of efficient computer codes. The Catia-Elfini software system is proposed as a possible code system for structural analysis and optimization purposes. ESA

N90-11059# Boeing Aerospace Co., Huntsville, AL. Space Station Program WP01.
SDM CHALLENGES FOR SPACE STATION
Eugene G. Cowart *In* ESA, Spacecraft Structures and Mechanical Testing Jan. 1989 p 557-569 (For primary document see N90-10986 02-18)
Copyright Avail: NTIS HC A99/MF E06

Various SDM (systems design methods) challenges in the design analysis of the Space Station are presented. The design areas considered include: thermal, load and stress analysis, mode shapes/dynamic excursions, atomic oxygen effects, radiation protection, acoustic drivers, and microgravity measurement. Design solutions and the rationale for their implementation are presented. The fabrication techniques for the various components used in the prototype module are described. ESA

N90-11060# Stuttgart Univ. (Germany, F.R.). Inst. for Aircraft Design.
WORKED-IN HOLES IN THREE-DIMENSIONAL REINFORCED COMPOSITES c24
F. J. Arendts and Klaus Drechsler *In* ESA, Spacecraft Structures and Mechanical Testing Jan. 1989 p 573-578 Prepared in cooperation with MBB G.m.b.H., Munich, Germany, Fed. Republic of Germany and Vorwerk und Co., Kulmbach, Fed. Republic of Germany (For primary document see N90-10986 02-18)
Copyright Avail: NTIS HC A99/MF E06

To improve notched-strength of composites, holes and pins were worked into two- and three-dimensional reinforced fiber composites. To judge the mechanical properties many aspects were taken into consideration. Tension specimens with worked-in holes have greater strength than those with drilled holes, but demonstrate less resistance during fatigue tests and pin-joint bearing tests. This is a result of the higher shear stresses and the lack of forty five degree fibers in the three-dimensional weaves. They demonstrate however, lower notch sensitivity than laminates. Interesting properties obtainable by weaving in pins and rings during the textile process are described. ESA

N90-11061# Deutsche Forschungs- und Versuchsanstalt fuer Luft- und Raumfahrt, Brunswick (Germany, F.R.). Inst. fuer Strukturmechanik.
DELAMINATION TESTS UNDER STATIC COMPRESSION LOADING c24
M. Gaedke *In* ESA, Spacecraft Structures and Mechanical Testing Jan. 1989 p 579-585 (For primary document see N90-10986 02-18)
Copyright Avail: NTIS HC A99/MF E06

The strength and stiffness of arbitrarily stacked multidirectional laminates are predicted from well defined characteristic properties of unidirectional laminates established by tests dependent on temperature and moisture content. Elasticity, first-ply failures and ultimate strengths are verified by tests. Prestresses caused by temperature and moisture must be included in the calculations. Excellent correspondence was found for the moduli of elasticity while for the ultimate strength it is sufficient for practical estimates. In the experimental program on the response of carbon fiber reinforced epoxy laminates containing artificial delaminations, four defect diameters at four ply interfaces in three multidirectional laminates were investigated. The results of the delamination growth show the influence of the delamination size, the stacking sequence, the thickness and the stiffness of the separated sublaminates. In all cases buckling of the delaminated areas occurred prior to failure depending on the level of compression loading. ESA

N90-11062# Deutsche Forschungs- und Versuchsanstalt fuer Luft- und Raumfahrt, Brunswick (Germany, F.R.). Inst. fuer Strukturmechanik.
DELAMINATION TESTS UNDER COMPRESSION-COMPRESSION AND TENSION-COMPRESSION LOADING c24
H. C. Goetting *In* ESA, Spacecraft Structures and Mechanical Testing Jan. 1989 p 587-592 (For primary document see N90-10986 02-18)
Copyright Avail: NTIS HC A99/MF E06

The delamination behavior of multidirectional CFRP (carbon fiber reinforced plastics) was investigated under compression-compression and tension-compression fatigue loading by means of artificially introduced delaminations. A computer aided test procedure enabled observation of the relevant damage mechanisms during the last cycles prior to failure without destroying the test specimens. The influence of the depth of location as well as of the diameter of delaminations are discussed with special reference to failure critical damage. With tension-compression fatigue the matrix crack formation in off-axis plies seems to induce the compressive failure more than the artificial delamination. With respect to damage tolerance considerations some configurations of delamination states prove to be non-critical. ESA

N90-11063# Katholieke Univ. te Leuven (Belgium). Dept. of Metallurgy and Materials Science.
THE 2.5D- AND 3D-FABRICS FOR DELAMINATION RESISTANT COMPOSITE LAMINATES AND SANDWICH STRUCTURES c24
I. Verpoest, M. Wevers, and P. deMeester *In* ESA, Spacecraft Structures and Mechanical Testing Jan. 1989 p 593-599 (For primary document see N90-10986 02-18)
Copyright Avail: NTIS HC A99/MF E06

A technique for making two and a half dimensional fabrics from three-dimensional fabrics woven in one step is described. These two and a half dimensional fabrics show better peel strength and interlaminar fracture toughness. Stronger three-dimensional

fabrics are formed by impregnation with polyurethane foam, creating a sandwich structure with interconnected skins. The results of peel tests, compression tests, and fracture toughness tests are given for these new materials. Preliminary results are encouraging. ESA

N90-11064# European Space Agency. European Space Research and Technology Center, ESTEC, Noordwijk (Netherlands).
THE ENVIRONMENTAL TEST CENTRE AT ESTEC (AN OVERVIEW) **c14**
E. Classen *In its* Spacecraft Structures and Mechanical Testing Jan. 1989 p 603-605 (For primary document see N90-10986 02-18)
Copyright Avail: NTIS HC A99/MF E06

The global tasks of the European Space Research and Technology Center (ESTEC) are outlined. The advantages of being able to carry out a wide series of tests all within one building complex are described. A diagram of the test center is provided. The test center will be capable of carrying out environmental tests on large satellites such as those to be launched on Ariane 4 and 5. ESA

N90-11065# European Space Agency. European Space Research and Technology Center, ESTEC, Noordwijk (Netherlands). Testing Div.
TWO YEARS EXPERIENCE WITH THE ESTEC MULTISHAKER SYSTEM **c14**
P. Bonnot *In its* Spacecraft Structures and Mechanical Testing Jan. 1989 p 607-612 (For primary document see N90-10986 02-18)
Copyright Avail: NTIS HC A99/MF E06

The ESTEC (European Space Research and Technology Center) 280 kN multishaker system is described. The performance of the system is summarized. The initial design of the system is explained. The utilization program of the system is outlined. It is concluded that on the whole the design options chosen in constructing the system were appropriate. Improvements on the original design are outlined and experience gained in utilizing the system summarized. ESA

N90-11066# European Space Agency. European Space Research and Technology Center, ESTEC, Noordwijk (Netherlands). Testing Div.
NEW DATA HANDLING SYSTEM (MDH) FOR MECHANICAL TESTS AT ESTEC **c14**
C. Fransen *In its* Spacecraft Structures and Mechanical Testing Jan. 1989 p 613-617 (For primary document see N90-10986 02-18)
Copyright Avail: NTIS HC A99/MF E06

The updated Mechanical Data Handling (MDH) system used for mechanical tests carried out at ESTEC (European Space Research and Technology Center) is described. The need for such a system in the analysis of larger and more complex space structures is outlined. During structural testing, fast processing of response data is required for a cost effective utilization of available test facilities. The planned capabilities, performance and methodologies applied in developing the updated MDH system are described. ESA

N90-11067# European Space Agency. European Space Research and Technology Center, ESTEC, Noordwijk (Netherlands).
THE LARGE EUROPEAN ACOUSTIC FACILITY AT ESTEC **c14**
W. E. Gruen and W. A. Shickle *In its* Spacecraft Structures and Mechanical Testing Jan. 1989 p 619-627 (For primary document see N90-10986 02-18)
Copyright Avail: NTIS HC A99/MF E06

The design of the reverberant acoustic chamber of ESTEC (European Space Research and Technology Center) with respect to the acoustic noise field is described. Design aspects for the noise generation system comprising horns and acoustic modulators using gaseous nitrogen as a working medium are discussed. Special attention is given to the nitrogen evaporating system where design alternatives are mentioned. Instrumentation and control systems are described with respect to noise control, safety and data handling. Considerations of the conceptual safety design in order to protect personnel and equipment from hazardous situations are discussed. ESA

N90-11068# Commissariat a l'Energie Atomique, Saclay (France).
TAMARIS: A NEW EUROPEAN FACILITY FOR LOW FREQUENCY MULTI-AXIS VIBRATION SIMULATION **c14**
P. Buland, C. Berriaud, and Ph. Jamet *In* ESA, Spacecraft Structures and Mechanical Testing Jan. 1989 p 631-634 (For primary document see N90-10986 02-18)
Copyright Avail: NTIS HC A99/MF E06

The main features of the Tamaris vibration simulation facility are outlined. Special attention is given to the 6 m by 6 m shaking table named Azalee. This table is presently a three Degrees of Freedom (DOF) facility and will be upgraded in the near future to be a full six DOF system with accurate control of rotations. The main characteristics of three other mono or multiaxial shaking tables are presented as well as the geometry of a 15 m deep testing pit for slender structures. A brief description of the digital data acquisition and control system is presented. ESA

N90-11069# Ometron Ltd., London (England).
ADVANCES IN INSTRUMENTATION FOR EXPERIMENTAL STRESS AND VIBRATION ANALYSIS AND ITS APPLICATIONS **c14**
A. J. Barker and D. J. Berry *In* ESA, Spacecraft Structures and Mechanical Testing Jan. 1989 p 635-639 (For primary document see N90-10986 02-18)
Copyright Avail: NTIS HC A99/MF E06

Instrumentation, utilizing the thermoelastic effect to provide full field stress data in a digitized form, that can be integrated with computer aided design methods for experimental optimization and validation of designs is described. The same full field data acquisition techniques have been applied to vibration measurements, and stress and vibration data can be obtained from the same experimental set up. Theoretical aspects of stress analysis using the thermoelastic effect are described. Laser Doppler interferometric methods are outlined. The combination of techniques for nondestructive testing of typical aerospace components, including composites, is illustrated. ESA

N90-11070# Intespace, Toulouse (France).
A NEW EUROPEAN VIBRATION TEST FACILITY FOR ARIANE 4 CLASS SATELLITES **c14**
Jean-Claude Pasquet and J. F. Imbert *In* ESA, Spacecraft Structures and Mechanical Testing Jan. 1989 p 643-648 (For primary document see N90-10986 02-18)
Copyright Avail: NTIS HC A99/MF E06

A vibration test facility for Ariane 4 class satellites is described. The design of this facility is unique in that it allows for minimization of test duration for heavy specimens weighing up to 4000 kg. A safety system associated with this equipment enables the testing of specimens containing up to 1000 liters of isopropyl alcohol. The test facility consists of two vertical 150 kN electrodynamic shakers, coupled with an expansion head 2100 mm in diameter and a 150 kN electrodynamic shaker coupled with a horizontal table of the same dimensions. A control and command system offers 8 control channels and 17 notching channels. A new generation measurement system, with a 256 channel capability, developed by Intespace, is connected to this equipment. ESA

N90-11071# Engineering System International, Rungis (France).
INTRINSIC DAMAGE AND STRENGTH CRITERIA FOR ADVANCED COMPOSITE LAMINATES IN SPACE APPLICATIONS **c24**
A. deRouvray, E. Haug, P. Dowlatyari, C. Stavrinidis, and A. Kreis (European Space Agency. European Space Research and Technology Center, ESTEC, Noordwijk, Netherlands) *In* ESA,

Spacecraft Structures and Mechanical Testing Jan. 1989 p 649-664 (For primary document see N90-10986 02-18)
Copyright Avail: NTIS HC A99/MF E06

Several classical strength criteria are evaluated on a large sample of test pieces with various stress concentrations and gradients loaded to ultimate failure. None of the strength criteria evaluated (K, G, Poe, Witney-Nuismer, etc) predicts satisfactorily the whole spectrum of test data. A new criterion is proposed, based on a damage mechanics concept, which fulfills the requirements of being intrinsic for both stress concentrations and stress gradients. Such a criterion is well suited for numerical simulations of composite damage and strength. Its effectiveness is demonstrated in the prediction of the scale effect on the ultimate tensile strength of center notched tensile test pieces of a cross ply laminate. It also allows to predict approximately, with the help of a simple analytical formula, the notch sensitivity effects in composite plates with cut-outs, and suggests thresholds for the applicability of low strain criteria in the analysis of the damage tolerance of composite components. ESA

N90-11072# Erno Raumfahrttechnik G.m.b.H. Bremen (Germany, F.R.).
KEY STRUCTURES MECHANICAL ISSUES OF THE EUROPEAN SPACE STATION AND PLATFORM PROGRAM COLUMBUS
S. Gazey and E. Winkelhoff *In* ESA, Spacecraft Structures and Mechanical Testing Jan. 1989 p 665-673 Previously announced as N89-28561 (For primary document see N90-10986 02-18)
Copyright Avail: NTIS HC A99/MF E06

The main technical features of the Columbus space segment: the Attached Pressurized Module (APM), integrated into NASA's Space Station Freedom; the Man Tended Free Flyer (MTFF), Europe's first step into autonomy in space, and the Polar Platform (PPF) are described. Because of the program requirements and operations scenario, Columbus elements will be subjected to new loads and environments. Operational loads/shocks induced by docking/berthing and ORU (orbital replaceable units) exchange, or crew and subsystem protection from meteoroids and space debris during very long life in orbit must be taken into consideration. These issues are discussed and solutions proposed from a systems point of view. ESA

N90-11073# Dynamic Engineering N.V., Heverlee (Belgium).
NUMERICAL MODELS FOR EXTERIOR AND INTERIOR FLUID-STRUCTURE INTERACTION PROBLEMS c34
J. P. Coyette *In* ESA, Spacecraft Structures and Mechanical Testing Jan. 1989 p 675-680 (For primary document see N90-10986 02-18)
Copyright Avail: NTIS HC A99/MF E06

The development of efficient numerical tools for acoustics and elasto-acoustics is discussed. Both finite element (FE) and boundary element (BE) methods are considered with their specific advantages and limitations. Emphasis is placed on the presentation of frequency formulations selected for software implementation. Special attention is devoted to extraction of acoustic modes from a BE model. The main features of related software are summarized and trends for future developments are outlined. ESA

N90-11074# Aerospatiale, Cannes (France).
DEPLOYMENT SIMULATION FOR 3rd GENERATION SOLAR ARRAY GSR3 c44
C. Verne and M. Rouchon *In* ESA, Spacecraft Structures and Mechanical Testing Jan. 1989 p 681-684 Sponsored by ESA (For primary document see N90-10986 02-18)
Copyright Avail: NTIS HC A99/MF E06

Deployment tests for different solar arrays are described. The Spacebus solar array deployment is tested in two dimensions. The Spot 4 array deployment is tested in three dimensions. A mock-up deployment test on an air cushion is compared to results obtained using simulation software. The third generation solar array concept equipped with Adele hinges is compared to previous solar array models. The need for greater accuracy and reliability in the deployment analysis of these third generation solar arrays is stressed. ESA

N90-11075# Engineering System International, Rungis (France).
NUMERICAL SIMULATION OF MICROMETEROIDS AND DEBRIS HYPERVELOCITY IMPACTS ON COLUMBUS PRESSURIZED MODULES
J. Dubois, F. Vogel, A. deRouvray, S. Falcone, H. G. Reimerdes, and D. Alwes (Erno Raumfahrttechnik G.m.b.H. Bremen, Germany, F.R.) *In* ESA, Spacecraft Structures and Mechanical Testing Jan. 1989 p 685-692 Sponsored by ESA/ESTEC, Noordwijk, Netherlands (For primary document see N90-10986 02-18)
Copyright Avail: NTIS HC A99/MF E06

Numerical work performed to illustrate and improve the physical mechanisms and hardening concepts for micrometeoroids and debris hypervelocity impacts, on the pressurized module and viewports of Columbus is presented. Aluminum debris particles are typically spheres 6 to 20 mm in diameter travelling at 0 to 20 km/s. Micrometeoroids are 1.5 to 6 mm in diameter and travel at over 10 km/s. Three bumper perforation calculations are presented at 3.7 and 10 km/s. A backup calculation is performed to illustrate the damage: cratering on the front face, spallation on the rear face and plastification inside. The correlation between the numerical simulation, analytical formulae and tests results is discussed. The methodology for studying the backup shield in the second phase of the research is presented. ESA

N90-11076# IKO Software Service G.m.b.H., Stuttgart (Germany, F.R.).
STSA-SPACE TELESCOPE SOLAR ARRAY INTERCONNECTORS: FROM SIMPLE APPROACHES TO COMPLEX MODELING. A CASE STUDY OF THE NECESSITY OF COMPLEX ANALYSIS c39
Ph. Deloo, M. Klein, and U. Wieland (AEG-Telefunken, Wedel, Germany, F.R.) *In* ESA, Spacecraft Structures and Mechanical Testing Jan. 1989 p 693-701 (For primary document see N90-10986 02-18)
Copyright Avail: NTIS HC A99/MF E06

The analysis of weld points in the interconnections between cells in the solar array of the Hubble space telescope is described. These welds, subjected to about 30,000 thermal cycles in the long duration low earth orbit mission, were first investigated using only locally focused two-dimensional models. The need to consider the spatial extension of the interconnectors between two cells, the layered nature of the cells, and the layered nature of the cell substrate result in large three-dimensional mathematical models. It is also shown that general effects that result from the non-linear material properties need to be considered in the low temperature range. ESA

N90-11077*# National Aeronautics and Space Administration. Marshall Space Flight Center, Huntsville, AL.
DERIVATION OF IMPROVED LOAD TRANSFORMATION MATRICES FOR LAUNCHERS-SPACECRAFT COUPLED ANALYSIS, AND DIRECT COMPUTATION OF MARGINS OF SAFETY
M. Klein, J. Reynolds (British Aerospace Public Ltd. Co., Bristol, England), and E. Ricks *In* ESA, Spacecraft Structures and Mechanical Testing Jan. 1989 p 703-719 (For primary document see N90-10986 02-18)
Copyright Avail: NTIS HC A99/MF E06 CSCL 22B

Load and stress recovery from transient dynamic studies are improved upon using an extended acceleration vector in the modal acceleration technique applied to structural analysis. Extension of the normal LTM (load transformation matrices) stress recovery to automatically compute margins of safety is presented with an application to the Hubble space telescope. ESA

N90-11078# Engineering System International, Rungis (France).
EXPLOITATION OF DATA MANAGEMENT FACILITIES FOR FINITE ELEMENT ANALYSIS IN AEROSPACE STRUCTURAL ENGINEERING APPLICATIONS c82
J. Dubois, R. Valent, J. L. Gregis, P. Carlier, M. Klein, and A.

Kreis (European Space Agency. European Space Research and Technology Center, ESTEC, Noordwijk, Netherlands) *In* ESA, Spacecraft Structures and Mechanical Testing Jan. 1989 p 721-728 Sponsored by ESA/ESTEC, Noordwijk, Netherlands (For primary document see N90-10986 02-18)
Copyright Avail: NTIS HC A99/MF E06

The ESA-CAR software system designed to reduce bottlenecks involved in the numerical analysis of spacecraft structures is described. The goals of this system are to reduce manpower and delays for such key activities as configuration and calculation control, increase quality, increase reutilization use for result replication, and facilitate heuristic knowledge transfer to individuals and organizations. ESA

19 SPACECRAFT INSTRUMENTATION

For related information see also *06 Aircraft Instrumentation* and *35 Instrumentation and Photography.*

No abstracts in this category.

20 SPACECRAFT PROPULSION AND POWER

Includes main propulsion systems and components, e.g., rocket engines; and spacecraft auxilliary power sources.

For related information see also *07 Aircraft Propulsion and Power, 28 Propellants and Fuels, 44 Energy Production and Conversion,* and *15 Launch Vehicles and Space Vehicles.*

N90-11079 Pennsylvania State Univ., University Park.
TURBULENT REACTING FLOWS IN SOLID-PROPELLANT DUCTED ROCKET COMBUSTORS Ph.D. Thesis
Dao-Lien Cherng 1988 122 p
Avail: Univ. Microfilms Order No. DA8909973

A theoretical model was developed to investigate turbulent mixing and combustion processes in the main combustion chamber of a solid-propellant ducted rocket. The formulation is based on the Favre-averaged conservation equations with a two-step chemical reaction scheme, and is solved by a semi-implicit finite-difference method. Turbulence closure is achieved using a well-known k-epsilon two-equation model. Calculated flow structures show good agreement with experimental results obtained from the flow visualization study and LDV measurements of turbulent velocity fields. Both two-dimensional and three-dimensional flow situations are considered. The influences of various parameters, including dome height and inlet inclination angle, on the propulsive performance of the system are investigated in detail. Dissert. Abstr.

N90-11080# Aeronautical Research Labs., Melbourne (Australia).
A SIMULATOR FOR A HYDROCARBON RAMROCKET FUEL GAS GENERATOR: FIRST PHASE DEVELOPMENT Propulsion Report No. 181
P. L. Buckley (Air Force Aero Propulsion Lab., Wright-Patterson AFB, OH.), S. A. Fisher, and L. W. Hillen May 1989 42 p
(AR-005-621; ARL-PROP-R-181) Avail: NTIS HC A03/MF A01

Development of a combustor to simulate the effluent of a solid hydrocarbon propellant ramrocket fuel gas generator, for use as a research tool, was undertaken. In this first phase of the work, the combustor was limited to an operating pressure of 350 kPa and was fuelled by a mixture of toluene, ethylene and oxygen. The exhaust effluent was analyzed for the compositions of both the gaseous and solid phases, and the results were compared with both theoretical predictions and published data from tests with a solid propellant gas generator. The work provides a basis for further development of simulator technology. Author

N90-11081*# National Aeronautics and Space Administration. Lewis Research Center, Cleveland, OH.
THE EFFECT OF ELECTRODE CONFIGURATION ON ARCJET PERFORMANCE
Frank M. Curran and David H. Manzella (Sverdrup Technology, Inc., Cleveland, OH.) 1989 14 p Presented at the 25th Joint Propulsion Conference, Monterey, CA, 10-12 Jul. 1989; cosponsored by AIAA, ASME, SAE, and ASEE Previously announced in IAA as A89-47044
(NASA-TM-102346; E-5054; NAS 1.15:102346) Avail: NTIS HC A03/MF A01 CSCL 21H

A radiation cooled, segmented anode was tested in a low power (1 kW class) arcjet thruster in order to study the current distribution in the attachment region of the nozzle of the thruster. The nozzle was composed of five segments insulated from one another with boron nitride spacers and matched the critical dimensions of nozzles commonly used in previous testing. The anode was configured so that the current could be collected across any combination of the segments and the potential difference between the cathode and each of the segments was monitored during testing. Author

N90-11082*# National Aeronautics and Space Administration. Lewis Research Center, Cleveland, OH.
HEAT TRANSFER TO THROAT TUBES IN A SQUARE-CHAMBERED ROCKET ENGINE AT THE NASA LEWIS RESEARCH CENTER
James A. Nesbitt and William J. Brindley Oct. 1989 33 p
(NASA-TM-102336; E-5045; NAS 1.15:102336) Avail: NTIS HC A03/MF A01 CSCL 21H

A gaseous H2/O2 rocket engine was constructed at the NASA-Lewis to provide a high heat flux source representative of the heat flux to the blades in the high pressure fuel turbopump (HPFTP) during startup of the space shuttle main engines. The high heat flux source was required to evaluate the durability of thermal barrier coatings being investigated for use on these blades. The heat transfer, and specifically, the heat flux to tubes located at the throat of the test rocket engine was evaluated and compared to the heat flux to the blades in the HPFTP during engine startup. Gas temperatures, pressures and heat transfer coefficients in the test rocket engine were measured. Near surface metal temperatures below thin thermal barrier coatings were also measured at various angular orientations around the throat tube to indicate the angular dependence of the heat transfer coefficients. A finite difference model for a throat tube was developed and a thermal analysis was performed using the measured gas temperatures and the derived heat transfer coefficients to predict metal temperatures in the tube. Near surface metal temperatures of an uncoated throat tube were measured at the stagnation point and showed good agreement with temperatures predicted by the thermal model. The maximum heat flux to the throat tube was calculated and compared to that predicted for the leading edge of an HPFTP blade. It is shown that the heat flux to an uncooled throat tube is slightly greater than the heat flux to an HPFTP blade during engine startup. Author

N90-11083# Air Force Occupational and Environmental Health Lab., Brooks AFB, TX. Human Systems Div.
EVALUATION OF ROCKET MOTOR EXHAUST AND LINER COMBUSTION BY-PRODUCTS Final Report, 3-6 Aug. 1988
Isaac Atkins, Jr. and Mark Dibben May 1989 33 p
(AD-A210747; AFOEHL-89-038EH0087EAC) Avail: NTIS HC A03/MF A01 CSCL 21/2

This laboratory conducted an evaluation of rocket motor exhaust and liner combustion by-products after four high speed rocket motor sled tests at the Holloman AFB Test Track. The Zuni, HVAR (High Velocity Air Rocket), and Nike rocket motors were evaluated. Results indicated airborne concentrations of nitric oxide, nitrogen dioxide, carbon monoxide, camphor and diethyl phthalate would

pose the greatest health risk to test track workers. Recommendations were made to have track crews wear personal protective equipment to control or reduce exposures. GRA

23 CHEMISTRY AND MATERIALS (GENERAL)

No abstracts in this category.

24 COMPOSITE MATERIALS

Includes physical, chemical, and mechanical properties of laminates and other composite materials.

For ceramic materials see *27 Nonmetallic Materials.*

N90-11084 Dayton Univ., OH.
FINITE ELEMENT ANALYSIS OF CURE-INDUCED RESIDUAL STRESS IN COMPOSITE MATERIALS Ph.D. Thesis
Habib Gerges Rai 1988 88 p
Avail: Univ. Microfilms Order No. DA8909276

Analyses of residual stresses in composites often employ the concept of a stress-free temperature, below which elastic behavior is assumed. In fact, the temperature at which gelation occurs and material memory begins depend upon the progress of the chemical reaction at a point, and in thick laminates different locations may exhibit different stress-free states. This research presents a method for predicting residual stresses in composite materials during the curing process. A heat transfer mode is employed to predict the time history of temperature and chemical reaction within the laminate. The mechanical model uses temperature as an independent variable in determining material properties, while the criterion for solidification depends upon degree of cure. This coupling of the chemical, heat transfer, and mechanical models allows more flexibility in describing the material, and eliminates the need for simplifying assumptions such as the existence of a uniform stress-free temperature. The residual stress analysis employs plate finite elements based on shear-flexible laminated plate theory. Residual deformations, strains forces, and moment resultants are obtained directly. Approximate methods for recovering pointwise residual stresses also have been implemented, and are useful for estimating interlaminar stress data. Several unsymmetric coupons have been fabricated to validate the residual stress analysis. Measurements of the residual curvature of such specimens provide indirect evidence about the residual stress states which can be compared directly with analytical results. The comparisons performed between analysis and experiment include variations in stacking sequence, coupon dimensions, and cure cycle temperature history. Author

N90-11085 Texas Univ., Austin.
ACCELERATED AGING OF METAL MATRIX COMPOSITES Ph.D. Thesis
Indranath Dutta 1988 153 p
Avail: Univ. Microfilms Order No. DA8909651

Accelerated aging of Metal Matrix Composites (MM's) with precipitation hardening matrices has often been attributed to an increase in the dislocation density in the immediate vicinity of the reinforcement. The plastic zone is generated due to differential thermal contraction of the matrix and the reinforcement during cooling from the solutionizing temperature. Here, a finite element approach was used to model the geometry of the plastic zone and the expended plastic work in the matrix and relate them to material parameters and reinforcement morphology. The information obtained was then used to relate the degree of accelerated aging to the state of plastic strain in the matrix. To identify the relative contributions of dislocations and the matrix residual stress field to accelerated aging, transmission electron miscroscopy and differential scanning calorimetry were done on 6061 Al-SiC MMCs. A theoretical model was developed to predict the rate of silicon clustering (the first step in the aging of 6061 Al) in the residual stress field around fibers in the MMC. The results were compared with the kinetics of clustering on an array of edge dislocations. It was concluded that for a given matrix dislocation density, there is a critical range of reinforcement sizes below which a residual stress mechanism dominates and above which a dislocation mechanism dominates. Dissert. Abstr.

N90-11086 Wisconsin Univ., Madison.
ON THE EFFECTIVE TRANSPORT PROPERTIES OF COMPOSITE MATERIALS Ph.D. Thesis
Shih-Yuan Lu 1988 218 p
Avail: Univ. Microfilms Order No. DA8903298

The effective thermal conductivity of a composite material containing the perfectly-conducting, perfectly-aligned, spheroidal inclusion was computed with an accuracy of up to the O(c squared) term, where c is the volume fraction of the inclusion, by taking into account the two-particle interactions. The non-absolutely convergent volume integral arising from the long-range decay of the thermal dipole was renormalized by adding a renormalization quantity which accounts for the screening effect of other particles. The relevant two-particle boundary value problems were solved by two numerical schemes: the boundary collocation method for the near field and the method-of-reflections for the far field. The necessary basis functions for the boundary collocation method and Faxen relations for the method-of-reflections were proposed and derived based on the general solution for the temperature fields in and outside an isolated ellipsoid driven by an arbitrary ambient field. Our calculations show that the use of spheroidal inclusions, when compared with spherical inclusions, results in a great enhancement in thermal conductivity in one direction while suffering only a slight decrease in the other direction. In addition, prolate spheroids are superior in enhancement to oblate spheroids. Dissert. Abstr.

N90-11087# Massachusetts Inst. of Tech., Cambridge.
STUDY OF THE APPLICATION OF AUTOMATION TO COMPOSITES MANUFACTURE Final Report, 31 Dec. 1984 - 1 Jun. 1989
Susan M. Krolewski May 1989 121 p
(Contract DAAG46-85-K-0001)
(AD-A211049; MTL-TR-89-47) Avail: NTIS HC A06/MF A01 CSCL 11/4

Several alternative manufacturing technologies were developed to replace current labor intensive manual fabrication methods for advanced thermoset composites. The objective as to evaluate the effect of direct labor savings, quality improvements and process flexibility on manufacturing cost and to identify desirable characteristics for new equipment. To estimate the cost benefits of replacing manual laborers with equipment, an economic model based on data from the literature and industry was developed. Knowledge of process physics and human error models was used to assess overall quality and estimate related costs such as rework, inspection and scrap. To evaluate process flexibility, system simulation techniques were used to analyze the tradeoffs between response time, work-in-progress inventory, equipment utilization and manufacturing cost. GRA

N90-11088# Army Lab. Command, Watertown, MA. Material Technology Lab.
Y-Si-Al-O-N GLASS FIBERS Final Report
Donald R. Messier, Robert P. Gleisner, and Ronald E. Rich May 1989 17 p
(AD-A211170; MTL-TR-89-44) Avail: NTIS HC A03/MF A01 CSCL 11/2

The excellent mechanical properties and outstanding water corrosion resistance of Y-Si-Al-O-N glasses indicate that they are attractive candidate materials for forming into high performance glass fibers. Fibers of glasses containing, respectively, 3.2 and 6.6 wt percent N were drawn freehand in air, and from glass rods

in N2. Continuous fibers (100-m long) of the former glass were melt-drawn in N2 while being wound in air outside of the glass-melting furnace. Some fibers had diameters as small as 10 um, and characterization data show that the fibers retain all of the desirable properties of the bulk glass. GRA

N90-11089# Massachusetts Univ., Amherst. Dept. of Polymer Science and Engineering.
COMPOSITES REINFORCED WITH THERMOTROPIC LIQUID CRYSTAL COPOLYESTER FIBERS
Richard L. Brady and Roger S. Porter 1 Aug. 1989 24 p
(Contract N00014-88-K-0224)
(AD-A211226; TR-38) Avail: NTIS HC A03/MF A01 CSCL 11/4

Composites reinforced with thermotropic liquid crystal copolyester fibers (Celanese Vectran) have been studied with regard to fiber properties and fiber matrix adhesion. As-spun (AS) and heat-treated (HT) fibers have been characterized. Heat treatment increases the crystal-to-nematic melting point by 40 C and increases modulus 18 percent while doubling strength. Composites made with Vectran fibers (HT) should be processed at or below 275 C, because fiber properties are significantly reduced on processing above this temperature, which corresponds to the AS melting point. GRA

N90-11090# Massachusetts Univ., Amherst. Dept. of Polymer Science and Engineering.
INTERFACIAL ADSORPTION AND CRYSTALLIZATION OF POLYCARBONATE IN CARBON FIBER COMPOSITES Interim Report
Richard L. Brady and Roger S. Porter 1 Aug. 1989 31 p
Submitted for publication
(Contract N00014-88-K-0224)
(AD-A211230; TR-37) Avail: NTIS HC A03/MF A01 CSCL 11/4

A polycarbonate (PC)/carbon fiber (CF) composite system has been examined with regard to interfacial adsorption and crystallization by altering times and temperature of annealing. Times up to 180 min and temperatures of 245, 275, and 300 C have been investigated. Transverse tensile, tranverse toughness, and scanning electron microscopy results on unidirectional, continuous-fiber composites indicate improved fiber/matrix adhesion at longer times and higher temperatures of annealing. Improvements in transverse toughness and transverse tensile strength of a factor of two is achieved. GRA

N90-11091# North Carolina Agricultural and Technical State Univ., Greensboro. Dept. of Mechanical Engineering.
EFFECT OF THERMAL AND CYCLIC LOADS ON SILICON CARBIDE YARN REINFORCED GLASS MATRIX COMPOSITES Final Report, 15 Aug. 1984 - 14 Feb. 1988
V. S. Avva and J. Sankar 11 Aug. 1989 81 p
(Contract DE-FG05-84ER-45140)
(DE89-016554; DOE/ER-45140/T1) Avail: NTIS HC A05/MF A01

This research investigated SiC fiber yarn in a borosilicate glass matrix. The following were objectives of the study: developing a suitable tabbing technique for room temperature and elevated temperature tensile testing of this new SiC yarn/glass composites; developing a procedure for specimen preparation after tabbing for proper alignment in test machine; tensile testing and development of S-N diagram at room temperature for this system; and scanning electron and optical microscopy study of fracture surfaces. DOE

N90-11092# Georgia Inst. of Tech., Atlanta. Research Inst.
LOW TEMPERATURE PROCESSING OF REACTION SINTERED SILICON NITRIDE
T. L. Starr, J. N. Harris, and D. L. Mohr Jul. 1989 31 p
(Contract DE-AC05-84OR-21400)
(DE89-017455; ORNL/Sub-87-00184/01) Avail: NTIS HC A03/MF A01

The reaction sintering process offers significant advantages for fabrication of silicon nitride matrix composites. It is a near-net-shape process, making it suitable for large and complex bodies, and its lower processing temperature, as compared to hot-pressing or sintering, is more conducive to fiber stability. Successful composites with silicon carbide reinforcement have used either randomly dispersed whiskers or oriented monofilaments. Complete nitridation of conventional silicon powders requires a long period (several days) at temperatures approaching the melting point of silicon (1410 C). Some results with ultrafine silicon powder indicate full conversion in a short time at dramatically lower temperatures. This report describes our efforts to develop an improved silicon powder for nitriding and optimized processing for this material. DOE

N90-11030# Deutsche Forschungs- und Versuchsanstalt fuer Luft- und Raumfahrt, Stuttgart (Germany, F.R.). Inst. for Structures and Design.
LIQUID INFILTRATED C/SiC: AN ALTERNATIVE MATERIAL FOR HOT SPACE STRUCTURES
W. Krenkel and H. Hald *In* ESA, Spacecraft Structures and Mechanical Testing Jan. 1989 p 325-330 (For primary document see N90-10986 02-18)
Copyright Avail: NTIS HC A99/MF E06

N90-11033# Rome Univ. (Italy). Dept. of Aerospace.
STUDY OF A GALLIUM ARSENIDE SOLAR CELL INTERCONNECTOR
R. S. Capitanio, M. Marchetti, and S. Tizzi *In* ESA, Spacecraft Structures and Mechanical Testing Jan. 1989 p 351-357 Sponsored by Fabrica Italiana Apparecchiature Radioelettriche S.p.A., Milan (For primary document see N90-10986 02-18)
Copyright Avail: NTIS HC A99/MF E06

N90-11036# Deutsche Forschungs- und Versuchsanstalt fuer Luft- und Raumfahrt, Brunswick (Germany, F.R.). Inst. fuer Strukturmechanik.
ANALYSIS OF DELAMINATION GROWTH
H. Eggers *In* ESA, Spacecraft Structures and Mechanical Testing Jan. 1989 p 377-381 (For primary document see N90-10986 02-18)
Copyright Avail: NTIS HC A99/MF E06

N90-11037# Katholieke Univ. te Leuven (Belgium). Dept. of Metallurgy and Materials Science.
INFLUENCE OF THE FIBER/MATRIX INTERFACE ON DAMAGE DEVELOPMENT IN CFRP
J. Ivens, M. Wevers, I. Verpoest, and P. DeMeester *In* ESA, Spacecraft Structures and Mechanical Testing Jan. 1989 p 383-386 (For primary document see N90-10986 02-18)
Copyright Avail: NTIS HC A99/MF E06

N90-11054# Centre National d'Etudes Spatiales, Toulouse (France).
DEVELOPMENT OF GRAPHITE-MAGNESIUM COMPOSITES FOR SPACE APPLICATIONS
Ph. Roy and J. F. Patin (Aerospatiale, Cannes, France) *In* ESA, Spacecraft Structures and Mechanical Testing Jan. 1989 p 521-527 (For primary document see N90-10986 02-18)
Copyright Avail: NTIS HC A99/MF E06

N90-11056# Aerospatiale Aquitaine, Saint-Medard en Jalles (France).
SPACE ENVIRONMENT EFFECTS ON CARBON/EPOXY MATERIALS
P. Plotard and C. Durin (Departement d'Etudes et de Recherches en Technologie Spatiale, Toulouse, France) *In* ESA, Spacecraft Structures and Mechanical Testing Jan. 1989 p 535-540 In FRENCH; ENGLISH summary (For primary document see N90-10986 02-18)
Copyright Avail: NTIS HC A99/MF E06

N90-11060# Stuttgart Univ. (Germany, F.R.). Inst. for Aircraft Design.
WORKED-IN HOLES IN THREE-DIMENSIONAL REINFORCED COMPOSITES

F. J. Arendts and Klaus Drechsler *In* ESA, Spacecraft Structures and Mechanical Testing Jan. 1989 p 573-578 Prepared in cooperation with MBB G.m.b.H., Munich, Germany, Fed. Republic of Germany and Vorwerk und Co., Kulmbach, Fed. Republic of Germany (For primary document see N90-10986 02-18)
Copyright Avail: NTIS HC A99/MF E06

N90-11061# Deutsche Forschungs- und Versuchsanstalt fuer Luft- und Raumfahrt, Brunswick (Germany, F.R.). Inst. fuer Strukturmechanik.
DELAMINATION TESTS UNDER STATIC COMPRESSION LOADING
M. Gaedke *In* ESA, Spacecraft Structures and Mechanical Testing Jan. 1989 p 579-585 (For primary document see N90-10986 02-18)
Copyright Avail: NTIS HC A99/MF E06

N90-11062# Deutsche Forschungs- und Versuchsanstalt fuer Luft- und Raumfahrt, Brunswick (Germany, F.R.). Inst. fuer Strukturmechanik.
DELAMINATION TESTS UNDER COMPRESSION-COMPRESSION AND TENSION-COMPRESSION LOADING
H. C. Goetting *In* ESA, Spacecraft Structures and Mechanical Testing Jan. 1989 p 587-592 (For primary document see N90-10986 02-18)
Copyright Avail: NTIS HC A99/MF E06

N90-11063# Katholieke Univ. te Leuven (Belgium). Dept. of Metallurgy and Materials Science.
THE 2.5D- AND 3D-FABRICS FOR DELAMINATION RESISTANT COMPOSITE LAMINATES AND SANDWICH STRUCTURES
I. Verpoest, M. Wevers, and P. deMeester *In* ESA, Spacecraft Structures and Mechanical Testing Jan. 1989 p 593-599 (For primary document see N90-10986 02-18)
Copyright Avail: NTIS HC A99/MF E06

N90-11071# Engineering System International, Rungis (France).
INTRINSIC DAMAGE AND STRENGTH CRITERIA FOR ADVANCED COMPOSITE LAMINATES IN SPACE APPLICATIONS
A. deRouvray, E. Haug, P. Dowlatyari, C. Stavrinidis, and A. Kreis (European Space Agency. European Space Research and Technology Center, ESTEC, Noordwijk, Netherlands) *In* ESA, Spacecraft Structures and Mechanical Testing Jan. 1989 p 649-664 (For primary document see N90-10986 02-18)
Copyright Avail: NTIS HC A99/MF E06

25 INORGANIC AND PHYSICAL CHEMISTRY

Includes chemical analysis, e.g., chromatography; combustion theory; electrochemistry; and photochemistry.

For related information see also *77 Thermodynamics and Statistical Physics.*.

N90-11093*# Research Inst. for Advanced Computer Science, Moffett Field, CA.
SIMPLIFIED RATE-LAW INTEGRATION FOR REACTIONS WHICH ARE FIRST ORDER IN EACH OF TWO REACTANTS
E. Levin and J. G. Eberhart (Colorado Univ., Colorado Springs.) Sep. 1988 5 p Submitted for publication
(Contract NCC2-387)
(NASA-CR-185408; NAS 1.26:185408; RIACS-TR-88.23) Avail: NTIS HC A01/MF A01 CSCL 07D

A simple procedure for integrating the rate law for chemical reactions which are first order in each of two reactants is presented. Author

N90-11094 Michigan Univ., Ann Arbor.
EVAPORATION AND COMBUSTION OF DENSE SPRAYS WITH A BIMODAL DROPLET SIZE DISTRIBUTION Ph.D. Thesis
Suk-Ho Lee 1988 144 p
Avail: Univ. Microfilms Order No. DA8907081

The evaporation and combustion of liquid fuel droplets in a stagnant atmosphere have been examined. Recently, both experiment and theory have shown that in many cases sufficiently dense fuel sprays may evaporate or burn as a group rather than as individual droplets because of the droplet interactions. The effect of the droplet interactions which arise in the interior of dense sprays can be studied by considering the vaporization of a single droplet in a confined region or bubble. Three approaches (thermodynamic, film theory and quasi-steady analyses) were used to deal with this problem. It was shown that the transition between complete and incomplete evaporation is very sensitive to the initial air temperature and to the ratio of the mass of the liquid to the air. The results of these studies were then related to the vaporization and burning characteristics of dense monodisperse sprays. In order to gain a preliminary indication of the effect of spray size distribution on the vaporization process the film analysis was extended to sprays with a bimodal droplet size distribution, and it was found that the kinetics of vaporization also depends on the ratio of the mass of the smaller to that of the larger droplets. The lowest order quasi-steady cloud behavior with a bimodal droplet size distribution showed that the cloud radius is found to decrease according to d(2)-law in analogy with single droplet theory, although with a modified vaporization constant for both purely vaporizing and burning clouds. The vaporization or burning characteristics were determined not by the droplet size distribution but by the ratio of the initial mass of the liquid to air and by the initial air temperature. Dissert. Abstr.

N90-11095# California Univ., Berkeley. Lawrence Berkeley Lab.
APPLICATIONS OF NMR SPECTROSCOPY TO THE STUDY OF ZEOLITE SYNTHESIS
Alexis T. Bell May 1989 20 p Presented at the ACS Meeting on Advances in Zeolite Synthesis, Los Angeles, CA, 25-30 Sep. 1988 Prepared in cooperation with California Univ., Berkeley
(Contract DE-AC03-76SF-00098)
(DE89-015226; LBL-26513; CONF-8809384-1) Avail: NTIS HC A03/MF A01

Nuclear magnetic resonance (NMR) spectroscopy is a powerful technique for identifying the structure and concentration of silicate and aluminosilicate anions in gels and solution used for zeolite synthesis. A review is presented of the types of species that have been observed and the dependence of the distribution of these species on pH and the nature of the cations present. DOE

N90-11096# State Univ. of New York, Buffalo. Dept. of Chemistry.
QUASI-DIFFUSION BETWEEN PHONON AND ROTON GASES IN TWO- AND THREE-DIMENSIONAL LIQUID HELIUM
Chung-In Um, Chul-Won Jun, Hyun Joon Shin (Research Inst. of Industrial Science and Technology, Pohang, Republic of Korea), and Thomas F. George Jul. 1989 28 p Submitted for publication
(Contract N00014-86-K-0043)
(AD-A210565; UBUFFALO/DC/89/TR-107) Avail: NTIS HC A03/MF A01 CSCL 20/10

Temperature variations of the quasi-diffusion constant and thermal diffusion ratio between phonon and roton gases in two and three-dimensional liquid helium are evaluated explicitly through the scattering of phonons by rotons. The diffusion constants in both dimensions decrease exponentially over the whole temperature range, while the thermal diffusion ratios increase and then decrease as temperature increases in the range from about 0.6 to about 1.1 K. GRA

N90-11097# Sandia National Labs., Albuquerque, NM. Fuel Science Div.
PHOTOCHEMICALLY-DRIVEN BIOMIMETIC OXIDATION OF ALKANES AND OLEFINS
J. A. Shelnutt and D. E. Trudell 1989 6 p Presented at the 1989 American Chemical Society National Meeting, Miami Beach, FL, 10-15 Sep. 1989
(Contract DE-AC04-76DP-00789)
(DE89-011536; SAND-89-0871C; CONF-890902-5) Avail: NTIS HC A02/MF A01

A photochemical reaction for oxidation of hydrocarbons that uses molecular oxygen as the oxidant is described. A reductive photoredox cycle that uses a tin(IV)- or antimony(V)-porphyrin photosensitizer generates the co-reductant equivalents required to activate oxygen. This 'artificial' photosynthesis system drives a second catalytic cycle, mimicking the cytochrome P sub 450 reaction, which oxidizes hydrocarbons. An iron (III)- or manganese(III)-porphyrin is used as the hydrocarbon-oxidation catalyst. Methylviologen can be used as a redox relay molecule to provide for electron-transfer from the reduced photosensitizer to the Fe or Mn porphyrin, but appears not to enhance efficiency of the process. The system is long-lived and may be used in time-resolved spectroscopic studies of the photo-initiated reaction to determine reaction rates and intermediates. DOE

N90-11098# Los Alamos National Lab., NM.
HOMOGENEOUS CATALYSTS IN HYPERSONIC COMBUSTION
David M. Harradine, John L. Lyman, Richard C. Oldenborg, Russell T. Pack, and Garry L. Schott 1989 12 p Presented at the American Physical Society Meeting, Miami, FL, 5-8 Sep. 1989
(Contract W-7405-eng-36)
(DE89-015258; LA-UR-89-2403; CONF-8909120-2) Avail: NTIS HC A03/MF A01

Density and residence time both become unfavorably small for efficient combustion of hydrogen fuel in ramjet propulsion in air at high altitude and hypersonic speed. Raising the density and increasing the transit time of the air through the engine necessitates stronger contraction of the air flow area. This enhances the kinetic and thermodynamic tendency of H2O to form completely, accompanied only by N2 and any excess H2 (or O2). The by-products to be avoided are the energetically expensive fragment species H and/or O atoms and OH radicals, and residual (2H2 plus O2). However, excessive area contraction raises air temperature and consequent combustion-product temperature by adiabatic compression. This counteracts and ultimately overwhelms the thermodynamic benefit by which higher density favors the triatomic product, H2O, over its monatomic and diatomic alternatives. For static pressures in the neighborhood of 1 atm, static temperature must be kept or brought below ca. 2400 K for acceptable stability of H2O. Another measure, whose requisite chemistry we address here, is to extract propulsive work from the combustion products early in the expansion. The objective is to lower the static temperature of the combustion stream enough for H2O to become adequately stable before the exhaust flow is massively expanded and its composition frozen. We proceed to address this mechanism and its kinetics, and then examine prospects for enhancing its rate by homogeneous catalysts.
DOE

N90-11099# Lawrence Livermore National Lab., CA.
THEORETICAL HUGONIOT OF LIQUID HYDROGEN FLUORIDE
Francis H. Ree and Daniel F. Calef Jul. 1989 5 p Presented at the American Physical Society Topical Conference on Shock Compression of Condensed Matter, Albuquerque, NM, 14-17 Aug. 1989
(Contract W-7405-eng-48)
(DE89-016504; UCRL-101434; CONF-890812-14) Avail: NTIS HC A01/MF A01

A new temperature dependent exponential-six potential for HF is presented for high temperature applications. It is used to examine effects of hydrogen bonding in liquid HF under shock conditions.
DOE

N90-11100# Sandia National Labs., Albuquerque, NM.
THERMOCHEMICAL MODEL FOR SHOCK-INDUCED CHEMICAL REACTIONS IN POROUS THERMITE: THE HEAT DETONATION MODEL
Mark B. Boslough 1989 4 p Presented at the American Physical Society Topical Conference on Shock Compression of Condensed Matter, Albuquerque, NM, 14-17 Aug. 1989
(Contract DE-AC04-76DP-00789)
(DE89-016528; SAND-89-0990C; CONF-890812-12) Avail: NTIS HC A01/MF A01

A thermochemical model was developed that treats a shock induced solid state chemical reaction as a special type of detonation, called a heat detonation to distinguish it from an ordinary explosive detonation and describe the final form that the chemical energy takes. According to shock temperature measurements, chemical energy can be released from porous reactive solids on a time scale shorter than shock-transit times in laboratory samples. By comparing the experimental shock temperature for porous thermite to that calculated by the model, the amount of thermite reacted when shocked to about 4 GPa was estimated to be between 60 and 70 percent. Calculated shock temperatures are extremely strong functions of the extent of reaction, but are relatively insensitive to the initial porosity and amount of volatile impurities. Thus, shock temperature measurements are the most useful for real time studies of shock induced exothermic chemical reactions in solids. DOE

N90-11101# Sandia National Labs., Albuquerque, NM. Dept. of Fluid and Thermal Sciences.
TIME-RESOLVED MASS SPECTROMETRY TECHNIQUE FOR STUDYING FAST TRANSIENT CHNO EXPLOSIVE DECOMPOSITION KINETICS
R. D. Skocypec and K. L. Erickson 1989 21 p Presented at the 9th International Symposium on Detonation, Portland, OR, 28 Aug. - 1 Sep. 1989
(Contract DE-AC04-76DP-00789)
(DE89-016540; SAND-88-2618C; CONF-890811-27) Avail: NTIS HC A03/MF A01

An experimental system is being developed to study the fast transient kinetics governing solid-phase decomposition and subsequent interaction with decomposition products. The first phase addresses the decomposition step. The experiment integrates a thin film sample configuration with two chemical diagnostic techniques, time-of-flight mass spectrometry and time resolved infrared spectral photography, and a pulsed laser heat source. The experiment has microsecond temporal resolution to examine both condensed phase mechanisms and concurrent gas phase species evolution from samples at temperatures up to 1000 C. Experiments are underway to demonstrate and assess the use of thin film samples with the experimental system. Results of these experiments, the diagnostic capabilities of the experimental system, and the advantages, preparation and characterization of thin film samples are presented. DOE

N90-11102# Maryland Univ., College Park. Inst. for Physical Science and Technology.
THERMOPHYSICAL PROPERTIES OF SUPERCRITICAL FLUIDS AND FLUID MIXTURES Progress Report, 15 May 1988 - 31 Jul. 1989
J. V. Sengers Aug. 1989 5 p
(Contract DE-FG05-88ER-13902)
(DE89-016568; DOE/ER-13902/1) Avail: NTIS HC A01/MF A01

The purpose of the research is to extend the theory of critical phenomena in fluids and fluid mixtures to obtain scientifically based equations that include the crossover from the asymptotic singular behavior of the thermophysical properties close to the critical point to the regular behavior of these properties far away from the critical point. DOE

N90-11103# Sandia National Labs., Albuquerque, NM. Thermomechanical and Physical Div.
EXPERIMENTAL MEASUREMENTS OF SHOCK-INDUCED VAPORIZATION IN CADMIUM AND LEAD
James R. Asay and Timothy G. Trucano 1989 4 p Presented at the American Physical Society Topical Conference on Shock Compression of Condensed Matter, Albuquerque, NM, 14-17 Aug. 1989
(Contract DE-AC04-76DP-00789)
(DE89-016877; SAND-89-0920C; CONF-890812-15) Avail: NTIS HC A01/MF A01

Time resolved techniques were used to study the shock-induced vaporization of lead and cadmium for partial states of vaporization ranging from 11 to 37 percent in lead and 42 to 56 percent in cadmium. The experimental results were compared with numerical simulations of the experiments which indicate that the expansion products are more dispersive than predicted with numerical calculations. The present data suggest that either diffusing flow between vapor and liquid phases or vaporization kinetics are important at these rates. DOE

N90-11104# Gandhi (Indira) Centre for Atomic Research, Kalpakkam (India). Radio Chemistry Programme.
A NEW INEXPENSIVE ELECTROCHEMICAL METER FOR OXYGEN IN SODIUM COOLANT
G. Periaswami, S. S. RajanBabu, and C. K. Mathews 1987 21 p
(DE89-630802; IGCAR-92) Avail: NTIS HC A03/MF A01

The development of an inexpensive oxygen meter for sodium coolant is described along with the results of the test experiments. Calcia stabilized zirconia was found to have necessary domain boundary characteristics at low temperatures for use as oxygen sensor in liquid sodium system. It is possible to obtain acceptable sensor cell resistance at temperatures as low as 230 C if K, K2O or Na, Na2O, is used as reference electrode. The performance of these cells was tested in bench top sodium loops over long periods. Their performance in terms of cell-out put variation with change in oxygen concentration in sodium was found to be satisfactory. They also have sufficently long life times since the kinetics of sodium attack on the electrolyte is slow at low temperatures. DOE

N90-11105# Connecticut Univ., Storrs. Dept. of Physics.
RADIATIONLESS TRANSITIONS AND EXCITED-STATE ABSORPTION OF LOW-FIELD CHROMIUM COMPLEXES IN SOLIDS Final Technical Report, 1 Jan. 1986 - 31 May 1989
Ralph H. Bartram 20 Jul. 1989 35 p
(Contract DAAL03-86-K-0017)
(AD-A210653; ARO-23118.6-PH) Avail: NTIS HC A03/MF A01 CSCL 09/3

The continuation of a coordinated experimental and theoretical investigation of photoluminescence quenching and excited-state absorption, major loss mechanisms in potential tunable laser materials, is reported. The materials investigated include chromium-doped crystals of cubic elpasolite structure: Cs2NaYCl6(prime), K2NaScF6, and K2NaGaF6. Photoluminescence lifetimes, measured as functions of temperature and pressure in a diamond-anvil cell, revealed a pressure-induced shift of the onset of thermal quenching to higher temperatures. This observation is consistent with the predictions of a theoretical model, proposed earlier, in which radiationless de-activation of the chromium complex is mediated by quadratic coupling to an asymmetric vibrational mode. Ab-initio embedded-molecular-cluster calculations yielded predictions of the pressure dependence of local compressibility and localized vibration frequencies in good accord with experiment, thus demonstrating the predictive capability of theoretical modeling. Raman-scattering measurements in the diamond-anvil cell provided information about the pressure dependence of both localized and host-lattice vibration frequencies. Two-photon absorption experiments designed to characterize the vibronic structure of excited states are in progress, as a prelude to the investigation of excited-state absorption spectra. GRA

N90-11106# North Carolina Central Univ., Durham. Dept. of Physics.
PRECISION MATERIALS CHARACTERIZATION IN THE NEAR MILLIMETER AND SUBMILLIMETER WAVELENGTH RANGE Final Report, 1 Oct. 1984 - 31 Dec. 1988
Jyotsna M. Dutta and Charles R. Jones 1 Jun. 1989 22 p
(Contract DAAG29-84-G-0089)
(AD-A210655; ARO-22368.3-PH-H) Avail: NTIS HC A03/MF A01 CSCL 20/2

Laser-based instrumentation which employs quasi-optical techniques to measure near millimeter wave dielectric properties was developed in this laboratory and successfully used to acquire a data base on a wide variety of materials. Included are the results for various crystalline and non-crystalline solids, semiconductor, and samples of various standard and advanced ceramics. Measurements are at 245 GHz and the results are compared with the data obtained by other researchers on similar samples. GRA

N90-11107# Washington State Univ., Pullman. Shock Dynamics Lab.
PRESSURE INDUCED RESONANCE RAMAN EFFECTS IN SHOCKED CARBON DISULFIDE Technical Report, 1 Jun. 1986 - 1 Mar. 1989
Y. M. Gupta, P. D. Horn, and C. S. Yoo 1 Mar. 1989 19 p Submitted for publication
(Contract N00014-86-K-0307)
(AD-A210665) Avail: NTIS HC A03/MF A01 CSCL 07/4

Understanding shock induced chemical processes in condensed materials requires knowledge about the molecular structure, chemical species and kinetics in these experiments. Hence, spectroscopic techniques have been used increasingly in recent years to complement the bulk or continuum measurements that are normally obtained in shock wave experiments. Time-resolved Raman spectroscopy applied to study shock-induced processes has been developed and as an example, studies of the solid carbon disulfide at 8 GPa and 160 K are presented. Pressure shifts of symmetric stretching mode, v1 and first overtone of the bending mode, 2v2 have been measured and the separation between two bands is decreased with pressure. Enhancement of the Raman cross section of carbon disulfide is observed at the higher pressures than 7 GPa and this will be explained in terms of pressure induced resonance Raman effect. GRA

N90-11108# Paris VI Univ. (France).
STUDY OF HIGH FREQUENCY WATER VAPOR ABSORPTION PARAMETERS Final Report, Jun. 1988 - Jun. 1989
Jean-Marie Flaud and Claude Camy-Peyret 30 Jun. 1989 107 p
(Grant AF-AFOSR-0190-86; AF Proj. 2310)
(AD-A210676; EOARD-TR-89-11) Avail: NTIS HC A06/MF A01 CSCL 07/4

Optical remote sensing and studies of the propagation of radiation through long atmospheric paths require a precise knowledge of the spectral parameters of molecular absorbers contributing to the opacity. Because of technological considerations, the first spectroscopic efforts were devoted to the mid and infrared regions. Recent advances in optics have now created a need for precise spectroscopic data from the near-infrared to the visible and the purpose of the project was to improve the spectroscopic parameters of water vapor which is, with oxygen, the main atmospheric absorber in this spectral region. This report summarizes the results obtained on the water absorption spectrum in the spectral regions 8000 to 11500/cm and 13500 to 22700/cm. The spectra were recorded at high resolution with a Fourier transform spectrometer using a multipath cell allowing path lengths up to 434 m. A thorough analysis has been performed and greatly improved line positions, intensities and assignments have been obtained providing a precise and complete picture of the water spectra in the concerned spectral regions. These results of important atmospheric interest will be included in the next version of the HITRAN data base. GRA

N90-11109# Cornell Univ., Ithaca, NY. Dept. of Chemistry.
DYNAMICS OF NUCLEATION AT ELECTROCHEMICAL INTERFACES VIA SURFACE EXAFS AND STANDING WAVE MEASUREMENTS Final Report, 1 Jun. 1986 - 31 May 1989
Hector D. Abruna 11 Jul. 1989 9 p
(Contract DAAL03-86-G-0038)
(AD-A210733; ARO-23782.11-CH-F) Avail: NTIS HC A02/MF A01 CSCL 07/4

We have been involved in the use of X-rays as in-situ probes of electrochemical interfaces in an attempt to gain some insights as to how interfacial structure affects electrochemical reactivity. X-rays provide an ideal tool for these studies because of their short wavelength and significant propagation distances even in the presence of a condensed phase. Our work on surface extended X-ray absorption fine structure (EXAFS) has centered on the study of the structure of underpotentially deposited metal and redox polymer films on electrodes. Underpotential deposition (UPD) refers to the deposition of metallic layers on an electrode of a different material. The X-ray standing wave (XSW) technique represents an extremely sensitive tool for determining the position of impurity atoms within a crystal or adsorbed onto crystal surfaces. GRA

N90-11110# Ecole Polytechnique Federale de Lausanne (Switzerland). Inst. de Chimie Physique.
ENHANCED OXIDATION AND SOLOVOLYSIS REACTIONS IN CHEMICALLY INERT MICROHETEROGENEOUS SYSTEMS Final Report
Andre M. Braun May 1989 23 p
(Contract DAJA45-85-C-0026; DA Proj. 1L1-61102-BH-57)
(AD-A210748; R/D-5038-CH-01) Avail: NTIS HC A03/MF A01 CSCL 07/4

The aim was to test the working hypothesis of an enhanced oxidative degradation of organic substrates solubilized in peroxide containing microemulsions. This work contains therefore three main topics: The stability of H2O2 containing microemulsions and the research for a potential catalytic effect of its decomposition; the qualitative and quantitative analysis of the intermediates of the H2O2 decomposition; and kinetic investigations on the reactivity of these intermediates towards solubilized organic substrates and evaluation of the efficiencies of these oxidation reactions. Both, the increased solubilization capability of microemulsions and an accelerated decomposition of H2O2 may be exploited for decontamination. The kinetic results of the reactivity of the superoxide anion will be reported as soon as the experiments are reproduced. The preliminary results are contained for the first pulsed radiolysis experiments. The quantitative analysis of hydroxyl radical in microemulsions and corresponding kinetic investigations will be the subject of a research proposal for a second project. GRA

N90-11111# Ohio State Univ., Columbus.
FORTY-FOURTH SYMPOSIUM ON MOLECULAR SPECTROSCOPY Final Report
K. Narahart Rao Jun. 1989 183 p Symposium held in Columbus, OH, 12-16 Jun. 1989
(Contract DAAL03-89-G-0020)
(AD-A210752; ARO-26430.1-PH-CF) Avail: NTIS HC A09/MF A01 CSCL 07/4

The forty-fourth symposium on Molecular Spectroscopy was held as scheduled. A report containing the abstracts of papers presented has been published by the Ohio State University. GRA

N90-11112# Army Lab. Command, Fort Monmouth, NJ. Electronics Technology and Devices Lab.
POLARIZATION MATRICES OF LITHIUM TETRABORATE Technical Report, Jan. 1988 - Jan. 1989
Arthur Ballato Jun. 1989 29 p
(AD-A210774; SLCET-TR-89-3) Avail: NTIS HC A03/MF A01 CSCL 09/1

In analytical treatments of piezoelectric-acoustic transducers, signal processors, and resonators, the electrochemical transduction mechanism is most often expressed in terms of the elements of the piezoelectric (e) or (d) matrices. Molecular interpretations of piezoelectricity, and especially electrooptical applications, usually involve polarization as the preferred variable, and consequently the alternative (a) and (b) matrices are of interest. The elements of these latter sets are calculated for lithium tetraborate from measured elastopiezodielectric constants taken from the literature. GRA

N90-11113# INTEL Corp., Santa Clara, CA.
REACTIVE ION ETCHING OF SIC THIN FILMS BY MIXTURES OF FLUORINATED GASES AND OXYGEN Interim Technical Report
W. S. Pan and A. J. Steckl 1989 43 p Prepared in cooperation with Cincinnati Univ., OH
(Contract N00014-81-K-0605; NR Proj. 056-768)
(AD-A211046; UC-TR-19; JECS-89-04-135) Avail: NTIS HC A03/MF A01 CSCL 07/4

Reactive ion etching (RIE) of SiC thin films was investigated in depth in a variety of fluorinated gas plasmas, such as SF6, CBrF3 and CHF3 mixed with oxygen. The optical emission spectrum of the RF plasma and the plasma-induced dc bias were monitored to explore the etching mechanisms. Argon actinometry was used to convert the plasma emission intensity to relative concentration of plasma species in order to more accurately quantify the etching process. Plasma conditions, such as composition of gas mixture, pressure, power were investigated in order to achieve selective SiC-to Si etching and anisotropic patterning of SiC thin films. A carbon-rich surface on the etched SiC films was found for all gases. The SiC etching mechanism in fluorinated gases was deduced from loading experiments, surface analysis and other etching phenomena. Evidence of the chemical reaction between carbon and oxygen is presented. No evidence of chemical reaction between fluorine and carbon was observed. A combined chemical and physical etching mode, supported by experiments, is suggested. A carbon blocking mechanism is proposed to understand the etching profile in all etching gases. GRA

N90-11114# Michigan State Univ., East Lansing. Dept. of Mathematics.
SOLIDIFICATION FRONT/VISCOUS PHASE TRANSITIONS, FORWARD-BACKWARD HEAT EQUATIONS Final Report, 1 Jun. 1987 - 28 Feb. 1989
Amy Novick-Cohen 26 Jul. 1989 4 p
(Grant AF-AFOSR-0267-87; AF Proj. 2304)
(AD-A211068; AFOSR-89-1064TR) Avail: NTIS HC A01/MF A01 CSCL 07/4

Topics addressed include: instability of periodic states for the Sivashinsky equation; the Cahn-Hillard equation; and the stable patterns in viscous diffusion equation. Each of the equations dealt with solidification and phase change/separation. Author

N90-11115# Johns Hopkins Univ., Laurel, MD. Applied Physics Lab.
MODIFICATIONS TO THE AEROTHERM CHARRING MATERIAL THERMAL RESPONSE AND ABLATION PROGRAM (CMA) FOR CARBON ABLATION ANALYSIS
C. C. Chan Mar. 1989 91 p
(Contract N00039-87-C-5301)
(AD-A211069; JHU/APL/TG-1373; DE89-015140) Avail: NTIS HC A05/MF A01 CSCL 07/2

Modifications to the Aerotherm Charring Material Thermal Response and Ablation Program (CMA) have been made to resolve deficiencies that were identified during the Aerospace Nuclear Safety Program's Galileo-VEEGA ablation studies. The primary modifications deal with integrating the Hunter carbon oxidation subroutine with the mainstream ablation calculations in CMA. The modified program uses a surface temperature criterion to determine when to switch between the Hunter oxidation subroutine and the sublimation routines in CMA. The user has the option to explicitly define this temperature criterion, indirectly define it via a mass loss parameter, or generate it via a search routine. A related feature uses Hunter's algorithm to compute an ablation threshold

temperature of the material for switching between abalation and non-ablator routines. A secondary modification permits blowing to attenuate the shock layer radiation to a carbon surface. GRA

N90-11116# University Coll., London (England).
A NEW METHOD FOR THE CHARACTERIZATION OF SOLUTES AND SOLVENT PHASES USING SOLVATOCHROMIC PARAMETERS Interim Progress Report No. 5
Michael H. Abraham and Gary S. Whiting 1989 45 p
(Contract DAJA45-87-C-0004)
(AD-A211238; R/D-5390-CH-01) Avail: NTIS HC A03/MF A01 CSCL 07/4

We now have an extensive data base of parameters that effectively characterize monofunctional solutes as regards solubility-related properties. Henceforth we shall be able to work on two concurrent lines of research, and in this report we set out our medium-term program and detail the results we have achieved so far. This research report contains data on the following subjects: determination of Sigma Beta 2 values by high performance liquid chromatography (HPLC); application to transfer of solutes from hexadecane to water; application to octanol/water partition coefficients; application to the characterization of iso-octane solvent and iso-octane/water partition coefficients; application to the characterization of methanol solvent; and application to the effect of airborne chemicals on respiratory tract irritation in mice. GRA

N90-11117# IIT Research Inst., Bartlesville, OK.
THE EFFECT OF DEGREE OF AROMATICITY AND ALKYL SUBSTITUTION OF POLYAROMATIC HYDROCARBONS ON INSTRUMENTAL RESPONSE FACTORS
J. S. Thomson, J. W. Reynolds, S. K. T. Yu, S. Y. Tang, and R. D. Grigsby Sep. 1989 61 p
(Contract DE-FC22-83FE-60149)
(DE89-000761; NIPER-200) Avail: NTIS HC A04/MF A01

Average gas chromatographic (flame ionization detection) and ultraviolet spectroscopic response factors and high resolution (HR) low voltage, electron impact, mass spectroscopic (MS) sensitivities were obtained for polyaromatic hydrocarbon mixtures from four different fossil fuels. These mixtures were obtained from neutral-aromatic fractions by heart-cutting 1-through 5-aromatic-ring compound types using charge-transfer liquid chromatography. Liquid chromatographic separation into fractions of a given number of condensed aromatic rings was verified independently using synchronized scanning fluorimetry. Gas chromatographic relative response factors for all fuels reached a minimum at three aromatic rings, and then increased again. Ultraviolet molar absorptivities of each ring number group at 254 nm were found to be similar for different boiling ranges within each fuel type studied, and generally agreed within a factor of two between fuel types. HR/MS sensitivities of 1- through 3-ring fractions were found to decrease for lower boiling fractions containing long alkyl chains, and increase as both boiling point and ring number of the fractions increased. DOE

N90-11118# Washington Univ., Seattle. Dept. of Physics.
X-RAY AND GAMMA-RAY SPECTROSCOPY OF SOLIDS UNDER PRESSURE Annual Technical Progress Report, Oct. 1988 - Oct. 1989
Robert L. Ingalls 30 Jun. 1989 8 p
(Contract DE-FG06-84ER-45163)
(DE89-017271; DOE/ER-45163/12) Avail: NTIS HC A02/MF A01

This report summarizes studies of various materials at high pressures by means of X-ray and (gamma)-ray absorption spectroscopy. It is to be recalled that pressure is a fundamental thermodynamic variable. In particular it enables one to control the state of the material, such as liquid or solid, insulating or conducting, para- or ferromagnetic, etc. We have developed such techniques suitable for use with synchrotron radiation such as at the Stanford Synchrotron Radiation Laboratory (SSRL). DOE

N90-11119# Brookhaven National Lab., Upton, NY. Dept. of Physics.
SPIN FLUCTUATIONS AND EXCITATIONS IN A 2D xy-FERROMAGNET: CoCl2 IN GRAPHITE
D. G. Wiesler, H. Zabel, and S. M. Shapiro 1989 7 p Presented at the 5th International Symposium on Graphite Intercalation Compounds, Berlin, Federal Rep. of Germany, 22-25 May 1989
(Contract DE-AC02-76CH-00016)
(DE89-017600; BNL-42810; CONF-890519-1) Avail: NTIS HC A02/MF A01

The spin fluctuations and excitations in the stage 2 CoCl2-graphite intercalation compound was investigated by neutron scattering. This compound has easy-plane anisotropy and sufficiently weak interplanar interaction to qualify as a test material for Kosterlitz-Thouless-Berezinsky type phase transitions. Quasi-elastic scattering measurements were performed to determine the temperature variation of the spin correlation length xi above the two dimensional ordering transition. The dependence on wave vector and temperature of the inelastic scattering cross section, consisting of both a central peak, associated with vortex diffusion, and spin wave, which become strongly damped above the transition temperature was also probed. DOE

N90-11120# Max-Planck-Institut fuer Stroemungsforschung, Goettingen (Germany, F.R.).
CHEMILUMINESCENT ION-MOLECULE REACTIONS OF GROUP-3 IONS WITH HALOGENS: NEW OPTICAL SPECTRA AND REACTION DYNAMICS Thesis [CHEMOLUMINESZENTE IONEN-MOLEKUELREAKTIONEN VON IONEN DER DRITTEN HAUPTGRUPPE MIT HALOGENEN: NEUE OPTISCHE SPEKTREN UND REAKTIONSDYNAMIK]
B. Mueller Aug. 1988 145 p In GERMAN
(MPIS-18/1988; ISSN-0436-1199; ETN-89-94570) Avail: NTIS HC A07/MF A01; Max-Planck Inst. fuer Stroemungsforschung, Boettinger Strasse 6-8, 3400 Goettingen, Fed; Republic of Germany, 30 DM

Molecular ions of the type AX(+), where A is an atom of group 3 (B, Al, Ga, In) and X is an halogen atom (F, Cl, Br) were investigated. The experiments were performed in an ion-beam-gas set-up under single-collision conditions, allowing the measurement of reaction cross sections. The observed spectra of ten ions AX(+) were analyzed, revealing band systems corresponding to several transitions in alkaline earth halogenides. The electronically excited states are explained by their electron structure. The types of binding can be classified in an ion or covalent way. This interpretation is completely in agreement with ab initio calculations. The absolute chemiluminescence cross sections for the reactions of Al(+) with F2 and Cl2, as well as the damping cross sections were determined, in good agreement with simple model calculations. ESA

N90-11121# Swedish Defence Research Establishment, Stockholm.
LASER RAMAN SPECTROSCOPY: A LITERATURE REVIEW
Helena Nilsson Apr. 1989 42 p In SWEDISH; ENGLISH summary
(FOA-C-20753-2.3; ISSN-0347-3694; ETN-89-94935) Avail: NTIS HC A03/MF A01

Laser Raman spectroscopy is reviewed and the possibilities of using the method for ignition studies are given. Ignition is a fast and transient sequence where intermediates with a short lifetime are common. The report covers forty different articles. The items addressed included combustion and even concentration measurements, the ways of measuring the ignition phenomena, the decomposition of explosives and the different ways of obtaining the decomposition chains, and the measuring methods. Raman spectroscopy is concluded to be a possible method for measuring decomposition processes. ESA

26 METALLIC MATERIALS

Includes physical, chemical, and mechanical properties of metals, e.g., corrosion; and metallurgy.

N90-11122# Pacific Northwest Lab., Richland, WA.
FREEZE-DRIED PROCESSING OF TUNGSTEN HEAVY ALLOYS
G. D. White and W. E. Gurwell Jun. 1989 41 p Sponsored by Army
(Contract DE-AC06-76RL-01830)
(DE89-015171; PNL-6887) Avail: NTIS HC A03/MF A01

Tungsten heavy alloy powders were produced from freeze-dried aqueous solutions of ammonium metatungstate and, principally, sulfates of Ni and Fe. The freeze-dried salts were calcined and hydrogen reduced to form very fine, homogeneous, low-density, W heavy alloy powders having a coral-like structure with elements of approximately 0.1 (mu)m in diameter. The powders yield high green strength and sinterability. Tungsten heavy alloy powders of 70, 90, and 96 percent W were prepared by freeze drying, compacted, and solid-state (SS) sintered to fully density at temperatures as low as 1200 C and also at conventional liquid-phase (LP) sintering temperatures. Solid-state sintered microstructures contained polygonal W grains with high contiguity; the matrix did not coat and separate the W grains to form low-contiguity, high-ductility structures. Liquid-phase sintered microstructures were very conventional in appearance, having W spheroids of low contiguity. All these materials were found to be brittle. High levels of residual S accompanied by segregation of the S to all the microstructural interfaces are principally responsible for the brittleness; problems with S could be eliminated by using Fe and Ni nitrates rather than the sulfates. DOE

N90-11123# General Electric Co., Schenectady, NY. Knolls Atomic Power Lab.
CORROSION RATES OF STRUCTURAL MATERIALS ON THE OCEAN FLOOR
Clyde H. Barth and Richard B. Sheldon Apr. 1989 33 p
(Contracts DE-AC02-76ET-34202; DE-AC12-76SN-00052)
(DE89-015211; KAPL-4701) Avail: NTIS HC A03/MF A01

Corrosion experiments were conducted to provide insight into the nature of corrosion on the deep ocean floor. Corrosion rates were determined for carbon steel, low alloy steel, carbon steel in contact with stainless steel, Ni-Cr-Fe alloy 600, and various stainless steels in deep ocean environments. Specimens for corrosion studies were deployed mostly by submersion at depths between 3000 and 3700 meters for exposure periods of up to seven years. Experimental conditions for determining corrosion behavior were flowing, stagnant, and semi-stagnant seawater. Specimens were also completely buried in sediment and buried in sediment with the addition of a steel cover plate to blanket the sediment surface. Mean long term rates as shown in the following graph ranged from .03 to 2.75 mils per year for carbon steel (CS-516) and low alloy steel (HY-80) and up to 8.49 mils per year for carbon steel in contact with stainless steel (galvanic effect). Specimens buried in the sediment demonstrated the largest variability with individual specimen corrosion rates for carbon steel as great as 6.5 mils per year. When a steel plate covered the sediment the corrosion rate decreased to a relatively constant rate of .15 mils per year. Experiments were conducted in shallow water sites for corrosion rate comparisons with deep water exposures. DOE

N90-11124# Sandia National Labs., Albuquerque, NM.
SHOCK-INDUCED ATOMIC-SCALE STRUCTURE IN METALS
Paul A. Taylor and Brian W. Dodson 1989 9 p Presented at the American Physical Society Topical Conference on Shock Compression of Condensed Matter, Albuquerque, NM, 14-17 Aug. 1989
(Contract DE-AC04-76DP-00789)
(DE89-016539; SAND-89-0998C; CONF-890812-20) Avail: NTIS HC A02/MF A01

The first atomic-scale simulations of shock propagation using accurate many-body atomic interactions were performed. Shock propagation in copper was modeled using the embedded-atom method. Lattice instabilities, consisting of crystallographic twinning boundaries and martensitic regions, were observed to form and propagate behind the shock front for impact velocities as low as 0.01 km/sec. The twinning boundary dislocations cause a loss of shear strength, resulting in a significant reduction in shock wave velocity without causing permanent crystallographic damage. This new mode of lattice deformation is qualitatively different from the behavior characteristic of pairwise atomic interactions. DOE

N90-11125# Pacific Northwest Lab., Richland, WA.
GRAIN BOUNDARY CHEMISTRY IN IRRADIATED STAINLESS STEEL AND ITS INFLUENCE ON ENVIRONMENTAL DEGRADATION
S. M. Bruemmer, E. P. Simonen, and L. A. Charlot Aug. 1989 16 p Presented at the 4th International Symposium on Environmental Degradation of Materials in Nuclear Power Systems: Water Reactors, Jekyll Island, GA, 6-10 Aug. 1989
(Contract DE-AC06-76RL-01830)
(DE89-016827; PNL-SA-17213; CONF-890820-3) Avail: NTIS HC A03/MF A01

Radiation-induced segregation (RIS) of chromium, silicon and phosphorus and its influence on intergranular stress corrosion cracking (IGSCC) of stainless steel (SS) was investigated. Material and irradiation effects on RIS to grain boundaries were studied using ion bombardment of fine-grained, sputter-deposited SS. Damage levels up to 10 dpa were produced in near-surface regions encompassing several grain diameters in depth. The resultant bulk damage promotes RIS of silicon and depletion of chromium at grain interfaces. Silicon enrichment and chromium depletion was highly localized to within 25 nm of the boundary in 316 SS heats as measured by analytical transmission electron microscopy. No significant grain boundary enrichment of phosphorus was observed in these heats even though heats contained very high levels of phosphorus in the bulk. Grain boundary chemistry effects on the IG corrosion and SCC of 316 SS were also examined by varying phosphorus segregation and chromium depletion through controlled thermal treatments. DOE

N90-11126# Oak Ridge National Lab., TN. Solid State Div.
NEUTRON SCATTERING STUDIES OF AMORPHOUS INVAR ALLOYS
J. A. Fernandez-Baca 1989 16 p Presented at the International Symposium on Magnetoelasticity and Electronic Structure of Transition Metals, Alloys, and Films, Duisburg, Fed. Republic of Germany, 20-22 Mar. 1989
(Contract DE-AC05-84OR-21400)
(DE89-016868; CONF-8903103-2) Avail: NTIS HC A03/MF A01

Recent inelastic neutron scattering experiments were performed to study the spin dynamics of two amorphous Invar systems: Fe(100-x)B(x) and Fe(90-x)Ni(x)Zr10. As in crystalline Invar Fe65Ni35 and Fe3Pt, the excitation of conventional long-wavelength spin waves in these amorphous systems cannot account for the relatively rapid change of their magnetization with temperature. These results are discussed in terms of additional low-lying excitations which apparently have a density of states similar to the spin waves. DOE

N90-11127# Oregon Graduate Center for Study and Research, Beaverton.
DEFORMATION INDUCED MICROSTRUCTURAL AND MICROCHEMICAL CHANGES DURING THERMOMECHANICAL TREATMENT Quarterly Progress Report, 1 Oct. 1988 - 31 Dec. 1988
D. G. Atteridge, S. M. Bruemmer, L. E. Murr, W. E. Wood, A. Advani, R. Chelakara, L. A. Charlot (Pacific Northwest Lab., Richland, WA.), and L. J. Venne 1988 27 p
(Contract DE-AC06-86NE-37963)
(DE89-017266; DOE/NE-37963/10) Avail: NTIS HC A03/MF A01

Considerable activity was focused in recent years on the structure and behavior of grain boundaries. Most of this activity has centered on atomistic aspects and has not enabled direct

interpolation of results toward mechanical properties in engineering materials. As a result, significant developments in basic understanding of grain boundary structure have not significantly impacted engineering practice. Topics examined are: thermomechanical effects on grain boundary microstructure, thermomechanical effects on grain boundary microchemistry, processing and fabrication characterizing, and integration and modeling. DOE

N90-11128# Associacao Latino-Americana de Metalurgia e Materiais, Rio de Janeiro (Brazil).
USE OF OVERLAPPED REFLECTION FOR DETERMINING THE RETAINED AUSTENITE BY X-RAY DIFFRACTION
J. L. Garin and C. F. Gonzalez 1988 13 p In SPANISH; ENGLISH summary Presented at the 3rd Latin-American Coll. About Fatigue and Fracture of Materials, Rio de Janeiro (Brazil), 27 Nov. - 2 Dec. 1988
(DE89-615450; INIS-BR-1530; CONF-8811214) Avail: NTIS (US Sales Only) HC A03/MF A01

Retainec austenite in high-carbon steels was determined by means of new computation techniques applied to the processing of X-ray diffraction data. Instead of using the traditional procedure based on the weak (200) reflections of martensite and austenite, intensity measurements of the overlapped (110) peak of martensite and (111) peak of austenite were performed. The separation of the peaks was based on a Pearson VII function, which is capable of describing all diffraction profiles. The accuracy of integrated intensities was then improved with the beneficial effects of higher precision in the calculation of the amount of retained austenite. DOE

N90-11129# Gandhi (Indira) Centre for Atomic Research, Kalpakkam (India). Radio Chemistry Programme.
COMPOSITIONAL ANALYSIS OF STEELS BY X-RAY FLUORESCENCE SPECTROMETRY
K. V. G. Kutty, S. Rajagopalan, S. K. Ananthakrishnan, and R. Asuvatharaman 1988 25 p
(DE89-630803; IGCAR-95) Avail: NTIS (US Sales Only) HC A03/MF A01

The X-ray fluorescence spectrometric method of determining Ni, Cr, Mn, Mo, Ti, Si and Co in austenitic, ferritic, titanium-stabilized and low alloy steels is described. Samples in the bulk solid form (25 to 50 mm diameter and up to 50 mm height) or very small samples having a flat surface at least 5 mm in diameter are analyzed as received after a brief surface treatment. The complex matrix effects affecting the determination of the various elements are discussed. The direct calibration method as well as the mathematical method of empirical coefficients of overcoming the matrix effects is described. The precision and accuracy of the analyses are discussed. DOE

N90-11130# Gandhi (Indira) Centre for Atomic Research, Kalpakkam (India). Radio Chemistry Programme.
THERMAL EXPANSION AND PHASE TRANSFORMATION STUDIES ON SOME MATERIALS BY HIGH TEMPERATURE X-RAY POWDER DIFFRACTOMETRY
S. Rajagopalan, K. V. G. Kutty, H. K. Jajoo, S. K. Ananthakrishnan, and R. Asuvatharaman 1988 27 p
(DE89-631032; IGCAR-96) Avail: NTIS (US Sales Only) HC A03/MF A01

A high temperature chamber based on electrical resistance heating was integrated to an existing X-ray powder diffractometer. The system is capable of going upto 2500 C at programmed rates of heating. Temperature measurement is carried out by means by Pt/Rh or W/Re thermocouples or by optical pyrometry depending upon the temperature range. Provision exists for performing high temperature X-ray diffractometry in vacuum or in a gaseous atmosphere of low X-ray absorption. The X-ray optical alignment was ensured by accurately measuring the unit cell lengths of X-ray diffraction standards like silicon and tungsten. The thermocouples were calibrated within the system by monitoring the melting points of gold and silver. The well characterized transformation of zirconia from the monoclinic to tetragonal structure occurring around 1100 C was satisfactorily reproduced. The high temperature phase transitions in some rare earth oxides were studied. Lattice parameter measurements on a variety of materials as a function of temperature up to 1500 C were carried out and the data found to be in agreement with the literature values. From the measured lattice parameter values, percentage thermal expansion and coefficients of thermal expansion were calculated for many substances from room temperature to 15000 C. DOE

N90-11131# Los Alamos National Lab., NM.
MICROSTRUCTURAL EFFECTS ON SPALL FRACTURE IN 1008 STEEL
Anna K. Zurek and Paul S. Follansbee 1989 5 p Presented at the American Physical Society Topical Conference on Shock Compression of Condensed Matter, Albuquerque, NM, 14-17 Aug. 1989
(Contract W-7405-eng-36)
(DE89-016770; LA-UR-89-2701; CONF-890812-39) Avail: NTIS HC A01/MF A01

The brittle fracture behavior of 1008 carbon steel was characterized under dynamic spall loading conditions. The role of grain size, carbide morphology, and high strain rate plastic deformation on the spall induced cleavage fracture were quantitatively estimated following the analysis of Lin, Evans, and Ritchie. DOE

N90-11132# Pacific Northwest Lab., Richland, WA.
FAILURE MODES AND MECHANISMS IN NICKEL ALLOYS: PRIMARILY AUSTENITIC STAINLESS STEEL
S. H. Bush Aug. 1989 25 p Presented at the Post Structural Materials and Reactor Technology Conference, Monterey, CA, 21-24 Aug. 1989
(Contract DE-AC06-76RL-01830)
(DE89-016823; PNL-SA-16974; CONF-8908125-5) Avail: NTIS HC A03/MF A01

Austenitic stainless steels and higher nickel alloys such as the Inconels are used extensively in the chemical and nuclear industries. Their behavior in nuclear reactors is reviewed because of the availability of information. Emphasis is given to the failure modes and mechanisms occurring in the context of causal mechanisms and the implications of alloy composition. Major use is made of the austenitic steels both AISI 304 and 316 in United States nuclear plants. This is true for both boiling water reactors (BWRs) and pressurized water reactors (PWRs). Over the years there have been many failures in these materials where failure is defined as cracking, leaking, and, rarely, catastrophic breakage. Failure mechanisms such as stress corrosion cracking, both transgranular and intergranular, fatigue, including vibrational and thermal, and other corrosion related failures are examined. DOE

N90-11133# EG and G Mound Applied Technologies, Miamisburg, OH.
ION IMPLANTATION OF TWO TITANIUM ALLOYS
Barrie D. Barton and Thomas N. Wittberg (Dayton Univ., OH.) 28 Aug. 1989 27 p
(Contract DE-AC04-88DP-43495)
(DE89-016958; MLM-3603) Avail: NTIS HC A03/MF A01

Samples of two titanium alloys, Ti-6Al-4V and Ti-15V-3Cr-3Sn-3Al, were ion implanted with a combination of nitrogen (N+) and oxygen (O+). For each alloy, implantation parameters were chosen to give implanted nitrogen concentrations of approximately 10 atom percent in one case and 50 atom percent in another, from a depth of 100 nm to a depth of 400 nm. In all but one case, dual energy (200 KeV and 90 KeV) implantations of nitrogen were used to give a relatively uniform nitrogen concentration over a region of 300 nm. In each case, oxygen was implanted at 35 KeV, following the nitrogen implantation, to give an oxygen-enriched region near the surface. The implanted samples were examined by optical microscopy and by Auger electron spectroscopy (AES). Depth profiles, determined by AES combined with argon ion sputtering, were in good agreement with theoretical predictions. Experimental observations were consistent with the

formation of a solid solution of nitrogen in a titanium alloy phase in the case of alloys implanted to a level of 10 atom percent; and compound formation was indicated in the case of alloys implanted to a level of 50 atom percent. DOE

N90-11134# Los Alamos National Lab., NM.
THE HEL (HUGONIOT ELASTIC LIMIT) AND RATE-DEPENDENT YIELD BEHAVIOR
Paul S. Follansbee 1989 6 p Presented at the American Physical Society Topical Conference on Shock Compression of Condensed Matter, Albuquerque, NM, 14-17 Aug. 1989
(Contract W-7405-eng-36)
(DE89-016981; LA-UR-89-2869; CONF-890812-24) Avail: NTIS HC A02/MF A01

Measurements of the Hugoniot Elastic Limit (HEL) are compared with measurements of the strain-rate dependent compressive yield stress in several metals. The measurements are analyzed according to standard thermal activation theory. In several cases, only data from material from a single lot are used in the comparison. Results in Ti-6Al-4V, W, Ta, and 1018 steel are presented. It is shown that in all of the materials investigated the HEL is below the mechanical threshold stress, or yield stress at 0K. Comparison of the HEL with compression measurements at low temperature and quasistatic strain rates and with compression measurements at room temperature and Hopkinson bar strain rates suggests that the strain rate associated with the HEL is on the order of 10(sup 4) to 10(sup 6) s(sup (minus)1). DOE

N90-11135# Technische Univ., Berlin (Germany, F.R.). Fachbereich Werkstoffwissenschaften.
INFLUENCE OF GRAIN REFINING ON THE CASTING, PHYSICAL, MECHANICAL, AND ELECTROCHEMICAL PROPERTIES OF TECHNICAL ALUMINUM Ph.D. Thesis [EINFLUSS DER KORNFEINUNG AUF DIE GIESSTECHNISCHEN, PHYSIKALISCHEN, MECHANISCHEN UND ELEKTROCHEMISCHEN EIGENSCHAFTEN VON TECHNISCHEM ALUMINIUM]
Wolfgang Krippahl 1988 229 p In GERMAN
(ETN-89-94661) Avail: NTIS HC A11/MF A01

The effects of grain refining additives on the casting engineering properties such as strength, deformability and corrosion resistance, are investigated using as an example technical aluminum and the additive AlTi5B1. The solidification behavior and the grain refining mechanisms are explained. For the tests, an AlTi5B1 master alloy (0 to 0.25 m percent) was added to the melt at 720 C. The effects of different percentages of additives on the properties of the casting are determined for the structure of the fine-grain Al sample, the electrical and thermal conductivity, cold working by tensile loading and rolling, hardness, hot working, surface finishing hardening, flowing property, form filling capability, heating crack sensitivity, porosity, and corrosion resistance. ESA

N90-11136# Technische Univ., Berlin (Germany, F.R.). Fachbereich Werkstoffwissenschaften.
INVESTIGATION OF COMMERCIAL Al-Ti AND Al-Ti-B MASTER ALLOYS AND DEVELOPMENT OF A NEW GRAIN REFINING AGENT BASED ON CARBIDES FOR ALUMINUM AND ALUMINUM ALLOYS Ph.D. Thesis [UNTERSUCHUNG DER HANDELSUEBLICHEN AL-TI- UND AL-TI-B-VORLEGIERUNGEN UND ENTWICKLUNG EINES NEUEN KORNFEINUNGSMITTELS AUF KARBIDBASIS FUER ALUMINIUM UND ALUMINIUMLEGIERUNGEN]
Abinash Banerji 1987 169 p In GERMAN
(ETN-89-94663) Avail: NTIS HC A08/MF A01

The growth phenomena of the different Al3Ti morphologies in Al-Ti alloys and the correlation between Al3Ti morphology and grain refining efficiency in the commercial master alloy Al-Ti5-B1 are investigated. A new grain refining master alloy on the basis of Al-Ti-C is developed. Due to problems with boron-containing alloys, boron is replaced by carbon which, in combination with Ti, is equally efficient as a grain refining agent. The different forms of the Al3Ti precipitations under different solidification conditions and the influence of the Al3Ti morphology on the grain refining of technical aluminum are determined. Chemical analyses of Al-Ti-C master alloys show insignificant quantities of free C, which are nevertheless significantly higher than the calculated equilibrium values. The Al4C3 phase is more stable than TiC. The occurrence of the ternary phase Ti3AlC is demonstrated. ESA

N90-11137# Dortmund Univ. (Germany, F.R.). Fachbereich Chemietechnik.
CONTRIBUTION TO THE TRANSCRYSTALLINE STRESS CRACK CORROSION OF AUSTENITE CHROMIUM-NICKEL STEELS Ph.D. Thesis [BEITRAG ZUR TRANSKRISTALLINEN SPANNUNGSRISSKORROSION AUSTENITISCHER CHROM-NICKEL-STAEHLE]
Reinhard Grefer 1988 138 p In GERMAN
(ETN-89-94665) Avail: NTIS HC A07/MF A01

The stress crack corrosion of austenitic Cr-Ni steels is investigated on single crystal samples, and a survey of findings is presented. The dominating effect of impurities (especially sulfides) on transcrystalline stress crack corrosion is demonstrated. Several models for the description of transcrystalline stress crack corrosion are presented. The passivation kinetics investigations allow only the demonstration of tendencies with respect to the effects of impurities on the propagation of stress corrosion cracks. ESA

N90-11138# Stuttgart Univ. (Germany, F.R.). Inst. fuer Metallkunde.
PRECIPITATION AND TRANSFORMATION TOUGHENING OF Al-Mg SIGNALS Ph.D. Thesis [AUSSCHEIDUNGS- UND UMWANDLUNGSVERSTAERKUNG VON AL-MG-SPINELLEN]
Karl-L. Weisskopf 1987 153 p In GERMAN
(ETN-89-94675) Avail: NTIS HC A08/MF A01

The technically and scientifically interesting combination of precipitation and transformation phenomena are investigated in Al-Mg-spinel ceramics. The sintering of Al-Mg spinels, the precipitation of Al2O3 in an Al-Mg spinel, the mechanical properties of Al-Mg spinels, and the structure toughening are treated. The powder treatment is characterized. The compression and grain formation during sintering of the Al-Mg-spinel mixed crystals and during the reaction sintering of the Al2O3-rich spinels is discussed. The precipitation kinetics of intergranular AlO2-particles, and the thermomechanical material properties are described. ESA

27 NONMETALLIC MATERIALS

Includes physical, chemical, and mechanical properties of plastics, elastomers, lubricants, polymers, textiles, adhesives, and ceramic materials.

For composite materials see *24 Composite Materials*.

N90-11139# Massachusetts Inst. of Tech., Cambridge. Ceramics Processing Research Lab.
BASIC RESEARCH ON PROCESSING OF CERAMICS FOR SPACE STRUCTURES Final Report, 1 Aug. 1984 - 15 Feb. 1988
H. Kent Bowen, Wendell E. Rhine, Anne Bagley Hardy, Christophe Zing, Mari-Ann Einarsrud, William C. Moffatt, Sumio Kamiya, Hyyun M. Jang (Pohang Inst. of Science and Technology, Republic of Korea), Bruce Bishop, and Mark Spotz 31 Jan. 1989 305 p Submitted for publication
(Contract F49620-84-C-0097)
(AD-A205954; AFOSR-89-0289TR) Avail: NTIS HC A14/MF A02 CSCL 11/2

The hydrolysis of alkoxide emulsion droplets was investigated for preparing un-agglomerated, submicrometer oxide ceramic particles with a homogeneous composition. This technique was used to prepare single- and mixed-oxide powders whose overall cation composition corresponded to the initial alkoxide cation composition. Uncalcined powders were amorphous, with high surface areas and low densities; upon calcination, powders densified and became crystalline. In other studies, a water-in-oil emulsion technique was investigated for preparing SrTiO3 and BaTiO3. Two AIN precursors were synthesized from

dimethylaminoalane and NH3 . Both AlN precursors gave fine, high purity AlN powders after heat-treatment; a colloidally pressed sample densified to 95 percent of theoretical density at 1750 C.
GRA

N90-11140 Ohio State Univ., Columbus.
TRANSPORT STUDIES OF CONDUCTING POLYMERS Ph.D. Thesis
Fulin Zuo 1988 156 p
Avail: Univ. Microfilms Order No. DA8907345

Experimental results of transport in emeraldine form of polyaniline are reported for the first time in the thesis. Possible models of different transport mechanisms are proposed and examined. Polyaniline family has been proven to be an interesting system in that it provides a means of systematically studying the electronic structure of polymers as a function of both the number of electrons and the number of protons on the polymer chains. Emeraldine form of polyaniline differs substantially from earlier studied polymers in several respects. First, it is not charge conjugation symmetric. Second, it is a A-B copolymer with nitrogen atoms and carbon rings in the same conjugation path. Third, it can be converted from insulating state to metallic state without change of the number of electrons on the chain. Experimental results in this thesis provides a direct evidence for insulator-to-metal transition of emeraldine with protonation. The dc conductivity, ac conductivity, thermopower, and electric field dependent conductivity measurements demonstrate that there is a phase segregation of protonated emeraldine into a fully protonated and a unprotonated phase. In the metallic state, metal particles are embedded in the insulating matrix. Charge conduction is through charging energy limited tunneling between the metallic particles. In the semiconducting region, polarons and bipolarons are being formed due to protonation, and the charge conduction is via the variable range-type hopping between localized states. Together with some preliminary work done on the new highly conducting poly-acetylene, it seems now possible that one can approach the intrinsic conductivity by decreasing the number of defect states to eliminate the barriers and increasing the size of metallic islands in the conducting polymers.
Dissert. Abstr.

N90-11141 Cornell Univ., Ithaca, NY.
LOW TEMPERATURE PROPERTIES OF GLASSES Ph.D. Thesis
Eric Ralph Grannan 1989 157 p
Avail: Univ. Microfilms Order No. DA8915103

We develop a numerical model to explain the universal low temperature properties of glasses. Elastic dipoles are placed randomly on a lattice in an elastic continuum, and local minima of the system are found through Monte Carlo annealing. The normal modes of the small angle oscillations of the dipoles about the ground state lead to a large density of low frequency modes. In this model, resonant scattering of the phonons from the normal modes causes the plateau in the thermal conductivity. Harmonic excitations of the modes are responsible for the excess specific heat. We compare with the glassy crystal KBr:KCN, and using known parameters achieve quantitative agreement with experimental thermal conductivities and specific heat. We determine the barriers to 180 deg reorientations of the dipoles, and find that these are in quantitative agreement with the barriers deduced from dielectric loss experiments. We also apply the model to a structural glasses, vitreous silica, and find that we can qualitatively explain the behavior in this material. Finally, we show that for a broad range of input parameters, this model leads naturally to a plateau in the thermal conductivity and discuss the relevance to the universality of the plateau.
Author

N90-11142# National Inst. of Standards and Technology, Boulder, CO. Chemical Engineering Science Div.
INTERLABORATORY COMPARISON OF TWO TYPES OF LINE-SOURCE THERMAL-CONDUCTIVITY APPARATUS MEASURING FIVE INSULATING MATERIALS
Jerome G. Hust and David R. Smith Jan. 1989 25 p
(Contract ORNL/IA-21428)
(PB89-218325; NISTIR-89/3908) Avail: NTIS HC A03/MF A01 CSCL 11C

Measurements of apparent thermal conductivity performed by five different laboratories are compared. Subcommittee C-16.30 (Thermal Measurements) of the American Society for Testing and Materials (ASTM) sponsored the interlaboratory comparison. Two different types of line-source apparatus were used: the needle and the hot wire. The five laboratories measured thermal conductivity of Ottawa silica sand, paraffin wax, and three insulating materials (fibrous glass, expanded polystyrene, and extruded polystyrene). Comparison of the test results illustrates the interlaboratory reproducibility. The standard deviation of the thermal conductivity results for the needle apparatus is 26 percent, whereas the standard deviation of the results for the hot-wire apparatus is 17 percent.
GRA

N90-11143# Johns Hopkins Univ., Baltimore, MD. Dept. of Chemistry.
QUANTUM CHEMICAL INVESTIGATIONS OF THE MECHANISM OF CATIONIC POLYMERIZATION AND THEORETICAL PREDICTION OF CRYSTAL DENSITIES AND DECOMPOSITION PATHWAYS OF ENERGETIC MOLECULES
Annual Report, 1 Oct. 1987 - 30 Sep. 1988
Joyce J. Kaufman 15 Nov. 1988 136 p
(Contract N00014-80-C-0003)
(AD-A210322; TR-9) Avail: NTIS HC A07/MF A01 CSCL 07/4

New program developments on the CRAY Supercomputer are reported. Multireference double excitation - configuration interaction (MRD-CI) calculations for cationic polymerization of energetic oxetanes is examined. Ab-initio MRD-CI calculations for breaking a chemical bond in a molecule in a crystal or other solid environment are also covered. Ab-initio multireference coupled cluster (MR-CC) and MRD-CI calculations for protonation NH3 / deprotonation NH4(+) are discussed. A state-of-the-theoretical-art multireference coupled cluster (for both closed and opened shell systems) was rewritten, vectorized and adapted for the CRAY XMP supercomputer. crystal in the presence of voids. (AW)
GRA

N90-11144*# National Aeronautics and Space Administration. Lewis Research Center, Cleveland, OH.
HYDROGEN-SILICON CARBIDE INTERACTIONS
Andrew J. Eckel, Nathan S. Jacobson, Ajay K. Misra, and Donald L. Humphrey Sep. 1989 12 p Presented at the 4th International Conference on Hydrogen Effects on Material Behavior, Moran, WY, 12-16 Sep. 1989; sponsored in part by The Metallurgical Society Prepared in cooperation with Sverdrup Technology, Inc., Cleveland, OH
(NASA-TM-102382; E-5120; NAS 1.15:102382) Avail: NTIS HC A03/MF A01 CSCL 11C

A study of the thermochemistry and kinetics of hydrogen environmental attack of silicon carbide was conducted for temperatures in the range from 1100 C to 1400 C. Thermodynamic maps based on the parameters of pressure and oxygen/moisture content were constructed. With increasing moisture levels, four distinct regions of attack were identified. Each region is defined by the thermodynamically stable solid phases. The theoretically stable solid phases of Region 1 are silicon carbide and silicon. Experimental evidence is provided to support this thermodynamic prediction. Silicon carbide is the single stable solid phase in Region 2. Active attack of the silicon carbide in this region occurs by the formation of gases of SiO, CO, CH4, SiH4, and SiH. Analysis of the kinetics of reaction for Region 2 at 1300 C show the attack of the silicon carbide to be controlled by gas phase diffusion of H2O to the sample. Silicon carbide and silica are the stable phases common to Regions 3 and 4. These two regions are characterized by the passive oxidation of silicon carbide and formation of a protective silica layer.
Author

N90-11145# Institut Franco-Allemand de Recherches, Saint-Louis (France).
BEHAVIOUR OF VF(SUB 2)/VF(SUB 3) PIEZOELECTRIC COPOLYMERS UNDER SHOCK LOADING
F. Bauer and R. A. Graham (Sandia National Labs., Albuquerque, NM.) 1989 5 p Presented at the American Physical Society Topical Conference on Shock Compression of Condensed Matter, Albuquerque, NM, 14-17 Aug. 1989
(Contract DE-AC04-76DP-00789)
(DE89-016538; SAND-89-1022C; CONF-890812-19) Avail: NTIS HC A01/MF A01

Vinylidene fluoride and trifluoroethylene (VF2/VF3) copolymers are known to be of ferroelectric nature. Their piezoelectric properties are strong dependent on the polarization process as well as on the value of the remanent polarization. VF2/VF3 films of 55 microns in thickness were pressed at ISL. The polarization process is based on that used for the homopolymer PVDF. Reproducible values of remanent polarization of 8 micro-C/sq cm were obtained for VF2/VF3 copolymers with 70 percent of VF2 in a shock gauge configuration. Properties of these copolymers are presented. First results of the piezoelectric response of VF2/VF3 shock gauges under shock loading are presented over the range 0 to 16 Gpa. They show that the response of the copolymers is a continuous function of the shock pressure. The results are discussed. DOE

N90-11146# Los Alamos National Lab., NM. Materials Science and Technology Div.
CHARACTERIZATIONS OF SHOCK-LOADED ALUMINUM-INFILTRATED BORON CARBIDE CERMETS
W. R. Blumenthal and G. T. Gray, III 1989 10 p Presented at the American Physical Society Topical Conference on Shock Compression of Condensed Matter, Albuquerque, NM, 14-17 Aug. 1989 Sponsored by DARPA
(Contract W-7405-eng-36)
(DE89-016773; LA-UR-89-2691; CONF-890812-31) Avail: NTIS HC A02/MF A01

Shock recovery experiments were performed on aluminum infiltrated B4C cermets as a function of shock pressure and composition. The effect of strain rate under uniaxial stress loading was also studied. Compressive strength was determined to be insensitive to strain rate between 10(-3) and 10(3)/s. TEM examination revealed dislocation debris and twins in a few B4C grains aftershock loading above an upper bound HEL estimate. Below this shock pressure the B4C substructure responded elastically. Elastic moduli and strengths were highly dependent on the fraction of B4C in the cermets. However, high yield and failure strains and limited fragmentation after shock loading attest that the aluminum phase contributes significantly to the strength and integrity. DOE

N90-11147# Oak Ridge National Lab., TN. Chemical Technology Div.
FIFTH INTERNATIONAL WORKSHOP ON GLASSES AND CERAMICS FROM GELS Foreign Trip Report
Michael T. Harris 15 Aug. 1989 5 p Workshop held in Rio de Janeiro, Brazil, 6-10 Aug. 1989
(Contract DE-AC05-84OR-21400)
(DE89-016899; ORNL/FTR-3351) Avail: NTIS HC A01/MF A01

The traveler attended the Fifth International Workshop on Glasses and Ceramics from Gels and presented a paper. Papers of specific interest to ORNL involved the sol-gel processing of sulfides, the formation of ceramic precursors from emulsions and sol-gel film formation. These papers may be useful in the synthesis of advanced ceramics and in improving thin film coatings. DOE

N90-11148# Texas Univ., Arlington. Dept. of Chemistry.
ELECTRONIC AND IONIC TRANSPORT IN POLYMERS Quarterly Technical Report No. 16, 1 Apr. 1989 - 30 Jun. 1989
Martin Pomerantz, John R. Reynolds, Krishnan Rajeshwar, Dennis S. Marynick, and Timothy D. Shaffer 24 Jul. 1989 7 p
(Contract N00014-86-K-0769)
(AD-A210654; TR-16) Avail: NTIS HC A02/MF A01 CSCL 07/6

A new family of conducting polymers, based on the thiophene-phenylene-thiophene repeat unit, was prepared via electrochemical and chemical polymerization routes. Optical gaps were correlated with calculated torsional angles. The benefit of this system lies in its facile derivatization of the phenyl ring. In addition to the unsubstituted polymer, the -CH3 and -OCH3 substituted polymers were prepared. The collaborative research on large scale preparations of electroactive polymers with General Dynamics Inc. has continued. Chemical modification of poly(pyrrole tosylate) and polypyrrole/poly(styrene sulfonate) films was investigated along with the preparation of polypyrrole/polyurethane composite foams. Soluble copolymers of 3-butylthiophene/3-octylthiophene, 3-methylthiophene/3-octylthiophene and 3-methylthiophene/3-hexylthiophene were prepared by FeCl3 polymerization and are being studied and evaluated. New polypyrrole/anthraquinone sulfonate polymers were synthesized. The release of the anion was monitored via UV/VIS spectroscopy, cycle voltammetry and hydrodynamic voltammetry. The quantity and rate of the anion released are dependent on the film thickness and the applied potential. The (open -circuit anion exchange kinetics of this system was also quantified. GRA

N90-11149# Air Force Systems Command, Wright-Patterson AFB, OH. Foreign Technology Div.
THERMODYNAMIC PRINCIPLES OF THE PROCESS OF THE EFFECT OF ELECTROMAGNETIC FIELDS ON A POLYMER MELT
V. F. Miroshnichenko and N. I. Semenyuk 23 Jun. 1989 12 p Transl. into ENGLISH from Plasticheskiye Massy (USSR), no. 10, 1970 p 35-36
(AD-A210698; FTD-ID(RS)T-1133-88) Avail: NTIS HC A03/MF A01 CSCL 07/4

The effect of electromagnetic fields on a polymer melt leads to an increase in the strength of polymers while magnetostatic field virtually does not have an effect on the immobile polymer melt. However, if relative motion of magnetic field and polymer melt occurs, then, according to the laws of electrodynamics, besides magnetic field in the polymer melt appears the electric field, which will interact with the macromolecules of polymer. As a result of this can be changed the structure of polymer melt, which will be fixed/recorded in proportion to cooling fusion/melt, which must immediately be reflected in the properties of solid polymer. Change in structure of polymer melt can be considered as peculiar phase transitions. Apparently, for the polymer melts besides the phase transformations of the first and second kind there are other, possibly, mixed phase transitions. We experimentally established presence of Delta T-effect in polymer melts, which is characteristic for phase second-order transformations. Therefore in this article we use theory of second-order phase transitions in application to the phenomena in question. GRA

N90-11150# Minnesota Univ., Minneapolis. Corrosion Research Center.
CAPACITIVE BEHAVIOR IN CONDUCTING POLYMERS: THE ac IMPEDANCE AND QUARTZ CRYSTAL MICROBALANCE STUDIES Technical Report No. 1, Jul. 1988 - Jun. 1989
Katsuhiko Naoi, William H. Smyrl, Boone B. Owens, and Mary M. Lien 15 Jun. 1989 3 p Submitted for publication
(Contract N00014-88-K-0360)
(AD-A210754; TR-1) Avail: NTIS HC A01/MF A01 CSCL 07/6

Conducting polymers (like polypyrrole) show super capacitive behavior (100-1000 F/cu. cm) at low frequencies. In practical application, these materials (thin films) may be utilized in high energy capacitors. The low-frequency capacitive behavior in such films is ill defined and still unclarified because of the superposition of capacitive currents on the redox process which occurs at electroactive sites. Low-frequency capacitive behavior as well as ionic transport of anions in electropolymerized conducting polymer films, such as polypyrrole, were investigated by using ac impedance

analysis. From the impedance spectra at two different frequency regions, the diffusion coefficient of the dopant (anions) and the redox capacity for the polymer films were estimated. The mass and volume changes during the charge-discharge process were also analyzed with a quartz crystal microbalance and phase detection interferometric microscopy. GRA

N90-11151# Minnesota Univ., Minneapolis. Corrosion Research Center.
CELL PERFORMANCE OF ULTRA-THIN POLYMER CATHODE SYSTEM: THEORETICAL ENERGY AND POWER DENSITY PROJECTIONS Technical Report No. 3, Jul. 1988 - Jun. 1989
Katsuhiko Naoi, Boone B. Owens, and William H. Smyrl 15 Jun. 1989 3 p
(Contract N00014-88-K-0360)
(AD-A210786) Avail: NTIS HC A01/MF A01 CSCL 07/1

Theoretical energy and power density values for thin film lithium/liquid electrolyte/polymer cell systems were calculated by designing a specific cell model for both a prismatic cell with only the basic cell elements (no hardware) and a bipolar-design cell with some idealized practical hardware. The cell performance is compared for three different cathode polymer materials, viz., polyaniline, polypyrrole, and polyvinylferrocene. The energy and power densities are estimated as a function of cathode thickness, active cell area, and initial concentration of electrolyte for very thin cathode films (cathode thickness: Lc=1 to 100 micrometer in both single cell and bipolar designs. The energy and the power estimated at 80 Wh/kg and 800 kW/kg for 10 micrometer cathodes. Problems of battery manufacturing process were not addressed. GRA

N90-11152# Minnesota Univ., Minneapolis. Corrosion Research Center.
ELECTROLYTE DEPENDENCE OF CHARGE INJECTION PROCESSES FOR ELECTROACTIVE POLYMER FILMS Technical Report No. 4, Jul. 1988 - Jun. 1989
Katsuhiko Naoi, Mary M. Lien, and William H. Smyrl 15 Jun. 1989 4 p
(Contract N00014-88-K-0360)
(AD-A210787) Avail: NTIS HC A01/MF A01 CSCL 07/4

Differences in cyclic voltammetric behavior when using acetonitrile as an electrolyte solvent as compared to water solutions have been reported for redox polymers such as poly(vinylferrocene) (PVF). These differences are attributed to the degree of solvent uptake into the polymer film, activity of anion in the solvent, changes in site-site interaction parameters for the polymer film, and differences in the reduction wave de-swelling process. Solvents penetrate glassy polymers and induce backbone motions of the polymer fibril. In the presence of any low molecular weight liquid, the polymer is swollen, and the free volume increases. The free volume may also change as the result of electrochemical cycling between the neutral and oxidized form of PVF. Reversibility of the charge-injection process for these films varies with the salt and choice of solvent. Cyclic voltammetry and quartz crystal microbalance (QCM) studies of NaCF3SO3 and NaPF6 in acetonitrile show irreversible degradation of PVF with charge capacity decreasing with each cycle and no net increase in mass. Degradation of polymer films by reaction with anions such as CF3So3(-) has been observed. This is contrasted by reversible, non-degrading charge injection processes with these same salts in water solutions. An examination of the nature of the degradation for the polymer polyvinylferrocene (PVF) by the techniques of ac impedance, quartz crystal microbalance gravimetry (QCM), and Phase Detection Microscopy (PDIM) will be presented. GRA

N90-11153# Illinois Univ., Urbana. Dept. of Materials Science and Engineering.
INFLUENCE OF CORE-SHELL GRAINS ON THE INTERNAL STRESS STATE AND PERMITTIVITY RESPONSE OF ZIRCONIA MODIFIED BARIUM TITANATE Final Report No. 16, 1 Oct. 1987 - 20 Apr. 1989
T. R. Armstrong and R. C. Buchanan Apr. 1989 25 p
(Contract N00014-87-K-0452)
(AD-A211245) Avail: NTIS HC A03/MF A01 CSCL 11/2

Ceramic multilayer capacitor formulations based on BaTiO3 can be chemically or physically modified to exhibit temperature-stable dielectric behavior over the temperature range -55 C to 125 C. The stability can result either from chemical substitution in the ceramic, from a small-grained microstructure, or from the presence of core-shell grains which may result from chemical inhomogeneities. Heywang, described the basic structure of these latter materials as being comprised of a microstructure made up of biphasic grains (i.e., core-shell grains). BaTiO3 modified with grain boundary resident ZrO2 results in substantial inhomogeneities in the microstructure when sintered at 1320 C for 2h. These inhomogeneous regions were seen as core-shell grains in the microstructure and were accompanied by an increase in the internal stress level. The shells had a variable composition (BaTi(1-x)Zr(x)O3) and a tetragonal structure. An expansion mismatch between the core and the shell placed the core in compression resulting in a decrease in the c lattice parameter and a pseudo-cubic structure. The combination of core-shell grains and increased internal stress resulted in an essentially flat permittivity response with temperature, a condition consistent with a distribution of Curie points within the ceramic. GRA

N90-11154# Los Alamos National Lab., NM. Center for Materials Science.
INTERGRANULAR AND INTERPHASE BOUNDARIES IN CERAMICS
T. E. Mitchell, T. Roy, and O. Unal 1989 7 p Presented at the International Congress on Intergranular and Interphase Boundaries in Materials, Paris, France, 4-8 Sep. 1989
(Contract W-7405-eng-36)
(DE89-016969; LA-UR-89-2929; CONF-890977-1) Avail: NTIS HC A02/MF A01

Interfaces are of great importance in both electronic and structural ceramics. The microstructure and microchemistry of interfaces can be studied by transmission electron microscopy, both high resolution and analytical. Examples are taken from both intergranular and interphase boundaries in ceramics. The former include low angle, twin and 90 degree boundaries in YBa2Cu3O7 superconductors. Interphase boundaries include epitactic layers of YBa2Cu3O7 on SrTiO3 and LaGaO3 and non-oriented interfaces such as those that occur in coatings and composites. DOE

N90-11155# Ruhr Univ., Bochum (Germany, F.R.). Abteilung fuer Physik und Astronomie.
INVESTIGATIONS OF THE INFLUENCE OF MAGNETICALLY LONG RANGE ORDERED PHASES ON THE ELECTRONIC CHARGE TRANSPORT IN METALLIC GLASSES Ph.D. Thesis [UNTERSUCHUNGEN ZUM EINFLUSS MAGNETISCH FERNGEORDNETER PHASEN AUF DEN ELEKTRONISCHEN LADUNGSTRANSPORT IN METALLISCHEN GLAESERN]
Wilhelm Heinrich Kettler 1988 148 p In GERMAN
(ETN-89-94672) Avail: NTIS HC A07/MF A01

The influence of the magnetic state on the transport properties of amorphous ferromagnets is investigated. A computer controlled measuring system for the determination of the temperature dependence of resistance and thermoforce is developed. The magnetic contribution to the specific electrical resistance of the amorphous alloys Fe80B(20-x)C(x) and Fe82B(18-x)Ge(x) are determined. The resistance of the magnetically diluted metallic glasses Fe(x)Ni(80-x)B16Si4, CO(x)Ni(80-x)B16Si4 and Fe(x)Ni(77-x)B13Si10 is measured. The temperature and concentration dependance of the absolute thermoforce of the amorphous alloys Fe(x)Ni(80-x)B19Si and Fe(x)Ni(80-x)B20 is discussed. ESA

N90-11156# Swedish Defence Research Establishment, Stockholm.
SYNTHESIS OF POWDER WITH GEL TECHNIQUE
Knut-Fredrik Alm Mar. 1989 38 p In SWEDISH; ENGLISH summary

(FOA-C-20752-2.4(2.1); ISSN-0347-3694; ETN-89-94934) Avail: NTIS HC A03/MF A01

In the sol-gel method a homogeneous solution of the raw material is polymerized. The reaction is catalyzed by water in acid or alkaline solution. The raw material preferred is organometallic (such as methyl or ethyl compounds) or propylene oxide but acetates and inorganics may also be used. With the sol-gel method very fine-grained compounds (10 to 100 nm) of high purity are produced. For some applications residual carbon may be a disadvantage of the method. The technique is simple but requires a relatively long time (1 to 4 weeks). The sol-gel method is used in making monolites (such as radomes or optical fibers) then layers on glass for reflection and absorption of light and studies of phase equilibria or other applications. A set of powders and monolites was made. ESA

28 PROPELLANTS AND FUELS

Includes rocket propellants, igniters, and oxidizers; their storage and handling procedures; and aircraft fuels.

For related information see also *07 Aircraft Propulsion and Power, 20 Spacecraft Propulsion and Power,* and *44 Energy Production and Conversion.*

N90-11157# Hazardous Materials Technical Center, Rockville, MD.

THE THIRD CONFERENCE ON THE ENVIRONMENTAL CHEMISTRY OF HYDRAZINE FUELS Final Report

Daniel A. Stone and Floyd L. Wiseman Jan. 1988 319 p Conference held at Panama City Beach, FL, 15-17 Sep. 1987 (Contract DLA900-82-C-4426; AF Proj. 1900; AF Proj. 2054) (AD-A197632; ESL-TR-87) Avail: NTIS HC A14/MF A02 CSCL 21/4

Gas phase kinetics and models; soil, surface and matrix isolation studies; hydrazine disposal studies; detection and modeling; and toxicity are discussed. For individual titles, see N90-11158 through N90-11182.

N90-11158# Statewide Air Pollution Research Center, Riverside, CA.

ATMOSPHERIC CHEMISTRY OF THE FUEL HYDRAZINES

E. C. Tuazon and W. P. L. Carter *In* Hazardous Materials Technical Center, The third Conference on the Environmental Chemistry of Hydrazine Fuels Jan. 1988 p 18-37 (For primary document see N90-11157 02-28)

Avail: NTIS HC A14/MF A02 CSCL 21D

Selected gas phase reactions of hydrazine (N sub 2 H sub 4), monomethyl hydrazine (MMH), and unsymmetrical dimethyl hydrazine (UDMH) have been investigated under simulated atmospheric conditions in -3800 and 6400-liter Teflon reaction chambers by FT-IR spectroscopy. Their reactions with ozone and nitrogen dioxide were extensively studied, and data were also obtained concerning their reactions with formaldehyde and nitric acid. The results of these experiments are summarized, and possible mechanisms for the reaction of these hydrazines with O sub 3 and NO sub 2 are discussed. Author

N90-11159*# Lockheed Engineering and Management Services Co., Inc., Las Cruces, NM.

SURFACE-CATALYZED AIR OXIDATION OF HYDRAZINES: ENVIRONMENTAL CHAMBER STUDIES

Jan E. Kilduff, Dennis D. Davis, and Steven L. Koontz (National Aeronautics and Space Administration. White Sands Test Facility, NM.) *In* Hazardous Materials Technical Center, The Third Conference on the Environmental Chemistry of Hydrazine Fuels Jan. 1988 p 38-49 (For primary document see N90-11157 02-28)

Avail: NTIS HC A14/MF A02 CSCL 21D

The surface-catalyzed air oxidation reactions of fuel hydrazines were studied in a 6500-liter fluorocarbon-film chamber at 80 to 100 ppm concentrations. First-order rate constants for the reactions catalyzed by aluminum, water-damaged aluminum (Al/Al2O3), stainless steel 304L, galvanized steel and titanium plates with surface areas of 2 to 24 sq m were determined. With 23.8 sq m of Al/Al2O3 the surface-catalyzed air oxidation of hydrazine had a half-life of 2 hours, diimide (N2H2) was observed as an intermediate and traces of ammonia were present in the final product mixture. The Al/Al2O3 catalyzed oxidation of monomethylhydrazine yielded methyldiazine (HN = NCH3) as an intermediate and traces of methanol. Unsymmetrical dimethylhydrazine gave no detectable products. The relative reactivities of hydrazine, MMH and UDMH were 130 : 7.3 : 1.0, respectively. The rate constants for Al/Al2O3-catalyzed oxidation of hydrazine and MMH were proportional to the square of the surface area of the plates. Mechanisms for the surface-catalyzed oxidation of hydrazine and diimide and the formation of ammonia are proposed. Author

N90-11160*# National Aeronautics and Space Administration. White Sands Test Facility, NM.

AN ATMOSPHERIC PRESSURE FLOW REACTOR: GAS PHASE KINETICS AND MECHANISM IN TROPOSPHERIC CONDITIONS WITHOUT WALL EFFECTS

Steven L. Koontz, Dennis D. Davis, and Merrill Hansen (Lockheed Engineering and Management Services Co., Inc., Las Cruces, NM.) *In* Hazardous Materials Technical Center, The Third Conference on the Environmental Chemistry of Hydrazine Fuels Jan. 1988 p 50-65 (For primary document see N90-11157 02-28)

Avail: NTIS HC A14/MF A02 CSCL 21D

A new type of gas phase flow reactor, designed to permit the study of gas phase reactions near 1 atm of pressure, is described. A general solution to the flow/diffusion/reaction equations describing reactor performance under pseudo-first-order kinetic conditions is presented along with a discussion of critical reactor parameters and reactor limitations. The results of numerical simulations of the reactions of ozone with monomethylhydrazine and hydrazine are discussed, and performance data from a prototype flow reactor are presented. Author

N90-11161# Air Force Engineering and Services Center, Tyndall AFB, FL.

THE BEHAVIOR OF HYDRAZINE VAPOR IN AN ENVIRONMENTAL CHAMBER UNDER SIMULATED ATMOSPHERIC CONDITIONS

Daniel A. Stone and Floyd L. Wiseman *In* Hazardous Materials Technical Center, The Third Conference on the Environmental Chemistry of Hydrazine Fuels Jan. 1988 p 66-75 (For primary document see N90-11157 02-28)

Avail: NTIS HC A14/MF A02 CSCL 21D

A series of experiments has been conducted to determine the decay kinetics of hydrazine vapor under simulated atmospheric conditions. These experiments were carried out in a 320-l environmental simulation chamber. Conditions studied included dry and humid air, and dry and humid nitrogen. The concentration of hydrazine was monitored with long-path FT-IR spectroscopy. In contrast to earlier studies in glass vessels, there was no detectable difference in the decay rate of hydrazine in humid air or humid nitrogen was also essentially identical, but was four to five times faster than in dry air or dry nitrogen. Adsorption and permeation appear to be the major controlling factors in the decay of hydrazine in this chamber. Author

N90-11162# Air Force Engineering and Services Center, Tyndall AFB, FL.

MODELING OF HYDRAZINE SURFACE INTERACTIONS IN ENVIRONMENTAL REACTION CHAMBERS

Floyd L. Wiseman and Daniel A. Stone *In* Hazardous Materials Technical Center, The Third Conference on the Environmental Chemistry of Hydrazine Fuels Jan. 1988 p 76-85 (For primary document see N90-11157 02-28)

Avail: NTIS HC A14/MF A02 CSCL 21D

Hydrazine vapor loss data generated from Teflon film reaction chambers have been successfully modeled. The data do not fit a simple first-order rate equation, but do fit a model which allows

for surface adsorption, desorption, and permeation through the Teflon film. This implies that the reaction between hydrazine vapor and oxygen is insignificant, and that surface interactions of hydrazine vapor are the significant avenues for hydrazine vapor losses in Teflon film chambers. In humid conditions, hydrazine vapor losses are more rapid and more deviant from first-order behavior than in dry conditions. This has been modeled by assuming a hydrazine-hydrate formation. At this point it is not known whether the hydrate forms in the vapor or on the Teflon film surface. Author

N90-11163# Cranfield Inst. of Tech., Bedford (England). Chemical Systems Group.
TRACE METAL CATALYSIS OF HYDRAZINE DECOMPOSITION: THE ROLE OF CHROMIUM
J. M. Bellerby, D. A. Edwards, and D. Thompsett (Bath Univ., England) *In* Hazardous Materials Technical Center, The Third Conference on the Environmental Chemistry of Hydrazine Fuels Jan. 1988 p 86-93 (For primary document see N90-11157 02-28)
Avail: NTIS HC A14/MF A02 CSCL 21D

A new chromium (II) carbazato- complex, Cr(N2H3 CO2).H2O, prepared by the reaction of aqueous carbazic acid with chromium (II) chloride, is described. The pale lilac solid, which has been fully characterized, is stable in air but undergoes oxidation to a chromium (III) carbazato- species on treatment with excess aqueous hydrazine in the presence of carbon dioxide. Evidence is presented showing that other complexes of chromium (II) are oxidized under similar conditions, leading to the conclusion that the stable oxidation state of chromium in anhydrous hydrazine is +3. Speculations are made regarding the significance of this in relation to the known activity of dissolved chromium as a homogeneous catalyst for the decomposition of propellant hydrazine. Author

N90-11164# Birmingham Univ. (England). Dept. of Chemistry.
INTERACTIONS OF HYDRAZINES WITH COLLOIDAL CONSTITUENTS OF SOILS
M. H. B. Hayes, K. Y. Chia, and T. B. R. Yormah *In* Hazardous Materials Technical Center, The Third Conference on the Environmental Chemistry of Hydrazine Fuels Jan. 1988 p 94-107 (For primary document see N90-11157 02-28)
Avail: NTIS HC A14/MF A02 CSCL 21D

Studies are described of interactions of hydrazine and of monomethyl hydrazine (MMH) with homoionic-exchanged clays, and with humic acid preparations. The hydrazines were shown to degrade in solution in the presence of oxygen. Degradation increased with pH and was enhanced by the heterogeneous surfaces provided by clays homoionically exchanged with K+, Na+, Mg2+ and Ca2+, Mn2+, Cu2+ and Fe3+ exchanged clays catalyzed the degradation because of the abilities of the cations to engage in redox reactions. In the presence of Cu2+ montimorillonite, degradation of hydrazine in solution was rapid and vigorous. Sorption by the Na+ clay decreased as pH increased, but sorption by Al3+ and Fe3+ clays, increased as the pH was raised from 4 to 8. This is explained in terms of oxyhydroxide species, and the mechanisms of sorption are discussed. Sorption by humic acids is governed by the shapes of the macromolecules, and these in turn are influenced by the charge neutralizing cations. Much of the hydrazines sorbed are irreversibly bound. Sorption in the soil environment will be strongly influenced by the humic substances and to a lesser extent by the clays. Interactions with oxyhydroxides are intermediate between those with clays and with humic substances. Author

N90-11165# Florida Univ., Gainesville. Dept. of Soil Science.
HYDRAZINE FATE AND TRANSFORMATION IN NATURAL WATERS AND SOILS
J. J. Street and A. M. Moliner *In* Hazardous Materials Technical Center, The Third Conference on the Environmental Chemistry of Hydrazine Fuels Jan. 1988 p 108-117 (For primary document see N90-11157 02-28)
Avail: NTIS HC A14/MF A02 CSCL 21D

Widespread use of hydrazine poses a potential environmental hazard from accidental spills and leakage of underground storage vessels. The inadvertant loss of hydrazine to soils may result in contamination of soils and/or subsurface waters. Although several papers have been published on the fate of hydrazine in the environment, the mechanisms of degradation and interaction of hydrazine with soil components may not be fully understood. The disagreements found among researchers appear to be due to the interaction between hydrazine solution and the reaction vessels used in various studies. The present work deals with the effect of several environmental factors on the fate of hydrazine. The effect of certain laboratory experimental conditions has also been evaluated. Author

N90-11166# Florida Univ., Gainesville. Dept. of Soil Science.
VIBRATIONAL SPECTROSCOPIC STUDY OF THE KAOLINITE-HYDRAZINE INTERCALATION COMPLEX
C. T. Johnston, Daniel A. Stone (Air Force Engineering and Services Center, Tyndall AFB, FL.), and L. A. Applewhite *In* Hazardous Materials Technical Center, The Third Conference on the Environmental Chemistry of Hydrazine Fuels Jan. 1988 p 118-127 (For primary document see N90-11157 02-28)
Avail: NTIS HC A14/MF A02 CSCL 21D

In-situ vibrational spectroscopic methods have been used to study the interaction of hydrazine with the kaolinite mineral surface. Non-invasive Raman and FT-IR spectra were obtained for the kaolinite-hydrazine (KH) intercalation complex at low temperatures and at reduced pressure values. Strong vibrational perturbations of the guest intercalate, hydrazine, and of the clay mineral kaolinite were observed. Upon expansion of the kaolinite structure by hydrazine, a significant reduction in the intensities of the inner-surface hydroxyl groups was observed which indicated that strong hydrogen bonds were formed between the intercalated hydrazine species and the kaolinite interlamellar surface. In addition, several Raman- and IR-active vibrational modes of hydrazine were influenced by the kaolinite surface. Author

N90-11167*# Florida Univ., Gainesville.
SURFACE-CATALYZED AIR OXIDATION REACTIONS OF HYDRAZINES: TUBULAR REACTOR STUDIES
Jan E. Kilduff, Dennis D. Davis, and Steven L. Koontz (National Aeronautics and Space Administration. White Sands Test Facility, NM.) *In* Hazardous Materials Technical Center, The Third Conference on the Environmental Chemistry of Hydrazine Fuels Jan. 1988 p 128-137 (For primary document see N90-11157 02-28)
Avail: NTIS HC A14/MF A02 CSCL 21D

The surface-catalyzed air oxidation reactions of hydrazine, monomethylhydrazine, unsymmetrical dimethylhydrazine, symmetrical dimethylhydrazine, trimethylhydrazine and tetramethylhydrazine were investigated in a metal-powder packed turbular flow reactor at 55 plus or minus 3 C. Hydrazine was completely reacted on all surfaces studied. The major products of monomethylhydrazine (MMH) oxidation were methanol, methane and methyldiazene. The di-, tri- and tetra-methyl hydrazines were essentially unreactive under these conditions. The relative catalytic reactivities toward MMH are: Fe greater than Al2O3 greater than Ti greater than Zn greater than 316 SS greater than Cr greater than Ni greater than Al greater than 304L SS. A kinetic scheme and mechanism involving adsorption, oxidative dehydrogenation and reductive elimination reactions on a metal oxide surface are proposed. Author

N90-11168# Florida Univ., Gainesville.
A MATRIX-ISOLATION FT-IR STUDY OF HYDRAZINE
T. Tipton, W. B. Person, K. Kubulat, M. Vala, and Daniel A. Stone *In* Hazardous Materials Technical Center, The Third Conference on the Environmental Chemistry of Hydrazine Fuels Jan. 1988 p 138-144 (For primary document see N90-11157 02-28)
Avail: NTIS HC A14/MF A02 CSCL 21D

FT-IR spectra (4000-420 cm(-1)) have been obtained for hydrazine in argon and nitrogen matrices over a concentration range of 1:200 to 1:5000, and a temperature range of 14 K to 30

K. This investigation, in conjunction with a concurrent ab initio calculation, has eliminated much of the uncertainty in the previous matrix and vapor-phase vibrational assignments for hydrazine.
Author

N90-11169# Florida Univ., Gainesville. Dept. of Chemistry.
LOW TEMPERATURE SPECTROSCOPE OF HYDRAZINE AND AMMONIA COMPLEXES
M. Vala, M. Szczesniak, J. Szczespanski, and W. B. Person *In* Hazardous Materials Technical Center, The Third Conference on the Environmental Chemistry of Hydrazine Fuels Jan. 1988 p 145-153 (For primary document see N90-11157 02-28)
Avail: NTIS HC A14/MF A02 CSCL 21D

Complexes of hydrazine and ammonia with the neutral transition metals, Cu and Fe, have been formed and investigated spectroscopically in solid argon matrices at 12 K. Fourier transform infrared spectra of the complexes have revealed large shifts for the metal ammonia complexes and substantially smaller shifts for the metal hydrazine complexes. Recent ab initio calculations have ascribed the bonding in Cu NH3 to an electrostatic interaction between the NH3 dipole moment and the induced effective dipole of the metal atom. All the present observations may be understood on the basis of this bonding picture. Author

N90-11170*# Lockheed Engineering and Management Services Co., Inc., Las Cruces, NM.
A DIFFUSE REFLECTANCE INFRARED FOURIER TRANSFORM SPECTROSCOPIC STUDY OF ADSORBED HYDRAZINES
Dennis D. Davis, Jan E. Kilduff, and Steven L. Koontz (National Aeronautics and Space Administration. White Sands Test Facility, NM.) *In* Hazardous Materials Technical Center, The Third Conference on the Environmental Chemistry of Hydrazine Fuels Jan. 1988 p 154-166 (For primary document see N90-11157 02-28)
Avail: NTIS HC A14/MF A02 CSCL 21D

Diffuse reflectance spectroscopy of fuel hydrazines adsorbed on silica, silica-alumina and alimina surfaces indicates that the primary surface-hydrazine interaction is hydrogen bonding. Hydrazine, on adsorption to a deuterated silica surface, undergoes a rapid H/D exchange with deuterated surface silanol (Si-OD) groups. Adsorption equilibria are rapidly established at room temperature. Monomethylhydrazine and unsymmetrical dimethylhydrazine are similarly adsorbed. On adsorption, the C-H stretching and methyl deformation modes of the methylhydrazines are shifted to higher frequencies by 10 to 20 cm(-1). These shifts are postulated to be due to changes in the lone-pair electro-density on the adjacent nitrogen atom and an electronegativity effect.
Author

N90-11171# Florida Univ., Gainesville. Dept. of Soil Science.
THE SOIL MICROBIOLOGY OF HYDRAZINES
L.-T. Ou and J. J. Street *In* Hazardous Materials Technical Center, The Third Conference on the Environmental Chemistry of Hydrazine Fuels Jan. 1988 p 167-176 (For primary document see N90-11157 02-28)
Avail: NTIS HC A14/MF A02 CSCL 21D

The object was to obtain information on the effects of hydrazine (HZ) and monomethylhydrazine (MMH) on soil microbial activity, microbial degradation of chemicals, and their persistence in soils.
Author

N90-11172# Florida Univ., Gainesville. Dept. of Soil Science.
NUMERICAL SIMULATION OF HYDRAZINE TRANSPORT IN A SANDY SOIL
R. S. Mansell, S. A. Bloom, and W. C. Downs *In* Hazardous Materials Technical Center, The Third Conference on the Environmental Chemistry of Hydrazine Fuels Jan. 1988 p 177-189 (For primary document see N90-11157 02-28)
Avail: NTIS HC A14/MF A02 CSCL 21D

Aqueous solutions of hydrazinium were miscibly displaced through columns of water saturated Arredondo fine sand in order to measure breakthrough curves (BTC) for concentration in column effluent. Solutions containing approximately 200 micro-g m1(-1) hydrazinium were applied as a wide pulse and as a continuous application. Two Darcy liquid velocities of 0.5 and 5.0 cm h(-1) were used to evaluate the importance of kinetics for physical sorption upon mobility of hydrazinium in the soil columns. A finite difference numerical transport model for hydrazinium was evaluated by comparing simulated and experimental breakthrough curves. Kinetic linear physical sorption and irreversible first order chemisorption components of the transport model were observed to be critical in providing adequate simulation of hydrazinium BTC. Initial breakthrough of hydrazinium in the effluent, general shape of BTC, tailing of BTC, and maximum hydrazinium concentrations in the effluent were particularly sensitive to the magnitudes of rate coefficients for sorption and degradation. Ion exchange appeared to be of minimal importance to the transport of hydrazinium under the conditions for the column experiments. Hydrazinium mobility in this soil is clearly dependent upon pore water velocity, and other work indicates that it is also highly dependent upon concentration of hydrazinium in the soil solution.
Author

N90-11173# Argonne National Lab., IL. Energy and Environmental Systems Div.
THE CHEMISTRY OF THE HYPOCHLORITE NEUTRALIZATION OF HYDRAZINE FUELS
Kenneth L. Brubaker *In* Hazardous Materials Technical Center, The Third Conference on the Environmental Chemistry of Hydrazine Fuels Jan. 1988 p 192-201 (For primary document see N90-11157 02-28)
(Contract MIPR-N-85-14)
Avail: NTIS HC A14/MF A02 CSCL 21D

Neutralization of hydrazine fuels with hypochlorite is a recommended procedure for the treatment of fuel spills prior to disposal. Various research workers have shown, however, that incomplete reaction of hypochlorite with the methylated hydrazine fuels monomethylhydrazine and unsymmetrical dimethylhydrazine leads to a wide variety of byproducts, including N-nitrosoalkylamines. The known reaction products and mechanisms are reviewed and summarized.
Author

N90-11174# Illinois Inst. of Tech., Chicago.
OZONATION OF HYDRAZINES AND THEIR ASSOCIATED IMPURITIES
B. J. Judy, P. Kosenka, S. Lewis, H. Takimoto, H. S. Judeikis, and J. Betschard (Air Force Space Div., Los Angeles, CA.) *In* Hazardous Materials Technical Center, The Third Conference on the Environmental Chemistry of Hydrazine Fuels Jan. 1988 p 202-215 (For primary document see N90-11157 02-28)
Avail: NTIS HC A14/MF A02 CSCL 21D

IIT Research Institute (IITRI) conducted a series of experiments on the ozonation of wastewater containing hydrazine fuels (hydrazine, HZ; monomethyl hydrazine, MMH; and unsymmetrical dimethyl hydrazine, UDMH). Experiments were performed on wastewater containing two different concentrations of hydrazine fuels (3 wt percent and 300 ppm) and using various pH levels, ozone flow rates, ultraviolet (UV) radiation levels, and metal catalysts. Ozone/UV treatment of wastewater containing hydrazine fuels was shown to be capable of destroying the three hydrazine fuels, their associated impurities, and oxidation products including dimethylnitrosamine (DMNA) to environmentably acceptable levels. The DMNA concentration was reduced to below 20 ppt, yielding a clean solution free of appreciable concentrations of any harmful species.
Author

N90-11175# Aerospace Corp., Los Angeles, CA.
MODELING THE OZONOLYSIS OF HYDRAZINES WASTEWATER
H. S. Judeikis *In* Hazardous Materials Technical Center, The Third Conference on the Environmental Chemistry of Hydrazine Fuels Jan. 1988 p 216-224 (For primary document see N90-11157 02-28)
Avail: NTIS HC A14/MF A02 CSCL 21D

Modeling of the ozonolysis of wastewaters containing hydrazine

propellants is described. Destruction of the hydrazines is rapid and leads to the production of intermediates, some of which help to destroy the hydrazines themselves. The rate limiting process in the overall ozonolysis treatment is, however, the destruction of dimethyl nitrosamine (DMNA), a potent animal carcinogen produced during the ozonolysis of the hydrazines. The data indicate that, especially at low (less than or equal to 1 ppm) DMNA concentrations, this process involves the slow conversion of another intermediate to DMNA which is then rapidly destroyed by ozone. Author

N90-11176*# Lockheed Engineering and Management Services Co., Inc., Las Cruces, NM.
FUEL NEUTRALIZATION BY OZONE OXIDATION
A. B. Swartz, R. E. Agthe, I. D. Smith, and J. P. Mulholland (National Aeronautics and Space Administration. White Sands Test Facility, NM.) *In* Hazardous Materials Technical Center, The Third Conference on the Environmental Chemistry of Hydrazine Fuels Jan. 1988 p 225-243 Previously announced as X88-71397 (For primary document see N90-11157 02-28)
Avail: NTIS HC A14/MF A02 CSCL 21D

The viability of a hazardous waste disposal system based on ozone oxidation of hydrazine fuels at low aqueous concentrations in the presence of ultraviolet light (UV at 2.537 x 10(exp -7) m or 8.324 x 10(exp -7) ft) excitation was investigated. Important parameters investigated include temperature, solution pH, and ultraviolet light power. Statistically relevant experimentation was done to estimate main factor effects on performance. The best available chemical analysis technology was used to evaluate the performance of the system. Author

N90-11177# Naval Research Lab., Washington, DC. Chemistry Div.
MICROSENSOR AND PATTERN RECOGNITION TECHNIQUES IN HYDRAZINE DETECTION
S. L. Rose-Pehrsson and J. W. Grate *In* Hazardous Materials Technical Center, The Third Conference on the Environmental Chemistry of Hydrazine Fuels Jan. 1988 p 244-251 (For primary document see N90-11157 02-28)
Avail: NTIS HC A14/MF A02 CSCL 21D

A new sensor technology combined with pattern recognition methods is being investigated for hydrazine vapor detection. The sensors, chemiresistors, use vapor-sensitive coatings on a set of interdigital electrodes. All of the coatings tested have a rapid response to hydrazine, but are slow to recover. Heating the sensors improves the response and the recovery times. A coating has been tested that is sensitive to part-per-billion (ppb) concentrations of hydrazine. The coating lacks the necessary selectivity, but when used with other coating will provide a fingerprint pattern for hydrazine. Pattern recognition methods combined with sensor arrays have been used to improve the selectivity of the new sensors. Author

N90-11178# Geo-Centers, Inc., Fort Washington, MD.
HYDRAZINE DOSIMETRY
P. A. Taffe, J. H. Callahan, K. P. Crossman, and S. L. Rose-Pehrsson (Naval Research Lab., Washington, DC.) *In* Hazardous Materials Technical Center, The Third Conference on the Environmental Chemistry of Hydrazine Fuels Jan. 1988 p 252-260 (For primary document see N90-11157 02-28)
Avail: NTIS HC A14/MF A02 CSCL 21D

Passive dosimetry methods applicable to personnel and area monitoring are being developed for hydrazine detection in ambient air at the part-per-billion (ppb) level. A new badge design, molded from polyethylene, consisting of a diffusion barrier and an organic acid collection medium provides quantitation of exposure when analyzed by the NIOSH colorimetric method or a coulometric titration procedure. The diffusion barrier containing 144 one millimeter diameter holes establishes a collection rate of approximately 30 ml/min. The accuracy of data collected with this badge is within 25 percent of actual values. The dosimeter has demonstrated accuracy for up to 65 hours of sampling monomethylhydrazine (MMH) at the threshold limit value (TLV) concentration (200 ppb) with minimal interference effects from ammonia, freons, and isopropyl alcohol. A new colorimetric dosimeter has given qualitative hydrazine measurements in 15 minutes for TLV levels of MMH in relative humidities (RH) of 0 to 55 percent. It has also shown no interference from ammonia and none is expected from freons and alcohols. The potential use of the color badge in combination with the quantitative dosimeter will be discussed. Author

N90-11179# Thermedics, Inc., Woburn, MA.
DESCRIPTION OF A CHEMILUMINESCENCE DETECTOR SYSTEM SPECIFICALLY DESIGNED FOR MONITORING AIRBORNE HYDRAZINE AND OXIDIZER PROPELLANT VAPORS
F. Frain, D. Rounbehler, D. Fine, J. Buckley, and P. Nama *In* Hazardous Materials Technical Center, The Third Conference on the Environmental Chemistry of Hydrazine Fuels Jan. 1988 p 261-275 Previously announced as X88-71429 (For primary document see N90-11157 02-28)
(Contract F04701-83-C-0069)
Avail: NTIS HC A14/MF A02 CSCL 21D

A new ambient air monitoring instrument designed specifically for detection of airborne levels of the three hydrazine propellants, hydrazine, monomethylhydrazine, and unsymmetrical dimethylhydrazine, has been developed under U.S. Air Force sponsorship. The objective of this work is a fast-response, wide-response range, sub-Titan Launch Vehicle (TLV) detector for these propellants, with high specificity, insuring interference-free monitoring at very low vapor levels. The detection method relies on the unique chemistry that occurs between the hydrazine fuel vapors and acetaldehyde. A two-channel fuel vapor detection system based on this chemistry and NO chemiluminescence has been demonstrated to meet many practical detection needs. This technology has now been applied to a multiple-channel system, which monitors for both fuel and oxidizer vapors, and is capable of fully automatic operation. Author

N90-11180# Lockheed Engineering and Management Services Co., Inc., Las Cruces, NM.
MEASUREMENT OF HYDRAZINE CONTAMINATION IN SOILS
C. S. Leasure and E. L. Miller *In* Hazardous Materials Technical Center, The Third Conference on the Environmental Chemistry of Hydrazine Fuels Jan. 1988 p 276-285 (For primary document see N90-11157 02-28)
Avail: NTIS HC A14/MF A02 CSCL 21D

A dilute acidic extraction method was developed to quantitatively extract three hydrazines (hydrazine, HZ; monomethylhydrazine, MMH; and unsymmetrical-dimethylhydrazine, UDMH) from soil. The soil used in the extraction is representative of local soil, and the calculated efficiency of extraction takes oxidation of the hydrazines by the soil into account. Derivatization of the hydrazines in the resulting aqueous extracts was unsuccessful with acetone and several other agents, but successful with 2,4-pentanedione. All three hydrazines were derivatized, including UDMH which formed 2-dimethylhydrazone-4-pentanone. The derivatized hydrazines were analyzed by gas chromatograph (GC) equipped with a thermionic ionization detector operating at nitrogen-sensitive conditions. The concentration of 2,4-pentanedione in the extract was found to affect the derivatization efficiency of the three hydrazines, especially UDMH. Detection limits of the hydrazines in the soil, without preconcentration, are 0.1 ppm for HZ, 0.2 ppm for MMH, and 0.5 ppm for UDMH. This method is also applicable to the determination of hydrazines in water. Author

N90-11181# Aerospace Corp., Los Angeles, CA. Chemistry and Physics Lab.
LOW ppb LEVEL DETECTION OF TOXIC COMPOUNDS WITH A FULLY AUTOMATED CO2 LASER PHOTOACOUSTIC DETECTOR
S. M. Beck, M. L. Takayama, R. L. Corbin, and G. L. Loper *In* Hazardous Materials Technical Center, The Third Conference on

the Environmental Chemistry of Hydrazine Fuels Jan. 1988 p 286-298 (For primary document see N90-11157 02-28)
Avail: NTIS HC A14/MF A02 CSCL 21D

Progress towards developing a breadboard CO2 laser photoacoustic detector capable of monitoring a wide variety of toxic compounds at less than 100 ppb in ambient air is described. Key achievements include: (1) development of an acoustic frequency tracking device which allows use of a sensitive conditions; (2) development of an electronic spectrum analyzer which provides a means for the computer to scan the CO2 laser; (3) development of software algorithms which allow efficient and accurate analysis of a gas sample; and (4) actual analysis of laboratory prepared gas mixtures. The instrument has been demonstrated in a laboratory environment to be capable of automatically and simultaneously monitoring several toxic compounds at low ppb concentrations in hydrazine at concentrations as low as five ppb in mixtures containing three other interferent gases at concentrations as high as 600 fold greater. Author

N90-11182# Aerospace Medical Research Labs., Wright-Patterson AFB, OH. Toxic Hazards Div.
OCCUPATIONAL SAFETY CONSIDERATIONS WITH HYDRAZINE
Harvey J. Clewell, III, James N. McDougal, Marilyn E. George, and Melvin E. Andersen *In* Hazardous Materials Technical Center, The Third Conference on the Environmental Chemistry of Hydrazine Fuels Jan. 1988 p 300-308 (For primary document see N90-11157 02-28)
Avail: NTIS HC A14/MF A02 CSCL 21D

Hydrazine is a reducing agent that is most commonly used as a propellant and as an oxygen scavenger in boilers. Hydrazine is extremely irritating and has been demonstrated to produce both acute and chronic toxicity. As a result, the established permissible inhalation exposure limits are very low, and respiratory protection is required whenever vapors are present. Liquid hydrazine penetrates the skin and produces a chemical burn; therefore, some protective measures must also be taken to protect the skin from liquid contact. Often, however, a cumbersome, whole-body protective suit is worn to protect against skin contact with vapor as well. To what extent it is actually necessary to protect skin from vapor penetration had not previously been demonstrated. In an attempt to answer this question, we conducted a study with rats to compare the dermal penetration of hydrazine vapor with inhalation. Pharmacokinetic modeling was used to compare body burdens resulting from these different routes of exposure. The analysis concluded that the vapor concentration during a skin-only exposure would have to be at least 200 times higher than that during inhalation to achieve the same body burden. This type of estimation illustrates the use of predictive toxicology in occupational exposures. Author

N90-11183 Purdue Univ., West Lafayette, IN.
NITRAMINE COMPOSITE SOLID PROPELLANT MODELING Ph.D. Thesis
Frederick Steele Blomshield 1988 234 p
Avail: Univ. Microfilms Order No. DA8911875

A theoretical model for the combustion of nitramine composite solid propellants is presented. An nitramine composite propellant typically consists of several distributions of cyclotetramethylene-tetranitramine crystals (HMX) and ammonium perchlorate crystals (AP) mixed in a hydrocarbon fuel binder such as polybutadiene (HTPB). The model, called the High Energy Petite Ensemble Model (HYPEM), is based upon a statistical treatment of the propellant's oxidizer crystals. It is a physiochemical combustion model with multiple flames situated over HMX and/or AP crystals. The HMX section of the model averages the propellant combustion in time while the AP portion averages the propellant combustion over the surface area of the propellant. Results from the HYPEM combustion model are compared with experimental burning rate, pressure exponent and temperature sensitivity for a wide variety of propellants containing multiple distributions of HMX and/or AP crystals. Composite propellant combustion properties are examined by parametrically varying particle size, pressure, oxidizer solids loading and formulation. Dissert. Abstr.

N90-11184# Allied-Signal Aerospace Co., Des Plaines, IL. Engineered Materials Research Center.
PRODUCTION OF JET FUELS FROM COAL-DERIVED LIQUIDS. VOLUME 11: PRODUCTION OF ADVANCED ENDOTHERMIC FUEL BLENDS FROM GREAT PLAINS GASIFICATION PLANT NAPHTHA BY-PRODUCT STREAM Final Report, Sep. 1987 - Dec. 1988
Russell W. Johnson, W. C. Zackro, G. Czajkowski, P. P. Shah, and A. P. Kelly (UOP, Inc., Des Plaines, IL.) Mar. 1989 130 p (Contracts MIPR-FY1455-86-N0655; DE-AC22-87PC-79810; DA Proj. 2480)
(AD-A210251; AFWAL-TR-87-2042-Vol-11) Avail: NTIS HC A07/MF A01 CSCL 21/4

The U.S. Air Force has an ongoing program to evaluate various endothermic fuels for cooling aircraft structures. The fuels will provide a heat sink by vaporization (latent heat) and endothermic reactions (dehydrogenation) before use as fuel in aircraft engines. Cycloparaffins hold the most promise for use as endothermic fuels. The U.S. Air Force is also evaluating various feedstock sources of endothermic fuels. The technical feasibility of producing endothermic fuel from the naphtha by-product from Great Plains Gasification Plant in Beulah, North Dakota was evaluated. The capital and operating costs of deriving the fuel from coal naphtha were also estimated. GRA

N90-11185# Sandia National Labs., Albuquerque, NM.
A SHOCK INITIATION MODEL FOR FINE-GRAINED HEXANITROSTILBENE
M. E. Kipp and R. E. Setchell 1989 17 p Presented at the 9th International Symposium on Detonation, Portland, OR, 28 Aug. - 1 Sep. 1989
(Contract DE-AC04-76DP-00789)
(DE89-007641; SAND-88-2385C; CONF-890811-5) Avail: NTIS HC A03/MF A01

An established body of data indicates that very fine-grained hexanitrostilbene (HNS), when pressed to 92 percent of crystal density, exhibits shock initiation characteristics unlike those typical of porous, granular explosives. That is, a progressive buildup towards detonation from an initial shock by hot spot formation and growth processes is not observed. Instead, this particular HNS exhibits shock initiation characteristics normally associated with homogeneous explosives (e.g., the formation of a superdetonation wave after an initial shock was introduced). A comprehensive effort was made to develop a predictive model for shock initiation in this material. This model is based on a theory of homogeneous reactive mixtures, and includes a refined equation of state for porous HNS reactant and a JWL equation of state for gaseous reaction products. The model was incorporated into wave propagation codes, and comparisons with available initiation data are made. DOE

N90-11186# Los Alamos National Lab., NM.
IN-SITU STUDY OF THE CHEMICALLY DRIVEN FLOW FIELDS IN INITIATING HOMOGENEOUS AND HETEROGENEOUS NITROMETHANE EXPLOSIVES
Stephen A. Sheffield, Ray Engelke, and Robert R. Alcon 1989 19 p Presented at the 9th International Symposium on Detonation, Portland, OR, 28 Aug. - 1 Sep. 1989
(Contract W-7405-eng-36)
(DE89-008415; LA-UR-89-602; CONF-890811-8) Avail: NTIS HC A03/MF A01

Electromagnetic gauging was used to make in-situ measurements of particle velocity and impulse at five Lagrangian positions in nitromethane (NM) during gas-gun-driven, shock-to-detonation experiments. Homogeneous initiation experiments were conducted using NM that was chemically sensitized (using an organic base) and heterogeneous initiation experiments were done with physically sensitized NM (using silica particles). In the homogeneous initiation experiments, some of the

features observed are consistent with the classical homogeneous initiation model, however, the measurements show that the superdetonation does not form immediately after an induction time. Considerably behind the initial shock, reaction causes a wave to build up over a discernible length and this wave evolves into a superdetonation which catches the initial shock. In the heterogeneous initiation experiments, the waveforms indicated that wave growth occurs primarily in the shock front, similar to earlier observations in other heterogeneous explosives. DOE

N90-11187# Sandia National Labs., Albuquerque, NM.
ESTIMATION OF THE C-J PRESSURE OF EXPLOSIVES
Paul W. Cooper 1989 13 p Presented at the 14th International Pyrotechnics Seminar, Jersey, England, 18-22 Sep. 1989
(Contract DE-AC04-76DP-00789)
(DE89-013811; SAND-89-0320C; CONF-8909113-2) Avail: NTIS HC A03/MF A01

The correlation of a broad experimental data base yields a power function relationship between rho sub cj and rho sub 0. Combining this function with the Rankine-Hugoniot equations for mass and momentum, an equation can be derived to estimate simply and accurately (within an average error of 5.7 percent) the value of P sub cj, when rho sub 0 and D are given. This estimating equation is P sub cj = rho sub 0 D squared (1 - 0.713 rho sub 0 sup 0.03). DOE

N90-11188# Sandia National Labs., Albuquerque, NM. Initiating and Pyrotechnic Components Div.
CONSEQUENCE OF CONDENSED-PHASE FORMATION IN TRANSIENT BURNING OF TiHx/KCIO IN A CLOSED SYSTEM
A. Razani, M. Shahinpoor (New Mexico Univ., Albuquerque.), and S. L. Hingorani-Norenberg 1989 10 p Presented at the 14th International Pyrotechnics Seminar, Jersey, England, 18-22 Sep. 1989
(Contract DE-AC04-76DP-00789)
(DE89-013922; SAND-89-0482C; CONF-8909113-3) Avail: NTIS HC A02/MF A01

Transient burning of TiH(x)/KCIO4 in a closed system is formulated including the effect of condensed species. Thermodynamic properties are evaluated using both BLAKE and TIGER computer codes. Three different equations of state for gaseous species are used and their effect on the burning rate is evaluated. For more accurate transient burning analysis, a pressure dependent covolume for gaseous species is generated. The effect of pressure dependent covolume as well as the condensed species on transient burning is evaluated. Both parameters are found to be important when the burning rate at high loading densities in a closed system is considered. At high loading densities, condensed species become important not only because of their effect on thermodynamic properties but also due to the volume occupied by these species. DOE

N90-11189# Los Alamos National Lab., NM.
CARBON IN DETONATIONS
James Daniel Johnson 1989 9 p Presented at the American Physical Society Topical Conference on Shock Compression of Condensed Matter, Albuquerque, NM, 14-17 Aug. 1989
(Contract W-7405-eng-36)
(DE89-016037; LA-UR-89-2773; CONF-890812-40) Avail: NTIS HC A02/MF A01

We review three principal results from a five year study of carbon and its properties in detonations and discuss the implications of these results to the behavior of explosives. We first present a new determination of the carbon melt line from release wave velocity measurements in the shocked state. We then outline a colloidal theory of carbon clustering which from diffusion limited coagulation predicts a slow energy release rate for the carbon chemistry. Finally, we show the results from the examination of recovered soot. Here we see support for the colloid theory and find the diamond phase of carbon. The main theme of this paper is that the carbon in detonation products is in the form of a colloidal suspension of carbon clusters which grow through diffusion limited collisions. Even the final state is not bulk graphite or diamond, but is a collection of small, less than 100 angstrom, diamond and graphitic clusters. DOE

N90-11190# Los Alamos National Lab., NM. Reaction Science Group.
CRYSTAL ORIENTATION EFFECTS IN PETN EXPLOSIVE WITH 4 GPa SHOCKS
J. J. Dick, D. R. Pettit, and W. J. Spencer 1989 3 p Presented at the American Physical Society Topical Conference on Shock Compression of Condensed Matter, Albuquerque, NM, 14-17 Aug. 1989
(Contract W-7405-eng-36)
(DE89-016996; LA-UR-89-2716; CONF-890812-32) Avail: NTIS HC A01/MF A01

Shock initiation of detonation has been observed in PETN crystals of (110) orientation at the low shock strength of 4.25 GPa. This result explains some observations by other workers at Los Alamos National Laboratory that were considered anomalous. Chemiluminescent emission from the shock-induced decomposition reactions has been observed using spectrographs, photodiodes, and image intensifier cameras. The emission is not seen in the insensitive orientations, (100) and (101); these orientations can deform using the primary slip plane, (110). DOE

N90-11191# Sandia National Labs., Albuquerque, NM.
POWDER MORPHOLOGY EFFECTS IN THE IGNITION OF TITANIUM-BASED PYROTECHNICS
K. L. Erickson, R. D. Skocypec, J. W. Rogers, Jr., and T. M. Massis 1989 16 p Presented at the 14th International Pyrotechnics Seminar, Jersey, England, 18-22 Sep. 1989
(Contract DE-AC04-76DP-00789)
(DE89-017229; SAND-89-0344C; CONF-8909113-4) Avail: NTIS HC A03/MF A01

The influence of powder morphology on the thermal ignition of uniformly heated titanium powders was examined theoretically using expressions for fundamental heat transfer and chemical reaction mechanisms. The basic effect of powder morphology is that critical conditions exist for which small relative decreases in the initial sample mass result in a major portion of the reactive surface area being depleted before the sample temperature is sufficient for a self-propagating reaction to occur. In these cases, ignition temperatures increase by 100 to 200 K relative to those for slightly larger samples. Similar effects are observed for small relative decreases in the heating rate. It appears that sample morphology accounts for similar effects that were previously observed experimentally. A practical aspect of powder morphology is the particle size distribution of the fines in different powder lots. A very small difference in particle size distribution can shift ignition temperatures by 100 K or more. DOE

N90-11192# Lawrence Livermore National Lab., CA. High Explosives Technology.
SHOCK INITIATION OF LX-17 AS A FUNCTION OF ITS INITIAL TEMPERATURE
P. A. Urtiew, L. M. Erickson, D. F. Aldis, and C. M. Tarver 24 Jul. 1989 11 p Presented at the 9th International Symposium on Detonation, Portland, OR, 28 Aug. - 1 Sep. 1989 Submitted for publication
(Contract W-7405-eng-48)
(DE89-017730; UCRL-101617; CONF-890811-29) Avail: NTIS HC A03/MF A01

The triaminotrinitrobenzene (TATB)-based pressed solid explosive LX-17 has been shown to exhibit significant differences in shock sensitivity as its initial temperature is varied from -54 C to 88 C. In this combined experimental-computational study, embedded gauges were used to measure the particle velocity and pressure histories in reacting LX-17 at various initial shock pressures and time durations at three initial temperatures: cold (-54 C), ambient (25 C), and hot (88 C). The ignition and growth reactive flow computer model, which had previously been normalized to a great deal of embedded gauge and other shock initiation data for ambient temperature LX-17, was then used to

determine the differences in chemical reaction rates which are required to calculate the cold and hot LX-17 data. The embedded gauge records clearly demonstrate that during shock compression at colder temperature there are fewer ignition hot spots and that the growth of reaction rates from these hot spots is also slower. At higher temperatures the ignition is more vigorous and the growth of reaction rates is also faster. However, the transition to detonation occurs as rapidly in cold LX-17 as it does in ambient or hot LX-17. The changes in the three reaction rate terms of the ignition and growth model necessary for accurate simulations are consistent with these experimental observations. DOE

N90-11193# Swedish Defence Research Establishment, Stockholm.
N-HEXYL CARBORANE (NHC) AS COMBUSTION CATALYST IN COMPOSITE PROPELLANTS
Tony Rosenquist and Roland Sanden May 1989 25 p In SWEDISH; ENGLISH summary
(FOA-C-20755-2.1; ISSN-0347-3694; ETN-89-95153) Avail: NTIS HC A03/MF A01

The feasibility of n-hexyl carborane as a combustion catalyst in composite propellants was investigated. The results indicate that NHC is an efficient combustion catalyst at high concentrations. Good bonding for NHC-containing HTPB propellants to liners and inhibitors was obtained. NHC migrates as easily as dioctyl seabacate or n-butyl ferrocene in the polymer. Despite a high boiling point, NHC evaporates noticeably at ambient temperatures. In contrast to n-butyl ferrocene, NHC does not seem to catalyze the thermal aging or the curing of HTPB. Thermal analyses show no indication that NHC should considerably enhance the sensitivity of ignition of the propellant. In other respects it seems to act mainly as a plasticizer. A great disadvantage of NHC is its high price. ESA

N90-11194# Swedish Defence Research Establishment, Stockholm.
TEST OF EED (ELECTRO-EXPLOSIVE DEVICES). PART 3: STATISTICAL ASPECTS ON THE ESTIMATION OF SENSITIVITY
Ola Hertzberg Feb. 1989 36 p In SWEDISH; ENGLISH summary
(FOA-C-20749-2.3-Pt-3; ISSN-0347-3694; ETN-89-95166-Pt-3)
Avail: NTIS HC A03/MF A01

The determination of a sensitivity curve of explosives is generally founded on quantal response data and each item gives either an ignition or a non-ignition when tested on a certain stimulus level. The ignition frequency is an estimate of the ignition probability. The reliability of the estimates is to a great extent influenced by the choice of stimuli levels. The up-and-down method gives an efficient estimate of the mean of the distribution but an inefficient estimate of its standard deviation. A modified method termed RMUD, was developed and its properties were investigated. The results demonstrate that RMUD is superior to the up-and-down method in estimating the standard deviation of the sensitivity curve and levels of safety handling and function. ESA

29 MATERIALS PROCESSING

Includes space-based development of products and processes for commercial applications.
For biological materials see *55 Space Biology*.

N90-11195*# National Aeronautics and Space Administration. Marshall Space Flight Center, Huntsville, AL.
CONCEPTS FOR MICROGRAVITY EXPERIMENTS UTILIZING GLOVEBOXES
Roger L. Kroes, Donald A. Reiss, and Barbara Facemire Sep. 1989 44 p
(NASA-TM-100378; NAS 1.15:100378) Avail: NTIS HC A03/MF A01 CSCL 22A

The need for glovebox facilities on spacecraft in which microgravity materials processing experiments are performed is discussed. At present such facilities are being designed, and some of their capabilities are briefly described. A list of experiment concepts which would require or benefit from such facilities is presented. Author

N90-11196*# National Aeronautics and Space Administration. Lewis Research Center, Cleveland, OH.
DROPLET COMBUSTION EXPERIMENT DROP TOWER TESTS USING MODELS OF THE SPACE FLIGHT APPARATUS
J. B. Haggard, M. H. Brace, J. L. Kropp, and F. L. Dryer (Princeton Univ., NJ.) 1989 13 p Presented at the 27th Aerospace Sciences Meeting, Reno, NV, 9-12 Jan. 1989; sponsored by AIAA Previously announced in IAA A89-28418
(NASA-TM-101472; E-4586; NAS 1.15:101472; AIAA-89-0501)
Avail: NTIS HC A03/MF A01 CSCL 22A

The Droplet Combustion Experiment (DCE) is an experiment that is being developed to ultimately operate in the shuttle environment (middeck or Spacelab). The current experiment implementation is for use in the 2.2 or 5 sec drop towers at NASA Lewis Research Center. Initial results were reported in the 1986 symposium of this meeting. Since then significant progress was made in drop tower instrumentation. The 2.2 sec drop tower apparatus, a conceptual level model, was improved to give more reproducible performance as well as operate over a wider range of test conditions. Some very low velocity deployments of ignited droplets were observed. An engineering model was built at TRW. This model will be used in the 5 sec drop tower operation to obtain science data. In addition, it was built using the flight design except for changes to accommodate the drop tower requirements. The mechanical and electrical assemblies have the same level of complexity as they will have in flight. The model was tested for functional operation and then delivered to NASA Lewis. The model was then integrated into the 5 sec drop tower. The model is currently undergoing initial operational tests prior to starting the science tests. Author

31 ENGINEERING (GENERAL)

Includes vacuum technology; control engineering; display engineering; cryogenics; and fire prevention.

N90-11197# Los Alamos National Lab., NM.
ACCELERATION OF METAL PLATES
S. P. Marsh, R. G. McQueen, and T. H. Tan 1989 3 p Presented at the American Physical Society Topical Conference on Shock Compression of Condensed Matter, Albuquerque, NM, 14-17 Aug. 1989
(Contract W-7405-eng-36)
(DE89-016816; LA-UR-89-2818; CONF-890812-36) Avail: NTIS HC A01/MF A01

High-explosive charges were used to accelerate stainless steel plates to velocities of 6 to 7 km/s. A two-stage system was used in which the first stage is a plane-wave detonating system that accelerates the plate down a short barrel. The second stage consists of a hollow cylindrical charge through which the moving plate passes. After an adjustable delay this charge is detonated on the outer circumference of the entry side of the charge. Flash radiographs and witness plates show no breakup in the first stage but bowing and frequent breakup in the second stage. DOE

N90-11198# United States Steel Corp., Monroeville, PA.
THIN SECTION CASTING PROGRAM. VOLUME 1: EXECUTIVE SUMMARY AND OVERVIEW Final Report
Jan. 1989 45 p Prepared in cooperation with Bethlehem Steel Corp., PA
(Contract DE-FC07-84ID-12545)
(DE89-009030; DOE/ID-12545/1-Vol-1) Avail: NTIS HC A03/MF A01

The objective of this project which started in September 1984 was to develop a new casting technology which could be both applied to the total range of hot- and cold-rolled sheet steels, and be successfully developed within a five-year project time scale.

These requirements resulted in the choice of a thin section casting (TSC) approach (casting around 1-inch-thick) over the alternative strip casting approach (casting around 0.1-inch-thick). The TSC approach was expected to result in significant capital cost, operating cost, and energy savings over current 10-inch-thick slab casting technology. DOE

N90-11199# United States Steel Corp., Monroeville, PA.
THIN SECTION CASTING PROGRAM. VOLUME 2: HORIZONTAL TSC (THIN-SECTION CASTING) APPROACH Final Report
Jan. 1989 484 p Prepared in cooperation with Bethlehem Steel Corp., PA
(Contract DE-FC07-84ID-12545)
(DE89-009031; DOE/ID-12545/1-Vol-2) Avail: NTIS HC A21

In horizontal thin-section casting (HTSC), 1-inch-thick steel sections are produced at speeds up to 600 ipm or about 60 tons per hour per foot of width (tphf). Liquid steel is fed from the ladle, and flows through a specially designed tundish, then flows through a refractory feeding tube and nozzle, with approximately the same external dimensions as the cast section, into a near-horizontal rectangular mold whose all four sides are traveling in the same direction and speed as the steel casting. This report is the second of a six volume set on thin section casting. This volume covers the research on horizontal thin section casting (TSC). DOE

N90-11200# United States Steel Corp., Monroeville, PA.
THIN SECTION CASTING PROGRAM. VOLUME 2-A: APPENDIX TO VOLUME 2 Final Report
Jan. 1989 788 p Prepared in cooperation with Bethlehem Steel Corp., PA
(Contract DE-FC07-84ID-12545)
(DE89-009032; DOE/ID-12545/1-Vol-2A) Avail: NTIS HC A99

This volume contains reports on the design, construction, and operation of the horizontal thin-section-casting dynamic simulator facility (H-DS) at the USS Technical Center's pilot facilities in Universal Pennsylvania (UPF). A dynamic simulator is a small-scale pilot facility that bridges the development gap between bench-scale work and a full-scale pilot facility. The main objectives of the H-DS program are: (1) to provide a critical proof-of-concept of closed-pool (injection) feeding, and (2) an evaluation of a near-full-scale casting system for steel (1-inch-thick by 17-inch-wide product) using a twin-belt caster. As originally configured, this phase also included a vertical feeding dynamic simulator to be operated concurrently with the H-DS. Based on the DS results, large-scale pilot facilities were to be constructed using the most successful of two feeding approaches for final evaluation. This plan was later modified by only building an H-DS facility at UPF. A smaller version of the V-DS called the V-rig was built at Bethlehem. Expanded casting campaigns are to be conducted independently on each casting approach at UPF and Bethlehem's Research Laboratory. DOE

N90-11201# United States Steel Corp., Monroeville, PA.
THIN SECTION CASTING PROGRAM. VOLUME 3: VERTICAL TSC (THIN-SECTION CASTING) APPROACH Final Report
Jan. 1989 301 p Prepared in cooperation with Bethlehem Steel Corp., PA
(Contract DE-FC07-84ID-12545)
(DE89-009033; DOE/ID-12545/1-Vol-3) Avail: NTIS HC A14/MF A02

A prototype vertical twin belt caster was designed, constructed and tested at Bethlehem Steel Corporation's Homer Research Laboratory for the development of a thin section casting process. In the prototype caster, the moving mold was aligned vertically and each of the two endless steel belts was tensioned around an upper and a lower large pulley by means of a third smaller pulley. The mold consisted of a long parallel lower section and a shorter V-shaped top section into which liquid steel was fed from a tundish via a submerged refractory nozzle. Mold length, defined as the distance from the meniscus in the V-mouth to the tangent point of the lower pulleys, was about eleven feet. The length of the V-mouth was 27 in. The belts were continuously supported between the upper and lower pulleys by a unique back-up system. Downstream support consisted of two pairs of foot rolls and a vertical water-cooled steel structure that would permit a cast length of about nineteen feet. A chain driven bar was used to start a cast and support the slab. The aim was to cast 1 in. by 17 in. sections at 250 in./min. The details of the prototype vertical caster, except the end walls, are given. DOE

N90-11202# United States Steel Corp., Monroeville, PA.
THIN SECTION CASTING PROGRAM. VOLUME 4: STATIC CAST PRODUCT BENDING, STRAIGHTENING, AND ROLLING Final Report
Jan. 1989 63 p Prepared in cooperation with Bethlehem Steel Corp., PA
(Contract DE-FC07-84ID-12545)
(DE89-009034; DOE/ID-12545/1-Vol-4) Avail: NTIS HC A04/MF A01

Statically cast 1/2 in., 3/4 in., and 1 in. thick steel slabs were subjected to hot rolling in a laboratory reversing mill and to simulated coiling-uncoiling on a three-point bender-unbender. Tensile properties and microstructures of hot bands thinner than 0.15 in. produced from the statically cast slabs were found to be independent of initial slab thickness and similar to those from conventionally cast 8 to 10 in. thick slabs. Cold rolled and batch annealed product from the statically cast slabs had mechanical properties equivalent to those of conventionally processed deep-drawing quality steel. Overall, the results of this task indicated that 1/2 to 1 in. thick steel sections produced in a twin belt caster can be coiled and uncoiled in a hot coiler box downstream of the caster without generating any cracks in the product, and that the total range of hot and cold rolled sheet and strip products with qualities equivalent to those of conventionally produced can be obtained from the 1/2 in. to 1 in. thick sections. This report is the fifth of a six volume set on thin section casting. DOE

N90-11203# United States Steel Corp., Monroeville, PA.
THIN SECTION CASTING PROGRAM. VOLUME 5: WESTINGHOUSE MHD PROJECT Final Report
Jan. 1989 303 p Prepared in cooperation with Bethlehem Steel Corp., PA
(Contract DE-FC07-84ID-12545)
(DE89-009035; DOE/ID-12545/1-Vol-5) Avail: NTIS HC A14

In September of 1984, the Research and Development Center entered into a 3-year contract to develop a magnetofluidynamically enhanced feeding system. This report describes the work conducted under this contract. A design for an MFD device to enhance the feeding system of a horizontal steel caster was conceived, analyzed, and successfully tested with a low melting point liquid metal. Difficulties with integrating the device into an existing demonstration caster led to a decision to forego MFD feeding enhancement. All work on the DOE contract was stopped in 1987 upon commercial demonstration of a vertical thin section steel caster. DOE

N90-11204# Fraunhofer Inst. fuer Werkstoffmechanik, Freiburg (Germany, F.R.).
BASIC INVESTIGATIONS OF CUTTING MACHINABILITY OF INORGANIC GLASSES USING SINGLE-POINT TOOLS Final Report [GRUNDLEGENDE UNTERSUCHUNGEN ZUR SPANENDEN BEARBEITBARKEIT VON ANORGANISCHEN GLAESERN MIT EINZAHNWERKZEUGEN]
M. G. Schinker and W. Doell 1987 132 p In GERMAN
(Contract AIF-6241)
(W-15/87; ETN-89-94613) Avail: NTIS HC A07/MF A01

The cutting machinability of inorganic glasses at room temperature was investigated with a view to the production of smooth, optically transparent surfaces with little eigenstresses and cracks. The removal of material in inorganic glasses, and the cutting depth, cutting microgeometry and cutting angle are discussed. The experimental set-up and the machinery are described. The characteristics of the different glasses are presented. The results show that optical glasses with very different chemical composition and physical properties can be machined

by viscoplastic removal of chips in such a way that new surfaces are obtained that are not only free of cracks but also have an excellent optical quality. ESA

32 COMMUNICATIONS AND RADAR

Includes radar; land and global communications; communications theory; and optical communications.

For related information see also *04 Aircraft Communications and Navigation* and *17 Space Communications, Spacecraft Communications, Command and Tracking.* For search and rescue see *03 Air Transportation and Safety,* and *16 Space Transportation.*

N90-11205*# Arizona State Univ., Tempe. Telecommunications Research Center.

NONPRINCIPAL-PLANE SCATTERING FROM FLAT PLATES: SECOND-ORDER AND CORNER DIFFRACTION AND PATTERN CONTROL OF HORN ANTENNAS Semiannual Progress Report, 1 Feb. - 31 Jul. 1989

Constantine A. Balanis 31 Jul. 1989 61 p
(Grant NAG1-562)
(NASA-CR-185485; NAS 1.26:185485) Avail: NTIS HC A04/MF A01 CSCL 20N

Several high-frequency models for nonprincipal-plane scattering from a rectangular, perfectly conducting plate are examined. Two methods, the Method of Equivalent Currents and corner diffraction coefficients, are considered. Formulations for second-order Physical Theory of Diffraction equivalent currents and for corner diffracted fields are presented. Comparisons are made among plate models. Results away from grazing are accurate using only first-order terms. Near grazing, second-order and corner diffraction terms improve the results for many cases. The pattern control of horn antennas using lossy materials to coat the inner walls of the horn is also investigated. Integral Equation and Moment Method techniques are used to formulate the problem. It is clearly demonstrated that side lobe level reduction can be achieved using impedance surfaces on the inner walls of the horn. For individual titles, see N90-11206 through N90-11207.

N90-11206*# Arizona State Univ., Tempe. Telecommunications Research Center.

PART A: NONPRINCIPAL-PLANE SCATTERING FROM FLAT PLATES: SECOND-ORDER AND CORNER DIFFRACTIONS

Constantine A. Balanis and Lesley A. Polka *In its* Nonprincipal-Plane Scattering From Flat Plates: Second-Order and Corner Diffraction and Pattern Control of Horn Antennas 31 Jul. 1989 p 2-49 (For primary document see N90-11205 02-32)
Avail: NTIS HC A04/MF A01 CSCL 20N

Two models of a flat plate for nonprincipal-plane scattering are explored. The first is a revised version of the Physical Optics/Physical Theory of Diffraction (PO/PTD) model with second-order PTD equivalent currents included to account for second-order interactions among the plate edges. The second model uses a heurisitcally derived corner diffraction coefficient to account for the corner scattering mechanism. The patterns obtained using the newer models were compared to the data of previously reported models, the Moment Method (MM), and experimental results. Near normal incidence, all the models agreed; however, near grazing incidence a need for higher-order and corner diffraction mechanisms was noted. In many instances the second-order and corner-scattered fields which were formulated improved the results. K.C.D.

N90-11207*# Arizona State Univ., Tempe. Telecommunications Research Center.

PART B: PATTERN CONTROL OF HORN ANTENNAS

Constantine A. Balanis and Kefeng Liu *In its* Nonprincipal-Plane Scattering From Flat Plates: Second-Order and Corner Diffraction and Pattern Control of Horn Antennas 31 Jul. 1989 p 50-60 (For primary document see N90-11205 02-32)
Avail: NTIS HC A04/MF A01 CSCL 20N

During this period, the computations of the impedance elements were completed. These include interactions between the two electric current modes, the elecric current mode and the magnetic current mode, and the two magnetic current modes. An accurate and efficient formulation of computing interactions between electric current mode and magnetic current mode was accomplished. This, together with other subroutines allows for the fill-in of all the elements in the matrix. After the fill-in of the impedance elements in the matrix, the forward problem is accomplished. That is, given the specification of the horn and the excitating waveguide mode, the radiation pattern of the antenna based on the integral equation can be obtained. An example case was run for a standard X-band gain-horn (DBG-520). The H- and E-plane patterns of this horn antenna with perfectly conducting walls are compared with the gain pattern available from the manufacturer for up to the first side lobe. Good agreements are obtained although the cross polarization has not yet been accounted for. The effect of the lossy coating on the radiation pattern was also investigated. The resulting E-plane pattern shows about 3-dB improvement in the first sidelobe and 4-dB improvement in the second sidelobe.
K.C.D.

N90-11208 British Broadcasting Corp., London (England). Engineering Div.

HDTV DISPLAYS: SUBJECTIVE EFFECTS OF SCANNING STANDARDS AND DOMESTIC PICTURE SIZES

N. E. Tanton and M. A. Stone 1989 13 p
(BBC-RD-1989/9) Avail: Issuing Activity

The results are described of two sets of subjective tests relating to High Definition TeleVision (HDTV) displays. The first set investigated the size of display and viewing distances which could or would be accommodated in the home, assuming that flat screen displays will be available in a mature HDTV service. For such a display it was found that a size of between 1 and 1.25 metres diagonal would be practicable and desirable, and that viewing distances of between four and six times picture height would be representative of domestic conditions. The second set of tests investigated the trade-off on perceived image quality between display field-rate and the number of displayed lines at a constant line frequency. It indicated that there are significant benefits to be had from higher field-rate displays but that perceived resolution is more important than scanning structure/field rate. Thus any increase of display field rate (e.g. by up-conversion) should not be at the expense of resolution. Author

N90-11209*# Ohio State Univ., Columbus. ElectroScience Lab.

NEAR ZONE-BASIC SCATTERING CODE USER'S MANUAL WITH SPACE STATION APPLICATIONS

R. J. Marhefka and J. W. Silvestro Mar. 1989 387 p
(Grant NsG-1498)
(NASA-CR-185925; NAS 1.26:185925; ESL-TR-716199-13)
Avail: NTIS HC A17/MF A02 CSCL 17B

The Numerical Electromagnetic Code-Basic Scattering Code, Version 3, is a user-oriented computer code to analyze near and far zone patterns of antennas in the presence of scattering structures, to provide coupling between antennas in a complex environment, and to determine radiation hazard calculations at UHF and above. The analysis is based on uniform asymptotic techniques formulated in terms of the Uniform Geometrical Theory of Diffraction (UTD). Complicated structures can be simulated by arbitrarily oriented flat plates and an infinite ground plane that can be perfectly conducting or dielectric. Also, perfectly conducting finite elliptic cylinder, elliptic cone frustum sections, and finite composite ellipsoids can be used to model the superstructure of a ship, the body of a truck, an airplane, a satellite, etc. This manual gives special consideration to space station modeling applications. This document is a user manual designed to give an overall view of the operation of the computer code, to instruct a user in how to model structures, and to show the validity of the code by comparing various computed results against measured and alternative calculations such as method of moments whenever available. It also describes in detail the input and output data for the code. Author

N90-11210*# Hughes Aircraft Co., El Segundo, CA. Space and Communications Group.
ANTENNA BEAMFORMING USING OPTICAL PROCESSING
L. P. Anderson, Jr., F. Boldissar, and D. C. D. Chang Jun. 1987 66 p Previously announced in IAA as A89-15844
(Contract NAS3-24889)
(NASA-CR-180844; NAS 1.26:180844) Avail: NTIS HC A04/MF A01 CSCL 20N

This work concerns itself with the analytical investigation into the feasibility of optical processor based beamforming for microwave array antennas. The primary focus is on systems utilizing the 20 and 30 GHz communications band and a transmit configuration exclusively to serve this band. A mathematical model is developed for computation of candidate design configurations. The model is capable of determination of the necessary design parameters required for both spatial aspects of the microwave footprint (beam) formation as well as transmitted signal quality. Computed example beams transmitted from geosynchronous orbit are presented to demonstrate network capabilities. A comprehensive device/component survey is also conducted in parallel to determine the feasibility of breadboarding a transmit processor. Recommendations are made for the configuration of such a processor and the components which would comprise such a network. Author

N90-11211*# Ohio State Univ., Columbus. ElectroScience Lab.
AN EXPERIMENTAL SMI ADAPTIVE ANTENNA ARRAY FOR WEAK INTERFERING SIGNALS
R. L. Dilsavor and I. J. Gupta Oct. 1989 89 p
(Grant NAG3-536)
(NASA-CR-185976; NAS 1.26:185976; ESL-TR-716111-7) Avail: NTIS HC A05/MF A01 CSCL 17B

A modified sample matrix inversion (SMI) algorithm designed to increase the suppression of weak interference is implemented on an existing experimental array system. The algorithm itself is fully described as are a number of issues concerning its implementation and evaluation, such as sample scaling, snapshot formation, weight normalization, power calculation, and system calibration. Several experiments show that the steady state performance (i.e., many snapshots are used to calculate the array weights) of the experimental system compares favorably with its theoretical performance. It is demonstrated that standard SMI does not yield adequate suppression of weak interference. Modified SMI is then used to experimentally increase this suppression by as much as 13dB. Author

N90-11212# Lawrence Livermore National Lab., CA.
VALIDATION OF NEC (NUMERICAL ELECTROMAGNETICS CODE) FOR ANTENNAS NEAR GROUND
G. J. Burke Jun. 1989 12 p Presented at the IEEE Antennas Propagation Society International Symposium, San Jose, CA, 26-30 Jun. 1989
(Contract W-7405-eng-48)
(DE89-016502; UCRL-101190; CONF-890660-9) Avail: NTIS HC A03/MF A01

Around 1980, a project was begun at LLNL to develop an accurate model for antennas above or buried in the ground in the general-purpose antenna code NEC. This effort started with a moderately complex formulation in which the field of a point source near ground was included in the kernel of the electric field integral equation. To maintain reasonable computation times, algorithms involving table lookup and least squares approximation were developed to supply the many field values needed in the moment method solution. The complexity and tradeoffs in this approach and the goal of modeling arbitrary wire antennas led to a need for extensive validation and testing of the code. Since little good experimental data or known ground parameters was available, much of the validation of the model has relied on internal self-consistency checks and comparisons with independent analytical or numerical results. The balance of input and radiated power, boundary values of the fields and reasonable behavior of the solution in convergence and other limits have provided valuable information. Initially, simple antennas such as a horizontal dipole or vertical wire penetrating the ground were modeled, followed by more complex cases such as a monopole on a radial wire ground screen. The code has since received an extensive wringing out in the hands of DOD users and contractors. Reasonable confidence in the code was built up for many types of antennas and some problems were uncovered. The history of debugging and validation of the NEC ground model is summarized. Although validation was not a separate task in this project, the steps were probably similar to what occurs with many other large codes. DOE

N90-11213# International Centre for Theoretical Physics, Trieste (Italy).
GENERATION OF HIGHER-ORDER SQUEEZING OF QUANTUM ELECTROMAGNETIC FIELDS BY DEGENERATE FOUR-WAVE MIXING AND OTHER PROCESSES
Li Xizeng, Shan Ying, and L. Mandel (Rochester Univ., NY.) Nov. 1988 7 p Submitted for publication
(DE89-618392; IC-88/353) Avail: NTIS (US Sales Only) HC A02/MF A01

It is found that the field of the combined mode of the probe wave and the phase conjugate wave in the process of degenerate four wave mixing exhibits higher order squeezing to all even order. The degree of squeezing increases with the order N, and the higher order squeeze parameter q sub N may approach -1. DOE

N90-11214# Naval Postgraduate School, Monterey, CA.
DEEP NULL ANTENNAS AND THEIR APPLICATIONS TO TACTICAL VHF RADIO COMMUNICATIONS M.S. Thesis
Kenneth A. Vincent Mar. 1989 99 p
(AD-A210656) Avail: NTIS HC A05/MF A01 CSCL 25/2

Antennas with a characteristic cardioid radiation pattern, their applications to VHF radio communications and their design, construction and performance are examined. Structures are investigated using both the Mini Numerical Electromagnetics Code (MININEC) and the Numerical Electromagnetics Code (NEC). A test structure is built, test data obtained, and a comparison of test results versus predicted results is made. GRA

N90-11215# Bolt, Beranek, and Newman, Inc., Cambridge, MA.
WIDEBAND CONNECTIVITY AND SUPPORT FOR CRONUS CLUSTER AT USAF ELECTRONIC SYSTEMS DIVISION Final Technical Report, 25 Sep. 1987 - 24 Mar. 1989
Steven B. Storch and Jonathan G. Cole 24 Mar. 1989 20 p
(Contract MDA903-87-C-0693; ARPA Order 4726)
(AD-A210749; BBN-7064) Avail: NTIS HC A03/MF A01 CSCL 25/5

The connection of a LAN-based Cronus Distributed Operating System Cluster at the USAF Electronic Systems Division to similar clusters at the Rome Air Development Center and at BBN via the DARPA Wideband Packet Satellite Network are described. Similar connectivity between ESD and the Jet Propulsion Laboratory, wide area network throughput measurement, performance studies, and network monitoring and control improvements are also described. GRA

N90-11216# Axiomatix, Los Angeles, CA.
NETWORK ANALYZER FOR NONSTATIC JAMMING Interim Report
Unjeng Cheng 30 Jun. 1989 23 p
(Contract DAAL03-87-C-0007)
(AD-A210759; R8906-3; ARO-24649.6-EL-S) Avail: NTIS HC A03/MF A01 CSCL 25/2

The survivability of a packet radio network (PRNET) under jamming attack is an important issue. The goal of this research is to develop the analytical methods for understanding as well as predicting the behavior of PRNETs under various jamming conditions. Jamming can be stationary or nonstationary. For the stationary jamming, the jamming strategy is fixed, but it can be described stochastically. For instance, we may say that a node is jammed with probability 0.5 in each slot. Therefore, although the jamming strategy is fixed, the actual jamming pattern changes from slot to slot. A subclass of the stationary jamming is the static jamming, where the jamming pattern is fixed. For the

nonstationary jamming, the jamming strategy changes from time to time. A subclass of the nonstationary jamming is the nonstatic jamming, where a fixed jamming pattern is applied in each block of time, but the jamming pattern changes from block to block. We analyzed the behavior of PRNETs under static jamming attack in our previous report. In this report, we introduce a method of analyzing the PRNET behavior under the nonstatic jamming attack. The analytical results for the static jamming attack scenario were presented in our previous report for both the transmitter-based code and the receiver-based code networks. The numerical results were given only for the receiver-based code case. Simulations were performed to verify the accuracy of the analytical approach. GRA

N90-11217# InterScience, Inc., Troy, NY.
EFFICIENT ALGORITHM FOR CALCULATION OF RADAR CROSS SECTION Final Report, 26 Sep. 1988 - 27 Mar. 1989
James T. Woo, Eduardo Saravia, D. M. Audet, James F. Pipkins, and Betriz Cassis 27 Mar. 1989 81 p
(Contract DAAH01-88-C-0863; ARPA Order 5916)
(AD-A210785) Avail: NTIS HC A05/MF A01 CSCL 17/9

A new formulation for the calculation of radar cross section of objects of arbitrary shape based on the solution of the electromagnetic wave equation in a natural coordinate system that conforms to the shape of the boundaries has been developed. The natural coordinate system is determined from the solution of an elliptical partial differential equation subject to Dirichlet boundary conditions. The basic approach is to solve the electromagnetic wave equation expressed in the natural coordinate system in a region between the scattering object and an fictitious interface that fully envelopes the object (a circle for two dimensional objects and a sphere for three dimensional objects). Outside the interface, the wave field can be expressed as infinite series of Bessel types of functions. A unique solution is obtained by matching the boundary conditions at the fictitious interface. GRA

N90-11218# Air Force Human Resources Lab., Brooks AFB, TX.
SIMULATION OF SYNTHETIC APERTURE RADAR 1: FEATURE DENSITY AND ACCURACY REQUIREMENTS Final Report, Jan. 1986 - Jan. 1988
Peter M. Crane, Herbert H. Bell, Robert G. Kalinyak, John Dooley, and David C. Hubbard (Dayton Univ., OH.) Jul. 1989 37 p
(AD-A211019; AFHRL-TR-88-42) Avail: NTIS HC A03/MF A01 CSCL 17/9

Simulations of ground mapping radar are generated from Defense Mapping Agency Digital Feature Analysis Data (DFAD) products which were developed to support real beam ground mapping radar. Criteria for inclusion of an object within a given level of DFAD are radar significance, height, and size. In general, level 1 includes objects 100m and larger and level 2 includes objects 30m and larger. A prototype DFAD incorporating features as small as 10m (level X) was developed to support the higher resolution Synthetic Aperture Radar (SAR); however, the minimum data base requirements for simulating SAR have not been determined. The present report describes three studies conducted to determine these requirements. In the first study, B-1B and F-15E radar operators rated SAR simulations produced from level 2 DFAD (30m) and level X (10m), plus two experimental data bases with 15m and 20m capture criteria. Eighty-two percent of SAR-experienced subjects found the 15m data acceptable. Simulations produced from level 2 depicted areas of high reflector density as a single feature with uniform brightness and were acceptable to only 18 percent of the subjects. A study of the Radar Scope Interpretation (RSI) cues used by B-1B Offensive Systems Officers (OSOs) found that roads and rivers were critical cues, whereas individual structures were used only in the immediate vicinity of the aimpoint. A third study compared B-1B OSO performance on a navigation update task using 10m and 15m feature data and generically enhanced 30m (level 2) and 100m (level 1) data. GRA

N90-11219# Georgia Inst. of Tech., Atlanta.
PERFORMANCE ANALYSIS OF HYBRID ARQ PROTOCOLS IN A SLOTTED CODE DIVISION MULTIPLE-ACCESS NETWORK Final Report Ph.D. Thesis
Joseph M. Hanratty Aug. 1989 155 p Sponsored by Army
(AD-A211078) Avail: NTIS HC A08/MF A01 CSCL 25/2

A link throughput-delay analysis is presented for a slotted direct-sequence spread-spectrum multiple-access packet radio network (PRN) operating in the presence of background noise, multiple-access interference, and pulsed jammer noise. The PRN is comprised of an arbitrary number of full-duplex radio units arranged in a paired-off topology. Slotted ALOHA random access is used in conjunction with CDMA for channel access and a type 1 hybrid ARQ is used for error control. Expression are derived for the link throughput-delay in terms of the channel cutoff rate and capacity. With the friendly objective of maximizing the link throughput, and the enemy objective of minimizing the link throughput, the dependency of the optimal retransmission probability, processing gain, code rate, and jamming fraction on the population size, traffic intensity, bit energy-to-background-noise ratio, is examined in detail. It is shown that properly designed (optimized) PRN using random-access CDMA offers a significantly larger heavy load throughput than a random-access PRN. GRA

N90-11220# Vermont Univ., Burlington. Dept. of Computer Science and Electrical Engineering.
ELECTROMAGNETIC PULSE INTERACTION AT A DIELECTRIC INTERFACE Final Report, 1 Mar. 1988 - 28 Feb. 1989
Kurt E. Oughstun 19 Apr. 1989 4 p
(Grant AF-AFOSR-0149-88; AF Proj. 2304)
(AD-A211081; AFOSR-89-1069TR) Avail: NTIS HC A01/MF A01 CSCL 20/15

The research on pulsed electromagnetic beam fields is nearing completion with some rather interesting results. In particular, the rigorous angular spectrum representation of pulsed beam fields was found to differ from the given by the simpler plane-wafe spectrum representation. This latter formulation (as given by W. H. Carter), Electromagnetic Beam Fields, Optica Acta, 21, 871-892 (1974) assumes the form of the propagated transverse field components for either the electric or magnetic field vector and then solves the Maxwell field equation for the remaining field components in a self-consistent manner. The rigorous derivation for a general pulsed electromagnetic beam field clearly shows that this assumption is valid only for very special cases of the spatial field distribution and polarization state. GRA

N90-11221# Mitre Corp., Bedford, MA.
A CALIBRATED, OMNIDIRECTIONAL, LF LOOP ANTENNA FOR GWEN (GROUND WAVE EMERGENCY NETWORK) Final Report
Patrick S. Debroux Jul. 1989 21 p
(Contract F19628-86-C-0001)
(AD-A211264; MTR-10403; ESD-TR-89-192) Avail: NTIS HC A03/MF A01 CSCL 25/5

This paper presents the design and performance characterization of a calibrated, omnidirectional, mobile low frequency (LF) receive antenna. This antenna is unique in its use of active circuitry to isolate two crossed-loop antenna elements from the combining network. A prototype was built for the Ground Wave Emergence Network (GWEN) in the 150 to 175 kHz band. The prototype has an effective height of 39 millimeters and is essentially omnidirectional over the GWEN frequency range. GRA

N90-11222# Massachusetts Inst. of Tech., Lexington. Lincoln Lab.
THE EFFECTIVENESS OF ADAPTIVE PRF (PULSE REPETITION FREQUENCY) SELECTION IN MINIMIZING RANGE OBSCURATION IN THE TDWR (TERMINAL DOPPLER WEATHER RADAR) SYSTEM
S. C. Crocker 27 Jul. 1989 51 p

(Contract F19628-85-C-0002)
(AD-A211267; ATC-164; DOT/FAA/PS-88/18) Avail: NTIS HC A04/MF A01 CSCL 17/9

An adaptive procedure for selecting radar pulse repetition frequency (PRF) has been developed as the primary means of minimizing the occurrence of range aliased echoes within operationally significant coverage areas (e.g., airport runways) of the Terminal Doppler Weather Radar (TDWR) system. This procedure underwent extensive testing at the S-Band TDWR testbed while located in Denver, CO, where it was judged to be highly successful at preserving the integrity of data collected within the vicinity of the Stapleton International Airport runways. The actual TDWR system will operate at a C-Band frequency, and an increase in potential range obscuration is expected over that experienced by the S-band testbed. This report discusses the anticipated performance of the PRF selection procedure in the C-Band environment by extrapolating results obtained using S-Band testbed data. The results conclusively demonstrates the efficacy of adaptive PRF selection as a method by which to reduce potential range obscuration. A worst-case scenario, for example, indicates that over 20 percent of the TDWR radar data collected about the airport runways has the potential for being contaminated with range aliased echoes at any given time during TDWR surveillance operations. With adaptive PRF selection, however, the expected obscuration is reduced to only 3 percent. GRA

N90-11223# Lawrence Livermore National Lab., CA. Physics Dept.
AUXILIARY-FIELD TRANSFORMATIONS FOR REPULSIVE POTENTIALS: A PHYSICAL APPROACH
K. Theilhaber Aug. 1989 15 p
(Contract W-7405-eng-48)
(DE89-016677; UCID-21767) Avail: NTIS HC A03/MF A01

It is shown that the imaginary coupling coefficient which arises in auxiliary field transformations on systems with repulsive Coulomb potentials is automatically obtained in the non-relativistic, electrostatic limit of the coupled electron-electromagnetic-field system. This suggests that the imaginary coupling term is not just a mathematical artifice, but that its appearance is deeply linked to the imaginary-time representation used for constructing the partition function of the electron-electromagnetic-field system. DOE

N90-11224# Technische Univ., Munich (Germany, F.R.). Fakultaet fuer Elektrotechnik.
CALCULATION, OPTIMIZATION AND COMPARISON OF OPTICAL TRANSMISSION SYSTEMS WITH SUPERHETERODYNE RECEPTION Ph.D. Thesis [BERECHNUNG, OPTIMIERUNG UND VERGLEICH OPTISCHER UEBERTRAGUNGSSYSTEME MIT UEBERLAGERUNGSEMPFANG]
Juergen Franz 1987 199 p In GERMAN
(ETN-89-94651) Avail: NTIS HC A09/MF A01

Five variants of optical transmission systems with heterodyne reception are calculated, optimized and compared, taking as a reference the conventional optical direct system with light power modulation and demodulation. The fundamentals of the operation of optical superheterodyne systems are explained. The calculation of optical superheterodyne systems is based on the statistical properties of laser phase noise and several deduced noise processes. The systems calculation results in the evolution of the signals in the optical transmitter, the transmission section, and the optical superheterodyne receiver, as well as in the error probabilities. Error rate floor occurs at high receiver light power densities. The system parameters which can be optimized and those which cannot be optimized are determined. The systems are compared with respect to error probability, sensitivity, maximum allowable laser line width, eye sample, and realizability. ESA

N90-11225# Universitaet der Bundeswehr, Neubiberg (Germany, F.R.). Fachbereich Maschinenbau.
UTILIZATION OF THE GENERALIZED LIKELIHOOD RATIO TEST FOR THE SUPPRESSION OF SYSTEMATIC ERRORS IN NOISY SYSTEMS Ph.D. Thesis [ANWENDUNG DES GENERALIZED LIKELIHOOD RATIO TESTS ZUR UNTERDRUECKUNG VON SYSTEMATISCHEN FEHLERN BEI VERRAUSCHTEN SYSTEMEN]
Peter Pagel 1988 93 p In GERMAN
(ETN-89-94656) Avail: NTIS HC A05/MF A01

The applicability of the generalized likelihood ratio (GLR) method, which is a powerful analytical redundancy method, in the suppression of systematic errors is investigated. Analytical redundancy methods for the detection of systematic errors are outlined. The principles and statistical properties of the GLR method are presented. The compensation and correction of detected errors are discussed. The utilization and implementation of the GLR method are outlined, and illustrated by the example of a bridge cranemodel. ESA

N90-11226# Technische Univ., Berlin (Germany, F.R.). Fachbereich fuer Elektrotechnik.
A CONTRIBUTION TO THE SYNTHESIS OF COMMUNICATION SWITCHING SYSTEMS WITH DECENTRALIZED CONTROL USING MODULAR COMPONENTS Ph.D. Thesis [EIN BEITRAG ZUR SYNTHESE VON DEZENTRAL GESTEUERTEN NACHRICHTENVERMITTLUNGSSYSTEMEN UNTER VERWENDUNG VON MODULAREN KOMPONENTEN]
Ruediger Weber 1988 128 p In GERMAN
(ETN-89-94660) Avail: NTIS HC A07/MF A01

Single components of a modular communication switching system with decentralized control are investigated and partly implemented. Only the maintenance functions are centralized. The basic principles of systems architecture are given. The systems concept, which is especially suited for spatially limited cases, special small networks, but is also applicable to public switching techniques, is presented. The characteristics of the concept, its efficiency, and its limitations are outlined. Some dimensioning examples are given. A subsystem is investigated in greater detail and partly implemented. ESA

N90-10881# Identification Friend, Foe, or Neutral Joint Test Force, Kirtland AFB, NM.
IDENTIFICATION FRIEND, FOE OR NEUTRAL JOINT TEST
James E. Haile *In* AGARD, Flight Test Techniques Jul. 1989 12 p (For primary document see N90-10860 02-05)
Copyright Avail: NTIS HC A18/MF A03

N90-11400# Centre National d'Etudes des Telecommunications, Lannion (France).
RADIO PROPAGATION CONDITIONS FORECAST ABOVE A LOW LATITUDE REGION
H. Sizun and M. Lissilour *In* AGARD, Ionospheric Structure and Variability on a Global Scale and Interactions with Atmosphere and Magnetosphere Apr. 1989 17 p (For primary document see N90-11361 02-46)
Copyright Avail: NTIS HC A20/MF A03

N90-11401# Millman (George H.), DeWitt, NY.
AN IONOSPHERIC MODEL FOR HF SKY-WAVE BACKSCATTER RADAR
George H. Millman, Carl A. Bowser, and Roger W. Swanson (General Electric Co., Syracuse, NY.) *In* AGARD, Ionospheric Structure and Variability on a Global Scale and Interactions with Atmosphere and Magnetosphere Apr. 1989 16 p (For primary document see N90-11361 02-46)
Copyright Avail: NTIS HC A20/MF A03

N90-11403# Andrews Antennas, Adelaide (Australia).
IONOSPHERIC LIMITATIONS TO THE ACCURACY OF SSL ESTIMATES OF HF TRANSMITTER LOCATIONS
L. F. McNamara *In* AGARD, Ionospheric Structure and Variability on a Global Scale and Interactions with Atmosphere and

Magnetosphere Apr. 1989 15 p (For primary document see N90-11361 02-46)
Copyright Avail: NTIS HC A20/MF A03

33 ELECTRONICS AND ELECTRICAL ENGINEERING

Includes test equipment and maintainability; components, e.g., tunnel diodes and transistors; microminiaturization; and integrated circuitry.

For related information see also *60 Computer Operations and Hardware* and *76 Solid-State Physics.*

N90-11227*# Texas A&M Univ., College Station. Dept. of Chemistry.
NEW SECONDARY BATTERIES UTILIZING ELECTRONICALLY CONDUCTIVE POLYMER CATHODES Semiannual Report, 1 Jan. - 30 Jun. 1989
Charles R. Martin and Ralph E. White Sep. 1989 43 p
(Grant NAG9-173)
(NASA-CR-185885; NAS 1.26:185885) Avail: NTIS HC A03/MF A01 CSCL 09C

The objectives of this project are to characterize the transport properties in electronically conductive polymers and to assess the utility of these films as cathodes in lithium/polymer secondary batteries. During this research period, progress has been made in a literature survey of the historical background, methods of preparation, the physical and chemical properties, and potential technological applications of polythiophene. Progress has also been made in the characterization of polypyrrole flat films and fibrillar films. Cyclic voltammetry and potential step chronocoulometry were used to gain information on peak currents and potentials switching reaction rates, charge capacity, and charge retention. Battery charge/discharge studies were also performed. Author

N90-11228# Science Applications International Corp., McLean, VA.
FREE-WORLD MICROELECTRONIC MANUFACTURING EQUIPMENT
J. S. Kilby, W. H. Arnold, W. T. Booth, J. A. Cunningham, J. D. Hutcheson, R. W. Owen, W. R. Runyan, Barbara L. McKenney, ed., Moira McGrain, ed., and Renee G. Taub, ed. Dec. 1988 353 p
(FASAC-TAR-4070) Avail: NTIS HC A16/MF A02

Equipment is examined and evaluated for the manufacture of microelectronic integrated circuit devices and sources for that equipment within the Free World. Equipment suitable for the following are examined: single-crystal silicon slice manufacturing and processing; required lithographic processes; wafer processing; device packaging; and test of digital integrated circuits. Availability of the equipment is also discussed, now and in the near future. Very adequate equipment for most stages of the integrated circuit manufacturing process is available from several sources, in different countries, although the best and most widely used versions of most manufacturing equipment are made in the United States or Japan. There is also an active market in used equipment, suitable for manufacture of capable integrated circuits with performance somewhat short of the present state of the art. Author

N90-11229# Fermi National Accelerator Lab., Batavia, IL.
A NEW SEMICUSTOM INTEGRATED BIPOLAR AMPLIFIER FOR SILICON STRIP DETECTORS
Tom Zimmerman 11 Jul. 1989 18 p
(Contract DE-AC02-76CH-03000)
(DE89-015585; FNAL-TM-1606) Avail: NTIS HC A03

The QPA02 is a four channel dc coupled two stage transimpedance amplifier designed at Fermilab on a semicustom linear array (Quickchip 2S) manufactured by Tektronix. The chip was developed as a silicon strip amplifier but may have other applications as well. Each channel consists of a preamplifier and a second stage amplifier/sharper with differential output which can directly drive a transmission line (90 to 140 ohms). External bypass capacitors are the only discrete components required. QPA02 has been tested and demonstrated to be an effective silicon strip amplifier. Other applications may exist which can use this amplifier or a modified version of this amplifier. For example, another design is now in progress for a wire chamber amplifier, QPA03, to be reported later. Only a relatively small effort was required to modify the design and layout for this application. DOE

N90-11230# Maryland Univ., College Park. Dept. of Physics.
ANALYSIS OF COAXIAL WIRE MEASUREMENT OF LONGITUDINAL COUPLING IMPEDANCE
R. L. Gluckstern and R. Li 1989 8 p Presented at the International Conference on High Energy Accelerators, Tsukuba (Japan), 20-26 Aug. 1989
(Contract DE-AS05-80ER-10660)
(DE89-015748; DOE/ER-10666/1; CONF-890803-7) Avail: NTIS HC A02/MF A01

In recent work, a method has been developed to calculate the longitudinal impedance for an azimuthally symmetric obstacle in a beam pipe of circular cross section. The method has been applied to a small obstacle, to an obstacle of general shape at high frequency, and to several obstacles, including a periodic structure at high frequency. Coupling impedances are difficult to measure directly. Instead, the reflection and transmission coefficients for a pulse carried through the obstacle on a thin coaxial wire are measured and the results approximate the longitudinal coupling impedance. In the present paper, an analysis is carried out including the coaxial wire and new boundary conditions for the fields at the surface of the wire. We then estimate the validity of the coaxial wire measurement for a variety of frequencies and geometries. Finally, several numerical calculations are carried out for both the beam and the wire pulse. The results confirm the predictions of the analysis. DOE

N90-11231# Sandia National Labs., Albuquerque, NM.
INTERNAL VOLTAGES AND CURRENTS IN WELL-SHIELDED CYLINDRICAL OBJECTS DUE TO SIMULATED DIRECT-STRIKE LIGHTNING
R. J. Fisher, L. K. Warne, and J. G. Kostas 1989 6 p Presented at the International Conference on Lightning and Static Electricity, Bath, England, 26-28 Sep. 1989
(Contract DE-AC04-76DP-00789)
(DE89-012664; SAND-88-3471C; CONF-8909124-3) Avail: NTIS HC A02/MF A01

A variety of cylindrical test objects of generic interest were tested through the use of simulated direct-strike lightning with the intent of bounding possible internal voltages due to joint leakage and currents through low-impedance loads due to diffusion. All the test objects would normally be considered to be high-quality Faraday shields. The highest voltage recorded was 21 V, which was developed across a flange-and-collar joint in a steel cylinder driven longitudinally by a test current of (approximately) 160 kA peak. A simple circuit model of the symmetric diffusion process, valid over the frequency range of lightning, is given. DOE

N90-11232# Sandia National Labs., Albuquerque, NM.
ASIC (APPLICATION SPECIFIC INTEGRATED CIRCUIT) REPLACEMENT FOR AN SSI (SMALL SCALE INTEGRATED) COMPONENT DESIGN: A CASE STUDY
Jeff Everts, David Gelet, Don Deatherage, and Manuel Contreras 1989 18 p Presented at the 2nd Annual IEEE/ASIC Seminar and Exhibit, Rochester, NY, 25-28 Sep. 1989
(Contract DE-AC04-76DP-00789)
(DE89-013494; SAND-89-0841C; CONF-8909146-1) Avail: NTIS HC A03/MF A01

The practical issues of design-for-functionality, design-for-simulation, and design-for-testability in replacing aging SSI component designs with ASIC gate arrays are covered. The replacement of a 169-TTL-component design with a CMOS ASIC gate array is presented. Maintaining existing functionality is accomplished through a series of ordered conversion steps that minimize the probability of error in the conversion. Design

modifications, such as the addition of initialization circuitry, were necessary to take advantage of CAE simulation tools. The faster ASIC technology coupled with design modifications allowed the time-to-simulate to be decreased by a factor of 10,000. A pseudo-random number generation/signature analysis technique is presented that interrogates highly sequential designs. The testability scheme and other design techniques improved stuck-at fault coverage by more than 640 percent. The economic advantages, knowledge gained, and the tools developed that are applicable to future design work are also discussed. DOE

N90-11233# Sandia National Labs., Albuquerque, NM.
A SEVERE HUMAN ESD (ELECTROSTATIC DISCHARGE) MODEL FOR SAFETY AND HIGH RELIABILITY SYSTEM QUALIFICATION TESTING
R. J. Fisher 1989 4 p Presented at the EOS Electrostatic Discharge Symposium, New Orleans, LA, 26-28 Sep. 1989
(Contract DE-AC04-76DP-00789)
(DE89-016177; SAND-89-0194C; CONF-8909176-1) Avail: NTIS HC A01/MF A01

A severe human electrostatic discharge (ESD) equivalent source model has been developed for use in qualification testing of systems that have stringent safety or very high reliability requirements. The model produces the now-acknowledged worst-case waveform, and the values of the constituent components have been selected from measured human body electrical parameters to maximize the peak amplitude and rate of rise of the short-circuit discharge current and energy transfer to the victim system. DOE

N90-11234# Technical Research Centre of Finland, Espoo.
COATINGS IN ELECTRICAL CONTACTS
I. Nieminen, S. Varjus, and H. Ronkainen Jan. 1989 24 p In FINNISH; ENGLISH summary
(DE89-787739; VTT-TUTK-576) Avail: NTIS (US Sales Only) HC A03

In this survey the suitability of titanium nitride (TiN) coatings for improving the wear resistance of electric connectors was studied. Traditional electroplated coatings and TiN-coatings prepared by an ion plating method were compared in the tests. Wear and contact resistance measurements were performed by modifying a scratch tester usually used for adhesion determination. Titanium nitride had a better wear resistance than gold, but contact resistance values for TiN-coated samples were not low enough for electro-mechanical components. It was not possible to prepare ion plated coatings on copper samples used in electric connectors. DOE

N90-11235# Minnesota Univ., Minneapolis. Corrosion Research Center.
LITHIUM POLYMER ELECTROLYTE BATTERY, ELECTROCHEMICAL BEHAVIOR OF CATHODE MATERIALS
Technical Report No. 2, Jul. 1988 - Jun. 1989
B. Scrosati, B. Selvaggi (Rome Univ., Italy), Boone B. Owens, and M. Z. A. Munshi 15 Jun. 1989 3 p Submitted for publication Sponsored by Italian National Research Council
(Contract N00014-88-K-0360)
(AD-A210755; TR-2) Avail: NTIS HC A01/MF A01 CSCL 10/3

Thin layer, lithium polymer electrolyte batteries have reached an advanced stage of development. All prototypes use insertion compounds of various composition and structures as the active cathode material. Titanium disulphide, vanadium oxide and lithium vanadium bronze, respectively, were tested under comparable conditions as the active electrode materials. The characteristics of the interfaces were examined by cyclic voltammetry, impedance spectroscopy and intercalation-deintercalation cycling and the results of this study are reported in this work. GRA

N90-11236# Aerospace Corp., El Segundo, CA. Lab. Operations.
A GENERAL-PURPOSE COMPUTER PROGRAM FOR THE VOLTERRA-SERIES ANALYSIS OF NONLINEAR MICROWAVE CIRCUITS
S. A. Maas 3 Jul. 1989 16 p
(Contract F04701-85-C-0086)
(AD-A210768; TR-0086A(2925-02)-5; SD-TR-89-37) Avail: NTIS HC A03/MF A01 CSCL 09/1

Volterra-series, or nonlinear transfer-function analysis, is an efficient and highly effective method for analyzing weakly nonlinear circuits under small-signal excitation. It has been used to analyze nonlinear effects in a wide variety of circuits, and is particularly useful for calculating intermodulation levels in MESFET amplifiers. Volterra-series techniques have also been used to analyze time-varying circuits such mixers and parametric upconverters. However, the large amount of algebraic effort necessary to generate analytical forms of the Volterra kernels of even simple circuits has prevented the wide application of Volterra-series analysis. This analytical complexity has forced many experimenters to employ simplifying assumptions, especially in the topology of the equivalent circuits of solid-state devices; these approximations limit the accuracy of the analysis. This report describes a general-purpose computer program that performs of Volterra-series analysis of a weakly nonlinear circuit. The program is intended primarily for use in the design of microwave circuits; its catalog of circuit elements includes the distributed elements necessary for such work. GRA

N90-11237# Naval Surface Warfare Center, Silver Spring, MD.
BATTERY ACTUATION OF NITINOL AT SUB-ZERO TEMPERATURES
David Goldstein Apr. 1989 22 p
(AD-A211254; NSWC-TR-89-110) Avail: NTIS HC A03/MF A01 CSCL 11/6

It is feasible to use batteries to produce rapid shape memory response in NITINOL wires which are in sub-zero temperature ambients. Data are presented on lithium thionyl chloride batteries used to joule heat 10 mil diameter wires of nominal transformation temperatures of 90 to 105 C. The batteries and wires were jointly tested in a -35 C ambient air environment. The wire contracted 5 percent in length (0.4 inch) and lifted a 1 pound load in 1/2 second. GRA

N90-11238# Lawrence Livermore National Lab., CA.
PERFORMANCE OF TRANSIENT LIMITERS UNDER LABORATORY, SIMULATED, AND ROCKET-TRIGGERED LIGHTNING CONDITIONS
R. T. Hasbrouck, J. P. Johnson, and J. Breitmeier (Diversified Electronic Services, Melbourne, FL.) 2 Jul. 1989 8 p Presented at the International Conference on Lightning and Static Electricity, Bath, England, 26-28 Sep. 1989
(Contract W-7405-eng-48)
(DE89-015773; UCRL-101192; CONF-8909124-4) Avail: NTIS HC A02/MF A01

A prototype system was designed and tested that implements a lightning protection method referred to as the fortress concept. The fortress, a structure similar to a Faraday cage, protects the critical system by surrounding it with a continuous metallic skin. Each electrical conductor that must enter the fortress is enclosed within a cable, which is, in turn, enclosed in a metallic shield that terminates at the entry point and is electrically bonded to the fortress' outer metallic surface. Within the fortress, each penetrating conductor is protected by a transient limiter. The system was tested by means of full-threat-level simulated lightning and actual lightening triggered by rockets. Several limited components were subsequently tested by using a laboratory-type surge generator to investigate certain anomalous responses. The fortress concept is reviewed, the operation of the limiters is discussed, and their performance are examined. Explanations are offered for the anomalous responses, and several important design considerations and trade-offs are offered. DOE

N90-11239# Los Alamos National Lab., NM. Applied Theoretical Physics Div.

ANTHEM SIMULATION OF PLASMA OPENING SWITCHES

Rodney J. Mason, Michael E. Jones, and Christy Bergman 1989 14 p Presented at the 7th Inst. of Electrical and Electronics Engineers Pulsed Power Conference, Monterey, CA, 12-14 Jun. 1989

(Contract W-7405-eng-36)

(DE89-016617; LA-UR-89-2877; CONF-890665-46) Avail: NTIS HC A03/MF A01

Plasma opening switches were examined numerically with the aid of the ANTHEM plasma simulation model. A generic bi-cylindrical switch is studied. The switching of generator pulses ranging from 50 ns to 1 microsec is reviewed, for a variety of plasma fill lengths and densities, and for a range of resistive loads. DOE

N90-11240# Sandia National Labs., Albuquerque, NM.

A COMPARISON OF FIXED-BASE AND DRIVEN-BASE MODAL TESTING OF AN ELECTRONICS PACKAGE

Thomas G. Carne, David R. Martinez, and Arlo R. Nord Aug. 1989 27 p

(Contract DE-AC04-76DP-00789)

(DE89-016673; SAND-88-1765) Avail: NTIS HC A03/MF A01

Results are compared for a fixed base and a driven base modal test of an electronics package. A fixed base modal test uses the common testing procedure of attaching the structure to a large inertial mass which is freely suspended. The problem with this approach is that the input levels are typically limited by the strength of the structure and stinger attachment. An attractive alternative to fixed base modal testing is to use high force shaker-tables to provide a driven base input. Some of the issues of concern are: properly simulating the fixed boundary conditions, applying modal estimation algorithms to motion-to-motion frequency response functions vs. motion-to-force frequency response functions, nonlinearity effects and testing at very low input levels vs. levels equal to those of the field environment, complications involved with shaker resonances, exciting the response critical modes of the structure, and consistency of the modal parameters using driven base tests vs. fixed base modal tests. Experimental results are presented which demonstrate the adequacy of using vibration shake tables to excite the fixed based modes of the system. A direct comparison of the modes acquired using fixed base and driven base excitation for the electronics package shows very close agreement. A discussion of the theory for driven-base testing is given, as well as a brief presentation of analytical predictions for the structure. DOE

N90-11241# Lawrence Livermore National Lab., CA.

HPW (HIGH POWER MICROWAVE) TESTING OF ELECTRONIC COMPONENTS

R. Antinone (BDM Corp., Albuquerque, NM.) and W. C. Ng 10 May 1989 79 p

(Contract W-7405-eng-48)

(DE89-016682; UCID-21687) Avail: NTIS HC A05/MF A01

This report documents the results of a study of high power microwave (HPM) vulnerability of electronic components commonly used in weapon systems. The study was carried out at the Lawrence Livermore National Laboratory from August through October 1988. The objective of this study was to determine the threshold levels for upset or disturbance and damage of the devices under test (DUT). In these tests pulsed microwave energy was directly injected into the terminal of the DUT and in most cases a 50-ohm microstrip test fixture was used to ensure that 50-ohm transmission was maintained as close to the DUT as possible. DOE

N90-11242# Sandia National Labs., Albuquerque, NM. Pulsed Power Research Div.

LIFETIME TESTING OF COMMERCIALLY AVAILABLE 3.0 (mu)f, 100 kV PULSED-POWER CAPACITORS

L. X. Schneider, S. R. Babcock, and G. E. Laderach 1989 5 p Presented at the 7th Inst. of Electrical and Electronics Engineers Pulsed Power Conference, Monterey, CA, 12-14 Jun. 1989

(Contract DE-AC04-76DP-00789)

(DE89-017230; SAND-89-0139C; CONF-890665-44) Avail: NTIS HC A01/MF A01

The lifetime characteristics of a small sample group of commercially available 3.0 microF, 100-kV pulsed-discharge capacitors were determined in an automated test facility. Both Maxwell Laboratories and Aerovox, Inc., capacitors were tested to failure to establish a data base on these new designs, which are a direct physical replacement for the present 1.3 microF, 100-kV, Syllac-style capacitor that are in wide spread use at Sandia and in the pulsed-power community. In conjunction with the lifetime testing a bipolar, 30-stage, 6-MV, Marx generator was constructed with these capacitors using conventional PBFA-II hardware and the Physics International Company, model T-508A spark gap. Capacitor failure mechanisms and lifetime statistics will be discussed. Electrode erosion rates in the 508A switches will be presented for the conventional brass electrodes and a copper/tungsten replacement set. DOE

N90-11243# Oak Ridge National Lab., TN. Solid State Theory Section.

THE THEORY OF ac IMPEDANCE OF ROUGH ELECTRODE-ELECTROLYTE INTERFACES Foreign Trip Report, 19 May - 5 Jun. 1989

S. H. Liu 19 Jun. 1989 7 p

(Contract DE-AC05-84OR-21400)

(DE89-017474; ORNL/FTR-3288) Avail: NTIS HC A02/MF A01

The author attended the First International Symposium on Electrochemical Impedance Spectroscopy and presented an invited lecture on the theory of ac impedance of rough electrode-electrolyte interfaces. After the symposium the author spent four days at Ecole Polytechnique, Palaiseau, on the outskirts of Paris to give an invited talk and to discuss the application of fractal concepts to a number of problems related to the physical properties of electrochemical systems. DOE

N90-11244# Swedish Defence Research Establishment, Linkoeping. Dept. of Information Technology.

A BRIEF DESCRIPTION OF TRAVELING WAVE TUBES

Veine Jernemalm Dec. 1988 57 p In SWEDISH; ENGLISH summary

(FOA-C-30522-3.6; ISSN-0347-3708; ETN-89-95154) Avail: NTIS HC A04/MF A01; Swedish Defence Research Establishment, P.O Box 1165, S-381 11 Linkoeping, Sweden, 50 Swedish crowns

The mechanical structure and function of traveling wave tubes are described. The part of the traveling wave tube (TWT) where the signal is amplified is called slow wave structure, and is carried through in two different forms: helix or coupled-cavity tube. The helix is made of tungsten or molybdenum with supports of ceramics. Cavity tubes are electrically coupled by means of holes or fissures. Efforts are made to build TWTs with a large bandwidth which at present for certain frequencies is up to 2 octaves. The glowing wire requires only a few volts as tension, but several thousand volts are necessary between anode and cathode. The performance is now between 40 percent and 50 percent which is due to the use of multiple stage collectors. TWTs are compared to solid state amplifiers. ESA

34 FLUID MECHANICS AND HEAT TRANSFER

Includes boundary layers; hydrodynamics; fluidics; mass transfer; and ablation cooling.

For related information see also *02 Aerodynamics* and *77 Thermodynamics and Statistical Physics.*

N90-11245*# National Aeronautics and Space Administration. Lewis Research Center, Cleveland, OH.
LASER ANEMOMETER MEASUREMENTS IN A TRANSONIC AXIAL-FLOW FAN ROTOR
Anthony J. Strazisar, Jerry R. Wood, Michael D. Hathaway, and Kenneth L. Suder Washington Nov. 1989 216 p
(NASA-TP-2879; E-4480; NAS 1.60:2879) Avail: NTIS HC A10/MF A02 CSCL 20D

Laser anemometer surveys were made of the 3-D flow field in NASA rotor 67, a low aspect ratio transonic axial-flow fan rotor. The test rotor has a tip relative Mach number of 1.38. The flowfield was surveyed at design speed at near peak efficiency and near stall operating conditions. Data is presented in the form of relative Mach number and relative flow angle distributions on surfaces of revolution at nine spanwise locations evenly spaced from hub to tip. At each spanwise location, data was acquired upstream, within, and downstream of the rotor. Aerodynamic performance measurements and detailed rotor blade and annulus geometry are also presented so that the experimental results can be used as a test case for 3-D turbomachinery flow analysis codes. Author

N90-11246 Texas Univ., Austin.
NUMERICAL SOLUTIONS OF TURBULENT FLOW WITH HEAT TRANSFER OVER ROUGH SURFACES Ph.D. Thesis
Hun Way Chen 1988 112 p
Avail: Univ. Microfilms Order No. DA8909632

A method for numerical prediction of the thermal field and associated convective heat transfer for turbulent flow over rough surfaces is presented. The rough surface is characterized by rectangular ribs placed transverse to the flow. Calculations were made for fully developed turbulent flow with either a constant temperature or a constant heat flux, applied at the lower surface of a wall for which the ribs form the upper surface. The solution of the energy equation included both conduction through the wall material as well as convection and conduction in the fluid region. Turbulent transport is characterized with a previously developed extension of the Spalding eddy viscosity model which depends on the well-known shifted-logarithmic velocity profile. Numerical solutions of the flow field are obtained from the stream function-vorticity formulation. An iterative solution scheme is developed to assure compatibility between the thermal fields of the wall material and the fluid region. Numerical results for various values of roughness Reynolds number, wall thickness and element spacing (pitch) are found to compare favorably with the available experimental data, which, though sparse, suggests that the present approach is viable. Dissert. Abstr.

N90-11247 Pennsylvania State Univ., University Park.
THE STRUCTURE OF REYNOLDS STRESS IN THE NEAR WALL REGION OF A TURBULENT PIPE FLOW Ph.D. Thesis
Paul-Andre Chevrin 1988 151 p
Avail: Univ. Microfilms Order No. DA8909974

The structure of Reynolds stress in the near-wall region of a fully developed turbulent pipe flow was investigated. The working fluid was glycerine, the high viscosity of which makes the viscous sublayer much larger than in water or air. The Reynolds number of the experiment, based on the diameter of the pipe, was close to 9000. The 0.285 m diameter test section is located 25 diameters downstream of the contraction to ensure a fully developed flow. A trip ring is used to fix the location of transition at the entrance of the pipe. The test section was built of acrylic to allow optical access for a laser Doppler velocimeter (LDV). Single point LDV measurements as close as one wall unit from the wall were made. Agreement with previous investigations was excellent. A two-component LDV and a one-component fiber optics LDV were combined to measure the two-point velocity correlation in the wall region. Separation distances as large as 900 wall units in the streamwise direction and 64 wall units in the normal direction were investigated. The effect of velocity bias on the correlation of coefficient was studied and it was found to be small in the conditions of the experiment. Two dimensional maps of the correlation coefficient between streamwise velocity and radial velocity were measured for 6 different distances of the two-component LDV from the wall. The results indicate that the turbulent structures resemble horseshoe vortices whose inclination angle to the wall increases as their distance from the wall increases. A simple model of the flow based on this interpretation was constructed. Agreement with experimental results was very good. Dissert. Abstr.

N90-11248 Lehigh Univ., Bethlehem, PA.
THE NEAR-WAKE FLOW STRUCTURE OF WAKE-CYLINDER INTERACTION AND SURFACE LOADING OF CYLINDER Ph.D. Thesis
Cheng-Hsiung Kuo 1989 193 p
Avail: Univ. Microfilms Order No. DA8909392

This investigation addresses the flow structure in the vicinity of, and the unsteady surface loading upon, a cylinder subjected to vortex streets of different frequency and circulation. Flow visualization, unsteady velocity fields, and surface pressure measurements are interrelated using a phase-referencing technique which allows reconstruction of the pseudo-instantaneous flow structure in relation to the corresponding surface loading on the cylinder. Two basic types of interactions are considered. They involve vortex streets having frequencies equal to and twice that of the inherent vortex shedding frequency from the cylinder. The interaction of the vortices incident upon the cylinder are shown to exhibit repetitive patterns of: incident vortex distortion over the upstream portion of the cylinder; and vortex-vortex interactions between the distorted incident vortices and the vortices shed from the surface of the cylinder. The instantaneous vorticity fields at each of the predominant spectral components in the downstream wake are compared with the corresponding vorticity field incident upon the cylinder. Knowledge of these vorticity fields allows the circulation and the degree of vorticity concentration to be related to the visualized interaction mechanisms. Dissert. Abstr.

N90-11249 Minnesota Univ., Minneapolis.
AN EXPERIMENTAL INVESTIGATION OF TRANSITION IN OSCILLATING PIPE FLOW Ph.D. Thesis
Joerg Reinhart Seume 1988 113 p
Avail: Univ. Microfilms Order No. DA8911026

Transition from laminar to turbulent oscillating pipe flow is investigated over a range of similarity parameters that corresponds to the operating conditions of many Stirling engine heaters and coolers. Hot film anemometry measurements of the absolute value of the local and instantaneous flow velocity are used to find the variation with time and profiles across the pipe of ensemble averaged velocity and rms velocity fluctuation. The results confirm the findings of other researchers that the critical amplitude Reynolds number above which transition from laminar to turbulent flow occurs, increases with Valensi number (dimensionless frequency). Once this critical amplitude Reynolds number is exceeded, transition occurs in each half-cycle. Transition may be caused by two mechanisms: (1) That fluid which was in the pipe at the time of flow reversal remains laminar. Incoming turbulent fluid remains turbulent as it displaces the laminar fluid in the pipe. As the turbulent fluid arrives, the flow locally undergoes a sudden transition from the laminar to the turbulent regime. (2) A boundary layer grows as that fluid which was in the pipe at the time of flow reversal is accelerated inside the tube. At axial locations sufficiently far from the inlet, this laminar boundary layer may undergo transition before the incoming turbulent fluid arrives. This study is the first, known to the author, that discusses these mechanisms in detail and provides supporting measurements. The transition process depends on the conditions of the fluid upstream of the pipe

entrance. The thesis recommends a method of predicting transition for various inflow conditions and discusses the limitations of the predictions. Dissert. Abstr.

N90-11250*# National Aeronautics and Space Administration. Lewis Research Center, Cleveland, OH.
WALL-LAYER ERUPTIONS IN TURBULENT FLOWS
J. D. A. Walker (Lehigh Univ., Bethlehem, PA.) Sep. 1989 13 p
(NASA Order C-99066-G)
(NASA-TM-102362; E-5078; ICOMP-89-26; NAS 1.15:102362)
Avail: NTIS HC A03/MF A01 CSCL 20D

The near-wall region of a turbulent flow is investigated in the limit of large Reynolds numbers. When low-speed streaks are present, the governing equations are shown to be of the boundary-layer type. Physical processes leading to local breakdown and a strong interaction with the outer region are considered. It is argued that convected vortices, predominantly of the hairpin type, will provoke eruptions and regenerative interactions with the outer region. Author

N90-11251 Tennessee Univ., Knoxville.
ON A TAYLOR WEAK STATEMENT FOR FINITE ELEMENT COMPUTATIONS IN GAS DYNAMICS Ph.D. Thesis
Jin Whan Kim 1988 155 p
Avail: Univ. Microfilms Order No. DA8911732

The Taylor Weak Statement has been developed as a potential unified approach for approximate computation of fluid flows. It is verified to contain a variety of numerical dissipative methods developed for advection problems by specific identification of its expansion parameters. Generalized Fourier modal analysis has been completed in one space dimension for both semi- and fully-discrete approximations, from which the flux limiter method is herein developed and evaluated for finite element computations. Its application to 1- and 2-dimensional scalar models is investigated for continuous and discontinuous initial value problems, and its use for the Euler equation system of gas dynamics in 1- and 2-dimensional cases is demonstrated. Dissert. Abstr.

N90-11252 Oklahoma Univ., Norman.
METHOD OF CHARACTERISTIC STUDIES FOR ROTATIONAL FLOW DOWNSTREAM OF A CURVED SHOCK WAVE Ph.D. Thesis
Min-Shan Liu 1988 196 p
Avail: Univ. Microfilms Order No. DA8911206

A number of different problems in gas dynamics have been solved by the method of characteristics (MOC). Here, both direct and inverse approaches by this method are used for determining the flow over an airfoil in supersonic flow. The Mach number, stagnation pressure, and streamline angle are used as dependent variables to develop the characteristic and compatibility equations. For checking the accuracy of numerically obtain MOC results, three integral relations are derived from the conservation equations. The derivatives of properties just downstream of an oblique curved shock wave are derived which also may be used to check the results. A mass integral is used in the interior of the rotational flow field to reduce the global errors. Although the global errors can be kept quite small, numerical results indicate that the inverse results are obtained with the direct approach. Several new techniques, such as the global error check and shock wave derivatives, are developed that should be of value in future studies. Dissert. Abstr.

N90-11253 Purdue Univ., West Lafayette, IN.
COMPUTATION OF TRANSIENT THREE-DIMENSIONAL INTERSTAGE FLOWFIELDS USING THE ARBITRARY LAGRANGIAN-EULERIAN METHOD Ph.D. Thesis
Richard Fred Harwood 1988 178 p
Avail: Univ. Microfilms Order No. DA8911914

The Arbitrary Lagrangian-Eulerian Method was used to compute the transient, 3-D flow field in the expanding interstage region between two missile stages during state separation. The governing equations employed were mass, momentum, and energy conservation for an inviscid gas. The perfect gas assumption was made. The upper stage motor ignition transient and the exterior flowfield were included in the model. Grid rezoning was employed to allow the mesh to follow the motion of the lower stage, and a grid remapping technique was developed to restructure the grid during the stage separation process. Shock tube flow, source flow, and steady shock reflection studies were performed to verify the numerical method. Full-scale and sub-scale interstage flow fields were simulated. Computational results compared favorably with experimental data from sub-scale separation tests. Dissert. Abstr.

N90-11254*# National Aeronautics and Space Administration. Ames Research Center, Moffett Field, CA.
A COMPUTATIONAL/EXPERIMENTAL STUDY OF THE FLOW AROUND A BODY OF REVOLUTION AT ANGLE OF ATTACK
Gregory G. Zilliac Sep. 1986 34 p
(NASA-TM-88329; A-86319; NAS 1.15:88329) Avail: NTIS HC A03/MF A01 CSCL 20D

The incompressible Navier-Stokes equations are numerically solved for steady flow around an ogive-cylinder (fineness ration 4.5) at angle of attack. The three-dimensional vortical flow is investigated with emphasis on the tip and the near wake region. The implicit, finite-difference computation is performed on the CRAY X-MP computer using the method of pseudo-compressibility. Comparisons of computational results with results of a companion towing tank experiment are presented for two symmetric leeside flow cases of moderate angles of attack. The topology of the flow is discussed and conclusions are drawn concerning the growth and stability of the primary vortices. Author

N90-11255*# Texas A&M Univ., College Station. Turbomachinery Labs.
RECTANGULAR SUBSONIC JET FLOW FIELD MEASUREMENTS
Gerald L. Morrison and David H. Swan Jan. 1989 164 p
(Grant NAG1-630)
(NASA-CR-185962; NAS 1.26:185962) Avail: NTIS HC A08/MF A01 CSCL 20D

Flow field measurements are presented of 3 subsonic rectangular cold air jets. The 3 cases presented had aspect ratios of 1 x 2, 1 x 4 at a Mach number of 0.09 and an aspect ratio of 1 x 2 at a Mach number of 0.9. All measurements were made using a 3-D laser Doppler anemoneter system. The presented data includes the mean velocity vector, all Reynolds stress tensor components, turbulent kinetic energy and velocity correlation coefficients. The data is presented in tabular and graphical form. No analysis of the measured data or comparison to other published data is made. All tabular data are available in ASCII format on MS-DOS compatible disks. Author

N90-11256*# Elrod (Harold G.), Old Saybrook, CT.
EFFICIENT NUMERICAL METHOD FOR COMPUTATION OF THERMOHYDRODYNAMICS OF LAMINAR LUBRICATING FILMS Final Report
Harold G. Elrod Aug. 1989 25 p
(NASA Order C-22406-M; DA Proj. 1L1-61102-AH-45)
(NASA-CR-185136; NAS 1.26:185136; AVSCOM-TR-89-C-015)
Avail: NTIS HC A03/MF A01 CSCL 20D

The purpose of this paper is to describe an accurate, yet economical, method for computing temperature effects in laminar lubricating films in two dimensions. The procedure presented here is a sequel to one presented in Leeds in 1986 that was carried out for the one-dimensional case. Because of the marked dependence of lubricant viscosity on temperature, the effect of viscosity variation both across and along a lubricating film can dwarf other deviations from ideal constant-property lubrication. In practice, a thermohydrodynamics program will involve simultaneous solution of the film lubrication problem, together with heat conduction in a solid, complex structure. The extent of computation required makes economy in numerical processing of utmost importance. In pursuit of such economy, we here use techniques similar to those for Gaussian quadrature. We show that, for many

purposes, the use of just two properly positioned temperatures (Lobatto points) characterizes well the transverse temperature distribution. Author

N90-11257# Lawrence Livermore National Lab., CA.
CELLULAR AUTOMATA AND MASSIVELY PARALLEL PHYSICS
C. E. Leith Mar. 1989 4 p Presented at the Whither Turbulence Conference, Ithaca, NY, 22-24 Mar. 1989
(Contract W-7405-eng-48)
(DE89-016506; UCRL-101562; CONF-8903159-1) Avail: NTIS HC A01/MF A01

Cellular automata and parallel processing are used for computer simulation of fluid dynamics. DOE

N90-11258# Lawrence Livermore National Lab., CA.
COMPUTATIONS OF THE REFRACTION OF A PLANE SHOCK WAVE AT A SLOW-FAST GAS INTERFACE
E. G. Puckett, P. Colella, and L. F. Henderson (Sydney Univ., Australia) 14 Jul. 1989 6 p Presented at the 17th International Symposium on Shock Waves and Shock Tubes, Bethlehem, PA, 17-21 Jul. 1989 Submitted for publication
(Contracts W-7405-eng-48; IACRO-88-873)
(DE89-016508; UCRL-101506; CONF-890756-1) Avail: NTIS HC A02/MF A01

An example is presented of the computations on a shock wave refracting from CO2 into CH4. The results are compared with the experiments of Abdel-Fattah and Henderson. The input data were the same as the parameters they measured and the same boundaries were used. Also taken into account was the mutual gas contamination present in the experiments and the effects of a separating membrane. All the principal properties of a free-precursor refraction were detected. DOE

N90-11259# Maryland Univ., College Park.
AN EXPERIMENTAL STUDY OF HELICITY AND RELATED PROPERTIES IN TURBULENT FLOWS
James M. Wallace and Jean-Louis Balint 1989 13 p Presented at the IUTAM Symposium on Topological Fluid Mechanics, Cambridge, England, Aug. 1989
(Contract DE-FG05-88ER-13838)
(DE89-016785; CONF-8908112-2) Avail: NTIS HC A03/MF A01

The measurement of the velocity and vorticity vectors in turbulent flow and the experimental results are discussed. DOE

N90-11260# Ballistic Research Labs., Aberdeen Proving Ground, MD.
JET-FLOW FROM SHOCK TUBES Technical Report, Sep. 1987 - Jul. 1988
Charles N. Kingery and Edmund J. Gion Jul. 1989 61 p
(AD-A210651; BRL-TR-3015) Avail: NTIS HC A04/MF A01 CSCL 19/9

This project was designed to map the magnitude and extent of the high velocity jet flow exiting shock tubes. The flow was measured by installing stagnation probes along three blast lines and by supplementing these measurements with calibrated displacement cubes. The side-on and stagnation overpressure versus time were measured, and from that, the side-on and stagnation impulse were calculated. The stagnation impulse showed a large drop in magnitude as the blast line was moved from the zero line to a 1.5 and then to a 3-diameter offset. A helium driver was used in the 2.54-cm-diameter shock tube to simulate an explosion in a storage magazine. Results are presented in the form of stagnation impulse versus distance along the three blast lines. The significance of these findings is that the present quantity-distance criteria for munitions stored in underground magazines are based on side-on peak overpressure, but our results show that the peak stagnation pressure and impulse are much greater. At a distance where 10.3-kPa (1.5 psi) side-on pressure was measured, a 49.6-kPa (7.2 psi) stagnation pressure was measured. At the same distance, a side-on impulse was 12.6 kPa-ms (1.83 psi-ms), while the stagnation impulse was 134 kPa-ms (20.2 psi-ms)--a dramatic difference. GRA

N90-11261# Ballistic Research Labs., Aberdeen Proving Ground, MD.
A LASER DOPPLER ANEMOMETRY INVESTIGATION OF SINGLE-PHASE AND PARTICLE-LADEN JET FLOWS Technical Report, Apr. 1989
Csaba K. Zoltani and Ali F. Bicen Jun. 1989 33 p
(DA Proj. 1L1-61102-AH-43)
(AD-A210660; BRL-TR-3005) Avail: NTIS HC A03/MF A01 CSCL 20/4

An experimental investigation of the near field of an axisymmetric single-phase and particle laden jet is described. A two-component laser Doppler anemometer was used to measure the turbulent flow characteristics. The second phase consisted of glass beads of 80 micron diameter with a mass loading of 1 percent. Typical flow Reynolds numbers were 29,000 at the jet exit. The measurements indicate that the particles lag behind the fluid by about 8 percent near the jet exit but lead the fluid by about 7 percent at 9 jet diameters downstream. The mean velocity profiles of the particle laden flow are flatter, exhibit lower radial rms velocities than those of the fluid and suggest a smaller spread of the beads in the cross-stream direction. Streamwise velocity fluctuations of the particles were found to be higher than the corresponding fluid fluctuations, especially near the jet exit, which can be attributed to the fan spreading of the particles. GRA

N90-11262# Miami Univ., Coral Gables, FL. Dept. of Mechanical Engineering.
INTERNATIONAL CONFERENCE ON NUMERICAL GRID GENERATION IN COMPUTATIONAL FLUID DYNAMICS Final Report, 1 Dec. 1987 - 30 Apr. 1989
Subrata Sengupta 30 Apr. 1989 31 p
(Grant AF-AFOSR-0082-88; AF Proj. 2304)
(AD-A211082; AFOSR-89-1070TR) Avail: NTIS HC A03/MF A01 CSCL 20/4

The International Conference series on Numerical Grid Generation in Computational Fluid Dynamics was started in July 1986 to recognize grid generation as an essential subject of Computational Fluid Dynamics which needs individual attention. The conference is held bi-annually with the purpose of disseminating new ideas, recent advances and difficulties encountered by researchers around the world while solving practical Computational Fluid Dynamics problems. The second conference in the series was held in Miami, Florida, USA, during the week of December 5 to 9, 1988. The main theme of the conference was 2-D and 3-D adaptive grid methods. Nevertheless, papers were invited from all relevant conventional areas such as algebraic, boundary fit, and conformal mapping methods and other areas including applications in computational mechanics. GRA

N90-11263# California Inst. of Tech., Pasadena. Graduate Aeronautical Labs.
CHEMICAL REACTIONS IN TURBULENT MIXING FLOWS Final Report, 1 Jan. 1986 - 31 Dec. 1988
Paul E. Dimotakis, James E. Broadwell, and Anthony Leonard 1 Jun. 1989 136 p
(Grant AF-AFOSR-0213-83; AF Proj. 2308)
(AD-A211240; AFOSR-89-1035TR) Avail: NTIS HC A07/MF A01 CSCL 20/4

The purpose of this research has been to conduct fundamental investigations of turbulent mixing, chemical reaction and combustion processes in turbulent, subsonic and supersonic flows. Progress in this effort thus far has uncovered important deficiencies in conventional modeling of these phenomena, and offered alternative suggestions and formulations to address some of these deficiencies. This program is comprised of an experimental effort, an analytical modeling effort, a computational effort, and a diagnostics development and data-acquisition effort, the latter as dictated by specific needs of our experiments. Our approach has been to carry out a series of detailed theoretical and experimental studies primarily in two, well-defined, fundamentally important flow

fields: free shear layers and axisymmetric jets. To elucidate molecular transport effects, experiments and theory concern themselves with both liquids and gases. Modeling efforts have been focused on both shear layers and turbulent jets, with an effort to include the physics of the molecular transport processes, as well as formulations of models that permit the full chemical kinetics of the combustion process to be incorporated. The computational studies are at present, focused at fundamental issues pertaining to the computational simulation of both compressible and incompressible flows. GRA

N90-11264# Texas Univ., Austin. Dept. of Mechanical Engineering.
QUESTIONS FROM THE WILLMARTH WORKSHOP ON NEW DIRECTIONS IN RESEARCH ON TURBULENT WALL-LAYER STRUCTURES Final Report
R. F. Blackwelder, Ronald L. Panton, and J. M. Wallace Aug. 1989 7 p Workshop held in Ann Arbor, MI, 18-19 Nov. 1988
(Contract N00014-88-J-1193)
(AD-A211282) Avail: NTIS HC A02/MF A01 CSCL 20/4

Certain patterns of motion are observed to occur repeatedly in turbulence. The search to identify these events, determine their interrelationships, and establish their importance is known as Structure Research. Important improvements have been seen in both experimental instrumentation and in the direct numerical simulation of turbulent flows with computers. Does the bursting process associate with a single, monolithic, eddy structure made up of many associated structure elements or is it composed of many smaller relatively independent structure elements. How are the low speed streaks and temporally related to Reynolds stress producing elements (such as ejections and sweeps) and to the wall stress. Experiments and numerical simulations reveal that there are frequently intense internal shear layers (in both the normal and span directions) in the near wall region. What are the sources and significance of these shear layers. Are the structure elements observed in wall layers part of a vortex structure, if so of what type. How can knowledge of vortex dynamics be applied to understanding the origin, evolution, and dynamics of these structures. What are the effects of Reynolds number on the structure elements and their characteristics. What are the effects of parameters such as wall-roughness, pressure-gradients, surface-curvature, and three-dimensionality on the structure elements. How do the evolutionary histories of structures change with the above parameters. GRA

N90-11265# Pacific Northwest Lab., Richland, WA. Energy Sciences Dept.
DESIGN OF CERAMIC FABRIC HEAT PIPE WITH WATER WORKING FLUID
Z. I. Antoniak, J. M. Bates, and B. J. Webb Aug. 1989 7 p Presented at the ASME/AIChE National Heat Transfer Conference, Philadelphia, PA, 6-9 Aug. 1989
(Contract DE-AC06-76RL-01830)
(DE89-016565; PNL-SA-16415; CONF-890819-20) Avail: NTIS HC A02/MF A01

A novel class of space radiators, constructed of ceramic fabric materials selected for their high-temperature strength and optical characteristics, is under development at Pacific Northwest Laboratory (PNL). An earlier study indicated that heat pipe radiators constructed of fabric tubes lined with metal foil will have superior performance characteristics with lower mass than most other radiator types. Test results confirm these earlier predictions. DOE

N90-11266# Los Alamos National Lab., NM.
SHARP SHOCK MODEL FOR PROPAGATING DETONATION WAVES
Bruce Bukiet and Ralph Menikoff 1989 5 p Presented at the American Physical Society Topical Conference on Shock Compression of Condensed Matter, Albuquerque, NM, 14-17 Aug. 1989
(Contract W-7405-eng-36)
(DE89-016772; LA-UR-89-2791; CONF-890812-38) Avail: NTIS HC A01/MF A01

Recent analyses of the reactive Euler equations have led to an understanding of the effect of curvature on an underdriven detonation wave. This advance can be incorporated into an improved sharp shock model for propagating detonation waves in hydrodynamic calculations. We illustrate the model with two simple examples: time dependent propagation of a diverging detonation wave in 1-D, and the steady 2-D propagation of a detonation wave in a rate stick. Incorporating this model into a 2-D front tracking code is discussed. DOE

N90-11267# Los Alamos National Lab., NM.
SHOCK INDUCED DISSOCIATION OF POLYETHYLENE
C. E. Morris, E. D. Loughran, G. F. Mortensen, G. T. Gray, III, and M. S. Shaw 1989 5 p Presented at the American Physical Society Topical Conference on Shock Compression of Condensed Matter, Albuquerque, NM, 14-17 Aug. 1989
(Contract W-7405-eng-36)
(DE89-016983; LA-UR-89-2864; CONF-890812-29) Avail: NTIS HC A01/MF A01

To identify the physical processes occurring on the Hugoniot, shock-recovery experiments were performed. Cylindrical recovery systems were used that enabled a wide range of single-shock Hugoniot states to be examined. Mass spectroscopy was used to examine the gaseous dissociation products. X-ray and TEM measurements were made to characterize the post-shock carbon structures. A dissociation product equation of state is presented to interpret the observed results. Polyethylene (PE) samples that were multiply shocked to their final states dissociated at much higher pressures than single-shocked samples. DOE

N90-11268# Los Alamos National Lab., NM.
IMPULSE TIME-INTEGRAL FUNCTION AND LAGRANGIAN ANALYSIS
Charles A. Forest 1989 5 p Presented at the American Physical Society Topical Conference on Shock Compression of Condensed Matter, Albuquerque, NM, 14-17 Aug. 1989
(Contract W-7405-eng-36)
(DE89-016997; LA-UR-89-2717; CONF-890812-33) Avail: NTIS HC A01/MF A01

In one-dimensional planar flow, the mechanical variables of stress, impulse, particle velocity, displacement and density are usual objects of measurement. They are related by conservation of mass and momentum, and it is shown here that they are partial derivatives of a single function of space and time. The function (alpha), which is defined on the Lagrangian space and time domain, is a double integral of the particle velocity over mass and time. By integration over the mass first, the function (alpha) is shown to be a time integral of impulse, which is chosen to name the function. Because the measured variables of Lagrangian gauge experiments are related to partial derivatives of (alpha), the entire data set may be least-square fit to the function (alpha) with a single parameter set. DOE

N90-11269# Washington Univ., Seattle. Dept. of Applied Mathematics.
ANALYTICAL AND NUMERICAL STUDIES IN FLOW DEVELOPMENT Progress Report, 1 Jul. - Present
W. O. Criminale and L. M. Adams 1989 5 p
(Contract DE-FG06-88ER-25061)
(DE89-017380; DOE/ER-25061/1) Avail: NTIS HC A01/MF A01

This paper discusses initial-value problems of the following topics: Couette flow; Viscous flow with boundaries; and Interface matching conditions. DOE

N90-11270# Technische Hochschule, Aachen (Germany, F.R.). Fakultaet fuer Maschinwesen.
THE DECAY OF VISCOELASTIC FLUID JETS Ph.D. Thesis [ZUM ZERFALL VISKOELASTISCHER FLUESSIGKEITSSTRAHLEN]

Hans-Guenter Thelen 11 Feb. 1988 165 p In GERMAN (ETN-89-94667) Avail: NTIS HC A08/MF A01

Particularities of the decay of a viscoelastic fluid are investigated. The experimental possibilities of dilatation rheometry using a decaying jet are discussed. A method for the investigation of monoaxial dilatation in diluted polymer solutions is proposed. A continuum concept for the preliminary calculation of the decay of viscoelastic fluid jets is presented. An equation system for the description of slim, non-Newtonian media under surface tension is developed, providing the boundary conditions for the numerical calculation of the harmonically perturbed free jet by a finite difference method. The results of the numerical simulation agree well with those of a decay experiment. The applied continuum theory combined with the numerical method is a useful aid for the engineering calculation of the jet decay of viscoelastic fluids. ESA

N90-11271# Center for Mathematics and Computer Science, Amsterdam (Netherlands). Dept. of Numerical Mathematics.
PRESSURE CORRECTION SPLITTING METHODS FOR THE COMPUTATION OF OSCILLATORY FREE CONVECTION IN LOW Pr FLUIDS
J. H. M. tenThijteBoonkkamp Nov. 1988 13 p Presented at the GAMM Workshop on Numerical Simulation of Oscillatory Convection in Low Pr Fluids, Marseille, France, 12-14 Oct. 1988 Submitted for publication
(CWI-NM-R8816; ETN-89-95106) Copyright Avail: NTIS HC A03/MF A01

Splitting methods for the time integration of the incompressible Navier-Stokes equations in the Boussinesq approximation are considered. These methods are combined with the pressure correction method in order to decouple the pressure computation from the velocity computation. The resulting pressure correction splitting methods are used to compute the (oscillatory) free convection of low Pr fluids in a long rectangular cavity. ESA

N90-11272# Swedish Defence Research Establishment, Stockholm.
NUMERICAL SIMULATION OF TURBULENT FLOW DOWNSTREAM A SUDDEN AXISYMMETRIC EXPANSION
Jan Eriksson Jun. 1989 54 p In SWEDISH; ENGLISH summary
(FOA-C-20758-2.1; ISSN-0347-3694; ETN-89-95167) Avail: NTIS HC A04/MF A01

Different turbulence models were tested, and the computational grid and other parameters were varied, using the FLUENT computer code. The computational results were compared with experimental data, from earlier measurements. The agreement was found to be fairly good, particularly for the mean velocities. None of the turbulence models had the ability to predict the flow entirely. This work contains a background for numerical control of the solid fuel ramjet flowfield. ESA

N90-11022# Industrieanlagen-Betriebsgesellschaft m.b.H., Ottobrunn (Germany, F.R.).
FLUID-STRUCTURE INTERACTION EFFECTS IN TANK STRUCTURES DUE TO SLOSHING AND HYDRODYNAMIC RAM: COUPLED LAGANGIAN-EULERIAN SIMULATIONS
W. W. Jarzab, R. Chwalinski, W. E. Pfrang, and G. Tokar *In* ESA, Spacecraft Structures and Mechanical Testing Jan. 1989 p 263-268 (For primary document see N90-10986 02-18)
Copyright Avail: NTIS HC A99/MF E06

N90-11023# Messerschmitt-Boelkow-Blohm G.m.b.H., Munich (Germany, F.R.). Space Communications and Propulsion Systems Div.
MODELING OF LIQUID SLOSHING EFFECTS IN MULTIBODY SYSTEMS
K. Ebert *In* ESA, Spacecraft Structures and Mechanical Testing Jan. 1989 p 269-275 (For primary document see N90-10986 02-18)
Copyright Avail: NTIS HC A99/MF E06

N90-11024# Ingenieurgesellschaft fuer Technische Software G.m.b.H., Stuttgart (Germany, F.R.).
MODAL ANALYSIS OF FLUID-STRUCTURE SYSTEMS BY PARALLEL SUBSPACE ITERATION
H. Wandinger *In* ESA, Spacecraft Structures and Mechanical Testing Jan. 1989 p 277-282 (For primary document see N90-10986 02-18)
Copyright Avail: NTIS HC A99/MF E06

N90-11073# Dynamic Engineering N.V., Heverlee (Belgium).
NUMERICAL MODELS FOR EXTERIOR AND INTERIOR FLUID-STRUCTURE INTERACTION PROBLEMS
J. P. Coyette *In* ESA, Spacecraft Structures and Mechanical Testing Jan. 1989 p 675-680 (For primary document see N90-10986 02-18)
Copyright Avail: NTIS HC A99/MF E06

35 INSTRUMENTATION AND PHOTOGRAPHY

Includes remote sensors; measuring instruments and gages; detectors; cameras and photographic supplies; and holography.

For aerial photography see *43 Earth Resources and Remote Sensing.* For related information see also *06 Aircraft Instrumentation,* and *19 Spacecraft Instrumentation.*

N90-11273 Salford Univ. (England).
DEVELOPMENT OF AN ADAPTIVE TIME OF FLIGHT SYSTEM FOR THE MEASUREMENT OF FLUID FLOW VELOCITY Ph.D. Thesis
Christopher Sodhi 1988 502 p
Avail: Univ. Microfilms Order No. BRD-84985

This thesis describes the construction of a flowmeter which measured the time taken for a fluid to travel between two stations. The flowmeter introduced markers into the flow at an ideal frequency which adapted as the flow rate changed. The ideal frequency property is proved using a classical analytical technique on the model of the system. Practical designs are considered and investigated using analytical and simulation techniques. The simulations involved simulation of a system with a transport lag and some of them employed novel techniques to do this. Systems and techniques for implementation are described some of which proved to be unsatisfactory. A system was designed to operate over the flow range of 0.06 to 7 m/s. It operated satisfactorily however, its range of operation was limited by problems with the flow in the testing duct. The cause of the problems was identified which showed the direction for further work. Chapter 12 provides an original and comprehensive exposition of the commonly used constant temperature anemometer bridge system. The analysis shows features not generally acknowledged and shows the potential of the system, which is far reaching, and how to control its behavior. Dissert Abstr.

N90-11274# National Inst. of Standards and Technology, Gaithersburg, MD. Temperature and Pressure Div.
NIST (NATIONAL INSTITUTE OF STANDARDS AND TECHNOLOGY) MEASUREMENT SERVICES: THE CALIBRATION OF THERMOCOUPLES AND THERMOCOUPLE MATERIALS Final Report
G. W. Burns and M. G. Scroger Apr. 1989 204 p
(PB89-209340; NIST/SP-250/35; LC-89-600732) Avail: NTIS HC A10/MF A02; SOD HC $10.00 as 003-003-02939-4
CSCL 14B

The document describes the calibration services for thermocouples and thermocouple materials presently provided by the NIST at temperatures from -210 to 2100 C. Three general calibration methods used at NIST, which provide traceability to the International Practical Temperature Scale of 1968, are outlined in detail. Consideration is given primarily to the calibration of type S (platinum-10 percent rhodium versus platinum) thermocouples at defining fixed points of the IPTS-68 as standard instruments,

and to the calibration of other letter-designated type thermocouples (types B, R, S, E, J, K, N. and T) by comparison with a calibrated reference thermocouple and by comparison with a standard platinum resistance thermometer. The procedures followed to maintain internal quality control of apparatus and standards in the NIST thermocouple calibration laboratories are covered, and statistical assessments of the uncertainties involved in the calibrations of type S thermocouples by the fixed-point method and by the comparison method are presented. GRA

N90-11275 Cornell Univ., Ithaca, NY.
A REMOTE SENSOR TO MONITOR COMBUSTION PRODUCTS USING A TUNABLE ACOUSTO-OPTIC FILTER Ph.D. Thesis
Michael Jay Bardash 1989 120 p
Avail: Univ. Microfilms Order No. DA8915155

An optical system using a tunable acousto-optic filter to measure the temperature and partial pressures of CO and CO2 in combustion gases was designed and operated. The system measures the infrared absorption over a linear path through the combustion products from several lines of the vibration-rotation band of CO at 4.7 microns. The temperature and partial pressure of CO is then calculated using these data. The infrared absorption due the asymmetric stretch mode of CO2 is then measured. The entire system, under computer control, is self calibrating and is well suited for remote process control applications. Dissert. Abstr.

N90-11276# National Aerospace Lab., Tokyo (Japan). Instrumentation and Control Div.
ON THE MOTION EQUATION OF AN ELASTICALLY SUPPORTED TWO DEGREE OF FREEDON GYRO
Hirokimi Shingu Apr. 1987 13 p In JAPANESE; ENGLISH summary
(NAL-TM-568; ISSN-0452-2982; JTN-88-80063) Avail: NTIS HC A03/MF A01

This report describes a method of deriving a stricter motion equation for TDG (Tuned Dry Gyro) than Craig's, which has been used in generalized solutions, and comparison is made between the two equations. In order to reduce the complexity of mathematical manipulation, Craig's solution for TDG is derived under the assumption that rotor displacement angle theta is very small, and the derived expressions are valid over a range where sin theta is approx. equal to theta and cos theta is aprrox. equal to 1. In this study, the motion of an ETG (Elastically Supportd Two Degree of Freedom Gyro), which is defined as a TDG where the above assumption is neglected, is theoretically analyzed, and the analytic solution about a single-gimballed model of ETG is presented. The behaviors of TDG and ETG are simulated using various parameters of TDG developed in Japan as attitude sensors of artificial satellites and their difference is quantitatively evaluated. The resulting numerical solution shows that Craig's solution becomes inaccurate with an increase in amplitude and frequency of input angle. NASDA

N90-11277*# National Aeronautics and Space Administration. Lewis Research Center, Cleveland, OH.
GAS-PHASE FLOWRATE EFFECT ON DISINTEGRATING CRYOGENIC LIQUID-JETS
Robert D. Ingebo 1989 8 p Prepared for presentation at the 3rd International Congress on Fluid Mechanics, Cairo, Egypt, 2-4 Jan. 1990
(NASA-TM-102357; E-5071; NAS 1.15:102357) Avail: NTIS HC A02/MF A01 CSCL 14B

Two phase liquid and gaseous nitrogen flow in a pneumatic two fluid atomizer was investigated. Characteristic dropsize for cryogenic sprays were measured with a scattered light scanning instrument developed at NASA-Lewis. Tests were conducted primarily in the aerodynamic stripping regime of liquid jet atomization. At a sampling distance of bar-x=1.3 cm, the Sauter mean, D(sub 32), and volume median, D(sub v.5), drop diameters were measured and correlated with nitrogen gas flowrate, W(sub n), to give the following expressions: D sub 32 to the -1=210W(sub n) to the -1.33 and D(sub v.5) to the -1=150 W(sub n to the -1.33, where reciprocal diameters and gas flowrate are in cm (-1) and g/sec, respectively. The exponent 1.33 for nitrogrn gas flowrate, W(sub n), is the same as that predicted by atomization theory for liquid-jet breakup in high velocity gasflow. When the spray was sampled at axial distances of bar-x=2.5 and 4.5 cm downstream of the atomizer, the exponent decreased to 1.2 and 0.9, respectively. This was attributed to the loss of small droplets due to their rapid vaporization. Author

N90-11278# Oak Ridge National Lab., TN. Instrumentation and Controls Div.
USING SELF-CALIBRATING THERMOCOUPLES IN INDUSTRY
F. R. Ruppel 1989 6 p Presented at the Sensor's Expo 1989, Cleveland, OH, 12-14 Sep. 1989
(Contract DE-AC05-84OR-21400)
(DE89-013539; CONF-890996-2) Avail: NTIS HC A02/MF A01

The self-calibrating thermocouple is a thermocouple with a low melting point, high-purity metal encapsulated near but metallurgically isolated from its thermojunction. It is designed to provide a single-point calibration of the thermocouple at the melting point of the encapsulated metal because the time-temperature curve of the thermocouple will plateau at this temperature during heating or cooling. The calibration procedure consists of comparing the plateau temperature with the known melting point temperature of the encapsulated metal. The difference between these two values is the thermocouple error at the calibration point. The device is commercially available, but to be effective in industry it must be augmented with a data acquisition system with an algorithm that will automatically report the calibration error. DOE

N90-11279# Oak Ridge National Lab., TN.
SENSORS FOR NONDESTRUCTIVE TESTING AND EVALUATION OF MATERIALS
R. W. McClung 1989 10 p Presented at the Sensor's Expo 1989, Cleveland, OH, 12-14 Sep. 9 1989
(Contract DE-AC05-84OR-21400)
(DE89-014763; CONF-890996-3) Avail: NTIS HC A02/MF A01

Basic principles, designs, and several applications are described for the use of ultrasonic and eddy-current sensors in the nondestructive testing and evaluation of materials. There are many other designs and applications that were used beneficially, and custom designing can be done to address specific needs or problems. The technology provides important tools for process control, product acceptance and assurance of continued integrity after periods of service. DOE

N90-11280*# National Aeronautics and Space Administration. Goddard Space Flight Center, Greenbelt, MD.
MOXE: AN X-RAY ALL-SKY MONITOR FOR SOVIET SPECTRUM-X-GAMMA MISSION
W. Priedhorsky, E. E. Fenimore, C. E. Moss (Los Alamos National Lab., NM.), R. L. Kelley, and S. S. Holt 1989 13 p Presented at the SPIE Conference on EUV, X-ray, and Gamma Ray Instrumentation for Astronomy and Atomic Physics, San Diego, CA, 7-11 Aug. 1989
(Contract W-7405-eng-36)
(NASA-TM-101266; NAS 1.15:101266; DE89-015241; LA-UR-89-2246; CONF-8908120-2) Avail: NTIS HC A03/MF A01 CSCL 14B

A Monitoring Monitoring X-Ray Equipment (MOXE) is being developed for the Soviet Spectrum-X-Gamma Mission. MOXE is an X-ray all-sky monitor based on array of pinhole cameras, to be provided via a collaboration between Goddard Space Flight Center and Los Alamos National Laboratory. The objectives are to alert other observers on Spectrum-X-Gamma and other platforms of interesting transient activity, and to synoptically monitor the X-ray sky and study long-term changes in X-ray binaries. MOXE will be sensitive to sources as faint as 2 milliCrab (5 sigma) in 1 day, and cover the 2 to 20 KeV band. DOE

N90-11281# Fermi National Accelerator Lab., Batavia, IL.
NEW TOOLS FOR THE SIMULATION AND DESIGN OF CALORIMETERS
W. J. Womersley (Florida Univ., Gainesville.) 10 Jul. 1989

16 p Presented at the 4th Pisa Meeting on Advanced Detectors: Frontier Detectors from Frontier Physics, La Biodola (Italy), 21-26 May 1989
(Contract DE-AC02-76CH-03000)
(DE89-016323; FNAL/C-89/155-E; CONF-8905194-3) Avail: NTIS HC A03/MF A01

Two new approaches to the simulation and design of large hermetic calorimeters are presented. Firstly, the Shower Library scheme used in the fast generation of showers in the Monte Carlo of the calorimeter for the D-Zero experiment at the Fermilab Tevatron is described. Secondly, a tool for the design of future calorimeters is described, which can be integrated with a computer aided design system to give engineering designers an immediate idea of the relative physics capabilities of different geometries. DOE

N90-11282# Sandia National Labs., Albuquerque, NM.
RESPONSE OF STANDARDIZED PVDF PIEZOELECTRIC POLYMER GAUGES TO DIRECT SHOCK PRESSURES BETWEEN 8 AND 32 GPa
L. M. Moore and R. A. Graham 1989 4 p Presented at the American Physical Society Topical Conference on Shock Compression of Condensed Matter, Albuquerque, NM, 14-17 Aug. 1989
(Contract DE-AC04-76DP-00789)
(DE89-016811; SAND-89-1043C; CONF-890812-37) Avail: NTIS HC A01/MF A01

Previous fundamental studies of the response of standardized piezoelectric polymer stress gauges were largely based on impact experiments in which peak pressures as high as 46 GPa are achieved by ringing up to peak pressure in times of about 60 nsec. The shock-induced increase in temperature is minimized in this case. In order to study thermal effects and other possible influences in PVDF piezoelectric response, direct shock loading to high pressures were carried out in high explosive plane-wave loading experiments. Measured piezoelectric charges to pressures up to 10 GPa are found to the the same in both ring-up and direct shock loading. At peak pressures of 32 GPa, the observed charge is reduced by about 20 percent in the direct shock experiments. DOE

N90-11283# Technion - Israel Inst. of Tech., Haifa. Dept. of Nuclear Engineering.
THE 3-D HEAT TRANSFER COMPUTER CALCULATIONS OF TH E PERFORMANCE OF THE IAEA'S AIR-BATH CALORIMETERS
E. Elias, S. Kaizermann, R. B. Perry, and S. Fiarman (Brookhaven National Lab., Upton, NY.) 1989 6 p Presented at the 30th Annual Meeting of the Institute of Nuclear Materials Management, Orlando, FL, 9-12 Jul. 1989
(Contract W-31-109-eng-38)
(DE89-016908; CONF-890736-64) Avail: NTIS HC A02/MF A01

A three dimensional (3-D) heat transfer computer code was developed to study and optimize the design parameters and to better understand the performance characteristics of the IAEA's air-bath calorimeters. The computer model accounts for heat conduction and radiation in the complex materials of the calorimeter and for heat convection and radiation at its outer surface. The temperature servo controller is modelled as an integral part of the heat balance equations in the system. The model predictions will be validated against test data using the Argonne National Laboratory (ANL) bulk calorimeter. DOE

N90-11284# Naval Medical Research Inst., Bethesda, MD.
ROBUST SPATIAL CALIBRATION OF A PLANAR POSITRON CAMERA Final Report, Oct. 1985 - Sep. 1987
Paul K. Weathersby, Shalini S. Survanshi, and Paul Meyer Oct. 1988 29 p
(AD-A210773; NMRI-88-23) Avail: NTIS HC A03/MF A01 CSCL 18/4

The planar positron camera is a three-dimensional imaging device with two parallel and planar large crystal detectors. The spatial calibration problem is to define the relation between the raw digitized detector output to a physical coordinate system in the imaged space. In a calibration procedure, a positron point source is placed in a series of known emission locations during data acquisition. Data is then fit to a mathematical model to estimate spatial offsets and gains in the detector. Fitting procedures require some assumptions about error distribution, and the assumption of normally distributed error used in least-squares estimation does not appear suitable for these detectors. In simulated data sets, alternative non-normal distributions (robust estimators) allowed successful recovery of camera spatial parameters even with a few hundred total detected positron emissions. With experimental data, the robust procedures avoided the unreasonable camera performance parameters estimated by least squares. GRA

N90-11285# Johns Hopkins Univ., Baltimore, MD. Dept. of Materials Science and Engineering.
THE INVESTIGATION OF THE FUNDAMENTAL LIMITS OF HETERODYNE HOLOGRAPHIC INTERFEROMETRY WITH THE APPLICATION OF IMAGING LASER GENERATED LAMB WAVES Technical Report, Jun. 1987 - Apr. 1989
Louis C. Phillips and James C. Wagner Apr. 1989 152 p
(Contract N00014-82-K-0741)
(AD-A211048) Avail: NTIS HC A08/MF A01 CSCL 14/2

Currently, the field of ultrasonic nondestructive testing uses primarily piezoelectric transducers for both the generation and detection of acoustic waves. However, contact transducers have several shortcomings that have inhibited their use in some applications. The major weakness of piezoelectric transducers is that they must be in physical contact with the specimen. There are many situations where direct contact is not desirable, and in some cases, not possible. An alternate technique which was explored and developed in his manuscript is the application of holographic interferometry to imaging acoustic waves. Past acoustic studies, involving holographic interferometry as the inspection tool, were restricted to large amplitude waves with displacements on the order of the wavelength of light. Heterodyne and quasi-heterodyne phase measurement techniques were employed to achieve the necessary resolution in order to image sub-fringe events. As previous researchers have shown, heterodyne holographic interferometry (HHI) can be a powerful technique in the accurate measurement of imaging full field object displacements. However, previous experimental obstacles have made HHI an impractical method for ultrasonic measurement on a diffusely reflecting surface, a requirement to make HHI a practical method in ultrasonic nondestructive testing. GRA

N90-11286# Naval Postgraduate School, Monterey, CA.
LASER ALTIMETER FOR USE OVER THE OCEAN Final Report, Oct. 1987 - Sep. 1988
Eugene C. Crittenden, Jr., G. W. Rodeback, A. W. Cooper, and C. M. Bourne Apr. 1989 78 p
(AD-A211252; NPS61-89-001) Avail: NTIS HC A05/MF A01 CSCL 17/9

A pilot model of a small size, mass, power, and cost, GaAs laser radar altimeter has been developed and tested for use over the ocean. Two versions have been developed, one for triggering a device at a predetermined altitude, and one for providing an altitude read out as an analog dc voltage. Field tests from a bridge over an inland reservoir indicate performance with negligible false-alarm rate up to an altitude of 400 meters over the ocean, under all sea-state conditions, from glassy calm to the worst-case rough sea state condition, and with the sun vertically overhead. A new remote sensing technique was developed to evaluate the roughness state of the water during field tests and to predict the mean laser return signal. This utilizes video imaging of the glitter pattern on the water from a bright point source light at night, or from the sun in the daytime. Tests of the altimeter over the ocean surface at sea are still needed, because extrapolation from ripples on the inland reservoir to full scale ocean waves is not fully understood. GRA

N90-11287# Sandia National Labs., Albuquerque, NM.
THE SANDIA STANDARD FOR PVDF (POLYVINYLIDENE DI-FLUORIDE) SHOCK SENSORS
R. P. Reed, R. A. Graham, L. M. Moore, L. M. Lee, D. J. Fogelson, and F. Bauer 1989 4 p Presented at the American Physical Society Topical Conference on Shock Compression of Condensed Matter, Albuquerque, NM, 14-17 Aug. 1989
(Contract DE-AC04-76DP-00789)
(DE89-016530; SAND-88-3338C; CONF-890812-11) Avail: NTIS HC A01/MF A01

A formal consensus standard for a version of the generic Bauer Polyvinylidene Di-Fluoride (PVDF) shock stress sensor is being defined by a panel broadly experienced in the techniques of PVDF sensor application. The evolving standard addresses points essential to accurate shock measurement with PVDF gauges. It covers the materials, dimensions, proportions, processing, inspection, calibration, certification, tolerances, and application for PVDF elements. The formal standard will be available for voluntary use by the shock stress community as a guide for selection procurement, application, and analysis of this useful new shock measurement tool. DOE

N90-11288# Los Alamos National Lab., NM.
LASER-DRIVEN MINIATURE FLYER PLATES FOR SHOCK INITIATION OF SECONDARY EXPLOSIVES
D. L. Paisley 1989 5 p Presented at the American Physical Society Topical Conference on Shock Compression of Condensed Matter, Albuquerque, NM, 14-17 Aug. 1989
(Contract W-7405-eng-36)
(DE89-016587; LA-UR-89-2723; CONF-890812-21) Avail: NTIS HC A01/MF A01

Miniature flyer plates (greater than 1-mm diameter X greater than 5-micron thick) of aluminum and other materials are accelerated by a 10-ns pulsed Nd:YAG laser to velocities less than 5 km/s. Velocity profiles are recorded by velocity interferometry (VISAR) techniques and impact planarity by electronic streak photography. Techniques for improving energy coupling from laser to flyer plate will be discussed. Flyer plate performance parameters will be compared with material properties. The P(sup n)t criteria for shock initiation of explosives will be compared for various flyer materials, pressure, and pulse duration. Performance of secondary explosives (PETN, HNS, HMX, various PBX, others) will be reported. These data will detail the experimental effect of t (in P(sup n)t) approaching values of a few nanoseconds. DOE

N90-11289# Sandia National Labs., Albuquerque, NM. Thermochemical and Physical Div.
GAS-ACCELERATED PLATE STABILITY STUDY
Lynn M. Barker and Lalit C. Chhabildas 1989 3 p Presented at the American Physical Society Topical Conference on Shock Compression of Condensed Matter, Albuquerque, NM, 14-17 Aug. 1989
(Contract DE-AC04-76DP-00789)
(DE89-016880; SAND-89-0781C; CONF-890812-18) Avail: NTIS HC A01/MF A01

Flier plates are launched to hypervelocities using gas pressures in the megabar range. Flash X-rays which record the integrity of the launched plates show that they normally disintegrate. Experiments to enhance the flier plate stability have included variations in plate material, the use of buffer materials, and various schemes for mitigating violent edge effects. The smoothness of the drive is also discussed, and the study which led to the launching of an intact plate to 5.7 km/s is described. DOE

N90-11290# Los Alamos National Lab., NM.
INTERFEROMETRY AND HIGH SPEED PHOTOGRAPHY OF LASER-DRIVEN FLYER PLATES
D. L. Paisley, N. I. Montoya, D. B. Stahl, and I. A. Garcia 1989 6 p Presented at the SPIE Conference on High Speed Photography, Videography, and Photonics, San Diego, CA, 8 Aug. 1989
(Contract W-7405-eng-36)
(DE89-016990; LA-UR-89-2657; CONF-8908140-1) Avail: NTIS HC A02/MF A01

Laser-driven thin (2 to10 mu thick) plates of aluminum and copper are accelerated to velocities (ge)5 km/s by a 1.06- mu wavelength Nd:YAG 8 to 10 ns FWHM laser pulse at power densities 0.7 to 4.0 GW/cm(sup 2). Accelerations (ge)10(sup 9) km/s(sup 2) have been achieved. The acceleration and velocity of these 0.4 to 1.0-mm-diameter plates are experimentally recorded by velocity interferometry (VISAR) and the planarity of impact by streak photography. DOE

N90-11291# Joint Inst. for Nuclear Research, Dubna (USSR). Lab. of Nuclear Reactions.
ION DETECTOR ON THE BASIS OF MICROCHANNEL PLATES FOR A HIGH-SENSITIVE MASS SPECTROMETER
A. M. Rodin, S. I. Sidorchuk, and V. A. Timakov 1988 8 p In RUSSIAN; ENGLISH summary
(DE89-620335; JINR-13-88-589) Avail: NTIS (US Sales Only) HC A02/MF A01

The parameters of low energy ion detector designed as tandem type microchannel plates (MCP) are measured. The measurements were performed both in the current mode and in the mode of single ion count. It is shown that using of the detector designed as tandem type MCP allows one to measure the pulsed ion flows in the range from 10(14)/sm(-2)x s(-1) to 10(-2)cm(-2) x s(-1). DOE

N90-11292# Stuttgart Univ. (Germany, F.R.). Inst. fuer Technische Optik.
UTILIZATION OF PHOTOREFRACTIVE CRYSTALS IN OPTICAL IMAGE PROCESSING Ph.D. Thesis [EINSATZ PHOTOREFRAKTIVER KRISTALLE IN DER OPTISCHEN BILDVERARBEITUNG]
Frank Stefan Hoeller Jun. 1988 148 p In GERMAN
(ISBN-3-923560-06-0; ETN-89-94676) Avail: NTIS HC A07/MF A01

A multipurpose image and object comparison system with analog optics realtime-processing and storage is developed and tested. The image storage effect, based on the principle of photoinduced birefringence is experimentally and theoretically investigated using Bi12SiO20 (BSO) crystals the time and space dependence of the Jones matrix of a photorefractive coplanar plate is deduced, and the theoretical formulas are experimentally confirmed. The BSO-crystals can be used for fields up to 10 kV/cm. Besides a BSO-crystal as optical storage element, illumination systems are built in to realize several image processing operations without modifications. The image quality of the crystal is no worse than that of an 875-lines TV camera. The applicability of the system for positioning (for aerial photography) and error mark extraction is demonstrated. ESA

N90-11293# Swedish Defence Research Establishment, Linkoeping. Dept. of Information Technology.
FIBER OPTIC TECHNIQUE FOR SURVEILLANCE AND CONTROL OF MINE FIELDS
Stefan Karlsson Mar. 1989 18 p In SWEDISH; ENGLISH summary
(FOA-C-30526-3.1; ISSN-0347-3708; ETN-89-95155) Avail: NTIS HC A03/MF A01; Swedish Defence Research Establishment, P.O. Box 1165, S-58/11 Linkoeping, Sweden, 50 Swedish crowns

By implementing the periodic disturbancies in an optical fiber cable, it is possible to make it sensitive to pressure variations (as a strain gage) but acting as a distributed sensor. Examples are shown of a track passing at 20 km/hour on the cable and also 2 m from the line. But for intensity modulating sensors it is difficult to separate variable losses from the measured data. The multiplex method overcomes that by using two cables and connecting optical fiber rings. Optical sensors are light and easy to place in the ground. They have no galvanomagnetic effects and cannot be discovered with the methods used today. ESA

36 LASERS AND MASERS

Includes parametric amplifiers.
For related information see also *76 Solid-State Physics.*

N90-11294 Texas Univ., Austin.
THE RECOVERY OF ORBITAL AND GEOPHYSICAL PARAMETERS USING A SPACEBORNE LASER RANGING SYSTEM Ph.D. Thesis
John Bertram McNamee, Jr. 1988 172 p
Avail: Univ. Microfilms Order No. DA8909713

The Geodynamics Laser Altimetry/Ranging System (GLRS) is a spaceborne laser instrument currently under development which combines a pointable, two color laser for centimeter level ranging to ground based, cube corner retroreflectors and a nadir viewing laser altimetry system for decimeter level determination of the spacecraft height relative to underlying surface features. Presently, GLRS is a candidate facility instrument for deployment onboard one of the Earth Observing System (EOS) polar orbiting platforms scheduled for launch in the latter half of the 1990's. The potential applications attributed to the spaceborne laser ranging system include the determination of precise satellite ephemerides, monitoring tectonic plate motions and crustal deformations at plate boundaries, observing intraplate deformations, refining models of the Earth's gravity field, improved modeling of solid earth and ocean tides, and monitoring polar motion and variations in the length of day. Two potential applications of the GLRS instrument are examined: (1) the use of GLRS range measurements to produce precision orbit solutions for the EOS platform in support the EOS altimetry missions, and (2) the use of GLRS range data to solve for accurate reflector coordinates and interreflector baselines in support of tectonic plate motion and crustal deformation studies in seismically active regions. Satellite orbits with a radial orbit accuracy on the order of 10 cm RMS are required to support the altimetry missions involved in EOS. Orbit determination simulation results indicate that radial orbit accuracies of better than 30 cm RMS may be obtained for EOS 16 day arcs using GLRS range data to a global network of 22 fiducial reflectors and a reference gravity model tuned to the EOS orbit. The results of the simulated baseline solutions indicate that subcentimeter baselines may be recovered for baseline distances extending to approximately 1000 km in length using GLRS range data in conjunction with short arc solution techniques involving nine EOS orbital passes over the region of interest. The results demonstrate a dependence of the recovered baseline accuracy on the level of measurement noise, the baseline length, and the orientation of the baseline relative to the satellite ground track. Dissert. Abstr.

N90-11295 Saint Andrew's Univ. (Scotland).
ELEMENTS OF A 200 WATT PULSED EXCIMER LASER Ph.D. Thesis
George Glen McDuff 1987 255 p
Avail: Univ. Microfilms Order No. BRDX85267

The theoretical and experimental investigation into many aspects of circuit and component design for high average power short pulse systems is examined. The primary objective is to develop both circuit design criteria and pulsed components for long life rare gas halide lasers. A pulsed system consists of 3 major components: energy storage, switches, and load. The type of circuit which uses capacitive energy storage in combination with a closing switch to transfer electrical power to a load is considered. Specific loads are not addressed but the implications of load characteristics that affect circuit/component design and life are considered. The physical and electrical characteristics and analysis of phenomena that adversely affect the performance and life of pulse duty components are described. In the area of capacitive storage, lifetimes of one particular design was improved by 3 orders of magnitude and a means of detecting the imminent failure of oil filled capacitors was devised and patented. In the area of switching, methods are described by which hydrogen thyratrons can be operated in parallel with equal current sharing without the need for inductive or resistive ballasting. The design and testing of a 200 watt XeCl laser modulator is presented. Dissert. Abstr.

N90-11296 California Univ., Berkeley.
LASER DYNAMICS: THE SYSTEM DYNAMICS AND NETWORK THEORY OF OPTOELECTRONIC INTEGRATED CIRCUIT DESIGN Ph.D. Thesis
Tom Shinming-T.K. Tarng 1988 209 p
Avail: Univ. Microfilms Order No. DA8902289

Laser dynamics is the system dynamics, communication and network theory for the design of opto-electronic integrated circuit (OEIC). Combining the optical network theory and optical communication theory, the system analysis and design for the OEIC fundamental building blocks is considered. These building blocks include the direct current modulation, inject light modulation, wideband filter, super-gain optical amplifier, E/O and O/O optical bistability and current-controlled optical oscillator. Based on the rate equations, the phase diagram and phase portrait analysis is applied to the theoretical studies and numerical simulation. The OEIC system design methodologies are developed for the OEIC design. Stimulating-field-dependent rate equations are used to model the line-width narrowing/broadening mechanism for the CW mode and frequency chirp of semiconductor lasers. The momentary spectra are carrier-density-dependent. Furthermore, the phase portrait analysis and the nonlinear refractive index is used to simulate the single mode frequency chirp. The average spectra of chaos, period doubling, period pulsing, multi-loops and analog modulation are generated and analyzed. The bifurcation-chirp design chart with modulation depth and modulation frequency as parameters is provided for design purpose. Dissert. Abstr.

N90-11297# Brookhaven National Lab., Upton, NY. Center for Accelerator Physics.
A COMPACT X-RAY FREE ELECTRON LASER
W. Barletta, M. Atac, D. B. Cline, J. Kolonko, X. Wang, A. Bhowmik, B. Bobbs, R. A. Cover, F. P. Dixon, and G. Rakowsky (Rockwell International Corp., Canoga Park, CA.) et al 9 Sep. 1988 8 p Presented at the 4th Topical Meeting on Short Wavelength Coherent Radiation: Generation and Applications, Cape Cod, MA, 26-29 Sep. 1988 and the American Optical Society Meeting, Cape Cod, MA, 9 Sep. 1988
(Contracts DE-AC02-76CH-00016; W-7405-eng-48)
(DE89-017236; BNL-42393; CONF-880904-11) Avail: NTIS HC A02/MF A01

A design concept and simulation of the performance of a compact X-ray, free electron laser driven by ultra-high gradient RF-linacs is presented. The accelerator design is based on recent advances in high gradient technology by a LLNL/SLAC/LBL collaboration and on the development of bright, high current electron sources by BNL and LANL. The GeV electron beams generated with such accelerators can be converted to soft X-rays in the range from 2 to 10 nm by passage through short period, high fields strength wigglers as are being designed at Rocketdyne. Linear light sources of this type can produce trains of picosecond (or shorter) pulses of extremely high spectral brilliance suitable for flash holography of biological specimens in vivo and for studies of fast chemical reactions. DOE

N90-11298# European Organization for Nuclear Research, Geneva (Switzerland). Dept. Tecnologie Intersettoriali di Base.
FREE-ELECTRON LASER THEORY
G. Dattoli and A. Torre 1 Mar. 1989 65 p
(DE89-620145; CERN-89-03) Avail: NTIS (US Sales Only) HC A04/MF A01

The essential features of the theory of the free electron laser (FEL) are given in some detail. Beginning with an explanation of the basic gain mechanism, the lectures continue with a discussion of the problems associated with single-passage and recirculated (storage-ring) operation. Pulse propagation effects and the so-called lethargic behavior are analyzed more completely. Finally, elements of FEL quantum theory are reported, in order to clarify the laser process from the microscopic point of view. Appendices

give a fuller treatment of optical cavities and undulator magnets. DOE

N90-11299# Illinois Univ., Urbana. Dept. of Electrical and Computer Engineering.
SEMICONDUCTOR QUANTUM WELL LASERS AND RELATED OPTOELECTRONIC DEVICES ON SILICON, III-V
N. Holonyak, Jr., K. C. Hsieh, and G. E. Stillman Jun. 1989 35 p
(Contract DAAL03-89-K-0008)
(AD-A210758; TR-1; ARO-26434.1-EL) Avail: NTIS HC A03/MF A01 CSCL 09/3

Although an ultimate goal of this work is to achieve long term reliable laser operation of Al(x)Ga(1-x)As-GaAs quantum well heterostructures (QWH's), or similar III-V QWH's, grown on Si, this has proven to be a formidable enough problem that to the best of our knowledge no one has exceeded the results we reported in 1987 and 1988. This problem is of such dimensions that it may not be solved for as much as 10 years, or even more. All we know so far is that continuous (CW) 300 K Al(x)Ga(1-x)As-GaAs QWH lasers can be grown on Si, and that, indeed, the heat sinking of an Al(x)Ga(1-x)As-GaAs QWH laser on Si is better than a similar laser on a GaAs substrate. Nevertheless, the problem of growing better versions of these devices (i.e., long-lived high performance CW 300 K lasers on Si) has run into the fundamental issue of the large GaAs-Si lattice and thermal expansion mismatch, and hence the built-in difficulty in reducing the defects guaranteed by mismatch. Accordingly, and as much as we have worked further on the problem of Al(x)Ga(1-x)As-GaAs QWH lasers on Si, we have worked as hard on other QWH laser problems, as well as a impurity-induced layer disordering (or layer intermixing, IILD) and its application in laser devices. We briefly describe this work below and append the titles and abstracts of the papers we have published on laser studies and IILD. GRA

N90-11300# Aerospace Corp., El Segundo, CA. Lab. Operations.
DISSOCIATION AND VIBRATIONAL RELAXATION OF XeF BY VARIOUS COLLISION PARTNERS
Jerry F. Bott, Raymond F. Heidner, John S. Holloway, John B. Koffend, and Munson A. Kwok 15 Jul. 1989 26 p
(Contract F04701-85-C-0086)
(AD-A210769; TR-0088(3930-04)-2; SD-TR-89-39) Avail: NTIS HC A03/MF A01 CSCL 07/4

The removal rates of the lower levels of XeF strongly affect the overall efficiency of the XeF excimer laser operating on the B yields X transitions. We have deduced the removal rates of XeF(X,v = 3) in krypton, xenon, nitrogen, and carbon dioxide and the removal rates of XeF(X,v = 0) in sulfur hexafluoride by monitoring the populations of vibrational levels formed by the photolysis XeF2. The time history of the selected vibrational population is monitored with a continuous-wave (CW) tunable dye laser tuned to an absorption feature of the selected vibrational/rotational level. The studies show a rapid vibrational relaxation followed by a common decay rate of the coupled vibrational levels. The rare gases were found to remove XeF (X) with rate coefficients that differed from one another by less than a factor of 1.6. Larger removal rate coefficients were measured for molecular collision partners, with XeF2 having the largest rate coefficient. Rate coefficients were also determined for the concerted vibrational relaxation of v = 3 although the values do not represent state-to-state rate coefficients. Fast vibrational relaxation is required to empty the lower levels of the laser transitions so the vibrational bottlenecking does not terminate laser action prematurely. GRA

N90-11301# Michigan Univ., Ann Arbor. Div. of Research Development and Administration.
NONLINEAR OPTICAL STUDIES OF RESONANT SYSTEMS Final Report, 1 Apr. 1986 - 30 Apr. 1989
Duncan G. Steel 14 Jun. 1989 25 p
(Contract DAAL03-86-K-0057)
(AD-A211032; DRDA-85-2478-P1; ARO-23357.2-PH) Avail: NTIS HC A03/MF A01 CSCL 20/5

This research program developed a new understanding of the fundamental nature of nonlinear laser spectroscopy of resonant systems in the presence of state specific reservoir coupling. Experimental studies to support this work were performed in atomic sodium. However, the results of this work were extended to more complex systems. In particular, these advanced nonlinear spectroscopy methods could be applied to obtain a new understanding of many body systems such as GaAs quantum well structures. For example, one of the most interesting achievements of this program was the first direct observation of the homogenous line shape of the HH1 exciton in a GaAs/AlGaAs multiple quantum well. Another interesting result of this work was the clear demonstration of the nature of exciton spectral diffusion. GRA

N90-11302# Stanford Univ., CA. Lab. of Physics.
LASER PHYSICS AND LASER TECHNIQUES Final Report
A. E. Siegman Jun. 1989 259 p
(Contract F49620-86-K-0013)
(AD-A211117; AFOSR-89-1073TR) Avail: NTIS HC A12/MF A02 CSCL 09/3

Several areas of Laser Physics and Laser Techniques are reported on, including ultrafast physical measurements; the development of a new subpicosecond time-response photodetector; identification and analysis of an important new quantum noise limit for unstable laser oscillators; and useful advances in stable and unstable laser resonator theory. GRA

N90-11303# Los Alamos National Lab., NM.
STABILITY REQUIREMENTS OF RF LINAC-DRIVEN FREE-ELECTRON LASERS
William E. Stein, W. Joel D. Johnson, John F. Power, and Thomas J. Russel (Boeing Aerospace Co., Seattle, WA.) 1989 15 p Presented at the 11th International Free Electron Laser Conference, Naples, FL, 28 Aug. - 1 Sep. 1989
(Contract W-7405-eng-36)
(DE89-016609; LA-UR-89-2915; CONF-8908134-4) Avail: NTIS HC A03/MF A01

Fluctuations in the output power and wavelength have been observed in two high-power, RF-driven, free-electron lasers (FELs): the 10-(mu)m FEL that has operated at the Los Alamos National Laboratory and the visible FEL at the Boeing Physical Sciences Research Center. The fluctuations have been traced primarily to instabilities in the electron beam. Specifically, these are variations in the electron energy, the charge per micropulse, and the time interval between micropulses. The effects of these instabilities on the performance of one of the FELs is demonstrated. Efforts made to minimize these instabilities are discussed and the subsequent improvements in the operation of each of the FELs are presented. DOE

N90-11304# Oregon Univ., Eugene. Inst. of Theoretical Science.
RESEARCH IN X-RAY OPTICS WITH THE ULTIMATE AIM OF CONSTRUCTING A SYNCHROTRON RADIATION PUMPED SOFT X-RAY LITHIUM LASER Final Report
P. L. Csonka 31 Aug. 1988 19 p
(Contract DE-FG06-85ER-13309)
(DE89-016788; DOE/ER-13309/4) Avail: NTIS HC A03/MF A01

One of the primary components of the proposed synchrotron radiation (SR) pumped Li X-Ray Laser was a vacuum based high density plasma of predominantly monatomic Lithium as the lasing medium. A monomer density in excess of 10(19) particles/cu cm at temperatures (gt) 1600 C, in volume of roughly 1 cm x 0.001 cm x 0.001 cm was estimated as being necessary for attaining useful gain. Originally two different methods of achieving this were considered, namely: laser driven ablation of solid Li, and steady state thermal emission of Li gas from an orifice in a suitable chamber. Due to uncertainties associated with the first option, the resources of the present development program were focused primarily on the latter technique. DOE

N90-11305# Los Alamos National Lab., NM.
MINIMIZED EMITTANCE GROWTH WITH ELLIPTICAL BEAM PIPES IN FEL (FREE-ELECTRON LASER)
K. C. D. Chan 1989 17 p Presented at the 11th International Free Electron Laser Conference, Naples, FL, 28 Aug. - 1 Sep. 1989
(Contract W-7405-eng-36)
(DE89-016982; LA-UR-89-2867; CONF-8908134-2) Avail: NTIS HC A03/MF A01

Wakefield effects can cause emittance growth in free-electron-laser systems and reduce free-electron-laser gain. This paper explains that, by using beam pipes with elliptical cross sections, discontinuities can be allowed along a beam pipe without introducing wakefields. To use a beam pipe with an elliptical cross section, wakefield-less transitions between beam pipes with circular and elliptical cross sections are also needed. A concept to achieve such a transition is discussed. DOE

N90-11306# Oak Ridge National Lab., TN. Physics Div.
SYNCHROTRON RADIATION, FREE ELECTRON LASER, AND NUCLEAR STRUCTURE Foreign Trip Report, 6 Apr. - 13 Apr. 1989
D. K. Olsen 1 May 1989 7 p
(Contract DE-AC05-84OR-21400)
(DE89-017352; ORNL/FTR-3218) Avail: NTIS HC A02/MF A01

The traveler attended the CERN Accelerator School and Daresbury Laboratory course on Synchrotron Radiation and Free Electron Lasers held at Chester College, Chester, England, from April 6 to 13, 1989. The course, attended by 89 people, was well conceived, well presented, and informative. Almost all aspects of accelerator-based light sources were discussed. The traveler also visited the Nuclear Structure Facility at Daresbury Laboratory, Daresbury, England. The tandem accelerator of the Nuclear Structure Facility runs routinely between 18 and 19 MV and, with difficulty, between 19 and 20 MV. Installation of the Oxford post-tandem superconducting RF cavities is nearly complete. These cavities will increase the effective accelerating potential by about 6 MV. In addition, Daresbury plans to add another 6 MV of superconducting RF cavities. When complete, the Daresbury tandem facility should be able, with three foil strippings, to accelerate lead to 5 MeV/nucleon. DOE

N90-11307# Oregon Univ., Eugene. Dept. of Physics.
NONLINEAR DYNAMICS OF BROAD-BAND LASERS Progress Report, 1 Sep. 1988 - 31 Aug. 1989
Michael G. Raymer Jun. 1989 5 p
(Contract DE-FG06-88ER-13973)
(DE89-017442; DOE/ER-13973/1) Avail: NTIS HC A01/MF A01

Progress was made on two fronts. First, a Ti:Sapphire laser and a micro-cavity dye laser were designed and constructed, and are now being tested. Second, a theoretical analysis was carried out on the effects of quantum noise on multimode lasers operating just above threshold. The prediction is that as threshold is approached from above, the mode intensity correlation time increases to a maximum value and then decreases when the quantum noise becomes dominant near threshold. The effects will be observed in the studies. DOE

N90-11308# Joint Inst. for Nuclear Research, Dubna (USSR).
DETERMINATION OF NEUTRAL PARTICLE CONCENTRATION AT EROSION LASER PLASMA EXPANSION INTO VACUUM
V. E. Mironov 1988 5 p In RUSSIAN; ENGLISH summary
(DE89-620128; JINR-13-88-486) Avail: NTIS (US Sales Only) HC A01/MF A01

Experimental setup and methods for erosion laser plasma neutral component by ion probing are described. Laser ion source was used. Time distribution of neutral particle density at 5 cm from a point of plasma forming at laser radiation flux density q in 2x10 sup 7 2x10 sup 9 Vxcm sup -2 range for various target materials were obtained. Obtained distributions were approximated by Maxwell velocity distributions. DOE

N90-11309# Swedish Defence Research Establishment, Linkoeping. Dept. of Information Technology.
LASER TECHNIQUES FOR GROUND TO AIR APPLICATIONS
Ove Steinvall Feb. 1989 35 p In SWEDISH; ENGLISH summary
(FOA-C-30524-3.1; ISSN-0347-3708; ETN-89-95170) Avail: NTIS HC A03/MF A01; Swedish Defence Research Establishment, Box 1165, S-581 11, Linkoeping, Sweden, 50 Swedish crowns

Laser techniques used in air defense for rangefinding, tracking, beamriding, and for ground to air applications are examined. Of special interest are the coherent systems which will add classical radar functions at optical wavelengths and allow imaging systems and Doppler functions. Besides target acquisition, future laser systems will also offer a possibility of atmospheric wind sounding and slant path measurements. Lasers can be used for jamming and destruction of optical sensors. Ordnance information about tactical laser weapons is included. ESA

37 MECHANICAL ENGINEERING

Includes auxiliary systems (nonpower); machine elements and processes; and mechanical equipment.

N90-11310*# National Inst. of Standards and Technology, Gaithersburg, MD. Robot System Div.
NASA/NBS (NATIONAL AERONAUTICS AND SPACE ADMINISTRATION/NATIONAL BUREAU OF STANDARDS) STANDARD REFERENCE MODEL FOR TELEROBOT CONTROL SYSTEM ARCHITECTURE (NASREM) Final Report
James S. Albus, Harry G. McCain, and Ronald Lumia Apr. 1989 85 p Sponsored by NASA, Goddard Space Flight Center, Greenbelt, Md
(NASA-CR-185078; NAS 1.26:185078; PB89-193940; NIST/TN-1235-89) Avail: NTIS HC A05/MF A01; SOD HC $4.25 as 003-003-02928-9 CSCL 13I

The document describes the NASA Standard Reference Model (NASREM) Architecture for the Space Station Telerobot Control System. It defines the functional requirements and high level specifications of the control system for the NASA space Station document for the functional specification, and a guideline for the development of the control system architecture, of the 10C Flight Telerobot Servicer. The NASREM telerobot control system architecture defines a set of standard modules and interfaces which facilitates software design, development, validation, and test, and make possible the integration of telerobotics software from a wide variety of sources. Standard interfaces also provide the software hooks necessary to incrementally upgrade future Flight Telerobot Systems as new capabilities develop in computer science, robotics, and autonomous system control. GRA

N90-11311 Cincinnati Univ., OH.
MODELING AND SIMULATION OF SPATIAL ROBOTIC MANIPULATORS WITH FLEXIBLE LINKS AND JOINT DRIVES FOR CONTROL STRATEGIES IMPLEMENTATION AND EVALUATION Ph.D. Thesis
Mohammad H. Fathalla Dado 1988 251 p
Avail: Univ. Microfilms Order No. DA8908466

A methodology is developed for the modeling and simulation of flexible robotic systems. The methodology consists of a comprehensive modeling procedure for robots with flexible links and joint derives and a procedure to determine the dynamic response of the robot for the purpose of control strategy evaluation. The link and joint flexibilities are modeled using finite element techniques. The robot links and joint shafts are considered to have distributed mass and elasticity properties and continuous loadings along their axes. The link cross-sectional dimensions can experience linear variations along the link axis. The joint model considers gear ratios, gear inertia and internal material damping. The link and joint models are integrated through automatic mesh generation and freedom number assignments. The global system matrices are partitioned in a manner that improves the speed of

computations for the simulation procedure. Simulation is provided in the kineto-elastodynamic mode. The objectives of the simulation procedure are: (1) to provide a direct relationship between the driving torques at the joints and the link accelerations in the kineto-elastodynamic mode, and (2) to determine the rigid body driving torques. The first objective is utilized in simulating and evaluating the dynamic behavior of the robot in response to different control strategies and under different operating conditions. The rigid body torques are used as part of the control strategy definition. Several numerical examples are provided to illustrate the applications of this development and future directions for research and development are identified. Dissert. Abstr.

N90-11312 Virginia Univ., Charlottesville.
DYNAMIC ANALYSIS OF ROTORS UNDER INTERFERENCE RUBS Ph.D. Thesis
Chihping Chester Lee 1987 308 p
Avail: Univ. Microfilms Order No. DA8902443

Theories and applications are developed for complex multi-level flexible rotor/bearing systems based on the finite element method. The complex system of equations is simplified by the static condensation method to reduce the number of degrees-of-freedom without losing much of the accuracy. An efficient subspace iteration technique for damped eigenvalue problem is applied to the damped natural frequency analysis of rotor systems. The method has been modified and extended to take advantage of the nature of the sparse matrix in a typical problem so that both the computer memory requirement and computation times can be reduced. Interference rub phenomenon between rotor and stator are studied using both linear and non-linear models. In a steady state linear model, the rub force is decomposed into harmonics using Fourier transformation. The overall response of the rotor is the summation of the individual rotor response at each of the harmonics. Non-linear models are also developed and the equations of motion are solved in the time domain to assess the overall response and stability of the system. Two example cases are presented to demonstrate the applications of the analysis. A computer program is developed based on the non-linear models presented. Author

N90-11313 Purdue Univ., West Lafayette, IN.
THE 3D-POLY: A ROBOT VISION SYSTEM FOR RECOGNIZING OBJECTS IN OCCLUDED ENVIRONMENTS Ph.D. Thesis
Chien-Huei Chen 1988 195 p
Avail: Univ. Microfilms Order No. DA8911888

The two factors that determine the time complexity associated with model-driven interpretation of range maps are: the particular strategy used for the generation of object hypotheses; and the manner in which both the model and the sensed data are organized, data organization being a primary determinant of the efficiency of verification of a given hypothesis. The 3D-POLY, a working system for recognizing objects in the presence of occlusion and against cluttered backgrounds, is presented. The time complexity of this system is only O(n(2)) for single object recognition, where n is the number of features on the object. The most novel aspect of this system is the manner in which the feature data are organized for the models. A data structure called the feature sphere is used for the purpose. Efficient algorithms are presented for assigning a feature to its proper place on a feature sphere, and for extracting the neighbors of a given feature from the feature sphere representation. For hypothesis generation, local feature sets are used, a notion similar to those used before us by Bolles, Shirai and others. The combination of the feature sphere idea for streamlining verification and the local feature sets for hypothesis generation results in a system whose time complexity has a polynomial bound. In addition to recognizing objects in occluded environments, 3D-POLY also possesses model learning capability. Model learning consists of looking at a model object from different views and integrating the resulting information. The 3D-POLY system also contains utilities for range image segmentation and classification of scene surfaces. Dissert. Abstr.

N90-11314 Cornell Univ., Ithaca, NY.
PLANAR SLIDING OF A RIGID BODY WITH DRY FRICTION: LIMIT SURFACES AND DYNAMICS OF MOTION Ph.D. Thesis
Suresh Goyal 1989 180 p
Avail: Univ. Microfilms Order No. DA8915177

We present a relation between friction load (force and torque) and slip motion (displacement and rotation) for a rigid planar object sliding on a flat surface, where the distribution of the normal contact forces between the object and the supporting surface is assumed to be known a priori and the friction is assumed to be independent of slip rate. Every point of frictional contact is assumed to obey a maximum work inequality which generalizes Coulomb friction. Then in analogy with the maximum plastic work inequality in classical plasticity, the relation between the total frictional load and slip motion for the given slider also obeys a loan motion inequality. The full relation between the frictional load and the slip motion for an object can thus be described by a convex limit surface in load space, with the instantaneous motion direction (in conjugate motion space) being normal to this surface, where it is smooth. The object's limit surface can be found by Minkowsky addition of the limit surfaces of the individual contact points or by other simple means. Attention is focussed on the cause of the occurrence of vertices on the limit surface (where motion is not unique for a given load) and flat regions (where load is not unique for a given motion). Dissert. Abstr.

N90-11315# Sandia National Labs., Livermore, CA. Process Development and Fabrication Div.
A CHARACTERIZATION OF THE SIDE BONDING, UPSET PLUG WELDING PROCESS
Samuel B. Johnson Aug. 1989 34 p
(Contract DE-AC04-76DR-00789)
(DE89-015181; SAND-89-8242) Avail: NTIS HC A03/MF A01

The goal was to characterize the side bonding variant of the upset plug welding process. In this process an oversized plug is driven into an opening where it is welded in place with the heat of electric current. The processing parameters studied in this work were weld current, closing force, weld time, plug fit, and interfacial cleanliness. The results were measured in terms of plug displacement, metallurgical structure, and bond length. The results of the experiments indicate that force has a modest influence on cold plug displacement, but little effect on ultimate bond quality. Plug fit has a moderate influence on cold displacement. Lubricous contamination can affect a sharp increase in cold displacement. With the passage of current, the weld structure is seen to develop quickly, then reach a point of equilibrium and become independent of weld time after that. Higher levels of current bring the process to completion sooner, but given sufficient time the end results can be the same for a wide range of currents. In a quantitative way, this work presents data which facilitates optimal selection of processing parameters. Qualitatively, the information provides insight into the basic mechanisms of the process. On a conceptual level, approaches for controlling quality are presented. Most significantly, the results of the work portray side bonding, upset plug welding as a remarkably robust process, extremely tolerant of major variations in processing parameters. DOE

N90-11316# Sunpower, Inc., Athens, OH.
FREE-PISTON STIRLING ENGINE MAGNETICALLY COUPLED HEAT PUMP: CRITICAL COMPONENT EVALUATION
G. Chen Aug. 1989 46 p
(Contract DE-AC05-84OR-21400)
(DE89-015646; ORNL/Sub-86-SA578/1) Avail: NTIS HC A03/MF A01

The Free-Piston Stirling Engine (FPSE) Magnetically Coupled Heat Pump Program at Sunpower involves the development of a FPSE/magnetic coupling/compressor (FPSE/MC/C) assembly for a gas residential heat pump application. The objectives of Phase 1 were: (1) to evaluate the feasibility and characteristics of critical components such as a linear magnetic coupling and hermetic sealing, (2) to demonstrate through tests the performance of a magnetic coupling/compressor assembly, and (3) to evaluate the system concept design by applying an air-charged FPSE. DOE

N90-11317# Sunpower, Inc., Athens, OH.
DYNAMIC CHARACTERISTICS CONCERNED IN THE DESIGN OF A FREE-PISTON STIRLING ENGINE/MAGNETIC COUPLING/COMPRESSOR SYSTEM
G. Chen 1989 7 p Presented at the 24th Intersociety Energy Conversion Engineering Conference, Arlington, VA, 6-11 Aug. 1989
(Contract DE-AC05-84OR-21400)
(DE89-015981; CONF-890815-23) Avail: NTIS HC A02

In a free-piston Stirling engine-driven heat pump, the engine power must be controlled to follow the compressor load. An axial magnetic coupling connecting the engine power piston and compressor piston acts like a nonlinear spring. The dynamic characteristics associated with the system design for this type of heat pump are considered in this paper. System concepts are described in terms of the engine power-load matching, system tuning, and identifying the load on the magnetic coupling. DOE

N90-11318# Allied-Signal Aerospace Co., Kansas City, MO.
ADVANCED TURBINE TECHNOLOGY APPLICATIONS PROGRAM, (ATTAP)
Apr. 1989 12 p
(DE89-016067; DOE/CE-50111/H1) Avail: NTIS HC A03/MF A01

A significant level of Research and Development and product development activities on ceramic materials is being carried on by the General Motors Corporation and the Allied-Signal Corporation, the parent companies of the ATTAP contractors, Allison Gas Turbine Division and Garrett Auxiliary Power Division, respectively. In continuing the automotive gas turbine program with both Allison and Garrett in the application of high temperature structural materials in advanced automotive gas turbine engines it was the intention of the Department of Energy to not only provide encouragement to these companies to continue their activities on ceramic materials which are providing important synergistic benefits to ATTAP but also to signal the developing U.S. ceramics industry of a continuing commitment to this program by important elements of the gas turbine industry and the automotive industry. DOE

N90-11319# Oak Ridge National Lab., TN. Engineering Technology Div.
RESULTS FROM THE SECOND YEAR OF OPERATION OF THE FEDERAL METHANOL FLEET AT ARGONNE NATIONAL LABORATORY
R. N. McGill, S. L. Hillis, B. H. West, and J. W. Hodgson (Tennessee Univ., Knoxville.) Aug. 1989 47 p
(Contract DE-AC05-84OR-21400)
(DE89-016935; ORNL/TM-11230) Avail: NTIS HC A03/MF A01

Argonne National Laboratory has completed two full years of operation of 19 vehicles in the Federal Methanol Fleet Project; ten of the vehicles are fueled with methanol. Over one-half million miles have been accumulated on the fleet vehicles so far, and comparisons of efficiency continue to show nearly equal performance between the methanol and gasoline vehicles. Emissions tests of some of the vehicles during the second year revealed degradations of emissions control systems for both the methanol and gasoline vehicle types, although emissions were still within limits. Methanol vehicles continued to require more maintenance, and the maintenance labor intensity (hours per 1000 miles) increased for all the vehicle types being monitored. Accumulation of metals in the lubricating oil of the methanol vehicles continued to be elevated compared to that of the gasoline vehicles although not at alarming levels. Drivers indicated less satisfaction with vehicles in the test during the second year, both for methanol as well as gasoline vehicles. DOE

N90-11320# Department of Energy, Washington, DC. Office of Transportation Systems.
ADVANCED TURBINE TECHNOLOGY APPLICATIONS PROGRAM, (ATTAP): A PLAN FOR IMPROVING THE PROTOTYPE PRODUCTION OF CERAMIC COMPONENTS FOR THE GAS TURBINE ENGINE, 1988--1992
Apr. 1989 18 p
(DE89-015566; DOE/CE-0257) Avail: NTIS HC A03/MF A01

This Advanced Turbine Technology Applications Project (ATTAP) Plan is intended to advance the technological readiness for commercialization of an automotive ceramic gas turbine engine, the feasibility of which was established and demonstrated during the recently concluded AGT Project. DOE

N90-11321# Welding Consultants, Inc., Columbus, OH.
THE META-LAX METHOD OF STRESS REDUCTION IN WELDS Quarterly Report No. 1
24 Jul. 1989 5 p
(Contract DE-FG01-89CE-15412)
(DE89-016437; DOE/CE-15412/T1) Avail: NTIS HC A01/MF A01

The objective of this program is to study the ability of the Meta-Lax process to replace thermal treatments commonly employed during welded fabrication of metals. The energy saving offered by the Meta-Lax process result in a twofold manner. First, the only energy input required is the small amount of 110 volt household current necessary to run an electric motor which drives the vibrator. Secondly, the time required to accomplish the necessary effect is minimal compared to the time for an equivalent thermally induced effect. DOE

N90-11322# Sandia National Labs., Albuquerque, NM.
RETHINKING SYNTHESIS OF FINE-MOTION STRATEGIES
D. Strip 2 Jun. 1989 11 p
(Contract DE-AC04-76DP-00789)
(DE89-016671; SAND-89-0547) Avail: NTIS HC A03/MF A01

In their influential paper, Automatic Synthesis of Fine Motion Strategies for Robots, Lozano-Perez, Mason, and Taylor hypothesize that fine motion strategies are inherently dependent on fine details of part geometry. They propose a complex algorithm which accounts for fine details in developing fine motion strategies. Recent work on insertions and grasping suggests that the use of force directed strategies allows the development of robust action primitives that are independent of all but the grossest details of geometry. DOE

N90-11323# Oak Ridge Y-12 Plant, TN. Dept. of Fabrication Systems.
ELECTRON BEAM WELDING: MODEL OF HIGH VOLTAGE BIAS TRANSMISSION LINE AND TERMINATION CIRCUITS
J. T. Greer Aug. 1989 15 p
(Contract DE-AC05-84OS-21400)
(DE89-016900; Y/DX-833) Avail: NTIS HC A03/MF A01

Three electron beam (EB) welding systems have experienced an excessive failure rate of the isolation transformer that supplies low voltage power to the high-deck control circuitry. The cost of this failure is $8K per transformer, plus installation, downtime expenses, etc. Nine transformers (twenty-two transformers since 1982) have been replaced in the last two years and represent a significant economic loss if this problem is not resolved. The commercial EB controller unit was purchased from Leybold-Heraeus Vacuum Systems, which has several other vendor-supplied parts. For example, the transmission line is a special build item and does not have published parameters. Off-line testing and model closure were required to attain these needed parameters. To obtain parameters for the transmission cable and to evaluate possible solutions, a model was constructed that predicts voltages and current for termination circuits and includes the four-conductor transmission cable used to bias and control the EB gun. To compound the problem, the entire high voltage deck is submerged in oil and limits the available space needed for termination circuits, etc. A low voltage test was performed that was used to attain good model closure and to provide critical cable parameters not previously available. The model was useful in assuring consistency for measured parameters and for estimating hard to measure parameters that were derived from test signals. Model closure was attained, and several possible termination circuits were

evaluated. A termination for the transmission cable is proposed in this report. DOE

N90-11324# Sandia National Labs., Albuquerque, NM.
LAND VEHICLE TELEOPERATION UNDER CONDITIONS OF REDUCED VIDEO RESOLUTION
J. Lee Schoeneman and Douglas E. McGovern Aug. 1989 60 p
(Contract DE-AC04-76DP-00789)
(DE89-016925; SAND-89-1256) Avail: NTIS HC A04/MF A01

Teleoperation of land vehicles was studied to investigate the effects of both spatial and temporal video resolution on the ability of the operator to effectively control the vehicle. Teleoperation extends part of a human operator's presence into remote or hazardous areas, and the predominant form of sensory feedback is that of vision. The quality of the transmitted video information has a significant effect on the operator's confidence and ability to effectively control the vehicle. Experiments were constructed to allow subjective evaluation of the lower limits of video quality necessary for degraded, yet effective, teleoperation. Subjects were asked to teleoperate a remote vehicle under varying conditions to degraded spatial and temporal resolution, and their comments were recorded along with the video driving scenes during teleoperation. Subjective assessments and teleoperation test data suggest the possibility of reducing the required video bandwidth for teleoperation by a factor of 28:1 over normal video standards. DOE

38 QUALITY ASSURANCE AND RELIABILITY

Includes product sampling procedures and techniques; and quality control.

N90-11325# Argonne National Lab., IL. Materials and Components Div.
A TECHNIQUE TO CORRELATE FRACTOGRAPHY WITH NDE (NON-DESTRUCTIVE EVALUATION) OF SMALL SAMPLES
J. J. Vaitekunas, R. A. Roberts, and W. A. Ellingson Dec. 1988 13 p Presented at the Joint ASME/JSME Pressure Vessel and Piping Conference, Honolulu, HI, 23-27 Jul. 1989
(Contract W-31-109-eng-38)
(DE89-016904; CONF-890721-41) Avail: NTIS HC A03/MF A01

Images are often produced from data obtained with nondestructive evaluation (NDE) techniques to take advantage of the human ability to visually detect patterns and changes in acquired data. An ultrasonic imaging technique was applied to detect flaws and predict failure locations in ceramic modulus-of-rupture (MOR) bars. After fracture and subsequent fractographic analysis, the ultrasonic NDE data were correlated with digitized optical images of the MOR bars to determine if the location of the failure-initiating flaw was detected by the ultrasonic technique. The microcomputer-based digital image processing method used to correlate the fractographic analysis with NDE data was described. An algorithm which can be used to implement the technique on most imaging workstations is presented, along with results obtained with an IBM-PC. DOE

N90-11326# Army Chemical Research and Development Center, Aberdeen Proving Ground, MD.
METHODOLOGY OF DEVELOPING A COMBINED ENVIRONMENTAL STRESS SCHEDULE FOR RELIABILITY GROWTH TESTING Special Publication
Louie J. Lipp Jun. 1989 57 p
(AD-A211053; CRDEC-SP-008) Avail: NTIS HC A04/MF A01 CSCL 14/2

Many U.S. Army systems require reliability growth testing to meet technical requirements for hardware durability during engineering development. Such tests are often performed in chambers that simulate multiple stressful environments. The usual environmental stresses include temperature, vibration, humidity, and power or voltage cycling. If it is apparent that other environments can cause or induce reliability-related failures, then they are also required. Because a combination of stresses will in most cases be experienced in actual use, these combined stresses are used in the environmental chambers. Hardware-related reliability weaknesses precipitated out during environmental testing will initiate the Failure Reporting and Corrective Action System (FRACAS) necessary to improve item design. The development of a test schedule that uses the user's mission profile when combining operational and storage environmental stresses is demonstrated. Blind application of test parameters or schedules from MIL-STD-810D, Environmental Test Methods and Engineering Guidelines, from International Test Operational Procedures (ITOPs) especially for vibration stresses, is not acceptable, because they are designed to cause short-term failures unrelated to either a mission profile or to determine a mean time between failure (MTBF) over thousands of hours of testing. GRA

N90-11053# Virginia Polytechnic Inst. and State Univ., Blacksburg. Materials Response Group.
THE USE OF DAMAGE CHARACTERIZATION FOR LIFE PREDICTION METHODOLOGIES
Kenneth L. Reifsnider *In* ESA, Spacecraft Structures and Mechanical Testing Jan. 1989 p 513-519 (For primary document see N90-10986 02-18)
(Contract N62269-85-C-2345; AF-AFOSR-0087-85)
Copyright Avail: NTIS HC A99/MF E06

39 STRUCTURAL MECHANICS

Includes structural element design and weight analysis; fatigue; and thermal stress.

For applications see *05 Aircraft Design, Testing and Performance* and *18 Spacecraft Design, Testing and Performance.*

N90-11327# Virginia Polytechnic Inst. and State Univ., Blacksburg.
COMPUTATIONAL ASPECTS OF SENSITIVITY CALCULATIONS IN LINEAR TRANSIENT STRUCTURAL ANALYSIS Ph.D. Thesis
William H. Greene Aug. 1989 109 p
Avail: NTIS HC A06/MF A01

A study has been performed focusing on the calculation of sensitivities of displacements, velocities, accelerations, and stresses in linear, structural, transient response problems. One significant goal was to develop and evaluate sensitivity calculation techniques suitable for large-order finite element analyses. Accordingly, approximation vectors such as vibration mode shapes are used to reduce the dimensionality of the finite element model. Much of the research focused on the accuracy of both response quantities and sensitivities as a function of number of vectors used. Two types of sensitivity calculation techniques were developed and evaluated. The first type of technique is an overall finite difference method where the analysis is repeated for perturbed designs. The second type of technique is termed semianalytical because it involves direct, analytical differentiation of the equations of motion with finite difference approximation of the coefficient matrices. To be computationally practical in large-order problems, the overall finite difference methods must use the approximation vectors from the original design in the analyses of the perturbed models. Author

N90-11328 Lehigh Univ., Bethlehem, PA.
A RE-EVALUATION OF FATIGUE THRESHOLD TEST PROCEDURES AND THE SIMULATION AND PREDICTION OF FATIGUE CRACK GROWTH UNDER CONDITIONS OF LOW CRACK CLOSURE Ph.D. Thesis
William Alexander Herman 1989 188 p
Avail: Univ. Microfilms Order No. DA8909386

Conventionally determined fatigue threshold information (ASTME647) can lead to nonconservative estimates of fatigue

lifetimes when these data are utilized in damage tolerant design assessments. The non-conservative nature of such data can be attributed primarily to the development of excessively large amounts of crack closure at low R-ratios, particularly at near threshold stress intensity factor levels. These high closure levels attenuate the effective stress intensity condition prevailing at the crack tip and confound attempts to predict in service crack propagation behavior which involve negligible crack closure levels. A modified test procedure, involving constant maximum stress intensity Delta K-decreasing test conditions (K(c)sub max) is described which identifies fatigue crack propagation (FCP) threshold behavior in the absence of detectable amounts of crack closure. These data have been generated with conventional long crack specimens for several aluminum, iron, and nickel base alloys and are shown to closely simulate the low closure FCP response of short cracks and weldments in these engineering materials. Furthermore, the deleterious effects of compressive underloads on crack propagation were demonstrated to be highly dependent on prior long crack closure levels. Dissert. Abstr.

N90-11329 Houston Univ., TX.
THE DYNAMICS OF CIRCULAR PLATES WITH PATCH DAMPING: A NUMERICAL AND EXPERIMENTAL STUDY Ph.D. Thesis
Mahmoud Mezache 1988 142 p
Avail: Univ. Microfilms Order No. DA8901483

The objective is to devise a procedure for studying the response of a vibrating structure and its acoustic radiation characteristics. The major goal is to arrange the damping treatment so as to obtain maximum reduction in the response of the structure. A finite-element approach is used and applied to a circular plate for which the first three axisymmetric modes are investigated. The plate is treated over selected areas, resulting in a nonproportional damping case. The damped elements are modeled so that their mass, loss factor and flexural rigidity are preserved. The finite-element program is linked to an existing program which is used to calculate the spatial distribution of the acoustic intensity and the radiated power. Two regions of interest are observed: first, the region within the first nodal circle, seen from the center of the plate, the second is in the region bounded by the first nodal circle and the free edge of the plate. The measured and calculated response quantities in the first region are in good agreement. The discrepancy increases as the size of the damping patch is reduced because of the boundary-element effect, particularly in the second mode. This discrepancy is less pronounced in this region for the third mode, as the wavelength is smaller and so is the boundary-element effect. Dissert. Abstr.

N90-11330 George Washington Univ., Washington, DC.
AN EVALUATION OF THE CHABOCHE AND BODNER-PARTOM VISCOPLASTIC CONSTITUTIVE THEORIES FOR STRAIN RATE SENSITIVE MATERIALS Ph.D. Thesis
Ahmed Mohamed El-Assal 1988 184 p
Avail: Univ. Microfilms Order No. DA8900487

Many unified viscoplastic constitutive theories were introduced during the recent decades to model the different inelastic behavioral aspects of engineering materials. These theories include in most cases many parameters associated with the complicated differential or integral equations describing the various deformation processes. Due to the sophistication associated with the formulation of constitutive equations, the task of evaluating their parameters is always a difficult one and in most cases involves many assumptions and approximations. A simple, systematic and straightforward procedure is developed to evaluate the parameters of two unified theories for strain rate sensitive materials. Two unified models were chosen to represent the two major classes of viscoplastic constitutive theories: the Chaboche theory was selected from the yield based class of theories, and the Bodner-Partom theory was selected from the nonyield based theories. A procedure for generating the experimental data required to achieve the material property evaluation task has been developed and corresponding tests were performed on two strain-rate sensitive materials, Ti-6A1-4V and Type 316 stainless steel. The predictive capabilitiues of both constitutive theories were demonstrated and compared with the experimental data for both materials. A generally good agreement was attained between the data and the predictions of both theories for the two materials even though the model parameters were not optimized. Dissert. Abstr.

N90-11331 University of South Florida, Tampa.
THE DYNAMIC STABILITY OF AN AXIALLY LOADED BEAM WITH LATERAL ELASTIC SUPPORT AND DAMPING Ph.D. Thesis
Renata Susan Engel 1988 101 p
Avail: Univ. Microfilms Order No. DA8907641

The dynamic stability of a simply supported beam which is subjected to a periodic axial load and supported laterally by an elastic foundation with damping is studied. The Winkler, Hetenyi and Pasternak foundation models are presented. The models are modified to include the viscous damping of the supporting medium. Stability studies are performed for the 1/2 subharmonic response by determining the conditions on the dynamic load which produce a periodic solution to the resulting differential equation of motion. Approximations to the critical dynamic loads and the regions of instability are employed to discuss the boundedness of the lateral displacements of the beam. Viscous damping is emphasized in the studies which illustrate the effect of the foundation properties on the stability behavior. The results indicate that an increase in the foundation stiffness or damping increases the critical dynamic load and shifts the region of instability to a higher applied frequency. The mode of vibration associated with the smallest critical dynamic load is shown to vary with either the foundation stiffness or flexural rigidity. A comparison of the Winkler model results with those obtained from the Pasternak or Hetenyi models shows that the inclusion of the foundation's shear or flexural stiffness properties increases the effect of damping. Dissert. Abstr.

N90-11332*# Case Western Reserve Univ., Cleveland, OH. Dept. of Civil Engineering.
THREE-DIMENSIONAL ANALYSIS OF SURFACE CRACK-HERTZIAN STRESS FIELD INTERACTION Final Report
R. Ballarini and Y. Hsu Washington NASA Oct. 1989 165 p (Grant NAG3-396)
(NASA-CR-4254; E-5013; NAS 1.26:4254) Avail: NTIS HC A08/MF A01 CSCL 20K

The results are presented of a stress intensity factor analysis of semicircular surface cracks in the inner raceway of an engine bearing. The loading consists of a moving spherical Hertzian contact load and an axial stress due to rotation and shrink fit. A 3-D linear elastic Boundary Element Method code was developed to perform the stress analysis. The element library includes linear and quadratic isoparametric surface elements. Singular quarter point elements were employed to capture the square root displacement variation and the inverse square root stress singularity along the crack front. The program also possesses the capability to separate the whole domain into two subregions. This procedure enables one to solve nonsymmetric fracture mechanics problems without having to separate the crack surfaces a priori. A wide range of configuration parameters was investigated. The ratio of crack depth to bearing thickness was varied from one-sixtieth to one-fifth for several different locations of the Hertzian load. The stress intensity factors for several crack inclinations were also investigated. The results demonstrate the efficiency and accuracy of the Boundary Element Method. Moreover, the results can provide the basis for crack growth calculations and fatigue life prediction. Author

N90-11333 Washington Univ., Seattle.
AN IMPROVED BEAM MODEL FOR THE VIBRATIONS OF ROTOR BLADES Ph.D. Thesis
Yousry Saleh Aboelnaga 1988 123 p
Avail: Univ. Microfilms Order No. DA8911599

The vibrations of unshrouded rotor blades are analytically modeled using a newly developed beam theory. This new theory has improved capabilities for treating deformation of cross-sections

during vibration; coupling between extensional, bending and torsional modes; realistically complicated geometries including pretwist, taper and camber; and including centrifugal effects due to blade rotation. Exact solutions obtained for non-rotating uniform beams show very good agreement with finite element analyses and Timoshenko Beam theory, but significant differences from Euler-Bernoulli theory are observed for beams which are not slender. Numerical methods are used to solve the resulting characteristic value problem for the modal frequencies of rotating blades. Vibration characteristics of rotating blades with doubly symmetric cross-sections are obtained to study the effects of changing rotation rate and geometric factors including setting angle, pretwist angle, and taper. Again good agreement with finite element analysis was obtained, but unexpected instabilities are predicted for highly twisted, flared blades over a range of rotation rates. The new equations of motion derived offer the first major improvement in beam theory for rotor blade applications since the work of Houbolt and Brooks which has been a standard since 1958. Dissert. Abstr.

N90-11334 Cornell Univ., Ithaca, NY.
A FINITE ELEMENT FORMULATION FOR INELASTIC PLATES AND SHELLS BASED ON A MIXED VARIATIONAL PRINCIPLE Ph.D. Thesis
Vicki Lynn Bergmann 1989 148 p
Avail: Univ. Microfilms Order No. DA8915098

A mixed variational principle is used to develop finite element formulations suitable for elastic and inelastic analysis of geometrically-linear plates and shells. Since the ultimate goal is inelastic analysis, the variational principle is written in terms of displacemant and strain rates. Two classes of elements are formulated and tested-axisymmetric elements and elements for analysis of more general shell geometries. Inelastic material behavior is modelled by a state variable theory which combines both creep and plasticity effects for metals. The axisymmetric elements are based on a conical geometry, with quadratic interpolations for displacement rates. In one case, the strain rates are modelled with linear interpolations and, in another, with quadratic functions. Numerical results for both elements are analyzed and compared to several analytical solutions from elasticity. These elements are shown to work well for thin plates and shells without resorting to the use of reduced integration. Numerical results for inelastic deformation of a capped steel cylinder under internal pressure are compared with an existing semi-analytical solution. The general plate and shell element is based on a nine-noded quadrilateral with biquadratic Lagrangian interpolations for the geometry and the displacement rates. The strain rate field is modelled with bilinear interpolations to which higher order terms are added. Specific higher order terms are selected for the elimination of spurious modes, without the introduction of shear or membrane locking effects. Numerical results and convergence studies are presented for several elastic test problems known to induce locking in plate and shell elements. Finally, numerical results for an element in which the plane stress assumption was imposed are compared with those for an element which includes the normal stress in the thickness. Dissert. Abstr.

N90-11335 Worcester Polytechnic Inst., MA.
DEVELOPMENT OF AN APPROXIMATE TECHNIQUE FOR THE NONLINEAR RANDOM VIBRATIONS ANALYSIS OF HYSTERETIC SYSTEMS Ph.D. Thesis
Hamid Davoodi 1989 295 p
Avail: Univ. Microfilms Order No. DA8912234

A cumulant-neglect closure scheme is developed for determining the stationary and nonstationary response of structural systems with hysteretic restoring force characteristics. The method is applied for the analysis of a hysteresis model with general strength/stiffness degradation capabilities. This model has been used in the past for stochastic seismic performance evaluation of buildings. Response statistics obtained for the model using this closure technique are compared with equivalent linearization results via Monte Carlo simulation. The study performed shows that the closure results are in better agreement with simulation than those obtained by linearization. This technique also provides information on higher order statistics for hysteresis models. These statistics were not obtainable previously using the existing approximation techniques. These higher order statistics are valuable in the reliability analysis and prediction of the probability of survival of hysteretically yielding structures. Dissert. Abstr.

N90-11336 Michigan State Univ., East Lansing.
AN ANALYTICAL AND EXPERIMENTAL STUDY OF THE ELASTODYNAMIC RESPONSE CHARACTERISTICS OF PLANAR LINKAGE MECHANISM WITH BEARING CLEARANCES Ph.D. Thesis
Kueiming Soong 1988 273 p
Avail: Univ. Microfilms Order No. DA8912641

A comprehensive investigation of the dynamic response characteristics of a general planar linkage mechanism featuring both rigid and flexible links with and without radial clearance in the revolute joints is presented. In the coherent combination of analytical, computational, and experimental work undertaken, the equations governing the dynamical behavior of this general mechanical system are established by incorporating a four-mode model of the phenomenological behavior of the principal elements of each revolute joint into the generalized form of Lagrange's equations. A displacement finite element formulation is developed for undertaking the nonlinear vibrational analysis of general flexible linkage mechanisms. This formulation incorporates elastic geometrical nonlinearities and also terms coupling the rigid-body kinematics of the linkage mechanism and the elastic deformations. The equations of motion for this class of mechanical system are composed of a mixed set of ordinary differential equations and algebraic constraint equations. These governing equations are solved by employing a quasi-static procedure, Adams numerical integration scheme and the mode superposition approach of vibrational analysis. Four different illustrative examples are considered and the analytical and experimental results show impressive correlation. Dissert. Abstr.

N90-11337# Sandia National Labs., Albuquerque, NM.
TECHNIQUES FOR RECOVERY OF SHOCK-LOADED SAMPLES
Brian W. Dodson and Mark B. Boslough 1989 8 p Presented at the American Physical Society Topical Conference on Shock Compression of Condensed Matter, Albuquerque, NM, 14-17 Aug. 1989
(Contract DE-AC04-76DP-00789)
(DE89-016881; SAND-89-1964C; CONF-890812-41) Avail: NTIS HC A02/MF A01

Recovery of impact loaded samples is extremely difficult owing to the highly destructive post-shock environment. A variety of techniques were introduced to accomplish this task for both organic and inorganic samples. The design principles underlying these techniques and the practical limitations encountered in applications are described. DOE

N90-10992# Deutsche Forschungs- und Versuchsanstalt fuer Luft- und Raumfahrt, Goettingen (Germany, F.R.). Inst. of Aeroelasticity.
UPDATING OF FINITE ELEMENT MODEL BY MEANS OF NORMAL MODE PARAMETERS
N. Niedbal, E. Klusowski, and W. Luber (Messerschmitt-Boelkow-Blohm G.m.b.H., Ottobrunn, Germany, F.R.) *In* ESA, Spacecraft Structures and Mechanical Testing Jan. 1989 p 47-53 (For primary document see N90-10986 02-18)
Copyright Avail: NTIS HC A99/MF E06

N90-10993# Imperial Coll. of Science and Technology, London (England).
A REVIEW OF THE ERROR OF MATRIX METHOD (EMM) FOR STRUCTURAL DYNAMIC MODEL COMPARISON
D. J. Ewins, J. He, and N. Lieven *In* ESA, Spacecraft Structures and Mechanical Testing Jan. 1989 p 55-62 (For primary

document see N90-10986 02-18)
Copyright Avail: NTIS HC A99/MF E06

N90-10994# Besancon Univ. (France). Lab. de Mecanique Appliquee.
PARAMETRIC IDENTIFICATION OF CONSERVATIVE SELF ADJOINT STRUCTURES
G. Lallement, J. Piranda, and R. Fillod *In* ESA, Spacecraft Structures and Mechanical Testing Jan. 1989 p 63-68 (For primary document see N90-10986 02-18)
Copyright Avail: NTIS HC A99/MF E06

N90-10995# Erno Raumfahrttechnik G.m.b.H. Bremen (Germany, F.R.).
OVERVIEW OF ACTUAL BUCKLING CALCULATION METHODS FOR SPACE VEHICLE STRUCTURES
W. Huessler and H. Oery (Technische Hochschule, Aachen, Germany, F.R.) *In* ESA, Spacecraft Structures and Mechanical Testing Jan. 1989 p 71-78 (For primary document see N90-10986 02-18)
Copyright Avail: NTIS HC A99/MF E06

N90-10996# Technische Univ., Brunswick (Germany, F.R.). Inst. fuer Flugzeugbau und Leichtbau.
THEORETICAL AND EXPERIMENTAL INVESTIGATION OF THIN-WALLED ALUMINUM PANELS UNDER CYCLIC SHEAR LOAD
P. Horst and H. Kossira *In* ESA, Spacecraft Structures and Mechanical Testing Jan. 1989 p 79-84 Sponsored by the Deutsche Forschungsgemeinschaft, Bonn, Fed. Republic of Germany (For primary document see N90-10986 02-18)
Copyright Avail: NTIS HC A99/MF E06

N90-10998# Politecnico di Torino (Italy). Dept. of Aerospace Engineering.
EQUILIBRIUM AND STABILITY IN COMPOSITE THIN SHELL
E. Antona and U. Icardi (Fiat Research Center, Orbassano, Turin, Italy) *In* ESA, Spacecraft Structures and Mechanical Testing Jan. 1989 p 91-97 (For primary document see N90-10986 02-18)
Copyright Avail: NTIS HC A99/MF E06

N90-10999# Ingemansson Anatrol A.B., Askim (Sweden).
VISCOELASTIC TUNED DAMPERS FOR CONTROL OF STRUCTURAL DYNAMICS
William G. Halvorsen *In* ESA, Spacecraft Structures and Mechanical Testing Jan. 1989 p 101-106 (For primary document see N90-10986 02-18)
Copyright Avail: NTIS HC A99/MF E06

N90-11001*# Jet Propulsion Lab., California Inst. of Tech., Pasadena. Applied Technologies.
ADAPTIVE STRUCTURES TO MEET FUTURE REQUIREMENTS FOR LARGE PRECISION STRUCTURES
B. K. Wada, J. L. Fanson, J. A. Garba, and G.-S. Chen *In* ESA, Spacecraft Structures and Mechanical Testing Jan. 1989 p 121-126 (For primary document see N90-10986 02-18) (Contract NAS7-918)
Copyright Avail: NTIS HC A99/MF E06 CSCL 20K

N90-11004# Liege Univ. (Belgium).
A SUPER ELEMENT FOR MULTIBODY DYNAMICS
A. Cardona and M. Geradin *In* ESA, Spacecraft Structures and Mechanical Testing Jan. 1989 p 143-148 (For primary document see N90-10986 02-18)
Copyright Avail: NTIS HC A99/MF E06

N90-11005# Aerospatiale, Cannes (France).
GEMMES: A NEW TOOL FOR DYNAMIC MODELING
C. Garnier and P. Rideau *In* ESA, Spacecraft Structures and Mechanical Testing Jan. 1989 p 149-154 Previously announced as N89-24078 (For primary document see N90-10986 02-18)
Copyright Avail: NTIS HC A99/MF E06

N90-11006# Katholieke Univ. te Leuven (Belgium). Mechanische Konstruktie en Produktie.
EMPLOYMENT OF MODAL SURVEY METHODOLOGIES IN DYNAMIC ANALYSIS PROCEDURES
W. Heyen, T. Janter, and P. Sas *In* ESA, Spacecraft Structures and Mechanical Testing Jan. 1989 p 155-159 (For primary document see N90-10986 02-18)
Copyright Avail: NTIS HC A99/MF E06

N90-11007# Intespace, Toulouse (France).
INTEGRATION OF ANALYTICAL AND TEST SOFTWARE FOR OPTIMAL STRUCTURAL DESIGN UNDER DYNAMIC LOADS
L. P. Bugeat, N. A. Roy, A. Girard, and J.-F. Imbert *In* ESA, Spacecraft Structures and Mechanical Testing Jan. 1989 p 161-166 (For primary document see N90-10986 02-18)
Copyright Avail: NTIS HC A99/MF E06

N90-11011# Texas Univ., Austin. Dept. of Aerospace Engineering and Engineering Mechanics.
USE OF LANCZOS VECTORS IN STRUCTURAL DYNAMICS
Roy R. Craig, Jr., Tzu-Jeng Su, and Hyoung M. Kim *In* ESA, Spacecraft Structures and Mechanical Testing Jan. 1989 p 187-192 (For primary document see N90-10986 02-18)
Copyright Avail: NTIS HC A99/MF E06

N90-11013# Industrieanlagen-Betriebsgesellschaft m.b.H., Ottobrunn (Germany, F.R.).
NUMERICAL ANALYSIS OF NONLINEAR VISCOELASTIC STRUCTURES: APPLICATION TO ELASTOMERS AND RUBBER-LIKE MATERIALS
W. W. Jarzab, J. Bauer, and P. Foros *In* ESA, Spacecraft Structures and Mechanical Testing Jan. 1989 p 201-206 (For primary document see N90-10986 02-18)
Copyright Avail: NTIS HC A99/MF E06

N90-11014# Rome Univ. (Italy). Dipt. Aerospaziale.
EVALUATION OF DISPERSIVE BEHAVIOR IN PERIODIC STRUCTURES BY DISCRETE FOURIER TRANSFORM
S. Sgubini and A. Agneni *In* ESA, Spacecraft Structures and Mechanical Testing Jan. 1989 p 207-212 Sponsored by the Italian Ministry of Public Education (For primary document see N90-10986 02-18)
Copyright Avail: NTIS HC A99/MF E06

N90-11016# Rome Univ. (Italy). Dipt. Aerospaziale.
NUMERICAL TREATMENT OF THE THERMO-STRUCTURAL-DYNAMIC PROBLEMS: THE INTERPOLATION TECHNIQUES
C. Arduini, G. Laneve, D. Mortari, and M. Parisse *In* ESA, Spacecraft Structures and Mechanical Testing Jan. 1989 p 219-224 (For primary document see N90-10986 02-18) (Contract ESA-6819/86/NL/PH(SC))
Copyright Avail: NTIS HC A99/MF E06

N90-11017# Centre National d'Etudes Spatiales, Toulouse (France).
THE THIRD GENERATION RIGID SOLAR ARRAY GSR3
A. Mamode, D. Gangloff, J. L. Bastard, and Ph. Auffray (Aerospatiale, Cannes, France) *In* ESA, Spacecraft Structures and Mechanical Testing Jan. 1989 p 227-232 (For primary document see N90-10986 02-18)
Copyright Avail: NTIS HC A99/MF E06

N90-11028# Old Dominion Univ., Norfolk, VA.
A DIRECT TWO RESPONSE APPROACH FOR UPDATING ANALYTICAL DYNAMIC MODELS OF STRUCTURES WITH EMPHASIS ON UNIQUENESS
S. R. Ibrahim, C. Stavrinidis, E. Fissette, and O. Brunner (European Space Agency. European Space Research and Technology Center, ESTEC, Noordwijk, Netherlands) *In* ESA, Spacecraft Structures and Mechanical Testing Jan. 1989 p 309-315 (For primary document see N90-10986 02-18)
Copyright Avail: NTIS HC A99/MF E06

N90-11029# European Space Agency. European Space Research and Technology Center, ESTEC, Noordwijk (Netherlands). Structural Design Section.
REVIEW OF THE ESA FRACTURE CONTROL POLICY
T. K. Henriksen *In its* Spacecraft Structures and Mechanical Testing Jan. 1989 p 319-324 (For primary document see N90-10986 02-18)
Copyright Avail: NTIS HC A99/MF E06

N90-11031# Deutsche Forschungs- und Versuchsanstalt fuer Luft- und Raumfahrt, Cologne (Germany, F.R.). Inst. for Materials Research.
FATIGUE CRACK GROWTH RATES AS A FUNCTION OF DELTA K: VARIABILITY AND MATERIAL PROPERTY
G. Marci, D. E. Castro, and V. Bachmann *In* ESA, Spacecraft Structures and Mechanical Testing Jan. 1989 p 331-342 (For primary document see N90-10986 02-18)
Copyright Avail: NTIS HC A99/MF E06

N90-11032# Aeritalia S.p.A., Turin (Italy). Space Systems Group.
MATERIAL PROPERTIES OF 2219-T851 ALUMINUM ALLOY PLASMA WELDED COMPARED TO TIG WELDING
Giorgio Banino and Edoardo Tacchino *In* ESA, Spacecraft Structures and Mechanical Testing Jan. 1989 p 343-348 (For primary document see N90-10986 02-18)
Copyright Avail: NTIS HC A99/MF E06

N90-11035# Veritas Research A.S., Hovik (Norway).
NONLINEAR COLLAPSE SIMULATION OF ANISOTROPIC PLATES AND CORRUGATED PANELS
P. G. Bergan, R. O. Bjoerum, and M. K. Nygard *In* ESA, Spacecraft Structures and Mechanical Testing Jan. 1989 p 369-376 (For primary document see N90-10986 02-18)
Copyright Avail: NTIS HC A99/MF E06

N90-11044# Rome Univ. (Italy). Dipt. Aerospaziale.
STRUCTURAL PROBLEMS OF ACCURATE INFLATABLE SURFACES
C. Arduini and U. Ponzi *In* ESA, Spacecraft Structures and Mechanical Testing Jan. 1989 p 439-445 Sponsored by Contraves Italiana, Rome (For primary document see N90-10986 02-18)
Copyright Avail: NTIS HC A99/MF E06

N90-11047# Rome Univ. (Italy). Dipt. Aerospaziale.
JOE: JORDAN OPTIMIZED EIGENSOLVER. A STEP TOWARD A NUMERICAL JORDAN FORM ANALYZER FOR CONTROL AND INTERACTIVE THERMO-STRUCTURAL-DYNAMIC APPLICATIONS
C. Arduini and D. Mortari *In* ESA, Spacecraft Structures and Machanical Testing Jan. 1989 p 461-465 (For primary document see N90-10986 02-18)
Copyright Avail: NTIS HC A99/MF E06

N90-11049# Centre National d'Etudes Spatiales, Toulouse (France).
MATHEMATICAL MODEL AND PREDICTIONS FOR STATIC AND DYNAMIC BEHAVIOR OF SOLAR ARRAY STRUCTURE
D. Gangloff, F. Mercier, N. Priou, and J. F. David (Aerospatiale, Les Mureaux, France) *In* ESA, Spacecraft Structures and Mechanical Testing Jan. 1989 p 483-489 (For primary document see N90-10986 02-18)
Copyright Avail: NTIS HC A99/MF E06

N90-11050# Mitsubishi Electric Corp., Tokyo (Japan).
TEST RESULTS ON CONCEPTUAL MODELS OF THE LARGE DEPLOYABLE ANTENNA FOR MOBILE COMMUNICATIONS SATELLITES
Yuichiro Baba, Yuji Tsutsumi, Akio Iso, and Kazuo Yamamoto *In* ESA, Spacecraft Structures and Mechanical Testing Jan. 1989 p 491-496 (For primary document see N90-10986 02-18)
Copyright Avail: NTIS HC A99/MF E06

N90-11051# IKO Software Service G.m.b.H., Stuttgart (Germany, F.R.).
SPACE TELESCOPE SOLAR ARRAY: NONLINEAR TEST AND ANALYSIS EFFECTS
Ph. Deloo and M. Klein (European Space Agency. European Space Research and Technology Center, ESTEC, Noordwijk, Netherlands) *In* ESA, Spacecraft Structures and Mechanical Testing Jan. 1989 p 497-504 (For primary document see N90-10986 02-18)
Copyright Avail: NTIS HC A99/MF E06

N90-11055# Katholieke Univ. te Leuven (Belgium). Dept. of Metallurgy and Materials Engineering.
HYGROTHERMAL DEFORMATIONS OF COMPOSITE SHELLS
Lawrence E. Doxsee, Jr. *In* ESA, Spacecraft Structures and Mechanical Testing Jan. 1989 p 529-534 Sponsored in part by the Hughes Space and Communications Group and General Motors Research Labs. (For primary document see N90-10986 02-18)
Copyright Avail: NTIS HC A99/MF E06

N90-11076# IKO Software Service G.m.b.H., Stuttgart (Germany, F.R.).
STSA-SPACE TELESCOPE SOLAR ARRAY INTERCONNECTORS: FROM SIMPLE APPROACHES TO COMPLEX MODELING. A CASE STUDY OF THE NECESSITY OF COMPLEX ANALYSIS
Ph. Deloo, M. Klein, and U. Wieland (AEG-Telefunken, Wedel, Germany, F.R.) *In* ESA, Spacecraft Structures and Mechanical Testing Jan. 1989 p 693-701 (For primary document see N90-10986 02-18)
Copyright Avail: NTIS HC A99/MF E06

42 GEOSCIENCES (GENERAL)

No abstracts in this category.

43 EARTH RESOURCES AND REMOTE SENSING

Includes remote sensing of earth resources by aircraft and spacecraft; photogrammetry; and aerial photography.

For instrumentation see *35 Instrumentation and Photography.*

N90-11338# National Weather Service, Minneapolis, MN. Office of Hydrology.
AIRBORNE GAMMA RADIATION SNOW WATER EQUIVALENT AND SOIL MOISTURE MEASUREMENTS AND SATELLITE AREAL EXTENT OF SNOW COVER MEASUERMENTS: A USER'S GUIDE, VERSION 3.0
Tom Carroll and Milan Allen 1 Nov. 1988 67 p
(PB89-177877) Avail: NTIS HC A04/MF A01 CSCL 08L

The National Remote Sensing Hydrology Program is managed by the Office of Hydrology and consists of the Airborne Snow Survey Section and the Satellite Hydrology Section. The Airborne Snow Survey Section makes airborne snow water equivalent and soil moisture measurements over large areas of the country subject to a severe and chronic snowmelt flooding threat. The User's Guide is intended primarily to provide field hydrologists with some background on the technical and administrative aspects of the National Remote Sensing Hydrology Program. The guide summarizes the techniques and procedures used to make and distribute real-time, operational airborne snow water equivalent measurements and satellite areal extent of snow cover measurements made over large areas of the country. The current

airborne and satellite databases are summarized, and procedures to access the real-time observations through both AFOS and through a commercial, electronic bulletin board system are given in the appendices. GRA

N90-11339# Naval Postgraduate School, Monterey, CA.
ANALYSIS OF FOREST FIRE SMOKE USING SATELLITE IMAGERY M.S. Thesis
Peter J. DeVries, Jr. Mar. 1989 81 p
(AD-A210657) Avail: NTIS HC A05/MF A01 CSCL 04/1

NOAA-9 AVHRR data from 17 and 18 September 1987 were used to perform forest fire smoke analysis and tracking. The analysis included alignment, subtraction and division of image digital values to produce an Aerosol Particle Size Index (S12) after Frost (1988). The S12 provides information about the slope of the aerosol particle size distribution curve and can be used to infer particle size distribution changes over time. The results provide evidence that the smoke aging process may be successfully studied using satellite imagery, provided careful analysis and removal of background effects are performed. GRA

N90-11340# Minnesota Univ., Minneapolis.
TOPOGRAPHIC MAP READING Final Report, 1 May 1988 - 31 Oct. 1989
Herbert L. Pick and William B. Thompson 20 Jun. 1989 9 p
(Grant AF-AFOSR-0187-86; AF Proj. 2313)
(AD-A211269; AFOSR-89-1029TR) Avail: NTIS HC A02/MF A01 CSCL 12/9

Efforts for the second six months of the subject project have continued to focus on determining how expert subjects solve map reading problems. A procedure for collecting and analyzing protocols of expert subjects as they solve problems has been worked out and this is being validated on new subjects. A simulated map reading situation has been developed for laboratory research and this is being exploited to manipulate information available in the map reading situation. Work is also continuing on the characterization of the map readings problem for computational modeling. GRA

N90-11341# Swedish Defence Research Establishment, Linkoeping. Dept. of Information Technology.
DEFINITION OF IMAGING PERFORMANCE FOR SATELLITE SURVEILLANCE, MODELS, AND SIMULATIONS
Sven Nyberg and Torleiv Orhaug Feb. 1989 78 p In SWEDISH; ENGLISH summary
(FOA-C-30493-9.4; ISSN-0347-3708; ETN-89-94936) Avail: NTIS HC A05/MF A01; Swedish Defence Research Establishment, P.O. Box 1165, S-581 11 Linkoeping, Sweden, 50 Swedish crowns

The definition of demands is studied for a satellite optical imaging system and an investigation of demands for detection, classification, and identification is presented. An important result shows that noise has to be taken into consideration if the imaging system is to be used at low light levels. Simulations of images have shown that normal vehicles can be detected and sometimes classified with a resolution of 2 meters. If the sensor is inclined, a slighly lower performance is obtained. ESA

N90-11342# Swedish Defence Research Establishment, Linkoeping. Dept. of Information Technology.
THERMAL RADIATION FROM TERRAIN: MEASUREMENTS AND FIRST RESULTS
Hans Pettersson 23 Mar. 1989 51 p In SWEDISH; ENGLISH summary
(FOA-C-30525-3.1; ISSN-0347-3708; ETN-89-95171) Avail: NTIS HC A04/MF A01; Swedish Defence Research Establishment, Box 1165, S-581 11 Linkoeping, Sweden, 50 Swedish crowns

For more than two years thermal images in the 3 to 5 and 8 to 12 micrometer bands were recorded. The terrain image recordings were carried out more or less daily together with registrations of ambient conditions. The purpose of the measurements was to form the basis of infrared radiance models of terrain background. The use of background models in simulation is described. Methodology and measurement equipment are presented with preliminary results. The limitations of the project are discussed. The most important disturbance is shown to be solar radiation. As the air temperature increases by degrees, the ground variance increases and contrasts in the background radiation result. ESA

44 ENERGY PRODUCTION AND CONVERSION

Includes specific energy conversion systems, e.g., fuel cells; global sources of energy; geophysical conversion; and windpower.

For related information see also *07 Aircraft Propulsion and Power, 20 Spacecraft Propulsion and Power,* and *28 Propellants and Fuels.*

N90-11343# National Inst. of Standards and Technology, Gaithersburg, MD. Center for Electronics and Electrical Engineering.
ASSESSMENT OF SPACE POWER RELATED MEASUREMENT REQUIREMENTS OF THE STRATEGIC DEFENSE INITIATIVE Final Report
James K. Olthoff and Robert E. Hebner Apr. 1989 147 p Sponsored by DNA, Washinton, DC Prepared for Strategic Defense Initiative Organization, Washington, DC
(PB89-209357; NIST/TN-1259) Avail: NTIS HC A07/MF A01; SOD HC $8.00 as 003-003-02930-1 CSCL 10B

A survey has been performed to determine the measurement requirements of space power related parameters for anticipated SDI system. These requirements have been compared to present state-of-the-art metrology capabilities as represented by the calibration capabilities of the National Instutute of Standards and Technology. Metrology areas where present state-of-the-art capabilities are inadequate to meet SDI requirements are discussed, and areas of metrology-related research which appear promising to meet these needs are examined. Particular attention is paid to the diffulties of long-term, unattended sensor calibrations and long-term measurement reliability. GRA

N90-11344# National Aerospace Lab., Tokyo (Japan).
TOWER WAKE/BLADE INTERACTION NOISE OF A WIND TURBINE
Hideo Nishiwaki and Katsumi Takeda Oct. 1987 10 p In JAPANESE; ENGLISH summary
(NAL-TR-945; ISSN-0389-4010) Avail: NTIS HC A02/MF A01

A scale model of a 1.5m dia. two-bladed windturbine was used in an anechoic chamber that provided a free-stream velocity of 8m/s. The blades used were a 1.5/8 scale model of a test machine for a local energy utilization project promoted by the Science and Technology Agency. The height of the tower from the ground level was 1.8m. The acoustic measurements were made in a circle of 1.6m downstream from the machine at the height of the windmill centerline. The noise level of the on-axis spectra was about 15dB larger than that of the off-axis. This is a result of the dipole nature of the acoustic impulse. The Wortmann airfoil (FX 77-W series) was employed for the blade profiles and the Reynolds number was 10(5), based on the tip chord length. The experiment revealed that the sound intensity at each harmonic was not proportional to the axial and radial extents of the wake. The elliptic slender configuration was the quietest, while the square configuration was the loudest. From a practical point of view, it is suggested that the circular section is most suitable for the tower leg. Author

N90-11345# Illinois Univ., Urbana.
CuInSe2 SOLAR CELL RESEARCH BY SPUTTER DEPOSITION
J. A. Thornton, A. Rockett, T. C. Lommasson, and H. Talieh Jul. 1989 66 p
(Contract DE-AC02-83CH-10093)
(DE89-009450; SERI/STR-211-3540) Avail: NTIS HC A04/MF A01

This is the final report for a program that began January 1, 1986 and ended November 10, 1987. The program focused on developing reactive sputtering as a technique for deposition of CuInSe sub 2 and high-efficiency CuInSe sub 2/CdS heterojunction solar cells. Most of the CuInSe sub 2/CdS devices fabricated thus far from CuInSe sub 2 deposited by reactive sputtering are characterized by relatively low efficiencies caused primarily by low open-circuit voltages, V sub oc. A contributor to the low V sub oc appears to be the lower In atom fraction relative to device layers prepared by evaporation, in the top layer of composite two-layer CuInSe sub 2 films (Cu-rich base layer, In-rich top layer) used in our cell fabrication attempts. The lower In fraction is caused by an In-rejection phenomenon that occurs at elevated growth temperatures. This program has focused significant effort on understanding and correcting the phenomenon. Variations in the relative currents to the Cu and In sputtering sources, the H sub 2 Se injection rate, and the substrate temperature have been explored. Slight reductions in the substrate temperature have been found to be effective for increasing the In fraction in the films. DOE

N90-11346# Pacific Northwest Lab., Richland, WA.
POTENTIAL INDUSTRIAL APPLICATIONS FOR COMPOSITE PHASE-CHANGE MATERIALS AS THERMAL ENERGY STORAGE MEDIA
G. E. Spanner and G. L. Wilfert Jul. 1989 44 p
(Contract DE-AC06-76RL-01830)
(DE89-015170; PNL-6935) Avail: NTIS HC A03/MF A01

Considerable effort has been spent by the U.S. Department of Energy and its contractors over the last few years to develop composite phase-change materials (CPCMs) for thermal energy storage (TES). This patented TES medium consists of a phase-change material (typically a salt or metal alloy) that is retained within the porous structure of a supporting material (typically a ceramic). The objectives of this study were to: (1) introduce CPCMs to industries that may not otherwise be aware of them, (2) identify potentially attractive applications for CPCM in industry, (3) determine technical requirements that will affect the design of CPCM's for specific applications, and (4) generate interest among industrial firms for employing CPCM TES in their processes. The approach in this study was to examine a wide variety of industries using a series of screens to select those industries that would be most likely to adopt CPCM TES in their processes. The screens used in this study were process temperature, presence of time-varying energy flows, energy intensity of the industry, and economic growth prospects over the next 5 years. After identifying industries that passed all of the screens, representatives of each industry were interviewed by telephone to introduce them to CPCM TES, assess technical requirements for CPCM TES in their industry, and determine their interest in pursuing applications for CPCM TES. DOE

N90-11347# New South Wales Univ., Kensington (Australia). Solar Photovoltaic Lab.
LASER GROOVED AND POLYCRYSTALLINE SILICON SOLAR CELL RESEARCH
M. A. Green, S. R. Wenham, C. M. Chong, S. Narayanan, Zhang Fuzu, J. C. Zolper, A. B. Sproul, and A. W. Blakers Aug. 1989 46 p Prepared in cooperation with Sandia National Labs., Albuquerque, NM
(Contract DE-AC04-76DP-00789)
(DE89-015196; SAND-89-7035) Avail: NTIS HC A03/MF A01

Research for the period August, 1987 to October, 1988 directed at improving the performance of laser grooved, buried contact crystalline silicon solar cells and of polycrystalline silicon cells is described. Key results include the demonstration of 20.6 percent energy conversion efficiency for 12 cm(2) laser grooved crystalline cells and 19.6 percent for 47 cm(2) cells of the same type. Several of the larger cells were encapsulated into 28 cm square mini-modules which demonstrated efficiencies up to 17 percent, significantly higher than previously established figures for silicon modules. Polycrystalline cell efficiency up to 17.8 percent was demonstrated during the project, again appreciably higher than previous results. DOE

N90-11348# Midwest Research Inst., Golden, CO.
PROCEEDINGS OF THE POLYCRYSTALLINE THIN FILM PROGRAM MEETING
1989 216 p Meeting held in Lakewood, CO, 16-17 Aug. 1989
(Contract DE-AC02-83CH-10093)
(DE89-009457; SERI/CP-211-3550; CONF-890851) Avail: NTIS HC A10/MF A02

Research programs in the following areas are presented: CdTe solar cells; CdTe devices; CuInSe2 fundamentals; and CuInSe2 solar cells. Individual projects are processed separately for the data bases. DOE

N90-11349# Argonne National Lab., IL. Energy and Environmental Systems Div.
PLANNING FOR HYBRID-CYCLE OTEC EXPERIMENTS USING THE HMTSTA TEST FACILITY AT THE NATURAL ENERGY LABORATORY OF HAWAII
C. Panchal, T. Rabas, and L. Genens 1989 5 p Presented at the Oceans 1989 Conference, Seattle, WA, 18-21 Sep. 1989
(Contract W-31-109-eng-38)
(DE89-013278; CONF-8909128-1) Avail: NTIS HC A01/MF A01

The U.S. Department of Energy has built an experimental apparatus for studying the open-cycle Ocean Thermal Energy Conversion (OC-OTEC) system. Experiments using warm and cold seawater are currently underway to validate the performance predictions for an OC-TEC flash evaporator, surface condenser, and direct-contact condenser. The hybrid cycle is another OTEC option that produces both power and desalinated water, it is comparable in capital cost to OC-OTEC, and it eliminates the problems associated with the large steam turbine. Means are presented or modifying the existing apparatus to conduct similar experiments on hybrid-cycle OTEC heat exchangers. These data are required to validate predictive methods of the components and for the system integration that were identified in an earlier study of hybrid-cycle OTEC power plants. DOE

N90-11074# Aerospatiale, Cannes (France).
DEPLOYMENT SIMULATION FOR 3rd GENERATION SOLAR ARRAY GSR3
C. Verne and M. Rouchon *In* ESA, Spacecraft Structures and Mechanical Testing Jan. 1989 p 681-684 Sponsored by ESA
(For primary document see N90-10986 02-18)
Copyright Avail: NTIS HC A99/MF E06

45 ENVIRONMENT POLLUTION

Includes atmospheric, noise, thermal, and water pollution.

N90-11350# Environmental Protection Agency, Washington, DC. Office of Policy, Planning and Evaluation.
POTENTIAL EFFECTS OF GLOBAL CLIMATE CHANGE ON THE UNITED STATES. EXECUTIVE SUMMARY. DRAFT
Joel B. Smith, ed. and Dennis A. Tirpak, ed. Oct. 1988 55 p
(PB89-161046) Avail: NTIS HC A04/MF A01; also available SOD HC $32.00 as 055-000-00280-1 CSCL 13B

Scientific theory suggests that the addition of greenhouse gases to the atmosphere will alter the global climate. The result will be increasing temperatures and consequent changes in rainfall and other weather patterns. To help identify the effects of such a climate change, Congress asked the U.S. Environmental Protection Agency to undertake two studies on the greenhouse effect. One of the studies would focus on the potential health and environmental effects of climate change including, but not be limited to the potential impacts on agricultural, forests, wetlands, human health, rivers, lakes, estuaries as well as societal impacts. The report used regional data from atmospheric models known as General Circulation Models (GCMs) as a basis for climate change

scenarios. The GCMs are large models of the ocean-atmosphere system that provide the best scientific estimates of the impacts of increased greenhouse gas concentrations on climate. The GCMs generally agree concerning general global and latitudinal increases in temperature, but they disagree concerning other areas such as the location of hydrological change. The temperature changes from three different GCMs are shown both for the United States and several regions. These results are estimates of changes caused by a doubling of carbon dioxide levels. Author

N90-11351# Environmental Protection Agency, Washington, DC. Office of Policy, Planning and Evaluation.
POTENTIAL EFFECTS OF GLOBAL CLIMATE CHANGE ON THE UNITED STATES. VOLUME 1: REGIONAL STUDIES. DRAFT
Joel B. Smith, ed. and Dennis A. Tirpak, ed. Oct. 1988 289 p
(PB89-161053) Avail: NTIS HC A13/MF A02 CSCL 13B

This report is an attempt to identify the sensitivities, direction and magnitude, linkages, regional differences, national impacts, policy implications, and uncertainties among the effects of global climate warming. It focuses on several systems that may be particularly affected by climate change: sea level rise, water resources, agriculture, forests, biodiversity and wildlife, energy demand, air pollution and health. This volume 1 contains an introduction to global climate change, the methodology used to study climate change and findings for California, the Great Lakes, the Southeast U.S., and the Great Plains. K.C.D.

N90-11352# Environmental Protection Agency, Washington, DC. Office of Policy, Planning and Evaluation.
POTENTIAL EFFECTS OF GLOBAL CLIMATE CHANGE ON THE UNITED STATES. VOLUME 2: NATIONAL STUDIES. DRAFT
Joel B. Smith, ed. and Dennis A. Tirpak, ed. Oct. 1988 414 p
(PB89-161061) Avail: NTIS HC A18/MF A03 CSCL 13B

This report is an attempt to identify the sensitivities, direction and magnitude, linkages, regional differences, national impacts, policy implications, and uncertainties among the effects of global climate warming. It focuses on several systems that may be particularly affected by climate change. This volume contains chapters on water resources, sea level rise, agriculture, forests, biological diversity, air quality, human health, urban infrastructure, climate variability, electricity demands and research needs. K.C.D.

N90-11353# NSI Technology Services Corp., Corvallis, OR.
INTERRELATION OF EXPERIMENTAL EXPOSURE AND AMBIENT AIR QUALITY DATA FOR COMPARISON OF OZONE EXPOSURE INDICES AND ESTIMATING AGRICULTURAL LOSSES
E. Henry Lee, David T. Tingey, and William E. Hogsett (Environmental Protection Agency, Corvallis, OR.) Jun. 1989 115 p
(Contract EPA-68-C8-0006)
(PB89-195036; EPA/600/3-89/047) Avail: NTIS HC A06/MF A01 CSCL 13B

The report evaluates ambient air quality indicators for ozone (O3) and estimates the exposure levels associated with agricultural losses. In support of the U.S. EPA Office of Air Quality Planning and Standards review and evaluation of a secondary National Ambient Air Quality Standard for ozone, the Terrestrial Branch within the Corvallis Environmental Research Laboratory investigated alternative exposure indices for characterizing the adverse effects of ozone on agriculture, using experimental data from the National Crop Loss Assessment Network program. Scientific and technical information on ozone and its effects on vegetation, natural ecosystems, natural and artificial materials, and human welfare necessitates a secondary standard that adequately describes the temporal variations of exposure and their effects on plant production and correlates well with short- and long-term exposures. The identification of an appropriate ozone standard that protects against crop yield losses proceeds along two lines: regression analysis of plant response data against various exposure indices to determine indices that best depict biological response, and ambient air quality analysis of ambient O3 data to identify indices that correlate well with various exposure patterns. GRA

N90-11354# Environmental Protection Agency, Washington, DC. Information Management and Services Div.
STRATOSPHERIC OZONE DEPLETION
May 1989 72 p
(PB89-207476; EPA/IMSD-89/001) Avail: NTIS HC A04/MF A01 CSCL 13B

The bibliography focuses solely on stratospheric ozone depletion. Global climate change, a related issue, is not within its scope. The first section contains an overview of stratospheric ozone issues. The second section, entitled science, discusses atmospheric chemistry and dynamics, specifically trace gas emissions and ozone/UVB levels. The third section contains citations relating to risk assessment for humans and other organisms. Section IV includes information on domestic and international public policy. The fifth section outlines research on substitutes and alternatives for ozone-depletion substances. World-wide participants in the Montreal Protocol are listed in the Appendix. GRA

N90-11355# Department of Energy, Washington, DC. Office of Energy Research.
EVALUATION OF MID-TO-LONG TERM BASIC RESEARCH FOR ENVIRONMENTAL RESTORATION
Sep. 1989 163 p
(DE89-015621; DOE/ER-0419) Avail: NTIS HC A08/MF A01

This document describes a long-term basic research program for the U.S. Department of Energy (DOE) that complements departmental initiatives in waste management and site cleanup. The most important problems faced by DOE are environmental restoration of waste sites and cleanup of inactive facilities. Environmental restoration is defined in this report as characterization, assessment, remediation, and post-closure verification within the waste/environmental system at DOE sites. Remediation of inactive, contaminated waste-disposal sites is the largest and most expensive task facing DOE. Immobilization, isolation, separation, and destruction of waste, either aboveground or in situ, are difficult and costly tasks. Technologies for these tasks are primitive or do not exist. Departmental problems in the long term are being analyzed scientifically and research needs are being identified. When completed, the Office of Energy Research's (OER's) basis research plan will describe potential scientific research needs for universities, national laboratories, and others as a basis for research proposals to DOE. Extensive interaction with the scientific community is planned to further refine and prioritize research needs. Basic research within DOE is directed toward fundamental knowledge leading to the discovery of new scientific or engineering concepts and principles that may or may not have immediate specific technological applications. However, because DOE is a mission-oriented agency, basic research in DOE is strongly influenced by national energy and environmental policy and may be multidisciplinary in nature. Basic research will provide innovative concepts and the fundamental knowledge base that facilitates the development and application of new and emerging technologies. DOE

N90-11356# Coastal Engineering Research Center, Vicksburg, MS.
PHYSIOGRAPHIC AND GEOLOGICAL SETTING OF THE COASTAL ENGINEERING RESEARCH CENTER'S FIELD RESEARCH FACILITY Final Report
Edward P. Meisburger, S. J. Williams, and Charles Judge Jul. 1989 32 p
(AD-A210772; CERC-MP-89-9) Avail: NTIS HC A03/MF A01 CSCL 08/7

This report describes, in general terms, aspects of the regional and local geology of the Coastal Engineering Research Center's Field Research Facility (FRF) in Duck, North Carolina. The FRF is located on the Outer Banks which form the seaward margin of the Atlantic Coastal Plain province in this region. The beach and

dunes of the barrier island at the site of the FRF are composed of fine to very coarse sand mixed with some granule and pebble-sized material. This lithology remains essentially unchanged beneath the barrier to a depth of more than 15.2 m (50 ft) below present sea level where finer grained sediments predominate. The inner continental shelf in the area is marked by irregular bottom topography with four large shoals interrupting seaward inclination of the shelf floor. The inner shelf is mantled by fine to very coarse sand with the coarser material occurring primarily on the shoals. GRA

N90-11357# Washington Univ., Seattle. Dept. of Statistics.
ARE OZONE EXCEEDANCE RATES DECREASING. COMMENT ON EXTREME VALUE ANALYSIS OF ENVIRONMENTAL TIME-SERIES: AN APPLICATION TO TREND DETECTION IN GROUND-LEVEL OZONE Technical Report, 1 Jan. - 31 Jul. 1989
Adrian E. Raftery Jul. 1989 14 p
(Contract N00014-88-K-0265)
(AD-A211029; TR-165) Avail: NTIS HC A03/MF A01 CSCL 04/1

In his Statistical Science discussion paper, R. L. Smith (1989) proposed new methods for analyzing extreme values based on the point process view of high-level exceedances, and illustrated them with a detailed analysis of ozone data from Houston, Texas. The methods are powerful and, in particular, the point process of cluster peaks over a high threshold, provides a remarkable condensation of the massive data set that he analyzes. It involves little loss of relevant information and permits fairly simple analyses. Smith's conclusion is that there is no trend in the overall levels of the series, but that there is a marked downward trend in the extreme values. It seems hard to find physical explanations for this, and here the evidence is reassessed in terms of a comparison between competing models for the intensity of a Poisson process. This suggests that there is some evidence for a decreasing trend in exceedance rates but that it is rather weak. If there is a trend, it seems more likely to consist of a fairly abrupt change than a gradual decrease. The possibility that such a change is due to an improvement in measurement technology is discussed. The possibility of long-memory dependence is also considered and the clustering method used is discussed. GRA

N90-11358# Jackson State Univ., MS. Dept. of Physics and Atmospheric Services.
DIAGNOSTIC STUDY OF ATMOSPHERE-TERRAIN INTERACTION LEADING TO THE FORMATION OF DUST CLOUDS AND POOR VISIBILITIES OVER NEAR EAST DESERT AREAS Final Report, 1 Sep. 1985 - 29 Feb. 1988
Lonzy J. Lewis and Pieter J. Feteris 30 Jun. 1989 21 p
(Contract DAAG29-85-G-0116)
(AD-A211243; ARO-23235.1-GS-H) Avail: NTIS HC A03/MF A01 CSCL 04/2

A comparison of the frequency of occurrence of poor visibilities in areas and during periods of intense agricultural, industrial and military activity with that in sparsely populated areas unaffected by war military maneuvers, has been undertaken. Three years of surface reports from 850 stations in the Near East and adjacent North Africa were screened for visibilities coded as 90 through 95 and 9 through 10 on FIGGE and NCC data bank tapes. Seasonal maps of the location of stations reporting poor visibilities, a calendar of poor visibility for each station and maps of the distribution of those stations reporting fog/rain, fog/snow/drifting snow and sand/dust were prepared for most of the three year period. Only the most reliable and important results are shown. In mountainous regions poor visibilities occurred frequently all year round. Low frequencies of poor visibility reports were found in Eastern Tunesia, Western Lybia, West Africa and the Sudan. (It must be remembered that during World War 2 the desert battle between the British and the German armies in North Africa caused noticeable deterioration of visibility in Western Egypt.) It is recommended that this climatology be completed. GRA

N90-11359# Edgerton, Germeshausen and Grier, Inc., Idaho Falls, ID.
REPORTING ENVIRONMENTAL DATA OF KNOWN QUALITY
P. N. Pink, J. S. Jessup, and D. K. Knight 1989 15 p Presented at the EPA Waste Testing and Quality Assurance Symposium, Washington, DC, 24-28 Jul. 1989
(Contract DE-AC07-76ID-01570)
(DE89-016214; EGG-M-89040; CONF-8907123-2) Avail: NTIS HC A03/MF A01

A comprehensive approach was developed for environmental program documents to integrate sampling, analytical chemical, quality control, and historical data when reporting results to accommodate technical and programmatic data users. The objective of this paper is to present this comprehensive and effective means of reporting the quality and usability of the analytical chemical data generated from the analysis of environmental samples. Most environmental programs require legally admissable data of known quality that will satisfy regulatory requirements and the rigors of potential litigation. Analytical chemical data generated using validated Environmental Protection Agency (EPA) protocols or their equivalent provide the supporting quality control (QC) information necessary to assess the quality of the data; however, no conclusion is drawn as to the programmatic usability of the data. The approach outlined in this paper details a mechanism for assessing, documenting, and reporting what is known about the data quality and consequently the usability of the analytical chemical data generated. DOE

N90-11360# Agricultural Research Service, Beltsville, MD.
ASSESSMENT OF CROP RESPONSE TO INCREASES IN ATMOSPHERIC CARBON DIOXIDE CONCENTRATIONS: SUMMARY OF RESEARCH PROGRESS REPORT, JULY 1, 1988--JUNE 30, 1989
1989 5 p
(Contract DE-AI05-88ER-69014)
(DE89-016251; DOE/ER-69014/T1) Avail: NTIS HC A01/MF A01

At Beltsville, the 2-dimensional soil model SOILSIM was purchased from a commercial company along with the rights to distribute our own modified version. The model as purchased dealt with the movement of water and solutes in both the unsaturated (rooted) and and saturated portions of the soil. It had simple empirical equations to simulate boundary conditions, no dictionary and very little comment in the code. However, it did have algorithms to predict correctly the movement of materials through a heterogeneous medium. In this respect it was much superior to the soil model RHIZOS incorporated in GLYCIM. Earlier use of the uncertainty analysis program PRISM had revealed how insensitive RHIZOS is to soil input variables and parameters. SOILSIM, has been adapted for use in crop models by inserting comments in the code, preparing a dictionary of variable and parameter names and units, stripping our code dealing with the deeper layers of the soil, and replacing the empirical boundary-condition equations with equations that link to the crop model. The modules dealing with soil water movement and root growth have been incorporated into GLYCIM. DOE

46 GEOPHYSICS

Includes aeronomy; upper and lower atmosphere studies; ionospheric and magnetospheric physics; and geomagnetism.

For space radiation see *93 Space Radiation.*

N90-11361# Advisory Group for Aerospace Research and Development, Neuilly-Sur-Seine (France). Electromagnetic Wave Propagation Panel.
IONOSPHERIC STRUCTURE AND VARIABILITY ON A GLOBAL SCALE AND INTERACTIONS WITH ATMOSPHERE AND MAGNETOSPHERE
Apr. 1989 468 p In ENGLISH and FRENCH Symposium held

in Munich, Fed. Republic of Germany, 16-20 May 1988 (AGARD-CP-441; ISBN-92-835-0500-X) Copyright Avail: NTIS HC A20/MF A03

Communications, Navigation and Surveillance Systems operating in/through the aerospace EM propagation environment are affected by the state/variability of the propagation media. The range of phenomena need for their elucidation, observations and analysis on a global scale since only an understanding of the complex global interaction can improve the means of predictability and assessment of localized phenomena suggesting methods for mitigating adverse propagation conditions. With this goal, ionospheric dynamics, ionosphere/magnetosphere and ionosphere/atmosphere interactions were analyzed and discussed. For individual titles, see N90-11362 through N90-11404.

N90-11362# Institut d'Aeronomie Spatiale de Belgique, Brussels.

SOLAR-TERRESTRIAL RELATIONS: FLARE AND SOLAR WIND EFFECTS **c92**

J. Lemaire *In* AGARD, Ionospheric Structure and Variability on a Global Scale and Interactions with Atmosphere and Magnetosphere Apr. 1989 11 p Sponsored in part by Ministere de l'Education Nationale et de la Culture Francaise and Fonds National de la Recherche Scientifique (For primary document see N90-11361 02-46)

Copyright Avail: NTIS HC A20/MF A03

The existence of solar terrestrial relations is clearly shown during solar flare events. During these catastrophic events the enhanced flux of XUV solar radiation as well as the sudden outburst of energetic solar cosmic ray particles induce a series of well identified effects in the Earth's magnetic field, in the terrestrial ionosphere and in the upper atmosphere. These geophysical effects and their solar origin are reviewed. Solar activity also perturbs the distribution of plasma and magnetic fields in the corona and in the interplanetary medium. Large-scale (low frequency) and small-scale (high frequency) inhomogeneities (perturbations) are produced in the expanding solar wind flow which then interacts with the Earth's magnetic field. The resulting variability of the impinging solar wind plasma triggers additional geophysical effects in the magnetosphere, in the terrestrial ionosphere, and in the upper atmosphere. Some of the geophysical consequences of this non-stationary interaction of the solar wind with the geomagnetic field, and, of impulsive penetration of small scale solar wind plasma irregularities into the magnetosphere are reviewed (e.g. polar cusp fields, currents, and related inospheric irregularities). Author

N90-11363# Alberta Univ., Edmonton. Inst. of Earth and Planetary Physics.

MAGNETOSPHERIC SUBSTORMS AS A SIGNATURE OF THE SOLAR TERRESTRIAL INTERACTION

Gordon Rostoker *In* AGARD, Ionospheric Structure and Variability on a Global Scale and Interactions with Atmosphere and Magnetosphere Apr. 1989 14 p Sponsored by Natural Sciences and Engineering Research Council of Canada (For primary document see N90-11361 02-46)

Copyright Avail: NTIS HC A20/MF A03

It is now well known that perturbations of the high latitude ionosphere are regulated by the properties of the solar wind and the interplanetary magnetic field. Variations in the direction of the interplanetary magnetic field lead to episodes normally lasting for a few minutes to a few hours in which large amounts of solar wind energy penetrate into the distant magnetosphere. This energy is stored in an intermediary form in the magnetotail magnetic field and in the kinetic drift energy of the Earth's boundary layers and plasma sheet before it is ultimately degraded to heat through the action of electric current systems which couple the magnetosphere to the ionosphere. The physical processes through which the solar wind energy, once it has entered the magnetosphere, is redistributed and dissipated through the process known as the magnetospheric substorm are discussed. Based on the nature of the physical processes involved, the possibility is discussed for being able to predict the locale and level of the high latitude ionospheric perturbations which result from the action of the precipitation of energetic particles into the upper atmosphere as part of the electromagnetic coupling of the outer magnetosphere to the ionosphere. Author

N90-11364# Duesseldorf Univ. (Germany, F.R.). Inst. for Theoretical Physics.

BALANCE EQUATIONS FOR IONOSPHERIC PLASMAS WITH DIFFERENT PARTIAL TEMPERATURES

K. Suchy *In* AGARD, Ionospheric Structure and Variability on a Global Scale and Interactions with Atmosphere and Magnetosphere Apr. 1989 11 p (For primary document see N90-11361 02-46)

Copyright Avail: NTIS HC A20/MF A03

Different expressions for pressure tensors in multispecies plasmas are investigated for their physical meaning. Partial temperatures are introduced proportional to the partial translational energies (per particle). This leads to the definitions of translational energy tensors and temperature tensors proportional to the pressure tensors. Stress tensors are defined as differences of the corresponding pressure tensors and their values in local thermodynamic equilibrium. Heat flux vectors are defined as quantities with vanishing divergence under adiabatic constraints. Balance equations are established for masses, momenta, pressures, temperatures, energies, enthalpy, stresses and heat fluxes. Author

N90-11365# Technische Hogeschool, Eindhoven (Netherlands). Dept. of Physics.

NON-LINEAR WAVE-EQUATIONS FOR LOW-FREQUENCY ACOUSTIC GRAVITY WAVES

R. H. M. Miesen, L. P. J. Kamp, and F. W. Sluijter *In* AGARD, Ionospheric Structure and Variability on a Global Scale and Interactions with Atmosphere and Magnetosphere Apr. 1989 9 p Previously announced in IAA as A89-16729 (For primary document see N90-11361 02-46)

Copyright Avail: NTIS HC A20/MF A03

It is shown that low-frequency (LF) acoustic gravity waves propagating parallel to the Earth's surface satisfy the Korteweg-DeVries (KdV) equation or the Kadomtsev-Petviashvili equation and have a discrete spectrum of group velocities. The nonlinear wave equations are obtained using the reductive perturbation technique, and changes for a compressible atmosphere are discussed. IAA

N90-11366# Freiburg Univ. (Germany, F.R.).

GLOBAL IONOSPHERIC DYNAMICS

E. Rawer *In* AGARD, Ionospheric Structure and Variability on a Global Scale and Interactions with Atmosphere and Magnetosphere Apr. 1989 21 p (For primary document see N90-11361 02-46)

Copyright Avail: NTIS HC A20/MF A03

Plasma (a minor constituent in planetary atmospheres) motion is narrowly linked with that of the neutrals as long as collisional coupling between neutral and charged particles is strong. At greater heights, both constituents are more and more decoupled and may move separately whenever forces are present which do only act upon charged particles. The most important difference between known planetary ionospheres is the absence or presence of a general magnetic field. While in the first condition the plasma moves freely, a magnetic field cannot provoke plasma motions of its own but restricts the motions provoked by other forces to one in either the direction parallel to the magnetic field or perpendicular to it. So, the motion patterns depend largely on the prevailing forces. Largely different conditions are found in the terrestrial ionosphere according to magnetic latitude. While at mid-latitudes mechanical forces mainly provoked by neutral winds are most important, electric forces cannot be neglected at low and high magnetic latitudes. Apart from such large scale motions, many small scale motions of more or less wave-like character are observed, in particular, internal gravity waves due to different causes. It is not always easy in local measurements to separate these localized motions from the large scale patterns. Different methods exist for observing plasma motions in the terrestrial

ionosphere. Unfortunately, all of these can only be applied with caution. The spatial and temporal density of such local observations is unsatisfactory. Author

N90-11367# Southampton Univ. (England). Dept. of Physics.
GLOBAL IONOSPHERIC DYNAMICS: A REVIEW
H. Rishbeth *In* AGARD, Ionospheric Structure and Variability on a Global Scale and Interactions with Atmosphere and Magnetosphere Apr. 1989 13 p (For primary document see N90-11361 02-46)
Copyright Avail: NTIS HC A20/MF A03

The ionosphere is a highly dynamic region of the Earth's environment, and its spatial and temporal variations are extremely complex. Practical needs call for a good description of the ionosphere and reliable predictions of its behavior. Some of the scientific problems and the principles behind them are reviewed. For practical and scientific purposes, the ionosphere is often modeled. The most important parameter for modeling is the electron density distribution N(h,t) which, at any one place, is primarily a function of height (h) and local time (t), but varies also with time of year, magnetic disturbance and solar activity. Thus time-scales ranging from minutes up to a solar cycle need to be considered. Many other parameters (such as temperature, composition and velocity) can be modeled and are needed for a physical understanding of the ionosphere. Aspects of ionospheric structure and behavior that are considered include the thermospheric wind system and its effects; sporadic E; the low latitude ionosphere; the high latitude ionosphere; and ionospheric storms. The references are illustrative rather than comprehensive. Author

N90-11368# Air Force Geophysics Lab., Hanscom AFB, MA.
A FULLY ANALYTIC, LOW AND MIDDLE LATITUDE IONOSPHERIC MODEL
D. N. Anderson and J. M. Forbes *In* AGARD, Ionospheric Structure and Variability on a Global Scale and Interactions with Atmosphere and Magnetosphere Apr. 1989 7 p (For primary document see N90-11361 02-46)
Copyright Avail: NTIS HC A20/MF A03

The well-known Chiu ionospheric model is a global empirical model which calculates electron density profiles as a function of latitude, local time, season and solar cycle. It is extensively used by thermospheric dynamicists because its analytic formulation can quickly provide global electron density values. The model, however has serious shortcomings. Recently, a fully analytic ionospheric model based on the Chiu formulation, was developed which provides much more realistic, low and mid-latitude electron density distributions. This is accomplished by redefining the latitude and local time dependence of parameters such as hmF2, nmF2, and the topside and bottomside scale heights. The modifications are based on a recently-developed Semi-empirical, Low-latitude Ionospheric Model (SLIM) and involves decomposing hmF2, nmF2 and plasma density scale heights into harmonic terms to describe the local time variations and then applying Hermite polynomials to obtain latitude variations. The analytic model generates electron density profiles under solar cycle minimum, moderate and maximum conditions for winter, summer and equinox periods. Differences between this model and the Chiu model are discussed and comparisons with observed, low-latitude electron density distributions are presented. Author

N90-11369# Max-Planck-Inst. fuer Aeronomie, Katlenburg-Lindau (Germany, F.R.).
GLOBAL MORPHOLOGY OF PLASMA BUBBLES IN THE LOW LATITUDE IONOSPHERE
K. Schlegel, K. Oyama, and T. Takahashi (Tohoku Univ., Sendai, Japan) *In* AGARD, Ionospheric Structure and Variability on a Global Scale and Interactions with Atmosphere and Magnetosphere Apr. 1989 6 p (For primary document see N90-11361 02-46)
Copyright Avail: NTIS HC A20/MF A03

The electron density and electron temperature structure in and around plasma bubbles in the low latitude ionosphere was studied with instruments on the Japanese satellite HINOTORI. Histograms are presented about the number of occurrence of certain types of bubbles in a latitude range of + or - 30 degrees around the equator. Particularly the temperature within the plasma bubbles which can be higher or lower than the temperature of the ambient plasma will be discussed and explanations will be proposed. A particular class of bubbles seem to occur over the South Atlantic magnetic anomaly and over the Hawaiian anomaly. Author

N90-11370# Centre National d'Etudes des Telecommunications, Issy-les-Moulineaux (France).
SIMULATION OF THE POLAR CAP F REGION IONIZATION USING AN EXPERIMENTAL CONVECTION ELECTRIC FIELD
Abstract Only
C. Taieb *In* AGARD, Ionospheric Structure and Variability on a Global Scale and Interactions with Atmosphere and Magnetosphere Apr. 1989 1 p (For primary document see N90-11361 02-46)
Copyright Avail: NTIS HC A20/MF A03

The electrons and ions concentration over the polar cap F region was calculated with a code running on a vectorial computer. Four coupled continuity equations, one for each ion specie, are solved together with the momentum equation, assuming that the in velocities and temperatures are the same for all species. The transportation of the ionization is due to neutral wind drag, the electric field and the ambipolar diffusion velocity which includes a stress tensor for taking account of the anisotropy created by the intense electric field encountered in the polar cap. The horizontal ion transportation is due to the planetary convection electric field which is deduced from 24 hours EISCAT observations during a quiet day. Because the observations are limited northward in latitude it is necessary to interpolate the equipotential lines providing reasonable physical assumption. Then the experimental convection electric field is replaced by a theoretical one. Results from the simulation of the ions concentration with the two convection models are compared. These results are compared also with the EISCAT electron density measurements. Author

N90-11371# Royal Aerospace Establishment, Farnborough (England). Space Dept.
AVERAGE DIURNAL AND SEASONAL PROFILES OF IONOSPHERIC STORMS
G. L. Wrenn, A. S. Rodger, and H. Rishbeth (Southampton Univ., England) *In* AGARD, Ionospheric Structure and Variability on a Global Scale and Interactions with Atmosphere and Magnetosphere Apr. 1989 9 p (For primary document see N90-11361 02-46) (Grant NERC-GST.02.112)
Copyright Avail: NTIS HC A20/MF A03

The reduction of Maximum Usable Frequency (MUF) during a geomagnetic storm represents a serious hindrance to the efficient operation of HF transmission links. Possible improvements in forecasting services are discussed. Statistical analyses of ionosonde data from Slough, U.K. (52 N) are used to define patterns for the main phase effects of ionospheric storms and these are compared with similar patterns derived for other midlatitude stations. The storm induced changes in foF2 are primarily dependent upon local time, season and the strength of the geomagnetic disturbance, as quantified by the geomagnetic index ap (tau). The phase of the solar cycle controls average ionization levels whilst short-term variations in solar activity have little effect. The computed mean patterns can be used to forecast foF2 for a few hours ahead, given the required geomagnetic input. Data from a complete solar cycle, 1971 through 1981, are used to determine the errors in the forecasts and to demonstrate that a useful advantage can be attained by this method. The root mean square error in foF2 for 89139 samples is 14.4 percent which compares favorably with the 17.0 percent that is obtained using forecasts based upon either quiet-time values or the previous day's measurements. Studies of error distributions highlight various limitations in the technique and indicate avenues to further improvement. Author

N90-11372# Naval Ocean Systems Center, San Diego, CA. Ocean and Atmospheric Sciences Div.
MEDIUM SCALE STRUCTURE OF THE F-REGION
Adolf K. Paul *In* AGARD, Ionospheric Structure and Variability

on a Global Scale and Interactions with Atmosphere and Magnetosphere Apr. 1989 8 p (For primary document see N90-11361 02-46)
Copyright Avail: NTIS HC A20/MF A03

The standard picture of the F-region is based on hourly observations by ionosondes. More frequent recordings with advanced digital instruments show that very often F-region variations take place with periods of less than half an hour. This means that even if ionograms are taken in 15 minute intervals the actual variations of the ionosphere are still undersampled. Assuming that the effects of propagating acoustic gravity waves are observed, the undersampling of the oscillations results in an overestimation of the periods and the wavelengths. This in turn means that distances between existing and planned ionospheric stations are too large for correct spatial sampling of the waves. Therefore, at this time the observed temporal variations in combination with an assumed propagation velocity provide the only means to obtain first order information about the medium scale spatial structure of the F-region on a routine basis. Digital ionograms recorded during 1980 to 1981 at Brighton, Colorado show characteristics (e.g. virtual height variations and Doppler profiles) supporting the hypothesis that short term F-region variations are caused by acoustic gravity waves which seem to be present all the time with varying amplitudes. In addition, some direct evidence for the spatial structure can be obtained from the angle of arrival observations and their frequency or height dependence. Comparisons of foF2 and MUF (3000) indicate that the main effect of gravity waves on the F-region structure is the variation of the height of the layer and to a lesser degree a variation of the maximum electron density. Author

N90-11373# Air Force Geophysics Lab., Hanscom AFB, MA. Ionospheric Physics Div.
VLF/LF RADIO WAVE STUDIES OF THE STRUCTURE AND VARIABILITY OF THE EQUATORIAL, MID-LATITUDE AND POLAR IONOSPHERE BELOW 100 km
P. A. Kossey, J. E. Rasmussen, and W. L. Klemetti *In* AGARD, Ionospheric Structure and Variability on a Global Scale and Interactions with Atmosphere and Magnetosphere Apr. 1989 14 p (For primary document see N90-11361 02-46)
Copyright Avail: NTIS HC A20/MF A03

The VLF/LF radio wave observations of structure and variability in the lower ionosphere are described. Emphasis is on data relating to the ionosphere below 100 km, obtained at equatorial, mid-latitude and polar locations, with a VLF/LF pulse ionosounder. The use of the data to help characterize the short- and long-term variability of the lower ionosphere is considered, in addition to its use to infer specific structural features of the ionosphere, such as the C-layer below 70 km altitude. Data obtained within the polar cap during a number of solar proton events (SPEs) are also described. Author

N90-11374# Technical Univ. of Istanbul (Turkey).
THE MIDDLE AND HIGH LATITUDE IONOSPHERE AT APPROXIMATELY 550 km ALTITUDE
Y. K. Tulunay *In* AGARD, Ionospheric Structure and Variability on a Global Scale and Interactions with Atmosphere and Magnetosphere Apr. 1989 5 p (For primary document see N90-11361 02-46)
Copyright Avail: NTIS HC A20/MF A03

Ambient electron density measurements made by the radio frequency capacitance probe on Ariel 4 satellite were analyzed in order to study the structures present at the satellite altitudes, i.e. between approximately 470 and 600 km, at latitudes poleward of + or - 50 degrees Lambda both during winter and equinox; data obtained on 94 days centered on the solstices, and March 1972 were used. The general morphology of and the extreme densities, the mid-latitude electron density trough, the polar cap depletions and the electron density enhancements associated with the cusp auroral zone were determined statistically. Analyses of the solstice and the equinox data acquired during quiet magnetic conditions show that the Northern and Southern Hemisphere ionospheres were significantly different. The global characteristics of the winter solstice and the equinox electron densities were similar although they differ from each other in fine details. Author

N90-11375*# Utah State Univ., Logan. Center for Atmospheric and Space Sciences.
MODELLING IONOSPHERIC DENSITY STRUCTURES
R. W. Schunk and J. J. Sojka *In* AGARD, Ionospheric Structure and Variability on a Global Scale and Interactions with Atmosphere and Magnetosphere Apr. 1989 12 p (For primary document see N90-11361 02-46)
(Contract NAGw-77; F49620-86-C-0109)
Copyright Avail: NTIS HC A20/MF A03 CSCL 04A

Large-scale density structures are a common feature in the high-latitude ionsphere. The structures were observed in the dayside cusp, polar cap, and nocturnal auroral region over a range of altitudes, including the E-region, F-region and topside ionosphere. The origins, lifetimes and transport characteristics of large-scale density structures were studied with the aid of a three-dimensional, time-dependent ionospheric model. Blob creation due to particle precipitation, the effect that structured electric fields have on the ionosphere, and the lifetimes and transport characteristics of density structures for different seasonal, solar cycle, and interplanetary magnetic field (IMF) conditions were studied. The main conclusions drawn are: (1) the observed precipitation energy fluxes are sufficient for blob creation if the plasma is exposed to the precipitation for 5 to 10 minutes; (2) structured electric fields produce structured electron densities, ion temperatures, and ion composition; (3) the lifetime of an F-region density structure depends on several factors, including the initial location where it was formed, the magnitude of the perturbation, season, solar cycle and IMF; and (4) depending on the IMF, horizontal plasma convection can cause an initial structure to break up into multiple structures of various sizes, remain as a single distorted structure, or become stretched into elongated segments. Author

N90-11376*# National Aeronautics and Space Administration. Goddard Space Flight Center, Greenbelt, MD.
OBSERVATIONS OF IONOSPHERE/MAGNETOSPHERE INTERACTIONS FROM THE DYNAMICS EXPLORER SATELLITES
R. A. Hoffman *In* AGARD, Ionospheric Structure and Variability on a Global Scale and Interactions with Atmosphere and Magnetosphere Apr. 1989 17 p (For primary document see N90-11361 02-46)
Copyright Avail: NTIS HC A20/MF A03 CSCL 04A

The Dynamics Explorer program was a dual spacecraft mission designed to study the interactions between the upper atmosphere, ionosphere and magnetosphere. The global auroral images acquired from the high altitude spacecraft have provided a revolutionary new time-dependent frame of reference for the interpretation of data acquired in situ. Using data especially from the low altitude spacecraft, interrelationships are developed between the various electrodynamic parameters measured. Ionospheric irregularities are found to be especially intense in regions of electric field convection shears, which are closely related to the dusk hemisphere field-aligned currents. These region 1 currents are spatially connected to the boundary plasma sheet electron precipitation. At all local times, there appears to be a universal relationship between regions where div E is less than 0 and electron precipitation structures. Depending upon the characteristics of the electrons bombarding the atmosphere, the atmosphere will radiate various spectral optical emissions, which can be imaged from high above the polar caps, with temporal resolution sufficient to follow the time-dependent evolution of a substorm. It is concluded that with further detailed analyses of the electrodynamic parameters obtained from in situ measurements, analyses of auroral images will yield specific information on many of the important ionospheric parameters over an entire auroral oval and polar cap, including regions of intense ionospheric irregularities. Author

N90-11377# Centre de Recherches en Physique de l'Environnement, Saint Maur des Fosses (France).
EMPIRICAL MODELS OF CONVECTION ELECTRIC FIELDS AND ELECTROSTATIC POTENTIAL AT HIGH LATITUDE FROM EISCAT OBSERVATIONS: PRELIMINARY RESULTS
Abstract Only
Catherine Senior, Dominique Fontaine, and Gerard Caudal *In* AGARD, Ionospheric Structure and Variability on a Global Scale and Interactions with Atmosphere and Mangetosphere Apr. 1989 1 p (For primary document see N90-11361 02-46)
Copyright Avail: NTIS HC A20/MF A03

Convection electric fields are observed with the EISCAT European Incoherent Scatter Common Program CP-3, which probes the F2 region of the aurorial ionosphere between 61 and 70 degrees invariant latitude for 24-hour runs. Average convection patterns were calculated from ion drift data gathered in several tens of these 24-hour experiments conducted between January 1982 and June 1987, for various levels of magnetospheric activity and orientation of the interplanetary magnetic field. The averaging technique is presented and the physical meaning of our criteria for selecting the data samples are discussed. Electrostatic potential distributions are computed from these statistical electric field models, using the method developed by Alcayde et al. These electrostatic potential patterns are compared to earlier models obtained from incoherent scatter radar or satellite data. Results are consistent with the well-known two-cell convection pattern with antisunward flow over the polar cap, and sunward flow in the auroral zone. The characteristics and variability of these two cells are discussed in the light of indices of magnetospheric activity and orientation of the interplanetary magnetic field. Particular emphasis is placed on the shape and position of the two cells, and on the intensity of the dawn to dusk potential drop applied to the ionospheric auroral zone probed by the radar. Author

N90-11378# Max-Planck-Inst. fuer Aeronomie, Katlenburg-Lindau (Germany, F.R.).
LOW FREQUENCY ELECTROSTATIC WAVES OBSERVED IN THE VICINITY OF AN AURORAL ARC
K. Rinnert *In* AGARD, Ionospheric Structure and Variability on a Global Scale and Interactions with Atmosphere and Magnetosphere Apr. 1989 7 p (For primary document see N90-11361 02-46)
Copyright Avail: NTIS HC A20/MF A03

Measurements of the electric field vector from d.c. to about 150 Hz were performed on board the CAESAR-2 payload. The payload flew over a faint localized auroral arc associated with an inverted-V precipitation event. Equatorward of this auroral disturbance intense electrostatic low frequency signals were observed with fundamental frequency below the ion cyclotron frequency. These signals had properties of wave fields of ion-beam-driven electrostatic ion cyclotron waves (EIC) described by Yamada et al. The spatially or temporarily limited occurrence of these signals may give an indication of the distribution of ion beams or field-aligned currents. Author

N90-11379# Centre National d'Etudes des Telecommunications, Issy-les-Moulineaux (France).
POLAR F LAYER LACUNA IRREGULARITIES AT DUMONT D'URVILLE
Paul Vila *In* AGARD, Ionospheric Structure and Variability on a Global Scale and Interactions with Atmosphere and Magnetosphere Apr. 1989 8 p (For primary document see N90-11361 02-46)
Copyright Avail: NTIS HC A20/MF A03

Polar F lacunae, a loss of F-region echoes by the vertical-incidence ionosondes are re-investigated. The Dumont D'Urville series including rapid-run sequences suggest the existence of three distinct classes of lacuna. Combining these morphological descriptions with some specific observations by backscatter radar, incoherent scatter meridian scans, angle-of-arrival ionosonde measurements and VIKING satellite, a dual mechanism was suggested for the propagation loss causing lacunae. This consists in a fine E-F sporadic screen structure sometimes identical to the Olesen Sec phenomenon, and of F-region fronts about 300 km wide which tilt the scattered ionosonde waves away from the captation cone of the ionosonde receiving antenna. The scant physical measurements available for this study allow a unifying model to be proposed for the front and screen formation, which needs checking up with more co-ordinated data. Author

N90-11380# University Coll., London (England). Dept. of Physics and Astronomy.
SEASONAL AND GEOMAGNETIC RESPONSE OF THE THERMOSPHERE AND IONOSPHERE
D. Rees and T. J. Fuller-Rowell *In* AGARD, Ionospheric Structure and Variability on a Global Scale and Interactions with Atmosphere and Magnetosphere Apr. 1989 27 p Sponsored in part by United Kingdom Science and Engineering Research Council (For primary document see N90-11361 02-46)
(Grant AF-AFOSR-0341-86)
Copyright Avail: NTIS HC A20/MF A03

A self-consistent coupled thermospheric/ionospheric model, a valuable diagnostic tool for examining thermospheric/ionospheric interactions was produced. The neutral thermospheric wind velocity, composition, density, and energy budget are computed, including their full interactions with the high-latitude ion drift and the evolution of the plasma density. A series of simulations was performed at high solar activity, for a level of moderate geomagnetic activity, for each of the June and December solstices, and positive and negative values of the IMF-BY component. In the winter polar region, ion transport and the dirunal migration of the polar convection pattern into and out of sunlight play a major role in the plasma density structure at F-region altitudes. In the summer polar region, an increase in the proportion of molecular to atomic species, created by the global seasonal thermospheric circulation and augmented by the geomagnetic forcing, controls the plasma densities at all Universal Times. The increased destruction of F-region ions in the summer polar region reduces the mean level of solar insolation. In the winter polar region at 300 km the dominant ion is O(+); in summer molecular and O(+) ions are of similar number densities. The summer ion temperature at 300 km exceeds the winter values by 500 K, due to change in neutral temperature. In the lower thermosphere auroral oval the ion density is dominated by auroral precipitation in both seasons, resulting in only a small seasonal dependence in the height-integrated Joule heating rate and field-aligned currents (FAC). Within the polar cap, solar ionization generates a large seasonal variation of conductivity, producing a threefold increase in peak Joule heating rates, changing the balance of FAC. Neglect of neutral winds increases dusk sector Joule heating. Most of the neutral and electrodynamic parameters considered also have strong IMF-BY dependence.
Author

N90-11381# Bonn Univ. (Germany, F.R.). Inst. fuer Astrophysik und Extraterrestrische Forschung.
STORMTIME COUPLING OF THE NEUTRAL AND IONIZED UPPER ATMOSPHERE AT MIDDLE LATITUDES
G. W. Proelss *In* AGARD, Ionospheric Structure and Variability on a Global Scale and Interactions with Atmosphere and Magnetosphere Apr. 1989 13 p (For primary document see N90-11361 02-46)
Copyright Avail: NTIS HC A20/MF A03

Present knowledge about the interaction between magnetic storm associated changes in the neutral gas composition and ionospheric storms is reviewed. After a brief description of ionospheric disturbance effects, it is shown that the negative phase is caused by a decrease of the atomic oxygen to molecular nitrogen (oxygen) density ratio. Local time variations are discussed as an example of systematic changes common to both disturbance phenomena. It is shown that negative ionospheric storms may be confused with ionospheric trough effects which are not produced by neutral composition changes. There is also no association between composition perturbations and positive ionospheric storm effects which again are attributed to the transport of ionization.
Author

N90-11382# Science Research Council, Chilton (England).
IONOSPHERE-THERMOSPHERE COUPLING AT HIGH LATITUDES: ASPECT ANGLE DEPENDENCE OF NON-THERMAL PLASMAS Abstract Only
K. J. Winser, M. Lockwood, A. D. Farmer, G. O. L. Jones, D. Rees, and A. Aruliah (University Coll., London, England) *In* AGARD, Ionospheric Structure and Variability on a Global Scale and Interactions with Atmosphere and Magnetosphere Apr. 1989 1 p (For primary document see N90-11361 02-46)
Copyright Avail: NTIS HC A20/MF A03

Recent observations with the EISCAT incoherent scatter radar have shown large, relatively short lived (approximately 1 hour), enhancements in the dayside, auroral convection flows over a side range of latitude. These are larger than the neutral thermal speed and represent the first experimental observations of non-thermal plasma over a range of observing angles, indicating a clear angular dependance. The observed ion temperature anisotropy, deduced by assuming a Maxwellian line-of-sight ion velocity distribution, exceeds the theoretical value for a bi-Maxwellian based on a realistic ion-neutral collision model. One of the main problems was that the neutral temperature and wind velocity had to be estimated from either the radar data or models, which may introduce a large source of error into the calculations described above. This problem is discussed and the possible consequences are illustrated by comparing the meridional and zonal components of the neutral wind derived from EISCAT observations with those measured simultaneously in the same volume, using a Fabry-Perot interferometer (FPI). A new experiment is planned which will combine low elevation EISCAT observations of the auroral zone/polar cap ionosphere with simultaneous FPI measurements of the neutral wind and temperature, which will address some previously unsolved problems on the collisional and plasma processes that occur in the high-latitude ionosphere/thermosphere system. Author

N90-11383# Auroral Observatory, Tromso (Norway).
QUIET TIME CONDUCTIVITIES OF THE AURORAL IONOSPHERE
Asgeir Brekke and Chris Hall *In* AGARD, Ionospheric Structure and Variability on a Global Scale and Interactions with Atmosphere and Magnetosphere Apr. 1989 17 p Sponsored in part by Norges Almenvitenskapelige Forskningsrad (For primary document see N90-11361 02-46)
Copyright Avail: NTIS HC A20/MF A03

EISCAT incoherent scatter data of the E- and F-region raw electron density profiles for 7 quiet days were used to derive the auroral ionosphere conductivities and conductances. Empirical formulas for the solar zenith angle dependence were obtained which are compared with earlier models and results. In particular, the Hall- to Pedersen-conductance ratio was found to be lower during quiet periods than usually reported from similar work on incoherent scatter data and model studies. For disturbed days, however, when the data are corrected for background ionization, this conductance ratio is much higher than models predict.
Author

N90-11384# Max-Planck-Inst. fuer Aeronomie, Katlenburg-Lindau (Germany, F.R.).
CALCULATION OF THE TEMPERATURE AND VELOCITY VECTOR OF THE NEUTRAL GAS USING EISCAT CP3-DATA
D. Figueroa and H. Kohl *In* AGARD, Ionospheric Structure and Variability on a Global Scale and Interactions with Atmosphere and Magnetosphere Apr. 1989 4 p (For primary document see N90-11361 02-46)
Copyright Avail: NTIS HC A20/MF A03

The CP3-mode of EISCAT is particularly appropriate for three-dimensional studies of the interaction between ionosphere and thermosphere, because of its good latitude, height and time coverage. Using mainly CP3-data of EISCAT as input, parameters of the neutral gas in the middle thermosphere in the latitudes of EISCAT, was calculated by solving the coupled transport equations for the neutral and ion gases for the heights between 150 and 500 km and latitudes between 66 and 72 degrees. By numerically solving the energy equation of the ions and the momentum equation of the neutral gas we obtained the temperature and the horizontal velocity of the neutral gas. This, used in combination with the energy equation of the neutral gas, allowed us to estimate the vertical neutral gas velocity. The calculated neutral gas temperatures sometimes deviate from those obtained by empirical models, which rather represent average conditions, and cannot be expected to described individual periods in the strong varying auroral thermosphere. Calculated neutral gas velocities show clearly the effect of the convection pattern of the ion gas, and little vertical variation. Estimated vertical neutral gas velocities look fairly reasonable, although they are subject to several sources of error. Author

N90-11385# Leicester Univ. (England). Ionospheric Physics Group.
ION HEATING EVENTS OBSERVED AT THE EISCAT RADAR
I. W. McCrea, T. R. Robinson, M. Lester, and T. B. Jones *In* AGARD, Ionospheric Structure and Variability on a Global Scale and Interactions with Atmosphere and Magnetosphere Apr. 1989 10 p (For primary document see N90-11361 02-46)
Copyright Avail: NTIS HC A20/MF A03

According to simple theory, a quadratic relationship should exist between ion temperature and ion velocity during frictional heating of the high-latitude ionosphere. A method of fitting the form of this relationship for a selection of EISCAT Common Program data is demonstrated, and the observed behavior is consistent with theoretical predictions. From the equation obtained, estimates are made of the neutral mass and one component of the neutral wind. These appear to be physically realistic. The validity and sensitivity of the technique is briefly discussed, and an attempt is made to account for possible errors due to changes in the ion composition and the presence of anistropic plasma velocity distributions. Author

N90-11386# Technische Hogeschool, Eindhoven (Netherlands). Dept. of Physics.
ON THE INFLUENCE OF IONOSPHERIC CONDUCTIVITY ON DISPERSION OF ACOUSTIC GRAVITY WAVES
L. P. J. Kamp, R. H. M. Miesen, P. C. deJagher, and F. W. Sluijter *In* AGARD, Ionospheric Structure and Variability on a Global Scale and Interactions with Atmosphere and Magnetosphere Apr. 1989 8 p (For primary document see N90-11361 02-46)
Copyright Avail: NTIS HC A20/MF A03

The influence of ionization and conduction on the dispersion of acoustic gravity waves in the upper atmosphere was investigated by means of a numerical analysis of the corresponding dispersion relation in which the Hall frequency is assumed to be much smaller than the Brunt-Vaisala frequency. It is shown that a significant consequence of the incorporation of ionospheric conduction is a relatively strong damping of gravity waves, unless propagating parallel to the Earth's magnet field with frequencies smaller than the Brunt-Vaisala frequency. Typically this damping takes place with a characteristic damping rate that scales with the Pedersen conductivity. Furthermore it turns out that waves that belong to the acoustic branch of the double-branch dispersion relation are also damped with a camping rate of the same order in magnitude when ionospheric conduction is taken into account. This is the case for waves propagating perpendicular to the Earth's magnetic field and for waves propagating parallel to the Earth's magnetic field but then with frequencies that are of the order of the acoustic cut-off frequency. Author

N90-11387# Max-Planck-Inst. fuer Aeronomie, Katlenburg-Lindau (Germany, F.R.).
ATMOSPHERIC GRAVITY WAVES IN THE AURORAL SOURCE REGION OF TIDs, STUDIED WITH THE EISCAT CP2-DATA
H.-P. Mauelshagen and K. Schlegel *In* AGARD, Ionospheric Structure and Variability on a Global Scale and Interactions with Atmosphere and Magnetosphere Apr. 1989 14 p (For primary document see N90-11361 02-46)
Copyright Avail: NTIS HC A20/MF A03

Atmospheric gravity waves and travelling ionospheric

disturbances (TIDs) with the data where the methods of estimating different TID-events, their direction and further aims of study presented, were studied. The time was confined more or less to a magnetically very quiet 38 hour period, 5 to 6 May 1987. Contrary to more active days it is possible in this period to show not only different TID-events but also to resolve a frequency-time evolution of sudden events. For this very weak magnetic activity it is unlikely that the present TIDs originate in auroral effects. Thereby the criteria were worked out to distinguish events of propagating waves and of waves which are just beginning. Summing up this work shows that it is possible to estimate the whole complex wave number as a function of time of every resolvable wave-like structure. This offers a possibility to test the theories of the generation, the propagation, and the dissipation of TIDs. Author

N90-11388# Bari Univ. (Italy). Dept. of Physics.
ON THE POSSIBILITY OF PRODUCING ARTIFICIAL IONIZATION AND POLAR AURORA IN THE IONOSPHERE BY RADIO-WAVES EMITTED FROM THE GROUND
Mario Cutolo and Angela Argenziano *In* AGARD, Ionospheric Structure and Variability on a Global Scale and Interactions with Atmosphere and Magnetosphere Apr. 1989 4 p Prepared in cooperation with Naples Univ., Italy (For primary document see N90-11361 02-46)
Copyright Avail: NTIS HC A20/MF A03

In 1938 Prof. V. A. Bailey demonstrated by calculations that some resonance may occur between electrons and a wave as the frequency of this wave varies around the local gyrofrequency, fh. A radio-wave having a frequency equal to the gyrofrequency is called a, gyro-wave. The resonance increases the collision frequency in the low ionosphere by an appreciable amount (I). There are two principal consequencies of the resonance: If a second wave unmodulated passes through the ionosphere region where the gyro-wave acts, an interaction is found between these two waves. This phenomenon is called gyrointeraction and was demonstrated experimentally. If the radiowave is a gyro-wave, with a carrier frequency varying around the local gyrofrequency and is powerful it could produce in the ionosphere an artificial aurora or airglow. The powerful gyro-wave would reduce strongly the electric voltage of the region illuminated by the gyro-wave as to generate an electrical discharge. Moreover with a suitable system of 800 aerial and with a power of 500 kW or of 1,000,000 kW it would be possible to generate an artificial aurora between 60 and 88 km in the ionosphere. Starting form the experiments of H. A. Wilson and D. M. Myers with high-frequency discharges on the lines developed by J. S Towsend and his associates, Bailey developed his theory. These experiments, made by Wilson and Myers, showed that the electric discharges can occur in the air when in the uniform column z/p the ratio of the electric force z to the gas pressure p is approximately 16. It is possible therefore to conclude that two of the necessary conditions for producing electrons and light, are satisfied when E/p 16. An investigation was made in 1959 of the possible increases of both the collision frequencies and the electron density N caused by a powerful extraordinary circular gyrowave in the nocturnal lower-E-region and in the daytime D-region. The principal process then freshly introduced was the attachment of the electrons to molecules in some collisions. According to this new thory the power density requirement for the excitations of an artificial airglow by means of gyrowaves were reconsidered. Author

N90-11389# California Univ., San Diego. Dept. of Electrical and Computer Engineering.
IONOSPHERIC IRREGULARITIES DUE TO POWERFUL HF RADIO TRANSMISSIONS
J. A. Fejer *In* AGARD, Ionospheric Structure and Variability on a Global Scale and Interactions with Atmosphere and Magnetosphere Apr. 1989 10 p (For primary document see N90-11361 02-46)
(Contract F19628-86-K-0031)
Copyright Avail: NTIS HC A20/MF A03

It was known for some time that sufficiently powerful HF radio transmissions produce a great variety of ionospheric irregularities. Ionospheric modification facilities with effective radiated powers of the order of 100 MW directed toward the ionosphere were used for the study of such irregularities since 1970. Such man-made irregularities were employed to establish experimental scatter communications links. Very powerful short wave broadcast transmitters must also produce man-made irregularities which affect the ionospheric propagation of short waves. All aspects of the physical phenomena which play a role in the production of ionospheric irregularities by powerful HF transmissions, are discussed. These include thermal self-focusing of radio waves, formation of short-scale field-aligned irregularities by a thermal parametric instability in which the scattering of the HF pump wave by the irregularities into Langmuir waves plays an important role, and those parametric instabilities in which the ponderomotive force dominates over thermal forces. The latter two parametric instabilities can lead to the acceleration of electrons to energies of tens of electron volts. Such accelerated electrons can produce artificial airglow and also additional ionization which under certain conditions could be significant. In their strongly nonlinear stage parametric instabilities can lead to the formation of localized electron density depletions (cavitons) maintained by the ponderomotive force of Langmuir waves trapped in them.
Author

N90-11390# Crete Univ., Iraklion (Greece). Dept. of Physics.
A REVIEW ON RADIO STUDIES OF AURORAL E-REGION IONOSPHERIC IRREGULARITIES
C. Haldoupis *In* AGARD, Ionospheric Structure and Variability on a Global Scale and Interactions with Atmosphere and Magnetosphere Apr. 1989 20 p Previously announced in IAA as A89-43027 (For primary document see N90-11361 02-46)
Copyright Avail: NTIS HC A20/MF A03

The physical significance of recent radar studies of auroral irregularities at different frequency bands in the VHF and UHF range is discussed, with emphasis on Doppler spectral studies. The results suggest that important differences exist between the 50 MHz equatorial and auroral backscatter processes, and that the role of altitude and of electron density in the generation and saturation of instabilities is much more important in the auroral than in the equatorial E region. The need for a general unified theory of radio aurora incorporating wave energy propagation characteristics and new nonlinear saturation mechanisms is emphasized. IAA

N90-11391# Illinois Univ., Urbana. Dept. of Electrical and Computer Engineering.
IONOSPHERIC IRREGULARITIES AND THEIR EFFECTS ON ELECTROMAGNETIC WAVES PROPAGATING THROUGH THEM
K. C. Yeh *In* AGARD, Ionospheric Structure and Variability on a Global Scale and Interactions with Atmosphere and Magnetosphere Apr. 1989 7 p (For primary document see N90-11361 02-46)
(Grant NSF ATM-84-14134)
Copyright Avail: NTIS HC A20/MF A03

Global sounding and probing of the ionosphere have revealed the frequent presence of irregularities throughout various ionospheric regions. Using the collected data, many comprehensive studies were made and reviewed. Models were constructed and continuously improved with additional data. Extensive morphological studies clearly indicate a strong dependence on the phase of solar cycle, the geomagnetic latitude, and the local time. Data were also collected that enable the characterization of the electron density fluctuations statistically in their space-time behavior. Such characterizations are necessary in connecting medium properties to wave properties. The ionosphere is known to be a dispersive medium. In the presence of irregularities, severe scattering may additionally take place. A radio wave propagating through such an environment may therefore experience fading and scintillation. The strength of a scintillating signal is usually measured by its scintillation index S4, defined as the normalized root-mean-square intensity fluctuations above the mean. The dependence of S4 on radio frequency was investigated by using

multifrequency data. The results are shown to agree with theory. The higher-order statistics that are used to describe the space-time signal were measured. Using spaced antennas, a cross correlation function can be calculated in addition to S4 and self spectrum. Several methods exist that connect the cross correlation function the ionospheric drift velocity and the velocity fluctuations. Several days of data obtained at an equatorial station will be shown as examples. Author

N90-11392# Centre de Recherches en Physique de l'Environnement, Saint Maur des Fosses (France).
ELECTROSTATIC TURBULENCE IN THE HIGH LATITUDE IONOSPHERE Abstract Only
J.-C. Cerisier, H. Mounir, and J.-J. Berthelier *In* AGARD, Ionospheric Structure and Variability on a Global Scale and Interactions with Atmosphere and Magnetosphere Apr. 1989 1 p (For primary document see N90-11361 02-46)
Copyright Avail: NTIS HC A20/MF A03

Two components of the Extremely Low Frequency (ELF) electric field are measured on board the low altitude (400 to 2000 km) polar orbiting satellite Aureol-3. At high latitude, the main wave-field component observed in the frequency range up to a few hundred Hertz is the electrostatic turbulence. The frequency spectrum measured in the satellite reference frame usually follows a power lay (E squared alpha E(sub 0) f sup -alpha), thus allowing to describe the turbulence with two parameters (amplitude and spectral index). These characteristic parameters will be discussed in relation with the possible free energy sources: field-aligned current, particle precipitation, electron density gradient. The relation between the frequency spectrum and the wave number spectrum is not unambiguous. However, under the hypothesis of time-independent turbulence, it is possible to deduce, from the measurement of two different components of the electric field, the anisotropy of the wave number spectrum of the turbulence. The method used for this determination will be described and applied to physical situations observed in the polar cap, in the auroral zone, and in sub-auroral regions. Author

N90-11393# Boston Univ., MA.
AURORAL AND SUB-AURORAL F-LAYER IRREGULARITY STUDIES IN THE NORTHERN AND SOUTHERN HEMISPHERE DURING THE EQUINOX TRANSITION STUDY SEPTEMBER 16-26, 1984
J. Aarons, J. C. Foster, L. Kersley, and A. S. Rodger (British Antarctic Survey, Cambridge, England) *In* AGARD, Ionospheric Structure and Variability on a Global Scale and Interactions with Atmosphere and Magnetosphere Apr. 1989 14 p Sponsored in part by ONR, Washington, DC (For primary document see N90-11361 02-46)
(Grant NSF ATM-84-19117)
Copyright Avail: NTIS HC A20/MF A03

A preliminary model detailing the auroral and sub-auroral nightly behavior of F-layer irregularities during the injection and recovery phases of magnetic storms is outlined. Initially the irregularities spread equatorwards from the auroral region. On subsequent nights in those storms where Dst slowly returns to its zero level there is activity at auroral latitudes at the end of the magnetic storm and finally, relatively high irregularity intensity primarily at sub-auroral latitudes. The model was tested with observations of the irregularities observed during the September 1984 Equinox Transition Study. Observations of irregularities and incoherent scatter were examined for the injection phase of the magnetic storm of Sep. 22 to 23. The concept was to determine what parameters are most important in indicating whether irregularities are present over a range of latitudes from 53 to 78 degrees CGL. The data set indicates distinct correlation with convection velocities in the early portion of the storm when a sub-storm was shown on magnetograms. In the latter half of the night with the magnetic storm fully developed, the data show good correlation with an electron density trough, high electron temperatures, and high velocities. For the recovery phase of a magnetic storm another period in the ETS is examined with sub-auroral irregularities observed during the recovery of Dst when quiet magnetic conditions prevailed. The general form of the model appears to be valid but many aspects of the timing and the magnitude of the irregularity intensity are to be determined. Author

N90-11394# Universite de Toulon et du Var (France).
SMALL-SCALE IRREGULARITIES AND GLOBAL PLASMA DYNAMICS IN THE HIGH-LATITUDE IONOSPHERE
C. Hanuise, R. A. Greenwald, K. B. Baker, J. M. Ruohoniemi, J. C. Cerisier, and Catherine Senior (Centre de Recherches en Physique de l'Environnement, Saint Maur des Fosses, France) *In* AGARD, Ionospheric Structure and Variability on a Global Scale and Interactions with Atmosphere and Magnetosphere Apr. 1989 14 p (For primary document see N90-11361 02-46)
Copyright Avail: NTIS HC A20/MF A03

New sophisticated HF coherent radars were installed in the past few years at very high latitudes. The APL Goose Bay radar and the French SHERPA radar in Schefferville are the two components of the Polar Region Ionospheric Structrure Monitor (PRISM) operating in Canada. These instruments detect irregularities within the three-dimensional volume covering much of northeastern Canada and Greenland. The instruments are capable of following the temporal variability of these irregularities as well as determining unambiguously the Doppler shift and spectral broadening of radar signals scattered by them. The scientific goals of the program concern both the physics of the small-scale structures and the mapping of large-scale plasma convection. Several case studies of plasma mechanisms generating the small-scale density structures were already published. The temporal and spatial variability of the large-scale irregularity structures, as seen by the radars, is also investigated. The relationship between the radar Doppler velocity and the plasma drift velocity were confirmed. The potential of the system for studying global ionospheric dynamics is emphasized. When combining the two radial velocities measured by each radar, a two-dimensional map of plasma convection and electric field is derived over a region as large as 2 million square kilometers, with a fine temporal and spatial resolution in the auroral region and over the polar cap. Author

N90-11395# Lowell Univ., MA. Center for Atmospheric Research.
EXAMPLES OF METEOROLOGICAL BEHAVIOR OF THE IONOSPHERE
K. Bibl *In* AGARD, Ionospheric Structure and Variability on a Global Scale and Interactions with Atmosphere and Magnetosphere Apr. 1989 6 p (For primary document see N90-11361 02-46)
(Contract CRL-61(052)-623)
Copyright Avail: NTIS HC A20/MF A03

For some time the network of ionosonde stations in Europe were dense enough to study the meteorological behavior of the ionosphere. Because the electron recombination near the maximum of the F-region ionization is sufficiently small, the maximum electron density and the profile are controlled substantially by dynamic processes. Gravity waves and vertical plasma drift and its vertical gradients change the F-layer ionization significantly. In fixed frequency ionosonde recordings the author has discovered direct oblique echoes from a hole in the ionosphere over the Alps. Maps were drawn to show the meteorological properties of this European Anomaly either as a time development of a cross-section of Europe from northern Germany to Rome, Italy using six stations, or as a sequence of a contour maps of the ionosphere over Europe using ten stations. A short animated movie was produced demonstrating the development of the hole in the ionosphere and its recovery with a curl developing. Even the average behavior of the F-region ionization shows substantial differences with location. In Europe the variations of the local gradients in ionization can be different by a factor of two over two locations separated by 1000 km. This behavior, important for understanding the meteorology of the ionosphere and for precise ionspheric radio predictions, certainly requires intense studies with digital sounders in Europe and at other locations. Author

N90-11396# Lowell Univ., MA. Center for Atmospheric Research.
MULTISTATION/MULTIPARAMETER OBSERVATIONS WITH A NETWORK OF DIGITAL IONOSONDES
B. W. Reinisch, J. Buchau (Air Force Geophysics Lab., Hanscom AFB, MA.), K. Bibl, and G. S. Sales *In* AGARD, Ionospheric Structure and Variability on a Global Scale and Interactions with Atmosphere and Magnetosphere Apr. 1989 9 p (For primary document see N90-11361 02-46)
Copyright Avail: NTIS HC A20/MF A03

The global network of modern ionosondes generates a data set of ionospheric characteristics that can serve as test bed for the developing ionospheric models. Remote access to each station make it possible to use real time data for project planning and radio communication tasks. New ionospheric parameters like ionospheric roughness, tilt angles and drift are now available for each Digisonde location. Author

N90-11397# Science Applications International Corp., McLean, VA. Lab. for Atmospheric and Space Sciences.
COORDINATED MULTI-PARAMETER MEASUREMENTS AND PREDICTIONS OF THE GLOBAL-SCALE IONOSPHERE
Edward P. Szuszczewicz, R. A. Wolf, B. G. Fejer, R. W. Schunk, and E. Roelof (Johns Hopkins Univ., Laurel, MD.) *In* AGARD, Ionospheric Structure and Variability on a Global Scale and Interactions with Atmosphere and Magnetosphere Apr. 1989 16 p (For primary document see N90-11361 02-46)
(Grant NSF ATM-85-13362)
Copyright Avail: NTIS HC A20/MF A03

The solar-terrestrial system involves a myriad of macro and microphysical processes that challenge the development of a unified physical description of solar, magnetrospheric, interplanetary, and thermospheric controls of the global-scale ionosphere. A well-planned interdisciplinary effort combining theoretical modelling with a coordinated measurement program should lead to significant advances in understanding of the solar-terrestrial system as a whole and the development of real-time predictive capability for a world-wide specification of ionospheric conditions as they are dictated by the controlling subsystem inputs. The SUNDIAL program has such a focus, with a combined modelling and measurement program that includes solar, solar wind, interplanetary and geomagnetic data, and nearly 70 ionospheric monitoring stations at high-, middle- and low-latitudes in the American, European/African, and Asian/Australian sectors. The program operates in an 8 to 14 day campaign mode with around-the-clock measurements. Campaigns were initiated in October 1984, and since September 1986 were conducted at 9-month intervals to study each of the four ionospheric seasons twice within the ascending phase of the current solar cycle. The measurement and modeling elements in the program were reviewed perspectives on global-scale ionospheric predictability discussed and some of the accumulating results which address magnetospheric substorms and the triggering of equatorial spread-F highlighted. Author

N90-11398# Centre National d'Etudes des Telecommunications, Lannion (France).
NORTH-SOUTH TROPICAL F2 LAYER ASYMMETRY AT WEST AFRICAN AND PACIFIC LONGITUDES
Colette Davy, Roland Fleury, Pierre Gourvez, Rudi Hanbaba, and Paul Vila (Centre National d'Etudes des Telecommunications, Issy-les-Moulineaux, France) *In* AGARD, Ionospheric Structure and Variability on a Global Scale and Interactions with Atmosphere and Magnetosphere Apr. 1989 6 p (For primary document see N90-11361 02-46)
Copyright Avail: NTIS HC A20/MF A03

Because in September to October 1986 the a sub p magnetic activity nearly changed with 24-hour steps, this period presents rather simple F2 layer day-to-day changes in the intertropical zone. Along the ten days selected for the equinox Sundial study, the CNET stations: Dakar (17.7 N, 17.2 W, northern subtropic, Ouagadougou (12.4 N, 1.6 W, magnetic eauator), Tahiti (17.4 S, 149.2 E, southern tropic) provide a sufficient latitude diversity to characterize the magnetic season asymmetry of generally dominant anti-solar tropical peak densities. On the basis of previous ground-based and satellite meridian-aligned surveys the F2 layer peak true height and foF2 evolution were investigated, here estimated from the Dakar variations of September 27, September 28 and October 4 1986. The evolution on the (moderately) disturbed day when the average kp values jumped from 1 plus the day before to 4 plus show everywhere the same single weaker maximum around 15 LT. The 1966 complete data along the Tamanrasset median help investigate the main processes of these two different types of evolutuion; the intertropical fountain and neutral drag mechanisms are investigated: the respective effects of the E X B dynamo, neutral wind from sub-solar atmospheric heating and from sub-auroral disturbance dynamo are deduced. Couplings between these processes and the conjugate photo-electron forced diffusion are discussed. Author

N90-11399# Royal Aerospace Establishment, Farnborough (England). Radio and Navigation Dept.
JOINT VHF COHERENT RADAR AND OBLIQUE SOUNDER OBSERVATIONS FOR SHORT TERM IONOSPHERE FORECASTING
P. S. Cannon, M. Lester, E. C. Thomas, A. H. Dickson, T. B. Jones, R. Maude, P. J. Rylah (Leicester Univ., England), and A. K. Shukla *In* AGARD, Ionospheric Structure and Variability on a Global Scale and Interactions with Atmosphere and Magnetosphere Apr. 1989 13 p (For primary document see N90-11361 02-46)
(Contract SERC-SGD/10696)
Copyright Avail: NTIS HC A20/MF A03

An experiment which utilizes two VHF coherent radars located in northern Scotland together with an oblique chirp sounder, operating over a path from Norway to northern Scotland is described. The expected sounder path falls within the radars field-of-view. Some initial results are described from the first in a series of experiments. A statistical correlation is found between the occurrence of radar backscatter and the occurrence of sporadic-E. On some occasions a positive correlation also exists between the backscatter signal to noise ratio and the highest frequency measured from the sporadic-E trace on the ionogram. On other occasions the correlation is poor. An initial interpretation of these data is presented which suggests that propagation of the HF sporadic-E signals via a simple plane ionosphere is inadequate to explain the observations. Author

N90-11400# Centre National d'Etudes des Telecommunications, Lannion (France).
RADIO PROPAGATION CONDITIONS FORECAST ABOVE A LOW LATITUDE REGION **c32**
H. Sizun and M. Lissillour *In* AGARD, Ionospheric Structure and Variability on a Global Scale and Interactions with Atmosphere and Magnetosphere Apr. 1989 17 p (For primary document see N90-11361 02-46)
Copyright Avail: NTIS HC A20/MF A03

The purpose is to present for the Tahiti region, a low latitude station, a method for determining monthly, weekly and daily forecasts of radio propagation conditions. The monthly forecasts are necessary to establish radio links in good conditions (antennas, frequencies, power and working hours determination) and are based on the forecast of the solar activity. The weekly and daily forecasts take into account the fine evolution of both solar and magnetic activities and also the influence of ionospheric storms. Author

N90-11401# Millman (George H.), DeWitt, NY.
AN IONOSPHERIC MODEL FOR HF SKY-WAVE BACKSCATTER RADAR **c32**
George H. Millman, Carl A. Bowser, and Roger W. Swanson (General Electric Co., Syracuse, NY.) *In* AGARD, Ionospheric Structure and Variability on a Global Scale and Interactions with Atmosphere and Magnetosphere Apr. 1989 16 p (For primary document see N90-11361 02-46)
Copyright Avail: NTIS HC A20/MF A03

The determination of target location by an HF over-the-horizon

backscatter radar is accomplished by the use of an ionospheric model in conjunction with ionogram transmission curves. An ionospheric model is described in terms of the temporal and spatial characteristics of the various ionospheric layers. The model includes the high-latitude region and is used with the transmission curve overlay process for HF backscatter radar-target coordinate registration. Author

N90-11402# Andrews Antennas, Adelaide (Australia).
ACCURATE MEASUREMENTS OF THE TOTAL ANGLE OF ARRIVAL OF HF SKYWAVES **c82**
Z. R. Jeffrey, P. T. Middleton, and C. Winkler *In* AGARD, Ionospheric Structure and Variability on a Global Scale and Interactions with Atmosphere and Magnetosphere Apr. 1989 10 p (For primary document see N90-11361 02-46)
Copyright Avail: NTIS HC A20/MF A03

The procedures adopted in the ANDREW Single Station Location (SSL) system, SKYLOC, to measure the azimuth and elevation angle of a skywave from an HF transmitter, with a view to determining the location of that transmitter by appropriate simulation of the ionosphere and the signals propagating through it are described. The procedures adopted are capable of providing very accurate measurements of the azimuth and elevation angle, well within the variability imposed by the ionosphere, and are able to process signals with very small signal-to-noise ratios. Author

N90-11403# Andrews Antennas, Adelaide (Australia).
IONOSPHERIC LIMITATIONS TO THE ACCURACY OF SSL ESTIMATES OF HF TRANSMITTER LOCATIONS **c32**
L. F. McNamara *In* AGARD, Ionospheric Structure and Variability on a Global Scale and Interactions with Atmosphere and Magnetosphere Apr. 1989 15 p (For primary document see N90-11361 02-46)
Copyright Avail: NTIS HC A20/MF A03

Procedures for determining the location of an HF transmitter using observations from a single DF site have improved greatly in recent years. The ability to measure angles of arrival of the incoming skywave has now progressed to the point where the accuracy of the postion estimation is set by the ionosphere and its variability, and by imperfect knowledge of these variations, rather than by errors in the measured angles of arrival. After discussing the levels of accuracy currently obtainable, some of the limits set by the inability to specify the ionosphere accurately enough are discussed and methods suggested by which some of these limitations can be overcome. Author

N90-11404# Laboratoire d'Etude des Transmissions Ionospheriques, Cachan (France).
INFLUENCE OF IONOSPHERIC VARIATIONS ON HIGH-RELIABILITY HF SYSTEMS UTILIZING LARGE BASES [INFLUENCE DES VARIATIONS IONOSPHERIQUES SUR LES SYSTEMES HF A HAUTE FIABILITE UTILISANT DE GRANDES BASES]
C. Goutelard and J. P. vanUffelen (Telecommunications Radioelectriques et Telephoniques, Le Plessis-Robinson, France) *In* AGARD, Ionospheric Structure and Variability on a Global Scale and Interactions with Atmosphere and Magnetosphere Apr. 1989 12 p In FRENCH (For primary document see N90-11361 02-46)
Copyright Avail: NTIS HC A20/MF A03

Transmission reliability is dependent on propagation parameters and interference. The use of wide bases provides a solution to this problem. The minimal base dimensions are determined by the interference. Management of the established network requires large scale modeling of the propagation medium and evaluation of interference. Optimal reception conditions are established for the case of bases composed of two to four receiving stations. Optimal coverage limits are determined and three hierarchical systems are defined for real-time network management. Author

N90-11405*# National Aeronautics and Space Administration. Goddard Space Flight Center, Greenbelt, MD.
TWO-DIMENSIONAL INTERCOMPARISON OF STRATOSPHERIC MODELS
Charles H. Jackman, ed., Robert K. Seals, Jr., ed., and Michael J. Prather, ed. (National Aeronautics and Space Administration. Goddard Inst. for Space Studies, New York, NY.) Aug. 1989 606 p Workshop held in Virginia Beach, VA, 11-16 Sep. 1988; sponsored by NASA, Washington
(NASA-CP-3042; Rept-89B00192; NAS 1.55:3042) Avail: NTIS HC A99/MF A04 CSCL 04A

A detailed record is provided for the examination of fundamental differences in photochemistry and transport among atmospheric models. The results of 16 different modeling groups are presented for several model experiments. For individual titles, see N90-11406 through N90-11409.

N90-11406*# National Aeronautics and Space Administration. Goddard Space Flight Center, Greenbelt, MD.
REPORT ON THE 2-D MODEL INTERCOMPARISON WORKSHOP HELD JANUARY 11-16, 1987 IN FORT MYERS BEACH, FLORIDA, CHAPTER 2
Paul D. Guthrie *In its* Two-Dimensional Intercomparison of Stratospheric Models Aug. 1989 p 31-41 (For primary document see N90-11405 02-46)
Avail: NTIS HC A99/MF A04 CSCL 04A

In the attempts to understand the processes which affect ozone in the stratosphere, and to predict future ozone levels, a variety of computer models were developed and employed. To oversimplify somewhat, the models range from 1-D models with intricately detailed photochemistry but only the crudest representation of transport, to 3-D general circulation models with intricately detailed dynamics and no photochemistry at all. Each of these has its appropriate uses. It was felt that there was much to be gained from intermediate models incorporating an extensive treatment of photochemistry with a dynamical framework which at least recognizes that atmospheric motions are advective as well as diffusive, and that both chemistry and dynamics are subject to latitudinal and seasonal variations. Thus the 2-D, zonally averaged models have begun to play a larger role in the last seven years, both in attempting to understand observed distributions of trace species and in attempting to assess the probable effects of antropogenic perturbations. There are many choices to be made in developing the model. It was the purpose of the 2-D model Intercomparison Workshop to permit discussion of the choices made and the behavior of the resulting models. The goal was not to identify a best set of choices, but rather to identify areas in which the models are sensitive to the choices made, and to develop a sense of where these models as a class do well or poorly in simulating the observed atmosphere. Author

N90-11407*# National Aeronautics and Space Administration. Goddard Space Flight Center, Greenbelt, MD.
REPORT OF THE 1988 2-D INTERCOMPARISON WORKSHOP, CHAPTER 3
Charles H. Jackman, Guy Brasseur, Susan Soloman, Paul D. Guthrie, Rolando Garcia, Yuk L. Yung, Lesley J. Gray, K. K. Tung, Malcolm K. W. Ko, and Ivar Isaken (Oslo Univ., Norway) et al *In its* Two-Dimensional Intercomparison of Stratospheric Models Aug. 1989 p 43-107 (For primary document see N90-11405 02-46)
Avail: NTIS HC A99/MF A04 CSCL 04A

Several factors contribute to the errors encountered. With the exception of the line-by-line model, all of the models employ simplifying assumptions that place fundamental limits on their accuracy and range of validity. For example, all 2-D modeling groups use the diffusivity factor approximation. This approximation produces little error in tropospheric H2O and CO2 cooling rates, but can produce significant errors in CO2 and O3 cooling rates at the stratopause. All models suffer from fundamental uncertainties in shapes and strengths of spectral lines. Thermal flux algorithms being used in 2-D tracer tranport models produce cooling rates that differ by as much as 40 percent for the same input model

atmosphere. Disagreements of this magnitude are important since the thermal cooling rates must be subtracted from the almost-equal solar heating rates to derive the net radiative heating rates and the 2-D model diabatic circulation. For much of the annual cycle, the net radiative heating rates are comparable in magnitude to the cooling rate differences described. Many of the models underestimate the cooling rates in the middle and lower stratosphere. The consequences of these errors for the net heating rates and the diabatic circulation will depend on their meridional structure, which was not tested here. Other models underestimate the cooling near 1 mbar. Suchs errors pose potential problems for future interactive ozone assessment studies, since they could produce artificially-high temperatures and increased O3 destruction at these levels. These concerns suggest that a great deal of work is needed to improve the performance of thermal cooling rate algorithms used in the 2-D tracer transport models. Author

N90-11408*# National Aeronautics and Space Administration. Goddard Space Flight Center, Greenbelt, MD.
MODEL DOCUMENTATION, CHAPTER 4
Malcolm K. W. Ko, Debra Weisenstein, Nien Dak Sze, Yuk L. Yung, David Crisp, Richard W. Zurek, J. A. Pyle, Richard Eckman, Lesley J. Gray, and V. Philushakin (State Committee on Hydrometeorology and Control of the Natural Environment, Moscow, USSR) et al *In its* Two-Dimensional Intercomparison of Stratospheric Models P 111-140 (SEE N90-11405 02-46) Aug. 1989 (For primary document see N90-11405 02-46)
Avail: NTIS HC A99/MF A04 CSCL 04A

The modeling groups are listed along with a brief description of the respective models. Author

N90-11409*# National Aeronautics and Space Administration. Goddard Space Flight Center, Greenbelt, MD.
INTRODUCTION AND DATA SUMMARY, CHAPTER 5
In its Two-Dimensional Intercomparison of Stratospheric Models Aug. 1989 p 141-151 (For primary document see N90-11405 02-46)
Avail: NTIS HC A99/MF A04 CSCL 04A

A subset of data representing most of the participating model groups was discussed and reviewed. The results are presented for intercomparisons of that subset of data. Subsequent to the workshop, the various modeling groups had the opportunity to either update or add to the data sets discussed at the workshop. The overall revised data sets as of December 1988 are presented. Data from all the models (where available) are grouped according to: (1) photochemistry and radiation (photodissociation coefficients, and ultraviolet heating and infrared cooling); (2) transport (net radiative heating, troposheric source tracer experiment, time-dependent source conserved tracer experiment, stratospheric source tracer experiment, and O3 column); (3) current atmosphere (integrated columns of trace gases, Cl(y) and NO(y), nitrogen gases, chlorine gases, O(x) and HO(x) gases, and source gases); and (4) perturbed circulations and temperatures. The data presented provide a detailed summary of the two-dimensional picture of the atmosphere as seen by current atmospheric models. Author

N90-11410 Tennessee Univ., Knoxville.
IONOSPHERIC TOTAL ELECTRON CONTENT, AND FAR ULTRAVIOLET, NEAR INFRARED OXYGEN EMISSION Ph.D. Thesis
Cyrus Aghanajafi 1988 87 p
Avail: Univ. Microfilms Order No. DA8911698

The total electron content and four oxygen emissions are calculated for solar cycle maximum at equinox season. It is shown that the total electron content reaches its maximum development at 2100 LT with the crest nearest to the equator beging the greatest. This asymmetry reverses at 0200 LT when the crest farthest from the equator is smallest. In spite of the fact that while Nmax decreases at noon, and the layer becomes greater in altitude under the influence of the upward drift, the noon bite out occurs at the equator around 1200 LT. The behavior of OI 6300 A, the brightest dayglow source is investigated. The oxygen at 6300 A is strongly a function of Nmax and hmax. The data for the OI 6300 A reveal that the latitudinal asymmetry is associated with the asymmetry in altitude of F2 peak. The maximum electron density height is strongly affected by vertical bar E x bar B drift velocity. The emission at 1356 A and 7774 A is calculated using the radiative recombination and ion-ion recombination processes. The ion-ion recombination has substantial effect in total emission rates. The intensity of OI 911 A due to direct recombination to the ground state is obtained. These emissions can be used as a way of remotely sensing the F region and exosphere plasma properties, and the winds responsible for plasma transport. Dissert. Abstr.

N90-11411# National Oceanic and Atmospheric Administration, Boulder, CO. Space Environment Lab.
USER'S GUIDE TO THE SPACE ENVIRONMENT SERVICES CENTER GEOPHYSICAL ALERT BROADCASTS
David A. Rosenthal and Joseph W. Hirman (Space Environment Services Center, Boulder, CO.) Mar. 1989 18 p
(PB89-194617; NOAA-TM-ERL-SEL-79) Avail: NTIS HC A03/MF A01 CSCL 04A

Intended for users with little or no scientific background as well as highly technical readers, the User's Guide provides an overview of the National Oceanic and Atmospheric Administration's hourly short-wave radio bulletins that provide continually updated information on solar-activity-induced effects on the near-Earth space environment. It also provides a step-by-step explanation of the standardized format and terminology of the bulletins. Specific terms are highlighted and defined in a glossary. Bulletins are 45 seconds or less in duration and contain a large amount of useful data. Until now, no attempt has been made to provide a systematic method of their use by other than highly technically trained listeners. GRA

N90-11412# National Oceanic and Atmospheric Administration, Silver Spring, MD. Air Resources Lab.
MICROMETEOROLOGICAL INVESTIGATION OF SURFACE EXCHANGE OF TRACE GASES: A CASE STUDY
B. B. Hicks, D. R. Matt, and R. T. McMillen Mar. 1989 78 p
(PB89-208375; NOAA-TM-ERL-ARL-172) Avail: NTIS HC A05/MF A01 CSCL 04A

Data obtained in an intensive field study of the dry deposition of sulfur dioxide, ozone, and nitrogen dioxide, conducted in 1985 in central Pennsylvania, are used to illustrate the factors that must be considered to assure that high quality rsults are derived. In particular, the quality of the site must be such that flux measurements made above the surface are representative of surface values. For this purpose, tests involving momentum transfer and the surface energy budget are especially useful. In addition, conditions must not be changing rapidly, and the statisitcal uncertainty associated with flux measurement must be low. For the set of data presented, conservative quality-assurance guidelines are used to reject potentially erroneous flux data. Author

N90-11413# National Center for Atmospheric Research, Boulder, CO. Atmospheric Chemistry Div.
NCAR (NATIONAL CENTER FOR ATMOSPHERIC RESEARCH) MASTER MECHANISM OF THE GAS PHASE CHEMISTRY, VERSION 2.0
Sasha Madronich and Jack G. Calvert May 1989 273 p
(Grant NSF ATM-87-09659)
(PB89-208979; NCAR/TN-333-STR) Avail: NTIS HC A12/MF A02 CSCL 04A

The NCAR Master Mechanism of the Gas Phase Chemistry is an explicit, highly detailed mechanism describing the gas phase chemical transformations that may occur in the atmosphere. The initial version (Version 1.0) was developed in 1984. Since that time, the number of chemical reactions considered has increased from 1964 to 4930. Most of the new reactions concern the photooxidation of hydrocarbons. Directly measured kinetic and mechanistic data were updated. For many reactions no direct kinetic or mechanistic measurements exist. For such reactions, similarity and analogy to known processes were used tio derive both product identity and the rate constants. One major departure from the Version 1.0 is the inclusion of the permutation reactions of organic

peroxy radicals. These reactions are handled using an exact counter method described by Madronich and Calvert (1989).
GRA

N90-11414# Sandia National Labs., Albuquerque, NM.
IRREVERSIBLE PHASE TRANSITION AND WAVE PROPAGATION IN SILICATE GEOLOGIC MATERIALS
J. W. Swegle 1989 4 p Presented at the American Physical Society Topical Conference on Shock Compression of Condensed Matter, Albuquerque, NM, 14-17 Aug. 1989
(Contract DE-AC04-76DP-00789)
(DE89-016031; SAND-89-0848C; CONF-890812-9) Avail: NTIS HC A01/MF A01

Shock and unloading experiments on quartz and silicate rocks indicate the release adiabats lie below the Hugoniot. The hysteresis and energy dissipation inherent in this situation have important wave propagation implications. On loading, there is pressure-induced transition to the stishovite phase which is not abrupt, with the Hugoniot passing through a metastable mixed phase region for several tens of GPa. One interpretation of the unloading data is that the transition is not reversible, and the material remains in a frozen phase mixture on initial unloading. However, material strength may also play a role. A complete thermodynamically consistent EOS which includes phase transitions and strength effects was developed and used to examine shock and release data on quartz and silicate rocks in order to quantify the kinetics of the reverse transition and to separate the hysteretic effects due to phase transition kinetics from those due to material strength. The model allows quantitative determination of the effect of transition kinetics on ground shock propagation in silicate materials. DOE

N90-11415# International Centre for Theoretical Physics, Trieste (Italy).
UPPER IONOSPHERE AND MAGNETOSPHERIC-IONOSPHERIC COUPLING
J. R. Manzano Feb. 1989 41 p
(DE89-619727; IC-89/36) Avail: NTIS (US Sales Only) HC A03/MF A01

After a presentation of the ionospheric physics and of the earth magnetosphere morphology, generation and dynamics, the magnetosphere-ionosphere coupling in quiet and perturbed conditions is discussed. Some summary information about other planetary magnetospheres, particularly Venus and Jupiter magnetospheres, are finally given. DOE

N90-11416# Los Alamos National Lab., NM.
SHORT WAVELENGTH STRIATIONS ON EXPANDING PLASMA CLOUDS
D. Winske and S. P. Gary 1989 25 p Presented at the Workshop on Theoretical Geoplasma Physics, Cambridge, MA, Jun. 1989
(Contract W-7405-eng-36)
(DE89-016585; LA-UR-89-2746; CONF-8906201-2) Avail: NTIS HC A03/MF A01

The growth and evolution of short wavelength (greater than ion gyroradius) flute modes on a plasma expanding across an ambient magnetic field have been actively studied in recent years, both by means of experiments in the laboratory as well as in space and through numerical simulations. We review the relevant observations and simulations results, discuss the instability mechanism and related linear theory, and describe recent work to bring experiments and theory into better agreement. DOE

N90-11417# Swedish Defence Research Establishment, Linkoeping. Dept. of Information Technology.
SOLAR RADIATION IN LINKOEPING (SWEDEN): VARIATIONS OVER HALF A YEAR IN IRRADIANCE AND SPECTRAL COMPOSITION IN THE INTERVAL 400-1000 NM
Carl Hugo Agren 15 Feb. 1989 24 p In SWEDISH; ENGLISH summary
(FOA-C-30521-3.1; ISSN-0347-3708; ETN-89-95168) Avail: NTIS HC A03/MF A01; Swedish Defence Research Establishment, Box 1165, S-581 11, Linkoeping, Sweden, 50 Swedish crowns

Knowledge about the variations of daylight is essential in all deliberations concerning reconnaissance in the visual wavelength range, for example aerial reconnaissance with photographic or electro-optical methods or video technique in remotely piloted vehicles. The variations of daylight on a horizontal surface are reported in irradiance and spectral composition from December to June. Overcast conditions are considered. The dynamic range of the irradiance turns out to be unexpectedly large, and color temperature is more constant than expected. ESA

47 METEOROLOGY AND CLIMATOLOGY

Includes weather forecasting and modification.

N90-11418# National Oceanic and Atmospheric Administration, Miami, FL. Oceanographic and Meteorological Labs.
HURRICANE RESEARCH DIVISION FISCAL YEAR 1988 PROGRAMS, FISCAL YEAR 1989 PROJECTIONS
Jan. 1989 65 p
(PB89-152268) Avail: NTIS HC A04/MF A01 CSCL 04B

The Hurricane Research Division (HRD) is NOAA's primary focus for research on hurricanes and tropical meteorology. HRD's research is directed at improved hurricane prediction through a detailed understanding of the structure and dynamics of these storms. HRD uses the NOAA P-3 research aircraft to acquire data sets that are analyzed to obtain a better understanding of the dynamics and energetics of the hurricane's inner core. Observational studies of the hurricane's synoptic environment are conducted. Theoretical and numerical modeling studies of hurricanes are also included in HRD's program. Hurricane Gilbert and tropical storms Florence and Floyd provided a substantial body of data this past year. K.C.D.

N90-11419# National Oceanic and Atmospheric Administration, Rockville, MD. Federal Coordinator for Meteorological Services and Supporting Research.
METEOROLOGICAL ROCKET OBSERVATIONS
Dec. 1988 140 p
(PB89-168769; FCM-H10-1988; FEDERAL-METEOROLOGICAL-HB-10) Avail: NTIS HC A07/MF A01 CSCL 04B

The handbook prescribes Federal standards for observing and reporting observations from the Cooperative Meteorological Rocket Network which provides valuable data for Federal agencies, aerospace contractors and universities concerned with diverse purposes such as the calibration and validation of data from meteorological satellites, design and reentry of space vehicles, performance of aerospace vehicles and understanding, monitoring, analyzing, and predicting atmospheric processes. The standards in the handbook apply to all agencies that participate in the network and provide a reference for users of these data. Topics discussed include the following: Metrocket systems and ground equipment; Metrocket launch and prelaunch procedures; Data reduction; coding and dissemination of rocketsonde observations; Records identification; Submission of records for publication; System performance; Manual application of temperature corrections to rocketsonde measurements; Acronyms and abbreviations. GRA

N90-11420 Iowa Univ., Iowa City.
OBSERVATIONAL STUDIES OF LOW-FREQUENCY OSCILLATIONS IN THE SOUTHERN HEMISPHERE Ph.D. Thesis
Charles Edward Graves 1988 100 p
Avail: Univ. Microfilms Order No. DA8909148

Forty to fifty day fluctuations in the Southern Hemisphere middle and high latitudes are examined. The existence of these fluctuations are established in rawinsonde data at Easter Island (27 S, 109 W) and in global geopotential heights fields. These fluctuations behave as quasi-stationary wavetrains that propagate energy along

an elliptical path from low latitudes in the Indian Ocean to the coast of Antarctica, near 70 W. The wavetrains exhibit vertical phase tilts from the surface to about 500 mb; above that, they are vertically in phase. However, the wavetrains are not observed in the middle and upper stratosphere. Over the Indian Ocean, there is also evidence suggesting that the wavetrains interact with the tropical 40 to 50 day oscillation. In addition, the extratropical 40 percent 50 day fluctuations extract energy from the mean zonal flow through baroclinic processes but lose energy to the mean zonal flow through barotropic processes. The results revealed increase the understanding of the global 40 to 50 day phenomena and may provide an important effect in the evolution of the tropical 40 to 50 day oscillation. Dissert. Abstr.

N90-11421 California Univ., Los Angeles.
STUDIES OF TIME-DEPENDENT POLAR CAP CONVECTION PATTERNS Ph.D. Thesis
Julie Joan Moses 1988 140 p
Avail: Univ. Microfilms Order No. DA8907578

A time dependent ionospheric convection model was developed for southward IMF conditions. The model consists of an adiaroic boundary with gaps through which fluid can enter or leave. The boundary expands when more flux enters the dayside gap and contracts when more flux leaves the nightside gap. This property of the model is based on observations of the auroral oval and polar cap expanding and contracting during southward IMF periods. Extensive model result comparisons and modelling with DE-2 data were done. A realistic day-night conductivity gradient added to the model for an expanding polar cap shows a curvature to the flow that is consistent with that predicted for positive B sub y. An extended merging line added to the model to create a lobe cell shows that the lobe cell has limited spatial extent and cannot account for curved flows in the nightside polar cap. Fitting the model to data reveals interesting possibilities for the dayside and nightside gap. The dayside gap appears spreadout in local time between 800 and 1400 MLT. Thirty five percent of the cases modelled cannot account for the data with a single throat. The results show a complicated, variable electric field pattern along the dayside polar cap boundary. On the nightside, it was determined that a nightside gap is necessary to fit 57 percent of the cases examined. Only 75 percent of the cases that occurred during the recovery phase of the substorm required the nightside gap while only 29 percent of the nightside gap cases happened during the expansive phase. This result implies that tail reconnection may occur through the recovery phase. Dissert. Abstr.

N90-11422 York Univ. (England).
SUBSTORM ASSOCIATED PULSATIONS: A STUDY OF PLASMASPHERIC CAVITY RESONANCE, MID-LATITUDE POLARISATION AND GEOSTATIONARY ORBIT SIGNATURES Ph.D. Thesis
Timothy Kenneth Yeoman 1988 226 p
Avail: Univ. Microfilms Order No. BRDX84789

A study has been made of substorm associated Pi2 magnetic pulsations at mid-latitudes. Pulsation frequency variation with longitude and power and phase variation with latitude are examined. Pulsations of constant frequency are found to exist over a large sector of local time. These pulsations are found to exhibit H component phase changes and ellipticity reversals apparently associated with the plasmaspheric cavity resonance and it is concluded that this is a likely mechanism for the mid-latitude Pi2 secondary amplitude maximum. Studies of mid-latitude Pi2 polarization patterns are undertaken on the net SAMNET array. These show new features in the latitudinal and longitudinal variation of the Pi2 signature. Considerable polarization ellipse asimuth rotation is seen with changing latitude, not just with changing longitude as previously observed. A modification of a travelling wave model is considered, which takes account of a low latitude secondary source. This model seems able to account for many of the new features seen. Magnetic and electric fields observed on GEOS-1 and GEOS-2 during substorm onset are also examined. One case study is made when both GEOS-2 data and data from a ground array is available. Much of the space signature is seen to be characterized by a highly compressional signal which does not appear to be directly related to the lower latitude pulsation, but could act as a source for it. No field guided energy flow is seen at ULF pulsation frequencies at geostationary orbit. Dissert. Abstr.

N90-11423 Colorado State Univ., Fort Collins.
SPATIAL AND TEMPORAL SHORT RANGE TOTAL CLOUD COVER ESTIMATION BY METRIC ANALYSIS OF COMPOSITE IMAGERY Ph.D. Thesis
Francis Peter Kelly 1988 169 p
Avail: Univ. Microfilms Order No. DA8911805

The compositing of regional scale satellite cloud imagery for the purpose of estimating climatological cloud occurrence frequencies is well formulated. Several studies by the author and colleagues within the last five years have combined image processing methods with digital satellite data to produce cloud climatologies. These efforts have investigated averaged cloud fields over areas of Montana, Colorado, Nebraska, Florida, and the Southeast U.S. Results are presented from an initial attempt to estimate future cloud cover based on cloud composites. Visible and infrared satellite data from the GOES satellite system are assembled into frequency and newly developed conditional probability of occurrence composites. The current research is extended on cloud cover estimation in new ways by generating cloud cover estimates for a one-hour time interval based on the combination of real time imagery with the frequency and conditional probability of occurrence composites. Recently developed non-classical statistical methods are also applied as they relate to: (1) the analysis of cloud imagery (Multi-Response Permutation Procedures, MRPP), and the (2) verification of the estimated cloud cover (Multi-Response Randomized Block Permutation Procedures, MRBP) by our method as contrasted to commonly used persistence approaches. Binary images generated by an objective cloud detection algorithm are quantitatively grouped based on the image structure derived from a method which applies MRPP to digital satellite imagery. Composites are then generated based on MRPP derived groupings and total cloud cover estimates are constructed for two case studies. The results of the estimation (i.e., ECI) are then tested with a verification (ground-truth) image by a metric imagery comparison technique. This method provides a measure of agreement between any two images and also p-value which quantifies the degree of significance of the test versus a null hypothesis of a completely random match. Dissert. Abstr.

N90-11424# National Weather Service, Garden City, NY. Scientific Services Div.
RELATION OF WIND FIELD AND BUOYANCY TO RAINFALL INFERRED FROM RADAR
Hugh M. Stone Apr. 1989 25 p
(PB89-208326; NOAA-TM-NWS-ER-81) Avail: NTIS HC A03/MF A01 CSCL 04B

Forecasting the potential for heavy rain, which may cause flash flooding is one of the most important activities of the National Weather Service. The problem is difficult because heavy rain events are usually the result of small scale convective storms and frequently occur with asynoptic map pattern that appears very benign. Maddox et al. (1979) complied a 5-year climatology of flash flood events from 1973 to 1977 and classified the heavy rain events into three types: synoptic, frontal, and mesohigh. The report investigates the relation of wind profile data and buoyancy to rainfall obtained from radar observations. Author

N90-11425# National Oceanic and Atmospheric Administration, Boulder, CO. Wave Propagation Lab.
LIDAR OBSERVATIONS OF THE STRATOSPHERIC AEROSOL: BOULDER, COLORADO, 1985 TO 1987
Jun Zhou, G. T. McNice, and W. L. Eberhard Apr. 1989 57 p
(PB89-203871; NOAA-TM-ERL-WPL-162) Avail: NTIS HC A04/MF A01 CSCL 04B

The lidar observations presented consist of 86 vertical profiles of backscatter measured by a ruby lidar (694.3-nm wavelength). Also presented are plots of scattering ratio profiles and tables

containing values of the scattering ratio, aerosol backscattering coefficient, and estimated aerosol optical depth versus altitude. Data acquisition and processing are briefly described. Some simple analyses of the lidar data are also discussed, including mean and peak aerosol backscatter characteristics, temperature versus aerosol structure, and trends in stratospheric aerosol optical depth. Author

N90-11426# National Climate Program Office, Rockville, MD.
NATIONAL CLIMATE PROGRAM FIVE-YEAR PLAN, 1989-1993
Dec. 1988 52 p
(PB89-207369) Avail: NTIS HC A04/MF A01 CSCL 04B

The Five-Year Plan for the National Climate Program fulfills the need as expressed by Congress, to create a framework for the nation to cope with, understand, and predict climate. The Plan presents broad outlines for program needs over the next few years and enumerates specific goals to be incorporated into plans of participating agencies. Scientists and administrators agree, the tasks ahead are far beyond what can be accomplished in a short time. The Plan recognizes resource and time limitations and attempts to set realistic priorities. The recommended program will produce early and useful results for the most immediate needs while building the scientific knowledge base required in the longer term. The Plan covers the fiscal years 1989 to 1993. It sets the goals and objectives for the coming half-decade and summarizes the present status of the U.S. National Climate Program. The most notable accomplishments over the past few years are briefly mentioned. More detailed information can be found in the National Climate Program's Annual Reports to Congress and the President. Author

N90-11427# Illinois State Water Survey, Champaign.
FREQUENCY DISTRIBUTIONS AND HYDROCLIMATIC CHARACTERISTICS OF HEAVY RAINSTORMS IN ILLINOIS
Floyd A. Huff and James R. Angel 1989 185 p Sponsored by Illinois Univ. at Urbana-Champaign
(PB89-203988; ISWS/BUL-70/89) Avail: NTIS HC A09/MF A01 CSCL 04B

The results are presented of an extensive investigation of the distribution of heavy rainstorms in Illinois based on data for 61 precipitation stations operated during 1901 to 1983. Results are presented in two forms: mean relations for 10 regions of approximately homogeneous precipitation climate, and statewide isohyetal maps based on the 61-station data. Frequency relations are presented on both an annual and seasonal basis. Results of a special investigation are presented for Chicago and the surrounding six counties subject to urban influences on precipitation distribution. Information is provided on the expected dispersion of point rainfall frequency distributions about the mean in the 10 regions of similar rainstorm climate. Information is also provided on the expected dispersion of point rainfall frequency distributions about the mean in the 10 regions of similar rainstorm climate. Information is also provided on the spatial and temporal characteristics of heavy rainstorms in Illinois. Author

N90-11428# National Center for Atmospheric Research, Boulder, CO.
NATIONAL CENTER FOR ATMOSPHERIC RESEARCH ANNUAL REPORT, FISCAL YEAR 1988 Report, 1 Oct. 1987 - 30 Sep. 1988
May 1989 50 p Original contains color illustrations
(Grant NSF ATM-87-09659)
(PB89-208987) Avail: NTIS HC A03/MF A01 CSCL 04B

Since its founding in 1960, the National Center for Atmospheric Research (NCAR) has been motivated by two equally important missions, science and service. Core staff and visiting university researchers carry out high-quality investigations on problems of national and international importance. These range from weather and climate studies to atmospheric chemistry and solar-terrestrial physics. NCAR's other mission is to provide service and facilities to the research community beyond its walls. These include the most advanced tools scientists need to carry out their work-everything from super-computing power to state-of-the-art instruments. Much of this technology, from computer models to advanced radars, is developed at NCAR. The universities are the bedrock of NCAR's existence. The University Corporation for Atmospheric Research (UCAR), a group of 57 institutions with doctoral-level programs in atmospheric and related sciences, manages the center. Funds for both organizations come largely from the federally supported National Science Foundation. This annual report covers fiscal year 1988, 1 October 1987 through 30 September 1988. GRA

N90-11429# Pacific Northwest Lab., Richland, WA.
HANFORD METEOROLOGICAL STATION COMPUTER CODES. VOLUME 10: THE ARCHIVE COMPUTER CODE
G. L. Andrews and K. W. Burk Aug. 1989 101 p
(Contract DE-AC06-76RL-01830)
(DE89-016175; PNL-6279-Vol-10) Avail: NTIS HC A06/MF A01

The purpose of the ARCHIVE computer program is twofold: (1) convert selected hourly binary data into formatted ASCII data, and (2) organize the converted data into monthly files. Formatted ASCII files are easier to access on a routine basis. The program is executed once a day and is initiated from a command file that submits itself to the SYS$BATCH queue on a daily basis. The monthly files are stored on the HMS computer's fixed hard disk and are merged into yearly files (located on removable disk packs) at the end of each year. This report describes the data bases maintained at the HMS, gives an overview of the ARCHIVE program, describes input and output files accessed by the ARCHIVE program, provides a description of program initiation, and discusses the limitations of the ARCHIVE program. A section on trouble-shooting is included. In addition, the appendixes contain flow charts, detailed descriptions, and source code listings for the ARCHIVE program and related subroutines. A description of the ARCHIVE command file and the data input and output files completes the report. DOE

N90-11430# ST Systems Corp., Monterey, CA.
GRIDDED ENVIRONMENTAL DATA COMPACTION: AN INVESTIGATION Final Report, Nov. 1988 - Apr. 1989
Harry D. Hamilton May 1989 151 p
(Contract N00228-86-D-3051)
(AD-A210580; NEPRF-CR-89-04) Avail: NTIS HC A08/MF A01 CSCL 04/2

Both graphical examples and tabulated statistics clearly indicate that regional environmental gridded data may be compacted with either delta-type or double fast Fourier transforms, when the field data approximate values that are continuous in the first derivative. The smoother the original field values are, the more the data can be compacted. Results also show that fields derived from compacted fields can retain required accuracy. The Fourier transforms take twice as long as the delta schemes, but provide better results for light (2:1) compaction. The delta scheme is better than the Fourier transforms for heavy (7:1) compaction. The heavily compacted fields, however, may not be operationally useful. GRA

N90-11431# Naval Research Lab., Washington, DC. Atmospheric Physics Branch.
ATMOSPHERIC AEROSOL SIZE DISTRIBUTIONS AND OPTICAL PROPERTIES FOUND IN THE MARINE BOUNDARY LAYER OVER THE ATLANTIC OCEAN Interim Report
William A. Hoppel, James W. Fitzgerald, Glendon M. Frick, Reginald E. Larson, and Eugene J. Mack (Calspan Advanced Technology Center, Buffalo, NY.) 30 Jun. 1989 81 p
(RR0330242)
(AD-A210800; NRL-9188) Avail: NTIS HC A05/MF A01 CSCL 04/2

Measurements and analyses of the aerosol size distributions and optical properties found in the marine boundary layer during the 1983 USNS Lynch cruise from Charleston SC to Scotland via the Canary Islands are presented. The data given in this report are the most extensive and accurate measurements of the submicron marine aerosol size distribution to date and are

supplemented by extensive meteorological observations, balloon soundings, satellite coverage, calculated air mass trajectories, and aerosol chemistry. Eight detailed case studies of the size distribution which occurred under different meteorological conditions are presented and discussed. The data indicates that repeated cycling of marine boundary layer (MBL) air through nonprecipitating clouds which are usually present at the top of the MBL is a major factor in shaping the size distribution and that new particle formation by hetermolecular, homogeneous nucleation is the most likely mechanism which sustains the concentration of particles found below 0.04 micron radius. Calculations of the scattering and extinction coefficients and optical depth of the MBL as a function of wavelength directly from the measured size distribution and MBL vertical structure are compared to measured values of the scattering coefficient and optical depth. These measured and calculated optical properties correlate well throughout the cruise and the results give a relatively consistent picture of the relationship between the aerosol size distribution and the electromagnetic properties in the MBL. GRA

N90-11432# Air Force Geophysics Lab., Hanscom AFB, MA. Atmospheric Sciences Div.
COMPOSITED LOCAL AREA FORECAST TECHNIQUES Final Report, Oct. 1985 - Oct. 1987
H. Stuart Muench 31 Aug. 1988 41 p
(AF Proj. 6670)
(AD-A210802; AFGL-TR-88-0216; AFGL-ERP-1012) Avail: NTIS HC A03/MF A01 CSCL 04/2

A previously developed advection forecast technique was modified to include data extracted from satellite imagery. A forecast experiment was then conducted using a data base gathered at AFGL during March 1984. This experiment was designed to test the usefulness of: (1) 3-hour forecast updates; (2) a biquadratic interpolation; and (3) cloud and precipitation information from satelliite imagery. The test results confirmed earlier tests in that advection using space-averaged 500-mb winds produced the best overall scores and that in general the scores for 1 to 15 hours were better than persistence. The age of the advection flow (3, 6 or 9 hours old) did not affect forecast score, making updates useful. The biquadratic interpolation procedure produced better fits to observation than bilinear and appears to have improved forecasts. There was but a small benefit from adding satellite information to surface observations when forecasting cloud cover and hourly precipitation. The difficulties of trying to forecast even 30 to 50 percent of the time-change variance suggest that alternative approaches such as mesoscale modeling will be needed for accurate, reliable short-range forecasts. GRA

N90-11433# Analytical Sciences Corp., Reading, MA.
DIRECT STATISTICAL THERMAL WIND ESTIMATION PROCEDURE Final Report, 17 Sep. 1987 - 16 Sep. 1988
Charles L. Medler 10 Mar. 1989 125 p
(Contract F19628-87-C-0248)
(AD-A211256; TASC-TR-5547-1; AFGL-TR-89-0076) Avail: NTIS HC A06/MF A01 CSCL 04/2

A procedure to estimate thermal wind profiles directly from multispectral satellite radiance data has been specified and implemented. A previous interim report which presented the theoretical formulation and statistical models for a baseline algorithm is included as Appendix G of this final report. Sensitivity of the Estimates and numerical evaluations of the baseline algorithm using NOAA-7 radiance data are the major topics of this final report, serving to demonstrate the procedure developed. Thermal winds derived independently from NMC temperature analyses provide a benchmark for verification. Results using a method from which this work was motivated are included for comparison. GRA

48 OCEANOGRAPHY

Includes biological, dynamic, and physical oceanography; and marine resources.

For related information see also *43 Earth Resources and Remote Sensing.*

N90-11434# National Marine Fisheries Service, La Jolla, CA. Fisheries Service.
INTERANNUAL VARIABILITY OF TEMPERATURE IN THE UPPER LAYER OF THE NORTH PACIFIC EASTERN BOUNDARY REGION, 1971-1987
David A. Cole and Douglas R. McLain (National Ocean Service, Monterey, CA.) Mar. 1989 25 p
(PB89-190227; NOAA-TM-NMFS-SWFC-125) Avail: NTIS HC A03/MF A01 CSCL 08C

A diagnostic study of large-scale interannual variability of surface and subsurface temperature along the eastern boundary region of the North Pacific Ocean is presented. The study involves analysis of archived surface marine weather reports and subsurface temperature profiles for the period from January 1971 to August 1987. Anomalous temperature conditions and events are compared between coastal and offshore regions. Effects of the major El Nino events of 1972-73, 1982-83, and the weaker 1976-77 and 1986-87 El Nino events are discussed. Monthly temperature anomalies are coherent in time and space over large portions of the study region, indicating the importance of large-scale ocean-atmosphere processes. In general, the 1971-76 period was anomalously cool over much of the region, excluding the 1972-73 El Nino event. In subsequent years, surface waters were warmer than average over much of the middle and high latitude regions, especially in the offshore areas during fall and winter. Negative anomalies predominated during the early part of the time series (1971-76), from the surface to at least 100m. GRA

N90-11435# Army Cold Regions Research and Engineering Lab., Hanover, NH.
COASTAL SUBSEA PERMAFROST AND BEDROCK OBSERVATIONS USING dc RESISTIVITY Final Report
Paul V. Sellmann, Allan J. Delaney, and Steven A. Arcone Jun. 1989 20 p
(AD-A210784; CRREL-89-13) Avail: NTIS HC A03/MF A01 CSCL 08/12

Measurements were made at several New England coastal sites and at three sites in Prudhoe Bay, Alaska, to evaluate dc resistivity techniques for mapping resistive seabed features: Bedrock and Subsea permafrost. The field studies employed the four-probe Wenner array technique, with electrode separations up to 50 m. The New England sites were selected to simulate permafrost conditions to help establish a feeling for the range of apparent resistivity in areas of subsea permafrost and for information on the vertical and lateral resolution of the technique. At Prudhoe Bay, offshore measurements were made with a floating cable, and inland measurements were made using electrodes driven into the ground. These observations indicate that the electrical properties of permafrost beneath the coastal bluff and adjacent tundra are rapidly modified by coastal erosion and periodic flooding during storms. Maximum apparent resistivity at the water's edge was around 50 Ohm-meters, and at distances greater than 100 m from shore all values were less than 20 Ohm-meters. Modeling supported by the drilling data permitted an interpretation of the position of the top of ice-bonded subsea permafrost. Real resistivities for the ice-bonded permafrost ranged from 200 to 1000 Ohm-meters. The techniques and equipment used for this study appear to have applications for studies in shallow coastal waters where permafrost is not more than 30 m below the seabed and where depths do not exceed 6 to 7 m. GRA

N90-11436# National Oceanic and Atmospheric Administration, Seattle, WA. Pacific Marine Environmental Lab.
THE SEA ICE MARGINS: A SUMMARY OF PHYSICAL PHENOMENA
Robin D. Muench (Science Applications International Corp., Bellevue, WA.) May 1989 60 p

(Contract N00014-82-C-0064)
(PB89-212328; NOAA-TM-ERL-PMEL-88; CONTRIB-1049) Avail: NTIS HC A04/MF A01 CSCL 08C

The sea ice margins, also referred to as the marginal ice zones (MIZs), are lateral transition regions between the ice-covered and ice-free portions of the world ocean. Global distribution of the sea ice margins is discussed. Small scale features and processes, as well as mesoscale oceanic features at the ice margins are also discussed. The effects of the ice margins in modifying water masses are presented. Meteorological effects associated with the ice margins are also considered. GRA

51 LIFE SCIENCES (GENERAL)

N90-11437# Department of Energy, Washington, DC. Office of Health and Environmental Research.
DOE/CEC WORKSHOP ON CRITICAL EVALUATION OF RADIOBIOLOGICAL DATA TO BIOPHYSICAL MODELING
1988 47 p Presented at the DOE/CEC Workshop, Oak Ridge, TN, 22-24 Jun. 1988 Prepared in cooperation with Commission of the European Communities, Brussels (Belgium)
(DE89-015214; CONF-8806237) Avail: NTIS HC A03/MF A01

The Department of Energy's Office of Health and Environmental Research and the Commission of the European Communities (CEC) Radiation Protection Program support the majority of research in the field of radiobiological modeling. This field of science develops models based on scientifically sound principles to predict biological response (at the cellular, molecular, and animal level) to exposure to low level ionizing radiation. Biophysical models are an important tool for estimating response of ionizing radiation at low doses and dose rates. Generally speaking, the biophysical models can be classified into two groups: (1) mechanistic models, and (2) phenomenological models. Mechanistic models are based on some assumptions about the physical, chemical, or biological mechanisms of action in association with radiobiological data whereas the phenomenological models are based solely on available experimental data on radiobiological effects with less emphasis on mechanisms of action. There are a number of these models which are being developed. Since model builders rely on radiobiological data available in the literature either to develop mechanistic or phenomenological models, it is essential that a critical evaluation of existing radiobiological data be made and data that is generally considered good and most appropriate for biophysical modeling be identified. DOE

N90-11438# Southwest Research Inst., San Antonio, TX.
STUDY OF THE BEHAVIORAL AND BIOLOGICAL EFFECTS OF HIGH INTENSITY 60 Hz ELECTRIC FIELDS Quarterly Progress Report No. 29
John L. Orr 14 Jul. 1989 141 p
(Contract DE-AC02-80RA-50219)
(DE89-015528; DOE/RA-50219/T9; SwRI-12-6253) Avail: NTIS HC A07/MF A01

Activities this quarter involved all phases of the project plus a meeting of the Joint Committee in Tokyo. Detailed mapping of the exposure facility is scheduled to be completed during the week of August 14, 1989. Both electric and magnetic fields should be available for tests of the components of the tether and blood sampling system for the neuroendocrine pilot study in September 1989. The groups for the social behavior study are stabilizing appropriately. Details on the formation of the groups and their status was provided. Information was included related to aspects of the social experiment ranging from age estimation in baboons through the cardiovascular consequences of psychosocial stress. In addition, a draft manuscript is included on the data from the previous experiments which describes the effects of 30 and 60 kV/m electric fields on the social behavior of baboons. Tests of the blood handling procedures and analysis methods were completed. With the exception of the catecholamine analyses, the handling procedures and variability in replicate measurements are satisfactory. Logistic and practical considerations now weigh strongly against including the analysis of the blood samples for catecholamines. Preliminary tests indicate that a sampling procedure which will work for the other compounds is probably not satisfactory for the catecholamines. DOE

52 AEROSPACE MEDICINE

Includes physiological factors; biological effects of radiation; and effects of weightlessness on man and animals.

N90-11439# Carnegie-Mellon Univ., Pittsburgh, PA. Dept. of Engineering and Public Policy.
BIOLOGICAL EFFECTS OF POWER FREQUENCY ELECTRIC AND MAGNETIC FIELDS: BACKGROUND PAPER
Indira Nair, M. Granger Morgan, and H. Keith Florig May 1989 114 p Sponsored by Office of Technology Assessment, Washington, DC
(PB89-209985; OTA-BP-E-53) Avail: NTIS HC A06/MF A01; SOD HC $4.75 as 052-003-01152-2 CSCL 06P

Electric and magnetic fields produced by electric power systems have recently been added to the list of environmental agents that are a potential threat to public health. The paper describes exposures to fields from power systems and other sources, reviews existing scientific evidence on the biological effects of these fields, presents a history of research support and of regulatory activity, and discusses problems and alternatives in regulatory action. If exposure to fields does turn out to pose a health risk, it is unlikely that high voltage transmission lines will be the only sources of concern. Power-frequency fields are also produced by distribution lines, wall wiring, appliances, and lighting fixtures. These non-transmission sources are much more common than transmission lines and could play a far greater role than transmission lines in any public health problem. Author

N90-11440# Naval Health Research Center, San Diego, CA.
TEST-RETEST RELIABILITY OF OXFORD MEDILOG 9000 SLEEP RECORDING AND SS-90-3 SLEEP STAGE SCORING Interim Report
David G. McDonald (Missouri Univ., Columbia.) and Lorene Irwin 13 Mar. 1989 11 p
(AD-A211165; NHRC-89-6) Avail: NTIS HC A03/MF A01 CSCL 06/4

Sleep was recorded in 19 normal sleepers (19.3 to 63.5 years of age) one night at home, using the Medilog 9000 system to assess the reliability of the Medilog SS-90-3 Sleep Stager by comparing sleep scoring of the same records scored five times. Primary results were: (1) Sleep Stager scoring of most sleep measures was highly reliable, with alpha coefficients ranging from .98 to 1.00 for total sleep time, movement time, sleep onset, waking after sleep onset, and both absolute and percentage amounts of sleep stages 1 to 4 and REM; and (2) scoring of latency measures was less reliable, although certainly acceptable for REM latency and marginally acceptable for stage 2 and 3 latencies, but not acceptable for an automated scoring of stage 4 latency. GRA

53 BEHAVIORAL SCIENCES

Includes psychological factors; individual and group behavior; crew training and evaluation; and psychiatric research.

N90-11441*# National Aeronautics and Space Administration. Ames Research Center, Moffett Field, CA.
TECHNIQUES FOR OPTIMIZING HUMAN-MACHINE INFORMATION TRANSFER RELATED TO REAL-TIME INTERACTIVE DISPLAY SYSTEMS
Michael M. Granaas and Donald C. Rhea Jan. 1989 16 p Presented at the 27th AIAA Aerospace Sciences Meeting, Reno,

NV, 9-12 Jan. 1989 Previously announced as N89-24599
(NASA-TM-100450; H-1506; NAS 1.15:100450; AIAA-89-0151)
Avail: NTIS HC A03/MF A01 CSCL 05I

In recent years the needs of ground-based researcher-analysts to access real-time engineering data in the form of processed information has expanded rapidly. Fortunately, the capacity to deliver that information has also expanded. The development of advanced display systems is essential to the success of a research test activity. Those developed at the National Aeronautics and Space Administration (NASA), Western Aeronautical Test Range (WATR), range from simple alphanumerics to interactive mapping and graphics. These unique display systems are designed not only to meet basic information display requirements of the user, but also to take advantage of techniques for optimizing information display. Future ground-based display systems will rely heavily not only on new technologies, but also on interaction with the human user and the associated productivity with that interaction. The psychological abilities and limitations of the user will become even more important in defining the difference between a usable and a useful display system. This paper reviews the requirements for development of real-time displays; the psychological aspects of design such as the layout, color selection, real-time response rate, and interactivity of displays; and an analysis of some existing WATR displays. Author

N90-11442# Case Western Reserve Univ., Cleveland, OH. Dept. of Psychology.
COMPREHENSION PROCESSES IN MECHANICAL REASONING Final Report, 1 Jun. 1985 - 31 May 1988
Patricia A. Carpenter and Marcel A. Just May 1989 16 p
(Contract N00014-85-K-0584)
(AD-A210459; ONR-89-1) Avail: NTIS HC A03/MF A01 CSCL 05/8

Several lines of research investigated how people reason about mechanical devices. One avenue explored the use of diagrams in conjunction with texts to understand a particular machine. Another project investigated the psychological processes that distinguish people who score high or low in a psychometric test of mechanical ability. A third project examined the visual scanning and decision processes that are used to evaluate a kinematic display of a machine in motion. A fourth project was a simulation model of how a person might generate the kinematic imagery to represent a machine in motion. A fifth project examined the cognitive processes in a visually-based test of pure reasoning (Raven Progressive Matrices). A sixth project examined the use of kinematic computer displays in understanding a complex device. These projects together provide an overview of the psychological processes used in mechanical comprehension, as well as indicating why some people are better at mechanical comprehension than others. GRA

N90-11443# Auburn Univ., AL. Dept. of Health and Human Performance.
STIMULUS-RESPONSE COMPATIBILITY IN SPATIAL PRECUING AND SYMBOLIC IDENTIFICATION: EFFECTS OF CODING PRACTICE, RETENTION, AND TRANSFER Final Report, 1 Oct. 1987 - 31 Mar. 1989
Robert W. Proctor (Purdue Univ., West Lafayette, IN.) and T. Gilmour Reeve 31 May 1989 111 p
(Grant AF-AFOSR-0002-88; AF Proj. 2313)
(AD-A210745; AFOSR-89-0810TR) Avail: NTIS HC A06/MF A01 CSCL 05/8

Research on stimulus-response compatibility effects is reviewed, with an integrated theoretical perspective provided that stresses mental coding of the stimulus and response sets. Eleven experiments, plus two follow-up experiments, are described in detail. The first six evaluate the nature of the codings used in spatial-precuing tasks. The remaining seven experiments examine the influence of practice on performance in the spatial-precuing tasks, as well as in symbolic-compatibility tasks. The experiments show that the codings used by subjects are affected by manipulations of the stimulus set but not of the response set. Compatibility effects within both tasks are reduced greatly by three sessions of practice. Transfer of these benefits to related tasks occurs in situations for which the response set is not altered. However, after more extended practice, partial transfer occurs even when the response set is changed. The results are interpreted in terms of an account that emphasizes salient-feature codings in a declarative stage of skill acquisition, with task-specific procedures acquired from practice. GRA

N90-11444# Naval Air Development Center, Warminster, PA. Air Vehicle and Crew Systems Technology Dept.
FILLING OR OUTLINING SHAPES WITH COLOR: THE EFFECTS ON A VISUAL SEARCH TASK Final Report
David Cohen Aug. 1988 18 p
(AD-A211067; NADC-89004-60) Avail: NTIS HC A03/MF A01 CSCL 06/4

Simplified tactical situation plots were created with shape symbology (i.e., ship, aircraft, submarine, unknown) outlined or filled with color to represent affiliation. Task times were recorded for subjects to identify quadrants which contained the greatest number of a specified target (e.g., hostile submarines, unknown aircraft, etc.) in each condition. Results confirmed that subjects' task times were significantly less in the color-filled condition. An explanation for the effect, how the search worked, and implications for coding tactical displays are discussed. GRA

54 MAN/SYSTEM TECHNOLOGY AND LIFE SUPPORT

Includes human engineering; biotechnology; and space suits and protective clothing.

For related information see also *16 Space Transportation.*

N90-11445*# Texas A&M Univ., College Station. Center for Electrochemical Systems and Hydrogen Research.
SELECTIVE REMOVAL OF ORGANICS FOR WATER RECLAMATION Semiannual Report
Oliver J. Murphy and G. Duncan Hitchens Sep. 1989 24 p
(Grant NAG9-350)
(NASA-CR-185959; NAS 1.26:185959) Avail: NTIS HC A03/MF A01 CSCL 06K

Electrolysis has been investigated as a means of purifying waste water. The feasibility of the direct electrochemical oxidation of urea has been demonstrated. Urea levels were reduced from 1200 ppm to 1 ppm forming the basis for a new approach to urine purification where the only consumable is electrical energy. Preliminary estimates of the energy requirements are 270 W/hr per liter of urine. Urea oxidation rates of around 350 mg urea/hr/m2 were observed. It is anticipated that a 1 m2 geometric area of electrode could treat urine for a crew of several persons. The low levels of organic contaminants resulting from this treatment indicate that the approach may have an impact as a post treatment process. Experiments are planned to investigate this later possibility. Author

N90-11446# Anacapa Sciences, Inc., Fort Rucker, AL.
TASK ANALYSIS OF THE UH-60 MISSION AND DECISION RULES FOR DEVELOPING A UH-60 WORKLOAD PREDICTION MODEL. VOLUME 1: SUMMARY REPORT Interim Report, Dec. 1986 - Dec. 1987
Carl R. Bierbaum, Sandra M. Szabo, and Theodore B. Aldrich Feb. 1989 43 p
(Contract MDA903-87-C-0523; AF Proj. 793)
(AD-A210763; ASI90-302-87-Vol-1; ARI-RP-89-08-Vol-1) Avail: NTIS HC A03/MF A01 CSCL 05/9

A composite scenario was used to conduct a comprehensive task analysis of the UH-60 mission. The analysis used a top-down approach to identify the mission's phases, functions, and tasks. Nine phases, 34 segments, 48 functions, and 138 tasks were identified. The crewmember performing each task was identified, and estimates of the sensory, cognitive, and psychomotor workload associated with the tasks were derived. Estimates of the task

times were also derived. The mission/task analysis data were used to develop a computer model of workload for UH-60 crewmembers. The model used a bottom-up approach to build mission functions from tasks and mission segments from functions. Decision rules were written to specify the procedure for combining the tasks into functions and the functions into segments. The model permitted an analysis of total workload experienced by each crewmember in the performance of both sequential and concurrent tasks. GRA

55 SPACE BIOLOGY

Includes exobiology; planetary biology; and extraterrestrial life.

No abstracts in this category.

59 MATHEMATICAL AND COMPUTER SCIENCES (GENERAL)

No abstracts in this category.

60 COMPUTER OPERATIONS AND HARDWARE

Includes hardware for computer graphics, firmware, and data processing.

For components see *33 Electronics and Electrical Engineering.*

N90-11447# Instituto de Pesquisas Espaciais, Sao Paulo (Brazil).
ANIMA: IMAGE ANALYZER APPLIED TO REMOTE SENSING
Sergio Rosim, Solange Pellegrina B Marcondes (Engespaco Industria e Comercio Ltda., Brazil), Antonio Miguel Vieir Monteiro, Junior Barrera, and Luciano Vieira Dutra Dec. 1988 8 p In PORTUGESE; ENGLISH summary Presented at the 5th Brazilian Symposium on Remote Sensing, Natal, Brazil, 11-15 Oct. 1988
(INPE-4766-PRE/1435) Avail: NTIS HC A02/MF A01

An image analyzer is presented called ANIMA that has a goal to automatize the attributes extraction of objects from an image to make it easier and to amplify the possibilities in getting the quantities results. It allows the image acquisition by TV, giving a book report to be followed by the expert. It presents also some areas that can use the system, giving emphasis to a remote sensing application. Author

N90-11448# National Inst. of Standards and Technology, Gaithersburg, MD. National Computer Systems Lab.
ELECTRONIC PUBLISHING: GUIDE TO SELECTION
Lynne S. Rosenthal Jun. 1989 39 p
(PB89-214753; NIST/SP-500/164) Avail: NTIS HC A03/MF A01; SOD HC $2.50 as 003-003-02938-6 CSCL 09B

The purpose of the report is to assist managers and users in making informed decisions on which systems are best for them. The report presents the technical and managerial choices and implications associated with selecting and using electronic publishing systems. A matrix of publishing capabilities and features is presented in the appendix to illustrate one method of comparing and selecting a publishing system. GRA

N90-11449# Sandia National Labs., Albuquerque, NM.
PERFORMANCE REPORTS FOR EIM (ENGINEERING INFORMATION MANAGEMENT) COMPUTER SYSTEMS: A MANAGERIAL PERSPECTIVE
Neal D. Wenderlich and R. A. Reid (New Mexico Univ., Albuquerque.) Jul. 1989 36 p
(Contract DE-AC04-76DP-00789)
(DE89-015194; SAND-89-1502) Avail: NTIS HC A03/MF A01

This document describes twelve different kinds of charts which have been designed to help manage the performance of the Engineering Information Management (EIM) computer systems at Sandia National Laboratories Albuquerque. Operational data generated by the two major software systems, Multiple Virtual Storage (MVS) and Integrated Database Management System (IDMS), are summarized to visually portray actual service levels and meaningful system performance characteristics. To demonstrate the potential utility of the resulting performance reports, summarized data in illustrative charts are evaluated from a managerial point of view. The resulting graphs can stimulate relevant analyses for modeling the impact of forecasted workloads on system service level objectives and identifying problems or trends that need the attention of system tuners. DOE

N90-11450# Los Alamos National Lab., NM.
COMPUTER SYMBIOSIS: EMERGENCE OF SYMBIOTIC BEHAVIOR THROUGH EVOLUTION
Takashi Ikegami and Kunihiko Kaneko 1989 8 p Presented at the Conference on Emergent Computation, Los Alamos, NM, 22-26 May 1989
(Contract W-7405-eng-36)
(DE89-015247; LA-UR-89-2456; CONF-8905201-1) Avail: NTIS HC A02

Symbiosis is altruistic cooperation between distinct species. It is one of the most effective evolutionary processes, but its dynamics are not well understood as yet. A simple model of symbiosis is introduced, where we consider interactions between hosts and parasites and also mutations of hosts and parasites. It is found that a symbiotic state emerges for a suitable range of mutation rates. The symbiotic state is not static, but dynamically oscillates. Harmful parasites violating symbiosis appear periodically, but are rapidly extinguished by hosts and other parasites, and the symbiotic state is recovered. The emergence of Tit for Tat strategy to maintain symbiosis is discussed. DOE

N90-11451*# National Aeronautics and Space Administration. Lyndon B. Johnson Space Center, Houston, TX.
CONSIDERATIONS FOR A DESIGN AND OPERATIONS KNOWLEDGE SUPPORT SYSTEM FOR SPACE STATION FREEDOM
Jon D. Erickson, Kenneth H. Crouse, Donald B. Wechsler, and Douglas R. Flaherty (Mitre Corp., Houston, TX.) Oct. 1989 73 p
(NASA-TM-102156; S-596; NAS 1.15:102156) Avail: NTIS HC A04/MF A01 CSCL 09B

Engineering and operations of modern engineered systems depend critically upon detailed design and operations knowledge that is accurate and authoritative. A design and operations knowledge support system (DOKSS) is a modern computer-based information system providing knowledge about the creation, evolution, and growth of an engineered system. The purpose of a DOKSS is to provide convenient and effective access to this multifaceted information. The complexity of Space Station Freedom's (SSF's) systems, elements, interfaces, and organizations makes convenient access to design knowledge especially important, when compared to simpler systems. The life cycle length, being 30 or more years, adds a new dimension to space operations, maintenance, and evolution. Provided here is a review and discussion of design knowledge support systems to be delivered and operated as a critical part of the engineered system. A concept of a DOKSS for Space Station Freedom (SSF) is presented. This is followed by a detailed discussion of a DOKSS for the Lyndon B. Johnson Space Center and Work Package-2 portions of SSF. Author

N90-11452# California Univ., Berkeley. Computer Science Div.
A PROTOTYPE SILICON COMPILER IN PROLOG
William R. Bush, Gino Cheng, Patrick C. McGeer, and Alvin M. Despain Dec. 1988 58 p
(Contract N00014-88-K-0579; ARPA Order 6501)
(AD-A210669; UCB/CSD-88/476) Avail: NTIS HC A04/MF A01 CSCL 12/5

The ASP effort is part of the Aquarius Project (Aquarius), which is aimed at producing high-performance Prolog engines, realized in part with specialized high-quality microprocessors. Thus the focus of ASP is microprocessor synthesis, with a design domain of single synchronous chips with a single data path and control path. ASP is also meant to test Prolog as an implementation language for design automation. Because a full behavior-to-silicon compiler is a complex undertaking, the silicon compilation problem is decomposed into three major abstract problem domains, ordered hierarchically (see CADDY and OCCAM, for other similar decompositions). GRA

N90-11453# Center for Mathematics and Computer Science, Amsterdam (Netherlands). Dept. of Computer Science.
A DISTRIBUTED DEBUGGER FOR AMOEBA
I. J. P. Elshoff Jul. 1988 15 p Presented at the ACM Workshop on Parallel and Distributed Debugging, Madison, WI, 5-6 May 1988
(CWI-CS-R8828; ETN-89-95093) Copyright Avail: NTIS HC A03/MF A01

A debugger under development for distributed programs in the capability based, distributed operating system Amoeba is described, and a method to make the debugger independent of the Amoeba kernel is attempted. The design integrates many facilities found in other debuggers such as execution replay, breakpointing, and an event based view of the execution of the target program. The influence of the system architecture on the target program, and the desired functionality of the debugger are discussed. Problems such as the handling of timeouts and interactions between the target program and its environment are considered. ESA

61 COMPUTER PROGRAMMING AND SOFTWARE

Includes computer programs, routines, alogorithms, and specific applications, e.g., CAD/CAM.

N90-11454*# National Aeronautics and Space Administration. Langley Research Center, Hampton, VA.
APPLICATIONS OF THE HYBRID AUTOMATED RELIABILITY PREDICTOR: REVISED EDITION
Salvatore J. Bavuso, Joanne Bechta Dugan, Kishor Trivedi, Beth Rothmann, and Mark Boyd (Duke Univ., Durham, NC.) Dec. 1988 30 p
(NASA-TP-2760-Rev; L-16304; NAS 1.60:2760-Rev) Avail: NTIS HC A03/MF A01 CSCL 09B

The Hybrid Automated Reliability Predictor (HARP) is a software package that implements advanced reliability modeling techniques. An overview of some of the problems that arise in modeling highly reliable fault tolerant systems is presented. The presentation is loosely divided into model construction and model solution problems. The HARP approach to these difficulties is described and facilitated by a technique called behavioral decomposition. The bulk of this paper presents examples of the evaluation of some typical fault tolerant systems, including a local area network, two fault tolerant computer systems (Carnegie-Mellon University multiprocessor system C.mmp and Software Implemented Fault Tolerance (SIFT)), and two examples of flight control systems.
Author

N90-11455*# Research Inst. for Advanced Computer Science, Moffett Field, CA.
TELESCIENCE TESTBED PILOT PROGRAM Quarterly Report No. 5, 1 Jun. - 31 Aug. 1988
Maria L. Gallagher, ed. and Barry M. Leiner, ed. 1 Sep. 1988 80 p
(Contract NASw-4234)
(NASA-CR-184594; NAS 1.26:184594; RIACS-M88.5) Avail: NTIS HC A05/MF A01 CSCL 09B

The Telescience Testbed Pilot Program is developing initial recommendations for requirements and design approaches for the information systems of the Space Station era. During this quarter, drafting of the final reports of the various participants was initiated. Several drafts are included in this report as the University technical reports. K.C.D.

N90-11456*# Missouri Univ., Columbia. Coll. of Engineering.
ENGINEERING SPECIFICATION AND SYSTEM DESIGN FOR CAD/CAM OF CUSTOM SHOES. PHASE 5: UMC INVOLVEMENT (JANUARY 1, 1989 - JUNE 30, 1989)
Han P. Bao Aug. 1989 50 p
(Grant NAG1-875)
(NASA-CR-185838; NAS 1.26:185838; UMC-IE-4-0889) Avail: NTIS HC A03/MF A01 CSCL 09B

The CAD/CAM of custom shoes is discussed. The solid object for machining is represented by a wireframe model with its nodes or vertices specified systematically in a grid pattern covering its entire length (point-to-point configuration). Two sets of data from CENCIT and CYBERWARE were used for machining purposes. It was found that the indexing technique (turning the stock by a small angle then moving the tool on a longitudinal path along the foot) yields the best result in terms of ease of programming, savings in wear and tear of the machine and cutting tools, and resolution of fine surface details. The work done using the LASTMOD last design system results in a shoe last specified by a number of congruent surface patches of different sizes. This data format was converted into a form amenable to the machine tool. It involves a series of sorting algorithms and interpolation algorithms to provide the grid pattern that the machine tool needs as was the case in the point to point configuration discussed above. This report also contains an in-depth treatment of the design and production technique of an integrated sole to complement the task of design and manufacture of the shoe last. Clinical data and essential production parameters are discussed. Examples of soles made through this process are given. K.C.D.

N90-11457*# National Aeronautics and Space Administration. Langley Research Center, Hampton, VA.
NEW COMPUTING SYSTEMS AND THEIR IMPACT ON STRUCTURAL ANALYSIS AND DESIGN
Ahmed K. Noor 1989 92 p Prepared in cooperation with George Washington Univ., Washington, DC
(Grant NAG1-730)
(NASA-CR-185831; NAS 1.26:185831) Avail: NTIS HC A05/MF A01 CSCL 09B

A review is given of the recent advances in computer technology that are likely to impact structural analysis and design. The computational needs for future structures technology are described. The characteristics of new and projected computing systems are summarized. Advances in programming environments, numerical algorithms, and computational strategies for new computing systems are reviewed, and a novel partitioning strategy is outlined for maximizing the degree of parallelism. The strategy is designed for computers with a shared memory and a small number of powerful processors (or a small number of clusters of medium-range processors). It is based on approximating the response of the structure by a combination of symmetric and antisymmetric response vectors, each obtained using a fraction of the degrees of freedom of the original finite element model. The strategy was implemented on the CRAY X-MP/4 and the Alliant FX/8 computers. For nonlinear dynamic problems on the CRAY X-MP with four CPUs, it resulted in an order of magnitude reduction in total analysis time, compared with the direct analysis on a single-CPU CRAY X-MP machine. K.C.D.

N90-11458# National Inst. of Standards and Technology, Gaithersburg, MD. National Computer Systems Lab.
SOFTWARE CONFIGURATION MANAGEMENT: AN OVERVIEW Final Report
Wilma M. Osborne Mar. 1989 34 p
(PB89-193833; NIST/SP-500/161; LC-89-600728) Avail: NTIS HC A03/MF A01; SOD HC $2.00 as 003-003-02927-1 CSCL 09B

The guide provides an overview of software configuration management, a support function dedicated to making both the technical and managerial software activities more effective. It addresses the problems associated with managing software changes; the importance of implementing Software Configuration Management (SCM) procedures early; and the application of those procedures throughout the software lifecycle. A brief summary of SCM tools and their applicable functionality is provided. SCM extends to more than just the code (source, relocatable, executable) and documentation (e.g., system and software requirements and design specifications). It also covers control files, test data, test suites, support tools, and other components used to develop and maintain the software product. GRA

N90-11459# Norwegian Defence Research Establishment, Kjeller.
ON ALGORITHMS FOR GENERATING COMPUTATIONALLY SIMPLE PIECEWISE LINEAR CLASSIFIERS
Hans Christian Palm May 1989 122 p
(NDRE/Publ-89/1001; ISSN-0800-4412) Avail: NTIS HC A06/MF A01

Piecewise linear classifiers constitute a group of classifiers often used in real time pattern recognition. In most cases they are reliable and sufficiently fast. New algorithms for generating piecewise linear classifiers are developed, which can easily handle multiclass problems. Using only a small number of discriminant functions, they attempt to create a classifier with low error rate. In brief, the concept consists of first splitting the sample space of a given class into two subsample spaces. The samples belonging to a given class which are lying in the same (sub) sample space are said to belong to the same subclass. Next, the (sub) classes are separated using linear classifiers. Then, a new (sub) class is split and a classifier based on this splitting, is created. Author

N90-11460*# North Carolina State Univ., Raleigh. Dept. of Computer Science.
EXPERIMENTS IN FAULT TOLERANT SOFTWARE RELIABILITY Annual Report, 1 Apr. 1988 - 31 Mar. 1989
David F. McAllister and Mladen A. Vouk 1 Apr. 1989 69 p
(Grant NAG1-667)
(NASA-CR-185927; NAS 1.26:185927; NCSU-5) Avail: NTIS HC A04/MF A01 CSCL 09B

Twenty functionally equivalent programs were built and tested in a multiversion software experiment. Following unit testing, all programs were subjected to an extensive system test. In the process sixty-one distinct faults were identified among the versions. Less than 12 percent of the faults exhibited varying degrees of positive correlation. The common-cause (or similar) faults spanned as many as 14 components. However, a majority of these faults were trivial, and easily detected by proper unit and/or system testing. Only two of the seven similar faults were difficult faults, and both were caused by specification ambiguities. One of these faults exhibited variable identical-and-wrong response span, i.e. response span which varied with the testing conditions and input data. Techniques that could have been used to avoid the faults are discussed. For example, it was determined that back-to-back testing of 2-tuples could have been used to eliminate about 90 percent of the faults. In addition, four of the seven similar faults could have been detected by using back-to-back testing of 5-tuples. It is believed that most, if not all, similar faults could have been avoided had the specifications been written using more formal notation, the unit testing phase was subject to more stringent standards and controls, and better tools for measuring the quality and adequacy of the test data (e.g. coverage) were used. Author

N90-11461# Sandia National Labs., Albuquerque, NM.
GaAs ASIC DESIGN CASE STUDY
James A. Heise 1989 3 p Presented at the 2nd Annual IEEE/ASIC Seminar and Exhibit, Rochester, NY, 25-28 Sep. 1989
(Contract DE-AC04-76DP-00789)
(DE89-013934; SAND-89-1542C; CONF-8909146-2) Avail: NTIS HC A01/MF A01

With increasing demands on system requirements, designers must look for new alternatives to successfully complete their goals. One alternative that offers designers many benefits is application specific integrated circuits (ASIC). They maximize device functionality while minimizing system space. Also as operating frequencies approach gigahertz speeds, ASICs allow specialized placement of functional blocks on chip to minimize propagation delays of the signal. At Sandia, we found these requirements forcing us to look at ASICs fabricated in GaAs. DOE

N90-11462# Cornell Univ., Ithaca, NY.
USING COMPUTER DESIGN AND SIMULATION TO IMPROVE MANUFACTURING PRODUCTIVITY, REPORT PERIOD 1, 2 AND 3 Quarterly Status Report No. 1
John E. Hopcroft Mar. 1989 5 p
(Contract N00014-88-K-0591; ARPA Order 6419)
(AD-A210255) Avail: NTIS HC A01/MF A01 CSCL 12/5

In the area of simulation, a system's ability to produce models of contact and collision was developed. These models are essential to research on gripping and manipulation of physical objects by electronic prototypes. Other areas being explored include anthropoid walking (a model of a human torso and legs); parallel, distributed control of complex systems (containing many degrees of freedom); solid modeler robustness; triangulations for the finite element method; and the problem of swept volumes (the volume swept by a polyhedral object as it moves). K.C.D.

N90-11463# Lawrence Livermore National Lab., CA.
AN INVESTIGATION OF THE USEFULNESS OF EARLEY'S ALGORITHM IN A GENERAL CONTEXT-FREE RECOGNIZER M.S. Thesis - Univ. of California, Davis
Cathleen M. Benedetti Jun. 1989 95 p
(Contract W-7405-eng-48)
(DE89-016498; UCRL-53921-th) Avail: NTIS HC A05/MF A01

The potential applications of a general context-free recognizer implemented using Earley's Algorithm are examined. First, several potential applications are identified. The recognizer is implemented, and tested using several grammars and input strings representative of these applications. The results of these tests are then examined to determine whether Earley's Algorithm can be successfully used in a general context-free recognizer. DOE

N90-11464# Gosudarstvennyj Komitet po Ispolzovaniyu Atomnoi Energii, Serpukhov (USSR).
PROGRAMS FOR NUMERICAL INTEGRATION OF PIECE-WISE SMOOTH FUNCTIONS
S. N. Sokolov 1988 12 p In RUSSIAN; ENGLISH summary
(DE89-620449; IFVE-OTF-88-110) Avail: NTIS (US Sales Only) HC A03/MF A01

A series of FORTRAN programs for the numerical integration of piece-wise smooth functions in the one- and many-dimensional spaces is described. The programs use Newton-Cotes quadrature formulas, make accuracy checks at each step, find efficiently the places of degraded smoothness (narrow peaks, splittings, breakpoints), optimize the step size and the degree of quadrature formula, assure the closeness of the actual accuracy of the result the asked one, and have improved reliability. DOE

N90-11465# Massachusetts Inst. of Tech., Cambridge. Dept. of Brain and Cognitive Sciences.
INFERENCES FROM IMAGES Final Report, Jul. 1984 - 30 Jun. 1987
Whitman Richards and Shimon Ullman Dec. 1988 104 p
(Contract N00014-84-K-0650; RR04209)
(AD-A210710) Avail: NTIS HC A06/MF A01 CSCL 12/5

How can a visual system make reliable inferences about surface

properties. To answer such questions, one can use computer graphics to generate a realistic rendition of a surface, such as water, clouds or rock. Such a rendition demonstrates that all the relevent psychophysical parameters have been indentified. Given these parameters, or rather their image correlates, we then proceed to show how the surface type can be inferred from the available image information (inverse optics). The surface we have studied most extensively is water, including some of its dynamical properties. Certain aspects of the motion of planar surfaces were also investigated. Our results suggest a simplification of the Cook-Torrance model for the reflection function. GRA

N90-11466# Norfolk State Univ., VA.
RESEARCH, DEVELOPMENT, TRAINING AND EDUCATION USING THE Ada PROGRAMMING LANGUAGE Final Report, 1 Sep. 1987 - 31 May 1989
George C. Harrison 16 Jul. 1989 18 p
(Contract DAAL03-87-G-0127)
(AD-A210760; ARO-25510.3-EL-H) Avail: NTIS HC A03/MF A01 CSCL 12/5

This research grant is titled Research, Development, Training and Education Using the Ada Programming Language and is hereafter called ReDTEA. The primary goal of this activity was to conduct research in the application and development of Ada, and in broader terms the objectives were as follows: (1) To develop numerical algorithms for parallel processing using the Ada language; (2) To develop new methodologies in reusing Ada software; (3) To solve select problems in applied mathematics using MACSYMA and Ada; (4) Simulate the interactions of nodes in a network using Ada; (5) To increase the cadre of educations available to provide Ada training by conducting Ada workshops for Norfolk State University faculty and staff; (6) To develop a series of in-class and individualized modules addressing Ada programming using computer assisted instruction; and (7) To disseminate research and computer aided instruction modules to other minority institutions through computer networking, workshops, and lecture series. GRA

N90-11467# Human Engineering Labs., Aberdeen Proving Ground, MD.
COMPUTER PROGRAMS FOR MEASURING VARIATIONS IN SPEECH Final Report
Christopher C. Smyth Jul. 1989 26 p
(AD-A211126; HEL-TN-6-89) Avail: NTIS HC A03/MF A01 CSCL 12/5

The measurement of variations in speech is investigated. Computer programs developed to study speech patterns determine the word boundaries and spacing, the fundamental pitch and the formants of words, and classification of the speech as voiced or unvoiced. The potential use of the computer programs is demonstrated using synthetic speech. A synthetic voice generator was used to generate voice patterns from a known speaker in two different voice patterns by changing pitch and breathing parameters. The patterns were digitized and processed on a VAX 11/780 computer for analysis. The computed parameters agree with those used to generate the synthetic speech. Use of these programs is planned for future investigations of the relation between worked load stress and voice variations in human factors testing of subjects who perform data entry tasks using automatic voice recognition systems. GRA

N90-11468# Digital Equipment Corp., Palo Alto, CA. Systems Research Center.
EVALUATING THE PERFORMANCE OF SOFTWARE CACHE COHERENCE
Susan Owicki and Anant Agarwal (Massachusetts Inst. of Tech., Cambridge.) Jun. 1989 25 p
(Contract N00014-87-K-0825)
(AD-A211164; MIT/LCS/TM-395) Avail: NTIS HC A03/MF A01 CSCL 12/5

In a shared memory multiprocessor with private caches, cached copies of a data item must be kept consistent. This is called cache coherence. Both hardware and software coherence schemes are proposed. Software techniques are attractive because they avoid hardware complexity and can be used with any processor-memory interconnection. An analytical model is presented of the performance of two software coherence schemes and, for comparison, snoopy-cache hardware. The model is validated against address traces from a bus-based multiprocessor. The behavior of the coherence schemes under various workloads is compared, and their sensitivity to variations in workload parameters is assessed. The analysis shows that the performance of software schemes is critically determined by certain parameters of the workload: the proportion of data accesses, the fraction of shared references, and the number of times a shared block is accessed before it is purged from the cache. Snoopy caches are more resilient to variations in these parameters. Thus when evaluating a software scheme as a design alternative, it is essential to consider the characteristics of the expected workload. The performance of the two software schemes with a multistage interconnection network is also evaluated, and it is determined that both scale well. GRA

N90-11469# Los Alamos National Lab., NM. Advanced Engineering Technology.
USING PATRAN: FROM EYEBALLS TO SUBMARINES AND MORE
Janine L. Fales and Daniel J. Weinacht 1989 18 p Presented at the PATRAN Users Conference, Costa Mesa, CA, 6-8 Sep. 1989
(Contract W-7405-eng-36)
(DE89-016989; LA-UR-89-2660; CONF-8909187-2) Avail: NTIS HC A03/MF A01

To maintain a position at the cutting edge of state of the art engineering mechanics, an engineer must develop a reliable set of powerful working tools. In the Advanced Engineering Technology group at Los Alamos National Laboratory, we have established such a basis. Our projects have run the gamut from eyeballs to submarines and more. We use a variety of finite element codes in our analyses with PATRAN playing a central role, both as a preprocessor and as a postprocessor. This paper will emphasize a few projects that have used PATRAN, will highlight useful and disappointing aspects of PATRAN, and finally, will demonstrate the use of PATRAN as an effective communications tool. DOE

N90-11470# Universiteit Twente, Enschede (Netherlands). Dept. of Computer Science.
TWO VAX-PASCAL TERMINAL INTERFACE MODULES FOR VISUALIZING SCANNING AND PARSING
Frans J. Faase Mar. 1989 25 p
(Memo-INF-89-17; ISSN-0923-1714; ETN-89-95067) Avail: NTIS HC A03/MF A01

Two VAX-PASCAL terminal interface modules are described which can be used to visualize a scanning and parsing process, both for educational and debugging purposes. They provide a stack-display mechanism, a scrolling screen (in which parts of the bottom line can be highlighted), a header line and an error-message line. The modules are designed in such way that they can also be used for other applications. The modules are used effectively in several compiler generation programs. Adding them to existing programs is shown to be simple and straightforward. ESA

N90-11471# Universiteit Twente, Enschede (Netherlands). Dept. of Computer Science.
A VERIFICATION EXERCISE RELATING TO SPECIFICATION STYLES IN LOTOS
Marten vanSinderen Mar. 1989 19 p
(Memo-INF-89-18; ISSN-0923-1714; ETN-89-95063) Avail: NTIS HC A03/MF A01

The design of complex distributed systems can be supported by a methodology where several, increasingly implementation-oriented, formal specifications are successfully developed. The relative verification of such specifications is discussed in the context of some example specifications in LOTOS. The adoption of common specification styles is claimed to simplify

the verificaton task. Two useful congruence laws which are not contained in the LOTOS standard are presented. ESA

N90-11472# Center for Mathematics and Computer Science, Amsterdam (Netherlands). Dept. of Computer Science.
BOOLEAN FUNCTIONS, INVARIANCE GROUPS AND PARALLEL COMPLEXITY
Peter Clote and Evangelos Kranakis Sep. 1988 44 p Submitted for publication
(Grant NSF DCR-86-06165)
(CWI-CS-R8836; ETN-89-95095) Copyright Avail: NTIS HC A03/MF A01

Invariance groups of boolean functions on a number of variables are studied. The necessary and sufficient conditions via Polya's cycle index for a general permutation group are given. An algorithm is given for cyclic groups for determining invariance of the group. The applicability of group theoretic techniques in the study of parallel complexity of languages is shown. The invariance groups of Dyck and palindrome languages are given, and an algorithm for testing membership in the invariance group of a regular language is provided. Problems of constructing languages with given invariance group structure are considered. ESA

N90-11473# Center for Mathematics and Computer Science, Amsterdam (Netherlands). Dept. of Computer Science.
COMPLETENESS OF RESOLUTION BY TRANSFINITE INDUCTION
Marc Bezem Oct. 1988 12 p Sponsored in part by the Dutch Stimulerings Projectteam Informatica-Onderzoek
(CWI-CS-R8837; ETN-89-95096) Copyright Avail: NTIS HC A03/MF A01

Completeness proofs of various strategies of ground resolution are unified using the principle of transfinite induction with respect to a well founded ordering. The ordering reflects the intuition that resolvents are somehow smaller than parent clauses. Redundancies in the completeness proofs are removed by choosing a better strategy. Zorn's lemma in dealing with infinite sets of ground clauses is applied, permitting a completeness proof of quantified resolution without using Herbrand's theorem. A proof theoretic argument, instead of the usual model theoretic argument, is given which proves the completeness of resolution combined with subsumption and the deletion of tautologies. ESA

N90-11474# Center for Mathematics and Computer Science, Amsterdam (Netherlands). Dept. of Computer Science/Dept. of Software Technology.
MODULE ALGEBRA (REVISED VERSION)
J. A. Bergstra (Amsterdam Univ., Netherlands), J. Heering, and P. Klint Nov. 1988 42 p Submitted for publication
(CWI-CS-R8844-Rev; CWI-CS-R8617; ETN-89-95100) Copyright Avail: NTIS HC A03/MF A01

The study of modules and modularization as a central issue in software engineering is discussed. An axiomatic algebraic calculus of modules is presented based on the operators combination/union, export, renaming, and taking the visible signature. Four different models of module algebra are discussed and compared. ESA

N90-11475# Center for Mathematics and Computer Science, Amsterdam (Netherlands). Dept. of Numerical Mathematics.
CHECKING THE GOLDBACH CONJECTURE ON A VECTOR COMPUTER
A. Granville, J. vandeLune, and H. J. J. teRiele Sep. 1988 14 p Submitted for publication
(CWI-NM-R8812; ETN-89-95103) Copyright Avail: NTIS HC A03/MF A01

Results of a numerical verification of the Goldbach conjecture on a Cyber 205 vector computer up to the bound 2 x 10 to the tenth power are described. Statistics and supporting results based on the prime k-tuplets conjecture of Hardy and Littlewood are presented. ESA

N90-11476# Center for Mathematics and Computer Science, Amsterdam (Netherlands). Dept. of Numerical Mathematics.
VARIABLE STEP ITERATION OF HIGH-ORDER RUNGE-KUTTA METHODS ON PARALLEL COMPUTERS
P. J. vanderHouwen and B. P. Sommeijer Nov. 1988 15 p
(CWI-NM-R8817; ETN-89-95107) Copyright Avail: NTIS HC A03/MF A01

Iterated Runge-Kutta methods of high order, designed in such a way that the righthand side evaluations can be computed in parallel, are investigated. A highly efficient code is developed using stepsize control based on embedded formulas. The eighth order mode of this code is shown to be more efficient than previous formulas on parallel computers, and the tenth order mode is shown to be twice as cheap for comparable accuracies. ESA

N90-11477# Technische Univ., Delft (Netherlands). Faculty of Technical Mathematics and Informatics.
MSP: MODELING OF CONCURRENT PROCESSES. VERSION 1.00 GENERAL INTRODUCTION AND DIRECTIONS FOR USE
J. E. Mebius 1989 22 p
(Rept-88-88; ISSN-0922-5641; ETN-89-95430) Copyright Avail: NTIS HC A03/MF A01

An interactive system for running models of systems of concurrent processes (concurrent systems) called MSP is described. The creation of models for concurrent systems and their forms are outlined. The representation of processes in MSP is explained. A description of MSP as an abstract machine is described. Unlike a real life operating system, in an MSP model, the operating system and tasks are integrated into a fixed whole. ESA

N90-11052# Aerospatiale, Cannes (France).
ESA-D: AN INTEGRATED SOFTWARE FOR ANTENNA DESIGN AND ANALYSIS
L. Marro, J. P. Boisset, and K. Pontoppidan (TICRA A/S, Copenhagen, Denmark) *In* ESA, Spacecraft Structures and Mechanical Testing Jan. 1989 p 505-510 Previously announced as N89-23784 (For primary document see N90-10986 02-18)
(Contract ESTEC-6659/86/NL/PH)
Copyright Avail: NTIS HC A99/MF E06

62 COMPUTER SYSTEMS

Includes computer networks and special application computer systems.

N90-11478# Los Alamos National Lab., NM. Computer Research and Applications.
AN INTEGRATED DISTRIBUTED PROCESSING INTERFACE FOR SUPERCOMPUTERS AND WORKSTATIONS
John Campbell and Lauren McGavran 1989 9 p Presented at the Conference on Applications of Supercomputers in Engineering, Southampton, England, 5-7 Sep. 1989
(Contract W-7405-eng-36)
(DE89-016769; LA-UR-89-2706; CONF-890941-2) Avail: NTIS HC A02/MF A01

Access to documentation, communication between multiple processes running on heterogeneous computers, and animation of simulations of engineering problems are typically weak in most supercomputer environments. This presentation will describe how we are improving this situation in the Computer Research and Applications group at Los Alamos National Laboratory. We have developed a tool using UNIX filters and a SunView interface that allows users simple access to documentation via mouse driven menus. We have also developed a distributed application that integrated a two point boundary value problem on one of our Cray Supercomputers. It is controlled and displayed graphically by a window interface running on a workstation screen. Our motivation for this research has been to improve the usual typewriter/static interface using language independent controls to show capabilities of the workstation/supercomputer combination. DOE

N90-11479# Universiteit Twente, Enschede (Netherlands). Dept. of Computer Science.
TRANSACTION THROUGHPUT IN DISTRIBUTED SYSTEMS: A MODELING STUDY USING DYNAMIC QUEUEING NETWORKS
Boundewijn R. Haverkort and Ignas G. Niemegeers Apr. 1989 17 p
(Memo-INF-89-25; ISSN-0923-1714; ETN-89-95072) Avail: NTIS HC A03/MF A01

Dynamic queueing network models are presented as an extension of classical performability models. Dynamic queueing networks, which combine product form queueing networks and generalized stochastic Petri nets are very suitable for the (extended) performability analysis of fault-tolerant gracefully degradable distributed computer systems. A dynamic queueing network model of a distributed transaction processing system is given and subsequently analyzed for various performability measures. The solution of dynamic queueing network models is based on behavioral decomposition (also called time scale decomposition). By making some assumptions concerning the symmetry in the model, a model is obtained whose state space size is linear in the number of nodes instead of exponential as it is without these assumptions. Performability measures of interest are indicated. By choosing some specific parameter values it is shown that an increase in the failure rate of a certain component does not always imply a decrease in performance for the customers using that component. By varying some of the model parameters the influence of the number of available repair units on the overall performance of the system is shown. By associating costs with repair units and loss of transaction throughput due to failed components the system is optimized with respect to the number of repair units. ESA

N90-11480# Center for Mathematics and Computer Science, Amsterdam (Netherlands). Dept. of Computer Science.
ON THE AMOEBA PROTOCOL
J. C. Mulder Jul. 1988 26 p
(ESPRIT Proj. 432)
(CWI-CS-R8827; ETN-89-95092) Copyright Avail: NTIS HC A03/MF A01

The Amoeba distributed operating system, which supports the transaction as its communication primitive, is addressed. The protocol that the Amoeba system uses to carry out sequences of transactions reliably and efficiently is analyzed in terms of process algebra. The design goals are formulated as process algebra equations and it is established that one of them is not met. This is repaired by adding an extra transition. The revised version is verified to meet its specifications. ESA

N90-11481# Center for Mathematics and Computer Science, Amsterdam (Netherlands). Dept. of Computer Science.
SYNCHRONY WITH EMPTY PROCESS
W. P. Weijland Aug. 1988 14 p
(CWI-CS-R8832; ETN-89-95094) Copyright Avail: NTIS HC A03/MF A01

The Algebra of Synchronous Processes (ASP) is extended with an extra constant which serves as a neutral element for sequential composition. In contrast to the asynchronous algebra of the communicating process, in the setting of ASP the extra empty process constant is shown to behave in a very natural way. ESA

N90-11482# Center for Mathematics and Computer Science, Amsterdam (Netherlands). Dept. of Computer Science.
PARALLEL INFERENCE BASED ON DELTA PROCESSING
A. Eliens Nov. 1988 14 p Sponsored in part by the Dutch Stimulerings Projectteam Informatica-Onderzoek
(CWI-CS-R8846; ETN-89-95101) Copyright Avail: NTIS HC A03/MF A01

The application of resolution based theorem proving techniques to expert system reasoning is addressed. Expert system reasoning can be considered a special form of resolution. The disadvantage of general resolution, involving full forward and backward subsumption is that it is rather costly. A technique is presented that effectively reduces the computational cost of resolution-based inference in expert system reasoning. The idea is to encode the effects of a resolution step as instructions to modify a set of clauses. The technique, moreover, allows efficient parallelism, both by simultaneously processing generated information (AND-parallelism), and by exploring different search paths when splitting on a positive disjunction (OR-parallelism). ESA

N90-11483# Center for Mathematics and Computer Science, Amsterdam (Netherlands). Dept. of Numerical Mathematics.
LINPACK ROUTINES BASED ON THE LEVEL 2 BLAS
Margreet Louter-Nool Sep. 1988 19 p Submitted for publication
(CWI-NM-R8811; ETN-89-95102) Copyright Avail: NTIS HC A03/MF A01

Extended or level two BLAS as an improvement on the performance of portable programs on high performance computers is addressed. The insertion of extended BLAS routines in LINPACK, such that no changes in the parameter list are required, is examined. The failure of simple restructuring in terms of level two BLAS in some algorithms is discussed. The translation of calls to original BLAS into calls to level two BLAS in order to improve readability, modularity, and efficiency, is detailed. This examination results in a still portable subset of the LINPACK with a better performance than the original routines. The measured performances of original and modified LINPACK routines on various machines are compared and analyzed. ESA

N90-11484# Technische Univ., Delft (Netherlands). Faculty of Technical Mathematics and Informatics.
A GENERALIZATION OF A. N. HABERMANN'S THEOREM FOR SEMAPHORES
J. E. Mebius 1988 13 p
(Rept-88-98; ISSN-0922-5641; ETN-89-95109) Copyright Avail: NTIS HC A03/MF A01

The use of semaphores as a means of implementing the safe execution of concurrent computer processes with synchronization and mutual exclusion requirements is addressed. The semaphore definition of A. N. Habermann precludes interim situations, so semaphores according to this definition are called strict. Where an interim situation is allowed to occur, semaphores are called relaxed. Habermann's formula, which is characteristic for strict semaphores, is generalized, and proved to be characteristic for relaxed semaphores. ESA

63 CYBERNETICS

Includes feedback and control theory, artificial intelligence, robotics and expert systems.

For related information see also *54 Man/System Technology and Life Support.*

N90-11485 Illinois Univ., Urbana-Champaign.
PERFORMANCE AND ROBUSTNESS OF ADAPTIVE CONTROLLERS FOR LINEAR STOCHASTIC SYSTEMS Ph.D. Thesis
Sheng-Fuu Lin 1988 129 p
Avail: Univ. Microfilms Order No. DA8908755

The twin questions of performance as well as robustness of an adaptive controller for linear stochastic systems are addressed. Regarding the performance problem, the issue is considered of convergence of the parameter estimates with respect to the stochastic gradient algorithm and the modified least squares algorithm. As to the linear model following problem, it was shown that under certain conditions, both algorithms are strongly consistent. For the general tracking problem, if the reference trajectory is sufficiently rich of order greater than or equal to a certain positive number, both algorithms are strongly consistent. As for the regulation problem, if the controller utilizes the stochastic gradient algorithm, the parameter estimates converge to a random scalar multiple of the true parameter vector. For the robustness problem, a robust adaptive controller is presented. Its mean square

stabilizes the ideal system optimally if the noise signal satisfied a positive real condition. It can also stabilize a non-ideal system if the system is in a certain graph topological neighborhood of an ideal system. Dissert. Abstr.

N90-11486 Purdue Univ., West Lafayette, IN.
APPLICATIONS OF ARTIFICIAL INTELLIGENCE TO DIGITAL PHOTOGRAMMETRY Ph.D. Thesis
Jeffrey Lee Kretsch 1988 287 p
Avail: Univ. Microfilms Order No. DA8911938

A great deal of interest has arisen lately in the application of expert systems to problems in which computer solutions were previously inapplicable. The application of expert systems to digital photogrammetry was studied, specifically to photogrammetric triangulation, feature extraction, and photogrammetric problem solving. In 1987, prototype expert systems were developed for doing system startup, interior orientation, and relative orientation in the mensuration stage. The system explored means of performing diagnostics during the process. In the area of feature extraction, the relationship of metric uncertainty to symbolic uncertainty was the topic of research. Error propagation through the Dempster-Shafer formalism for representing evidence was performed in order to find the variance in the calculated belief values due to errors in measurements made to gather the initial evidence needed to begin labeling of observed image features with features in an object model. In Photogrammetric problem solving, an expert system is under continuous development which seeks to solve photogrammetric problems using mathematical reasoning. The key to the approach used is the representation of knowledge directly in the form of equations, rather than in the form of if-then rules. Then each variable in the equations is treated as a goal to be solved. Once the solution set of equations able to solve the problem is determined, the set is submitted to the Vaxima (MACSYMA) expert system for solution. Development of a rule-based part to deal with the heuristic knowledge needed in solving the equations, such as choosing optimum equations, and selecting suitable approximations, is described. Dissert. Abstr.

N90-11487*# Integrated Systems, Inc., Palo Alto, CA.
NONLINEAR MANEUVER AUTOPILOT FOR THE F-15 AIRCRAFT Final Report
P. K. A. Menon, M. E. Badgett, and R. A. Walker Jun. 1989 90 p
(Contract NAS2-11877)
(NASA-CR-179442; H-1541; NAS 1.26:179442) Avail: NTIS HC A05/MF A01 CSCL 09B

A methodology is described for the development of flight test trajectory control laws based on singular perturbation methodology and nonlinear dynamic modeling. The control design methodology is applied to a detailed nonlinear six degree-of-freedom simulation of the F-15 and results for a level accelerations, pushover/pullup maneuver, zoom and pushover maneuver, excess thrust windup turn, constant thrust windup turn, and a constant dynamic pressure/constant load factor trajectory are presented. Author

N90-11488# Los Alamos National Lab., NM.
SPOKEN COMMANDS CONTROL ROBOT THAT HANDLES RADIOACTIVE MATERIALS
Patrick F. Phelan, Christopher Keddy, and Tony J. Beugelsdijk 1989 9 p Presented at the American Voice Input/Output Society Meeting, Newport Beach, CA, Sep. 1989
(Contract W-7405-eng-36)
(DE89-012632; LA-UR-89-1833; CONF-8909147-1) Avail: NTIS HC A02/MF A01

Several robotic systems have been developed by Los Alamos National Laboratory to handle radioactive material. Because of safety considerations, the robotic system must be under direct human supervision and interactive control continuously. In this paper, we describe the implementation of a voice-recognition system that permits this control, yet allows the robot to perform complex preprogrammed manipulations without the operator's intervention. To provide better interactive control, we connected to the robot's control computer, a speech synthesis unit, which provides audible feedback to the operator. Thus upon completion of a task or if an emergency arises, an appropriate spoken message can be reported by the control computer. The training programming and operation of this commercially available system are discussed, as are the practical problems encountered during operations. DOE

N90-11489# Pacific Northwest Lab., Richland, WA.
PRINCIPAL COMPONENTS IN MULTIVARIATE CONTROL CHARTS
D. L. Eggett and B. A. Pulsipher Aug. 1989 22 p Presented at the American Statistical Association Meeting, Washington, DC, 7-10 Aug. 1989
(Contract DE-AC06-76RL-01830)
(DE89-016828; PNL-SA-17221; CONF-8908108-2) Avail: NTIS HC A03/MF A01

Principal components were used as a variable reduction technique. The principal component scores have desirable statistical properties when the original variables are distributed as multivariate normal. Three statistics derived from the PC scores and used to form multivariate control charts are examined. These statistics are outlined and their distributional properties reviewed. The effectiveness of control charts using the three statistics was examined through Monte Carlo simulations. Several parameters were varied including correlation pattern, size of changes in means and variances, number of means or variances changed, change in the correlation for one variable, and the number of PCs retained. DOE

N90-11490# Oak Ridge National Lab., TN. Chemical Technology Div.
SYSTEMS ANALYSIS CONSIDERATIONS IN ARTIFICIAL INTELLIGENCE/EXPERT SYSTEMS TECHNOLOGY APPLICATIONS
Angel L. Rivera 1989 12 p Presented at the American Institute of Chemical Engineer's Summer National Meeting, Philadelphia, PA, 20-23 Aug. 1989
(Contract DE-AC05-84OR-21400)
(DE89-016847; CONF-890814-6) Avail: NTIS HC A03/MF A01

The concept of artificial intelligence (AI) represents a challenging opportunity in expanding the potential benefits from computer systems. The potential of this concept lies in facilitating the development of intelligent computer systems to help analysts and decision-makers in problem solving in the same way that machines support the laborer. Because the knowledge of human experts is an essential input to many parts of chemical process planning, development, and operation, there are numerous opportunities for the applications of expert systems (a product from AI) in chemical engineering. Intelligent computer systems could be developed by chemical engineers to increase the contribution of computer technology to the advancement of the profession, particularly in the strategic management of the scientific and technological aspects of chemical engineering applications. System analysis is introduced as a framework for the planning and development of intelligent computer systems in those areas where chemical engineering could play a significant role. DOE

N90-11491# Institute for Defense Analyses, Alexandria, VA.
A SURVEY OF RESEARCH METHODS TO STUDY DESIGN Final Report, Oct. 1987 - Sep. 1988
Marylouise Brei, David A. Dierolf, and Karen J. Richter Jun. 1989 123 p
(Contract MDA903-84-C-0031)
(AD-A211213; AD-E501143; IDA-P-2155; IDA/HQ-88-33821)
Avail: NTIS HC A06/MF A01 CSCL 05/1

This report identifies and evaluates methods used by the design research community that could be used to establish requirements for improving the effectiveness of the engineering design process in a Unified Life Cycle Engineering (ULCE) environment. More than 50 design research projects were reviewed to develop an understanding of the scope of design research during the 1970s and 1980s. Reports on these diverse projects are included in an annotated bibliography, which is an appendix to this report. Reviews

of the strengths and weaknesses of 18 specific design research projects comprise the body of the report. The methods used in these 18 projects include systems analysis, field observation and participation, retrospective analysis, knowledge representation, protocol analysis, and computational experiments of problem-solving behavior. GRA

N90-11492# Center for Mathematics and Computer Science, Amsterdam (Netherlands). Dept. of Computer Science.
DETERMINISM YIELDS (EVENT STRUCTURE ISOMORPHISM EQUALS STEP SEQUENCE EQUIVALENCE)
Fritz W. Vaandrager Oct. 1988 20 p Sponsored in part by the Commission of the European Communities ESPRIT Project 432 METEOR
(CWI-CS-R8839; ETN-89-95098) Copyright Avail: NTIS HC A03/MF A01

For deterministic concurrent systems most of the interleaved equivalences (bisimulation, failure, trace) coincide. In the setting of event structures, most non-interleaved equivalences are proved to coincide on this domain. As a consequence of the result, the casual structure of a deterministic concurrent system is unravelled by observers capable of observing the beginning and termination of events. ESA

64 NUMERICAL ANALYSIS

Includes iteration, difference equations, and numerical approximation.

N90-11493# Illinois Univ., Urbana. Dept. of Computer Science.
ASYNCHRONOUS INTEGRATION OF ORDINARY DIFFERENTIAL EQUATIONS ON MULTIPROCESSORS
Sohail Aslam and C. W. Gear Jul. 1989 35 p
(Contract DE-FG02-87ER-25026)
(DE89-014169; DOE/ER-25026/31; UIUCDCS-R-89-1525; UILU-ENG-89-1744) Avail: NTIS HC A03/MF A01

Asynchronous iteration methods have been shown to offer significant speedups in multiprocessing environments for the class of iterative methods $x = F(x)$. For a system of equations, parallel implementation on a multiprocessor with no minimal synchronization between cooperating processes yields the most advantage. Picard or Picard-like iteration schemes for solving ordinary differential equations (ODEs) fall into such a class of iterative methods. A preliminary report on the use of Picard-like integration methods for solving initial value problems (IVP) from a class of ODEs is presented. An algorithm has been implemented on an Encore Multimax which is a multiprocessor shared-memory machine. The computer code is designed to solve a given system of ODEs. The user interface to the code is similar to traditional ODEs solvers. DOE

N90-11494*# Institute for Computer Applications in Science and Engineering, Hampton, VA.
ESTIMATION ON NONLINEAR DAMPING IN SECOND ORDER DISTRIBUTED PARAMETER SYSTEMS Final Report
H. T. Banks, Simeon Reich, and I. G. Rosen (University of Southern California, Los Angeles.) Aug. 1989 32 p Prepared in cooperation with Technion Research and Development Foundation Ltd., Haifa (Israel)
(Contracts NAS1-18107; NAS1-18605; NAG1-517; F49620-86-C-0111; AF-AFOSR-0356-87; NSF MCS-85-04316)
(NASA-CR-181890; ICASE-89-16; NAS 1.26:181890) Avail: NTIS HC A03/MF A01 CSCL 12A

An approximation and convergence theory for the identification of nonlinear damping in abstract wave equations is developed. It is assumed that the unknown dissipation mechanism to be identified can be described by a maximal monotone operator acting on the generalized velocity. The stiffness is assumed to be linear and symmetric. Functional analytic techniques are used to establish that solutions to a sequence of finite dimensional (Galerkin) approximating identification problems in some sense approximate a solution to the original infinite dimensional inverse problem. Author

N90-11495*# Institute for Computer Applications in Science and Engineering, Hampton, VA.
A CONFORMING SPECTRAL COLLOCATION STRATEGY FOR STOKES FLOW THROUGH A CHANNEL CONTRACTION Final Report
Timothy N. Phillips and Andreas Karageorghis (University Coll. of Wales, Aberystwyth.) Sep. 1989 22 p
(Contract NAS1-18605)
(NASA-CR-181912; NAS 1.26:181912; ICASE-89-60) Avail: NTIS HC A03/MF A01 CSCL 12A

A formula expressing the coefficients of an expansion of ultraspherical polynomials which has been differentiated an arbitrary number of times in terms of the coefficients of the original expansion is proved. The particular examples of Chebyshev and Legendre polynomials are considered. Author

N90-11496# Wisconsin Univ., Madison. Center for Mathematical Sciences.
SUBHARMONIC SOLUTIONS NEAR AN EQUILIBRIUM POINT FOR HAMILTONIAN SYSTEMS Summary Report
Patricio L. Felmer Apr. 1989 77 p Prepared in cooperation with Chile Univ., Santiago
(Grant AF-AFOSR-0202-87)
(AD-A210558; CMS-TSR-89-30) Avail: NTIS HC A05/MF A01 CSCL 12/2

This document studies subharmonic solutions near an equilibrium point for a Hamiltonian system. On the linear part of the system we impose a condition expressed in terms of its symplectic invariants. The higher order term is assumed to be superquadratic near the equilibrium point, and we show that this condition can be reduced to the center manifold. We transform the Hamiltonian system to a variational problem and we apply a minimax argument to find critical points. GRA

N90-11497*# National Aeronautics and Space Administration. Lewis Research Center, Cleveland, OH.
A NONOSCILLATORY, CHARACTERISTICALLY CONVECTED, FINITE VOLUME SCHEME FOR MULTIDIMENSIONAL CONVECTION PROBLEMS
Jeffrey W. Yokota and Hung T. Huynh 1989 20 p Prepared for presentation at the 28th Aerospace Sciences Meeting, Reno, NV, 8-11 Jan. 1990; sponsored in part by AIAA Prepared in cooperation with Sverdrup Technology, Inc., Cleveland, OH
(NASA-TM-102354; E-5069; NAS 1.15:102354) Avail: NTIS HC A03/MF A01 CSCL 12A

A new, nonoscillatory upwind scheme is developed for the multidimensional convection equation. The scheme consists of an upwind, nonoscillatory interpolation of data to the surfaces of an intermediate finite volume; a characteristic convection of surface data to a midpoint time level; and a conservative time integration based on the midpoint rule. This procedure results in a convection scheme capable of resolving discontinuities neither aligned with, nor convected along, grid lines. Author

N90-11498*# Institute for Computer Applications in Science and Engineering, Hampton, VA.
DIRECT DISCRETIZATION OF PLANAR div-curl PROBLEMS Final Report
R. A. Nicolaides (Carnegie-Mellon Univ., Pittsburgh, PA.) Oct. 1989 32 p Submitted for publication
(Contract NAS1-18605; AF-AFOSR-0359-89)
(NASA-CR-181935; ICASE-89-76; NAS 1.26:181935) Avail: NTIS HC A03/MF A01 CSCL 12A

A control volume method is proposed for planar div-curl systems. The method is independent of potential and least squares formulations, and works directly with the div-curl system. The novelty of the technique lies in its use of a single local vector field component and two control volumes rather than the other way around. A discrete vector field theory comes quite naturally

from this idea and is developed. Error estimates are proved for the method, and other ramifications investigated. Author

N90-11499# Sandia National Labs., Albuquerque, NM.
EVALUATION OF INTEGRALS RELATED TO THE DEBYE FUNCTION
Donald E. Amos Jul. 1989 8 p
(Contract DE-AC04-76DP-00789)
(DE89-016930; SAND-88-2896) Avail: NTIS HC A02/MF A01

Certain models for the penetration and perforation of metal plate targets impacted by high velocity projectiles lead to integrals related to the Debye function. These integrals are numerically evaluated by a combination of series expansions near singularities and numerical quadrature away from singularities. Numerical evaluation of the Riemann zeta function and dilogarithm function for small parameters are by-products of this analysis. DOE

N90-11500# International Centre for Theoretical Physics, Trieste (Italy).
ON THE AREAS OF VARIOUS BODIES IN THE EUCLIDEAN SPACE: THE CASE OF IRREGULAR CONVEX POLYGONS
P. C. Ozoemena (Anambra State Univ. of Technology, Enugu, Nigeria) Nov. 1988 20 p
(DE89-618377; IC-88/383) Avail: NTIS (US Sales Only) HC A03/MF A01

A theorem is proposed for the areas of n-sided irregular convex polygons, of given length of sides. The theorem is illustrated as a simple but powerful one in estimating the areas of irregular polygons, being dependent only on the number of sides n (and not on any of the explicit angles) of the irregular polygon. Finally, because of the global symmetry shown by equilateral triangles, squares and circles under group (gauge) theory, the relationships governing their areas, when they are inscribed or escribed in one another are discussed as riders, and some areas of their applications in graph theory, ratios and maxima and minima problems of differential calculus briefly mentioned. DOE

N90-11501# International Centre for Theoretical Physics, Trieste (Italy).
LOCAL STRUCTURE OF A 2-CODIMENSIONAL CONFORMALLY FLAT SUBMANIFOLD IN AN EUCLIDEAN SPACE R(SUP n+2)
G. Zafindratafa Dec. 1988 27 p
(DE89-618379; IC-88/392) Avail: NTIS (US Sales Only) HC A03/MF A01

Since 1917, many mathematicians studied conformally flat submanifolds. In 1917, E. Cartan showed that the second fundamental form of a conformally flat hypersurface of R sup n+1 admits an eigenvalue of multiplicity greater than or = to n-1. In 1972, B. Y. Chen introduced the notion of quasiumbilical submanifold. A submanifold M of codimension N in R sup n+N is quasiumbilical if and only if there exists, locally at each point of M, an orthonormal frame field (xi sub 1,..., xi sub N) of the normal space so that the Weingarten tensor of each xi sub alpha possesses an eigenvalue of multiplicity greater than or = to n-1. The purpose of this work is to resolve the following problem: Is there any equivalent definition of quasiumbilicity which does not use either any local frame field on the normal bundle or any particular sections on the tangent bundle. B. Y. Chen and K. Yano proved in 1972 that a quasiumbilical submanifold of codimension N is greater than or = to 1 in R sup n+N is conformally flat; moreover in the case of codimension N=1, the notion of quasiumbilicity is equivalent to the conformal flatness. J. D. Moore and J. M. Morvan improved this last equivalence in 1978 by proving that, if 1 is less than or = to N is less than or = to inf (4,n - 3), a N-codimensional submanifold of R sup n+N is conformally flat if and only if it is quasiumbilical. But two years before, B. Y. Chen and L. Verstraelen demonstrated that any N-codimensional conformally flat submanifold of R sup n+N (1 is less than or = to N is less than or equal to n - 3) with a null normal curvature is quasiumbilical. In 1985, M. do Carmo and his coworkers determined the local geometry of a conformally flat hypersurface of R sup n+1. The purpose of this work is to generalize M. do Carmo's result. DOE

N90-11502# International Centre for Theoretical Physics, Trieste (Italy).
COMPACT SURFACE IN THREE-DIMENSIONAL ELLIPSOID WITH PRESCRIBED MEAN CURVATURE (I)
Xuanguo Huang (Fudan Univ., Shanghai, China) Dec. 1988 10 p Submitted for publication
(DE89-618381; IC-88/410) Avail: NTIS (US Sales Only) HC A02/MF A01

It is proved that torus S sup 1 (1) x S sup 1 (1) can be embedded into three-dimensional ellipsoid M sub 3 with suitable mean curvature function. DOE

N90-11503# International Centre for Theoretical Physics, Trieste (Italy).
ON SUFFICIENT CONDITIONS FOR A FUNCTION TO BE ANALYTIC
F. M. Diab (Cairo Univ., Giza, Egypt) Dec. 1988 8 p Submitted for publication
(DE89-618382; IC-88/420) Avail: NTIS (US Sales Only) HC A02/MF A01

The object of this note is to discuss the minimal requirements for monogeneity (and in particular, for analyticity) of schlicht continuous mappings in the sense that the slightest alteration in these requirements endangers the possibly analytical character of such mappings. DOE

N90-11504# International Centre for Theoretical Physics, Trieste (Italy).
GENERAL HULLS IN UNIFORM ALGEBRAS
Toma V. Tonev (Bulgarian Academy of Sciences, Sofia.) Dec. 1988 10 p Submitted for publication Sponsored in part by Ministry of Culture, Science, and Education of Bulgaria
(DE89-618383; IC-88/428) Avail: NTIS (US Sales Only) HC A02/MF A01

An approach is given for introducing general hulls of closed subsets of the spectrum of a given uniform algebra, that relates to n-th Shilov-Sibony-Basener boundaries. DOE

N90-11505# International Centre for Theoretical Physics, Trieste (Italy).
ANALYTIC MANIFOLDS IN UNIFORM ALGEBRAS
Toma V. Tonev (Bulgarian Academy of Sciences, Sofia.) Dec. 1988 8 p Submitted for publication Sponsored in part by Ministry of Culture, Science, and Education of Bulgaria
(DE89-618384; IC-88/429) Avail: NTIS (US Sales Only) HC A02/MF A01

Bear-Hile's results are extended concerning the version of famous Bishop's theorem for 1-D analytic structures in two directions: for n-dimensional complex analytic manifolds, n greater than 1, and for generalized analytic manifolds. DOE

N90-11506# Carnegie-Mellon Univ., Pittsburgh, PA. Robotics Inst.
PREFERENCE PROPAGATION IN TEMPORAL/CAPACITY CONSTRAINT GRAPHS
Norman Sadeh and Mark S. Fox Jan. 1989 58 p Sponsored by McDonnell Aircraft Co.
(Contract F30602-88-C-0001)
(AD-A210668; CMU-RI-TR-89-2) Avail: NTIS HC A04/MF A01 CSCL 12/4

Scheduling can be formalized as a constraint satisfaction problem. Within this framework activities in a plan are interconnected via temporal relation constraints a la Allen, thereby defining a temporal constraint graph (TCG). Additionally there are capacity constraints restricting the use of each resource to only one activity at a time. Together these constraints form a temporal/capacity constraint graph (T/CCG). Preferences such as meeting due dates, reducing order flowtime, or selecting accurate machines are modeled as utility functions over the domain of possible start times and durations of activities and over the sets

of possible resources activities can use. These preferences interact via the TCG and via the resource capacity constraints. Hence, in general, they cannot be simultaneously optimized. The objective of preference propagation techniques is to transform such local a priori preferences so as to account for their interactions. This paper describes a probabilistic framework in which start time, duration and resource preferences are propagated across T/CCGs in order to focus attention in an incremental scheduler. GRA

N90-11507# Teledyne Geotechnical, Alexandria, VA.
ITERATIVE NETWORK MAGNITUDE ESTIMATION AND UNCERTAINTY ASSESSMENT WITH NOISY AND CLIPPED DATA Final Report, Jun. 1987 - Jun. 1989
R.-S. Jih and R. H. Shumway Jun. 1989 62 p
(Contract MDA903-87-C-0069; ARPA Order 5143)
(AD-A210707; TGAL-88-06) Avail: NTIS HC A04/MF A01 CSCL 12/3

This document discusses the similarities and differences between two iterative estimators that are suitable for the network m sub b estimation problem, namely a modification of the Iterative Least-Squares method (ILS) due to Scheme and Hahn (1979) and the Maximum-Likihood Estimator (MLE). Both methods reduce to the usual Least Square Multiple Factors (LSMF) method when the censored data are deleted from the network observational data. For the censored case, the standard deviation (sigma) of the obscuring noise must be solved through iteration along with the event magnitudes and the station corrections. An extra constraint on sigma is necessary to determine which optimal estimation scheme is of interest. The final value of sigma for each iterative scheme can be used as a good approximation to the unbiased estimate of the standard deviation of the perturbing noise. By scaling this sigma value by the square root of the number of observations associated with each unknown parameter, the uncertainty in each estimated parameter can be approximated efficiently. These error estimates seem to differ from the unbiased standard errors only by a common multiplying constant across all stations and all event m sub b's. The bootstrap method is reviewed and adapted to the case of multivariate estimation with doubly censored data. GRA

N90-11508# Stanford Univ., CA. Dept. of Operations Research.
STOCHASTIC OPTIMIZATION BY SIMULATION: SOME EXPERIMENTS WITH A SIMPLE STEADY-STATE QUEUE
Pierre LEcuyer, Nataly Giroux (Laval Univ., Quebec), and Peter W. Glynn Feb. 1989 36 p
(Contract DAAL03-88-K-0063)
(AD-A210762; TR-31; ARO-25839.4-MA) Avail: NTIS HC A03/MF A01 CSCL 12/4

New approaches like perturbation analysis and the likelihood ratio method have been proposed recently to estimate the gradient of a performance measure with respect to some continuous parameters in a dynamic stochastic system. In this paper, we experiment the use of these estimators in stochastic approximation algorithms, to perform so-called single-run optimizations. We also compare them to finite difference estimators, with and without common random numbers. The experiments are done on a simple M/M/1 queue. The performance measure involves the average system time per customer, and the optimal solution is easy to compute analytically, which facilitates the evaluation of the algorithms. We also demonstrate some properties of the algorithms. In particular, we show that using perturbation analysis, the single-run optimization converges to the optimum even with a fixed (and small) number of ends of service per iteration, while under the same conditions, the algorithm that uses the finite difference estimators converges to the wrong answer. GRA

N90-11509# Nova Univ., Dania, FL. Oceanographic Center.
NONLINEAR ADJUSTMENT WITH OR WITHOUT CONSTRAINTS, APPLICABLE TO GEODETIC MODELS Final Report, 4 Mar. 1987 - 3 Mar. 1989
Georges Blaha Mar. 1989 53 p
(Contract F19628-87-K-0030)
(AD-A210820; AFGL-TR-89-0118) Avail: NTIS HC A04/MF A01 CSCL 12/3

This study concentrates on the least-squares resolution of the parametric adjustment model. In general this model may occur in a linear or a nonlinear form, and may or may not have constraints associated with it. The constraints, if present, may be linear or nonlinear. Furthermore, two basic categories of constraints are available, namely the familiar equality constraints (i.e., exact relations which must be fulfilled by the parameters), and the relatively new category of inequality constraints. With the exception of the inequality constraints, which are treated in the linear version in conjunction with the linear parametric model, the adjustment model and the eventual (equality) constraints are presented here in the nonlinear version. But in every case, the least-squares solution is achieved via an isomorphic geometrical setup with tensor structure and notation. This is possible due to the fact that in the geometrical context the least-squares criterion translates into the minimum-distance property, which, in turn, entails an orthogonal projection of the observational point onto the pertinent model surface. GRA

N90-11510# Brown Univ., Providence, RI. Div. of Applied Mathematics.
WAVEFRONT PROPAGATION FOR REACTION-DIFFUSION SYSTEMS OF PDE
G. Barles, L. C. Evans (Maryland Univ., College Park.), and P. E. Souganidis Mar. 1989 36 p
(Contracts N00014-83-K-0542; DAAL03-86-K-0074; AF-AFOSR-ISSA-86-0078; NSF DMS-86-01532; NSF DMS-86-01258; NSF DMS-86-57464)
(AD-A210862; LCDS-89-3; AFOSR-89-0574TR) Avail: NTIS HC A03/MF A01 CSCL 12/1

The theory of viscosity solutions for Hamilton-Jacobi equations is used to study the asymptotic behavior of solutions to certain systems of reaction-diffusion partial differential equations (PDE). Our principal result characterizes the region of convergence of the solution to an unstable rest point as the set where the solution of an appropriate Hamilton-Jacobi equation is positive. GRA

N90-11511# North Carolina Univ., Chapel Hill. Dept. of Mathematics.
PARAMETER ESTIMATION IN FUNCTIONAL AND PARTIAL DIFFERENTIAL EQUATIONS Final Report, 1 Sep. 1986 - 30 Apr. 1989
Katherine A. Murphy 31 May 1989 13 p
(Grant AF-AFOSR-0256-86; AF Proj. 2304)
(AD-A211040; AFOSR-89-1068TR) Avail: NTIS HC A03/MF A01 CSCL 12/2

Research focused on theoretical and computational methods for estimation of unknown variable parameters in nonlinear partial differential equations. Also methods for estimating time delays in functional differential equations and boundary parameters in moving boundary problems were developed. Seven publications were produced under this grant, including estimation of discontinuous coefficients and boundary parameters for hyperbolic systems and estimation of time - and state - dependent delays and other parameters in functional differential equations. GRA

N90-11512# Florida Univ., Gainesville. Center for Mathematical System Theory.
REALIZATION THEORETIC SOLUTION OF TWO ANALYTIC MATRIX EQUATIONS WITH APPLICATIONS TO STABILIZATION OF INFINITE-DIMENSIONAL SYSTEMS
Erol Emre and Jin H. Seo 1988 22 p
(Contract DAAG29-85-K-0099)
(AD-A211118; CM-875; ARO-22356.3-MA) Avail: NTIS HC A03/MF A01 CSCL 12/3

A realization theoretic approach is proposed for the solutions of two matrix analytic equations arising in the control of infinite-dimensional systems. The realization proposed here is based on the operator theoretic machinery described by Fuhrmann (1981). With this form of realization, we extend to infinite-

dimensional systems the solutions given by Emre (1980) and Emre and Silverman (1981) for finite-dimensional systems. A systematic characterization of all H to the 2nd power solutions of the Bezout-type equation are given in terms of a realization and the Hankel map of the given system. H to the 2nd power solutions are shown to be an intermediate step for H to infinity solutions of such equations. This provides a parametrization of all H to infinity, H to the 2nd power solutions, and solutions with Y polynomials. All H to the 2nd power solutions of the skew matrix equation are given. All H to infinity solutions and solutions with X polynomials of the skew matrix equation can also be obtained under certain conditions. A new criterion is developed for Bezout type equations to have H to infinity solutions in the cases where the Corona condition (Fuhrmann 1981) is not necessarily satisfied. Approximate polynomial solutions for Bezout type equations are also given. This approach provides an explicit link between the state-space descriptions of the open-loop systems and stabilizing compensators. GRA

N90-11513# Colorado Univ., Boulder. Dept. of Electrical and Computer Engineering.
CONTROL AND OPTIMIZATION FOR OBSERVATIONS OF SYSTEMS GOVERNED BY CONTROLLED PARTIAL DIFFERENTIAL EQUATIONS Final Report, 1 Aug. 1986 - 15 Dec. 1988
Renjeng Su 19 May 1989 9 p
(Grant AF-AFOSR-0198-86; AF Proj. 2304)
(AD-A211122; AFOSR-89-1067TR) Avail: NTIS HC A02/MF A01 CSCL 12/9

This project was focused on fundamental issues of modeling and control of flexible structures. Particular problems considered were: patterns of transmission zeroes, sensor placement, robust control, and high-performance control using iterative learning approach. During the grant period a flexible beam control devise for experimental purpose was also developed. With most of the work carried out to the extent of laboratory implementation, the following results were concluded: (1) For flexible structure control the location of transmission zeroes in the mathematical models critically depend on the location of sensors. For flexible beams the movement of zeroes were mapped out for control design; (2) For flexible structures a class of new compensators called generalized lead/lag compensators were developed. Their implementation is very simple with delay elements; and (3) Optimal sensor placement can be based on the robustness of the dynamic observer to parameter uncertainty. A design procedure was developed for this purpose. GRA

N90-11514# Pacific Fleet, Camp Smith, HI. Strategic Planning and Policy Directorate.
TWO ENHANCEMENTS OF THE LOGARITHMIC LEAST-SQUARES METHOD FOR ANALYZING SUBJECTIVE COMPARISONS Final Report
Michael L. McCurdy 25 Mar. 1989 72 p Presented at the 57th Military Operations Research Society Symposium, Fort Leavenworth, KS, 6-8 Jun. 1989
(AD-A211192) Avail: NTIS HC A04/MF A01 CSCL 12/3

This memorandum presents two extension of the logarithmic least-squares method for analyzing subjective comparisons. The first is a test of consistency that is based on analysis-of-variance techniques. Unlike Saaty's eigenvalue-based consistency ratio, the consistency metric developed here is independent of any scale used to elicit comparisons. It is easily applied to sets of comparisons that are incomplete or contain multiple comparisons. This metric provides valuable insights into the trade-off between data set completeness and our ability to detect inconsistency. The second extension is to use robust regression for calculating the ratio scale that best represents most of the data. These extensions combine to make the logarithmic least-squares method an attractive alternative to Saaty's eigenvalue method. GRA

N90-11515# Georgia Inst. of Tech., Atlanta. School of Industrial and Systems Engineering.
STOCHASTIC FLOWS IN NETWORKS Final Technical Report, 16 Feb. 1988 - 15 Apr. 1989
Richard F. Serfozo 15 Jun. 1989 10 p
(Grant AF-AFOSR-0137-88; AF Proj. 2304)
(AD-A211209; AFOSR-89-1066TR) Avail: NTIS HC A02/MF A01 CSCL 12/4

This report summarizes research accomplishments on stochastic flows in networks. The highlight is a new family of probability distributions for describing the numbers of units at the nodes in partially balanced stochastic networks. Such a distribution is a key tool for evaluating the performance and design of a network. Another major accomplishment is the solution of a long-standing problem of finding an expression for the mean time for one unit to move from one sector of a network to another sector. We also developed several models for concurrent movement of units in networks and batch processing at nodes. GRA

N90-11516# Yale Univ., New Haven, CT. Dept. of Computer Science.
ON THE NUMERICAL SOLUTION OF TWO-POINT BOUNDARY VALUE PROBLEMS
Leslie Greengard and V. Rokhlin May 1989 32 p
(Contract N00014-89-J-1527)
(AD-A211244; YALEU/DCS/RR-692) Avail: NTIS HC A03/MF A01 CSCL 12/1

This paper, presents a new numerical method for the solution of linear two-point boundary value problems of ordinary differential equations. After reducing the differential equation to a second kind integral equation. The latter are discretized via a high order Nystrom scheme. A somewhat involved analytical apparatus is then constructed which allows for the solution of the discrete system using O(N x p2) operations, where N is the number of nodes on the interval and p is the desired order of convergence. Thus, the advantages of the integral equation formulation (small condition number, insensitivity to boundary layers, insensitivity to end-point singularities, etc.) are retained, while achieving a computational efficiency previously available only to finite difference or finite element methods. GRA

N90-11517# Yale Univ., New Haven, CT. Dept. of Computer Science.
THE FAST GAUSS TRANSFORM
Leslie Greengard and John Strain (New York Univ., New York.) Jul. 1989 20 p Sponsored in part by NSF, Washington, DC
(Contracts N00014-89-J-1527; F49620-87-C-0065; IBM-P00038437)
(AD-A211287; YALEU/DCS/RR-718) Avail: NTIS HC A03/MF A01 CSCL 12/1

Many problems in applied mathematics require the evaluation of the sum of N Gaussians at M points in space. The work required for direct evaluation grows like N M as N and M increase; this makes it very expensive to carry out such calculations on a large scale. In this paper, we present an algorithm which evaluates the sum of N Gaussians at M arbitrarily distributed points in C (dot) (N + M) work, where C depends only on the precision required. When N = M = 100,000, our algorithm is several thousand times faster than direct evaluation. It is based on a divide and conquer strategy, combined with the manipulation of Hermite expansions and Taylor series. GRA

N90-11518# Lawrence Livermore National Lab., CA.
COMPUTING THE TWO DIMENSIONAL FAST FOURIER TRANSFORM ON A GENERAL PURPOSE MESH CONNECTED MULTIPROCESSOR
E. M. Johansson, A. J. DeGroot, and S. R. Parker 1989 11 p Presented at the 12th SPIE Conference on Real-Time Signal Processing, San Diego, CA, 10-11 Aug. 1989
(Contract W-7405-eng-48)
(DE89-016515; UCRL-100283; CONF-8908130-1) Avail: NTIS HC A03/MF A01

This paper discusses an implementation of the two dimensional fast Fourier transform (FFT) on SPRINT, the Systolic Processor with a Reconfigurable Interconnection Network of Transputers. SPRINT is a 64 element multiprocessor developed at Lawrence Livermore National Laboratory for the experimental evaluation of systolic algorithms and architectures. The implementation is a radix two decimation in time algorithm, valid for an arbitrary sized p times q mesh of processors and an arbitrary sized P times Q complex input array (P, Q, p, and q must all be powers of two). The processors are interconnected with their nearest neighbors along North-South-East-West communication links. The problems of array partitioning, bit reversal, sub-array transform computation, and weighed (butterfly) combinations are all discussed. Finally, benchmark results are presented, and speedup and efficiency are discussed. DOE

N90-11519# Lawrence Livermore National Lab., CA.
DOMAIN DECOMPOSITION FOR PARTIAL DIFFERENTIAL EQUATIONS Ph.D. Thesis - California Univ., Davis
Louise Perkins 1989 56 p
(Contract W-7405-eng-48)
(DE89-016669; UCID-21695) Avail: NTIS HC A04/MF A01

A cursory look is given at partial differential equations and methods of solving them on digital computers. A brief discussion if presened of mapping complex geometric domains to simpler ones. The second chapter is a discussion about domain decomposition and it's current directions. Chapter three introduces some of the physical Fluid Dynamics problems. Chapters four and five discuss current research work in domain decomposition for elliptic and hyperbolic equations. DOE

N90-11520# Lawrence Livermore National Lab., CA.
AN INTERACTIVE PROGRAM FOR CONSTRAINED SPLINE APPROXIMATION OF NUMERICAL DATA
Donald E. Amos Jul. 1989 32 p
(Contract DE-AC04-76DP-00789)
(DE89-016674; SAND-88-1218) Avail: NTIS HC A03/MF A01

A portable FORTRAN program for (weighted) least squares curve fitting of data using piecewise cubic polynomials is presented. Menu options for equality and inequality constraints can be applied to produce smooth curves whose first and second derivatives match qualitative aspects of the data. Addition and deletion of knots by menu selection allows considerable flexibility. The code is distributed on a 360K-formatted diskette. A PC with a FORTRAN compiler will suffice to execute the code. DOE

N90-11521# Department of Energy, Washington, DC. Scientific Computing Staff.
SUMMARIES OF THE FY 1989 APPLIED MATHEMATICAL SCIENCES RESEARCH PROGRAM
Sep. 1989 62 p
(DE89-016694; DOE/ER-0422) Avail: NTIS HC A04/MF A01

This report is a compilation of summaries of the individual research projects that constitute the Applied Mathematical Sciences research subprogram managed by the Director, Scientific Computing Staff in the Office of the Director of Energy Research, U.S. Department of Energy. Major topics covered are: analytical and numerical methods; information analysis and display; advanced computing concepts; energy sciences advanced computation; and capital equipment for national laboratories. DOE

N90-11522# Illinois Univ., Urbana. Dept. of Computer Science.
GENERALIZED BDF (BACKWARD DIFFERENTIATION FORMULA) METHODS APPLIED TO HESSENBERG FORM DAES Ph.D. Thesis
Jerry Bruce Keiper Aug. 1989 113 p
(Contract DE-FG02-87ER-25026)
(DE89-017328; DOE/ER-25026/33; UIUCDCS-R-89-1534; UILU-ENG-89-1753) Avail: NTIS HC A06/MF A01

We study the numerical solution of Hessenberg form differential algebraic equations by variable stepsize generalized backward difference formulae (GBDF). GBDF methods of sufficiently high order are shown to converge for problems of index two, three, or four. The proof techniques developed are not sufficiently powerful to show convergence for index five problems. In addition we perform very high precision numerical experiments on problems of index two, three, four, and five using the standard six step backward difference formula. The experiments confirm the analysis regarding the error behavior of the index two and three problems, but suggest that the analysis of the index four problem is too pessimistic. It appears from the experiments that index five problems can also be solved by GBDF methods. DOE

N90-11523# Illinois Univ., Urbana. Dept. of Computer Science.
POTENTIAL FOR PARALLELISM IN EXPLICIT LINEAR METHODS
Robert D. Skeel and Hon-Wah Tam Jul. 1989 11 p Presented at the Conference on Computational Ordinary Differential Equations, London, England, 3-7 Jul. 1989
(Contract DE-FG02-87ER-25026)
(DE89-017329; DOE/ER-25026/32; CONF-8907106-3) Avail: NTIS HC A03/MF A01

Numerical methods for ordinary initial value problems that do not depend on special properties of the system are usually found in the class of linear multi-stage multi-value methods, first formulated by J.C. Butcher. Among these the explicit methods are easiest to implement. For these reasons there has been considerable research activity devoted to generating methods of this class which utilize independent function evaluations that can be performed in parallel. Each such group of concurrent function evaluations can be regarded as a stage of the method. It turns out that parallelism afford only limited opportunity for reducing the computing time with such methods. This is most evident for the simple linear homogenous constant coefficient test problem, which is essentially a matter of approximating the exponential by an algebraic function. For a given number of stages and a given number of saved values, parallelism offers a somewhat enlarged set of algebraic functions from which to choose. However there is absolutely no benefit in having the degree of parallelism (number of processors) exceed the number of saved values of the method. Thus, in particular, parallel one-step methods offer no speedup over serial one-step methods for the standard linear test problem. Because of the fairly remarkable modelling ability of the standard test problem, one should not expect much better speedups for general nonlinear problems. DOE

N90-11524# Joint Inst. for Nuclear Research, Dubna (USSR). Lab. of Theoretical Physics.
SOME EXACT SOLUTIONS OF THE THREE-IDENTICAL-PARTICLE PROBLEM WITH S-WAVE INVERSE SQUARE POTENTIALS
V. V. Pupyshev 1988 7 p Submitted for publication
(DE89-618402; JINR-E-5-88-456) Avail: NTIS (US Sales Only) HC A02/MF A01

The existence criterion of exact solutions to the Schroedinger equation as a product of the Bessel function of the hyperradius and a finite sum hyperharmonics is proved within the Faddeev integrodifferential approach. DOE

N90-11525# Joint Inst. for Nuclear Research, Dubna (USSR). Lab. of Theoretical Physics.
ON SOME STOCHASTIC PROPERTIES OF THE INFINITELY DIMENSIONAL HAMILTONIAN SYSTEMS OF CLASSICAL MECHANICS
D. P. Sankovich 1988 10 p In RUSSIAN; ENGLISH summary
(DE89-618403; JINR-R-17-88-349) Avail: NTIS (US Sales Only) HC A02/MF A01

Some simplest systems of the classical 1-D field theory is considered. For the nonlinear Schroedinger model the kinetic and hydrodynamic equations are obtained. For the 1-D Ginzburg-Landau type system by Bogolubov inequality the lower bound for the pair correlation function and average total momentum is obtained. In case of the cubic non-linearity (KdV-model), a hydrodynamic interpretation is attempted of the conservation laws and reductions which arised in the model. DOE

N90-11526# Universiteit Twente, Enschede (Netherlands). Dept. of Computer Science.
BACKWARD ANALYSIS ON HIGHER ORDER FUNCTIONS
G. F. v.d.Hoeven and M. Ramaer Apr. 1989 23 p
(Memo-INF-89-19; ISSN-0923-1714; ETN-89-95069) Avail: NTIS HC A03/MF A01

The problem of strictness analysis is considered through a backward analysis technique, especially for higher functions. A two step method is proposed to avoid the exponential increase of complexity of the analysis in the presence of such functions. The presentation of the method is reviewed for flat domains and lists. Consideration of strictness analysis is strongly operational but is found to be more intuitively appealing, especially from an implementation viewpoint, without formal loss of rigor. ESA

N90-11527# Universiteit Twente, Enschede (Netherlands). Dept. of Computer Science.
AN AXIOMATIC THEORY FOR PARTIAL FUNCTIONS
Jan Kuper Mar. 1989 48 p Submitted for publication
(Memo-INF-89-22; ISSN-0923-1714; ETN-89-95070) Avail: NTIS HC A03/MF A01

An axiomatic theory for the concept of one-place, partial functions, where a function is taken in its extensional sense, is described. The structure of such a theory can be rather like ZF set theory. The equi-consistency of the theory with ZF set theory is shown and some commonly applied mechanisms for functions are derived. The theory is described in the language of classical first order predicate logic with equality and one non-logical predicate symbol for function application. By means of some notational conventions, a method within this logic to handle undefinedness in a natural way is developed. ESA

N90-11528# Center for Mathematics and Computer Science, Amsterdam (Netherlands). Dept. of Computer Science.
AN INTERPOLATION THEOREM IN EQUATIONAL LOGIC
P. H. Rondenburg (Amsterdam Univ., Netherlands) and R. J. vanGlabbeek Oct. 1988 16 p Sponsored in part by the Dutch Stimulerings Projectteam Informatica-Onderzoek and the Commission of the European Communities ESPRIT Project METEOR
(CWI-CS-R8838; ETN-89-95097) Copyright Avail: NTIS HC A03/MF A01

In pronouncement on the behavior of equational logic with respect to interpolation, a suitable statement of Craig's lemma as a proposition about first order logic, must be found. Using a natural formulation, Craig's interpolation theorem is shown to hold for equational logic. Prevalent claims that equational logic does not have the interpolation property are discussed. ESA

N90-11529# Center for Mathematics and Computer Science, Amsterdam (Netherlands). Dept. of Numerical Mathematics.
NOTE ON EXPLICIT PARALLEL MULTISTEP RUNGE-KUTTA METHODS
P. J. vanderHouwen, B. P. Sommeijer, and P. A. vanMourik Nov. 1988 13 p
(CWI-NM-R8814; ETN-89-95104) Copyright Avail: NTIS HC A03/MF A01

A family of explicit two-step, two-stage Runge-Kutta methods is investigated in which the two righthand side evaluations can be computed in parallel, so that effectively only one righthand side evaluation per step is required. This family is compared with the family of explicit linear two-step methods of Adams type. Examples of methods with increased stability intervals and methods with increased order of accuracy are given. These methods are applied to test problems taken from the test set of Hull et al. and compared with conventional linear multistep methods. A rather general class of k-step, m-stage Runge-Kutta methods in which the m righthand side evaluations can also be computed in parallel is described. Derivation of the order equations and stability region is described. ESA

N90-11530# Center for Mathematics and Computer Science, Amsterdam (Netherlands). Dept. of Numerical Mathematics.
ON THE EQUIVALENCE OF BS-STABILITY AND B-CONSISTENCY
W. H. Hundsdorfer and J. Schneid (Technische Univ., Vienna, Austria) Nov. 1988 10 p Sponsored in part by the Fonds zur Foerderung des wissenschaftlichen Forschung, Vienna, Austria
(CWI-NM-R8815; ETN-89-95105) Copyright Avail: NTIS HC A02/MF A01

Several stability and consistency concepts for Runge-Kutta methods are applied to stiff initial value problems. BS-stability and B-consistency are shown to be equivalent for initial value problems with a one-sided Lipschitz constant greater than or equal to zero. The same is shown to hold for their internal counterparts. ESA

N90-11003# Rome Univ. (Italy). Dipt. Aerospaziale.
ANALYTIC SIGNALS IN THE DAMPING COEFFICIENT ESTIMATION
Alessandro Agenni and Luigi Balis Crema *In* ESA, Spacecraft Structures and Mechanical Testing Jan. 1989 p 133-139 Sponsored in part by the Italian Ministry of Public Education (For primary document see N90-10986 02-18)
(Grant CNR-85/01244/11)
Copyright Avail: NTIS HC A99/MF E06

65 STATISTICS AND PROBABILITY

Includes data sampling and smoothing; Monte Carlo method; and stochastic processes.

N90-11531# Princeton Univ., NJ. Dept. of Statistics.
PROCEDURES FOR SEPARATIONS WITHIN BATCHES OF VALUES, 1. THE ORDERLY TOOL KIT AND SOME HEURISTICS Technical Report No. 293
Thu Hoang (Paris V Univ., France) and John W. Tukey Mar. 1989 109 p
(Contract DAAL03-86-K-0073)
(AD-A210652; TR-293; ARO-23360.12-MA) Avail: NTIS HC A06/MF A01 CSCL 12/3

First of several reports studying techniques to answer the question of the desirability of treating this batch of values together, or to separate them into at least two parts (called below the canyon problem). The focus is on tools to help answer the question, primarily on the orderly tool kit in which the simple general properties of order statistics from any reasonable distribution are identified and arranged for use. Once the values of a set of observations are ordered, attention needs to shift from values to gaps (differences of adjacent ordered values). Rescaling gaps toward a common scale allows easy combination into measures of spread. Like other measures of spread, these measures of spread are well described in terms of degrees of freedom, which can be defined for both linear and quadratic expressions. (Linear d.f. will be slightly less than 4 times quadratic d.f.) It can be natural and useful to order the rescaled gaps, when dealing with gaps of rescaled gaps. (Various quantitative matters are also addressed.) Application of the orderly tool kit to the canyon problem leads to test statistics for whose distribution a well-chosen F-distribution is a natural approximation. While the orderly tool kit provides a rough idea of the power of the procedure, simulation will be required to anchor and modify the approximation. GRA

N90-11532# Texas A&M Univ., College Station. Dept. of Statistics.
BOUNDARY KERNEL ESTIMATION OF THE TWO SAMPLE COMPARISON DENSITY FUNCTION
William P. Alexander May 1989 250 p
(Contract DAAL03-87-K-0003; AF Proj. 5641)
(AD-A210757; TR-56; ARO-23010.5-MA) Avail: NTIS HC A11/MF A02 CSCL 12/3

The focus of this work is to derive functional and graphical statistical techniques for the two sample problem suitable for

implementation in modern computing environments. In the two sample problem, it is desired to test the null hypothesis that two independent random samples have a common distribution function. Assuming certain conditions on the distribution functions, a procedure is proposed which has strong graphical elements, a sound theoretical foundation, and estimates the relation of the two distributions if the null hypothesis is rejected. The proposed procedure has as its motivation the estimation of the comparison density and inference concerning its uniformity. GRA

N90-11533# Naval Underwater Systems Center, New London, CT.
ALIAS-FREE WIGNER DISTRIBUTION FUNCTION AND COMPLEX AMBIGUITY FUNCTION FOR DISCRETE-TIME SAMPLES
Albert H. Nuttall 14 Apr. 1989 94 p
(AD-A211050; NUSC-TR-8533) Avail: NTIS HC A05/MF A01 CSCL 12/3

If an arbitrary complex continuous waveform s(t) with finite overall frequency extent F Hertz is sampled with time increment Delta is less than 1/F, the aliasing can be controlled and the continuous time waveform s(t) reconstructed exactly at any desired time instant from waveform samples (s(kDelta)). On the other hand, it is commonly believed that aliasing of the corresponding Wigner distribution function (WDF) can only be avoided by sampling twice as fast; i.e., Delta is less than 1/(2F) is thought to be required. Alternatively, interpolation of the time data has been suggested as a means of circumventing aliasing of the WDF; however, the computational burden has proven excessive if done by sinc function interpolation. It is demonstrated here that this conjecture is false, and that the usual sampling criterion, Delta is less than 1/F, suffices for exact reconstruction of the original continuous WDF, as well as the complex ambiguity function (CAF), at all time, frequency locations, without an excessive amount of computational effort. GRA

N90-11534# Stanford Univ., CA. Dept. of Statistics.
AN EXTENSION OF COCHRAN'S TEST FOR HOMOGENEITY OF VARIANCES
Herbert Solomon and M. A. Stephens 8 Aug. 1989 34 p
(Contract N00014-89-J-1627; NR Proj. 042-267)
(AD-A211054; TR-419) Avail: NTIS HC A03/MF A01 CSCL 12/3

Cochran's test for equality of k normal population variances consists of comparing the largest of the set of k sample variances, all based on the same number of degrees of freedom n, with the sum of the sample variances. More generally, it may sometimes be advantageous to compare the m-th largest sample variance with the total. GRA

N90-11535# Universiteit Twente, Enschede (Netherlands). Dept. of Computer Science.
FIXED POINT ITERATION ON POINT-SYMMETRIC INTERFERENCE GRAPHS
J. Peter Veltkamp (Technische Univ., Eindhoven, Netherlands) and Ruud vanDamme Mar. 1989 30 p
(Memo-INF-89-23; ISSN-0923-1714; ETN-89-95071) Avail: NTIS HC A03/MF A01

Interference graphs are used for performance analysis of multiprocessor interconnection networks. In order to model blocked transmissions, nodes can have three states: idle, active or blocked. The resulting steady state probability distribution has a non-product form. Macro states are introduced to calculate performance measures, and the corresponding macro state probability distribution is approximated by a special type of fixed point iteration: the macro-approximation, which proves to be very efficient for point-symmetic interference graphs. ESA

N90-11536# Center for Mathematics and Computer Science, Amsterdam (Netherlands). Dept. of Computer Science.
PARTIALLY SPECIFIED PROBABILITY MEASURES IN EXPERT SYSTEMS
L. C. vanderGaag Oct. 1988 24 p
(CWI-CS-R8842; ETN-89-95099) Copyright Avail: NTIS HC A03/MF A01

Plausible reasoning as an important issue in expert systems research and artificial intelligence research in general is discussed. Bayesian probability theory as a foundation for the development of models for handling uncertain information in expert systems is addressed and the availability of a fully specified probability measure in the problem domains in which expert systems are developed is considered. A model is presented in which partially and even inconsistently specified probability measures are employed to establish upper and lower bounds on probability of interest. ESA

66 SYSTEMS ANALYSIS

Includes mathematical modeling; network analysis; and operations research.

N90-11537# Swedish Defence Research Establishment, Linkoeping. Dept. of Information Technology.
LINKOEPING'S A.I. CONSORTIUM (LAIC) FOR PLAN GUIDED SYSTEMS. REVIEW OF THE FIRST 18 MONTHS Progress Report, 1 Jul. 1987 - 31 Dec. 1988
Erik Sandewall, ed. Apr. 1989 25 p In SWEDISH; ENGLISH summary
(FOA-C-30528-3.4; LAIC-IDA-89-B1; LAIC-IDA-89-B2; ISSN-0347-3708; ETN-89-95172) Avail: NTIS HC A03/MF A01

An overview of the activities is given. An analysis of the traffic in the streets, crossings, and strategies for vehicle maneuvers is presented, based on the ETL method (Explicit Temporal Logic) created in 1988. A chapter is related to itinerary planning, which requires another design of map data structures. Even maps in three dimensions are suggested, altitude being important. Planning may be considered also for aircrafts, as a study proposes a system for a real-time planning agent in an autonomous aircraft. For interpreting the multisensors data, which is often incomplete, methods for uncertain reasoning may be used. Algorithms for the analysis of the planning are also treated, with the aid of the ETL method. ESA

67 THEORETICAL MATHEMATICS

Includes topology and number theory.

N90-11538# Massachusetts Inst. of Tech., Cambridge. Center for Theoretical Physics.
SINGULARITY THEORY AND N = 2 SUPERCONFORMAL FIELD THEORIES
N. P. Warner 1989 7 p Presented at the Superstring '89 Workshop, College Station, TX, 13-18 Mar. 1989
(Contract DE-AC02-76ER-03069)
(DE89-016582; CONF-8903130-2; CTP-1745) Avail: NTIS HC A02/MF A01

The N = 2 superconformal field theories that appear at the fixed points of the renormalization group flows of Landau-Ginsburg models are discussed. Some of the techniques of singularity theory are employed to deduce properties of these superconformal theories. These ideas are then used to deduce the relationship between Calabi-Yau compactifications and tensored discrete series models. The chiral rings of general N = 2 superconformal theories are also described. DOE

N90-11539# International Centre for Theoretical Physics, Trieste (Italy).
S7 WITHOUT ANY CONSTRUCTION OF LIE GROUP
Jian Zhou (Academia Sinica, Hefei, China) and Senlin Xu Dec. 1988 7 p

(DE89-618380; IC-88/404) Avail: NTIS (US Sales Only) HC A02/MF A01

It was proved that the sphere S sup n is a parallelizable manifold if and only if n = 1, 3, or 7, and that S sup n is an H-space if and only if n = 0, 1, 3, or 7. Because a Lie group must necessarily be a parallelizable manifold and also an H-space, naturally it is asked that S sup n is a Lie group for n = 0, 1, 3, or 7. It is proven that S sup 7 is not a Lie group, and it is not even a topological group. Therefore, S sup n is a Lie group (or a topological group) if and only if n = 0, 1, 3. DOE

N90-11540# International Centre for Theoretical Physics, Trieste (Italy).

MARKOV PROCESSES IN HILBERT SPACE AND CONTINUOUS SPONTANEOUS LOCALIZATION OF SYSTEMS OF IDENTICAL PARTICLES

Gian Carlo Ghirardi, Philip Pearle, and Alberto Rimini (Pavia Univ., Italy) Mar. 1989 28 p Prepared in cooperation with Trieste Univ. (Italy) Sponsored by Istituto Nazionale di Fisica Nucleare Sezioni di Pavia e Trieste

(DE89-618396; IC-89/44) Avail: NTIS (US Sales Only) HC A03/MF A01

Stochastic differential equations describing the Markovian evolution of state vectors in the quantum Hilbert space are studied as possible expressions of a universal dynamical principle. The general features of the considered class of equations as well as their dynamical consequences are investigated in detail. The stochastic evolution is proved to induce continuous dynamical reduction of the state vector onto mutually orthogonal subspaces. A specific choice, expressed in terms of creation and annihilation operators, of the operators defining the Markov process is then proved to be appropriate to describe continuous spontaneous localization of systems of identical particles. The dynamics obtained in such a way leaves practically unaffected the standard quantum evolution of microscopic systems and induces a very rapid suppression of coherence among macroscopically distinguishable states. The classical behaviour of macroscopic objects as well as the reduction of the wave packet in a quantum measurement process can be consistently derived from the postulated universal dynamical principle. DOE

N90-11541# Joint Inst. for Nuclear Research, Dubna (USSR). Lab. of Theoretical Physics.

REDUCTION OF THE DIRAC EQUATION TO THE DIRAC-KAEHLER EQUATION

A. B. Pestov, I. A. Satikov, and V. I. Strazhev 1988 4 p In RUSSIAN; ENGLISH summary

(DE89-630111; JINR-R-2-88-454) Avail: NTIS (US Sales Only) HC A01/MF A01

Relation is established between spinors of the space of dimensionality d=2 m and antisymmetric tensors of the space of dimensionality d=m. It is shown that there exists a dimensional reduction of the Dirac equation to the Dirac-Kahler equation. DOE

70 PHYSICS (GENERAL)

For precision time and time interval (PTTI) see *35 Instrumentation and Photography;* for geophysics, astrophysics or solar physics see *46 Geophysics, 90 Astrophysics,* or *92 Solar Physics.*

N90-11542 Texas Univ., Austin.

MAGNETICALLY LEVITATED MICRO-ROBOTICS Ph.D. Thesis

Ronald Edward Pelrine 1988 199 p

Avail: Univ. Microfilms Order No. DA8909721

The use of magnetic levitation (maglev) as a microrobot drive is examined theoretically and experimentally. Microrobots are small, programmable, multi-degree of freedom mechanical devices. Maglev drive appears capable of addressing a number of important microrobotics issues, including friction, wear, material transport, and ability to tolerate adverse environments. These issues, often involving problems beyond the technical feasibility of single microrobots, must be dealt with effectively in order to realize the goal of low cost, integrated, multi-manipulator systems operating on small scales. Maglev microrobot drive is compared with other possible microrobot drives, particularly electrostatic drive. Various magnetic levitation systems are examined next, showing the rich variety of possible maglev microrobots. Out of 48 physically distinct maglev drive systems, the focus is narrowed using the requirements of an integrated micro-factory (IMF). These requirements suggest that at the present level of technical development the maglev system of primary interest is one which uses air core electromagnets driving a permanent magnet manipulator. Various air core electromagnets are discussed, including planar electromagnets suitable for a high level of silicon integration. Several force/torque environments are considered, such as solid and liquid surfaces. These different environments primarily affect the control strategy's performance and requirements, such as the ability to operate in open loop modes. The analysis was used to build a number of experimental prototypes, including a planar type, 1-D manipulator transport path, and 4. degree of freedom microrobots capable of 0.5 micron resolutions. Finally, future trends in the field such as superconductive systems are discussed. Dissert. Abstr.

N90-11543# Sandia National Labs., Albuquerque, NM. Applied Mechanics Div.

DMC (DISTINCT MOTION CODE): A RIGID BODY MOTION CODE FOR DETERMINING THE INTERACTION OF MULTIPLE SPHERICAL PARTICLES

L. M. Taylor and D. S. Preece Jul. 1989 38 p

(Contract DE-AC04-76DP-00789)
(DE89-016929; SAND-88-3482) Avail: NTIS HC A03/MF A01

The computer program Distinct Motion Code (DMC) determines the two-dimensional planar rigid body motion of an arbitrary number of spherical shaped particles. The code uses an explicit central difference time integration algorithm to calculate the motion of the particles. Contact constraints between the particles are enforced using the penalty method. Coulomb friction and viscous damping are included in the collisions. The explicit time integration is conditionally stable with a time increment size which is dependent on the mass of the smallest particle in the mesh and the penalty stiffness used for the contact forces. The code chooses the spring stiffness based on the Young's modulus and Poisson's ratio of the material. The ability to tie spheres in pairs with a constraint condition is included in the code. The code has been written in an extremely efficient manner with particular emphasis placed on vector processing. While this does not impose any restrictions on non-vector processing computers, it does provide extremely fast results on vector processing computers. A bucket sorting or boxing algorithm is used to reduce the number of comparisons which must be made between spheres to determine the contact pairs. The sorting algorithm is completely algebraic and contains no logical branching. DOE

N90-11544# Los Alamos National Lab., NM.

A SOLUTION TO NONLINEARITY PROBLEMS

David V. Neuffer 1989 7 p Presented at the International Conference on High Energy Accelerators, Tsukuba, Japan, 20-26 Aug. 1989

(Contract W-7405-eng-36)
(DE89-016975; LA-UR-89-2795; CONF-890803-5) Avail: NTIS HC A02/MF A01

New methods of correcting dynamic nonlinearities resulting from the multipole content of a synchrotron or transport line are presented. In a simplest form, correction elements are places at the center (C) of the accelerator half-cells as well as near the focusing (F) and defocusing (D) quadrupoles. In a first approximation, the corrector strengths follow Simpson's Rule, forming an accurate quasi-local canceling approximation to the nonlinearity. The F, C, and D correctors may also be used to obtain precise control of the horizontal, coupled, and vertical motion. Correction by three or more orders of magnitude can be

obtained, and simple solutions to a fundamental problem in beam transport have been obtained. DOE

N90-11545# California Inst. of Tech., Pasadena. Lab. of Chemical Physics.
[ELECTRON TRANSFER REACTIONS] Final Report, 1 Dec. 1986 - 30 Nov. 1988
R. A. Marcus 24 Jul. 1989 4 p
(Contract N00014-87-K-0064)
(AD-A210711) Avail: NTIS HC A01/MF A01 CSCL 07/4

During the tenure of this contract research was performed on a number of aspects of electron transfer reactions (solvent dynamics including vibrational effects, non-Debye solvent dynamics, early steps in bacterial photosynthesis) and of the use of artificial intelligence searching methods, the latter, in part, as a prelude to our current study of electron transfer reactions in structurally complicated systems such as proteins. Seven Technical Reports were issued during this period, and research on several topics was initiated: the study of the relation between charge transfer absorption and fluorescence spectra and the inverted region, a nonadiabatic/adiabatic coherent mechanism for electron transfers, and electron transfers between two immiscible-liquid phases and between a semiconductor and an electrolyte. GRA

N90-11546# Los Alamos National Lab., NM.
MAGNETIC FLUX COMPRESSION
C. M. Fowler 1989 13 p Presented at the American Physical Society Topical Conference on Shock Compression of Condensed Matter, Albuquerque, NM, 14-17 Aug. 1989
(Contract W-7405-eng-36)
(DE89-016991; LA-UR-89-2656; CONF-890812-30) Avail: NTIS HC A03/MF A01

Magnetic Flux Compression, as treated in this paper, is accomplished by high explosives. Flux is first captured in a closed conducting circuit, of which some or all of the conducting elements are overlaid with high explosives. Upon detonation of the explosives, these elements are driven in such a fashion as to compress the flux into regions of smaller areas or, in engineering terminology, into regions of lower inductance. The magnetic energy associated with the flux is increased by the flux compression. The additional energy is ultimately supplied by the explosive as it drives the conductors against the magnetic field pressure, which in some cases may be in the megabar range. Various names in common use for flux compression devices are flux compression generators (FCG), magneto-cumulative generators (MCG), particularly in the USSR, or simply, flux compressors. FCGs are generally used in two broadly defined categories: as compact, high-power sources to drive various loads and as generators of very large magnetic fields. In this talk, general principles of flux compression are first discussed. This is followed by a description of several applications in which different types of FCGs are used to supply pulsed power to various devices. DOE

N90-11547# Brookhaven National Lab., Upton, NY. National Synchrotron Light Source.
X-RAY LITHOGRAPHY SOURCES: A REVIEW
James B. Murphy 1989 4 p Presented at the 13th Particle Accelerator Conference, Chicago, IL, 20-23 Mar. 1989
(Contract DE-AC02-76CH-00016)
(DE89-017610; BNL-42004; CONF-890335-251) Avail: NTIS HC A01/MF A01

Synchrotron radiation from dipole magnets in electron storage rings has emerged as a useful source of X-rays for lithography. To meet the need for these sources numerous groups around the world have embarked on projects to design and construct storage rings for X-ray lithography. Both conventional electromagnets as well as superconducting (SC) dipoles have been incorporated into the various designs. An overview of the worldwide effort to produce commercial X-ray sources will be presented. To better illustrate the elements involved in these sources a closer examination of the Superconducting X-ray Lithography Source Project (SXLS) at BNL will be presented. DOE

N90-11548# Academy of Sciences (USSR), Novosibirsk. Inst. Yadernoj Fiziki.
RESONANCE EFFECT ON THE OSCILLATOR DISTRIBUTION FUNCTION
A. L. Gerasimov 1988 16 p In RUSSIAN
(DE89-630105; IYaF-88-34) Avail: NTIS (US Sales Only) HC A03/MF A01

A problem on the equilibrium distribution function (EDF) of a multi-dimensional non-linear oscillator with external perturbation, periodic in time, in the presence of dissipation and external noise is considered. A situation with the resonance of an arbitrary (indefinitely low) V(sub e) harmonic is considered. The Fokker-Planck equation is used as a model. It is shown that the resonance starts to effect the EDF exponential tails only when its width p(sub r) becomes of the order of the noise force. DOE

71 ACOUSTICS

Includes sound generation, transmission and attenuation. For noise pollution see *45 Environmental Pollution.*

N90-11549*# General Electric Co., Cincinnati, OH. Advanced Engineering Technologies Dept.
AN INVESTIGATION OF COUNTERROTATING TIP VORTEX INTERACTION
R. K. Majjigi, K. Uenishi, and P. R. Gliebe Oct. 1989 124 p
(Contract NAS3-24080)
(NASA-CR-185135; NAS 1.26:185135) Avail: NTIS HC A06/MF A01 CSCL 20A

A tip vortex interaction model originally developed for compressors has been extended and adapted for use with counterrotating open rotors. Comparison of available acoustic data with predictions (made with and without the tip vortex model included) illustrate the importance of this interaction effect. This report documents the analytical modeling, a limited experimental verification, and certain key parametric studies pertaining to the tip vortex as a noise source mechanism for the unsteady loading noise of counterrotating properllers. Author

N90-11550# Texas Univ., Austin. Applied Research Lab.
NONLINEAR ACOUSTICS: REFLECTION AND REFRACTION, PROPAGATION IN A PERIODIC WAVEGUIDE, SCATTERING OF SOUND BY SOUND AND ELLIPSOIDAL FOCUSING Annual Summary Report No. 1, 1 Oct. 1988 - 30 Sep. 1989
David T. Blackstock 31 Jul. 1989 30 p
(Contract N00014-89-J-1109)
(AD-A211224; ARL-TR-89-38) Avail: NTIS HC A03/MF A01 CSCL 20/1

Reflection and refraction of plane finite amplitude waves at a plane interface between two fluids. The nonlinear equation for 3-D waves in a thermoviscous, relaxing fluid was derived. A second order perturbation solution was obtained for the reflection-refraction problem for the case of lossless fluid and an arbitrary source signal. Propagation was measured in a plane wave tube loaded periodically with reactive branch elements. Experiments with small-signal waves verify in fine detail the dispersion relation that has been derived earlier (and this year modified to include thermoviscous boundary layer effects and the end correction for the branch elements). Development of an experimental facility with which to perform single beam and crossed beams experiments in the megahertz range is in progress. Ellipsoidal focusing has applications to lithotripsy. The experiments are carried out in air. An electric spark located at the near focus of an ellipsoidal reflector generates an N wave. The reflector concentrates the sound at the remote focus. Near the reflector the reflected pulse is N shaped, but strong interaction of nonlinear distortion and focusing (and to some extent diffraction) produces gross changes in the waveform as the pulse travels to the remote focus and beyond. GRA

N90-11551# Pennsylvania State Univ., University Park. Dept. of Physics.
ACOUSTIC STUDIES OF NEW MATERIALS: QUASICRYSTALS, LOW-LOSS GLASSES AND HIGH Tc SUPERCONDUCTORS Annual Summary Report, 1 Oct. 1988 - 30 Sep. 1989
Julian D. Maynard 1 Aug. 1989 19 p
(Contract N00014-85-K-0701)
(AD-A211281) Avail: NTIS HC A03/MF A01 CSCL 20/1

The goals of this project involve the development and application of new techniques in acoustics. The goals are: (1) to study the properties of single crystal high temperature superconductor oxide materials with ultrasonic measurements; (2) to study the properties of quasicrystals using ultrasound and acoustic analog systems; and (3) to develop and apply a new resonant photoacoustic technique to measure optical absorption in very low-loss glasses and crystals. Major accomplishments include the development of a new method of ultrasound measurement which permits the determination of all of the independent elastic constants of very small samples (a few hundred microns in size), and the development and test of a new technique for measuring optical absorption with more than an order of magnitude improvement in sensitivity over existing methods.
GRA

N90-11009# Aeronautical Research Inst. of Sweden, Bromma.
CALCULATION OF SOUND TRANSMISSION THROUGH A CYLINDRICAL SHELL USING ASKA ACOUSTICS
P. Goransson *In* ESA, Spacecraft Structures and Mechanical Testing Jan. 1989 p 175-180 (For primary document see N90-10986 02-18)
Copyright Avail: NTIS HC A99/MF E06

N90-11010# Centre National d'Etudes Spatiales, Toulouse (France).
ACOUSTIC RESPONSE ANALYSIS IN THE LOW FREQUENCY DOMAIN
F. Mercier, D. Gangloff, and A. Mamode *In* ESA, Spacecraft Structures and Mechanical Testing Jan. 1989 p 181-185 (For primary document see N90-10986 02-18)
Copyright Avail: NTIS HC A99/MF E06

72 ATOMIC AND MOLECULAR PHYSICS

Includes atomic structure, electron properties, and molecular spectra.

N90-11552*# Eloret Corp., Sunnyvale, CA.
THEORETICAL INVESTIGATION OF GAS-SURFACE INTERACTIONS Progress Report, 1 Sep. 1988 - 31 Jan. 1989
Timothy J. Lee 31 Jan. 1989 58 p
(Contract NCC2-552)
(NASA-CR-185492; NAS 1.26:185492) Avail: NTIS HC A04/MF A01 CSCL 20H

Four reprints are presented from four projects which are to be published in a refereed journal. Two are of interest to us and are presented herein. One is a description of a very detailed theoretical study of four anionic hydrogen bonded complexes. The other is a detailed study of the first generally reliable diagnostic for determining the quality of results that may be expected from single reference based electron correlation methods. For individual titles, see N90-11553 through N90-11554.

N90-11553*# Eloret Corp., Sunnyvale, CA.
A HIGH LEVEL Ab INITIO STUDY OF THE ANIONIC HYDROGEN-BONDED COMPLEXES FH-CN-, FH-NC-, H2O-CN- AND H2O-NC-
Timothy J. Lee *In its* Theoretical Investigation of Gas-Surface Interactions 31 Jan. 1989 p 1-42 Prepared in cooperation with University Chemical Labs., Cambridge (England) (For primary document see N90-11552 02-72)
Avail: NTIS HC A04/MF A01 CSCL 20H

HF, H2O, CN- and their hydrogen-bonded complexes were studied using state-of-the-art ab initio quantum mechanical methods. A large Gaussian one particle basis set consisting of triple zeta plus double polarization plus diffuse s and p functions (TZ2P + diffuse) was used. The theoretical methods employed include self consistent field, second order Moller-Plesset perturbation theory, singles and doubles configuration interaction theory and the singles and doubles coupled cluster approach. The FH-CN- and FH-NC- and H2O-CN-, H2O-NC- pairs of complexes are found to be essentially isoenergetic. The first pair of complexes are predicted to be bound by approx. 24 kcal/mole and the latter pair bound by approximately 15 kcal/mole. The ab initio binding energies are in good agreement with the experimental values. The two being shorter than the analogous C-N hydrogen bond. The infrared (IR) spectra of the two pairs of complexes are also very similar, though a severe perturbation of the potential energy surface by proton exchange means that the accurate prediction of the band center of the most intense IR mode requires a high level of electronic structure theory as well as a complete treatment of anharmonic effects. The bonding of anionic hydrogen-bonded complexes is discussed and contrasted with that of neutral hydrogen-bonded complexes.
Author

N90-11554*# Eloret Corp., Sunnyvale, CA.
A DIAGNOSTIC FOR DETERMINING THE QUALITY OF SINGLE-REFERENCE ELECTRON CORRELATION METHODS
Timothy J. Lee and Peter R. Taylor *In its* Theoretical Investigation of Gas-Surface Interactions 31 Jan. 1989 p 1-15 Prepared in cooperation with NASA. Ames Research Center, Moffett Field, CA (For primary document see N90-11552 02-72)
Avail: NTIS HC A04/MF A01 CSCL 20H

It was recently proposed that the Euclidian norm of the t sub 1 vector of the coupled cluster wave function (normalized by the number of electrons included in the correlation procedure) could be used to determine whether a single-reference-based electron correlation procedure is appropriate. This diagnostic, T sub 1, is defined for use with self consistent field molecular orbitals and is invariant to the same orbital rotations as the coupled cluster energy. T sub 1 is investigated for several different chemical systems which exhibit a range of multireference behavior, and is shown to be an excellent measure of the importance of nondynamical electron correlation and is far superior to C sub 0 from a singles and doubles configuration interaction wave function. It is further suggested that when the aim is to recover a large fraction of the dynamical electron correlation energy, a large T sub 1 (i.e., greater than 0.02) probably indicates the need for a multireference electron correlation procedure.
Author

N90-11555# Lund Univ. (Sweden). Cosmic and Subatomic Physics.
GLOBAL AND LOCAL FLUCTUATIONS IN MULTIPLICITY AND TRANSVERSE ENERGY FOR CENTRAL ULTRA-RELATIVISTIC HEAVY-ION INTERACTIONS
R. Albrecht, T. C. Awes, C. Baktash, P. Beckmann, F. Berger, R. Bock, G. Claesson, G. Clewing, L. Dragon (Muenster Univ., Germany, F.R.), and A. Eklund et al May 1989 19 p
(LUIP-8903; LUNFD6/(NFFK-7100)1-18(1989); ISSN-0348-9329)
Avail: NTIS HC A03/MF A01

The results are presented from a comparison between experimental data and model calculations, in this case represented by the Fritiof model, regarding global and local fluctuations in the distributions of transverse energy and charged particle multiplicity. The results indicate that the observed fluctuations originate predominantly from the distribution of sources, i.e., either the number of participating nucleons or the number of binary collisions. The apparently larger widths of the distributions observed in restricted regions of phase space, are explained to be of purely statistical nature. As a result of the analysis the cross section for events with energy densities much larger than the typical value for a central collision is limited. The results of the analysis are essentially independent of whether intermittence is of importance in the reactions or not. The very small scales, normally associated with studies of intermittent behavior, are not within the scope of this study.
Author

N90-11556# Rice Univ., Houston, TX.
STUDIES OF ULTRATHIN MAGNETIC FILMS AND PARTICLE-SURFACE INTERACTIONS WITH SPIN-SENSITIVE ELECTRON SPECTROSCOPIES Progress Report, 1 Jan. 1989 - 30 Nov. 1989
G. K. Walters and F. B. Dunning Aug. 1989 9 p
(Contract DE-FG05-86ER-45233)
(DE89-016741; DOE/ER-45233/4) Avail: NTIS HC A02/MF A01

Investigations were made of: spin-exchange in electron scattering from nonmagnetic metallic surfaces by means of Spin-Polarized Electron Energy Loss Spectroscopy (SPEELS); and magnetic properties of the Fe(110) surface, and the effect of an oxygen overlayer, utilizing Spin-Polarized Metastable Atom De-excitation Spectroscopy (SPMDS). DOE

N90-11557# Los Alamos National Lab., NM.
STRUCTURE AND PROPERTIES OF SIMPLE MOLECULAR SYSTEMS AT VERY HIGH DENSITY
Richard LeSar 1989 8 p Presented at the AIRAPT and EHPRG International High Pressure Science and Technology Conference, Paderborn, Fed. Republic of Germany, 17-21 Jul. 1989
(Contract W-7405-eng-36)
(DE89-016974; LA-UR-89-2798; CONF-890798-10) Avail: NTIS HC A02/MF A01

The use of computer simulations in the study of molecular systems at very high density is reviewed. Applications to the thermodynamics of dense fluid nitrogen and phase transitions in solid oxygen are presented. The effects of changes in the atomic electronic structure on the equation of state of very dense helium are discussed. DOE

N90-11558# Lawrence Livermore National Lab., CA.
NEW THEORETICAL APPROACHES FOR STUDYING ELECTRON COLLISIONS WITH SMALL MOLECULES
T. N. Rescigno Jun. 1989 8 p Presented at the NATO Advanced Study Institute on Non-Equilibrium Processes in Partially Ionized Gases, Acquafredda di Maratea, Italy, 4-17 Jun. 1989
(Contract W-7405-eng-48)
(DE89-017543; UCRL-101228; CONF-890697-3) Avail: NTIS HC A02/MF A01

There has been a recent resurgence of interest in the use of algebraic variational methods for studying a variety of collision problems. Much of this interest stems from the discovery that spurious singularities, which plagued the traditional methods, can be eliminated when the variational principle is formulated with outgoing-wave boundary conditions. Another reason for the recent activity is the obvious suitability of these methods to present-day supercomputers. My purpose here is to describe an implementation of the complex Kohn method, an algebraic variational technique, for studying electron collisions with small molecules, both linear and non-linear, unlike variational principles based on the integral form of the Schroedinger equation (Lippmann-Schwinger equation), the method only requires Hamiltonian matrix elements. I will also show how the formalism allows one to develop a variational principle for computing first-order properties, such as bound-free dipole transition amplitudes. I will show results for the electron-impact dissociation of hydrogen as a function of initial vibrational quantum number. I will also illustrate the method for polyatomic molecules with results for elastic scattering of electrons by formaldehyde. DOE

N90-11559# Oak Ridge National Lab., TN.
EXTRACTION INDUCED EMITTANCE GROWTH FOR NEGATIVE ION SOURCES
J. H. Whealton, P. S. Meszaros, R. J. Raridon, and K. E. Rothe 1989 15 p Presented at the International Conference on Ion Sources, Berkeley, CA, 9-15 Jul. 1989
(Contract DE-AC05-84OR-21400)
(DE89-017586; CONF-890703-18) Avail: NTIS HC A03/MF A01

Nonlinear emittance growth produced by ion extraction is considered by a 3-D analysis in a Vlasov-Poisson-Boltzmann formulation. Phenomena considered include: presheath effects, including electron depletion, electron sheath accumulation (for large transverse magnetic fields), nonlinear sheath fields (obtained by a self-consistent solution with an assumed quasi-equilibrium positive ion distribution and at least one Vlasov distribution), nonlinear fringe fields produced by the accelerator-extractor itself obtained self-consistently with item 3 above, nonlinear space charge of the beam itself, and beam in conjunction with extracted electrons. For specific volume negative ion source configurations, an investigation of the contribution of aberrations caused by an electron trap and electron accumulation in the extraction sheath are studied. Either of these effects can contribute significantly to the beam emittance, possibly dominating the contribution of the negative ion temperature in the source. DOE

N90-11560# Joint Inst. for Nuclear Research, Dubna (USSR). Lab. of Nuclear Reactions.
SIMULATION OF AN AXIALLY SYMMETRIC ION-OPTICAL SYSTEM
S. Biri and S. L. Bogomolov 1988 10 p In RUSSIAN; ENGLISH summary
(DE89-620129; JINR-9-88-533) Avail: NTIS (US Sales Only) HC A02/MF A01

The simulation of an electrostatic axially symmetric ion-optical system designed for forming an ion beam extracted from an ion source was carried out. The design of an ion-optical system with an axial electric potential distribution consisting of linear and cosine terms is considered. The electrode shape and electric potentials are determined from the given potential distribution on the axis. The properties of the ion-optical system designed in this manner were verified using the code ELENS. It is shown that the ion-optical systems constructed by the proposed method practically provide the same quality of the beam as do other systems known from the literature. The proposed method of constructing an ion-optical system does not require bulky numerical calculations. DOE

N90-11561# Technische Univ., Berlin (Germany, F.R.). Fachbereich Physik.
INVESTIGATIONS INTO THE INFLUENCE OF THE STATE FUNCTIONS ON THE CROSS SECTIONS OF THE DIRECT P,GAMMA REACTIONS AT ENERGIES IN THE 100 keV RANGE, AND PROJECT OF A CASCADE ACCELERATOR FOR THE MEASUREMENT OF THE P,GAMMA CAPTURE CROSS SECTIONS Ph.D. Thesis [UNTERSUCHUNGEN ZUM EINFLUSS DER ZUSTANDSFUNKTIONEN AUF WIRKUNGSQUERSCHNITTE DIREKTER P,GAMMA-REAKTIONEN BEI ENERGIEN IM 100 KEV-BEREICH UND PROJEKTIERUNG EINES KASKADENBESCHLEUNIGERS ZUR MESSUNG VON P,GAMMA-EINFANGWIRKUNGSQUERSCHNITTEN]
Huschang Heydari 1988 163 p In GERMAN
(ETN-89-94662) Avail: NTIS HC A08/MF A01

The approximate deduction of cross sections of gamma quanta capture reactions with light nuclei at low energies, and the experimental construction of an accelerator for electrically charged slow particles with a view to the measurement of small gamma capture cross sections, are investigated. Direct transitions of light ions from the continuum to bound nuclear energy states at low energy are theoretically described. The radial function of the Schroedinger equation in the Coulomb field is solved. The transition probability and coupling of several nucleons are determined. The calculations agree with experimental results with a view to the experimental construction, particle beams in the phase space are characterized, and a 400 keV particle accelerator and beam guiding components are designed, and the current density of the RF ion source calculated. ESA

73 NUCLEAR AND HIGH-ENERGY PHYSICS

Includes elementary and nuclear particles; and reactor theory.

For space radiation see *93 Space Radiation.*

N90-11562# Brookhaven National Lab., Upton, NY.
ION SOURCES, ELECTRON GUNS AND BEAM OPTICS
Krsto Prelec Aug. 1989 4 p
(Contract DE-AC02-76CH-00016)
(DE89-015526; DOE/FTR-9015526) Avail: NTIS HC A01/MF A01

The Advanced Source Development Group at BNL is currently involved in feasibility studies to replace heavy ion beams from a tandem accelerator with a possibly much more efficient and reliable EBIS, coupled with an RFQ accelerator. Discussions with Dr. Liljeby of the M. Siegbahn Institute and with Professor M. Sedlacek of the Royal Institute of Technology were focused on the BNL approach in the design of an electron gun or such a source. CERN Laboratory in Geneva, Switzerland, is presently considering acceleration of lead ions in their SPS (with a fixed target), as well as acceleration of heavy ions in the proposed Large Hadron Collider (LHC), in the colliding mode similar to BNL's RHIC project. Discussions were held with Drs. H. Haseroth and K. Schindl on both the LHC and RHIC projects. With Ch. Hill, who is in charge of the CERN preinjectors, experiences were compared with volume H(-) ion sources, while discussions with M. Weiss were a follow-up of the joint work going on since 1984 on ion optics and RFQ acceleration. DOE

N90-11563# Auburn Univ., AL. Dept. of Physics.
THEORETICAL ATOMIC PHYSICS FOR FUSION Annual Report, 1989
Michael S. Pindzola 1989 7 p
(Contract DE-FG05-86ER-53217)
(DE89-017363; DOE/ER-53217/3) Avail: NTIS HC A02/MF A01

Electron-ion collision processes play a major role in many plasma research efforts to understand particle and energy transport in magnetic fusion experiments. The 1989 efforts are summarized in several areas of electron-ion scattering theory. DOE

74 OPTICS

Includes light phenomena; and optical devices.

For lasers see *36 Lasers and Masers.*

N90-11564# Colorado Univ., Boulder. Optoelectronic Computing Systems Center.
A METHODOLOGY FOR THE DESIGN OF CONTINUOUS-DATAFLOW SYNCHRONOUS SYSTEMS
Jonathan P. Pratt and Vincent P. Heuring Mar. 1989 28 p Sponsored in part by Colorado Advanced Technology Inst. Prepared in cooperation with Colorado State Univ., Fort Collins
(Grant NSF CDR-86-22236)
(PB89-184360; OCS-TR-89-23) Avail: NTIS HC A03/MF A01 CSCL 20F

Increasingly it is the propagation velocity of information that limits processing speed rather than the inherent delays in processing elements. One consequence is that optimal processing throughput is not possible when memory elements are employed to synchronize information parcels. In the paper the design of systems lacking such memory elements is discussed. Such systems are characterized by the need for precise control over data propagation delays. Synchronization in the context of the systems is characterized and related to existing graph theory. An algorithm is presented that allows efficient distribution of lumped delay designs while preserving synchronization. Applications in optical computing are discussed. The techniques described are also applicable to existing data processing architectures, particularly those based on pipelining. GRA

N90-11565 Wisconsin Univ., Madison.
NOVEL PHYSICAL EFFECTS IN INTERSECTING OPTICAL WAVEGUIDES Ph.D. Thesis
Niraj Agrawal 1988 160 p
Avail: Univ. Microfilms Order No. DA8906509

A description of the interaction between two intersecting waveguides is an important problem in integrated optics. Small and large intersection angles offer the possibility of making switches and crossovers, respectively. The guided-guided and guided-radiation mode interactions are studied experimentally in Ti:LiNbO3 single-mode intersecting waveguides. These measurements cannot be interpreted in terms of any existing theory for intersecting waveguides. A multiple scattering interaction analysis was developed which is in good agreement with all the experimental data on intersecting waveguides known to-date. In addition, the theory points out novel physical effects associated with this geometry. For example, it is found that the crosstalk vanishes for an intersection angle which is twice the angle of rays corresponding to guided modes in the individual waveguides. A sharply peaked radiation pattern from the intersection region of the two waveguides is both predicted and observed for the first time. A recipe to fabricate low-loss switches by fractional doping of the intersection region is also suggested. Dissert. Abstr.

N90-11566# National Aerospace Lab., Tokyo (Japan). Instrumentation and Control Div.
EVALUATION TEST OF CCD AREA SENSOR FOR STAR SENSOR
Yoshio Sakurai and Takeo Kimura Apr. 1987 43 p In JAPANESE
(NAL-TM-570; ISSN-0452-2982; JTN-88-80065) Avail: NTIS HC A03/MF A01

The star sensor permits the determination of the posture of an artificial satellite or space vehicle. Coupled with the recent progress of semi- conductor technologies, the desire to develop the charge coupled device (CCD) star sensor has been expressed. This sensor is expected to be small-sized and lightweight, to consume little power, to provide high accuracy and to have a long life expectancy. In proceeding with the R and D on the CCD star sensor, it is essentially necessary to fully grasp the photoelectric characteristics of a CCD area sensor, which serves as the eye of the CCD star sensor. To increase their sensitivity, those sensors which are employed in the CCD star sensor require a longer accumulation time than a TV camera generally employed and they require cooling as well. Such usage, however, is rather special. The photoelectric characteristics of a sensor measured under such working conditions as referred to above, therefore, have been very rarely reported. National Aerospace Laboratory (NAL) has been conducting the research related to the trial manufacture and tests of CCD star sensors since 1982, including a joint research with Toshiba Corporation. To obtain the basic data for designing and trial manufacturing a CCD star sensor to be borne on an artificial satellite, an evaluation test relating to the photoelectronic characteristics of a CCD area sensor, was carried out. NASDA

N90-11567# EG and G Energy Measurements, Inc., Idaho Falls.
FIBER OPTICS: A BRIEF INTRODUCTION
Michael E. Gruchalla 1989 14 p Presented at the Sensor's Expo 1989, Cleveland, OH, 12-14 Sep. 1989
(Contract DE-AC08-88NV-10617)
(DE89-009337; EGG-10617-6055; CONF-890996-1) Avail: NTIS HC A03

A basic introduction into the principles of fiber optics is presented. A review of both the underlying physical principles and the individual elements of typical fiber optic systems are presented. The optical phenomenon of total internal reflection is reviewed. The basic construction of the optical fiber is presented. Both step index and graded index fiber designs are reviewed. Multimode and single mode fiber constructions are considered and typical performance parameters given. Typical optical fiber bandwidth and loss characteristics are compared to various common coaxial cables, waveguides, and air transmission. The constructions of

optical fiber cables are reviewed. Both loose tube and tightly buffered designs are considered. Several optical connection approaches are presented. Photographs of several representative optical connectors are included. Light Emitting Diode and Laser Diode emitters for fiber optic applications are reviewed, and some advantages and shortcomings of each are considered. The phenomenon of modal noise is briefly explained. Both PIN and Avalanche photodetectors are reviewed and their performance parameters compared. Methods of data transmission over optical fiber are introduced. Principles of Wavelength, Frequency, and Time Division Multiplexing are briefly presented. The technology of fiber optic sensors is briefly reviewed with basic principles introduced. The performance of a fiber optic strain sensor is included as a practical example. DOE

N90-11568# Sandia National Labs., Albuquerque, NM.
OPTICAL COHERENCE MULTIPLEXING FOR INTERPROCESSOR COMMUNICATIONS
K. W. Chu and F. M. Dickey 1989 13 p Presented at the Optical Engineering/Fibers '89 Meeting, Boston MA, 5-8 Sep. 1989
(Contract DE-AC04-76DP-00789)
(DE89-016186; SAND-89-0220C; CONF-8909177-1) Avail: NTIS HC A03/MF A01

The development of an optical circuit that multiplexes gigabit-per-second electronic data streams into a very broad bandwidth (greater than 10 Gbit/s) optical signal would greatly enhance interprocessor communications in a parallel computer. One possibility that we are investigating is coherence multiplexing. In this method, time delays exceeding the coherence time of the light source are used to achieve multiplexing. We have analyzed the limitations of coherence multiplexing for high-speed data links. For the geometry that we are investigating, the analysis shows that the signal decreases inversely as the square of the number of channels. Noise sources include photon shot noise, excess noise (classical optical field fluctuations) and detector noise. A suitable optical source must have a smooth broad spectrum. Superluminescent diodes or edge emitting diodes are the best candidates. We show how all these factors affect the total information transfer rate. An integrated optical circuit for coherence multiplexing is being designed and built. This device is an array of four Mach-Zehnder interferometers integrated on a lithium niobate substrate. The differential delays will be achieved using proton exchange. Each interferometer will have two sets of electrodes, one for signal modulation and a second for fine adjustments of the delay. DOE

N90-11569# Sandia National Labs., Albuquerque, NM.
ACCELERATION OF THIN FOIL TARGETS USING FIBER-COUPLED OPTICAL PULSES
Wayne M. Trott and Kent D. Meeks 1989 4 p Presented at the American Physical Society Topical Conference on Shock Compression of Condensed Matter, Albuquerque, NM, 14-17 Aug. 1989
(Contract DE-AC04-76DP-00789)
(DE89-016526; SAND-89-1056C; CONF-890812-13) Avail: NTIS HC A01/MF A01

Commercially available optical fibers can reliably transmit Nd:Glass laser pulses of high irradiance (greater than 3.5 GW/sq cm) without damage. The optical energy at the fiber output can be used for efficient acceleration of thin foil targets. An optically recording velocity interferometer system (ORVIS) was used to determine velocity-time histories for aluminum foils accelerated in this manner. Flyer performance was examined as a function of laser energy and pulse duration. The measured velocities indicate that the efficiency of coupling optical energy into flyer kinetic energy can be as high as 35 percent. For 0.005-mm-thick Al coupled to a 0.4-mm-diameter fiber, foil velocities greater than 3 km/s were achieved with modest laser energies (less than 30 mJ). Preliminary results of particle velocity measurements on flyer-impacted witness plates are also given. DOE

N90-11570# RDP, Inc., Waltham, MA.
OFFAXIS RADIANCE STUDIES FOR INFRARED SENSORS
Report, 3 Feb. 1987 - 2 Feb. 1988
Andrew J. Mazzella, Jr. and Steven A. Lacaire 27 Dec. 1988 47 p
(Contract F19628-87-C-0039)
(AD-A210790; AFGL-TR-89-0038; SR-1) Avail: NTIS HC A03/MF A01 CSCL 17/5

The calculation of offaxis radiance for a sensor involves two programs, LOWFILT and OAREJ, and a set of data files specifying the sensor spectral response, sensor offaxis rejection response, and the radiance profile for the earth limb. For this description, the earth limb profile is provided as data generated by the LOWTRAN4 program, although more recent or alternative limb profile data could be used, provided the data format is preserved. For this study, a series of models of offaxis response functions has been developed to characterize the performance of several infrared sensors, including the Zodiacal Infrared Project (ZIP) telescopes, which were used for both the ZIP and Earth Limb Clutter (ELC) missions, and the SPIRE telescope. A number of observational and theoretical considerations were incorporated into the development of these models, and comparisons of the computed offaxis in-band radiance to actual flight data have been performed. Further investigations are still in progress. GRA

N90-11571# California Univ., Los Angeles. School of Engineering and Applied Science.
ADAPTIVE GIGABIT FIBER OPTICS LOCAL AREA NETWORK
Final Report, 1 Apr. 1985 - 14 Apr. 1989
Cavour Yeh and Mario Gerla 11 Jul. 1989 14 p
(Contract DAAG29-85-K-0101)
(AD-A210794; UCLA/EE-ARO-1001; ARO-21885.1-EL) Avail: NTIS HC A03/MF A01 CSCL 25/5

This is a final report on the investigation of adaptive gigabit fiber optics local area network. The following tasks were completed: (1) exploration of tree topologies with passive taps (Tree-Net); (2) investigation of novel, adaptive access scheduling mechanisms (Virtual Queue); (3) use of time division slot switching for the interconnection of FOLANs and the implementation of regular network topologies (e.g., Manhattan grid); (4) use of wavelength division multiplexing (WDM) in order to increase the throughput capacity and functionality of Tree-Net; (5) development of a simple (from the implementation standpoint) and yet efficient protocol - RATO-NET - for a twin, unidirectional fiber bus architecture; and (6) implementation of an experimental RATO-NET, and comparison of the experimental results with analysis simulation. GRA

N90-11572# Naval Research Lab., Washington, DC. Surface Modification Branch.
THE Si(1-x)Nx RUGATE Memorandum Report, Feb. 1986 - Feb. 1988
R. H. Bassel 8 Aug. 1989 18 p
(AD-A211236; NRL-MR-6510) Avail: NTIS HC A03/MF A01 CSCL 20/6

With the advent of lasers, intense sources of monochromatic light are now available. The problem of eye and sensor protection from these devices is now crucial to the field operations of troops and military weapons systems. In other words it is necessary to construct a filter which will reject particular laser lines from impinging upon a material. The results are presented in the infrared and near infrared region of the spectrum. The effectiveness of a Rugate filter constructed of a silicon nitrogen alloy is calculated. Single and double line rugates are discussed. The dependence on the rugate on the various parameters such as the number of cycles, the amplitudes of the sine waves and the phase angle are presented. The effects of absorption, constructional malfunctions, and the angle of incidence of the laser beam are studied. It is found that quite large optical densities can be achieved with rather thin films, thus the silicon nitrogen rugate is a viable candidate for a laser rejection filter. GRA

N90-11573# Universal Energy Systems, Inc., Dayton, OH.
DIAMONDLIKE CARBON COATINGS FOR OPTICAL SYSTEMS Final Report, Sep. 1986 - Sep. 1988
R. Wu, D. Ingram, A. McCormick, A. Rai, P. Pronko, and J. Woollam Feb. 1989 118 p
(Contract DAAL04-86-C-0030)
(AD-A211255; MTL-TR-89-13) Avail: NTIS HC A06/MF A01 CSCL 20/6

Diamondlike carbon (DLC) coatings have been deposited on seven infrared transmitting substrates utilizing three different techniques: ion-beam deposition, RF-plasma discharge, and hollow cathode discharge methods. Optimum deposition parameters for each technique have been established as a function of substrate material. Extensive characterization of the DLC films was also performed. Rutherford backscattering and proton recoil detection techniques were used to analyze carbon and hydrogen content and impurities. These films contain typically 70 percent C and 30 percent H. Transmission electron microscopy was used to analyze the crystallinity, void structure, surface microstructure, and thickness of the films which were found to be amorphous and dense. Optical properties such as refractive index, extinction coefficient, and optical band gap of the films were determined by variable angle spectroscopic ellipsometry (VASE) over the special range from 300 nm to 10.6 micron. Optical properties were found to be related to the preparation procedure used. The thermal stability, moisture penetration, rain erosion, and sand ballistic impact effects on these DLC films were extensively investigated. The effect of high energy ion radiation on DLC films was studied. Details of preparation methods and characterization of DLC films are presented. GRA

N90-11574# Center for Night Vision and Electro-Optics, Fort Belvoir, VA.
NIGHT SKY RADIOMETRIC MEASUREMENTS DURING FOLLOW-ON-EVALUATION TESTING OF AN/PVS-7 (A, B) AT FORT BENNING, GEORGIA Final Report, Oct. - Dec. 1986
Raymond J. Stefanik May 1989 120 p
(AD-A211273; AMSEL-NV-TR-0079) Avail: NTIS HC A06/MF A01 CSCL 17/5

The characterization of the lighting conditions during field testing on night vision intensifier systems requires more information than can be obtained by a photometer. The Follow-on-Evaluation (FOE) testing of AN/PVS-7 Night Vision Goggles at Fort Benning, GA (Oct. 1986 to Dec. 1986) required a radiometric characterization of the nighttime spectral content in the region encompassing that of the generation two and generation three image intensifier photocathodes (400 to 920nm) used in the goggles. A night sky radiometer (NSR) measuring system was designed and fabricated by the Center for Night Vision and Electro-Optics for the purpose of characterizing the night sky spectral content during the FOE test. This report discusses the design features of the NSR, its measuring techniques, and the results of the night sky conditions during the FOE test at Fort Benning. GRA

N90-11575# Swedish Defence Research Establishment, Linkoeping. Dept. of Information Technology.
TURBULENCE EFFECTS FOR RETROREFLECTION
Ove Steinvall Feb. 1989 26 p In SWEDISH; ENGLISH summary
(FOA-C-30523-3.1; ISSN-0347-3708; ETN-89-95169) Avail: NTIS HC A03/MF A01; Swedish Defence Research Establishment, Box 1165, S-581 11, Linkoeping, Sweden, 50 Swedish crowns

Atmospheric turbulence influences the performances of many kinds of optical systems of both passive and active type, for example in the widening of the laser beam in the air. There are many types of disturbances, scintillations, phase distortion, angular fluctuation, and shifting of the beam (the latter may occur if the temperature varies very much above the ground). To characterize the turbulence strength an optical link is constructed with the transceiver unit at one end and a reflector (point reflector, angular reflector, or a flat mirror) at the other. Some relevant questions in conjunction with testing and calibration of the optical link are reported. Theoretical results from the literature are illustrated in diagram form. ESA

N90-10853# Air Force Inst. of Tech., Wright-Patterson AFB, OH. Dept. of Electrical and Computer Engineering.
ADAPTIVE TRACKING OF MANEUVERING TARGETS BASED ON IR IMAGE DATA
Peter S. Maybeck *In* AGARD, Kalman Filter Integration of Modern Guidance and Navigation Systems Jun. 1989 18 p (For primary document see N90-10847 02-04)
Copyright Avail: NTIS HC A09/MF A01

75 PLASMA PHYSICS

Includes magnetohydrodynamics and plasma fusion.
For ionospheric plasmas see *46 Geophysics*. For space plasmas see *90 Astrophysics*.

N90-11576# Wisconsin Univ., Madison. Plasma Physics Research.
BOUNDARY EFFECTS ON THE MHD DYNAMO IN LABORATORY PLASMAS
Y. L. Ho and S. C. Prager Jul. 1989 11 p Presented at the IUTAM Symposium on Topological Fluid Mechanics, Cambridge, England, Aug. 1989
(Contract DE-FG02-85ER-05321)
(DE89-015207; DOE/ER-53212/142; CONF-8908112-1) Avail: NTIS HC A03/MF A01

In recent laboratory experiments, a dynamo-like mechanism has been demonstrated in which a portion of the axisymmetric component of the magnetic field is believed to be sustained by 3D spatial fluctuations in the field and flow. With a conducting shell at the plasma surface, past MHD computation shows that sustainment arises from fluctuations which cause magnetic reconnection. If the conducting wall is retracted from the plasma surface, the fluctuations are amplified and the dynamo sustainment is still active for the times studied, but an increased energy input to the plasma is required through the applied electric field. The retraction of the conducting wall enhances the helicity dissipation rate by the intersection of the fields with the resistive surface which bounds the plasma. This enhanced helicity dissipation is balanced by the helicity injection that accompanies the increased applied electric field. DOE

N90-11577# Los Alamos National Lab., NM.
THE REVERSED-FIELD-PINCH (RFP) FUSION NEUTRON SOURCE: A CONCEPTUAL DESIGN
C. G. Bathke, R. A. Krakowski, R. L. Miller, and K. A. Werley 1989 25 p Presented at the International Energy Agency Workshop on Fusion Materials Irradiation Facilities, San Diego, CA, 14-17 Feb. 1989 Submitted for publication
(Contract W-7405-eng-36)
(DE89-015297; LA-UR-89-2489; CONF-8902118-2) Avail: NTIS HC A03/MF A01

The conceptual design of an ohmically heated, reversed-field pinch (RFP) operating at approximately 5-MW/m(2) steady-state DT fusion neutron wall loading and approximately 124-MW total fusion power is presented. These results are useful in projecting the development of a cost effective, low input power, approximately 206 MW, source of DT neutrons for large-volume approximately 10 m(3), high-fluence, 3.4 MW yr/m(2), fusion nuclear materials and technology testing. DOE

N90-11578# California Univ., Los Angeles. Inst. for Plasma and Fusion Research.
PISCES PROGRAM PLASMA-SURFACE INTERACTIONS RESEARCH
May 1989 51 p
(Contract DE-FG03-86ER-05213)
(DE89-015622; UCLA/PPG-1247) Avail: NTIS HC A04/MF A01

The following topics of the Pisces program are discussed: major objectives of the program; staff in the PISCES program at UCLA; highlights in the program; collaborations with other institutions; PISCES-A facility; PISCES-B facility; fast scanning Langmuir probe; Omegatron mass spectrometer; spectroscopic diagnostics; data acquisition system; redeposition effect on carbon chemical erosion; erosion of carbon tokamakium from TFTR; effect of boron-doping on carbon chemical erosion; radiation enhanced sublimation of carbon; surface analysis of TEXTOR titles; spectroscopic analysis of carbon impurities; biased limiter and divertor; biased divertor channel; gaseous divertor experiments; presheath profile measurements; particle transport in CCT tokamak; and biased divertor experiments in CCT. DOE

N90-11579# Oak Ridge National Lab., TN.
HYBRID PARTICLE-FLUID APPROACH TO LOW-FREQUENCY TURBULENCE IN MAGNETICALLY CONFINED PLASMAS
J. N. Leboeuf, R. H. Fowler, J. H. Han, and P. M. Lyster (Texas Univ., Austin.) 1989 4 p Presented at the 13th Conference on the Numerical Simulation of Plasmas, Santa Fe, NM, 17-20 Sep. 1989
(Contract DE-AC05-84OR-21400)
(DE89-015904; CONF-890931-1) Avail: NTIS HC A01/MF A01

A hybrid particle-fluid computer model was developed for quasineutral microinstabilities in magnetically confined plasmas. The ions are treated in the fluid approximation. The electrons are taken as guiding-center macroparticles. The model was extensively tested for frequency and fluctuation spectra. Linear and nonlinear studies of drift waves, eta sub i modes, interchange modes, and trapped electron modes were also carried out. DOE

N90-11580# Columbia Univ., New York, NY.
ION TEMPERATURE GRADIENT INSTABILITY Progress Report
1989 3 p
(Contract DE-FG02-87ER-53257)
(DE89-016574; DOE/ER-53257/2) Avail: NTIS HC A01/MF A01

Anomalous ion thermal conductivity remains an open physics issue for the present generation of high temperature tokamaks. It is generally believed to be due to Ion Temperature Gradient Instability (eta sub i mode). However, it was difficult, if not impossible to identify this instability and study the anomalous transport due to it, directly. Therefore the production and identification of the mode is pursued in the simpler and experimentally convenient configuration of the Columbia Linear Machine (CLM). CLM is a steady state machine which already has all the appropriate parameters, except (eta sub i). This parameter is being increased to the appropriate value of the order of 1 by feathering a tungsten screen located between the plasma source and the experimental cell to flatten the density profile and appropriate redesign of heating antennas to steepen the ion temperature profile. Once the instability is produced and identified, a thorough study of the characteristics of the mode can be done via a wide range of variation of all the critical parameters: (eta sub i), parallel wavelength, etc. DOE

N90-11581# Los Alamos National Lab., NM. Physics Div.
STUDIES OF A STRONGLY COUPLED PLASMA PRODUCED IN A CAPILLARY DISCHARGE
John F. Benage, Jr., Larry A. Jones, R. James Trainor, Jr., William R. Shanahan, Ronnie L. Shepherd (Lawrence Livermore National Lab., CA.), and David P. Nothwang 1989 6 p Presented at the 24th Yamada Conference on Strongly Coupled Plasma Physics, Tokyo, Japan, 29 Aug. - 2 Sep. 1989
(Contract W-7405-eng-36)
(DE89-016611; LA-UR-89-2899; CONF-8908133-1) Avail: NTIS HC A02/MF A01

An experiment was carried to measure the properties of a strongly coupled (Gamma approx. 0.8) plasma produced in a capillary discharge. Using an analytical model and some 1-D MHD calculations along with the measurements, the density, temperature, strong coupling parameter (Gamma), and the resistivity of this plasma were determined. The resistivity measurements were compared to various theories. DOE

N90-11582# Texas Univ., Austin. Inst. for Fusion Studies.
THEORY OF HIGH-n TOROIDICITY-INDUCED SHEAR ALFVEN EIGENMODE IN TOKAMAKS
G. Y. Fu and C. Z. Cheng (Princeton Univ., NJ.) Jul. 1989 35 p Sponsored by Texas Advanced Technology Program and Texas Atomic Energy Research Foundation
(Contracts DE-AC02-76CH-03073; DE-FG05-80ET-53088)
(DE89-016726; DOE/ET-53088/385; IFSR-385) Avail: NTIS HC A03/MF A01

High-n WKB ballooning mode equation is employed to study toroidicity induced shear Alfven eigenmodes (TAE) in the delta - alpha space, where delta = r/q dq/dr is the magnetic shear, and alpha = -2Rq sup 2/B sup 2 dp/dr is the normalized pressure gradient for tokamak plasmas. In the ballooning mode first stability region, TAE modes are found to exist only for alpha less than some critical value alpha sub c. It was also found that these TAE modes reappear in the ballooning mode second stability region for bands of alpha values. The global envelope structures of these TAE modes are studied by WKB method and are found to be bounded radially if the local mode frequency has a maximum in radius. DOE

N90-11583# Texas Univ., Austin. Dept. of Physics.
PARTICLE SIMULATION IN CURVILINEAR COORDINATE SYSTEMS
M. J. LeBrun and T. Tajima Jun. 1989 76 p
(Contract DE-FG05-80ET-53088; NSF ATM-88-11128)
(DE89-016727; DOE/ET-53088/374; IFSR-374) Avail: NTIS HC A05/MF A01

Methods are presented for particle simulation of plasmas in a nearly arbitrary coordinate metric and describe a toroidal electrostatic simulation code that evolved from this effort. A Mercier-type coordinate system is used, with a nonuniform radial grid for improved cross-field resolution. A fast iterative method for solving the Poisson equation is employed, and the interpolation and/or filtering technique shown to be momentum and energy conserving in the continuum limit. Lorentz ion and drift electron species are used. The code was thoroughly tested for its reproduction of linear and nonlinear physics, and was applied to the toroidal drift wave problem and its impact on anomalous transport in tokamaks. DOE

N90-11584# Texas Univ., Austin. Inst. for Fusion Studies.
A STUDY OF RUNAWAY ELECTRON CONFINEMENT AND THEORY OF NEOCLASSICAL MHD TURBULENCE Ph.D. Thesis
Oh Jin Kwon Jul. 1989 150 p
(Contract DE-FG05-80ET-53088)
(DE89-016728; DOE/ET-53088/386; IFSR-386) Avail: NTIS HC A07/MF A01

Two major studies are presented: a study of runaway electron confinement and a theory of neoclassical MHD turbulence. The aim of the former is to study the structure of internal magnetic turbulence in tokamaks, which is thought by many to be responsible for the heat transport. The aim of the latter is to extend existing theories of MHD turbulence in tokamaks into experimentally relevant low collisionality regimes. This section contains a theory of neoclassical pressure gradient driven turbulence and a theory of neoclassical resistivity gradient driven turbulence. DOE

N90-11585# Los Alamos National Lab., NM.
ANTHEM SIMULATION OF THE EARLY TIME MAGNETIC FIELD PENETRATION OF THE PLASMA SURROUNDING A HIGH DENSITY Z-PINCH
Rodney J. Mason 1989 7 p Presented at the 2nd International Conference on High-Density Pinches (ICHDP-2), Laguna Beach, CA, 26-27 Apr. 1989
(Contract W-7405-eng-36)

(DE89-016980; LA-UR-89-2782; CONF-8904107-8) Avail: NTIS HC A02/MF A01

The early time penetration of magnetic field into the low density coronal plasma of a Z-pinch fiber is studied with the implicit plasma simulation code ANTHEM. Calculations show the emission of electrons from the cathode, pinching of the electron flow, magnetic insulation of the electrons near the anode, and low density ion blow off. PIC-particle ion calculations show a late time clumping of the ion density not seen with a fluid ion treatment. DOE

N90-11586# International Centre for Theoretical Physics, Trieste (Italy).

PRODUCING OF AN ECR PLASMA USING 2450MHz WHISTLER WAVE AND THE INVESTIGATING OF ITS PARAMETERS

Yude Fang, Jiande Zhang, Keming Fu, Xiangyu Lu, Dengcheng Liu, Xianyu Wang, Weidong Xie, Dinghua Bao, and Xiejin Yin (Academia Sinica, Hefei, China) Dec. 1988 16 p Submitted for publication

(DE89-618689; IC-88/384) Avail: NTIS (US Sales Only) HC A03/MF A01

A stable ECR plasma was produced and sustained in HER mirror using 2450MHz Whistler wave. The parameters of the ECR plasma and their chaining characters were studied in detail and were compared with those of the dc discharge plasmas. The conclusion is that the ECR plasma is a high ionizability, low temperature, middle density plasma, its peak density may much exceed the cutoff density of the pump wave (when omega = omega sub pe) and arrive at the order of 10(12)/cu cm. The ECR plasma includes some high energy hot electrons (20 KeV-200 KeV) and middle energy warm electrons (less than 20 KeV). Those two kinds of electron created some strong X-ray emissions in a wide frequency range. The ECR plasma has higher edge density and can strongly interact with the wall. DOE

N90-11587# Iowa Univ., Iowa City. Dept. of Physics and Astronomy.

CRRES (COMBINED RELEASE AND RADIATION EFFECTS SATELLITE) SPACERAD PLASMA WAVE EXPERIMENT Final Report, 20 Apr. 1982 - 30 Jun. 1988

Roger R. Anderson and Donald A. Gurnett Oct. 1988 43 p (Contract F19628-82-K-0028)

(AD-A210791; AFGL-TR-88-0299) Avail: NTIS HC A03/MF A01 CSCL 20/3

This document discusses the Main Electronics Package, two Electric Field Preamps and Search Coil Magnetometer for the AFGL 701 SPACERAD instrumentation on the CRRES (Combined Release and Radiation Effects Satellite) project. This document discusses the scientific objectives and the importance of the Plasma Wave Experiment in the CRRES SPACERAD mission and describes the instrument design rational and the instrument development philosophy. This document also discusses the testing and operations of the experiment and contains a schematic drawing of the instrumentation electronics and lists of the schematics, drawings, and wiring diagrams that describe the as-built configuration of the Plasma Wave Experiment instrumentation. Problems encountered during the construction and testing of the instrument and their resolutions are discussed. Test results from already completed environmental and EMC/RFI tests have already been submitted to AFGL and to the Air Force Headquarters Space Division Space Test Program. The recertification of the calibration of the instrument is recommended in the near future under a new contract covering the re-delivery (necessitated due to the removal during the launch-delay storage period), pre-launch, and launch operations. GRA

N90-11588# Los Alamos National Lab., NM.

COMPUTER SIMULATIONS OF ELECTROMAGNETIC ION INSTABILITIES IN THE PLASMA SHEET BOUNDARY LAYER

S. P. Gary and D. Winske 1989 7 p Presented at the Workshop on Theoretical Geoplasma Physics, Cambridge, MA, Jun. 1989

(Contract W-7405-eng-36)

(DE89-016596; LA-UR-89-2740; CONF-8906201-1) Avail: NTIS HC A02/MF A01

Linear Vlasov dispersion theory and one-dimensional hybrid computer simulations are used to study electromagnetic instabilities driven by hot, anisotropic counterstreaming proton components which model those observed from ISEE in the plasma sheet boundary layer of the near-Earth magnetotail. The proton anisotropies lead to the ion cyclotron anisotropy instability, which saturates at a low level of fluctuating fields and yields only weak proton scattering. Modest increases of the proton/proton relative drift, which might correspond to deeper tail conditions, excite the proton/proton nonresistant instability which attains larger fluctuation levels and more strongly heats the protons. If a relatively dense oxygen ion component is also introduced, the ion/ion right-hand resonant instability is excited; the consequent pitch-angle scattering of the protons resembles that indicated in the ISEE data. DOE

N90-11589# Lawrence Livermore National Lab., CA.

PROJECTIONS FOR A STEADY-STATE TOKAMAK REACTOR BASED ON ITER

R. S. Devoto, W. L. Barr, R. H. Bulmer, R. B. Campbell, M. E. Fenstermacher, J. D. Lee, B. G. Logan, J. R. Miller, L. L. Reginato, and R. A. Krakowski (Los Alamos National Lab., NM.) 20 Jul. 1989 64 p Prepared in cooperation with California Univ., Berkeley, Lawrence Berkeley Lab.; Massachusetts Inst. of Tech.; Oak Ridge Natl. Lab.; Negion, Inc.; and Argonne Natl. Lab. (Contract W-7405-eng-48)

(DE89-016678; UCID-21519-Rev-1) Avail: NTIS HC A04/MF A01

The extensions of the physics and engineering guidelines for the ITER device needed for acceptable operating points for a steady state tokamak power reactor are examined. Noninductive current drive is provided in steady state by high energy neutral beam injection in the plasma core, lower hybrid slow waves in the outer regions of the plasma and (30 percent) bootstrap current. Three different levels of extension of the ITER physics/engineering guidelines, with differing assumptions on the possible plasma beta, elongation and aspect ratio, are considered for power reactor applications. Plasma gain, Q sub p = fusion power/input power, in excess of 20 and average neutron wall fluxes from 2.3 to 3.6 MW/sq m are predicted in devices with major radii varying from 7.0 to 6.0 m and aspect ratios from 2.9 to 4.3. Peak divertor heat fluxes range up to 12.2 MW/sq m which is somewhat higher than the current ITER design limit of 10 MW/sq m with a magnetically swept divertor. These designs were selected on the basis of improvements in physics/engineering consistent with time scales for development of future reactors. The design re-optimization on the basis of cost of electricity (COE) was then examined using a reactor systems model. This analysis generally verified the original estimates for the required extensions of the ITER guidelines. Cost of electricity is projected to be less than 66 mills/kW sub e h in all of the configurations. The smallest reactor, which has the largest neutron wall flux and mass power density, yields the lowest COE, 56 mills/kW sub e h. DOE

N90-11590# Lawrence Livermore National Lab., CA.

TESTING RESULTS OF THE MIT PROBE

S. S. Shen and M. R. Chaplin 11 Aug. 1989 18 p (Contract W-7405-eng-48)

(DE89-016679; UCID-21737) Avail: NTIS HC A03/MF A01

The MIT Probe is a noninductively wound coil of Cable-in-Conduit Conductor (CICC) designed and fabricated by the MIT Plasma Fusion Center for testing at the High Field Test Facility (HFTF) as a cooperative testing of high current conductors for fusion applications. Test objectives mainly include measurement of Lorentz force degradation in such practical conductors. The probe was received in January 1988. It first went through a series of checkouts and was then connected to a 40-kA power supply system and installed in HFTF. Testing of the probe started on May 12, 1989, and ended on June 16, 1989. Results of all tests are summarized. DOE

N90-11591# Argonne National Lab., IL. High Energy Physics Div.
EXPERIMENTAL STUDIES OF PLASMA WAKE-FIELD ACCELERATION AND FOCUSING
J. B. Rosenzweig, B. Cole, C. Ho, W. Gai, R. Konecny, S. Mtingwa, J. Norem, M. Rosing, P. Schoessow, and J. Simpson 18 Jul. 1989 49 p Presented at the International Centre for Theoretical Physics Conference, Trieste, Italy, 22-26 May 1989 Submitted for publication
(Contract W-31-109-eng-38)
(DE89-016718; ANL-HEP-CP-89-75; CONF-8905156-2) Avail: NTIS HC A03/MF A01

More than four years after the initial proposal of the Plasma Wake-Field Accelerator (PWFA), it continues to be the object of much investigation, due to the promise of the ultra-high accelerating gradients that can exist in relativistic plasma waves driven in the wake of charged particle beams. These large amplitude plasma wake-fields are of interest in the laboratory, both for the wealth of basic nonlinear plasma wave phenomena which can be studied, as well as for the applications of acceleration of focusing of electrons and positrons in future linear colliders. Plasma wake-field waves are also of importance in nature, due to their possible role in direct cosmic ray acceleration. The purpose of the present work is to review the recent experimental advances made in PWFA research at Argonne National Laboratory, in which many interesting beam and plasma phenomena have been observed. Emphasis is given to discussion of the nonlinear aspects of the PWFA beam-plasma interaction. DOE

N90-11592# Los Alamos National Lab., NM.
SOLID FIBER Z-PINCHES: COLD-START COMPUTATIONS
Irvin R. Lindemuth 1989 11 p Presented at the 2nd International Conference on High-Density Plasmas, Laguna Beach, CA, 24-28 Apr. 1989
(Contract W-7405-eng-36)
(DE89-016768; LA-UR-89-2710; CONF-890454-1) Avail: NTIS HC A03/MF A01

One- and two-dimensional magnetohydrodynamic computations have been performed to study the behavior of solid deuterium fiber Z-pinch experiments performed at Los Alamos and the Naval Research Laboratory. The computations use a tabulated atomic data base and cold-start initial conditions. The computations predict that the solid fiber persists longer in existing experiments than previously expected and that the discharge actually consists of a relatively low-density, hot plasma which has been ablated from the fiber. The computations exhibit m = 0 behavior in the hot, exterior plasma prior to complete ablation of the solid fiber. The m = 0 behavior enhances the fiber ablation rate. DOE

N90-11593# Los Alamos National Lab., NM.
A FULLY ELECTROMAGNETIC HYBRID MODEL FOR HIGH DENSITY PLASMA SIMULATIONS
Michael E. Jones, V. A. Thomas, R. J. Mason, and D. Winske 1989 5 p Presented at the 13th Conference on the Numerical Simulation of Plasmas, Santa Fe, NM, 17-20 Sep. 1989
(DE89-016771; LA-UR-89-2687; CONF-890931-5) Avail: NTIS HC A01/MF A01

Hybrid simulation methods in which ions are treated by particle-in-cell and electrons are treated as a massless fluid have proven to be useful for modeling a variety of low frequency plasma phenomena. In addition to the massless electron approximation, usually the models assume quasineutrality and the Darwin approximation to Maxwell's equations. We have considered a hybrid model in which the Darwin approximation is not used. Rather the full set of Maxwell's equations are solved. This model appears to be particularly suited to modeling situations in which the plasma has a finite extent i.e., where high density plasma is next to vacuum. This model allows electromagnetic waves to propagate in the vacuum and to be properly handled in the plasma. DOE

N90-11594# Sandia National Labs., Albuquerque, NM.
HYDROGEN-ASSISTED THERMAL DONOR FORMATION IN SILICON
H. J. Stein and S. Hahn (Siltec Corp., Menlo Park, CA.) 1989 10 p Presented at the 3rd Meeting on Defect Recognition and Image Processing in Semiconductors, Yokohama, Japan, 17-22 Sep. 1989
(Contract DE-AC04-76DP-00789)
(DE89-016809; SAND-88-3307C; CONF-890946-1) Avail: NTIS HC A02/MF A01

Energetic hydrogen or deuterium ions from a plasma can increase the thermal donor, TD, formation rate in Czochralski Si at 400 C by more than an order of magnitude above that for exposure in H2 or in a He plasma. Infrared absorption techniques were used to identify the donors, and donors concentrations and penetration depths were determined from spreading resistance probe measurements. The concentration and penetration depth for hydrogen-assisted TD formation are dependent upon the annealing history. Hydrogen-assisted formation rates can extend through a 0.5 mm depth of an as-grown wafer, whereas the hydrogen-assisted rate decreases markedly with depth when the plasma exposure occurs after a rapid thermal anneal cycle at 850 C. Hydrogen-assisted TD formation is attributed to H(deuterium) diffusion and catalyzed conversion of oxygen-related nuclei to TD's in as-grown Si. Hydrogen-assisted regrowth of nuclei is suggested for the rate-limiting step in TD formation after a rapid thermal anneal cycle. Assisted TD formation in a hydrogen-plasma was observed beyond a buried oxide layer in Si, but not beyond a buried nitride layer which is consistent with relative hydrogen diffusivities in SiO2 and silicon nitride. DOE

N90-11595# Sandia National Labs., Albuquerque, NM.
PULSED-POWER SWITCHING FOR INERTIAL CONFINEMENT FUSION WITH LIGHT ION BEAMS
J. Pace Vandevender, M. T. Buttram, H. C. Harjes, D. L. Johnson, T. H. Martin, E. L. Neau, K. R. Prestwich, J. J. Ramirez, G. J. Rohwein, and L. X. Schneider et al 1989 13 p Presented at the International Workshop on High Power Opening Switches, Novosibirsk, USSR, 1-2 Jul. 1989
(Contract DE-AC04-76DP-00789)
(DE89-016810; SAND-89-1270C; CONF-890796-3) Avail: NTIS HC A03/MF A01

Inertial confinement fusion requires 100 to 1000 terawatts of power be generated by sequentially storing and switching between 2 and 4 mj of energy to compress the pulse duration to approximately 10 ns. The status and promise of the switching technologies for light ion driven inertial fusion are presented. Experiments on the Particle Beam Fusion Accelerator II (PBFA II) at Sandia National Laboratories will attempt to find the threshold for igniting thermonuclear fuel in the laboratory and, if the threshold is within the range of PBFA II experiments, to achieve ignition. These experiments are possible because of advances in electrically triggered and laser triggered gas switching and in untriggered water dielectric switching. The advances permit reliable operation of the 36-module PBFA II with module jitters of 4 ns and first-to-last spreads of 15 ns. The modules are combined in series and parallel combinations to give an effective asynchrony of (approx) 1 ns. The next major facility in the inertial fusion program will be the Laboratory Microfusion Facility for producing 200 to 1000 mj of thermonuclear yield. The laser triggered gas switching and water dielectric switching demonstrated on the Hermes III accelerator are adequate for this next step. The high efficiency and low cost of large pulsed power accelerators result in a low cost reactor concept. Development of the high average power and high peak power necessary for 3 to 5 Hz operation will require further advances in high power switching. Saturable inductors offer a promising option. Photoconductive semiconductor switching offer the possibility of substantially reducing the number of required pulse compression stages. DOE

N90-11596# Sandia National Labs., Albuquerque, NM.
LAUNCHED ELECTRONS IN PLASMA OPENING SWITCHES
C. W. Mendel, Jr., G. E. Rochau, M. A. Sweeney, D. H. McDaniel, J. P. Quintenz, M. E. Savage, E. L. Lindman, and J. M. Kindel (Mission Research Corp., Los Alamos, NM.) 1989 26 p Presented at the International Workshop on Physics and

Techniques of High Power Opening Switches, Novosibirsk, USSR, 30 Jun. - 2 Jul. 1989
(Contract DE-AC04-76DP-00789)
(DE89-016886; SAND-89-0283C; CONF-8906208-1) Avail: NTIS HC A03/MF A01

Plasma opening switches have provided a means to improve the characteristics of super-power pulse generators. Recent advances involving plasma control with fast and slow magnetic fields have made these switches more versatile, allowing for improved switch uniformity, triggering, and opening current levels that are set by the level of auxiliary fields. Such switches necessarily involve breaks in the translational symmetry of the transmission line geometry and therefore affect the electron flow characteristics of the line. These symmetry breaks are the result of high electric field regions caused by plasma conductors remaining in the transmission line, ion beams crossing the line, or auxilliary magnetic field regions. Symmetry breaks cause the canonical momentum of the electrons to change, thereby moving them away from the cathode. Additional electrons are pulled from the cathode into the magnetically insulated flow, resulting in an excess of electron flow over that expected for the voltage and line current downstream of the switch. These electrons are called launched electrons. Unless they are recaptured at the cathode or else are fed into the load and used beneficially, they cause a large power loss downstream. Examples are shown of SuperMite and PBFA II data showing these losses, the tools used to study them are explained, and the mechanisms employed to mitigate the problem are discussed. The losses will be reduced primarily by reducing the amount of launched electron flow. DOE

N90-11597# Ukrainian Regional Research Inst., Kiev (USSR). Inst. Yadernykh Issledovanij.
BEAM-PLASMA DISCHARGE IN PENETRATING PLASMA
A. V. Opanasenko, G. V. Pitatelev, and L. I. Romanyuk 1988 24 p In RUSSIAN; ENGLISH summary
(DE89-630481; KIYI-88-9) Avail: NTIS (US Sales Only) HC A03/MF A01

The beam-plasma interaction in plasma penetrating towards an electron beam injected into the symmetrically opened penning type plasma system is investigated. The ignition of the beam-plasma discharge by upper hybrid wave excited by the electron beam is found. The behaviors of the amplitude-frequency spectra, oscillation localizations and steady-state plasma parameters while the the beam-plasma discharge developing are determined. It is shown that the strong relaxation of the energy spectrum of beam electrons and the heating of plasma electrons occur in the beam-plasma discharge region. The beam-plasma discharge is determined to be nonstationary and relaxation behavior. DOE

N90-11598# Essen Univ. (Germany, F.R.). Fachbereich Physik.
COMPACT TORUS CONFIGURATIONS WITH HIGH FREQUENCY DRIVEN CURRENTS Ph.D. Thesis [KOMPAKTTORUS KONFIGURATIONEN MIT HOCHFREQUENZGETRIEBEN STROEMEN]
Michael Kuehnapfel Nov. 1988 88 p In GERMAN
(ETN-89-94674) Avail: NTIS HC A05/MF A01

Two methods for the generation of compact torus configurations using HF (high frequency) magnetic fields are investigated. Following the tokamak principle, a static circular current is driven in a preheated and magnetized plasma using a rotating magnetic field, whose 1MW power was produced by a two-channel HF tramsmitter during 1.5 ms. The second method uses an HF magnetic AC field and is based on the Blevin-Thonemann effect; a 500 kW, 200 micros HF transmitter was used. Both methods allow a plasma current of up to 2.5 kA to be driven, which, together with an external static magnetic field, generates a stable compact torus configuration. Under certain conditions another magnetic configuration with two concentric current rings in the plasma is obtained. This result questions the validity of the present models explaining the tokamak principle and Blevin-Thonemann effect. ESA

N90-11599# Swedish Inst. of Space Physics, Umea.
QUANTITATIVE METHODS FOR WAVES IN SPACE PLASMAS
Kjell Roennmark Apr. 1989 74 p
(PB89-210256; IRF-Preprint-112; ETN-89-95160) Avail: NTIS HC A04/MF A01

Methods that bring the theoretical and observational descriptions closer together are reviewed. Standard techniques employed to measure wave fields in space and the analysis of wave data are described. The dynamics of observed waves cannot be described by methods of spectral analysis developed for random stationary processes. Attempts to define time dependent spectra are discussed. Direct satellite observations of wave vectors are scarce. The reconstruction of the wave distribution function from observed frequency spectra is possible. Developed phase space methods allow equations governing the evolution of the wave distribution function in weakly inhomogeneous plasmas to be derived. ESA

N90-11600# Swedish Inst. of Space Physics, Umea.
CAN ION ACCELERATION BY DOUBLE-CYCLOTRON ABSORPTION PRODUCE O(+) ION CONICS
Lewis Ball (Sydney Univ., Australia) Jun. 1989 19 p Submitted for publication
(IRF-Preprint-114; ETN-89-95161) Avail: NTIS HC A03/MF A01

The feasibility of double cyclotron absorption as a source mechanism for oxygen (O(+)) conic distributions in the Earth's magnetosphere is investigated. The appropriate values of the relevant wave and plasma parameters are discussed. The applicability of approximate expressions for the average rate of perpendicular acceleration of O(+) ions due to double cyclotron absorption, is reviewed. The acceleration rate which results from the approximations is shown to be exactly a factor of five larger than the corresponding result of Temerin and Roth. An explanation for this discrepancy is presented. Rough numerical estimates of the average rate of perpendicular acceleration of O(+) ions along auroral field lines are considered. It is shown that double cyclotron absorption is capable of producing O(+) ions at energies comparable to those observed by spacecraft. ESA

76 SOLID-STATE PHYSICS

Includes superconductivity.

For related information, see also *33 Electronics and Electrical Engineering* and *36 Lasers and Masers.*

N90-11601 California Univ., Los Angeles.
STUDY OF DISORDER AND STRAIN IN SEMICONDUCTOR HETEROSTRUCTURES AND SUPERLATTICES BY RAMAN SCATTERING Ph.D. Thesis
Mahmoud Rocco Abdelouhab 1989 172 p
Avail: Univ. Microfilms Order No. DA8907556

Raman scattering was employed in this thesis to study the substitutional disorder and strain in semiconductor heterostructures and superlattices. The details of the In sub 0.52 Al sub 0.48 As/InP longitudinal optical phonon line shape are interpreted in terms of a Spatial Correlation Model with a Gaussian correlation function. This model quantitatively explained the broadening and asymmetry of the LO phonon lines induced by alloy potential fluctuations. The stress, calculated from the pressure coefficient and the observed frequency shift for GaP-like LO phonon in In sub xGa sub 1-xP heterostructures, is larger than the one obtained from the lattice mismatch given by the elastic theory; the possibility of other type of defects responsible for this difference is considered. The presence of internal stress in the epitaxial layer could induce a switch over from one to two-mode behavior. The modified random element isodisplacement model is used to explore this possibility. The strain induced shifts of the GaP-like LO phonons indicate the misfit strains which are known to exist in the (GaP)1(InP)1 monolayer superlattices grown by MBE at two different substrate temperatures. At T sub s = 505 C the strain calculated from the observed frequency shift agrees with the lattice mismatch given

by the elastic theory, whereas for the sample that was grown at a substrate temperature T sub s = 560 C the agreement is quite poor. Dissert Abstr.

N90-11602 Virginia Polytechnic Inst. and State Univ., Blacksburg.
EFFECTS OF GRAVITY ON EQUILIBRIUM CRYSTAL SHAPES Ph.D. Thesis
Apostolos Georgios Gittis 1988 112 p
Avail: Univ. Microfilms Order No. DA8904955

The effects of gravity on the 2-D equilibrium shapes (ES) of crystals and menisci are investigated for different geometries (positions) of the substrate. In the gravity free case, the equilibrium crystal shape (ECS) is characterized by a scale invariance. The presence of gravity breaks the scale invariance and the resulting ECS changes as the volume of the crystal V is changed. Moreover, the presence of gravity breaks the translational invariance along the direction it acts. Physically realized by the necessity of a support, this is manifested by the existence of an inhomogeneous effective pressure P sub eff, which divides the space into two regions, with P sub eff either negative or positive. The ECS changes as the crystal passes from one region to another, being concave where P sub eff less than 0, and convex where P sub eff greater than 0. In all cases it was possible to express the corresponding ECS in terms of the gravity free one. For the hung crystal, i.e., a crystal pinned to a vertical wall at the top, it is shown that some orientations are missing from the ECS that otherwise will be present in the gravity free ECS, adsorbed on the same substrate. Thus, facets could disappear from the crystal shape as the volume V or the gravitational acceleration g is increased. A critical volume V sub c is found, so that if the crystal volume V exceeds V sub c, the crystal cannot be pinned. The ECS can exhibit both concave and convex portions. For a crystal, pinned to a vertical wall at its lower end, it was found that it will never develop a concave part. On the other hand, new orientations, absent from the gravity free crystal, will be present on its ECS. The ES of a free and pinned crystal meniscus is also solved and an expression for the excess (depleted) volume Del V is derived. The solution for the crystal meniscus between two walls is also presented. For the pendant crystal, i.e., a crystal hanging from a horizontal support, it was found that it can exhibit both concave and convex portions on its ECS. An expression for the facet length in the presence of gravity is obtained that is valid for all types of support. Dissert. Abstr.

N90-11603*# Ohio State Univ., Columbus. ElectroScience Lab.
CONSTITUTIVE PARAMETER MEASUREMENTS OF LOSSY MATERIALS
A. Dominek and A. Park Sep. 1989 45 p
(Grant NAG3-1000)
(NASA-CR-183398; NAS 1.26:183398; ESL-721837-1) Avail: NTIS HC A03/MF A01 CSCL 20L

The electrical constitutive parameters of lossy materials are considered. A discussion of the NRL arch for lossy coatings is presented involving analytical analyses of the reflected field using the geometrical theory of diffraction (GTD) and physical optics (PO). The actual values for these parameters can be obtained through a traditional transmission technique which is examined from an error analysis standpoint. Alternate sample geometries are suggested for this technique to reduce sample tolerance requirements for accurate parameter determination. The performance for one alternate geometry is given. Author

N90-11604# Midwest Research Inst., Golden, CO. Solar Energy Research Inst.
NOVEL THIN-FILM CuInSe2 FABRICATION
G. D. Mooney and A. M. Hermann (Arkansas Univ., Fayetteville.) Jun. 1989 7 p
(Contract DE-AC02-83CH-10093)
(DE89-009440; SERI/STR-211-3529) Avail: NTIS HC A02/MF A01

This work studies the feasibility of fabricating CuInSe sub 2 (CIS) solar cells by laser annealing sandwiched layers of elemental Cu, In, and Se. The chalcopyrite phase of CIS is now obtained by thermal annealing elemental Cu and In layers in H sub 2 Se. This process is hazardous because the H sub 2 Se gas is highly toxic. The ability to form the desired chalcopyrite structure by laser annealing would be safer and more conductive to large-scale production. Initial studies of the feasibility of laser annealing the elemental layered structures were performed using a CW argon laser on films fabricated by means of electrodeposition. Characterization of the post-annealed films by X-ray diffraction analysis has shown encouraging results. The laser annealed films have all contained the chalcopyrite phase of CIS. The percentage of the chalcopyrite phase has been small however. Undesirable binary oxides have also formed. To produce higher quality films, future work will concentrate on increasing the percentage of the desirable phase and eliminating all binary compounds. DOE

N90-11605# Los Alamos National Lab., NM.
ON THE PHOTOEMISSION SPECTRUM AND OPTICAL GAP IN La2CuO4
R. L. Martin 1989 17 p Presented at the International Conference on the Physics of Highly Correlated Electron Systems, Santa Fe, NM, 11-15 Sep. 1989
(Contract W-7405-eng-36)
(DE89-015281; LA-UR-89-2564; CONF-890953-1) Avail: NTIS HC A03/MF A01

The photoemission and optical spectrum of La sub 2 CuO sub 4 are computed for a CuO sub 6 cluster model using the techniques of ab initio quantum chemistry. Evidence for a near degeneracy and strong electronic coupling between the configurations Cu(3) plus O(2) minus ((1) A sub g) and Cu(2) plus O(1 minus) (sup 1 A sub g) is presented. This interaction leads to d(8) character at the Fermi energy as well as in the 12eV satellite. DOE

N90-11606*# Case Western Reserve Univ., Cleveland, OH.
SUPERCONDUCTING CERAMICS IN THE Bi1.5SrCaCu2O SUB x SYSTEM BY MELT QUENCHING TECHNIQUE Final Report
Narottam P. Bansal and Mark R. DeGuire Oct. 1989 20 p Presented at the 91st Annual Meeting of the American Ceramic Society, Indianapolis, IN, 23-27 Apr. 1989
(Contract NCC3-133)
(NASA-CR-185139; E-5064; NAS 1.26:185139) Avail: NTIS HC A03/MF A01 CSCL 20L

Bi sub 1.5 SrCaCu sub 2 O sub x has been prepared in the glassy state by rapid quenching of the melt. The kinetics of crystallization of various phases in the glass have been evaluated by a variable heating rate differential scanning calorimetry method. The formation various phases on thermal treatments of the glass has been investigated by powder X-ray diffraction and electrical resistivity measurements. Heating at 450 C formed Bi sub 2 Sr sub 2 CuO sub 6, which disappeared on further heating at 765 C, where Bi sub 2 Sr sub 2 CaCu sub 2 O sub 8 formed. Prolonged heating at 845 C resulted in the formation of a small amount of a phase with T sub c onset of approx. 108 K, believed to be Bi sub 2 Sr sub 2 Ca sub 2 Cu sub 3 O sub 10. This specimen showed zero resistivity at 54 K. The glass ceramic approach could offer several advantages in the fabrication of the high-T sub c superconductors in desired practical shapes such as continuous fibers, wires, tapes, etc. Author

N90-11607# Oak Ridge National Lab., TN.
A STUDY OF THE TRIBOLOGICAL AND SURFACE MICROMECHANICAL PROPERTIES OF YBa2Cu3O7-x
P. J. Blau, C. E. DeVore, D. F. Wilson, and J. R. Keiser Jul. 1989 40 p
(Contract DE-AC05-84OR-21400)
(DE89-015680; ORNL/TM-11053) Avail: NTIS HC A03/MF A01

The burgeoning interest in high critical temperature (T sub c) superconductors has created a need to examine the technological properties of these materials for the purpose of defining potential applications and handling characteristics. While new superconducting compounds continue to be developed, the perovskite-structure oxide ceramics form the basis for these new materials. The information obtained about the reciprocating sliding

friction coefficients (self-mated and on gold), scratch resistance, microindentation hardness, and wear damage mechanisms in YBa2Cu3O(7-x) fabricated in several ways is discussed. As expected, the materials are quite brittle. Knoop microindentation hardness numbers for single crystals can exceed 4.41 GPa (450 kg/sq mm). Low-load, precision indentation experiments provided information on the hardness of thin surface regions less than 300 nm deep, as well as on the modulus of elasticity. The modulus of elasticity obtained by indentation experiments was 78 to 81 GPa, which is in relatively good agreement with density-corrected published values obtained by ultrasonic methods. Scratch resistance using a diamond stylus test falls with increasing load because both intergranular and transgranular cracking increase with load. The abrasion rate of YBa2Cu3O(7-x) on 180-grit silicon carbide papers is linearly proportional to normal load. Overall results confirm that the YBa2Cu3O(7-x) materials are brittle in their monolithic form, and their use in tribological applications should be avoided unless a suitable, more damage-tolerant composite can be developed. DOE

N90-11608# Lawrence Livermore National Lab., CA.
ADAPTATION OF THE THEORY OF SUPERCONDUCTIVITY TO THE BEHAVIOR OF OXIDES
Edward Teller Jul. 1989 12 p Presented at the NATO Advanced Study Institute International Advanced Course on the Nuclear Equation of State, Peniscola, Spain, 12 May - 3 Jun. 1989
(Contract W-7405-eng-48)
(DE89-016518; UCRL-101545; CONF-8905143-11) Avail: NTIS HC A03/MF A01

An adaptation of the conventional theory to high temperature superconductors is proposed. Excitation of electrons from below the Fermi surface to above the Fermi surface (according to Bardeen, Copper and Schrieffer) is replaced by excitation from a filled energy band into an empty one. The energy bands are constructed from 2-D Bloch functions in neighboring layers of the oxide lattices. Strong coupling with lattice displacements is due to the removal of the topmost electrons from the O(2-) ions in the perovskite planes. The main methods of the BCS theory are retained. The formation and observability of a super-lattice is discussed. DOE

N90-11609# Florida Univ., Gainesville. Dept. of Physics.
STUDIES OF NOVEL SUPERCONDUCTORS Progress Report, 1 Jan. 1989 - 31 Dec. 1989
G. R. Stewart Aug. 1989 18 p
(Contract DE-FG05-86ER-45268)
(DE89-016744; DOE/ER-45268/T1) Avail: NTIS HC A03/MF A01

Important progress was made in understanding the formation of the heavy fermion ground state via specific heat, susceptibility, and resistivity studies of U sub 1-x M sub x Be13, 0 less than or = x less than or = .995 and M = Hf, Zr, Sc, Y, La, Ce, Pr, Lu and Th. The high effective mass, m*, in UBe13 was found to be caused both by single ion effects, which contribute about 50 percent of the large specific heat gamma (alpha m*), and also by a many body correlation which depends on complete occupation of the U sites by U, i.e., the Kondo-lattice model. This is the first such demonstration of how the large m* ground state is formed in a heavy fermion compound. In the single ion regime, it was found that it is the U-Be separation that is the controlling factor, not the effective U-U distance ((alpha) dilution) nor the identity of the doping metal M. Progress was also made on other heavy fermion research projects, including the response of T sub c in UPt3 to non-magnetic impurities, the T sub c of super-pure UBe13, and the behavior of C in high field of CeCu6. Additionally, a new heavy fermion compound, NpPt4Au, was discovered, improving the understanding of the temperature dependence of the formation of m* at low temperatures. DOE

N90-11610# Oak Ridge National Lab., TN. Solid State Div.
ION BEAM ANNEALING OF Ga-IMPLANTED Si
S. P. Withrow, O. W. Holland, and S. J. Pennycook 1989 11 p Presented at the European Materials Research Society Spring Meeting, Strasbourg, France, 30 May - 2 Jun. 1989 Submitted for publication
(Contract DE-AC05-84OR-21400)
(DE89-016857; CONF-890579-1) Avail: NTIS HC A03/MF A01

Rutherford backscattering/ion channeling and transmission electron microscopy were used to investigate regrowth effects which occur during high-energy ion bombardment of amorphous silicon layers implanted with 1 x 10(16) Ga/sq cm. At both 300 and 400 C the Si lattice initially regrows epitaxially. However, at this high dopant level, Ga is segregated at the crystalline-amorphous interface and eventually disrupts epitaxy. Transmission electron microscopy had been used to characterize the lattice morphology and monitor movement of the Ga. The results are compared with thermal annealing effects in Ga-implanted Si samples. DOE

N90-11611# Oak Ridge National Lab., TN.
PROPAGATION OF NORMAL ZONES OF FINITE SIZE IN LARGE, COMPOSITE SUPERCONDUCTORS
Lawrence Dresner 1989 14 p Presented at the 11th International Conference on Magnet Technology, Tsukuba, Japan, 28 Aug. - 1 Sep. 1989
(Contract DE-AC05-84OR-21400)
(DE89-016866; CONF-890850-1) Avail: NTIS HC A03/MF A01

Very large, composite superconductors were proposed for use in energy storage magnets. A typical conductor, rated at 230 kA, was discussed by J. Waynert, Y. Eyssa, and X. Huang, namely, a 6-cm aluminum cylinder with superconducting filaments on its outer surface. Owing to its large size and nonuniform distribution of filaments, such a conductor can sustain normal zones of finite size that travel at a uniform velocity along the conductor. A simple, analytical model was presented that permits determination of the conditions under which such zones can exist and the size and velocity of such zones. It was shown that the transport current has a threshold value below which finite normal zones cannot exist and that the propagation velocity corresponding to this threshold current, though not zero, is the smallest possible. DOE

N90-11612# Argonne National Lab., IL. Materials Science Div.
DEFECT STRUCTURES PRECEDING AMORPHIZATION BY ION IRRADIATIONS IN YBa2Cu3O(7-DELTA)
M. A. Kirk, M. C. Frischherz, J. Z. Liu, L. L. Funk, L. J. Thompson, E. A. Ryan, S. T. Ockers, and H. W. Weber (Atominstitut der Oesterreichischen Hochschulen, Vienna.) Jun. 1989 3 p Presented at the International Conference on Materials and Mechanisms of Superconductivity - High-Temperature Superconductors, Stanford, CA, 23-28 July 1989
(Contract W-31-109-eng-38)
(DE89-016905; CONF-890718-25) Avail: NTIS HC A01/MF A01

Transmission electron microscopy was used to investigate defect microstructures in single crystals of YBa2Cu3O(7-delta) as a function of ion irradiation dose at 300 K. Two qualitatively different defect microstructures were observed to precede amorphization. The transition between microstructures occurs at a damage level where published resistance versus temperature measurements indicate a transition from superconducting to insulating behavior. DOE

N90-11613# Gosudarstvennyi Komitet po Ispolzovaniyu Atomnoi Energii, Moscow (USSR). Inst. Atomnoj Ehnergii.
PASSAGE OF ULTRARELATIVISTIC ELECTRONS THROUGH REAL CRYSTALS
V. A. Starostin 1988 5 p In RUSSIAN; ENGLISH summary
(DE89-618624; IAE-4677/1) Avail: NTIS (US Sales Only) HC A01/MF A01

A theory was developed on passage of fast charged particles through single crystals of any nature. Necessity of allowance for defect influence in choosing the crystal, the source of directional radiation, is shown. DOE

N90-11614# International Centre for Theoretical Physics, Trieste (Italy).
PINNING OF CURVED FLUX LINES ON THE BOUNDARY BETWEEN TWO PHASES OF HIGH TEMPERATURE SUPERCONDUCTORS
A. G. Saif (Atomic Energy Establishment, Cairo, Egypt) Jan. 1989 11 p Submitted for publication
(DE89-618865; IC-89/11) Avail: NTIS (US Sales Only) HC A03/MF A01

The distribution of the magnetic fields and the current density in a system of two phases of high temperature superconductors (HTS) are determined. Recently, this system was confirmed experimentally. The energy of the interaction between curved flux lines (FLs) and the interface is calculated. It is shown that for positive Delta G (the change in the flux line (FL) energy at the interface) the FLs will be pinned by the interface and the pinning force is formulated. Moreover, this force will be different according to the movement of the FL to the right or to the left. Agreements with the previous results (in special cases) are obtained. This study may serve to test the pinning experimentally. DOE

N90-11615# Rensselaer Polytechnic Inst., Troy, NY. Dept. of Materials Engineering.
EXPLORATORY STUDY OF NIOBIUM, TITANIUM, ZIRCONIUM AND TANTALUM ALUMINIDES Final Report, 1 Mar. 1988 - 31 May 1989
Norman S. Stoloff 1 Jul. 1989 24 p
(Contract N00014-88-K-0275)
(AD-A210658) Avail: NTIS HC A03/MF A01 CSCL 20/2

The microstructure, crystal structures of existing phases, hardness and slip systems for several binary and ternary aluminides were determined. Arc melted samples purchased from an external supplier invariably cracked upon cooling in the arc melting unit, thereby hampering the ability to prepare mechanical test specimens. Homogenization heat treatments in vacuum usually led to significant porosity, apparently due to loss of aluminum. The properties of arc melted material are compared to those derived from similar compositions prepared by powder metallurgical techniques. GRA

N90-11616# North Carolina State Univ., Raleigh. Dept. of Materials Science and Engineering.
KINETICS AND MECHANISMS OF PRIMARY AND STEADY STATE CREEP IN B- AND Al-CONTAINING ALPHA SILICON CARBIDE Final Report, 15 Nov. 1985 - 15 Jul. 1989
Robert F. Davis and Calvin H. Carter, Jr. Jul. 1989 12 p
(Contract DAAL03-86-K-0013)
(AD-A210739; ARO-23025.1-MS) Avail: NTIS HC A03/MF A01 CSCL 11/2

The steady state creep behavior of a number of high temperature structural ceramics has been measured and the results analyzed to determine the controlling mechanism. Pure polycrystalline silicon carbide, devoid of sintering aids, creeps by dislocation motion and climb. Silicon carbide containing B- and Al- sintering aids, creeps by grain boundary sliding controlled by diffusion mechanisms (grain boundary diffusion - Coble creep - below 1920 K; lattice diffusion - Nabarro-Herring creep-above 1920 K). The difference in behavior is attributed to the high concentration of vacancies accompanying impurity substitution in the sintered silicon carbide. Experimental measurements of grain boundary sliding offsets on polycrystalline silicon carbide have shown that the primary, transient, creep stage in this material is primarily due to plastic strain within the grains, and that the secondary, steady state, creep stage is primarily due to grain boundary sliding between the grains. The creep of a single crystal and polycrystalline niobium carbide in the 1570 to 1850 K range is controlled by dislocation glide and climb. The creep of hot pressed silicon nitrate and mullite in the 1470 to 1800 K range is controlled by grain boundary sliding due to the amorphous phase present as a consequence of Y2O3 and Al2O3 sintering aids. GRA

N90-11617# Centre National de la Recherche Scientifique, Toulouse (France).
INTERNATIONAL WORKSHOP ON BEAM INJECTION ASSESSMENT OF DEFECTS IN SEMICONDUCTORS
20 Jul. 1989 52 p Workshop held in Meudon-Bellevue (France), 18-20 Jul. 1988
(Contract DAJA45-88-M-0202)
(AD-A210842; R/D-6047-MS-02) Avail: NTIS HC A04/MF A01 CSCL 20/12

The following topics were addressed at the International Workshop on beam injection assessment of defects in semiconductors: scanning electron microscopy (SEM) microcharacterization of semiconductors; electron and photon-matter interaction; modelling of the elctron beam induced current (EBIC) measurements of diffusion lengths and the recombination contrast; minority carrier diffusion length (measurement by EBIC, connection to material microstructure); STEM-catholuminescence; intrinsic or extrinsic origin of the recombinations at defects; LBIC (light beam induced current) quantitative mapping; scanning deep level transient spectroscopy (DLTS); cathodoluminescence (CL) in laser heterojunctions; CL in quantum-wells;and electron and optical beam testing of integrated circuits. GRA

N90-11618# General Atomic Co., San Diego, CA.
HIGH-TEMPERATURE CERAMIC SUPERCONDUCTORS Annual Technical Report, 24 May 1988 - 30 Jun. 1989
K. S. Mazdiyasni, K. C. Chen, W. J. DeHope, D. M. Duggan, E. Y. Glatter, Y. R. Lin-Liu, B. W. McQuillan, F. C. Montgomery, S. S. Pak, and R. B. Stephens et al 15 Jul. 1989 111 p
(Contract N00014-88-C-0714)
(AD-A211070; GA-A19800) Avail: NTIS HC A06/MF A01 CSCL 20/3

The principal goals of this program are: (1) to demonstrate fabrication of high-temperature ceramic superconductors via sol-gel method that can operate at or above 90 K with appropriate current density, Jc, in forms useful for application in resonant cavities, magnets, motors, sensors, computers, and other devices; and (2) to fabricate and demonstrate selected components made of these materials, including microwave cavities and magnetic shields. The chemical pathways for preparation of 123 powder, fiber and film were identified. GRA

N90-11619# Applied Research Lab., State College, PA.
PHYSICS AND MATERIALS SCIENCE OF HIGH TEMPERATURE SUPERCONDUCTORS Final Report
Ram Rossowsky and Siegfried Methfessel (Ruhr Univ., Bochum, Germany, F.R.) 26 Aug. 1989 165 p
(Contract MIPR-ARO-135-89)
(AD-A211246; ARO-26564.1-MS-CF) Avail: NTIS HC A08/MF A01 CSCL 20/3

This report contains the conference program, a list of the abstracts of papers, the poster session abstracts and a list of the participants. The program stressed the physics and materials science of high temperature superconductors. GRA

N90-11620# Los Alamos National Lab., NM.
HIGH PRESSURE 129I MOESSBAUER STUDIES OF GeI4 MOLECULAR CRYSTALS
M. P. Pasternak (Tel-Aviv Univ., Israel) and R. Dean Taylor 1989 12 p Presented at the International Conference on the Applications of the Mossbauer Effect (ICAME '89), Budapest, Hungary, 4-8 Sep. 1989
(Contract W-7405-eng-36)
(DE89-015269; LA-UR-89-2324; CONF-890933-1) Avail: NTIS HC A03/MF A01

The Moessbauer effect in (129)I in conjunction with Diamond-Anvil-Cell high pressure techniques was applied to investigate the high pressure phase(s) of the molecular crystal GeI sub 4. The (129)I Quadrupole Interaction was the main probe for characterizing the intermolecular structural transformation with pressure. With increasing pressure, at about 15 GPAa, the onset of a partial molecular-association phase (HP1) is first observed. In

HP1 two out of the four iodines strongly overlap to form linear chains of GeI(sub 4). The HP1 phase coexists with the low pressure (LP) molecular phase, but its population increases with increasing pressure. At P (approx)20 GPa a second high pressure phase (HP2) is identified where all four iodines strongly overlap to form a three dimensional, fully molecular-associated structure. With increasing pressure and at P less than 20 GPa, HP2 is the only phase up to P = 34 GPa, the highest pressure used. A significant hysteresis of the relative abundances with pressure is observed. The isomer shift of the HP2 and HP1 structures is considerably larger than that of the LP one. DOE

N90-11621# Wisconsin Univ., Madison.
THERMODYNAMICS, KINETICS, AND INTERFACE MORPHOLOGIES OF PHASE FORMATION REACTIONS BETWEEN METALS AND GALLIUM ARSENIDE: BULK VS THIN-FILM STUDIES
Y. A. Chang 1989 7 p
(Contract DE-FG02-86ER-45274)
(DE89-016469; DOE/ER-45274/3) Avail: NTIS HC A02/MF A01

During the past two years or so, we have been carrying out the following studies: (1) investigation of the thermodynamic stabilities of selected GaAs/M couples by determining the Ga-M-As phase diagrams at one temperature in the composition region of importance to the metallization of GaAs, and (2) determination of the kinetics and morphologies of reactions between GaAs and M for both bulk and thin-film cases. The metallic elements which have been studied are Pd, Pt, Ir, Rh, Nb, Co and Ni. In the following, we will summarize briefly our accomplishments. DOE

N90-11622# Oak Ridge National Lab., TN.
ORIGINS OF HIGH-TEMPERATURE SUPERCONDUCTIVITY IN THE NEW COPPER OXIDE BASED CERAMIC SUPERCONDUCTORS Foreign Trip Report, 20 Jul. 1988 - 29 Jul. 1989
R. F. Wood 14 Aug. 1989 24 p
(Contract DE-AC05-84OR-21400)
(DE89-016543; ORNL/FTR-3349) Avail: NTIS HC A03/MF A01

The traveler spent a year at the University of Erlangen-Nuernberg, FRG, funded by a Senior U.S. Scientist Award from the Alexander von Humboldt Foundation. Brief background information on the von Humboldt Foundation and on the Friedrich-Alexander- Universitaet Erlangen-Nuernberg is given. The traveler's theoretical work on high-T sub c superconductivity at Erlangen, carried out primarily at the Chair for Theoretical Chemistry, was concentrated on excitonic and spin-polaron mechanisms for superconductivity. Brief comments and observations related to interactions and travel during the year are given. Finally, some general observations about science and the university system in the Federal Republic of Germany are made. DOE

N90-11623# Argonne National Lab., IL. Materials and Components Technology Div.
TRANSPORT PROPERTIES OF THERMALLY GROWN Cr2O3
J. H. Park and K. Natesan May 1989 33 p
(Contract W-31-109-eng-38)
(DE89-016703; ANL/FE-89/5) Avail: NTIS HC A03/MF A01

The electrical conductivity of thermally grown chromium oxide (Cr2O3) has been measured as a function of temperature and over a range of oxygen partial pressures from that of air to that of the Cr/Cr2O3 equilibrium. The conductivity showed p-type behavior over the range of conditions of the present investigation. At temperatures above 1000 C, the conductivity values were independent of oxygen partial pressure and indicated intrinsic semiconductor behavior. The mobility of holes, determined by measuring conductivity at fixed compositions increased with temperature. The oxidation kinetics of Cr were determined by measuring the electrical conductivity and electromotive force across the oxide layer at 875 C. The result agreed well with the oxidation data obtained in thermogravimetric tests. The diffusivities of oxygen and sulfur in thermally grown chromium oxide were determined by means of electrical conductivity measurements. The measured diffusivity of sulfur in chromium oxide is at least one to two orders of magnitude higher than that of oxygen. The solubility of sulfur was also determined from the conductivity measurements. The solubility of sulfur decreased with an increase in temperature, but was almost constant below 800 C. DOE

N90-11624# Los Alamos National Lab., NM.
A FERMI LIQUID ELECTRIC STRUCTURE AND THE NATURE OF THE CARRIERS IN HIGH-T(SUB c) CUPRATES: A PHOTOEMISSION STUDY
A. J. Arko, R. S. List, R. J. Bartlett, S. W. Cheong, Z. Fisk, J. D. Thompson, C. G. Olson, A. B. Yang, R. Liu, and C. Gu (Iowa State Univ. of Science and Technology, Ames.) et al 1989 32 p Presented at the 9th Vacuum Ultraviolet Radiation Conference, Honolulu, HI, 17-21 Jul. 1989 Prepared in cooperation with Argonne National Lab., IL; and Sandia National Labs, Albuquerque, NM
(Contracts W-7405-eng-36; W-31-109-eng-38; W-7405-eng-82)
(DE89-016774; LA-UR-89-2680; CONF-8907130-2) Avail: NTIS HC A03/MF A01

We have performed angle-integrated and angle-resolved photoemission measurements at 20 K on well-characterized single crystals of high-T(sub c) cuprates (both 1:2:3-type and 2:2:1:2-type) cleaved in situ, and find a relatively large, resolution limited Fermi edge which shows large amplitude variations with photon energy, indicative of band structure final state effects. The lineshapes of the spectra of the 1:2:3 materials as a function of photon energy are well reproduced by band structure predictions, indicating a correct mix of 2p and 3d orbitals on the calculations, while the energy positions of the peaks agree with calculated bands only to within (approx)0.5 eV. This may yet prove to reflect the effects of Coulomb correlation. We nevertheless conclude that a Fermi liquid approach to conductivity is appropriate. Angle-resolved data, while still incomplete, suggest agreement with the Fermi surface predicted by the local density approximation (LDA) calculations. A BCS-like energy gap is observed in the 2:2:1:2 materials, whose magnitude is twice the weak coupling BCS value (i.e., 2(Delta) = 7 KT(sub c)). DOE

N90-11625# Oak Ridge National Lab., TN.
DIELECTRONIC EXCITATION AND RECOMBINATION IN CRYSTAL CHANNELS
S. Datz, C. R. Vane, P. F. Dittner, J. P. Giese, J. GomezdelCampo, N. L. Jones, H. F. Krause, P. D. Miller, M. Schulz, and H. Schone et al 1989 24 p Presented at the 13th International Conference on Atomic Collisions in Solids, Aarhus, Denmark, 7-11 Aug. 1989
(Contract DE-AC05-84OR-21400)
(DE89-016864; CONF-890821-2) Avail: NTIS HC A03/MF A01

Dielectronic excitation and recombination have been observed during the interaction of channeled ions (H-like S, Ca, and Ti and He-like Ti) with the electrons contained in less than 110 greater than less than 100 greater than channels in Si. As in dielectronic recombination, the products of the reaction are an ion of reduced charge state and the emission of a photon(s). However, the high electron density in the channel introduces collisional mechanisms for the destruction of the doubly excited intermediate state and even the formation of ions with increased charge state. The experiments prove that crystal channels may be treated quantitatively as a dense electron target for ions with velocity v(sub i) much greater than v(sub f), the Fermi velocity of the electrons in the channel. DOE

N90-11626# Oak Ridge National Lab., TN.
RATIONAL DESIGN OF HIGH-CURRENT CABLE-IN-CONDUIT SUPERCONDUCTORS
Lawrence Dresner 1989 21 p Presented at the IAEA Specialists Meeting on Superconducting Materials and Magnets, Tokyo, Japan, 4-6 Sep. 1989
(Contract DE-AC05-84OR-21400)
(DE89-016867; CONF-8909184-1) Avail: NTIS HC A03/MF A01

Cable-in-conduit superconductors are composed of a cable of many fine composite strands encased in a strong, protective jacket, with helium coolant filling the interstices of the cable. Because of the high degree of subdivision of the composite and its consequent large cooled surface, such conductors are capable of stable operation at quite high current densities. The designer of such conductors is frequently given the field at the conductor and the overall current density and asked to specify the remaining variables of the conductor (e.g., the strand diameter, the hydraulic path length, the void fraction of the cable, and the Cu/SC ratio). A rational procedure is outlined for determining the most problematic variables, the two composition variables that determine the proportions of copper, superconductor, and helium in the cable space. All other variables of the conductor are assumed known.
DOE

N90-11627# Sandia National Labs., Albuquerque, NM.
STRAIN AND DENSITY DEPENDENT VALENCE-BAND MASSES IN InGaAs/GaAs AND GaAs/GaAsP STRAINED-LAYER STRUCTURES
E. D. Jones, R. M. Biefeld, J. F. Klem, and S. K. Lyo 1989 6 p Presented at the 16th Symposium on Gallium Arsenide and Related Compounds, Karuizawa, Japan, 25-29 Sep. 1989
(Contract DE-AC04-76DP-00789)
(DE89-016882; SAND-89-1116C; CONF-8909185-1) Avail: NTIS HC A02/MF A01

Low temperature magnetoluminescence measurements were performed in several n-type InGaAs/GaAs single strained quantum wells with varying internal strain and a n-type GaAs/GaAsP strained layer superlattice. Using newly discovered selection rules, an analysis of the data yields simultaneous information about the conduction and valence band dispersion curves from a single sample. It was found that the conduction-bands are parabolic for all of our structures, with effective mass in the range of 0.068 to 0.074m sub 0. The valence-bands are found to be nonparabolic and strain dependent. A simple two band model is used to analyze the nonparabolicity in terms of a zone-center mass m and a parameter C which is expressed in terms of the light-hole and heavy-hole energy difference. From the two-band model, predictions for the valence-band mass as a function of the 2D-carrier concentration can be made. These predictions are found to be in good agreement with recent cyclotron resonance measurements of the mass in p-type samples. DOE

N90-11628# Los Alamos National Lab., NM. Neutron Scattering Center.
CHEVRON LAYER STRUCTURES IN SURFACE STABILIZED FERROELECTRIC LIQUID CRYSTAL (SSFLC) CELLS FILLED WITTH A MATERIAL WHICH EXHIBITS THE CHIRAL NEMATIC TO SMECTIC C* PHASE TRANSITION
T. P. Rieker, N. A. Clark, and C. R. Safinya (Exxon Research and Engineering Co., Annandale, NJ.) 1989 17 p Presented at the Symposium on Ferroelectric Liquid Crystals, Goteborg, Sweden, 27-30 Jun. 1989
(Contracts W-7405-eng-36; DAAL03-86-0053; NSF DMR-83-07157; NSF CDR-86-22236)
(DE89-016985; LA-UR-89-2840; CONF-8906207-1) Avail: NTIS HC A03/MF A01

In this paper we report on the layer structure in Surface Stabilized Ferroelectric Liquid Crystal (SSFLC) electro-optic cells, adopted by a compound which exhibit the smectic C asterisk (SC asterisk) to chiral nematic (N asterisk) phase transition. This class of compounds is unique in that the SC asterisk layers form directly from the N asterisk phase. These materials demonstrate a large tilt ((Theta)) of the director ((cflx n)) from the layer normal ((cflx z)(prime)) immediately upon cooling into the SC asterisk phase. Recent high resolution X-ray experiments have demonstrated the presence of a chevron layer structure of tilted layers in compounds which exhibit the smectic A (SA) to SC asterisk and the N asterisk-SC asterisk phase transitions, and also in a compound which has a very broad smectic A Phase. Chevron formation in smectic samples is a result of the layers anchoring normal or nearly normal to the bounding plates and subsequent layer contraction in the absence of dislocations. Patel and Goodby have demonstrated that compounds which exhibit the N asterisk-SC asterisk phase transition in the SSFLC geometry can be aligned by the application of an electric field across a cell with a buffed polymer surface treatment. With this method two domains of smectic layers form at large angles to the buffing direction normal.
DOE

N90-11629# Sandia National Labs., Albuquerque, NM.
EFFECTS OF SHOCK-MODIFICATION ON SUPERCONDUCTIVITY IN Tl2Ca2Ba2Cu3Oy AND Bi2CaSr2Cu2Ox
E. L. Venturini, R. A. Graham, D. S. Ginley, and B. Morosin 1989 4 p Presented at the American Physical Society Topical Conference on Shock Compression of Condensed Matter, Albuquerque, NM, 14-17 Aug. 1989
(Contract DE-AC04-76DP-00789)
(DE89-017231; SAND-89-1115C; CONF-890812-28) Avail: NTIS HC A01/MF A01

Powder compacts of superconducting Tl2 Ca2 Ba2 Cu3 O sub y Tl-2223 and Bi2 CaSr2 Cu2 O sub x Bi-2122 were subjected to controlled, quantitative high-pressure shock-wave loading in gas-tight copper recovery capsules and preserved for post-shock analysis. Magnetization data show a substantial decrease in both diamagnetic shielding and Meissner effect for both compounds following shock modification over a range of peak pressures from 7.5 to 27 GPa and peak temperatures from 150 to 850 C. There is a 5 K increase in the onset of superconductivity in shock-modified Tl-2223, while Bi-2122 shows no measurable change. Magnetic flux creep measurements at low temperature reveal a three-fold increase in the flux pinning energy for Tl-2223 following shock modification.
DOE

N90-11630# Oak Ridge National Lab., TN. Solid State Div.
NEUTRON SCATTERING EXPERIMENTS ON HIGH-TEMPERATURE SUPERCONDUCTING MATERIALS: FOREIGN TRIP REPORT, SEPTEMBER 13, 1988--OCTOBER 4, 1988
H. A. Mook 21 Oct. 1988 7 p
(Contract DE-AC05-84OR-21400)
(DE89-017451; ORNL/FTR-3092) Avail: NTIS HC A02/MF A01

The trip to the Institut Laue-Langevin (ILL) was made to perform neutron scattering experiments on the new high temperature superconducting materials. Part of this work could have been accomplished at the High Flux Isotope Reactor (HFIR) at ORNL had it been operational; other parts utilized the special instrumentation at the ILL available at no other place. Experiments performed were the following: high energy magnetic excitations in pure and Ba-doped La2CuO4, magnetic excitations and structural phase transitions in the Bi2Ba2Cu1O6 superconductor, search for the fluxoid lattice in the high temperature materials, and magnetic spin structures in ErBa2Cu3O7 and GdBa2Cu3O6.5. Measurements were also made on supermirrors important for polarizing and neutron guide applications.
DOE

N90-11631# Hokkaido Univ., Sapporo (Japan).
REPORT OF THE SPECIALISTS' WORKSHOP ON PHASE TRANSITION STUDIES ON HYDROGEN-BONDED CRYSTALS BY NEUTRON AND X-RAY DIFFRACTOMETRIES
M. Tokunaga, ed. and I. Shibuya, ed. (Kyoto Univ., Kumatori, Japan) Jan. 1989 56 p In JAPANESE Workshop held in Kumatori, Japan, 12-13 Dec. 1988
(DE89-906638; KURRI-TR-311; CONF-8812101) Avail: NTIS (US Sales Only) HC A04/MF A01

A total of 15 studies on hydrogen bonded crystals made by means of neutron/X-ray diffraction which were presented at a technical study meeting are presented. Areas covered are: introduction; linear relation between transition temperature and hydrogen bond length in KDP type crystals; X-ray study of crystal structure under high pressure in DKDP; crystal structure of ADP in the paraelectric phase; crystal structure of Rochelle salt in the paraelectric phase; distortion of AsO4 in KDA; study of phase

transition in KDP family by dielectric dispersion; dielectric relaxation and phase transition in ice Ih; Raman scattering study of KDP; mechanism of phase transition in KDP by Raman scattering study under high pressure reinvestigation of the Peercy's conclusion; localized modes of proton in KDP; hyper-Raman scattering study of hydrogen bonded crystals; phase transition of CDP; the 180 deg law in phase diagram; and comments. DOE

N90-11632# Essen Univ. (Germany, F.R.). Fachbereich Chemie.
DESIGN AND CONSTRUCTION OF SYSTEMS FOR THE SINGLE-CRYSTALS GROWTH OF TERNARY SILVER HALIDES, ALKALI HALIDES, AND ALKALINE EARTH FLUORIDES, AND THE DIELECTRIC INVESTIGATION OF SILVER HALIDE Ph.D. Thesis [ENTWICKLUNG UND AUFBAU VON ANLAGEN FUER DIE EINKRISTALLZUCHT VON TERNAERN SILBERHALOGENIDEN, ALKALIHALOGENIDEN UND ERDALKALIFLUORIDEN UND DIELEKTRISCHE UNTERSUCHUNG DER SILBERHALOGENIDE]
Werner Hueben-Riechert 1988 174 p In GERMAN
(ETN-89-94673) Avail: NTIS HC A08/MF A01

Large single crystals of several congruently melting and incongruently melting compounds are produced for optics applications. The state diagrams of the quasi-binary silver halide system, are described and verified. The methods for the growth of single crystals from the melt, and from melting solutions, are outlined. The different developed crystal growth apparatus are described. Large single crystals of the congruently melting compounds NaCl, KBr, CsI, MgF2, CaF2, and the incongruently melting compounds RbAg4I5, Rb2AgBr3, AgPb2Br5, Ag3PbI5 are produced. The ionic conductivity of these synthetic ternary silver compounds is measured using a dielectric spectrometer. ESA

77 THERMODYNAMICS AND STATISTICAL PHYSICS

Includes quantum mechanics; theoretical physics; and Bose and Fermi statistics.

For related information see also *25 Inorganic and Physical Chemistry* and *34 Fluid Mechanics and Heat Transfer.*

N90-11633# Lawrence Livermore National Lab., CA. Dept. of Physics.
GENERAL COVARIANCE AND STRINGS
Frans R. Klinkhamer (Nationaal Inst. voor Kernfysica en Hoge Energiefysica, Amsterdam, Netherlands) Jul. 1989 5 p Presented at the NATO Advanced Research Workshop on Physics and Geometry, Lake Tahoe, CA, 2-8 Jul. 1989
(Contract W-7405-eng-48)
(DE89-016505; UCRL-101586; CONF-8907129-2) Avail: NTIS HC A01/MF A01

It may be that (super)strings are part of the elusive quantum theory of gravity. If so, one obvious question is whether or not string field theory is generally covariant. Recall that string field theory involves the string creation/annihilation operator Phi (X), where, for brevity, the ghost coordinates is omitted. The action of the free open string is (integral) DX Phi (X) Q Phi (X), where Q = Q(X, delta/delta X) is the so called BRST operator and (integral)DX integrates over the space of all strings, i.e., loop space. Since both DX and Q involve the Minkowski metric eta sub mu nu the action is clearly not generally covariant. Actually, we are interested in covariance not only over the finite dimensional target space but over the infinite dimensional loop space. The most straight forward thing to do is to introduce a background loop space metric and to follow, as closely as possible, the steps of standard general relativity. Only the basic results are listed. DOE

N90-11634# Stanford Linear Accelerator Center, CA.
THREE LEVEL CONSTRAINTS ON CONFORMAL FIELD THEORIES AND STRING MODELS
David C. Lewellen May 1989 8 p Presented at the Superstring 1989 Workshop, College Station, TX, 13-18 Mar. 1989
(Contract DE-AC03-76SF-00515)
(DE89-016942; SU-SLAC-Pub-5022; CONF-8903130-3) Avail: NTIS HC A02/MF A01

Simple tree level constraints for conformal field theories which follow from the requirement of crossing symmetry of four-point amplitudes are presented, and their utility for probing general properties of string models is briefly illustrated and discussed. DOE

N90-11635# Instituto de Fisica Teorica, Sao Paulo (Brazil).
GRAVITATIONAL NONMINIMALLY COUPLED ELECTROMAGNETIC FIELDS: A POSSIBLE SOLUTION TO SOME IDIOSINCRASIES OF EINSTEIN-MAXWELL THEORY
A. J. Accioly, U. F. Michoski, and N. L. P. PereiradaSilva (Universidade Federal do Rio de Janeiro, Brazil) 1988 37 p
(DE89-618430; IFT-P-28/88) Avail: NTIS (US Sales Only) HC A03/MF A01

A theory of nonminimal coupling of electromagnetism and gravitation in the framework of Riomannian geometry is constructed. As a consequence the main difficulties concerning the Einstein-Maxwell theory are cleared away. The theory works as a kind of correction to the Einstein-Maxwell one for regions with strong curvature and for times much greater than the Planck time. A Reissner-Nordstroem-type solution is exhibited and comments are made on a parameter which somewhat resembles the Schwarzschild radius. A mechanism of charge creation via nonminimal coupling is also discussed. The propagation of photons in a Robertson-Walker background was calculated and it was found that the effect of the nonminimal coupling in this case may be to deviate the photon from the null geodesics, increasing its velocity beyond the flat-space value. Taking into account this result, the observed isotropy of the background radiation can be explained in a simple way, regardless of any assumption about the state of the Universe prior to the Planck time. DOE

N90-11636# International Centre for Theoretical Physics, Trieste (Italy).
SUPERFILED FORMULATION OF CHERN-SIMONS SUPERSYMMETRY
Danny Birmingham and Mark Rakowski (Oklahoma Univ., Norman.) Mar. 1989 10 p Submitted for publication
(DE89-618459; IC-89/38) Avail: NTIS (US Sales Only) HC A02/MF A01

An an extra supersymmetry present in the covariantly quantized Chern-Simons action within the superfield formalism is discussed. By introducing scalar superfields, it is shown how the component transformations are naturally reproduced from the superfield transformation. When the superspace is extended to include an additional odd coordinate for the BRST symmetry, the entire theory is described by a single odd scalar superfield. The implications of this supersymmetry for the renormalized theory are also discussed. DOE

N90-11637# International Centre for Theoretical Physics, Trieste (Italy).
GENERAL ACTION FOR TOPOLOGICAL QUANTUM FIELD THEORIES
Oemer F. Dayi Mar. 1989 18 p Submitted for publication
(DE89-618460; IC-89/47) Avail: NTIS (US Sales Only) HC A03/MF A01

Topological field theories can be formulated by beginning from a higher dimensional action. The additional dimension is an unphysical time parameter and the action is the derivative of a functional W with respect to this variable. In the d = 4 case, it produces actions which are shown to give topological quantum field theory after gauge fixing. In d = 3 this action leads to the Hamiltonian, which yields the Floer groups if the additional parameter is treated as physical when W is the pure Chern-Simons action. This W can be used to define a topological quantum field theory in d = 3 by treating the additional parameter as unphysical. The BFV-BRST operator quantization of this theory yields to an enlarged system which has only first class constraints. This is not identical to the previously introduced d = 3 topological quantum

field theory, even if it is shown that the latter theory also gives the theory which was began with, after a partial gauge fixing. DOE

N90-11638# International Centre for Theoretical Physics, Trieste (Italy).
THE THERMAL STABILITY BETWEEN ROTATING CYLINDERS IN A RADIALLY SYMMETRICAL GRAVITATIONAL FIELD
A. R. Bestman (Port Harcourt Univ., Nigeria) Dec. 1988 6 p Submitted for publication
(DE89-618548; IC-88/421) Avail: NTIS (US Sales Only) HC A02/MF A01

The flow in a porous medium confined between two rotating heated cylinders in a radially symmetrical gravitational field is examined. Particular attention is focussed on the critical point for the onset of instability. The effect of porosity and heating on the stability boundary is discussed quantitatively. The results are important to geophysics. DOE

N90-11639# Stanford Linear Accelerator Center, CA.
MODULI SPACES AND TOPOLOGICAL QUANTUM FIELD THEORIES
Jacob Sonnenschein (California Univ., Los Angeles.) Jul. 1989 13 p Presented at the 18th International Conference on Differential Geometric Methods in Theoretical Physics: Physics and Geometry, Tahoe City, CA, 2-8 Jul. 1989
(Contract DE-AC03-76SF-00515)
(DE89-016943; SU-SLAC-PUB-5031; CONF-8907140-1) Avail: NTIS HC A03/MF A01

We show how to construct a topological quantum field theory which corresponds to a given moduli space. This method is applied to several cases. In particular we discuss the moduli space of flat gauge connections over a Riemann surface which is related to the phase space of the Chern-Simons theory. The observables of these theories are derived. Geometrical properties are invoked to prove that the global invariants are not trivial. DOE

N90-11640# Joint Inst. for Nuclear Research, Dubna (USSR). Lab. of Theoretical Physics.
ON THE CONSTRUCTION OF THE SCATTERING MATRIX FOR LOCALLY-NONCOMMUTATIVE INTERACTIONS OF RELATIVISTIC FIELDS
A. V. Zorin, V. V. Kuryshkin, and E. E. Entralgo 1988 16 p In RUSSIAN; ENGLISH summary
(DE89-630138; JINR-R-4-88-587) Avail: NTIS (US Sales Only) HC A03/MF A01

It is shown that a covariant, unitary and causal scattering matrix for relativistic quantum-field models with locally-noncommutative interaction lagrangians can be constructed by the Bogolubov method when a new covariant chronological ordering operation is introduced. The explicit form for the required ordering is obtained, its main properties are studied, the comparison with the standard (noncovariant) time-ordering, as well as with the covariant chronological orderings proposed earlier by Yukawa, Koba and Golfand is performed. DOE

N90-11641# Swedish Inst. of Space Physics, Kiruna.
THEORY OF ATOMIC SPECTRAL EMISSION INTENSITY
Sten Yngstroem Feb. 1989 34 p
(IRF-Preprint-110; ETN-89-95159) Avail: NTIS HC A03/MF A01

The theoretical derivation of a spectral line intensity formula for atomic radiative emission is presented. The theory is based on first principles of quantum physics and statistical physics. The formulation of the theory provides an example of the manner in which quantum logic transforms into common sense logic. Experimental evidence is given. The analysis of the optical emission data concerning the expanding barium clouds released by rockets in the upper atmosphere, supports the suggestion that the intensity of auroral emissions depends on an exponential function of the energy. ESA

80 SOCIAL SCIENCES (GENERAL)

Includes educational matters.

N90-11642# Office of Technology Assessment, Washington, DC.
HIGHER EDUCATION FOR SCIENCE AND TECHNOLOGY: A BACKGROUND PAPER
Mar. 1989 280 p
(PB89-191290; OTA-BP-SET-52) Avail: NTIS HC A13/MF A02; SOD HC $12.00 as 052-003-01148-4 CSCL 05I

The background paper focuses on the end point of educational preparation for science and engineering careers-undergraduate and graduate study. It places the issue of future supply in the broad cultural context of changing demographics, labor market adjustments, and intervention policies. In a dynamic economy and an increasingly technological society, planning is essential. GRA

81 ADMINISTRATION AND MANAGEMENT

Includes management planning and research.

N90-11643 Colorado Univ., Boulder.
GUARANTEED COST CONTROL OF FLEXIBLE SPACE STRUCTURES Ph.D. Thesis
Donald Lee Mackison 1988 140 p
Avail: Univ. Microfilms Order No. DA8912205

The control of flexible space structures is complicated by the uncertain nature of the system to be controlled. The design of control laws which are intended to control both the inertial orientation (attitude) and shape (flexures) must be robust against anticipated variations in the system parameters (modal frequencies, shapes, locations of nodes of the flexures). The only control synthesis technique which includes a priori measures of the uncertainties of system parameters is guaranteed cost control (GCC). Guaranteed cost controllers are generated for a variety of flexible space structures. The stability robustness of the resulting closed loop systems is determined using singular value methods. The system dynamics are modeled as a linear system whose coefficients contain time varying parameters of bounded variation. Linear state feedback is used to minimize an integral quadratic cost function. Dissert. Abstr.

N90-11644# National Academy of Sciences - National Research Council, Washington, DC. Commission on Physical Sciences, Mathematics and Resources.
TOWARD A NATIONAL RESEARCH NETWORK
1988 61 p
(Grant NSF NCR-87-22333)
(PB89-198709) Avail: NTIS HC A04/MF A01 CSCL 05A

The United States would benefit significantly from the creation of a national research network (NRN). The National Research Network Review Committee has evaluated the proposal for an NRN submitted by the Office of Science and Technology Policy (OSTP), and the committee strongly supports the concept presented. An NRN would create a computer network infrastructure to provide much-needed support to the scientific research community. Data obtained by the committee regarding current and anticipated research activities demonstrate that an NRN could dramatically improve the productivity and quality of output of the U.S. research community. Through these direct benefits, plus commercial spinoffs from associated computer and network research, an NRN could greatly promote U.S. competitiveness in a multiplicity of disciplines. The OSTP proposals for an NRN have three phases, a structure the committee supports. The committee viewed the OSTP proposals as providing a general direction for the NRN, not a set of design specifications (which they were not) to be evaluated. Four areas of concern were addressed: technical considerations, funding, management, and commercial and specialty networks. The recommendations are presented. GRA

N90-11645# National Academy of Sciences - National Research Council, Washington, DC.
GLOBALIZATION OF TECHNOLOGY: INTERNATIONAL PERSPECTIVES. PROCEEDINGS OF THE 6TH CONVOCATION OF THE COUNCIL OF ACADEMIES OF ENGINEERING AND TECHNOLOGICAL SCIENCES
Janet H. Muroyama, ed. and H. Guyford Stever, ed. 1988 226 p Convocation held in Washington, DC, 30 Mar. - 1 Apr. 1987
(PB89-198840; LC-88-12090; ISBN-0-309-03842-1; ISBN-0-309-03843-X) Avail: NTIS HC A11/MF A02 CSCL 05A

The proceedings contains: Globalization of industry and implications for the future; The technology revolution and the restructuring of the global economy; Global flows and barriers; Driving technologies; Information technologies in industry and society; Technological advances and challenges in the telecommunications sector; Technological advances in the construction section; Fifteen years of major structural changes in manufacturing; Globalization of industry through production sharing; Regional and national consequences of globalizing industries of the Pacific Rim; Technology and the world economy: The case of the American hemisphere; Strategies for U.S. economic growth; and Improving the quality of life through technology. Author

82 DOCUMENTATION AND INFORMATION SCIENCE

Includes information management; information storage and retrieval technology; technical writing; graphic arts; and micrography.

For computer documentation see *61 Computer Programming and Software.*

N90-11646 Texas Univ., Austin.
INFERRING DATA BASE REQUIREMENTS FROM EXAMPLES IN FORMS Ph.D. Thesis
Veronica Peng Tseng 1988 147 p
Avail: Univ. Microfilms Order No. DA8816592

To reduce the communication problems and support end user involvement, an approach based on combining the paradigms of electronic forms and the strategy of learning from examples is proposed. The aim is the development of both theoretical and practical issues for combining these two paradigms. This approach permits an expert to state requirements directly or a novice to provide examples of requirements. To help with inferences, rules, heuristics and algorithms are designed. To control the burden of providing lengthy examples, the feature of system examples generation is employed. The explanatory feedback facility provided may upgrade a novice to an expert over time. The inference strategies support the collection of application specific requirements such as the hierarchical structure on a form and invariant properties such as dependencies between form fields. The feasibility of this approach is demonstrated by implementing a prototype. The validation of this prototype based on a real situation is conducted to examine its utility. Dissert. Abstr.

N90-11647*# National Aeronautics and Space Administration. Langley Research Center, Hampton, VA.
TECHNICAL COMMUNICATIONS IN AERONAUTICS: RESULTS OF AN EXPLORATORY STUDY. AN ANALYSIS OF MANAGERS' AND NONMANAGERS' RESPONSES
Thomas E. Pinelli, Myron Glassman, Rebecca O. Barclay, and Walter E. Oliu (Nuclear Regulatory Commission, Washington, DC.) Aug. 1989 61 p
(NASA-TM-101625; NAS 1.15:101625) Avail: NTIS HC A04/MF A01 CSCL 05B

Data collected from an exploratory study concerned with the technical communications practices of aerospace engineers and scientists were analyzed to test the primary assumption that aerospace managers and nonmanagers have different technical communications practices. Five assumptions were established for the analysis. Aerospace managers and nonmanagers were found to have different technical communications practices for three of the five assumptions tested. Although aerospace managers and nonmanagers were found to have different technical communications practices, the evidence was neither conclusive nor compelling that the presumption of difference in practices could be attributed to the duties performed by aerospace managers and nonmanagers. Author

N90-11648# Carnegie-Mellon Univ., Pittsburgh, PA.
PLANNING IN WRITING: THE COGNITION OF A CONSTRUCTIVE PROCESS
Linda Flower, John R. Hayes, Karen A. Schriver, Christina Haas, and Linda Carey May 1989 56 p
(Contract N00014-85-K-0423)
(AD-A210434) Avail: NTIS HC A04/MF A01 CSCL 05/7

Planning in writing is a strategic response to both the writing situation and the writer's own knowledge. This paper describes the process adult writers bring to ill-defined, expository tasks, such as writing essays, articles, reports and proposals. In planning, writers draw on (nest and integrate) three executive level strategies: knowledge-driven planning, script- or schema-driven planning, and constructive planning. Research in both instructional and academic writing suggests that writers may fail to turn to a constructive strategy even when ill-defined tasks demand it. This paper presents a theory of constructive planning based on a detailed analysis of expert and novice writers. It isolates five critical features of this constructive strategy, in which writers must create a unique network of working goals and deal with the special problems of integration, conflict resolution and instantiation this constructive process entails. The paper describes the strategies writers use to meet these demands and some expert/novice differences that affect the integration of the entire plan. This theoretical framework also suggests some goals for instruction and the support of planning. GRA

N90-11649# Sandia National Labs., Albuquerque, NM.
LEXER: A TOOL FOR LEXICAL ANALYSIS OF PROGRAM INPUT
Elisa M. Kephart (RE/SPEC, Inc., Albuquerque, NM.) and Colin B. Selleck Aug. 1989 28 p
(Contract DE-AC04-76DP-00789)
(DE89-016924; SAND-89-1055; RSI-0327) Avail: NTIS HC A03/MF A01

LEXER is a useful tool for lexical analysis. It is designed to give an application programmer the ability to write code that will quickly parse commands to an interactive program. It is also useful in parsing character data stored in a file. This is done by lexically analyzing the input character string and placing its components and related information into arrays stored in common blocks. The code is written in FORTRAN which conforms to the ANSI Standard FORTRAN 77 in all but a few carefully documented areas. DOE

N90-11650# University of Southern California, Marina del Rey. Information Sciences Inst.
THE KNOWLEDGE REPRESENTATION PROJECT
Robert McGregor and John Yen Jul. 1989 26 p
(Contract F30602-85-C-0221)
(AD-A211288; ISI/RR-89-199) Avail: NTIS HC A03/MF A01 CSCL 12/5

This report describes ISI's knowledge representation research, which can be divided into two phases. The initial phase produced the NIKL classifier, a system that provides competent and efficient capability for inference applied to terminological knowledge. The second phase began with a study of how NIKL could be improved, and is now in the process of producing LOOM, a new knowledge representation system with significantly broader inference capabilities. This report describes these two current research efforts and discusses some future plans for ISI's research in knowledge representation. GRA

N90-11651# Oak Ridge National Lab., TN.
TECHNOLOGY APPLICATIONS BULLETINS

Walter Koncinski, Jr., ed. Feb. 1989 74 p
(Contract DE-AC05-84OR-21400)
(DE89-017454; ORNL/M-772) Avail: NTIS HC A04/MF A01

Martin Marietta Energy Systems, Inc. (Energy Systems), operates five facilities for the U.S. Department of Energy (DOE): the Oak Ridge National Laboratory (ORNL), which is a large, multidisciplinary research and development (R and D) center whose primary mission is energy research; the Oak Ridge Y-12 Plant, which engages in defense research, development, and production; and the uranium-enrichment plants at Oak Ridge; Paducah, Kentucky; and Portsmouth, Ohio. Much of the research carried out at these facilities is of interest to industry and to state or local governments. To make information about this research available, the Energy Systems Office of Technology Applications publishes brief descriptions of selected technologies and reports. These technology applications bulletins describe the new technology and inform the reader about how to obtain further information, gain access to technical resources, and initiate direct contact with Energy Systems researchers. DOE

N90-11652# Japan Atomic Energy Research Inst., Tokyo. Dept. of Large Tokamak Research.
EXPERIMENTAL DATABASE RETRIEVAL SYSTEM DARTS (HA NDLING MANUAL)
Tetsuo Aoyagi, Keiji Tani, Hirobumi Haginoya, and Shinjiro Naito Feb. 1989 96 p In JAPANESE and ENGLISH
(DE89-906473; JAERI-M-89-015) Avail: NTIS (US Sales Only) HC A05/MF A01

In JT-60, a large tokamak device of Japan Atomic Energy Research Institute (JAERI), a plasma is fired for 5 to approx 10 seconds at intervals of about 10 minutes. The each firing is called a shot. Plasma diagnostic data are edited as JT-60 experimental database at every shot cycle and are stored in a large-scale computer (FACOM-M780). Experimentalists look up the data for specific shots which they want to analyze and consider. As the total number of shots increases, they find a difficulty in the looking-up work. In order that they can easily access to their objective shot data or shot group data by using a computer terminal, DARTS (DAtabase ReTrieval System) was developed. Enough information is possibly provided on DARTS handling for users. DOE

N90-11078# Engineering System International, Rungis (France).
EXPLOITATION OF DATA MANAGEMENT FACILITIES FOR FINITE ELEMENT ANALYSIS IN AEROSPACE STRUCTURAL ENGINEERING APPLICATIONS
J. Dubois, R. Valent, J. L. Gregis, P. Carlier, M. Klein, and A. Kreis (European Space Agency. European Space Research and Technology Center, ESTEC, Noordwijk, Netherlands) *In* ESA, Spacecraft Structures and Mechanical Testing Jan. 1989 p 721-728 Sponsored by ESA/ESTEC, Noordwijk, Netherlands
(For primary document see N90-10986 02-18)
Copyright Avail: NTIS HC A99/MF E06

N90-11402# Andrews Antennas, Adelaide (Australia).
ACCURATE MEASUREMENTS OF THE TOTAL ANGLE OF ARRIVAL OF HF SKYWAVES
Z. R. Jeffrey, P. T. Middleton, and C. Winkler *In* AGARD, Ionospheric Structure and Variability on a Global Scale and Interactions with Atmosphere and Magnetosphere Apr. 1989 10 p (For primary document see N90-11361 02-46)
Copyright Avail: NTIS HC A20/MF A03

83 ECONOMICS AND COST ANALYSIS

Includes cost effectiveness studies.

N90-11653# National Aerospace Lab., Tokyo (Japan). Aircraft Noise and Emission Research Group.
VIEW ON RECENT FUEL COSTS IN AIRLINES
Yoshikazu Tanabe Apr. 1987 22 p In JAPANESE
(NAL-TM-569; ISSN-0452-2982; JTN-88-80064) Avail: NTIS HC A03/MF A01

The ratio of fuel oil to the total cost of the air lines was increased to about 20 percent from 10 percent at the turning point in the first oil crisis in 1973 to 1974. Then, the rate was reduced down to about 15 percent by energy conservation measures. The second oil crisis in the period 1979 to 1981 turned this down trend upward to 30 percent or more. While the crude oil price is down and stable at low levels, the rate has been fluctuating at high price levels. In the U.S., where the airline rate has already been decontrolled, the airline service control relaxation law went into effect in 1978, which shook 229 airlines in 1984 down to 97 in March 1986. The merging of airline companies is still going on. After the 1990's, 130- to 180-seated medium sized aircraft are expected to be replaced on a large scale. The A320 will be put into commission in 1989 and the YXX/B.7J7 (150-seated) in 1992. These aircraft are forerunners of energy-saving, low-contamination aircraft. For a period before 1990 or so, there will be no other adequate measures than to provide the existing aircraft with energy-saving means. In this regard, it is essential to know the actual conditions. The data given here is limited, compared to that for Japan. Now the effort of improvement in the U.S. airlines has come to a certain stable stage. A view is shown under this circumstance. NASDA

84 LAW, POLITICAL SCIENCE AND SPACE POLICY

Includes NASA appropriation hearings; aviation law; space law and policy; international law; international cooperation; and patent policy.

N90-10905# Joint Publications Research Service, Arlington, VA.
USSR AND INTERNATIONAL COOPERATION IN SPACE
S. A. Nikitin *In its* JPRS Report: Science and Technology. USSR: Space 28 Jun. 1989 p 64-69 Transl. into ENGLISH from Novoye v Zhizni, Nauke, Tekhnike: Seriya Kosmonavtika, Astronomiya (Moscow, USSR), No. 12, Dec. 1988 p 32-47 (For primary document see N90-10900 02-12)
Copyright Avail: NTIS HC A06/MF A01

85 URBAN TECHNOLOGY AND TRANSPORTATION

Includes applications of space technology to urban problems; technology transfer; technology assessment; and surface and mass transportation.

For related information see also *03 Air Transportation and Safety, 16 Space Transportation,* and *44 Energy Production and Conversion.*

N90-11654*# Mechanical Technology, Inc., Latham, NY. Stirling Engine Systems Div.
AUTOMOTIVE STIRLING ENGINE DEVELOPMENT PROGRAM Semiannual Technical Progress Report, 1 Jul. - 31 Dec. 1986
R. Farrell, C. Hindes, R. Battista, M. Connelly, M. Cronin, R. Howarth, A. Donahue, E. Slate, R. Stotts, and R. Lacy et al Feb. 1988 59 p
(Contracts DEN3-32; DE-AI01-85CE-50112)
(NASA-CR-180839; DOE/NASA/0032-30; NAS 1.26:180839; MTI-87ASE555SA11) Avail: NTIS HC A04/MF A01 CSCL 13I

The study of high power kinematic Stirling engines for transportation use, testing of Mod I and Mod II Stirling engines, and component development activities are summarized. Mod II development testing was performed to complete the development of the basic engine and begin characterization of performance. Mod I engines were used for Mod II component development and to obtain independent party (U.S. Air Force) evaluation of Stirling engine vehicle performance. Author

N90-11655# Oak Ridge National Lab., TN. Energy Div.
THE TRANSFER AND DIFFUSION OF NEW TECHNOLOGIES: A REVIEW OF THE ECONOMICS LITERATURE
T. Randall Curlee and Rajeev K. Goel Jun. 1989 54 p
(Contract DE-AC05-84OR-21400)
(DE89-015671; ORNL/TM-11155) Avail: NTIS HC A04/MF A01

A general overview is presented of the economics literature on technological change and focuses particularly on the interface between the public and private sectors in promoting the transfer and diffusion of new technologies. The ability to transfer and diffuse new technologies is generally recognized as a key to increased productivity in the United States and this country's ability to compete internationally. A great deal of research was done on technology transfer and diffusion by various disciplines and from numerous perspectives. Unfortunately, the policy implications of those different works are not always consistent. Further, the different disciplines have difficulty in communicating even when addressing the same issues and drawing the same general conclusions. The primary objective is to lessen the chasm among the disciplines with respect to technology transfer and diffusion by summarizing the perspectives presented in the economics literature. The document is intended primarily for an interdisciplinary audience. DOE

88 SPACE SCIENCES (GENERAL)

No abstracts in this category.

89 ASTRONOMY

Includes radio, gamma-ray, and infrared astronomy, and astrometry.

N90-11656 Edinburgh Univ. (Scotland).
ASPECTS OF THE DEVELOPMENT OF A 1-5 MICRON INFRARED CAMERA FOR ASTRONOMY Ph.D. Thesis
John Thornton Rayner 1988 170 p
Avail: Univ. Microfilms Order No. BRD-85067

Aspects of the design, development and evaluation of a 1 to 5 micron near-infrared camera for a large ground-based telescope are described and discussed. In particular the detailed cryogenic design and the closely inter-related areas of the optical and mechanical design are described. Also discussed is near-infrared imaging and imaging polarimetry of the star forming region OMC2, acquired during the astronomical commissioning of the camera. Dissert. Abstr.

N90-11657 Leeds Univ. (England).
IRAS OBSERVATIONS OF THE EXTENDED GALACTIC OBJECTS Cas A AND W80 Ph.D. Thesis
Stephen Roger Marley 1988 303 p
Avail: Univ. Microfilms Order No. BRD-84837

This thesis presents work on objects at either end of the stellar evolutionary scale. We endeavor to reconstruct images in the mid-infrared of both the young supernova remnant Cas A, and the evolved H II region W80. We analyze both the intensity and temperature distribution within both objects, from which we determine several parameters concerning the nature of their infrared dust emission. It has been necessary to divide the thesis into two halves, and to provide separate introductions and results chapters for the work on W80 and Cas A. In Chapter 1 we discuss general theory of supernova remnant evolution, paying particular attention to modelling the reverse shock, from which the current models of Cas A are derived. The results of the IRAS observations of Cas A are presented in Chapter 4. Here we determine that the embedded dust is heated by collision with electrons in the shock heated plasma. We also determine that the dust is likely to have been swept up from the interstellar medium, and not condensed from the supernova ejecta. Both results chapters make extensive use of dust emission theory as given in Chapter 2. In Chapter 5 we discuss the general evolution of H II regions, including sequential star formation and blister evolution of asymmetrical ionization fronts. The current observational models of W80 are then compared and criticised in the light of this review. In Chapter 7 we discuss the IRAS observations of W80. We find a number of new point sources, of which one is a candidate for the powering source of the complex. We find that the dust emission in general is consistent with the dust being embedded within the ionized plasma, and not within the surrounding molecular material. In addition to the observational results, we have made a number of important advances in data analysis techniques (particularly with the reconstructed survey data). These techniques are discussed in Chapters 3 and 6, and applied in Chapters 4 and 7. Author

N90-11658 Florida Univ., Gainesville.
AN IMPROVED ALGORITHM FOR THE DETERMINATION OF THE SYSTEM PARAMTERS OF A VISUAL BINARY BY LEAST SQUARES Ph.D. Thesis
Yu-Lin Xu 1988 151 p
Avail: Univ. Microfilms Order No. DA8908293

The problem of computing the orbit of a visual binary from a set of observed positions is reconsidered. It is a least squares adjustment problem, if the observational errors follow a bias-free multivariate Gaussian distribution and the covariance matrix of the observations is assumed to be known. The condition equations are constructed to satisfy both the conic section equation and the area theorem, which are nonlinear in both the observations and the adjustment parameters. The traditional least squares algorithm, which employs condition equations that are solved with respect to the uncorrelated observations and either linear in the adjustment parameters or linearized by developing them in Taylor series by first-order approximation, is inadequate in our orbit problem. D.C. Brown proposed an algorithm solving a more general least squares adjustment problem in which the scalar residual function, however, is still constructed by first-order approximation. Not long ago, a completely general solution was published by W.H Jefferys, who proposed a rigorous adjustment algorithm for models in which the observations appear nonlinearly in the condition equations and may be correlated, and in which construction of the normal equations and the residual function involves no approximation. This method was successfully applied in our problem. The normal equations were first solved by Newton's scheme. Practical examples show that this converges fast if the observational errors are sufficiently small and the initial approximate solution is sufficiently accurate, and that it fails otherwise. Newton's method was modified to yield a definitive solution in the case the normal approach fails, by combination with the method of steepest descent and other sophisticated algorithms. Practical examples show that the modified Newton scheme can always lead to a final solution. The weighting of observations, the orthogonal parameters and the efficiency of a set of adjustment parameters are also considered. The definition of efficiency is revised. Author

N90-11659 Edinburgh Univ. (Scotland).
INTEGRATING DETECTORS AND THEIR APPLICATION TO INFRARED ASTRONOMY Ph.D. Thesis
Mark Christopher Bird 1988 183 p
Avail: Univ. Microfilms Order No. BRD-85012

The work contained in this thesis is concerned with the preformance of infrared integrating detector arrays, within the context of astronomical spectroscopy. A linear array of thirty-two InSb photodiodes is investigated. It is found to exhibit good capacitance and dark current uniformity across the array. By applying the principle of charge conservation to the multiplexed readout arrangement of this device, the signal response of the detector to different levels of illumination is derived. It is found from this, and confirmed experimentally, that the device has a highly linear radiation response over a range of reverse biases. The interaction between dark current and photo-current is studied,

primarily by the application of a simple model. The results indicate that the effective signal gain of a detector can vary in the situation where dark current dominates the discharge processes, since in this instance accurate dark current subtraction becomes difficult. The predictions of the model are compared with experiments performed on two integrating arrays; one under study in the laboratory, and the other installed in the low background environment of a cooled grating spectrometer. Finally, suggestions are presented of ways of avoiding this problem, the simplest of which involves utilizing, where possible, low dark current detector materials. The importance of achieving good dark current uniformity with arrays is stressed, since this will improve the ability to flat-field faint object spectra. To illustrate the importance of these devices, infrared spectra obtained with array detectors, covering a range of astronomical objects, are presented and discussed.

Dissert. Abstr.

N90-11660 Saint Andrew's Univ. (Scotland).
THE ASTRONOMY OF ANDEAN MYTH: THE HISTORY OF A COSMOLOGY Ph.D. Thesis
William F. Sullivan 1986 417 p
Avail: Univ. Microfilms Order No. BRDX85320

It is shown that Andean myth, on one level, represents a technical language recording astronomical observations of precession and, at the same time, an historical record of simultaneous social and celestial transformations. Topographic and architectural terms of Andean myth are interpreted as a metaphor for the organization of and locations on the celestial sphere. Via ethoastronomical date, mythical animals are identified as stars and placed on the celestial sphere according to their topographical location. Tested in the planetarium, these arrays generate cluster of dates - 200 B.C. and 650 A.D. Analysis of the names of Wiraqocha and Manco Capac indicates they represent Saturn and Jupiter and that their mythical meeting represents their conjunction in 650 A.D. The astronomy of Andean myth is then used as an historical tool to examine how the Andean priest-astronomers recorded the simultaneous creation of the avllu and of this distinctive astronomical system about 200 B.C. The idea that the agricultural avllu, with its double descent system stressing the importance of paternity, represents a transformation of society from an earlier matrilineal/horticultural era is examined in light of the sexual imagery employed in myth. Wiraqocha's androgyny and the division of the celestial sphere into male (ecliptic) and female (celestial equator = earth) are interpreted as cosmological validations of the new social structure. Dissert. Abstr.

N90-11661*# Washington Univ., Seattle. Dept. of Astronomy.
UV OBSERVATIONS OF NGC 205 Final Report
Eric M. Wilcots, Paul W. Hodge, Paul B. Eskridge, Erika Boehm-Vitense, and Francesco Bertola (Padua Univ., Italy) 2 Nov. 1989 19 p
(Grant NAG5-1020)
(NASA-CR-185975; NAS 1.26:185975) Avail: NTIS HC A03/MF A01 CSCL 03A

Low resolution IUE observations of the dwarf elliptical galaxy NGC 205 show that the UV spectral energy distribution (SED) of the galaxy is relatively flat. Spectra centered on the nucleus and on a region north of the nucleus show evidence of recent bursts of star formation which contribute strongly to the UV spectral energy distribution. The UV spectra was fit with a composite spectrum based on a Miller-Scalo initial mass function, an underlying older population (modelled using the UV spectrum of 47 Tuc), and an extinction based on a SMC-like extinction cure. This fit implies that the total mass of young stars (with M equal to or greater than 1 solar mass) in the galaxy is approx. 7x10(5) solar mass, which can be compared to the total mass of globular cluster like stars in the galaxy of approx. 8x10(7) solar mass.

Author

N90-11662*# Columbia Univ., New York, NY. Astrophysics Lab.
A LIQUID XENON IMAGING TELESCOPE FOR 1-30 MeV GAMMA-RAY ASTROPHYSICS Semiannual Technical Report, 1 May 1989 - 31 Oct. 1989
Elena Aprile, Reshmi Mukherjee, and Masayo Suzuki 13 Nov. 1989 15 p Presented at the 33rd Annual International Symposium on Optical and Optoelectronic Applied Science and Engineering, San Diego, CA, 6-11 Aug. 1989
(Contract NAGw-1370; N00014-86-C-0086)
(NASA-CR-185999; NAS 1.26:185999; CAL-1792) Avail: NTIS HC A03/MF A01 CSCL 03A

A study of the primary scintillation light in liquid xenon excited by 241 Am alpha particles and 207 Bi internal conversion electrons are discussed. The time dependence and the intensity of the light at different field strengths have been measured with a specifically designed chamber, equipped with a CaF sub 2 light transmitting window coupled to a UV sensitive PMT. The time correlation between the fast light signal and the charge signal shows that the scintillation signals produced in liquid xenon by ionizing particles provides an ideal trigger in a Time Projection type LXe detector aiming at full imaging of complex gamma-ray events. Researchers also started Monte Carlo calculations to establish the performance of a LXe imaging telescope for high energy gamma-rays. Author

N90-11002# MATRA Espace, Toulouse (France). Dept. of Mechanical Engineering.
SYSTEM AND PERFORMANCE ANALYSIS OF A LOW DENSITY ACTIVELY CONTROLLED MIRROR FOR ASTRONOMIC OBSERVATION
B. Laviron and M. Duran *In* ESA, Spacecraft Structures and Mechanical Testing Jan. 1989 p 127-132 (For primary document see N90-10986 02-18)
Copyright Avail: NTIS HC A99/MF E06

N90-11019# Aerospatiale, Chatillon (France).
TELESCOPE STRUCTURE FOR CRYOGENIC APPLICATION
J. A. Massoni *In* ESA, Spacecraft Structures and Mechanical Testing Jan. 1989 p 239-245 In FRENCH; ENGLISH summary Previously announced as N89-23940 (For primary document see N90-10986 02-18)
Copyright Avail: NTIS HC A99/MF E06

90 ASTROPHYSICS

Includes cosmology; celestial mechanics; space plasmas; and interstellar and interplanetary gases and dust.
For related information see also *75 Plasma Physics*.

N90-11663# Onsala Space Observatory (Sweden).
THE MASS DISTRIBUTION IN THE GALACTIC CENTRE ESTIMATED FROM OH/IR STARS
M. Lindqvist, A. Winnberg, H. J. Habing, H. E. Matthews, and F. M. Olnon (Radio Sterrenwacht, Dwingeloo, Netherlands) 1988 7 p Submitted for publication Sponsored by Swedish Natural Research Council
(PB89-154884; Rept-88/32) Avail: NTIS HC A02/MF A01 CSCL 03B

The preliminary results of a search for OH/IR stars in the Galactic Center using the VLA are presented. The goal of the project is to determine the mass density distribution from a few parsecs up to about 120 pc of the Galactic Center using stellar kinematics. Up to now 125 Oh/IR stars have been found. The distribution of the stars is clearly elongated with the major axis parallel to the galactic equator. The stars show a rotation of 117 km/s/deg with a dispersion of 90 km/s. Two preliminary models have been applied in order to determine the enclosed mass, resulting in M(r) equals 4 million (r to the 1.4 power)Mo, where r is the galactocentric distance in parsecs. GRA

N90-11664 Texas Univ., Austin.
CARBON ISOTOPE RATIOS AND LITHIUM ABUNDANCES IN OPEN CLUSTER GIANTS Ph.D. Thesis
Kalpana Krishnaswamy Gilroy 1988 207 p
Avail: Univ. Microfilms Order No. DA8909660

Carbon isotope ratios and lithium abundances were obtained in giants of about 20 galactic open clusters. Both these quantities are important indicators of the extent of convective mixing in a red giant since, their surface abundances are reduced when the star undergoes first dredge up phase. The ages and turn off masses of these open clusters were determined by fitting theoretical isochrones to their color magnitude diagrams. Plots of the C-12/C-13 ratios and Li abundances agains the cluster turn off masses indicated the following: (1) Older clusters with lower turn off masses showed lower C-12/C-13 ratios than the intermediate aged and younger clusters; (2) The C-12/C-13 ratios in these low mass stars were much lower than the theoretically predicted values whereas, the younger clusters exhibited the predicted ratios; (3) Examination of the various theories put forth over the years to predict the low isotope ratios in field giants allowed the elmination of some of these theories on the basis of being inconsistent with the observed results; and (4) The plot of the lithium abundance against the cluster turn off mass did not show a prominent trend and no definite conclusions could be made, based on this plot.
Dissert. Abstr.

N90-11665 Princeton Univ., NJ.
THE STABILITY OF MAGNETOHYDRODYNAMIC SHOCK WAVES IN MOLECULAR CLOUDS Ph.D. Thesis
Mark John Wardle 1989 141 p
Avail: Univ. Microfilms Order No. DA8909065

A linear analysis of the stability of isothermal magneto-hydrodynamic C-type shocks propagating perpendicular to a magnetic field shows that shocks with Alfven numbers greater than about 5 are unstable. The fastest-growing modes form clumps on a scale of about half the shock thickness-about 0.01 pc for parameters typical of molecular clouds. The growth rate rises rapidly with increasing shock strength, reaching about 40 times the inverse flow time through the front at the point where shocks are sufficiently strong to be J or C*-type. Radiative shocks are considered, assuming that neutral gas is heated by ion-neutral friction and cools by rotational transitions of H(2). Ion inertia and pressure are neglected. The growth rate and wave number of the fastest growing mode is reduced by at most 30 percent in reasonably strong (25 km s(-1)) shocks. The clumps of neutral gas forming within the shock front are cooler than the gas at the same point in the unperturbed flow, and the magnitude of the fractional changes in the neutral temperature and density are of the same order. When the C-type shock is near to C* or J-type and the gas pressure is dynamically important the clumps are less centrally concentrated. The clumps are expected to eventually drift behind the front, where they will be cool, poorly coupled to the magnetic field and possibly unstable to gravitational collapse: the instability may trigger low-mass star formation. Finally, the stability of oblique shocks is examined. As the angle between the ambient magnetic field and the direction of shock propagation is reduced, the steady shocks become stronger and more unstable. The growing perturbations propagate across the face of the shock front at a speed of order the Alfven speed in the preshock gas (typically 2 km s(-1) in molecular clouds). It is noted that a similar instability may arise in other situations in which ambipolar diffusion is important. Author

N90-11666 Columbia Univ. Teachers Coll., New York, NY.
MATHEMATICAL METHOD FOR THE STUDY AND TEACHING OF STELLAR AND PROTOSTELLAR STRUCTURE Ed.D. Thesis
John Francis Doorish 1988 137 p
Avail: Univ. Microfilms Order No. DA8906448

The purpose of this thesis is to develop a relatively simple yet effective method of teaching stellar and protostellar structure. There are four differential equations describing the structure of a star. They are: These equations are linearly approximated in the following form: W = W sub o (1 plus or minus wx). Here, W represents the pressure (P), temperature (T), mass (M), and/or luminosity (L) gradients within the star; W represents some initial value of these parameters expanded inwardly or outwardly from an initial point, r sub o; and w represents what is called the Motz Dimensionless Variables (MDV) which are directly derivable from the above set of equations. They are dimensionless, so, in the expansion, W has the same units as w sub o. The MDV appear below: As yet, there is no MDV for luminosity owing to the complicating energy generation factor, epsilon. In the above sets of equations, the mean molecular weight is micro; the opacity is kappa; the ratio of gas pressure to total pressure is beta; and the other symbols have their usual meanings. In the above set of equations describing the MDV, if the surface of the star is expanded to larger values, representing earlier, and therefore, protostellar stages of the star, by theoretically halting accretion, no dynamical factors need to be considered. The above set of equations describing a stellar structure in static equilibrium may then be used. This method was designed for college and early graduate students who have never before encountered the topic of stellar structure. This method was taught to a class of college physics majors in a local New York City college. The students had never before seen these equations. After the presentation, they were asked to attempt construction of sample stellar model using this method and also to complete a questionnaire concerning their general academic history and their opinions of the method. According to the questionnaire, most subjects felt that it was effective, yet simple enough, as an introductory method for the topic. Author

N90-11667 California Univ., Santa Cruz.
SPECTROPOLARIMETRY, VARIABILITY, AND THE TAXONOMY OF ACTIVE GALACTIC NUCLEI Ph.D. Thesis
Robert W. Goodrich 1988 99 p
Avail: Univ. Microfilms Order No. DA8906797

Two subclasses of active galactic nuclei (AGN) are studied using spectropolarimetry, with the intent of defining the relationships of the subclasses to other classes of AGNs, and to study the physics of the objects themselves. In the Seyfert 1.8/1.9 class there is good evidence for dust just outside of the broad-line regions in two objects. IRAS 1958-183 and NGC 2622. Spectropolarimetry of the latter object reveals the presence of dust moving at similar to -800 s(-1) along our line-of-sight, and causing much of the polarization in this object. In addition, three of these objects have undergone extreme variability. Combining IDS data from Osterbrock and collaborators with the more recent CCD data it is shown that in all three cases the changes in both broad emission line fluxes and featureless continuum are consistent with changes in the line-of-sight reddening to the broad-line region. Together with the polarimetric evidence for dust and IRAS photometry this strongly suggests that the Seyfert 1.8/1.9 character is caused by dust and the consequent reddening and extinction. Variability occurs when dust clouds evaporate or move out of line-of-sight, and the extinction then changes. In the so-called narrow line Seyfert 1s spectropolarimetry reveals seven highly-polarized objects. In Mrk 1239 there is evidence for at least two components of polarization, one probably due to dust reflection. In this Seyfert there is also a highly polarized red excess wing on the Balmer lines. In two other objects, Mrk 766 (= NGC 4253) and IRAS 1509-211, the polarization also appears to indicate dust reflection as the polarigenic mechanism. There is a weak circumstantial evidence for an association of the low-density region (the (O III)-emitting region) and the polarizing source, provided by comparison of the radio axes and polarization position angles in Mrk 766 and Mrk 1126. This conclusion is also supported by the tendency of the highly-polarized objects to have large (O III) lambda 5007/H beta sub b ratios. The correlation of W lambda (H beta sub b) with the FWHM of H beta is confirmed, and it is noted that X-ray selected Seyfert 1s have lower values of W lambda (H beta sub b) than do optically-selected Seyfert 1s. Author

N90-11668 California Univ., Berkeley.
ROCKET AND SATELLITE OBSERVATIONS OF THE LOCAL

INTERSTELLAR MEDIUM Ph.D. Thesis
Patrick Neal Jelinsky 1988 161 p
Avail: Univ. Microfilms Order No. DA8902135

The purpose of the study described in this thesis was to obtain new information on the structure of the local interstellar medium (ISM). Two separate experiments using different instruments were used in this study. The first experiment employed a spectrometer with a spectral bandpass from 350 to 1150 A which was placed at the focus of a 95 cm, f/2.8 normal incidence telescope flown on an Aries sounding rocket. The purpose of this experiment was to measure the interstellar absorption edges, due to neutral helium and neutral hydrogen, in the spectrum of a hot white dwarf. The hot white dwarf G191-B2B was observed for 87 seconds during the flight. Unfortunately, due to high pressure in the rocket, no scientifically useful data was obtained during the flight. Had the experiment worked, it could have measured the neutral helium column density, the neutral hydrogen column density, the hydrogen ionization fraction, and limits on the abundance of helium and the interstellar radiation field. The second experiment utilized the high resolution spectrometer on the International Ultraviolet Explorer satellite. The purpose of the experiment was to observe interstellar absorption lines in the spectrum of hot white dwarfs. A new method of determining the equivalent widths of absorption lines and their uncertainties was developed. This method along with the reduction method used to determine the column densities and velocity dispersions for the observed absorption lines are discussed. The neutral hydrogen column density is estimated from the N I, Si II, and C II columns. Unfortunately, the uncertainties in the neutral hydrogen columns are very large, only two are constrained to better than an order of magnitude. High ionization species (N V, Si IV, and C IV) are seen in five of the stars. Upper limits to the temperature of the ISM are determined from the velocity dispersions. The temperature of the low ionization gas toward four of the stars is constrained to be less than 50,000 K. The temperature of the high ionization gas to two of the stars is constrained to be less than 10 (5) K suggesting that this gas is either in a photoionized region around the star or in the photosphere of the star. Author

N90-11669*# Colorado Univ., Boulder. Dept. of Astrophysical, Planetary and Atmospheric Sciences.
NUMERICAL STUDY OF THE CURRENT SHEET AND PSBL IN A MAGNETOTAIL MODEL
I. Doxas, W. Horton, K. Sandusky, T. Tajima, and R. Steinolfson (Texas Univ., Austin.) 1989 30 p
(Grant NAGw-1176)
(NASA-CR-183289; NAS 1.26:183289) Avail: NTIS HC A03/MF A01 CSCL 03B

The current sheet and plasma sheet boundary layer (PSBL) in a magnetotail model are discussed. A test particle code is used to study the response of ensembles of particles to a two-dimensional, time-dependent model of the geomagnetic tail, and test the proposition (Coroniti, 1985a, b; Buchner and Zelenyi, 1986; Chen and Palmadesso, 1986; Martin, 1986) that the stochasticity of the particle orbits in these fields is an important part of the physical mechanism for magnetospheric substorms. The realistic results obtained for the fluid moments of the particle distribution with this simple model, and their insensitivity to initial conditions, is consistent with this hypothesis. Author

N90-11670 Colorado Univ., Boulder.
RADIATIVE SHOCKS WITH ELECTRON THERMAL CONDUCTION Ph.D. Thesis
Kazimierz Jan Borkowski 1988 130 p
Avail: Univ. Microfilms Order No. DA8912179

The influence of electron thermal conduction on radiative shock structure for both one- and two-temperature plasmas is studied. The dimensionless ratio of the conductive length to the cooling length determines whether or not conduction is important, and shock jump conditions with conduction are established for a collisionless shock front. Approximate solutions are obtained with the assumptions that the ionization state of the gas is constant and the cooling rate is a function of temperature alone. In the absence of magnetic fields, these solutions indicate that conduction noticeably influences normal-abundance interstellar shocks with velocities 50 to 100 km/s and dramatically affects metal dominated shocks over a wide range of shock velocities. Magnetic fields inhibit conduction, but the conductive energy flux and the corresponding decrease in the post-shock electron temperature may still be appreciable. Detailed steady state radiative shock models are calculated in gas composed entirely of oxygen, with the purpose of explaining observations of fast-moving knots in Cas A and other oxygen-rich supernova remnants (SNRs). Conduction reduces post-shock electron temperatures by a factor of 7 to 10 and flattens temperature gradients. The O III ion, whose forbidden emission usually dominates the observed spectra, is present over a wide range of shock velocities, from 100 to 170/kms. The electron temperature in the (O III) line formation region is 3 x 10(4) K, in agreement with the 2 x 10(4) K derived from observations. All models with conduction have extensive warm (T greater than 4000 K) photoionization zones, which provides better agreement with observed optical (O I) line strengths. However, the temperatures in these zones could be lowered by (Si II) 34.8 microns and (Ne II) 12.8 microns cooling if Si and Ne are present in appreciable abundance relative to O. Such low temperatures would be inconsistent with the observed (O I) emission in oxygen-rich SNRs. Dissert. Abstr.

N90-11671 Virginia Univ., Charlottesville.
THE INTERACTION OF SUPERNOVAE AND PULSARS WITH THE CIRCUMSTELLAR ENVIRONMENT Ph.D. Thesis
Robert Thoms Emmering 1988 128 p
Avail: Univ. Microfilms Order No. DA8913909

Self-similar solutions for the time dependent behavior of a shocked spherically, symmetric, relativistic fluid with tangential magnetic field in the case where the boundaries of the shocked fluid move at a constant velocity are found. These solutions can be applied to the evolution of the shocked relativistic pulsar winds which are probably observed as Crab-like supernova remnants. In the case of the Crab Nebula itself, the solutions suggest that ratio of magnetic to particle energy in the wind, as measured in the fluid frame, is only a few tenths of 1 percent. This is rough agreement with a steady state model developed by Kennel and Coroniti. Since the models include time evolution, they can be applied to young objects and may be relevant to a possible pulsar nebula in SN1987a. The development of models for the infrared echo from Type II supernovae arising from the heating of circumstellar dust is discussed. In these models, ellipsoidial dust distributions are considered (previous models considered only spherically symmetric dust distributions) since some red supergiants, the likely progenitors of most Type II supernovae, are known to have asymmetric circumstellar envelopes. The models show that an asymmetric dust distribution can have a substantial effect on the time evolution of the echo. The properties to be expected of the infrared and scattered light echoes from SN1987A are derived. These echoes are expected to arise from the dust formed within the wind given off by the progenitor during a previous red supergiant phase. The models take into account the emission and scattering properties of the dust grains, in particular silicate dust grains, and the observed supernova light curve. The predictions of the models are compared with the available observations. Dissert. Abstr.

N90-11672 Colorado Univ., Boulder.
SMALL GRAINS IN REFLECTION NEBULAE: A STUDY OF DIFFUSE INTERSTELLAR BANDS, ELEMENTAL DEPLETIONS AND INFRARED FLUX Ph.D. Thesis
Karl Hinrik Josafatsson 1988 146 p
Avail: Univ. Microfilms Order No. DA8912197

A study is presented of interstellar absorption and emission features that arise in either very small dust grains (10 to 100 A) or large molecules. Most of the observed stars are in reflection nebulae where the relatively high density and high UV flux provides a very favorable regions for the study of small grains. The data cover three different wavelength bands. In the optical regime, high quality data was observed for 59 stars on the diffuse interstellar

absorption bands (DIBs) between 5690 and 5870 A. In the ultraviolet, both new and archival high dispersion images are used from both cameras of the International Ultraviolet Explorer (IUE) satellite to calculate the depletion of sulphur (S), silicon (Si), manganese (Mn), and iron (Fe). In the infrared, the shape was determined of the emission spectrum from the nebulae surrounding the target stars by using the available data in all four bands of the Infrared Astronomical Satellite (IRAS). The presence of tiny grains will show up as excess IR flux at 12 and 25 microns. Large grains that are not heated as much as small grains will contribute more to the 60 and 100 micron bands. It was found that the DIBs can be divided into three groups, each of which must arise in a different carrier or through a different physical process. A study of the band profiles leads to the prediction that the narrow bands most likely arise from rotational levels of a large molecule and not from absorption on small grains. The depletion analysis shows a surprising range of depletion values, with the highest depletion found in the line of sight toward two stars in the Pleiades cluster. The IR data shows that the ratio of the 12 to 100 micron flux varies considerably between nebulae, indicating the the proportion of tiny grains is not constant. The number of tiny grains appears to vary with distance from the star as well. Dissert. Abstr.

N90-11673 Texas Univ., Austin.
GAS DYNAMICAL PROCESSES IN THE THEORY OF GALAXY FORMATION Ph.D. Thesis
Hyesung Kang 1988 262 p
Avail: Univ. Microfilms Order No. DA8909685

The hydrodynamical conservation equations was solved along with the rate equations for nonequilibrium ionization, recombination, and molecule formation and the equation of radiative transfer, for steady state shocks in a gas of primordial composition. The calculation self-consistently includes the effects of the diffuse postshock emission as well as a possible external radiation flux on the postshock flow. It is shown that the shocked gas cools faster than it can recombine and, as a result, is able to form an H2 concentration as high as 10(-3) via the formation of H- and H2+ intermediaries due to the enhanced nonequilibrium ionization fraction at 10(4) K. With such an H2 concentration, the gas cools by rotational-vibrational line excitation of H2 molecules to well below the canonical final temperature of 10(4) K for a molecule-free gas without metals. This cooling below 10(4) K significantly lowers the characteristic gravitational fragment mass estimated for shocks relative to the value if the gas cooling stops at 10(4) K. The shock calculation was applied to explore the hypothesis that globular clusters were formed by gravitational instability behind radiative shocks inside protogalaxies. The results indicate that, in the absence of a strong external source of UV radiation, the shock heated gas radiatively cools below 10(4) K as a result of H2 formation and cooling to approximately 10(2) K before the globular cluster mass can be imprinted on the gas by Jeans instability. In this case the suggestion of globular cluster formation behind such protogalactic shocks fails. The presence of a source of UV radiation such as a quasar with L greater than 5 x 10(44 erg/s) or a distribution of early type stars with L greater than 3 x 10(44) erg/s is found to be necessary in order to inhibit this rapid cooling below 10(4) K for a time longer than the free fall time for the gas when it reaches 10(4) K. A 3D hydrodynamical N-body code was developed along with the merger of a Smoothed Particle Hydrodynamics code with a hierarchical N-body Particle-Mesh code. The code was applied to the problem of pancake formation and compared the results to previous detailed, 1D, planar, numerical hydrodynamic simulations. Dissert. Abstr.

N90-11674 Sussex Univ., Brighton (England).
NEW STATISTICAL APPROACHES TO GALAXY CLUSTERING Ph.D. Thesis
Edward Nigel Ling 1987 143 p
Avail: Univ. Microfilms Order No. BRDX85467

The bootstrap resampling technique is used to estimate the sampling errors in the two-point correlation function. The spatial correlation functions is calculated for a subset of the CfA redshift survey of galaxies and a redshift sample of 104 Abell clusters. The angular correlation function is also calculated for a sample of 1664 Abell clusters. The best estimate for the ratio of the correlation length for Abell clusters (richness class R equal to or less than 1, distance class D equal to or less than 4) to that of CfA galaxies is 4.2 + 1.5/-1.1 (68 percent error). The enhancement of cluster clustering over galaxy clustering is statistically significant in the presence of resampling errors. The bootstrap is applied to calculations of the spatial and angular correlation functions of galaxy morphological types in the CfA catalogue. It was found that elliptical correlation function is steeper than that of lenticular or spiral galaxies. In general, the standard errors in the correlation function estimated with the bootstrap technique are considerably larger than the quoted Poisson errors. The uncertainties do not include the effects of possible additional systematic biases in the catalogues. Two spatial statistics are used to study the large scale clustering. The Voronoi tessellation and the Minimal Spanning Tree (MST) are applied to the CfA survey, the neutrino and cold dark matter N-body models and some artificial patterns. It was found that the tessellation is able to quantify voids and indicate dominant linear features. The MST was constructed for the original data sets and again after randomly permuting the samples on selected scales. The MST is shown to be sensitive to filamentary structures. It was concluded that the MST of the CfA data provides the first objective evidence for filaments in the galaxy distribution. The CDM model is a better match to the observations than the neutrino universe. Dissert. Abstr.

N90-11675 Cornell Univ., Ithaca, NY.
ELECTROMAGNETIC JETS IN PULSAR MAGNETOSPHERES AND NEAR MAGNETIZED ACCRETION DISKS Ph.D. Thesis
Martin Erick Sulkanen 1989 267 p
Avail: Univ. Microfilms Order No. DA8915063

The structure of the electromagnetic fields that surround a rotating, magnetized neutron star or that may be in and near the accretion disk of an active galactic nucleus is examined. The method developed was used for time independent axisymmetric fusion plasma equilibria, the Grad-Shafranov equation. In the case of the pulsar magnetosphere the Grad-Shafranov equation is identical to the pulsar equation. Here, it is derived from a variational principle that minimizes the field energy subject to fixed angular momentum and magnetic helicity for the configuration. This procedure allows one to apply a powerful result from fusion plasma equilibria to constrain the form of the magnetic helicity for the configuration, Taylor's hypothesis. This removes an indeterminacy from the pulsar equation that has plagued all earlier attempts to find a unique equation to describe the fields. The pulsar equation is fixed to be a piecewise linear partial differential equation with a class of solutions that include self-collimated electromagnetic jets along the rotation axis of the star. These jets carry energy, angular momentum, and electric current away from the star. A finite difference scheme is employed to solve for the entire field structure for these jet magnetospheres. For the structure of the accretion disk fields, the formalism was developed to describe the equilibria of a thin, viscous, resistive, and nonrelativistic accretion disk, leading to simplified equations for the poloidal and toroidal magnetic field. The coronal plasms that surrounds the disk was treated like the magnetospheric plasma of the pulsar, and a pulsar equation was found that determines the fields there. A Green's function method is used to determine the far field solution for the coronal fields. Energy conservation for the disk-jet system yields a global consistency condition which restricts the amount of gravitational accretion power that can be carried away by the jets for a given field symmetry. Dissert. Abstr.

N90-11676 Tennessee Univ., Knoxville.
ON TRANSONIC FLOW OVER SEGMENTED SLOTTED WIND TUNNEL WALL WITH MASS TRANSFER Ph.D. Thesis
Maharaj Krishen Bhat 1988 144 p
Avail: Univ. Microfilms Order No. DA8911707

The flowfield on a single and a segmented multi-slotted wind tunnel wall was studied at transonic speeds by traversing the wall viscous layer using five port cone probes. As expected, the slotted

wall flowfield was observed to be three-dimensional in nature for a significant distance above the slot. The boundary layer characteristics measured on the single slotted wall have been found to be very sensitive to the applied suction through the slot. The velocity component perturbations generated due to the flow through the slot decay rapidly in the transverse direction. A vortex-like flow existed on the single slotted wall for natural ventilation but diminished with increased section flow rate. For flow on a segmented multi-slotted wall, the normal velocity component changes were found to be maximum for measurement points located between the segmented slots atop the active chamber. The lateral influence due to applied suction and blowing, through a compartment, exceeded only slightly that in the downstream direction. Limited upstream influence was observed. Influence coefficients were determined from the data in the least-square sense for blowing and suction applied through one and two compartments. This was found to be an adequate determination of the influence coefficients for the range of mass flows considered. Dissert. Abstr.

N90-11677# International Centre for Theoretical Physics, Trieste (Italy).
STUDYING SHOCKS IN MODEL ASTROPHYSICAL FLOWS
Sandip K. Chakrabarti Jan. 1989 9 p
(DE89-618786; IC-89/2) Avail: NTIS (US Sales Only) HC A02/MF A01

Some properties of the shocks in the existing models for quasi two-dimensional astrophysical flows are discussed. All of these models which allow the study of shock analytically have some unphysical characteristics due to inherent assumptions made. A hybrid model is proposed for a thin flow which has fewer unpleasant features and is suitable for the study of shocks. DOE

N90-11678# Los Alamos National Lab., NM. Applied Theoretical Physics Div.
EFFECTS OF MAIN-SEQUENCE MASS LOSS ON THE TURNOFF AGES OF GLOBULAR CLUSTERS
Joyce A. Guzik 1989 9 p Presented at the 5th IAP Astrophysics Meeting on Astrophysical Ages and Dating Methods, Paris, France, 26-29 Jun. 1989
(Contract W-7405-eng-36)
(DE89-016784; LA-UR-89-2962; CONF-8906206-2) Avail: NTIS HC A02/MF A01

Willson, Bowen, and Struck-Marcell have proposed that globular cluster main-sequence turnoff ages can be reconciled with the lower ages of the Galaxy and universe deduced from other methods by incorporating an epoch of early main-sequence mass-loss by stars of spectral types A through early-F. The proposed mass loss is pulsation-driven, and facilitated by rapid rotation. This paper presents stellar evolution calculations of Pop. 2 (Z = 0.001) mass-losing stars of initial mass 0.8 to 1.6 solar mass, with exponentially-decreasing mass loss rates of e-folding times 0.5 to 2.0 Gyr, evolving to a final mass of 0.7 solar mass. The calculations indicate that a globular cluster with apparent turnoff age 18 Gyr could have an actual age as low as (approximately) 12 Gyr. Observational implications that may help to verify the hypothesis, e.g., low C/N abundance ratios among red giants following first dredge-up, blue stragglers, red giant deficiencies, and signatures in cluster mass/luminosity functions, are also discussed. DOE

N90-11679# Hiroshima Univ., Takehara (Japan). Research Inst. for Theoretical Physics.
GAUGE INVARIANT COSMOLOGICAL PERTURBATIONS WITH COLD DARK MATTER
Naoshi Sugiyama Feb. 1989 33 p
(DE89-790940; RRK-89-9) Avail: NTIS (US Sales Only) HC A03/MF A01

In the gauge-invariant formalism, the evolution of adiabatic and baryonic isocurvature density perturbations in a universe dominated by cold dark matter (CDM) is thoroughly investigated. Anisotropies are evaluated in the cosmic microwave background (CMB) and large scale peculiar velocities. From the recent observations of CMB fluctuations, new and stringent constraint is obtained for adiabatic CDM models as Omega sub 0 h sup -1 greater than 0.3. As for baryonic isocurvature perturbations, though the constraint is required as Omega sub 0 h sup -1 greater than or approx 0.6, these baryonic isocurvature models are more viable than axion isocurvature models. However it is difficult for both adiabatic and baryonic isocurvature CDM models to explain to observed large scale velocity field at greater than or approx 50h sup -1 Mpc while being consistent with the observations of CMB anisotropies. DOE

N90-10901# Joint Publications Research Service, Arlington, VA.
PROJECT RADIOASTRON
V. V. Andreyanov *In its* JPRS Report: Science and Technology. USSR: Space 28 Jun. 1989 p 13-17 Transl. into ENGLISH from Zemlya i Vselennaya (Moscow, USSR), no. 1, Jan.-Feb. 1989 p 13-17 (For primary document see N90-10900 02-12)
Copyright Avail: NTIS HC A06/MF A01

N90-10902# Joint Publications Research Service, Arlington, VA.
MEETING OF INTERCOSMOS SPACE PHYSICS GROUP
N. A. Frolova *In its* JPRS Report: Science and Technology. USSR: Space 28 Jun. 1989 p 17-19 Transl. into ENGLISH from Zemlya i Vselennaya (Moscow, USSR), no. 1, Jan.-Feb. 1989 p 46-48 (For primary document see N90-10900 02-12)
Copyright Avail: NTIS HC A06/MF A01

91 LUNAR AND PLANETARY EXPLORATION

Includes planetology; and manned and unmanned flights. For spacecraft design or space stations see *18 Spacecraft Design, Testing and Performance.*

N90-11680*# RAND Corp., Santa Monica, CA.
PHOEBE: A PRELIMINARY CONTROL NETWORK AND ROTATIONAL ELEMENTS
Tim R. Colvin, Merton E. Davies, Patricia G. Rogers, and Jeanne Heller, ed. May 1989 12 p
(Grant NAGw-1309)
(NASA-CR-185716; NAS 1.26:185716; N-2934-NASA) Avail: NTIS HC A03/MF A01 CSCL 03B

A preliminary control network for the Saturnian satellite Phoebe was determined based upon 6 distinct albedo features mapped on 16 Voyager 2 images. Using an existing map and an analytical triangulation program which minimized the measurement error, the north pole of Phoebe was calculated to be alpha sub 0 = 355.0 deg + or - 9.6 deg, delta sub 0 = 68.7 deg + or - 7.9 deg, where alpha sub 0, delta sub 0 are standard equatorial coordinates with equinox J2000 at epoch J2000. The prime meridian of Phoebe was computed to be W = 304.7 deg + 930.833872d, where d is the interval in days from JD 2451545.0 TDB. Author

N90-11681 California Inst. of Tech., Pasadena.
A DYNAMICAL STUDY OF JUPITER'S GREAT RED SPOT Ph.D. Thesis
Timothy Edward Dowling 1989 145 p
Avail: Univ. Microfilms Order No. DA8908413

This work is presented in the form of two related papers. In the first paper we investigate layer thickness variations in Jupiter's atmosphere by tracking absolute vorticity (zeta + f) along streamlines of the Great Red Spot (GRS) and White Oval BC. The ratio of absolute vorticity to layer thickness, called the potential vorticity, is conserved following the motion. By observing Lagrangian variations of absolute vorticity, we may infer variations in layer thickness. The data thus obtained are a useful diagnostic that will help differentiate between models of Jovian vortices. We interpret the observed layer thickness variations using a simple 1-1/2 layer model in which a thin upper weather layer, which contains the vortices, overlies a much deeper layer, which is meant to model the deep atmosphere. In this model, layer thickness variations are directly coupled to motions in the deep atmosphere, and we use the data to infer the deep motions. In the first paper

we interpret the data, using the quasi-geostrophic equations. In the second paper we reinterpret the data, using the more general shallow water equations. Most current models of the GRS are cast in terms of the 1-1/2 layer model, and they start by prescribing the motions in the deep atmosphere. Here we are able to derive the deep motions using the same 1-1/2 layer model assumptions, up to a constant that depends on the unknown static stability of Jupiter's troposphere. None of the current prescriptions for the deep motions are in qualitative agreement with the observations over the full range of latitudes observed. We study the 1-1/2 layer model numerically, using both the derived deep motions and the prescribed deep motions of current models. Only the present model, based on observations, yields Lagrangian absolute vorticity profiles that agree with those obtained in the first paper. A model run that starts with the observed zonally averaged cloud-top winds and derived deep motions shows instability, which naturally leads to the genesis and maintenance of a large, isolated vortex similar to the GRS. Author

N90-11682 Virginia Univ., Charlottesville.
ION BOMBARDMENT OF Io AND MERCURY Ph.D. Thesis
Melissa Ann McGrath 1988 111 p
Avail: Univ. Microfilms Order No. DA8909575

The existence of an atmosphere at Io is presumed and used to generate nonthermal coronae by ion bombardment of the atmosphere exobase. Several different exobase heights, temperatures, and compositions are used to characterize the neutral and ion ejection processes associated with possible atmospheres. The net injection rates are compared with estimates of the rates required to populate the plasma torus. The supply rate to the torus can be satisfied with an exobase very close to the surface if an unattenuated incident ion flux is assumed. A high exobase is consistent with the estimated supply rates only if the incident plasma flux is significantly attenuated or deflected. The results presented scale approximately with the magnitude of the incident ion flux and can be used as knowledge of both the plasma flow and atmospheric composition improve. The non-thermal corona model is compared with a thermal corona model and with recent observations of the variation in Na column density versus distance from Io. The effect of an E x B velocity drift on the magnitude of the incident ion flux and, subsequently, the plasma supply rates from Io's atmosphere and corona are investigated. Significant reduction of the supply rates is found by using reasonable values for the parameters describing Io's atmosphere and the plasma medium surrounding it. This relaxes constraints on the atmospheric exobase height mentioned above. New charge exchange cross sections which are important for the plasma supply scenarios and for determining ion partitioning and energy supply in the Io plasma torus are calculated. Finally, investigation of the ion and photon bombardment of Mercury is carried out, in analogy with the situation at Io, to determine possible supply and loss mechanisms for the Na recently observed in the atmosphere of Mercury. Author

N90-11683# Lawrence Livermore National Lab., CA.
EQUATION-OF-STATE DATA OF SYNTHETIC URANUS
W. J. Nellis and A. C. Mitchell Jun. 1989 3 p Presented at the AIRAPT and EHPRG International High Pressure Science and Technology Conference, Paderborn, Fed. Republic of Germany, 17-21 Jul. 1989
(Contract W-7405-eng-48)
(DE89-016509; UCRL-100983; CONF-890798-8) Avail: NTIS HC A01/MF A01

New equation-of-state data for the liquid mixture called synthetic Uranus is discussed. This liquid was double shocked to 220 GPa and 3 g/cu cm. These data are coincident with the adiabat of Uranus calculated by Hubbard and Marley. DOE

92 SOLAR PHYSICS

Includes solar activity, solar flares, solar radiation and sunspots.

For related information see *93 Space Radiation.*

N90-11684# National Geophysical Data Center, Boulder, CO.
SOLAR-GEOPHYSICAL DATA NUMBER 536, PART 1. DATA FOR MARCH, FEBUARY 1989 AND LATE DATA Prompt Reports, Apr. 1989
Helen E. Coffey, ed. Apr. 1989 185 p
(PB89-194716; SGD-536-Pt-1; LC-79-640375; ISSN-0038-0911)
Avail: NTIS HC A09/MF A01 CSCL 03B

A detailed solar-geophysical index for 1988-1989 is presented. Data for March 1989 includes: (1) International Ursigram and World Days Service (IUWDS) alert periods (advance and worldwide); (2) solar activity indices; (3) solar flares; (4) solar radio emission; and (5) Stanford mean solar magnetic field. Data for February 1989 includes: (1) solar active regions; (2) sudden ionospheric disturbances; (3) solar radio spectral observations; (4) geomagnetic indices; (5) cosmic ray measurements by neutron monitor; and (6) radio propagation indices. Other data includes: (1) H-alpha solar synoptic charts 1809-1810 for Nov-Dec 88; (2) cosmic rays (Huancayo) Jan 89; (3) geomagnetic sudden commencements/solar flare effects Jan 89; (4) Pioneer 12 interplanetary magnetic field magnitudes July 88; (5) Pioneer 12 solar wind data for Jan-Dec 88; and (6) March special event data. GRA

N90-11685 National Geophysical Data Center, Boulder, CO.
SOLAR-GEOPHYSICAL DATA NUMBER 537, PART 1. DATA FOR APRIL, MARCH 1989 AND LATE DATA Prompt Reports, May 1989
Helen E. Coffey, ed. Jul. 1987 151 p
(PB89-207393; SGD-537-Pt-1; LC-79-640375; ISSN-0038-0911)
Avail: NTIS HC A08/MF A01 CSCL 03B

Solar data are presented for March and April, 1989. The data include sunspot activity indices; solar flares in the H-alpha line; solar radio emissions at 3, 10, 21, and 43 cm; and mean solar magnetic fields. GRA

N90-11686 Colorado Univ., Boulder.
A SOLAR EXTREME ULTRAVIOLET FLUX MODEL Ph.D. Thesis
William Kent Tobiska 1988 306 p
Avail: Univ. Microfilms Order No. DA8912226

Solar extreme ultraviolet (EUV) flux for 37 discrete wavelengths or wavelength intervals is modeled during the decline of solar cycle 21. The primary modeling input parameters are the two indices of the filtered daily values of solar Lyman-alpha photon flux and the natural logarithm of solar 1 to 8 A X-ray energy flux. These two emissions were measured on a daily basis by the Solar Mesosphere Explorer (SME) and Geostationary Operational Environmental Satellites (GOES), respectively. The EUV data from the Atmosphere Explorer E (AE-E) satellite is correlated with AE-E Lyman-alpha flux, Ottawa 10.7 cm flux (F sub 10.7), and GOES 1 to 8 A X-ray flux. Linear relations are established between the EUV and Lyman-alpha emissions and between the EUV and the natural logarithm of 1 to 8 A X-ray emissions during the rising phase of cycle 21. Nine dominant EUV energy emissions are detailed which contribute nearly 50 percent of the thermospheric heating for solar minimum and maximum conditions. These EUV emissions are used as energy inputs into a 1-D, time dependent thermospheric model to solve for temperatures and constituent densities. The resulting densities are compared with satellite derived densities and MSIS 83 modeled densities for the period between January 1982 and May 1983. The two-indices method of modeling EUV flux is validated by this comparison although the 1 to 8 A X-ray index tends to overestimate the energy flux during certain time periods. It is shown that chromospheric emissions contribute the 27-day variability in atmospheric density at satellite altitudes during high solar activity. Through the use of a long term orbit predictor, the two indices method of modeling EUV flux is further validated by a comparison of the modeled orbit decay to the

actual satellite orbit decay. In the orbit decay calculation, it is additionally suggested that the satellite drag coefficient, C sub d, has a small variation due to the long term solar EUV flux variation and its effects upon neutral thermospheric gas temperatures.
Dissert. Abstr.

N90-11687# Los Alamos National Lab., NM. Theoretical Div.
SOLAR OPACITIES CONSTRAINED BY SOLAR NEUTRINOS AND SOLAR OSCILLATIONS
Arthur N. Cox 15 Aug. 1989 15 p Presented at the Inside the Sun International Conference, Versailles, France, 22-26 May 1989
(Contract W-7405-eng-36)
(DE89-016988; LA-UR-89-2825; CONF-890520-1) Avail: NTIS HC A03/MF A01

This review discusses the current situation for opacities at the solar center, the solar surface, and for the few million kelvin temperatures that occur below the convection zone. The solar center conditions are important because they are crucial for the neutrino production, which continues to be predicted about 4 times that observed. The main extinction effects there are free-free photon absorption in the electric fields of the hydrogen, helium and the CNO atoms, free electron scattering of photons, and the bound-free and bound-bound absorption of photons by iron atoms with two electrons in the 1s bound level. An assumption that the iron is condensed-out below the convection zone, and the opacity in the central regions is thereby reduced, results in about a 25 percent reduction in the central opacity but only a 5 percent reduction at the base of the convection zone. Furthermore, the p-mode solar oscillations are changed with this assumption, and do not fit the observed ones as well as for standard models. A discussion of the large effective opacity reduction by weakly interacting massive particles also results in poor agreement with observed p-mode oscillation frequencies. The much larger opacities for the solar surface layers from the Los Alamos Astrophysical Opacity Library instead of the widely used Cox and Tabor values show small improvements in oscillation frequency predictions, but the largest effect is in the discussion of p-mode stability. Solar oscillation frequencies can serve as an opacity experiment for the temperatures and densities, respectively, of a few million kelvin and between 0.1 and 10 g/cu cm. Current oscillation frequency calculations indicate that possibly the Opacity Library values need an increase of typically 15 percent just at the bottom of the convection zone at 3 x 10(6) K. DOE

N90-11362# Institut d'Aeronomie Spatiale de Belgique, Brussels.
SOLAR-TERRESTRIAL RELATIONS: FLARE AND SOLAR WIND EFFECTS
J. Lemaire *In* AGARD, Ionospheric Structure and Variability on a Global Scale and Interactions with Atmosphere and Magnetosphere Apr. 1989 11 p Sponsored in part by Ministere de l'Education Nationale et de la Culture Francaise and Fonds National de la Recherche Scientifique (For primary document see N90-11361 02-46)
Copyright Avail: NTIS HC A20/MF A03

93 SPACE RADIATION

Includes cosmic radiation; and inner and outer earth's radiation belts.

For biological effects of radiation see *52 Aerospace Medicine*. For theory see *73 Nuclear and High-Energy Physics*.

N90-11688 Council for National Academic Awards (England).
THE RATIO TO X-RAY SPECTRAL SHAPE AND VARIABILITY OF BLAZARS Ph.D. Thesis
Lucinda Mary Joanna Brown 1988 203 p
Avail: Univ. Microfilms Order No. BRDX85338

The results are presented of analysis of the spectral shape and variability properties of the radio to X-ray continua of a sample of BL Lac objects and OVV quasars (blazars). These results have important implications for the unification of BL Lac objects, OVV quasars and low polarization quasars into a single class of objects showing a smoothly continuous distribution of properties. The spectral shape of the violently variable millimetre to ultraviolet emission indicates that in this wavelength region the blazar emission is dominated by a very compact, single synchrotron component which becomes self-absorbed at wavelenghts longer than approx. 3 mm. The centimeter emission can be attributed to a separate, more slowly varying component, which can be identified with an underlying quiescent component, similar to that observed in the low polarization quasar 3C273. The OVV quasars also exhibit evidence of an optical excess, which was identified with the optical excesses which are observed in low polarization quasars. The variability behavior of the BL Lac objects is consistent with repeated injections or reaccelerations of electrons within in a small flaring synchrotron component, with subsequent radiative energy loss. In the case of the OVV quasars, however, the variability behavior at near infrared wavelengths is not consistent with emission from a single synchrotron component. It is shown that the behavior of the OVV quasars provides evidence for the presence of an additional non-variable, near infrared spectral component, reminiscent of that observed in 3C273. The sizes of the regions responsible for the flaring and quiescent emission are deduced to the approx. 10(-2) and 10(-1) parsecs, respectively. It is suggested that the flaring regions may represent regions of enhanced emission within a relativistic jet, possibly due to shock waves within the jet.
Dissert. Abstr.

N90-11689*# National Aeronautics and Space Administration. Marshall Space Flight Center, Huntsville, AL.
GAMMA RADIATION BACKGROUND MEASUREMENTS FROM SPACELAB 2 Annual Report
William S. Paciesas, John C. Gregory (Alabama Univ., Huntsville.), and Gerald J. Fishman 1988 10 p
(Contract NAS8-35354)
(NASA-CR-183782; NAS 1.26:183782; SSL-Preprint-88-136)
Avail: NTIS HC A02/MF A01 CSCL 03B

A Nuclear Radiation Monitor incorporating a NaI(Tl) scintillation detector was flown as part of the verification flight instrumentation on the Spacelab 2 mission, July 29 to August 6, 1985. Gamma-ray spectra were measured with better than 20 s resolution throughout most of the mission in the energy range 0.1 to 30 MeV. Knowledge of the decay characteristics and the geomagnetic dependence of the counting rates enable measurement of the various components of the Spacelab gamma-ray background: prompt secondary radiation, Earth albedo, and delayed induced radioactivity. The status of the data analysis and present relevant examples of typical background behavior are covered. Author

99 GENERAL

N90-11690# Indiana Univ., Bloomington. Dept. of West European Studies.
A HISTORY OF WEST EUROPEAN ROCKETRY AND SPACE RESEARCH M.A. Thesis
Lee C. Jorde Dec. 1988 139 p
(AD-A211191) Avail: NTIS HC A07/MF A01 CSCL 19/7

The purpose of this thesis is to document and analyze steps taken by West Europeans in the rocketry and space field that have played a significant role in world politics and in the development of West Europe as a more integrated power. Through this chronological study, covering a period from the years immediately before the rise of the Nazis to power in Germany until the mid-1980's, the author portrays the three most salient European nations, namely Great Britain, France, and West Germany, in their political roles with one another and, to a lesser extent, with the two superpowers. It is also my intention for this study to act as a reminder that growth, economic well-being, and national security are the rewards of a continued, uninterrupted,

generously-funded program of research and development that is organized for efficiency, that is well led, and that is staffed by well educated personnel. GRA

N90-11691# Swedish Defence Research Establishment, Linkoeping. Dept. of Information Technology.

THE SWEDISH DEFENSE RESEARCH NEEDS: FOR SURVEILLANCE AND SEEKER APPLICATIONS

Jan Kjellgren, ed., Staffan Gadd, Per Grahn, Hans Hellsten, Bjoern Larsson, Staffan Lindstroem, Hans Ottersten, Gunnar Rosenquist, and Ain Sume Jan. 1989 26 p In SWEDISH; ENGLISH summary

(FOA-C-30520-3.3; ISSN-0347-3708; ETN-89-94937) Avail: NTIS HC A03/MF A01; Swedish Defence Research Establishment, P.O. Box 1165, S-581 11 Linkoeping, Sweden, 50 Swedish crowns

The methods used in surveillance (including local radar surveillance) and in air, sea, and ground target acquisition are surveyed. Special notice is given to data processing, optical data processing, microwave technique, microelectronics and rapid digital systems, adaptive control, multisensors, infrared tracking, target following and identification of the target, jamming, and confusion. The applied methods are: the theoretical analysis (as electromagnetic wave transmission is a difficult problem to be treated exactly theoretically), models and computerized simulation, experimental research, and tests in the field. Suggestions are presented for choice criteria, having in mind the possibilities of the future technique. ESA

SUBJECT INDEX

Typical Subject Index Listing

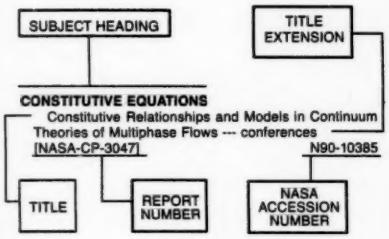

The subject heading is a key to the subject content of the document. Titles, report numbers, and accession numbers of pertinent documents are provided under each subject heading. When the title is insufficiently descriptive of the document content, a title extension has been added, separated from the title by three hyphens. The report number helps to indicate the type of document cited (e.g., NASA report, NASA translation, NASA contractor report). The NASA accession number is the number by which the document abstracts are arranged in this journal and by which the document is sold or requested. The titles, with title extensions if present, are arranged under each subject heading in ascending accession number order. The subject headings have been selected from the latest revision of the *NASA Thesaurus* (NASA SP-7064).

A

A-320 AIRCRAFT
A320 flight tests: Particularities and innovations N90-10864

ABILITIES
Comprehension processes in mechanical reasoning [AD-A210459] N90-11442
Stimulus-response compatibility in spatial precuing and symbolic identification: Effects of coding practice, retention, and transfer [AD-A210745] N90-11443

ABLATION
Modifications to the aerotherm charring material thermal response and ablation program (CMA) for carbon ablation analysis [AD-A211069] N90-11115

ABSORPTION CROSS SECTIONS
Investigations into the influence of the state functions on the cross sections of the direct p,gamma reactions at energies in the 100 keV range, and project of a cascade accelerator for the measurement of the p,gamma capture cross sections [ETN-89-94662] N90-11561

ABSORPTION SPECTRA
Spectropolarimetry, variability, and the taxonomy of active galactic nuclei N90-11667
Small grains in reflection nebulae: A study of diffuse interstellar bands, elemental depletions and infrared flux N90-11672

ABSORPTION SPECTROSCOPY
Study of high frequency water vapor absorption parameters [AD-A210676] N90-11108

ABUNDANCE
Carbon isotope ratios and lithium abundances in open cluster giants N90-11664

ACCELERATED LIFE TESTS
Accelerated aging of metal matrix composites N90-11085

ACCELERATION (PHYSICS)
Acceleration of metal plates [DE89-016816] N90-11197
Interferometry and high speed photography of laser-driven flyer plates [DE89-016990] N90-11290
Computational aspects of sensitivity calculations in linear transient structural analysis N90-11327

ACCESS CONTROL
Performance analysis of hybrid ARQ protocols in a slotted code division multiple-access network [AD-A211078] N90-11219

ACCRETION DISKS
Electromagnetic jets in pulsar magnetospheres and near magnetized accretion disks N90-11675

ACCURACY
High accuracy coordinate determination using the global positioning system N90-10858
Adaptive structures to meet future requirements for large precision structures N90-11001
Simulation of synthetic aperture radar 1: Feature density and accuracy requirements [AD-A211019] N90-11218

ACOUSTIC ATTENUATION
Calculation of sound transmission through a cylindrical shell using ASKA acoustics N90-11009

ACOUSTIC FREQUENCIES
Low ppb level detection of toxic compounds with a fully automated CO2 laser photoacoustic detector N90-11181

ACOUSTIC MEASUREMENT
Tower wake/blade interaction noise of a wind turbine [NAL-TR-945] N90-11344

ACOUSTIC PROPAGATION
Non-linear wave-equations for low-frequency acoustic gravity waves N90-11365
Medium scale structure of the F-region N90-11372

ACOUSTIC PROPERTIES
The dynamics of circular plates with patch damping: A numerical and experimental study N90-11329
Acoustic studies of new materials: Quasicrystals, low-loss glasses and high Tc superconductors [AD-A211281] N90-11551

ACOUSTIC SCATTERING
Nonlinear acoustics: Reflection and refraction, propagation in a periodic waveguide, scattering of sound by sound and ellipsoidal focusing [AD-A211224] N90-11550

ACOUSTIC SIMULATION
Acoustic response analysis in the low frequency domain N90-11010
The large European Acoustic Facility at ESTEC N90-11067

ACOUSTICAL HOLOGRAPHY
The investigation of the fundamental limits of heterodyne holographic interferometry with the application of imaging laser generated lamb waves [AD-A211048] N90-11285

ACOUSTICS
Development of a thermoacoustic test facility N90-11041

ACOUSTO-OPTICS
A remote sensor to monitor combustion products using a tunable acousto-optic filter N90-11275
Acoustic studies of new materials: Quasicrystals, low-loss glasses and high Tc superconductors [AD-A211281] N90-11551

ACTIVATION ENERGY
Quasi-diffusion between phonon and roton gases in two- and three-dimensional liquid helium [AD-A210565] N90-11096

ACTIVE CONTROL
The active control of an unstable canard aircraft N90-10894
Independent Orbiter Assessment (IOA): CIL issues resolution report, volume 1 [NASA-CR-185524-VOL-1] N90-10954
Independent Orbiter Assessment (IOA): Assessment of the active thermal control system [NASA-CR-185573] N90-10979

ACTIVE GALAXIES
Spectropolarimetry, variability, and the taxonomy of active galactic nuclei N90-11667

ACTUATION
Battery actuation of NITINOL at sub-zero temperatures [AD-A211254] N90-11237

ACTUATORS
Independent Orbiter Assessment (IOA): Analysis of the elevon subsystem [NASA-CR-185576] N90-10935
Independent Orbiter Assessment (IOA): Analysis of the mechanical actuation subsystem [NASA-CR-185525] N90-10944
Independent Orbiter Assessment (IOA): Assessment of the mechanical actuation subsystem, volume 1 [NASA-CR-185527-VOL-1] N90-10952
Independent Orbiter Assessment (IOA): Assessment of the mechanical actuation subsystem, volume 2 [NASA-CR-185527-VOL-2] N90-10953
Independent Orbiter Assessment (IOA): Assessment of the ascent thrust vector control actuator subsystem FMEA/CIL [NASA-CR-185590] N90-10959
Independent Orbiter Assessment (IOA): Assessment of the elevon actuator subsystem FMEA/CIL [NASA-CR-185578] N90-10970

ADA (PROGRAMMING LANGUAGE)
Research, development, training and education using the Ada programming language [AD-A210760] N90-11466

ADAPTIVE CONTROL
Performance and robustness of adaptive controllers for linear stochastic systems N90-11485

ADAPTIVE FILTERS
Adaptive tracking of maneuvering targets based on IR image data N90-10853

ADAPTIVE OPTICS
Adaptive gigabit fiber optics local area network [AD-A210794] N90-11571

ADDITIVES
Influence of grain refining on the casting, physical, mechanical, and electrochemical properties of technical aluminum [ETN-89-94661] N90-11135

ADSORPTION
Interfacial adsorption and crystallization of polycarbonate in carbon fiber composites [AD-A211230] N90-11090
Modeling of hydrazine surface interactions in environmental reaction chambers N90-11162
A diffuse reflectance infrared Fourier transform spectroscopic study of adsorbed hydrazines N90-11170

ADVECTION
Composited local area forecast techniques [AD-A210802] N90-11432

AERIAL RUDDERS
Independent Orbiter Assessment (IOA): Assessment of the rudder/speed brake subsystem FMEA/CIL [NASA-CR-185558] N90-10975

AEROACOUSTICS
An investigation of counterrotating tip vortex interaction [NASA-CR-185135] N90-11549

AERODYNAMIC CHARACTERISTICS
Low-speed, high-lift aerodynamic characteristics of slender, hypersonic accelerator-type configurations [NASA-TP-2945] N90-10830
An experimental investigation of the aerodynamic characteristics of slanted base ogive cylinders using magnetic suspension technology [NASA-CR-181708] N90-10834
P-180 AVANTI: Project and flight test program comprehensive overview N90-10863

AERODYNAMIC COEFFICIENTS
Independent Orbiter Assessment (IOA): Assessment of the Orbiter Experiment (OEX) subsystem [NASA-CR-185587] N90-10962
Independent Orbiter Assessment (IOA): Analysis of the Orbiter Experiment (OEX) subsystem [NASA-CR-185586] N90-10963

On transonic flow over segmented slotted wind tunnel wall with mass transfer N90-11676

AERODYNAMIC CONFIGURATIONS

US Navy principal site testing concept and the F-18 N90-10861

P-180 AVANTI: Project and flight test program comprehensive overview N90-10863

AERODYNAMIC FORCES

A scalar/vector potential solution for aerodynamic coefficients in wind shear N90-10838

AERODYNAMICS

The spinning of aircraft: A discussion of spin prediction techniques including a chronological bibliography [ARL-AERO-R-177] N90-10888

Analytical study of mistuning/friction/aerodynamics interaction in a bladed disk assembly [AD-A211139] N90-10893

AERONAUTICAL ENGINEERING

Technical communications in aeronautics: Results of an exploratory study. An analysis of managers' and nonmanagers' responses [NASA-TM-101625] N90-11647

AEROSOLS

Analysis of forest fire smoke using satellite imagery [AD-A210657] N90-11339

Lidar observations of the stratospheric aerosol: Boulder, Colorado, 1985 to 1987 [PB89-203871] N90-11425

Atmospheric aerosol size distributions and optical properties found in the marine boundary layer over the Atlantic Ocean [AD-A210800] N90-11431

AEROSPACE ENGINEERING

The Environmental Test Centre at ESTEC (an overview) N90-11064

AEROSPACE PLANES

Low-speed, high-lift aerodynamic characteristics of slender, hypersonic accelerator-type configurations [NASA-TP-2945] N90-10830

AEROSPACE SAFETY

Evaluation of tests and design factors N90-10987

AEROTHERMOCHEMISTRY

Modifications to the aerotherm charring material thermal response and ablation program (CMA) for carbon ablation analysis [AD-A211069] N90-11115

AEROTHERMODYNAMICS

Development of a thermoacoustic test facility N90-11041

AGING (MATERIALS)

Space environment effects on carbon/epoxy materials N90-11056

AGING (METALLURGY)

Accelerated aging of metal matrix composites N90-11085

AIR

Surface-catalyzed air oxidation of hydrazines: Environmental chamber studies N90-11159

Surface-catalyzed air oxidation reactions of hydrazines: Tubular reactor studies N90-11167

AIR DATA SYSTEMS

Independent Orbiter Assessment (IOA): Assessment of the Orbiter Experiment (OEX) subsystem [NASA-CR-185587] N90-10962

Independent Orbiter Assessment (IOA): Analysis of the Orbiter Experiment (OEX) subsystem [NASA-CR-185586] N90-10963

Independent Orbiter Assessment (IOA): Assessment of the backup flight system FMEA/CIL [NASA-CR-185566] N90-10973

AIR JETS

Rectangular subsonic jet flow field measurements [NASA-CR-185962] N90-11255

AIR LOCKS

Independent Orbiter Assessment (IOA): Assessment of the life support and airlock support systems, volume 1 [NASA-CR-185581-VOL-1] N90-10977

Independent Orbiter Assessment (IOA): Assessment of the life support and airlock support systems, volume 2 [NASA-CR-185581-VOL-2] N90-10978

AIR MASSES

Are ozone exceedance rates decreasing. Comment on extreme value analysis of environmental time-series: An application to trend detection in ground-level ozone [AD-A211029] N90-11357

Atmospheric aerosol size distributions and optical properties found in the marine boundary layer over the Atlantic Ocean [AD-A210800] N90-11431

AIR NAVIGATION

Federal Radionavigation Plan, 1988 [PB89-163075] N90-10846

Design of a Kalman filter for transfer alignment N90-10848

AIR POLLUTION

Hydrazine dosimetry N90-11178

Potential effects of global climate change on the United States. Executive summary. Draft [PB89-161046] N90-11350

Potential effects of global climate change on the United States. Volume 1: Regional studies. Draft [PB89-161053] N90-11351

Potential effects of global climate change on the United States. Volume 2: National studies. Draft [PB89-161061] N90-11352

AIR PURIFICATION

Independent Orbiter Assessment (IOA): CIL issues resolution report, volume 2 [NASA-CR-185524-VOL-2] N90-10955

AIR QUALITY

Interrelation of experimental exposure and ambient air quality data for comparison of ozone exposure indices and estimating agricultural losses [PB89-195036] N90-11353

AIR SAMPLING

Interrelation of experimental exposure and ambient air quality data for comparison of ozone exposure indices and estimating agricultural losses [PB89-195036] N90-11353

AIR START

In flight relight tests on AM-X single engine fly-by-wire aircraft N90-10869

AIR TO AIR MISSILES

Optimal and on-board near-optimal midcourse guidance N90-10857

AIR TRAFFIC CONTROL

Design of a final approach spacing tool for TRACON air traffic control [NASA-TM-102229] N90-10841

Ground and Obstacle Avoidance (GOA) concept of operations [DOT/FAA/DS-89/08] N90-10855

AIRBORNE/SPACEBORNE COMPUTERS

Optimal and on-board near-optimal midcourse guidance N90-10857

Realtime processing and display N90-10886

Independent Orbiter Assessment (IOA): Analysis of the backup flight system [NASA-CR-185567] N90-10932

AIRCRAFT APPROACH SPACING

Design of a final approach spacing tool for TRACON air traffic control [NASA-TM-102229] N90-10841

AIRCRAFT CONTROL

The active control of an unstable canard aircraft N90-10894

AIRCRAFT DESIGN

Low-speed, high-lift aerodynamic characteristics of slender, hypersonic accelerator-type configurations [NASA-TP-2945] N90-10830

See and avoid/cockpit visibility [DOT/FAA/CT-TN89/18] N90-10843

ATTAS flight testing experiences N90-10862

P-180 AVANTI: Project and flight test program comprehensive overview N90-10863

The Experimental Aircraft Flight Test Programme N90-10865

Flight test techniques adopted by Avions Marcel Dassault-Breguet Aviation N90-10867

Flight testing and flight research: From the age of the tower jumper to the age of the astronaut N90-10882

Integrated multidisciplinary design optimization of rotorcraft [NASA-TM-101642] N90-10889

AIRCRAFT DETECTION

Identification Friend, Foe or Neutral Joint Test N90-10881

AIRCRAFT ENGINES

Advanced technologies impact on compressor design and development: A perspective [NASA-TM-102341] N90-10891

AIRCRAFT HAZARDS

Remote sensing techniques of the Wave Propagation Laboratory for the measurement of supercooled liquid water: Applications to aircraft icing [PB89-208102] N90-10842

AIRCRAFT INSTRUMENTS

Flight simulator evaluation of a head-down display [NAL-TM-573] N90-10898

AIRCRAFT MANEUVERS

Nonlinear maneuver autopilot for the F-15 aircraft [NASA-CR-179442] N90-11487

AIRCRAFT MODELS

Measurements of pressures on the tail and aft fuselage of an airplane model during rotary motions at spin attitudes [NASA-TP-2939] N90-10829

The spinning of aircraft: A discussion of spin prediction techniques including a chronological bibliography [ARL-AERO-R-177] N90-10888

AIRCRAFT SAFETY

Design of a final approach spacing tool for TRACON air traffic control [NASA-TM-102229] N90-10841

Test and evaluation: Reducing risks to military aircraft from bird collisions. Report to the Chairman, Legislation, and National Security Subcommittee, Committee on Goverment Operations, House of Representatives [AD-A210870] N90-10845

AIRCRAFT STABILITY

The active control of an unstable canard aircraft N90-10894

AIRCRAFT SURVIVABILITY

Aircraft live fire testing N90-10879

AIRGLOW

Ionospheric irregularities due to powerful HF radio transmissions N90-11389

AIRLINE OPERATIONS

View on recent fuel costs in airlines [NAL-TM-569] N90-11653

AIRLOCK MODULES

Independent Orbiter Assessment (IOA): Assessment of the life support and airlock support systems, volume 1 [NASA-CR-185581-VOL-1] N90-10977

Independent Orbiter Assessment (IOA): Assessment of the life support and airlock support systems, volume 2 [NASA-CR-185581-VOL-2] N90-10978

ALGEBRA

Module algebra (revised version) [CWI-CS-R8844-REV] N90-11474

Synchrony with empty process — the algebra of synchronous processes [CWI-CS-R8832] N90-11481

On sufficient conditions for a function to be analytic [DE89-618382] N90-11503

General hulls in uniform algebras [DE89-618383] N90-11504

Analytic manifolds in uniform algebras [DE89-618384] N90-11505

Generalized BDF (Backward Differentiation Formula) methods applied to Hessenberg form DAEs [DE89-017328] N90-11522

An interpolation theorem in equational logic [CWI-CS-R8838] N90-11526

ALGORITHMS

High accuracy coordinate determination using the global positioning system N90-10858

Frequency domain design of robust controllers for space structures [AD-A211172] N90-10985

Modal analysis of space structures with the Ibrahim Time Domain method N90-11026

An experimental SMI adaptive antenna array for weak interfering signals [NASA-CR-185976] N90-11211

Validation of NEC (Numerical Electromagnetics Code) for antennas near ground [DE89-016502] N90-11212

Rethinking synthesis of fine-motion strategies [DE89-016671] N90-11322

A technique to correlate fractography with NDE (Non-Destructive Evaluation) of small samples [DE89-016904] N90-11325

On algorithms for generating computationally simple piecewise linear classifiers [NDRE/PUBL-89/1001] N90-11459

An investigation of the usefulness of Earley's Algorithm in a general context-free recognizer [DE89-016498] N90-11463

Programs for numerical integration of piece-wise smooth functions [DE89-620449] N90-11464

Parameter estimation in functional and partial differential equations [AD-A211040] N90-11511

ALIGNMENT

Design of a Kalman filter for transfer alignment N90-10848

ALKALI HALIDES

Design and construction of systems for the single-crystals growth of ternary silver halides, alkali halides, and alkaline earth fluorides, and the dielectric investigation of silver halide [ETN-89-94673] N90-11632

ALKALINE EARTH COMPOUNDS

Chemiluminescent ion-molecule reactions of group-3 ions with halogens: New optical spectra and reaction dynamics [MPIS-18/1988] N90-11120

ALKANES

A new method for the characterization of solutes and solvent phases using solvatochromic parameters [AD-A211238] N90-11116

ALKYL COMPOUNDS
The effect of degree of aromaticity and alkyl substitution of polyaromatic hydrocarbons on instrumental response factors
[DE89-000761] N90-11117
ALL-WEATHER AIR NAVIGATION
Kalman Filter Integration of Modern Guidance and Navigation Systems
[AGARD-LS-166] N90-10847
Development of the integrated all-weather navigation system for Tornado N90-10849
ALTERNATING CURRENT
Capacitive behavior in conducting polymers: The ac impedance and quartz crystal microbalance studies
[AD-A210754] N90-11150
The theory of ac impedance of rough electrode-electrolyte interfaces
[DE89-017474] N90-11243
ALTERNATING DIRECTION IMPLICIT METHODS
Pressure correction splitting methods for the computation of oscillatory free convection in low Pr fluids
[CWI-NM-R8816] N90-11271
ALTITUDE
Laser altimeter for use over the ocean
[AD-A211252] N90-11286
ALUMINIDES
Exploratory study of niobium, titanium, zirconium and tantalum aluminides
[AD-A210658] N90-11615
ALUMINUM
Influence of grain refining on the casting, physical, mechanical, and electrochemical properties of technical aluminum
[ETN-89-94661] N90-11135
ALUMINUM ALLOYS
Theoretical and experimental investigation of thin-walled aluminum panels under cyclic shear load N90-10996
Material properties of 2219-T851 aluminum alloy plasma welded compared to TIG welding N90-11032
ALUMINUM CARBIDES
Investigation of commercial Al-Ti and Al-Ti-B master alloys and development of a new grain refining agent based on carbides for aluminum and aluminum alloys
[ETN-89-94663] N90-11136
ALUMINUM COMPOUNDS
Y-Si-Al-O-N glass fibers
[AD-A211170] N90-11088
ALUMINUM NITRIDES
Basic research on processing of ceramics for space structures
[AD-A205954] N90-11139
ALUMINUM OXIDES
A diffuse reflectance infrared Fourier transform spectroscopic study of adsorbed hydrazines N90-11170
Kinetics and mechanisms of primary and steady state creep in B- and Al-containing alpha silicon carbide
[AD-A210739] N90-11616
AMBIGUITY
Alias-free Wigner distribution function and complex ambiguity function for discrete-time samples
[AD-A211050] N90-11533
AMMONIA
Low temperature spectroscope of hydrazine and ammonia complexes N90-11169
Equation-of-state data of synthetic Uranus
[DE89-016509] N90-11683
AMORPHOUS MATERIALS
Neutron scattering studies of amorphous Invar alloys
[DE89-016868] N90-11126
AMPLIFICATION
Minimized emittance growth with elliptical beam pipes in FEL (Free-Electron Laser)
[DE89-016982] N90-11305
AMPLIFIERS
A new semicustom integrated bipolar amplifier for silicon strip detectors
[DE89-015585] N90-11229
ANALOG DATA
Acoustic studies of new materials: Quasicrystals, low-loss glasses and high Tc superconductors
[AD-A211281] N90-11551
ANALYSIS (MATHEMATICS)
Summaries of the FY 1989 Applied Mathematical Sciences Research program
[DE89-016694] N90-11521
Backward analysis on higher order functions
[MEMO-INF-89-19] N90-11526
ANALYTIC FUNCTIONS
On sufficient conditions for a function to be analytic
[DE89-618382] N90-11503
General hulls in uniform algebras
[DE89-618383] N90-11504
ANECHOIC CHAMBERS
Tower wake/blade interaction noise of a wind turbine
[NAL-TR-945] N90-11344
ANGLE OF ATTACK
A computational/experimental study of the flow around a body of revolution at angle of attack
[NASA-TM-88329] N90-11254
ANILINE
Transport studies of conducting polymers N90-11140
Cell performance of ultra-thin polymer cathode system: Theoretical energy and power density projections
[AD-A210786] N90-11151
ANISOTROPIC PLATES
Nonlinear collapse simulation of anisotropic plates and corrugated panels N90-11035
ANISOTROPIC SHELLS
Nonlinear collapse simulation of anisotropic plates and corrugated panels N90-11035
ANNEALING
Thin section casting program. Volume 4: Static cast product bending, straightening, and rolling
[DE89-009034] N90-11202
Ion beam annealing of Ga-implanted Si
[DE89-016857] N90-11610
ANNUAL VARIATIONS
Diagnostic study of atmosphere-terrain interaction leading to the formation of dust clouds and poor visibilities over near east desert areas
[AD-A211243] N90-11358
Average diurnal and seasonal profiles of ionospheric storms N90-11371
Solar radiation in Linkoeping (Sweden): Variations over half a year in irradiance and spectral composition in the interval 400-1000 nm
[FOA-C-30521-3.1] N90-11417
ANTARCTIC OCEAN
The sea ice margins: A summary of physical phenomena
[PB89-212328] N90-11436
ANTENNA ARRAYS
Antenna beamforming using optical processing
[NASA-CR-180844] N90-11210
An experimental SMI adaptive antenna array for weak interfering signals
[NASA-CR-185976] N90-11211
ANTENNA COMPONENTS
Structural problems of accurate inflatable surfaces N90-11044
ANTENNA DESIGN
A high precision gravity compensation system for the deployment test of the ERS-1 SAR antenna N90-11038
Structural problems of accurate inflatable surfaces N90-11044
Test results on conceptual models of the large deployable antenna for mobile communications satellites N90-11050
ESA-D: An integrated software for antenna design and analysis N90-11052
A calibrated, omnidirectional, LF loop antenna for GWEN (Ground Wave Emergency Network)
[AD-A211264] N90-11221
ANTENNA RADIATION PATTERNS
Nonprincipal-plane scattering from flat plates: Second-order and corner diffraction and pattern control of horn antennas
[NASA-CR-185485] N90-11205
Part B: Pattern control of horn antennas N90-11207
Near zone-basic scattering code user's manual with space station applications
[NASA-CR-185925] N90-11209
ANTENNAS
An experimental SMI adaptive antenna array for weak interfering signals
[NASA-CR-185976] N90-11211
Validation of NEC (Numerical Electromagnetics Code) for antennas near ground
[DE89-016502] N90-11212
ANTIREFLECTION COATINGS
Diamondlike carbon coatings for optical systems
[AD-A211255] N90-11573
APPLICATION SPECIFIC INTEGRATED CIRCUITS
ASIC (Application Specific Integrated Circuit) replacement for an SSI (Small Scale Integrated) component design: A case study
[DE89-013494] N90-11232
GaAs ASIC design case study
[DE89-013934] N90-11461
APPLICATIONS OF MATHEMATICS
The fast Gauss transform
[AD-A211287] N90-11517
APPLICATIONS PROGRAMS (COMPUTERS)
User's manual for PEPSIG NASA tip vortex version
[NASA-CR-182178] N90-10835
A parallel numerical simulation for supersonic flows using zonal overlapped grids and local time steps for common and distributed memory multiprocessors
[DE89-015252] N90-10839
Independent Orbiter Assessment (IOA): Analysis of the backup flight system
[NASA-CR-185567] N90-10932
Modifications to the aerotherm charring material thermal response and ablation program (CMA) for carbon ablation analysis
[AD-A211069] N90-11115
Near zone-basic scattering code user's manual with space station applications
[NASA-CR-185925] N90-11209
Applications of the hybrid automated reliability predictor: Revised edition
[NASA-TP-2760-REV] N90-11454
Two VAX-PASCAL terminal interface modules for visualizing scanning and parsing
[MEMO-INF-89-17] N90-11470
Offaxis radiance studies for infrared sensors
[AD-A210790] N90-11570
APPROACH INDICATORS
Helicopter Visual Segment Approach Lighting System (HALS)
[ACD-330] N90-10856
APPROXIMATION
An interactive program for constrained spline approximation of numerical data
[DE89-016674] N90-11520
ARC JET ENGINES
The effect of electrode configuration on arcjet performance
[NASA-TM-102346] N90-11081
ARCHITECTURE
The astronomy of Andean myth: The history of a cosmology N90-11660
ARCHITECTURE (COMPUTERS)
Realtime processing and display N90-10886
Hanford Meteorological Station computer codes. Volume 10: The ARCHIVE computer code
[DE89-016175] N90-11429
Performance reports for EIM (Engineering Information Management) computer systems: A managerial perspective
[DE89-015194] N90-11449
New computing systems and their impact on structural analysis and design
[NASA-CR-185831] N90-11457
An investigation of the usefulness of Earley's Algorithm in a general context-free recognizer
[DE89-016498] N90-11463
Computing the two dimensional fast Fourier transform on a general purpose mesh connected multiprocessor
[DE89-016515] N90-11518
An interactive program for constrained spline approximation of numerical data
[DE89-016674] N90-11520
Summaries of the FY 1989 Applied Mathematical Sciences Research program
[DE89-016694] N90-11521
Adaptive gigabit fiber optics local area network
[AD-A210794] N90-11571
LEXER: A tool for lexical analysis of program input
[DE89-016924] N90-11649
ARCTIC OCEAN
The sea ice margins: A summary of physical phenomena
[PB89-212328] N90-11436
AREA
On the areas of various bodies in the Euclidean space: The case of irregular convex polygons
[DE89-618377] N90-11500
ARIANE LAUNCH VEHICLE
Dynamic substructuring for modular analysis and testing N90-11015
Induced shock loads during the separation of the Ariane 5 VEB structure N90-11045
Flight-mechanical environment on Ariane launch vehicle payloads N90-11048
Ariane 5 structural design and development N90-11057
ARIES SOUNDING ROCKET
Rocket and satellite observations of the local interstellar medium N90-11668
AROMATIC COMPOUNDS
The effect of degree of aromaticity and alkyl substitution of polyaromatic hydrocarbons on instrumental response factors
[DE89-000761] N90-11117
ARTIFICIAL INTELLIGENCE
Flight testing a newly-designed stand-off weapon dispenser N90-10880
Systems analysis considerations in artificial intelligence/expert systems technology applications
[DE89-016847] N90-11490

A survey of research methods to study design
[AD-A211213] N90-11491
Electron transfer reactions
[AD-A210711] N90-11545

ASIA

Diagnostic study of atmosphere-terrain interaction leading to the formation of dust clouds and poor visibilities over near east desert areas
[AD-A211243] N90-11358

ASSESSMENTS

Independent Orbiter Assessment (IOA): Analysis of the Orbiter Experiment (OEX) subsystem
[NASA-CR-185586] N90-10963

ASTRONOMICAL CATALOGS

New statistical approaches to galaxy clustering
N90-11674

ASTRONOMICAL OBSERVATORIES

System and performance analysis of a low density actively controlled mirror for astronomic observation
N90-11002

ASTRONOMICAL SPECTROSCOPY

Integrating detectors and their application to infrared astronomy N90-11659

ASTRONOMY

Meeting of intercosmos space physics group
N90-10902
The astronomy of Andean myth: The history of a cosmology N90-11660

ASTROPHYSICS

Meeting of intercosmos space physics group
N90-10902
A liquid xenon imaging telescope for 1-30 MeV gamma-ray astrophysics
[NASA-CR-185999] N90-11662
Studying shocks in model astrophysical flows
[DE89-618786] N90-11677

ASYMMETRY

Radiationless transitions and excited-state absorption of low-field chromium complexes in solids
[AD-A210653] N90-11105
Ionospheric total electron content, and far ultraviolet, near infrared oxygen emission N90-11410

ATLANTIC OCEAN

Atmospheric aerosol size distributions and optical properties found in the marine boundary layer over the Atlantic Ocean
[AD-A210800] N90-11431

ATLANTIS (ORBITER)

Shuttle Atlantis to deploy Galileo probe toward Jupiter
[NASA-TM-101888] N90-10982

ATMOSPHERIC CHEMISTRY

Study of high frequency water vapor absorption parameters
[AD-A210676] N90-11108
The Third Conference on the Environmental Chemistry of Hydrazine Fuels
[AD-A197632] N90-11157
Atmospheric chemistry of the fuel hydrazines
N90-11158
An atmospheric pressure flow reactor: Gas phase kinetics and mechanism in tropospheric conditions without wall effects N90-11160
The behavior of hydrazine vapor in an environmental chamber under simulated atmospheric conditions
N90-11161
Potential effects of global climate change on the United States. Executive summary. Draft
[PB89-161046] N90-11350
NCAR (National Center for Atmospheric Research) master mechanism of the gas phase chemistry, version 2.0
[PB89-208979] N90-11413
National Climate Program five-year plan, 1989-1993
[PB89-207369] N90-11426
National Center For Atmospheric Research annual report, fiscal year 1988
[PB89-208987] N90-11428
Atmospheric aerosol size distributions and optical properties found in the marine boundary layer over the Atlantic Ocean
[AD-A210800] N90-11431
Ion bombardment of Io and Mercury N90-11682

ATMOSPHERIC CIRCULATION

Atmospheric environment for space shuttle (STS-29) launch
[NASA-TM-100376] N90-10980
Atmospheric environment for space shuttle (STS-30) launch
[NASA-TM-100381] N90-10981
Global ionospheric dynamics N90-11366
Global ionospheric dynamics: A review N90-11367
A fully analytic, low and middle latitude ionospheric model N90-11368
Seasonal and geomagnetic response of the thermosphere and ionosphere N90-11380

ATMOSPHERIC COMPOSITION

Atmospheric chemistry of the fuel hydrazines
N90-11158
Stratospheric ozone depletion
[PB89-207476] N90-11354
Report of the 1988 2-D Intercomparison Workshop, chapter 3 N90-11407
Micrometeorological investigation of surface exchange of trace gases: A case study
[PB89-208375] N90-11412
NCAR (National Center for Atmospheric Research) master mechanism of the gas phase chemistry, version 2.0
[PB89-208979] N90-11413
Lidar observations of the stratospheric aerosol: Boulder, Colorado, 1985 to 1987
[PB89-203871] N90-11425
A dynamical study of Jupiter's Great Red Spot
N90-11681
Ion bombardment of Io and Mercury N90-11682

ATMOSPHERIC EFFECTS

Diagnostic study of atmosphere-terrain interaction leading to the formation of dust clouds and poor visibilities over near east desert areas
[AD-A211243] N90-11358
Ionospheric irregularities and their effects on electromagnetic waves propagating through them
N90-11391
Small-scale irregularities and global plasma dynamics in the high-latitude ionosphere N90-11394
Accurate measurements of the total angle of arrival of HF skywaves N90-11402
Ionospheric limitations to the accuracy of SSL estimates of HF transmitter locations N90-11403
NCAR (National Center for Atmospheric Research) master mechanism of the gas phase chemistry, version 2.0
[PB89-208979] N90-11413
Turbulence effects for retroreflection
[FOA-C-30523-3.1] N90-11575

ATMOSPHERIC ENTRY SIMULATION

Liquid infiltrated C/SiC: An alternative material for hot space structures N90-11030

ATMOSPHERIC HEATING

Ion heating events observed at the EISCAT radar
N90-11385
North-south tropical F2 layer asymmetry at west African and Pacific longitudes N90-11398

ATMOSPHERIC MODELS

Potential effects of global climate change on the United States. Volume 1: Regional studies. Draft
[PB89-161053] N90-11351
Ionospheric Structure and Variability on a Global Scale and Interactions with Atmosphere and Magnetosphere
[AGARD-CP-441] N90-11361
Global ionospheric dynamics: A review N90-11367
A fully analytic, low and middle latitude ionospheric model N90-11368
Modelling ionospheric density structures N90-11375
Seasonal and geomagnetic response of the thermosphere and ionosphere N90-11380
Ionospheric irregularities and their effects on electromagnetic waves propagating through them
N90-11391
Auroral and sub-auroral F-layer irregularity studies in the Northern and Southern Hemisphere during the equinox transition study September 16-26, 1984 N90-11393
Multistation/multiparameter observations with a network of digital ionosondes N90-11396
Coordinated multi-parameter measurements and predictions of the global-scale ionosphere N90-11397
An ionospheric model for HF sky-wave backscatter radar N90-11401
Ionospheric limitations to the accuracy of SSL estimates of HF transmitter locations N90-11403
Two-Dimensional Intercomparison of Stratospheric Models
[NASA-CP-3042] N90-11405
Report on the 2-D Model Intercomparison Workshop held January 11-16, 1987 in Fort Myers Beach, Florida, chapter 2 N90-11406
Report of the 1988 2-D Intercomparison Workshop, chapter 3 N90-11407
Model documentation, chapter 4 N90-11408
Introduction and data summary, chapter 5
N90-11409

ATMOSPHERIC OPTICS

Turbulence effects for retroreflection
[FOA-C-30523-3.1] N90-11575

ATMOSPHERIC PHYSICS

Study of high frequency water vapor absorption parameters
[AD-A210676] N90-11108
Ionospheric Structure and Variability on a Global Scale and Interactions with Atmosphere and Magnetosphere
[AGARD-CP-441] N90-11361
Atmospheric gravity waves in the auroral source region of TIDs, studied with the EISCAT CP2-data N90-11387
Small-scale irregularities and global plasma dynamics in the high-latitude ionosphere N90-11394
Meteorological rocket observations
[PB89-168769] N90-11419
National Center For Atmospheric Research annual report, fiscal year 1988
[PB89-208987] N90-11428
Interannual variability of temperature in the upper layer of the North Pacific eastern boundary region, 1971-1987
[PB89-190227] N90-11434

ATMOSPHERIC PRESSURE

Independent Orbiter Assessment (IOA): Analysis of the electrical power generation/power reactant storage and distribution subsystem
[NASA-CR-185556] N90-10918
Independent Orbiter Assessment (IOA): Assessment of the atmospheric revitalization pressure control subsystem FMEA/CIL
[NASA-CR-185594] N90-10957
An atmospheric pressure flow reactor: Gas phase kinetics and mechanism in tropospheric conditions without wall effects N90-11160

ATMOSPHERIC SCATTERING

Lidar observations of the stratospheric aerosol: Boulder, Colorado, 1985 to 1987
[PB89-203871] N90-11425
Atmospheric aerosol size distributions and optical properties found in the marine boundary layer over the Atlantic Ocean
[AD-A210800] N90-11431

ATMOSPHERIC TURBULENCE

Turbulence effects for retroreflection
[FOA-C-30523-3.1] N90-11575

ATOMIC COLLISIONS

Dielectronic excitation and recombination in crystal channels
[DE89-016864] N90-11625

ATOMIC EXCITATIONS

Dielectronic excitation and recombination in crystal channels
[DE89-016864] N90-11625

ATOMIC PHYSICS

Theoretical atomic physics for fusion
[DE89-017363] N90-11563

ATOMIC SPECTRA

Theory of atomic spectral emission intensity
[IRF-PREPRINT-110] N90-11641

ATOMIC STRUCTURE

Shock-induced atomic-scale structure in metals
[DE89-016539] N90-11124
Proceedings of the Polycrystalline Thin Film Program Meeting
[DE89-009457] N90-11348
Structure and properties of simple molecular systems at very high density
[DE89-016974] N90-11557
A fermi liquid electric structure and the nature of the carriers in high-T(sub c) cuprates: A photoemission study
[DE89-016774] N90-11624

ATOMS

Dynamics of nucleation at electrochemical interfaces via surface EXAFS and standing wave measurements
[AD-A210733] N90-11109

ATTITUDE CONTROL

Independent Orbiter Assessment (IOA): Analysis of the ascent thrust vector control actuator subsystem
[NASA-CR-185579] N90-10929
Independent Orbiter Assessment (IOA): Analysis of the reaction control system, volume 1
[NASA-CR-185532-VOL-1] N90-10938

AUDITORY PERCEPTION

Inferences from images
[AD-A210710] N90-11465

AURORAL ARCS

Low frequency electrostatic waves observed in the vicinity of an auroral arc N90-11378

AURORAL ZONES

A review on radio studies of auroral E-region ionospheric irregularities N90-11390
Auroral and sub-auroral F-layer irregularity studies in the Northern and Southern Hemisphere during the equinox transition study September 16-26, 1984 N90-11393
An ionospheric model for HF sky-wave backscatter radar N90-11401

AURORAS

Observations of ionosphere/magnetosphere interactions from the Dynamics Explorer satellites
N90-11376
Empirical models of convection electric fields and electrostatic potential at high latitude from EISCAT observations: Preliminary results N90-11377
Polar F layer lacuna irregularities at Dumont d'Urville
N90-11379

Quiet time conductivities of the auroral ionosphere N90-11383
Atmospheric gravity waves in the auroral source region of TIDs, studied with the EISCAT CP2-data N90-11387
On the possibility of producing artificial ionization and polar aurora in the ionosphere by radio-waves emitted from the ground N90-11388
North-south tropical F2 layer asymmetry at west AFrican and Pacific longitudes N90-11398

AUSTENITE
Use of overlapped reflection for determining the retained austenite by X-ray diffraction
[DE89-615450] N90-11128
Contribution to the transcrystalline stress crack corrosion of austenite chromium-nickel steels
[ETN-89-94665] N90-11137

AUTOMATA THEORY
Cellular automata and massively parallel physics
[DE89-016506] N90-11257

AUTOMATIC PILOTS
Nonlinear maneuver autopilot for the F-15 aircraft
[NASA-CR-179442] N90-11487

AUTOMOBILE ENGINES
Automotive Stirling engine development program
[NASA-CR-180839] N90-11654

AUTOMOBILES
Advanced Turbine Technology Applications Program, (ATTAP): A plan for improving the prototype production of ceramic components for the gas turbine engine, 1988--1992
[DE89-015566] N90-11320

AUXILIARY POWER SOURCES
Independent Orbiter Assessment (IOA): Analysis of the auxiliary power unit
[NASA-CR-185568] N90-10931
Independent Orbiter Assessment (IOA): Weibull analysis report
[NASA-CR-185534] N90-10948
Independent Orbiter Assessment (IOA): Assessment of the auxiliary power unit
[NASA-CR-185580] N90-10976

AVIATION METEOROLOGY
A scalar/vector potential solution for aerodynamic coefficients in wind shear N90-10838

AVIONICS
Kalman Filter Integration of Modern Guidance and Navigation Systems
[AGARD-LS-166] N90-10847
Development of the integrated all-weather navigation system for Tornado N90-10849
The development of mission-specific advanced inertially-based avionics system N90-10851
Flight Test Techniques
[AGARD-CP-452] N90-10860
Flight testing of the Tornado Terrain Following System N90-10875
Air Combat Environment Test and Evaluation Facility (ACETEF) N90-10883
Flight test instrumentation and data processing at British Aerospace, Warton, U.K. N90-10887

AXIAL FLOW
Laser anemometer measurements in a transonic axial-flow fan rotor
[NASA-TP-2879] N90-11245

AXISYMMETRIC FLOW
Chemical reactions in turbulent mixing flows
[AD-A211240] N90-11263

AZIMUTH
Passive trajectography by azimuth: Improvement of estimation quality N90-10854

B

BACKGROUND RADIATION
Thermal radiation from terrain: Measurements and first results
[FOA-C-30525-3.1] N90-11342
Gamma radiation background measurements from Spacelab 2
[NASA-CR-183782] N90-11689

BACKSCATTERING
Global ionospheric dynamics N90-11366
An ionospheric model for HF sky-wave backscatter radar N90-11401

BACKUPS
Independent Orbiter Assessment (IOA): Assessment of the backup flight system FMEA/CIL
[NASA-CR-185566] N90-10973

BACKWARD DIFFERENCING
Generalized BDF (Backward Differentiation Formula) methods applied to Hessenberg form DAEs
[DE89-017328] N90-11522
Backward analysis on higher order functions
[MEMO-INF-89-19] N90-11526

BALLISTICS
Aircraft live fire testing N90-10879

BALLOONING MODES
Theory of high-n toroidicity-induced shear Alfven eigenmode in tokamaks
[DE89-016726] N90-11582

BAND STRUCTURE OF SOLIDS
A fermi liquid electric structure and the nature of the carriers in high-T(sub c) cuprates: A photoemission study
[DE89-016774] N90-11624

BARIUM OXIDES
A study of the tribological and surface micromechanical properties of YBa2Cu3O7-x
[DE89-015680] N90-11607

BARIUM TITANATES
Influence of core-shell grains on the internal stress state and permittivity response of zirconia modified barium titanate
[AD-A211245] N90-11153

BAYS (STRUCTURAL UNITS)
Independent Orbiter Assessment (IOA): Assessment of the mechanical actuation subsystem, volume 1
[NASA-CR-185527-VOL-1] N90-10952
Independent Orbiter Assessment (IOA): Assessment of the mechanical actuation subsystem, volume 2
[NASA-CR-185527-VOL-2] N90-10953

BEAM CURRENTS
Simulation of an axially symmetric ion-optical system
[DE89-620129] N90-11560

BEAM INJECTION
Simulation of an axially symmetric ion-optical system
[DE89-620129] N90-11560
Projections for a steady-state tokamak reactor based on ITER
[DE89-016678] N90-11589
Beam-plasma discharge in penetrating plasma
[DE89-630481] N90-11597
International workshop on Beam Injection Assessment of Defects in Semiconductors
[AD-A210842] N90-11617

BEAM INTERACTIONS
Novel physical effects in intersecting optical waveguides N90-11565

BEAM SWITCHING
Antenna beamforming using optical processing
[NASA-CR-180844] N90-11210

BEAMS (RADIATION)
Electromagnetic pulse interaction at a dielectric interface
[AD-A211081] N90-11220
A solution to nonlinearity problems
[DE89-016975] N90-11544
International workshop on Beam Injection Assessment of Defects in Semiconductors
[AD-A210842] N90-11617

BEAMS (SUPPORTS)
Analysis of delamination growth N90-11036
The dynamic stability of an axially loaded beam with lateral elastic support and damping N90-11331

BEARINGS
Three-dimensional analysis of surface crack-Hertzian stress field interaction
[NASA-CR-4254] N90-11332

BEHAVIOR
Study of the behavioral and biological effects of high intensity 60 Hz electric fields
[DE89-015528] N90-11438

BEND TESTS
Liquid infiltrated C/SiC: An alternative material for hot space structures N90-11030

BENDING
Thin section casting program. Volume 4: Static cast product bending, straightening, and rolling
[DE89-009034] N90-11202

BERING SEA
The sea ice margins: A summary of physical phenomena
[PB89-212328] N90-11436

BESSEL FUNCTIONS
Some exact solutions of the three-identical-particle problem with S-wave inverse square potentials
[DE89-618402] N90-11524

BINARY MIXTURES
Solidification front/viscous phase transitions, forward-backward heat equations
[AD-A211068] N90-11114

BINARY STARS
MOXE: An X-ray all-sky monitor for Soviet Spectrum-X-Gamma Mission
[NASA-TM-101266] N90-11280
An improved algorithm for the determination of the system paramters of a visual binary by least squares N90-11658

BIOLOGICAL EFFECTS
Study of the behavioral and biological effects of high intensity 60 Hz electric fields
[DE89-015528] N90-11438

BIOPHYSICS
DOE/CEC Workshop on Critical Evaluation of Radiobiological Data to Biophysical Modeling
[DE89-015214] N90-11437

BIPOLARITY
A new semicustom integrated bipolar amplifier for silicon strip detectors
[DE89-015585] N90-11229

BIRD-AIRCRAFT COLLISIONS
Test and evaluation: Reducing risks to military aircraft from bird collisions. Report to the Chairman, Legislation, and National Security Subcommittee, Committee on Goverment Operations, House of Representatives
[AD-A210670] N90-10845

BIREFRINGENCE
Utilization of photorefractive crystals in optical image processing
[ISBN-3-923560-06-0] N90-11292

BL LACERTAE OBJECTS
The ratio to X-ray spectral shape and variability of blazars N90-11688

BLADE TIPS
User's manual for PEPSIG NASA tip vortex version
[NASA-CR-182178] N90-10835
Computation of the tip vortex flowfield for advanced aircraft propellers
[NASA-CR-182179] N90-10836

BLADE-VORTEX INTERACTION
User's manual for PEPSIG NASA tip vortex version
[NASA-CR-182178] N90-10835
Computation of the tip vortex flowfield for advanced aircraft propellers
[NASA-CR-182179] N90-10836
An investigation of counterrotating tip vortex interaction
[NASA-CR-185135] N90-11549

BODIES OF REVOLUTION
A computational/experimental study of the flow around a body of revolution at angle of attack
[NASA-TM-88329] N90-11254

BODY-WING CONFIGURATIONS
Low-speed, high-lift aerodynamic characteristics of slender, hypersonic accelerator-type configurations
[NASA-TP-2945] N90-10830

BOGOLIUBOV THEORY
On the construction of the scattering matrix for locally-noncommutative interactions of relativistic fields
[DE89-630138] N90-11640

BOILERS
Independent Orbiter Assessment (IOA): Analysis of the hydraulics/water spray boiler subsystem
[NASA-CR-185541] N90-10934

BOMBS (ORDNANCE)
Flight testing a newly-designed stand-off weapon dispenser N90-10880

BONDING
A characterization of the side bonding, upset plug welding process
[DE89-015181] N90-11315

BOOLEAN FUNCTIONS
Boolean functions, invariance groups and parallel complexity
[CWI-CS-R8836] N90-11472

BOOMS (EQUIPMENT)
Space telescope solar array: Nonlinear test and analysis effects N90-11051

BORON CARBIDES
Characterizations of shock-loaded aluminum-infiltrated boron carbide cermets
[DE89-016773] N90-11146

BORON REINFORCED MATERIALS
Kinetics and mechanisms of primary and steady state creep in B- and Al-containing alpha silicon carbide
[AD-A210739] N90-11616

BOUNDARIES
Parameter estimation in functional and partial differential equations
[AD-A211040] N90-11511
Boundary effects on the MHD dynamo in laboratory plasmas
[DE89-015207] N90-11576

BOUNDARY ELEMENT METHOD
Numerical models for exterior and interior fluid-structure interaction problems N90-11073
Three-dimensional analysis of surface crack-Hertzian stress field interaction
[NASA-CR-4254] N90-11332

BOUNDARY LAYER FLOW
Low-Reynolds-number modeling of complex flows with and without density variation N90-10832

BOUNDARY LAYER PLASMAS
Numerical study of the current sheet and PSBL in a magnetotail model
[NASA-CR-183289] N90-11669
BOUNDARY LAYER STABILITY
Wall-layer eruptions in turbulent flows
[NASA-TM-102362] N90-11250
BOUNDARY LAYER TRANSITION
An experimental investigation of transition in oscillating pipe flow N90-11249
BOUNDARY LAYERS
Atmospheric aerosol size distributions and optical properties found in the marine boundary layer over the Atlantic Ocean
[AD-A210800] N90-11431
Computer simulations of electromagnetic ion instabilities in the plasma sheet boundary layer
[DE89-016596] N90-11588
BOUNDARY VALUE PROBLEMS
Efficient algorithm for calculation of radar cross section
[AD-A210785] N90-11217
Analytical and numerical studies in flow development
[DE89-017380] N90-11269
Parameter estimation in functional and partial differential equations
[AD-A211040] N90-11511
On the numerical solution of two-point boundary value problems
[AD-A211244] N90-11516
Potential for parallelism in explicit linear methods
[DE89-017329] N90-11523
On the equivalence of BS-stability and B-consistency
[CWI-NM-R8815] N90-11530
BRAKES (FOR ARRESTING MOTION)
Independent Orbiter Assessment (IOA): Analysis of the rudder/speed brake subsystem
[NASA-CR-185560] N90-10916
Independent Orbiter Assessment (IOA): Assessment of the rudder/speed brake subsystem FMEA/CIL
[NASA-CR-185558] N90-10975
BRAKING
Independent Orbiter Assessment (IOA): Analysis of the nose wheel steering subsystem
[NASA-CR-185548] N90-10921
Independent Orbiter Assessment (IOA): Analysis of the landing/deceleration subsystem
[NASA-CR-185569] N90-10943
BRITTLENESS
Microstructural effects on spall fracture in 1008 steel
[DE89-016770] N90-11131
BROADBAND
Comparison of sine dwell and broadband methods for modal testing N90-11025
Wideband connectivity and support for Cronus cluster at USAF Electronic Systems Division
[AD-A210749] N90-11215
BUBBLES
Global morphology of plasma bubbles in the low latitude ionosphere N90-11369
BUCKLING
Overview of actual buckling calculation methods for space vehicle structures N90-10995
BUOYANCY
Relation of wind field and buoyancy to rainfall inferred from radar
[PB89-208326] N90-11424

C

C BAND
The effectiveness of adaptive PRF (Pulse Repetition Frequency) selection in minimizing range obscuration in the TDWR (Terminal Doppler Weather Radar) system
[AD-A211267] N90-11222
CADMIUM
Experimental measurements of shock-induced vaporization in cadmium and lead
[DE89-016877] N90-11103
CALCULUS OF VARIATIONS
New theoretical approaches for studying electron collisions with small molecules
[DE89-017543] N90-11558
CALIBRATING
NIST (National Institute of Standards and Technology) measurement services: The calibration of thermocouples and thermocouple materials
[PB89-209340] N90-11274
Using self-calibrating thermocouples in industry
[DE89-013539] N90-11278
CALORIMETERS
New tools for the simulation and design of calorimeters
[DE89-016323] N90-11281
The 3-D heat transfer computer calculations of th e performance of the IAEA's air-bath calorimeters
[DE89-016908] N90-11283
CAMERAS
Robust spatial calibration of a planar positron camera
[AD-A210773] N90-11284
Aspects of the development of a 1-5 micron infrared camera for astronomy N90-11656
CANADAIR AIRCRAFT
CF 18 480 Gallon External Fuel Tank Stores Clearance Program N90-10877
CANARD CONFIGURATIONS
The active control of an unstable canard aircraft N90-10894
CAPACITORS
Capacitive behavior in conducting polymers: The ac impedance and quartz crystal microbalance studies
[AD-A210754] N90-11150
Lifetime testing of commercially available 3.0 (mu)f, 100 kV pulsed-power capacitors
[DE89-017230] N90-11242
CAPE KENNEDY LAUNCH COMPLEX
Atmospheric environment for space shuttle (STS-29) launch
[NASA-TM-100378] N90-10980
Atmospheric environment for space shuttle (STS-30) launch
[NASA-TM-100381] N90-10981
CARBON
Modifications to the aerotherm charring material thermal response and ablation program (CMA) for carbon ablation analysis
[AD-A211069] N90-11115
Carbon in detonations
[DE89-016037] N90-11189
Diamondlike carbon coatings for optical systems
[AD-A211255] N90-11573
CARBON DIOXIDE
Potential effects of global climate change on the United States. Executive summary. Draft
[PB89-161046] N90-11350
CARBON DIOXIDE CONCENTRATION
Assessment of crop response to increases in atmospheric carbon dioxide concentrations: Summary of research progress report, July 1, 1988--June 30, 1989
[DE89-016251] N90-11360
CARBON DIOXIDE LASERS
Low ppb level detection of toxic compounds with a fully automated CO2 laser photoacoustic detector N90-11181
CARBON DIOXIDE REMOVAL
Dissociation and vibrational relaxation of XeF by various collision partners
[AD-A210769] N90-11300
CARBON DISULFIDE
Pressure induced resonance Raman effects in shocked carbon disulfide
[AD-A210665] N90-11107
CARBON FIBER REINFORCED PLASTICS
Influence of the fiber/matrix interface on damage development in CFRP N90-11037
Delamination tests under compression-compression and tension-compression loading N90-11062
CARBON FIBERS
Interfacial adsorption and crystallization of polycarbonate in carbon fiber composites
[AD-A211230] N90-11090
CARBON ISOTOPES
Carbon isotope ratios and lithium abundances in open cluster giants N90-11664
CARBON STEELS
Corrosion rates of structural materials on the ocean floor
[DE89-015211] N90-11123
Microstructural effects on spall fracture in 1008 steel
[DE89-016770] N90-11131
CARBONACEOUS MATERIALS
Modifications to the aerotherm charring material thermal response and ablation program (CMA) for carbon ablation analysis
[AD-A211069] N90-11115
Diamondlike carbon coatings for optical systems
[AD-A211255] N90-11573
CARBORANE
N-Hexyl Carborane (NHC) as combustion catalyst in composite propellants
[FOA-C-20755-2.1] N90-11193
CAST ALLOYS
Influence of grain refining on the casting, physical, mechanical, and electrochemical properties of technical aluminum
[ETN-89-94661] N90-11135
CASTING
Thin section casting program. Volume 1: Executive summary and overview
[DE89-009030] N90-11198
Thin section casting program. Volume 2: Horizontal TSC (Thin-Section Casting) approach
[DE89-009031] N90-11199
Thin section casting program. Volume 2-A: Appendix to volume 2
[DE89-009032] N90-11200
Thin section casting program. Volume 3: Vertical TSC (Thin-Section Casting) approach
[DE89-009033] N90-11201
Thin section casting program. Volume 4: Static cast product bending, straightening, and rolling
[DE89-009034] N90-11202
Thin section casting program. Volume 5: Westinghouse MHD Project
[DE89-009035] N90-11203
CASTINGS
Influence of grain refining on the casting, physical, mechanical, and electrochemical properties of technical aluminum
[ETN-89-94661] N90-11135
CATALYSIS
Enhanced oxidation and solovolysis reactions in chemically inert microheterogeneous systems
[AD-A210748] N90-11110
Surface-catalyzed air oxidation reactions of hydrazines: Tubular reactor studies N90-11167
CATALYSTS
Photochemically-driven biomimetic oxidation of alkanes and olefins
[DE89-011536] N90-11097
Homogeneous catalysts in hypersonic combustion
[DE89-015258] N90-11098
Surface-catalyzed air oxidation of hydrazines: Environmental chamber studies N90-11159
Trace metal catalysis of hydrazine decomposition: The role of chromium N90-11163
N-Hexyl Carborane (NHC) as combustion catalyst in composite propellants
[FOA-C-20755-2.1] N90-11193
CATHODES
New secondary batteries utilizing electronically conductive polymer cathodes
[NASA-CR-185885] N90-11227
CATHODIC COATINGS
Diamondlike carbon coatings for optical systems
[AD-A211255] N90-11573
CATHODOLUMINESCENCE
International workshop on Beam Injection Assessment of Defects in Semiconductors
[AD-A210842] N90-11617
CATIONS
Quantum chemical investigations of the mechanism of cationic polymerization and theoretical prediction of crystal densities and decomposition pathways of energetic molecules
[AD-A210322] N90-11143
CAVITIES
Worked-in holes in three-dimensional reinforced composites N90-11060
CCD STAR TRACKER
Evaluation test of CCD area sensor for star sensor
[NAL-TM-570] N90-11566
CDC CYBER 205 COMPUTER
Checking the Goldbach conjecture on a vector computer
[CWI-NM-R8812] N90-11475
CELL CATHODES
Cell performance of ultra-thin polymer cathode system: Theoretical energy and power density projections
[AD-A210786] N90-11151
CERAMIC MATRIX COMPOSITES
Liquid infiltrated C/SiC: An alternative material for hot space structures N90-11030
CERAMICS
Precision materials characterization in the near millimeter and submillimeter wavelength range
[AD-A210655] N90-11106
Basic research on processing of ceramics for space structures
[AD-A205954] N90-11139
Fifth International Workshop on Glasses and Ceramics from Gels
[DE89-016899] N90-11147
Influence of core-shell grains on the internal stress state and permittivity response of zirconia modified barium titanate
[AD-A211245] N90-11153
Intergranular and interphase boundaries in ceramics
[DE89-016969] N90-11154
Design of ceramic fabric heat pipe with water working fluid
[DE89-016565] N90-11265
Advanced Turbine Technology Applications Program, (ATTAP)
[DE89-016067] N90-11318

Advanced Turbine Technology Applications Program, (ATTAP): A plan for improving the prototype production of ceramic components for the gas turbine engine, 1988--1992
[DE89-015566] N90-11320
Superconducting ceramics in the Bi1.5SrCaCu2O sub x system by melt quenching technique
[NASA-CR-185139] N90-11606
Kinetics and mechanisms of primary and steady state creep in B- and Al-containing alpha silicon carbide
[AD-A210739] N90-11616
High-temperature ceramic superconductors
[AD-A211070] N90-11618
Physics and materials science of high temperature superconductors
[AD-A211246] N90-11619
Origins of high-temperature superconductivity in the new copper oxide based ceramic superconductors
[DE89-016543] N90-11622

CERMETS
Characterizations of shock-loaded aluminum-infiltrated boron carbide cermets
[DE89-016773] N90-11146

CERTIFICATION
CF 18 480 Gallon External Fuel Tank Stores Clearance Program N90-10877
Realtime processing and display N90-10886

CHARACTERIZATION
A new method for the characterization of solutes and solvent phases using solvatochromic parameters
[AD-A211238] N90-11116

CHARGE CARRIERS
International workshop on Beam Injection Assessment of Defects in Semiconductors
[AD-A210842] N90-11617
A fermi liquid electric structure and the nature of the carriers in high-T(sub c) cuprates: A photoemission study
[DE89-016774] N90-11624

CHARGE COUPLED DEVICES
Evaluation test of CCD area sensor for star sensor
[NAL-TM-570] N90-11566

CHARGE TRANSFER
Electron transfer reactions
[AD-A210711] N90-11545

CHARRING
Modifications to the aerotherm charring material thermal response and ablation program (CMA) for carbon ablation analysis
[AD-A211069] N90-11115

CHECKOUT
A distributed debugger for Amoeba
[CWI-CS-R8828] N90-11453

CHEMICAL ANALYSIS
A simulator for a hydrocarbon ramrocket fuel gas generator: First phase development
[AR-005-621] N90-11080
Reporting environmental data of known quality
[DE89-016214] N90-11359

CHEMICAL BONDS
Quantum chemical investigations of the mechanism of cationic polymerization and theoretical prediction of crystal densities and decomposition pathways of energetic molecules
[AD-A210322] N90-11143
Vibrational spectroscopic study of the kaolinite-hydrazine intercalation complex N90-11166
Low temperature spectroscope of hydrazine and ammonia complexes N90-11169

CHEMICAL COMPOSITION
Evaluation of rocket motor exhaust and liner combustion by-products
[AD-A210747] N90-11083
Compositional analysis of steels by X-ray fluorescence spectrometry
[DE89-630803] N90-11129
Interactions of hydrazines with colloidal constituents of soils N90-11164

CHEMICAL ENGINEERING
Systems analysis considerations in artificial intelligence/expert systems technology applications
[DE89-016847] N90-11490

CHEMICAL EXPLOSIONS
Time-resolved mass spectrometry technique for studying fast transient CHNO explosive decomposition kinetics
[DE89-016540] N90-11101
Shock initiation of LX-17 as a function of its initial temperature
[DE89-017730] N90-11192

CHEMICAL PROPERTIES
Electronic and ionic transport in polymers
[AD-A210654] N90-11148

CHEMICAL REACTIONS
Critical reaction rates in hypersonic combustion chemistry
[DE89-014278] N90-10892
Finite element analysis of cure-induced residual stress in composite materials N90-11084
Simplified rate-law integration for reactions which are first order in each of two reactants
[NASA-CR-185408] N90-11093
Thermochemical model for shock-induced chemical reactions in porous thermite: The heat detonation model
[DE89-016528] N90-11100
Pressure induced resonance Raman effects in shocked carbon disulfide
[AD-A210665] N90-11107
Reactive ion etching of SiC thin films by mixtures of fluorinated gases and oxygen
[AD-A211046] N90-11113
Atmospheric chemistry of the fuel hydrazines N90-11158
Modeling of hydrazine surface interactions in environmental reaction chambers N90-11162
Interactions of hydrazines with colloidal constituents of soils N90-11164
In-situ study of the chemically driven flow fields in initiating homogeneous and heterogeneous nitromethane explosives
[DE89-008415] N90-11186
Chemical reactions in turbulent mixing flows
[AD-A211240] N90-11263

CHEMILUMINESCENCE
Chemiluminescent ion-molecule reactions of group-3 ions with halogens: New optical spectra and reaction dynamics
[MPIS-18/1988] N90-11120
Description of a chemiluminescence detector system specifically designed for monitoring airborne hydrazine and oxidizer propellant vapors N90-11179

CHIPS (ELECTRONICS)
A new semicustom integrated bipolar amplifier for silicon strip detectors
[DE89-015585] N90-11229

CHLORINE COMPOUNDS
The chemistry of the hypochlorite neutralization of hydrazine fuels N90-11173

CHROMIUM
Radiationless transitions and excited-state absorption of low-field chromium complexes in solids
[AD-A210653] N90-11105
Trace metal catalysis of hydrazine decomposition: The role of chromium N90-11163

CHROMIUM OXIDES
Transport properties of thermally grown Cr2O3
[DE89-016703] N90-11623

CHROMIUM STEELS
Contribution to the transcrystalline stress crack corrosion of austenite chromium-nickel steels
[ETN-89-94665] N90-11137

CHRONOLOGY
Carbon isotope ratios and lithium abundances in open cluster giants N90-11664

CIRCUIT BREAKERS
Independent Orbiter Assessment (IOA): Analysis of the backup flight system
[NASA-CR-185567] N90-10932

CIRCUIT DIAGRAMS
Elements of a 200 watt pulsed excimer laser N90-11295

CIRCUIT PROTECTION
Performance of transient limiters under laboratory, simulated, and rocket-triggered lightning conditions
[DE89-015773] N90-11238

CIRCUITS
Independent Orbiter Assessment (IOA): Analysis of the backup flight system
[NASA-CR-185567] N90-10932

CIRCULAR CYLINDERS
The near-wake flow structure of wake-cylinder interaction and surface loading of cylinder N90-11248

CIRCULAR PLATES
The dynamics of circular plates with patch damping: A numerical and experimental study N90-11329

CIVIL AVIATION
Flight testing in the Netherlands: An overview N90-10884

CLASSICAL MECHANICS
On some stochastic properties of the infinitely dimensional Hamiltonian systems of classical mechanics
[DE89-618403] N90-11525

CLAYS
Interactions of hydrazines with colloidal constituents of soils N90-11164

CLEARANCES
CF 18 480 Gallon External Fuel Tank Stores Clearance Program N90-10877
Heliport surface maneuvering test results
[ACD-330] N90-10897

CLIMATE CHANGE
Potential effects of global climate change on the United States. Executive summary. Draft
[PB89-161046] N90-11350
Potential effects of global climate change on the United States. Volume 1: Regional studies. Draft
[PB89-161053] N90-11351
Potential effects of global climate change on the United States. Volume 2: National studies. Draft
[PB89-161061] N90-11352

CLIMATOLOGY
Potential effects of global climate change on the United States. Volume 1: Regional studies. Draft
[PB89-161053] N90-11351
Potential effects of global climate change on the United States. Volume 2: National studies. Draft
[PB89-161061] N90-11352
Spatial and temporal short range total cloud cover estimation by metric analysis of composite imagery N90-11423
National Center For Atmospheric Research annual report, fiscal year 1988
[PB89-208987] N90-11428

CLOSURES
Fatigue crack growth rates as a function of delta K: Variability and material property N90-11031

CLOUD COVER
Spatial and temporal short range total cloud cover estimation by metric analysis of composite imagery N90-11423

CLOUD PHYSICS
Remote sensing techniques of the Wave Propagation Laboratory for the measurement of supercooled liquid water: Applications to aircraft icing
[PB89-206102] N90-10842

CLUSTER ANALYSIS
On algorithms for generating computationally simple piecewise linear classifiers
[NDRE/PUBL-89/1001] N90-11459

COAL DERIVED LIQUIDS
Production of jet fuels from coal-derived liquids. Volume 11: Production of advanced endothermic fuel blends from Great Plains Gasification Plant naphtha by-product stream
[AD-A210251] N90-11184

COASTS
Coastal subsea permafrost and bedrock observations using dc resistivity
[AD-A210784] N90-11435

COATINGS
Coatings in electrical contacts
[DE89-787739] N90-11234
Constitutive parameter measurements of lossy materials
[NASA-CR-183398] N90-11603

COAXIAL CABLES
Analysis of coaxial wire measurement of longitudinal coupling impedance
[DE89-015748] N90-11230
Fiber optics: A brief introduction
[DE89-009337] N90-11567

COCKPIT SIMULATORS
Flight simulation test facility: Function and specification of the simulator cockpit system
[NAL-TM-577] N90-10899

COCKPITS
See and avoid/cockpit visibility
[DOT/FAA/CT-TN89/18] N90-10843
Flight simulation test facility: Function and specification of the simulator cockpit system
[NAL-TM-577] N90-10899

CODING
Deep null antennas and their applications to tactical VHF radio communications
[AD-A210656] N90-11214
Performance analysis of hybrid ARQ protocols in a slotted code division multiple-access network
[AD-A211078] N90-11219

COGNITION
Comprehension processes in mechanical reasoning
[AD-A210459] N90-11442
Planning in writing: The cognition of a constructive process
[AD-A210434] N90-11648

COHERENCE
Optical coherence multiplexing for interprocessor communications
[DE89-016186] N90-11568

COHERENT RADAR
Joint VHF coherent radar and oblique sounder observations for short term ionosphere forecasting N90-11399

COLD ROLLING
Thin section casting program. Volume 1: Executive summary and overview
[DE89-009030] N90-11198

COLD WEATHER
Definition of research needs to address airport pavement distress in cold regions
[DOT/FAA/DS-89/13] N90-10896
COLD WEATHER TESTS
Battery actuation of NITINOL at sub-zero temperatures
[AD-A211254] N90-11237
COLLAPSE
Nonlinear collapse simulation of anisotropic plates and corrugated panels N90-11035
COLLIMATION
Antenna beamforming using optical processing
[NASA-CR-180844] N90-11210
COLLISION AVOIDANCE
See and avoid/cockpit visibility
[DOT/FAA/CT-TN89/18] N90-10843
Test and evaluation: Reducing risks to military aircraft from bird collisions. Report to the Chairman, Legislation, and National Security Subcommittee, Committee on Goverment Operations, House of Representatives
[AD-A210670] N90-10845
Ground and Obstacle Avoidance (GOA) concept of operations
[DOT/FAA/DS-89/08] N90-10855
COLLISION RATES
Dissociation and vibrational relaxation of XeF by various collision partners
[AD-A210769] N90-11300
COLLISIONLESS PLASMAS
Hybrid particle-fluid approach to low-frequency turbulence in magnetically confined plasmas
[DE89-015904] N90-11579
Radiative shocks with electron thermal conduction N90-11670
COLLOIDS
Interactions of hydrazines with colloidal constituents of soils N90-11164
COLOR VISION
Filling or outlining shapes with color: The effects on a visual search task
[AD-A211067] N90-11444
COLUMBUS SPACE STATION
Aeritalia Space Systems Group, Turin, Italy
[EOARD-LR-89-041] N90-10908
Key structures mechanical issues of the European Space Station and platform program Columbus N90-11072
COMBAT
Aircraft live fire testing N90-10879
Air Combat Environment Test and Evaluation Facility (ACETEF) N90-10883
COMBUSTIBLE FLOW
Chemical reactions in turbulent mixing flows
[AD-A211240] N90-11263
COMBUSTION
Consequence of condensed-phase formation in transient burning of TiHx/KClO in a closed system
[DE89-013922] N90-11188
COMBUSTION CHAMBERS
Evaluation of rocket motor exhaust and liner combustion by-products
[AD-A210747] N90-11063
COMBUSTION CHEMISTRY
Critical reaction rates in hypersonic combustion chemistry
[DE89-014278] N90-10892
COMBUSTION CONTROL
Evaporation and combustion of dense sprays with a bimodal droplet size distribution N90-11094
COMBUSTION EFFICIENCY
Homogeneous catalysts in hypersonic combustion
[DE89-015258] N90-11098
COMBUSTION PHYSICS
Evaporation and combustion of dense sprays with a bimodal droplet size distribution N90-11094
Droplet combustion experiment drop tower tests using models of the space flight apparatus
[NASA-TM-101472] N90-11196
COMBUSTION PRODUCTS
A simulator for a hydrocarbon ramrocket fuel gas generator: First phase development
[AR-005-621] N90-11080
Evaluation of rocket motor exhaust and liner combustion by-products
[AD-A210747] N90-11063
Homogeneous catalysts in hypersonic combustion
[DE89-015258] N90-11098
A remote sensor to monitor combustion products using a tunable acousto-optic filter N90-11275
COMMAND AND CONTROL
Identification Friend, Foe or Neutral Joint Test N90-10881
COMMUNICATION
Technical communications in aeronautics: Results of an exploratory study. An analysis of managers' and nonmanagers' responses
[NASA-TM-101625] N90-11647
COMMUNICATION EQUIPMENT
Independent Orbiter Assessment (IOA) CIL issues resolution report, volume 3
[NASA-CR-185524-VOL-3] N90-10956
Independent Orbiter Assessment (IOA): Analysis of the communication and tracking subsystem
[NASA-CR-185582] N90-10967
COMMUNICATION NETWORKS
Network analyzer for nonstatic jamming
[AD-A210759] N90-11216
A contribution to the synthesis of communication switching systems with decentralized control using modular components
[ETN-89-94660] N90-11226
Influence of ionospheric variations on high-reliability HF systems utilizing large bases N90-11404
COMMUNICATION SATELLITES
Test results on conceptual models of the large deployable antenna for mobile communications satellites N90-11050
COMMUNICATION THEORY
Determinism yields (event structure isomorphism equals step sequence equivalence)
[CWI-CS-R8839] N90-11492
COMPILERS
A prototype silicon compiler in prolog
[AD-A210669] N90-11452
COMPLETENESS
Completeness of resolution by transfinite induction
[CWI-CS-R8837] N90-11473
COMPLEX COMPOUNDS
Theoretical investigation of gas-surface interactions
[NASA-CR-185492] N90-11552
A high level Ab initio study of the anionic hydrogen-bonded complexes FH-CN-, FH-NC-, H2O-CN- and H2O-NC- N90-11553
COMPLEXITY
Boolean functions, invariance groups and parallel complexity
[CWI-CS-R8836] N90-11472
COMPONENT RELIABILITY
Independent Orbiter Assessment (IOA) CIL issues resolution report, volume 3
[NASA-CR-185524-VOL-3] N90-10956
Independent Orbiter Assessment (IOA): FMEA/CIL assessment
[NASA-CR-185589] N90-10960
Independent Orbiter Assessment (IOA): Analysis of the communication and tracking subsystem
[NASA-CR-185582] N90-10967
COMPOSITE MATERIALS
Finite element analysis of cure-induced residual stress in composite materials N90-11084
On the effective transport properties of composite materials N90-11086
Effect of thermal and cyclic loads on silicon carbide yarn reinforced glass matrix composites
[DE89-016554] N90-11091
Potential industrial applications for composite phase-change materials as thermal energy storage media
[DE89-015170] N90-11346
COMPOSITE PROPELLANTS
Nitramine composite solid propellant modeling N90-11183
N-Hexyl Carborane (NHC) as combustion catalyst in composite propellants
[FOA-C-20755-2.1] N90-11193
COMPOSITE STRUCTURES
Equilibrium and stability in composite thin shell N90-10998
Transverse shear stiffness of composite and sandwich finite elements N90-11034
Study of the application of automation to composites manufacture
[AD-A211049] N90-11087
Rational design of high-current cable-in-conduit superconductors
[DE89-016867] N90-11626
COMPRESSING
The HEL (Hugoniot Elastic Limit) and rate-dependent yield behavior
[DE89-016981] N90-11134
Magnetic flux compression
[DE89-016991] N90-11546
COMPRESSION TESTS
Delamination tests under static compression loading N90-11061
Delamination tests under compression-compression and tension-compression loading N90-11062
COMPRESSIVE STRENGTH
Characterizations of shock-loaded aluminum-infiltrated boron carbide cermets
[DE89-016773] N90-11146
COMPRESSOR BLADES
Dynamic analysis of rotors under interference rubs N90-11312
COMPRESSOR ROTORS
Advanced technologies impact on compressor design and development: A perspective
[NASA-TM-102341] N90-10891
Dynamic analysis of rotors under interference rubs N90-11312
COMPUTATION
Computational aspects of sensitivity calculations in linear transient structural analysis N90-11327
COMPUTATIONAL FLUID DYNAMICS
Linear instability of supersonic plane wakes
[NASA-CR-181911] N90-10833
An experimental investigation of the aerodynamic characteristics of slanted base ogive cylinders using magnetic suspension technology
[NASA-CR-181708] N90-10834
Computation of the tip vortex flowfield for advanced aircraft propellers
[NASA-CR-182179] N90-10836
A parallel numerical simulation for supersonic flows using zonal overlapped grids and local time steps for common and distributed memory multiprocessors
[DE89-015252] N90-10839
International conference on numerical grid generation in computational fluid dynamics
[AD-A211082] N90-11262
Chemical reactions in turbulent mixing flows
[AD-A211240] N90-11263
Pressure correction splitting methods for the computation of oscillatory free convection in low Pr fluids
[CWI-NM-R8816] N90-11271
A conforming spectral collocation strategy for Stokes flow through a channel contraction
[NASA-CR-181912] N90-11495
COMPUTATIONAL GRIDS
A parallel numerical simulation for supersonic flows using zonal overlapped grids and local time steps for common and distributed memory multiprocessors
[DE89-015252] N90-10839
Computation of transient three-dimensional interstage flowfields using the arbitrary Lagrangian-Eulerian method N90-11253
COMPUTER AIDED DESIGN
Qualification by simulation: Dream or reality N90-10990
Experimental identification of modal momentum coefficients and modal identity parameters of the FLECS structure N90-10991
Overview of actual buckling calculation methods for space vehicle structures N90-10995
ASIC (Application Specific Integrated Circuit) replacement for an SSI (Small Scale Integrated) component design: A case study
[DE89-013494] N90-11232
New tools for the simulation and design of calorimeters
[DE89-016323] N90-11281
Considerations for a design and operations knowledge support system for Space Station Freedom
[NASA-TM-102156] N90-11451
Engineering specification and system design for CAD/CAM of custom shoes. Phase 5: UMC involvement (January 1, 1989 - June 30, 1989)
[NASA-CR-185838] N90-11456
Using PATRAN: From eyeballs to submarines and more
[DE89-016989] N90-11469
A survey of research methods to study design
[AD-A211213] N90-11491
COMPUTER AIDED MANUFACTURING
Engineering specification and system design for CAD/CAM of custom shoes. Phase 5: UMC involvement (January 1, 1989 - June 30, 1989)
[NASA-CR-185838] N90-11456
Using computer design and simulation to improve manufacturing productivity, report period 1, 2 and 3
[AD-A210255] N90-11462
COMPUTER ASSISTED INSTRUCTION
Research, development, training and education using the Ada programming language
[AD-A210760] N90-11466
COMPUTER GRAPHICS
Using PATRAN: From eyeballs to submarines and more
[DE89-016989] N90-11469
Summaries of the FY 1989 Applied Mathematical Sciences Research program
[DE89-016694] N90-11521

COMPUTER NETWORKS
Transaction throughput in distributed systems: A modeling study using dynamic queueing networks
[MEMO-INF-89-25] N90-11479
Fixed point iteration on point-symmetric interference graphs
[MEMO-INF-89-23] N90-11535
Toward a national research network
[PB89-198709] N90-11644

COMPUTER PROGRAMMING
Rethinking synthesis of fine-motion strategies
[DE89-016671] N90-11322
An investigation of the usefulness of Earley's Algorithm in a general context-free recognizer
[DE89-016498] N90-11463
Checking the Goldbach conjecture on a vector computer
[CWI-NM-R8812] N90-11475
A generalization of A. N. Habermann's theorem for semaphores
[REPT-88-98] N90-11484
LEXER: A tool for lexical analysis of program input
[DE89-016924] N90-11649
The Knowledge Representation Project
[AD-A211288] N90-11650

COMPUTER PROGRAMS
A preliminary sensitivity analysis of the Generalized Escape System Simulation (GESS) computer program
[DE89-016891] N90-10844
High accuracy coordinate determination using the global positioning system N90-10858
GRATE: A new flight test tool for flying qualities evaluation N90-10868
Results and practical experience using parameter identification techniques on the AM-X program at Aermacchi N90-10873
Flight testing of the Tornado Terrain Following System N90-10875
Independent Orbiter Assessment (IOA): Analysis of the guidance, navigation, and control subsystem
[NASA-CR-185555] N90-10920
Independent Orbiter Assessment (IOA): Analysis of the remote manipulator system
[NASA-CR-185585] N90-10926
Frequency domain design of robust controllers for space structures
[AD-A211172] N90-10985
GEMMES: A new tool for dynamic modeling N90-11005
Integration of analytical and test software for optimal structural design under dynamic loads N90-11007
Experiences using a major FEM package interactively for spacecraft applications N90-11008
Calculation of sound transmission through a cylindrical shell using ASKA acoustics N90-11009
Numerical analysis of nonlinear viscoelastic structures: Application to elastomers and rubber-like materials N90-11013
Automated stress analysis of Shuttle orbiter thermal protection system N90-11043
JOE: Jordan Optimized Eigensolver. A step toward a numerical Jordan form analyzer for control and interactive thermo-structural-dynamic applications N90-11047
ESA-D: An integrated software for antenna design and analysis N90-11052
Thermal and structural analysis of Hermes N90-11058
Exploitation of data management facilities for finite element analysis in aerospace structural engineering applications N90-11078
Consequence of condensed-phase formation in transient burning of TiHx/KClO in a closed system
[DE89-013922] N90-11188
Validation of NEC (Numerical Electromagnetics Code) for antennas near ground
[DE89-016502] N90-11212
A general-purpose computer program for the Volterra-series analysis of nonlinear microwave circuits
[AD-A210768] N90-11236
The 3D-POLY; A robot vision system for recognizing objects in occluded environments N90-11313
Simulation of the polar cap F region ionization using an experimental convection electric field N90-11370
Empirical models of convection electric fields and electrostatic potential at high latitude from EISCAT observations: Preliminary results N90-11377
Calculation of the temperature and velocity vector of the neutral gas using EISCAT CP3-data N90-11384
Ion heating events observed at the EISCAT radar N90-11385
Coordinated multi-parameter measurements and predictions of the global-scale ionosphere N90-11397
Hanford Meteorological Station computer codes. Volume 10: The ARCHIVE computer code
[DE89-016175] N90-11429
ANIMA: Image analyzer applied to remote sensing
[INPE-4766-PRE/1435] N90-11447
Software configuration management: An overview
[PB89-193833] N90-11458
Experiments in fault tolerant software reliability
[NASA-CR-185927] N90-11460
Programs for numerical integration of piece-wise smooth functions
[DE89-620449] N90-11464
Research, development, training and education using the Ada programming language
[AD-A210760] N90-11466
Computer programs for measuring variations in speech
[AD-A211126] N90-11467
Evaluating the performance of software cache coherence
[AD-A211164] N90-11468
LINPACK routines based on the level 2 BLAS
[CWI-NM-R8811] N90-11483
An interactive program for constrained spline approximation of numerical data
[DE89-016674] N90-11520
Simulation of an axially symmetric ion-optical system
[DE89-620129] N90-11560
LEXER: A tool for lexical analysis of program input
[DE89-016924] N90-11649
Experimental database retrieval system DARTS (Handling Manual)
[DE89-906473] N90-11652

COMPUTER STORAGE DEVICES
Evaluating the performance of software cache coherence
[AD-A211164] N90-11468

COMPUTER SYSTEMS DESIGN
Independent Orbiter Assessment (IOA): Assessment of the data processing system FMEA/CIL
[NASA-CR-185546] N90-10917
Evaluating the performance of software cache coherence
[AD-A211164] N90-11468
A verification exercise relating to specification styles in LOTOS
[MEMO-INF-89-18] N90-11471

COMPUTER SYSTEMS PERFORMANCE
Independent Orbiter Assessment (IOA): Assessment of the data processing system FMEA/CIL
[NASA-CR-185546] N90-10917
The 3-D heat transfer computer calculations of th e performance of the IAEA's air-bath calorimeters
[DE89-016908] N90-11283
Evaluating the performance of software cache coherence
[AD-A211164] N90-11468
LINPACK routines based on the level 2 BLAS
[CWI-NM-R8811] N90-11483

COMPUTER SYSTEMS PROGRAMS
Flight Test Techniques
[AGARD-CP-452] N90-10860
Software configuration management: An overview
[PB89-193833] N90-11458

COMPUTER TECHNIQUES
Topographic map reading
[AD-A211269] N90-11340
Applications of the hybrid automated reliability predictor: Revised edition
[NASA-TP-2760-REV] N90-11454
Using computer design and simulation to improve manufacturing productivity, report period 1, 2 and 3
[AD-A210255] N90-11462
Research, development, training and education using the Ada programming language
[AD-A210760] N90-11466
Preference propagation in temporal/capacity constraint graphs
[AD-A210668] N90-11506

COMPUTER VISION
The 3D-POLY: A robot vision system for recognizing objects in occluded environments N90-11313

COMPUTERIZED SIMULATION
A parallel numerical simulation for supersonic flows using zonal overlapped grids and local time steps for common and distributed memory multiprocessors
[DE89-015252] N90-10839
A preliminary sensitivity analysis of the Generalized Escape System Simulation (GESS) computer program
[DE89-016891] N90-10844
Design of a Kalman filter for transfer alignment N90-10848
Qualification by simulation: Dream or reality N90-10990
Experimental identification of modal momentum coefficients and modal identity parameters of the FLECS structure N90-10991
GEMMES: A new tool for dynamic modeling N90-11005
Calculation of sound transmission through a cylindrical shell using ASKA acoustics N90-11009
Numerical treatment of the thermo-structural-dynamic problems: The interpolation techniques N90-11018
Fluid-structure interaction effects in tank structures due to sloshing and hydrodynamic ram: Coupled Lagangian-Eulerian simulations N90-11022
Modeling of liquid sloshing effects in multibody systems N90-11023
Nonlinear collapse simulation of anisotropic plates and corrugated panels N90-11035
Automated stress analysis of Shuttle orbiter thermal protection system N90-11043
Numerical simulation of micrometeroids and debris hypervelocity impacts on Columbus pressurized modules N90-11075
ANTHEM simulation of plasma opening switches
[DE89-016617] N90-11239
Cellular automata and massively parallel physics
[DE89-016506] N90-11257
Numerical simulation of turbulent flow downstream a sudden axisymmetric expansion
[FOA-C-20758-2.1] N90-11272
New tools for the simulation and design of calorimeters
[DE89-016323] N90-11281
A compact X-ray free electron laser
[DE89-017236] N90-11297
Simulation of the polar cap F region ionization using an experimental convection electric field N90-11370
Short wavelength striations on expanding plasma clouds
[DE89-016585] N90-11416
Task analysis of the UH-60 mission and decision rules for developing a UH-60 workload prediction model. Volume 1: Summary report
[AD-A210763] N90-11446
On algorithms for generating computationally simple piecewise linear classifiers
[NDRE/PUBL-89/1001] N90-11459
Using computer design and simulation to improve manufacturing productivity, report period 1, 2 and 3
[AD-A210255] N90-11462
Using PATRAN: From eyeballs to submarines and more
[DE89-016989] N90-11469
DMC (Distinct Motion Code): A rigid body motion code for determining the interaction of multiple spherical particles
[DE89-016929] N90-11543
Structure and properties of simple molecular systems at very high density
[DE89-016974] N90-11557
Simulation of an axially symmetric ion-optical system
[DE89-620129] N90-11560
Particle simulation in curvilinear coordinate systems
[DE89-016727] N90-11583
Computer simulations of electromagnetic ion instabilities in the plasma sheet boundary layer
[DE89-016596] N90-11588

CONCURRENT PROCESSING
MSP: Modeling of concurrent processes. Version 1.00 General introduction and directions for use
[REPT-88-88] N90-11477
Synchrony with empty process — the algebra of synchronous processes
[CWI-CS-R8832] N90-11481
A generalization of A. N. Habermann's theorem for semaphores
[REPT-88-98] N90-11484
Determinism yields (event structure isomorphism equals step sequence equivalence)
[CWI-CS-R8839] N90-11492

CONDENSING
Consequence of condensed-phase formation in transient burning of TiHx/KClO in a closed system
[DE89-013922] N90-11188

CONDUCTION BANDS
Strain and density dependent valence-band masses in InGaAs/GaAs and GaAs/GaAsP strained-layer structures
[DE89-016882] N90-11627

CONDUCTION ELECTRONS
Radiative shocks with electron thermal conduction N90-11670

CONDUCTIVE HEAT TRANSFER
Interlaboratory comparison of two types of line-source thermal-conductivity apparatus measuring five insulating materials
[PB89-218325] N90-11142

CONFERENCES
Kalman Filter Integration of Modern Guidance and Navigation Systems
[AGARD-LS-166] N90-10847
Flight Test Techniques
[AGARD-CP-452] N90-10860

Meeting of intercosmos space physics group
N90-10902
Spacecraft Structures and Mechanical Testing
[ESA-SP-289] N90-10986
Fifth International Workshop on Glasses and Ceramics from Gels
[DE89-016899] N90-11147
The Third Conference on the Environmental Chemistry of Hydrazine Fuels
[AD-A197632] N90-11157
International conference on numerical grid generation in computational fluid dynamics
[AD-A211082] N90-11262
Proceedings of the Polycrystalline Thin Film Program Meeting
[DE89-009457] N90-11348
Ionospheric Structure and Variability on a Global Scale and Interactions with Atmosphere and Magnetosphere
[AGARD-CP-441] N90-11361
Two-Dimensional Intercomparison of Stratospheric Models
[NASA-CP-3042] N90-11405
DOE/CEC Workshop on Critical Evaluation of Radiobiological Data to Biophysical Modeling
[DE89-015214] N90-11437
Report of the Specialists' Workshop on Phase Transition Studies on Hydrogen-Bonded Crystals by Neutron and X-ray Diffractometries
[DE89-906538] N90-11631
Globalization of Technology: International Perspectives. Proceedings of the 6th Convocation of the Council of Academies of Engineering and Technological Sciences
[PB89-198840] N90-11645

CONFIGURATION MANAGEMENT
Independent Orbiter Assessment (IOA): FMEA/CIL assessment
[NASA-CR-185589] N90-10960

CONFORMAL MAPPING
Local structure of a 2-codimensional conformally flat submanifold in an Euclidean space R(sup n+2)
[DE89-618379] N90-11501
On sufficient conditions for a function to be analytic
[DE89-618382] N90-11503
Singularity theory and N = 2 superconformal field theories
[DE89-016582] N90-11538

CONICS
Can ion acceleration by double-cyclotron absorption produce O(+) ion conics
[IRF-PREPRINT-114] N90-11600

CONSISTENCY
On the equivalence of BS-stability and B-consistency
[CWI-NM-R8815] N90-11530

CONSTITUTIVE EQUATIONS
An evaluation of the Chaboche and Bodner-Partom viscoplastic constitutive theories for strain rate sensitive materials N90-11330

CONSTRAINTS
Nonlinear adjustment with or without constraints, applicable to geodetic models
[AD-A210820] N90-11509
Three level constraints on conformal field theories and string models
[DE89-016942] N90-11634

CONSTRUCTION
S7 without any construction of Lie group
[DE89-618380] N90-11539

CONTAMINANTS
Measurement of hydrazine contamination in soils
N90-11180

CONTEXT FREE LANGUAGES
An investigation of the usefulness of Earley's Algorithm in a general context-free recognizer
[DE89-016498] N90-11463

CONTINENTAL SHELVES
Physiographic and geological setting of the Coastal Engineering Research Center's field research facility
[AD-A210772] N90-11356

CONTINUOUS WAVE LASERS
Dissociation and vibrational relaxation of XeF by various collision partners
[AD-A210769] N90-11300
Novel thin-film CuInSe2 fabrication
[DE89-009440] N90-11604

CONTROL EQUIPMENT
Independent Orbiter Assessment (IOA): Assessment of instrumental subsystem FMEA/CIL
[NASA-CR-185572] N90-10972

CONTROL SIMULATION
An assessment of robustness of flight control systems based on variable structure techniques N90-10895

CONTROL SYSTEMS DESIGN
ATTAS flight testing experiences N90-10862
The active control of an unstable canard aircraft
N90-10894
An assessment of robustness of flight control systems based on variable structure techniques N90-10895
Independent Orbiter Assessment (IOA): Analysis of the ascent thrust vector control actuator subsystem
[NASA-CR-185579] N90-10929
Independent Orbiter Assessment (IOA): Analysis of the electrical power distribution and control/electrical power generation subsystem
[NASA-CR-185538] N90-10933
Independent Orbiter Assessment (IOA): Analysis of the reaction control system, volume 1
[NASA-CR-185532-VOL-1] N90-10938
Independent Orbiter Assessment (IOA): Analysis of the reaction control system, volume 2
[NASA-CR-185532-VOL-2] N90-10939
Independent Orbiter Assessment (IOA): Analysis of the reaction control system, volume 3
[NASA-CR-185532-VOL-3] N90-10940
Independent Orbiter Assessment (IOA): Analysis of the electrical power distribution and control subsystem, volume 1
[NASA-CR-185529-VOL-1] N90-10941
Independent Orbiter Assessment (IOA): Analysis of the electrical power distribution and control subsystem, volume 2
[NASA-CR-185529-VOL-2] N90-10942
Independent Orbiter Assessment (IOA): CIL issues resolution report, volume 1
[NASA-CR-185524-VOL-1] N90-10954
Independent Orbiter Assessment (IOA) CIL issues resolution report, volume 3
[NASA-CR-185524-VOL-3] N90-10956
Independent Orbiter Assessment (IOA): Assessment of the atmospheric revitalization pressure control subsystem FMEA/CIL
[NASA-CR-185594] N90-10957
Independent Orbiter Assessment (IOA): Assessment of the ascent thrust vector control actuator subsystem FMEA/CIL
[NASA-CR-185590] N90-10959
Independent Orbiter Assessment (IOA): Assessment of the displays and controls subsystem
[NASA-CR-185588] N90-10961
Independent Orbiter Assessment (IOA): Assessment of the EPD and C/remote manipulator system FMEA/CIL
[NASA-CR-185583] N90-10965
Frequency domain design of robust controllers for space structures
[AD-A211172] N90-10985
System and performance analysis of a low density actively controlled mirror for astronomic observation
N90-11002
The large European Acoustic Facility at ESTEC
N90-11067
A contribution to the synthesis of communication switching systems with decentralized control using modular components
[ETN-89-94660] N90-11226
Modeling and simulation of spatial robotic manipulators with flexible links and joint drives for control strategies implementation and evaluation N90-11311
Using computer design and simulation to improve manufacturing productivity, report period 1, 2 and 3
[AD-A210255] N90-11462
Control and optimization for observations of systems governed by controlled partial differential equations
[AD-A211122] N90-11513
Guaranteed cost control of flexible space structures
N90-11643

CONTROL THEORY
Frequency domain design of robust controllers for space structures
[AD-A211172] N90-10985
Performance and robustness of adaptive controllers for linear stochastic systems N90-11485
Nonlinear maneuver autopilot for the F-15 aircraft
[NASA-CR-179442] N90-11487
Principal components in multivariate control charts
[DE89-016828] N90-11489

CONTROL VALVES
Independent Orbiter Assessment (IOA): Analysis of the hydraulics/water spray boiler subsystem
[NASA-CR-185541] N90-10934

CONTROLLED FUSION
Compact torus configurations with high frequency driven currents
[ETN-89-94674] N90-11598

CONTROLLERS
Independent Orbiter Assessment (IOA): Analysis of the manned maneuvering unit
[NASA-CR-185565] N90-10913
Independent Orbiter Assessment (IOA): Analysis of the electrical power generation/fuel cell powerplant subsystem
[NASA-CR-185561] N90-10915
Independent Orbiter Assessment (IOA): Analysis of the electrical power generation/power reactant storage and distribution subsystem
[NASA-CR-185556] N90-10918
Independent Orbiter Assessment (IOA): Analysis of the electrical power distribution and control/electrical power generation subsystem
[NASA-CR-185538] N90-10933
Independent Orbiter Assessment (IOA): Analysis of the electrical power distribution and control/remote manipulator system subsystem
[NASA-CR-185526] N90-10936
Independent Orbiter Assessment (IOA): Analysis of the reaction control system, volume 1
[NASA-CR-185532-VOL-1] N90-10938
Independent Orbiter Assessment (IOA): Analysis of the reaction control system, volume 2
[NASA-CR-185532-VOL-2] N90-10939
Independent Orbiter Assessment (IOA): Analysis of the reaction control system, volume 3
[NASA-CR-185532-VOL-3] N90-10940
Independent Orbiter Assessment (IOA): Analysis of the electrical power distribution and control subsystem, volume 1
[NASA-CR-185529-VOL-1] N90-10941
Independent Orbiter Assessment (IOA): Analysis of the electrical power distribution and control subsystem, volume 2
[NASA-CR-185529-VOL-2] N90-10942
Independent Orbiter Assessment (IOA): Assessment of the backup flight system FMEA/CIL
[NASA-CR-185566] N90-10973
Performance and robustness of adaptive controllers for linear stochastic systems N90-11485

CONVECTION
Simulation of the polar cap F region ionization using an experimental convection electric field N90-11370

CONVECTIVE FLOW
Studies of time-dependent polar cap convection patterns N90-11421
A nonosciliatory, characteristically convected, finite volume scheme for multidimensional convection problems
[NASA-TM-102354] N90-11497

CONVECTIVE HEAT TRANSFER
Numerical solutions of turbulent flow with heat transfer over rough surfaces N90-11246

CONVERGENCE
Estimation on nonlinear damping in second order distributed parameter systems
[NASA-CR-181890] N90-11494
Generalized BDF (Backward Differentiation Formula) methods applied to Hessenberg form DAEs
[DE89-017328] N90-11522

CONVEXITY
On the areas of various bodies in the Euclidean space: The case of irregular convex polygons
[DE89-618377] N90-11500

COOLANTS
A new inexpensive electrochemical meter for oxygen in sodium coolant
[DE89-630802] N90-11104

COORDINATES
Wave-mode coordinate analysis of L junction in LSS
[AD-A211116] N90-10984

COORDINATION POLYMERS
Transport studies of conducting polymers N90-11140

COPOLYMERS
Composites reinforced with thermotropic liquid crystal copolyester fibers
[AD-A211226] N90-11089
Behaviour of VF(sub 2)/VF(sub 3) piezoelectric copolymers under shock loading
[DE89-016538] N90-11145
Electronic and ionic transport in polymers
[AD-A210654] N90-11148

COPPER
Shock-induced atomic-scale structure in metals
[DE89-016539] N90-11124

COPPER OXIDES
Adaptation of the theory of superconductivity to the behavior of oxides
[DE89-016518] N90-11608
Defect structures preceding amorphization by ion irradiations in YBa2Cu3O(7-delta)
[DE89-016905] N90-11612
Origins of high-temperature superconductivity in the new copper oxide based ceramic superconductors
[DE89-016543] N90-11622
A fermi liquid electric structure and the nature of the carriers in high-T(sub c) cuprates: A photoemission study
[DE89-016774] N90-11624

CORRECTION
Pressure correction splitting methods for the computation of oscillatory free convection in low Pr fluids
[CWI-NM-R8816] N90-11271
CORROSION
Corrosion rates of structural materials on the ocean floor
[DE89-015211] N90-11123
CORROSION RESISTANCE
Corrosion rates of structural materials on the ocean floor
[DE89-015211] N90-11123
CORRUGATED PLATES
Nonlinear collapse simulation of anisotropic plates and corrugated panels N90-11035
CORRUGATED SHELLS
Nonlinear collapse simulation of anisotropic plates and corrugated panels N90-11035
COSMIC DUST
Small grains in reflection nebulae: A study of diffuse interstellar bands, elemental depletions and infrared flux N90-11672
COSMIC PLASMA
Ion bombardment of Io and Mercury N90-11682
COSMOLOGY
The astronomy of Andean myth: The history of a cosmology N90-11660
Gauge invariant cosmological perturbations with cold dark matter
[DE89-790940] N90-11679
COST ANALYSIS
Lessons learned from the integration of flight systems N90-10874
Guaranteed cost control of flexible space structures N90-11643
COST EFFECTIVENESS
Environmental testing: An approach to more cost efficiency N90-10988
Study of the application of automation to composites manufacture
[AD-A211049] N90-11087
COST ESTIMATES
Projections for a steady-state tokamak reactor based on ITER
[DE89-016678] N90-11589
COST REDUCTION
US Navy principal site testing concept and the F-18 N90-10861
Environmental testing: An approach to more cost efficiency N90-10988
Qualification by simulation: Dream or reality N90-10990
COUETTE FLOW
Analytical and numerical studies in flow development
[DE89-017380] N90-11269
The thermal stability between rotating cylinders in a radially symmetrical gravitational field
[DE89-618548] N90-11638
COULOMB POTENTIAL
Auxiliary-field transformations for repulsive potentials: A physical approach
[DE89-016677] N90-11223
COUNTER ROTATION
An investigation of counterrotating tip vortex interaction
[NASA-CR-185135] N90-11549
COUPLING
Stormtime coupling of the neutral and ionized upper atmosphere at middle latitudes N90-11381
Ionosphere-thermosphere coupling at high latitudes: Aspect angle dependence of non-thermal plasmas N90-11382
COUPLING COEFFICIENTS
Transfer functions for nonlinear systems via Fourier-Borel transforms
[NASA-TM-100034] N90-10828
Auxiliary-field transformations for repulsive potentials: A physical approach
[DE89-016677] N90-11223
Dissociation and vibrational relaxation of XeF by various collision partners
[AD-A210769] N90-11300
COUPLINGS
Dynamic characteristics concerned in the design of a free-piston Stirling engine/magnetic coupling/compressor system
[DE89-015981] N90-11317
COVARIANCE
General covariance and strings
[DE89-016505] N90-11633
CRACK CLOSURE
A re-evaluation of fatigue threshold test procedures and the simulation and prediction of fatigue crack growth under conditions of low crack closure N90-11328
CRACK INITIATION
Review of the ESA fracture control policy N90-11029
Influence of the fiber/matrix interface on damage development in CFRP N90-11037
CRACK PROPAGATION
Review of the ESA fracture control policy N90-11029
Fatigue crack growth rates as a function of delta K: Variability and material property N90-11031
A re-evaluation of fatigue threshold test procedures and the simulation and prediction of fatigue crack growth under conditions of low crack closure N90-11328
CRACKS
Effect of thermal and cyclic loads on silicon carbide yarn reinforced glass matrix composites
[DE89-016554] N90-11091
CRAY COMPUTERS
New computing systems and their impact on structural analysis and design
[NASA-CR-185831] N90-11457
CREWS
Evaluation of rocket motor exhaust and liner combustion by-products
[AD-A210747] N90-11083
CRITICAL POINT
Thermophysical properties of supercritical fluids and fluid mixtures
[DE89-016568] N90-11102
CRITICAL TEMPERATURE
Physics and materials science of high temperature superconductors
[AD-A211246] N90-11619
CRYOGENIC FLUID STORAGE
Evaluation of supercritical cryogen storage and transfer systems for future NASA missions
[NASA-TM-102394] N90-10912
Independent Orbiter Assessment (IOA): Analysis of the electrical power distribution and control/electrical power generation subsystem
[NASA-CR-185538] N90-10933
Evolutionary space station fluids management strategies
[NASA-CR-185137] N90-10983
CRYOGENIC FLUIDS
Evolutionary space station fluids management strategies
[NASA-CR-185137] N90-10983
Gas-phase flowrate effect on disintegrating cryogenic liquid-jets
[NASA-TM-102357] N90-11277
CRYOGENIC ROCKET PROPELLANTS
Evaluation of supercritical cryogen storage and transfer systems for future NASA missions
[NASA-TM-102394] N90-10912
Evolutionary space station fluids management strategies
[NASA-CR-185137] N90-10983
CRYOGENICS
Telescope structure for cryogenic application N90-11019
Aspects of the development of a 1-5 micron infrared camera for astronomy N90-11656
CRYSTAL DEFECTS
Defect structures preceding amorphization by ion irradiations in YBa2Cu3O(7-delta)
[DE89-016905] N90-11612
Passage of ultrarelativistic electrons through real crystals
[DE89-618624] N90-11613
CRYSTAL GROWTH
Effects of gravity on equilibrium crystal shapes N90-11602
Design and construction of systems for the single-crystals growth of ternary silver halides, alkali halides, and alkaline earth fluorides, and the dielectric investigation of silver halide
[ETN-89-94673] N90-11632
CRYSTAL LATTICES
Shock-induced atomic-scale structure in metals
[DE89-016539] N90-11124
Ion beam annealing of Ga-implanted Si
[DE89-016857] N90-11610
CRYSTAL STRUCTURE
X-ray and gamma-ray spectroscopy of solids under pressure
[DE89-017271] N90-11118
Intergranular and interphase boundaries in ceramics
[DE89-016969] N90-11154
Effects of gravity on equilibrium crystal shapes N90-11602
Defect structures preceding amorphization by ion irradiations in YBa2Cu3O(7-delta)
[DE89-016905] N90-11612
Exploratory study of niobium, titanium, zirconium and tantalum aluminides
[AD-A210658] N90-11615
High pressure 129I Moessbauer studies of GeI4 molecular crystals
[DE89-015269] N90-11620
Chevron layer structures in Surface Stabilized Ferroelectric Liquid Crystal (SSFLC) cells filled with a material which exhibits the chiral nematic to smectic C* phase transition
[DE89-016985] N90-11628
Report of the Specialists' Workshop on Phase Transition Studies on Hydrogen-Bonded Crystals by Neutron and X-ray Diffractometries
[DE89-906638] N90-11631
CRYSTAL SURFACES
Dynamics of nucleation at electrochemical interfaces via surface EXAFS and standing wave measurements
[AD-A210733] N90-11109
CRYSTALLIZATION
Interfacial adsorption and crystallization of polycarbonate in carbon fiber composites
[AD-A211230] N90-11090
CRYSTALS
Crystal orientation effects in PETN explosive with 4 GPa shocks
[DE89-016996] N90-11190
Utilization of photorefractive crystals in optical image processing
[ISBN-3-923560-06-0] N90-11292
Acoustic studies of new materials: Quasicrystals, low-loss glasses and high Tc superconductors
[AD-A211281] N90-11551
High pressure 129I Moessbauer studies of GeI4 molecular crystals
[DE89-015269] N90-11620
Dielectronic excitation and recombination in crystal channels
[DE89-016864] N90-11625
CURL (VECTORS)
Direct discretization of planar div-curl problems
[NASA-CR-181935] N90-11498
CURRENT DENSITY
Pinning of curved flux lines on the boundary between two phases of high temperature superconductors
[DE89-618865] N90-11614
CURRENT SHEETS
Numerical study of the current sheet and PSBL in a magnetotail model
[NASA-CR-183289] N90-11669
CURVATURE
Compact surface in three-dimensional ellipsoid with prescribed mean curvature (I)
[DE89-618381] N90-11502
CURVE FITTING
An interactive program for constrained spline approximation of numerical data
[DE89-016674] N90-11520
CUTTING
Basic investigations of cutting machinability of inorganic glasses using single-point tools
[W-15/87] N90-11204
CYCLIC LOADS
Theoretical and experimental investigation of thin-walled aluminum panels under cyclic shear load N90-10996
Effect of thermal and cyclic loads on silicon carbide yarn reinforced glass matrix composites
[DE89-016554] N90-11091
CYCLOTRON RESONANCE
Producing of an ECR plasma using 2450MHz Whistler wave and the investigating of its parameters
[DE89-618689] N90-11586
CYLINDRICAL BODIES
An experimental investigation of the aerodynamic characteristics of slanted base ogive cylinders using magnetic suspension technology
[NASA-CR-181708] N90-10834
Internal voltages and currents in well-shielded cylindrical objects due to simulated direct-strike lightning
[DE89-012664] N90-11231
A computational/experimental study of the flow around a body of revolution at angle of attack
[NASA-TM-88329] N90-11254
CYLINDRICAL SHELLS
Overview of actual buckling calculation methods for space vehicle structures N90-10995
Calculation of sound transmission through a cylindrical shell using ASKA acoustics N90-11009

D

DAMAGE
Influence of the fiber/matrix interface on damage development in CFRP N90-11037
Numerical simulation of micrometeroids and debris hypervelocity impacts on Columbus pressurized modules N90-11075

DAMAGE ASSESSMENT
Aircraft live fire testing N90-10879
The use of damage characterization for life prediction methodologies N90-11053
Delamination tests under compression-compression and tension-compression loading N90-11062
Intrinsic damage and strength criteria for advanced composite laminates in space applications N90-11071

DAMPING
Use of Lanczos vectors in structural dynamics N90-11011
Numerical analysis of nonlinear viscoelastic structures: Application to elastomers and rubber-like materials N90-11013
The dynamic stability of an axially loaded beam with lateral elastic support and damping N90-11331
Estimation on nonlinear damping in second order distributed parameter systems [NASA-CR-181890] N90-11494

DARK MATTER
Rocket and satellite observations of the local interstellar medium N90-11668
Gauge invariant cosmological perturbations with cold dark matter [DE89-790940] N90-11679

DATA ACQUISITION
Independent Orbiter Assessment (IOA): Analysis of the DPS subsystem [NASA-CR-185549] N90-10924
Robust spatial calibration of a planar positron camera [AD-A210773] N90-11284
Reporting environmental data of known quality [DE89-016214] N90-11359
Meteorological rocket observations [PB89-168769] N90-11419

DATA BASE MANAGEMENT SYSTEMS
Performance reports for EIM (Engineering Information Management) computer systems: A managerial perspective [DE89-015194] N90-11449
Software configuration management: An overview [PB89-193833] N90-11458
The Knowledge Representation Project [AD-A211288] N90-11650
Experimental database retrieval system DARTS (Handling Manual) [DE89-906473] N90-11652

DATA BASES
Precision materials characterization in the near millimeter and submillimeter wavelength range [AD-A210655] N90-11106
Robust spatial calibration of a planar positron camera [AD-A210773] N90-11284
Multistation/multiparameter observations with a network of digital ionosondes N90-11396
Two-Dimensional Intercomparison of Stratospheric Models [NASA-CP-3042] N90-11405
Introduction and data summary, chapter 5 N90-11409
Two enhancements of the logarithmic least-squares method for analyzing subjective comparisons [AD-A211192] N90-11514
Experimental database retrieval system DARTS (Handling Manual) [DE89-906473] N90-11652

DATA COMPRESSION
Gridded environmental data compaction: An investigation [AD-A210580] N90-11430

DATA FLOW ANALYSIS
Stochastic flows in networks [AD-A211209] N90-11515

DATA LINKS
Toward a national research network [PB89-198709] N90-11644

DATA MANAGEMENT
Exploitation of data management facilities for finite element analysis in aerospace structural engineering applications N90-11078
Toward a national research network [PB89-198709] N90-11644

DATA PROCESSING
Flight Test Techniques [AGARD-CP-452] N90-10860
The Experimental Aircraft Flight Test Programme N90-10865
Flight test techniques adopted by Avions Marcel Dassault-Breguet Aviation N90-10867
Flight test instrumentation and data processing at British Aerospace, Warton, U.K. N90-10887
New data handling system (MDH) for mechanical tests at ESTEC N90-11066
The large European Acoustic Facility at ESTEC N90-11067
Hanford Meteorological Station computer codes. Volume 10: The ARCHIVE computer code [DE89-016175] N90-11429
Gridded environmental data compaction: An investigation [AD-A210580] N90-11430
Quantitative methods for waves in space plasmas [PB89-210256] N90-11599
Inferring data base requirements from examples in forms N90-11646
The Knowledge Representation Project [AD-A211288] N90-11650

DATA PROCESSING EQUIPMENT
Independent Orbiter Assessment (IOA): Assessment of the data processing system FMEA/CIL [NASA-CR-185546] N90-10917
Independent Orbiter Assessment (IOA): Analysis of the DPS subsystem [NASA-CR-185549] N90-10924
Independent Orbiter Assessment (IOA): CIL issues resolution report, volume 1 [NASA-CR-185524-VOL-1] N90-10954
A methodology for the design of continuous-dataflow synchronous systems [PB89-184360] N90-11564

DATA REDUCTION
The Experimental Aircraft Flight Test Programme N90-10865
The Knowledge Representation Project [AD-A211288] N90-11650

DATA SAMPLING
Boundary kernel estimation of the two sample comparison density function [AD-A210757] N90-11532

DATA STORAGE
A methodology for the design of continuous-dataflow synchronous systems [PB89-184360] N90-11564

DATA SYSTEMS
The large European Acoustic Facility at ESTEC N90-11067
A methodology for the design of continuous-dataflow synchronous systems [PB89-184360] N90-11564

DATA TRANSMISSION
A prototype silicon compiler in prolog [AD-A210669] N90-11452
A methodology for the design of continuous-dataflow synchronous systems [PB89-184360] N90-11564

DECAY
The behavior of hydrazine vapor in an environmental chamber under simulated atmospheric conditions N90-11161
The decay of viscoelastic fluid jets [ETN-89-94667] N90-11270

DECAY RATES
Dissociation and vibrational relaxation of XeF by various collision partners [AD-A210769] N90-11300

DECELERATION
Independent Orbiter Assessment (IOA): Assessment of the landing/deceleration (LDG/DEC) subsystem FMEA/CIL [NASA-CR-185570] N90-10966

DECISION MAKING
Comprehension processes in mechanical reasoning [AD-A210459] N90-11442
Electronic publishing: Guide to selection [PB89-214753] N90-11448
Preference propagation in temporal/capacity constraint graphs [AD-A210668] N90-11506

DECISION THEORY
Task analysis of the UH-60 mission and decision rules for developing a UH-60 workload prediction model. Volume 1: Summary report [AD-A210763] N90-11446

DECOMPOSITION
Time-resolved mass spectrometry technique for studying fast transient CHNO explosive decomposition kinetics [DE89-016540] N90-11101
Enhanced oxidation and solovolysis reactions in chemically inert microheterogeneous systems [AD-A210748] N90-11110
Quantum chemical investigations of the mechanism of cationic polymerization and theoretical prediction of crystal densities and decomposition pathways of energetic molecules [AD-A210322] N90-11143
Trace metal catalysis of hydrazine decomposition: The role of chromium N90-11163
A prototype silicon compiler in prolog [AD-A210669] N90-11452

DECONTAMINATION
Evaluation of mid-to-long term basic research for environmental restoration [DE89-015621] N90-11355

DEFORMATION
Hygrothermal deformations of composite shells N90-11055
Deformation induced microstructural and microchemical changes during thermomechanical treatment [DE89-017266] N90-11127
An improved beam model for the vibrations of rotor blades N90-11333
Evaluation of integrals related to the Debye function [DE89-016930] N90-11499

DEGRADATION
Grain boundary chemistry in irradiated stainless steel and its influence on environmental degradation [DE89-016827] N90-11125

DEGREES OF FREEDOM
Dynamic analysis of rotors under interference rubs N90-11312

DELAMINATING
Analysis of delamination growth N90-11036
Delamination tests under static compression loading N90-11061
Delamination tests under compression-compression and tension-compression loading N90-11062
The 2.5D- and 3D-fabrics for delamination resistant composite laminates and sandwich structures N90-11063

DEMODULATORS
Robust spatial calibration of a planar positron camera [AD-A210773] N90-11284

DENSE PLASMAS
A fully electromagnetic hybrid model for high density plasma simulations [DE89-016771] N90-11593

DENSITY MEASUREMENT
The middle and high latitude ionosphere at approximately 550 km altitude N90-11374
Modelling ionospheric density structures N90-11375

DEPLOYMENT
The third generation rigid solar array GSR3 N90-11017
A high precision gravity compensation system for the deployment test of the ERS-1 SAR antenna N90-11038
Deployment simulation for 3rd generation solar array GSR3 N90-11074

DEPOSITION
CuInSe2 solar cell research by sputter deposition [DE89-009450] N90-11345
The Si(1-x)Nx Rugate [AD-A211236] N90-11572
Diamondlike carbon coatings for optical systems [AD-A211255] N90-11573

DESALINIZATION
Planning for hybrid-cycle OTEC experiments using the HMTSTA test facility at the Natural Energy Laboratory of Hawaii [DE89-013278] N90-11349

DESERTS
Diagnostic study of atmosphere-terrain interaction leading to the formation of dust clouds and poor visibilities over near east desert areas [AD-A211243] N90-11358

DESIGN ANALYSIS
Integrated multidisciplinary design optimization of rotorcraft [NASA-TM-101642] N90-10889
An assessment of robustness of flight control systems based on variable structure techniques N90-10895
Spacecraft Structures and Mechanical Testing [ESA-SP-289] N90-10986
Qualification by simulation: Dream or reality N90-10990
Overview of actual buckling calculation methods for space vehicle structures N90-10995
Viscoelastic tuned dampers for control of structural dynamics N90-10999
Integration of analytical and test software for optimal structural design under dynamic loads N90-11007
Advances in design and testing of spacecraft structures N90-11018
ESA-D: An integrated software for antenna design and analysis N90-11052
Two years experience with the ESTEC multishaker system N90-11065
Deployment simulation for 3rd generation solar array GSR3 N90-11074
ASIC (Application Specific Integrated Circuit) replacement for an SSI (Small Scale Integrated) component design: A case study [DE89-013494] N90-11232

Laser dynamics: The system dynamics and network theory of optoelectronic integrated circuit design N90-11296
GaAs ASIC design case study
[DE89-013934] N90-11461
A survey of research methods to study design
[AD-A211213] N90-11491

DESORPTION
Modeling of hydrazine surface interactions in environmental reaction chambers N90-11162

DETECTORS
A new semicustom integrated bipolar amplifier for silicon strip detectors
[DE89-015585] N90-11229

DETONATION
Thermochemical model for shock-induced chemical reactions in porous thermite: The heat detonation model
[DE89-016528] N90-11100
A shock initiation model for fine-grained hexanitrostilbene
[DE89-007641] N90-11185
In-situ study of the chemically driven flow fields in initiating homogeneous and heterogeneous nitromethane explosives
[DE89-008415] N90-11186
Estimation of the C-J pressure of explosives
[DE89-013811] N90-11187
Carbon in detonations
[DE89-016037] N90-11189
Crystal orientation effects in PETN explosive with 4 GPa shocks
[DE89-016996] N90-11190
Shock initiation of LX-17 as a function of its initial temperature
[DE89-017730] N90-11192
Acceleration of metal plates
[DE89-016816] N90-11197
Sharp shock model for propagating detonation waves
[DE89-016772] N90-11266
Shock induced dissociation of polyethylene
[DE89-016983] N90-11267
Response of standardized PVDF piezoelectric polymer gauges to direct shock pressures between 8 and 32 GPa
[DE89-016811] N90-11282
Laser-driven miniature flyer plates for shock initiation of secondary explosives
[DE89-016587] N90-11288
Effects of shock-modification on superconductivity in Tl2Ca2Ba2Cu3Oy and Bi2CaSr2Cu2Ox
[DE89-017231] N90-11629

DETONATION WAVES
Sharp shock model for propagating detonation waves
[DE89-016772] N90-11266

DEUTERIUM
Solid fiber Z-pinches: Cold-start computations
[DE89-016768] N90-11592

DIAMONDS
Diamondlike carbon coatings for optical systems
[AD-A211255] N90-11573

DIATOMIC MOLECULES
Particle kinetic simulation of high altitude hypervelocity flight
[NASA-CR-186003] N90-10840

DIELECTRIC POLARIZATION
Electromagnetic pulse interaction at a dielectric interface
[AD-A211081] N90-11220

DIELECTRIC PROPERTIES
Precision materials characterization in the near millimeter and submillimeter wavelength range
[AD-A210655] N90-11106
Design and construction of systems for the single-crystals growth of ternary silver halides, alkali halides, and alkaline earth fluorides, and the dielectric investigation of silver halide
[ETN-89-94673] N90-11632

DIELECTRICS
Influence of core-shell grains on the internal stress state and permittivity response of zirconia modified barium titanate
[AD-A211245] N90-11153
Electromagnetic pulse interaction at a dielectric interface
[AD-A211081] N90-11220

DIFFERENTIAL EQUATIONS
Asynchronous integration of ordinary differential equations on multiprocessors
[DE89-014169] N90-11493
Parameter estimation in functional and partial differential equations
[AD-A211040] N90-11511
On the numerical solution of two-point boundary value problems
[AD-A211244] N90-11516
Generalized BDF (Backward Differentiation Formula) methods applied to Hessenberg form DAEs
[DE89-017328] N90-11522
Some exact solutions of the three-identical-particle problem with S-wave inverse square potentials
[DE89-618402] N90-11524

DIFFERENTIAL GEOMETRY
Compact surface in three-dimensional ellipsoid with prescribed mean curvature (I)
[DE89-618381] N90-11502

DIFFRACTION
Nonprincipal-plane scattering from flat plates: Second-order and corner diffraction and pattern control of horn antennas
[NASA-CR-185485] N90-11205
Part A: Nonprincipal-plane scattering from flat plates: Second-order and corner diffractions N90-11206

DIFFRACTION PATTERNS
Part A: Nonprincipal-plane scattering from flat plates: Second-order and corner diffractions N90-11206

DIFFUSION
Wavefront propagation for reaction-diffusion systems of PDE
[AD-A210862] N90-11510

DIFFUSIVITY
Transport properties of thermally grown Cr2O3
[DE89-016703] N90-11623

DIGITAL DATA
Applications of artificial intelligence to digital photogrammetry N90-11486
Inferring data base requirements from examples in forms N90-11646

DIGITAL ELECTRONICS
Free-world microelectronic manufacturing equipment
[FASAC-TAR-4070] N90-11228
Inferring data base requirements from examples in forms N90-11646

DIGITAL RADAR SYSTEMS
Simulation of synthetic aperture radar 1: Feature density and accuracy requirements
[AD-A211019] N90-11218

DIGITAL SIMULATION
Numerical simulation of leading-edge vortex rollup and bursting N90-10831

DIGITAL SYSTEMS
Flight test results of a complex precise digital flight control system N90-10870
Analysis of forest fire smoke using satellite imagery
[AD-A210657] N90-11339

DIMENSIONAL ANALYSIS
Realization theoretic solution of two analytic matrix equations with applications to stabilization of infinite-dimensional systems
[AD-A211118] N90-11512

DIMETHYLHYDRAZINES
Ozonation of hydrazines and their associated impurities N90-11174

DIRAC EQUATION
Reduction of the Dirac equation to the Dirac-Kaehler equation
[DE89-630111] N90-11541

DIRECT CURRENT
A new semicustom integrated bipolar amplifier for silicon strip detectors
[DE89-015585] N90-11229

DIRECTIONAL CONTROL
Independent Orbiter Assessment (IOA): Analysis of the rudder/speed brake subsystem
[NASA-CR-185560] N90-10916
Independent Orbiter Assessment (IOA): Analysis of the guidance, navigation, and control subsystem
[NASA-CR-185555] N90-10920
Independent Orbiter Assessment (IOA): Analysis of the ascent thrust vector control actuator subsystem
[NASA-CR-185579] N90-10929

DISEASES
Evaluation of rocket motor exhaust and liner combustion by-products
[AD-A210747] N90-11083

DISPLACEMENT
Planar sliding of a rigid body with dry friction: Limit surfaces and dynamics of motion N90-11314
Computational aspects of sensitivity calculations in linear transient structural analysis N90-11327

DISPLAY DEVICES
Flight simulator evaluation of a head-down display
[NAL-TM-573] N90-10898
Independent Orbiter Assessment (IOA): Analysis of the backup flight system
[NASA-CR-185567] N90-10932
Independent Orbiter Assessment (IOA): Assessment of the displays and controls subsystem
[NASA-CR-185588] N90-10961
HDTV displays: Subjective effects of scanning standards and domestic picture sizes
[BBC-RD-1989/9] N90-11208
Techniques for optimizing human-machine information transfer related to real-time interactive display systems
[NASA-TM-100450] N90-11441
Filling or outlining shapes with color: The effects on a visual search task
[AD-A211067] N90-11444

DISSOCIATION
Shock induced dissociation of polyethylene
[DE89-016983] N90-11267

DISTRIBUTED PARAMETER SYSTEMS
Transaction throughput in distributed systems: A modeling study using dynamic queueing networks
[MEMO-INF-89-25] N90-11479
Estimation on nonlinear damping in second order distributed parameter systems
[NASA-CR-181890] N90-11494
Parameter estimation in functional and partial differential equations
[AD-A211040] N90-11511

DISTRIBUTED PROCESSING
Advanced manned space flight simulation and training: An investigation of simulation host computer system concepts
[NASA-CR-185998] N90-10911
A distributed debugger for Amoeba
[CWI-CS-R8828] N90-11453
A verification exercise relating to specification styles in LOTOS
[MEMO-INF-89-18] N90-11471
An integrated distributed processing interface for supercomputers and workstations
[DE89-016769] N90-11478
On the Amoeba protocol
[CWI-CS-R8827] N90-11480
Fixed point iteration on point-symmetric interference graphs
[MEMO-INF-89-23] N90-11535

DISTRIBUTION FUNCTIONS
Balance equations for ionospheric plasmas with different partial temperatures N90-11364
Boundary kernel estimation of the two sample comparison density function
[AD-A210757] N90-11532
Resonance effect on the oscillator distribution function
[DE89-630105] N90-11548

DIURNAL VARIATIONS
Average diurnal and seasonal profiles of ionospheric storms N90-11371

DOCUMENTATION
Laser Raman spectroscopy: A literature review
[FOA-C-20753-2.3] N90-11121
Electronic publishing: Guide to selection
[PB89-214753] N90-11448

DONOR MATERIALS
Hydrogen-assisted thermal donor formation in silicon
[DE89-016809] N90-11594

DOORS
Independent Orbiter Assessment (IOA): Analysis of the mechanical actuation subsystem
[NASA-CR-185525] N90-10944
Independent Orbiter Assessment (IOA): Assessment of the mechanical actuation subsystem, volume 1
[NASA-CR-185527-VOL-1] N90-10952
Independent Orbiter Assessment (IOA): Assessment of the mechanical actuation subsystem, volume 2
[NASA-CR-185527-VOL-2] N90-10953

DOPPLER EFFECT
A laser Doppler anemometry investigation of single-phase and particle-laden jet flows
[AD-A210660] N90-11261

DOPPLER NAVIGATION
Development of the integrated all-weather navigation system for Tornado N90-10849

DOPPLER RADAR
The effectiveness of adaptive PRF (Pulse Repetition Frequency) selection in minimizing range obscuration in the TDWR (Terminal Doppler Weather Radar) system
[AD-A211267] N90-11222

DOSIMETERS
Hydrazine dosimetry N90-11178

DRAINAGE
Independent Orbiter Assessment (IOA): Assessment of the purge, vent and drain subsystem
[NASA-CR-185535] N90-10949
Independent Orbiter Assessment (IOA): Analysis of the purge, vent and drain subsystem
[NASA-CR-185547] N90-10969

DRILLING
Coastal subsea permafrost and bedrock observations using dc resistivity
[AD-A210784] N90-11435

DROP SIZE
Evaporation and combustion of dense sprays with a bimodal droplet size distribution N90-11094

DROP TOWERS
Droplet combustion experiment drop tower tests using models of the space flight apparatus
[NASA-TM-101472] N90-11196
DRY FRICTION
Planar sliding of a rigid body with dry friction: Limit surfaces and dynamics of motion N90-11314
DRYING
Freeze-dried processing of tungsten heavy alloys
[DE89-015171] N90-11122
DUCTED ROCKET ENGINES
A simulator for a hydrocarbon ramrocket fuel gas generator: First phase development
[AR-005-621] N90-11080
DUCTS
Turbulent reacting flows in solid-propellant ducted rocket combustors N90-11079
DUST
Diagnostic study of atmosphere-terrain interaction leading to the formation of dust clouds and poor visibilities over near east desert areas
[AD-A211243] N90-11358
DWARF GALAXIES
UV observations of NGC 205
[NASA-CR-185975] N90-11661
DYE LASERS
Nonlinear dynamics of broad-band lasers
[DE89-017442] N90-11307
DYES
Flow visualization techniques for flight research N90-10878
DYNAMIC CHARACTERISTICS
A review of the Error of Matrix Method (EMM) for structural dynamic model comparison N90-10993
Dynamic characteristics concerned in the design of a free-piston Stirling engine/magnetic coupling/compressor system
[DE89-015981] N90-11317
Stochastic optimization by simulation: Some experiments with a simple steady-state queue
[AD-A210762] N90-11508
Markov processes in Hilbert space and continuous spontaneous localization of systems of identical particles
[DE89-618396] N90-11540
DYNAMIC CONTROL
Viscoelastic tuned dampers for control of structural dynamics N90-10999
DYNAMIC LOADS
Integration of analytical and test software for optimal structural design under dynamic loads N90-11007
The dynamic stability of an axially loaded beam with lateral elastic support and damping N90-11331
DYNAMIC MODELS
GEMMES: A new tool for dynamic modeling N90-11005
A direct two response approach for updating analytical dynamic models of structures with emphasis on uniqueness N90-11028
DYNAMIC RESPONSE
Frequency domain design of robust controllers for space structures
[AD-A211172] N90-10985
Reduction of dynamic response of spacecraft structures and payloads N90-11000
DYNAMIC STABILITY
The dynamic stability of an axially loaded beam with lateral elastic support and damping N90-11331
DYNAMIC STRUCTURAL ANALYSIS
Updating of finite element model by means of normal mode parameters N90-10992
Viscoelastic tuned dampers for control of structural dynamics N90-10999
A super element for multibody dynamics N90-11004
Employment of modal survey methodologies in dynamic analysis procedures N90-11006
Integration of analytical and test software for optimal structural design under dynamic loads N90-11007
Use of Lanczos vectors in structural dynamics N90-11011
Numerical treatment of the thermo-structural-dynamic problems: The interpolation techniques N90-11016
Comparison of sine dwell and broadband methods for modal testing N90-11025
Induced shock loads during the separation of the Ariane 5 VEB structure N90-11045
The dynamics of circular plates with patch damping: A numerical and experimental study N90-11329
DYNAMIC TESTS
Dynamic substructuring for modular analysis and testing N90-11015
Comparison of phase resonance, mode separation, and driven-base modal identification methods applied to the FLECS test structure N90-11027
Transient tests for spacecraft structures N90-11040

E

E REGION
Quiet time conductivities of the auroral ionosphere N90-11383
A review on radio studies of auroral E-region ionospheric irregularities N90-11390
An ionospheric model for HF sky-wave backscatter radar N90-11401
EARTH (PLANET)
Offaxis radiance studies for infrared sensors
[AD-A210790] N90-11570
EARTH ATMOSPHERE
Potential effects of global climate change on the United States. Volume 1: Regional studies. Draft
[PB89-161053] N90-11351
Potential effects of global climate change on the United States. Volume 2: National studies. Draft
[PB89-161061] N90-11352
EARTH IONOSPHERE
Balance equations for ionospheric plasmas with different partial temperatures N90-11364
Global ionospheric dynamics: A review N90-11367
A fully analytic, low and middle latitude ionospheric model N90-11368
VLF/LF radio wave studies of the structure and variability of the equatorial, mid-latitude and polar ionosphere below 100 km N90-11373
Seasonal and geomagnetic response of the thermosphere and ionosphere N90-11380
Ionosphere-thermosphere coupling at high latitudes: Aspect angle dependence of non-thermal plasmas N90-11382
Calculation of the temperature and velocity vector of the neutral gas using EISCAT CP3-data N90-11384
Ion heating events observed at the EISCAT radar N90-11385
Small-scale irregularities and global plasma dynamics in the high-latitude ionosphere N90-11394
Short wavelength striations on expanding plasma clouds
[DE89-016585] N90-11416
EARTH LIMB
Offaxis radiance studies for infrared sensors
[AD-A210790] N90-11570
EARTH MAGNETOSPHERE
User's guide to the Space Environment Services Center geophysical alert broadcasts
[PB89-194617] N90-11411
Substorm associated pulsations: A study of plasmaspheric cavity resonance, mid-latitude polarisation and geostationary orbit signatures N90-11422
EARTH RESOURCES
Potential effects of global climate change on the United States. Volume 1: Regional studies. Draft
[PB89-161053] N90-11351
Potential effects of global climate change on the United States. Volume 2: National studies. Draft
[PB89-161061] N90-11352
ECONOMIC ANALYSIS
Study of the application of automation to composites manufacture
[AD-A211049] N90-11087
View on recent fuel costs in airlines
[NAL-TM-569] N90-11653
ECONOMICS
The transfer and diffusion of new technologies: A review of the economics literature
[DE89-015871] N90-11655
EDDY CURRENTS
Questions from the Willmarth Workshop on New Directions in Research on Turbulent Wall-Layer Structures
[AD-A211282] N90-11264
Sensors for nondestructive testing and evaluation of materials
[DE89-014763] N90-11279
EDITING
An investigation of the usefulness of Earley's Algorithm in a general context-free recognizer
[DE89-016498] N90-11463
EDUCATION
Higher education for science and technology: A background paper
[PB89-191290] N90-11642
Planning in writing: The cognition of a constructive process
[AD-A210434] N90-11648
EIGENVALUES
JOE: Jordan Optimized Eigensolver. A step toward a numerical Jordan form analyzer for control and interactive thermo-structural-dynamic applications N90-11047
Two enhancements of the logarithmic least-squares method for analyzing subjective comparisons
[AD-A211192] N90-11514
EIGENVECTORS
JOE: Jordan Optimized Eigensolver. A step toward a numerical Jordan form analyzer for control and interactive thermo-structural-dynamic applications N90-11047
EINSTEIN EQUATIONS
Gravitational nonminimally coupled electromagnetic fields: A possible solution to some idiosincrasies of Einstein-Maxwell theory
[DE89-618430] N90-11635
EJECTION SEATS
A preliminary sensitivity analysis of the Generalized Escape System Simulation (GESS) computer program
[DE89-016891] N90-10844
EL NINO
Interannual variability of temperature in the upper layer of the North Pacific eastern boundary region, 1971-1987
[PB89-190227] N90-11434
ELASTIC ANISOTROPY
Low temperature properties of glasses N90-11141
ELASTIC PLATES
A finite element formulation for inelastic plates and shells based on a mixed variational principle N90-11334
ELASTIC PROPERTIES
Acoustic studies of new materials: Quasicrystals, low-loss glasses and high Tc superconductors
[AD-A211281] N90-11551
ELASTIC SCATTERING
New theoretical approaches for studying electron collisions with small molecules
[DE89-017543] N90-11558
ELASTIC SHELLS
A finite element formulation for inelastic plates and shells based on a mixed variational principle N90-11334
ELASTODYNAMICS
An analytical and experimental study of the elastodynamic response characteristics of planar linkage mechanism with bearing clearances N90-11336
ELASTOMERS
Numerical analysis of nonlinear viscoelastic structures: Application to elastomers and rubber-like materials N90-11013
ELECTRIC BATTERIES
New secondary batteries utilizing electronically conductive polymer cathodes
[NASA-CR-185885] N90-11227
Lithium polymer electrolyte battery, electrochemical behavior of cathode materials
[AD-A210755] N90-11235
Battery actuation of NITINOL at sub-zero temperatures
[AD-A211254] N90-11237
ELECTRIC CHARGE
Capacitive behavior in conducting polymers: The ac impedance and quartz crystal microbalance studies
[AD-A210754] N90-11150
ELECTRIC CONDUCTORS
Testing results of the MIT Probe
[DE89-016679] N90-11590
ELECTRIC CONTACTS
Coatings in electrical contacts
[DE89-787739] N90-11234
ELECTRIC CURRENT
Internal voltages and currents in well-shielded cylindrical objects due to simulated direct-strike lightning
[DE89-012664] N90-11231
ELECTRIC DISCHARGES
Capacitive behavior in conducting polymers: The ac impedance and quartz crystal microbalance studies
[AD-A210754] N90-11150
A severe human ESD (Electrostatic Discharge) model for safety and high reliability system qualification testing
[DE89-016177] N90-11233
ELECTRIC EQUIPMENT TESTS
Testing results of the MIT Probe
[DE89-016679] N90-11590
ELECTRIC FIELDS
Thermodynamic principles of the process of the effect of electromagnetic fields on a polymer melt
[AD-A210698] N90-11149
Simulation of the polar cap F region ionization using an experimental convection electric field N90-11370
Empirical models of convection electric fields and electrostatic potential at high latitude from EISCAT observations: Preliminary results N90-11377
Substorm associated pulsations: A study of plasmaspheric cavity resonance, mid-latitude polarisation and geostationary orbit signatures N90-11422
Biological effects of power frequency electric and magnetic fields: Background paper
[PB89-209985] N90-11439
Chevron layer structures in Surface Stabilized Ferroelectric Liquid Crystal (SSFLC) cells filled with a material which exhibits the chiral nematic to smectic C* phase transition
[DE89-016985] N90-11628

ELECTRIC POTENTIAL
Internal voltages and currents in well-shielded cylindrical objects due to simulated direct-strike lightning
[DE89-012664] N90-11231
Empirical models of convection electric fields and electrostatic potential at high latitude from EISCAT observations: Preliminary results N90-11377
ELECTRIC POWER SUPPLIES
Biological effects of power frequency electric and magnetic fields: Background paper
[PB89-209985] N90-11439
ELECTRIC POWER TRANSMISSION
Independent Orbiter Assessment (IOA): Analysis of the electrical power distribution and control/electrical power generation subsystem
[NASA-CR-185538] N90-10933
Independent Orbiter Assessment (IOA): Analysis of the electrical power distribution and control/remote manipulator system subsystem
[NASA-CR-185526] N90-10936
Independent Orbiter Assessment (IOA): Analysis of the reaction control system, volume 2
[NASA-CR-185532-VOL-2] N90-10939
Independent Orbiter Assessment (IOA): Analysis of the reaction control system, volume 3
[NASA-CR-185532-VOL-3] N90-10940
Independent Orbiter Assessment (IOA): Analysis of the electrical power distribution and control subsystem, volume 1
[NASA-CR-185529-VOL-1] N90-10941
Independent Orbiter Assessment (IOA): Analysis of the electrical power distribution and control subsystem, volume 2
[NASA-CR-185529-VOL-2] N90-10942
Electron beam welding: Model of high voltage bias transmission line and termination circuits
[DE89-016900] N90-11323
ELECTRIC PULSES
Elements of a 200 watt pulsed excimer laser N90-11295
ELECTRIC WELDING
A characterization of the side bonding, upset plug welding process
[DE89-015181] N90-11315
ELECTRICAL MEASUREMENT
Coastal subsea permafrost and bedrock observations using dc resistivity
[AD-A210784] N90-11435
ELECTRICAL PROPERTIES
Coastal subsea permafrost and bedrock observations using dc resistivity
[AD-A210784] N90-11435
ELECTRICAL RESISTANCE
Coastal subsea permafrost and bedrock observations using dc resistivity
[AD-A210784] N90-11435
ELECTRICAL RESISTIVITY
Transport studies of conducting polymers N90-11140
New secondary batteries utilizing electronically conductive polymer cathodes
[NASA-CR-185885] N90-11227
Studies of a strongly coupled plasma produced in a capillary discharge
[DE89-016611] N90-11581
Transport properties of thermally grown Cr2O3
[DE89-016703] N90-11623
ELECTRO-OPTICS
Polarization matrices of lithium tetraborate
[AD-A210774] N90-11112
ELECTROCATALYSTS
Electronic and ionic transport in polymers
[AD-A210654] N90-11148
ELECTROCHEMISTRY
Dynamics of nucleation at electrochemical interfaces via surface EXAFS and standing wave measurements
[AD-A210733] N90-11109
Polarization matrices of lithium tetraborate
[AD-A210774] N90-11112
Electronic and ionic transport in polymers
[AD-A210654] N90-11148
Electrolyte dependence of charge injection processes for electroactive polymer films
[AD-A210787] N90-11152
Lithium polymer electrolyte battery, electrochemical behavior of cathode materials
[AD-A210755] N90-11235
The theory of ac impedance of rough electrode-electrolyte interfaces
[DE89-017474] N90-11243
ELECTRODEPOSITION
Proceedings of the Polycrystalline Thin Film Program Meeting
[DE89-009457] N90-11348
ELECTRODES
Microsensor and pattern recognition techniques in hydrazine detection N90-11177
Lithium polymer electrolyte battery, electrochemical behavior of cathode materials
[AD-A210755] N90-11235
The theory of ac impedance of rough electrode-electrolyte interfaces
[DE89-017474] N90-11243
ELECTRODYNAMICS
Observations of ionosphere/magnetosphere interactions from the Dynamics Explorer satellites N90-11376
Polar F layer lacuna irregularities at Dumont d'Urville N90-11379
Biological effects of power frequency electric and magnetic fields: Background paper
[PB89-209985] N90-11439
ELECTROENCEPHALOGRAPHY
Test-retest reliability of oxford Medilog 9000 sleep recording and SS-90-3 sleep stage scoring
[AD-A211165] N90-11440
ELECTROJETS
A review on radio studies of auroral E-region ionospheric irregularities N90-11390
ELECTROLYSIS
Selective removal of organics for water reclamation
[NASA-CR-185959] N90-11445
ELECTROLYTES
Lithium polymer electrolyte battery, electrochemical behavior of cathode materials
[AD-A210755] N90-11235
The theory of ac impedance of rough electrode-electrolyte interfaces
[DE89-017474] N90-11243
ELECTROLYTIC CELLS
Cell performance of ultra-thin polymer cathode system: Theoretical energy and power density projections
[AD-A210786] N90-11151
ELECTROMAGNETIC ABSORPTION
Radiationless transitions and excited-state absorption of low-field chromium complexes in solids
[AD-A210653] N90-11105
ELECTROMAGNETIC FIELDS
Thermodynamic principles of the process of the effect of electromagnetic fields on a polymer melt
[AD-A210698] N90-11149
Generation of higher-order squeezing of quantum electromagnetic fields by degenerate four-wave mixing and other processes
[DE89-618392] N90-11213
Deep null antennas and their applications to tactical VHF radio communications
[AD-A210656] N90-11214
Auxiliary-field transformations for repulsive potentials: A physical approach
[DE89-016677] N90-11223
New tools for the simulation and design of calorimeters
[DE89-016323] N90-11281
Study of the behavioral and biological effects of high intensity 60 Hz electric fields
[DE89-015528] N90-11438
Biological effects of power frequency electric and magnetic fields: Background paper
[PB89-209985] N90-11439
Computer simulations of electromagnetic ion instabilities in the plasma sheet boundary layer
[DE89-016596] N90-11588
A fully electromagnetic hybrid model for high density plasma simulations
[DE89-016771] N90-11593
Gravitational nonminimally coupled electromagnetic fields: A possible solution to some idiosincrasies of Einstein-Maxwell theory
[DE89-618430] N90-11635
Numerical study of the current sheet and PSBL in a magnetotail model
[NASA-CR-183289] N90-11669
Electromagnetic jets in pulsar magnetospheres and near magnetized accretion disks N90-11675
ELECTROMAGNETIC INTERACTIONS
Electromagnetic pulse interaction at a dielectric interface
[AD-A211081] N90-11220
ELECTROMAGNETIC NOISE
Nonlinear dynamics of broad-band lasers
[DE89-017442] N90-11307
ELECTROMAGNETIC PROPERTIES
High-temperature ceramic superconductors
[AD-A211070] N90-11618
ELECTROMAGNETIC PULSES
Electromagnetic pulse interaction at a dielectric interface
[AD-A211081] N90-11220
Acceleration of thin foil targets using fiber-coupled optical pulses
[DE89-016526] N90-11569
ELECTROMAGNETIC RADIATION
Efficient algorithm for calculation of radar cross section
[AD-A210785] N90-11217
Ionospheric irregularities and their effects on electromagnetic waves propagating through them N90-11391
ELECTROMAGNETIC SCATTERING
Near zone-basic scattering code user's manual with space station applications
[NASA-CR-185925] N90-11209
ELECTROMAGNETIC WAVE TRANSMISSION
Validation of NEC (Numerical Electromagnetics Code) for antennas near ground
[DE89-016502] N90-11212
ELECTROMAGNETISM
Magnetically levitated micro-robotics N90-11542
ELECTROMECHANICS
Coatings in electrical contacts
[DE89-787739] N90-11234
ELECTRON BEAM WELDING
Electron beam welding: Model of high voltage bias transmission line and termination circuits
[DE89-016900] N90-11323
ELECTRON BEAMS
A compact X-ray free electron laser
[DE89-017236] N90-11297
Free-electron laser theory
[DE89-620145] N90-11298
Stability requirements of RF linac-driven free-electron lasers
[DE89-016609] N90-11303
Minimized emittance growth with elliptical beam pipes in FEL (Free-Electron Laser)
[DE89-016982] N90-11305
Launched electrons in plasma opening switches
[DE89-016886] N90-11596
Beam-plasma discharge in penetrating plasma
[DE89-630481] N90-11597
International workshop on Beam Injection Assessment of Defects in Semiconductors
[AD-A210842] N90-11617
ELECTRON DENSITY (CONCENTRATION)
A diagnostic for determining the quality of single-reference electron correlation methods N90-11554
ELECTRON ENERGY
Global morphology of plasma bubbles in the low latitude ionosphere N90-11369
Radiative shocks with electron thermal conduction N90-11670
ELECTRON GUNS
Stability requirements of RF linac-driven free-electron lasers
[DE89-016609] N90-11303
Ion sources, electron guns and beam optics
[DE89-015526] N90-11562
ELECTRON RUNAWAY (PLASMA PHYSICS)
A study of runaway electron confinement and theory of neoclassical MHD turbulence
[DE89-016728] N90-11584
ELECTRON SCATTERING
Studies of ultrathin magnetic films and particle-surface interactions with spin-sensitive electron spectroscopies
[DE89-016741] N90-11556
New theoretical approaches for studying electron collisions with small molecules
[DE89-017543] N90-11558
Theoretical atomic physics for fusion
[DE89-017363] N90-11563
ELECTRON SOURCES
A compact X-ray free electron laser
[DE89-017236] N90-11297
ELECTRON SPECTROSCOPY
Studies of ultrathin magnetic films and particle-surface interactions with spin-sensitive electron spectroscopies
[DE89-016741] N90-11556
ELECTRON STATES
Forty-fourth symposium on molecular spectroscopy
[AD-A210752] N90-11111
ELECTRON TRANSFER
Investigations of the influence of magnetically long range ordered phases on the electronic charge transport in metallic glasses
[ETN-89-94672] N90-11155
Electron transfer reactions
[AD-A210711] N90-11545
ELECTRON TRANSITIONS
Forty-fourth symposium on molecular spectroscopy
[AD-A210752] N90-11111
ELECTRON-ION RECOMBINATION
Dielectronic excitation and recombination in crystal channels
[DE89-016364] N90-11625

ELECTRONIC CONTROL
Independent Orbiter Assessment (IOA): Assessment of the body flap subsystem FMEA/CIL
[NASA-CR-185575] N90-10968
ELECTRONIC COUNTERMEASURES
Network analyzer for nonstatic jamming
[AD-A210759] N90-11216
ELECTRONIC EQUIPMENT
A comparison of fixed-base and driven-base modal testing of an electronics package
[DE89-016673] N90-11240
HPW (High Power Microwave) testing of electronic components
[DE89-016682] N90-11241
Electronic publishing: Guide to selection
[PB89-214753] N90-11448
ELECTRONIC EQUIPMENT TESTS
A comparison of fixed-base and driven-base modal testing of an electronics package
[DE89-016673] N90-11240
ELECTRONIC PACKAGING
A comparison of fixed-base and driven-base modal testing of an electronics package
[DE89-016673] N90-11240
ELECTRONS
Auxiliary-field transformations for repulsive potentials: A physical approach
[DE89-016677] N90-11223
Observations of ionosphere/magnetosphere interactions from the Dynamics Explorer satellites N90-11376
ANTHEM simulation of the early time magnetic field penetration of the plasma surrounding a high density Z-pinch
[DE89-016960] N90-11585
Passage of ultrarelativistic electrons through real crystals
[DE89-618624] N90-11613
ELECTROPHYSICS
Physics and materials science of high temperature superconductors
[AD-A211246] N90-11619
ELECTROSTATIC PROBES
PISCES program plasma-surface interactions research
[DE89-015622] N90-11578
ELECTROSTATIC WAVES
Low frequency electrostatic waves observed in the vicinity of an auroral arc N90-11378
ELECTROSTATICS
A severe human ESD (Electrostatic Discharge) model for safety and high reliability system qualification testing
[DE89-016177] N90-11233
Empirical models of convection electric fields and electrostatic potential at high latitude from EISCAT observations: Preliminary results N90-11377
Electrostatic turbulence in the high latitude ionosphere N90-11392
ELEVONS
Independent Orbiter Assessment (IOA): Analysis of the elevon subsystem
[NASA-CR-185576] N90-10935
Independent Orbiter Assessment (IOA): Analysis of the mechanical actuation subsystem
[NASA-CR-185525] N90-10944
Independent Orbiter Assessment (IOA): Assessment of the mechanical actuation subsystem, volume 1
[NASA-CR-185527-VOL-1] N90-10952
Independent Orbiter Assessment (IOA): Assessment of the mechanical actuation subsystem, volume 2
[NASA-CR-185527-VOL-2] N90-10953
Independent Orbiter Assessment (IOA): Assessment of the elevon actuator subsystem FMEA/CIL
[NASA-CR-185578] N90-10970
ELLIPSOIDS
Compact surface in three-dimensional ellipsoid with prescribed mean curvature (I)
[DE89-618381] N90-11502
ELLIPTICAL GALAXIES
UV observations of NGC 205
[NASA-CR-185975] N90-11661
EMISSION SPECTRA
Small grains in reflection nebulae: A study of diffuse interstellar bands, elemental depletions and infrared flux N90-11672
EMITTANCE
Minimized emittance growth with elliptical beam pipes in FEL (Free-Electron Laser)
[DE89-016982] N90-11305
Extraction induced emittance growth for negative ion sources
[DE89-017586] N90-11559
EMULSIONS
Basic research on processing of ceramics for space structures
[AD-A205954] N90-11139
ENDOTHERMIC FUELS
Production of jet fuels from coal-derived liquids. Volume 11: Production of advanced endothermic fuel blends from Great Plains Gasification Plant naphtha by-product stream
[AD-A210251] N90-11184
ENERGY CONSERVATION
Technology applications bulletins
[DE89-017454] N90-11651
ENERGY CONSUMPTION
Technology applications bulletins
[DE89-017454] N90-11651
ENERGY CONVERSION EFFICIENCY
Laser grooved and polycrystalline silicon solar cell research
[DE89-015196] N90-11347
ENERGY DISTRIBUTION
Global and local fluctuations in multiplicity and transverse energy for central ultra-relativistic heavy-ion interactions
[LUIP-8903] N90-11555
ENERGY GAPS (SOLID STATE)
A fermi liquid electric structure and the nature of the carriers in high-T(sub c) cuprates: A photoemission study
[DE89-016774] N90-11624
ENERGY LEVELS
Quantum chemical investigations of the mechanism of cationic polymerization and theoretical prediction of crystal densities and decomposition pathways of energetic molecules
[AD-A210322] N90-11143
ENERGY SPECTRA
A solar extreme ultraviolet flux model N90-11686
ENERGY STORAGE
Propagation of normal zones of finite size in large, composite superconductors
[DE89-016866] N90-11611
ENERGY TECHNOLOGY
Summaries of the FY 1989 Applied Mathematical Sciences Research program
[DE89-016694] N90-11521
Technology applications bulletins
[DE89-017454] N90-11651
ENERGY TRANSFER
Particle kinetic simulation of high altitude hypervelocity flight
[NASA-CR-186003] N90-10840
A severe human ESD (Electrostatic Discharge) model for safety and high reliability system qualification testing
[DE89-016177] N90-11233
ENGINE CONTROL
Independent Orbiter Assessment (IOA): Analysis of the hydraulics/water spray boiler subsystem
[NASA-CR-185541] N90-10934
ENGINE DESIGN
Advanced technologies impact on compressor design and development: A perspective
[NASA-TM-102341] N90-10891
Automotive Stirling engine development program
[NASA-CR-180839] N90-11654
ENGINE PARTS
Advanced Turbine Technology Applications Program, (ATTAP): A plan for improving the prototype production of ceramic components for the gas turbine engine, 1988--1992
[DE89-015566] N90-11320
Automotive Stirling engine development program
[NASA-CR-180839] N90-11654
ENGINE TESTS
Test and evaluation: Reducing risks to military aircraft from bird collisions. Report to the Chairman, Legislation, and National Security Subcommittee, Committee on Goverment Operations, House of Representatives
[AD-A210670] N90-10845
The effect of electrode configuration on arcjet performance
[NASA-TM-102346] N90-11081
Automotive Stirling engine development program
[NASA-CR-180839] N90-11654
ENGINEERING DRAWINGS
CRRES (Combined Release and Radiation Effects Satellite) SPACERAD plasma wave experiment
[AD-A210791] N90-11587
ENVIRONMENT EFFECTS
Hydrazine fate and transformation in natural waters and soils N90-11165
Methodology of developing a combined environmental stress schedule for reliability growth testing
[AD-A211053] N90-11326
Potential effects of global climate change on the United States. Executive summary. Draft
[PB89-161046] N90-11350
Interrelation of experimental exposure and ambient air quality data for comparison of ozone exposure indices and estimating agricultural losses
[PB89-195036] N90-11353
ENVIRONMENT MANAGEMENT
Evaluation of mid-to-long term basic research for environmental restoration
[DE89-015621] N90-11355
ENVIRONMENT POLLUTION
The Third Conference on the Environmental Chemistry of Hydrazine Fuels
[AD-A197632] N90-11157
Measurement of hydrazine contamination in soils N90-11180
ENVIRONMENT PROTECTION
National Climate Program five-year plan, 1989-1993
[PB89-207369] N90-11426
ENVIRONMENT SIMULATION
The Environmental Test Centre at ESTEC (an overview) N90-11064
The behavior of hydrazine vapor in an environmental chamber under simulated atmospheric conditions N90-11161
Modeling of hydrazine surface interactions in environmental reaction chambers N90-11162
ENVIRONMENTAL ENGINEERING
National Climate Program five-year plan, 1989-1993
[PB89-207369] N90-11426
ENVIRONMENTAL MONITORING
National Climate Program five-year plan, 1989-1993
[PB89-207369] N90-11426
ENVIRONMENTAL QUALITY
Reporting environmental data of known quality
[DE89-016214] N90-11359
ENVIRONMENTAL SURVEYS
Stratospheric ozone depletion
[PB89-207476] N90-11354
ENVIRONMENTAL TESTS
Spacecraft Structures and Mechanical Testing
[ESA-SP-289] N90-10986
Environmental testing: An approach to more cost efficiency N90-10988
The Environmental Test Centre at ESTEC (an overview) N90-11064
Methodology of developing a combined environmental stress schedule for reliability growth testing
[AD-A211053] N90-11326
EPITAXY
Intergranular and interphase boundaries in ceramics
[DE89-016969] N90-11154
EQUATIONS OF MOTION
On the motion equation of an elastically supported two degree of freedon gyro
[NAL-TM-568] N90-11276
A nonoscillatory, characteristically convected, finite volume scheme for multidimensional convection problems
[NASA-TM-102354] N90-11497
DMC (Distinct Motion Code): A rigid body motion code for determining the interaction of multiple spherical particles
[DE89-016929] N90-11543
EQUATIONS OF STATE
Experimental measurements of shock-induced vaporization in cadmium and lead
[DE89-016877] N90-11103
Consequence of condensed-phase formation in transient burning of TiHx/KClO in a closed system
[DE89-013922] N90-11188
Acceleration of metal plates
[DE89-016816] N90-11197
Irreversible phase transition and wave propagation in silicate geologic materials
[DE89-016031] N90-11414
Equation-of-state data of synthetic Uranus
[DE89-016509] N90-11683
Solar opacities constrained by solar neutrinos and solar oscillations
[DE89-016988] N90-11687
EQUILIBRIUM EQUATIONS
Electromagnetic jets in pulsar magnetospheres and near magnetized accretion disks N90-11675
EQUILIBRIUM METHODS
Equilibrium and stability in composite thin shell N90-10998
EQUIPMENT SPECIFICATIONS
Free-world microelectronic manufacturing equipment
[FASAC-TAR-4070] N90-11228
EQUIVALENCE
Determinism yields (event structure isomorphism equals step sequence equivalence)
[CWI-CS-R8839] N90-11492
On the equivalence of BS-stability and B-consistency
[CWI-NM-R8815] N90-11530

EQUIVALENT CIRCUITS
A general-purpose computer program for the Volterra-series analysis of nonlinear microwave circuits
[AD-A210768] N90-11236
ERGODIC PROCESS
Stochastic flows in networks
[AD-A211209] N90-11515
EROSION
Determination of neutral particle concentration at erosion laser plasma expansion into vacuum
[DE89-620128] N90-11308
PISCES program plasma-surface interactions research
[DE89-015622] N90-11578
ERROR ANALYSIS
Using self-calibrating thermocouples in industry
[DE89-013539] N90-11278
Iterative network magnitude estimation and uncertainty assessment with noisy and clipped data
[AD-A210707] N90-11507
New statistical approaches to galaxy clustering N90-11674
ERROR CORRECTING DEVICES
Utilization of the generalized likelihood ratio test for the suppression of systematic errors in noisy systems
[ETN-89-94656] N90-11225
ERROR DETECTION CODES
Utilization of the generalized likelihood ratio test for the suppression of systematic errors in noisy systems
[ETN-89-94656] N90-11225
ESCAPE SYSTEMS
A preliminary sensitivity analysis of the Generalized Escape System Simulation (GESS) computer program
[DE89-016891] N90-10844
ESTIMATES
Passive trajectography by azimuth: Improvement of estimation quality N90-10854
Estimation on nonlinear damping in second order distributed parameter systems
[NASA-CR-181890] N90-11494
ESTIMATING
Analytic signals in the damping coefficient estimation N90-11003
Parameter estimation in functional and partial differential equations
[AD-A211040] N90-11511
ETCHING
Reactive ion etching of SiC thin films by mixtures of flucrinated gases and oxygen
[AD-A211046] N90-11113
EUCLIDEAN GEOMETRY
On the areas of various bodies in the Euclidean space: The case of irregular convex polygons
[DE89-618377] N90-11500
Local structure of a 2-codimensional conformally flat submanifold in an Euclidean space R(sup n+2)
[DE89-618379] N90-11501
EULER EQUATIONS OF MOTION
Numerical simulation of leading-edge vortex rollup and bursting N90-10831
EULER-LAGRANGE EQUATION
Fluid-structure interaction effects in tank structures due to sloshing and hydrodynamic ram: Coupled Lagangian-Eulerian simulations N90-11022
Computation of transient three-dimensional interstage flowfields using the arbitrary Lagrangian-Eulerian method N90-11253
EUROPE
A history of West European rocketry and space research
[AD-A211191] N90-11690
EUROPEAN SPACE PROGRAMS
Aeritalia Space Systems Group, Turin, Italy
[EOARD-LR-89-041] N90-10908
EVAPORATION
Experimental measurements of shock-induced vaporization in cadmium and lead
[DE89-016877] N90-11103
EVENTS
Determinism yields (event structure isomorphism equals step sequence equivalence)
[CWI-CS-R8839] N90-11492
EXCIMER LASERS
Elements of a 200 watt pulsed excimer laser N90-11295
Dissociation and vibrational relaxation of XeF by various collision partners
[AD-A210769] N90-11300
EXCITATION
Radiationless transitions and excited-state absorption of low-field chromium complexes in solids
[AD-A210653] N90-11105
EXCITONS
Nonlinear optical studies of resonant systems
[AD-A211032] N90-11301
EXHAUST GASES
A simulator for a hydrocarbon ramrocket fuel gas generator: First phase development
[AR-005-621] N90-11080
EXPERT SYSTEMS
Parallel inference based on delta processing
[CWI-CS-R8846] N90-11482
Applications of artificial intelligence to digital photogrammetry N90-11486
Nonlinear maneuver autopilot for the F-15 aircraft
[NASA-CR-179442] N90-11487
Systems analysis considerations in artificial intelligence/expert systems technology applications
[DE89-016847] N90-11490
Partially specified probability measures in expert systems
[CWI-CS-R8842] N90-11536
EXPLORER SATELLITES
Rocket and satellite observations of the local interstellar medium N90-11668
EXPLOSIONS
Carbon in detonations
[DE89-016037] N90-11189
EXPLOSIVE DEVICES
Test of EED (Electro-Explosive Devices). Part 3: Statistical aspects on the estimation of sensitivity
[FOA-C-20749-2.3-PT-3] N90-11194
EXPLOSIVES
In-situ study of the chemically driven flow fields in initiating homogeneous and heterogeneous nitromethane explosives
[DE89-008415] N90-11186
Estimation of the C-J pressure of explosives
[DE89-013811] N90-11187
Laser-driven miniature flyer plates for shock initiation of secondary explosives
[DE89-016587] N90-11288
Magnetic flux compression
[DE89-016991] N90-11546
EXPOSURE
Occupational safety considerations with hydrazine N90-11182
EXTERNAL STORE SEPARATION
Evaluation of store carriage (and release) environment using flight instrumented stores N90-10876
EXTERNAL STORES
Evaluation of store carriage (and release) environment using flight instrumented stores N90-10876
CF 18 480 Gallon External Fuel Tank Stores Clearance Program N90-10877
EXTERNAL TANKS
Independent Orbiter Assessment (IOA): Analysis of the orbiter main propulsion system
[NASA-CR-185584] N90-10927
Independent Orbiter Assessment (IOA): Assessment of the mechanical actuation subsystem, volume 1
[NASA-CR-185527-VOL-1] N90-10952
Independent Orbiter Assessment (IOA): Assessment of the mechanical actuation subsystem, volume 2
[NASA-CR-185527-VOL-2] N90-10953
EXTRACTION
Measurement of hydrazine contamination in soils N90-11180
Extraction induced emittance growth for negative ion sources
[DE89-017586] N90-11559
EXTRAVEHICULAR ACTIVITY
Independent Orbiter Assessment (IOA): Analysis of the extravehicular mobility unit
[NASA-CR-185540] N90-10937
Independent Orbiter Assessment (IOA): Analysis of the crew equipment subsystem
[NASA-CR-185591] N90-10958
Independent Orbiter Assessment (IOA): Assessment of the crew equipment subsystem
[NASA-CR-185577] N90-10971
EXTRAVEHICULAR MOBILITY UNITS
Independent Orbiter Assessment (IOA): Analysis of the extravehicular mobility unit
[NASA-CR-185540] N90-10937
Independent Orbiter Assessment (IOA): Assessment of the extravehicular mobility unit, volume 1
[NASA-CR-185536-VOL-1] N90-10950
Independent Orbiter Assessment (IOA): Assessment of the extravehicular mobility unit, volume 2
[NASA-CR-185536-VOL-2] N90-10951
Independent Orbiter Assessment (IOA): CIL issues resolution report, volume 2
[NASA-CR-185524-VOL-2] N90-10955
EXTREME ULTRAVIOLET RADIATION
A solar extreme ultraviolet flux model N90-11686
EYE PROTECTION
The Si(1-x)Nx Rugate
[AD-A211236] N90-11572

F

F REGION
Simulation of the polar cap F region ionization using an experimental convection electric field N90-11370
Medium scale structure of the F-region N90-11372
Polar F layer lacuna irregularities at Dumont d'Urville N90-11379
Seasonal and geomagnetic response of the thermosphere and ionosphere N90-11380
Quiet time conductivities of the auroral ionosphere N90-11383
Auroral and sub-auroral F-layer irregularity studies in the Northern and Southern Hemisphere during the equinox transition study September 16-26, 1984 N90-11393
Examples of meteorological behavior of the ionosphere N90-11395
Multistation/multiparameter observations with a network of digital ionosondes N90-11396
Coordinated multi-parameter measurements and predictions of the global-scale ionosphere N90-11397
An ionospheric model for HF sky-wave backscatter radar N90-11401
Ionospheric total electron content, and far ultraviolet, near infrared oxygen emission N90-11410
F 2 REGION
North-south tropical F2 layer asymmetry at west AFrican and Pacific longitudes N90-11398
Radio propagation conditions forecast above a low latitude region N90-11400
F-15 AIRCRAFT
Nonlinear maneuver autopilot for the F-15 aircraft
[NASA-CR-179442] N90-11487
F-18 AIRCRAFT
CF 18 480 Gallon External Fuel Tank Stores Clearance Program N90-10877
FABRICATION
CuInSe2 solar cell research by sputter deposition
[DE89-009450] N90-11345
Novel thin-film CuInSe2 fabrication
[DE89-009440] N90-11604
FABRICS
Design of ceramic fabric heat pipe with water working fluid
[DE89-016565] N90-11265
FADDEEV EQUATIONS
Some exact solutions of the three-identical-particle problem with S-wave inverse square potentials
[DE89-618402] N90-11524
FAILURE MODES
Independent Orbiter Assessment (IOA): Analysis of the manned maneuvering unit
[NASA-CR-185565] N90-10913
Independent Orbiter Assessment (IOA): Assessment of the electrical power generation/fuel cell powerplant subsystem FMEA/CIL
[NASA-CR-185562] N90-10914
Independent Orbiter Assessment (IOA): Analysis of the electrical power generation/fuel cell powerplant subsystem
[NASA-CR-185561] N90-10915
Independent Orbiter Assessment (IOA): Analysis of the rudder/speed brake subsystem
[NASA-CR-185560] N90-10916
Independent Orbiter Assessment (IOA): Assessment of the data processing system FMEA/CIL
[NASA-CR-185546] N90-10917
Independent Orbiter Assessment (IOA): Analysis of the electrical power generation/power reactant storage and distribution subsystem
[NASA-CR-185556] N90-10918
Independent Orbiter Assessment (IOA): Analysis of the orbital maneuvering system
[NASA-CR-185554] N90-10919
Independent Orbiter Assessment (IOA): Analysis of the guidance, navigation, and control subsystem
[NASA-CR-185555] N90-10920
Independent Orbiter Assessment (IOA): Analysis of the nose wheel steering subsystem
[NASA-CR-185548] N90-10921
Independent Orbiter Assessment (IOA): FMEA/CIL instructions and ground rules
[NASA-CR-185551] N90-10922
Independent Orbiter Assessment (IOA): Assessment of the electrical power generation/power reactant storage and distribution subsystem FMEA/CIL
[NASA-CR-185545] N90-10923
Independent Orbiter Assessment (IOA): Analysis of the DPS subsystem
[NASA-CR-185549] N90-10924
Independent Orbiter Assessment (IOA): Analysis of the atmospheric revitalization pressure control subsystem
[NASA-CR-185593] N90-10925

Independent Orbiter Assessment (IOA): Analysis of the remote manipulator system
[NASA-CR-185585] N90-10926
Independent Orbiter Assessment (IOA): Analysis of the orbiter main propulsion system
[NASA-CR-185584] N90-10927
Independent Orbiter Assessment (IOA): Analysis of the instrumentation subsystem
[NASA-CR-185571] N90-10928
Independent Orbiter Assessment (IOA): Analysis of the ascent thrust vector control actuator subsystem
[NASA-CR-185579] N90-10929
Independent Orbiter Assessment (IOA): Analysis of the body flap subsystem
[NASA-CR-185574] N90-10930
Independent Orbiter Assessment (IOA): Analysis of the auxiliary power unit
[NASA-CR-185568] N90-10931
Independent Orbiter Assessment (IOA): Analysis of the backup flight system
[NASA-CR-185567] N90-10932
Independent Orbiter Assessment (IOA): Analysis of the electrical power distribution and control/electrical power generation subsystem
[NASA-CR-185538] N90-10933
Independent Orbiter Assessment (IOA): Analysis of the hydraulics/water spray boiler subsystem
[NASA-CR-185541] N90-10934
Independent Orbiter Assessment (IOA): Analysis of the elevon subsystem
[NASA-CR-185576] N90-10935
Independent Orbiter Assessment (IOA): Analysis of the electrical power distribution and control/remote manipulator system subsystem
[NASA-CR-185526] N90-10936
Independent Orbiter Assessment (IOA): Analysis of the extravehicular mobility unit
[NASA-CR-185540] N90-10937
Independent Orbiter Assessment (IOA): Analysis of the reaction control system, volume 1
[NASA-CR-185532-VOL-1] N90-10938
Independent Orbiter Assessment (IOA): Analysis of the reaction control system, volume 2
[NASA-CR-185532-VOL-2] N90-10939
Independent Orbiter Assessment (IOA): Analysis of the reaction control system, volume 3
[NASA-CR-185532-VOL-3] N90-10940
Independent Orbiter Assessment (IOA): Analysis of the electrical power distribution and control subsystem, volume 1
[NASA-CR-185529-VOL-1] N90-10941
Independent Orbiter Assessment (IOA): Analysis of the electrical power distribution and control subsystem, volume 2
[NASA-CR-185529-VOL-2] N90-10942
Independent Orbiter Assessment (IOA): Analysis of the landing/deceleration subsystem
[NASA-CR-185569] N90-10943
Independent Orbiter Assessment (IOA): Analysis of the mechanical actuation subsystem
[NASA-CR-185525] N90-10944
Independent Orbiter Assessment (IOA): Analysis of the pyrotechnics subsystem
[NASA-CR-185530] N90-10945
Independent Orbiter Assessment (IOA): Assessment of the pyrotechnics subsystem
[NASA-CR-185531] N90-10946
Independent Orbiter Assessment (IOA): Assessment of the nose wheel steering subsystem
[NASA-CR-185533] N90-10947
Independent Orbiter Assessment (IOA): Weibull analysis report
[NASA-CR-185534] N90-10948
Independent Orbiter Assessment (IOA): Assessment of the purge, vent and drain subsystem
[NASA-CR-185535] N90-10949
Independent Orbiter Assessment (IOA): Assessment of the extravehicular mobility unit, volume 1
[NASA-CR-185536-VOL-1] N90-10950
Independent Orbiter Assessment (IOA): Assessment of the extravehicular mobility unit, volume 2
[NASA-CR-185536-VOL-2] N90-10951
Independent Orbiter Assessment (IOA): Assessment of the mechanical actuation subsystem, volume 1
[NASA-CR-185527-VOL-1] N90-10952
Independent Orbiter Assessment (IOA): Assessment of the mechanical actuation subsystem, volume 2
[NASA-CR-185527-VOL-2] N90-10953
Independent Orbiter Assessment (IOA): CIL issues resolution report, volume 1
[NASA-CR-185524-VOL-1] N90-10954
Independent Orbiter Assessment (IOA): CIL issues resolution report, volume 2
[NASA-CR-185524-VOL-2] N90-10955
Independent Orbiter Assessment (IOA) CIL issues resolution report, volume 3
[NASA-CR-185524-VOL-3] N90-10956
Independent Orbiter Assessment (IOA): Assessment of the atmospheric revitalization pressure control subsystem FMEA/CIL
[NASA-CR-185594] N90-10957
Independent Orbiter Assessment (IOA): Analysis of the crew equipment subsystem
[NASA-CR-185591] N90-10958
Independent Orbiter Assessment (IOA): Assessment of the ascent thrust vector control actuator subsystem FMEA/CIL
[NASA-CR-185590] N90-10959
Independent Orbiter Assessment (IOA): FMEA/CIL assessment
[NASA-CR-185589] N90-10960
Independent Orbiter Assessment (IOA): Assessment of the displays and controls subsystem
[NASA-CR-185588] N90-10961
Independent Orbiter Assessment (IOA): Assessment of the Orbiter Experiment (OEX) subsystem
[NASA-CR-185587] N90-10962
Independent Orbiter Assessment (IOA): Analysis of the Orbiter Experiment (OEX) subsystem
[NASA-CR-185586] N90-10963
Independent Orbiter Assessment (IOA): Assessment of the remote manipulator system FMEA/CIL
[NASA-CR-185592] N90-10964
Independent Orbiter Assessment (IOA): Assessment of the EPD and C/remote manipulator system FMEA/CIL
[NASA-CR-185583] N90-10965
Independent Orbiter Assessment (IOA): Assessment of the landing/deceleration (LDG/DEC) subsystem FMEA/CIL
[NASA-CR-185570] N90-10966
Independent Orbiter Assessment (IOA): Analysis of the communication and tracking subsystem
[NASA-CR-185582] N90-10967
Independent Orbiter Assessment (IOA): Assessment of the body flap subsystem FMEA/CIL
[NASA-CR-185575] N90-10968
Independent Orbiter Assessment (IOA): Analysis of the purge, vent and drain subsystem
[NASA-CR-185547] N90-10969
Independent Orbiter Assessment (IOA): Assessment of the elevon actuator subsystem FMEA/CIL
[NASA-CR-185578] N90-10970
Independent Orbiter Assessment (IOA): Assessment of the crew equipment subsystem
[NASA-CR-185577] N90-10971
Independent Orbiter Assessment (IOA): Assessment of instrumental subsystem FMEA/CIL
[NASA-CR-185572] N90-10972
Independent Orbiter Assessment (IOA): Assessment of the backup flight system FMEA/CIL
[NASA-CR-185566] N90-10973
Independent Orbiter Assessment (IOA): Assessment of the manned maneuvering unit
[NASA-CR-185564] N90-10974
Independent Orbiter Assessment (IOA): Assessment of the rudder/speed brake subsystem FMEA/CIL
[NASA-CR-185558] N90-10975
Independent Orbiter Assessment (IOA): Assessment of the auxiliary power unit
[NASA-CR-185580] N90-10976
Independent Orbiter Assessment (IOA): Assessment of the life support and airlock support systems, volume 1
[NASA-CR-185581-VOL-1] N90-10977
Independent Orbiter Assessment (IOA): Assessment of the life support and airlock support systems, volume 2
[NASA-CR-185581-VOL-2] N90-10978
Independent Orbiter Assessment (IOA): Assessment of the active thermal control system
[NASA-CR-185573] N90-10979
Failure modes and mechanisms in nickel alloys: Primarily austenitic stainless steel
[DE89-016823] N90-11132

FAN BLADES
Laser anemometer measurements in a transonic axial-flow fan rotor
[NASA-TP-2879] N90-11245

FAR ULTRAVIOLET RADIATION
Ionospheric total electron content, and far ultraviolet, near infrared oxygen emission N90-11410

FARADAY EFFECT
Sensors for nondestructive testing and evaluation of materials
[DE89-014763] N90-11279

FARM CROPS
Assessment of crop response to increases in atmospheric carbon dioxide concentrations: Summary of research progress report, July 1, 1988--June 30, 1989
[DE89-016251] N90-11360

FATIGUE LIFE
Study of a gallium arsenide solar cell interconnector N90-11033

FATIGUE TESTS
Worked-in holes in three-dimensional reinforced composites N90-11060

FAULT TOLERANCE
Applications of the hybrid automated reliability predictor: Revised edition
[NASA-TP-2760-REV] N90-11454
Experiments in fault tolerant software reliability
[NASA-CR-185927] N90-11460

FEASIBILITY
Can ion acceleration by double-cyclotron absorption produce O(+) ion conics
[IRF-PREPRINT-114] N90-11600

FEASIBILITY ANALYSIS
Development of the large spacecraft structure N90-11020
Transient vibration testing of spacecraft structures. Experience with multiaxial base motion and combined base motion and point force excitation N90-11039
Advanced Turbine Technology Applications Program, (ATTAP): A plan for improving the prototype production of ceramic components for the gas turbine engine, 1988--1992
[DE89-015566] N90-11320

FEED SYSTEMS
Thin section casting program. Volume 5: Westinghouse MHD Project
[DE89-009035] N90-11203

FEEDBACK CIRCUITS
Transfer functions for nonlinear systems via Fourier-Borel transforms
[NASA-TM-100034] N90-10828

FEEDBACK CONTROL
Optimal and on-board near-optimal midcourse guidance N90-10857
Flight test results of a complex precise digital flight control system N90-10870

FERMI LIQUIDS
A fermi liquid electric structure and the nature of the carriers in high-T(sub c) cuprates: A photoemission study
[DE89-016774] N90-11624

FERMIONS
Studies of novel superconductors
[DE89-016744] N90-11609

FERROELECTRICITY
Behaviour of VF(sub 2)/VF(sub 3) piezoelectric copolymers under shock loading
[DE89-016538] N90-11145
Chevron layer structures in Surface Stabilized Ferroelectric Liquid Crystal (SSFLC) cells filled with a material which exhibits the chiral nematic to smectic C* phase transition
[DE89-016985] N90-11628

FERROMAGNETIC MATERIALS
Spin fluctuations and excitations in a 2D xy-ferromagnet: CoCl2 in graphite
[DE89-017600] N90-11119
Investigations of the influence of magnetically long range ordered phases on the electronic charge transport in metallic glasses
[ETN-89-94672] N90-11155

FIBER COMPOSITES
Hygrothermal deformations of composite shells N90-11055
Composites reinforced with thermotropic liquid crystal copolyester fibers
[AD-A211226] N90-11089
Interfacial adsorption and crystallization of polycarbonate in carbon fiber composites
[AD-A211230] N90-11090

FIBER OPTICS
Fiber optic technique for surveillance and control of mine fields
[FOA-C-30526-3.1] N90-11293
Fiber optics: A brief introduction
[DE89-009337] N90-11567
Adaptive gigabit fiber optics local area network
[AD-A210794] N90-11571

FIBERS
Solid fiber Z-pinches: Cold-start computations
[DE89-016768] N90-11592

FIELD ALIGNED CURRENTS
Electrostatic turbulence in the high latitude ionosphere N90-11392

FIELD THEORY (PHYSICS)
On some stochastic properties of the infinitely dimensional Hamiltonian systems of classical mechanics
[DE89-618403] N90-11525
Three level constraints on conformal field theories and string models
[DE89-016942] N90-11634

Superfiled formulation of Chern-Simons supersymmetry
[DE89-618459] N90-11636
General action for topological quantum field theories
[DE89-618460] N90-11637
Moduli spaces and topological quantum field theories
[DE89-016943] N90-11639

FINITE DIFFERENCE THEORY
Direct discretization of planar div-curl problems
[NASA-CR-181935] N90-11498

FINITE ELEMENT METHOD
Updating of finite element model by means of normal mode parameters N90-10992
Parametric identification of conservative self adjoint structures N90-10994
Employment of modal survey methodologies in dynamic analysis procedures N90-11006
Experiences using a major FEM package interactively for spacecraft applications N90-11008
Numerical analysis of nonlinear viscoelastic structures: Application to elastomers and rubber-like materials N90-11013
Nonlinear collapse simulation of anisotropic plates and corrugated panels N90-11035
Numerical models for exterior and interior fluid-structure interaction problems N90-11073
Exploitation of data management facilities for finite element analysis in aerospace structural engineering applications N90-11078
Accelerated aging of metal matrix composites N90-11085
On a Taylor Weak Statement for finite element computations in gas dynamics N90-11251
A finite element formulation for inelastic plates and shells based on a mixed variational principle N90-11334
An analytical and experimental study of the elastodynamic response characteristics of planar linkage mechanism with bearing clearances N90-11336

FINITE VOLUME METHOD
A nonoscillatory, characteristically convected, finite volume scheme for multidimensional convection problems
[NASA-TM-102354] N90-11497
Direct discretization of planar div-curl problems
[NASA-CR-181935] N90-11498

FIXED POINTS (MATHEMATICS)
Fixed point iteration on point-symmetric interference graphs
[MEMO-INF-89-23] N90-11535

FLAMEOUT
In flight relight tests on AM-X single engine fly-by-wire aircraft N90-10869

FLAPS (CONTROL SURFACES)
Independent Orbiter Assessment (IOA): Analysis of the body flap subsystem
[NASA-CR-185574] N90-10930
Independent Orbiter Assessment (IOA): Assessment of the body flap subsystem FMEA/CIL
[NASA-CR-185575] N90-10968

FLAT PLATES
Linear instability of supersonic plane wakes
[NASA-CR-181911] N90-10833
Nonprincipal-plane scattering from flat plates: Second-order and corner diffraction and pattern control of horn antennas
[NASA-CR-185485] N90-11205
Part A: Nonprincipal-plane scattering from flat plates: Second-order and corner diffractions N90-11206

FLEXIBLE BODIES
Frequency domain design of robust controllers for space structures
[AD-A211172] N90-10985
GEMMES: A new tool for dynamic modeling N90-11005
Use of Lanczos vectors in structural dynamics N90-11011
Control and optimization for observations of systems governed by controlled partial differential equations
[AD-A211122] N90-11513
Guaranteed cost control of flexible space structures N90-11643

FLIGHT CHARACTERISTICS
GRATE: A new flight test tool for flying qualities evaluation N90-10868

FLIGHT CONTROL
A320 flight tests: Particularities and innovations N90-10864
Real-time flight test analysis and display techniques for the X-29A aircraft N90-10866
Flight test results of a complex precise digital flight control system N90-10870
An assessment of robustness of flight control systems based on variable structure techniques N90-10895
Independent Orbiter Assessment (IOA): Analysis of the body flap subsystem
[NASA-CR-185574] N90-10930
Independent Orbiter Assessment (IOA): Analysis of the backup flight system
[NASA-CR-185567] N90-10932
Independent Orbiter Assessment (IOA): Analysis of the hydraulics/water spray boiler subsystem
[NASA-CR-185541] N90-10934
Independent Orbiter Assessment (IOA): Assessment of the ascent thrust vector control actuator subsystem FMEA/CIL
[NASA-CR-185590] N90-10959
Independent Orbiter Assessment (IOA): Assessment of the backup flight system FMEA/CIL
[NASA-CR-185566] N90-10973

FLIGHT CREWS
Task analysis of the UH-60 mission and decision rules for developing a UH-60 workload prediction model. Volume 1: Summary report
[AD-A210763] N90-11446

FLIGHT INSTRUMENTS
Flight simulator evaluation of a head-down display
[NAL-TM-573] N90-10898
On the motion equation of an elastically supported two degree of freedon gyro
[NAL-TM-568] N90-11276

FLIGHT MECHANICS
On the development of a basic flight test capability and some related research projects N90-10885
Realtime processing and display N90-10886
Flight-mechanical environment on Ariane launch vehicle payloads N90-11048

FLIGHT PLANS
Ground and Obstacle Avoidance (GOA) concept of operations
[DOT/FAA/DS-89/08] N90-10855

FLIGHT SAFETY
See and avoid/cockpit visibility
[DOT/FAA/CT-TN89/18] N90-10843
The Air Force Flight Test Center Flight Test Safety Program N90-10872

FLIGHT SIMULATION
Flight Test Techniques
[AGARD-CP-452] N90-10860
ATTAS flight testing experiences N90-10862
GRATE: A new flight test tool for flying qualities evaluation N90-10868
Flight testing of the Tornado Terrain Following System N90-10875
Identification Friend, Foe or Neutral Joint Test N90-10881
Flight simulator evaluation of a head-down display
[NAL-TM-573] N90-10898
Flight simulation test facility: Function and specification of the simulator cockpit system
[NAL-TM-577] N90-10899
Advanced manned space flight simulation and training: An investigation of simulation host computer system concepts
[NASA-CR-185998] N90-10911

FLIGHT SIMULATORS
Advanced manned space flight simulation and training: An investigation of simulation host computer system concepts
[NASA-CR-185998] N90-10911

FLIGHT TESTS
Flight Test Techniques
[AGARD-CP-452] N90-10860
US Navy principal site testing concept and the F-18 N90-10861
ATTAS flight testing experiences N90-10862
P-180 AVANTI: Project and flight test program comprehensive overview N90-10863
A320 flight tests: Particularities and innovations N90-10864
The Experimental Aircraft Flight Test Programme N90-10865
Real-time flight test analysis and display techniques for the X-29A aircraft N90-10866
Flight test techniques adopted by Avions Marcel Dassault-Breguet Aviation N90-10867
GRATE: A new flight test tool for flying qualities evaluation N90-10868
In flight relight tests on AM-X single engine fly-by-wire aircraft N90-10869
Flight test results of a complex precise digital flight control system N90-10870
Analysis of flutter tests with the use of a telemetry system N90-10871
The Air Force Flight Test Center Flight Test Safety Program N90-10872
Results and practical experience using parameter identification techniques on the AM-X program at Aermacchi N90-10873
Lessons learned from the integration of flight systems N90-10874
Flight testing of the Tornado Terrain Following System N90-10875
Evaluation of store carriage (and release) environment using flight instrumented stores N90-10876
CF 18 480 Gallon External Fuel Tank Stores Clearance Program N90-10877
Flow visualization techniques for flight research N90-10878
Flight testing a newly-designed stand-off weapon dispenser N90-10880
Flight testing and flight research: From the age of the tower jumper to the age of the astronaut N90-10882
Flight testing in the Netherlands: An overview N90-10884
On the development of a basic flight test capability and some related research projects N90-10885
Flight test instrumentation and data processing at British Aerospace, Warton, U.K. N90-10887
Heliport surface maneuvering test results
[ACD-330] N90-10897

FLOOD PREDICTIONS
Relation of wind field and buoyancy to rainfall inferred from radar
[PB89-208326] N90-11424

FLOW CHARACTERISTICS
Wall-layer eruptions in turbulent flows
[NASA-TM-102362] N90-11250
A computational/experimental study of the flow around a body of revolution at angle of attack
[NASA-TM-88329] N90-11254
Development of an adaptive time of flight system for the measurement of fluid flow velocity N90-11273

FLOW DIRECTION INDICATORS
Study for optimization of redundant vane-type flow-direction sensing systems and numerical analysis for design of the systems
[NAL-TM-571] N90-10890

FLOW DISTRIBUTION
Low-Reynolds-number modeling of complex flows with and without density variation N90-10832
Linear instability of supersonic plane wakes
[NASA-CR-181911] N90-10833
User's manual for PEPSIG NASA tip vortex version
[NASA-CR-182178] N90-10835
Computation of the tip vortex flowfield for advanced aircraft propellers
[NASA-CR-182179] N90-10836
In-situ study of the chemically driven flow fields in initiating homogeneous and heterogeneous nitromethane explosives
[DE89-008415] N90-11186
Numerical solutions of turbulent flow with heat transfer over rough surfaces N90-11246
An experimental investigation of transition in oscillating pipe flow N90-11249
Method of characteristic studies for rotational flow downstream of a curved shock wave N90-11252
Computation of transient three-dimensional interstage flowfields using the arbitrary Lagrangian-Eulerian method N90-11253
Rectangular subsonic jet flow field measurements
[NASA-CR-185962] N90-11255
A laser Doppler anemometry investigation of single-phase and particle-laden jet flows
[AD-A210660] N90-11261
Questions from the Willmarth Workshop on New Directions in Research on Turbulent Wall-Layer Structures
[AD-A211282] N90-11264
A nonoscillatory, characteristically convected, finite volume scheme for multidimensional convection problems
[NASA-TM-102354] N90-11497
On transonic flow over segmented slotted wind tunnel wall with mass transfer N90-11676

FLOW EQUATIONS
A conforming spectral collocation strategy for Stokes flow through a channel contraction
[NASA-CR-181912] N90-11495
Direct discretization of planar div-curl problems
[NASA-CR-181935] N90-11498

FLOW GEOMETRY
A parallel numerical simulation for supersonic flows using zonal overlapped grids and local time steps for common and distributed memory multiprocessors
[DE89-015252] N90-10839

FLOW MEASUREMENT
Jet-flow from shock tubes
[AD-A210651] N90-11260
Development of an adaptive time of flight system for the measurement of fluid flow velocity N90-11273

FLOW VELOCITY
Laser anemometer measurements in a transonic axial-flow fan rotor
[NASA-TP-2879] N90-11245
The structure of Reynolds stress in the near wall region of a turbulent pipe flow N90-11247

An experimental study of helicity and related properties in turbulent flows
[DE89-016785] N90-11259
Gas-phase flowrate effect on disintegrating cryogenic liquid jets
[NASA-TM-102357] N90-11277

FLOW VISUALIZATION
Flow visualization techniques for flight research N90-10878
The near-wake flow structure of wake-cylinder interaction and surface loading of cylinder N90-11248

FLOWMETERS
Development of an adaptive time of flight system for the measurement of fluid flow velocity N90-11273

FLUID DYNAMICS
Quasi-diffusion between phonon and roton gases in two- and three-dimensional liquid helium
[AD-A210565] N90-11096

FLUID FLOW
An atmospheric pressure flow reactor: Gas phase kinetics and mechanism in tropospheric conditions without wall effects N90-11160
On a Taylor Weak Statement for finite element computations in gas dynamics N90-11251
Development of an adaptive time of flight system for the measurement of fluid flow velocity N90-11273

FLUID JETS
The decay of viscoelastic fluid jets
[ETN-89-94667] N90-11270

FLUID MANAGEMENT
Evaluation of supercritical cryogen storage and transfer systems for future NASA missions
[NASA-TM-102394] N90-10912
Evolutionary space station fluids management strategies
[NASA-CR-185137] N90-10983

FLUID MECHANICS
Flow visualization techniques for flight research N90-10878

FLUID-SOLID INTERACTIONS
Modal analysis of fluid-structure systems by parallel subspace iteration N90-11024
Numerical models for exterior and interior fluid-structure interaction problems N90-11073

FLUORIDES
Design and construction of systems for the single-crystals growth of ternary silver halides, alkali halides, and alkaline earth fluorides, and the dielectric investigation of silver halide
[ETN-89-94673] N90-11632

FLUORINATION
Reactive ion etching of SiC thin films by mixtures of fluorinated gases and oxygen
[AD-A211046] N90-11113

FLUORINE COMPOUNDS
Electrolyte dependence of charge injection processes for electroactive polymer films
[AD-A210787] N90-11152

FLUTTER ANALYSIS
Analysis of flutter tests with the use of a telemetry system N90-10871

FLUX PINNING
Pinning of curved flux lines on the boundary between two phases of high temperature superconductors
[DE89-618865] N90-11614

FLY BY WIRE CONTROL
ATTAS flight testing experiences N90-10862
In flight relight tests on AM-X single engine fly-by-wire aircraft N90-10869

FOCUSING
Nonlinear acoustics: Reflection and refraction, propagation in a periodic waveguide, scattering of sound by sound and ellipsoidal focusing
[AD-A211224] N90-11550

FOLDING STRUCTURES
Test results on conceptual models of the large deployable antenna for mobile communications satellites N90-11050

FORECASTING
Joint VHF coherent radar and oblique sounder observations for short term ionosphere forecasting N90-11399
Radio propagation conditions forecast above a low latitude region N90-11400

FOREST FIRES
Analysis of forest fire smoke using satellite imagery
[AD-A210657] N90-11339

FOSSIL FUELS
The effect of degree of aromaticity and alkyl substitution of polyaromatic hydrocarbons on instrumental response factors
[DE89-000761] N90-11117

FOURIER SERIES
Transfer functions for nonlinear systems via Fourier-Borel transforms
[NASA-TM-100034] N90-10828

FOURIER TRANSFORMATION
Frequency domain aerodynamic analysis of interacting rotating systems N90-10837
Evaluation of dispersive behavior in periodic structures by discrete Fourier transform N90-11014
Gridded environmental data compaction: An investigation
[AD-A210580] N90-11430
Computing the two dimensional fast Fourier transform on a general purpose mesh connected multiprocessor
[DE89-016515] N90-11518

FRACTOGRAPHY
Effect of thermal and cyclic loads on silicon carbide yarn reinforced glass matrix composites
[DE89-016554] N90-11091
A technique to correlate fractography with NDE (Non-Destructive Evaluation) of small samples
[DE89-016904] N90-11325

FRACTURE MECHANICS
Review of the ESA fracture control policy N90-11029
A re-evaluation of fatigue threshold test procedures and the simulation and prediction of fatigue crack growth under conditions of low crack closure N90-11328

FRACTURES (MATERIALS)
Review of the ESA fracture control policy N90-11029

FRACTURING
Review of the ESA fracture control policy N90-11029
Microstructural effects on spall fracture in 1008 steel
[DE89-016770] N90-11131

FREE CONVECTION
Pressure correction splitting methods for the computation of oscillatory free convection in low Pr fluids
[CWI-NM-R8816] N90-11271

FREE ELECTRON LASERS
A compact X-ray free electron laser
[DE89-017236] N90-11297
Free-electron laser theory
[DE89-620145] N90-11298
Stability requirements of RF linac-driven free-electron lasers
[DE89-016609] N90-11303
Minimized emittance growth with elliptical beam pipes in FEL (Free-Electron Laser)
[DE89-016982] N90-11305
Synchrotron radiation, free electron laser, and nuclear structure
[DE89-017352] N90-11306

FREE FLOW
Chemical reactions in turbulent mixing flows
[AD-A211240] N90-11263

FREE-PISTON ENGINES
Free-Piston Stirling Engine magnetically coupled heat pump: Critical component evaluation
[DE89-015646] N90-11316
Dynamic characteristics concerned in the design of a free-piston Stirling engine/magnetic coupling/compressor system
[DE89-015981] N90-11317

FREQUENCY DIVISION MULTIPLEXING
Adaptive gigabit fiber optics local area network
[AD-A210794] N90-11571

FREQUENCY MEASUREMENT
Quantitative methods for waves in space plasmas
[PB89-210256] N90-11599

FREQUENCY MODULATION
Laser dynamics: The system dynamics and network theory of optoelectronic integrated circuit design N90-11296

FRICTION
Analytical study of mistuning/friction/aerodynamics interaction in a bladed disk assembly
[AD-A211139] N90-10893

FROST DAMAGE
Definition of research needs to address airport pavement distress in cold regions
[DOT/FAA/DS-89/13] N90-10896

FUEL CELLS
Independent Orbiter Assessment (IOA): Assessment of the electrical power generation/fuel cell powerplant subsystem FMEA/CIL
[NASA-CR-185562] N90-10914
Independent Orbiter Assessment (IOA): Analysis of the electrical power generation/fuel cell powerplant subsystem
[NASA-CR-185561] N90-10915
Independent Orbiter Assessment (IOA): Analysis of the electrical power generation/power reactant storage and distribution subsystem
[NASA-CR-185556] N90-10918

FUEL COMBUSTION
Turbulent reacting flows in solid-propellant ducted rocket combustors N90-11079
Evaporation and combustion of dense sprays with a bimodal droplet size distribution N90-11094

FUEL CONSUMPTION
Results from the second year of operation of the Federal Methanol Fleet at Argonne National Laboratory
[DE89-016935] N90-11319
View on recent fuel costs in airlines
[NAL-TM-569] N90-11653

FUEL PRODUCTION
Production of jet fuels from coal-derived liquids. Volume 11: Production of advanced endothermic fuel blends from Great Plains Gasification Plant naphtha by-product stream
[AD-A210251] N90-11184

FUEL SPRAYS
Evaporation and combustion of dense sprays with a bimodal droplet size distribution N90-11094

FUEL TANKS
CF 18 480 Gallon External Fuel Tank Stores Clearance Program N90-10877

FUELS
View on recent fuel costs in airlines
[NAL-TM-569] N90-11653

FUNCTIONAL ANALYSIS
Impulse time-integral function and Lagrangian analysis
[DE89-016997] N90-11268

FUNCTIONAL DESIGN SPECIFICATIONS
Ariane 5 structural design and development N90-11057
Engineering specification and system design for CAD/CAM of custom shoes. Phase 5: UMC involvement (January 1, 1989 - June 30, 1989)
[NASA-CR-185838] N90-11456

FUNCTIONS (MATHEMATICS)
Impulse time-integral function and Lagrangian analysis
[DE89-016997] N90-11268
Backward analysis on higher order functions
[MEMO-INF-89-19] N90-11526
An axiomatic theory for partial functions
[MEMO-INF-89-22] N90-11527

FUSELAGES
Measurements of pressures on the tail and aft fuselage of an airplane model during rotary motions at spin attitudes
[NASA-TP-2939] N90-10829

FUSION (MELTING)
Thermodynamic principles of the process of the effect of electromagnetic fields on a polymer melt
[AD-A210698] N90-11149

G

GALACTIC CLUSTERS
New statistical approaches to galaxy clustering N90-11674

GALACTIC EVOLUTION
IRAS observations of the extended galactic objects Cas A and W80 N90-11657

GALACTIC NUCLEI
Spectropolarimetry, variability, and the taxonomy of active galactic nuclei N90-11667

GALACTIC STRUCTURE
The mass distribution in the galactic centre estimated from OH/IR stars
[PB89-154884] N90-11663

GALERKIN METHOD
Estimation on nonlinear damping in second order distributed parameter systems
[NASA-CR-181890] N90-11494

GALILEO PROJECT
Shuttle Atlantis to deploy Galileo probe toward Jupiter
[NASA-TM-101888] N90-10982

GALILEO SPACECRAFT
Shuttle Atlantis to deploy Galileo probe toward Jupiter
[NASA-TM-101888] N90-10982

GALLIUM
Ion beam annealing of Ga-implanted Si
[DE89-016857] N90-11610

GALLIUM ARSENIDES
Study of a gallium arsenide solar cell interconnector N90-11033
Laser altimeter for use over the ocean
[AD-A211252] N90-11286
Semiconductor quantum well lasers and related optoelectronic devices on silicon, III-V
[AD-A210758] N90-11299
GaAs ASIC design case study
[DE89-013934] N90-11461
Thermodynamics, kinetics, and interface morphologies of phase formation reactions between metals and Gallium Arsenide: Bulk vs thin-film studies
[DE89-016469] N90-11621
Strain and density dependent valence-band masses in InGaAs/GaAs and GaAs/GaAsP strained-layer structures
[DE89-016882] N90-11627

GALLIUM PHOSPHIDES
Strain and density dependent valence-band masses in InGaAs/GaAs and GaAs/GaAsP strained-layer structures
[DE89-016882] N90-11627
GAMMA RAY BEAMS
Investigations into the influence of the state functions on the cross sections of the direct p,gamma reactions at energies in the 100 keV range, and project of a cascade accelerator for the measurement of the p,gamma capture cross sections
[ETN-89-94662] N90-11561
GAMMA RAY OBSERVATORY
A liquid xenon imaging telescope for 1-30 MeV gamma-ray astrophysics
[NASA-CR-185999] N90-11662
GAMMA RAY SPECTRA
Gamma radiation background measurements from Spacelab 2
[NASA-CR-183782] N90-11689
GAMMA RAY SPECTROMETERS
X-ray and gamma-ray spectroscopy of solids under pressure
[DE89-017271] N90-11118
GAMMA RAYS
MOXE: An X-ray all-sky monitor for Soviet Spectrum-X-Gamma Mission
[NASA-TM-101266] N90-11280
Airborne gamma radiation snow water equivalent and soil moisture measurements and satellite areal extent of snow cover measuerments: A user's guide, version 3.0
[PB89-177877] N90-11338
Gamma radiation background measurements from Spacelab 2
[NASA-CR-183782] N90-11689
GAS CHROMATOGRAPHY
The effect of degree of aromaticity and alkyl substitution of polyaromatic hydrocarbons on instrumental response factors
[DE89-000761] N90-11117
GAS COMPOSITION
NCAR (National Center for Atmospheric Research) master mechanism of the gas phase chemistry, version 2.0
[PB89-208979] N90-11413
GAS DETECTORS
Independent Orbiter Assessment (IOA): Assessment of the purge, vent and drain subsystem
[NASA-CR-185535] N90-10949
Independent Orbiter Assessment (IOA): Analysis of the purge, vent and drain subsystem
[NASA-CR-185547] N90-10969
The Third Conference on the Environmental Chemistry of Hydrazine Fuels
[AD-A197632] N90-11157
Microsensor and pattern recognition techniques in hydrazine detection N90-11177
Hydrazine dosimetry N90-11178
Description of a chemiluminescence detector system specifically designed for monitoring airborne hydrazine and oxidizer propellant vapors N90-11179
Low ppb level detection of toxic compounds with a fully automated CO2 laser photoacoustic detector N90-11181
GAS DYNAMICS
Particle kinetic simulation of high altitude hypervelocity flight
[NASA-CR-186003] N90-10840
On a Taylor Weak Statement for finite element computations in gas dynamics N90-11251
Method of characteristic studies for rotational flow downstream of a curved shock wave N90-11252
Gas dynamical processes in the theory of galaxy formation N90-11673
GAS EXCHANGE
Micrometeorological investigation of surface exchange of trace gases: A case study
[PB89-208375] N90-11412
GAS FLOW
Gas-phase flowrate effect on disintegrating cryogenic liquid-jets
[NASA-TM-102357] N90-11277
GAS GENERATORS
Independent Orbiter Assessment (IOA): Weibull analysis report
[NASA-CR-185534] N90-10948
A simulator for a hydrocarbon ramrocket fuel gas generator: First phase development
[AR-005-621] N90-11080
GAS JETS
Gas-phase flowrate effect on disintegrating cryogenic liquid-jets
[NASA-TM-102357] N90-11277
GAS METERS
A new inexpensive electrochemical meter for oxygen in sodium coolant
[DE89-630802] N90-11104
GAS MIXTURES
Reactive ion etching of SiC thin films by mixtures of fluorinated gases and oxygen
[AD-A211046] N90-11113
GAS SPECTROSCOPY
Forty-fourth symposium on molecular spectroscopy
[AD-A210752] N90-11111
GAS TUNGSTEN ARC WELDING
Material properties of 2219-T851 aluminum alloy plasma welded compared to TIG welding N90-11032
GAS TURBINE ENGINES
Advanced technologies impact on compressor design and development: A perspective
[NASA-TM-102341] N90-10891
Advanced Turbine Technology Applications Program, (ATTAP): A plan for improving the prototype production of ceramic components for the gas turbine engine, 1988--1992
[DE89-015566] N90-11320
GAS-SOLID INTERACTIONS
Theoretical investigation of gas-surface interactions
[NASA-CR-185492] N90-11552
GASEOUS DIFFUSION
Quasi-diffusion between phonon and roton gases in two- and three-dimensional liquid helium
[AD-A210565] N90-11096
GASES
Reactive ion etching of SiC thin films by mixtures of fluorinated gases and oxygen
[AD-A211046] N90-11113
GASIFICATION
Production of jet fuels from coal-derived liquids. Volume 11: Production of advanced endothermic fuel blends from Great Plains Gasification Plant naphtha by-product stream
[AD-A210251] N90-11184
GAUGE INVARIANCE
Gauge invariant cosmological perturbations with cold dark matter
[DE89-790940] N90-11679
GAUSS EQUATION
The fast Gauss transform
[AD-A211287] N90-11517
GEARS
Independent Orbiter Assessment (IOA): Weibull analysis report
[NASA-CR-185534] N90-10948
GELS
Applications of NMR spectroscopy to the study of zeolite synthesis
[DE89-015226] N90-11095
Fifth International Workshop on Glasses and Ceramics from Gels
[DE89-016899] N90-11147
GENERAL AVIATION AIRCRAFT
The spinning of aircraft: A discussion of spin prediction techniques including a chronological bibliography
[ARL-AERO-R-177] N90-10888
GEODESIC LINES
Local structure of a 2-codimensional conformally flat submanifold in an Euclidean space R(sup n+2)
[DE89-618379] N90-11501
GEODESY
Nonlinear adjustment with or without constraints, applicable to geodetic models
[AD-A210820] N90-11509
GEOMAGNETIC TAIL
Numerical study of the current sheet and PSBL in a magnetotail model
[NASA-CR-183289] N90-11669
GEOMAGNETISM
Short wavelength striations on expanding plasma clouds
[DE89-016585] N90-11416
GEOMETRICAL THEORY OF DIFFRACTION
Constitutive parameter measurements of lossy materials
[NASA-CR-183398] N90-11603
GEOMORPHOLOGY
Physiographic and geological setting of the Coastal Engineering Research Center's field research facility
[AD-A210772] N90-11356
GEOPOTENTIAL HEIGHT
Observational studies of low-frequency oscillations in the Southern Hemisphere N90-11420
GEOS 1 SATELLITE
Substorm associated pulsations: A study of plasmaspheric cavity resonance, mid-latitude polarisation and geostationary orbit signatures N90-11422
GEOS 2 SATELLITE
Substorm associated pulsations: A study of plasmaspheric cavity resonance, mid-latitude polarisation and geostationary orbit signatures N90-11422
GERMANIUM
High pressure 129I Moessbauer studies of GeI4 molecular crystals
[DE89-015269] N90-11620
GLASS
Effect of thermal and cyclic loads on silicon carbide yarn reinforced glass matrix composites
[DE89-016554] N90-11091
Fifth International Workshop on Glasses and Ceramics from Gels
[DE89-016899] N90-11147
Electrolyte dependence of charge injection processes for electroactive polymer films
[AD-A210787] N90-11152
Basic investigations of cutting machinability of inorganic glasses using single-point tools
[W-15/87] N90-11204
Acoustic studies of new materials: Quasicrystals, low-loss glasses and high Tc superconductors
[AD-A211281] N90-11551
GLASS COATINGS
Superconducting ceramics in the Bi1.5SrCaCu2O sub x system by melt quenching technique
[NASA-CR-185139] N90-11606
GLASS FIBERS
Y-Si-Al-O-N glass fibers
[AD-A211170] N90-11088
GLASSWARE
Low temperature properties of glasses N90-11141
GLIDE LANDINGS
Landing tests for Buran shuttle with jet engine-equipped mock-up N90-10904
GLOBAL POSITIONING SYSTEM
A high performance airborne INS/GPS Integrated Navigation System N90-10850
High accuracy coordinate determination using the global positioning system N90-10858
STS-GPS (Space Transportation System - Global Positioning System) tracking experiment for gravitation estimation: Feasibility study
[AD-A211265] N90-10859
GLOBULAR CLUSTERS
Effects of main-sequence mass loss on the turnoff ages of globular clusters
[DE89-016784] N90-11678
GLOVES
Concepts for microgravity experiments utilizing gloveboxes
[NASA-TM-100378] N90-11195
GOALS
PISCES program plasma-surface interactions research
[DE89-015622] N90-11578
GOGGLES
Night sky radiometric measurements during follow-on-evaluation testing of AN/PVS-7 (A, B) at Fort Benning, Georgia
[AD-A211273] N90-11574
GOVERNMENTS
The transfer and diffusion of new technologies: A review of the economics literature
[DE89-015671] N90-11655
GRAIN BOUNDARIES
Grain boundary chemistry in irradiated stainless steel and its influence on environmental degradation
[DE89-016827] N90-11125
Deformation induced microstructural and microchemical changes during thermomechanical treatment
[DE89-017266] N90-11127
Influence of core-shell grains on the internal stress state and permittivity response of zirconia modified barium titanate
[AD-A211245] N90-11153
Intergranular and interphase boundaries in ceramics
[DE89-016969] N90-11154
Kinetics and mechanisms of primary and steady state creep in B- and Al-containing alpha silicon carbide
[AD-A210739] N90-11616
GRAIN SIZE
Influence of grain refining on the casting, physical, mechanical, and electrochemical properties of technical aluminum
[ETN-89-94661] N90-11135
Investigation of commercial Al-Ti and Al-Ti-B master alloys and development of a new grain refining agent based on carbides for aluminum and aluminum alloys
[ETN-89-94663] N90-11136
GRAPHITE
Development of graphite-magnesium composites for space applications N90-11054

Modifications to the aerotherm charring material thermal response and ablation program (CMA) for carbon ablation analysis
[AD-A211069] N90-11115
Spin fluctuations and excitations in a 2D xy-ferromagnet: CoCl2 in graphite
[DE89-017600] N90-11119
Carbon in detonations
[DE89-016037] N90-11189

GRAPHITE-EPOXY COMPOSITES
Space environment effects on carbon/epoxy materials N90-11056
Delamination tests under static compression loading N90-11061

GRAVITATIONAL EFFECTS
A high precision gravity compensation system for the deployment test of the ERS-1 SAR antenna N90-11038
Effects of gravity on equilibrium crystal shapes N90-11602

GRAVITATIONAL FIELDS
STS-GPS (Space Transportation System - Global Positioning System) tracking experiment for gravitation estimation: Feasibility study
[AD-A211265] N90-10859
Gravitational nonminimally coupled electromagnetic fields: A possible solution to some idiosincrasies of Einstein-Maxwell theory
[DE89-618430] N90-11635
The thermal stability between rotating cylinders in a radially symmetrical gravitational field
[DE89-618548] N90-11638

GRAVITY WAVES
Non-linear wave-equations for low-frequency acoustic gravity waves N90-11365
Medium scale structure of the F-region N90-11372
On the influence of ionospheric conductivity on dispersion of acoustic gravity waves N90-11386
Atmospheric gravity waves in the auroral source region of TIDs, studied with the EISCAT CP2-data N90-11387

GREENHOUSE EFFECT
Potential effects of global climate change on the United States. Executive summary. Draft
[PB89-161046] N90-11350
Potential effects of global climate change on the United States. Volume 1: Regional studies. Draft
[PB89-161053] N90-11351
Potential effects of global climate change on the United States. Volume 2: National studies. Draft
[PB89-161061] N90-11352
Assessment of crop response to increases in atmospheric carbon dioxide concentrations: Summary of research progress report, July 1, 1988--June 30, 1989
[DE89-016251] N90-11360

GRID GENERATION (MATHEMATICS)
International conference on numerical grid generation in computational fluid dynamics
[AD-A211082] N90-11262

GROUND OPERATIONAL SUPPORT SYSTEM
Independent Orbiter Assessment (IOA): Assessment of the electrical power generation/power reactant storage and distribution subsystem FMEA/CIL
[NASA-CR-185545] N90-10023

GROUND SUPPORT EQUIPMENT
Design of a final approach spacing tool for TRACON air traffic control
[NASA-TM-102229] N90-10841

GROUND WATER
Hydrazine fate and transformation in natural waters and soils N90-11165
Numerical simulation of hydrazine transport in a sandy soil N90-11172

GROUND WAVE PROPAGATION
A calibrated, omnidirectional, LF loop antenna for GWEN (Ground Wave Emergency Network)
[AD-A211264] N90-11221

GROUP THEORY
Boolean functions, invariance groups and parallel complexity
[CWI-CS-R8836] N90-11472

GROUP 3A COMPOUNDS
Chemiluminescent ion-molecule reactions of group-3 ions with halogens: New optical spectra and reaction dynamics
[MPIS-18/1988] N90-11120

GUIDANCE (MOTION)
Rethinking synthesis of fine-motion strategies
[DE89-016671] N90-11322

GUIDANCE SENSORS
Evaluation test of CCD area sensor for star sensor
[NAL-TM-570] N90-11566

GYROFREQUENCY
On the possibility of producing artificial ionization and polar aurora in the ionosphere by radio-waves emitted from the ground N90-11388

GYROSCOPES
On the motion equation of an elastically supported two degree of freedon gyro
[NAL-TM-568] N90-11276

H

HALOGENS
Chemiluminescent ion-molecule reactions of group-3 ions with halogens: New optical spectra and reaction dynamics
[MPIS-18/1988] N90-11120

HAMILTONIAN FUNCTIONS
Subharmonic solutions near an equilibrium point for Hamiltonian systems
[AD-A210558] N90-11496
On some stochastic properties of the infinitely dimensional Hamiltonian systems of classical mechanics
[DE89-618403] N90-11525

HANDLING EQUIPMENT
Spoken commands control robot that handles radioactive materials
[DE89-012632] N90-11488

HARDNESS TESTS
Worked-in holes in three-dimensional reinforced composites N90-11060

HARMONIC EXCITATION
Low temperature properties of glasses N90-11141

HARMONICS
Subharmonic solutions near an equilibrium point for Hamiltonian systems
[AD-A210558] N90-11496

HATCHES
Independent Orbiter Assessment (IOA): Analysis of the mechanical actuation subsystem
[NASA-CR-185525] N90-10944
Independent Orbiter Assessment (IOA): Assessment of the mechanical actuation subsystem, volume 1
[NASA-CR-185527-VOL-1] N90-10952
Independent Orbiter Assessment (IOA): Assessment of the mechanical actuation subsystem, volume 2
[NASA-CR-185527-VOL-2] N90-10953

HAZARDS
Measurement of hydrazine contamination in soils N90-11180

HEALTH
Evaluation of rocket motor exhaust and liner combustion by-products
[AD-A210747] N90-11083

HEALTH PHYSICS
Biological effects of power frequency electric and magnetic fields: Background paper
[PB89-209985] N90-11439

HEAT FLUX
Heat transfer to throat tubes in a square-chambered rocket engine at the NASA Lewis Research Center
[NASA-TM-102336] N90-11082

HEAT PIPES
Design of ceramic fabric heat pipe with water working fluid
[DE89-016565] N90-11265

HEAT PUMPS
Free-Piston Stirling Engine magnetically coupled heat pump: Critical component evaluation
[DE89-015646] N90-11316
Dynamic characteristics concerned in the design of a free-piston Stirling engine/magnetic coupling/compressor system
[DE89-015981] N90-11317

HEAT STORAGE
Potential industrial applications for composite phase-change materials as thermal energy storage media
[DE89-015170] N90-11346

HEAT TRANSFER
Heat transfer to throat tubes in a square-chambered rocket engine at the NASA Lewis Research Center
[NASA-TM-102336] N90-11082
Thin section casting program. Volume 4: Static cast product bending, straightening, and rolling
[DE89-009034] N90-11202
Design of ceramic fabric heat pipe with water working fluid
[DE89-016565] N90-11265
The 3-D heat transfer computer calculations of th e performance of the IAEA's air-bath calorimeters
[DE89-016908] N90-11283
Advanced Turbine Technology Applications Program, (ATTAP)
[DE89-016067] N90-11318

HEAT TREATMENT
Composites reinforced with thermotropic liquid crystal copolyester fibers
[AD-A211226] N90-11089

HEAVY IONS
Global and local fluctuations in multiplicity and transverse energy for central ultra-relativistic heavy-ion interactions
[LUIP-8903] N90-11555

HELICAL FLOW
An experimental study of helicity and related properties in turbulent flows
[DE89-016785] N90-11259

HELICOPTER PERFORMANCE
Helicopter Visual Segment Approach Lighting System (HALS)
[ACD-330] N90-10856
Heliport surface maneuvering test results
[ACD-330] N90-10897

HELIPORTS
Heliport surface maneuvering test results
[ACD-330] N90-10897

HERMES MANNED SPACEPLANE
Thermal and structural analysis of Hermes N90-11058

HERMITIAN POLYNOMIAL
The fast Gauss transform
[AD-A211287] N90-11517

HETERODYNING
The investigation of the fundamental limits of heterodyne holographic interferometry with the application of imaging laser generated lamb waves
[AD-A211048] N90-11285

HETEROJUNCTIONS
CuInSe2 solar cell research by sputter deposition
[DE89-009450] N90-11345
International workshop on Beam Injection Assessment of Defects in Semiconductors
[AD-A210842] N90-11617

HEURISTIC METHODS
Procedures for separations within batches of values, 1. The orderly tool kit and some heuristics
[AD-A210652] N90-11531

HEXANITROSTILBENE
A shock initiation model for fine-grained hexanitrostilbene
[DE89-007641] N90-11185

HIGH ALTITUDE
Particle kinetic simulation of high altitude hypervelocity flight
[NASA-CR-186003] N90-10840

HIGH FREQUENCIES
Study of high frequency water vapor absorption parameters
[AD-A210676] N90-11108
An ionospheric model for HF sky-wave backscatter radar N90-11401
Accurate measurements of the total angle of arrival of HF skywaves N90-11402
Ionospheric limitations to the accuracy of SSL estimates of HF transmitter locations N90-11403

HIGH PRESSURE
High pressure 129I Moessbauer studies of GeI4 molecular crystals
[DE89-015269] N90-11620

HIGH RESOLUTION
HDTV displays: Subjective effects of scanning standards and domestic picture sizes
[BBC-RD-1989/9] N90-11208

HIGH SPEED PHOTOGRAPHY
Interferometry and high speed photography of laser-driven flyer plates
[DE89-016990] N90-11290

HIGH TEMPERATURE
High-temperature ceramic superconductors
[AD-A211070] N90-11618

HIGH TEMPERATURE SUPERCONDUCTORS
Acoustic studies of new materials: Quasicrystals, low-loss glasses and high Tc superconductors
[AD-A211281] N90-11551
Adaptation of the theory of superconductivity to the behavior of oxides
[DE89-016518] N90-11608
Studies of novel superconductors
[DE89-016744] N90-11609
Pinning of curved flux lines on the boundary between two phases of high temperature superconductors
[DE89-618865] N90-11614
High-temperature ceramic superconductors
[AD-A211070] N90-11618
Physics and materials science of high temperature superconductors
[AD-A211246] N90-11619
Origins of high-temperature superconductivity in the new copper oxide based ceramic superconductors
[DE89-016543] N90-11622
A fermi liquid electric structure and the nature of the carriers in high-T(sub c) cuprates: A photoemission study
[DE89-016774] N90-11624

Neutron scattering experiments on high-temperature superconducting materials: Foreign trip report, September 13, 1988--October 4, 1988
[DE89-017451] N90-11630

HIGH TEMPERATURE TESTS
Liquid infiltrated C/SiC: An alternative material for hot space structures N90-11030

HIGH VACUUM
Determination of neutral particle concentration at erosion laser plasma expansion into vacuum
[DE89-620128] N90-11308

HILBERT SPACE
S7 without any construction of Lie group
[DE89-618380] N90-11539
Markov processes in Hilbert space and continuous spontaneous localization of systems of identical particles
[DE89-618396] N90-11540

HILBERT TRANSFORMATION
Analytic signals in the damping coefficient estimation N90-11003

HINGES
The third generation rigid solar array GSR3 N90-11017

HIPPARCOS SATELLITE
Aeritalia Space Systems Group, Turin, Italy
[EOARD-LR-89-041] N90-10908

HISTORIES
Flight testing and flight research: From the age of the tower jumper to the age of the astronaut N90-10882
The astronomy of Andean myth: The history of a cosmology N90-11660
A history of West European rocketry and space research
[AD-A211191] N90-11690

HOLE MOBILITY
Transport properties of thermally grown Cr2O3
[DE89-016703] N90-11623

HOLOGRAPHIC INTERFEROMETRY
The investigation of the fundamental limits of heterodyne holographic interferometry with the application of imaging laser generated lamb waves
[AD-A211048] N90-11285

HOMING DEVICES
The Swedish defense research needs: For surveillance and seeker applications
[FOA-C-30520-3.3] N90-11691

HOMOGENEITY
An extension of Cochran's test for homogeneity of variances
[AD-A211054] N90-11534

HORN ANTENNAS
Nonprincipal-plane scattering from flat plates: Second-order and corner diffraction and pattern control of horn antennas
[NASA-CR-185485] N90-11205
Part B: Pattern control of horn antennas N90-11207

HOT WORKING
Thin section casting program. Volume 2: Horizontal TSC (Thin-Section Casting) approach
[DE89-009031] N90-11199
Thin section casting program. Volume 2-A: Appendix to volume 2
[DE89-009032] N90-11200
Thin section casting program. Volume 4: Static cast product bending, straightening, and rolling
[DE89-009034] N90-11202

HUBBLE SPACE TELESCOPE
Space telescope solar array: Nonlinear test and analysis effects N90-11051
STSA-Space Telescope solar array interconnectors: From simple approaches to complex modeling. A case study of the necessity of complex analysis N90-11076
Derivation of improved load transformation matrices for launchers-spacecraft coupled analysis, and direct computation of margins of safety N90-11077

HUGONIOT EQUATION OF STATE
Shock induced dissociation of polyethylene
[DE89-016983] N90-11267

HUMAN BODY
A severe human ESD (Electrostatic Discharge) model for safety and high reliability system qualification testing
[DE89-016177] N90-11233

HUMAN FACTORS ENGINEERING
See and avoid/cockpit visibility
[DOT/FAA/CT-TN89/18] N90-10843
NASA/NBS (National Aeronautics and Space Administration/National Bureau of Standards) standard reference model for telerobot control system architecture (NASREM)
[NASA-CR-185078] N90-11310
Techniques for optimizing human-machine information transfer related to real-time interactive display systems
[NASA-TM-100450] N90-11441
Selective removal of organics for water reclamation
[NASA-CR-185959] N90-11445
Task analysis of the UH-60 mission and decision rules for developing a UH-60 workload prediction model. Volume 1: Summary report
[AD-A210763] N90-11446

HUMIDITY
Methodology of developing a combined environmental stress schedule for reliability growth testing
[AD-A211053] N90-11326

HURRICANES
Hurricane Research Division fiscal year 1988 programs, fiscal year 1989 projections
[PB89-152268] N90-11418

HYDRAULIC EQUIPMENT
Independent Orbiter Assessment (IOA): Analysis of the hydraulics/water spray boiler subsystem
[NASA-CR-185541] N90-10934
Independent Orbiter Assessment (IOA): Analysis of the elevon subsystem
[NASA-CR-185576] N90-10935
Independent Orbiter Assessment (IOA): Analysis of the landing/deceleration subsystem
[NASA-CR-185569] N90-10943
Independent Orbiter Assessment (IOA): Weibull analysis report
[NASA-CR-185534] N90-10948

HYDRAULIC FLUIDS
Test and evaluation: Reducing risks to military aircraft from bird collisions. Report to the Chairman, Legislation, and National Security Subcommittee, Committee on Goverment Operations, House of Representatives
[AD-A210670] N90-10845

HYDRAZINES
The Third Conference on the Environmental Chemistry of Hydrazine Fuels
[AD-A197632] N90-11157
Surface-catalyzed air oxidation of hydrazines: Environmental chamber studies N90-11159
An atmospheric pressure flow reactor: Gas phase kinetics and mechanism in tropospheric conditions without wall effects N90-11160
The behavior of hydrazine vapor in an environmental chamber under simulated atmospheric conditions N90-11161
Modeling of hydrazine surface interactions in environmental reaction chambers N90-11162
Trace metal catalysis of hydrazine decomposition: The role of chromium N90-11163
Interactions of hydrazines with colloidal constituents of soils N90-11164
Hydrazine fate and transformation in natural waters and soils N90-11165
Vibrational spectroscopic study of the kaolinite-hydrazine intercalation complex N90-11166
Surface-catalyzed air oxidation reactions of hydrazines: Tubular reactor studies N90-11167
A matrix-isolation FT-IR study of hydrazine N90-11168
Low temperature spectroscope of hydrazine and ammonia complexes N90-11169
A diffuse reflectance infrared Fourier transform spectroscopic study of adsorbed hydrazines N90-11170
Numerical simulation of hydrazine transport in a sandy soil N90-11172
The chemistry of the hypochlorite neutralization of hydrazine fuels N90-11173
Modeling the ozonolysis of hydrazines wastewater N90-11175
Fuel neutralization by ozone oxidation N90-11176
Microsensor and pattern recognition techniques in hydrazine detection N90-11177
Hydrazine dosimetry N90-11178
Description of a chemiluminescence detector system specifically designed for monitoring airborne hydrazine and oxidizer propellant vapors N90-11179
Measurement of hydrazine contamination in soils N90-11180
Occupational safety considerations with hydrazine N90-11182

HYDROCARBON FUELS
A simulator for a hydrocarbon ramrocket fuel gas generator: First phase development
[AR-005-621] N90-11080

HYDROCARBONS
The effect of degree of aromaticity and alkyl substitution of polyaromatic hydrocarbons on instrumental response factors
[DE89-000761] N90-11117

HYDROCLIMATOLOGY
Frequency distributions and hydroclimatic characteristics of heavy rainstorms in Illinois
[PB89-203988] N90-11427

HYDRODYNAMIC RAM EFFECT
Fluid-structure interaction effects in tank structures due to sloshing and hydrodynamic ram: Coupled Lagangian-Eulerian simulations N90-11022

HYDRODYNAMICS
Electronic and ionic transport in polymers
[AD-A210654] N90-11148
Carbon in detonations
[DE89-016037] N90-11189
Acceleration of metal plates
[DE89-016816] N90-11197

HYDROFLUORIC ACID
Theoretical Hugoniot of liquid hydrogen fluoride
[DE89-016504] N90-11099
A high level Ab initio study of the anionic hydrogen-bonded complexes FH-CN-, FH-NC-, H2O-CN- and H2O-NC- N90-11553

HYDROGEN
Hydrogen-silicon carbide interactions
[NASA-TM-102382] N90-11144

HYDROGEN BONDS
Theoretical Hugoniot of liquid hydrogen fluoride
[DE89-016504] N90-11099
Theoretical investigation of gas-surface interactions
[NASA-CR-185492] N90-11552
A high level Ab initio study of the anionic hydrogen-bonded complexes FH-CN-, FH-NC-, H2O-CN- and H2O-NC- N90-11553
Report of the Specialists' Workshop on Phase Transition Studies on Hydrogen-Bonded Crystals by Neutron and X-ray Diffractometries
[DE89-906638] N90-11631

HYDROGEN OXYGEN ENGINES
Heat transfer to throat tubes in a square-chambered rocket engine at the NASA Lewis Research Center
[NASA-TM-102336] N90-11082

HYDROGEN PEROXIDE
A thermochemical analysis of proposed working fluids for electrothermal guns
[AD-A210661] N90-10910

HYDROGEN PLASMA
Hydrogen-assisted thermal donor formation in silicon
[DE89-016809] N90-11594

HYDROGEOLOGY
Physiographic and geological setting of the Coastal Engineering Research Center's field research facility
[AD-A210772] N90-11356

HYDROTHERMAL STRESS ANALYSIS
Hygrothermal deformations of composite shells N90-11055

HYPERBOLIC DIFFERENTIAL EQUATIONS
Domain decomposition for partial differential equations
[DE89-016669] N90-11519

HYPERSONIC COMBUSTION
Critical reaction rates in hypersonic combustion chemistry
[DE89-014278] N90-10892
Homogeneous catalysts in hypersonic combustion
[DE89-015258] N90-11098

HYPERSONIC FLOW
Low-speed, high-lift aerodynamic characteristics of slender, hypersonic accelerator-type configurations
[NASA-TP-2945] N90-10830
Homogeneous catalysts in hypersonic combustion
[DE89-015258] N90-11098
Gas-accelerated plate stability study
[DE89-016880] N90-11289

HYPERSONIC SPEED
Particle kinetic simulation of high altitude hypervelocity flight
[NASA-CR-186003] N90-10840

HYPERVELOCITY GUNS
A thermochemical analysis of proposed working fluids for electrothermal guns
[AD-A210661] N90-10910

I

ICE ENVIRONMENTS
The sea ice margins: A summary of physical phenomena
[PB89-212328] N90-11436

ICE FORMATION
Remote sensing techniques of the Wave Propagation Laboratory for the measurement of supercooled liquid water: Applications to aircraft icing
[PB89-208102] N90-10842

ICE MAPPING
Coastal subsea permafrost and bedrock observations using dc resistivity
[AD-A210784] N90-11435

IDEAL GAS
Computation of transient three-dimensional interstage flowfields using the arbitrary Lagrangian-Eulerian method N90-11253

IDENTIFYING
Stimulus-response compatibility in spatial precuing and symbolic identification: Effects of coding practice, retention, and transfer
[AD-A210745] N90-11443
IFF SYSTEMS (IDENTIFICATION)
Identification Friend, Foe or Neutral Joint Test
N90-10881
IGNITION
Powder morphology effects in the ignition of titanium-based pyrotechnics
[DE89-017229] N90-11191
IMAGE ANALYSIS
Spatial and temporal short range total cloud cover estimation by metric analysis of composite imagery
N90-11423
ANIMA: Image analyzer applied to remote sensing
[INPE-4766-PRE/1435] N90-11447
IMAGE INTENSIFIERS
Night sky radiometric measurements during follow-on-evaluation testing of AN/PVS-7 (A, B) at Fort Benning, Georgia
[AD-A211273] N90-11574
IMAGE PROCESSING
Utilization of photorefractive crystals in optical image processing
[ISBN-3-923560-06-0] N90-11292
Filling or outlining shapes with color: The effects on a visual search task
[AD-A211067] N90-11444
Computing the two dimensional fast Fourier transform on a general purpose mesh connected multiprocessor
[DE89-016515] N90-11518
IMAGE RESOLUTION
HDTV displays: Subjective effects of scanning standards and domestic picture sizes
[BBC-RD-1989/9] N90-11208
Definition of imaging performance for satellite surveillance, models, and simulations
[FOA-C-30493-9.4] N90-11341
IMAGE TRANSDUCERS
The investigation of the fundamental limits of heterodyne holographic interferometry with the application of imaging laser generated lamb waves
[AD-A211048] N90-11285
IMAGES
Robust spatial calibration of a planar positron camera
[AD-A210773] N90-11284
A technique to correlate fractography with NDE (Non-Destructive Evaluation) of small samples
[DE89-016904] N90-11325
Analysis of forest fire smoke using satellite imagery
[AD-A210657] N90-11339
IMAGING TECHNIQUES
The investigation of the fundamental limits of heterodyne holographic interferometry with the application of imaging laser generated lamb waves
[AD-A211048] N90-11285
Definition of imaging performance for satellite surveillance, models, and simulations
[FOA-C-30493-9.4] N90-11341
IMPACT DAMAGE
Aircraft live fire testing N90-10879
IMPACT LOADS
Techniques for recovery of shock-loaded samples
[DE89-016881] N90-11337
Irreversible phase transition and wave propagation in silicate geologic materials
[DE89-016031] N90-11414
IMPACT RESISTANCE
The 2.5D- and 3D-fabrics for delamination resistant composite laminates and sandwich structures
N90-11063
IMPACT TESTS
Numerical simulation of micrometeroids and debris hypervelocity impacts on Columbus pressurized modules
N90-11075
IMPEDANCE
The theory of ac impedance of rough electrode-electrolyte interfaces
[DE89-017474] N90-11243
IMPEDANCE MEASUREMENT
Analysis of coaxial wire measurement of longitudinal coupling impedance
[DE89-015748] N90-11230
IMPULSES
Impulse time-integral function and Lagrangian analysis
[DE89-016997] N90-11268
IMPURITIES
Dynamics of nucleation at electrochemical interfaces via surface EXAFS and standing wave measurements
[AD-A210733] N90-11109
Ozonation of hydrazines and their associated impurities N90-11174
PISCES program plasma-surface interactions research
[DE89-015622] N90-11578
IN-FLIGHT MONITORING
Independent Orbiter Assessment (IOA): Assessment of the Orbiter Experiment (OEX) subsystem
[NASA-CR-185587] N90-10962
Independent Orbiter Assessment (IOA): Analysis of the Orbiter Experiment (OEX) subsystem
[NASA-CR-185586] N90-10963
Independent Orbiter Assessment (IOA): Assessment of instrumental subsystem FMEA/CIL
[NASA-CR-185572] N90-10972
INCOMPRESSIBLE FLUIDS
Pressure correction splitting methods for the computation of oscillatory free convection in low Pr fluids
[CWI-NM-R8816] N90-11271
INDIUM ARSENIDES
Strain and density dependent valence-band masses in InGaAs/GaAs and GaAs/GaAsP strained-layer structures
[DE89-016882] N90-11627
INDUCTION (MATHEMATICS)
Completeness of resolution by transfinite induction
[CWI-CS-R8837] N90-11473
INDUSTRIAL ENERGY
Potential industrial applications for composite phase-change materials as thermal energy storage media
[DE89-015170] N90-11346
INDUSTRIES
Using self-calibrating thermocouples in industry
[DE89-013539] N90-11278
INELASTIC SCATTERING
Neutron scattering studies of amorphous Invar alloys
[DE89-016868] N90-11126
INELASTIC STRESS
A finite element formulation for inelastic plates and shells based on a mixed variational principle N90-11334
INERTIAL CONFINEMENT FUSION
Pulsed-power switching for inertial confinement fusion with light ion beams
[DE89-016810] N90-11595
INERTIAL GUIDANCE
The development of mission-specific advanced inertially-based avionics system N90-10851
INERTIAL NAVIGATION
Design of a Kalman filter for transfer alignment
N90-10848
Development of the integrated all-weather navigation system for Tornado N90-10849
A high performance airborne INS/GPS Integrated Navigation System N90-10850
INERTIAL PLATFORMS
STS-GPS (Space Transportation System - Global Positioning System) tracking experiment for gravitation estimation: Feasibility study
[AD-A211265] N90-10859
INFERENCE
Parallel inference based on delta processing
[CWI-CS-R8846] N90-11482
INFINITY
Realization theoretic solution of two analytic matrix equations with applications to stabilization of infinite-dimensional systems
[AD-A211118] N90-11512
INFLATABLE SPACECRAFT
Structural problems of accurate inflatable surfaces
N90-11044
INFORMATION DISSEMINATION
Toward a national research network
[PB89-198709] N90-11644
The transfer and diffusion of new technologies: A review of the economics literature
[DE89-015671] N90-11655
INFORMATION MANAGEMENT
Reporting environmental data of known quality
[DE89-016214] N90-11359
Techniques for optimizing human-machine information transfer related to real-time interactive display systems
[NASA-TM-100450] N90-11441
Electronic publishing: Guide to selection
[PB89-214753] N90-11448
A methodology for the design of continuous-dataflow synchronous systems
[PB89-184360] N90-11564
INFORMATION RETRIEVAL
Experimental database retrieval system DARTS (Handling Manual)
[DE89-906473] N90-11652
INFORMATION SYSTEMS
Techniques for optimizing human-machine information transfer related to real-time interactive display systems
[NASA-TM-100450] N90-11441
Electronic publishing: Guide to selection
[PB89-214753] N90-11448
Performance reports for EIM (Engineering Information Management) computer systems: A managerial perspective
[DE89-015194] N90-11449
Considerations for a design and operations knowledge support system for Space Station Freedom
[NASA-TM-102156] N90-11451
INFORMATION THEORY
Completeness of resolution by transfinite induction
[CWI-CS-R8837] N90-11473
Summaries of the FY 1989 Applied Mathematical Sciences Research program
[DE89-016694] N90-11521
INFORMATION TRANSFER
User's guide to the Space Environment Services Center geophysical alert broadcasts
[PB89-194617] N90-11411
INFRARED ASTRONOMY
Aspects of the development of a 1-5 micron infrared camera for astronomy N90-11656
Integrating detectors and their application to infrared astronomy N90-11659
INFRARED ASTRONOMY SATELLITE
Telescope structure for cryogenic application
N90-11019
IRAS observations of the extended galactic objects Cas A and W80 N90-11657
INFRARED DETECTORS
Offaxis radiance studies for infrared sensors
[AD-A210790] N90-11570
Integrating detectors and their application to infrared astronomy N90-11659
INFRARED IMAGERY
Adaptive tracking of maneuvering targets based on IR image data N90-10853
INFRARED SIGNATURES
Thermal radiation from terrain: Measurements and first results
[FOA-C-30525-3.1] N90-11342
INFRARED SPACE OBSERVATORY (ISO)
Telescope structure for cryogenic application
N90-11019
The service module structure of the IOS spacecraft development and qualification program N90-11021
INFRARED SPECTRA
Vibrational spectroscopic study of the kaolinite-hydrazine intercalation complex N90-11166
INFRARED SPECTROSCOPY
Forty-fourth symposium on molecular spectroscopy
[AD-A210752] N90-11111
Atmospheric chemistry of the fuel hydrazines
N90-11158
A matrix-isolation FT-IR study of hydrazine
N90-11168
Low temperature spectroscope of hydrazine and ammonia complexes N90-11169
Integrating detectors and their application to infrared astronomy N90-11659
INFRARED STARS
The mass distribution in the galactic centre estimated from OH/IR stars
[PB89-154884] N90-11663
INFRARED TELESCOPES
Telescope structure for cryogenic application
N90-11019
INITIATION
Shock initiation of LX-17 as a function of its initial temperature
[DE89-017730] N90-11192
INITIATORS (EXPLOSIVES)
A shock initiation model for fine-grained hexanitrostilbene
[DE89-007641] N90-11185
Test of EED (Electro-Explosive Devices). Part 3: Statistical aspects on the estimation of sensitivity
[FOA-C-20749-2.3-PT-3] N90-11194
INPUT
LEXER: A tool for lexical analysis of program input
[DE89-016924] N90-11649
INSTRUMENT COMPENSATION
A high precision gravity compensation system for the deployment test of the ERS-1 SAR antenna
N90-11038
INSTRUMENT RECEIVERS
CRRES (Combined Release and Radiation Effects Satellite) SPACERAD plasma wave experiment
[AD-A210791] N90-11587
INTEGRAL CALCULUS
Programs for numerical integration of piece-wise smooth functions
[DE89-620449] N90-11464
INTEGRAL EQUATIONS
An evaluation of the Chaboche and Bodner-Partom viscoplastic constitutive theories for strain rate sensitive materials N90-11330

On the numerical solution of two-point boundary value problems
[AD-A211244] N90-11516
Some exact solutions of the three-identical-particle problem with S-wave inverse square potentials
[DE89-618402] N90-11524

INTEGRALS
Evaluation of integrals related to the Debye function
[DE89-016930] N90-11499

INTEGRATED CIRCUITS
Free-world microelectronic manufacturing equipment
[FASAC-TAR-4070] N90-11228
A new semicustom integrated bipolar amplifier for silicon strip detectors
[DE89-015585] N90-11229
Laser dynamics: The system dynamics and network theory of optoelectronic integrated circuit design N90-11296
Optical coherence multiplexing for interprocessor communications
[DE89-016186] N90-11568

INTEGRATED OPTICS
Novel physical effects in intersecting optical waveguides N90-11565

INTELSAT SATELLITES
Advances in design and testing of spacecraft structures N90-11018

INTERACTIONAL AERODYNAMICS
Frequency domain aerodynamic analysis of interacting rotating systems N90-10837

INTERACTIVE CONTROL
Adaptive structures to meet future requirements for large precision structures N90-11001
System and performance analysis of a low density actively controlled mirror for astronomic observation N90-11002
Experiences using a major FEM package interactively for spacecraft applications N90-11008
MSP: Modeling of concurrent processes. Version 1.00 General introduction and directions for use
[REPT-88-88] N90-11477
Spoken commands control robot that handles radioactive materials
[DE89-012632] N90-11488

INTERFACES
Interfacial adsorption and crystallization of polycarbonate in carbon fiber composites
[AD-A211230] N90-11090
Intergranular and interphase boundaries in ceramics
[DE89-016969] N90-11154
An integrated distributed processing interface for supercomputers and workstations
[DE89-016769] N90-11478

INTERFEROMETRY
Project Radioastron N90-10901
Interferometry and high speed photography of laser-driven flyer plates
[DE89-016990] N90-11290

INTERGRANULAR CORROSION
Failure modes and mechanisms in nickel alloys: Primarily austenitic stainless steel
[DE89-016823] N90-11132

INTERIM STAGES (SPACECRAFT)
Aeritalia Space Systems Group, Turin, Italy
[EOARD-LR-89-041] N90-10908

INTERNAL WAVES
Non-linear wave-equations for low-frequency acoustic gravity waves N90-11365

INTERNATIONAL COOPERATION
Meeting of intercosmos space physics group N90-10902
USSR and international cooperation in space N90-10905
Globalization of Technology: International Perspectives. Proceedings of the 6th Convocation of the Council of Academies of Engineering and Technological Sciences
[PB89-198840] N90-11645

INTERPLANETARY FLIGHT
JPRS Report: Science and Technology. USSR: Space
[JPRS-USP-89-007] N90-10900

INTERPLANETARY MAGNETIC FIELDS
Studies of time-dependent polar cap convection patterns N90-11421

INTERPLANETARY SPACECRAFT
USSR and international cooperation in space N90-10905

INTERPOLATION
Numerical treatment of the thermo-structural-dynamic problems: The interpolation techniques N90-11016
An interpolation theorem in equational logic
[CWI-CS-R8838] N90-11528
Alias-free Wigner distribution function and complex ambiguity function for discrete-time samples
[AD-A211050] N90-11533

INTERPROCESSOR COMMUNICATION
An integrated distributed processing interface for supercomputers and workstations
[DE89-016769] N90-11478
Optical coherence multiplexing for interprocessor communications
[DE89-016186] N90-11568

INTERSTELLAR CHEMISTRY
Rocket and satellite observations of the local interstellar medium N90-11668

INTERSTELLAR GAS
Rocket and satellite observations of the local interstellar medium N90-11668

INTERSTELLAR MAGNETIC FIELDS
The interaction of supernovae and pulsars with the circumstellar environment N90-11671

INTERSTELLAR MATTER
IRAS observations of the extended galactic objects Cas A and W80 N90-11657
Rocket and satellite observations of the local interstellar medium N90-11668
Small grains in reflection nebulae: A study of diffuse interstellar bands, elemental depletions and infrared flux N90-11672

INTERSTELLAR SPACE
IRAS observations of the extended galactic objects Cas A and W80 N90-11657

INVARIANCE
Boolean functions, invariance groups and parallel complexity
[CWI-CS-R8836] N90-11472

IO
Ion bombardment of Io and Mercury N90-11682

IODINE ISOTOPES
High pressure 129I Moessbauer studies of GeI4 molecular crystals
[DE89-015269] N90-11620

ION BEAMS
Reactive ion etching of SiC thin films by mixtures of fluorinated gases and oxygen
[AD-A211046] N90-11113
Simulation of an axially symmetric ion-optical system
[DE89-620129] N90-11560
Ion sources, electron guns and beam optics
[DE89-015526] N90-11562
The Si(1-x)Nx Rugate
[AD-A211236] N90-11572
Pulsed-power switching for inertial confinement fusion with light ion beams
[DE89-016810] N90-11595
Ion beam annealing of Ga-implanted Si
[DE89-016857] N90-11610
Ion bombardment of Io and Mercury N90-11682

ION CYCLOTRON RADIATION
Can ion acceleration by double-cyclotron absorption produce O(+) ion conics
[IRF-PREPRINT-114] N90-11600

ION DENSITY (CONCENTRATION)
Determination of neutral particle concentration at erosion laser plasma expansion into vacuum
[DE89-620128] N90-11308
ANTHEM simulation of the early time magnetic field penetration of the plasma surrounding a high density Z-pinch
[DE89-016980] N90-11585

ION IMPLANTATION
Ion implantation of two titanium alloys
[DE89-016958] N90-11133
Hydrogen-assisted thermal donor formation in silicon
[DE89-016809] N90-11594
Ion beam annealing of Ga-implanted Si
[DE89-016857] N90-11610

ION IRRADIATION
Defect structures preceding amorphization by ion irradiations in YBa2Cu3O(7-delta)
[DE89-016905] N90-11612

ION SOURCES
Determination of neutral particle concentration at erosion laser plasma expansion into vacuum
[DE89-620128] N90-11308
Extraction induced emittance growth for negative ion sources
[DE89-017586] N90-11559
Simulation of an axially symmetric ion-optical system
[DE89-620129] N90-11560
Ion sources, electron guns and beam optics
[DE89-015526] N90-11562

ION TEMPERATURE
Ion temperature gradient instability
[DE89-016574] N90-11580

IONIZATION
Simulation of the polar cap F region ionization using an experimental convection electric field N90-11370
On the possibility of producing artificial ionization and polar aurora in the ionosphere by radio-waves emitted from the ground N90-11388

IONOSONDES
Multistation/multiparameter observations with a network of digital ionosondes N90-11396

IONOSPHERIC CONDUCTIVITY
On the influence of ionospheric conductivity on dispersion of acoustic gravity waves N90-11386

IONOSPHERIC DISTURBANCES
Atmospheric gravity waves in the auroral source region of TIDs, studied with the EISCAT CP2-data N90-11387
Ionospheric irregularities due to powerful HF radio transmissions N90-11389
A review on radio studies of auroral E-region ionospheric irregularities N90-11390
Ionospheric irregularities and their effects on electromagnetic waves propagating through them N90-11391
Electrostatic turbulence in the high latitude ionosphere N90-11392
Examples of meteorological behavior of the ionosphere N90-11395
North-south tropical F2 layer asymmetry at west African and Pacific longitudes N90-11398

IONOSPHERIC ELECTRON DENSITY
Global ionospheric dynamics: A review N90-11367
A fully analytic, low and middle latitude ionospheric model N90-11368
Global morphology of plasma bubbles in the low latitude ionosphere N90-11369
The middle and high latitude ionosphere at approximately 550 km altitude N90-11374
Modelling ionospheric density structures N90-11375
Quiet time conductivities of the auroral ionosphere N90-11383
Electrostatic turbulence in the high latitude ionosphere N90-11392
Examples of meteorological behavior of the ionosphere N90-11395
Ionospheric total electron content, and far ultraviolet, near infrared oxygen emission N90-11410

IONOSPHERIC PROPAGATION
Atmospheric gravity waves in the auroral source region of TIDs, studied with the EISCAT CP2-data N90-11387
On the possibility of producing artificial ionization and polar aurora in the ionosphere by radio-waves emitted from the ground N90-11388
Influence of ionospheric variations on high-reliability HF systems utilizing large bases N90-11404

IONOSPHERIC STORMS
Average diurnal and seasonal profiles of ionospheric storms N90-11371
Stormtime coupling of the neutral and ionized upper atmosphere at middle latitudes N90-11381

IONS
Electronic and ionic transport in polymers
[AD-A210654] N90-11148
Computer simulations of electromagnetic ion instabilities in the plasma sheet boundary layer
[DE89-016596] N90-11588

IRIDIUM
Thermodynamics, kinetics, and interface morphologies of phase formation reactions between metals and Gallium Arsenide: Bulk vs thin-film studies
[DE89-016469] N90-11621

IRRADIANCE
Solar radiation in Linkoeping (Sweden): Variations over half a year in irradiance and spectral composition in the interval 400-1000 nm
[FOA-C-30521-3.1] N90-11417

IRRADIATION
Grain boundary chemistry in irradiated stainless steel and its influence on environmental degradation
[DE89-016827] N90-11125

IRREVERSIBLE PROCESSES
Electrolyte dependence of charge injection processes for electroactive polymer films
[AD-A210787] N90-11152
Irreversible phase transition and wave propagation in silicate geologic materials
[DE89-016031] N90-11414

ISOPROPYL ALCOHOL
Equation-of-state data of synthetic Uranus
[DE89-016509] N90-11683

ITERATION
Modal analysis of fluid-structure systems by parallel subspace iteration N90-11024
Asynchronous integration of ordinary differential equations on multiprocessors
[DE89-014169] N90-11493
Fixed point iteration on point-symmetric interference graphs
[MEMO-INF-89-23] N90-11535

ITERATIVE NETWORKS
Iterative network magnitude estimation and uncertainty assessment with noisy and clipped data
[AD-A210707] N90-11507

ITERATIVE SOLUTION
Numerical solutions of turbulent flow with heat transfer over rough surfaces N90-11246
Variable step iteration of high-order Runge-Kutta methods on parallel computers [CWI-NM-R8817] N90-11476
Particle simulation in curvilinear coordinate systems [DE89-016727] N90-11583

J

JAMMING
Network analyzer for nonstatic jamming [AD-A210759] N90-11216
Performance analysis of hybrid ARQ protocols in a slotted code division multiple-access network [AD-A211078] N90-11219
JET BLAST EFFECTS
Jet-flow from shock tubes [AD-A210651] N90-11260
JET ENGINE FUELS
Production of jet fuels from coal-derived liquids. Volume 11: Production of advanced endothermic fuel blends from Great Plains Gasification Plant naphtha by-product stream [AD-A210251] N90-11184
JET FLOW
Rectangular subsonic jet flow field measurements [NASA-CR-185962] N90-11255
JET NOZZLES
The effect of electrode configuration on arcjet performance [NASA-TM-102346] N90-11081
JETTISONING
Independent Orbiter Assessment (IOA): Analysis of the electrical power distribution and control/remote manipulator system subsystem [NASA-CR-185526] N90-10936
JOINING
Study of a gallium arsenide solar cell interconnector N90-11033
JOINTS (JUNCTIONS)
Modeling and simulation of spatial robotic manipulators with flexible links and joint drives for control strategies implementation and evaluation N90-11311
An analytical and experimental study of the elastodynamic response characteristics of planar linkage mechanism with bearing clearances N90-11336
JORDAN FORM
JOE: Jordan Optimized Eigensolver. A step toward a numerical Jordan form analyzer for control and interactive thermo-structural-dynamic applications N90-11047
JUPITER (PLANET)
Upper ionosphere and magnetospheric-ionospheric coupling [DE89-619727] N90-11415
A dynamical study of Jupiter's Great Red Spot N90-11681
Ion bombardment of Io and Mercury N90-11682
JUPITER ATMOSPHERE
A dynamical study of Jupiter's Great Red Spot N90-11681
JUPITER RED SPOT
A dynamical study of Jupiter's Great Red Spot N90-11681

K

K-EPSILON TURBULENCE MODEL
Turbulent reacting flows in solid-propellant ducted rocket combustors N90-11079
KALMAN FILTERS
Kalman Filter Integration of Modern Guidance and Navigation Systems [AGARD-LS-166] N90-10847
Design of a Kalman filter for transfer alignment N90-10848
Development of the integrated all-weather navigation system for Tornado N90-10849
A high performance airborne INS/GPS Integrated Navigation System N90-10850
The development of mission-specific advanced inertially-based avionics system N90-10851
Development of a marine integrated navigation system N90-10852
Adaptive tracking of maneuvering targets based on IR image data N90-10853
KAOLINITE
Vibrational spectroscopic study of the kaolinite-hydrazine intercalation complex N90-11166
KERNEL FUNCTIONS
Boundary kernel estimation of the two sample comparison density function [AD-A210757] N90-11532
KERR MAGNETOOPTICAL EFFECT
Laser physics and laser techniques [AD-A211117] N90-11302
KINETICS
Particle kinetic simulation of high altitude hypervelocity flight [NASA-CR-186003] N90-10840
Enhanced oxidation and solovolysis reactions in chemically inert microheterogeneous systems [AD-A210748] N90-11110
An atmospheric pressure flow reactor: Gas phase kinetics and mechanism in tropospheric conditions without wall effects N90-11160
Numerical simulation of hydrazine transport in a sandy soil N90-11172
Kinetics and mechanisms of primary and steady state creep in B- and Al-containing alpha silicon carbide [AD-A210739] N90-11616
KNOWLEDGE BASES (ARTIFICIAL INTELLIGENCE)
Considerations for a design and operations knowledge support system for Space Station Freedom [NASA-TM-102156] N90-11451
KNOWLEDGE REPRESENTATION
A survey of research methods to study design [AD-A211213] N90-11491
The Knowledge Representation Project [AD-A211288] N90-11650

L

LABORATORIES
Research and test facilities for development of technologies and experiments with commercial applications [NASA-TM-101789] N90-10909
LABORATORY EQUIPMENT
Interlaboratory comparison of two types of line-source thermal-conductivity apparatus measuring five insulating materials [PB89-218325] N90-11142
LAGRANGE MULTIPLIERS
On the construction of the scattering matrix for locally-noncommutative interactions of relativistic fields [DE89-630138] N90-11640
LAMB WAVES
The investigation of the fundamental limits of heterodyne holographic interferometry with the application of imaging laser generated lamb waves [AD-A211048] N90-11285
LAMINATES
Analysis of delamination growth N90-11036
Delamination tests under static compression loading N90-11061
The 2.5D- and 3D-fabrics for delamination resistant composite laminates and sandwich structures N90-11063
Intrinsic damage and strength criteria for advanced composite laminates in space applications N90-11071
LANDAU-GINZBURG EQUATIONS
Singularity theory and N = 2 superconformal field theories [DE89-016582] N90-11538
LANDING GEAR
Independent Orbiter Assessment (IOA): Analysis of the landing/deceleration subsystem [NASA-CR-185569] N90-10943
Independent Orbiter Assessment (IOA): Assessment of the landing/deceleration (LDG/DEC) subsystem FMEA/CIL [NASA-CR-185570] N90-10966
LANTHANUM COMPOUNDS
On the photoemission spectrum and optical gap in La2CuO4 [DE89-015281] N90-11605
LARGE SPACE STRUCTURES
Wave-mode coordinate analysis of L junction in LSS [AD-A211116] N90-10984
Frequency domain design of robust controllers for space structures [AD-A211172] N90-10985
A contribution to the stability analysis of large space structures N90-10997
Adaptive structures to meet future requirements for large precision structures N90-11001
Thermoelastic behavior of large space structures: Modeling and control N90-11012
Evaluation of dispersive behavior in periodic structures by discrete Fourier transform N90-11014
Development of the large spacecraft structure N90-11020
Basic research on processing of ceramics for space structures [AD-A205954] N90-11139
Guaranteed cost control of flexible space structures N90-11643
LASER ALTIMETERS
Laser altimeter for use over the ocean [AD-A211252] N90-11286
The recovery of orbital and geophysical parameters using a spaceborne laser ranging system N90-11294
LASER ANEMOMETERS
Laser anemometer measurements in a transonic axial-flow fan rotor [NASA-TP-2879] N90-11245
LASER ANNEALING
Novel thin-film CuInSe2 fabrication [DE89-009440] N90-11604
LASER APPLICATIONS
Precision materials characterization in the near millimeter and submillimeter wavelength range [AD-A210655] N90-11106
Laser physics and laser techniques [AD-A211117] N90-11302
LASER DOPPLER VELOCIMETERS
Advances in instrumentation for experimental stress and vibration analysis and its applications N90-11069
A laser Doppler anemometry investigation of single-phase and particle-laden jet flows [AD-A210660] N90-11261
LASER OUTPUTS
Semiconductor quantum well lasers and related optoelectronic devices on silicon, III-V [AD-A210758] N90-11299
Acceleration of thin foil targets using fiber-coupled optical pulses [DE89-016526] N90-11569
LASER PLASMAS
Determination of neutral particle concentration at erosion laser plasma expansion into vacuum [DE89-620128] N90-11308
LASER RANGE FINDERS
The recovery of orbital and geophysical parameters using a spaceborne laser ranging system N90-11294
LASER SPECTROMETERS
Forty-fourth symposium on molecular spectroscopy [AD-A210752] N90-11111
LASER SPECTROSCOPY
Laser Raman spectroscopy: A literature review [FOA-C-20753-2.3] N90-11121
Nonlinear optical studies of resonant systems [AD-A211032] N90-11301
LASER WEAPONS
Laser techniques for ground to air applications [FOA-C-30524-3.1] N90-11309
Assessment of space power related measurement requirements of the Strategic Defense Initiative [PB89-209357] N90-11343
LASERS
Laser grooved and polycrystalline silicon solar cell research [DE89-015196] N90-11347
International workshop on Beam Injection Assessment of Defects in Semiconductors [AD-A210842] N90-11617
LATCHES
Independent Orbiter Assessment (IOA): Analysis of the electrical power distribution and control/remote manipulator system subsystem [NASA-CR-185526] N90-10936
LATTICE PARAMETERS
Thermal expansion and phase transformation studies on some materials by high temperature X-ray powder diffractometry [DE89-631032] N90-11130
LATTICE VIBRATIONS
Study of disorder and strain in semiconductor heterostructures and superlattices by Raman scattering N90-11601
LAUNCH VEHICLE CONFIGURATIONS
Ariane 5 structural design and development N90-11057
LEAD (METAL)
Experimental measurements of shock-induced vaporization in cadmium and lead [DE89-016877] N90-11103
LEADING EDGES
Numerical simulation of leading-edge vortex rollup and bursting N90-10831
LEAKAGE
Hydrazine fate and transformation in natural waters and soils N90-11165
LEARNING THEORY
Inferring data base requirements from examples in forms N90-11648
LEAST SQUARES METHOD
Robust spatial calibration of a planar positron camera [AD-A210773] N90-11284
Iterative network magnitude estimation and uncertainty assessment with noisy and clipped data [AD-A210707] N90-11507

Nonlinear adjustment with or without constraints, applicable to geodetic models
[AD-A210820] N90-11509
Two enhancements of the logarithmic least-squares method for analyzing subjective comparisons
[AD-A211192] N90-11514
An improved algorithm for the determination of the system paramters of a visual binary by least squares
N90-11658

LIE GROUPS
S7 without any construction of Lie group
[DE89-618380] N90-11539

LIFE (DURABILITY)
The use of damage characterization for life prediction methodologies N90-11053
Lifetime testing of commercially available 3.0 (mu)f, 100 kV pulsed-power capacitors
[DE89-017230] N90-11242
A re-evaluation of fatigue threshold test procedures and the simulation and prediction of fatigue crack growth under conditions of low crack closure N90-11328

LIFE SUPPORT SYSTEMS
Independent Orbiter Assessment (IOA): Analysis of the extravehicular mobility unit
[NASA-CR-185540] N90-10937
Independent Orbiter Assessment (IOA): CIL issues resolution report, volume 1
[NASA-CR-185524-VOL-1] N90-10954
Independent Orbiter Assessment (IOA): Assessment of the atmospheric revitalization pressure control subsystem FMEA/CIL
[NASA-CR-185594] N90-10957
Independent Orbiter Assessment (IOA): Assessment of the life support and airlock support systems, volume 1
[NASA-CR-185581-VOL-1] N90-10977
Independent Orbiter Assessment (IOA): Assessment of the life support and airlock support systems, volume 2
[NASA-CR-185581-VOL-2] N90-10978
Selective removal of organics for water reclamation
[NASA-CR-185959] N90-11445

LIFT
Low-speed, high-lift aerodynamic characteristics of slender, hypersonic accelerator-type configurations
[NASA-TP-2945] N90-10830

LIGHT IONS
Pulsed-power switching for inertial confinement fusion with light ion beams
[DE89-016810] N90-11595

LIGHT SCATTERING
The interaction of supernovae and pulsars with the circumstellar environment N90-11671

LIGHTNING
Internal voltages and currents in well-shielded cylindrical objects due to simulated direct-strike lightning
[DE89-012664] N90-11231
Performance of transient limiters under laboratory, simulated, and rocket-triggered lightning conditions
[DE89-015773] N90-11238

LIGHTNING SUPPRESSION
Performance of transient limiters under laboratory, simulated, and rocket-triggered lightning conditions
[DE89-015773] N90-11238

LIKELIHOOD RATIO
Utilization of the generalized likelihood ratio test for the suppression of systematic errors in noisy systems
[ETN-89-94656] N90-11225

LINE SPECTRA
Nonlinear optical studies of resonant systems
[AD-A211032] N90-11301
The Si(1-x)Nx Rugate
[AD-A211236] N90-11572

LINEAR PROGRAMMING
Partially specified probability measures in expert systems
[CWI-CS-R8842] N90-11536

LINKAGES
Modeling and simulation of spatial robotic manipulators with flexible links and joint drives for control strategies implementation and evaluation N90-11311
An analytical and experimental study of the elastodynamic response characteristics of planar linkage mechanism with bearing clearances N90-11336

LIQUID CHROMATOGRAPHY
A new method for the characterization of solutes and solvent phases using solvatochromic parameters
[AD-A211238] N90-11116

LIQUID CRYSTALS
Flow visualization techniques for flight research
N90-10878
Composites reinforced with thermotropic liquid crystal copolyester fibers
[AD-A211226] N90-11089
Chevron layer structures in Surface Stabilized Ferroelectric Liquid Crystal (SSFLC) cells filled with a material which exhibits the chiral nematic to smectic C* phase transition
[DE89-016985] N90-11628

LIQUID HELIUM
Quasi-diffusion between phonon and roton gases in two- and three-dimensional liquid helium
[AD-A210565] N90-11096

LIQUID INJECTION
Electrolyte dependence of charge injection processes for electroactive polymer films
[AD-A210787] N90-11152

LIQUID ROCKET PROPELLANTS
The Third Conference on the Environmental Chemistry of Hydrazine Fuels
[AD-A197632] N90-11157
Surface-catalyzed air oxidation of hydrazines: Environmental chamber studies N90-11159
Modeling the ozonolysis of hydrazines wastewater
N90-11175
Fuel neutralization by ozone oxidation N90-11176
Description of a chemiluminescence detector system specifically designed for monitoring airborne hydrazine and oxidizer propellant vapors N90-11179
Measurement of hydrazine contamination in soils
N90-11180

LIQUID SLOSHING
Fluid-structure interaction effects in tank structures due to sloshing and hydrodynamic ram: Coupled Lagangian-Eulerian simulations N90-11022
Modeling of liquid sloshing effects in multibody systems N90-11023

LIQUID-SOLID INTERFACES
Hybrid particle-fluid approach to low-frequency turbulence in magnetically confined plasmas
[DE89-015904] N90-11579

LITHIUM
New secondary batteries utilizing electronically conductive polymer cathodes
[NASA-CR-185885] N90-11227
Research in X-ray optics with the ultimate aim of constructing a synchrotron radiation pumped soft X-ray lithium laser
[DE89-016788] N90-11304
Carbon isotope ratios and lithium abundances in open cluster giants N90-11664

LITHIUM BORATES
Polarization matrices of lithium tetraborate
[AD-A210774] N90-11112

LITHIUM COMPOUNDS
A thermochemical analysis of proposed working fluids for electrothermal guns
[AD-A210661] N90-10910
Polarization matrices of lithium tetraborate
[AD-A210774] N90-11112

LITHIUM OXIDES
Lithium polymer electrolyte battery, electrochemical behavior of cathode materials
[AD-A210755] N90-11235

LITHOGRAPHY
X-ray lithography sources: A review
[DE89-017610] N90-11547

LITHOLOGY
Physiographic and geological setting of the Coastal Engineering Research Center's field research facility
[AD-A210772] N90-11356

LOAD TESTS
STS payload design load evolution N90-10989
Equilibrium and stability in composite thin shell
N90-10998
Multi-axis transient testing: Experimental investigations
N90-11042

LOADS (FORCES)
Overview of actual buckling calculation methods for space vehicle structures N90-10995
Key structures mechanical issues of the European Space Station and platform program Columbus N90-11072
Derivation of improved load transformation matrices for launchers-spacecraft coupled analysis, and direct computation of margins of safety N90-11077
Planar sliding of a rigid body with dry friction: Limit surfaces and dynamics of motion N90-11314

LOCAL AREA NETWORKS
Adaptive gigabit fiber optics local area network
[AD-A210794] N90-11571

LOGIC DESIGN
An axiomatic theory for partial functions
[MEMO-INF-89-22] N90-11527
An interpolation theorem in equational logic
[CWI-CS-R8838] N90-11528

LOGIC PROGRAMMING
An axiomatic theory for partial functions
[MEMO-INF-89-22] N90-11527
An interpolation theorem in equational logic
[CWI-CS-R8838] N90-11528

LOGISTICS
US Navy principal site testing concept and the F-18
N90-10861

LONG DURATION SPACE FLIGHT
Space Station Freedom: A foothold on the future
[NASA-NP-107/10-88] N90-10907

LONGITUDINAL CONTROL
The active control of an unstable canard aircraft
N90-10894

LOOP ANTENNAS
A calibrated, omnidirectional, LF loop antenna for GWEN (Ground Wave Emergency Network)
[AD-A211264] N90-11221

LORENTZ FORCE
On the influence of ionospheric conductivity on dispersion of acoustic gravity waves N90-11388
Testing results of the MIT Probe
[DE89-016679] N90-11590

LOSSY MEDIA
Part B: Pattern control of horn antennas N90-11207
Constitutive parameter measurements of lossy materials
[NASA-CR-183398] N90-11603

LOW GRAVITY MANUFACTURING
Concepts for microgravity experiments utilizing gloveboxes
[NASA-TM-100378] N90-11195

LOW REYNOLDS NUMBER
Low-Reynolds-number modeling of complex flows with and without density variation N90-10832

LOW TEMPERATURE
Low temperature processing of reaction sintered silicon nitride
[DE89-017455] N90-11092
Low temperature properties of glasses N90-11141
Low temperature spectroscope of hydrazine and ammonia complexes N90-11169

LUBRICATION
Efficient numerical method for computation of thermohydrodynamics of laminar lubricating films
[NASA-CR-185136] N90-11256

M

MACHINING
Basic investigations of cutting machinability of inorganic glasses using single-point tools
[W-15/87] N90-11204
Engineering specification and system design for CAD/CAM of custom shoes. Phase 5: UMC involvement (January 1, 1989 - June 30, 1989)
[NASA-CR-185838] N90-11456

MAGNESIUM
Development of graphite-magnesium composites for space applications N90-11054

MAGNET COILS
Testing results of the MIT Probe
[DE89-016679] N90-11590

MAGNETIC COOLING
Thermodynamic principles of the process of the effect of electromagnetic fields on a polymer melt
[AD-A210698] N90-11149

MAGNETIC DISTURBANCES
User's guide to the Space Environment Services Center geophysical alert broadcasts
[PB89-194617] N90-11411
Solar-geophysical data number 536, part 1. Data for March, Febuary 1989 and late data
[PB89-194716] N90-11684

MAGNETIC FIELD CONFIGURATIONS
Compact torus configurations with high frequency driven currents
[ETN-89-94674] N90-11598

MAGNETIC FIELDS
Substorm associated pulsations: A study of plasmaspheric cavity resonance, mid-latitude polarisation and geostationary orbit signatures N90-11422
Extraction induced emittance growth for negative ion sources
[DE89-017586] N90-11559
Boundary effects on the MHD dynamo in laboratory plasmas
[DE89-015207] N90-11576
ANTHEM simulation of the early time magnetic field penetration of the plasma surrounding a high density Z-pinch
[DE89-016980] N90-11585
Launched electrons in plasma opening switches
[DE89-016886] N90-11596
Physics and materials science of high temperature superconductors
[AD-A211246] N90-11619
The stability of magnetohydrodynamic shock waves in molecular clouds N90-11665

MAGNETIC FILMS
Studies of ultrathin magnetic films and particle-surface interactions with spin-sensitive electron spectroscopies
[DE89-016741] N90-11556
MAGNETIC FLUX
Magnetic flux compression
[DE89-016991] N90-11546
Pinning of curved flux lines on the boundary between two phases of high temperature superconductors
[DE89-618865] N90-11614
MAGNETIC LEVITATION VEHICLES
Magnetically levitated micro-robotics N90-11542
MAGNETIC PROPERTIES
Neutron scattering studies of amorphous Invar alloys
[DE89-016868] N90-11126
Investigations of the influence of magnetically long range ordered phases on the electronic charge transport in metallic glasses
[ETN-89-94672] N90-11155
Studies of ultrathin magnetic films and particle-surface interactions with spin-sensitive electron spectroscopies
[DE89-016741] N90-11556
MAGNETIC STORMS
Magnetospheric substorms as a signature of the solar terrestrial interaction N90-11363
Stormtime coupling of the neutral and ionized upper atmosphere at middle latitudes N90-11381
Auroral and sub-auroral F-layer irregularity studies in the Northern and Southern Hemisphere during the equinox transition study September 16-26, 1984 N90-11393
Radio propagation conditions forecast above a low latitude region N90-11400
Substorm associated pulsations: A study of plasmaspheric cavity resonance, mid-latitude polarisation and geostationary orbit signatures N90-11422
Numerical study of the current sheet and PSBL in a magnetotail model
[NASA-CR-183289] N90-11669
MAGNETIC SUSPENSION
An experimental investigation of the aerodynamic characteristics of slanted base ogive cylinders using magnetic suspension technology
[NASA-CR-181708] N90-10834
Magnetically levitated micro-robotics N90-11542
MAGNETIZATION
Effects of shock-modification on superconductivity in Tl2Ca2Ba2Cu3Oy and Bi2CaSr2Cu2Ox
[DE89-017231] N90-11629
MAGNETOHYDRODYNAMIC STABILITY
Low frequency electrostatic waves observed in the vicinity of an auroral arc N90-11378
A review on radio studies of auroral E-region ionospheric irregularities N90-11390
Short wavelength striations on expanding plasma clouds
[DE89-016585] N90-11416
Ion temperature gradient instability
[DE89-016574] N90-11580
Computer simulations of electromagnetic ion instabilities in the plasma sheet boundary layer
[DE89-016596] N90-11588
MAGNETOHYDRODYNAMIC TURBULENCE
A study of runaway electron confinement and theory of neoclassical MHD turbulence
[DE89-016728] N90-11584
The stability of magnetohydrodynamic shock waves in molecular clouds N90-11665
MAGNETOHYDRODYNAMIC WAVES
Theory of high-n toroidicity-induced shear Alfven eigenmode in tokamaks
[DE89-016726] N90-11582
The stability of magnetohydrodynamic shock waves in molecular clouds N90-11665
MAGNETOHYDRODYNAMICS
Thin section casting program. Volume 1: Executive summary and overview
[DE89-009030] N90-11198
Thin section casting program. Volume 2: Horizontal TSC (Thin-Section Casting) approach
[DE89-009031] N90-11199
Thin section casting program. Volume 5: Westinghouse MHD Project
[DE89-009035] N90-11203
Boundary effects on the MHD dynamo in laboratory plasmas
[DE89-015207] N90-11576
Solid fiber Z-pinches: Cold-start computations
[DE89-016768] N90-11592
MAGNETOMETERS
CRRES (Combined Release and Radiation Effects Satellite) SPACERAD plasma wave experiment
[AD-A210791] N90-11587
MAGNETOSPHERE-IONOSPHERE COUPLING
Ionospheric Structure and Variability on a Global Scale and Interactions with Atmosphere and Magnetosphere
[AGARD-CP-441] N90-11361
Magnetospheric substorms as a signature of the solar terrestrial interaction N90-11363
Observations of ionosphere/magnetosphere interactions from the Dynamics Explorer satellites N90-11376
Quiet time conductivities of the auroral ionosphere N90-11383
Upper ionosphere and magnetospheric-ionospheric coupling
[DE89-619727] N90-11415
MAGNETS
Free-Piston Stirling Engine magnetically coupled heat pump: Critical component evaluation
[DE89-015646] N90-11316
MAGNONS
Spin fluctuations and excitations in a 2D xy-ferromagnet: CoCl2 in graphite
[DE89-017600] N90-11119
MAIN SEQUENCE STARS
Effects of main-sequence mass loss on the turnoff ages of globular clusters
[DE89-016784] N90-11678
MAINTENANCE
Results from the second year of operation of the Federal Methanol Fleet at Argonne National Laboratory
[DE89-016935] N90-11319
MAN ENVIRONMENT INTERACTIONS
Evaluation of mid-to-long term basic research for environmental restoration
[DE89-015621] N90-11355
MAN MACHINE SYSTEMS
Independent Orbiter Assessment (IOA): Assessment of the remote manipulator system FMEA/CIL
[NASA-CR-185592] N90-10964
Techniques for optimizing human-machine information transfer related to real-time interactive display systems
[NASA-TM-100450] N90-11441
Filling or outlining shapes with color: The effects on a visual search task
[AD-A211067] N90-11444
Task analysis of the UH-60 mission and decision rules for developing a UH-60 workload prediction model. Volume 1: Summary report
[AD-A210763] N90-11446
MAN-COMPUTER INTERFACE
Filling or outlining shapes with color: The effects on a visual search task
[AD-A211067] N90-11444
MANAGEMENT
Technical communications in aeronautics: Results of an exploratory study. An analysis of managers' and nonmanagers' responses
[NASA-TM-101625] N90-11647
MANAGEMENT METHODS
The Air Force Flight Test Center Flight Test Safety Program N90-10872
MANAGEMENT PLANNING
Preference propagation in temporal/capacity constraint graphs
[AD-A210668] N90-11506
MANAGEMENT SYSTEMS
Preference propagation in temporal/capacity constraint graphs
[AD-A210668] N90-11506
MANEUVERS
Passive trajectography by azimuth: Improvement of estimation quality N90-10854
MANIFOLDS (MATHEMATICS)
Local structure of a 2-codimensional conformally flat submanifold in an Euclidean space R(sup n+2)
[DE89-618379] N90-11501
Analytic manifolds in uniform algebras
[DE89-618384] N90-11505
MANIPULATORS
Independent Orbiter Assessment (IOA): Assessment of the EPD and C/remote manipulator system FMEA/CIL
[NASA-CR-185583] N90-10965
Modeling and simulation of spatial robotic manipulators with flexible links and joint drives for control strategies implementation and evaluation N90-11311
Rethinking synthesis of fine-motion strategies
[DE89-016671] N90-11322
Telescience Testbed Pilot Program
[NASA-CR-184594] N90-11455
Magnetically levitated micro-robotics N90-11542
MANNED MANEUVERING UNITS
Independent Orbiter Assessment (IOA): Analysis of the manned maneuvering unit
[NASA-CR-185565] N90-10913
Independent Orbiter Assessment (IOA): Assessment of the manned maneuvering unit
[NASA-CR-185564] N90-10974
MANNED SPACE FLIGHT
JPRS Report: Science and Technology. USSR: Space
[JPRS-USP-89-007] N90-10900
USSR and international cooperation in space N90-10905
Advanced manned space flight simulation and training: An investigation of simulation host computer system concepts
[NASA-CR-185998] N90-10911
MANUFACTURING
Study of the application of automation to composites manufacture
[AD-A211049] N90-11087
Free-world microelectronic manufacturing equipment
[FASAC-TAR-4070] N90-11228
MANY BODY PROBLEM
Modeling of liquid sloshing effects in multibody systems N90-11023
MAPS
Linkoeping's A.I. Consortium (LAIC) for plan guided systems. Review of the first 18 months
[FOA-C-30528-3.4] N90-11537
MARKOV PROCESSES
Markov processes in Hilbert space and continuous spontaneous localization of systems of identical particles
[DE89-618396] N90-11540
MARS (PLANET)
Soviet Mars program N90-10903
Sagdeyev discusses space missions, policy, Mars plans N90-10906
MARTENSITE
Use of overlapped reflection for determining the retained austenite by X-ray diffraction
[DE89-615450] N90-11128
MASS
Estimation of the C-J pressure of explosives
[DE89-013811] N90-11187
MASS SPECTRA
Time-resolved mass spectrometry technique for studying fast transient CHNO explosive decomposition kinetics
[DE89-016540] N90-11101
MASS SPECTROMETERS
Ion detector on the basis of microchannel plates for a high-sensitive mass spectrometer
[DE89-620335] N90-11291
MASS SPECTROSCOPY
The effect of degree of aromaticity and alkyl substitution of polyaromatic hydrocarbons on instrumental response factors
[DE89-000761] N90-11117
MASS TRANSFER
On transonic flow over segmented slotted wind tunnel wall with mass transfer N90-11676
MATERIALS TESTS
Research and test facilities for development of technologies and experiments with commercial applications
[NASA-TM-101789] N90-10909
MATHEMATICAL MODELS
Low-Reynolds-number modeling of complex flows with and without density variation N90-10832
A preliminary sensitivity analysis of the Generalized Escape System Simulation (GESS) computer program
[DE89-016891] N90-10844
Results and practical experience using parameter identification techniques on the AM-X program at Aermacchi N90-10873
On the development of a basic flight test capability and some related research projects N90-10885
Environmental testing: An approach to more cost efficiency N90-10988
STS payload design load evolution N90-10989
A review of the Error of Matrix Method (EMM) for structural dynamic model comparison N90-10993
Parametric identification of conservative self adjoint structures N90-10994
A contribution to the stability analysis of large space structures N90-10997
A super element for multibody dynamics N90-11004
GEMMES: A new tool for dynamic modeling N90-11005
Use of Lanczos vectors in structural dynamics N90-11011
Evaluation of dispersive behavior in periodic structures by discrete Fourier transform N90-11014
A direct two response approach for updating analytical dynamic models of structures with emphasis on uniqueness N90-11028
Study of a gallium arsenide solar cell interconnector N90-11033
Analysis of delamination growth N90-11036
Induced shock loads during the separation of the Ariane 5 VEB structure N90-11045
Mathematical model and predictions for static and dynamic behavior of solar array structure N90-11049
Space telescope solar array: Nonlinear test and analysis effects N90-11051
Hygrothermal deformations of composite shells N90-11055

Numerical models for exterior and interior fluid-structure interaction problems N90-11073
STSA-Space Telescope solar array interconnectors: From simple approaches to complex modeling. A case study of the necessity of complex analysis N90-11076
Thermochemical model for shock-induced chemical reactions in porous thermite: The heat detonation model [DE89-016528] N90-11100
Modeling of hydrazine surface interactions in environmental reaction chambers N90-11162
Numerical simulation of hydrazine transport in a sandy soil N90-11172
Nitramine composite solid propellant modeling N90-11183
A shock initiation model for fine-grained hexanitrostilbene [DE89-007641] N90-11185
Estimation of the C-J pressure of explosives [DE89-013811] N90-11187
Sharp shock model for propagating detonation waves [DE89-016772] N90-11266
Modeling and simulation of spatial robotic manipulators with flexible links and joint drives for control strategies implementation and evaluation N90-11311
An evaluation of the Chaboche and Bodner-Partom viscoplastic constitutive theories for strain rate sensitive materials N90-11330
The dynamic stability of an axially loaded beam with lateral elastic support and damping N90-11331
An improved beam model for the vibrations of rotor blades N90-11333
Empirical models of convection electric fields and electrostatic potential at high latitude from EISCAT observations: Preliminary results N90-11377
Studies of time-dependent polar cap convection patterns N90-11421
DOE/CEC Workshop on Critical Evaluation of Radiobiological Data to Biophysical Modeling [DE89-015214] N90-11437
Computer symbiosis: Emergence of symbiotic behavior through evolution [DE89-015247] N90-11450
Control and optimization for observations of systems governed by controlled partial differential equations [AD-A211122] N90-11513
Summaries of the FY 1989 Applied Mathematical Sciences Research program [DE89-016694] N90-11521
Partially specified probability measures in expert systems [CWI-CS-R8842] N90-11536
Singularity theory and N = 2 superconformal field theories [DE89-016582] N90-11538
Hybrid particle-fluid approach to low-frequency turbulence in magnetically confined plasmas [DE89-015904] N90-11579
Propagation of normal zones of finite size in large, composite superconductors [DE89-016866] N90-11611
General covariance and strings [DE89-016505] N90-11633

MATRICES (MATHEMATICS)
LINPACK routines based on the level 2 BLAS [CWI-NM-R8811] N90-11483
Realization theoretic solution of two analytic matrix equations with applications to stabilization of infinite-dimensional systems [AD-A211118] N90-11512
An improved algorithm for the determination of the system paramters of a visual binary by least squares N90-11658

MATRIX MATERIALS
Composites reinforced with thermotropic liquid crystal copolyester fibers [AD-A211226] N90-11089

MATRIX METHODS
A review of the Error of Matrix Method (EMM) for structural dynamic model comparison N90-10993

MAXIMUM LIKELIHOOD ESTIMATES
The use of damage characterization for life prediction methodologies N90-11053
Iterative network magnitude estimation and uncertainty assessment with noisy and clipped data [AD-A210707] N90-11507

MAXIMUM USABLE FREQUENCY
Average diurnal and seasonal profiles of ionospheric storms N90-11371

MAXWELL EQUATION
Gravitational nonminimally coupled electromagnetic fields: A possible solution to some idiosincrasies of Einstein-Maxwell theory [DE89-618430] N90-11635

MEASURE AND INTEGRATION
Asynchronous integration of ordinary differential equations on multiprocessors [DE89-014169] N90-11493

MEASURING INSTRUMENTS
Flight test instrumentation and data processing at British Aerospace, Warton, U.K. N90-10887
Response of standardized PVDF piezoelectric polymer gauges to direct shock pressures between 8 and 32 GPa [DE89-016811] N90-11282
The Sandia standard for PVDF (Polyvinylidene Di-Fluoride) shock sensors [DE89-016530] N90-11287

MECHANICAL DEVICES
Comprehension processes in mechanical reasoning [AD-A210459] N90-11442

MECHANICAL DRIVES
Magnetically levitated micro-robotics N90-11542

MECHANICAL PROPERTIES
Liquid infiltrated C/SiC: An alternative material for hot space structures N90-11030
Worked-in holes in three-dimensional reinforced composites N90-11060
A study of the tribological and surface micromechanical properties of YBa2Cu3O7-x [DE89-015680] N90-11607
Exploratory study of niobium, titanium, zirconium and tantalum aluminides [AD-A210658] N90-11615

MELTING POINTS
Composites reinforced with thermotropic liquid crystal copolyester fibers [AD-A211226] N90-11089

MEMORY (COMPUTERS)
New computing systems and their impact on structural analysis and design [NASA-CR-185831] N90-11457

MENISCI
Effects of gravity on equilibrium crystal shapes N90-11602

MENTAL PERFORMANCE
Comprehension processes in mechanical reasoning [AD-A210459] N90-11442
Stimulus-response compatibility in spatial precuing and symbolic identification: Effects of coding practice, retention, and transfer [AD-A210745] N90-11443

METAL FATIGUE
Fatigue crack growth rates as a function of delta K: Variability and material property N90-11031
Failure modes and mechanisms in nickel alloys: Primarily austenitic stainless steel [DE89-016823] N90-11132
A re-evaluation of fatigue threshold test procedures and the simulation and prediction of fatigue crack growth under conditions of low crack closure N90-11328

METAL FOILS
Acceleration of thin foil targets using fiber-coupled optical pulses [DE89-016526] N90-11569

METAL MATRIX COMPOSITES
Development of graphite-magnesium composites for space applications N90-11054
Accelerated aging of metal matrix composites N90-11085

METAL PLATES
Surface-catalyzed air oxidation of hydrazines: Environmental chamber studies N90-11159
Acceleration of metal plates [DE89-016816] N90-11197
Thin section casting program. Volume 4: Static cast product bending, straightening, and rolling [DE89-009034] N90-11202
Laser-driven miniature flyer plates for shock initiation of secondary explosives [DE89-016587] N90-11288
Interferometry and high speed photography of laser-driven flyer plates [DE89-016990] N90-11290

METAL SHEETS
Thin section casting program. Volume 1: Executive summary and overview [DE89-009030] N90-11198

METALLIC GLASSES
Investigations of the influence of magnetically long range ordered phases on the electronic charge transport in metallic glasses [ETN-89-94672] N90-11155

METEOROID HAZARDS
Numerical simulation of micrometeroids and debris hypervelocity impacts on Columbus pressurized modules N90-11075

METEOROID PROTECTION
Key structures mechanical issues of the European Space Station and platform program Columbus N90-11072
Numerical simulation of micrometeroids and debris hypervelocity impacts on Columbus pressurized modules N90-11075

METEOROLOGICAL CHARTS
Diagnostic study of atmosphere-terrain interaction leading to the formation of dust clouds and poor visibilities over near east desert areas [AD-A211243] N90-11358

METEOROLOGICAL PARAMETERS
Atmospheric environment for space shuttle (STS-29) launch [NASA-TM-100376] N90-10980
Atmospheric environment for space shuttle (STS-30) launch [NASA-TM-100381] N90-10981
Hurricane Research Division fiscal year 1988 programs, fiscal year 1989 projections [PB89-152268] N90-11418
National Center For Atmospheric Research annual report, fiscal year 1988 [PB89-208987] N90-11428
Interannual variability of temperature in the upper layer of the North Pacific eastern boundary region, 1971-1987 [PB89-190227] N90-11434
The sea ice margins: A summary of physical phenomena [PB89-212328] N90-11436

METEOROLOGICAL RADAR
The effectiveness of adaptive PRF (Pulse Repetition Frequency) selection in minimizing range obscuration in the TDWR (Terminal Doppler Weather Radar) system [AD-A211267] N90-11222

METEOROLOGICAL SATELLITES
Meteorological rocket observations [PB89-168769] N90-11419
Composited local area forecast techniques [AD-A210802] N90-11432

METEOROLOGICAL SERVICES
Meteorological rocket observations [PB89-168769] N90-11419

METEOROLOGY
Examples of meteorological behavior of the ionosphere N90-11395
Hanford Meteorological Station computer codes. Volume 10: The ARCHIVE computer code [DE89-016175] N90-11429

METHOD OF CHARACTERISTICS
Method of characteristic studies for rotational flow downstream of a curved shock wave N90-11252

METHYL ALCOHOL
Results from the second year of operation of the Federal Methanol Fleet at Argonne National Laboratory [DE89-016935] N90-11319

METHYLHYDRAZINE
Atmospheric chemistry of the fuel hydrazines N90-11158

MICROBIOLOGY
The soil microbiology of hydrazines N90-11171

MICROBURSTS (METEOROLOGY)
A scalar/vector potential solution for aerodynamic coefficients in wind shear N90-10838

MICROCHANNEL PLATES
Ion detector on the basis of microchannel plates for a high-sensitive mass spectrometer [DE89-620335] N90-11291

MICROGRAVITY APPLICATIONS
Space Station Freedom: A foothold on the future [NASA-NP-107/10-88] N90-10907
Telescience Testbed Pilot Program [NASA-CR-184594] N90-11455

MICROMECHANICS
A study of the tribological and surface micromechanical properties of YBa2Cu3O7-x [DE89-015680] N90-11607

MICROMETEOROLOGY
Micrometeorological investigation of surface exchange of trace gases: A case study [PB89-208375] N90-11412

MICROORGANISMS
The soil microbiology of hydrazines N90-11171

MICROPROCESSORS
A prototype silicon compiler in prolog [AD-A210669] N90-11452

MICROSTRUCTURE
Fatigue crack growth rates as a function of delta K: Variability and material property N90-11031
Deformation induced microstructural and microchemical changes during thermomechanical treatment [DE89-017266] N90-11127
Microstructural effects on spall fracture in 1008 steel [DE89-016770] N90-11131
Ion implantation of two titanium alloys [DE89-016958] N90-11133
Characterizations of shock-loaded aluminum-infiltrated boron carbide cermets [DE89-016773] N90-11146

Intergranular and interphase boundaries in ceramics
[DE89-016969] N90-11154
Basic investigations of cutting machinability of inorganic glasses using single-point tools
[W-15/87] N90-11204
A characterization of the side bonding, upset plug welding process
[DE89-015181] N90-11315
A study of the tribological and surface micromechanical properties of YBa2Cu3O7-x
[DE89-015680] N90-11607
Defect structures preceding amorphization by ion irradiations in YBa2Cu3O(7-delta)
[DE89-016905] N90-11612
Exploratory study of niobium, titanium, zirconium and tantalum aluminides
[AD-A210658] N90-11615
High-temperature ceramic superconductors
[AD-A211070] N90-11618
Transport properties of thermally grown Cr2O3
[DE89-016703] N90-11623

MICROWAVE ANTENNAS
Antenna beamforming using optical processing
[NASA-CR-180844] N90-11210

MICROWAVE CIRCUITS
A general-purpose computer program for the Volterra-series analysis of nonlinear microwave circuits
[AD-A210768] N90-11236

MICROWAVE LANDING SYSTEMS
Helicopter Visual Segment Approach Lighting System (HALS)
[ACD-330] N90-10856

MICROWAVES
HPW (High Power Microwave) testing of electronic components
[DE89-016682] N90-11241
High-temperature ceramic superconductors
[AD-A211070] N90-11618

MIDCOURSE GUIDANCE
Optimal and on-board near-optimal midcourse guidance N90-10857

MIDLATITUDE ATMOSPHERE
Substorm associated pulsations: A study of plasmaspheric cavity resonance, mid-latitude polarisation and geostationary orbit signatures N90-11422

MILITARY OPERATIONS
Flight testing in the Netherlands: An overview N90-10884

MILITARY TECHNOLOGY
Laser techniques for ground to air applications
[FOA-C-30524-3.1] N90-11309

MILLIMETER WAVES
Precision materials characterization in the near millimeter and submillimeter wavelength range
[AD-A210655] N90-11106

MINERALOGY
Physiographic and geological setting of the Coastal Engineering Research Center's field research facility
[AD-A210772] N90-11356

MINES (ORDNANCE)
Fiber optic technique for surveillance and control of mine fields
[FOA-C-30526-3.1] N90-11293

MINIMAX TECHNIQUE
Subharmonic solutions near an equilibrium point for Hamiltonian systems
[AD-A210556] N90-11496

MIRRORS
System and performance analysis of a low density actively controlled mirror for astronomic observation N90-11002

MISSILE CONTROL
Design of a Kalman filter for transfer alignment N90-10848

MISSION PLANNING
Task analysis of the UH-60 mission and decision rules for developing a UH-60 workload prediction model. Volume 1: Summary report
[AD-A210763] N90-11446

MODAL RESPONSE
Analytic signals in the damping coefficient estimation N90-11003
Acoustic response analysis in the low frequency domain N90-11010
Comparison of sine dwell and broadband methods for modal testing N90-11025

MODELS
A fully electromagnetic hybrid model for high density plasma simulations
[DE89-016771] N90-11593
Inferring data base requirements from examples in forms N90-11646

MODULARITY
Module algebra (revised version)
[CWI-CS-R8844-REV] N90-11474

MODULES
Evaluation of dispersive behavior in periodic structures by discrete Fourier transform N90-11014
Dynamic substructuring for modular analysis and testing N90-11015

MODULUS OF ELASTICITY
Composites reinforced with thermotropic liquid crystal copolyester fibers
[AD-A211226] N90-11089

MOISTURE CONTENT
Airborne gamma radiation snow water equivalent and soil moisture measurements and satellite areal extent of snow cover measuerments: A user's guide, version 3.0
[PB89-177877] N90-11338

MOLECULAR ABSORPTION
Study of high frequency water vapor absorption parameters
[AD-A210676] N90-11108

MOLECULAR BIOLOGY
DOE/CEC Workshop on Critical Evaluation of Radiobiological Data to Biophysical Modeling
[DE89-015214] N90-11437

MOLECULAR CLOUDS
The stability of magnetohydrodynamic shock waves in molecular clouds N90-11665

MOLECULAR COLLISIONS
Particle kinetic simulation of high altitude hypervelocity flight
[NASA-CR-186003] N90-10840

MOLECULAR ENERGY LEVELS
Dissociation and vibrational relaxation of XeF by various collision partners
[AD-A210769] N90-11300

MOLECULAR EXCITATION
Quantum chemical investigations of the mechanism of cationic polymerization and theoretical prediction of crystal densities and decomposition pathways of energetic molecules
[AD-A210322] N90-11143

MOLECULAR ORBITALS
A diagnostic for determining the quality of single-reference electron correlation methods N90-11554

MOLECULAR OSCILLATIONS
Forty-fourth symposium on molecular spectroscopy
[AD-A210752] N90-11111

MOLECULAR ROTATION
Forty-fourth symposium on molecular spectroscopy
[AD-A210752] N90-11111

MOLECULAR SPECTRA
Chemiluminescent ion-molecule reactions of group-3 ions with halogens: New optical spectra and reaction dynamics
[MPIS-18/1988] N90-11120

MOLECULAR SPECTROSCOPY
Forty-fourth symposium on molecular spectroscopy
[AD-A210752] N90-11111

MOLECULAR STRUCTURE
Pressure induced resonance Raman effects in shocked carbon disulfide
[AD-A210665] N90-11107

MOLECULES
Structure and properties of simple molecular systems at very high density
[DE89-016974] N90-11557
New theoretical approaches for studying electron collisions with small molecules
[DE89-017543] N90-11558

MOMENTUM
Experimental identification of modal momentum coefficients and modal identity parameters of the FLECS structure N90-10991
Estimation of the C-J pressure of explosives
[DE89-013811] N90-11187

MOMENTUM TRANSFER
Questions from the Willmarth Workshop on New Directions in Research on Turbulent Wall-Layer Structures
[AD-A211282] N90-11264

MONITORS
The Third Conference on the Environmental Chemistry of Hydrazine Fuels
[AD-A197632] N90-11157
Description of a chemiluminescence detector system specifically designed for monitoring airborne hydrazine and oxidizer propellant vapors N90-11179

MONTE CARLO METHOD
Auxiliary-field transformations for repulsive potentials: A physical approach
[DE89-016677] N90-11223
Development of an approximate technique for the nonlinear random vibrations analysis of hysteretic systems N90-11335
On algorithms for generating computationally simple piecewise linear classifiers
[NDRE/PUBL-89/1001] N90-11459
Principal components in multivariate control charts
[DE89-016828] N90-11489

MORPHOLOGY
Global morphology of plasma bubbles in the low latitude ionosphere N90-11369
The middle and high latitude ionosphere at approximately 550 km altitude N90-11374
Modelling ionospheric density structures N90-11375
Polar F layer lacuna irregularities at Dumont d'Urville N90-11379
Upper ionosphere and magnetospheric-ionospheric coupling
[DE89-619727] N90-11415
Ion beam annealing of Ga-implanted Si
[DE89-016857] N90-11610

MOTION PERCEPTION
Inferences from images
[AD-A210710] N90-11465

MOTION SIMULATION
On the motion equation of an elastically supported two degree of freedon gyro
[NAL-TM-568] N90-11276

MRCA AIRCRAFT
Development of the integrated all-weather navigation system for Tornado N90-10849

MULTIPATH TRANSMISSION
Study of high frequency water vapor absorption parameters
[AD-A210676] N90-11108

MULTIPHASE FLOW
Gas-phase flowrate effect on disintegrating cryogenic liquid-jets
[NASA-TM-102357] N90-11277

MULTIPLE ACCESS
Performance analysis of hybrid ARQ protocols in a slotted code division multiple-access network
[AD-A211078] N90-11219

MULTIPLEXING
Independent Orbiter Assessment (IOA): Analysis of the instrumentation subsystem
[NASA-CR-185571] N90-10928
Optical coherence multiplexing for interprocessor communications
[DE89-016186] N90-11568

MULTIPROCESSING (COMPUTERS)
Evaluating the performance of software cache coherence
[AD-A211164] N90-11468
Asynchronous integration of ordinary differential equations on multiprocessors
[DE89-014169] N90-11493
Computing the two dimensional fast Fourier transform on a general purpose mesh connected multiprocessor
[DE89-016515] N90-11518
Fixed point iteration on point-symmetric interference graphs
[MEMO-INF-89-23] N90-11535

MULTISENSOR APPLICATIONS
Linkoeping's A.I. Consortium (LAIC) for plan guided systems. Review of the first 18 months
[FOA-C-30528-3.4] N90-11537

MULTIVARIATE STATISTICAL ANALYSIS
Evaluation of tests and design factors N90-10987
Principal components in multivariate control charts
[DE89-016828] N90-11489
Iterative network magnitude estimation and uncertainty assessment with noisy and clipped data
[AD-A210707] N90-11507

MUTATIONS
Computer symbiosis: Emergence of symbiotic behavior through evolution
[DE89-015247] N90-11450

N

NAPHTHALENE
Production of jet fuels from coal-derived liquids. Volume 11: Production of advanced endothermic fuel blends from Great Plains Gasification Plant naphtha by-product stream
[AD-A210251] N90-11184

NATIONAL AIRSPACE SYSTEM
Ground and Obstacle Avoidance (GOA) concept of operations
[DOT/FAA/DS-89/08] N90-10855

NAVIER-STOKES EQUATION
A parallel numerical simulation for supersonic flows using zonal overlapped grids and local time steps for common and distributed memory multiprocessors
[DE89-015252] N90-10839
An experimental study of helicity and related properties in turbulent flows
[DE89-016785] N90-11259

NAVIGATION AIDS
Federal Radionavigation Plan, 1988
[PB89-163075] N90-10846
NAVIGATION INSTRUMENTS
Development of a marine integrated navigation system N90-10852
NAVY
US Navy principal site testing concept and the F-18 N90-10861
NEAR FIELDS
Near zone-basic scattering code user's manual with space station applications
[NASA-CR-185925] N90-11209
NEAR INFRARED RADIATION
Study of high frequency water vapor absorption parameters
[AD-A210676] N90-11108
Ionospheric total electron content, and far ultraviolet, near infrared oxygen emission N90-11410
NEAR WAKES
Linear instability of supersonic plane wakes
[NASA-CR-181911] N90-10833
NEGATIVE IONS
Extraction induced emittance growth for negative ion sources
[DE89-017586] N90-11559
NEODYMIUM LASERS
Laser-driven miniature flyer plates for shock initiation of secondary explosives
[DE89-016587] N90-11288
Interferometry and high speed photography of laser-driven flyer plates
[DE89-016990] N90-11290
NETHERLANDS
Flight testing in the Netherlands: An overview N90-10884
NETWORK ANALYSIS
Transaction throughput in distributed systems: A modeling study using dynamic queueing networks
[MEMO-INF-89-25] N90-11479
Stochastic flows in networks
[AD-A211209] N90-11515
Phoebe: A preliminary control network and rotational elements
[NASA-CR-185716] N90-11680
NETWORK CONTROL
A contribution to the synthesis of communication switching systems with decentralized control using modular components
[ETN-89-94660] N90-11226
NETWORK SYNTHESIS
Adaptive gigabit fiber optics local area network
[AD-A210794] N90-11571
NEUTRAL GASES
Stormtime coupling of the neutral and ionized upper atmosphere at middle latitudes N90-11381
Calculation of the temperature and velocity vector of the neutral gas using EISCAT CP3-data N90-11384
NEUTRAL PARTICLES
Determination of neutral particle concentration at erosion laser plasma expansion into vacuum
[DE89-620128] N90-11308
NEUTRALIZERS
The chemistry of the hypochlorite neutralization of hydrazine fuels N90-11173
NEUTRON DIFFRACTION
Neutron scattering experiments on high-temperature superconducting materials: Foreign trip report, September 13, 1988--October 4, 1988
[DE89-017451] N90-11630
Report of the Specialists' Workshop on Phase Transition Studies on Hydrogen-Bonded Crystals by Neutron and X-ray Diffractometries
[DE89-906638] N90-11631
NEUTRON SCATTERING
Spin fluctuations and excitations in a 2D xy-ferromagnet: CoCl2 in graphite
[DE89-017600] N90-11119
Neutron scattering studies of amorphous Invar alloys
[DE89-016868] N90-11126
Neutron scattering experiments on high-temperature superconducting materials: Foreign trip report, September 13, 1988--October 4, 1988
[DE89-017451] N90-11630
NEUTRON SOURCES
The Reversed-Field-Pinch (RFP) fusion neutron source: A conceptual design
[DE89-015297] N90-11577
NEWTON METHODS
An improved algorithm for the determination of the system paramters of a visual binary by least squares N90-11658
NICKEL ALLOYS
Failure modes and mechanisms in nickel alloys: Primarily austenitic stainless steel
[DE89-016823] N90-11132
NICKEL STEELS
Contribution to the transcrystalline stress crack corrosion of austenite chromium-nickel steels
[ETN-89-94665] N90-11137
NIGHT SKY
Night sky radiometric measurements during follow-on-evaluation testing of AN/PVS-7 (A, B) at Fort Benning, Georgia
[AD-A211273] N90-11574
NIGHT VISION
Night sky radiometric measurements during follow-on-evaluation testing of AN/PVS-7 (A, B) at Fort Benning, Georgia
[AD-A211273] N90-11574
NIOBIUM
Exploratory study of niobium, titanium, zirconium and tantalum aluminides
[AD-A210658] N90-11615
NIOBIUM CARBIDES
Kinetics and mechanisms of primary and steady state creep in B- and Al-containing alpha silicon carbide
[AD-A210739] N90-11616
NITINOL ALLOYS
Battery actuation of NITINOL at sub-zero temperatures
[AD-A211254] N90-11237
NITRAMINE PROPELLANTS
Nitramine composite solid propellant modeling N90-11183
NITRIDES
Ion implantation of two titanium alloys
[DE89-016958] N90-11133
NITROGEN COMPOUNDS
Y-Si-Al-O-N glass fibers
[AD-A211170] N90-11088
NITROGEN DIOXIDE
Atmospheric chemistry of the fuel hydrazines N90-11158
Micrometeorological investigation of surface exchange of trace gases: A case study
[PB89-208375] N90-11412
NITROGEN IONS
Ion implantation of two titanium alloys
[DE89-016958] N90-11133
NITROMETHANE
In-situ study of the chemically driven flow fields in initiating homogeneous and heterogeneous nitromethane explosives
[DE89-008415] N90-11186
NOISE GENERATORS
Development of a thermoacoustic test facility N90-11041
The large European Acoustic Facility at ESTEC N90-11067
NOISE REDUCTION
Calculation of sound transmission through a cylindrical shell using ASKA acoustics N90-11009
NONDESTRUCTIVE TESTS
Wave-mode coordinate analysis of L junction in LSS
[AD-A211116] N90-10984
Advances in instrumentation for experimental stress and vibration analysis and its applications N90-11069
Sensors for nondestructive testing and evaluation of materials
[DE89-014763] N90-11279
The investigation of the fundamental limits of heterodyne holographic interferometry with the application of imaging laser generated lamb waves
[AD-A211048] N90-11285
A technique to correlate fractography with NDE (Non-Destructive Evaluation) of small samples
[DE89-016904] N90-11325
NONEQUILIBRIUM FLOW
Particle kinetic simulation of high altitude hypervelocity flight
[NASA-CR-186003] N90-10840
NONEQUILIBRIUM IONIZATION
Gas dynamical processes in the theory of galaxy formation N90-11673
NONFLAMMABLE MATERIALS
Test and evaluation: Reducing risks to military aircraft from bird collisions. Report to the Chairman, Legislation, and National Security Subcommittee, Committee on Goverment Operations, House of Representatives
[AD-A210670] N90-10845
NONLINEAR EQUATIONS
Non-linear wave-equations for low-frequency acoustic gravity waves N90-11365
NONLINEAR OPTICS
Generation of higher-order squeezing of quantum electromagnetic fields by degenerate four-wave mixing and other processes
[DE89-618392] N90-11213
Nonlinear optical studies of resonant systems
[AD-A211032] N90-11301
NONLINEAR SYSTEMS
A general-purpose computer program for the Volterra-series analysis of nonlinear microwave circuits
[AD-A210768] N90-11236
Nonlinear adjustment with or without constraints, applicable to geodetic models
[AD-A210820] N90-11509
NONLINEARITY
Passive trajectography by azimuth: Improvement of estimation quality N90-10854
Development of an approximate technique for the nonlinear random vibrations analysis of hysteretic systems N90-11335
Estimation on nonlinear damping in second order distributed parameter systems
[NASA-CR-181890] N90-11494
Nonlinear adjustment with or without constraints, applicable to geodetic models
[AD-A210820] N90-11509
Potential for parallelism in explicit linear methods
[DE89-017329] N90-11523
A solution to nonlinearity problems
[DE89-016975] N90-11544
NONPARAMETRIC STATISTICS
Boundary kernel estimation of the two sample comparison density function
[AD-A210757] N90-11532
NONTHERMAL RADIATION
Ionosphere-thermosphere coupling at high latitudes: Aspect angle dependence of non-thermal plasmas N90-11382
NORMAL DENSITY FUNCTIONS
Efficient numerical method for computation of thermohydrodynamics of laminar lubricating films
[NASA-CR-185136] N90-11256
NORMAL SHOCK WAVES
The stability of magnetohydrodynamic shock waves in molecular clouds N90-11665
NORTHERN HEMISPHERE
Auroral and sub-auroral F-layer irregularity studies in the Northern and Southern Hemisphere during the equinox transition study September 16-26, 1984 N90-11393
NOSE WHEELS
Independent Orbiter Assessment (IOA): Analysis of the nose wheel steering subsystem
[NASA-CR-185548] N90-10921
Independent Orbiter Assessment (IOA): Analysis of the landing/deceleration subsystem
[NASA-CR-185569] N90-10943
Independent Orbiter Assessment (IOA): Assessment of the nose wheel steering subsystem
[NASA-CR-185533] N90-10947
Independent Orbiter Assessment (IOA): CIL issues resolution report, volume 2
[NASA-CR-185524-VOL-2] N90-10955
NUCLEAR FUSION
Theoretical atomic physics for fusion
[DE89-017363] N90-11563
The Reversed-Field-Pinch (RFP) fusion neutron source: A conceptual design
[DE89-015297] N90-11577
NUCLEAR MAGNETIC RESONANCE
Applications of NMR spectroscopy to the study of zeolite synthesis
[DE89-015226] N90-11095
NUCLEAR REACTORS
Boundary effects on the MHD dynamo in laboratory plasmas
[DE89-015207] N90-11576
NUCLEAR STRUCTURE
Synchrotron radiation, free electron laser, and nuclear structure
[DE89-017352] N90-11306
NUCLEATION
Dynamics of nucleation at electrochemical interfaces via surface EXAFS and standing wave measurements
[AD-A210733] N90-11109
NULL ZONES
Deep null antennas and their applications to tactical VHF radio communications
[AD-A210656] N90-11214
Boundary kernel estimation of the two sample comparison density function
[AD-A210757] N90-11532
NUMERICAL ANALYSIS
Study for optimization of redundant vane-type flow-direction sensing systems and numerical analysis for design of the systems
[NAL-TM-571] N90-10890
Numerical treatment of the thermo-structural-dynamic problems: The interpolation techniques N90-11016
International conference on numerical grid generation in computational fluid dynamics
[AD-A211082] N90-11262
Analytical and numerical studies in flow development
[DE89-017380] N90-11269

On the numerical solution of two-point boundary value problems
[AD-A211244] N90-11516
NUMERICAL CONTROL
Numerical simulation of turbulent flow downstream a sudden axisymmetric expansion
[FOA-C-20758-2.1] N90-11272
NUMERICAL INTEGRATION
STS-GPS (Space Transportation System - Global Positioning System) tracking experiment for gravitation estimation: Feasibility study
[AD-A211265] N90-10859
An analytical and experimental study of the elastodynamic response characteristics of planar linkage mechanism with bearing clearances N90-11336
Programs for numerical integration of piece-wise smooth functions
[DE89-620449] N90-11464
NUMERICAL STABILITY
A nonoscillatory, characteristically convected, finite volume scheme for multidimensional convection problems
[NASA-TM-102354] N90-11497
Note on explicit parallel multistep Runge-Kutta methods
[CWI-NM-R8814] N90-11529
On the equivalence of BS-stability and B-consistency
[CWI-NM-R8815] N90-11530

O

OBLIQUE SHOCK WAVES
The stability of magnetohydrodynamic shock waves in molecular clouds N90-11665
OCCLUSION
The 3D-POLY: A robot vision system for recognizing objects in occluded environments N90-11313
OCCUPATIONAL DISEASES
Occupational safety considerations with hydrazine N90-11182
OCEAN BOTTOM
Corrosion rates of structural materials on the ocean floor
[DE89-015211] N90-11123
Physiographic and geological setting of the Coastal Engineering Research Center's field research facility
[AD-A210772] N90-11356
Coastal subsea permafrost and bedrock observations using dc resistivity
[AD-A210784] N90-11435
OCEAN SURFACE
Laser altimeter for use over the ocean
[AD-A211252] N90-11286
Interannual variability of temperature in the upper layer of the North Pacific eastern boundary region, 1971-1987
[PB89-190227] N90-11434
OCEAN TEMPERATURE
Interannual variability of temperature in the upper layer of the North Pacific eastern boundary region, 1971-1987
[PB89-190227] N90-11434
OCEAN THERMAL ENERGY CONVERSION
Planning for hybrid-cycle OTEC experiments using the HMTSTA test facility at the Natural Energy Laboratory of Hawaii
[DE89-013278] N90-11349
OCEANOGRAPHIC PARAMETERS
The sea ice margins: A summary of physical phenomena
[PB89-212328] N90-11436
OCEANOGRAPHY
Coastal subsea permafrost and bedrock observations using dc resistivity
[AD-A210784] N90-11435
OCEANS
Laser altimeter for use over the ocean
[AD-A211252] N90-11286
OGIVES
An experimental investigation of the aerodynamic characteristics of slanted base ogive cylinders using magnetic suspension technology
[NASA-CR-181708] N90-10834
OILS
Flow visualization techniques for flight research N90-10878
OMNIDIRECTIONAL ANTENNAS
A calibrated, omnidirectional, LF loop antenna for GWEN (Ground Wave Emergency Network)
[AD-A211264] N90-11221
OPACITY
Solar opacities constrained by solar neutrinos and solar oscillations
[DE89-016988] N90-11687
OPEN CLUSTERS
Carbon isotope ratios and lithium abundances in open cluster giants N90-11684
OPERATING COSTS
View on recent fuel costs in airlines
[NAL-TM-569] N90-11653
OPERATING SYSTEMS (COMPUTERS)
A distributed debugger for Amoeba
[CWI-CS-R8828] N90-11453
MSP: Modeling of concurrent processes. Version 1.00 General introduction and directions for use
[REPT-88-88] N90-11477
On the Amoeba protocol
[CWI-CS-R8827] N90-11480
OPERATIONAL CALCULUS
Module algebra (revised version)
[CWI-CS-R8844-REV] N90-11474
Backward analysis on higher order functions
[MEMO-INF-89-19] N90-11526
OPERATIONS RESEARCH
Checking the Goldbach conjecture on a vector computer
[CWI-NM-R8812] N90-11475
Variable step iteration of high-order Runge-Kutta methods on parallel computers
[CWI-NM-R8817] N90-11476
Transaction throughput in distributed systems: A modeling study using dynamic queueing networks
[MEMO-INF-89-25] N90-11479
On the Amoeba protocol
[CWI-CS-R8827] N90-11480
LINPACK routines based on the level 2 BLAS
[CWI-NM-R8811] N90-11483
Fixed point iteration on point-symmetric interference graphs
[MEMO-INF-89-23] N90-11535
OPTICAL COMMUNICATION
Calculation, optimization and comparison of optical transmission systems with superheterodyne reception
[ETN-89-94651] N90-11224
Laser dynamics: The system dynamics and network theory of optoelectronic integrated circuit design N90-11296
Optical coherence multiplexing for interprocessor communications
[DE89-016186] N90-11568
OPTICAL COMPUTERS
Antenna beamforming using optical processing
[NASA-CR-180844] N90-11210
OPTICAL DATA PROCESSING
Utilization of photorefractive crystals in optical image processing
[ISBN-3-923560-06-0] N90-11292
OPTICAL FIBERS
Fiber optic technique for surveillance and control of mine fields
[FOA-C-30526-3.1] N90-11293
Fiber optics: A brief introduction
[DE89-009337] N90-11567
Acceleration of thin foil targets using fiber-coupled optical pulses
[DE89-016526] N90-11569
OPTICAL FILTERS
A remote sensor to monitor combustion products using a tunable acousto-optic filter N90-11275
The Si(1-x)Nx Rugate
[AD-A211236] N90-11572
OPTICAL MEASURING INSTRUMENTS
Evaluation test of CCD area sensor for star sensor
[NAL-TM-570] N90-11566
OPTICAL PATHS
Study of high frequency water vapor absorption parameters
[AD-A210676] N90-11108
OPTICAL PROPERTIES
Study of high frequency water vapor absorption parameters
[AD-A210676] N90-11108
Atmospheric aerosol size distributions and optical properties found in the marine boundary layer over the Atlantic Ocean
[AD-A210800] N90-11431
Acoustic studies of new materials: Quasicrystals, low-loss glasses and high Tc superconductors
[AD-A211281] N90-11551
OPTICAL PUMPING
Precision materials characterization in the near millimeter and submillimeter wavelength range
[AD-A210655] N90-11106
OPTICAL RADAR
Laser altimeter for use over the ocean
[AD-A211252] N90-11286
Laser techniques for ground to air applications
[FOA-C-30524-3.1] N90-11309
Lidar observations of the stratospheric aerosol: Boulder, Colorado, 1985 to 1987
[PB89-203871] N90-11425
OPTICAL REFLECTION
Fiber optics: A brief introduction
[DE89-009337] N90-11567
OPTICAL WAVEGUIDES
Novel physical effects in intersecting optical waveguides N90-11565
OPTIMAL CONTROL
Performance analysis of hybrid ARQ protocols in a slotted code division multiple-access network
[AD-A211078] N90-11219
OPTIMIZATION
Optimal and on-board near-optimal midcourse guidance N90-10857
Integrated multidisciplinary design optimization of rotorcraft
[NASA-TM-101642] N90-10889
Study for optimization of redundant vane-type flow-direction sensing systems and numerical analysis for design of the systems
[NAL-TM-571] N90-10890
A review of the Error of Matrix Method (EMM) for structural dynamic model comparison N90-10993
JOE: Jordan Optimized Eigensolver. A step toward a numerical Jordan form analyzer for control and interactive thermo-structural-dynamic applications N90-11047
New data handling system (MDH) for mechanical tests at ESTEC N90-11066
Thin section casting program. Volume 3: Vertical TSC (Thin-Section Casting) approach
[DE89-009033] N90-11201
Calculation, optimization and comparison of optical transmission systems with superheterodyne reception
[ETN-89-94651] N90-11224
Stochastic optimization by simulation: Some experiments with a simple steady-state queue
[AD-A210762] N90-11508
Control and optimization for observations of systems governed by controlled partial differential equations
[AD-A211122] N90-11513
Reduction of the Dirac equation to the Dirac-Kaehler equation
[DE89-630111] N90-11541
OPTOELECTRONIC DEVICES
Laser dynamics: The system dynamics and network theory of optoelectronic integrated circuit design N90-11296
Semiconductor quantum well lasers and related optoelectronic devices on silicon, III-V
[AD-A210758] N90-11299
ORBIT CALCULATION
The recovery of orbital and geophysical parameters using a spaceborne laser ranging system N90-11294
ORBITAL ASSEMBLY
Space Station Freedom: A foothold on the future
[NASA-NP-107/10-88] N90-10907
ORBITAL MANEUVERING VEHICLES
Independent Orbiter Assessment (IOA): Analysis of the orbital maneuvering system
[NASA-CR-185554] N90-10919
ORBITAL MECHANICS
Adaptive structures to meet future requirements for large precision structures N90-11001
An improved algorithm for the determination of the system paramters of a visual binary by least squares N90-11658
ORGANIC MATERIALS
Interactions of hydrazines with colloidal constituents of soils N90-11164
Selective removal of organics for water reclamation
[NASA-CR-185959] N90-11445
ORGANOMETALLIC COMPOUNDS
Synthesis of powder with gel technique
[FOA-C-20752-2.4(2.1)] N90-11156
ORTHOTROPIC SHELLS
Equilibrium and stability in composite thin shell N90-10998
OSCILLATING FLOW
An experimental investigation of transition in oscillating pipe flow N90-11249
OSCILLATORS
Resonance effect on the oscillator distribution function
[DE89-630105] N90-11548
OXIDATION
Photochemically-driven biomimetic oxidation of alkanes and olefins
[DE89-011536] N90-11097
Enhanced oxidation and solovolysis reactions in chemically inert microheterogeneous systems
[AD-A210748] N90-11110
Hydrogen-silicon carbide interactions
[NASA-TM-102382] N90-11144
Surface-catalyzed air oxidation of hydrazines: Environmental chamber studies N90-11159
Trace metal catalysis of hydrazine decomposition: The role of chromium N90-11163

Surface-catalyzed air oxidation reactions of hydrazines: Tubular reactor studies N90-11167
The chemistry of the hypochlorite neutralization of hydrazine fuels N90-11173
Fuel neutralization by ozone oxidation N90-11176
Powder morphology effects in the ignition of titanium-based pyrotechnics
[DE89-017229] N90-11191
Transport properties of thermally grown Cr2O3
[DE89-016703] N90-11623

OXIDATION-REDUCTION REACTIONS
Dynamics of nucleation at electrochemical interfaces via surface EXAFS and standing wave measurements
[AD-A210733] N90-11109
Enhanced oxidation and solvolysis reactions in chemically inert microheterogeneous systems
[AD-A210748] N90-11110
Capacitive behavior in conducting polymers: The ac impedance and quartz crystal microbalance studies
[AD-A210754] N90-11150

OXYGEN
A new inexpensive electrochemical meter for oxygen in sodium coolant
[DE89-630802] N90-11104
Ionospheric total electron content, and far ultraviolet, near infrared oxygen emission N90-11410

OXYGEN IONS
Ion implantation of two titanium alloys
[DE89-016958] N90-11133
Can ion acceleration by double-cyclotron absorption produce O(+) ion conics
[IRF-PREPRINT-114] N90-11600

OXYNITRIDES
Y-Si-Al-O-N glass fibers
[AD-A211170] N90-11088

OZONE
Atmospheric chemistry of the fuel hydrazines N90-11158
Ozonation of hydrazines and their associated impurities N90-11174
Modeling the ozonolysis of hydrazines wastewater N90-11175
Fuel neutralization by ozone oxidation N90-11176
Interrelation of experimental exposure and ambient air quality data for comparison of ozone exposure indices and estimating agricultural losses
[PB89-195036] N90-11353
Are ozone exceedance rates decreasing. Comment on extreme value analysis of environmental time-series: An application to trend detection in ground-level ozone
[AD-A211029] N90-11357
Micrometeorological investigation of surface exchange of trace gases: A case study
[PB89-208375] N90-11412
Theoretical investigation of gas-surface interactions
[NASA-CR-185492] N90-11552

OZONE DEPLETION
Stratospheric ozone depletion
[PB89-207476] N90-11354

P

PACIFIC OCEAN
Interannual variability of temperature in the upper layer of the North Pacific eastern boundary region, 1971-1987
[PB89-190227] N90-11434

PACKETS (COMMUNICATION)
Network analyzer for nonstatic jamming
[AD-A210759] N90-11216

PANEL METHOD (FLUID DYNAMICS)
Frequency domain aerodynamic analysis of interacting rotating systems N90-10837

PARALLEL COMPUTERS
Variable step iteration of high-order Runge-Kutta methods on parallel computers
[CWI-NM-R8817] N90-11476

PARALLEL PROCESSING (COMPUTERS)
A parallel numerical simulation for supersonic flows using zonal overlapped grids and local time steps for common and distributed memory multiprocessors
[DE89-015252] N90-10839
Advanced manned space flight simulation and training: An investigation of simulation host computer system concepts
[NASA-CR-185998] N90-10911
Modal analysis of fluid-structure systems by parallel subspace iteration N90-11024
Cellular automata and massively parallel physics
[DE89-016506] N90-11257
New computing systems and their impact on structural analysis and design
[NASA-CR-185831] N90-11457
Research, development, training and education using the Ada programming language
[AD-A210760] N90-11466
Parallel inference based on delta processing
[CWI-CS-R8846] N90-11482
A generalization of A. N. Habermann's theorem for semaphores
[REPT-88-98] N90-11484
Asynchronous integration of ordinary differential equations on multiprocessors
[DE89-014169] N90-11493
Computing the two dimensional fast Fourier transform on a general purpose mesh connected multiprocessor
[DE89-016515] N90-11518
Potential for parallelism in explicit linear methods
[DE89-017329] N90-11523
Note on explicit parallel multistep Runge-Kutta methods
[CWI-NM-R8814] N90-11529

PARALLEL PROGRAMMING
Boolean functions, invariance groups and parallel complexity
[CWI-CS-R8836] N90-11472

PARAMETER IDENTIFICATION
STS-GPS (Space Transportation System - Global Positioning System) tracking experiment for gravitation estimation: Feasibility study
[AD-A211265] N90-10859
Results and practical experience using parameter identification techniques on the AM-X program at Aermacchi N90-10873
Experimental identification of modal momentum coefficients and modal identity parameters of the FLECS structure N90-10991
Updating of finite element model by means of normal mode parameters N90-10992
Parametric identification of conservative self adjoint structures N90-10994
Employment of modal survey methodologies in dynamic analysis procedures N90-11006
Comparison of phase resonance, mode separation, and driven-base modal identification methods applied to the FLECS test structure N90-11027
Performance and robustness of adaptive controllers for linear stochastic systems N90-11485

PARAMETERIZATION
An evaluation of the Chaboche and Bodner-Partom viscoplastic constitutive theories for strain rate sensitive materials N90-11330
Parameter estimation in functional and partial differential equations
[AD-A211040] N90-11511
Constitutive parameter measurements of lossy materials
[NASA-CR-183398] N90-11603

PARASITES
Computer symbiosis: Emergence of symbiotic behavior through evolution
[DE89-015247] N90-11450

PARSING ALGORITHMS
Two VAX-PASCAL terminal interface modules for visualizing scanning and parsing
[MEMO-INF-89-17] N90-11470

PARTIAL DIFFERENTIAL EQUATIONS
Wavefront propagation for reaction-diffusion systems of PDE
[AD-A210862] N90-11510
Control and optimization for observations of systems governed by controlled partial differential equations
[AD-A211122] N90-11513
Domain decomposition for partial differential equations
[DE89-016869] N90-11519

PARTICLE ACCELERATION
Ionospheric irregularities due to powerful HF radio transmissions N90-11389
Can ion acceleration by double-cyclotron absorption produce O(+) ion conics
[IRF-PREPRINT-114] N90-11600

PARTICLE ACCELERATORS
Lifetime testing of commercially available 3.0 (mu)f, 100 kV pulsed-power capacitors
[DE89-017230] N90-11242
Investigations into the influence of the state functions on the cross sections of the direct p,gamma reactions at energies in the 100 keV range, and project of a cascade accelerator for the measurement of the p,gamma capture cross sections
[ETN-89-94662] N90-11561

PARTICLE BEAMS
Ion sources, electron guns and beam optics
[DE89-015526] N90-11562

PARTICLE COLLISIONS
Global ionospheric dynamics N90-11366
Ion heating events observed at the EISCAT radar N90-11385
Theoretical atomic physics for fusion
[DE89-017363] N90-11563

PARTICLE INTERACTIONS
On the effective transport properties of composite materials N90-11086
Global and local fluctuations in multiplicity and transverse energy for central ultra-relativistic heavy-ion interactions
[LUIP-8903] N90-11555

PARTICLE MOTION
DMC (Distinct Motion Code): A rigid body motion code for determining the interaction of multiple spherical particles
[DE89-016929] N90-11543

PARTICLE PRECIPITATION
Magnetospheric substorms as a signature of the solar terrestrial interaction N90-11363
Modelling ionospheric density structures N90-11375
Observations of ionosphere/magnetosphere interactions from the Dynamics Explorer satellites N90-11378
Electrostatic turbulence in the high latitude ionosphere N90-11392

PARTICLE SIZE DISTRIBUTION
Powder morphology effects in the ignition of titanium-based pyrotechnics
[DE89-017229] N90-11191
Analysis of forest fire smoke using satellite imagery
[AD-A210657] N90-11339
Atmospheric aerosol size distributions and optical properties found in the marine boundary layer over the Atlantic Ocean
[AD-A210800] N90-11431

PARTICLES
A laser Doppler anemometry investigation of single-phase and particle-laden jet flows
[AD-A210660] N90-11261
DMC (Distinct Motion Code): A rigid body motion code for determining the interaction of multiple spherical particles
[DE89-016929] N90-11543

PASCAL (PROGRAMMING LANGUAGE)
Two VAX-PASCAL terminal interface modules for visualizing scanning and parsing
[MEMO-INF-89-17] N90-11470

PATTERN RECOGNITION
Microsensor and pattern recognition techniques in hydrazine detection N90-11177
Simulation of synthetic aperture radar 1: Feature density and accuracy requirements
[AD-A211019] N90-11218
The 3D-POLY: A robot vision system for recognizing objects in occluded environments N90-11313
ANIMA: Image analyzer applied to remote sensing
[INPE-4766-PRE/1435] N90-11447
On algorithms for generating computationally simple piecewise linear classifiers
[NDRE/PUBL-89/1001] N90-11459
Inferences from images
[AD-A210710] N90-11465
Applications of artificial intelligence to digital photogrammetry N90-11486

PAVEMENTS
Definition of research needs to address airport pavement distress in cold regions
[DOT/FAA/DS-89/13] N90-10896

PAYLOAD CONTROL
Independent Orbiter Assessment (IOA): Analysis of the remote manipulator system
[NASA-CR-185585] N90-10926
STS payload design load evolution N90-10989
Reduction of dynamic response of spacecraft structures and payloads N90-11000
Flight-mechanical environment on Ariane launch vehicle payloads N90-11048

PAYLOAD INTEGRATION
STS payload design load evolution N90-10989

PAYLOAD INTEGRATION PLAN
Flight-mechanical environment on Ariane launch vehicle payloads N90-11048

PENETRATION
Evaluation of integrals related to the Debye function
[DE89-016930] N90-11499

PENNING DISCHARGE
Beam-plasma discharge in penetrating plasma
[DE89-630481] N90-11597

PERFORMANCE PREDICTION
The third generation rigid solar array GSR3 N90-11017
Planning for hybrid-cycle OTEC experiments using the HMTSTA test facility at the Natural Energy Laboratory of Hawaii
[DE89-013278] N90-11349

PERFORMANCE TESTS
Development of a marine integrated navigation system N90-10852
Aircraft live fire testing N90-10879

Deep null antennas and their applications to tactical VHF radio communications
[AD-A210656] N90-11214
Wideband connectivity and support for Cronus cluster at USAF Electronic Systems Division
[AD-A210749] N90-11215
ASIC (Application Specific Integrated Circuit) replacement for an SSI (Small Scale Integrated) component design: A case study
[DE89-013494] N90-11232
Lifetime testing of commercially available 3.0 (mu)f, 100 kV pulsed-power capacitors
[DE89-017230] N90-11242

PERMEATING
Modeling of hydrazine surface interactions in environmental reaction chambers N90-11162

PERMITTIVITY
Influence of core-shell grains on the internal stress state and permittivity response of zirconia modified barium titanate
[AD-A211245] N90-11153

PERSONNEL
Hydrazine dosimetry N90-11178

PERSONNEL DEVELOPMENT
Higher education for science and technology: A background paper
[PB89-191290] N90-11642

PERTURBATION
Report on the 2-D Model Intercomparison Workshop held January 11-16, 1987 in Fort Myers Beach, Florida, chapter 2 N90-11406
Gauge invariant cosmological perturbations with cold dark matter
[DE89-790940] N90-11679

PETN
Crystal orientation effects in PETN explosive with 4 GPa shocks
[DE89-016996] N90-11190

PHASE CHANGE MATERIALS
Potential industrial applications for composite phase-change materials as thermal energy storage media
[DE89-015170] N90-11346

PHASE TRANSFORMATIONS
Time-resolved mass spectrometry technique for studying fast transient CHNO explosive decomposition kinetics
[DE89-016540] N90-11101
Solidification front/viscous phase transitions, forward-backward heat equations
[AD-A211068] N90-11114
X-ray and gamma-ray spectroscopy of solids under pressure
[DE89-017271] N90-11118
Thermal expansion and phase transformation studies on some materials by high temperature X-ray powder diffractometry
[DE89-631032] N90-11130
Precipitation and transformation toughening of Al-Mg signals
[ETN-89-94675] N90-11138
Shock induced dissociation of polyethylene
[DE89-016983] N90-11267
Structure and properties of simple molecular systems at very high density
[DE89-016974] N90-11557
Chevron layer structures in Surface Stabilized Ferroelectric Liquid Crystal (SSFLC) cells filled witth a material which exhibits the chiral nematic to smectic C* phase transition
[DE89-016985] N90-11628
Neutron scattering experiments on high-temperature superconducting materials: Foreign trip report, September 13, 1988--October 4, 1988
[DE89-017451] N90-11630
Report of the Specialists' Workshop on Phase Transition Studies on Hydrogen-Bonded Crystals by Neutron and X-ray Diffractometries
[DE89-906638] N90-11631

PHASED ARRAYS
Antenna beamforming using optical processing
[NASA-CR-180844] N90-11210

PHOBOS
Soviet Mars program N90-10903

PHOEBE
Phoebe: A preliminary control network and rotational elements
[NASA-CR-185716] N90-11680

PHONONS
Quasi-diffusion between phonon and roton gases in two- and three-dimensional liquid helium
[AD-A210565] N90-11096
Study of disorder and strain in semiconductor heterostructures and superlattices by Raman scattering N90-11601

PHOTOCHEMICAL OXIDANTS
Stratospheric ozone depletion
[PB89-207476] N90-11354

PHOTOCHEMICAL REACTIONS
Photochemically-driven biomimetic oxidation of alkanes and olefins
[DE89-011536] N90-11097
Two-Dimensional Intercomparison of Stratospheric Models
[NASA-CP-3042] N90-11405
Report on the 2-D Model Intercomparison Workshop held January 11-16, 1987 in Fort Myers Beach, Florida, chapter 2 N90-11406
Report of the 1988 2-D Intercomparison Workshop, chapter 3 N90-11407
Model documentation, chapter 4 N90-11408
Introduction and data summary, chapter 5 N90-11409
Electron transfer reactions
[AD-A210711] N90-11545

PHOTOELECTRIC EMISSION
On the photoemission spectrum and optical gap in La2CuO4
[DE89-015281] N90-11605
A fermi liquid electric structure and the nature of the carriers in high-T(sub c) cuprates: A photoemission study
[DE89-016774] N90-11624

PHOTOGRAMMETRY
Applications of artificial intelligence to digital photogrammetry N90-11486

PHOTOLUMINESCENCE
Radiationless transitions and excited-state absorption of low-field chromium complexes in solids
[AD-A210653] N90-11105

PHOTOMETERS
Laser physics and laser techniques
[AD-A211117] N90-11302

PHOTON-ELECTRON INTERACTION
International workshop on Beam Injection Assessment of Defects in Semiconductors
[AD-A210842] N90-11617

PHOTONS
Dielectronic excitation and recombination in crystal channels
[DE89-016864] N90-11625
Solar opacities constrained by solar neutrinos and solar oscillations
[DE89-016988] N90-11687

PHOTOSYNTHESIS
Photochemically-driven biomimetic oxidation of alkanes and olefins
[DE89-011536] N90-11097

PHYSICAL OPTICS
Nonprincipal-plane scattering from flat plates: Second-order and corner diffraction and pattern control of horn antennas
[NASA-CR-185485] N90-11205
Part A: Nonprincipal-plane scattering from flat plates: Second-order and corner diffractions N90-11206
Constitutive parameter measurements of lossy materials
[NASA-CR-183398] N90-11603

PHYSIOLOGICAL EFFECTS
Biological effects of power frequency electric and magnetic fields: Background paper
[PB89-209985] N90-11439

PIEZOELECTRIC TRANSDUCERS
Polarization matrices of lithium tetraborate
[AD-A210774] N90-11112

PIEZOELECTRICITY
Behaviour of VF(sub 2)/VF(sub 3) piezoelectric copolymers under shock loading
[DE89-016538] N90-11145
Response of standardized PVDF piezoelectric polymer gauges to direct shock pressures between 8 and 32 GPa
[DE89-016811] N90-11282
The Sandia standard for PVDF (Polyvinylidene Di-Fluoride) shock sensors
[DE89-016530] N90-11287

PILOT PERFORMANCE
Helicopter Visual Segment Approach Lighting System (HALS)
[ACD-330] N90-10856
Heliport surface maneuvering test results
[ACD-330] N90-10897

PILOT PLANTS
Thin section casting program. Volume 2-A: Appendix to volume 2
[DE89-009032] N90-11200

PINS
Worked-in holes in three-dimensional reinforced composites N90-11060

PIPE FLOW
The structure of Reynolds stress in the near wall region of a turbulent pipe flow N90-11247
An experimental investigation of transition in oscillating pipe flow N90-11249

PIPES (TUBES)
Surface-catalyzed air oxidation reactions of hydrazines: Tubular reactor studies N90-11167
Analysis of coaxial wire measurement of longitudinal coupling impedance
[DE89-015748] N90-11230

PITCH (INCLINATION)
The dynamics of circular plates with patch damping: A numerical and experimental study N90-11329

PLANAR STRUCTURES
Robust spatial calibration of a planar positron camera
[AD-A210773] N90-11284
Planar sliding of a rigid body with dry friction: Limit surfaces and dynamics of motion N90-11314
An analytical and experimental study of the elastodynamic response characteristics of planar linkage mechanism with bearing clearances N90-11336
Inferences from images
[AD-A210710] N90-11485

PLANE WAVES
Computations of the refraction of a plane shock wave at a slow-fast gas interface
[DE89-016508] N90-11258

PLANETARY IONOSPHERES
Global ionospheric dynamics N90-11366

PLANETARY MAPPING
Phoebe: A preliminary control network and rotational elements
[NASA-CR-185716] N90-11680

PLANETARY SURFACES
A dynamical study of Jupiter's Great Red Spot N90-11681

PLANNING
The Air Force Flight Test Center Flight Test Safety Program N90-10872
Advanced Turbine Technology Applications Program, (ATTAP): A plan for improving the prototype production of ceramic components for the gas turbine engine, 1988--1992
[DE89-015566] N90-11320
Linkoeping's A.I. Consortium (LAIC) for plan guided systems. Review of the first 18 months
[FOA-C-30528-3.4] N90-11537
Planning in writing: The cognition of a constructive process
[AD-A210434] N90-11648

PLASMA ACCELERATION
Experimental studies of plasma wake-field acceleration and focusing
[DE89-016718] N90-11591

PLASMA ARC WELDING
Material properties of 2219-T851 aluminum alloy plasma welded compared to TIG welding N90-11032

PLASMA CLOUDS
Short wavelength striations on expanding plasma clouds
[DE89-016585] N90-11416

PLASMA CONTROL
Hybrid particle-fluid approach to low-frequency turbulence in magnetically confined plasmas
[DE89-015904] N90-11579
A study of runaway electron confinement and theory of neoclassical MHD turbulence
[DE89-016728] N90-11584
Launched electrons in plasma opening switches
[DE89-016886] N90-11596
Compact torus configurations with high frequency driven currents
[ETN-89-94674] N90-11598

PLASMA CURRENTS
Compact torus configurations with high frequency driven currents
[ETN-89-94674] N90-11598

PLASMA DENSITY
ANTHEM simulation of plasma opening switches
[DE89-016617] N90-11239
Studies of a strongly coupled plasma produced in a capillary discharge
[DE89-016611] N90-11581
ANTHEM simulation of the early time magnetic field penetration of the plasma surrounding a high density Z-pinch
[DE89-016980] N90-11585
Producing of an ECR plasma using 2450MHz Whistler wave and the investigating of its parameters
[DE89-618689] N90-11586
Experimental studies of plasma wake-field acceleration and focusing
[DE89-016718] N90-11591
Beam-plasma discharge in penetrating plasma
[DE89-630481] N90-11597

PLASMA DIAGNOSTICS
PISCES program plasma-surface interactions research
[DE89-015622] N90-11578
PLASMA DRIFT
Particle simulation in curvilinear coordinate systems
[DE89-016727] N90-11583
PLASMA EQUILIBRIUM
Electromagnetic jets in pulsar magnetospheres and near magnetized accretion disks N90-11675
PLASMA ETCHING
Reactive ion etching of SiC thin films by mixtures of fluorinated gases and oxygen
[AD-A211046] N90-11113
PLASMA FOCUS
Experimental studies of plasma wake-field acceleration and focusing
[DE89-016718] N90-11591
PLASMA HEATING
Projections for a steady-state tokamak reactor based on ITER
[DE89-016678] N90-11589
PLASMA JETS
Diamondlike carbon coatings for optical systems
[AD-A211255] N90-11573
Studies of a strongly coupled plasma produced in a capillary discharge
[DE89-016611] N90-11581
Electromagnetic jets in pulsar magnetospheres and near magnetized accretion disks N90-11675
PLASMA LAYERS
Computer simulations of electromagnetic ion instabilities in the plasma sheet boundary layer
[DE89-016596] N90-11588
Numerical study of the current sheet and PSBL in a magnetotail model
[NASA-CR-183289] N90-11669
PLASMA TEMPERATURE
Studies of a strongly coupled plasma produced in a capillary discharge
[DE89-016611] N90-11581
PLASMA WAVES
Hybrid particle-fluid approach to low-frequency turbulence in magnetically confined plasmas
[DE89-015904] N90-11579
Producing of an ECR plasma using 2450MHz Whistler wave and the investigating of its parameters
[DE89-618689] N90-11586
CRRES (Combined Release and Radiation Effects Satellite) SPACERAD plasma wave experiment
[AD-A210791] N90-11587
Experimental studies of plasma wake-field acceleration and focusing
[DE89-016718] N90-11591
Beam-plasma discharge in penetrating plasma
[DE89-630481] N90-11597
Quantitative methods for waves in space plasmas
[PB89-210256] N90-11599
PLASMA-PARTICLE INTERACTIONS
Beam-plasma discharge in penetrating plasma
[DE89-630481] N90-11597
The interaction of supernovae and pulsars with the circumstellar environment N90-11671
PLASMAS (PHYSICS)
ANTHEM simulation of plasma opening switches
[DE89-016617] N90-11239
Ionospheric Structure and Variability on a Global Scale and Interactions with Atmosphere and Magnetosphere
[AGARD-CP-441] N90-11361
Balance equations for ionospheric plasmas with different partial temperatures N90-11364
Global morphology of plasma bubbles in the low latitude ionosphere N90-11369
Ionosphere-thermosphere coupling at high latitudes: Aspect angle dependence of non-thermal plasmas N90-11382
Small-scale irregularities and global plasma dynamics in the high-latitude ionosphere N90-11394
Boundary effects on the MHD dynamo in laboratory plasmas
[DE89-015207] N90-11576
ANTHEM simulation of the early time magnetic field penetration of the plasma surrounding a high density Z-pinch
[DE89-016980] N90-11585
CRRES (Combined Release and Radiation Effects Satellite) SPACERAD plasma wave experiment
[AD-A210791] N90-11587
Solid fiber Z-pinches: Cold-start computations
[DE89-016768] N90-11592
A fully electromagnetic hybrid model for high density plasma simulations
[DE89-016771] N90-11593
Beam-plasma discharge in penetrating plasma
[DE89-630481] N90-11597
Ion bombardment of Io and Mercury N90-11682
PLASMASPHERE
Short wavelength striations on expanding plasma clouds
[DE89-016585] N90-11416
PLASTIC DEFORMATION
Microstructural effects on spall fracture in 1008 steel
[DE89-016770] N90-11131
PLATES (TECTONICS)
The recovery of orbital and geophysical parameters using a spaceborne laser ranging system N90-11294
PLUGGING
A characterization of the side bonding, upset plug welding process
[DE89-015181] N90-11315
PODS (EXTERNAL STORES)
Independent Orbiter Assessment (IOA): Analysis of the orbital maneuvering system
[NASA-CR-185554] N90-10919
Independent Orbiter Assessment (IOA): Analysis of the reaction control system, volume 3
[NASA-CR-185532-VOL-3] N90-10940
POISSON EQUATION
Particle simulation in curvilinear coordinate systems
[DE89-016727] N90-11583
POLAR CAPS
Studies of time-dependent polar cap convection patterns N90-11421
POLAR REGIONS
Simulation of the polar cap F region ionization using an experimental convection electric field N90-11370
VLF/LF radio wave studies of the structure and variability of the equatorial, mid-latitude and polar ionosphere below 100 km N90-11373
Observations of ionosphere/magnetosphere interactions from the Dynamics Explorer satellites N90-11376
Empirical models of convection electric fields and electrostatic potential at high latitude from EISCAT observations: Preliminary results N90-11377
Polar F layer lacuna irregularities at Dumont d'Urville N90-11379
On the possibility of producing artificial ionization and polar aurora in the ionosphere by radio-waves emitted from the ground N90-11388
POLARIMETERS
Spectropolarimetry, variability, and the taxonomy of active galactic nuclei N90-11667
POLICIES
Sagdeyev discusses space missions, policy, Mars plans N90-10906
The transfer and diffusion of new technologies: A review of the economics literature
[DE89-015671] N90-11655
POLLUTION MONITORING
Interrelation of experimental exposure and ambient air quality data for comparison of ozone exposure indices and estimating agricultural losses
[PB89-195036] N90-11353
POLYATOMIC MOLECULES
A diagnostic for determining the quality of single-reference electron correlation methods N90-11554
POLYCARBONATES
Interfacial adsorption and crystallization of polycarbonate in carbon fiber composites
[AD-A211230] N90-11090
POLYCRYSTALS
Laser grooved and polycrystalline silicon solar cell research
[DE89-015196] N90-11347
Proceedings of the Polycrystalline Thin Film Program Meeting
[DE89-009457] N90-11348
POLYETHYLENES
Shock induced dissociation of polyethylene
[DE89-016983] N90-11267
POLYMER CHEMISTRY
Transport studies of conducting polymers N90-11140
Thermodynamic principles of the process of the effect of electromagnetic fields on a polymer melt
[AD-A210698] N90-11149
POLYMER PHYSICS
Lithium polymer electrolyte battery, electrochemical behavior of cathode materials
[AD-A210755] N90-11235
POLYMERIC FILMS
Dynamics of nucleation at electrochemical interfaces via surface EXAFS and standing wave measurements
[AD-A210733] N90-11109
Capacitive behavior in conducting polymers: The ac impedance and quartz crystal microbalance studies
[AD-A210754] N90-11150
Cell performance of ultra-thin polymer cathode system: Theoretical energy and power density projections
[AD-A210786] N90-11151
Electrolyte dependence of charge injection processes for electroactive polymer films
[AD-A210787] N90-11152
New secondary batteries utilizing electronically conductive polymer cathodes
[NASA-CR-185885] N90-11227
POLYMERIZATION
Quantum chemical investigations of the mechanism of cationic polymerization and theoretical prediction of crystal densities and decomposition pathways of energetic molecules
[AD-A210322] N90-11143
Electronic and ionic transport in polymers
[AD-A210654] N90-11148
POROSITY
Thermochemical model for shock-induced chemical reactions in porous thermite: The heat detonation model
[DE89-016528] N90-11100
PORPHYRINS
Photochemically-driven biomimetic oxidation of alkanes and olefins
[DE89-011536] N90-11097
PORTABLE EQUIPMENT
Test-retest reliability of oxford Medilog 9000 sleep recording and SS-90-3 sleep stage scoring
[AD-A211165] N90-11440
POSITION (LOCATION)
Ionospheric limitations to the accuracy of SSL estimates of HF transmitter locations N90-11403
Markov processes in Hilbert space and continuous spontaneous localization of systems of identical particles
[DE89-618396] N90-11540
Evaluation test of CCD area sensor for star sensor
[NAL-TM-570] N90-11566
POSITION ERRORS
Robust spatial calibration of a planar positron camera
[AD-A210773] N90-11284
POSTFLIGHT ANALYSIS
Independent Orbiter Assessment (IOA): Analysis of the instrumentation subsystem
[NASA-CR-185571] N90-10928
POTABLE WATER
Selective removal of organics for water reclamation
[NASA-CR-185959] N90-11445
POTASSIUM PERCHLORATES
Consequence of condensed-phase formation in transient burning of TiHx/KClO in a closed system
[DE89-013922] N90-11188
POWDER (PARTICLES)
Low temperature processing of reaction sintered silicon nitride
[DE89-017455] N90-11092
Freeze-dried processing of tungsten heavy alloys
[DE89-015171] N90-11122
Basic research on processing of ceramics for space structures
[AD-A205954] N90-11139
Synthesis of powder with gel technique
[FOA-C-20752-2.4(2.1)] N90-11156
Powder morphology effects in the ignition of titanium-based pyrotechnics
[DE89-017229] N90-11191
Effects of shock-modification on superconductivity in Tl2Ca2Ba2Cu3Oy and Bi2CaSr2Cu2Ox
[DE89-017231] N90-11629
POWDER METALLURGY
Exploratory study of niobium, titanium, zirconium and tantalum aluminides
[AD-A210658] N90-11615
POWER CONDITIONING
Assessment of space power related measurement requirements of the Strategic Defense Initiative
[PB89-209357] N90-11343
POWER EFFICIENCY
The effect of electrode configuration on arcjet performance
[NASA-TM-102346] N90-11081
PRECIPITATION HARDENING
Accelerated aging of metal matrix composites N90-11085
Precipitation and transformation toughening of Al-Mg signals
[ETN-89-94675] N90-11138
PREDICTION ANALYSIS TECHNIQUES
A review of the Error of Matrix Method (EMM) for structural dynamic model comparison N90-10993
Mathematical model and predictions for static and dynamic behavior of solar array structure N90-11049
The use of damage characterization for life prediction methodologies N90-11053
Intrinsic damage and strength criteria for advanced composite laminates in space applications N90-11071
Numerical simulation of turbulent flow downstream a sudden axisymmetric expansion
[FOA-C-20758-2.1] N90-11272

Coordinated multi-parameter measurements and predictions of the global-scale ionosphere N90-11397

PREDICTIONS

Applications of the hybrid automated reliability predictor: Revised edition
[NASA-TP-2760-REV] N90-11454

PREFLIGHT ANALYSIS

Mathematical model and predictions for static and dynamic behavior of solar array structure N90-11049

PRELAUNCH SUMMARIES

Atmospheric environment for space shuttle (STS-29) launch
[NASA-TM-100376] N90-10980

Atmospheric environment for space shuttle (STS-30) launch
[NASA-TM-100381] N90-10981

PRELAUNCH TESTS

A high precision gravity compensation system for the deployment test of the ERS-1 SAR antenna N90-11038

PRESSURE

Pressure correction splitting methods for the computation of oscillatory free convection in low Pr fluids
[CWI-NM-R8816] N90-11271

PRESSURE CHAMBERS

Aeritalia Space Systems Group, Turin, Italy
[EOARD-LR-89-041] N90-10908

PRESSURE DEPENDENCE

Structure and properties of simple molecular systems at very high density
[DE89-016974] N90-11557

PRESSURE EFFECTS

Pressure induced resonance Raman effects in shocked carbon disulfide
[AD-A210665] N90-11107

Balance equations for ionospheric plasmas with different partial temperatures N90-11364

PRESSURE MEASUREMENT

Measurements of pressures on the tail and aft fuselage of an airplane model during rotary motions at spin attitudes
[NASA-TP-2939] N90-10829

The near-wake flow structure of wake-cylinder interaction and surface loading of cylinder N90-11248

Jet-flow from shock tubes
[AD-A210651] N90-11260

A remote sensor to monitor combustion products using a tunable acousto-optic filter N90-11275

PRESSURE OSCILLATIONS

Development of a thermoacoustic test facility N90-11041

Observational studies of low-frequency oscillations in the Southern Hemisphere N90-11420

PRESSURIZED CABINS

Independent Orbiter Assessment (IOA): Analysis of the atmospheric revitalization pressure control subsystem
[NASA-CR-185593] N90-10925

Independent Orbiter Assessment (IOA): Assessment of the atmospheric revitalization pressure control subsystem FMEA/CIL
[NASA-CR-185594] N90-10957

Numerical simulation of micrometeroids and debris hypervelocity impacts on Columbus pressurized modules N90-11075

PRESSURIZING

Independent Orbiter Assessment (IOA): Analysis of the reaction control system, volume 2
[NASA-CR-185532-VOL-2] N90-10939

Independent Orbiter Assessment (IOA): Analysis of the reaction control system, volume 3
[NASA-CR-185532-VOL-3] N90-10940

PRINTERS (DATA PROCESSING)

Electronic publishing: Guide to selection
[PB89-214753] N90-11448

PROBABILITY DENSITY FUNCTIONS

Analytical study of mistuning/friction/aerodynamics interaction in a bladed disk assembly
[AD-A211139] N90-10893

Boundary kernel estimation of the two sample comparison density function
[AD-A210757] N90-11532

PROBABILITY DISTRIBUTION FUNCTIONS

Stochastic flows in networks
[AD-A211209] N90-11515

Alias-free Wigner distribution function and complex ambiguity function for discrete-time samples
[AD-A211050] N90-11533

Fixed point iteration on point-symmetric interference graphs
[MEMO-INF-89-23] N90-11535

PROBABILITY THEORY

Development of an approximate technique for the nonlinear random vibrations analysis of hysteretic systems N90-11335

Partially specified probability measures in expert systems
[CWI-CS-R8842] N90-11536

PROBLEM SOLVING

On the effective transport properties of composite materials N90-11086

A survey of research methods to study design
[AD-A211213] N90-11491

Domain decomposition for partial differential equations
[DE89-016669] N90-11519

PROCESS CONTROL (INDUSTRY)

Thin section casting program. Volume 3: Vertical TSC (Thin-Section Casting) approach
[DE89-009033] N90-11201

Sensors for nondestructive testing and evaluation of materials
[DE89-014763] N90-11279

An extension of Cochran's test for homogeneity of variances
[AD-A211054] N90-11534

PRODUCT DEVELOPMENT

The service module structure of the IOS spacecraft development and qualification program N90-11021

PRODUCTIVITY

Using computer design and simulation to improve manufacturing productivity, report period 1, 2 and 3
[AD-A210255] N90-11462

PROGRAM VERIFICATION (COMPUTERS)

High accuracy coordinate determination using the global positioning system N90-10858

ATTAS flight testing experiences N90-10862

Validation of NEC (Numerical Electromagnetics Code) for antennas near ground
[DE89-016502] N90-11212

A distributed debugger for Amoeba
[CWI-CS-R8828] N90-11453

A verification exercise relating to specification styles in LOTOS
[MEMO-INF-89-18] N90-11471

PROGRAMMING LANGUAGES

A verification exercise relating to specification styles in LOTOS
[MEMO-INF-89-18] N90-11471

Boolean functions, invariance groups and parallel complexity
[CWI-CS-R8836] N90-11472

PROJECT MANAGEMENT

Evaluation of mid-to-long term basic research for environmental restoration
[DE89-015621] N90-11355

Preference propagation in temporal/capacity constraint graphs
[AD-A210668] N90-11506

PROJECTILES

Gas-accelerated plate stability study
[DE89-016880] N90-11289

Evaluation of integrals related to the Debye function
[DE89-016930] N90-11499

PROPAGATION MODES

Wave-mode coordinate analysis of L junction in LSS
[AD-A211116] N90-10984

PROPELLANT ADDITIVES

Homogeneous catalysts in hypersonic combustion
[DE89-015258] N90-11098

N-Hexyl Carborane (NHC) as combustion catalyst in composite propellants
[FOA-C-20755-2.1] N90-11193

PROPELLANT COMBUSTION

Nitramine composite solid propellant modeling N90-11183

PROPELLANT STORAGE

Evaluation of supercritical cryogen storage and transfer systems for future NASA missions
[NASA-TM-102394] N90-10912

Independent Orbiter Assessment (IOA): Analysis of the reaction control system, volume 2
[NASA-CR-185532-VOL-2] N90-10939

Independent Orbiter Assessment (IOA): Analysis of the reaction control system, volume 3
[NASA-CR-185532-VOL-3] N90-10940

Evolutionary space station fluids management strategies
[NASA-CR-185137] N90-10983

PROPELLANT TANKS

Independent Orbiter Assessment (IOA): Assessment of the electrical power generation/power reactant storage and distribution subsystem FMEA/CIL
[NASA-CR-185545] N90-10923

PROPELLANT TRANSFER

Evaluation of supercritical cryogen storage and transfer systems for future NASA missions
[NASA-TM-102394] N90-10912

Independent Orbiter Assessment (IOA): Analysis of the orbiter main propulsion system
[NASA-CR-185584] N90-10927

PROPELLER BLADES

User's manual for PEPSIG NASA tip vortex version
[NASA-CR-182178] N90-10835

Computation of the tip vortex flowfield for advanced aircraft propellers
[NASA-CR-182179] N90-10836

PROPELLER NOISE

An investigation of counterrotating tip vortex interaction
[NASA-CR-185135] N90-11549

PROPULSION SYSTEM CONFIGURATIONS

Independent Orbiter Assessment (IOA): Assessment of the manned maneuvering unit
[NASA-CR-185564] N90-10974

PROPULSIVE EFFICIENCY

Independent Orbiter Assesment (IOA): Analysis of the manned maneuvering unit
[NASA-CR-185565] N90-10913

PROTECTIVE CLOTHING

Concepts for microgravity experiments utilizing gloveboxes
[NASA-TM-100378] N90-11195

PROTECTIVE COATINGS

Diamondlike carbon coatings for optical systems
[AD-A211255] N90-11573

PROTECTORS

Independent Orbiter Assessment (IOA): Analysis of the backup flight system
[NASA-CR-185567] N90-10932

PROTEINS

Electron transfer reactions
[AD-A210711] N90-11545

PROTOCOL (COMPUTERS)

Performance analysis of hybrid ARQ protocols in a slotted code division multiple-access network
[AD-A211078] N90-11219

On the Amoeba protocol
[CWI-CS-R8827] N90-11480

A survey of research methods to study design
[AD-A211213] N90-11491

Adaptive gigabit fiber optics local area network
[AD-A210794] N90-11571

PROTOSTARS

The stability of magnetohydrodynamic shock waves in molecular clouds N90-11665

Mathematical method for the study and teaching of stellar and protostellar structure N90-11666

PROTOTYPES

The Experimental Aircraft Flight Test Programme N90-10865

Flight testing a newly-designed stand-off weapon dispenser N90-10880

Realtime processing and display N90-10886

Thin section casting program. Volume 3: Vertical TSC (Thin-Section Casting) approach
[DE89-009033] N90-11201

A prototype silicon compiler in prolog
[AD-A210669] N90-11452

PROVING

Checking the Goldbach conjecture on a vector computer
[CWI-NM-R8812] N90-11475

PSYCHOLOGY

Comprehension processes in mechanical reasoning
[AD-A210459] N90-11442

PSYCHOPHYSICS

Inferences from images
[AD-A210710] N90-11465

PULSAR MAGNETOSPHERES

Electromagnetic jets in pulsar magnetospheres and near magnetized accretion disks N90-11675

PULSARS

The interaction of supernovae and pulsars with the circumstellar environment N90-11671

PULSE CODE MODULATION

Independent Orbiter Assessment (IOA): Analysis of the instrumentation subsystem
[NASA-CR-185571] N90-10928

PULSE GENERATORS

Magnetic flux compression
[DE89-016991] N90-11546

PULSE RADAR

The effectiveness of adaptive PRF (Pulse Repetition Frequency) selection in minimizing range obscuration in the TDWR (Terminal Doppler Weather Radar) system
[AD-A211267] N90-11222

PULSE RATE

The effectiveness of adaptive PRF (Pulse Repetition Frequency) selection in minimizing range obscuration in the TDWR (Terminal Doppler Weather Radar) system
[AD-A211267] N90-11222

PULSED LASERS

Elements of a 200 watt pulsed excimer laser N90-11295

Research in X-ray optics with the ultimate aim of constructing a synchrotron radiation pumped soft X-ray lithium laser
[DE89-016788] N90-11304

PURGING
Independent Orbiter Assessment (IOA): Analysis of the purge, vent and drain subsystem
[NASA-CR-185547] N90-10969

PYROTECHNICS
Independent Orbiter Assessment (IOA): Analysis of the pyrotechnics subsystem
[NASA-CR-185530] N90-10945
Independent Orbiter Assessment (IOA): Assessment of the pyrotechnics subsystem
[NASA-CR-185531] N90-10946
Powder morphology effects in the ignition of titanium-based pyrotechnics
[DE89-017229] N90-11191

PYRROLES
Cell performance of ultra-thin polymer cathode system: Theoretical energy and power density projections
[AD-A210786] N90-11151

Q

QUADRUPOLES
A solution to nonlinearity problems
[DE89-016975] N90-11544

QUALITATIVE ANALYSIS
A new inexpensive electrochemical meter for oxygen in sodium coolant
[DE89-630802] N90-11104
Enhanced oxidation and solovolysis reactions in chemically inert microheterogeneous systems
[AD-A210748] N90-11110
Compositional analysis of steels by X-ray fluorescence spectrometry
[DE89-630803] N90-11129

QUALITY CONTROL
Lifetime testing of commercially available 3.0 (mu)f, 100 kV pulsed-power capacitors
[DE89-017230] N90-11242
Principal components in multivariate control charts
[DE89-016828] N90-11489
An extension of Cochran's test for homogeneity of variances
[AD-A211054] N90-11534

QUANTITATIVE ANALYSIS
Enhanced oxidation and solovolysis reactions in chemically inert microheterogeneous systems
[AD-A210748] N90-11110

QUANTUM ELECTRODYNAMICS
Free-electron laser theory
[DE89-620145] N90-11298

QUANTUM ELECTRONICS
Nonlinear optical studies of resonant systems
[AD-A211032] N90-11301

QUANTUM MECHANICS
Generation of higher-order squeezing of quantum electromagnetic fields by degenerate four-wave mixing and other processes
[DE89-618392] N90-11213
Alias-free Wigner distribution function and complex ambiguity function for discrete-time samples
[AD-A211050] N90-11533
Markov processes in Hilbert space and continuous spontaneous localization of systems of identical particles
[DE89-618396] N90-11540
A high level Ab initio study of the anionic hydrogen-bonded complexes FH-CN-, FH-NC-, H2O-CN- and H2O-NC- N90-11553
Origins of high-temperature superconductivity in the new copper oxide based ceramic superconductors
[DE89-016543] N90-11622

QUANTUM THEORY
Semiconductor quantum well lasers and related optoelectronic devices on silicon, III-V
[AD-A210758] N90-11299
A diagnostic for determining the quality of single-reference electron correlation methods N90-11554
Superfiled formulation of Chern-Simons supersymmetry
[DE89-618459] N90-11636
General action for topological quantum field theories
[DE89-618460] N90-11637
Moduli spaces and topological quantum field theories
[DE89-016943] N90-11639

QUANTUM WELLS
Semiconductor quantum well lasers and related optoelectronic devices on silicon, III-V
[AD-A210758] N90-11299
Nonlinear optical studies of resonant systems
[AD-A211032] N90-11301

QUARTZ CRYSTALS
Capacitive behavior in conducting polymers: The ac impedance and quartz crystal microbalance studies
[AD-A210754] N90-11150

QUASARS
The ratio to X-ray spectral shape and variability of blazars N90-11688

QUEUEING THEORY
Network analyzer for nonstatic jamming
[AD-A210759] N90-11216
Transaction throughput in distributed systems: A modeling study using dynamic queueing networks
[MEMO-INF-89-25] N90-11479
Stochastic optimization by simulation: Some experiments with a simple steady-state queue
[AD-A210762] N90-11508

R

RADAR
The Swedish defense research needs: For surveillance and seeker applications
[FOA-C-30520-3.3] N90-11691

RADAR APPROACH CONTROL
Design of a final approach spacing tool for TRACON air traffic control
[NASA-TM-102229] N90-10841

RADAR CROSS SECTIONS
Efficient algorithm for calculation of radar cross section
[AD-A210785] N90-11217

RADAR ECHOES
Small-scale irregularities and global plasma dynamics in the high-latitude ionosphere N90-11394

RADAR IMAGERY
Ionosphere-thermosphere coupling at high latitudes: Aspect angle dependence of non-thermal plasmas N90-11382
An ionospheric model for HF sky-wave backscatter radar N90-11401

RADAR MAPS
Simulation of synthetic aperture radar 1: Feature density and accuracy requirements
[AD-A211019] N90-11218

RADAR TRACKING
Relation of wind field and buoyancy to rainfall inferred from radar
[PB89-208326] N90-11424

RADIANCE
Offaxis radiance studies for infrared sensors
[AD-A210790] N90-11570

RADIATION ABSORPTION
Acoustic studies of new materials: Quasicrystals, low-loss glasses and high Tc superconductors
[AD-A211281] N90-11551

RADIATION BELTS
CRRES (Combined Release and Radiation Effects Satellite) SPACERAD plasma wave experiment
[AD-A210791] N90-11587

RADIATION COUNTERS
Ion detector on the basis of microchannel plates for a high-sensitive mass spectrometer
[DE89-620335] N90-11291

RADIATION DETECTORS
A liquid xenon imaging telescope for 1-30 MeV gamma-ray astrophysics
[NASA-CR-185999] N90-11662

RADIATION DOSAGE
Ozonation of hydrazines and their associated impurities N90-11174

RADIATION EFFECTS
Grain boundary chemistry in irradiated stainless steel and its influence on environmental degradation
[DE89-016827] N90-11125
Report of the 1988 2-D Intercomparison Workshop, chapter 3 N90-11407
Introduction and data summary, chapter 5 N90-11409
PISCES program plasma-surface interactions research
[DE89-015622] N90-11578
CRRES (Combined Release and Radiation Effects Satellite) SPACERAD plasma wave experiment
[AD-A210791] N90-11587

RADIATION PROTECTION
DOE/CEC Workshop on Critical Evaluation of Radiobiological Data to Biophysical Modeling
[DE89-015214] N90-11437

RADIATIVE TRANSFER
Two-Dimensional Intercomparison of Stratospheric Models
[NASA-CP-3042] N90-11405
Introduction and data summary, chapter 5 N90-11409
Gas dynamical processes in the theory of galaxy formation N90-11673

RADIO ALTIMETERS
Laser altimeter for use over the ocean
[AD-A211252] N90-11286

RADIO ANTENNAS
Deep null antennas and their applications to tactical VHF radio communications
[AD-A210656] N90-11214

RADIO ASTRONOMY
Project Radioastron N90-10901
Integrating detectors and their application to infrared astronomy N90-11659

RADIO COMMUNICATION
Deep null antennas and their applications to tactical VHF radio communications
[AD-A210656] N90-11214
Network analyzer for nonstatic jamming
[AD-A210759] N90-11216

RADIO FREQUENCY INTERFERENCE
An experimental SMI adaptive antenna array for weak interfering signals
[NASA-CR-185976] N90-11211
Offaxis radiance studies for infrared sensors
[AD-A210790] N90-11570

RADIO NAVIGATION
Federal Radionavigation Plan, 1988
[PB89-163075] N90-10846

RADIO RECEPTION
Influence of ionospheric variations on high-reliability HF systems utilizing large bases N90-11404

RADIO TELESCOPES
Project Radioastron N90-10901

RADIO TRANSMISSION
Ionospheric irregularities due to powerful HF radio transmissions N90-11389

RADIO WAVES
VLF/LF radio wave studies of the structure and variability of the equatorial, mid-latitude and polar ionosphere below 100 km N90-11373
On the possibility of producing artificial ionization and polar aurora in the ionosphere by radio-waves emitted from the ground N90-11388
Radio propagation conditions forecast above a low latitude region N90-11400

RADIOACTIVE DECAY
Gamma radiation background measurements from Spacelab 2
[NASA-CR-183782] N90-11689

RADIOACTIVE MATERIALS
Spoken commands control robot that handles radioactive materials
[DE89-012632] N90-11488

RADIOBIOLOGY
DOE/CEC Workshop on Critical Evaluation of Radiobiological Data to Biophysical Modeling
[DE89-015214] N90-11437

RAIN
Relation of wind field and buoyancy to rainfall inferred from radar
[PB89-208326] N90-11424

RAINSTORMS
Frequency distributions and hydroclimatic characteristics of heavy rainstorms in Illinois
[PB89-203988] N90-11427

RAMAN SPECTRA
Vibrational spectroscopic study of the kaolinite-hydrazine intercalation complex N90-11166
Study of disorder and strain in semiconductor heterostructures and superlattices by Raman scattering N90-11601

RAMAN SPECTROSCOPY
Pressure induced resonance Raman effects in shocked carbon disulfide
[AD-A210665] N90-11107
Laser Raman spectroscopy: A literature review
[FOA-C-20753-2.3] N90-11121

RAMJET ENGINES
A simulator for a hydrocarbon ramrocket fuel gas generator: First phase development
[AR-005-621] N90-11080

RANDOM ACCESS MEMORY
Performance analysis of hybrid ARQ protocols in a slotted code division multiple-access network
[AD-A211078] N90-11219

RANGE (EXTREMES)
Are ozone exceedance rates decreasing. Comment on extreme value analysis of environmental time-series: An application to trend detection in ground-level ozone
[AD-A211029] N90-11357

RANGEFINDING
Laser techniques for ground to air applications
[FOA-C-30524-3.1] N90-11309

RANGES (FACILITIES)
Research and test facilities for development of technologies and experiments with commercial applications
[NASA-TM-101789] N90-10909

RANKINE CYCLE
Shock induced dissociation of polyethylene
[DE89-016983] N90-11267
RANKINE-HUGONIOT RELATION
Theoretical Hugoniot of liquid hydrogen fluoride
[DE89-016504] N90-11099
Estimation of the C-J pressure of explosives
[DE89-013811] N90-11187
RAPID EYE MOVEMENT STATE
Test-retest reliability of oxford Medilog 9000 sleep recording and SS-90-3 sleep stage scoring
[AD-A211165] N90-11440
RARE GAS-HALIDE LASERS
Elements of a 200 watt pulsed excimer laser N90-11295
RARE GASES
Dissociation and vibrational relaxation of XeF by various collision partners
[AD-A210769] N90-11300
REACTION KINETICS
Critical reaction rates in hypersonic combustion chemistry
[DE89-014278] N90-10892
Simplified rate-law integration for reactions which are first order in each of two reactants
[NASA-CR-185408] N90-11093
Time-resolved mass spectrometry technique for studying fast transient CHNO explosive decomposition kinetics
[DE89-016540] N90-11101
Chemiluminescent ion-molecule reactions of group-3 ions with halogens: New optical spectra and reaction dynamics
[MPIS-18/1988] N90-11120
Hydrogen-silicon carbide interactions
[NASA-TM-102382] N90-11144
A shock initiation model for fine-grained hexanitrostilbene
[DE89-007641] N90-11185
Shock initiation of LX-17 as a function of its initial temperature
[DE89-017730] N90-11192
NCAR (National Center for Atmospheric Research) master mechanism of the gas phase chemistry, version 2.0
[PB89-208979] N90-11413
Theoretical investigation of gas-surface interactions
[NASA-CR-185492] N90-11552
Thermodynamics, kinetics, and interface morphologies of phase formation reactions between metals and Gallium Arsenide: Bulk vs thin-film studies
[DE89-016469] N90-11621
Transport properties of thermally grown Cr2O3
[DE89-016703] N90-11623
REACTION PRODUCTS
Surface-catalyzed air oxidation reactions of hydrazines: Tubular reactor studies N90-11167
The chemistry of the hypochlorite neutralization of hydrazine fuels N90-11173
REACTOR DESIGN
The Reversed-Field-Pinch (RFP) fusion neutron source: A conceptual design
[DE89-015297] N90-11577
REACTOR TECHNOLOGY
The Reversed-Field-Pinch (RFP) fusion neutron source: A conceptual design
[DE89-015297] N90-11577
READING
Topographic map reading
[AD-A211269] N90-11340
REAL TIME OPERATION
Real-time flight test analysis and display techniques for the X-29A aircraft N90-10866
Identification Friend, Foe or Neutral Joint Test N90-10881
Realtime processing and display N90-10886
Flight test instrumentation and data processing at British Aerospace, Warton, U.K. N90-10887
RECOMBINATION REACTIONS
Gas dynamical processes in the theory of galaxy formation N90-11673
RECONNAISSANCE
Solar radiation in Linkoeping (Sweden): Variations over half a year in irradiance and spectral composition in the interval 400-1000 nm
[FOA-C-30521-3.1] N90-11417
RECONSTRUCTION
Quantitative methods for waves in space plasmas
[PB89-210256] N90-11599
RECORDING
Test-retest reliability of oxford Medilog 9000 sleep recording and SS-90-3 sleep stage scoring
[AD-A211165] N90-11440
RED SHIFT
New statistical approaches to galaxy clustering N90-11674
REDUCED GRAVITY
Concepts for microgravity experiments utilizing gloveboxes
[NASA-TM-100378] N90-11195
REDUNDANT COMPONENTS
Study for optimization of redundant vane-type flow-direction sensing systems and numerical analysis for design of the systems
[NAL-TM-571] N90-10890
REENTRY EFFECTS
Modifications to the aerotherm charring material thermal response and ablation program (CMA) for carbon ablation analysis
[AD-A211069] N90-11115
REFINING
Influence of grain refining on the casting, physical, mechanical, and electrochemical properties of technical aluminum
[ETN-89-94661] N90-11135
Investigation of commercial Al-Ti and Al-Ti-B master alloys and development of a new grain refining agent based on carbides for aluminum and aluminum alloys
[ETN-89-94663] N90-11136
REFLECTING TELESCOPES
System and performance analysis of a low density actively controlled mirror for astronomic observation N90-11002
REFLECTION NEBULAE
Small grains in reflection nebulae: A study of diffuse interstellar bands, elemental depletions and infrared flux N90-11672
REFLECTOR ANTENNAS
Test results on conceptual models of the large deployable antenna for mobile communications satellites N90-11050
ESA-D: An integrated software for antenna design and analysis N90-11052
REFRACTED WAVES
Computations of the refraction of a plane shock wave at a slow-fast gas interface
[DE89-016508] N90-11258
Nonlinear acoustics: Reflection and refraction, propagation in a periodic waveguide, scattering of sound by sound and ellipsoidal focusing
[AD-A211224] N90-11550
REFRACTORY COATINGS
Superconducting ceramics in the Bi1.5SrCaCu2O sub x system by melt quenching technique
[NASA-CR-185139] N90-11606
REGULATIONS
Review of the ESA fracture control policy N90-11029
RELATIVISTIC PARTICLES
Global and local fluctuations in multiplicity and transverse energy for central ultra-relativistic heavy-ion interactions
[LUIP-8903] N90-11555
RELIABILITY
Methodology of developing a combined environmental stress schedule for reliability growth testing
[AD-A211053] N90-11326
Applications of the hybrid automated reliability predictor: Revised edition
[NASA-TP-2760-REV] N90-11454
Experiments in fault tolerant software reliability
[NASA-CR-185927] N90-11480
RELIABILITY ANALYSIS
Evaluation of tests and design factors N90-10987
RELIEF MAPS
Topographic map reading
[AD-A211269] N90-11340
REMOTE CONTROL
NASA/NBS (National Aeronautics and Space Administration/National Bureau of Standards) standard reference model for telerobot control system architecture (NASREM)
[NASA-CR-185078] N90-11310
Land vehicle teleoperation under conditions of reduced video resolution
[DE89-016925] N90-11324
Spoken commands control robot that handles radioactive materials
[DE89-012632] N90-11488
REMOTE HANDLING
Telescience Testbed Pilot Program
[NASA-CR-184594] N90-11455
Spoken commands control robot that handles radioactive materials
[DE89-012632] N90-11488
REMOTE MANIPULATOR SYSTEM
Independent Orbiter Assessment (IOA): Analysis of the remote manipulator system
[NASA-CR-185585] N90-10926
Independent Orbiter Assessment (IOA): Analysis of the electrical power distribution and control/remote manipulator system subsystem
[NASA-CR-185526] N90-10936
Independent Orbiter Assessment (IOA): CIL issues resolution report, volume 2
[NASA-CR-185524-VOL-2] N90-10955
Independent Orbiter Assessment (IOA): Assessment of the remote manipulator system FMEA/CIL
[NASA-CR-185592] N90-10964
Independent Orbiter Assessment (IOA): Assessment of the EPD and C/remote manipulator system FMEA/CIL
[NASA-CR-185583] N90-10965
REMOTE SENSING
Remote sensing techniques of the Wave Propagation Laboratory for the measurement of supercooled liquid water: Applications to aircraft icing
[PB89-208102] N90-10842
Airborne gamma radiation snow water equivalent and soil moisture measurements and satellite areal extent of snow cover measuerments: A user's guide, version 3.0
[PB89-177877] N90-11338
ANIMA: Image analyzer applied to remote sensing
[INPE-4766-PRE/1435] N90-11447
Telescience Testbed Pilot Program
[NASA-CR-184594] N90-11455
REMOTE SENSORS
Study of high frequency water vapor absorption parameters
[AD-A210676] N90-11108
A remote sensor to monitor combustion products using a tunable acousto-optic filter N90-11275
REMOTELY PILOTED VEHICLES
Land vehicle teleoperation under conditions of reduced video resolution
[DE89-016925] N90-11324
REPLACING
ASIC (Application Specific Integrated Circuit) replacement for an SSI (Small Scale Integrated) component design: A case study
[DE89-013494] N90-11232
REQUIREMENTS
Key structures mechanical issues of the European Space Station and platform program Columbus N90-11072
Methodology of developing a combined environmental stress schedule for reliability growth testing
[AD-A211053] N90-11326
RESEARCH
Technology applications bulletins
[DE89-017454] N90-11651
A history of West European rocketry and space research
[AD-A211191] N90-11690
RESEARCH AND DEVELOPMENT
On the development of a basic flight test capability and some related research projects N90-10885
Ariane 5 structural design and development N90-11057
SDM challenges for space station N90-11059
The Swedish defense research needs: For surveillance and seeker applications
[FOA-C-30520-3.3] N90-11691
RESEARCH FACILITIES
Research and test facilities for development of technologies and experiments with commercial applications
[NASA-TM-101789] N90-10909
Physiographic and geological setting of the Coastal Engineering Research Center's field research facility
[AD-A210772] N90-11356
National Center For Atmospheric Research annual report, fiscal year 1988
[PB89-208987] N90-11428
RESEARCH MANAGEMENT
National Climate Program five-year plan, 1989-1993
[PB89-207369] N90-11426
Toward a national research network
[PB89-198709] N90-11644
RESEARCH PROJECTS
Assessment of space power related measurement requirements of the Strategic Defense Initiative
[PB89-209357] N90-11343
National Center For Atmospheric Research annual report, fiscal year 1988
[PB89-208987] N90-11428
Toward a national research network
[PB89-198709] N90-11644
The Knowledge Representation Project
[AD-A211288] N90-11650
RESIDUAL STRESS
Finite element analysis of cure-induced residual stress in composite materials N90-11084
Influence of core-shell grains on the internal stress state and permittivity response of zirconia modified barium titanate
[AD-A211245] N90-11153
Questions from the Willmarth Workshop on New Directions in Research on Turbulent Wall-Layer Structures
[AD-A211282] N90-11264

The Meta-Lax method of stress reduction in welds
[DE89-016437] N90-11321

RESISTANCE HEATING
Battery actuation of NITINOL at sub-zero temperatures
[AD-A211254] N90-11237

RESISTORS
Microsensor and pattern recognition techniques in hydrazine detection N90-11177

RESOLUTION
Completeness of resolution by transfinite induction
[CWI-CS-R8837] N90-11473
Parallel inference based on delta processing
[CWI-CS-R8846] N90-11482

RESONANCE
Nonlinear optical studies of resonant systems
[AD-A211032] N90-11301
Resonance effect on the oscillator distribution function
[DE89-630105] N90-11548

RESONANT VIBRATION
An improved beam model for the vibrations of rotor blades N90-11333

RESPONSES
Stimulus-response compatibility in spatial precuing and symbolic identification: Effects of coding practice, retention, and transfer
[AD-A210745] N90-11443

RETROREFLECTION
Turbulence effects for retroreflection
[FOA-C-30523-3.1] N90-11575

REVERSE FIELD PINCH
The Reversed-Field-Pinch (RFP) fusion neutron source: A conceptual design
[DE89-015297] N90-11577

REYNOLDS STRESS
The structure of Reynolds stress in the near wall region of a turbulent pipe flow N90-11247
Wall-layer eruptions in turbulent flows
[NASA-TM-102362] N90-11250
Questions from the Willmarth Workshop on New Directions in Research on Turbulent Wall-Layer Structures
[AD-A211282] N90-11264

RHODIUM COMPOUNDS
Thermodynamics, kinetics, and interface morphologies of phase formation reactions between metals and Gallium Arsenide: Bulk vs thin-film studies
[DE89-016469] N90-11621

ROBOTICS
Modeling and simulation of spatial robotic manipulators with flexible links and joint drives for control strategies implementation and evaluation N90-11311
Using computer design and simulation to improve manufacturing productivity, report period 1, 2 and 3
[AD-A210255] N90-11462

ROBOTS
NASA/NBS (National Aeronautics and Space Administration/National Bureau of Standards) standard reference model for telerobot control system architecture (NASREM)
[NASA-CR-185078] N90-11310
The 3D-POLY: A robot vision system for recognizing objects in occluded environments N90-11313
Rethinking synthesis of fine-motion strategies
[DE89-016671] N90-11322
Spoken commands control robot that handles radioactive materials
[DE89-012632] N90-11488
Magnetically levitated micro-robotics N90-11542

ROBUSTNESS (MATHEMATICS)
Performance and robustness of adaptive controllers for linear stochastic systems N90-11485

ROCKET ENGINES
Evaluation of rocket motor exhaust and liner combustion by-products
[AD-A210747] N90-11083

ROCKET EXHAUST
Evaluation of rocket motor exhaust and liner combustion by-products
[AD-A210747] N90-11083

ROCKET PROPELLED SLEDS
Evaluation of rocket motor exhaust and liner combustion by-products
[AD-A210747] N90-11083

ROCKETS
A history of West European rocketry and space research
[AD-A211191] N90-11690

RODS
Wave-mode coordinate analysis of L junction in LSS
[AD-A211116] N90-10984

ROTARY WINGS
Integrated multidisciplinary design optimization of rotorcraft
[NASA-TM-101642] N90-10889

ROTATING CYLINDERS
The thermal stability between rotating cylinders in a radially symmetrical gravitational field
[DE89-618548] N90-11638

ROTATION
A super element for multibody dynamics N90-11004

ROTONS
Quasi-diffusion between phonon and roton gases in two- and three-dimensional liquid helium
[AD-A210565] N90-11096

ROTOR AERODYNAMICS
An investigation of counterrotating tip vortex interaction
[NASA-CR-185135] N90-11549

ROTOR BLADES (TURBOMACHINERY)
Laser anemometer measurements in a transonic axial-flow fan rotor
[NASA-TP-2879] N90-11245
An improved beam model for the vibrations of rotor blades N90-11333

ROTORCRAFT AIRCRAFT
Integrated multidisciplinary design optimization of rotorcraft
[NASA-TM-101642] N90-10889

RUDDERS
Independent Orbiter Assessment (IOA): Analysis of the rudder/speed brake subsystem
[NASA-CR-185560] N90-10916

RUNGE-KUTTA METHOD
Variable step iteration of high-order Runge-Kutta methods on parallel computers
[CWI-NM-R8817] N90-11476
Note on explicit parallel multistep Runge-Kutta methods
[CWI-NM-R8814] N90-11529
On the equivalence of BS-stability and B-consistency
[CWI-NM-R8815] N90-11530

RUNWAY LIGHTS
Helicopter Visual Segment Approach Lighting System (HALS)
[ACD-330] N90-10856

RUNWAYS
Definition of research needs to address airport pavement distress in cold regions
[DOT/FAA/DS-89/13] N90-10896

S

S MATRIX THEORY
On the construction of the scattering matrix for locally-noncommutative interactions of relativistic fields
[DE89-630138] N90-11640

SAFETY
A severe human ESD (Electrostatic Discharge) model for safety and high reliability system qualification testing
[DE89-016177] N90-11233

SAFETY FACTORS
Evaluation of tests and design factors N90-10987

SAFETY MANAGEMENT
Derivation of improved load transformation matrices for launchers-spacecraft coupled analysis, and direct computation of margins of safety N90-11077

SAMPLES
Techniques for recovery of shock-loaded samples
[DE89-016881] N90-11337

SAMPLING
A technique to correlate fractography with NDE (Non-Destructive Evaluation) of small samples
[DE89-016904] N90-11325
Alias-free Wigner distribution function and complex ambiguity function for discrete-time samples
[AD-A211050] N90-11533

SANDS
Numerical simulation of hydrazine transport in a sandy soil N90-11172
Diagnostic study of atmosphere-terrain interaction leading to the formation of dust clouds and poor visibilities over near east desert areas
[AD-A211243] N90-11358

SANDWICH STRUCTURES
Transverse shear stiffness of composite and sandwich finite elements N90-11034
The 2.5D- and 3D-fabrics for delamination resistant composite laminates and sandwich structures N90-11063

SATELLITE ANTENNAS
Test results on conceptual models of the large deployable antenna for mobile communications satellites N90-11050
ESA-D: An integrated software for antenna design and analysis N90-11052

SATELLITE ATMOSPHERES
Ion bombardment of Io and Mercury N90-11682

SATELLITE DESIGN
Telescope structure for cryogenic application N90-11019
Development of the large spacecraft structure N90-11020
The service module structure of the IOS spacecraft development and qualification program N90-11021

SATELLITE IMAGERY
Analysis of forest fire smoke using satellite imagery
[AD-A210657] N90-11339
Definition of imaging performance for satellite surveillance, models, and simulations
[FOA-C-30493-9.4] N90-11341
Ionospheric Structure and Variability on a Global Scale and Interactions with Atmosphere and Magnetosphere
[AGARD-CP-441] N90-11361
The middle and high latitude ionosphere at approximately 550 km altitude N90-11374
North-south tropical F2 layer asymmetry at west AFrican and Pacific longitudes N90-11398
Composited local area forecast techniques
[AD-A210802] N90-11432
Phoebe: A preliminary control network and rotational elements
[NASA-CR-185716] N90-11680

SATELLITE NAVIGATION SYSTEMS
High accuracy coordinate determination using the global positioning system N90-10858

SATELLITE NETWORKS
Wideband connectivity and support for Cronus cluster at USAF Electronic Systems Division
[AD-A210749] N90-11215

SATELLITE OBSERVATION
Airborne gamma radiation snow water equivalent and soil moisture measurements and satellite areal extent of snow cover measuerments: A user's guide, version 3.0
[PB89-177877] N90-11338
Composited local area forecast techniques
[AD-A210802] N90-11432

SATELLITE SOUNDING
Meteorological rocket observations
[PB89-168769] N90-11419
Direct statistical thermal wind estimation procedure
[AD-A211256] N90-11433

SCALE MODELS
The spinning of aircraft: A discussion of spin prediction techniques including a chronological bibliography
[ARL-AERO-R-177] N90-10888

SCANNING
HDTV displays: Subjective effects of scanning standards and domestic picture sizes
[BBC-RD-1989/9] N90-11208
Two VAX-PASCAL terminal interface modules for visualizing scanning and parsing
[MEMO-INF-89-17] N90-11470

SCATTERING
X-ray and gamma-ray spectroscopy of solids under pressure
[DE89-017271] N90-11118
Nonprincipal-plane scattering from flat plates: Second-order and corner diffraction and pattern control of horn antennas
[NASA-CR-185485] N90-11205
Part A: Nonprincipal-plane scattering from flat plates: Second-order and corner diffractions N90-11206

SCATTERING CROSS SECTIONS
Spin fluctuations and excitations in a 2D xy-ferromagnet: CoCl2 in graphite
[DE89-017600] N90-11119
Investigations into the influence of the state functions on the cross sections of the direct p,gamma reactions at energies in the 100 keV range, and project of a cascade accelerator for the measurement of the p,gamma capture cross sections
[ETN-89-94662] N90-11561

SCHROEDINGER EQUATION
Some exact solutions of the three-identical-particle problem with S-wave inverse square potentials
[DE89-618402] N90-11524
On some stochastic properties of the infinitely dimensional Hamiltonian systems of classical mechanics
[DE89-618403] N90-11525

SCIENTISTS
Higher education for science and technology: A background paper
[PB89-191290] N90-11642

SCINTILLATION
A liquid xenon imaging telescope for 1-30 MeV gamma-ray astrophysics
[NASA-CR-185999] N90-11662

SCINTILLATION COUNTERS
Gamma radiation background measurements from Spacelab 2
[NASA-CR-183782] N90-11689

SCORING
Test-retest reliability of oxford Medilog 9000 sleep recording and SS-90-3 sleep stage scoring
[AD-A211165] N90-11440
SEA ICE
The sea ice margins: A summary of physical phenomena
[PB89-212328] N90-11436
SEA ROUGHNESS
Laser altimeter for use over the ocean
[AD-A211252] N90-11286
SEA WATER
Corrosion rates of structural materials on the ocean floor
[DE89-015211] N90-11123
SEALS (STOPPERS)
Independent Orbiter Assessment (IOA): Assessment of the mechanical actuation subsystem, volume 1
[NASA-CR-185527-VOL-1] N90-10952
Independent Orbiter Assessment (IOA): Assessment of the mechanical actuation subsystem, volume 2
[NASA-CR-185527-VOL-2] N90-10953
SEARCHING
Filling or outlining shapes with color: The effects on a visual search task
[AD-A211067] N90-11444
SEGMENTS
On transonic flow over segmented slotted wind tunnel wall with mass transfer N90-11676
SELF ADAPTIVE CONTROL SYSTEMS
Adaptive structures to meet future requirements for large precision structures N90-11001
SELF CONSISTENT FIELDS
A diagnostic for determining the quality of single-reference electron correlation methods N90-11554
SEMANTICS
Determinism yields (event structure isomorphism equals step sequence equivalence)
[CWI-CS-R8839] N90-11492
SEMICONDUCTOR DEVICES
Proceedings of the Polycrystalline Thin Film Program Meeting
[DE89-009457] N90-11348
Pulsed-power switching for inertial confinement fusion with light ion beams
[DE89-016810] N90-11595
SEMICONDUCTOR LASERS
Laser dynamics: The system dynamics and network theory of optoelectronic integrated circuit design N90-11296
Semiconductor quantum well lasers and related optoelectronic devices on silicon, III-V
[AD-A210758] N90-11299
SEMICONDUCTORS (MATERIALS)
Study of disorder and strain in semiconductor heterostructures and superlattices by Raman scattering N90-11601
International workshop on Beam Injection Assessment of Defects in Semiconductors
[AD-A210642] N90-11617
SENSITIVITY
Test of EED (Electro-Explosive Devices). Part 3: Statistical aspects on the estimation of sensitivity
[FOA-C-20749-2.3-PT-3] N90-11194
HPW (High Power Microwave) testing of electronic components
[DE89-016682] N90-11241
Ion detector on the basis of microchannel plates for a high-sensitive mass spectrometer
[DE89-620335] N90-11291
SEPARATED FLOW
Flow visualization techniques for flight research N90-10878
SERIES EXPANSION
Evaluation of integrals related to the Debye function
[DE89-016930] N90-11499
SERVICE MODULES
The service module structure of the IOS spacecraft development and qualification program N90-11021
SET THEORY
An axiomatic theory for partial functions
[MEMO-INF-89-22] N90-11527
SEYFERT GALAXIES
Spectropolarimetry, variability, and the taxonomy of active galactic nuclei N90-11667
SHAKERS
Two years experience with the ESTEC multishaker system N90-11065
Tamaris: A new European facility for low frequency multi-axis vibration simulation N90-11068
A new European vibration test facility for Ariane 4 class satellites N90-11070
SHAPES
Filling or outlining shapes with color: The effects on a visual search task
[AD-A211067] N90-11444
SHEAR FLOW
Chemical reactions in turbulent mixing flows
[AD-A211240] N90-11263
SHEAR LAYERS
Chemical reactions in turbulent mixing flows
[AD-A211240] N90-11263
Questions from the Willmarth Workshop on New Directions in Research on Turbulent Wall-Layer Structures
[AD-A211282] N90-11264
SHEAR PROPERTIES
Transverse shear stiffness of composite and sandwich finite elements N90-11034
SHEAR STRAIN
Theoretical and experimental investigation of thin-walled aluminum panels under cyclic shear load N90-10996
SHELLS (STRUCTURAL FORMS)
Hygrothermal deformations of composite shells N90-11055
SHOCK ABSORBERS
Numerical analysis of nonlinear viscoelastic structures: Application to elastomers and rubber-like materials N90-11013
SHOCK FRONTS
Radiative shocks with electron thermal conduction N90-11670
SHOCK LOADS
Induced shock loads during the separation of the Ariane 5 VEB structure N90-11045
Techniques for recovery of shock-loaded samples
[DE89-016881] N90-11337
SHOCK TESTS
Pressure induced resonance Raman effects in shocked carbon disulfide
[AD-A210665] N90-11107
SHOCK TUBES
Jet-flow from shock tubes
[AD-A210651] N90-11260
SHOCK WAVE PROPAGATION
Sharp shock model for propagating detonation waves
[DE89-016772] N90-11266
Impulse time-integral function and Lagrangian analysis
[DE89-016997] N90-11268
Gas dynamical processes in the theory of galaxy formation N90-11673
SHOCK WAVES
Theoretical Hugoniot of liquid hydrogen fluoride
[DE89-016504] N90-11099
Thermochemical model for shock-induced chemical reactions in porous thermite: The heat detonation model
[DE89-016528] N90-11100
Experimental measurements of shock-induced vaporization in cadmium and lead
[DE89-016877] N90-11103
Pressure induced resonance Raman effects in shocked carbon disulfide
[AD-A210665] N90-11107
Shock-induced atomic-scale structure in metals
[DE89-016539] N90-11124
The HEL (Hugoniot Elastic Limit) and rate-dependent yield behavior
[DE89-016981] N90-11134
Behaviour of VF(sub 2)/VF(sub 3) piezoelectric copolymers under shock loading
[DE89-016538] N90-11145
Characterizations of shock-loaded aluminum-infiltrated boron carbide cermets
[DE89-016773] N90-11146
A shock initiation model for fine-grained hexanitrostilbene
[DE89-007641] N90-11185
In-situ study of the chemically driven flow fields in initiating homogeneous and heterogeneous nitromethane explosives
[DE89-008415] N90-11186
Crystal orientation effects in PETN explosive with 4 GPa shocks
[DE89-016996] N90-11190
Shock initiation of LX-17 as a function of its initial temperature
[DE89-017730] N90-11192
Method of characteristic studies for rotational flow downstream of a curved shock wave N90-11252
Computations of the refraction of a plane shock wave at a slow-fast gas interface
[DE89-016508] N90-11258
Shock induced dissociation of polyethylene
[DE89-016983] N90-11267
Response of standardized PVDF piezoelectric polymer gauges to direct shock pressures between 8 and 32 GPa
[DE89-016811] N90-11282
The Sandia standard for PVDF (Polyvinylidene Di-Fluoride) shock sensors
[DE89-016530] N90-11287
Laser-driven miniature flyer plates for shock initiation of secondary explosives
[DE89-016587] N90-11288
Gas-accelerated plate stability study
[DE89-016880] N90-11289
Effects of shock-modification on superconductivity in Tl2Ca2Ba2Cu3Oy and Bi2CaSr2Cu2Ox
[DE89-017231] N90-11629
Studying shocks in model astrophysical flows
[DE89-618786] N90-11677
Equation-of-state data of synthetic Uranus
[DE89-016509] N90-11683
SHOES
Engineering specification and system design for CAD/CAM of custom shoes. Phase 5: UMC involvement (January 1, 1989 - June 30, 1989)
[NASA-CR-185838] N90-11456
SHORT CIRCUIT CURRENTS
A severe human ESD (Electrostatic Discharge) model for safety and high reliability system qualification testing
[DE89-016177] N90-11233
SHORT TAKEOFF AIRCRAFT
Flight simulator evaluation of a head-down display
[NAL-TM-573] N90-10898
SIGNAL DETECTION
Polarization matrices of lithium tetraborate
[AD-A210774] N90-11112
SIGNAL PROCESSING
Adaptive tracking of maneuvering targets based on IR image data N90-10853
Analytic signals in the damping coefficient estimation N90-11003
Polarization matrices of lithium tetraborate
[AD-A210774] N90-11112
An experimental SMI adaptive antenna array for weak interfering signals
[NASA-CR-185976] N90-11211
SIGNAL RECEPTION
Accurate measurements of the total angle of arrival of HF skywaves N90-11402
SILICATES
Applications of NMR spectroscopy to the study of zeolite synthesis
[DE89-015226] N90-11095
Irreversible phase transition and wave propagation in silicate geologic materials
[DE89-016031] N90-11414
SILICON
A new semicustom integrated bipolar amplifier for silicon strip detectors
[DE89-015585] N90-11229
A prototype silicon compiler in prolog
[AD-A210669] N90-11452
Hydrogen-assisted thermal donor formation in silicon
[DE89-016809] N90-11594
Ion beam annealing of Ga-implanted Si
[DE89-016857] N90-11610
SILICON CARBIDES
Effect of thermal and cyclic loads on silicon carbide yarn reinforced glass matrix composites
[DE89-016554] N90-11091
Hydrogen-silicon carbide interactions
[NASA-TM-102382] N90-11144
Kinetics and mechanisms of primary and steady state creep in B- and Al-containing alpha silicon carbide
[AD-A210739] N90-11616
SILICON COMPOUNDS
Y-Si-Al-O-N glass fibers
[AD-A211170] N90-11088
SILICON DIOXIDE
A diffuse reflectance infrared Fourier transform spectroscopic study of adsorbed hydrazines N90-11170
SILICON NITRIDES
Low temperature processing of reaction sintered silicon nitride
[DE89-017455] N90-11092
The Si(1-x)Nx Rugate
[AD-A211236] N90-11572
SILVER HALIDES
Design and construction of systems for the single-crystals growth of ternary silver halides, alkali halides, and alkaline earth fluorides, and the dielectric investigation of silver halide
[ETN-89-94673] N90-11632
SIMULATION
Particle kinetic simulation of high altitude hypervelocity flight
[NASA-CR-186003] N90-10840
Deployment simulation for 3rd generation solar array GSR3 N90-11074

Study of the application of automation to composites manufacture
[AD-A211049] N90-11087
Atmospheric chemistry of the fuel hydrazines N90-11158
Numerical simulation of hydrazine transport in a sandy soil N90-11172
Simulation of synthetic aperture radar 1: Feature density and accuracy requirements
[AD-A211019] N90-11218
Internal voltages and currents in well-shielded cylindrical objects due to simulated direct-strike lightning
[DE89-012664] N90-11231
Modeling and simulation of spatial robotic manipulators with flexible links and joint drives for control strategies implementation and evaluation N90-11311
A re-evaluation of fatigue threshold test procedures and the simulation and prediction of fatigue crack growth under conditions of low crack closure N90-11328
Development of an approximate technique for the nonlinear random vibrations analysis of hysteretic systems N90-11335
Definition of imaging performance for satellite surveillance, models, and simulations
[FOA-C-30493-9.4] N90-11341
ANTHEM simulation of the early time magnetic field penetration of the plasma surrounding a high density Z-pinch
[DE89-016980] N90-11585
A fully electromagnetic hybrid model for high density plasma simulations
[DE89-016771] N90-11593

SIMULATORS
A simulator for a hydrocarbon ramrocket fuel gas generator: First phase development
[AR-005-621] N90-11080
Thin section casting program. Volume 2-A: Appendix to volume 2
[DE89-009032] N90-11200

SINE WAVES
Comparison of sine dwell and broadband methods for modal testing N90-11025
The Si(1-x)Nx Rugate
[AD-A211236] N90-11572

SINGLE CRYSTALS
Defect structures preceding amorphization by ion irradiations in YBa2Cu3O(7-delta)
[DE89-016905] N90-11612
Passage of ultrarelativistic electrons through real crystals
[DE89-618624] N90-11613
Design and construction of systems for the single-crystals growth of ternary silver halides, alkali halides, and alkaline earth fluorides, and the dielectric investigation of silver halide
[ETN-89-94673] N90-11632

SINGULARITY (MATHEMATICS)
Singularity theory and N = 2 superconformal field theories
[DE89-016582] N90-11538

SINTERED ALUMINUM POWDER
Kinetics and mechanisms of primary and steady state creep in B- and Al-containing alpha silicon carbide
[AD-A210739] N90-11616

SINTERING
Low temperature processing of reaction sintered silicon nitride
[DE89-017455] N90-11092
Freeze-dried processing of tungsten heavy alloys
[DE89-015171] N90-11122

SKIN (ANATOMY)
Occupational safety considerations with hydrazine N90-11182

SKY SURVEYS (ASTRONOMY)
MOXE: An X-ray all-sky monitor for Soviet Spectrum-X-Gamma Mission
[NASA-TM-101266] N90-11280

SKY WAVES
Accurate measurements of the total angle of arrival of HF skywaves N90-11402
Ionospheric limitations to the accuracy of SSL estimates of HF transmitter locations N90-11403

SLEEP
Test-retest reliability of oxford Medilog 9000 sleep recording and SS-90-3 sleep stage scoring
[AD-A211165] N90-11440

SLIDING
Planar sliding of a rigid body with dry friction: Limit surfaces and dynamics of motion N90-11314

SLOTTED WIND TUNNELS
On transonic flow over segmented slotted wind tunnel wall with mass transfer N90-11676

SMOKE
Analysis of forest fire smoke using satellite imagery
[AD-A210657] N90-11339

SNOW COVER
Airborne gamma radiation snow water equivalent and soil moisture measurements and satellite areal extent of snow cover measuerments: A user's guide, version 3.0
[PB89-177877] N90-11338

SOCIOLOGY
The astronomy of Andean myth: The history of a cosmology N90-11660

SODIUM
A new inexpensive electrochemical meter for oxygen in sodium coolant
[DE89-630802] N90-11104

SOFTWARE ENGINEERING
Considerations for a design and operations knowledge support system for Space Station Freedom
[NASA-TM-102156] N90-11451
Software configuration management: An overview
[PB89-193833] N90-11458
Module algebra (revised version)
[CWI-CS-R8844-REV] N90-11474

SOFTWARE TOOLS
A distributed debugger for Amoeba
[CWI-CS-R8828] N90-11453
Software configuration management: An overview
[PB89-193833] N90-11458

SOIL SCIENCE
The soil microbiology of hydrazines N90-11171

SOILS
The Third Conference on the Environmental Chemistry of Hydrazine Fuels
[AD-A197632] N90-11157
Hydrazine fate and transformation in natural waters and soils N90-11165
Vibrational spectroscopic study of the kaolinite-hydrazine intercalation complex N90-11166
The soil microbiology of hydrazines N90-11171
Measurement of hydrazine contamination in soils N90-11180

SOL-GEL PROCESSES
Fifth International Workshop on Glasses and Ceramics from Gels
[DE89-016899] N90-11147
Synthesis of powder with gel technique
[FOA-C-20752-2.4(2.1)] N90-11156

SOLAR ACTIVITY
Meeting of intercosmos space physics group N90-10902
Solar-geophysical data number 536, part 1. Data for March, Febuary 1989 and late data
[PB89-194716] N90-11684

SOLAR ACTIVITY EFFECTS
Radio propagation conditions forecast above a low latitude region N90-11400
User's guide to the Space Environment Services Center geophysical alert broadcasts
[PB89-194617] N90-11411

SOLAR ARRAYS
Acoustic response analysis in the low frequency domain N90-11010
The third generation rigid solar array GSR3 N90-11017
Mathematical model and predictions for static and dynamic behavior of solar array structure N90-11049
Space telescope solar array: Nonlinear test and analysis effects N90-11051
Deployment simulation for 3rd generation solar array GSR3 N90-11074
STSA-Space Telescope solar array interconnectors: From simple approaches to complex modeling. A case study of the necessity of complex analysis N90-11076

SOLAR CELLS
Study of a gallium arsenide solar cell interconnector N90-11033
CuInSe2 solar cell research by sputter deposition
[DE89-009450] N90-11345
Laser grooved and polycrystalline silicon solar cell research
[DE89-015196] N90-11347
Proceedings of the Polycrystalline Thin Film Program Meeting
[DE89-009457] N90-11348
Novel thin-film CuInSe2 fabrication
[DE89-009440] N90-11604

SOLAR FLARES
Solar-terrestrial relations: Flare and solar wind effects N90-11362
Solar-geophysical data number 536, part 1. Data for March, Febuary 1989 and late data
[PB89-194716] N90-11684
Solar-geophysical data number 537, part 1. Data for April, March 1989 and late data
[PB89-207393] N90-11685

SOLAR FLUX DENSITY
A solar extreme ultraviolet flux model N90-11686

SOLAR MAGNETIC FIELD
Solar-geophysical data number 536, part 1. Data for March, Febuary 1989 and late data
[PB89-194716] N90-11684

SOLAR NEUTRINOS
Solar opacities constrained by solar neutrinos and solar oscillations
[DE89-016988] N90-11687

SOLAR OSCILLATIONS
Solar opacities constrained by solar neutrinos and solar oscillations
[DE89-016988] N90-11687

SOLAR PHYSICS
Solar-geophysical data number 537, part 1. Data for April, March 1989 and late data
[PB89-207393] N90-11685

SOLAR PLANETARY INTERACTIONS
User's guide to the Space Environment Services Center geophysical alert broadcasts
[PB89-194617] N90-11411
National Center For Atmospheric Research annual report, fiscal year 1988
[PB89-208987] N90-11428

SOLAR RADIATION
Solar radiation in Linkoeping (Sweden): Variations over half a year in irradiance and spectral composition in the interval 400-1000 nm
[FOA-C-30521-3.1] N90-11417
A solar extreme ultraviolet flux model N90-11686

SOLAR RADIO EMISSION
Solar-geophysical data number 536, part 1. Data for March, Febuary 1989 and late data
[PB89-194716] N90-11684
Solar-geophysical data number 537, part 1. Data for April, March 1989 and late data
[PB89-207393] N90-11685

SOLAR SEA POWER PLANTS
Planning for hybrid-cycle OTEC experiments using the HMTSTA test facility at the Natural Energy Laboratory of Hawaii
[DE89-013278] N90-11349

SOLAR TEMPERATURE
Solar opacities constrained by solar neutrinos and solar oscillations
[DE89-016988] N90-11687

SOLAR TERRESTRIAL INTERACTIONS
Ionospheric Structure and Variability on a Global Scale and Interactions with Atmosphere and Magnetosphere
[AGARD-CP-441] N90-11361
Solar-terrestrial relations: Flare and solar wind effects N90-11362
Magnetospheric substorms as a signature of the solar terrestrial interaction N90-11363
Stormtime coupling of the neutral and ionized upper atmosphere at middle latitudes N90-11381
Coordinated multi-parameter measurements and predictions of the global-scale ionosphere N90-11397

SOLAR WIND
Solar-terrestrial relations: Flare and solar wind effects N90-11362
Magnetospheric substorms as a signature of the solar terrestrial interaction N90-11363

SOLID CRYOGENS
Solid fiber Z-pinches: Cold-start computations
[DE89-016768] N90-11592

SOLID ELECTRODES
The effect of electrode configuration on arcjet performance
[NASA-TM-102346] N90-11081

SOLID PROPELLANT ROCKET ENGINES
Turbulent reacting flows in solid-propellant ducted rocket combustors N90-11079

SOLID STATE DEVICES
A general-purpose computer program for the Volterra-series analysis of nonlinear microwave circuits
[AD-A210768] N90-11236

SOLID STATE LASERS
Nonlinear dynamics of broad-band lasers
[DE89-017442] N90-11307

SOLID STATE PHYSICS
Superconducting ceramics in the Bi1.5SrCaCu2O sub x system by melt quenching technique
[NASA-CR-185139] N90-11606

SOLID-SOLID INTERFACES
Influence of the fiber/matrix interface on damage development in CFRP N90-11037

SOLIDIFICATION
Solidification front/viscous phase transitions, forward-backward heat equations
[AD-A211068] N90-11114

SOLIDS
Radiationless transitions and excited-state absorption of low-field chromium complexes in solids
[AD-A210653] N90-11105

X-ray and gamma-ray spectroscopy of solids under pressure
[DE89-017271] N90-11118
SOLUBILITY
A new method for the characterization of solutes and solvent phases using solvatochromic parameters
[AD-A211238] N90-11116
SOLUTES
A new method for the characterization of solutes and solvent phases using solvatochromic parameters
[AD-A211238] N90-11116
SOLUTIONS
Wavefront propagation for reaction-diffusion systems of PDE
[AD-A210862] N90-11510
SOLVENTS
A new method for the characterization of solutes and solvent phases using solvatochromic parameters
[AD-A211238] N90-11116
SOLVOLYSIS
Enhanced oxidation and solovolysis reactions in chemically inert microheterogeneous systems
[AD-A210748] N90-11110
SORPTION
Numerical simulation of hydrazine transport in a sandy soil N90-11172
SOS (SEMICONDUCTORS)
Precision materials characterization in the near millimeter and submillimeter wavelength range
[AD-A210655] N90-11106
SOUND TRANSMISSION
Calculation of sound transmission through a cylindrical shell using ASKA acoustics N90-11009
SOUND WAVES
The dynamics of circular plates with patch damping: A numerical and experimental study N90-11329
Nonlinear acoustics: Reflection and refraction, propagation in a periodic waveguide, scattering of sound by sound and ellipsoidal focusing
[AD-A211224] N90-11550
SOUND-SOUND INTERACTIONS
Nonlinear acoustics: Reflection and refraction, propagation in a periodic waveguide, scattering of sound by sound and ellipsoidal focusing
[AD-A211224] N90-11550
SOUNDING ROCKETS
Meteorological rocket observations
[PB89-168769] N90-11419
SOUTHERN HEMISPHERE
Auroral and sub-auroral F-layer irregularity studies in the Northern and Southern Hemiaphere during the equinox transition study September 16-26, 1984 N90-11393
Observational studies of low-frequency oscillations in the Southern Hemisphere N90-11420
SOUTHERN OSCILLATION
Observational studies of low-frequency oscillations in the Southern Hemisphere N90-11420
SOVIET SPACECRAFT
USSR and international cooperation in space N90-10905
SPACE CHARGE
Extraction induced emittance growth for negative ion sources
[DE89-017586] N90-11559
SPACE COMMERCIALIZATION
Research and test facilities for development of technologies and experiments with commercial applications
[NASA-TM-101789] N90-10909
SPACE COMMUNICATION
Telescience Testbed Pilot Program
[NASA-CR-184594] N90-11455
SPACE ENVIRONMENT SIMULATION
Space environment effects on carbon/epoxy materials N90-11056
Droplet combustion experiment drop tower tests using models of the space flight apparatus
[NASA-TM-101472] N90-11196
SPACE ERECTABLE STRUCTURES
A super element for multibody dynamics N90-11004
Thermoelastic behavior of large space structures: Modeling and control N90-11012
SPACE EXPLORATION
A history of West European rocketry and space research
[AD-A211191] N90-11690
SPACE FLIGHT TRAINING
Advanced manned space flight simulation and training: An investigation of simulation host computer system concepts
[NASA-CR-185998] N90-10911
SPACE INDUSTRIALIZATION
Research and test facilities for development of technologies and experiments with commercial applications
[NASA-TM-101789] N90-10909
SPACE MANUFACTURING
Meeting of intercosmos space physics group N90-10902
SPACE MISSIONS
JPRS Report: Science and Technology. USSR: Space
[JPRS-USP-89-007] N90-10900
Soviet Mars program N90-10903
USSR and international cooperation in space N90-10905
Sagdeyev discusses space missions, policy, Mars plans N90-10906
SPACE NAVIGATION
Independent Orbiter Assessment (IOA): Analysis of the guidance, navigation, and control subsystem
[NASA-CR-185555] N90-10920
SPACE PLASMAS
Quantitative methods for waves in space plasmas
[PB89-210256] N90-11599
Can ion acceleration by double-cyclotron absorption produce O(+) ion conics
[IRF-PREPRINT-114] N90-11600
Numerical study of the current sheet and PSBL in a magnetotail model
[NASA-CR-183289] N90-11669
SPACE PROCESSING
Space Station Freedom: A foothold on the future
[NASA-NP-107/10-88] N90-10907
Concepts for microgravity experiments utilizing gloveboxes
[NASA-TM-100378] N90-11195
SPACE PROGRAMS
Federal Radionavigation Plan, 1988
[PB89-163075] N90-10846
SPACE SHUTTLE ASCENT STAGE
Atmospheric environment for space shuttle (STS-29) launch
[NASA-TM-100376] N90-10980
Atmospheric environment for space shuttle (STS-30) launch
[NASA-TM-100381] N90-10981
SPACE SHUTTLE MAIN ENGINE
Independent Orbiter Assessment (IOA): Analysis of the orbiter main propulsion system
[NASA-CR-185584] N90-10927
SPACE SHUTTLE MISSION 61-A
Atmospheric environment for space shuttle (STS-29) launch
[NASA-TM-100376] N90-10980
Atmospheric environment for space shuttle (STS-30) launch
[NASA-TM-100381] N90-10981
SPACE SHUTTLE MISSIONS
Shuttle Atlantis to deploy Galileo probe toward Jupiter
[NASA-TM-101888] N90-10982
SPACE SHUTTLE ORBITERS
Independent Orbiter Assessment (IOA): Analysis of the manned maneuvering unit
[NASA-CR-185565] N90-10913
Independent Orbiter Assessment (IOA): Assessment of the electrical power generation/fuel cell powerplant subsystem FMEA/CIL
[NASA-CR-185562] N90-10914
Independent Orbiter Assesment (IOA): Analysis of the electrical power generation/fuel cell powerplant subsystem
[NASA-CR-185561] N90-10915
Independent Orbiter Assessment (IOA): Analysis of the rudder/speed brake subsystem
[NASA-CR-185560] N90-10916
Independent Orbiter Assessment (IOA): Assessment of the data processing system FMEA/CIL
[NASA-CR-185546] N90-10917
Independent Orbiter Assessment (IOA): Analysis of the electrical power generation/power reactant storage and distribution subsystem
[NASA-CR-185556] N90-10918
Independent Orbiter Assesment (IOA): Analysis of the orbital maneuvering system
[NASA-CR-185554] N90-10919
Independent Orbiter Assessment (IOA): Analysis of the guidance, navigation, and control subsystem
[NASA-CR-185555] N90-10920
Independent Orbiter Assessment (IOA): Analysis of the nose wheel steering subsystem
[NASA-CR-185548] N90-10921
Independent Orbiter Assessment (IOA): FMEA/CIL instructions and ground rules
[NASA-CR-185551] N90-10922
Independent Orbiter Assesment (IOA): Assessment of the electrical power generation/power reactant storage and distribution subsystem FMEA/CIL
[NASA-CR-185545] N90-10923
Independent Orbiter Assessment (IOA): Analysis of the DPS subsystem
[NASA-CR-185549] N90-10924
Independent Orbiter Assessment (IOA): Analysis of the atmospheric revitalization pressure control subsystem
[NASA-CR-185593] N90-10925
Independent Orbiter Assessment (IOA): Analysis of the remote manipulator system
[NASA-CR-185585] N90-10926
Independent Orbiter Assessment (IOA): Analysis of the orbiter main propulsion system
[NASA-CR-185584] N90-10927
Independent Orbiter Assessment (IOA): Analysis of the instrumentation subsystem
[NASA-CR-185571] N90-10928
Independent Orbiter Assessment (IOA): Analysis of the ascent thrust vector control actuator subsystem
[NASA-CR-185579] N90-10929
Independent Orbiter Assessment (IOA): Analysis of the body flap subsystem
[NASA-CR-185574] N90-10930
Independent Orbiter Assessment (IOA): Analysis of the auxiliary power unit
[NASA-CR-185568] N90-10931
Independent Orbiter Assessment (IOA): Analysis of the backup flight system
[NASA-CR-185567] N90-10932
Independent Orbiter Assessment (IOA): Analysis of the electrical power distribution and control/electrical power generation subsystem
[NASA-CR-185538] N90-10933
Independent Orbiter Assessment (IOA): Analysis of the hydraulics/water spray boiler subsystem
[NASA-CR-185541] N90-10934
Independent Orbiter Assessment (IOA): Analysis of the elevon subsystem
[NASA-CR-185576] N90-10935
Independent Orbiter Assessment (IOA): Analysis of the electrical power distribution and control/remote manipulator system subsystem
[NASA-CR-185526] N90-10936
Independent Orbiter Assessment (IOA): Analysis of the extravehicular mobility unit
[NASA-CR-185540] N90-10937
Independent Orbiter Assessment (IOA): Analysis of the reaction control system, volume 1
[NASA-CR-185532-VOL-1] N90-10938
Independent Orbiter Assessment (IOA): Analysis of the reaction control system, volume 2
[NASA-CR-185532-VOL-2] N90-10939
Independent Orbiter Assessment (IOA): Analysis of the reaction control system, volume 3
[NASA-CR-185532-VOL-3] N90-10940
Independent Orbiter Assessment (IOA): Analysis of the electrical power distribution and control subsystem, volume 1
[NASA-CR-185529-VOL-1] N90-10941
Independent Orbiter Assessment (IOA): Analysis of the electrical power distribution and control subsystem, volume 2
[NASA-CR-185529-VOL-2] N90-10942
Independent Orbiter Assessment (IOA): Analysis of the landing/deceleration subsystem
[NASA-CR-185569] N90-10943
Independent Orbiter Assessment (IOA): Analysis of the mechanical actuation subsystem
[NASA-CR-185525] N90-10944
Independent Orbiter Assessment (IOA): Analysis of the pyrotechnics subsystem
[NASA-CR-185530] N90-10945
Independent Orbiter Assessment (IOA): Assessment of the pyrotechnics subsystem
[NASA-CR-185531] N90-10946
Independent Orbiter Assessment (IOA): Assessment of the nose wheel steering subsystem
[NASA-CR-185533] N90-10947
Independent Orbiter Assessment (IOA): Weibull analysis report
[NASA-CR-185534] N90-10948
Independent Orbiter Assessment (IOA): Assessment of the purge, vent and drain subsystem
[NASA-CR-185535] N90-10949
Independent Orbiter Assessment (IOA): Assessment of the extravehicular mobility unit, volume 1
[NASA-CR-185536-VOL-1] N90-10950
Independent Orbiter Assessment (IOA): Assessment of the extravehicular mobility unit, volume 2
[NASA-CR-185536-VOL-2] N90-10951
Independent Orbiter Assessment (IOA): Assessment of the mechanical actuation subsystem, volume 1
[NASA-CR-185527-VOL-1] N90-10952
Independent Orbiter Assessment (IOA): Assessment of the mechanical actuation subsystem, volume 2
[NASA-CR-185527-VOL-2] N90-10953
Independent Orbiter Assessment (IOA): CIL issues resolution report, volume 1
[NASA-CR-185524-VOL-1] N90-10954

Independent Orbiter Assessment (IOA): CIL issues resolution report, volume 2
[NASA-CR-185524-VOL-2] N90-10955
Independent Orbiter Assessment (IOA) CIL issues resolution report, volume 3
[NASA-CR-185524-VOL-3] N90-10956
Independent Orbiter Assessment (IOA): Assessment of the atmospheric revitalization pressure control subsystem FMEA/CIL
[NASA-CR-185594] N90-10957
Independent Orbiter Assessment (IOA): Analysis of the crew equipment subsystem
[NASA-CR-185591] N90-10958
Independent Orbiter Assessment (IOA): Assessment of the ascent thrust vector control actuator subsystem FMEA/CIL
[NASA-CR-185590] N90-10959
Independent Orbiter Assessment (IOA): FMEA/CIL assessment
[NASA-CR-185589] N90-10960
Independent Orbiter Assessment (IOA): Assessment of the displays and controls subsystem
[NASA-CR-185588] N90-10961
Independent Orbiter Assessment (IOA): Assessment of the Orbiter Experiment (OEX) subsystem
[NASA-CR-185587] N90-10962
Independent Orbiter Assessment (IOA): Analysis of the Orbiter Experiment (OEX) subsystem
[NASA-CR-185586] N90-10963
Independent Orbiter Assessment (IOA): Assessment of the remote manipulator system FMEA/CIL
[NASA-CR-185592] N90-10964
Independent Orbiter Assessment (IOA): Assessment of the EPD and C/remote manipulator system FMEA/CIL
[NASA-CR-185583] N90-10965
Independent Orbiter Assessment (IOA): Assessment of the landing/deceleration (LDG/DEC) subsystem FMEA/CIL
[NASA-CR-185570] N90-10966
Independent Orbiter Assessment (IOA): Analysis of the communication and tracking subsystem
[NASA-CR-185582] N90-10967
Independent Orbiter Assessment (IOA): Assessment of the body flap subsystem FMEA/CIL
[NASA-CR-185575] N90-10968
Independent Orbiter Assessment (IOA): Analysis of the purge, vent and drain subsystem
[NASA-CR-185547] N90-10969
Independent Orbiter Assessment (IOA): Assessment of the elevon actuator subsystem FMEA/CIL
[NASA-CR-185578] N90-10970
Independent Orbiter Assessment (IOA): Assessment of the crew equipment subsystem
[NASA-CR-185577] N90-10971
Independent Orbiter Assessment (IOA): Assessment of instrumental subsystem FMEA/CIL
[NASA-CR-185572] N90-10972
Independent Orbiter Assessment (IOA): Assessment of the backup flight system FMEA/CIL
[NASA-CR-185566] N90-10973
Independent Orbiter Assessment (IOA): Assessment of the manned maneuvering unit
[NASA-CR-185564] N90-10974
Independent Orbiter Assessment (IOA): Assessment of the rudder/speed brake subsystem FMEA/CIL
[NASA-CR-185558] N90-10975
Independent Orbiter Assessment (IOA): Assessment of the auxiliary power unit
[NASA-CR-185580] N90-10976
Independent Orbiter Assessment (IOA): Assessment of the life support and airlock support systems, volume 1
[NASA-CR-185581-VOL-1] N90-10977
Independent Orbiter Assessment (IOA): Assessment of the life support and airlock support systems, volume 2
[NASA-CR-185581-VOL-2] N90-10978
Independent Orbiter Assessment (IOA): Assessment of the active thermal control system
[NASA-CR-185573] N90-10979
Automated stress analysis of Shuttle orbiter thermal protection system N90-11043

SPACE SHUTTLE PAYLOADS
Shuttle Atlantis to deploy Galileo probe toward Jupiter
[NASA-TM-101888] N90-10982

SPACE SHUTTLES
STS-GPS (Space Transportation System - Global Positioning System) tracking experiment for gravitation estimation: Feasibility study
[AD-A211265] N90-10859
Landing tests for Buran shuttle with jet engine-equipped mock-up N90-10904

SPACE STATION POLAR PLATFORMS
Key structures mechanical issues of the European Space Station and platform program Columbus N90-11072

SPACE STATION STRUCTURES
SDM challenges for space station N90-11059

SPACE STATIONS
Space Station Freedom: A foothold on the future
[NASA-NP-107/10-88] N90-10907
Advanced manned space flight simulation and training: An investigation of simulation host computer system concepts
[NASA-CR-185998] N90-10911
Evolutionary space station fluids management strategies
[NASA-CR-185137] N90-10983
SDM challenges for space station N90-11059
Near zone-basic scattering code user's manual with space station applications
[NASA-CR-185925] N90-11209
NASA/NBS (National Aeronautics and Space Administration/National Bureau of Standards) standard reference model for telerobot control system architecture (NASREM)
[NASA-CR-185078] N90-11310
Considerations for a design and operations knowledge support system for Space Station Freedom
[NASA-TM-102156] N90-11451

SPACE STORAGE
Evolutionary space station fluids management strategies
[NASA-CR-185137] N90-10983

SPACE SUITS
Independent Orbiter Assessment (IOA): Analysis of the extravehicular mobility unit
[NASA-CR-185540] N90-10937
Independent Orbiter Assessment (IOA): Analysis of the crew equipment subsystem
[NASA-CR-185591] N90-10958
Independent Orbiter Assessment (IOA): Assessment of the crew equipment subsystem
[NASA-CR-185577] N90-10971

SPACE TRANSPORTATION SYSTEM
STS-GPS (Space Transportation System - Global Positioning System) tracking experiment for gravitation estimation: Feasibility study
[AD-A211265] N90-10859
STS payload design load evolution N90-10989

SPACE WEAPONS
Assessment of space power related measurement requirements of the Strategic Defense Initiative
[PB89-209357] N90-11343

SPACE-TIME FUNCTIONS
On the construction of the scattering matrix for locally-noncommutative interactions of relativistic fields
[DE89-630138] N90-11640

SPACEBORNE ASTRONOMY
Project Radioastron N90-10901

SPACEBORNE EXPERIMENTS
Space Station Freedom: A foothold on the future
[NASA-NP-107/10-88] N90-10907
Shuttle Atlantis to deploy Galileo probe toward Jupiter
[NASA-TM-101888] N90-10982
Concepts for microgravity experiments utilizing gloveboxes
[NASA-TM-100378] N90-11195
Droplet combustion experiment drop tower tests using models of the space flight apparatus
[NASA-TM-101472] N90-11196

SPACEBORNE LASERS
The recovery of orbital and geophysical parameters using a spaceborne laser ranging system N90-11294

SPACEBORNE TELESCOPES
Project Radioastron N90-10901

SPACECRAFT CABIN ATMOSPHERES
Independent Orbiter Assessment (IOA): Analysis of the atmospheric revitalization pressure control subsystem
[NASA-CR-185593] N90-10925

SPACECRAFT COMPONENTS
Independent Orbiter Assessment (IOA): FMEA/CIL assessment
[NASA-CR-185589] N90-10960
The use of damage characterization for life prediction methodologies N90-11053

SPACECRAFT CONFIGURATIONS
Dynamic substructuring for modular analysis and testing N90-11015

SPACECRAFT CONSTRUCTION MATERIALS
Liquid infiltrated C/SiC: An alternative material for hot space structures N90-11030
Material properties of 2219-T851 aluminum alloy plasma welded compared to TIG welding N90-11032
Development of graphite-magnesium composites for space applications N90-11054
Space environment effects on carbon/epoxy materials N90-11056

SPACECRAFT CONTROL
Independent Orbiter Assessment (IOA): Analysis of the guidance, navigation, and control subsystem
[NASA-CR-185555] N90-10920
Independent Orbiter Assessment (IOA): Analysis of the backup flight system
[NASA-CR-185567] N90-10932
Independent Orbiter Assessment (IOA): Assessment of the rudder/speed brake subsystem FMEA/CIL
[NASA-CR-185558] N90-10975
Use of Lanczos vectors in structural dynamics N90-11011
Thermoelastic behavior of large space structures: Modeling and control N90-11012
Guaranteed cost control of flexible space structures N90-11643

SPACECRAFT DESIGN
Flight testing and flight research: From the age of the tower jumper to the age of the astronaut N90-10882
Qualification by simulation: Dream or reality N90-10990
Experimental identification of modal momentum coefficients and modal identity parameters of the FLECS structure N90-10991
Experiences using a major FEM package interactively for spacecraft applications N90-11008
Numerical treatment of the thermo-structural-dynamic problems: The interpolation techniques N90-11016
Modeling of liquid sloshing effects in multibody systems N90-11023
Comparison of sine dwell and broadband methods for modal testing N90-11025
Thermal and structural analysis of Hermes N90-11058
Exploitation of data management facilities for finite element analysis in aerospace structural engineering applications N90-11078

SPACECRAFT ELECTRONIC EQUIPMENT
Evaluation test of CCD area sensor for star sensor
[NAL-TM-570] N90-11566
CRRES (Combined Release and Radiation Effects Satellite) SPACERAD plasma wave experiment
[AD-A210791] N90-11587

SPACECRAFT ENVIRONMENTS
Space Station Freedom: A foothold on the future
[NASA-NP-107/10-88] N90-10907
Independent Orbiter Assessment (IOA): Assessment of the life support and airlock support systems, volume 1
[NASA-CR-185581-VOL-1] N90-10977
Independent Orbiter Assessment (IOA): Assessment of the life support and airlock support systems, volume 2
[NASA-CR-185581-VOL-2] N90-10978

SPACECRAFT GUIDANCE
Independent Orbiter Assessment (IOA): Analysis of the guidance, navigation, and control subsystem
[NASA-CR-185555] N90-10920
Evaluation test of CCD area sensor for star sensor
[NAL-TM-570] N90-11566

SPACECRAFT INSTRUMENTS
Independent Orbiter Assessment (IOA): Assessment of the Orbiter Experiment (OEX) subsystem
[NASA-CR-185587] N90-10962
Independent Orbiter Assessment (IOA): Analysis of the Orbiter Experiment (OEX) subsystem
[NASA-CR-185586] N90-10963
Independent Orbiter Assessment (IOA): Analysis of the communication and tracking subsystem
[NASA-CR-185582] N90-10967
Independent Orbiter Assessment (IOA): Assessment of instrumental subsystem FMEA/CIL
[NASA-CR-185572] N90-10972
Evaluation test of CCD area sensor for star sensor
[NAL-TM-570] N90-11566

SPACECRAFT LANDING
Landing tests for Buran shuttle with jet engine-equipped mock-up N90-10904
Independent Orbiter Assessment (IOA): Analysis of the nose wheel steering subsystem
[NASA-CR-185548] N90-10921
Independent Orbiter Assessment (IOA): Assessment of the landing/deceleration (LDG/DEC) subsystem FMEA/CIL
[NASA-CR-185570] N90-10966

SPACECRAFT LAUNCHING
Flight-mechanical environment on Ariane launch vehicle payloads N90-11048

SPACECRAFT MANEUVERS
Independent Orbiter Assessment (IOA): Analysis of the reaction control system, volume 1
[NASA-CR-185532-VOL-1] N90-10938

SPACECRAFT MODELS
Landing tests for Buran shuttle with jet engine-equipped mock-up N90-10904
Spacecraft Structures and Mechanical Testing
[ESA-SP-289] N90-10986
Thermoelastic behavior of large space structures: Modeling and control N90-11012

SPACECRAFT PERFORMANCE
Independent Orbiter Assessment (IOA): FMEA/CIL instructions and ground rules
[NASA-CR-185551] N90-10922
SPACECRAFT POWER SUPPLIES
Independent Orbiter Assessment (IOA): Assessment of the electrical power generation/fuel cell powerplant subsystem FMEA/CIL
[NASA-CR-185562] N90-10914
Independent Orbiter Assessment (IOA): Analysis of the electrical power generation/fuel cell powerplant subsystem
[NASA-CR-185561] N90-10915
Independent Orbiter Assessment (IOA): Analysis of the electrical power generation/power reactant storage and distribution subsystem
[NASA-CR-185556] N90-10918
Independent Orbiter Assessment (IOA): Analysis of the orbital maneuvering system
[NASA-CR-185554] N90-10919
Independent Orbiter Assessment (IOA): Assessment of the electrical power generation/power reactant storage and distribution subsystem FMEA/CIL
[NASA-CR-185545] N90-10923
Independent Orbiter Assessment (IOA): Analysis of the electrical power distribution and control/electrical power generation subsystem
[NASA-CR-185538] N90-10933
Independent Orbiter Assessment (IOA): Analysis of the electrical power distribution and control/remote manipulator system subsystem
[NASA-CR-185526] N90-10936
Independent Orbiter Assessment (IOA): Analysis of the reaction control system, volume 2
[NASA-CR-185532-VOL-2] N90-10939
Independent Orbiter Assessment (IOA): Analysis of the reaction control system, volume 3
[NASA-CR-185532-VOL-3] N90-10940
Independent Orbiter Assessment (IOA): Analysis of the electrical power distribution and control subsystem, volume 1
[NASA-CR-185529-VOL-1] N90-10941
Independent Orbiter Assessment (IOA): Analysis of the electrical power distribution and control subsystem, volume 2
[NASA-CR-185529-VOL-2] N90-10942
Independent Orbiter Assessment (IOA): CIL issues resolution report, volume 2
[NASA-CR-185524-VOL-2] N90-10955
Independent Orbiter Assessment (IOA): Assessment of the auxiliary power unit
[NASA-CR-185580] N90-10976
SPACECRAFT PROPULSION
Independent Orbiter Assessment (IOA) CIL issues resolution report, volume 3
[NASA-CR-185524-VOL-3] N90-10956
The effect of electrode configuration on arcjet performance
[NASA-TM-102346] N90-11081
SPACECRAFT RADIATORS
Design of ceramic fabric heat pipe with water working fluid
[DE89-016565] N90-11265
SPACECRAFT RELIABILITY
Independent Orbiter Assessment (IOA): Analysis of the manned maneuvering unit
[NASA-CR-185565] N90-10913
Independent Orbiter Assessment (IOA): Assessment of the electrical power generation/fuel cell powerplant subsystem FMEA/CIL
[NASA-CR-185562] N90-10914
Independent Orbiter Assessment (IOA): Analysis of the electrical power generation/fuel cell powerplant subsystem
[NASA-CR-185561] N90-10915
Independent Orbiter Assessment (IOA): Analysis of the rudder/speed brake subsystem
[NASA-CR-185560] N90-10916
Independent Orbiter Assessment (IOA): Assessment of the data processing system FMEA/CIL
[NASA-CR-185546] N90-10917
Independent Orbiter Assessment (IOA): Analysis of the electrical power generation/power reactant storage and distribution subsystem
[NASA-CR-185556] N90-10918
Independent Orbiter Assessment (IOA): Analysis of the orbital maneuvering system
[NASA-CR-185554] N90-10919
Independent Orbiter Assessment (IOA): Analysis of the nose wheel steering subsystem
[NASA-CR-185548] N90-10921
Independent Orbiter Assessment (IOA): FMEA/CIL instructions and ground rules
[NASA-CR-185551] N90-10922
Independent Orbiter Assessment (IOA): Assessment of the electrical power generation/power reactant storage and distribution subsystem FMEA/CIL
[NASA-CR-185545] N90-10923
Independent Orbiter Assessment (IOA): Analysis of the DPS subsystem
[NASA-CR-185549] N90-10924
Independent Orbiter Assessment (IOA): Analysis of the atmospheric revitalization pressure control subsystem
[NASA-CR-185593] N90-10925
Independent Orbiter Assessment (IOA): Analysis of the remote manipulator system
[NASA-CR-185585] N90-10926
Independent Orbiter Assessment (IOA): Analysis of the instrumentation subsystem
[NASA-CR-185571] N90-10928
Independent Orbiter Assessment (IOA): Analysis of the ascent thrust vector control actuator subsystem
[NASA-CR-185579] N90-10929
Independent Orbiter Assessment (IOA): Analysis of the body flap subsystem
[NASA-CR-185574] N90-10930
Independent Orbiter Assessment (IOA): Analysis of the auxiliary power unit
[NASA-CR-185568] N90-10931
Independent Orbiter Assessment (IOA): Analysis of the backup flight system
[NASA-CR-185567] N90-10932
Independent Orbiter Assessment (IOA): Analysis of the electrical power distribution and control/electrical power generation subsystem
[NASA-CR-185538] N90-10933
Independent Orbiter Assessment (IOA): Analysis of the hydraulics/water spray boiler subsystem
[NASA-CR-185541] N90-10934
Independent Orbiter Assessment (IOA): Analysis of the elevon subsystem
[NASA-CR-185576] N90-10935
Independent Orbiter Assessment (IOA): Analysis of the electrical power distribution and control/remote manipulator system subsystem
[NASA-CR-185526] N90-10936
Independent Orbiter Assessment (IOA): Analysis of the extravehicular mobility unit
[NASA-CR-185540] N90-10937
Independent Orbiter Assessment (IOA): Analysis of the reaction control system, volume 1
[NASA-CR-185532-VOL-1] N90-10938
Independent Orbiter Assessment (IOA): Analysis of the reaction control system, volume 2
[NASA-CR-185532-VOL-2] N90-10939
Independent Orbiter Assessment (IOA): Analysis of the reaction control system, volume 3
[NASA-CR-185532-VOL-3] N90-10940
Independent Orbiter Assessment (IOA): Analysis of the electrical power distribution and control subsystem, volume 1
[NASA-CR-185529-VOL-1] N90-10941
Independent Orbiter Assessment (IOA): Analysis of the electrical power distribution and control subsystem, volume 2
[NASA-CR-185529-VOL-2] N90-10942
Independent Orbiter Assessment (IOA): Analysis of the landing/deceleration subsystem
[NASA-CR-185569] N90-10943
Independent Orbiter Assessment (IOA): Analysis of the mechanical actuation subsystem
[NASA-CR-185525] N90-10944
Independent Orbiter Assessment (IOA): Analysis of the pyrotechnics subsystem
[NASA-CR-185530] N90-10945
Independent Orbiter Assessment (IOA): Assessment of the pyrotechnics subsystem
[NASA-CR-185531] N90-10946
Independent Orbiter Assessment (IOA): Assessment of the nose wheel steering subsystem
[NASA-CR-185533] N90-10947
Independent Orbiter Assessment (IOA): Weibull analysis report
[NASA-CR-185534] N90-10948
Independent Orbiter Assessment (IOA): Assessment of the purge, vent and drain subsystem
[NASA-CR-185535] N90-10949
Independent Orbiter Assessment (IOA): Assessment of the extravehicular mobility unit, volume 1
[NASA-CR-185536-VOL-1] N90-10950
Independent Orbiter Assessment (IOA): Assessment of the extravehicular mobility unit, volume 2
[NASA-CR-185536-VOL-2] N90-10951
Independent Orbiter Assessment (IOA): Assessment of the mechanical actuation subsystem, volume 1
[NASA-CR-185527-VOL-1] N90-10952
Independent Orbiter Assessment (IOA): Assessment of the mechanical actuation subsystem, volume 2
[NASA-CR-185527-VOL-2] N90-10953
Independent Orbiter Assessment (IOA): CIL issues resolution report, volume 2
[NASA-CR-185524-VOL-2] N90-10955
Independent Orbiter Assessment (IOA) CIL issues resolution report, volume 3
[NASA-CR-185524-VOL-3] N90-10958
Independent Orbiter Assessment (IOA): Assessment of the atmospheric revitalization pressure control subsystem FMEA/CIL
[NASA-CR-185594] N90-10957
Independent Orbiter Assessment (IOA): Analysis of the crew equipment subsystem
[NASA-CR-185591] N90-10958
Independent Orbiter Assessment (IOA): Assessment of the ascent thrust vector control actuator subsystem FMEA/CIL
[NASA-CR-185590] N90-10959
Independent Orbiter Assessment (IOA): FMEA/CIL assessment
[NASA-CR-185589] N90-10960
Independent Orbiter Assessment (IOA): Assessment of the displays and controls subsystem
[NASA-CR-185588] N90-10961
Independent Orbiter Assessment (IOA): Assessment of the Orbiter Experiment (OEX) subsystem
[NASA-CR-185587] N90-10962
Independent Orbiter Assessment (IOA): Analysis of the Orbiter Experiment (OEX) subsystem
[NASA-CR-185586] N90-10963
Independent Orbiter Assessment (IOA): Assessment of the remote manipulator system FMEA/CIL
[NASA-CR-185592] N90-10964
Independent Orbiter Assessment (IOA): Assessment of the EPD and C/remote manipulator system FMEA/CIL
[NASA-CR-185583] N90-10965
Independent Orbiter Assessment (IOA): Assessment of the landing/deceleration (LDG/DEC) subsystem FMEA/CIL
[NASA-CR-185570] N90-10966
Independent Orbiter Assessment (IOA): Analysis of the communication and tracking subsystem
[NASA-CR-185582] N90-10967
Independent Orbiter Assessment (IOA): Assessment of the body flap subsystem FMEA/CIL
[NASA-CR-185575] N90-10968
Independent Orbiter Assessment (IOA): Analysis of the purge, vent and drain subsystem
[NASA-CR-185547] N90-10969
Independent Orbiter Assessment (IOA): Assessment of the elevon actuator subsystem FMEA/CIL
[NASA-CR-185578] N90-10970
Independent Orbiter Assessment (IOA): Assessment of the crew equipment subsystem
[NASA-CR-185577] N90-10971
Independent Orbiter Assessment (IOA): Assessment of instrumental subsystem FMEA/CIL
[NASA-CR-185572] N90-10972
Independent Orbiter Assessment (IOA): Assessment of the backup flight system FMEA/CIL
[NASA-CR-185566] N90-10973
Independent Orbiter Assessment (IOA): Assessment of the manned maneuvering unit
[NASA-CR-185564] N90-10974
Independent Orbiter Assessment (IOA): Assessment of the rudder/speed brake subsystem FMEA/CIL
[NASA-CR-185558] N90-10975
Independent Orbiter Assessment (IOA): Assessment of the auxiliary power unit
[NASA-CR-185580] N90-10976
Independent Orbiter Assessment (IOA): Assessment of the life support and airlock support systems, volume 1
[NASA-CR-185581-VOL-1] N90-10977
Independent Orbiter Assessment (IOA): Assessment of the life support and airlock support systems, volume 2
[NASA-CR-185581-VOL-2] N90-10978
Independent Orbiter Assessment (IOA): Assessment of the active thermal control system
[NASA-CR-185573] N90-10979
SPACECRAFT STRUCTURES
Spacecraft Structures and Mechanical Testing
[ESA-SP-289] N90-10986
Updating of finite element model by means of normal mode parameters N90-10992
Reduction of dynamic response of spacecraft structures and payloads N90-11000
Acoustic response analysis in the low frequency domain N90-11010
Advances in design and testing of spacecraft structures N90-11018
Development of the large spacecraft structure N90-11020
Modal analysis of space structures with the Ibrahim Time Domain method N90-11026
Transient vibration testing of spacecraft structures. Experience with multiaxial base motion and combined base motion and point force excitation N90-11039

Transient tests for spacecraft structures N90-11040
Multi-axis transient testing: Experimental investigations N90-11042
A new aspect for the use of thin walled beams as shell stiffeners of spacecraft structures N90-11046
New data handling system (MDH) for mechanical tests at ESTEC N90-11066
Exploitation of data management facilities for finite element analysis in aerospace structural engineering applications N90-11078
Basic research on processing of ceramics for space structures
[AD-A205954] N90-11139

SPACECRAFT TEMPERATURE
Independent Orbiter Assessment (IOA): Analysis of the electrical power distribution and control/electrical power generation subsystem
[NASA-CR-185538] N90-10933
Independent Orbiter Assessment (IOA): Assessment of the active thermal control system
[NASA-CR-185573] N90-10979

SPACECRAFT TRACKING
Independent Orbiter Assessment (IOA) CIL issues resolution report, volume 3
[NASA-CR-185524-VOL-3] N90-10956

SPACECREWS
Independent Orbiter Assessment (IOA): Analysis of the extravehicular mobility unit
[NASA-CR-185540] N90-10937
Independent Orbiter Assessment (IOA): Analysis of the crew equipment subsystem
[NASA-CR-185591] N90-10958
Independent Orbiter Assessment (IOA): Assessment of the crew equipment subsystem
[NASA-CR-185577] N90-10971

SPACELAB
Gamma radiation background measurements from Spacelab 2
[NASA-CR-183782] N90-11689

SPACELAB PAYLOADS
Gamma radiation background measurements from Spacelab 2
[NASA-CR-183782] N90-11689

SPALLING
Microstructural effects on spall fracture in 1006 steel
[DE89-016770] N90-11131

SPATIAL DISTRIBUTION
Spatial and temporal short range total cloud cover estimation by metric analysis of composite imagery N90-11423

SPATIAL RESOLUTION
Land vehicle teleoperation under conditions of reduced video resolution
[DE89-016925] N90-11324

SPECIFIC HEAT
Studies of novel superconductors
[DE89-016744] N90-11609

SPECIFICATIONS
A verification exercise relating to specification styles in LOTOS
[MEMO-INF-89-18] N90-11471

SPECTRA
On the photoemission spectrum and optical gap in La2CuO4
[DE89-015281] N90-11605

SPECTRAL EMISSION
Theory of atomic spectral emission intensity
[IRF-PREPRINT-110] N90-11641
A solar extreme ultraviolet flux model N90-11686
The ratio to X-ray spectral shape and variability of blazars N90-11688

SPECTRAL ENERGY DISTRIBUTION
UV observations of NGC 205
[NASA-CR-185975] N90-11661

SPECTRAL METHODS
A conforming spectral collocation strategy for Stokes flow through a channel contraction
[NASA-CR-181912] N90-11495

SPECTRAL THEORY
Theory of atomic spectral emission intensity
[IRF-PREPRINT-110] N90-11641

SPECTROSCOPIC ANALYSIS
A diffuse reflectance infrared Fourier transform spectroscopic study of adsorbed hydrazines N90-11170

SPECTROSCOPY
Applications of NMR spectroscopy to the study of zeolite synthesis
[DE89-015226] N90-11095
A diffuse reflectance infrared Fourier transform spectroscopic study of adsorbed hydrazines N90-11170
The theory of ac impedance of rough electrode-electrolyte interfaces
[DE89-017474] N90-11243

SPECTRUM ANALYSIS
Low ppb level detection of toxic compounds with a fully automated CO2 laser photoacoustic detector N90-11181
Solar radiation in Linkoeping (Sweden): Variations over half a year in irradiance and spectral composition in the interval 400-1000 nm
[FOA-C-30521-3.1] N90-11417
Quantitative methods for waves in space plasmas
[PB89-210256] N90-11599
Theory of atomic spectral emission intensity
[IRF-PREPRINT-110] N90-11641
Rocket and satellite observations of the local interstellar medium N90-11668

SPEECH
Computer programs for measuring variations in speech
[AD-A211126] N90-11467

SPEECH RECOGNITION
Computer programs for measuring variations in speech
[AD-A211126] N90-11467
Spoken commands control robot that handles radioactive materials
[DE89-012632] N90-11488

SPEED CONTROL
Independent Orbiter Assessment (IOA): Analysis of the rudder/speed brake subsystem
[NASA-CR-185560] N90-10916

SPHERES
DMC (Distinct Motion Code): A rigid body motion code for determining the interaction of multiple spherical particles
[DE89-016929] N90-11543

SPHERICAL COORDINATES
Particle simulation in curvilinear coordinate systems
[DE89-016727] N90-11583

SPIN
The spinning of aircraft: A discussion of spin prediction techniques including a chronological bibliography
[ARL-AERO-R-177] N90-10888

SPIN DYNAMICS
Spin fluctuations and excitations in a 2D xy-ferromagnet: CoCl2 in graphite
[DE89-017600] N90-11119
Neutron scattering studies of amorphous Invar alloys
[DE89-016868] N90-11126

SPIN EXCHANGE
Studies of ultrathin magnetic films and particle-surface interactions with spin-sensitive electron spectroscopies
[DE89-016741] N90-11556

SPIN TESTS
Measurements of pressures on the tail and aft fuselage of an airplane model during rotary motions at spin attitudes
[NASA-TP-2939] N90-10829
The spinning of aircraft: A discussion of spin prediction techniques including a chronological bibliography
[ARL-AERO-R-177] N90-10888

SPINEL
Precipitation and transformation toughening of Al-Mg signals
[ETN-89-94675] N90-11138

SPINOR GROUPS
Reduction of the Dirac equation to the Dirac-Kaehler equation
[DE89-630111] N90-11541

SPLINE FUNCTIONS
An interactive program for constrained spline approximation of numerical data
[DE89-016674] N90-11520

SPRAYERS
Independent Orbiter Assessment (IOA): Analysis of the hydraulics/water spray boiler subsystem
[NASA-CR-185541] N90-10934

SPUTTERING
Ion implantation of two titanium alloys
[DE89-016958] N90-11133
CuInSe2 solar cell research by sputter deposition
[DE89-009450] N90-11345

STABILITY
Gas-accelerated plate stability study
[DE89-016880] N90-11289
Stability requirements of RF linac-driven free-electron lasers
[DE89-016609] N90-11303
An extension of Cochran's test for homogeneity of variances
[AD-A211054] N90-11534

STABILITY TESTS
A contribution to the stability analysis of large space structures N90-10997

STABILIZATION
Realization theoretic solution of two analytic matrix equations with applications to stabilization of infinite-dimensional systems
[AD-A211118] N90-11512

STAGE SEPARATION
Independent Orbiter Assessment (IOA): Analysis of the electrical power distribution and control subsystem, volume 1
[NASA-CR-185529-VOL-1] N90-10941
Computation of transient three-dimensional interstage flowfields using the arbitrary Lagrangian-Eulerian method N90-11253

STAGNATION PRESSURE
Jet-flow from shock tubes
[AD-A210651] N90-11260

STAINLESS STEELS
Grain boundary chemistry in irradiated stainless steel and its influence on environmental degradation
[DE89-016827] N90-11125
Compositional analysis of steels by X-ray fluorescence spectrometry
[DE89-630803] N90-11129

STANDARDIZATION
Response of standardized PVDF piezoelectric polymer gauges to direct shock pressures between 8 and 32 GPa
[DE89-016811] N90-11282

STANDARDS
Intrinsic damage and strength criteria for advanced composite laminates in space applications N90-11071

STANDING WAVES
Dynamics of nucleation at electrochemical interfaces via surface EXAFS and standing wave measurements
[AD-A210733] N90-11109

STAR FORMATION
UV observations of NGC 205
[NASA-CR-185975] N90-11661
The stability of magnetohydrodynamic shock waves in molecular clouds N90-11665
Gas dynamical processes in the theory of galaxy formation N90-11673

STATIC TESTS
Delamination tests under static compression loading N90-11061

STATISTICAL ANALYSIS
Analytical study of mistuning/friction/aerodynamics interaction in a bladed disk assembly
[AD-A211139] N90-10893
Development of an approximate technique for the nonlinear random vibrations analysis of hysteretic systems N90-11335
Joint VHF coherent radar and oblique sounder observations for short term ionosphere forecasting N90-11399
Spatial and temporal short range total cloud cover estimation by metric analysis of composite imagery N90-11423
Direct statistical thermal wind estimation procedure
[AD-A211256] N90-11433
Procedures for separations within batches of values, 1. The orderly tool kit and some heuristics
[AD-A210652] N90-11531
Boundary kernel estimation of the two sample comparison density function
[AD-A210757] N90-11532

STATISTICAL CORRELATION
New statistical approaches to galaxy clustering N90-11674

STATISTICAL DISTRIBUTIONS
Frequency distributions and hydroclimatic characteristics of heavy rainstorms in Illinois
[PB89-203988] N90-11427
Procedures for separations within batches of values, 1. The orderly tool kit and some heuristics
[AD-A210652] N90-11531

STATISTICAL MECHANICS
Theory of atomic spectral emission intensity
[IRF-PREPRINT-110] N90-11641

STATISTICAL TESTS
Comparison of sine dwell and broadband methods for modal testing N90-11025
Utilization of the generalized likelihood ratio test for the suppression of systematic errors in noisy systems
[ETN-89-94656] N90-11225
Two enhancements of the logarithmic least-squares method for analyzing subjective comparisons
[AD-A211192] N90-11514
An extension of Cochran's test for homogeneity of variances
[AD-A211054] N90-11534

STATORS
Dynamic analysis of rotors under interference rubs N90-11312

STEADY STATE
Stochastic optimization by simulation: Some experiments with a simple steady-state queue
[AD-A210762] N90-11508
STEADY STATE CREEP
Kinetics and mechanisms of primary and steady state creep in B- and Al-containing alpha silicon carbide
[AD-A210739] N90-11616
STEELS
Thin section casting program. Volume 1: Executive summary and overview
[DE89-009030] N90-11198
Thin section casting program. Volume 2: Horizontal TSC (Thin-Section Casting) approach
[DE89-009031] N90-11199
Thin section casting program. Volume 3: Vertical TSC (Thin-Section Casting) approach
[DE89-009033] N90-11201
Thin section casting program. Volume 4: Static cast product bending, straightening, and rolling
[DE89-009034] N90-11202
Thin section casting program. Volume 5: Westinghouse MHD Project
[DE89-009035] N90-11203
STEERING
Independent Orbiter Assessment (IOA): Analysis of the nose wheel steering subsystem
[NASA-CR-185548] N90-10921
Independent Orbiter Assessment (IOA): Analysis of the landing/deceleration subsystem
[NASA-CR-185569] N90-10943
Independent Orbiter Assessment (IOA): Assessment of the nose wheel steering subsystem
[NASA-CR-185533] N90-10947
Independent Orbiter Assessment (IOA): CIL issues resolution report, volume 2
[NASA-CR-185524-VOL-2] N90-10955
STELLAR COMPOSITION
The mass distribution in the galactic centre estimated from OH/IR stars
[PB89-154884] N90-11663
Mathematical method for the study and teaching of stellar and protostellar structure N90-11666
STELLAR EVOLUTION
IRAS observations of the extended galactic objects Cas A and W80 N90-11657
Mathematical method for the study and teaching of stellar and protostellar structure N90-11666
Effects of main-sequence mass loss on the turnoff ages of globular clusters
[DE89-016784] N90-11678
STELLAR MASS
The mass distribution in the galactic centre estimated from OH/IR stars
[PB89-154884] N90-11663
Effects of main-sequence mass loss on the turnoff ages of globular clusters
[DE89-016784] N90-11678
STELLAR PHYSICS
The mass distribution in the galactic centre estimated from OH/IR stars
[PB89-154884] N90-11663
STELLAR ROTATION
Phoebe: A preliminary control network and rotational elements
[NASA-CR-185716] N90-11680
STELLAR SPECTRA
The ratio to X-ray spectral shape and variability of blazars N90-11688
STELLAR STRUCTURE
Mathematical method for the study and teaching of stellar and protostellar structure N90-11666
STIFFENING
A new aspect for the use of thin walled beams as shell stiffeners of spacecraft structures N90-11046
STIFFNESS
Transverse shear stiffness of composite and sandwich finite elements N90-11034
STIFFNESS MATRIX
Parametric identification of conservative self adjoint structures N90-10994
On the equivalence of BS-stability and B-consistency
[CWI-NM-R8815] N90-11530
STIMULATION
Stimulus-response compatibility in spatial precuing and symbolic identification: Effects of coding practice, retention, and transfer
[AD-A210745] N90-11443
STIRLING CYCLE
Dynamic characteristics concerned in the design of a free-piston Stirling engine/magnetic coupling/compressor system
[DE89-015981] N90-11317
STIRLING ENGINES
An experimental investigation of transition in oscillating pipe flow N90-11249
Free-Piston Stirling Engine magnetically coupled heat pump: Critical component evaluation
[DE89-015646] N90-11316
Automotive Stirling engine development program
[NASA-CR-180839] N90-11654
STOCHASTIC PROCESSES
Performance and robustness of adaptive controllers for linear stochastic systems N90-11485
Stochastic optimization by simulation: Some experiments with a simple steady-state queue
[AD-A210762] N90-11508
Stochastic flows in networks
[AD-A211209] N90-11515
On some stochastic properties of the infinitely dimensional Hamiltonian systems of classical mechanics
[DE89-618403] N90-11525
STOKES FLOW
A conforming spectral collocation strategy for Stokes flow through a channel contraction
[NASA-CR-181912] N90-11495
STORAGE RINGS (PARTICLE ACCELERATORS)
X-ray lithography sources: A review
[DE89-017610] N90-11547
STORAGE TANKS
Fluid-structure interaction effects in tank structures due to sloshing and hydrodynamic ram: Coupled Lagangian-Eulerian simulations N90-11022
Modeling of liquid sloshing effects in multibody systems N90-11023
Hydrazine fate and transformation in natural waters and soils N90-11165
STRAIN ENERGY RELEASE RATE
Analysis of delamination growth N90-11036
STRAIN RATE
The HEL (Hugoniot Elastic Limit) and rate-dependent yield behavior
[DE89-016981] N90-11134
Characterizations of shock-loaded aluminum-infiltrated boron carbide cermets
[DE89-016773] N90-11146
An evaluation of the Chaboche and Bodner-Partom viscoplastic constitutive theories for strain rate sensitive materials N90-11330
Strain and density dependent valence-band masses in InGaAs/GaAs and GaAs/GaAsP strained-layer structures
[DE89-016882] N90-11627
STRATOSPHERE
Stratospheric ozone depletion
[PB89-207476] N90-11354
Two-Dimensional Intercomparison of Stratospheric Models
[NASA-CP-3042] N90-11405
Report on the 2-D Model Intercomparison Workshop held January 11-16, 1987 in Fort Myers Beach, Florida, chapter 2 N90-11406
Report of the 1988 2-D Intercomparison Workshop, chapter 3 N90-11407
Model documentation, chapter 4 N90-11408
Lidar observations of the stratospheric aerosol: Boulder, Colorado, 1985 to 1987
[PB89-203871] N90-11425
STREAK CAMERAS
Interferometry and high speed photography of laser-driven flyer plates
[DE89-016990] N90-11290
STREAM FUNCTIONS (FLUIDS)
A conforming spectral collocation strategy for Stokes flow through a channel contraction
[NASA-CR-181912] N90-11495
STRESS (PSYCHOLOGY)
Study of the behavioral and biological effects of high intensity 60 Hz electric fields
[DE89-015528] N90-11438
Computer programs for measuring variations in speech
[AD-A211126] N90-11467
STRESS ANALYSIS
Transverse shear stiffness of composite and sandwich finite elements N90-11034
Automated stress analysis of Shuttle orbiter thermal protection system N90-11043
Advances in instrumentation for experimental stress and vibration analysis and its applications N90-11069
Finite element analysis of cure-induced residual stress in composite materials N90-11084
Methodology of developing a combined environmental stress schedule for reliability growth testing
[AD-A211053] N90-11326
A finite element formulation for inelastic plates and shells based on a mixed variational principle N90-11334
Study of disorder and strain in semiconductor heterostructures and superlattices by Raman scattering N90-11601
STRESS CORROSION
Contribution to the transcrystalline stress crack corrosion of austenite chromium-nickel steels
[ETN-89-94665] N90-11137
STRESS CORROSION CRACKING
Grain boundary chemistry in irradiated stainless steel and its influence on environmental degradation
[DE89-016827] N90-11125
Deformation induced microstructural and microchemical changes during thermomechanical treatment
[DE89-017266] N90-11127
Failure modes and mechanisms in nickel alloys: Primarily austenitic stainless steel
[DE89-016823] N90-11132
Contribution to the transcrystalline stress crack corrosion of austenite chromium-nickel steels
[ETN-89-94665] N90-11137
STRESS CYCLES
Methodology of developing a combined environmental stress schedule for reliability growth testing
[AD-A211053] N90-11326
STRESS DISTRIBUTION
Multi-axis transient testing: Experimental investigations N90-11042
Three-dimensional analysis of surface crack-Hertzian stress field interaction
[NASA-CR-4254] N90-11332
STRESS INTENSITY FACTORS
A re-evaluation of fatigue threshold test procedures and the simulation and prediction of fatigue crack growth under conditions of low crack closure N90-11328
Three-dimensional analysis of surface crack-Hertzian stress field interaction
[NASA-CR-4254] N90-11332
STRESS MEASUREMENT
The Sandia standard for PVDF (Polyvinylidene Di-Fluoride) shock sensors
[DE89-016530] N90-11287
STRESS RELAXATION
Derivation of improved load transformation matrices for launchers-spacecraft coupled analysis, and direct computation of margins of safety N90-11077
The Meta-Lax method of stress reduction in welds
[DE89-016437] N90-11321
STRESS RELIEVING
Study of a gallium arsenide solar cell interconnector N90-11033
STRESSES
The HEL (Hugoniot Elastic Limit) and rate-dependent yield behavior
[DE89-016981] N90-11134
Impulse time-integral function and Lagrangian analysis
[DE89-016997] N90-11268
The Sandia standard for PVDF (Polyvinylidene Di-Fluoride) shock sensors
[DE89-016530] N90-11287
STRING THEORY
General covariance and strings
[DE89-016505] N90-11633
Three level constraints on conformal field theories and string models
[DE89-016942] N90-11634
STRINGS
General covariance and strings
[DE89-016505] N90-11633
STRONGLY COUPLED PLASMAS
Studies of a strongly coupled plasma produced in a capillary discharge
[DE89-016611] N90-11581
STRUCTURAL ANALYSIS
Spacecraft Structures and Mechanical Testing
[ESA-SP-289] N90-10986
Parametric identification of conservative self adjoint structures N90-10994
Overview of actual buckling calculation methods for space vehicle structures N90-10995
Theoretical and experimental investigation of thin-walled aluminum panels under cyclic shear load N90-10996
A contribution to the stability analysis of large space structures N90-10997
Adaptive structures to meet future requirements for large precision structures N90-11001
Acoustic response analysis in the low frequency domain N90-11010
Dynamic substructuring for modular analysis and testing N90-11015
Advances in design and testing of spacecraft structures N90-11018
Modal analysis of fluid-structure systems by parallel subspace iteration N90-11024
Modal analysis of space structures with the Ibrahim Time Domain method N90-11026
A direct two response approach for updating analytical dynamic models of structures with emphasis on uniqueness N90-11028

Thermal and structural analysis of Hermes N90-11058
Derivation of improved load transformation matrices for launchers-spacecraft coupled analysis, and direct computation of margins of safety N90-11077
Computational aspects of sensitivity calculations in linear transient structural analysis N90-11327
Development of an approximate technique for the nonlinear random vibrations analysis of hysteretic systems N90-11335
An analytical and experimental study of the elastodynamic response characteristics of planar linkage mechanism with bearing clearances N90-11336
New computing systems and their impact on structural analysis and design [NASA-CR-185831] N90-11457
Estimation on nonlinear damping in second order distributed parameter systems [NASA-CR-181890] N90-11494

STRUCTURAL DESIGN
Environmental testing: An approach to more cost efficiency N90-10988
Reduction of dynamic response of spacecraft structures and payloads N90-11000
Employment of modal survey methodologies in dynamic analysis procedures N90-11006
Integration of analytical and test software for optimal structural design under dynamic loads N90-11007
Experiences using a major FEM package interactively for spacecraft applications N90-11008
Advances in design and testing of spacecraft structures N90-11018
Development of the large spacecraft structure N90-11020
Ariane 5 structural design and development N90-11057
SDM challenges for space station N90-11059
Key structures mechanical issues of the European Space Station and platform program Columbus N90-11072
New computing systems and their impact on structural analysis and design [NASA-CR-185831] N90-11457
Aspects of the development of a 1-5 micron infrared camera for astronomy N90-11656

STRUCTURAL DESIGN CRITERIA
Evaluation of tests and design factors N90-10987
Transient tests for spacecraft structures N90-11040
Multi-axis transient testing: Experimental investigations N90-11042

STRUCTURAL ENGINEERING
Exploitation of data management facilities for finite element analysis in aerospace structural engineering applications N90-11078

STRUCTURAL MEMBERS
Structural problems of accurate inflatable surfaces N90-11044

STRUCTURAL RELIABILITY
Evaluation of tests and design factors N90-10987

STRUCTURAL STABILITY
Theoretical and experimental investigation of thin-walled aluminum panels under cyclic shear load N90-10996
A contribution to the stability analysis of large space structures N90-10997

STRUCTURAL STRAIN
Analysis of delamination growth N90-11036

STRUCTURAL VIBRATION
Thermoelastic behavior of large space structures: Modeling and control N90-11012
Evaluation of dispersive behavior in periodic structures by discrete Fourier transform N90-11014
Computational aspects of sensitivity calculations in linear transient structural analysis N90-11327
Development of an approximate technique for the nonlinear random vibrations analysis of hysteretic systems N90-11335
An analytical and experimental study of the elastodynamic response characteristics of planar linkage mechanism with bearing clearances N90-11336

STUDENTS
Higher education for science and technology: A background paper [PB89-191290] N90-11642

SUBMILLIMETER WAVES
Precision materials characterization in the near millimeter and submillimeter wavelength range [AD-A210655] N90-11106

SUBSONIC FLOW
Rectangular subsonic jet flow field measurements [NASA-CR-185962] N90-11255

SUBSTRUCTURES
Structural problems of accurate inflatable surfaces N90-11044

SUBZERO TEMPERATURE
Battery actuation of NITINOL at sub-zero temperatures [AD-A211254] N90-11237

SUDDEN IONOSPHERIC DISTURBANCES
User's guide to the Space Environment Services Center geophysical alert broadcasts [PB89-194617] N90-11411
Solar-geophysical data number 536, part 1. Data for March, Febuary 1989 and late data [PB89-194716] N90-11684

SUDDEN STORM COMMENCEMENTS
Solar-geophysical data number 536, part 1. Data for March, Febuary 1989 and late data [PB89-194716] N90-11684

SULFIDES
Fifth International Workshop on Glasses and Ceramics from Gels [DE89-016899] N90-11147

SULFUR DIOXIDES
Micrometeorological investigation of surface exchange of trace gases: A case study [PB89-208375] N90-11412

SULFUR FLUORIDES
Dissociation and vibrational relaxation of XeF by various collision partners [AD-A210769] N90-11300

SUNSPOTS
Solar-geophysical data number 537, part 1. Data for April, March 1989 and late data [PB89-207393] N90-11685

SUPERCOMPUTERS
An integrated distributed processing interface for supercomputers and workstations [DE89-016769] N90-11478

SUPERCONDUCTING MAGNETS
A solution to nonlinearity problems [DE89-016975] N90-11544
X-ray lithography sources: A review [DE89-017610] N90-11547
Propagation of normal zones of finite size in large, composite superconductors [DE89-016866] N90-11611

SUPERCONDUCTING SUPER COLLIDER
New tools for the simulation and design of calorimeters [DE89-016323] N90-11281

SUPERCONDUCTIVITY
Superconducting ceramics in the Bi1.5SrCaCu2O sub x system by melt quenching technique [NASA-CR-185139] N90-11606
Adaptation of the theory of superconductivity to the behavior of oxides [DE89-016518] N90-11608
Physics and materials science of high temperature superconductors [AD-A211246] N90-11619
Origins of high-temperature superconductivity in the new copper oxide based ceramic superconductors [DE89-016543] N90-11622
Effects of shock-modification on superconductivity in Tl2Ca2Ba2Cu3Oy and Bi2CaSr2Cu2Ox [DE89-017231] N90-11629
Neutron scattering experiments on high-temperature superconducting materials: Foreign trip report, September 13, 1988--October 4, 1988 [DE89-017451] N90-11630

SUPERCONDUCTORS
X-ray and gamma-ray spectroscopy of solids under pressure [DE89-017271] N90-11118
A study of the tribological and surface micromechanical properties of YBa2Cu3O7-x [DE89-015680] N90-11607
Propagation of normal zones of finite size in large, composite superconductors [DE89-016866] N90-11611
Rational design of high-current cable-in-conduit superconductors [DE89-016867] N90-11626

SUPERCOOLING
Remote sensing techniques of the Wave Propagation Laboratory for the measurement of supercooled liquid water: Applications to aircraft icing [PB89-208102] N90-10842

SUPERCRITICAL FLUIDS
Evaluation of supercritical cryogen storage and transfer systems for future NASA missions [NASA-TM-102394] N90-10912
Thermophysical properties of supercritical fluids and fluid mixtures [DE89-016568] N90-11102

SUPERHETERODYNE RECEIVERS
Calculation, optimization and comparison of optical transmission systems with superheterodyne reception [ETN-89-94651] N90-11224

SUPERHIGH FREQUENCIES
The effectiveness of adaptive PRF (Pulse Repetition Frequency) selection in minimizing range obscuration in the TDWR (Terminal Doppler Weather Radar) system [AD-A211267] N90-11222

SUPERLATTICES
Intergranular and interphase boundaries in ceramics [DE89-016969] N90-11154
Adaptation of the theory of superconductivity to the behavior of oxides [DE89-016518] N90-11608
Strain and density dependent valence-band masses in InGaAs/GaAs and GaAs/GaAsP strained-layer structures [DE89-016882] N90-11627

SUPERNOVA REMNANTS
IRAS observations of the extended galactic objects Cas A and W80 N90-11657

SUPERNOVAE
The interaction of supernovae and pulsars with the circumstellar environment N90-11671

SUPERSONIC FLOW
A parallel numerical simulation for supersonic flows using zonal overlapped grids and local time steps for common and distributed memory multiprocessors [DE89-015252] N90-10839

SUPERSYMMETRY
Superfiled formulation of Chern-Simons supersymmetry [DE89-018459] N90-11636

SUPPORT SYSTEMS
Wideband connectivity and support for Cronus cluster at USAF Electronic Systems Division [AD-A210749] N90-11215
Considerations for a design and operations knowledge support system for Space Station Freedom [NASA-TM-102156] N90-11451

SURFACE CRACKS
Definition of research needs to address airport pavement distress in cold regions [DOT/FAA/DS-89/13] N90-10896
Three-dimensional analysis of surface crack-Hertzian stress field interaction [NASA-CR-4254] N90-11332

SURFACE DEFECTS
Structural problems of accurate inflatable surfaces N90-11044

SURFACE NAVIGATION
Federal Radionavigation Plan, 1988 [PB89-163075] N90-10846

SURFACE PROPERTIES
Reactive ion etching of SiC thin films by mixtures of fluorinated gases and oxygen [AD-A211046] N90-11113
A study of the tribological and surface micromechanical properties of YBa2Cu3O7-x [DE89-015680] N90-11607

SURFACE REACTIONS
Dynamics of nucleation at electrochemical interfaces via surface EXAFS and standing wave measurements [AD-A210733] N90-11109
Surface-catalyzed air oxidation of hydrazines: Environmental chamber studies N90-11159
Vibrational spectroscopic study of the kaolinite-hydrazine intercalation complex N90-11166
Surface-catalyzed air oxidation reactions of hydrazines: Tubular reactor studies N90-11167
A diffuse reflectance infrared Fourier transform spectroscopic study of adsorbed hydrazines N90-11170

SURFACE ROUGHNESS
Numerical solutions of turbulent flow with heat transfer over rough surfaces N90-11246

SURFACE TO AIR MISSILES
Laser techniques for ground to air applications [FOA-C-30524-3.1] N90-11309

SURFACE VEHICLES
Land vehicle teleoperation under conditions of reduced video resolution [DE89-016925] N90-11324

SURFACE WAVES
Dynamics of nucleation at electrochemical interfaces via surface EXAFS and standing wave measurements [AD-A210733] N90-11109

SURVEILLANCE
Fiber optic technique for surveillance and control of mine fields [FOA-C-30526-3.1] N90-11293
The Swedish defense research needs: For surveillance and seeker applications [FOA-C-30520-3.3] N90-11691

SURVEYS
Laser anemometer measurements in a transonic axial-flow fan rotor [NASA-TP-2879] N90-11245

SWITCHES
Independent Orbiter Assessment (IOA): Analysis of the backup flight system
[NASA-CR-185567] N90-10932
ANTHEM simulation of plasma opening switches
[DE89-016617] N90-11239
SWITCHING CIRCUITS
A contribution to the synthesis of communication switching systems with decentralized control using modular components
[ETN-89-94660] N90-11226
Pulsed-power switching for inertial confinement fusion with light ion beams
[DE89-016810] N90-11595
Launched electrons in plasma opening switches
[DE89-016886] N90-11596
SYMBIOSIS
Computer symbiosis: Emergence of symbiotic behavior through evolution
[DE89-015247] N90-11450
SYMBOLS
Stimulus-response compatibility in spatial precuing and symbolic identification: Effects of coding practice, retention, and transfer
[AD-A210745] N90-11443
SYMMETRY
Moduli spaces and topological quantum field theories
[DE89-016943] N90-11639
SYNCHRONISM
Synchrony with empty process — the algebra of synchronous processes
[CWI-CS-R8832] N90-11481
Asynchronous integration of ordinary differential equations on multiprocessors
[DE89-014169] N90-11493
SYNCHROTRON RADIATION
Research in X-ray optics with the ultimate aim of constructing a synchrotron radiation pumped soft X-ray lithium laser
[DE89-016788] N90-11304
Synchrotron radiation, free electron laser, and nuclear structure
[DE89-017352] N90-11306
X-ray lithography sources: A review
[DE89-017610] N90-11547
SYNCHROTRONS
A solution to nonlinearity problems
[DE89-016975] N90-11544
SYNTHETIC APERTURE RADAR
The development of mission-specific advanced inertially-based avionics system N90-10851
A high precision gravity compensation system for the deployment test of the ERS-1 SAR antenna N90-11038
Simulation of synthetic aperture radar 1: Feature density and accuracy requirements
[AD-A211019] N90-11218
SYSTEM EFFECTIVENESS
Air Combat Environment Test and Evaluation Facility (ACETEF) N90-10683
SYSTEM FAILURES
Independent Orbiter Assessment (IOA): FMEA/CIL assessment
[NASA-CR-185589] N90-10960
Independent Orbiter Assessment (IOA): Assessment of the body flap subsystem FMEA/CIL
[NASA-CR-185575] N90-10968
Independent Orbiter Assessment (IOA): Assessment of the elevon actuator subsystem FMEA/CIL
[NASA-CR-185578] N90-10970
SYSTEMS ANALYSIS
Modal analysis of fluid-structure systems by parallel subspace iteration N90-11024
Comparison of phase resonance, mode separation, and driven-base modal identification methods applied to the FLECS test structure N90-11027
New data handling system (MDH) for mechanical tests at ESTEC N90-11066
Laser dynamics: The system dynamics and network theory of optoelectronic integrated circuit design N90-11296
Systems analysis considerations in artificial intelligence/expert systems technology applications
[DE89-016847] N90-11490
A survey of research methods to study design
[AD-A211213] N90-11491
SYSTEMS ENGINEERING
Kalman Filter Integration of Modern Guidance and Navigation Systems
[AGARD-LS-166] N90-10847
Design of a Kalman filter for transfer alignment N90-10848
Development of the integrated all-weather navigation system for Tornado N90-10849
A high performance airborne INS/GPS Integrated Navigation System N90-10850
The development of mission-specific advanced inertially-based avionics system N90-10851
Flight Test Techniques
[AGARD-CP-452] N90-10860
Flight test techniques adopted by Avions Marcel Dassault-Breguet Aviation N90-10867
Identification Friend, Foe or Neutral Joint Test N90-10881
On the development of a basic flight test capability and some related research projects N90-10885
Independent Orbiter Assessment (IOA): FMEA/CIL assessment
[NASA-CR-185589] N90-10960
The third generation rigid solar array GSR3 N90-11017
Dynamic characteristics concerned in the design of a free-piston Stirling engine/magnetic coupling/compressor system
[DE89-015961] N90-11317
Methodology of developing a combined environmental stress schedule for reliability growth testing
[AD-A211053] N90-11326
Considerations for a design and operations knowledge support system for Space Station Freedom
[NASA-TM-102156] N90-11451
Engineering specification and system design for CAD/CAM of custom shoes. Phase 5: UMC involvement (January 1, 1989 - June 30, 1989)
[NASA-CR-185838] N90-11456
A survey of research methods to study design
[AD-A211213] N90-11491
SYSTEMS INTEGRATION
Kalman Filter Integration of Modern Guidance and Navigation Systems
[AGARD-LS-166] N90-10847
A high performance airborne INS/GPS Integrated Navigation System N90-10850
The development of mission-specific advanced inertially-based avionics system N90-10851
Development of a marine integrated navigation system N90-10852
Flight Test Techniques
[AGARD-CP-452] N90-10860
Real-time flight test analysis and display techniques for the X-29A aircraft N90-10866
Flight test techniques adopted by Avions Marcel Dassault-Breguet Aviation N90-10867
Lessons learned from the integration of flight systems N90-10874
Planning for hybrid-cycle OTEC experiments using the HMTSTA test facility at the Natural Energy Laboratory of Hawaii
[DE89-013278] N90-11349
SYSTEMS SIMULATION
A super element for multibody dynamics N90-11004
Induced shock loads during the separation of the Ariane 5 VEB structure N90-11045
MSP: Modeling of concurrent processes. Version 1.00 General introduction and directions for use
[REPT-88-88] N90-11477

T

TABULATION PROCESSES
Gridded environmental data compaction: An investigation
[AD-A210580] N90-11430
TAIL ASSEMBLIES
Measurements of pressures on the tail and aft fuselage of an airplane model during rotary motions at spin attitudes
[NASA-TP-2939] N90-10829
TANTALUM
Exploratory study of niobium, titanium, zirconium and tantalum aluminides
[AD-A210658] N90-11615
TARGET ACQUISITION
Adaptive tracking of maneuvering targets based on IR image data N90-10853
TARGETS
Evaluation of integrals related to the Debye function
[DE89-016930] N90-11499
Acceleration of thin foil targets using fiber-coupled optical pulses
[DE89-016526] N90-11569
TATB
Shock initiation of LX-17 as a function of its initial temperature
[DE89-017730] N90-11192
TAYLOR SERIES
The fast Gauss transform
[AD-A211287] N90-11517
TECHNICAL WRITING
Technical communications in aeronautics: Results of an exploratory study. An analysis of managers' and nonmanagers' responses
[NASA-TM-101625] N90-11647
Planning in writing: The cognition of a constructive process
[AD-A210434] N90-11648
TECHNOLOGY ASSESSMENT
Advanced Turbine Technology Applications Program, (ATTAP)
[DE89-016067] N90-11318
TECHNOLOGY TRANSFER
Toward a national research network
[PB89-198709] N90-11644
Globalization of Technology: International Perspectives. Proceedings of the 6th Convocation of the Council of Academies of Engineering and Technological Sciences
[PB89-198840] N90-11645
Technology applications bulletins
[DE89-017454] N90-11651
The transfer and diffusion of new technologies: A review of the economics literature
[DE89-015671] N90-11655
TECHNOLOGY UTILIZATION
Advanced Turbine Technology Applications Program, (ATTAP)
[DE89-016067] N90-11318
Systems analysis considerations in artificial intelligence/expert systems technology applications
[DE89-016847] N90-11490
Globalization of Technology: International Perspectives. Proceedings of the 6th Convocation of the Council of Academies of Engineering and Technological Sciences
[PB89-198840] N90-11645
Technology applications bulletins
[DE89-017454] N90-11651
TELECOMMUNICATION
Deep null antennas and their applications to tactical VHF radio communications
[AD-A210656] N90-11214
TELEMETRY
Analysis of flutter tests with the use of a telemetry system N90-10871
Flight test instrumentation and data processing at British Aerospace, Warton, U.K. N90-10887
TELEOPERATORS
NASA/NBS (National Aeronautics and Space Administration/National Bureau of Standards) standard reference model for telerobot control system architecture (NASREM)
[NASA-CR-185078] N90-11310
Land vehicle teleoperation under conditions of reduced video resolution
[DE89-016925] N90-11324
Telescience Testbed Pilot Program
[NASA-CR-184594] N90-11455
TELESCOPES
A liquid xenon imaging telescope for 1-30 MeV gamma-ray astrophysics
[NASA-CR-185999] N90-11662
TELEVISION SYSTEMS
HDTV displays: Subjective effects of scanning standards and domestic picture sizes
[BBC-RD-1989/9] N90-11208
TEMPERATURE CONTROL
Independent Orbiter Assessment (IOA): Analysis of the electrical power distribution and control/electrical power generation subsystem
[NASA-CR-185538] N90-10933
Independent Orbiter Assessment (IOA): CIL issues resolution report, volume 1
[NASA-CR-185524-VOL-1] N90-10954
Independent Orbiter Assessment (IOA): Assessment of the active thermal control system
[NASA-CR-185573] N90-10979
TEMPERATURE DEPENDENCE
Theoretical Hugoniot of liquid hydrogen fluoride
[DE89-016504] N90-11099
Thermal expansion and phase transformation studies on some materials by high temperature X-ray powder diffractometry
[DE89-631032] N90-11130
TEMPERATURE EFFECTS
Accelerated aging of metal matrix composites N90-11085
Effect of thermal and cyclic loads on silicon carbide yarn reinforced glass matrix composites
[DE89-016554] N90-11091
Shock initiation of LX-17 as a function of its initial temperature
[DE89-017730] N90-11192
Efficient numerical method for computation of thermohydrodynamics of laminar lubricating films
[NASA-CR-185136] N90-11256

Interannual variability of temperature in the upper layer of the North Pacific eastern boundary region, 1971-1987 [PB89-190227] N90-11434
Hydrogen-assisted thermal donor formation in silicon [DE89-016809] N90-11594
Superconducting ceramics in the Bi1.5SrCaCu2O sub x system by melt quenching technique [NASA-CR-185139] N90-11606

TEMPERATURE GRADIENTS
Ion temperature gradient instability [DE89-016574] N90-11580

TEMPERATURE MEASUREMENT
NIST (National Institute of Standards and Technology) measurement services: The calibration of thermocouples and thermocouple materials [PB89-209340] N90-11274
A remote sensor to monitor combustion products using a tunable acousto-optic filter N90-11275

TEMPERATURE PROBES
NIST (National Institute of Standards and Technology) measurement services: The calibration of thermocouples and thermocouple materials [PB89-209340] N90-11274

TEMPERATURE PROFILES
Direct statistical thermal wind estimation procedure [AD-A211256] N90-11433

TEMPERATURE SENSORS
Independent Orbiter Assessment (IOA): Assessment of the Orbiter Experiment (OEX) subsystem [NASA-CR-185587] N90-10962

TEMPORAL DISTRIBUTION
Spatial and temporal short range total cloud cover estimation by metric analysis of composite imagery N90-11423

TEMPORAL RESOLUTION
Land vehicle teleoperation under conditions of reduced video resolution [DE89-016925] N90-11324

TENSILE TESTS
Influence of the fiber/matrix interface on damage development in CFRP N90-11037
Worked-in holes in three-dimensional reinforced composites N90-11060

TENSOR ANALYSIS
Nonlinear adjustment with or without constraints, applicable to geodetic models [AD-A210820] N90-11509

TERNARY SYSTEMS
Design and construction of systems for the single-crystals growth of ternary silver halides, alkali halides, and alkaline earth fluorides, and the dielectric investigation of silver halide [ETN-89-94673] N90-11632

TERRAIN
Thermal radiation from terrain: Measurements and first results [FOA-C-30525-3.1] N90-11342
Diagnostic study of atmosphere-terrain interaction leading to the formation of dust clouds and poor visibilities over near east desert areas [AD-A211243] N90-11358

TERRAIN ANALYSIS
Flight testing of the Tornado Terrain Following System N90-10875

TEST CHAMBERS
The Environmental Test Centre at ESTEC (an overview) N90-11064
An atmospheric pressure flow reactor: Gas phase kinetics and mechanism in tropospheric conditions without wall effects N90-11160
The behavior of hydrazine vapor in an environmental chamber under simulated atmospheric conditions N90-11161
Modeling of hydrazine surface interactions in environmental reaction chambers N90-11162
Surface-catalyzed air oxidation reactions of hydrazines: Tubular reactor studies N90-11167

TEST FACILITIES
US Navy principal site testing concept and the F-18 N90-10861
The Air Force Flight Test Center Flight Test Safety Program N90-10872
Air Combat Environment Test and Evaluation Facility (ACETEF) N90-10883
Flight simulation test facility: Function and specification of the simulator cockpit system [NAL-TM-577] N90-10899
Research and test facilities for development of technologies and experiments with commercial applications [NASA-TM-101789] N90-10909
Spacecraft Structures and Mechanical Testing [ESA-SP-289] N90-10986
Comparison of phase resonance, mode separation, and driven-base modal identification methods applied to the FLECS test structure N90-11027
Development of a thermoacoustic test facility N90-11041
Space environment effects on carbon/epoxy materials N90-11058
The Environmental Test Centre at ESTEC (an overview) N90-11064
Two years experience with the ESTEC multishaker system N90-11065
New data handling system (MDH) for mechanical tests at ESTEC N90-11066
The large European Acoustic Facility at ESTEC N90-11067
Tamaris: A new European facility for low frequency multi-axis vibration simulation N90-11068
A new European vibration test facility for Ariane 4 class satellites N90-11070

TETHERED SATELLITES
Aeritalia Space Systems Group, Turin, Italy [EOARD-LR-89-041] N90-10908

THEOREM PROVING
Parallel inference based on delta processing [CWI-CS-R8846] N90-11482

THEORETICAL PHYSICS
Theoretical atomic physics for fusion [DE89-017363] N90-11563

THERMAL ABSORPTION
Radiationless transitions and excited-state absorption of low-field chromium complexes in solids [AD-A210653] N90-11105

THERMAL ANALYSIS
Thermal and structural analysis of Hermes N90-11058
Low temperature processing of reaction sintered silicon nitride [DE89-017455] N90-11092

THERMAL CONDUCTIVITY
On the effective transport properties of composite materials N90-11086

THERMAL CONDUCTIVITY GAGES
Interlaboratory comparison of two types of line-source thermal-conductivity apparatus measuring five insulating materials [PB89-218325] N90-11142

THERMAL CONDUCTORS
Radiative shocks with electron thermal conduction N90-11670

THERMAL CONTROL COATINGS
Heat transfer to throat tubes in a square-chambered rocket engine at the NASA Lewis Research Center [NASA-TM-102336] N90-11082

THERMAL DIFFUSION
Quasi-diffusion between phonon and roton gases in two- and three-dimensional liquid helium [AD-A210565] N90-11096

THERMAL DIFFUSIVITY
A study of runaway electron confinement and theory of neoclassical MHD turbulence [DE89-016728] N90-11584

THERMAL EXPANSION
Thermal expansion and phase transformation studies on some materials by high temperature X-ray powder diffractometry [DE89-631032] N90-11130

THERMAL MAPPING
Thermal radiation from terrain: Measurements and first results [FOA-C-30525-3.1] N90-11342

THERMAL PROTECTION
Automated stress analysis of Shuttle orbiter thermal protection system N90-11043
Thermal and structural analysis of Hermes N90-11058

THERMAL RADIATION
Thermal radiation from terrain: Measurements and first results [FOA-C-30525-3.1] N90-11342

THERMAL STABILITY
The thermal stability between rotating cylinders in a radially symmetrical gravitational field [DE89-618548] N90-11638

THERMITES
Thermochemical model for shock-induced chemical reactions in porous thermite: The heat detonation model [DE89-016528] N90-11100

THERMOCHEMISTRY
A thermochemical analysis of proposed working fluids for electrothermal guns [AD-A210661] N90-10910
Hydrogen-silicon carbide interactions [NASA-TM-102382] N90-11144
Thermodynamic principles of the process of the effect of electromagnetic fields on a polymer melt [AD-A210698] N90-11149

THERMOCOUPLES
NIST (National Institute of Standards and Technology) measurement services: The calibration of thermocouples and thermocouple materials [PB89-209340] N90-11274
Using self-calibrating thermocouples in industry [DE89-013539] N90-11278

THERMODYNAMIC EQUILIBRIUM
Balance equations for ionospheric plasmas with different partial temperatures N90-11364

THERMODYNAMIC PROPERTIES
Interlaboratory comparison of two types of line-source thermal-conductivity apparatus measuring five insulating materials [PB89-218325] N90-11142
Consequence of condensed-phase formation in transient burning of TiHx/KClO in a closed system [DE89-013922] N90-11188
Efficient numerical method for computation of thermohydrodynamics of laminar lubricating films [NASA-CR-185136] N90-11256
Direct statistical thermal wind estimation procedure [AD-A211256] N90-11433
Physics and materials science of high temperature superconductors [AD-A211246] N90-11619

THERMODYNAMICS
Solidification front/viscous phase transitions, forward-backward heat equations [AD-A211068] N90-11114
Thermodynamic principles of the process of the effect of electromagnetic fields on a polymer melt [AD-A210698] N90-11149
A shock initiation model for fine-grained hexanitrostilbene [DE89-007641] N90-11185
Thermodynamics, kinetics, and interface morphologies of phase formation reactions between metals and Gallium Arsenide: Bulk vs thin-film studies [DE89-016469] N90-11621

THERMOELASTICITY
Thermoelastic behavior of large space structures: Modeling and control N90-11012

THERMOELECTRICITY
A thermochemical analysis of proposed working fluids for electrothermal guns [AD-A210661] N90-10910

THERMOMECHANICAL TREATMENT
Deformation induced microstructural and microchemical changes during thermomechanical treatment [DE89-017266] N90-11127

THERMOPHYSICAL PROPERTIES
Finite element analysis of cure-induced residual stress in composite materials N90-11084
Low temperature properties of glasses N90-11141
Interlaboratory comparison of two types of line-source thermal-conductivity apparatus measuring five insulating materials [PB89-218325] N90-11142

THERMOPLASTIC RESINS
Interfacial adsorption and crystallization of polycarbonate in carbon fiber composites [AD-A211230] N90-11090

THERMOSETTING RESINS
Study of the application of automation to composites manufacture [AD-A211049] N90-11087

THERMOSPHERE
Seasonal and geomagnetic response of the thermosphere and ionosphere N90-11380
Ionosphere-thermosphere coupling at high latitudes: Aspect angle dependence of non-thermal plasmas N90-11382
Calculation of the temperature and velocity vector of the neutral gas using EISCAT CP3-data N90-11384

THIN FILMS
Reactive ion etching of SiC thin films by mixtures of fluorinated gases and oxygen [AD-A211046] N90-11113
Capacitive behavior in conducting polymers: The ac impedance and quartz crystal microbalance studies [AD-A210754] N90-11150
Cell performance of ultra-thin polymer cathode system: Theoretical energy and power density projections [AD-A210786] N90-11151
Intergranular and interphase boundaries in ceramics [DE89-016969] N90-11154
Efficient numerical method for computation of thermohydrodynamics of laminar lubricating films [NASA-CR-185136] N90-11256
CuInSe2 solar cell research by sputter deposition [DE89-009450] N90-11345
Proceedings of the Polycrystalline Thin Film Program Meeting [DE89-009457] N90-11348

Diamondlike carbon coatings for optical systems
[AD-A211255] N90-11573
Novel thin-film CuInSe2 fabrication
[DE89-009440] N90-11604
Physics and materials science of high temperature superconductors
[AD-A211246] N90-11619
Thermodynamics, kinetics, and interface morphologies of phase formation reactions between metals and Gallium Arsenide: Bulk vs thin-film studies
[DE89-016469] N90-11621

THIN WALLED SHELLS
Theoretical and experimental investigation of thin-walled aluminum panels under cyclic shear load N90-10996
Equilibrium and stability in composite thin shell N90-10998

THIN WALLS
A new aspect for the use of thin walled beams as shell stiffeners of spacecraft structures N90-11046

THREE DIMENSIONAL COMPOSITES
Worked-in holes in three-dimensional reinforced composites N90-11060

THREE DIMENSIONAL FLOW
A computational/experimental study of the flow around a body of revolution at angle of attack
[NASA-TM-88329] N90-11254

THREE DIMENSIONAL MODELS
The 3D-POLY: A robot vision system for recognizing objects in occluded environments N90-11313
Modelling ionospheric density structures N90-11375

THROATS
Heat transfer to throat tubes in a square-chambered rocket engine at the NASA Lewis Research Center
[NASA-TM-102336] N90-11082

THRUST VECTOR CONTROL
Independent Orbiter Assessment (IOA): Analysis of the ascent thrust vector control actuator subsystem
[NASA-CR-185579] N90-10929
Independent Orbiter Assessment (IOA): Assessment of the ascent thrust vector control actuator subsystem FMEA/CIL
[NASA-CR-185590] N90-10959

TILES
Automated stress analysis of Shuttle orbiter thermal protection system N90-11043

TIME DEPENDENCE
An assessment of robustness of flight control systems based on variable structure techniques N90-10895
Studies of time-dependent polar cap convection patterns N90-11421

TIME MARCHING
A parallel numerical simulation for supersonic flows using zonal overlapped grids and local time steps for common and distributed memory multiprocessors
[DE89-015252] N90-10839

TIME SERIES ANALYSIS
Are ozone exceedance rates decreasing. Comment on extreme value analysis of environmental time-series: An application to trend detection in ground-level ozone
[AD-A211029] N90-11357
Task analysis of the UH-60 mission and decision rules for developing a UH-60 workload prediction model. Volume 1: Summary report
[AD-A210763] N90-11446

TIMOSHENKO BEAMS
Wave-mode coordinate analysis of L junction in LSS
[AD-A211116] N90-10984
A new aspect for the use of thin walled beams as shell stiffeners of spacecraft structures N90-11046
An improved beam model for the vibrations of rotor blades N90-11333

TIN COMPOUNDS
Photochemically-driven biomimetic oxidation of alkanes and olefins
[DE89-011536] N90-11097

TITANIUM
Powder morphology effects in the ignition of titanium-based pyrotechnics
[DE89-017229] N90-11191
Exploratory study of niobium, titanium, zirconium and tantalum aluminides
[AD-A210658] N90-11615

TITANIUM ALLOYS
Ion implantation of two titanium alloys
[DE89-016958] N90-11133

TITANIUM CARBIDES
Investigation of commercial Al-Ti and Al-Ti-B master alloys and development of a new grain refining agent based on carbides for aluminum and aluminum alloys
[ETN-89-94663] N90-11136

TITANIUM COMPOUNDS
Consequence of condensed-phase formation in transient burning of TiHx/KClO in a closed system
[DE89-013922] N90-11188
Lithium polymer electrolyte battery, electrochemical behavior of cathode materials
[AD-A210755] N90-11235

TITANIUM OXIDES
Basic research on processing of ceramics for space structures
[AD-A205954] N90-11139

TOKAMAK DEVICES
Theory of high-n toroidicity-induced shear Alfven eigenmode in tokamaks
[DE89-016726] N90-11582
A study of runaway electron confinement and theory of neoclassical MHD turbulence
[DE89-016728] N90-11584
Projections for a steady-state tokamak reactor based on ITER
[DE89-016678] N90-11589

TOLERANCES (MECHANICS)
Adaptive structures to meet future requirements for large precision structures N90-11001

TOLERANCES (PHYSIOLOGY)
Evaluation of rocket motor exhaust and liner combustion by-products
[AD-A210747] N90-11083

TOPOGRAPHY
Topographic map reading
[AD-A211269] N90-11340
The astronomy of Andean myth: The history of a cosmology N90-11660

TOPOLOGY
General action for topological quantum field theories
[DE89-018460] N90-11637
Moduli spaces and topological quantum field theories
[DE89-016943] N90-11639

TOROIDAL PLASMAS
Theory of high-n toroidicity-induced shear Alfven eigenmode in tokamaks
[DE89-016726] N90-11582
Particle simulation in curvilinear coordinate systems
[DE89-016727] N90-11583
Compact torus configurations with high frequency driven currents
[ETN-89-94674] N90-11598

TOROIDAL WHEELS
Structural problems of accurate inflatable surfaces N90-11044

TOXIC HAZARDS
The Third Conference on the Environmental Chemistry of Hydrazine Fuels
[AD-A197632] N90-11157
The soil microbiology of hydrazines N90-11171
Fuel neutralization by ozone oxidation N90-11176
Low ppb level detection of toxic compounds with a fully automated CO2 laser photoacoustic detector N90-11181
Occupational safety considerations with hydrazine N90-11182

TOXICITY
A matrix-isolation FT-IR study of hydrazine N90-11168

TRACE CONTAMINANTS
Potential effects of global climate change on the United States. Volume 1: Regional studies. Draft
[PB89-161053] N90-11351

TRACE ELEMENTS
Micrometeorological investigation of surface exchange of trace gases: A case study
[PB89-208375] N90-11412

TRACKING (POSITION)
Kalman Filter Integration of Modern Guidance and Navigation Systems
[AGARD-LS-166] N90-10847
Adaptive tracking of maneuvering targets based on IR image data N90-10853
Passive trajectography by azimuth: Improvement of estimation quality N90-10854
Independent Orbiter Assessment (IOA): Analysis of the communication and tracking subsystem
[NASA-CR-185582] N90-10967
Analysis of forest fire smoke using satellite imagery
[AD-A210657] N90-11339

TRACKING PROBLEM
Passive trajectography by azimuth: Improvement of estimation quality N90-10854

TRAFFIC
Linkoeping's A.I. Consortium (LAIC) for plan guided systems. Review of the first 18 months
[FOA-C-30528-3.4] N90-11537

TRAINING ANALYSIS
Higher education for science and technology: A background paper
[PB89-191290] N90-11642

TRAINING EVALUATION
Higher education for science and technology: A background paper
[PB89-191290] N90-11642

TRAJECTORIES
Passive trajectography by azimuth: Improvement of estimation quality N90-10854
Optimal and on-board near-optimal midcourse guidance N90-10857

TRAJECTORY OPTIMIZATION
Nonlinear maneuver autopilot for the F-15 aircraft
[NASA-CR-179442] N90-11487

TRANSFER FUNCTIONS
Transfer functions for nonlinear systems via Fourier-Borel transforms
[NASA-TM-100034] N90-10828

TRANSFORMATIONS (MATHEMATICS)
The fast Gauss transform
[AD-A211287] N90-11517

TRANSFORMERS
Electron beam welding: Model of high voltage bias transmission line and termination circuits
[DE89-016900] N90-11323

TRANSIENT LOADS
Transient tests for spacecraft structures N90-11040
Multi-axis transient testing: Experimental investigations N90-11042

TRANSITION PRESSURE
Radiationless transitions and excited-state absorption of low-field chromium complexes in solids
[AD-A210653] N90-11105

TRANSITION TEMPERATURE
Studies of novel superconductors
[DE89-016744] N90-11609

TRANSMISSION CIRCUITS
Electron beam welding: Model of high voltage bias transmission line and termination circuits
[DE89-016900] N90-11323

TRANSMISSION LINES
Electron beam welding: Model of high voltage bias transmission line and termination circuits
[DE89-016900] N90-11323
Rational design of high-current cable-in-conduit superconductors
[DE89-016867] N90-11626

TRANSMITTERS
Ionospheric limitations to the accuracy of SSL estimates of HF transmitter locations N90-11403

TRANSONIC FLOW
Laser anemometer measurements in a transonic axial-flow fan rotor
[NASA-TP-2879] N90-11245

TRANSONIC SPEED
On transonic flow over segmented slotted wind tunnel wall with mass transfer N90-11676

TRANSPARENCE
Basic investigations of cutting machinability of inorganic glasses using single-point tools
[W-15/87] N90-11204

TRANSPORT PROPERTIES
On the effective transport properties of composite materials N90-11086
Transport studies of conducting polymers N90-11140
Electronic and ionic transport in polymers
[AD-A210654] N90-11148
Capacitive behavior in conducting polymers: The ac impedance and quartz crystal microbalance studies
[AD-A210754] N90-11150
Numerical simulation of hydrazine transport in a sandy soil N90-11172
New secondary batteries utilizing electronically conductive polymer cathodes
[NASA-CR-185885] N90-11227
A solution to nonlinearity problems
[DE89-016975] N90-11544
Transport properties of thermally grown Cr2O3
[DE89-016703] N90-11623

TRAPPED PARTICLES
Hybrid particle-fluid approach to low-frequency turbulence in magnetically confined plasmas
[DE89-015904] N90-11579

TRAVELING WAVE AMPLIFIERS
A brief description of traveling wave tubes
[FOA-C-30522-3.6] N90-11244

TRAVELING WAVE TUBES
A brief description of traveling wave tubes
[FOA-C-30522-3.6] N90-11244

TRAVELING WAVES
Atmospheric gravity waves in the auroral source region of TIDs, studied with the EISCAT CP2-data N90-11387

TRENDS
Are ozone exceedance rates decreasing. Comment on extreme value analysis of environmental time-series: An application to trend detection in ground-level ozone
[AD-A211029] N90-11357

TRIANGULATION
Applications of artificial intelligence to digital photogrammetry N90-11486

TRIBOLOGY
A study of the tribological and surface micromechanical properties of YBa2Cu3O7-x
[DE89-015680] N90-11607
TRINITROTOLUENE
Carbon in detonations
[DE89-016037] N90-11189
TROPICAL METEOROLOGY
Hurricane Research Division fiscal year 1988 programs, fiscal year 1989 projections
[PB89-152268] N90-11418
TROPICAL REGIONS
North-south tropical F2 layer asymmetry at west AFrican and Pacific longitudes N90-11398
TROPICAL STORMS
Hurricane Research Division fiscal year 1988 programs, fiscal year 1989 projections
[PB89-152268] N90-11418
TROPOSPHERE
An atmospheric pressure flow reactor: Gas phase kinetics and mechanism in tropospheric conditions without wall effects N90-11160
TRUSSES
Test results on conceptual models of the large deployable antenna for mobile communications satellites N90-11050
TUNGSTEN ALLOYS
Freeze-dried processing of tungsten heavy alloys
[DE89-015171] N90-11122
TUNING
Analytical study of mistuning/friction/aerodynamics interaction in a bladed disk assembly
[AD-A211139] N90-10893
TURBINE BLADES
Analytical study of mistuning/friction/aerodynamics interaction in a bladed disk assembly
[AD-A211139] N90-10893
Heat transfer to throat tubes in a square-chambered rocket engine at the NASA Lewis Research Center
[NASA-TM-102336] N90-11082
TURBINE WHEELS
Advanced technologies impact on compressor design and development: A perspective
[NASA-TM-102341] N90-10891
Independent Orbiter Assessment (IOA): Weibull analysis report
[NASA-CR-185534] N90-10948
TURBINES
Advanced Turbine Technology Applications Program, (ATTAP)
[DE89-016067] N90-11318
TURBOCOMPRESSORS
Dynamic analysis of rotors under interference rubs N90-11312
TURBOFAN ENGINES
Advanced technologies impact on compressor design and development: A perspective
[NASA-TM-102341] N90-10891
TURBOPROP AIRCRAFT
P-180 AVANTI: Project and flight test program comprehensive overview N90-10863
TURBULENCE EFFECTS
Turbulence effects for retroreflection
[FOA-C-30523-3.1] N90-11575
TURBULENT BOUNDARY LAYER
Wall-layer eruptions in turbulent flows
[NASA-TM-102362] N90-11250
TURBULENT FLOW
Thermophysical properties of supercritical fluids and fluid mixtures
[DE89-016568] N90-11102
Numerical solutions of turbulent flow with heat transfer over rough surfaces N90-11246
The structure of Reynolds stress in the near wall region of a turbulent pipe flow N90-11247
Wall-layer eruptions in turbulent flows
[NASA-TM-102362] N90-11250
Cellular automata and massively parallel physics
[DE89-016506] N90-11257
An experimental study of helicity and related properties in turbulent flows
[DE89-016785] N90-11259
Chemical reactions in turbulent mixing flows
[AD-A211240] N90-11263
Questions from the Willmarth Workshop on New Directions in Research on Turbulent Wall-Layer Structures
[AD-A211282] N90-11264
Numerical simulation of turbulent flow downstream a sudden axisymmetric expansion
[FOA-C-20758-2.1] N90-11272
TURBULENT JETS
A laser Doppler anemometry investigation of single-phase and particle-laden jet flows
[AD-A210660] N90-11261
Chemical reactions in turbulent mixing flows
[AD-A211240] N90-11263
TURBULENT MIXING
Turbulent reacting flows in solid-propellant ducted rocket combustors N90-11079
Chemical reactions in turbulent mixing flows
[AD-A211240] N90-11263
TURBULENT WAKES
Linear instability of supersonic plane wakes
[NASA-CR-181911] N90-10833
The near-wake flow structure of wake-cylinder interaction and surface loading of cylinder N90-11248
TWO DIMENSIONAL BODIES
A scalar/vector potential solution for aerodynamic coefficients in wind shear N90-10838
TWO DIMENSIONAL BOUNDARY LAYER
Wall-layer eruptions in turbulent flows
[NASA-TM-102362] N90-11250
TWO DIMENSIONAL MODELS
Two-Dimensional Intercomparison of Stratospheric Models
[NASA-CP-3042] N90-11405
Report on the 2-D Model Intercomparison Workshop held January 11-16, 1987 in Fort Myers Beach, Florida, chapter 2 N90-11406
Report of the 1988 2-D Intercomparison Workshop, chapter 3 N90-11407
Model documentation, chapter 4 N90-11408
Introduction and data summary, chapter 5 N90-11409
Studying shocks in model astrophysical flows
[DE89-618786] N90-11677
TWO PHASE FLOW
A laser Doppler anemometry investigation of single-phase and particle-laden jet flows
[AD-A210660] N90-11261

U

U.S.S.R. SPACE PROGRAM
JPRS Report: Science and Technology. USSR: Space
[JPRS-USP-89-007] N90-10900
Meeting of intercosmos space physics group N90-10902
Soviet Mars program N90-10903
USSR and international cooperation in space N90-10905
Sagdeyev discusses space missions, policy, Mars plans N90-10906
UH-60A HELICOPTER
Task analysis of the UH-60 mission and decision rules for developing a UH-60 workload prediction model. Volume 1: Summary report
[AD-A210763] N90-11446
ULTRAHIGH FREQUENCIES
The effectiveness of adaptive PRF (Pulse Repetition Frequency) selection in minimizing range obscuration in the TDWR (Terminal Doppler Weather Radar) system
[AD-A211267] N90-11222
ULTRASONIC FLAW DETECTION
Sensors for nondestructive testing and evaluation of materials
[DE89-014763] N90-11279
A technique to correlate fractography with NDE (Non-Destructive Evaluation) of small samples
[DE89-016904] N90-11325
ULTRASONIC WAVE TRANSDUCERS
The investigation of the fundamental limits of heterodyne holographic interferometry with the application of imaging laser generated lamb waves
[AD-A211048] N90-11285
ULTRAVIOLET RADIATION
Fuel neutralization by ozone oxidation N90-11176
ULTRAVIOLET SPECTRA
UV observations of NGC 205
[NASA-CR-185975] N90-11661
ULTRAVIOLET SPECTROSCOPY
The effect of degree of aromaticity and alkyl substitution of polyaromatic hydrocarbons on instrumental response factors
[DE89-000761] N90-11117
UMBILICAL CONNECTORS
Independent Orbiter Assessment (IOA): Assessment of the mechanical actuation subsystem, volume 1
[NASA-CR-185527-VOL-1] N90-10952
UNDERGROUND STORAGE
Hydrazine fate and transformation in natural waters and soils N90-11165
UNIQUENESS
A direct two response approach for updating analytical dynamic models of structures with emphasis on uniqueness N90-11028
UNIVERSITIES
Origins of high-temperature superconductivity in the new copper oxide based ceramic superconductors
[DE89-016543] N90-11622
UNSTEADY AERODYNAMICS
An investigation of counterrotating tip vortex interaction
[NASA-CR-185135] N90-11549
UPPER IONOSPHERE
Upper ionosphere and magnetospheric-ionospheric coupling
[DE89-619727] N90-11415
URANIUM COMPOUNDS
Studies of novel superconductors
[DE89-016744] N90-11609
USER MANUALS (COMPUTER PROGRAMS)
User's manual for PEPSIG NASA tip vortex version
[NASA-CR-182178] N90-10835
Near zone-basic scattering code user's manual with space station applications
[NASA-CR-185925] N90-11209
Experimental database retrieval system DARTS (Ha ndling Manual)
[DE89-906473] N90-11652

V

VACANCIES (CRYSTAL DEFECTS)
Kinetics and mechanisms of primary and steady state creep in B- and Al-containing alpha silicon carbide
[AD-A210739] N90-11616
VALENCE
Strain and density dependent valence-band masses in InGaAs/GaAs and GaAs/GaAsP strained-layer structures
[DE89-016882] N90-11627
VALUE
Procedures for separations within batches of values, 1. The orderly tool kit and some heuristics
[AD-A210652] N90-11531
VANADIUM OXIDES
Lithium polymer electrolyte battery, electrochemical behavior of cathode materials
[AD-A210755] N90-11235
VANES
Study for optimization of redundant vane-type flow-direction sensing systems and numerical analysis for design of the systems
[NAL-TM-571] N90-10890
Tower wake/blade interaction noise of a wind turbine
[NAL-TR-945] N90-11344
VAPOR PHASES
An atmospheric pressure flow reactor: Gas phase kinetics and mechanism in tropospheric conditions without wall effects N90-11160
The behavior of hydrazine vapor in an environmental chamber under simulated atmospheric conditions N90-11161
Modeling of hydrazine surface interactions in environmental reaction chambers N90-11162
A matrix-isolation FT-IR study of hydrazine N90-11168
VAPORIZING
Evaporation and combustion of dense sprays with a bimodal droplet size distribution N90-11094
Experimental measurements of shock-induced vaporization in cadmium and lead
[DE89-016877] N90-11103
VARIABLE GEOMETRY STRUCTURES
An assessment of robustness of flight control systems based on variable structure techniques N90-10895
VARIATIONAL PRINCIPLES
A finite element formulation for inelastic plates and shells based on a mixed variational principle N90-11334
VAX COMPUTERS
Two VAX-PASCAL terminal interface modules for visualizing scanning and parsing
[MEMO-INF-89-17] N90-11470
VECTOR PROCESSING (COMPUTERS)
Checking the Goldbach conjecture on a vector computer
[CWI-NM-R8812] N90-11475
VECTORS (MATHEMATICS)
Use of Lanczos vectors in structural dynamics N90-11011
Calculation of the temperature and velocity vector of the neutral gas using EISCAT CP3-data N90-11384
LINPACK routines based on the level 2 BLAS
[CWI-NM-R8811] N90-11483
VELOCITY
Interferometry and high speed photography of laser-driven flyer plates
[DE89-016990] N90-11290

VELOCITY DISTRIBUTION
Frequency domain aerodynamic analysis of interacting rotating systems N90-10837
Laser anemometer measurements in a transonic axial-flow fan rotor
[NASA-TP-2879] N90-11245
A laser Doppler anemometry investigation of single-phase and particle-laden jet flows
[AD-A210660] N90-11261
VELOCITY MEASUREMENT
Development of an adaptive time of flight system for the measurement of fluid flow velocity N90-11273
VENTING
Independent Orbiter Assessment (IOA): Analysis of the purge, vent and drain subsystem
[NASA-CR-185547] N90-10969
VENTS
Independent Orbiter Assessment (IOA): Assessment of the purge, vent and drain subsystem
[NASA-CR-185535] N90-10949
Independent Orbiter Assessment (IOA): Assessment of the mechanical actuation subsystem, volume 1
[NASA-CR-185527-VOL-1] N90-10952
Independent Orbiter Assessment (IOA): Assessment of the mechanical actuation subsystem, volume 2
[NASA-CR-185527-VOL-2] N90-10953
VENUS (PLANET)
Upper ionosphere and magnetospheric-ionospheric coupling
[DE89-619727] N90-11415
VERY HIGH FREQUENCIES
Joint VHF coherent radar and oblique sounder observations for short term ionosphere forecasting N90-11399
VIBRATION
Analytical study of mistuning/friction/aerodynamics interaction in a bladed disk assembly
[AD-A211139] N90-10893
VIBRATION DAMPING
Frequency domain design of robust controllers for space structures
[AD-A211172] N90-10985
Reduction of dynamic response of spacecraft structures and payloads N90-11000
The dynamics of circular plates with patch damping: A numerical and experimental study N90-11329
VIBRATION EFFECTS
A contribution to the stability analysis of large space structures N90-10997
Electron transfer reactions
[AD-A210711] N90-11545
VIBRATION ISOLATORS
Frequency domain design of robust controllers for space structures
[AD-A211172] N90-10985
Viscoelastic tuned dampers for control of structural dynamics N90-10999
Reduction of dynamic response of spacecraft structures and payloads N90-11000
VIBRATION MEASUREMENT
Advances in instrumentation for experimental stress and vibration analysis and its applications N90-11069
VIBRATION METERS
Advances in instrumentation for experimental stress and vibration analysis and its applications N90-11069
VIBRATION MODE
Computational aspects of sensitivity calculations in linear transient structural analysis N90-11327
VIBRATION SIMULATORS
Employment of modal survey methodologies in dynamic analysis procedures N90-11006
Transient vibration testing of spacecraft structures. Experience with multiaxial base motion and combined base motion and point force excitation N90-11039
Two years experience with the ESTEC multishaker system N90-11065
Tamaris: A new European facility for low frequency multi-axis vibration simulation N90-11068
A new European vibration test facility for Ariane 4 class satellites N90-11070
A comparison of fixed-base and driven-base modal testing of an electronics package
[DE89-016673] N90-11240
VIBRATION TESTS
Modal analysis of space structures with the Ibrahim Time Domain method N90-11026
Transient vibration testing of spacecraft structures. Experience with multiaxial base motion and combined base motion and point force excitation N90-11039
Tamaris: A new European facility for low frequency multi-axis vibration simulation N90-11068
A new European vibration test facility for Ariane 4 class satellites N90-11070
VIBRATIONAL SPECTRA
A matrix-isolation FT-IR study of hydrazine N90-11168
Theoretical investigation of gas-surface interactions
[NASA-CR-185492] N90-11552
Study of disorder and strain in semiconductor heterostructures and superlattices by Raman scattering N90-11601
VIBRATIONAL STRESS
Methodology of developing a combined environmental stress schedule for reliability growth testing
[AD-A211053] N90-11326
VIDEO SIGNALS
Land vehicle teleoperation under conditions of reduced video resolution
[DE89-016925] N90-11324
VINYL POLYMERS
The Sandia standard for PVDF (Polyvinylidene Di-Fluoride) shock sensors
[DE89-016530] N90-11287
VISCOELASTIC DAMPING
Viscoelastic tuned dampers for control of structural dynamics N90-10999
VISCOELASTICITY
Numerical analysis of nonlinear viscoelastic structures: Application to elastomers and rubber-like materials N90-11013
The decay of viscoelastic fluid jets
[ETN-89-94667] N90-11270
VISCOPLASTICITY
An evaluation of the Chaboche and Bodner-Partom viscoplastic constitutive theories for strain rate sensitive materials N90-11330
VISCOSITY
Numerical simulation of leading-edge vortex rollup and bursting N90-10831
VISCOUS DAMPING
Analytic signals in the damping coefficient estimation N90-11003
VISCOUS FLOW
Analytical and numerical studies in flow development
[DE89-017380] N90-11269
VISCOUS FLUIDS
Nonlinear acoustics: Reflection and refraction, propagation in a periodic waveguide, scattering of sound by sound and ellipsoidal focusing
[AD-A211224] N90-11550
VISIBILITY
Diagnostic study of atmosphere-terrain interaction leading to the formation of dust clouds and poor visibilities over near east desert areas
[AD-A211243] N90-11358
VISUAL DISCRIMINATION
Night sky radiometric measurements during follow-on-evaluation testing of AN/PVS-7 (A, B) at Fort Benning, Georgia
[AD-A211273] N90-11574
VISUAL PERCEPTION
Inferences from images
[AD-A210710] N90-11465
VISUAL TASKS
Filling or outlining shapes with color: The effects on a visual search task
[AD-A211067] N90-11444
VOICE COMMUNICATION
Computer programs for measuring variations in speech
[AD-A211126] N90-11467
Spoken commands control robot that handles radioactive materials
[DE89-012632] N90-11488
VOICE DATA PROCESSING
Computer programs for measuring variations in speech
[AD-A211126] N90-11467
VORTEX BREAKDOWN
Numerical simulation of leading-edge vortex rollup and bursting N90-10831
VORTEX SHEDDING
The near-wake flow structure of wake-cylinder interaction and surface loading of cylinder N90-11248
VORTEX SHEETS
Numerical simulation of leading-edge vortex rollup and bursting N90-10831
The near-wake flow structure of wake-cylinder interaction and surface loading of cylinder N90-11248
VORTICES
Computation of the tip vortex flowfield for advanced aircraft propellers
[NASA-CR-182179] N90-10836
Method of characteristic studies for rotational flow downstream of a curved shock wave N90-11252
A computational/experimental study of the flow around a body of revolution at angle of attack
[NASA-TM-88329] N90-11254
Questions from the Willmarth Workshop on New Directions in Research on Turbulent Wall-Layer Structures
[AD-A211282] N90-11264
An investigation of counterrotating tip vortex interaction
[NASA-CR-185135] N90-11549
VULNERABILITY
HPW (High Power Microwave) testing of electronic components
[DE89-016682] N90-11241

W

WALL FLOW
Low-Reynolds-number modeling of complex flows with and without density variation N90-10832
The structure of Reynolds stress in the near wall region of a turbulent pipe flow N90-11247
On transonic flow over segmented slotted wind tunnel wall with mass transfer N90-11676
WALLS
Questions from the Willmarth Workshop on New Directions in Research on Turbulent Wall-Layer Structures
[AD-A211282] N90-11264
WARNING SYSTEMS
See and avoid/cockpit visibility
[DOT/FAA/CT-TN89/18] N90-10843
Independent Orbiter Assessment (IOA): Analysis of the extravehicular mobility unit
[NASA-CR-185540] N90-10937
Independent Orbiter Assessment (IOA): Assessment of the displays and controls subsystem
[NASA-CR-185588] N90-10961
Hydrazine dosimetry N90-11178
Description of a chemiluminescence detector system specifically designed for monitoring airborne hydrazine and oxidizer propellant vapors N90-11179
WASTE DISPOSAL
The Third Conference on the Environmental Chemistry of Hydrazine Fuels
[AD-A197632] N90-11157
The chemistry of the hypochlorite neutralization of hydrazine fuels N90-11173
Fuel neutralization by ozone oxidation N90-11176
Evaluation of mid-to-long term basic research for environmental restoration
[DE89-015621] N90-11355
WASTE TREATMENT
The chemistry of the hypochlorite neutralization of hydrazine fuels N90-11173
Ozonation of hydrazines and their associated impurities N90-11174
Modeling the ozonolysis of hydrazines wastewater N90-11175
WASTE WATER
Ozonation of hydrazines and their associated impurities N90-11174
Modeling the ozonolysis of hydrazines wastewater N90-11175
WASTES
Evaluation of mid-to-long term basic research for environmental restoration
[DE89-015621] N90-11355
WATER
Independent Orbiter Assessment (IOA): Analysis of the electrical power distribution and control/electrical power generation subsystem
[NASA-CR-185538] N90-10933
Independent Orbiter Assessment (IOA): Analysis of the hydraulics/water spray boiler subsystem
[NASA-CR-185541] N90-10934
A new method for the characterization of solutes and solvent phases using solvatochromic parameters
[AD-A211238] N90-11116
Design of ceramic fabric heat pipe with water working fluid
[DE89-016565] N90-11265
A high level Ab initio study of the anionic hydrogen-bonded complexes FH-CN-, FH-NC-, H2O-CN- and H2O-NC- N90-11553
Equation-of-state data of synthetic Uranus
[DE89-016509] N90-11683
WATER POLLUTION
Hydrazine fate and transformation in natural waters and soils N90-11165
WATER TREATMENT
Selective removal of organics for water reclamation
[NASA-CR-185959] N90-11445
WAVE DISPERSION
Evaluation of dispersive behavior in periodic structures by discrete Fourier transform N90-11014
On the influence of ionospheric conductivity on dispersion of acoustic gravity waves N90-11386
WAVE EQUATIONS
Efficient algorithm for calculation of radar cross section
[AD-A210785] N90-11217

Non-linear wave-equations for low-frequency acoustic gravity waves N90-11365
Estimation on nonlinear damping in second order distributed parameter systems [NASA-CR-181890] N90-11494
Theory of high-n toroidicity-induced shear Alfven eigenmode in tokamaks [DE89-016726] N90-11582

WAVE FRONTS
Wavefront propagation for reaction-diffusion systems of PDE [AD-A210862] N90-11510

WAVE FUNCTIONS
Markov processes in Hilbert space and continuous spontaneous localization of systems of identical particles [DE89-618396] N90-11540
Structure and properties of simple molecular systems at very high density [DE89-016974] N90-11557
New theoretical approaches for studying electron collisions with small molecules [DE89-017543] N90-11558

WAVE PROPAGATION
Wave-mode coordinate analysis of L junction in LSS [AD-A211116] N90-10984
Shock-induced atomic-scale structure in metals [DE89-016539] N90-11124
VLF/LF radio wave studies of the structure and variability of the equatorial, mid-latitude and polar ionosphere below 100 km N90-11373
On the influence of ionospheric conductivity on dispersion of acoustic gravity waves N90-11386
Ionospheric irregularities and their effects on electromagnetic waves propagating through them N90-11391
Joint VHF coherent radar and oblique sounder observations for short term ionosphere forecasting N90-11399
Radio propagation conditions forecast above a low latitude region N90-11400
Irreversible phase transition and wave propagation in silicate geologic materials [DE89-016031] N90-11414
Wavefront propagation for reaction-diffusion systems of PDE [AD-A210862] N90-11510
Nonlinear acoustics: Reflection and refraction, propagation in a periodic waveguide, scattering of sound by sound and ellipsoidal focusing [AD-A211224] N90-11550

WAVE REFLECTION
Nonlinear acoustics: Reflection and refraction, propagation in a periodic waveguide, scattering of sound by sound and ellipsoidal focusing [AD-A211224] N90-11550

WAVEGUIDES
Constitutive parameter measurements of lossy materials [NASA-CR-183398] N90-11603

WEAPON SYSTEMS
Development of a marine integrated navigation system N90-10852
Flight testing a newly-designed stand-off weapon dispenser N90-10880
Air Combat Environment Test and Evaluation Facility (ACETEF) N90-10883
HPW (High Power Microwave) testing of electronic components [DE89-016682] N90-11241

WEAR RESISTANCE
Coatings in electrical contacts [DE89-787739] N90-11234

WEATHER
Diagnostic study of atmosphere-terrain interaction leading to the formation of dust clouds and poor visibilities over near east desert areas [AD-A211243] N90-11358

WEATHER FORECASTING
Average diurnal and seasonal profiles of ionospheric storms N90-11371
Hurricane Research Division fiscal year 1988 programs, fiscal year 1989 projections [PB89-152268] N90-11418
Composited local area forecast techniques [AD-A210802] N90-11432

WEATHER STATIONS
Hanford Meteorological Station computer codes. Volume 10: The ARCHIVE computer code [DE89-016175] N90-11429

WEIBULL DENSITY FUNCTIONS
Independent Orbiter Assessment (IOA): Weibull analysis report [NASA-CR-185534] N90-10948

WELD STRENGTH
STSA-Space Telescope solar array interconnectors: From simple approaches to complex modeling. A case study of the necessity of complex analysis N90-11076
A re-evaluation of fatigue threshold test procedures and the simulation and prediction of fatigue crack growth under conditions of low crack closure N90-11328

WELDED JOINTS
The Meta-Lax method of stress reduction in welds [DE89-016437] N90-11321

WHISKERS (CRYSTALS)
Kinetics and mechanisms of primary and steady state creep in B- and Al-containing alpha silicon carbide [AD-A210739] N90-11616

WHISTLERS
Producing of an ECR plasma using 2450MHz Whistler wave and the investigating of its parameters [DE89-618689] N90-11586

WHITE DWARF STARS
MOXE: An X-ray all-sky monitor for Soviet Spectrum-X-Gamma Mission [NASA-TM-101266] N90-11280
Rocket and satellite observations of the local interstellar medium N90-11668

WIGNER COEFFICIENT
Alias-free Wigner distribution function and complex ambiguity function for discrete-time samples [AD-A211050] N90-11533

WIND (METEOROLOGY)
Hurricane Research Division fiscal year 1988 programs, fiscal year 1989 projections [PB89-152268] N90-11418
Direct statistical thermal wind estimation procedure [AD-A211256] N90-11433

WIND EFFECTS
Solar-terrestrial relations: Flare and solar wind effects N90-11362

WIND PROFILES
A scalar/vector potential solution for aerodynamic coefficients in wind shear N90-10838
Relation of wind field and buoyancy to rainfall inferred from radar [PB89-208326] N90-11424
Direct statistical thermal wind estimation procedure [AD-A211256] N90-11433

WIND SHEAR
A scalar/vector potential solution for aerodynamic coefficients in wind shear N90-10838

WIND TUNNEL MODELS
An experimental investigation of the aerodynamic characteristics of slanted base ogive cylinders using magnetic suspension technology [NASA-CR-181708] N90-10834

WIND TUNNEL TESTS
Tower wake/blade interaction noise of a wind turbine [NAL-TR-945] N90-11344

WINDMILLS (WINDPOWERED MACHINES)
Tower wake/blade interaction noise of a wind turbine [NAL-TR-945] N90-11344

WINGS
Independent Orbiter Assessment (IOA): Analysis of the elevon subsystem [NASA-CR-185576] N90-10935

WIRE
Analysis of coaxial wire measurement of longitudinal coupling impedance [DE89-015748] N90-11230
Battery actuation of NITINOL at sub-zero temperatures [AD-A211254] N90-11237

WORD PROCESSING
Computer programs for measuring variations in speech [AD-A211126] N90-11467

WORKING FLUIDS
A thermochemical analysis of proposed working fluids for electrothermal guns [AD-A210661] N90-10910
Design of ceramic fabric heat pipe with water working fluid [DE89-016565] N90-11265

WORKLOADS (PSYCHOPHYSIOLOGY)
Computer programs for measuring variations in speech [AD-A211126] N90-11467

WORKSTATIONS
An integrated distributed processing interface for supercomputers and workstations [DE89-016769] N90-11478

X

X RAY DIFFRACTION
Use of overlapped reflection for determining the retained austenite by X-ray diffraction [DE89-615450] N90-11128
Thermal expansion and phase transformation studies on some materials by high temperature X-ray powder diffractometry [DE89-631032] N90-11130
Report of the Specialists' Workshop on Phase Transition Studies on Hydrogen-Bonded Crystals by Neutron and X-ray Diffractometries [DE89-906638] N90-11631

X RAY FLUORESCENCE
Compositional analysis of steels by X-ray fluorescence spectrometry [DE89-630803] N90-11129

X RAY LASERS
A compact X-ray free electron laser [DE89-017236] N90-11297
Research in X-ray optics with the ultimate aim of constructing a synchrotron radiation pumped soft X-ray lithium laser [DE89-016788] N90-11304

X RAY SOURCES
X-ray lithography sources: A review [DE89-017610] N90-11547

X RAY SPECTRA
The ratio to X-ray spectral shape and variability of blazars N90-11688

X RAY SPECTROSCOPY
Dynamics of nucleation at electrochemical interfaces via surface EXAFS and standing wave measurements [AD-A210733] N90-11109
X-ray and gamma-ray spectroscopy of solids under pressure [DE89-017271] N90-11118
Compositional analysis of steels by X-ray fluorescence spectrometry [DE89-630803] N90-11129

X RAYS
MOXE: An X-ray all-sky monitor for Soviet Spectrum-X-Gamma Mission [NASA-TM-101266] N90-11280

X-29 AIRCRAFT
Real-time flight test analysis and display techniques for the X-29A aircraft N90-10866

XENON
A liquid xenon imaging telescope for 1-30 MeV gamma-ray astrophysics [NASA-CR-185999] N90-11662

Y

YARNS
Effect of thermal and cyclic loads on silicon carbide yarn reinforced glass matrix composites [DE89-016554] N90-11091

YIELD STRENGTH
The HEL (Hugoniot Elastic Limit) and rate-dependent yield behavior [DE89-016981] N90-11134

YTTRIUM COMPOUNDS
Y-Si-Al-O-N glass fibers [AD-A211170] N90-11088

YTTRIUM OXIDES
A study of the tribological and surface micromechanical properties of YBa2Cu3O7-x [DE89-015680] N90-11607

Z

ZEOLITES
Applications of NMR spectroscopy to the study of zeolite synthesis [DE89-015226] N90-11095

ZETA PINCH
Solid fiber Z-pinches: Cold-start computations [DE89-016768] N90-11592

ZIRCONIUM
Exploratory study of niobium, titanium, zirconium and tantalum aluminides [AD-A210658] N90-11615

ZIRCONIUM OXIDES
Influence of core-shell grains on the internal stress state and permittivity response of zirconia modified barium titanate [AD-A211245] N90-11153

ZONAL FLOW (METEOROLOGY)
Global ionospheric dynamics N90-11366

Report on the 2-D Model Intercomparison Workshop held January 11-16, 1987 in Fort Myers Beach, Florida, chapter 2 N90-11406
Observational studies of low-frequency oscillations in the Southern Hemisphere N90-11420

PERSONAL AUTHOR INDEX

Typical Personal Author Index Listing

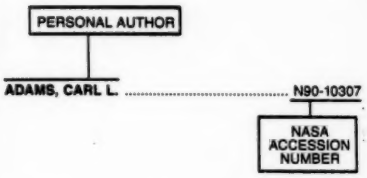

Listings in this index are arranged alphabetically by personal author. The NASA accession number denotes the number by which the citation is identified.

A

AARONS, J. N90-11393
ABDELOUHAB, MAHMOUD ROCCO N90-11601
ABOELNAGA, YOUSRY SALEH N90-11333
ABRAHAM, MICHAEL H. N90-11116
ABRUNA, HECTOR D. N90-11109
ACCIOLY, A. J. N90-11635
ADAMS, KELLY J. N90-10872
ADAMS, L. M. N90-11269
ADDIS, A. W. N90-10972
ADELMAN, HOWARD M. N90-10889
ADVANI, A. N90-11127
AGARWAL, ANANT N90-11468
AGENNI, ALESSANDRO N90-11003
AGHANAJAFI, CYRUS N90-11410
AGNENI, A. N90-11014
AGRAWAL, BRIJ N. N90-11018
AGRAWAL, NIRAJ N90-11565
AGREN, CARL HUGO N90-11417
AGTHE, R. E. N90-11176
ALARCON, E. N90-11045
ALBRECHT, R. N90-11555
ALBUS, JAMES S. N90-11310
ALCON, ROBERT R. N90-11186
ALCORN, CHARLES W. N90-10834
ALDIS, D. F. N90-11192
ALDRICH, THEODORE B. N90-11446
ALEXANDER, WILLIAM P. N90-11532
ALFONSO, F. N90-11043
ALLEN, MILAN N90-11338
ALM, KNUT-FREDRIK N90-11156
ALWES, D. N90-11075
AMES, B. E. N90-10923
AMOS, DONALD E. N90-11499
N90-11520
ANANTHAKRISHNAN, S. K. N90-11129
N90-11130
ANDERSEN, MELVIN E. N90-11182
ANDERSON, D. N. N90-11368
ANDERSON, L. P., JR. N90-11210
ANDERSON, ROGER R. N90-11587
ANDREWS, G. L. N90-11429
ANDREYANOV, V. V. N90-10901
ANGEL, JAMES R. N90-11427
ANTINONE, R. N90-11241
ANTONA, E. N90-10997
N90-10998
ANTONIAK, Z. I. N90-11265
AOYAGI, TETSUO N90-11652
APPLEWHITE, L. A. N90-11166
APRILE, ELENA N90-11662
ARBET, J. D. N90-10977
ARCONE, STEVEN A. N90-11435
ARDUINI, C. N90-11016
N90-11044
N90-11047
ARENDTS, F. J. N90-11060
ARGENZIANO, ANGELA N90-11388
ARIF, HUGH N90-10912
ARKO, A. J. N90-11624
ARMOUR, MICHAEL F. N90-10887
ARMSTRONG, T. R. N90-11153
ARNOLD, W. H. N90-11228
ARULIAH, A. N90-11382
ASAY, JAMES R. N90-11103
ASLAM, SOHAIL N90-11493
ASUVATHARAMAN, R. N90-11129
N90-11130
ATAC, M. N90-11297
ATKINS, ISAAC, JR. N90-11083
ATTERIDGE, D. G. N90-11127
AUDET, D. M. N90-11217
AUFFRAY, PH. N90-11017
AVVA, V. S. N90-11091
AWES, T. C. N90-11555
AYDELOTT, JOHN C. N90-10912

B

BABA, YUICHIRO N90-11050
BABCOCK, S. R. N90-11242
BACHER, J. L. N90-10944
BACHMANN, V. N90-11031
BADGETT, M. E. N90-11487
BAIER, H. N90-11000
BAILEY, P. S. N90-10913
BAKER, K. B. N90-11394
BAKTASH, C. N90-11555
BALANIS, CONSTANTINE A. N90-11205
N90-11206
N90-11207
BALINT, JEAN-LOUIS N90-11259
BALL, CALVIN L. N90-10891
BALL, LEWIS N90-11600
BALLARINI, R. N90-11332
BALLATO, ARTHUR N90-11112
BANDO, TOSHIO N90-10899
BANERJI, ABINASH N90-11136
BANINO, GIORGIO N90-11032
BANKS, H. T. N90-11494
BANSAL, NAROTTAM P. N90-11606
BAO, DINGHUA N90-11586
BAO, HAN P. N90-11456
BARCLAY, REBECCA O. N90-11647
BARDASH, MICHAEL JAY N90-11275
BARICKMAN, K. N90-10977
N90-10978
BARKER, A. J. N90-11069
BARKER, LYNN M. N90-11289
BARLES, G. N90-11510
BARLETTA, W. N90-11297
BARNES, J. E. N90-10931
N90-10954
N90-10960
N90-10976
BARR, W. L. N90-11589
BARRERA, JUNIOR N90-11447
BARTH, CLYDE H. N90-11123
BARTLETT, R. J. N90-11624
BARTON, BARRIE D. N90-11133
BARTRAM, RALPH H. N90-11105
BASSEL, R. H. N90-11572
BASTARD, J. L. N90-11017
BATES, J. M. N90-11265
BATHKE, C. G. N90-11577
BATTISTA, R. N90-11654
BATTS, G. W. N90-10980
N90-10981
BAUER, F. N90-11145
N90-11287
BAUER, J. N90-11013
BAVUSO, SALVATORE J. N90-11454
BAYERDOERFER, G. N90-11041
BEAIRD, H. G. N90-10943
BECK, S. M. N90-11181
BECKMANN, P. N90-11555
BELL, ALEXIS T. N90-11095
BELL, HERBERT H. N90-11218
BELLERBY, J. M. N90-11163
BENAGE, JOHN F., JR. N90-11581
BENEDETTI, CATHLEEN M. N90-11463
BENNETT, WILLIAM H. N90-10985
BERG, R. L. N90-10896
BERGAN, P. G. N90-11035
BERGER, F. N90-11555
BERGERON, HUGH N90-10841
BERGMAN, CHRISTY N90-11239
BERGMANN, VICKI LYNN N90-11334
BERGSTRA, J. A. N90-11474
BERNELLI-ZAZZERA, F. N90-11012
BERRIAUD, C. N90-11068
BERRY, D. J. N90-11069
BERTHELIER, J.-J. N90-11392
BERTOLA, FRANCESCO N90-11661
BERTRAM, A. N90-11027
BERTSCH, P. J. N90-10914
N90-10915
BESTMAN, A. R. N90-11638
BETSCHARD, J. N90-11174
BEUGELSDIJK, TONY J. N90-11488
BEZEM, MARC N90-11473
BHAT, MAHARAJ KRISHEN N90-11676
BHOWMIK, A. N90-11297
BIBL, K. N90-11395
N90-11396
BICEN, ALI F. N90-11261
BIEFELD, R. M. N90-11627
BIERBAUM, CARL R. N90-11446
BIEZAD, D. J. N90-10868
BILLMANN, BARRY R. N90-10858
BIRD, MARK CHRISTOPHER N90-11659
BIRI, S. N90-11560
BIRMINGHAM, DANNY N90-11636
BISHOP, ALFRED M. N90-10911
BISHOP, BRUCE N90-11139
BJOERUM, R. O. N90-11035
BLACKSTOCK, DAVID T. N90-11550
BLACKWELDER, R. F. N90-11264
BLAHA, GEORGES N90-11509
BLAKERS, A. W. N90-11347
BLAU, P. J. N90-11607
BLOMSHIELD, FREDERICK STEELE N90-11183
BLOOM, S. A. N90-11172
BLUMENTHAL, W. R. N90-11146
BOBBS, B. N90-11297
BOCK, R. N90-11555
BOEHM-VITENSE, ERIKA N90-11661
BOGOMOLOV, S. L. N90-11560
BOISSET, J. P. N90-11052
BOLDISSAR, F. N90-11210
BONNOT, P. N90-11065
BOOTH, W. T. N90-11228
BORKOWSKI, KAZIMIERZ JAN N90-11670
BOSLOUGH, MARK B. N90-11100
N90-11337
BOTT, JERRY F. N90-11300
BOURNE, C. M. N90-11286
BOWEN, H. KENT N90-11139
BOWMAN, JAMES S., JR. N90-10829
BOWSER, CARL A. N90-11401
BOYD, IAIN D. N90-10840
BOYD, MARK N90-11454
BRACE, M. H. N90-11196
BRADWAY, M. W. N90-10944
N90-10952
N90-10953
BRADY, RICHARD L. N90-11089
N90-11090
BRANDT, STEVEN ALLAN N90-10831
BRASSEUR, GUY N90-11407
BRAUN, ANDRE M. N90-11110
BREI, MARYLOUISE N90-11491
BREITMEIER, J. N90-11238
BREKKE, ASGEIR N90-11383
BRINDLEY, WILLIAM J. N90-11082
BRITCHER, COLIN N90-10834
BROADWELL, JAMES E. N90-11263
BROWN, K. L. N90-10914
N90-10915
BROWN, LUCINDA MARY JOANNA N90-11688
BRUBAKER, KENNETH L. N90-11173
BRUEMMER, S. M. N90-11125
N90-11127
BRUNNER, O. N90-11028
BUCHACKER, E. N90-10868
BUCHANAN, R. C. N90-11153

BUCHARLES, ALAIN N90-10871
BUCHAU, J. N90-11396
BUCKLEY, J. N90-11179
BUCKLEY, P. L. N90-11080
BUGEAT, L. P. N90-11007
N90-11015
BUGEAT, L.-P. N90-11040
BUKIET, BRUCE N90-11266
BULAND, P. N90-11068
BULMER, R. H. N90-11589
BUNTE, STEVEN W. N90-10910
BURK, K. W. N90-11429
BURKE, G. J. N90-11212
BURKE, W. R. N90-10986
BURKEMPER, V. J. N90-10919
N90-10938
N90-10939
N90-10940
BURNS, G. W. N90-11274
BUSH, S. H. N90-11132
BUSH, WILLIAM R. N90-11452
BUTTRAM, M. T. N90-11595
BYNUM, M. C., III N90-10949
N90-10969

C

CALEF, DANIEL F. N90-11099
CALLAHAN, J. H. N90-11178
CALLENDER, DAVID I. N90-10850
CALVERT, JACK G. N90-11413
CAMPBELL, JOHN N90-11478
CAMPBELL, R. B. N90-11589
CAMPOS, L. M. B. C. N90-10885
CAMY-PEYRET, CLAUDE N90-11108
CAN, SUMER N90-10828
CANEILLES, J. L. N90-11048
CANNON, P. S. N90-11399
CAPITANIO, R. S. N90-11033
CARDONA, A. N90-11004
CAREY, LINDA N90-11648
CARLIER, P. N90-11078
CARNE, THOMAS G. N90-11240
CARPENTER, PATRICIA A. N90-11442
CARROLL, TOM N90-11338
CARTER, CALVIN H., JR. N90-11616
CARTER, W. P. L. N90-11158
CASSAN, HENRI N90-10871
CASSIS, BETRIZ N90-11217
CASTILLO, B. A. N90-11043
CASTRO, D. E. N90-11031
CAUDAL, GERARD N90-11377
CERISIER, J. C. N90-11394
CERISIER, J.-C. N90-11392
CHAKRABARTI, SANDIP K. N90-11677
CHAN, C. C. N90-11115
CHAN, K. C. D. N90-11305
CHANG, D. C. D. N90-11210
CHANG, Y. A. N90-11621
CHAPLIN, M. R. N90-11590
CHARLES, D. N90-10876
CHARLOT, L. A. N90-11125
N90-11127
CHATO, DAVID J. N90-10912
CHELAKARA, R. N90-11127
CHEN, CHIEN-HUEI N90-11313
CHEN, G. N90-11316
N90-11317
CHEN, G.-S. N90-11001
CHEN, HUN WAY N90-11246
CHEN, JAY-CHUNG N90-11025
CHEN, K. C. N90-11618
CHEN, SHING N90-10893
CHENG, C. Z. N90-11582
CHENG, GINO N90-11452
CHENG, UNJENG N90-11216
CHEONG, S. W. N90-11624
CHERNG, DAO-LIEN N90-11079
CHEVRIN, PAUL-ANDRE N90-11247
CHHABILDAS, LALIT C. N90-11289
CHIA, K. Y. N90-11164
CHIMETTO, P. N90-10873
CHO, JINSOO N90-10837
CHONG, C. M. N90-11347
CHU, K. W. N90-11568
CHWALINSKI, R. N90-11022
CLAESSON, G. N90-11555
CLARK, N. A. N90-11628
CLASSEN, E. N90-11064
CLEWELL, HARVEY J., III N90-11182
CLEWING, G. N90-11555
CLINE, D. B. N90-11297
CLOTE, PETER N90-11472
COFFEY, HELEN E. N90-11684
N90-11685
COHEN, DAVID N90-11444
COLE, B. N90-11591
COLE, DAVID A. N90-11434
COLE, JONATHAN G. N90-11215
COLELLA, P. N90-11258
COLVIN, TIM R. N90-11680
COMPTON, J. M. N90-10943
N90-10962
N90-10963
CONNELLY, M. N90-11654
CONTRERAS, MANUEL N90-11232
COOPER, A. W. N90-11286
COOPER, PAUL W. N90-11187
CORBIN, R. L. N90-11181
COSTARD, JEAN N90-10867
COVER, R. A. N90-11297
COWART, EUGENE G. N90-11059
COWLING, DAVID A. N90-10894
COX, ARTHUR N. N90-11687
COYETTE, J. P. N90-11073
CRAIG, ROY R., JR. N90-11011
CRANE, PETER M. N90-11218
CRAWFORD, MARK R. N90-10872
CREMA, LUIGI BALIS N90-11003
CRIMINALE, W. O. N90-11269
CRISP, DAVID N90-11408
CRITTENDEN, EUGENE C., JR. N90-11286
CROCKER, S. C. N90-11222
CRONIN, M. N90-11654
CROSSMAN, K. P. N90-11178
CROUSE, KENNETH H. N90-11451
CSONKA, P. L. N90-11304
CUNNINGHAM, J. A. N90-11228
CURLEE, T. RANDALL N90-11655
CURRAN, FRANK M. N90-11081
CUTOLO, MARIO N90-11388
CZAJKOWSKI, G. N90-11184

D

DADO, MOHAMMAD H. FATHALLA N90-11311
DALEY, E. S. N90-10967
DATTOLI, G. N90-11298
DATZ, S. N90-11625
DAVID, J. F. N90-11049
DAVIDSON, W. R. N90-10934
DAVIES, MERTON E. N90-11680
DAVIS, DENNIS D. N90-11159
N90-11160
N90-11167
N90-11170
DAVIS, ROBERT F. N90-11616
DAVIS, THOMAS J. N90-10841
DAVOODI, HAMID N90-11335
DAVY, COLETTE N90-11398
DAYI, OEMER F. N90-11637
DEATHERAGE, DON N90-11232
DEBROUX, PATRICK S. N90-11221
DEGENER, M. N90-11027
DEGROOT, A. J. N90-11518
DEGUIRE, MARK R. N90-11606
DEHOPE, W. J. N90-11618
DEJAGHER, P. C. N90-11386
DEJONG, FREDERICK J. N90-10835
N90-10836
DELAFUENTE, CLIVE N90-10858
DELANEY, ALLAN J. N90-11435
DELOO, PH. N90-11051
N90-11076
DEMEESTER, P. N90-11037
N90-11063
DEMOLLERAT, T. N90-10987
DEPOMPEIS, R. N90-10863
DEROUVRAY, A. N90-11071
N90-11075
DESPAIN, ALVIN M. N90-11452
DEVORE, C. E. N90-11607
DEVOTO, R. S. N90-11589
DEVRIES, PETER J., JR. N90-11339
DIAB, F. M. N90-11503
DIBBEN, MARK N90-11083
DICK, J. J. N90-11190
DICKERSON, WALTER E. N90-10897
DICKEY, F. M. N90-11568
DICKSON, A. H. N90-11399
DIEROLF, DAVID A. N90-11491
DIFILIPPO, D. J. N90-10851
DILSAVOR, R. L. N90-11211
DIMOTAKIS, PAUL E. N90-11263
DISCIUVA, M. N90-10997
DITTNER, P. F. N90-11625
DIXON, F. P. N90-11297
DODSON, BRIAN W. N90-11124
N90-11337
DOELL, W. N90-11204
DOMINEK, A. N90-11603
DONAHUE, A. N90-11654
DONLAN, VINCENT N90-10908
DOOLEY, JOHN N90-11218
DOORISH, JOHN FRANCIS N90-11666
DOWLATYARI, P. N90-11071
DOWLING, TIMOTHY EDWARD N90-11681
DOWNS, W. C. N90-11172
DOXAS, I. N90-11669
DOXSEE, LAWRENCE E., JR. N90-11055
DRAGON, L. N90-11555
DRECHSLER, KLAUS N90-11060
DRESNER, LAWRENCE N90-11611
N90-11626
DRIFFILL, P. J. N90-10876
DRYER, F. L. N90-11196
DUBOIS, J. N90-11075
N90-11078
DUFFY, R. E. N90-10925
N90-10974
N90-10977
DUGAN, JOANNE BECHTA N90-11454
DUGGAN, D. M. N90-11618
DUNN, JOE L. N90-10861
DUNNING, F. B. N90-11556
DURAN, M. N90-11002
DURANTI, P. N90-10880
DURIN, C. N90-11056
DUTRA, LUCIANO VIEIRA N90-11447
DUTTA, INDRANATH N90-11085
DUTTA, JYOTSNA M. N90-11106
DUVAL, J. D. N90-10934

E

EBERHARD, W. L. N90-11425
EBERHART, J. G. N90-11093
EBERT, K. N90-11023
ECKEL, ANDREW J. N90-11144
ECKHARDT, K. N90-11042
ECKMAN, RICHARD N90-11408
EDWARDS, D. A. N90-11163
EGGERS, H. N90-11036
EGGETT, D. L. N90-11489
EINARSRUD, MARI-ANN N90-11139
EKLUND, A. N90-11555
EL-ASSAL, AHMED MOHAMED N90-11330
ELIAS, E. N90-11283
ELIENS, A. N90-11482
ELLINGSON, W. A. N90-11325
ELROD, HAROLD G. N90-11256
ELSHOFF, I. J. P. N90-11453
EMMERING, ROBERT THOMS N90-11671
EMMONS, T. E. N90-10927
EMRE, EROL N90-11512
ENGEL, RENATA SUSAN N90-11331
ENGELKE, RAY N90-11186
ENTRALGO, E. E. N90-11640
ERCOLI-FINZI, A. N90-11012
ERICKSON, JON D. N90-11451
ERICKSON, K. L. N90-11101
N90-11191
ERICKSON, L. M. N90-11192
ERIKSSON, JAN N90-11272
ERLICHMAN, SCOTT L. N90-10897
ERZBERGER, HEINZ N90-10841
ESKRIDGE, PAUL B. N90-11661
EVANS, L. C. N90-11510
EVERTS, JEFF N90-11232
EWELL, J. J., JR. N90-10973
EWINS, D. J. N90-10993

F

FAASE, FRANS J. N90-11470
FACEMIRE, BARBARA N90-11195
FALCONE, S. N90-11075
FALES, JANINE L. N90-11469
FANG, YUDE N90-11586
FANSON, J. L. N90-11001
FARMER, A. D. N90-11382
FARRELL, R. N90-11654
FEJER, B. G. N90-11397
FEJER, J. A. N90-11389
FELMER, PATRICIO L. N90-11496
FENIMORE, E. E. N90-11280
FENSTERMACHER, M. E. N90-11589
FERNANDEZ-BACA, J. A. N90-11126
FERRETTI, G. N90-10880
FETERIS, PIETER J. N90-11358
FIARMAN, S. N90-11283
FIGUEROA, D. N90-11384
FILLOD, R. N90-10994
FINE, D. N90-11179

FISHER, DAVID F. N90-10878
FISHER, R. J. N90-11231
N90-11233
FISHER, S. A. N90-11080
FISHMAN, GERALD J. N90-11689
FISK, Z. N90-11624
FISSETTE, E. N90-11028
FITZGERALD, JAMES W. N90-11431
FLAHERTY, DOUGLAS R. N90-11451
FLAUD, JEAN-MARIE N90-11108
FLECK, THOMAS N90-10875
FLEURY, ROLAND N90-11398
FLORIG, H. KEITH N90-11439
FLOWER, LINDA N90-11648
FOGELSON, D. J. N90-11287
FOLLANSBEE, PAUL S. N90-11131
N90-11134
FONSECA, A. A. N90-10885
FONTAINE, DOMINIQUE N90-11377
FORBES, J. M. N90-11368
FOREST, CHARLES A. N90-11268
FOROS, P. N90-11013
FOSTER, J. C. N90-11393
FOWLER, C. M. N90-11546
FOWLER, R. H. N90-11579
FOX, MARK S. N90-11506
FRAIN, F. N90-11179
FRANSEN, C. N90-11066
FRANZ, JUERGEN N90-11224
FRICK, GLENDON M. N90-11431
FRISCHHERZ, M. C. N90-11612
FROLOVA, N. A. N90-10902
FU, G. Y. N90-11582
FU, KEMING N90-11586
FULLER-ROWELL, T. J. N90-11380
FUNK, L. L. N90-11612
FUZU, ZHANG N90-11347

G

GADD, STAFFAN N90-11691
GAEDKE, M. N90-11061
GAI, W. N90-11591
GALLAGHER, MARIA L. N90-11455
GAMALERO, G. N90-10869
GANGLOFF, D. N90-11010
N90-11017
N90-11049
GARBA, J. A. N90-11001
GARCIA, I. A. N90-11290
GARCIA, ROLANDO N90-11407
GARDNER, J. R. N90-10967
N90-10972
GARIN, J. L. N90-11128
GARNIER, C. N90-11005
GARY, S. P. N90-11416
N90-11588
GATLIN, GREGORY M. N90-10830
GAUVRIT, MICHEL N90-10854
GAZEY, S. N90-11072
GEAR, C. W. N90-11493
GELET, DAVID N90-11232
GENENS, L. N90-11349
GEORGE, MARILYN E. N90-11182
GEORGE, THOMAS F. N90-11096
GERADIN, M. N90-11004
GERASIMOV, A. L. N90-11548
GERLA, MARIO N90-11571
GHIRARDI, GIAN CARLO N90-11540
GIESE, J. P. N90-11625
GILROY, KALPANA KRISHNASWAMY N90-11664
GINLEY, D. S. N90-11629
GION, EDMUND J. N90-11260
GIRARD, A. N90-11007
N90-11015
N90-11040
GIROUX, NATALY N90-11508
GITTIS, APOSTOLOS GEORGIOS N90-11602
GLASSMAN, MYRON N90-11647
GLATTER, E. Y. N90-11618
GLEISNER, ROBERT P. N90-11088
GLIEBE, P. R. N90-11549
GLUCKSTERN, R. L. N90-11230
GLYNN, PETER W. N90-11508
GOEL, RAJEEV K. N90-11655
GOETTING, H. C. N90-11062
GOLDSTEIN, DAVID N90-11237
GOMEZDELCAMPO, J. N90-11625
GOMEZLERA, S. N90-11045
GOMEZMOLINERO, V. N90-11008
N90-11045
GONZALES, FRANCISCO N90-11021
GONZALEZ, C. F. N90-11128
GONZALEZBLASQUEZ, A. L. N90-11057
GOODRICH, ROBERT W. N90-11667
GORANSSON, P. N90-11009
GOTCH, S. M. N90-10918
GOURVEZ, PIERRE N90-11398
GOUTELARD, C. N90-11404
GOYAL, SURESH N90-11314
GRAHAM, L. N90-10958
GRAHAM, R. A. N90-11145
N90-11282
N90-11287
N90-11629
GRAHAM, WALTON N90-10843
GRAHN, PER N90-11691
GRANAAS, MICHAEL M. N90-11441
GRANNAN, ERIC RALPH N90-11141
GRANVILLE, A. N90-11475
GRASMEDER, R. F. N90-10926
N90-10964
GRATE, J. W. N90-11177
GRAVES, CHARLES EDWARD N90-11420
GRAY, G. T., III N90-11146
N90-11267
GRAY, LESLEY J. N90-11407
N90-11408
GREEN, M. A. N90-11347
GREENE, WILLIAM H. N90-11327
GREENGARD, LESLIE N90-11516
N90-11517
GREENWALD, R. A. N90-11394
GREER, J. T. N90-11323
GREFER, REINHARD N90-11137
GREGIS, J. L. N90-11078
GREGORY, JOHN C. N90-11689
GRIGSBY, R. D. N90-11117
GRUCHALLA, MICHAEL E. N90-11567
GRUEN, W. E. N90-11067
GU, C N90-11624
GUPTA, I. J. N90-11211
GUPTA, Y. M. N90-11107
GURNETT, DONALD A. N90-11587
GURWELL, W. E. N90-11122
GUTHRIE, PAUL D. N90-11406
N90-11407
GUYOT, GERARD N90-10864
GUZIK, JOYCE A. N90-11678

H

HAAS, CHRISTINA N90-11648
HAAS, W. N90-10896
HABING, H. J. N90-11663
HAGGARD, J. B. N90-11196
HAGINOYA, HIROBUMI N90-11652
HAHN, S. N90-11594
HAILE, JAMES E. N90-10881
HALD, H. N90-11030
HALDOUPIS, C. N90-11390
HALL, CHRIS N90-11383
HALLINGSTAD, ODDVAR N90-10648
HALLION, RICHARD P. N90-10882
HALVORSEN, WILLIAM G. N90-10999
HAMILTON, DAVID A. N90-10989
HAMILTON, HARRY D. N90-11430
HAN, J. H. N90-11579
HANBABA, RUDI N90-11398
HANRATTY, JOSEPH M. N90-11219
HANSEN, MERRILL N90-11160
HANUISE, C. N90-11394
HARDY, ANNE BAGLEY N90-11139
HARJES, H. C. N90-11595
HARRADINE, DAVID M. N90-10892
N90-11098
HARRIS, J. N. N90-11092
HARRIS, MICHAEL T. N90-11147
HARRIS, S. D. N90-10883
HARRISON, GEORGE C. N90-11466
HARTLEY, R. A. N90-10865
HARWOOD, RICHARD FRED N90-11253
HASBROUCK, R. T. N90-11238
HATHAWAY, MICHAEL D. N90-11245
HAUFLER, W. A. N90-10917
N90-10924
N90-10938
N90-10939
N90-10940
HAUG, E. N90-11071
HAVERKORT, BOUNDEWIJN R. N90-11479
HAYES, JOHN R. N90-11648
HAYES, M. H. B. N90-11164
HE, J. N90-10993
HEBNER, ROBERT E. N90-11343
HEERING, J. N90-11474
HEIDNER, RAYMOND F. N90-11300
HEISE, JAMES A. N90-11461
HELLER, JEANNE N90-11680
HELLSTEN, HANS N90-11691
HENDERSON, L. F. N90-11258
HENRIKSEN, T. K. N90-11029
HERMAN, WILLIAM ALEXANDER N90-11328
HERMANN, A. M. N90-11604
HERTZBERG, OLA N90-11194
HEURING, VINCENT P. N90-11564
HEYDARI, HUSCHANG N90-11561
HEYEN, W. N90-11006
HICKS, B. B. N90-11412
HICKS, JOHN W. N90-10866
HILLEN, L. W. N90-11080
HILLIS, S. L. N90-11319
HINDES, C. N90-11654
HINGORANI-NORENBERG, S. L. N90-11188
HINSDALE, L. W. N90-10932
N90-10954
N90-10960
N90-10973
HIOTT, J. M. N90-10920
HIRMAN, JOSEPH W. N90-11411
HIROMOTO, ROBERT N90-10839
HITCHENS, G. DUNCAN N90-11445
HO, C. N90-11591
HO, Y. L. N90-11576
HOANG, THU N90-11531
HODGE, PAUL W. N90-11661
HODGSON, J. W. N90-11319
HOELLER, FRANK STEFAN N90-11292
HOFFMAN, R. A. N90-11376
HOGSETT, WILLIAM E. N90-11353
HOLDEMAN, JONAS T. N90-10844
HOLDEN, K. A. N90-10927
HOLLAND, O. W. N90-11610
HOLLOWAY, JOHN S. N90-11300
HOLONYAK, N., JR. N90-11299
HOLT, S. S. N90-11280
HOPCROFT, JOHN E. N90-11462
HOPPEL, WILLIAM A. N90-11431
HORN, P. D. N90-11107
HORST, P. N90-10996
HORTON, W. N90-11669
HOWARD, B. S. N90-10928
HOWARTH, R. N90-11654
HSIEH, K. C. N90-11299
HSU, Y. N90-11332
HUANG, XUANGUO N90-11502
HUBBARD, DAVID C. N90-11218
HUEBEN-RIECHERT, WERNER N90-11632
HUERTA, C. N90-11045
HUESSLER, W. N90-10995
HUFF, FLOYD A. N90-11427
HULTBERG, RANDY S. N90-10829
HUMPHREY, DONALD L. N90-11144
HUNDSDORFER, W. H. N90-11530
HUPKE, FRANK N90-10849
HUST, JEROME G. N90-11142
HUTCHESON, J. D. N90-11228
HUYNH, HUNG T. N90-11497
HUYNH, M. N90-10974

I

IBRAHIM, S. R. N90-11028
ICARDI, U. N90-10998
IKEGAMI, TAKASHI N90-11450
IMBERT, J. F. N90-11070
IMBERT, J.-F. N90-11007
INGALLS, ROBERT L. N90-11118
INGEBC, ROBERT D. N90-11277
INGRAM, D. N90-11573
IRWIN, LORENE N90-11440
ISAKEN, IVAR N90-11407
ISO, AKIO N90-11050
IVENS, J. N90-11037

J

JACKMAN, CHARLES H. N90-11405
N90-11407
JACOBSON, NATHAN S. N90-11144
JAIN, M. N90-11043
JAJOO, H. K. N90-11130
JAMET, PH. N90-11068
JANG, HYYUN M. N90-11139
JANTER, T. N90-11006
JARZAB, W. W. N90-11013
N90-11022
JASPER, G. L. N90-10980
N90-10981
JEFFREY, Z. R. N90-11402
JELINSKY, PATRICK NEAL N90-11668
JERNEMALM, VEINE N90-11244
JESSUP, J. S. N90-11359
JIH, R.-S. N90-11507

JOHANSSON, E. M. N90-11518
JOHNSON, D. L. N90-11595
JOHNSON, J. P. N90-11238
JOHNSON, JAMES DANIEL N90-11189
JOHNSON, RUSSELL W. N90-11184
JOHNSON, SAMUEL B. N90-11315
JOHNSON, W. JOEL D. N90-11303
JOHNSTON, C. T. N90-11166
JONES, CHARLES R. N90-11106
JONES, E. D. N90-11627
JONES, G. O. L. N90-11382
JONES, LARRY A. N90-11581
JONES, MICHAEL E. N90-11239
N90-11593
JONES, N. L. N90-11625
JONES, T. B. N90-11385
N90-11399
JORDE, LEE C. N90-11690
JOSAFATSSON, KARL HINRIK N90-11672
JUDEIKIS, H. S. N90-11174
N90-11175
JUDGE, CHARLES N90-11356
JUDY, B. J. N90-11174
JUN, CHUL-WON N90-11096
JUST, MARCEL A. N90-11442

K

KAIZERMANN, S. N90-11283
KALINYAK, ROBERT G. N90-11218
KAMIYA, SUMIO N90-11139
KAMP, L. P. J. N90-11365
N90-11386
KANEKO, KUNIHIKO N90-11450
KANG, HYESUNG N90-11673
KARAGEORGHIS, ANDREAS N90-11495
KARLSSON, STEFAN N90-11293
KATOH, T. N90-11020
KATZIR, SHEVACH N90-10857
KAUFMAN, JOYCE J. N90-11143
KAWAHARA, HIROYASU N90-10898
N90-10899
KEDDY, CHRISTOPHER N90-11488
KEIPER, JERRY BRUCE N90-11522
KEISER, J. R. N90-11607
KELLEY, R. L. N90-11280
KELLY, A. P. N90-11184
KELLY, FRANCIS PETER N90-11423
KEPHART, ELISA M. N90-11649
KERSLEY, L. N90-11393
KETTLER, WILHELM HEINRICH N90-11155
KILBY, J. S. N90-11228
KILDUFF, JAN E. N90-11159
N90-11167
N90-11170
KIM, HYOUNG M. N90-11011
KIM, JIN WHAN N90-11251
KIMURA, TAKEO N90-10890
N90-11586
KINDEL, J. M. N90-11596
KINGERY, CHARLES N. N90-11260
KIPP, M. E. N90-11185
KIRK, M. A. N90-11612
KISS, FERENC N90-11046
KJELLGREN, JAN N90-11681
KLEIN, M. N90-10967
N90-11051
N90-11076
N90-11077
N90-11078
KLEM, J. F. N90-11627
KLEMETTI, W. L. N90-11373
KLINKHAMER, FRANS R. N90-11633
KLINT, P. N90-11474
KLUSOWSKI, E. N90-10992
KNIGHT, D. K. N90-11359
KO, MALCOLM K. W. N90-11407
N90-11408
KOBAYASHI, DOUGLAS N. N90-10877
KOEHLER, R. N90-10868
KOFFEND, JOHN B. N90-11300
KOHL, H. N90-11384
KOLONKO, J. N90-11297
KOLSCH, L. N90-11000
KONCINSKI, WALTER, JR. N90-11651
KONECNY, R. N90-11591
KOONTZ, STEVEN L. N90-11159
N90-11160
N90-11167
N90-11170
KOSENKA, P. N90-11174
KOSSEY, P. A. N90-11373
KOSSIRA, H. N90-10996
KOSTAS, J. G. N90-11231
KRAKOWSKI, R. A. N90-11577
N90-11589
KRANAKIS, EVANGELOS N90-11472
KRAUSE, H. F. N90-11625
KREIS, A. N90-11071
N90-11078
KRENKEL, W. N90-11030
KRETSCH, JEFFREY LEE N90-11486
KRIPPAHL, WOLFGANG N90-11135
KROES, ROGER L. N90-11195
KROLEWSKI, SUSAN M. N90-11087
KROPFLI, R. A. N90-10842
KROPP, J. L. N90-11196
KUBULAT, K. N90-11168
KUEHNAPFEL, MICHAEL N90-11598
KUHN, RODNEY N90-10855
KUO, CHENG-HSIUNG N90-11248
KUPER, JAN N90-11527
KURYSHKIN, V. V. N90-11640
KUTTY, K. V. G. N90-11129
N90-11130
KUWAO, F. N90-11020
KWOK, MUNSON A. N90-11300
KWON, OH JIN N90-11584

L

LACAIRE, STEVEN A. N90-11570
LACY, R. N90-11654
LADERACH, G. E. N90-11242
LALLEMENT, G. N90-10994
LANEVE, G. N90-11016
LANGE, H.-H. N90-10862
LARSON, REGINALD E. N90-11431
LARSSON, BJOERN N90-11691
LAUZZE, R. W. N90-10879
LAVIGNA, C. N90-10985
LAVIRON, B. N90-11002
LEASURE, C. S. N90-11180
LEBOEUF, J. N. N90-11579
LEBRUN, M. J. N90-11583
LECUYER, PIERRE N90-11508
LEE, CHIMPING CHESTER N90-11312
LEE, E. HENRY N90-11353
LEE, J. D. N90-11589
LEE, L. M. N90-11287
LEE, SUK-HO N90-11094
LEE, TIMOTHY J. N90-11552
N90-11553
N90-11554
LEINER, BARRY M. N90-11455
LEITH, C. E. N90-11257
LEMAIRE, J. N90-11362
LEONARD, ANTHONY N90-11263
LESAR, RICHARD N90-11557
LESTER, M. N90-11385
N90-11399
LEVIN, E. N90-11093
LEVY, RALPH N90-10835
N90-10836
LEWELLEN, DAVID C. N90-11634
LEWIS, LONZY J. N90-11358
LEWIS, S. N90-11174
LI, R. N90-11230
LIANG, D. F. N90-10851
N90-10852
LIEN, MARY M. N90-11150
N90-11152
LIEPINS, GUNAR E. N90-10844
LIEVEN, N. N90-10993
LIGNON, GERALD N90-10871
LIN-LIU, Y. R. N90-11618
LIN, SHENG-FUU N90-11485
LINDEMUTH, IRVIN R. N90-11592
LINDMAN, E. L. N90-11596
LINDQVIST, M. N90-11663
LINDSTROEM, STAFFAN N90-11691
LING, EDWARD NIGEL N90-11674
LIPP, LOUIE J. N90-11326
LISSILLOUR, M. N90-11400
LIST, R. S. N90-11624
LIU, DENGCHENG N90-11586
LIU, J. Z. N90-11612
LIU, KEFENG N90-11207
LIU, MIN-SHAN N90-11252
LIU, R. N90-11624
LIU, S. H. N90-11243
LOCKWOOD, M. N90-11382
LOGAN, B. G. N90-11589
LOGE, GARY W. N90-10892
LOMMASSON, T. C. N90-11345
LONG, W. C. N90-10967
LOPER, G. L. N90-11181
LOUGHRAN, E. D. N90-11267
LOUTER-NOOL, MARGREET N90-11483
LOWERY, H. J. N90-10917
N90-10924
N90-10927
LU, SHIH-YUAN N90-11086
LU, XIANGYU N90-11586
LUBER, W. N90-10992
LUCCHESINI, M. N90-10873
LUMIA, RONALD N90-11310
LYMAN, JOHN L. N90-10892
N90-11098
LYO, S. K. N90-11627
LYSTER, P. M. N90-11579

M

MAAS, S. A. N90-11236
MACK, EUGENE J. N90-11431
MACKISON, DONALD LEE N90-11643
MADRONICH, SASHA N90-11413
MAESTRELLI, P. N90-10873
MAJJIGI, R. K. N90-11549
MAMODE, A. N90-11010
N90-11017
MANDEL, L. N90-11213
MANFRIANI, L. N90-10873
MANSELL, R. S. N90-11172
MANTAY, WAYNE R. N90-10889
MANZANO, J. R. N90-11415
MANZELLA, DAVID H. N90-11081
MARCHETTI, M. N90-11033
MARCI, G. N90-11031
MARCONDES, SOLANGE PELLEGRINA BUENO N90-11447
MARCUS, R. A. N90-11545
MARHEFKA, R. J. N90-11209
MARLEY, STEPHEN ROGER N90-11657
MARRO, L. N90-11052
MARSH, S. P. N90-11197
MARTIN, CHARLES R. N90-11227
MARTIN, COLIN A. N90-10829
N90-10888
MARTIN, R. L. N90-11605
MARTIN, T. H. N90-11595
MARTINEZ, DAVID R. N90-11240
MARYNICK, DENNIS S. N90-11148
MASON, R. J. N90-11593
MASON, RODNEY J. N90-11239
N90-11585
MASSIS, T. M. N90-11191
MASSONI, J. A. N90-11019
MATHEWS, C. K. N90-11104
MATT, D. R. N90-11412
MATTHEWS, H. E. N90-11663
MAUDE, R. N90-11399
MAUELSHAGEN, H.-P. N90-11387
MAYBECK, PETER S. N90-10853
MAYNARD, JULIAN D. N90-11551
MAYNARDDELAVALETTE, GUY N90-10854
MAZDIYASNI, K. S. N90-11618
MAZZELLA, ANDREW J., JR. N90-11570
MCALLISTER, DAVID F. N90-11460
MCCAIN, HARRY G. N90-11310
MCCLUNG, R. W. N90-11279
MCCORMICK, A. N90-11573
MCCREA, I. W. N90-11385
MCCURDY, MICHAEL L. N90-11514
MCDANIEL, D. H. N90-11596
MCDONALD, DAVID G. N90-11440
MCDOUGAL, JAMES N. N90-11182
MCDUFF, GEORGE GLEN N90-11295
MCGAVRAN, LAUREN N90-11478
MCGEER, PATRICK C. N90-11452
MCGILL, R. N. N90-11319
MCGOVERN, DOUGLAS E. N90-11324
MCGRAIN, MOIRA N90-11228
MCGRATH, MELISSA ANN N90-11682
MCGREGOR, ROBERT N90-11650
MCKENNEY, BARBARA L. N90-11228
MCLAIN, DOUGLAS R. N90-11434
MCLAUGHLIN, T. D. N90-10925
MCMILLAN, J. C. N90-10852
MCMILLEN, R. T. N90-11412
MCNAMARA, L. F. N90-11403
MCNAMEE, JOHN BERTRAM, JR. N90-11294
MCNEELY, M. N90-10927
MCNICE, G. T. N90-11425
MCNICOLL, W. J. N90-10927
MCQUEEN, R. G. N90-11197
MCQUILLAN, B. W. N90-11618
MEBIUS, J. E. N90-11477
N90-11484
MEDIAVILLA, ANTHONY SCOTT N90-10921
N90-10947
MEDLER, CHARLES L. N90-11433
MEEKS, KENT D. N90-11569
MEISBURGER, EDWARD P. N90-11356
MENDEL, C. W., JR. N90-11596
MENIKOFF, RALPH N90-11266

MENNECIER, PHILIPPE N90-10854
MENON, P. K. A. N90-11487
MENSO, G. N90-10869
MERCIER, F. N90-11010
N90-11049
MERLET, J. N90-11040
MESSIER, DONALD R. N90-11088
MESZAROS, P. S. N90-11559
METHFESSEL, SIEGFRIED N90-11619
MEYER, H.-L. N90-10862
MEYER, PAUL N90-11284
MEYER, ROBERT R., JR. N90-10678
MEZACHE, MAHMOUD N90-11329
MICHOSKI, U. F. N90-11635
MIDDLETON, P. T. N90-11402
MIELKE, R. W. N90-10932
MIESEN, R. H. M. N90-11365
N90-11386
MIKOYAN, STEPAN ANASTASOVICH N90-10904
MILLER, E. L. N90-11180
MILLER, J. R. N90-11589
MILLER, P. D. N90-11625
MILLER, R. L. N90-11577
MILLMAN, GEORGE H. N90-11401
MIRONOV, V. E. N90-11308
MIROSHNICHENKO, V. F. N90-11149
MISRA, AJAY K. N90-11144
MITCHELL, A. C. N90-11683
MITCHELL, T. E. N90-11154
MITSUMA, H. N90-11020
MOFFATT, WILLIAM C. N90-11139
MOHR, D. L. N90-11092
MOLINA, J. N90-11045
MOLINER, A. M. N90-11165
MONTAG, BRUCE C. N90-10911
MONTEGAZZA, P. N90-11012
MONTEIRO, ANTONIO MIGUEL VIEIRA N90-11447
MONTGOMERY, A. D. N90-10926
N90-10944
N90-10964
MONTGOMERY, F. C. N90-11618
MONTOYA, N. I. N90-11290
MOOK, H. A. N90-11630
MOONEY, G. D. N90-11604
MOORE, L. M. N90-11282
N90-11287
MORGAN, M. GRANGER N90-11439
MOROSIN, B. N90-11629
MORRIS, C. E. N90-11267
MORRISON, GERALD L. N90-11255
MORROW, JOHN G. N90-10897
MORTARI, D. N90-11016
N90-11047
MORTENSEN, G. F. N90-11267
MOSES, JULIE JOAN N90-11421
MOSS, C. E. N90-11280
MOUNIR, H. N90-11392
MTINGWA, S. N90-11591
MUEHLBAUER, K. N90-11039
MUELLER, B. N90-11120
MUENCH, H. STUART N90-11432
MUENCH, ROBIN D. N90-11436
MUKHERJEE, RESHMI N90-11662
MULDER, J. C. N90-11480
MULHOLLAND, J. P. N90-11176
MUNSHI, M. Z. A. N90-11235
MUROYAMA, JANET H. N90-11645
MURPHY, BRIAN D. N90-10844
MURPHY, JAMES B. N90-11547
MURPHY, KATHERINE A. N90-11511
MURPHY, OLIVER J. N90-11445
MURR, L. E. N90-11127

N

NAIR, INDIRA N90-11439
NAITO, SHINJIRO N90-11652
NAKAMURA, K. N90-11020
NAMA, P. N90-11179
NAOI, KATSUHIKO N90-11150
N90-11151
N90-11152
NARAYANAN, S. N90-11347
NATESAN, K. N90-11623
NEAU, E. L. N90-11595
NELLIS, W. J. N90-11683
NESBITT, JAMES A. N90-11082
NEUFFER, DAVID V. N90-11544
NG, W. C. N90-11241
NICOLAIDES, R. A. N90-11498
NIEDBAL, N. N90-10992
NIEMEGEERS, IGNAS G. N90-11479
NIEMINEN, I. N90-11234
NIEUWENHUIZEN, M. P. N90-10990
NIKITIN, S. A. N90-10905
NILSSON, HELENA N90-11121
NISHIWAKI, HIDEO N90-11344
NOOR, AHMED K. N90-11457
NORD, ARLO R. N90-11240
NOREM, J. N90-11591
NOTHWANG, DAVID P. N90-11581
NOVICK-COHEN, AMY N90-11114
NUTTALL, ALBERT H. N90-11533
NYBERG, SVEN N90-11341
NYGARD, M. K. N90-11035

O

OBERLE, WILLIAM F. N90-10910
OCKERS, S. T. N90-11612
ODONNELL, R. A. N90-10920
N90-10938
N90-10939
N90-10940
N90-10966
OERY, H. N90-10995
OHR, SANG Y. N90-10844
OKABE, MASANORI N90-10899
OLDENBORG, RICHARD C. N90-10892
N90-11098
OLIU, WALTER E. N90-11647
OLNON, F. M. N90-11663
OLSEN, D. K. N90-11306
OLSON, C. G. N90-11624
OLTHOFF, JAMES K. N90-11343
OPANASENKO, A. V. N90-11597
ORHAUG, TORLEIV N90-11341
ORR, JOHN L. N90-11438
OSBORNE, WILMA M. N90-11458
OTTERSTEN, HANS N90-11691
OU, L.-T. N90-11171
OUGHSTUN, KURT E. N90-11220
OWEN, R. W. N90-11228
OWENS, BOONE B. N90-11150
N90-11151
N90-11235
OWICKI, SUSAN N90-11468
OYAMA, K. N90-11369
OZOEMENA, P. C. N90-11500

P

PACIESAS, WILLIAM S. N90-11689
PACK, RUSSELL T. N90-11098
PAGEL, PETER N90-11225
PAISLEY, D. L. N90-11288
N90-11290
PAK, S. S. N90-11618
PALM, HANS CHRISTIAN N90-11459
PAN, W. S. N90-11113
PANCHAL, C. N90-11349
PANTON, RONALD L. N90-11264
PAPAGEORGIOU, D. T. N90-10833
PARISSE, M. N90-11016
PARK, A. N90-11603
PARK, J. H. N90-11623
PARKER, S. R. N90-11518
PARKMAN, WILLIAM E. N90-10934
PASQUET, JEAN-CLAUDE N90-11070
PASTERNAK, M. P. N90-11620
PATEL, N. R. N90-10839
PATIN, J. F. N90-11054
PATTON, JEFF A. N90-10933
PAUL, ADOLF K. N90-11372
PAUL, D. J. N90-10919
N90-10938
N90-10939
N90-10940
PEARLE, PHILIP N90-11540
PELRINE, RONALD EDWARD N90-11542
PENNYCOOK, S. J. N90-11610
PEREIRADASILVA, N. L. P. N90-11635
PERIASWAMI, G. N90-11104
PERKINS, LOUISE N90-11519
PERRY, R. B. N90-11283
PERSON, W. B. N90-11168
N90-11169
PESTOV, A. B. N90-11541
PETERSEN, KEVIN L. N90-10866
PETIAU, C. N90-11058
PETTERSSON, HANS N90-11342
PETTIT, D. R. N90-11190
PFRANG, W. E. N90-11022
PHELAN, PATRICK F. N90-11488
PHILLIPS, LOUIS C. N90-11285
PHILLIPS, TIMOTHY N. N90-11495
PHILUSHAKIN, V. N90-11408
PICK, HERBERT L. N90-11340
PICKERELL, THOMAS N90-10855
PIETZ, K. C. N90-10920
N90-10924
PINDZOLA, MICHAEL S. N90-11563
PINELLI, THOMAS E. N90-11647
PINK, P. N. N90-11359
PIPKINS, JAMES F. N90-11217
PIRANDA, J. N90-10994
PITATELEV, G. V. N90-11597
PLOTARD, P. N90-11056
POLKA, LESLEY A. N90-11206
POMERANTZ, MARTIN N90-11148
PONTOPPIDAN, K. N90-11052
PONZI, U. N90-11044
PORTER, ROGER E. N90-10887
PORTER, ROGER S. N90-11089
N90-11090
POWER, JOHN F. N90-11303
PRAGER, S. C. N90-11576
PRATHER, MICHAEL J. N90-11405
PRATT, JONATHAN P. N90-11564
PREECE, D. S. N90-11543
PRELEC, KRSTO N90-11562
PRESTWICH, K. R. N90-11595
PRIEDHORSKY, W. N90-11280
PRIOU, N. N90-11049
PRIOVOLOS, GEORGE N90-10859
PROCTOR, ROBERT W. N90-11443
PROELSS, G. W. N90-11381
PRONKO, P. N90-11573
PRUST, C. D. N90-10919
PRUST, E. E. N90-10932
N90-10961
N90-10973
PUCKETT, E. G. N90-11258
PULSIPHER, B. A. N90-11489
PUPYSHEV, V. V. N90-11524
PYLE, J. A. N90-11408

Q

QUINTENZ, J. P. N90-11596

R

RAASCH, W. N90-11039
RABAS, T. N90-11349
RAFFAELLI, GARY G. N90-10937
N90-10948
N90-10950
N90-10951
RAFTERY, ADRIAN E. N90-11357
RAI, A. N90-11573
RAI, HABIB GERGES N90-11084
RAJAGOPALAN, S. N90-11129
N90-11130
RAJANBABU, S. S. N90-11104
RAJESHWAR, KRISHNAN N90-11148
RAKOWSKI, MARK N90-11636
RAKOWSKY, G. N90-11297
RAMAER, M. N90-11526
RAMIREZ, J. J. N90-11595
RAMOS, H. F. N90-10885
RAO, K. NARAHART N90-11111
RARIDON, R. J. N90-11559
RASMUSSEN, J. E. N90-11373
RAWER, E. N90-11366
RAYMER, MICHAEL G. N90-11307
RAYNER, JOHN THORNTON N90-11656
RAZANI, A. N90-11188
REDEKER, A. N90-10886
REDFIELD, JOE B. N90-10911
REE, FRANCIS H. N90-11099
REED, R. P. N90-11287
REES, D. N90-11380
N90-11382
REEVE, T. GILMOUR N90-11443
REGINATO, L. L. N90-11589
REICH, SIMEON N90-11494
REID, R. A. N90-11449
REIFSNIDER, KENNETH L. N90-11053
REIMERDES, H. G. N90-11075
REINISCH, B. W. N90-11396
REISS, DONALD A. N90-11195
RESCIGNO, T. N. N90-11558
REYNOLDS, J. N90-11077
REYNOLDS, J. W. N90-11117
REYNOLDS, JOHN R. N90-11148
RHEA, DONALD C. N90-11441
RHINE, WENDELL E. N90-11139
RHODEHAMEL, HARLEY N90-10859
RICCIO, J. R. N90-10916
N90-10929
N90-10930
N90-10935

RICH, RONALD E. N90-11088
RICHARD, BILL N90-10958
N90-10971
RICHARDS, WHITMAN N90-11465
RICHTER, KAREN J. N90-11491
RICKS, E. N90-11077
RIDEAU, P. N90-11005
RIEKER, T. P. N90-11628
RIMINI, ALBERTO N90-11540
RINNERT, K. N90-11378
RISHBETH, H. N90-11367
N90-11371
RIVERA, ANGEL L. N90-11490
ROBERTS, R. A. N90-11325
ROBINSON, T. R. N90-11385
ROBINSON, W. M. N90-10946
N90-10967
ROBINSON, W. W. N90-10936
N90-10945
N90-10965
ROCHAU, G. E. N90-11596
ROCKETT, A. N90-11345
RODEBACK, G. W. N90-11286
RODGER, A. S. N90-11371
N90-11393
RODIN, A. M. N90-11291
ROELOF, E. N90-11397
ROENNMARK, KJELL N90-11599
ROGERS, J. W., JR. N90-11191
ROGERS, PATRICIA G. N90-11680
ROHLF, D. N90-10862
ROHWEIN, G. J. N90-11595
ROHWER, K. N90-11034
ROKHLIN, V. N90-11516
ROMANYUK, L. I. N90-11597
RONDENBURG, P. H. N90-11528
RONKAINEN, H. N90-11234
ROSE-PEHRSSON, S. L. N90-11177
N90-11178
ROSEN, I. G. N90-11494
ROSENQUIST, GUNNAR N90-11691
ROSENQUIST, TONY N90-11193
ROSENTHAL, DAVID A. N90-11411
ROSENTHAL, LYNNE S. N90-11448
ROSENZWEIG, J. B. N90-11591
ROSIM, SERGIO N90-11447
ROSING, M. N90-11591
ROSSOWSKY, RAM N90-11619
ROSTOKER, GORDON N90-11363
ROTHE, K. E. N90-11559
ROTHMANN, BETH N90-11454
ROUCHON, M. N90-11074
ROUNBEHLER, D. N90-11179
ROWE, J. N90-11043
ROY, N. A. N90-11007
ROY, PH. N90-11054
ROY, T. N90-11154
RUNYAN, W. R. N90-11228
RUOHONIEMI, J. M. N90-11394
RUPPEL, F. R. N90-11278
RUSSEL, THOMAS J. N90-11303
RYAN, E. A. N90-11612
RYLAH, P. J. N90-11399

S

SACH, E. D. N90-10988
SADEH, NORMAN N90-11506
SAFINYA, C. R. N90-11628
SAGDEYEV, ROALD ZINNUROVICH N90-10906
SAIF, A. G. N90-11614
SAIIDI, M. J. N90-10925
N90-10957
N90-10974
N90-10977
SAKURAI, YOSHIO N90-11566
SALES, G. S. N90-11396
SANCHEZCERCOS, J. N90-11008
SANDEN, ROLAND N90-11193
SANDEWALL, ERIK N90-11537
SANDUSKY, K. N90-11669
SANKAR, J. N90-11091
SANKOVICH, D. P. N90-11525
SARAVIA, EDUARDO N90-11217
SAS, P. N90-11006
SATIKOV, I. A. N90-11541
SAVAGE, M. E. N90-11596
SAXON, H. N90-10958
N90-10971
SCHAENZER, GUNTHER N90-10870
SCHENK, A. N90-11026
SCHILDT, U. N90-11039
SCHINKER, M. G. N90-11204
SCHLEGEL, K. N90-11369
N90-11387
SCHMECKPEPER, K. R. N90-10941
N90-10942
SCHMIDT, G. N90-11042
SCHNEID, J. N90-11530
SCHNEIDER, L. X. N90-11242
N90-11595
SCHOENEMAN, J. LEE N90-11324
SCHOESSOW, P. N90-11591
SCHONE, H. N90-11625
SCHOTT, GARRY L. N90-10892
N90-11098
SCHRIVER, KAREN A. N90-11648
SCHULZ, M. N90-11625
SCHUNK, R. W. N90-11375
N90-11397
SCHWEGLER, FLORIAN N90-10849
SCROGER, M. G. N90-11274
SCROSATI, B. N90-11235
SEALS, ROBERT K., JR. N90-11405
SELLECK, COLIN B. N90-11649
SELLMANN, PAUL V. N90-11435
SELVAGGI, B. N90-11235
SEMENYUK, N. I. N90-11149
SENGERS, J. V. N90-11102
SENGUPTA, SUBRATA N90-11262
SENIOR, CATHERINE N90-11377
N90-11394
SEO, JIN H. N90-11512
SERFOZO, RICHARD F. N90-11515
SETCHELL, R. E. N90-11185
SEUME, JOERG REINHART N90-11249
SGUBINI, S. N90-11014
SHAFFER, TIMOTHY D. N90-11148
SHAH, P. P. N90-11184
SHAHINPOOR, M. N90-11188
SHANAHAN, WILLIAM R. N90-11581
SHAPIRO, S. M. N90-11119
SHAW, M. S. N90-11267
SHEFFIELD, STEPHEN A. N90-11186
SHELDON, RICHARD B. N90-11123
SHELNUTT, J. A. N90-11097
SHEN, S. S. N90-11590
SHEPHERD, RONNIE L. N90-11581
SHIBUYA, I. N90-11631
SHICKLE, W. A. N90-11087
SHIN, HYUN JOON N90-11096
SHINGU, HIROKIMI N90-11276
SHOLLENBERGER, SCOTT N90-10856
SHUKLA, A. K. N90-11399
SHUMWAY, R. H. N90-11507
SIDORCHUK, S. I. N90-11291
SIEGMAN, A. E. N90-11302
SILVESTRO, J. W. N90-11209
SIMONEN, E. P. N90-11125
SIMPSON, J. N90-11591
SINCLAIR, S. K. N90-10971
N90-10979
SINCLAIR, SUSAN N90-10958
SINGAL, R. K. N90-10991
N90-11027
SINHA, ALOK N90-10893
SIPPEL, R. N90-11038
SIZUN, H. N90-11400
SKEEL, ROBERT D. N90-11523
SKOCYPEC, R. D. N90-11101
N90-11191
SLATE, E. N90-11654
SLAUGHTER, W. T. N90-10944
N90-10952
N90-10953
SLUIJTER, F. W. N90-11365
N90-11386
SMITH, DAVID R. N90-11142
SMITH, I. D. N90-11176
SMITH, JOEL B. N90-11350
N90-11351
N90-11352
SMULLEN, R. R. N90-10883
SMYRL, WILLIAM H. N90-11150
N90-11151
N90-11152
SMYTH, CHRISTOPHER C. N90-11467
SODHI, CHRISTOPHER N90-11273
SOJKA, J. J. N90-11375
SOKOLOV, S. N. N90-11464
SOLOMAN, SUSAN N90-11407
SOLOMON, HERBERT N90-11534
SOMMEIJER, B. P. N90-11476
N90-11529
SONNENSCHEIN, JACOB N90-11639
SOONG, KUEIMING N90-11336
SOUCY, Y. N90-10991
SOUGANIDIS, P. E. N90-11510
SPANNER, G. E. N90-11346
SPENCER, W. J. N90-11190
SPOTZ, MARK N90-11139
SPROUL, A. B. N90-11347
SPURGEON, SARAH KATHERINE N90-10895
STAHL, D. B. N90-11290
STAROSTIN, V. A. N90-11613
STARR, T. L. N90-11092
STAVRINIDIS, C. N90-11028
N90-11071
STECKL, A. J. N90-11113
STEEL, DUNCAN G. N90-11301
STEELE, T. N90-11027
STEFANIK, RAYMOND J. N90-11574
STEIN, H. J. N90-11594
STEIN, WILLIAM E. N90-11303
STEINOLFSON, R. N90-11669
STEINVALL, OVE N90-11309
N90-11575
STEPHENS, M. A. N90-11534
STEPHENS, R. B. N90-11618
STEVER, H. GUYFORD N90-11645
STEWART, G. R. N90-11609
STILLMAN, G. E. N90-11299
STOLOFF, NORMAN S. N90-11615
STONE, DANIEL A. N90-11157
N90-11161
N90-11162
N90-11166
N90-11168
STONE, HUGH M. N90-11424
STONE, M. A. N90-11208
STORCH, STEVEN B. N90-11215
STOTTS, R. N90-11654
STRAIN, JOHN N90-11517
STRAZHEV, V. I. N90-11541
STRAZISAR, ANTHONY J. N90-11245
STREET, J. J. N90-11165
N90-11171
STRIP, D. N90-11322
STUREK, W. B. N90-10839
SU, RENJENG N90-11513
SU, TZU-JENG N90-11011
SUCHY, K. N90-11364
SUDER, KENNETH L. N90-11245
SUGIYAMA, NAOSHI N90-11679
SULKANEN, MARTIN ERICK N90-11675
SULLIVAN, WILLIAM F. N90-11660
SUME, AIN N90-11691
SURVANSHI, SHALINI S. N90-11284
SUZUKI, MASAYO N90-11662
SWAIN, L. J. N90-10960
SWAN, DAVID H. N90-11255
SWANSON, ROGER W. N90-11401
SWARTZ, A. B. N90-11176
SWEENEY, M. A. N90-11596
SWEGLE, J. W. N90-11414
SWORSKI, THOMAS J. N90-10844
SZABO, SANDRA M. N90-11448
SZCZESNIAK, M. N90-11169
SZCZESPANSKI, J. N90-11169
SZE, NIEN DAK N90-11408
SZUSZCZEWICZ, EDWARD P. N90-11397

T

TACCHINO, EDOARDO N90-11032
TAFFE, P. A. N90-11178
TAIEB, C. N90-11370
TAJIMA, T. N90-11583
N90-11669
TAKAHASHI, T. N90-11369
TAKAYAMA, M. L. N90-11181
TAKEDA, KATSUMI N90-11344
TAKIMOTO, H. N90-11174
TAKIZAWA, MINORU N90-10890
TALIEH, H. N90-11345
TAM, HON-WAH N90-11523
TAN, T. H. N90-11197
TANABE, YOSHIKAZU N90-11653
TANAKA, KEIJI N90-10898
TANG, S. Y. N90-11117
TANGORRA, F. N90-10926
N90-10964
TANI, KEIJI N90-11652
TANTON, N. E. N90-11208
TARNG, TOM SHINMING-T.K. N90-11296
TARVER, C. M. N90-11192
TAUB, RENEE G. N90-11228
TAYLOR, L. M. N90-11543
TAYLOR, PAUL A. N90-11124
TAYLOR, PETER R. N90-11554
TAYLOR, R. DEAN N90-11620
TELLER, EDWARD N90-11608
TENTHIJTEBOONKKAMP, J. H. M. N90-11271
TERIELE, H. J. J. N90-11475
THEILHABER, K. N90-11223
THELEN, HANS-GUENTER N90-11270

THOMAS, E. C. N90-11399
THOMAS, V. A. N90-11593
THOMPSETT, D. N90-11163
THOMPSON, J. D. N90-11624
THOMPSON, L. J. N90-11612
THOMPSON, WILLIAM B. N90-11340
THOMSON, J. S. N90-11117
THORNTON, J. A. N90-11345
TIMAKOV, V. A. N90-11291
TINGEY, DAVID T. N90-11353
TIPTON, T. N90-11168
TIRPAK, DENNIS A. N90-11350
N90-11351
N90-11352
TIZZI, S. N90-11033
TOBISKA, WILLIAM KENT N90-11686
TOKAR, G. N90-11022
TOKUNAGA, M. N90-11631
TONEV, TOMA V. N90-11504
N90-11505
TORODE, H. A. N90-10876
TORRE, A. N90-11298
TRAHAN, W. H. N90-10920
N90-10961
N90-10967
TRAINI, E. N90-10863
TRAINOR, R. JAMES, JR. N90-11581
TRAVES, S. T. N90-10922
TRENT, WILLIAM N90-10855
TRESSET, JACQUES N90-10874
TRIVEDI, KISHOR N90-11454
TROTT, WAYNE M. N90-11569
TRUCANO, TIMOTHY G. N90-11103
TRUDELL, D. E. N90-11097
TSAI, TOMMY M. N90-10835
N90-10836
TSENG, VERONICA PENG N90-11646
TSUJIHATA, A. N90-11020
TSUKASHIMA, T. N90-11020
TSUTSUMI, YUJI N90-11050
TUAZON, E. C. N90-11158
TUKEY, JOHN W. N90-11531
TULUNAY, Y. K. N90-11374
TUNG, K. K. N90-11407

U

UCHIDA, TADAO N90-10890
UENISHI, K. N90-11549
ULLMAN, SHIMON N90-11465
UM, CHUNG-IN N90-11096
UNAL, AYNUR N90-10828
UNAL, O. N90-11154
UPADHYAY, TRIVENI N. N90-10859
URBANOWICZ, KENNETH J. N90-10954
URTIEW, P. A. N90-11192

V

V.D.HOEVEN, G. F. N90-11526
VAANDRAGER, FRITZ W. N90-11492
VACHER, PIERRE N90-10854
VAITEKUNAS, J. J. N90-11325
VALA, M. N90-11168
N90-11169
VALENT, R. N90-11078
VANDAMME, RUUD N90-11535
VANDELUNE, J. N90-11475
VANDERGAAG, L. C. N90-11536
VANDERHOUWEN, P. J. N90-11476
N90-11529
VANDERVELDE, R. L. N90-10884
VANDERVELDE, WALLACE E. N90-10859
VANDEVENDER, J. PACE N90-11595
VANDOORN, J. T. M. N90-10884
VANE, C. R. N90-11625
VANGLABBEEK, R. J. N90-11528
VANMOURIK, P. A. N90-11529
VANSINDEREN, MARTEN N90-11471
VANUFFELEN, J. P. N90-11404
VARJUS, S. N90-11234
VELTKAMP, J. PETER N90-11535
VENNE, L. J. N90-11127
VENTURINI, E. L. N90-11629
VERNE, C. N90-11074
VERPOEST, I. N90-11037
N90-11063
VIDAL, C. N90-10987
VIGNERON, F. R. N90-10991
N90-11027
VILA, PAUL N90-11379
N90-11398
VINCENT, KENNETH A. N90-11214
VINSON, T. S. N90-10896
VOGEL, F. N90-11075
VOUK, MLADEN A. N90-11460

W

WADA, B. K. N90-11001
WADDELL, M. D. N90-10879
WADE, DONALD C. N90-10989
WAGNER, JAMES C. N90-11285
WAKAIRO, KAORU N90-10899
WALKER, J. D. A. N90-11250
WALKER, R. A. N90-11487
WALLACE, J. M. N90-11264
WALLACE, JAMES M. N90-11259
WALTERS, G. K. N90-11556
WANDINGER, H. N90-11024
WANG, JYH-CHYANG ALEX N90-10838
WANG, X. N90-11297
WANG, XIANYU N90-11586
WARDLE, MARK JOHN N90-11665
WARNE, L. K. N90-11231
WARNER, GORDON E. N90-10844
WARNER, N. P. N90-11538
WATANABE, AKIRA N90-10899
WEATHERSBY, PAUL K. N90-11284
WEBB, B. J. N90-11265
WEBB, DERRICK S. N90-10984
WEBER, H. W. N90-11612
WEBER, RUEDIGER N90-11226
WECHSLER, DONALD B. N90-11451
WEIJLAND, W. P. N90-11481
WEINACHT, DANIEL J. N90-11469
WEISENSTEIN, DEBRA N90-11408
WEISS, ROSANNE M. N90-10897
WEISSINGER, D. N90-10966
WEISSINGER, W. D. N90-10943
WEISSKOPF, KARL-L. N90-11138
WENDERLICH, NEAL D. N90-11449
WENHAM, S. R. N90-11347
WERLEY, K. A. N90-11577
WEST, B. H. N90-11319
WESTWATER, E. R. N90-10842
WEVERS, M. N90-11037
N90-11063
WHEALTON, J. H. N90-11559
WHITE, G. D. N90-11122
WHITE, RALPH E. N90-11227
WHITING, GARY S. N90-11116
WIELAND, U. N90-11076
WIESLER, D. G. N90-11119
WILCOTS, ERIC M. N90-11661
WILFERT, G. L. N90-11346
WILLIAMS, JAMES H., JR. N90-10984
WILLIAMS, S. J. N90-11356
WILSON, D. F. N90-11607
WILSON, R. E. N90-10916
N90-10929
N90-10930
N90-10935
N90-10959
N90-10968
N90-10970
N90-10975
WINKELHOFF, E. N90-11072
WINKLER, C. N90-11402
WINN, KENNETH R. N90-10892
WINNBERG, A. N90-11683
WINSER, K. J. N90-11382
WINSKE, D. N90-11416
N90-11588
N90-11593
WISEMAN, FLOYD L. N90-11157
N90-11161
N90-11162
WITHROW, S. P. N90-11610
WITTBERG, THOMAS N. N90-11133
WOLF, CHRISTOPHER J. N90-10897
WOLF, R. A. N90-11397
WOMERSLEY, W. J. N90-11281
WOO, JAMES T. N90-11217
WOOD, JERRY R. N90-11245
WOOD, R. F. N90-11622
WOOD, W. E. N90-11127
WOOLLAM, J. N90-11573
WRENN, G. L. N90-11371
WU, R. N90-11573

X

XIE, WEIDONG N90-11586
XIZENG, LI N90-11213
XU, SENLIN N90-11539
XU, YU-LIN N90-11658

Y

YAMAMOTO, KAZUO N90-11050
YANG, A. B. N90-11624
YEH, CAVOUR N90-11571
YEH, K. C. N90-11391
YEN, JOHN N90-11650
YEOMAN, TIMOTHY KENNETH N90-11422
YIN, XIEJIN N90-11586
YING, SHAN N90-11213
YNGSTROEM, STEN N90-11641
YOKOTA, JEFFREY W. N90-11497
YOO, C. S. N90-11107
YOO, GEUN JONG N90-10832
YORMAH, T. B. R. N90-11164
YU, S. K. T. N90-11117
YUNG, YUK L. N90-11407
N90-11408

Z

ZABEL, H. N90-11119
ZACH, A. N90-10862
ZACKRO, W. C. N90-11184
ZAFINDRATAFA, G. N90-11501
ZAYTSEV, YU. I. N90-10903
ZGELA, MIRKO B. N90-10877
ZHANG, JIANDE N90-11586
ZHOU, JIAN N90-11539
ZHOU, JUN N90-11425
ZILLIAC, GREGORY G. N90-11254
ZIMMERMAN, TOM N90-11229
ZING, CHRISTOPHE N90-11139
ZOLPER, J. C. N90-11347
ZOLTANI, CSABA K. N90-11261
ZOMERMAN, I. N90-10896
ZORIN, A. V. N90-11640
ZUO, FULIN N90-11140
ZUREK, ANNA K. N90-11131
ZUREK, RICHARD W. N90-11408

Typical Corporate Source Index Listing

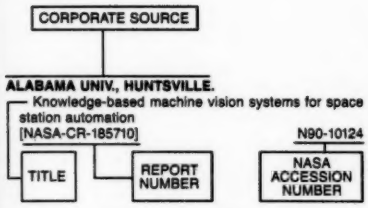

Listings in this index are arranged alphabetically by corporate source. The title of the document provides the user with a brief description of the subject matter. The report number helps to indicate the type of document cited (e.g., NASA report, translation, NASA contractor report). The NASA accession number denotes the number by which the citation is identified. The titles are arranged under each corporate source in ascending accession number order.

A

ACADEMY OF SCIENCES (USSR), NOVOSIBIRSK.
Resonance effect on the oscillator distribution function [DE89-630105] N90-11548

ADVISORY GROUP FOR AEROSPACE RESEARCH AND DEVELOPMENT, NEUILLY-SUR-SEINE (FRANCE).
Kalman Filter Integration of Modern Guidance and Navigation Systems [AGARD-LS-166] N90-10847
Flight Test Techniques [AGARD-CP-452] N90-10860
Ionospheric Structure and Variability on a Global Scale and Interactions with Atmosphere and Magnetosphere [AGARD-CP-441] N90-11361

AERITALIA S.P.A., CASELLE TORINESE (ITALY).
In flight relight tests on AM-X single engine fly-by-wire aircraft N90-10869
Flight testing a newly-designed stand-off weapon dispenser N90-10880

AERITALIA S.P.A., TURIN (ITALY).
Material properties of 2219-T851 aluminum alloy plasma welded compared to TIG welding N90-11032

AERODATA FLUGMESSTECHNIK G.M.B.H., BRUNSWICK (GERMANY, F.R.).
Realtime processing and display N90-10886

AERONAUTICA MACCHI S.P.A., VARESE (ITALY).
Results and practical experience using parameter identification techniques on the AM-X program at Aermacchi N90-10873

AERONAUTICAL RESEARCH INST. OF SWEDEN, BROMMA.
Calculation of sound transmission through a cylindrical shell using ASKA acoustics N90-11009

AERONAUTICAL RESEARCH LABS., MELBOURNE (AUSTRALIA).
The spinning of aircraft: A discussion of spin prediction techniques including a chronological bibliography [ARL-AERO-R-177] N90-10888
A simulator for a hydrocarbon ramrocket fuel gas generator: First phase development [AR-005-621] N90-11080

AEROSPACE CORP., EL SEGUNDO, CA.
A general-purpose computer program for the Volterra-series analysis of nonlinear microwave circuits [AD-A210768] N90-11236
Dissociation and vibrational relaxation of XeF by various collision partners [AD-A210769] N90-11300

AEROSPACE CORP., LOS ANGELES, CA.
Modeling the ozonolysis of hydrazines wastewater N90-11175
Low ppb level detection of toxic compounds with a fully automated CO2 laser photoacoustic detector N90-11181

AEROSPACE ENGINEERING TEST ESTABLISHMENT, COLD LAKE (ALBERTA).
CF 18 480 Gallon External Fuel Tank Stores Clearance Program N90-10877

AEROSPACE MEDICAL RESEARCH LABS., WRIGHT-PATTERSON AFB, OH.
Occupational safety considerations with hydrazine N90-11182

AEROSPATIALE, CANNES (FRANCE).
Evaluation of tests and design factors N90-10987
GEMMES: A new tool for dynamic modeling N90-11005
ESA-D: An integrated software for antenna design and analysis N90-11052
Deployment simulation for 3rd generation solar array GSR3 N90-11074

AEROSPATIALE, CHÂTILLON (FRANCE).
Telescope structure for cryogenic application N90-11019

AEROSPATIALE AQUITAINE, SAINT-MEDARD EN JALLES (FRANCE).
Space environment effects on carbon/epoxy materials N90-11056

AGRICULTURAL RESEARCH SERVICE, BELTSVILLE, MD.
Assessment of crop response to increases in atmospheric carbon dioxide concentrations: Summary of research progress report, July 1, 1988--June 30, 1989 [DE89-016251] N90-11360

AIR FORCE ENGINEERING AND SERVICES CENTER, TYNDALL AFB, FL.
The behavior of hydrazine vapor in an environmental chamber under simulated atmospheric conditions N90-11161
Modeling of hydrazine surface interactions in environmental reaction chambers N90-11162

AIR FORCE FLIGHT TEST CENTER, EDWARDS AFB, CA.
The Air Force Flight Test Center Flight Test Safety Program N90-10872

AIR FORCE GEOPHYSICS LAB., HANSCOM AFB, MA.
A fully analytic, low and middle latitude ionospheric model N90-11368
VLF/LF radio wave studies of the structure and variability of the equatorial, mid-latitude and polar ionosphere below 100 km N90-11373
Composited local area forecast techniques [AD-A210802] N90-11432

AIR FORCE HUMAN RESOURCES LAB., BROOKS AFB, TX.
Simulation of synthetic aperture radar 1: Feature density and accuracy requirements [AD-A211019] N90-11218

AIR FORCE INST. OF TECH., WRIGHT-PATTERSON AFB, OH.
Adaptive tracking of maneuvering targets based on IR image data N90-10853

AIR FORCE OCCUPATIONAL AND ENVIRONMENTAL HEALTH LAB., BROOKS AFB, TX.
Evaluation of rocket motor exhaust and liner combustion by-products [AD-A210747] N90-11083

AIR FORCE SYSTEMS COMMAND, WRIGHT-PATTERSON AFB, OH.
Thermodynamic principles of the process of the effect of electromagnetic fields on a polymer melt [AD-A210598] N90-11149

AIR FORCE WRIGHT AERONAUTICAL LABS., WRIGHT-PATTERSON AFB, OH.
Aircraft live fire testing N90-10879

AIRBUS INDUSTRIE, BLAGNAC (FRANCE).
A320 flight tests: Particularities and innovations N90-10864

ALBERTA UNIV., EDMONTON.
Magnetospheric substorms as a signature of the solar terrestrial interaction N90-11363

ALLIED-SIGNAL AEROSPACE CO., DES PLAINES, IL.
Production of jet fuels from coal-derived liquids. Volume 11: Production of advanced endothermic fuel blends from Great Plains Gasification Plant naphtha by-product stream [AD-A210251] N90-11184

ALLIED-SIGNAL AEROSPACE CO., KANSAS CITY, MO.
Advanced Turbine Technology Applications Program, (ATTAP) [DE89-016067] N90-11318

ANACAPA SCIENCES, INC., FORT RUCKER, AL.
Task analysis of the UH-60 mission and decision rules for developing a UH-60 workload prediction model. Volume 1: Summary report [AD-A210763] N90-11446

ANALYTICAL SCIENCES CORP., READING, MA.
Direct statistical thermal wind estimation procedure [AD-A211256] N90-11433

ANDREWS ANTENNAS, ADELAIDE (AUSTRALIA).
Accurate measurements of the total angle of arrival of HF skywaves N90-11402
Ionospheric limitations to the accuracy of SSL estimates of HF transmitter locations N90-11403

APPLIED RESEARCH LAB., STATE COLLEGE, PA.
Physics and materials science of high temperature superconductors [AD-A211246] N90-11619

ARGONNE NATIONAL LAB., IL.
The chemistry of the hypochlorite neutralization of hydrazine fuels N90-11173
A technique to correlate fractography with NDE (Non-Destructive Evaluation) of small samples [DE89-016904] N90-11325
Planning for hybrid-cycle OTEC experiments using the HMTSTA test facility at the Natural Energy Laboratory of Hawaii [DE89-013278] N90-11349
Projections for a steady-state tokamak reactor based on ITER [DE89-016678] N90-11589
Experimental studies of plasma wake-field acceleration and focusing [DE89-016718] N90-11591
Defect structures preceding amorphization by ion irradiations in YBa2Cu3O(7-delta) [DE89-016905] N90-11612
Transport properties of thermally grown Cr2O3 [DE89-016703] N90-11623
A fermi liquid electric structure and the nature of the carriers in high-T(sub c) cuprates: A photoemission study [DE89-016774] N90-11624

ARIANESPACE, EVRY (FRANCE).
Flight-mechanical environment on Ariane launch vehicle payloads N90-11048

ARIZONA STATE UNIV., TEMPE.
Low-Reynolds-number modeling of complex flows with and without density variation N90-10832
Nonprincipal-plane scattering from flat plates: Second-order and corner diffraction and pattern control of horn antennas [NASA-CR-185485] N90-11205
Part A: Nonprincipal-plane scattering from flat plates: Second-order and corner diffractions N90-11206
Part B: Pattern control of horn antennas N90-11207

ARMY AVIATION SYSTEMS COMMAND, MOFFETT FIELD, CA.
Transfer functions for nonlinear systems via Fourier-Borel transforms [NASA-TM-100034] N90-10828

ARMY CHEMICAL RESEARCH AND DEVELOPMENT CENTER, ABERDEEN PROVING GROUND, MD.
Methodology of developing a combined environmental stress schedule for reliability growth testing [AD-A211053] N90-11326

ARMY COLD REGIONS RESEARCH AND ENGINEERING LAB., HANOVER, NH.
Definition of research needs to address airport pavement distress in cold regions [DOT/FAA/DS-89/13] N90-10896
Coastal subsea permafrost and bedrock observations using dc resistivity [AD-A210784] N90-11435

ARMY LAB. COMMAND, FORT MONMOUTH, NJ.
Polarization matrices of lithium tetraborate [AD-A210774] N90-11112

ARMY LAB. COMMAND, WATERTOWN, MA.
Y-Si-Al-O-N glass fibers
[AD-A211170] N90-11088
ARMY WAR COLL., CARLISLE BARRACKS, PA.
Flight testing and flight research: From the age of the tower jumper to the age of the astronaut N90-10882
ASSOCIACAO LATINO-AMERICANA DE METALURGIA E MATERIAIS, RIO DE JANEIRO (BRAZIL).
Use of overlapped reflection for determining the retained austenite by X-ray diffraction
[DE89-615450] N90-11126
AUBURN UNIV., AL.
Stimulus-response compatibility in spatial precuing and symbolic identification: Effects of coding practice, retention, and transfer
[AD-A210745] N90-11443
Theoretical atomic physics for fusion
[DE89-017363] N90-11563
AURORAL OBSERVATORY, TROMSO (NORWAY).
Quiet time conductivities of the auroral ionosphere N90-11383
AVIONS MARCEL DASSAULT-BREGUET AVIATION, ISTRES (FRANCE).
Flight test techniques adopted by Avions Marcel Dassault-Breguet Aviation N90-10867
AVIONS MARCEL DASSAULT-BREGUET AVIATION, SAINT-CLOUD (FRANCE).
Thermal and structural analysis of Hermes N90-11058
AXIOMATIX, LOS ANGELES, CA.
Network analyzer for nonstatic jamming
[AD-A210759] N90-11216

B

BALLISTIC RESEARCH LABS., ABERDEEN PROVING GROUND, MD.
A thermochemical analysis of proposed working fluids for electrothermal guns
[AD-A210681] N90-10910
Jet-flow from shock tubes
[AD-A210651] N90-11260
A laser Doppler anemometry investigation of single-phase and particle-laden jet flows
[AD-A210660] N90-11261
BARI UNIV. (ITALY).
On the possibility of producing artificial ionization and polar aurora in the ionosphere by radio-waves emitted from the ground N90-11388
BESANCON UNIV. (FRANCE).
Parametric identification of conservative self adjoint structures N90-10994
BETHLEHEM STEEL CO., PA.
Thin section casting program. Volume 1: Executive summary and overview
[DE89-009030] N90-11198
Thin section casting program. Volume 2: Horizontal TSC (Thin-Section Casting) approach
[DE89-009031] N90-11199
Thin section casting program. Volume 2-A: Appendix to volume 2
[DE89-009032] N90-11200
Thin section casting program. Volume 3: Vertical TSC (Thin-Section Casting) approach
[DE89-009033] N90-11201
Thin section casting program. Volume 4: Static cast product bending, straightening, and rolling
[DE89-009034] N90-11202
Thin section casting program. Volume 5: Westinghouse MHD Project
[DE89-009035] N90-11203
BIRMINGHAM UNIV. (ENGLAND).
Interactions of hydrazines with colloidal constituents of soils N90-11164
BOEING AEROSPACE CO., HUNTSVILLE, AL.
SDM challenges for space station N90-11059
BOLT, BERANEK, AND NEWMAN, INC., CAMBRIDGE, MA.
Wideband connectivity and support for Cronus cluster at USAF Electronic Systems Division
[AD-A210749] N90-11215
BONN UNIV. (GERMANY, F.R.).
Stormtime coupling of the neutral and ionized upper atmosphere at middle latitudes N90-11381
BOSTON UNIV., MA.
Auroral and sub-auroral F-layer irregularity studies in the Northern and Southern Hemisphere during the equinox transition study September 16-26, 1984 N90-11393
BRISTOL UNIV. (ENGLAND).
The active control of an unstable canard aircraft N90-10894
BRITISH AEROSPACE PUBLIC LTD. CO., PRESTON (ENGLAND).
The Experimental Aircraft Flight Test Programme N90-10865
Flight test instrumentation and data processing at British Aerospace, Warton, U.K. N90-10887
BRITISH BROADCASTING CORP., LONDON (ENGLAND).
HDTV displays: Subjective effects of scanning standards and domestic picture sizes
[BBC-RD-1989/9] N90-11208
BROOKHAVEN NATIONAL LAB., UPTON, NY.
Spin fluctuations and excitations in a 2D xy-ferromagnet: CoCl2 in graphite
[DE89-017600] N90-11119
A compact X-ray free electron laser
[DE89-017236] N90-11297
X-ray lithography sources: A review
[DE89-017610] N90-11547
Ion sources, electron guns and beam optics
[DE89-015526] N90-11562
BROWN UNIV., PROVIDENCE, RI.
Wavefront propagation for reaction-diffusion systems of PDE
[AD-A210662] N90-11510

C

CALIFORNIA INST. OF TECH., PASADENA.
Chemical reactions in turbulent mixing flows
[AD-A211240] N90-11263
Electron transfer reactions
[AD-A210711] N90-11545
A dynamical study of Jupiter's Great Red Spot N90-11681
CALIFORNIA UNIV., BERKELEY.
Applications of NMR spectroscopy to the study of zeolite synthesis
[DE89-015226] N90-11095
Laser dynamics: The system dynamics and network theory of optoelectronic integrated circuit design N90-11296
A prototype silicon compiler in prolog
[AD-A210669] N90-11452
Rocket and satellite observations of the local interstellar medium N90-11668
CALIFORNIA UNIV., BERKELEY. LAWRENCE BERKELEY LAB.
Applications of NMR spectroscopy to the study of zeolite synthesis
[DE89-015226] N90-11095
Projections for a steady-state tokamak reactor based on ITER
[DE89-016678] N90-11589
CALIFORNIA UNIV., DAVIS.
Iterative network magnitude estimation and uncertainty assessment with noisy and clipped data
[AD-A210707] N90-11507
CALIFORNIA UNIV., LOS ANGELES.
Studies of time-dependent polar cap convection patterns N90-11421
Adaptive gigabit fiber optics local area network
[AD-A210794] N90-11571
PISCES program plasma-surface interactions research
[DE89-015622] N90-11578
Study of disorder and strain in semiconductor heterostructures and superlattices by Raman scattering N90-11601
CALIFORNIA UNIV., SAN DIEGO.
Ionospheric irregularities due to powerful HF radio transmissions N90-11389
CALIFORNIA UNIV., SANTA CRUZ.
Spectropolarimetry, variability, and the taxonomy of active galactic nuclei N90-11667
CARNEGIE-MELLON UNIV., PITTSBURGH, PA.
Biological effects of power frequency electric and magnetic fields: Background paper
[PB89-209985] N90-11439
Preference propagation in temporal/capacity constraint graphs
[AD-A210668] N90-11506
Planning in writing: The cognition of a constructive process
[AD-A210434] N90-11648
CASE WESTERN RESERVE UNIV., CLEVELAND, OH.
Three-dimensional analysis of surface crack-Hertzian stress field interaction
[NASA-CR-4254] N90-11332
Comprehension processes in mechanical reasoning
[AD-A210459] N90-11442
Superconducting ceramics in the Bi1.5SrCaCu2O sub x system by melt quenching technique
[NASA-CR-185139] N90-11606
CENTER FOR MATHEMATICS AND COMPUTER SCIENCE, AMSTERDAM (NETHERLANDS).
Pressure correction splitting methods for the computation of oscillatory free convection in low Pr fluids
[CWI-NM-R8816] N90-11271
A distributed debugger for Amoeba
[CWI-CS-R8828] N90-11453
Boolean functions, invariance groups and parallel complexity
[CWI-CS-R8836] N90-11472
Completeness of resolution by transfinite induction
[CWI-CS-R8837] N90-11473
Module algebra (revised version)
[CWI-CS-R8844-REV] N90-11474
Checking the Goldbach conjecture on a vector computer
[CWI-NM-R8812] N90-11475
Variable step iteration of high-order Runge-Kutta methods on parallel computers
[CWI-NM-R8817] N90-11476
On the Amoeba protocol
[CWI-CS-R8827] N90-11480
Synchrony with empty process
[CWI-CS-R8832] N90-11481
Parallel inference based on delta processing
[CWI-CS-R8846] N90-11482
LINPACK routines based on the level 2 BLAS
[CWI-NM-R8811] N90-11483
Determinism yields (event structure isomorphism equals step sequence equivalence)
[CWI-CS-R8839] N90-11492
An interpolation theorem in equational logic
[CWI-CS-R8838] N90-11528
Note on explicit parallel multistep Runge-Kutta methods
[CWI-NM-R8814] N90-11529
On the equivalence of BS-stability and B-consistency
[CWI-NM-R8815] N90-11530
Partially specified probability measures in expert systems
[CWI-CS-R8842] N90-11536
CENTER FOR NIGHT VISION AND ELECTRO-OPTICS, FORT BELVOIR, VA.
Night sky radiometric measurements during follow-on-evaluation testing of AN/PVS-7 (A, B) at Fort Benning, Georgia
[AD-A211273] N90-11574
CENTRE D'ESSAIS EN VOL, BRETIGNY-SUR-ORGE (FRANCE).
Lessons learned from the integration of flight systems N90-10874
CENTRE D'ETUDES ET DE RECHERCHES, TOULOUSE (FRANCE).
Passive trajectography by azimuth: Improvement of estimation quality N90-10854
CENTRE DE RECHERCHES EN PHYSIQUE DE L'ENVIRONNEMENT, SAINT MAUR DES FOSSES (FRANCE).
Empirical models of convection electric fields and electrostatic potential at high latitude from EISCAT observations: Preliminary results N90-11377
Electrostatic turbulence in the high latitude ionosphere N90-11392
CENTRE NATIONAL D'ETUDES DES TELECOMMUNICATIONS, ISSY-LES-MOULINEAUX (FRANCE).
Simulation of the polar cap F region ionization using an experimental convection electric field N90-11370
Polar F layer lacuna irregularities at Dumont d'Urville N90-11379
CENTRE NATIONAL D'ETUDES DES TELECOMMUNICATIONS, LANNION (FRANCE).
North-south tropical F2 layer asymmetry at west AFrican and Pacific longitudes N90-11398
Radio propagation conditions forecast above a low latitude region N90-11400
CENTRE NATIONAL D'ETUDES SPATIALES, TOULOUSE (FRANCE).
Acoustic response analysis in the low frequency domain N90-11010
The third generation rigid solar array GSR3 N90-11017
Mathematical model and predictions for static and dynamic behavior of solar array structure N90-11049
Development of graphite-magnesium composites for space applications N90-11054
CENTRE NATIONAL DE LA RECHERCHE SCIENTIFIQUE, TOULOUSE (FRANCE).
International workshop on Beam Injection Assessment of Defects in Semiconductors
[AD-A210842] N90-11617
CHILE UNIV., SANTIAGO.
Subharmonic solutions near an equilibrium point for Hamiltonian systems
[AD-A210558] N90-11496
CINCINNATI UNIV., OH.
Reactive ion etching of SiC thin films by mixtures of fluorinated gases and oxygen
[AD-A211046] N90-11113

Modeling and simulation of spatial robotic manipulators with flexible links and joint drives for control strategies implementation and evaluation N90-11311

COASTAL ENGINEERING RESEARCH CENTER, VICKSBURG, MS.

Physiographic and geological setting of the Coastal Engineering Research Center's field research facility [AD-A210772] N90-11356

COLORADO STATE UNIV., FORT COLLINS.

Spatial and temporal short range total cloud cover estimation by metric analysis of composite imagery N90-11423

A methodology for the design of continuous-dataflow synchronous systems [PB89-184360] N90-11564

COLORADO UNIV., BOULDER.

Control and optimization for observations of systems governed by controlled partial differential equations [AD-A211122] N90-11513

A methodology for the design of continuous-dataflow synchronous systems [PB89-184360] N90-11564

Guaranteed cost control of flexible space structures N90-11643

Numerical study of the current sheet and PSBL in a magnetotail model [NASA-CR-183289] N90-11669

Radiative shocks with electron thermal conduction N90-11670

Small grains in reflection nebulae: A study of diffuse interstellar bands, elemental depletions and infrared flux N90-11672

A solar extreme ultraviolet flux model N90-11686

COLUMBIA UNIV., NEW YORK, NY.

Ion temperature gradient instability [DE89-016574] N90-11580

A liquid xenon imaging telescope for 1-30 MeV gamma-ray astrophysics [NASA-CR-185999] N90-11662

COLUMBIA UNIV. TEACHERS COLL., NEW YORK, NY.

Mathematical method for the study and teaching of stellar and protostellar structure N90-11666

COMMISSARIAT A L'ENERGIE ATOMIQUE, SACLAY (FRANCE).

Tamaris: A new European facility for low frequency multi-axis vibration simulation N90-11068

COMMUNICATIONS RESEARCH CENTRE, OTTAWA (ONTARIO).

Experimental identification of modal momentum coefficients and modal identity parameters of the FLECS structure N90-10991

Comparison of phase resonance, mode separation, and driven-base modal identification methods applied to the FLECS test structure N90-11027

COMPUTER RESOURCE MANAGEMENT, INC., VIENNA, VA.

Ground and Obstacle Avoidance (GOA) concept of operations [DOT/FAA/DS-89/08] N90-10855

CONNECTICUT UNIV., STORRS.

Radiationless transitions and excited-state absorption of low-field chromium complexes in solids [AD-A210653] N90-11105

CONSTRUCCIONES AERONAUTICAS S.A., MADRID (SPAIN).

Experiences using a major FEM package interactively for spacecraft applications N90-11008

The service module structure of the IOS spacecraft development and qualification program N90-11021

Induced shock loads during the separation of the Ariane 5 VEB structure N90-11045

CORNELL UNIV., ITHACA, NY.

Dynamics of nucleation at electrochemical interfaces via surface EXAFS and standing wave measurements [AD-A210733] N90-11109

Low temperature properties of glasses N90-11141

A remote sensor to monitor combustion products using a tunable acousto-optic filter N90-11275

Planar sliding of a rigid body with dry friction: Limit surfaces and dynamics of motion N90-11314

A finite element formulation for inelastic plates and shells based on a mixed variational principle N90-11334

Using computer design and simulation to improve manufacturing productivity, report period 1, 2 and 3 [AD-A210255] N90-11462

Electromagnetic jets in pulsar magnetospheres and near magnetized accretion disks N90-11675

COUNCIL FOR NATIONAL ACADEMIC AWARDS (ENGLAND).

The ratio to X-ray spectral shape and variability of blazars N90-11688

CRANFIELD INST. OF TECH., BEDFORD (ENGLAND).

Trace metal catalysis of hydrazine decomposition: The role of chromium N90-11163

CRETE UNIV., IRAKLION (GREECE).

A review on radio studies of auroral E-region ionospheric irregularities N90-11390

D

DAYTON UNIV., OH.

Finite element analysis of cure-induced residual stress in composite materials N90-11084

DEFENCE RESEARCH ESTABLISHMENT, OTTAWA (ONTARIO).

The development of mission-specific advanced inertially-based avionics system N90-10851

Development of a marine integrated navigation system N90-10852

DEPARTMENT OF DEFENSE, WASHINGTON, DC.

Federal Radionavigation Plan, 1988 [PB89-163075] N90-10846

DEPARTMENT OF ENERGY, WASHINGTON, DC.

Advanced Turbine Technology Applications Program, (ATTAP): A plan for improving the prototype production of ceramic components for the gas turbine engine, 1988--1992 [DE89-015566] N90-11320

Evaluation of mid-to-long term basic research for environmental restoration [DE89-015621] N90-11355

DOE/CEC Workshop on Critical Evaluation of Radiobiological Data to Biophysical Modeling [DE89-015214] N90-11437

Summaries of the FY 1989 Applied Mathematical Sciences Research program [DE89-016694] N90-11521

DEPARTMENT OF TRANSPORTATION, WASHINGTON, DC.

Federal Radionavigation Plan, 1988 [PB89-163075] N90-10846

DEUTSCHE FORSCHUNGS- UND VERSUCHSANSTALT FUER LUFT- UND RAUMFAHRT, BRUNSWICK (GERMANY, F.R.).

ATTAS flight testing experiences N90-10862

GRATE: A new flight test tool for flying qualities evaluation N90-10868

Transverse shear stiffness of composite and sandwich finite elements N90-11034

Analysis of delamination growth N90-11036

Delamination tests under static compression loading N90-11061

Delamination tests under compression-compression and tension-compression loading N90-11062

DEUTSCHE FORSCHUNGS- UND VERSUCHSANSTALT FUER LUFT- UND RAUMFAHRT, COLOGNE (GERMANY, F.R.).

Fatigue crack growth rates as a function of delta K: Variability and material property N90-11031

DEUTSCHE FORSCHUNGS- UND VERSUCHSANSTALT FUER LUFT- UND RAUMFAHRT, GOETTINGEN (GERMANY, F.R.).

Updating of finite element model by means of normal mode parameters N90-10992

Modal analysis of space structures with the Ibrahim Time Domain method N90-11026

DEUTSCHE FORSCHUNGS- UND VERSUCHSANSTALT FUER LUFT- UND RAUMFAHRT, PORZ (GERMANY, F.R.).

Experimental identification of modal momentum coefficients and modal identity parameters of the FLECS structure N90-10991

DEUTSCHE FORSCHUNGS- UND VERSUCHSANSTALT FUER LUFT- UND RAUMFAHRT, STUTTGART (GERMANY, F.R.).

Liquid infiltrated C/SiC: An alternative material for hot space structures N90-11030

DIGITAL EQUIPMENT CORP., PALO ALTO, CA.

Evaluating the performance of software cache coherence [AD-A211164] N90-11468

DORNIER SYSTEM G.M.B.H., FRIEDRICHSHAFEN (GERMANY, F.R.).

Reduction of dynamic response of spacecraft structures and payloads N90-11000

A high precision gravity compensation system for the deployment test of the ERS-1 SAR antenna N90-11038

DORTMUND UNIV. (GERMANY, F.R.).

Contribution to the transcrystalline stress crack corrosion of austenite chromium-nickel steels [ETN-89-94665] N90-11137

DUESSELDORF UNIV. (GERMANY, F.R.).

Balance equations for ionospheric plasmas with different partial temperatures N90-11364

DYNAMIC ENGINEERING N.V., HEVERLEE (BELGIUM).

Numerical models for exterior and interior fluid-structure interaction problems N90-11073

E

ECOLE POLYTECHNIQUE FEDERALE DE LAUSANNE (SWITZERLAND).

Enhanced oxidation and solovolysis reactions in chemically inert microheterogeneous systems [AD-A210748] N90-11110

EDGERTON, GERMESHAUSEN AND GRIER, INC., IDAHO FALLS, ID.

Reporting environmental data of known quality [DE89-016214] N90-11359

EDINBURGH UNIV. (SCOTLAND).

Aspects of the development of a 1-5 micron infrared camera for astronomy N90-11656

Integrating detectors and their application to infrared astronomy N90-11659

EG AND G ENERGY MEASUREMENTS, INC., IDAHO FALLS.

Fiber optics: A brief introduction [DE89-009337] N90-11567

EG AND G MOUND APPLIED TECHNOLOGIES, MIAMISBURG, OH.

Ion implantation of two titanium alloys [DE89-016958] N90-11133

ELORET CORP., SUNNYVALE, CA.

Particle kinetic simulation of high altitude hypervelocity flight [NASA-CR-186003] N90-10840

Theoretical investigation of gas-surface interactions [NASA-CR-185492] N90-11552

A high level Ab initio study of the anionic hydrogen-bonded complexes FH-CN-, FH-NC-, H2O-CN- and H2O-NC- N90-11553

A diagnostic for determining the quality of single-reference electron correlation methods N90-11554

ELROD (HAROLD G.), OLD SAYBROOK, CT.

Efficient numerical method for computation of thermohydrodynamics of laminar lubricating films [NASA-CR-185136] N90-11256

ENGINEERING SYSTEM INTERNATIONAL, RUNGIS (FRANCE).

Intrinsic damage and strength criteria for advanced composite laminates in space applications N90-11071

Numerical simulation of micrometeroids and debris hypervelocity impacts on Columbus pressurized modules N90-11075

Exploitation of data management facilities for finite element analysis in aerospace structural engineering applications N90-11078

ENVIRONMENTAL PROTECTION AGENCY, WASHINGTON, DC.

Potential effects of global climate change on the United States. Executive summary. Draft [PB89-161046] N90-11350

Potential effects of global climate change on the United States. Volume 1: Regional studies. Draft [PB89-161053] N90-11351

Potential effects of global climate change on the United States. Volume 2: National studies. Draft [PB89-161061] N90-11352

Stratospheric ozone depletion [PB89-207476] N90-11354

ERNO RAUMFAHRTTECHNIK G.M.B.H. BREMEN (GERMANY, F.R.).

Overview of actual buckling calculation methods for space vehicle structures N90-10995

Key structures mechanical issues of the European Space Station and platform program Columbus N90-11072

ESSEN UNIV. (GERMANY, F.R.).

Compact torus configurations with high frequency driven currents [ETN-89-94674] N90-11598

Design and construction of systems for the single-crystals growth of ternary silver halides, alkali halides, and alkaline earth fluorides, and the dielectric investigation of silver halide [ETN-89-94673] N90-11632

EUROPEAN OFFICE OF AEROSPACE RESEARCH AND DEVELOPMENT, LONDON (ENGLAND).

Aeritalia Space Systems Group, Turin, Italy [EOARD-LR-89-041] N90-10908

EUROPEAN ORGANIZATION FOR NUCLEAR RESEARCH, GENEVA (SWITZERLAND).

Free-electron laser theory [DE89-620145] N90-11298

EUROPEAN SPACE AGENCY, PARIS (FRANCE).

Spacecraft Structures and Mechanical Testing [ESA-SP-289] N90-10986

EUROPEAN SPACE AGENCY. EUROPEAN SPACE RESEARCH AND TECHNOLOGY CENTER, ESTEC, NOORDWIJK (NETHERLANDS).

Review of the ESA fracture control policy N90-11029

Ariane 5 structural design and development N90-11057

The Environmental Test Centre at ESTEC (an overview) N90-11064
Two years experience with the ESTEC multishaker system N90-11065
New data handling system (MDH) for mechanical tests at ESTEC N90-11066
The large European Acoustic Facility at ESTEC N90-11067

F

FEDERAL AVIATION ADMINISTRATION, ATLANTIC CITY, NJ.
Helicopter Visual Segment Approach Lighting System (HALS)
[ACD-330] N90-10856
Heliport surface maneuvering test results
[ACD-330] N90-10897
FERMI NATIONAL ACCELERATOR LAB., BATAVIA, IL.
A new semicustom integrated bipolar amplifier for silicon strip detectors
[DE89-015585] N90-11229
New tools for the simulation and design of calorimeters
[DE89-016323] N90-11281
FERRANTI DEFENCE SYSTEMS LTD., EDINBURGH (SCOTLAND).
A high performance airborne INS/GPS Integrated Navigation System N90-10850
FLORIDA UNIV., GAINESVILLE.
Hydrazine fate and transformation in natural waters and soils N90-11165
Vibrational spectroscopic study of the kaolinite-hydrazine intercalation complex N90-11166
Surface-catalyzed air oxidation reactions of hydrazines: Tubular reactor studies N90-11167
A matrix-isolation FT-IR study of hydrazine N90-11168
Low temperature spectroscope of hydrazine and ammonia complexes N90-11169
The soil microbiology of hydrazines N90-11171
Numerical simulation of hydrazine transport in a sandy soil N90-11172
Realization theoretic solution of two analytic matrix equations with applications to stabilization of infinite-dimensional systems
[AD-A211118] N90-11512
Studies of novel superconductors
[DE89-016744] N90-11609
An improved algorithm for the determination of the system paramters of a visual binary by least squares N90-11658
FOKKER B.V., AMSTERDAM (NETHERLANDS).
Qualification by simulation: Dream or reality N90-10990
FRAUNHOFER INST. FUER WERKSTOFFMECHANIK, FREIBURG (GERMANY, F.R.).
Basic investigations of cutting machinability of inorganic glasses using single-point tools
[W-15/87] N90-11204
FREIBURG UNIV. (GERMANY, F.R.).
Global ionospheric dynamics N90-11366

G

GANDHI (INDIRA) CENTRE FOR ATOMIC RESEARCH, KALPAKKAM (INDIA).
A new inexpensive electrochemical meter for oxygen in sodium coolant
[DE89-630802] N90-11104
Compositional analysis of steels by X-ray fluorescence spectrometry
[DE89-630803] N90-11129
Thermal expansion and phase transformation studies on some materials by high temperature X-ray powder diffractometry
[DE89-631032] N90-11130
GENERAL ACCOUNTING OFFICE, WASHINGTON, DC.
Test and evaluation: Reducing risks to military aircraft from bird collisions. Report to the Chairman, Legislation, and National Security Subcommittee, Committee on Goverment Operations, House of Representatives
[AD-A210670] N90-10845
GENERAL ATOMIC CO., SAN DIEGO, CA.
High-temperature ceramic superconductors
[AD-A211070] N90-11618
GENERAL DYNAMICS CORP., SAN DIEGO, CA.
Evolutionary space station fluids management strategies
[NASA-CR-185137] N90-10983
GENERAL ELECTRIC CO., CINCINNATI, OH.
An investigation of counterrotating tip vortex interaction
[NASA-CR-185135] N90-11549
GENERAL ELECTRIC CO., SCHENECTADY, NY.
Corrosion rates of structural materials on the ocean floor
[DE89-015211] N90-11123
GEO-CENTERS, INC., FORT WASHINGTON, MD.
Hydrazine dosimetry N90-11178
GEORGE WASHINGTON UNIV., WASHINGTON, DC.
An evaluation of the Chaboche and Bodner-Partom viscoplastic constitutive theories for strain rate sensitive materials N90-11330
New computing systems and their impact on structural analysis and design
[NASA-CR-185831] N90-11457
GEORGIA INST. OF TECH., ATLANTA.
Low temperature processing of reaction sintered silicon nitride
[DE89-017455] N90-11092
Performance analysis of hybrid ARQ protocols in a slotted code division multiple-access network
[AD-A211078] N90-11219
Stochastic flows in networks
[AD-A211209] N90-11515
GOSUDARSTVENNYI KOMITET PO ISPOLZOVANIYU ATOMNOI ENERGII, MOSCOW (USSR).
Passage of ultrarelativistic electrons through real crystals
[DE89-618624] N90-11613
GOSUDARSTVENNYJ KOMITET PO ISPOLZOVANIYU ATOMNOI ENERGII, SERPUKHOV (USSR).
Programs for numerical integration of piece-wise smooth functions
[DE89-620449] N90-11464

H

HAZARDOUS MATERIALS TECHNICAL CENTER, ROCKVILLE, MD.
The Third Conference on the Environmental Chemistry of Hydrazine Fuels
[AD-A197632] N90-11157
HIROSHIMA UNIV., TAKEHARA (JAPAN).
Gauge invariant cosmological perturbations with cold dark matter
[DE89-790940] N90-11679
HOKKAIDO UNIV., SAPPORO (JAPAN).
Report of the Specialists' Workshop on Phase Transition Studies on Hydrogen-Bonded Crystals by Neutron and X-ray Diffractometries
[DE89-906638] N90-11631
HOUSTON UNIV., TX.
The dynamics of circular plates with patch damping: A numerical and experimental study N90-11329
HUGHES AIRCRAFT CO., EL SEGUNDO, CA.
Antenna beamforming using optical processing
[NASA-CR-180844] N90-11210
HUMAN ENGINEERING LABS., ABERDEEN PROVING GROUND, MD.
Computer programs for measuring variations in speech
[AD-A211126] N90-11467

I

I.A.M. RINALDO PIAGGIO, FINALE LIGURE (ITALY).
P-180 AVANTI: Project and flight test program comprehensive overview N90-10863
IDENTIFICATION FRIEND, FOE, OR NEUTRAL JOINT TEST FORCE, KIRTLAND AFB, NM.
Identification Friend, Foe or Neutral Joint Test N90-10881
IIT RESEARCH INST., BARTLESVILLE, OK.
The effect of degree of aromaticity and alkyl substitution of polyaromatic hydrocarbons on instrumental response factors
[DE89-000761] N90-11117
IKO SOFTWARE SERVICE G.M.B.H., STUTTGART (GERMANY, F.R.).
A new aspect for the use of thin walled beams as shell stiffeners of spacecraft structures N90-11046
Space telescope solar array: Nonlinear test and analysis effects N90-11051
STSA-Space Telescope solar array interconnectors: From simple approaches to complex modeling. A case study of the necessity of complex analysis N90-11076
ILLINOIS INST. OF TECH., CHICAGO.
Ozonation of hydrazines and their associated impurities N90-11174
ILLINOIS STATE WATER SURVEY, CHAMPAIGN.
Frequency distributions and hydroclimatic characteristics of heavy rainstorms in Illinois
[PB89-203988] N90-11427
ILLINOIS UNIV. AT URBANA-CHAMPAIGN, SAVOY.
Numerical simulation of leading-edge vortex rollup and bursting N90-10831
ILLINOIS UNIV., URBANA.
Influence of core-shell grains on the internal stress state and permittivity response of zirconia modified barium titanate
[AD-A211245] N90-11153
Semiconductor quantum well lasers and related optoelectronic devices on silicon, III-V
[AD-A210758] N90-11299
CuInSe2 solar cell research by sputter deposition
[DE89-009450] N90-11345
Ionospheric irregularities and their effects on electromagnetic waves propagating through them N90-11391
Asynchronous integration of ordinary differential equations on multiprocessors
[DE89-014169] N90-11493
Generalized BDF (Backward Differentiation Formula) methods applied to Hessenberg form DAEs
[DE89-017328] N90-11522
Potential for parallelism in explicit linear methods
[DE89-017329] N90-11523
ILLINOIS UNIV., URBANA-CHAMPAIGN.
Performance and robustness of adaptive controllers for linear stochastic systems N90-11485
IMPERIAL COLL. OF SCIENCE AND TECHNOLOGY, LONDON (ENGLAND).
A review of the Error of Matrix Method (EMM) for structural dynamic model comparison N90-10993
INDIANA UNIV., BLOOMINGTON.
A history of West European rocketry and space research
[AD-A211191] N90-11690
INDUSTRIEANLAGEN-BETRIEBSGESELLSCHAFT M.B.H., OTTOBRUNN (GERMANY, F.R.).
Numerical analysis of nonlinear viscoelastic structures: Application to elastomers and rubber-like materials N90-11013
Fluid-structure interaction effects in tank structures due to sloshing and hydrodynamic ram: Coupled Lagangian-Eulerian simulations N90-11022
Transient vibration testing of spacecraft structures. Experience with multiaxial base motion and combined base motion and point force excitation N90-11039
Development of a thermoacoustic test facility N90-11041
INGEMANSSON ANATROL A.B., ASKIM (SWEDEN).
Viscoelastic tuned dampers for control of structural dynamics N90-10999
INGENIEURGESELLSCHAFT FUER TECHNISCHE SOFTWARE G.M.B.H., STUTTGART (GERMANY, F.R.).
Modal analysis of fluid-structure systems by parallel subspace iteration N90-11024
INSTITUT D'AERONOMIE SPATIALE DE BELGIQUE, BRUSSELS.
Solar-terrestrial relations: Flare and solar wind effects N90-11362
INSTITUT FRANCO-ALLEMAND DE RECHERCHES, SAINT-LOUIS (FRANCE).
Behaviour of VF(sub 2)/VF(sub 3) piezoelectric copolymers under shock loading
[DE89-016538] N90-11145
INSTITUTE FOR COMPUTER APPLICATIONS IN SCIENCE AND ENGINEERING, HAMPTON, VA.
Linear instability of supersonic plane wakes
[NASA-CR-181911] N90-10833
Estimation on nonlinear damping in second order distributed parameter systems
[NASA-CR-181890] N90-11494
A conforming spectral collocation strategy for Stokes flow through a channel contraction
[NASA-CR-181912] N90-11495
Direct discretization of planar div-curl problems
[NASA-CR-181935] N90-11498
INSTITUTE FOR DEFENSE ANALYSES, ALEXANDRIA, VA.
A survey of research methods to study design
[AD-A211213] N90-11491
INSTITUTO DE FISICA TEORICA, SAO PAULO (BRAZIL).
Gravitational nonminimally coupled electromagnetic fields: A possible solution to some idiosincrasies of Einstein-Maxwell theory
[DE89-618430] N90-11635
INSTITUTO DE PESQUISAS ESPACIAIS, SAO PAULO (BRAZIL).
ANIMA: Image analyzer applied to remote sensing
[INPE-4766-PRE/1435] N90-11447
INTEGRATED SYSTEMS, INC., PALO ALTO, CA.
Nonlinear maneuver autopilot for the F-15 aircraft
[NASA-CR-179442] N90-11487
INTEL CORP., SANTA CLARA, CA.
Reactive ion etching of SiC thin films by mixtures of fluorinated gases and oxygen
[AD-A211046] N90-11113

INTERNATIONAL CENTRE FOR THEORETICAL PHYSICS, TRIESTE (ITALY).
Generation of higher-order squeezing of quantum electromagnetic fields by degenerate four-wave mixing and other processes
[DE89-618392] N90-11213
Upper ionosphere and magnetospheric-ionospheric coupling
[DE89-619727] N90-11415
On the areas of various bodies in the Euclidean space: The case of irregular convex polygons
[DE89-618377] N90-11500
Local structure of a 2-codimensional conformally flat submanifold in an Euclidean space R(sup n+2)
[DE89-618379] N90-11501
Compact surface in three-dimensional ellipsoid with prescribed mean curvature (I)
[DE89-618381] N90-11502
On sufficient conditions for a function to be analytic
[DE89-618382] N90-11503
General hulls in uniform algebras
[DE89-618383] N90-11504
Analytic manifolds in uniform algebras
[DE89-618384] N90-11505
S7 without any construction of Lie group
[DE89-618380] N90-11539
Markov processes in Hilbert space and continuous spontaneous localization of systems of identical particles
[DE89-618396] N90-11540
Producing of an ECR plasma using 2450MHz Whistler wave and the investigating of its parameters
[DE89-618689] N90-11586
Pinning of curved flux lines on the boundary between two phases of high temperature superconductors
[DE89-618865] N90-11614
Superfiled formulation of Chern-Simons supersymmetry
[DE89-618459] N90-11636
General action for topological quantum field theories
[DE89-618460] N90-11637
The thermal stability between rotating cylinders in a radially symmetrical gravitational field
[DE89-618548] N90-11638
Studying shocks in model astrophysical flows
[DE89-618786] N90-11677

INTERNATIONAL TELECOMMUNICATIONS SATELLITE ORGANIZATION, WASHINGTON, DC.
Advances in design and testing of spacecraft structures N90-11018

INTERSCIENCE, INC., TROY, NY.
Efficient algorithm for calculation of radar cross section
[AD-A210785] N90-11217

INTESPACE, TOULOUSE (FRANCE).
Integration of analytical and test software for optimal structural design under dynamic loads N90-11007
Dynamic substructuring for modular analysis and testing N90-11015
Transient tests for spacecraft structures N90-11040
A new European vibration test facility for Ariane 4 class satellites N90-11070

IOWA UNIV., IOWA CITY.
Observational studies of low-frequency oscillations in the Southern Hemisphere N90-11420
CRRES (Combined Release and Radiation Effects Satellite) SPACERAD plasma wave experiment
[AD-A210791] N90-11587

J

JACKSON STATE UNIV., MS.
Diagnostic study of atmosphere-terrain interaction leading to the formation of dust clouds and poor visibilities over near east desert areas
[AD-A211243] N90-11358

JAPAN ATOMIC ENERGY RESEARCH INST., TOKYO.
Experimental database retrieval system DARTS (Handling Manual)
[DE89-906473] N90-11652

JET PROPULSION LAB., CALIFORNIA INST. OF TECH., PASADENA.
Adaptive structures to meet future requirements for large precision structures N90-11001
Comparison of sine dwell and broadband methods for modal testing N90-11025

JOHNS HOPKINS UNIV., BALTIMORE, MD.
Quantum chemical investigations of the mechanism of cationic polymerization and theoretical prediction of crystal densities and decomposition pathways of energetic molecules
[AD-A210322] N90-11143
The investigation of the fundamental limits of heterodyne holographic interferometry with the application of imaging laser generated lamb waves
[AD-A211048] N90-11285

JOHNS HOPKINS UNIV., LAUREL, MD.
Modifications to the aerotherm charring material thermal response and ablation program (CMA) for carbon ablation analysis
[AD-A211069] N90-11115

JOINT INST. FOR NUCLEAR RESEARCH, DUBNA (USSR).
Ion detector on the basis of microchannel plates for a high-sensitive mass spectrometer
[DE89-620335] N90-11291
Determination of neutral particle concentration at erosion laser plasma expansion into vacuum
[DE89-620128] N90-11308
Some exact solutions of the three-identical-particle problem with S-wave inverse square potentials
[DE89-618402] N90-11524
On some stochastic properties of the infinitely dimensional Hamiltonian systems of classical mechanics
[DE89-618403] N90-11525
Reduction of the Dirac equation to the Dirac-Kaehler equation
[DE89-630111] N90-11541
Simulation of an axially symmetric ion-optical system
[DE89-620129] N90-11560
On the construction of the scattering matrix for locally-noncommutative interactions of relativistic fields
[DE89-630138] N90-11640

JOINT PUBLICATIONS RESEARCH SERVICE, ARLINGTON, VA.
JPRS Report: Science and Technology. USSR: Space
[JPRS-USP-89-007] N90-10900
Project Radioastron N90-10901
Meeting of intercosmos space physics group N90-10902
Soviet Mars program N90-10903
Landing tests for Buran shuttle with jet engine-equipped mock-up N90-10904
USSR and international cooperation in space N90-10905
Sagdeyev discusses space missions, policy, Mars plans N90-10906

K

KATHOLIEKE UNIV. TE LEUVEN (BELGIUM).
Employment of modal survey methodologies in dynamic analysis procedures N90-11006
Influence of the fiber/matrix interface on damage development in CFRP N90-11037
Hygrothermal deformations of composite shells N90-11055
The 2.5D- and 3D-fabrics for delamination resistant composite laminates and sandwich structures N90-11063

L

LABORATOIRE D'ETUDE DES TRANSMISSIONS IONOSPHERIQUES, CACHAN (FRANCE).
Influence of ionospheric variations on high-reliability HF systems utilizing large bases N90-11404

LAWRENCE LIVERMORE NATIONAL LAB., CA.
Theoretical Hugoniot of liquid hydrogen fluoride
[DE89-016504] N90-11099
Shock initiation of LX-17 as a function of its initial temperature
[DE89-017730] N90-11192
Validation of NEC (Numerical Electromagnetics Code) for antennas near ground
[DE89-016502] N90-11212
Auxiliary-field transformations for repulsive potentials: A physical approach
[DE89-016677] N90-11223
Performance of transient limiters under laboratory, simulated, and rocket-triggered lightning conditions
[DE89-015773] N90-11238
HPW (High Power Microwave) testing of electronic components
[DE89-016682] N90-11241
Cellular automata and massively parallel physics
[DE89-016506] N90-11257
Computations of the refraction of a plane shock wave at a slow-fast gas interface
[DE89-016508] N90-11258
An investigation of the usefulness of Earley's Algorithm in a general context-free recognizer
[DE89-016498] N90-11463
Computing the two dimensional fast Fourier transform on a general purpose mesh connected multiprocessor
[DE89-016515] N90-11518
Domain decomposition for partial differential equations
[DE89-016669] N90-11519
An interactive program for constrained spline approximation of numerical data
[DE89-016674] N90-11520
New theoretical approaches for studying electron collisions with small molecules
[DE89-017543] N90-11558
Projections for a steady-state tokamak reactor based on ITER
[DE89-016678] N90-11589
Testing results of the MIT Probe
[DE89-016679] N90-11590
Adaptation of the theory of superconductivity to the behavior of oxides
[DE89-016518] N90-11608
General covariance and strings
[DE89-016505] N90-11633
Equation-of-state data of synthetic Uranus
[DE89-016509] N90-11683

LEEDS UNIV. (ENGLAND).
IRAS observations of the extended galactic objects Cas A and W80 N90-11657

LEHIGH UNIV., BETHLEHEM, PA.
The near-wake flow structure of wake-cylinder interaction and surface loading of cylinder N90-11248
A re-evaluation of fatigue threshold test procedures and the simulation and prediction of fatigue crack growth under conditions of low crack closure N90-11328

LEICESTER UNIV. (ENGLAND).
Ion heating events observed at the EISCAT radar N90-11385

LIEGE UNIV. (BELGIUM).
A super element for multibody dynamics N90-11004

LISBON UNIV. (PORTUGAL).
On the development of a basic flight test capability and some related research projects N90-10885

LOCKHEED ENGINEERING AND MANAGEMENT SERVICES CO., INC., LAS CRUCES, NM.
Surface-catalyzed air oxidation of hydrazines: Environmental chamber studies N90-11159
A diffuse reflectance infrared Fourier transform spectroscopic study of adsorbed hydrazines N90-11170
Fuel neutralization by ozone oxidation N90-11176
Measurement of hydrazine contamination in soils N90-11180

LOS ALAMOS NATIONAL LAB., NM.
A parallel numerical simulation for supersonic flows using zonal overlapped grids and local time steps for common and distributed memory multiprocessors
[DE89-015252] N90-10839
Critical reaction rates in hypersonic combustion chemistry
[DE89-014278] N90-10892
Homogeneous catalysts in hypersonic combustion
[DE89-015258] N90-11098
Microstructural effects on spall fracture in 1008 steel
[DE89-016770] N90-11131
The HEL (Hugoniot Elastic Limit) and rate-dependent yield behavior
[DE89-016981] N90-11134
Characterizations of shock-loaded aluminum-infiltrated boron carbide cermets
[DE89-016773] N90-11146
Intergranular and interphase boundaries in ceramics
[DE89-016969] N90-11154
In-situ study of the chemically driven flow fields in initiating homogeneous and heterogeneous nitromethane explosives
[DE89-008415] N90-11186
Carbon in detonations
[DE89-016037] N90-11189
Crystal orientation effects in PETN explosive with 4 GPa shocks
[DE89-016996] N90-11190
Acceleration of metal plates
[DE89-016816] N90-11197
ANTHEM simulation of plasma opening switches
[DE89-016617] N90-11239
Sharp shock model for propagating detonation waves
[DE89-016772] N90-11266
Shock induced dissociation of polyethylene
[DE89-016983] N90-11267
Impulse time-integral function and Lagrangian analysis
[DE89-016997] N90-11268
Laser-driven miniature flyer plates for shock initiation of secondary explosives
[DE89-016587] N90-11288
Interferometry and high speed photography of laser-driven flyer plates
[DE89-016990] N90-11290
Stability requirements of RF linac-driven free-electron lasers
[DE89-016609] N90-11303
Minimized emittance growth with elliptical beam pipes in FEL (Free-Electron Laser)
[DE89-016982] N90-11305

Short wavelength striations on expanding plasma clouds
[DE89-016585] N90-11416
Computer symbiosis: Emergence of symbiotic behavior through evolution
[DE89-015247] N90-11450
Using PATRAN: From eyeballs to submarines and more
[DE89-016989] N90-11469
An integrated distributed processing interface for supercomputers and workstations
[DE89-016769] N90-11478
Spoken commands control robot that handles radioactive materials
[DE89-012632] N90-11488
A solution to nonlinearity problems
[DE89-016975] N90-11544
Magnetic flux compression
[DE89-016991] N90-11546
Structure and properties of simple molecular systems at very high density
[DE89-016974] N90-11557
The Reversed-Field-Pinch (RFP) fusion neutron source: A conceptual design
[DE89-015297] N90-11577
Studies of a strongly coupled plasma produced in a capillary discharge
[DE89-016611] N90-11581
ANTHEM simulation of the early time magnetic field penetration of the plasma surrounding a high density Z-pinch
[DE89-016980] N90-11585
Computer simulations of electromagnetic ion instabilities in the plasma sheet boundary layer
[DE89-016596] N90-11588
Solid fiber Z-pinches: Cold-start computations
[DE89-016768] N90-11592
A fully electromagnetic hybrid model for high density plasma simulations
[DE89-016771] N90-11593
On the photoemission spectrum and optical gap in La2CuO4
[DE89-015281] N90-11605
High pressure 129I Moessbauer studies of GeI4 molecular crystals
[DE89-015269] N90-11620
A fermi liquid electric structure and the nature of the carriers in high-T(sub c) cuprates: A photoemission study
[DE89-016774] N90-11624
Chevron layer structures in Surface Stabilized Ferroelectric Liquid Crystal (SSFLC) cells filled witth a material which exhibits the chiral nematic to smectic C* phase transition
[DE89-016985] N90-11628
Effects of main-sequence mass loss on the turnoff ages of globular clusters
[DE89-016784] N90-11678
Solar opacities constrained by solar neutrinos and solar oscillations
[DE89-016988] N90-11687

LOWELL UNIV., MA.
Examples of meteorological behavior of the ionosphere N90-11395
Multistation/multiparameter observations with a network of digital ionosondes N90-11396

LUND UNIV. (SWEDEN).
Global and local fluctuations in multiplicity and transverse energy for central ultra-relativistic heavy-ion interactions
[LUIP-8903] N90-11555

M

MARYLAND UNIV., COLLEGE PARK.
Thermophysical properties of supercritical fluids and fluid mixtures
[DE89-016568] N90-11102
Analysis of coaxial wire measurement of longitudinal coupling impedance
[DE89-015748] N90-11230
An experimental study of helicity and related properties in turbulent flows
[DE89-016785] N90-11259

MASSACHUSETTS INST. OF TECH., CAMBRIDGE.
Study of the application of automation to composites manufacture
[AD-A211049] N90-11087
Basic research on processing of ceramics for space structures
[AD-A205954] N90-11139
Inferences from images
[AD-A210710] N90-11455
Singularity theory and N = 2 superconformal field theories
[DE89-016582] N90-11538
Projections for a steady-state tokamak reactor based on ITER
[DE89-016678] N90-11589

MASSACHUSETTS INST. OF TECH., LEXINGTON.
The effectiveness of adaptive PRF (Pulse Repetition Frequency) selection in minimizing range obscuration in the TDWR (Terminal Doppler Weather Radar) system
[AD-A211267] N90-11222

MASSACHUSETTS UNIV., AMHERST.
Composites reinforced with thermotropic liquid crystal copolyester fibers
[AD-A211226] N90-11089
Interfacial adsorption and crystallization of polycarbonate in carbon fiber composites
[AD-A211230] N90-11090

MATRA ESPACE, TOULOUSE (FRANCE).
System and performance analysis of a low density actively controlled mirror for astronomic observation N90-11002

MAX-PLANCK-INST. FUER AERONOMIE, KATLENBURG-LINDAU (GERMANY, F.R.).
Global morphology of plasma bubbles in the low latitude ionosphere N90-11369
Low frequency electrostatic waves observed in the vicinity of an auroral arc N90-11378
Calculation of the temperature and velocity vector of the neutral gas using EISCAT CP3-data N90-11384
Atmospheric gravity waves in the auroral source region of TIDs, studied with the EISCAT CP2-data N90-11387

MAX-PLANCK-INSTITUT FUER STROEMUNGSFORSCHUNG, GOETTINGEN (GERMANY, F.R.).
Chemiluminescent ion-molecule reactions of group-3 ions with halogens: New optical spectra and reaction dynamics
[MPIS-18/1988] N90-11120

MAYFLOWER COMMUNICATIONS CO., INC., READING, MA.
STS-GPS (Space Transportation System - Global Positioning System) tracking experiment for gravitation estimation: Feasibility study
[AD-A211265] N90-10859

MCDONNELL-DOUGLAS ASTRONAUTICS CO., HOUSTON, TX.
Independent Orbiter Assessment (IOA): Analysis of the manned maneuvering unit
[NASA-CR-185565] N90-10913
Independent Orbiter Assessment (IOA): Assessment of the electrical power generation/fuel cell powerplant subsystem FMEA/CIL
[NASA-CR-185562] N90-10914
Independent Orbiter Assessment (IOA): Analysis of the electrical power generation/fuel cell powerplant subsystem
[NASA-CR-185561] N90-10915
Independent Orbiter Assessment (IOA): Analysis of the rudder/speed brake subsystem
[NASA-CR-185560] N90-10916
Independent Orbiter Assessment (IOA): Assessment of the data processing system FMEA/CIL
[NASA-CR-185546] N90-10917
Independent Orbiter Assessment (IOA): Analysis of the electrical power generation/power reactant storage and distribution subsystem
[NASA-CR-185556] N90-10918
Independent Orbiter Assessment (IOA): Analysis of the orbital maneuvering system
[NASA-CR-185554] N90-10919
Independent Orbiter Assessment (IOA): Analysis of the guidance, navigation, and control subsystem
[NASA-CR-185555] N90-10920
Independent Orbiter Assessment (IOA): Analysis of the nose wheel steering subsystem
[NASA-CR-185548] N90-10921
Independent Orbiter Assessment (IOA): FMEA/CIL instructions and ground rules
[NASA-CR-185551] N90-10922
Independent Orbiter Assessment (IOA): Assessment of the electrical power generation/power reactant storage and distribution subsystem FMEA/CIL
[NASA-CR-185545] N90-10923
Independent Orbiter Assessment (IOA): Analysis of the DPS subsystem
[NASA-CR-185549] N90-10924
Independent Orbiter Assessment (IOA): Analysis of the atmospheric revitalization pressure control subsystem
[NASA-CR-185593] N90-10925
Independent Orbiter Assessment (IOA): Analysis of the remote manipulator system
[NASA-CR-185585] N90-10926
Independent Orbiter Assessment (IOA): Analysis of the orbiter main propulsion system
[NASA-CR-185584] N90-10927
Independent Orbiter Assessment (IOA): Analysis of the auxiliary power unit
[NASA-CR-185568] N90-10931
Independent Orbiter Assessment (IOA): Analysis of the backup flight system
[NASA-CR-185567] N90-10932
Independent Orbiter Assessment (IOA): Analysis of the electrical power distribution and control/electrical power generation subsystem
[NASA-CR-185538] N90-10933
Independent Orbiter Assessment (IOA): Analysis of the hydraulics/water spray boiler subsystem
[NASA-CR-185541] N90-10934
Independent Orbiter Assessment (IOA): Analysis of the electrical power distribution and control/remote manipulator system subsystem
[NASA-CR-185526] N90-10936
Independent Orbiter Assessment (IOA): Analysis of the extravehicular mobility unit
[NASA-CR-185540] N90-10937
Independent Orbiter Assessment (IOA): Analysis of the reaction control system, volume 1
[NASA-CR-185532-VOL-1] N90-10938
Independent Orbiter Assessment (IOA): Analysis of the reaction control system, volume 2
[NASA-CR-185532-VOL-2] N90-10939
Independent Orbiter Assessment (IOA): Analysis of the reaction control system, volume 3
[NASA-CR-185532-VOL-3] N90-10940
Independent Orbiter Assessment (IOA): Analysis of the electrical power distribution and control subsystem, volume 1
[NASA-CR-185529-VOL-1] N90-10941
Independent Orbiter Assessment (IOA): Analysis of the electrical power distribution and control subsystem, volume 2
[NASA-CR-185529-VOL-2] N90-10942
Independent Orbiter Assessment (IOA): Analysis of the landing/deceleration subsystem
[NASA-CR-185569] N90-10943
Independent Orbiter Assessment (IOA): Analysis of the mechanical actuation subsystem
[NASA-CR-185525] N90-10944
Independent Orbiter Assessment (IOA): Analysis of the pyrotechnics subsystem
[NASA-CR-185530] N90-10945
Independent Orbiter Assessment (IOA): Assessment of the pyrotechnics subsystem
[NASA-CR-185531] N90-10946
Independent Orbiter Assessment (IOA): Assessment of the nose wheel steering subsystem
[NASA-CR-185533] N90-10947
Independent Orbiter Assessment (IOA): Weibull analysis report
[NASA-CR-185534] N90-10948
Independent Orbiter Assessment (IOA): Assessment of the purge, vent and drain subsystem
[NASA-CR-185535] N90-10949
Independent Orbiter Assessment (IOA): Assessment of the extravehicular mobility unit, volume 1
[NASA-CR-185536-VOL-1] N90-10950
Independent Orbiter Assessment (IOA): Assessment of the extravehicular mobility unit, volume 2
[NASA-CR-185536-VOL-2] N90-10951
Independent Orbiter Assessment (IOA): Assessment of the mechanical actuation subsystem, volume 1
[NASA-CR-185527-VOL-1] N90-10952
Independent Orbiter Assessment (IOA): Assessment of the mechanical actuation subsystem, volume 2
[NASA-CR-185527-VOL-2] N90-10953
Independent Orbiter Assessment (IOA): CIL issues resolution report, volume 1
[NASA-CR-185524-VOL-1] N90-10954
Independent Orbiter Assessment (IOA): CIL issues resolution report, volume 2
[NASA-CR-185524-VOL-2] N90-10955
Independent Orbiter Assessment (IOA) CIL issues resolution report, volume 3
[NASA-CR-185524-VOL-3] N90-10956
Independent Orbiter Assessment (IOA): Assessment of the atmospheric revitalization pressure control subsystem FMEA/CIL
[NASA-CR-185594] N90-10957
Independent Orbiter Assessment (IOA): Analysis of the crew equipment subsystem
[NASA-CR-185591] N90-10958
Independent Orbiter Assessment (IOA): Assessment of the ascent thrust vector control actuator subsystem FMEA/CIL
[NASA-CR-185590] N90-10959
Independent Orbiter Assessment (IOA): FMEA/CIL assessment
[NASA-CR-185589] N90-10960
Independent Orbiter Assessment (IOA): Assessment of the displays and controls subsystem
[NASA-CR-185588] N90-10961

Independent Orbiter Assessment (IOA): Assessment of the Orbiter Experiment (OEX) subsystem
[NASA-CR-185587] N90-10962
Independent Orbiter Assessment (IOA): Analysis of the Orbiter Experiment (OEX) subsystem
[NASA-CR-185586] N90-10963
Independent Orbiter Assessment (IOA): Assessment of the remote manipulator system FMEA/CIL
[NASA-CR-185592] N90-10964
Independent Orbiter Assessment (IOA): Assessment of the EPD and C/remote manipulator system FMEA/CIL
[NASA-CR-185583] N90-10965
Independent Orbiter Assessment (IOA): Analysis of the communication and tracking subsystem
[NASA-CR-185582] N90-10967
Independent Orbiter Assessment (IOA): Analysis of the purge, vent and drain subsystem
[NASA-CR-185547] N90-10969
Independent Orbiter Assessment (IOA): Assessment of the backup flight system FMEA/CIL
[NASA-CR-185586] N90-10973
Independent Orbiter Assessment (IOA): Assessment of the manned maneuvering unit
[NASA-CR-185564] N90-10974
Independent Orbiter Assessment (IOA): Assessment of the rudder/speed brake subsystem FMEA/CIL
[NASA-CR-185558] N90-10975
Independent Orbiter Assessment (IOA): Assessment of the auxiliary power unit
[NASA-CR-185580] N90-10976
Independent Orbiter Assessment (IOA): Assessment of the life support and airlock support systems, volume 1
[NASA-CR-185581-VOL-1] N90-10977
Independent Orbiter Assessment (IOA): Assessment of the life support and airlock support systems, volume 2
[NASA-CR-185581-VOL-2] N90-10978

MCDONNELL-DOUGLAS CORP., HOUSTON, TX.

Independent Orbiter Assessment (IOA): Analysis of the instrumentation subsystem
[NASA-CR-185571] N90-10928
Independent Orbiter Assessment (IOA): Analysis of the ascent thrust vector control actuator subsystem
[NASA-CR-185579] N90-10929
Independent Orbiter Assessment (IOA): Analysis of the body flap subsystem
[NASA-CR-185574] N90-10930
Independent Orbiter Assessment (IOA): Analysis of the elevon subsystem
[NASA-CR-185576] N90-10935
Independent Orbiter Assessment (IOA): Assessment of the landing/deceleration (LDG/DEC) subsystem FMEA/CIL
[NASA-CR-185570] N90-10966
Independent Orbiter Assessment (IOA): Assessment of the body flap subsystem FMEA/CIL
[NASA-CR-185575] N90-10968
Independent Orbiter Assessment (IOA): Assessment of the elevon actuator subsystem FMEA/CIL
[NASA-CR-185578] N90-10970
Independent Orbiter Assessment (IOA): Assessment of the crew equipment subsystem
[NASA-CR-185577] N90-10971
Independent Orbiter Assessment (IOA): Assessment of instrumental subsystem FMEA/CIL
[NASA-CR-185572] N90-10972
Independent Orbiter Assessment (IOA): Assessment of the active thermal control system
[NASA-CR-185573] N90-10979

MECHANICAL TECHNOLOGY, INC., LATHAM, NY.

Automotive Stirling engine development program
[NASA-CR-180839] N90-11654

MESSERSCHMITT-BOELKOW-BLOHM G.M.B.H., BREMEN (GERMANY, F.R.).

Multi-axis transient testing: Experimental investigations N90-11042

MESSERSCHMITT-BOELKOW-BLOHM G.M.B.H., MUNICH (GERMANY, F.R.).

Development of the integrated all-weather navigation system for Tornado N90-10849
Flight testing of the Tornado Terrain Following System N90-10875
Environmental testing: An approach to more cost efficiency N90-10988
Modeling of liquid sloshing effects in multibody systems N90-11023
Worked-in holes in three-dimensional reinforced composites N90-11060

MIAMI UNIV., CORAL GABLES, FL.

International conference on numerical grid generation in computational fluid dynamics
[AD-A211082] N90-11262

MICHIGAN STATE UNIV., EAST LANSING.

Solidification front/viscous phase transitions, forward-backward heat equations
[AD-A211068] N90-11114
An analytical and experimental study of the elastodynamic response characteristics of planar linkage mechanism with bearing clearances N90-11336

MICHIGAN UNIV., ANN ARBOR.

Evaporation and combustion of dense sprays with a bimodal droplet size distribution N90-11094
Nonlinear optical studies of resonant systems
[AD-A211032] N90-11301

MIDWEST RESEARCH INST., GOLDEN, CO.

Proceedings of the Polycrystalline Thin Film Program Meeting
[DE89-009457] N90-11348
Novel thin-film CuInSe2 fabrication
[DE89-009440] N90-11604

MILLMAN (GEORGE H.), DEWITT, NY.

An ionospheric model for HF sky-wave backscatter radar N90-11401

MINNESOTA UNIV., MINNEAPOLIS.

Capacitive behavior in conducting polymers: The ac impedance and quartz crystal microbalance studies
[AD-A210754] N90-11150
Cell performance of ultra-thin polymer cathode system: Theoretical energy and power density projections
[AD-A210786] N90-11151
Electrolyte dependence of charge injection processes for electroactive polymer films
[AD-A210787] N90-11152
Lithium polymer electrolyte battery, electrochemical behavior of cathode materials
[AD-A210755] N90-11235
An experimental investigation of transition in oscillating pipe flow N90-11249
Topographic map reading
[AD-A211269] N90-11340

MISSOURI UNIV., COLUMBIA.

Engineering specification and system design for CAD/CAM of custom shoes. Phase 5: UMC involvement (January 1, 1989 - June 30, 1989)
[NASA-CR-185838] N90-11456

MITRE CORP., BEDFORD, MA.

A calibrated, omnidirectional, LF loop antenna for GWEN (Ground Wave Emergency Network)
[AD-A211264] N90-11221

MITSUBISHI ELECTRIC CORP., TOKYO (JAPAN).

Test results on conceptual models of the large deployable antenna for mobile communications satellites N90-11050

N

NAPLES UNIV. (ITALY).

On the possibility of producing artificial ionization and polar aurora in the ionosphere by radio-waves emitted from the ground N90-11388

NATIONAL ACADEMY OF SCIENCES - NATIONAL RESEARCH COUNCIL, WASHINGTON, DC.

Toward a national research network
[PB89-198709] N90-11644
Globalization of Technology: International Perspectives. Proceedings of the 6th Convocation of the Council of Academies of Engineering and Technological Sciences
[PB89-198840] N90-11645

NATIONAL AERONAUTICS AND SPACE ADMINISTRATION, WASHINGTON, DC.

Space Station Freedom: A foothold on the future
[NASA-NP-107/10-88] N90-10907
Shuttle Atlantis to deploy Galileo probe toward Jupiter
[NASA-TM-101888] N90-10982

NATIONAL AERONAUTICS AND SPACE ADMINISTRATION. AMES RESEARCH CENTER, MOFFETT FIELD, CA.

Transfer functions for nonlinear systems via Fourier-Borel transforms
[NASA-TM-100034] N90-10828
Design of a final approach spacing tool for TRACON air traffic control
[NASA-TM-102229] N90-10841
Real-time flight test analysis and display techniques for the X-29A aircraft N90-10866
Flow visualization techniques for flight research N90-10878
A computational/experimental study of the flow around a body of revolution at angle of attack
[NASA-TM-88329] N90-11254
Techniques for optimizing human-machine information transfer related to real-time interactive display systems
[NASA-TM-100450] N90-11441
A diagnostic for determining the quality of single-reference electron correlation methods N90-11554

NATIONAL AERONAUTICS AND SPACE ADMINISTRATION. GODDARD SPACE FLIGHT CENTER, GREENBELT, MD.

Research and test facilities for development of technologies and experiments with commercial applications
[NASA-TM-101789] N90-10909
MOXE: An X-ray all-sky monitor for Soviet Spectrum-X-Gamma Mission
[NASA-TM-101266] N90-11280
Observations of ionosphere/magnetosphere interactions from the Dynamics Explorer satellites N90-11376
Two-Dimensional Intercomparison of Stratospheric Models
[NASA-CP-3042] N90-11405
Report on the 2-D Model Intercomparison Workshop held January 11-16, 1987 in Fort Myers Beach, Florida, chapter 2 N90-11406
Report of the 1988 2-D Intercomparison Workshop, chapter 3 N90-11407
Model documentation, chapter 4 N90-11408
Introduction and data summary, chapter 5 N90-11409

NATIONAL AERONAUTICS AND SPACE ADMINISTRATION. LYNDON B. JOHNSON SPACE CENTER, HOUSTON, TX.

STS payload design load evolution N90-10989
Considerations for a design and operations knowledge support system for Space Station Freedom
[NASA-TM-102156] N90-11451

NATIONAL AERONAUTICS AND SPACE ADMINISTRATION. LANGLEY RESEARCH CENTER, HAMPTON, VA.

Measurements of pressures on the tail and aft fuselage of an airplane model during rotary motions at spin attitudes
[NASA-TP-2939] N90-10829
Low-speed, high-lift aerodynamic characteristics of slender, hypersonic accelerator-type configurations
[NASA-TP-2945] N90-10830
Design of a final approach spacing tool for TRACON air traffic control
[NASA-TM-102229] N90-10841
Integrated multidisciplinary design optimization of rotorcraft
[NASA-TM-101642] N90-10889
Applications of the hybrid automated reliability predictor: Revised edition
[NASA-TP-2760-REV] N90-11454
New computing systems and their impact on structural analysis and design
[NASA-CR-185831] N90-11457
Technical communications in aeronautics: Results of an exploratory study. An analysis of managers' and nonmanagers' responses
[NASA-TM-101625] N90-11647

NATIONAL AERONAUTICS AND SPACE ADMINISTRATION. LEWIS RESEARCH CENTER, CLEVELAND, OH.

Advanced technologies impact on compressor design and development: A perspective
[NASA-TM-102341] N90-10891
Evaluation of supercritical cryogen storage and transfer systems for future NASA missions
[NASA-TM-102394] N90-10912
The effect of electrode configuration on arcjet performance
[NASA-TM-102346] N90-11081
Heat transfer to throat tubes in a square-chambered rocket engine at the NASA Lewis Research Center
[NASA-TM-102336] N90-11082
Hydrogen-silicon carbide interactions
[NASA-TM-102382] N90-11144
Droplet combustion experiment drop tower tests using models of the space flight apparatus
[NASA-TM-101472] N90-11196
Laser anemometer measurements in a transonic axial-flow fan rotor
[NASA-TP-2879] N90-11245
Wall-layer eruptions in turbulent flows
[NASA-TM-102362] N90-11250
Gas-phase flowrate effect on disintegrating cryogenic liquid-jets
[NASA-TM-102357] N90-11277
A nonoscillatory, characteristically convected, finite volume scheme for multidimensional convection problems
[NASA-TM-102354] N90-11497

NATIONAL AERONAUTICS AND SPACE ADMINISTRATION. MARSHALL SPACE FLIGHT CENTER, HUNTSVILLE, AL.

Atmospheric environment for space shuttle (STS-29) launch
[NASA-TM-100376] N90-10980

Atmospheric environment for space shuttle (STS-30) launch
[NASA-TM-100381] N90-10981

Derivation of improved load transformation matrices for launchers-spacecraft coupled analysis, and direct computation of margins of safety N90-11077

Concepts for microgravity experiments utilizing gloveboxes
[NASA-TM-100378] N90-11195

Gamma radiation background measurements from Spacelab 2
[NASA-CR-183782] N90-11689

NATIONAL AERONAUTICS AND SPACE ADMINISTRATION. WHITE SANDS TEST FACILITY, NM.

An atmospheric pressure flow reactor: Gas phase kinetics and mechanism in tropospheric conditions without wall effects N90-11160

NATIONAL AEROSPACE LAB., AMSTERDAM (NETHERLANDS).

Flight testing in the Netherlands: An overview N90-10884

NATIONAL AEROSPACE LAB., TOKYO (JAPAN).

Study for optimization of redundant vane-type flow-direction sensing systems and numerical analysis for design of the systems
[NAL-TM-571] N90-10890

Flight simulator evaluation of a head-down display
[NAL-TM-573] N90-10898

Flight simulation test facility: Function and specification of the simulator cockpit system
[NAL-TM-577] N90-10899

On the motion equation of an elastically supported two degree of freedon gyro
[NAL-TM-568] N90-11276

Tower wake/blade interaction noise of a wind turbine
[NAL-TR-945] N90-11344

Evaluation test of CCD area sensor for star sensor
[NAL-TM-570] N90-11566

View on recent fuel costs in airlines
[NAL-TM-569] N90-11653

NATIONAL CENTER FOR ATMOSPHERIC RESEARCH, BOULDER, CO.

NCAR (National Center for Atmospheric Research) master mechanism of the gas phase chemistry, version 2.0
[PB89-208979] N90-11413

National Center For Atmospheric Research annual report, fiscal year 1988
[PB89-208987] N90-11428

NATIONAL CLIMATE PROGRAM OFFICE, ROCKVILLE, MD.

National Climate Program five-year plan, 1989-1993
[PB89-207369] N90-11426

NATIONAL GEOPHYSICAL DATA CENTER, BOULDER, CO.

Solar-geophysical data number 536, part 1. Data for March, Febuary 1989 and late data
[PB89-194716] N90-11684

Solar-geophysical data number 537, part 1. Data for April, March 1989 and late data
[PB89-207393] N90-11685

NATIONAL INST. OF STANDARDS AND TECHNOLOGY, BOULDER, CO.

Interlaboratory comparison of two types of line-source thermal-conductivity apparatus measuring five insulating materials
[PB89-218325] N90-11142

NATIONAL INST. OF STANDARDS AND TECHNOLOGY, GAITHERSBURG, MD.

NIST (National Institute of Standards and Technology) measurement services: The calibration of thermocouples and thermocouple materials
[PB89-209340] N90-11274

NASA/NBS (National Aeronautics and Space Administration/National Bureau of Standards) standard reference model for telerobot control system architecture (NASREM)
[NASA-CR-185078] N90-11310

Assessment of space power related measurement requirements of the Strategic Defense Initiative
[PB89-209357] N90-11343

Electronic publishing: Guide to selection
[PB89-214753] N90-11448

Software configuration management: An overview
[PB89-193833] N90-11458

NATIONAL MARINE FISHERIES SERVICE, LA JOLLA, CA.

Interannual variability of temperature in the upper layer of the North Pacific eastern boundary region, 1971-1987
[PB89-190227] N90-11434

NATIONAL OCEANIC AND ATMOSPHERIC ADMINISTRATION, BOULDER, CO.

Remote sensing techniques of the Wave Propagation Laboratory for the measurement of supercooled liquid water: Applications to aircraft icing
[PB89-208102] N90-10842

User's guide to the Space Environment Services Center geophysical alert broadcasts
[PB89-194617] N90-11411

Lidar observations of the stratospheric aerosol: Boulder, Colorado, 1985 to 1987
[PB89-203871] N90-11425

NATIONAL OCEANIC AND ATMOSPHERIC ADMINISTRATION, MIAMI, FL.

Hurricane Research Division fiscal year 1988 programs, fiscal year 1989 projections
[PB89-152268] N90-11418

NATIONAL OCEANIC AND ATMOSPHERIC ADMINISTRATION, ROCKVILLE, MD.

Meteorological rocket observations
[PB89-168769] N90-11419

NATIONAL OCEANIC AND ATMOSPHERIC ADMINISTRATION, SEATTLE, WA.

The sea ice margins: A summary of physical phenomena
[PB89-212328] N90-11436

NATIONAL OCEANIC AND ATMOSPHERIC ADMINISTRATION, SILVER SPRING, MD.

Micrometeorological investigation of surface exchange of trace gases: A case study
[PB89-208375] N90-11412

NATIONAL SPACE DEVELOPMENT AGENCY, TOKYO (JAPAN).

Development of the large spacecraft structure N90-11020

NATIONAL WEATHER SERVICE, GARDEN CITY, NY.

Relation of wind field and buoyancy to rainfall inferred from radar
[PB89-208326] N90-11424

NATIONAL WEATHER SERVICE, MINNEAPOLIS, MN.

Airborne gamma radiation snow water equivalent and soil moisture measurements and satellite areal extent of snow cover measuerments: A user's guide, version 3.0
[PB89-177877] N90-11338

NAVAL AIR DEVELOPMENT CENTER, WARMINSTER, PA.

Filling or outlining shapes with color: The effects on a visual search task
[AD-A211067] N90-11444

NAVAL AIR TEST CENTER, PATUXENT RIVER, MD.

US Navy principal site testing concept and the F-18 N90-10861

Air Combat Environment Test and Evaluation Facility (ACETEF) N90-10883

NAVAL HEALTH RESEARCH CENTER, SAN DIEGO, CA.

Test-retest reliability of oxford Medilog 9000 sleep recording and SS-90-3 sleep stage scoring
[AD-A211165] N90-11440

NAVAL MEDICAL RESEARCH INST., BETHESDA, MD.

Robust spatial calibration of a planar positron camera
[AD-A210773] N90-11284

NAVAL OCEAN SYSTEMS CENTER, SAN DIEGO, CA.

Medium scale structure of the F-region N90-11372

NAVAL POSTGRADUATE SCHOOL, MONTEREY, CA.

Deep null antennas and their applications to tactical VHF radio communications
[AD-A210656] N90-11214

Laser altimeter for use over the ocean
[AD-A211252] N90-11286

Analysis of forest fire smoke using satellite imagery
[AD-A210657] N90-11339

NAVAL RESEARCH LAB., WASHINGTON, DC.

Microsensor and pattern recognition techniques in hydrazine detection N90-11177

Atmospheric aerosol size distributions and optical properties found in the marine boundary layer over the Atlantic Ocean
[AD-A210800] N90-11431

The Si(1-x)Nx Rugate
[AD-A211236] N90-11572

NAVAL SURFACE WARFARE CENTER, SILVER SPRING, MD.

Battery actuation of NiTINOL at sub-zero temperatures
[AD-A211254] N90-11237

NAVAL UNDERWATER SYSTEMS CENTER, NEW LONDON, CT.

Alias-free Wigner distribution function and complex ambiguity function for discrete-time samples
[AD-A211050] N90-11533

NEGION, INC., HAYWARD, CA.

Projections for a steady-state tokamak reactor based on ITER
[DE89-016678] N90-11589

NEW SOUTH WALES UNIV., KENSINGTON (AUSTRALIA).

Laser grooved and polycrystalline silicon solar cell research
[DE89-015196] N90-11347

NORFOLK STATE UNIV., VA.

Research, development, training and education using the Ada programming language
[AD-A210760] N90-11486

NORTH CAROLINA AGRICULTURAL AND TECHNICAL STATE UNIV., GREENSBORO.

Effect of thermal and cyclic loads on silicon carbide yarn reinforced glass matrix composites
[DE89-016554] N90-11091

NORTH CAROLINA CENTRAL UNIV., DURHAM.

Precision materials characterization in the near millimeter and submillimeter wavelength range
[AD-A210655] N90-11106

NORTH CAROLINA STATE UNIV., RALEIGH.

Experiments in fault tolerant software reliability
[NASA-CR-185927] N90-11460

Kinetics and mechanisms of primary and steady state creep in B- and Al-containing alpha silicon carbide
[AD-A210739] N90-11616

NORTH CAROLINA UNIV., CHAPEL HILL.

Parameter estimation in functional and partial differential equations
[AD-A211040] N90-11511

NORWEGIAN DEFENCE RESEARCH ESTABLISHMENT, KJELLER.

Design of a Kalman filter for transfer alignment N90-10848

On algorithms for generating computationally simple piecewise linear classifiers
[NDRE/PUBL-89/1001] N90-11459

NOTTINGHAM UNIV. (ENGLAND).

High accuracy coordinate determination using the global positioning system N90-10858

NOVA UNIV., DANIA, FL.

Nonlinear adjustment with or without constraints, applicable to geodetic models
[AD-A210820] N90-11509

NSI TECHNOLOGY SERVICES CORP., CORVALLIS, OR.

Interrelation of experimental exposure and ambient air quality data for comparison of ozone exposure indices and estimating agricultural losses
[PB89-195036] N90-11353

O

OAK RIDGE NATIONAL LAB., TN.

A preliminary sensitivity analysis of the Generalized Escape System Simulation (GESS) computer program
[DE89-016891] N90-10844

Neutron scattering studies of amorphous Invar alloys
[DE89-016868] N90-11126

Fifth International Workshop on Glasses and Ceramics from Gels
[DE89-016899] N90-11147

The theory of ac impedance of rough electrode-electrolyte interfaces
[DE89-017474] N90-11243

Using self-calibrating thermocouples in industry
[DE89-013539] N90-11278

Sensors for nondestructive testing and evaluation of materials
[DE89-014763] N90-11279

Synchrotron radiation, free electron laser, and nuclear structure
[DE89-017352] N90-11306

Results from the second year of operation of the Federal Methanol Fleet at Argonne National Laboratory
[DE89-016935] N90-11319

Systems analysis considerations in artificial intelligence/expert systems technology applications
[DE89-016847] N90-11490

Extraction induced emittance growth for negative ion sources
[DE89-017586] N90-11559

Hybrid particle-fluid approach to low-frequency turbulence in magnetically confined plasmas
[DE89-015904] N90-11579

Projections for a steady-state tokamak reactor based on ITER
[DE89-016678] N90-11589

A study of the tribological and surface micromechanical properties of YBa2Cu3O7-x
[DE89-015680] N90-11607

Ion beam annealing of Ga-implanted Si
[DE89-016857] N90-11610

Propagation of normal zones of finite size in large, composite superconductors
[DE89-016866] N90-11611

Origins of high-temperature superconductivity in the new copper oxide based ceramic superconductors
[DE89-016543] N90-11622
Dielectronic excitation and recombination in crystal channels
[DE89-016864] N90-11625
Rational design of high-current cable-in-conduit superconductors
[DE89-016867] N90-11626
Neutron scattering experiments on high-temperature superconducting materials: Foreign trip report, September 13, 1988--October 4, 1988
[DE89-017451] N90-11630
Technology applications bulletins
[DE89-017454] N90-11651
The transfer and diffusion of new technologies: A review of the economics literature
[DE89-015671] N90-11655

OAK RIDGE Y-12 PLANT, TN.
Electron beam welding: Model of high voltage bias transmission line and termination circuits
[DE89-016900] N90-11323

OFFICE NATIONAL D'ETUDES ET DE RECHERCHES AEROSPATIALES, TOULOUSE (FRANCE).
Analysis of flutter tests with the use of a telemetry system N90-10871

OFFICE OF TECHNOLOGY ASSESSMENT, WASHINGTON, DC.
Higher education for science and technology: A background paper
[PB89-191290] N90-11642

OHIO STATE UNIV., COLUMBUS.
Forty-fourth symposium on molecular spectroscopy
[AD-A210752] N90-11111
Transport studies of conducting polymers N90-11140
Near zone-basic scattering code user's manual with space station applications
[NASA-CR-185925] N90-11209
An experimental SMI adaptive antenna array for weak interfering signals
[NASA-CR-185976] N90-11211
Constitutive parameter measurements of lossy materials
[NASA-CR-183398] N90-11603

OKLAHOMA UNIV., NORMAN.
Method of characteristic studies for rotational flow downstream of a curved shock wave N90-11252

OLD DOMINION UNIV., NORFOLK, VA.
An experimental investigation of the aerodynamic characteristics of slanted base ogive cylinders using magnetic suspension technology
[NASA-CR-181708] N90-10834
A direct two response approach for updating analytical dynamic models of structures with emphasis on uniqueness N90-11028

OMETRON LTD., LONDON (ENGLAND).
Advances in instrumentation for experimental stress and vibration analysis and its applications N90-11069

ONSALA SPACE OBSERVATORY (SWEDEN).
The mass distribution in the galactic centre estimated from OH/IR stars
[PB89-154884] N90-11663

OREGON GRADUATE CENTER FOR STUDY AND RESEARCH, BEAVERTON.
Deformation induced microstructural and microchemical changes during thermomechanical treatment
[DE89-017266] N90-11127

OREGON UNIV., EUGENE.
Research in X-ray optics with the ultimate aim of constructing a synchrotron radiation pumped soft X-ray lithium laser
[DE89-016788] N90-11304
Nonlinear dynamics of broad-band lasers
[DE89-017442] N90-11307

P

PACIFIC FLEET, CAMP SMITH, HI.
Two enhancements of the logarithmic least-squares method for analyzing subjective comparisons
[AD-A211192] N90-11514

PACIFIC NORTHWEST LAB., RICHLAND, WA.
Freeze-dried processing of tungsten heavy alloys
[DE89-015171] N90-11122
Grain boundary chemistry in irradiated stainless steel and its influence on environmental degradation
[DE89-016827] N90-11125
Failure modes and mechanisms in nickel alloys: Primarily austenitic stainless steel
[DE89-016823] N90-11132
Design of ceramic fabric heat pipe with water working fluid
[DE89-016565] N90-11265
Potential industrial applications for composite phase-change materials as thermal energy storage media
[DE89-015170] N90-11346
Hanford Meteorological Station computer codes. Volume 10: The ARCHIVE computer code
[DE89-016175] N90-11429
Principal components in multivariate control charts
[DE89-016828] N90-11489

PARIS VI UNIV. (FRANCE).
Study of high frequency water vapor absorption parameters
[AD-A210676] N90-11108

PENNSYLVANIA STATE UNIV., UNIVERSITY PARK.
Analytical study of mistuning/friction/aerodynamics interaction in a bladed disk assembly
[AD-A211139] N90-10893
Turbulent reacting flows in solid-propellant ducted rocket combustors N90-11079
The structure of Reynolds stress in the near wall region of a turbulent pipe flow N90-11247
Acoustic studies of new materials: Quasicrystals, low-loss glasses and high Tc superconductors
[AD-A211281] N90-11551

POLITECNICO DI MILANO (ITALY).
Thermoelastic behavior of large space structures: Modeling and control N90-11012

POLITECNICO DI TORINO (ITALY).
A contribution to the stability analysis of large space structures N90-10997
Equilibrium and stability in composite thin shell N90-10998

PRINCETON UNIV., NJ.
Procedures for separations within batches of values, 1. The orderly tool kit and some heuristics
[AD-A210652] N90-11531
The stability of magnetohydrodynamic shock waves in molecular clouds N90-11665

PURDUE UNIV., WEST LAFAYETTE, IN.
Frequency domain aerodynamic analysis of interacting rotating systems N90-10837
Nitramine composite solid propellant modeling N90-11183
Computation of transient three-dimensional interstage flowfields using the arbitrary Lagrangian-Eulerian method N90-11253
The 3D-POLY: A robot vision system for recognizing objects in occluded environments N90-11313
Applications of artificial intelligence to digital photogrammetry N90-11486

Q

QUESTEK, INC., CENTERPORT, NY.
See and avoid/cockpit visibility
[DOT/FAA/CT-TN89/18] N90-10843

R

RAND CORP., SANTA MONICA, CA.
Phoebe: A preliminary control network and rotational elements
[NASA-CR-185716] N90-11680

RDP, INC., WALTHAM, MA.
Offaxis radiance studies for infrared sensors
[AD-A210790] N90-11570

RENSSELAER POLYTECHNIC INST., TROY, NY.
Exploratory study of niobium, titanium, zirconium and tantalum aluminides
[AD-A210658] N90-11615

RESEARCH INST. FOR ADVANCED COMPUTER SCIENCE, MOFFETT FIELD, CA.
Simplified rate-law integration for reactions which are first order in each of two reactants
[NASA-CR-185408] N90-11093
Telescience Testbed Pilot Program
[NASA-CR-184594] N90-11455

RICE UNIV., HOUSTON, TX.
Studies of ultrathin magnetic films and particle-surface interactions with spin-sensitive electron spectroscopies
[DE89-016741] N90-11556

ROCKWELL INTERNATIONAL CORP., DOWNEY, CA.
Automated stress analysis of Shuttle orbiter thermal protection system N90-11043

ROME UNIV. (ITALY).
Analytic signals in the damping coefficient estimation N90-11003
Evaluation of dispersive behavior in periodic structures by discrete Fourier transform N90-11014
Numerical treatment of the thermo-structural-dynamic problems: The interpolation techniques N90-11016
Study of a gallium arsenide solar cell interconnector N90-11033
Structural problems of accurate inflatable surfaces N90-11044
JOE: Jordan Optimized Eigensolver. A step toward a numerical Jordan form analyzer for control and interactive thermo-structural-dynamic applications N90-11047

ROYAL AEROSPACE ESTABLISHMENT, FARNBOROUGH (ENGLAND).
Evaluation of store carriage (and release) environment using flight instrumented stores N90-10876
Average diurnal and seasonal profiles of ionospheric storms N90-11371
Joint VHF coherent radar and oblique sounder observations for short term ionosphere forecasting N90-11399

RUHR UNIV., BOCHUM (GERMANY, F.R.).
Investigations of the influence of magnetically long range ordered phases on the electronic charge transport in metallic glasses
[ETN-89-94672] N90-11155

S

SAINT ANDREW'S UNIV. (SCOTLAND).
Elements of a 200 watt pulsed excimer laser N90-11295
The astronomy of Andean myth: The history of a cosmology N90-11660

SALFORD UNIV. (ENGLAND).
Development of an adaptive time of flight system for the measurement of fluid flow velocity N90-11273

SANDIA NATIONAL LABS., ALBUQUERQUE, NM.
Photochemically-driven biomimetic oxidation of alkanes and olefins
[DE89-011536] N90-11097
Thermochemical model for shock-induced chemical reactions in porous thermite: The heat detonation model
[DE89-016528] N90-11100
Time-resolved mass spectrometry technique for studying fast transient CHNO explosive decomposition kinetics
[DE89-016540] N90-11101
Experimental measurements of shock-induced vaporization in cadmium and lead
[DE89-016877] N90-11103
Shock-induced atomic-scale structure in metals
[DE89-016539] N90-11124
A shock initiation model for fine-grained hexanitrostilbene
[DE89-007641] N90-11185
Estimation of the C-J pressure of explosives
[DE89-013811] N90-11187
Consequence of condensed-phase formation in transient burning of TiHx/KClO in a closed system
[DE89-013922] N90-11188
Powder morphology effects in the ignition of titanium-based pyrotechnics
[DE89-017229] N90-11191
Internal voltages and currents in well-shielded cylindrical objects due to simulated direct-strike lightning
[DE89-012664] N90-11231
ASIC (Application Specific Integrated Circuit) replacement for an SSI (Small Scale Integrated) component design: A case study
[DE89-013494] N90-11232
A severe human ESD (Electrostatic Discharge) model for safety and high reliability system qualification testing
[DE89-016177] N90-11233
A comparison of fixed-base and driven-base modal testing of an electronics package
[DE89-016673] N90-11240
Lifetime testing of commercially available 3.0 (mu)f, 100 kV pulsed-power capacitors
[DE89-017230] N90-11242
Response of standardized PVDF piezoelectric polymer gauges to direct shock pressures between 8 and 32 GPa
[DE89-016811] N90-11282
The Sandia standard for PVDF (Polyvinylidene Di-Fluoride) shock sensors
[DE89-016530] N90-11287
Gas-accelerated plate stability study
[DE89-016880] N90-11289
Rethinking synthesis of fine-motion strategies
[DE89-016671] N90-11322
Land vehicle teleoperation under conditions of reduced video resolution
[DE89-016925] N90-11324
Techniques for recovery of shock-loaded samples
[DE89-016881] N90-11337
Laser grooved and polycrystalline silicon solar cell research
[DE89-015196] N90-11347
Irreversible phase transition and wave propagation in silicate geologic materials
[DE89-016031] N90-11414

Performance reports for EIM (Engineering Information Management) computer systems: A managerial perspective
[DE89-015194] N90-11449
GaAs ASIC design case study
[DE89-013934] N90-11461
Evaluation of integrals related to the Debye function
[DE89-016930] N90-11499
DMC (Distinct Motion Code): A rigid body motion code for determining the interaction of multiple spherical particles
[DE89-016929] N90-11543
Optical coherence multiplexing for interprocessor communications
[DE89-016186] N90-11568
Acceleration of thin foil targets using fiber-coupled optical pulses
[DE89-016526] N90-11569
Hydrogen-assisted thermal donor formation in silicon
[DE89-016809] N90-11594
Pulsed-power switching for inertial confinement fusion with light ion beams
[DE89-016810] N90-11595
Launched electrons in plasma opening switches
[DE89-016886] N90-11596
A fermi liquid electric structure and the nature of the carriers in high-T(sub c) cuprates: A photoemission study
[DE89-016774] N90-11624
Strain and density dependent valence-band masses in InGaAs/GaAs and GaAs/GaAsP strained-layer structures
[DE89-016882] N90-11627
Effects of shock-modification on superconductivity in Tl2Ca2Ba2Cu3Oy and Bi2Ca5r2Cu2Ox
[DE89-017231] N90-11629
LEXER: A tool for lexical analysis of program input
[DE89-016924] N90-11649

SANDIA NATIONAL LABS., LIVERMORE, CA.
A characterization of the side bonding, upset plug welding process
[DE89-015181] N90-11315

SCIENCE APPLICATIONS INTERNATIONAL CORP., MCLEAN, VA.
Free-world microelectronic manufacturing equipment
[FASAC-TAR-4070] N90-11228
Coordinated multi-parameter measurements and predictions of the global-scale ionosphere N90-11397

SCIENCE APPLICATIONS INTERNATIONAL CORP., SAN DIEGO, CA.
Free-world microelectronic manufacturing equipment
[FASAC-TAR-4070] N90-11228

SCIENCE RESEARCH COUNCIL, CHILTON (ENGLAND).
Ionosphere-thermosphere coupling at high latitudes: Aspect angle dependence of non-thermal plasmas N90-11382

SCIENTIFIC RESEARCH ASSOCIATES, INC., GLASTONBURY, CT.
User's manual for PEPSIG NASA tip vortex version
[NASA-CR-182178] N90-10835
Computation of the tip vortex flowfield for advanced aircraft propellers
[NASA-CR-182179] N90-10836

SOUTHAMPTON UNIV. (ENGLAND).
Global ionospheric dynamics: A review N90-11367

SOUTHWEST RESEARCH INST., SAN ANTONIO, TX.
Advanced manned space flight simulation and training: An investigation of simulation host computer system concepts
[NASA-CR-185998] N90-10911
Study of the behavioral and biological effects of high intensity 60 Hz electric fields
[DE89-015528] N90-11436

ST SYSTEMS CORP., MONTEREY, CA.
Gridded environmental data compaction: An investigation
[AD-A210580] N90-11430

STANFORD LINEAR ACCELERATOR CENTER, CA.
Three level constraints on conformal field theories and string models
[DE89-016942] N90-11634
Moduli spaces and topological quantum field theories
[DE89-016943] N90-11639

STANFORD UNIV., CA.
Laser physics and laser techniques
[AD-A211117] N90-11302
Stochastic optimization by simulation: Some experiments with a simple steady-state queue
[AD-A210762] N90-11508
An extension of Cochran's test for homogeneity of variances
[AD-A211054] N90-11534

STATE UNIV. OF NEW YORK, BUFFALO.
Quasi-diffusion between phonon and roton gases in two- and three-dimensional liquid helium
[AD-A210565] N90-11096

STATEWIDE AIR POLLUTION RESEARCH CENTER, RIVERSIDE, CA.
Atmospheric chemistry of the fuel hydrazines N90-11158

STUTTGART UNIV. (GERMANY, F.R.).
Worked-in holes in three-dimensional reinforced composites N90-11060
Precipitation and transformation toughening of Al-Mg signals
[ETN-89-94675] N90-11138
Utilization of photorefractive crystals in optical image processing
[ISBN-3-923560-06-0] N90-11292

SUNPOWER, INC., ATHENS, OH.
Free-Piston Stirling Engine magnetically coupled heat pump: Critical component evaluation
[DE89-015646] N90-11316
Dynamic characteristics concerned in the design of a free-piston Stirling engine/magnetic coupling/compressor system
[DE89-015981] N90-11317

SUSSEX UNIV., BRIGHTON (ENGLAND).
New statistical approaches to galaxy clustering N90-11674

SVERDRUP TECHNOLOGY, INC., CLEVELAND, OH.
Hydrogen-silicon carbide interactions
[NASA-TM-102382] N90-11144
A nonoscillatory, characteristically convected, finite volume scheme for multidimensional convection problems
[NASA-TM-102354] N90-11497

SWEDISH DEFENCE RESEARCH ESTABLISHMENT, LINKOEPING.
A brief description of traveling wave tubes
[FOA-C-30522-3.6] N90-11244
Fiber optic technique for surveillance and control of mine fields
[FOA-C-30526-3.1] N90-11293
Laser techniques for ground to air applications
[FOA-C-30524-3.1] N90-11309
Definition of imaging performance for satellite surveillance, models, and simulations
[FOA-C-30493-9.4] N90-11341
Thermal radiation from terrain: Measurements and first results
[FOA-C-30525-3.1] N90-11342
Solar radiation in Linkoeping (Sweden): Variations over half a year in irradiance and spectral composition in the interval 400-1000 nm
[FOA-C-30521-3.1] N90-11417
Linkoeping's A.I. Consortium (LAIC) for plan guided systems. Review of the first 18 months
[FOA-C-30528-3.4] N90-11537
Turbulence effects for retroreflection
[FOA-C-30523-3.1] N90-11575
The Swedish defense research needs: For surveillance and seeker applications
[FOA-C-30520-3.3] N90-11691

SWEDISH DEFENCE RESEARCH ESTABLISHMENT, STOCKHOLM.
Laser Raman spectroscopy: A literature review
[FOA-C-20753-2.3] N90-11121
Synthesis of powder with gel technique
[FOA-C-20752-2.4(2.1)] N90-11156
N-Hexyl Carborane (NHC) as combustion catalyst in composite propellants
[FOA-C-20755-2.1] N90-11193
Test of EED (Electro-Explosive Devices). Part 3: Statistical aspects on the estimation of sensitivity
[FOA-C-20749-2.3-PT-3] N90-11194
Numerical simulation of turbulent flow downstream a sudden axisymmetric expansion
[FOA-C-20758-2.1] N90-11272

SWEDISH INST. OF SPACE PHYSICS, KIRUNA.
Theory of atomic spectral emission intensity
[IRF-PREPRINT-110] N90-11641

SWEDISH INST. OF SPACE PHYSICS, UMEA.
Quantitative methods for waves in space plasmas
[PB89-210256] N90-11599
Can ion acceleration by double-cyclotron absorption produce O(+) ion conics
[IRF-PREPRINT-114] N90-11600

SYSTEMS ENGINEERING LABS., INC., GREENBELT, MD.
Frequency domain design of robust controllers for space structures
[AD-A211172] N90-10985

T

TECHNICAL RESEARCH CENTRE OF FINLAND, ESPOO.
Coatings in electrical contacts
[DE89-787739] N90-11234

TECHNICAL UNIV. OF ISTANBUL (TURKEY).
The middle and high latitude ionosphere at approximately 550 km altitude N90-11374

TECHNION - ISRAEL INST. OF TECH., HAIFA.
The 3-D heat transfer computer calculations of th e performance of the IAEA's air-bath calorimeters
[DE89-016908] N90-11283

TECHNION RESEARCH AND DEVELOPMENT FOUNDATION LTD., HAIFA (ISRAEL).
Estimation on nonlinear damping in second order distributed parameter systems
[NASA-CR-181890] N90-11494

TECHNISCHE HOCHSCHULE, AACHEN (GERMANY, F.R.).
The decay of viscoelastic fluid jets
[ETN-89-94667] N90-11270

TECHNISCHE HOGESCHOOL, EINDHOVEN (NETHERLANDS).
Non-linear wave-equations for low-frequency acoustic gravity waves N90-11365
On the influence of ionospheric conductivity on dispersion of acoustic gravity waves N90-11386

TECHNISCHE UNIV., BERLIN (GERMANY, F.R.).
Influence of grain refining on the casting, physical, mechanical, and electrochemical properties of technical aluminum
[ETN-89-94661] N90-11135
Investigation of commercial Al-Ti and Al-Ti-B master alloys and development of a new grain refining agent based on carbides for aluminum and aluminum alloys
[ETN-89-94663] N90-11136
A contribution to the synthesis of communication switching systems with decentralized control using modular components
[ETN-89-94660] N90-11226
Investigations into the influence of the state functions on the cross sections of the direct p,gamma reactions at energies in the 100 keV range, and project of a cascade accelerator for the measurement of the p,gamma capture cross sections
[ETN-89-94662] N90-11561

TECHNISCHE UNIV., BRUNSWICK (GERMANY, F.R.).
Flight test results of a complex precise digital flight control system N90-10870
Theoretical and experimental investigation of thin-walled aluminum panels under cyclic shear load N90-10996

TECHNISCHE UNIV., DELFT (NETHERLANDS).
MSP: Modeling of concurrent processes. Version 1.00 General introduction and directions for use
[REPT-88-88] N90-11477
A generalization of A. N. Habermann's theorem for semaphores
[REPT-88-98] N90-11484

TECHNISCHE UNIV., MUNICH (GERMANY, F.R.).
Calculation, optimization and comparison of optical transmission systems with superheterodyne reception
[ETN-89-94651] N90-11224

TELEDYNE GEOTECHNICAL, ALEXANDRIA, VA.
Iterative network magnitude estimation and uncertainty assessment with noisy and clipped data
[AD-A210707] N90-11507

TENNESSEE UNIV., KNOXVILLE.
A scalar/vector potential solution for aerodynamic coefficients in wind shear N90-10838
On a Taylor Weak Statement for finite element computations in gas dynamics N90-11251
Ionospheric total electron content, and far ultraviolet, near infrared oxygen emission N90-11410
On transonic flow over segmented slotted wind tunnel wall with mass transfer N90-11676

TEXAS A&M UNIV., COLLEGE STATION.
New secondary batteries utilizing electronically conductive polymer cathodes
[NASA-CR-185885] N90-11227
Rectangular subsonic jet flow field measurements
[NASA-CR-185962] N90-11255
Selective removal of organics for water reclamation
[NASA-CR-185959] N90-11445
Boundary kernel estimation of the two sample comparison density function
[AD-A210757] N90-11532

TEXAS UNIV., ARLINGTON.
Electronic and ionic transport in polymers
[AD-A210654] N90-11148

TEXAS UNIV., AUSTIN.
Use of Lanczos vectors in structural dynamics N90-11011
Accelerated aging of metal matrix composites N90-11085
Numerical solutions of turbulent flow with heat transfer over rough surfaces N90-11246
Questions from the Willmarth Workshop on New Directions in Research on Turbulent Wall-Layer Structures
[AD-A211282] N90-11264

The recovery of orbital and geophysical parameters using a spaceborne laser ranging system N90-11294
Magnetically levitated micro-robotics N90-11542
Nonlinear acoustics: Reflection and refraction, propagation in a periodic waveguide, scattering of sound by sound and ellipsoidal focusing
[AD-A211224] N90-11550
Theory of high-n toroidicity-induced shear Alfven eigenmode in tokamaks
[DE89-016726] N90-11582
Particle simulation in curvilinear coordinate systems
[DE89-016727] N90-11583
A study of runaway electron confinement and theory of neoclassical MHD turbulence
[DE89-016728] N90-11584
Inferring data base requirements from examples in forms N90-11646
Carbon isotope ratios and lithium abundances in open cluster giants N90-11684
Gas dynamical processes in the theory of galaxy formation N90-11673

THERMEDICS, INC., WOBURN, MA.
Description of a chemiluminescence detector system specifically designed for monitoring airborne hydrazine and oxidizer propellant vapors N90-11179

TRIESTE UNIV. (ITALY).
Markov processes in Hilbert space and continuous spontaneous localization of systems of identical particles
[DE89-618396] N90-11540

U

UKRAINIAN REGIONAL RESEARCH INST., KIEV (USSR).
Beam-plasma discharge in penetrating plasma
[DE89-630481] N90-11597

UNITED STATES STEEL CORP., MONROEVILLE, PA.
Thin section casting program. Volume 1: Executive summary and overview
[DE89-009030] N90-11198
Thin section casting program. Volume 2: Horizontal TSC (Thin-Section Casting) approach
[DE89-009031] N90-11199
Thin section casting program. Volume 2-A: Appendix to volume 2
[DE89-009032] N90-11200
Thin section casting program. Volume 3: Vertical TSC (Thin-Section Casting) approach
[DE89-009033] N90-11201
Thin section casting program. Volume 4: Static cast product bending, straightening, and rolling
[DE89-009034] N90-11202
Thin section casting program. Volume 5: Westinghouse MHD Project
[DE89-009035] N90-11203

UNIVERSAL ENERGY SYSTEMS, INC., DAYTON, OH.
Diamondlike carbon coatings for optical systems
[AD-A211255] N90-11573

UNIVERSITAET DER BUNDESWEHR, NEUBIBERG (GERMANY, F.R.).
Utilization of the generalized likelihood ratio test for the suppression of systematic errors in noisy systems
[ETN-89-94656] N90-11225

UNIVERSITE DE TOULON ET DU VAR (FRANCE).
Small-scale irregularities and global plasma dynamics in the high-latitude ionosphere N90-11394

UNIVERSITEIT TWENTE, ENSCHEDE (NETHERLANDS).
Two VAX-PASCAL terminal interface modules for visualizing scanning and parsing
[MEMO-INF-89-17] N90-11470
A verification exercise relating to specification styles in LOTOS
[MEMO-INF-89-18] N90-11471
Transaction throughput in distributed systems: A modeling study using dynamic queueing networks
[MEMO-INF-89-25] N90-11479
Backward analysis on higher order functions
[MEMO-INF-89-19] N90-11526
An axiomatic theory for partial functions
[MEMO-INF-89-22] N90-11527
Fixed point iteration on point-symmetric interference graphs
[MEMO-INF-89-23] N90-11535

UNIVERSITY CHEMICAL LABS., CAMBRIDGE (ENGLAND).
A high level Ab initio study of the anionic hydrogen-bonded complexes FH-CN-, FH-NC-, H2O-CN- and H2O-NC- N90-11553

UNIVERSITY COLL., LONDON (ENGLAND).
A new method for the characterization of solutes and solvent phases using solvatochromic parameters
[AD-A211238] N90-11116
Seasonal and geomagnetic response of the thermosphere and ionosphere N90-11380

UNIVERSITY OF SOUTH FLORIDA, TAMPA.
The dynamic stability of an axially loaded beam with lateral elastic support and damping N90-11331

UNIVERSITY OF SOUTHERN CALIFORNIA, MARINA DEL REY.
The Knowledge Representation Project
[AD-A211288] N90-11650

UTAH STATE UNIV., LOGAN.
Modelling ionospheric density structures N90-11375

V

VERITAS RESEARCH A.S., HOVIK (NORWAY).
Nonlinear collapse simulation of anisotropic plates and corrugated panels N90-11035

VERMONT UNIV., BURLINGTON.
Electromagnetic pulse interaction at a dielectric interface
[AD-A211081] N90-11220

VIRGINIA POLYTECHNIC INST. AND STATE UNIV., BLACKSBURG.
Optimal and on-board near-optimal midcourse guidance N90-10857
The use of damage characterization for life prediction methodologies N90-11053
Computational aspects of sensitivity calculations in linear transient structural analysis N90-11327
Effects of gravity on equilibrium crystal shapes N90-11602

VIRGINIA UNIV., CHARLOTTESVILLE.
Dynamic analysis of rotors under interference rubs N90-11312
The interaction of supernovae and pulsars with the circumstellar environment N90-11671
Ion bombardment of Io and Mercury N90-11682

VORWERK UND CO., KULMBACH (GERMANY, F.R.).
Worked-in holes in three-dimensional reinforced composites N90-11060

W

WASHINGTON STATE UNIV., PULLMAN.
Pressure induced resonance Raman effects in shocked carbon disulfide
[AD-A210665] N90-11107

WASHINGTON UNIV., SEATTLE.
X-ray and gamma-ray spectroscopy of solids under pressure
[DE89-017271] N90-11118
Analytical and numerical studies in flow development
[DE89-017380] N90-11269
An improved beam model for the vibrations of rotor blades N90-11333
Are ozone exceedance rates decreasing. Comment on extreme value analysis of environmental time-series: An application to trend detection in ground-level ozone
[AD-A211029] N90-11357
UV observations of NGC 205
[NASA-CR-185975] N90-11661

WEA, CAMBRIDGE, MA.
Wave-mode coordinate analysis of L junction in LSS
[AD-A211116] N90-10984

WELDING CONSULTANTS, INC., COLUMBUS, OH.
The Meta-Lax method of stress reduction in welds
[DE89-016437] N90-11321

WISCONSIN UNIV., MADISON.
On the effective transport properties of composite materials N90-11086
Subharmonic solutions near an equilibrium point for Hamiltonian systems
[AD-A210558] N90-11496
Novel physical effects in intersecting optical waveguides N90-11565
Boundary effects on the MHD dynamo in laboratory plasmas
[DE89-015207] N90-11576
Thermodynamics, kinetics, and interface morphologies of phase formation reactions between metals and Gallium Arsenide: Bulk vs thin-film studies
[DE89-016469] N90-11621

WORCESTER POLYTECHNIC INST., MA.
Development of an approximate technique for the nonlinear random vibrations analysis of hysteretic systems N90-11335

Y

YALE UNIV., NEW HAVEN, CT.
On the numerical solution of two-point boundary value problems
[AD-A211244] N90-11516
The fast Gauss transform
[AD-A211287] N90-11517

YORK UNIV. (ENGLAND).
An assessment of robustness of flight control systems based on variable structure techniques N90-10895
Substorm associated pulsations: A study of plasmaspheric cavity resonance, mid-latitude polarisation and geostationary orbit signatures N90-11422

Typical Contract Number Index Listing

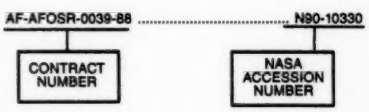

Listings in this index are arranged alphanumerically by contract number. Under each contract number the NASA accession numbers denoting documents that have been produced as a result of research done under that contract are arranged in ascending order. The NASA accession number denotes the number by which the citation is identified.

AF PROJ. 793 ..... N90-11446
AF PROJ. 1900 ..... N90-11157
AF PROJ. 2054 ..... N90-11157
AF PROJ. 2302 ..... N90-10893
N90-10984
AF PROJ. 2304 ..... N90-11114
N90-11220
N90-11262
N90-11511
N90-11513
N90-11515
AF PROJ. 2308 ..... N90-11263
AF PROJ. 2310 ..... N90-11108
AF PROJ. 2313 ..... N90-11340
N90-11443
AF PROJ. 5641 ..... N90-11532
AF PROJ. 6670 ..... N90-11432
AF-AFOSR-ISSA-86-0078 ..... N90-11510
AF-AFOSR-0002-88 ..... N90-11443
AF-AFOSR-0082-88 ..... N90-11262
AF-AFOSR-0087-85 ..... N90-11053
AF-AFOSR-0137-88 ..... N90-11515
AF-AFOSR-0142-87 ..... N90-10893
AF-AFOSR-0149-88 ..... N90-11220
AF-AFOSR-0187-88 ..... N90-11340
AF-AFOSR-0190-86 ..... N90-11108
AF-AFOSR-0198-86 ..... N90-11513
AF-AFOSR-0202-87 ..... N90-11496
AF-AFOSR-0213-83 ..... N90-11263
AF-AFOSR-0256-86 ..... N90-11511
AF-AFOSR-0267-87 ..... N90-11114
AF-AFOSR-0341-86 ..... N90-11380
AF-AFOSR-0356-87 ..... N90-11494
AF-AFOSR-0359-89 ..... N90-11498
AIF-6241 ..... N90-11204
ARPA ORDER 4726 ..... N90-11215
ARPA ORDER 5143 ..... N90-11507
ARPA ORDER 5916 ..... N90-11217
ARPA ORDER 6419 ..... N90-11462
ARPA ORDER 6501 ..... N90-11452
CNR-85/01244/11 ..... N90-11003
CRL-61(052)-623 ..... N90-11395
DA PROJ. 1L1-61102-AH-43 ..... N90-11261
DA PROJ. 1L1-61102-AH-45 ..... N90-11256
DA PROJ. 1L1-61102-BH-57 ..... N90-11110
DA PROJ. 2480 ..... N90-11184
DAAG29-84-G-0089 ..... N90-11106
DAAG29-85-G-0116 ..... N90-11358
DAAG29-85-K-0099 ..... N90-11512
DAAG29-85-K-0101 ..... N90-11571
DAAG46-85-K-0001 ..... N90-11087
DAAH01-88-C-0863 ..... N90-11217
DAAL03-86-G-0038 ..... N90-11109
DAAL03-86-K-0013 ..... N90-11616
DAAL03-86-K-0017 ..... N90-11105
DAAL03-86-K-0057 ..... N90-11301
DAAL03-86-K-0073 ..... N90-11531
DAAL03-86-K-0074 ..... N90-11510
DAAL03-86-0053 ..... N90-11628
DAAL03-87-C-0007 ..... N90-11216
DAAL03-87-G-0127 ..... N90-11466
DAAL03-87-K-0003 ..... N90-11532
DAAL03-88-K-0063 ..... N90-11508
DAAL03-89-G-0020 ..... N90-11111
DAAL03-89-K-0008 ..... N90-11299
DAAL04-86-C-0030 ..... N90-11573
DAJA45-85-C-0026 ..... N90-11110
DAJA45-87-C-0004 ..... N90-11116
DAJA45-88-M-0202 ..... N90-11617
DE-AC02-76CH-00016 ..... N90-11119
N90-11297
N90-11547
N90-11562
DE-AC02-76CH-03000 ..... N90-11229
N90-11281
DE-AC02-76CH-03073 ..... N90-11582
DE-AC02-76ER-03069 ..... N90-11538
DE-AC02-76ET-34202 ..... N90-11123
DE-AC02-80RA-50219 ..... N90-11438
DE-AC02-83CH-10093 ..... N90-11345
N90-11348
N90-11604
DE-AC03-76SF-00098 ..... N90-11095
DE-AC03-76SF-00515 ..... N90-11634
N90-11639
DE-AC04-76DP-00789 ..... N90-11097
N90-11100
N90-11101
N90-11103
N90-11124
N90-11145
N90-11185
N90-11187
N90-11188
N90-11191
N90-11231
N90-11232
N90-11233
N90-11240
N90-11242
N90-11282
N90-11287
N90-11289
N90-11322
N90-11324
N90-11337
N90-11347
N90-11414
N90-11449
N90-11461
N90-11499
N90-11520
N90-11543
N90-11568
N90-11569
N90-11594
N90-11595
N90-11596
N90-11627
N90-11629
N90-11649
DE-AC04-76DR-00789 ..... N90-11315
DE-AC04-88DP-43495 ..... N90-11133
DE-AC05-84OR-21400 ..... N90-10844
N90-11092
N90-11126
N90-11147
N90-11243
N90-11278
N90-11279
N90-11306
N90-11316
N90-11317
N90-11319
N90-11490
N90-11559
N90-11579
N90-11607
N90-11610
N90-11611
N90-11622
N90-11625
N90-11626
N90-11630
N90-11651
N90-11655
DE-AC05-84OS-21400 ..... N90-11323
DE-AC06-76RL-01830 ..... N90-11122
N90-11125
N90-11132
N90-11265
N90-11346
N90-11429
N90-11489
DE-AC06-86NE-37963 ..... N90-11127
DE-AC07-76ID-01570 ..... N90-11359
DE-AC08-88NV-10617 ..... N90-11567
DE-AC12-76SN-00052 ..... N90-11123
DE-AC22-87PC-79810 ..... N90-11184
DE-AI01-85CE-50112 ..... N90-11654
DE-AI05-88ER-69014 ..... N90-11360
DE-AS05-80ER-10660 ..... N90-11230
DE-FC07-84ID-12545 ..... N90-11198
N90-11199
N90-11200
N90-11201
N90-11202
N90-11203
DE-FC22-83FE-60149 ..... N90-11117
DE-FG01-89CE-15412 ..... N90-11321
DE-FG02-85ER-05321 ..... N90-11576
DE-FG02-86ER-45274 ..... N90-11621
DE-FG02-87ER-25026 ..... N90-11493
N90-11522
N90-11523
DE-FG02-87ER-53257 ..... N90-11580
DE-FG03-86ER-05213 ..... N90-11578
DE-FG05-80ET-53088 ..... N90-11582
N90-11583
N90-11584
DE-FG05-84ER-45140 ..... N90-11091
DE-FG05-86ER-45233 ..... N90-11556
DE-FG05-86ER-45268 ..... N90-11609
DE-FG05-86ER-53217 ..... N90-11563
DE-FG05-88ER-13838 ..... N90-11259
DE-FG05-88ER-13902 ..... N90-11102
DE-FG06-84ER-45163 ..... N90-11118
DE-FG06-85ER-13309 ..... N90-11304
DE-FG06-88ER-13973 ..... N90-11307
DE-FG06-88ER-25061 ..... N90-11269
DEN3-32 ..... N90-11654
DLA900-82-C-4426 ..... N90-11157
DTFA01-84-Z-02038 ..... N90-10896
DTFA01-88-Y-10173 ..... N90-10855
EPA-68-C8-0006 ..... N90-11353
ESA-6819/86/NL/PH(SC) N90-11015
N90-11016
ESPRIT PROJ. 432 ..... N90-11480
ESTEC-6659/86/NL/PH N90-11052
FAA-T0701-R N90-10897
FAA-T0701-U N90-10856
F04701-83-C-0069 ..... N90-11179
F04701-85-C-0086 ..... N90-11236
N90-11300
F19628-82-K-0028 ..... N90-11587
F19628-85-C-0002 ..... N90-11222
F19628-86-C-0001 ..... N90-11221
F19628-86-C-0136 ..... N90-10859
F19628-86-K-0031 ..... N90-11389
F19628-87-C-0039 ..... N90-11570
F19628-87-C-0248 ..... N90-11433
F19628-87-K-0030 ..... N90-11509
F30602-85-C-0221 ..... N90-11650
F30602-88-C-0001 ..... N90-11506
F33615-88-C-3215 ..... N90-10985
F49620-84-C-0097 ..... N90-11139
F49620-86-C-0109 ..... N90-11375
F49620-86-C-0111 ..... N90-11494
F49620-86-K-0013 ..... N90-11302
F49620-87-C-0065 ..... N90-11517
F49620-88-C-0036 ..... N90-10984
IACRO-88-873 ..... N90-11258
IBM-P00038437 ..... N90-11517
MDA903-84-C-0031 ..... N90-11491
MDA903-87-C-0069 ..... N90-11507
MDA903-87-C-0523 ..... N90-11448
MDA903-87-C-0693 ..... N90-11215

MIPR-ARO-135-89 ..... N90-11619
MIPR-FY1455-86-N0655 ..... N90-11184
MIPR-N-85-14 ..... N90-11173
NAGW-77 ..... N90-11375
NAGW-1176 ..... N90-11669
NAGW-1309 ..... N90-11680
NAGW-1370 ..... N90-11682
NAG1-517 ..... N90-11494
NAG1-562 ..... N90-11205
NAG1-630 ..... N90-11255
NAG1-667 ..... N90-11460
NAG1-716 ..... N90-10834
NAG1-730 ..... N90-11457
NAG1-875 ..... N90-11456
NAG3-396 ..... N90-11332
NAG3-536 ..... N90-11211
NAG3-1000 ..... N90-11603
NAG5-1020 ..... N90-11661
NAG9-173 ..... N90-11227
NAG9-350 ..... N90-11445
NAG9-394 ..... N90-10911
NASA ORDER C-22406-M N90-11256
NASA ORDER C-99068-G N90-11250
NASW-4234 ..... N90-11455
NAS1-18107 ..... N90-11494
NAS1-18605 ..... N90-10833
N90-11494
N90-11495
N90-11498
NAS2-11877 ..... N90-11487
NAS3-24060 ..... N90-11549
NAS3-24881 ..... N90-10835
N90-10836
NAS3-24889 ..... N90-11210
NAS3-25354 ..... N90-10983
NAS7-918 ..... N90-11001
NAS8-35354 ..... N90-11689
NAS9-17650 ..... N90-10913
N90-10914
N90-10915
N90-10916
N90-10917
N90-10918
N90-10919
N90-10920
N90-10921
N90-10922
N90-10923
N90-10924
N90-10925
N90-10926
N90-10927
N90-10928
N90-10929
N90-10930
N90-10931
N90-10932
N90-10933
N90-10934
N90-10935
N90-10936
N90-10937
N90-10938
N90-10939
N90-10940
N90-10941
N90-10942
N90-10943
N90-10944
N90-10945
N90-10946
N90-10947
N90-10948
N90-10949
N90-10950
N90-10951
N90-10952
N90-10953
N90-10954
N90-10955
N90-10956
N90-10957
N90-10958
N90-10959
N90-10960
N90-10961
N90-10962
N90-10963
N90-10964
N90-10965
N90-10966
N90-10967
N90-10968
N90-10969
N90-10970
N90-10971
N90-10972
N90-10973
N90-10974
N90-10975
N90-10976
N90-10977
N90-10978
N90-10979
NCC2-387 ..... N90-11093
NCC2-552 ..... N90-11552
NCC2-582 ..... N90-10840
NCC3-133 ..... N90-11606
NERC-GST.02.112 ..... N90-11371
NR PROJ. 042-267 ..... N90-11534
NR PROJ. 056-768 ..... N90-11113
NSF ATM-84-14134 ..... N90-11391
NSF ATM-84-19117 ..... N90-11393
NSF ATM-85-13362 ..... N90-11397
NSF ATM-87-09659 ..... N90-11413
N90-11428
NSF ATM-88-11128 ..... N90-11583
NSF CDR-86-22236 ..... N90-11564
N90-11628
NSF DCR-86-06165 ..... N90-11472
NSF DMR-83-07157 ..... N90-11628
NSF DMS-86-01258 ..... N90-11510
NSF DMS-86-01532 ..... N90-11510
NSF DMS-86-57464 ..... N90-11510
NSF MCS-85-04316 ..... N90-11494
NSF NCR-87-22333 ..... N90-11644
NSG-1498 ..... N90-11209
N00014-80-C-0003 ..... N90-11143
N00014-81-K-0605 ..... N90-11113
N00014-82-C-0064 ..... N90-11436
N00014-82-K-0741 ..... N90-11285
N00014-83-K-0542 ..... N90-11510
N00014-84-K-0650 ..... N90-11465
N00014-85-K-0423 ..... N90-11648
N00014-85-K-0584 ..... N90-11442
N00014-85-K-0701 ..... N90-11551
N00014-86-C-0086 ..... N90-11682
N00014-86-K-0043 ..... N90-11096
N00014-86-K-0307 ..... N90-11107
N00014-86-K-0769 ..... N90-11148
N00014-87-K-0064 ..... N90-11545
N00014-87-K-0452 ..... N90-11153
N00014-87-K-0825 ..... N90-11468
N00014-88-C-0714 ..... N90-11618
N00014-88-J-1193 ..... N90-11264
N00014-88-K-0224 ..... N90-11089
N90-11090
N00014-88-K-0265 ..... N90-11357
N00014-88-K-0275 ..... N90-11615
N00014-88-K-0360 ..... N90-11150
N90-11151
N90-11152
N90-11235
N00014-88-K-0579 ..... N90-11452
N00014-88-K-0591 ..... N90-11462
N00014-89-J-1109 ..... N90-11550
N00014-89-J-1527 ..... N90-11516
N90-11517
N00014-89-J-1627 ..... N90-11534
N00039-87-C-5301 ..... N90-11115
N00228-86-D-3051 ..... N90-11430
N62269-85-C-2345 ..... N90-11053
ORNL/IA-21428 ..... N90-11142
RR04209 ..... N90-11465
RR0330242 ..... N90-11431
SERC-SGD/10696 ..... N90-11399
SWRI PROJ. 05-3050 ..... N90-10911
W-31-109-ENG-38 ..... N90-11283
N90-11325
N90-11349
N90-11591
N90-11612
N90-11623
N90-11624
W-7405-ENG-36 ..... N90-10839
N90-10892
N90-11098
N90-11131
N90-11134
N90-11146
N90-11154
N90-11186
N90-11189
N90-11190
N90-11197
N90-11239
N90-11266
N90-11267
N90-11268
N90-11280
N90-11288
N90-11290
N90-11303
N90-11305
N90-11416
N90-11450
N90-11469
N90-11478
N90-11488
N90-11544
N90-11546
N90-11557
N90-11577
N90-11581
N90-11585
N90-11588
N90-11592
N90-11605
N90-11620
N90-11624
N90-11628
N90-11678
N90-11687
W-7405-ENG-48 ..... N90-11099
N90-11192
N90-11212
N90-11223
N90-11238
N90-11241
N90-11257
N90-11258
N90-11297
N90-11463
N90-11518
N90-11519
N90-11558
N90-11589
N90-11590
N90-11608
N90-11633
N90-11683
W-7405-ENG-82 ..... N90-11624
307-51-00 ..... N90-11606
314-50-20 ..... N90-11441
505-03-01 ..... N90-10835
N90-10836
505-42-31 ..... N90-11081
505-60-31 ..... N90-11254
505-61-71 ..... N90-10829
505-62-0K N90-11256
505-62-21 ..... N90-11250
N90-11277
N90-11497
505-62-61 ..... N90-11245
505-63-1A N90-11082
505-63-1B N90-11332
505-63-51-10 ..... N90-10889
505-66-21-02 ..... N90-11454
505-66-71 ..... N90-11487
505-67-21 ..... N90-10841
505-90-21-01 ..... N90-10833
N90-11494
N90-11495
N90-11498
506-48-21 ..... N90-10912
535-03-01 ..... N90-11549
535-505-01 ..... N90-10891
582-01-11 ..... N90-11144
673-62-12 ..... N90-11405
694-22-00 ..... N90-11196
763-01-31-22 ..... N90-10830
992-21-01 ..... N90-10828

REPORT/ACCESSION NUMBER INDEX

Typical Report Number Index Listing

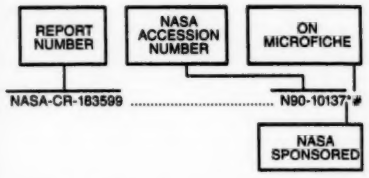

Listings in this index are arranged alphanumerically by report number. The NASA accession number denotes the number by which the citation is identified. An asterisk (*) indicates that the itemis a NASA report. A pound sign (#) indicates that the item is available on microfiche.

A-86319 ..... N90-11254* #
A-88002 ..... N90-10828* #
A-89235 ..... N90-10841* #

ACD-330 ..... N90-10856 #
ACD-330 ..... N90-10897 #

AD-A197632 ..... N90-11157 #
AD-A205954 ..... N90-11139 #
AD-A210251 ..... N90-11184 #
AD-A210255 ..... N90-11462 #
AD-A210322 ..... N90-11143 #
AD-A210434 ..... N90-11648 #
AD-A210459 ..... N90-11442 #
AD-A210558 ..... N90-11496 #
AD-A210565 ..... N90-11096 #
AD-A210580 ..... N90-11430 #
AD-A210651 ..... N90-11260 #
AD-A210652 ..... N90-11531 #
AD-A210653 ..... N90-11105 #
AD-A210654 ..... N90-11148 #
AD-A210655 ..... N90-11106 #
AD-A210656 ..... N90-11214 #
AD-A210657 ..... N90-11339 #
AD-A210658 ..... N90-11615 #
AD-A210660 ..... N90-11261 #
AD-A210661 ..... N90-10910 #
AD-A210665 ..... N90-11107 #
AD-A210668 ..... N90-11506 #
AD-A210669 ..... N90-11452 #
AD-A210670 ..... N90-10845 #
AD-A210676 ..... N90-11108 #
AD-A210698 ..... N90-11149 #
AD-A210707 ..... N90-11507 #
AD-A210710 ..... N90-11465 #
AD-A210711 ..... N90-11545 #
AD-A210733 ..... N90-11109 #
AD-A210739 ..... N90-11616 #
AD-A210745 ..... N90-11443 #
AD-A210747 ..... N90-11083 #
AD-A210748 ..... N90-11110 #
AD-A210749 ..... N90-11215 #
AD-A210752 ..... N90-11111 #
AD-A210754 ..... N90-11150 #
AD-A210755 ..... N90-11235 #
AD-A210757 ..... N90-11532 #
AD-A210758 ..... N90-11299 #
AD-A210759 ..... N90-11216 #
AD-A210760 ..... N90-11466 #
AD-A210762 ..... N90-11508 #
AD-A210763 ..... N90-11446 #
AD-A210768 ..... N90-11236 #
AD-A210769 ..... N90-11300 #
AD-A210772 ..... N90-11356 #
AD-A210773 ..... N90-11284 #
AD-A210774 ..... N90-11112 #
AD-A210784 ..... N90-11435 #
AD-A210785 ..... N90-11217 #
AD-A210786 ..... N90-11151 #
AD-A210787 ..... N90-11152 #
AD-A210790 ..... N90-11570 #
AD-A210791 ..... N90-11587 #
AD-A210794 ..... N90-11571 #
AD-A210800 ..... N90-11431 #
AD-A210802 ..... N90-11432 #
AD-A210820 ..... N90-11509 #
AD-A210842 ..... N90-11617 #
AD-A210862 ..... N90-11510 #
AD-A211019 ..... N90-11218 #
AD-A211029 ..... N90-11357 #
AD-A211032 ..... N90-11301 #
AD-A211040 ..... N90-11511 #
AD-A211046 ..... N90-11113 #
AD-A211048 ..... N90-11285 #
AD-A211049 ..... N90-11087 #
AD-A211050 ..... N90-11533 #
AD-A211053 ..... N90-11326 #
AD-A211054 ..... N90-11534 #
AD-A211067 ..... N90-11444 #
AD-A211068 ..... N90-11114 #
AD-A211069 ..... N90-11115 #
AD-A211070 ..... N90-11618 #
AD-A211078 ..... N90-11219 #
AD-A211081 ..... N90-11220 #
AD-A211082 ..... N90-11262 #
AD-A211116 ..... N90-10984 #
AD-A211117 ..... N90-11302 #
AD-A211118 ..... N90-11512 #
AD-A211122 ..... N90-11513 #
AD-A211126 ..... N90-11467 #
AD-A211139 ..... N90-10893 #
AD-A211164 ..... N90-11468 #
AD-A211165 ..... N90-11440 #
AD-A211170 ..... N90-11088 #
AD-A211172 ..... N90-10985 #
AD-A211191 ..... N90-11690 #
AD-A211192 ..... N90-11514 #
AD-A211209 ..... N90-11515 #
AD-A211213 ..... N90-11491 #
AD-A211224 ..... N90-11550 #
AD-A211226 ..... N90-11089 #
AD-A211230 ..... N90-11090 #
AD-A211236 ..... N90-11572 #
AD-A211238 ..... N90-11116 #
AD-A211240 ..... N90-11263 #
AD-A211243 ..... N90-11358 #
AD-A211244 ..... N90-11516 #
AD-A211245 ..... N90-11153 #
AD-A211246 ..... N90-11619 #
AD-A211252 ..... N90-11286 #
AD-A211254 ..... N90-11237 #
AD-A211255 ..... N90-11573 #
AD-A211256 ..... N90-11433 #
AD-A211264 ..... N90-11221 #
AD-A211265 ..... N90-10859 #
AD-A211267 ..... N90-11222 #
AD-A211269 ..... N90-11340 #
AD-A211273 ..... N90-11574 #
AD-A211281 ..... N90-11551 #
AD-A211282 ..... N90-11264 #
AD-A211287 ..... N90-11517 #
AD-A211288 ..... N90-11650 #

AD-E501143 ..... N90-11491 #

AFGL-ERP-1012 ..... N90-11432 #

AFGL-TR-88-0216 ..... N90-11432 #
AFGL-TR-88-0299 ..... N90-11587 #
AFGL-TR-89-0035 ..... N90-10859 #
AFGL-TR-89-0038 ..... N90-11570 #
AFGL-TR-89-0076 ..... N90-11433 #
AFGL-TR-89-0118 ..... N90-11509 #

AFHRL-TR-88-42 ..... N90-11218 #

AFOEHL-89-038EH0087EAC ..... N90-11083 #

AFOSR-89-0289TR ..... N90-11139 #
AFOSR-89-0574TR ..... N90-11510 #
AFOSR-89-0810TR ..... N90-11443 #
AFOSR-89-1029TR ..... N90-11340 #
AFOSR-89-1035TR ..... N90-11263 #
AFOSR-89-1059TR ..... N90-10893 #
AFOSR-89-1063TR ..... N90-10984 #
AFOSR-89-1064TR ..... N90-11114 #
AFOSR-89-1066TR ..... N90-11515 #
AFOSR-89-1067TR ..... N90-11513 #
AFOSR-89-1068TR ..... N90-11511 #
AFOSR-89-1069TR ..... N90-11220 #
AFOSR-89-1070TR ..... N90-11262 #
AFOSR-89-1073TR ..... N90-11302 #

AFWAL-TR-87-2042-VOL-11 ..... N90-11184 #

AGARD-CP-441 ..... N90-11361 #
AGARD-CP-452 ..... N90-10860 #

AGARD-LS-166 ..... N90-10847 #

AIAA-89-0151 ..... N90-11441* #
AIAA-89-0501 ..... N90-11196* #
AIAA-90-0719 ..... N90-10912* #

AMSEL-NV-TR-0079 ..... N90-11574 #

ANL-HEP-CP-89-75 ..... N90-11591 #

ANL/FE-89/5 ..... N90-11623 #

AR-005-530 ..... N90-10888 #
AR-005-621 ..... N90-11080 #

ARI-RP-89-08-VOL-1 ..... N90-11446 #

ARL-AERO-R-177 ..... N90-10888 #

ARL-PROP-R-181 ..... N90-11080 #

ARL-TR-89-38 ..... N90-11550 #

ARO-21885.1-EL ..... N90-11571 #
ARO-22356.3-MA ..... N90-11512 #
ARO-22368.3-PH-H ..... N90-11106 #
ARO-23010.5-MA ..... N90-11532 #
ARO-23025.1-MS ..... N90-11616 #
ARO-23118.6-PH ..... N90-11105 #
ARO-23235.1-GS-H ..... N90-11358 #
ARO-23357.2-PH ..... N90-11301 #
ARO-23360.12-MA ..... N90-11531 #
ARO-23782.11-CH-F ..... N90-11109 #
ARO-24649.6-EL-S ..... N90-11216 #
ARO-25510.3-EL-H ..... N90-11466 #
ARO-25839.4-MA ..... N90-11508 #
ARO-26430.1-PH-CF ..... N90-11111 #
ARO-26434.1-EL ..... N90-11299 #
ARO-26564.1-MS-CF ..... N90-11619 #

ASI90-302-87-VOL-1 ..... N90-11446 #

ATC-164 ..... N90-11222 #

AV-235-4376 ..... N90-10908 #

AVSCOM-TM-89-B-008 ..... N90-10889* #

AVSCOM-TR-89-C-015 ..... N90-11256* #

BBC-RD-1989/9 ..... N90-11208

BBN-7064 ..... N90-11215 #

BNL-42004 ..... N90-11547 #
BNL-42393 ..... N90-11297 #
BNL-42810 ..... N90-11119 #

BRL-TR-3000 ..... N90-10910 #
BRL-TR-3005 ..... N90-11261 #
BRL-TR-3015 ..... N90-11260 #

CAL-1792 ..... N90-11662* #

CERC-MP-89-9 ..... N90-11356 #

CERN-89-03 ..... N90-11298 #

CM-875 ..... N90-11512 #

CMS-TSR-89-30 ..... N90-11496 #

CMU-RI-TR-89-2 ..... N90-11506 #

CONF-880904-11 ..... N90-11297 #
CONF-890335-251 ..... N90-11547 #
CONF-890454-1 ..... N90-11592 #
CONF-890519-1 ..... N90-11119 #
CONF-890520-1 ..... N90-11687 #
CONF-890579-1 ..... N90-11610 #
CONF-890660-9 ..... N90-11212 #
CONF-890665-44 ..... N90-11242 #
CONF-890665-46 ..... N90-11239 #
CONF-890697-3 ..... N90-11558 #
CONF-890703-18 ..... N90-11559 #
CONF-890718-25 ..... N90-11612 #
CONF-890721-41 ..... N90-11325 #
CONF-890736-84 ..... N90-11283 #
CONF-890756-1 ..... N90-11258 #
CONF-890796-3 ..... N90-11595 #
CONF-890796-8 ..... N90-11683 #
CONF-890796-10 ..... N90-11557 #
CONF-890803-5 ..... N90-11544 #
CONF-890803-7 ..... N90-11230 #
CONF-890811-5 ..... N90-11185 #
CONF-890811-8 ..... N90-11186 #
CONF-890811-27 ..... N90-11101 #
CONF-890811-29 ..... N90-11192 #
CONF-890812-9 ..... N90-11414 #
CONF-890812-11 ..... N90-11287 #
CONF-890812-12 ..... N90-11100 #
CONF-890812-13 ..... N90-11569 #
CONF-890812-14 ..... N90-11099 #
CONF-890812-15 ..... N90-11103 #
CONF-890812-18 ..... N90-11289 #
CONF-890812-19 ..... N90-11145 #
CONF-890812-20 ..... N90-11124 #
CONF-890812-21 ..... N90-11288 #
CONF-890812-24 ..... N90-11134 #
CONF-890812-28 ..... N90-11629 #
CONF-890812-29 ..... N90-11267 #
CONF-890812-30 ..... N90-11546 #
CONF-890812-31 ..... N90-11146 #
CONF-890812-32 ..... N90-11190 #
CONF-890812-33 ..... N90-11268 #
CONF-890812-36 ..... N90-11197 #
CONF-890812-37 ..... N90-11282 #
CONF-890812-38 ..... N90-11266 #
CONF-890812-39 ..... N90-11131 #
CONF-890812-40 ..... N90-11189 #
CONF-890812-41 ..... N90-11337 #
CONF-890814-6 ..... N90-11490 #
CONF-890815-23 ..... N90-11317 #
CONF-890819-20 ..... N90-11265 #
CONF-890820-3 ..... N90-11125 #
CONF-890821-2 ..... N90-11625 #
CONF-890850-1 ..... N90-11611 #
CONF-890851 ..... N90-11348 #
CONF-890902-5 ..... N90-11097 #
CONF-890902-12 ..... N90-10892 #
CONF-890931-1 ..... N90-11579 #
CONF-890931-5 ..... N90-11593 #
CONF-890933-1 ..... N90-11620 #
CONF-890941-1 ..... N90-10839 #
CONF-890941-2 ..... N90-11478 #
CONF-890946-1 ..... N90-11594 #
CONF-890953-1 ..... N90-11605 #
CONF-890977-1 ..... N90-11154 #
CONF-890996-1 ..... N90-11567 #
CONF-890996-2 ..... N90-11278 #
CONF-890996-3 ..... N90-11279 #
CONF-8806237 ..... N90-11437 #
CONF-8809384-1 ..... N90-11095 #
CONF-8811214 ..... N90-11128 #
CONF-8812101 ..... N90-11631 #
CONF-8902118-2 ..... N90-11577 #
CONF-8903103-2 ..... N90-11126 #
CONF-8903130-2 ..... N90-11538 #
CONF-8903130-3 ..... N90-11634 #
CONF-8903159-1 ..... N90-11257 #
CONF-8904107-8 ..... N90-11585 #
CONF-8905143-11 ..... N90-11608 #
CONF-8905156-2 ..... N90-11591 #
CONF-8905194-3 ..... N90-11281 #
CONF-8905201-1 ..... N90-11450 #
CONF-8906201-1 ..... N90-11588 #
CONF-8906201-2 ..... N90-11416 #
CONF-8906206-2 ..... N90-11678 #
CONF-8906207-1 ..... N90-11628 #
CONF-8906208-1 ..... N90-11596 #
CONF-8907106-3 ..... N90-11523 #
CONF-8907123-2 ..... N90-11359 #
CONF-8907129-2 ..... N90-11633 #
CONF-8907130-2 ..... N90-11624 #
CONF-8907140-1 ..... N90-11639 #
CONF-8908108-2 ..... N90-11489 #

CONF-8908112-1 ..... N90-11576 #
CONF-8908112-2 ..... N90-11259 #
CONF-8908120-2 ..... N90-11280* #
CONF-8908125-5 ..... N90-11132 #
CONF-8908130-1 ..... N90-11518 #
CONF-8908133-1 ..... N90-11581 #
CONF-8908134-2 ..... N90-11305 #
CONF-8908134-4 ..... N90-11303 #
CONF-8908140-1 ..... N90-11290 #
CONF-8909113-2 ..... N90-11187 #
CONF-8909113-3 ..... N90-11188 #
CONF-8909113-4 ..... N90-11191 #
CONF-8909120-2 ..... N90-11098 #
CONF-8909124-3 ..... N90-11231 #
CONF-8909124-4 ..... N90-11238 #
CONF-8909128-1 ..... N90-11349 #
CONF-8909146-1 ..... N90-11232 #
CONF-8909146-2 ..... N90-11461 #
CONF-8909147-1 ..... N90-11488 #
CONF-8909176-1 ..... N90-11233 #
CONF-8909177-1 ..... N90-11568 #
CONF-8909184-1 ..... N90-11626 #
CONF-8909185-1 ..... N90-11627 #
CONF-8909187-2 ..... N90-11469 #

CONTRIB-1049 ..... N90-11436 #

CRDEC-SP-006 ..... N90-11326 #

CRREL-89-10 ..... N90-10896 #
CRREL-89-13 ..... N90-11435 #

CTP-1745 ..... N90-11538 #

CWI-CS-R8617 ..... N90-11474 #
CWI-CS-R8827 ..... N90-11480 #
CWI-CS-R8828 ..... N90-11453 #
CWI-CS-R8832 ..... N90-11481 #
CWI-CS-R8836 ..... N90-11472 #
CWI-CS-R8837 ..... N90-11473 #
CWI-CS-R8838 ..... N90-11528 #
CWI-CS-R8839 ..... N90-11492 #
CWI-CS-R8842 ..... N90-11536 #
CWI-CS-R8844-REV ..... N90-11474 #
CWI-CS-R8846 ..... N90-11482 #

CWI-NM-R8811 ..... N90-11483 #
CWI-NM-R8812 ..... N90-11475 #
CWI-NM-R8814 ..... N90-11529 #
CWI-NM-R8815 ..... N90-11530 #
CWI-NM-R8816 ..... N90-11271 #
CWI-NM-R8817 ..... N90-11476 #

DE89-000761 ..... N90-11117 #
DE89-007641 ..... N90-11185 #
DE89-008415 ..... N90-11186 #
DE89-009030 ..... N90-11198 #
DE89-009031 ..... N90-11199 #
DE89-009032 ..... N90-11200 #
DE89-009033 ..... N90-11201 #
DE89-009034 ..... N90-11202 #
DE89-009035 ..... N90-11203 #
DE89-009337 ..... N90-11567 #
DE89-009440 ..... N90-11604 #
DE89-009450 ..... N90-11345 #
DE89-009457 ..... N90-11348 #
DE89-011536 ..... N90-11097 #
DE89-012632 ..... N90-11488 #
DE89-012664 ..... N90-11231 #
DE89-013278 ..... N90-11349 #
DE89-013494 ..... N90-11232 #
DE89-013539 ..... N90-11278 #
DE89-013811 ..... N90-11187 #
DE89-013922 ..... N90-11188 #
DE89-013934 ..... N90-11461 #
DE89-014169 ..... N90-11493 #
DE89-014278 ..... N90-10892 #
DE89-014763 ..... N90-11279 #
DE89-015140 ..... N90-11115 #
DE89-015170 ..... N90-11346 #
DE89-015171 ..... N90-11122 #
DE89-015181 ..... N90-11315 #
DE89-015194 ..... N90-11449 #
DE89-015196 ..... N90-11347 #
DE89-015207 ..... N90-11576 #
DE89-015211 ..... N90-11123 #
DE89-015214 ..... N90-11437 #
DE89-015226 ..... N90-11095 #
DE89-015241 ..... N90-11280* #
DE89-015247 ..... N90-11450 #
DE89-015252 ..... N90-10839 #
DE89-015258 ..... N90-11098 #
DE89-015269 ..... N90-11620 #
DE89-015281 ..... N90-11605 #
DE89-015297 ..... N90-11577 #
DE89-015526 ..... N90-11562 #

DE89-015528 ..... N90-11438 #
DE89-015566 ..... N90-11320 #
DE89-015585 ..... N90-11229 #
DE89-015621 ..... N90-11355 #
DE89-015622 ..... N90-11578 #
DE89-015646 ..... N90-11316 #
DE89-015671 ..... N90-11655 #
DE89-015680 ..... N90-11607 #
DE89-015748 ..... N90-11230 #
DE89-015773 ..... N90-11238 #
DE89-015904 ..... N90-11579 #
DE89-015981 ..... N90-11317 #
DE89-016031 ..... N90-11414 #
DE89-016037 ..... N90-11189 #
DE89-016067 ..... N90-11318 #
DE89-016175 ..... N90-11429 #
DE89-016177 ..... N90-11233 #
DE89-016186 ..... N90-11568 #
DE89-016214 ..... N90-11359 #
DE89-016251 ..... N90-11360 #
DE89-016323 ..... N90-11281 #
DE89-016437 ..... N90-11321 #
DE89-016469 ..... N90-11621 #
DE89-016498 ..... N90-11463 #
DE89-016502 ..... N90-11212 #
DE89-016504 ..... N90-11099 #
DE89-016505 ..... N90-11633 #
DE89-016506 ..... N90-11257 #
DE89-016508 ..... N90-11258 #
DE89-016509 ..... N90-11683 #
DE89-016515 ..... N90-11518 #
DE89-016518 ..... N90-11608 #
DE89-016526 ..... N90-11569 #
DE89-016528 ..... N90-11100 #
DE89-016530 ..... N90-11287 #
DE89-016538 ..... N90-11145 #
DE89-016539 ..... N90-11124 #
DE89-016540 ..... N90-11101 #
DE89-016543 ..... N90-11622 #
DE89-016554 ..... N90-11091 #
DE89-016565 ..... N90-11265 #
DE89-016568 ..... N90-11102 #
DE89-016574 ..... N90-11580 #
DE89-016582 ..... N90-11538 #
DE89-016585 ..... N90-11416 #
DE89-016587 ..... N90-11288 #
DE89-016596 ..... N90-11588 #
DE89-016609 ..... N90-11303 #
DE89-016611 ..... N90-11581 #
DE89-016617 ..... N90-11239 #
DE89-016669 ..... N90-11519 #
DE89-016671 ..... N90-11322 #
DE89-016673 ..... N90-11240 #
DE89-016674 ..... N90-11520 #
DE89-016677 ..... N90-11223 #
DE89-016678 ..... N90-11589 #
DE89-016679 ..... N90-11590 #
DE89-016682 ..... N90-11241 #
DE89-016694 ..... N90-11521 #
DE89-016703 ..... N90-11623 #
DE89-016718 ..... N90-11591 #
DE89-016726 ..... N90-11582 #
DE89-016727 ..... N90-11583 #
DE89-016728 ..... N90-11584 #
DE89-016741 ..... N90-11556 #
DE89-016744 ..... N90-11609 #
DE89-016768 ..... N90-11592 #
DE89-016769 ..... N90-11478 #
DE89-016770 ..... N90-11131 #
DE89-016771 ..... N90-11593 #
DE89-016772 ..... N90-11266 #
DE89-016773 ..... N90-11146 #
DE89-016774 ..... N90-11624 #
DE89-016784 ..... N90-11678 #
DE89-016785 ..... N90-11259 #
DE89-016788 ..... N90-11304 #
DE89-016809 ..... N90-11594 #
DE89-016810 ..... N90-11595 #
DE89-016811 ..... N90-11282 #
DE89-016816 ..... N90-11197 #
DE89-016823 ..... N90-11132 #
DE89-016827 ..... N90-11125 #
DE89-016828 ..... N90-11489 #
DE89-016847 ..... N90-11490 #
DE89-016857 ..... N90-11610 #
DE89-016864 ..... N90-11625 #
DE89-016866 ..... N90-11611 #
DE89-016867 ..... N90-11626 #
DE89-016868 ..... N90-11126 #
DE89-016877 ..... N90-11103 #
DE89-016880 ..... N90-11289 #
DE89-016881 ..... N90-11337 #
DE89-016882 ..... N90-11627 #
DE89-016886 ..... N90-11596 #
DE89-016891 ..... N90-10844 #
DE89-016899 ..... N90-11147 #

DE89-016900 ..... N90-11323 #
DE89-016904 ..... N90-11325 #
DE89-016905 ..... N90-11612 #
DE89-016908 ..... N90-11283 #
DE89-016924 ..... N90-11649 #
DE89-016925 ..... N90-11324 #
DE89-016929 ..... N90-11543 #
DE89-016930 ..... N90-11499 #
DE89-016935 ..... N90-11319 #
DE89-016942 ..... N90-11634 #
DE89-016943 ..... N90-11639 #
DE89-016958 ..... N90-11133 #
DE89-016969 ..... N90-11154 #
DE89-016974 ..... N90-11557 #
DE89-016975 ..... N90-11544 #
DE89-016980 ..... N90-11585 #
DE89-016981 ..... N90-11134 #
DE89-016982 ..... N90-11305 #
DE89-016983 ..... N90-11267 #
DE89-016985 ..... N90-11628 #
DE89-016988 ..... N90-11687 #
DE89-016989 ..... N90-11469 #
DE89-016990 ..... N90-11290 #
DE89-016991 ..... N90-11546 #
DE89-016996 ..... N90-11190 #
DE89-016997 ..... N90-11268 #
DE89-017229 ..... N90-11191 #
DE89-017230 ..... N90-11242 #
DE89-017231 ..... N90-11629 #
DE89-017236 ..... N90-11297 #
DE89-017266 ..... N90-11127 #
DE89-017271 ..... N90-11118 #
DE89-017328 ..... N90-11522 #
DE89-017329 ..... N90-11523 #
DE89-017352 ..... N90-11306 #
DE89-017363 ..... N90-11563 #
DE89-017380 ..... N90-11269 #
DE89-017442 ..... N90-11307 #
DE89-017451 ..... N90-11630 #
DE89-017454 ..... N90-11651 #
DE89-017455 ..... N90-11092 #
DE89-017474 ..... N90-11243 #
DE89-017543 ..... N90-11558 #
DE89-017586 ..... N90-11559 #
DE89-017600 ..... N90-11119 #
DE89-017610 ..... N90-11547 #
DE89-017730 ..... N90-11192 #
DE89-615450 ..... N90-11128 #
DE89-618377 ..... N90-11500 #
DE89-618379 ..... N90-11501 #
DE89-618380 ..... N90-11539 #
DE89-618381 ..... N90-11502 #
DE89-618382 ..... N90-11503 #
DE89-618383 ..... N90-11504 #
DE89-618384 ..... N90-11505 #
DE89-618392 ..... N90-11213 #
DE89-618396 ..... N90-11540 #
DE89-618402 ..... N90-11524 #
DE89-618403 ..... N90-11525 #
DE89-618430 ..... N90-11635 #
DE89-618459 ..... N90-11636 #
DE89-618460 ..... N90-11637 #
DE89-618548 ..... N90-11638 #
DE89-618624 ..... N90-11613 #
DE89-618689 ..... N90-11586 #
DE89-618786 ..... N90-11677 #
DE89-618865 ..... N90-11614 #
DE89-619727 ..... N90-11415 #
DE89-620128 ..... N90-11308 #
DE89-620129 ..... N90-11560 #
DE89-620145 ..... N90-11298 #
DE89-620335 ..... N90-11291 #
DE89-620449 ..... N90-11464 #
DE89-630105 ..... N90-11548 #
DE89-630111 ..... N90-11541 #
DE89-630138 ..... N90-11640 #
DE89-630481 ..... N90-11597 #
DE89-630802 ..... N90-11104 #
DE89-630803 ..... N90-11129 #
DE89-631032 ..... N90-11130 #
DE89-787739 ..... N90-11234 #
DE89-790940 ..... N90-11679 #
DE89-906473 ..... N90-11652 #
DE89-906638 ..... N90-11631 #

DOD-4650.4 ..... N90-10846 #

DOE/CE-0257 ..... N90-11320 #
DOE/CE-15412/T1 ..... N90-11321 #
DOE/CE-50111/H1 ..... N90-11318 #

DOE/ER-0419 ..... N90-11355 #
DOE/ER-0422 ..... N90-11521 #
DOE/ER-10666/1 ..... N90-11230 #
DOE/ER-13309/4 ..... N90-11304 #
DOE/ER-13902/1 ..... N90-11102 #
DOE/ER-13973/1 ..... N90-11307 #
DOE/ER-25026/31 ..... N90-11493 #
DOE/ER-25026/32 ..... N90-11523 #
DOE/ER-25026/33 ..... N90-11522 #
DOE/ER-25061/1 ..... N90-11269 #
DOE/ER-45140/T1 ..... N90-11091 #
DOE/ER-45163/12 ..... N90-11118 #
DOE/ER-45233/4 ..... N90-11556 #
DOE/ER-45268/T1 ..... N90-11609 #
DOE/ER-45274/3 ..... N90-11621 #
DOE/ER-53212/142 ..... N90-11576 #
DOE/ER-53217/3 ..... N90-11563 #
DOE/ER-53257/2 ..... N90-11580 #
DOE/ER-69014/T1 ..... N90-11360 #

DOE/ET-53088/374 ..... N90-11583 #
DOE/ET-53088/385 ..... N90-11582 #
DOE/ET-53088/386 ..... N90-11584 #

DOE/FTR-9015526 ..... N90-11562 #

DOE/ID-12545/1-VOL-1 ..... N90-11198 #
DOE/ID-12545/1-VOL-2 ..... N90-11199 #
DOE/ID-12545/1-VOL-2A ..... N90-11200 #
DOE/ID-12545/1-VOL-3 ..... N90-11201 #
DOE/ID-12545/1-VOL-4 ..... N90-11202 #
DOE/ID-12545/1-VOL-5 ..... N90-11203 #

DOE/NASA/0032-30 ..... N90-11654* #

DOE/NE-37963/10 ..... N90-11127 #

DOE/RA-50219/T9 ..... N90-11438 #

DOT-TSC-RSPA-88-4 ..... N90-10846 #

DOT/FAA/CT-TN88/30 ..... N90-10897 #
DOT/FAA/CT-TN89/18 ..... N90-10843 #
DOT/FAA/CT-TN89/21 ..... N90-10856 #

DOT/FAA/DS-89/08 ..... N90-10855 #
DOT/FAA/DS-89/13 ..... N90-10896 #

DOT/FAA/PS-88/18 ..... N90-11222 #

DRDA-85-2478-P1 ..... N90-11301 #

E-4480 ..... N90-11245* #
E-4586 ..... N90-11196* #
E-5013 ..... N90-11332* #
E-5039 ..... N90-10891* #
E-5045 ..... N90-11082* #
E-5054 ..... N90-11081* #
E-5064 ..... N90-11606* #
E-5069 ..... N90-11497* #
E-5071 ..... N90-11277* #
E-5078 ..... N90-11250* #
E-5120 ..... N90-11144* #
E-5144 ..... N90-10912* #

EGG-M-89040 ..... N90-11359 #

EGG-10617-6055 ..... N90-11567 #

EOARD-LR-89-041 ..... N90-10908 #

EOARD-TR-89-11 ..... N90-11108 #

EPA/IMSD-89/001 ..... N90-11354 #

EPA/600/3-89/047 ..... N90-11353 #

ESA-SP-289 ..... N90-10986 #

ESD-TR-89-192 ..... N90-11221 #

ESL-TR-87 ..... N90-11157 #
ESL-TR-716111-7 ..... N90-11211* #
ESL-TR-716199-13 ..... N90-11209* #

ESL-721837-1 ..... N90-11603* #

ETN-89-94570 ..... N90-11120 #
ETN-89-94613 ..... N90-11204 #
ETN-89-94651 ..... N90-11224 #
ETN-89-94656 ..... N90-11225 #
ETN-89-94660 ..... N90-11226 #
ETN-89-94661 ..... N90-11135 #
ETN-89-94662 ..... N90-11561 #
ETN-89-94663 ..... N90-11136 #
ETN-89-94665 ..... N90-11137 #
ETN-89-94667 ..... N90-11270 #
ETN-89-94672 ..... N90-11155 #
ETN-89-94673 ..... N90-11632 #
ETN-89-94674 ..... N90-11598 #
ETN-89-94675 ..... N90-11138 #
ETN-89-94676 ..... N90-11292 #
ETN-89-94934 ..... N90-11156 #
ETN-89-94935 ..... N90-11121 #
ETN-89-94936 ..... N90-11341 #
ETN-89-94937 ..... N90-11691 #
ETN-89-95067 ..... N90-11470 #
ETN-89-95068 ..... N90-11471 #
ETN-89-95069 ..... N90-11526 #
ETN-89-95070 ..... N90-11527 #
ETN-89-95071 ..... N90-11535 #
ETN-89-95072 ..... N90-11479 #
ETN-89-95092 ..... N90-11480 #
ETN-89-95093 ..... N90-11453 #
ETN-89-95094 ..... N90-11481 #
ETN-89-95095 ..... N90-11472 #
ETN-89-95096 ..... N90-11473 #
ETN-89-95097 ..... N90-11528 #
ETN-89-95098 ..... N90-11482 #
ETN-89-95099 ..... N90-11536 #
ETN-89-95100 ..... N90-11474 #
ETN-89-95101 ..... N90-11482 #
ETN-89-95102 ..... N90-11483 #
ETN-89-95103 ..... N90-11475 #
ETN-89-95104 ..... N90-11529 #
ETN-89-95105 ..... N90-11530 #
ETN-89-95106 ..... N90-11271 #
ETN-89-95107 ..... N90-11476 #
ETN-89-95109 ..... N90-11484 #
ETN-89-95153 ..... N90-11193 #
ETN-89-95154 ..... N90-11244 #
ETN-89-95155 ..... N90-11293 #
ETN-89-95159 ..... N90-11641 #
ETN-89-95160 ..... N90-11599 #
ETN-89-95161 ..... N90-11600 #
ETN-89-95166-PT-3 ..... N90-11194 #
ETN-89-95167 ..... N90-11272 #
ETN-89-95168 ..... N90-11417 #
ETN-89-95169 ..... N90-11575 #
ETN-89-95170 ..... N90-11309 #
ETN-89-95171 ..... N90-11342 #
ETN-89-95172 ..... N90-11537 #
ETN-89-95384 ..... N90-10986 #
ETN-89-95430 ..... N90-11477 #

FASAC-TAR-4070 ..... N90-11228 #

FCM-H10-1988 ..... N90-11419 #

FEDERAL-METEOROLOGICAL-HB-10 ..... N90-11419 #

FNAL-TM-1606 ..... N90-11229 #

FNAL/C-89/155-E ..... N90-11281 #

FOA-C-20749-2.3-PT-3 ..... N90-11194 #
FOA-C-20752-2.4(2.1) ..... N90-11156 #
FOA-C-20753-2.3 ..... N90-11121 #
FOA-C-20755-2.1 ..... N90-11193 #
FOA-C-20758-2.1 ..... N90-11272 #
FOA-C-30493-9.4 ..... N90-11341 #
FOA-C-30520-3.3 ..... N90-11691 #
FOA-C-30521-3.1 ..... N90-11417 #
FOA-C-30522-3.6 ..... N90-11244 #
FOA-C-30523-3.1 ..... N90-11575 #
FOA-C-30524-3.1 ..... N90-11309 #
FOA-C-30525-3.1 ..... N90-11342 #
FOA-C-30526-3.1 ..... N90-11293 #
FOA-C-30528-3.4 ..... N90-11537 #

FTD-ID(RS)T-1133-88 ..... N90-11149 #

GA-A19800 ..... N90-11618 #

GAO/NSIAD-89-127 ..... N90-10845 #

GDSS-CRAD-89-002 ..... N90-10983* #

H-1506 ..... N90-11441* #
H-1541 ..... N90-11487* #

HEL-TN-6-89 ..... N90-11467 #

IAE-4677/1 ..... N90-11613 #

IC-88/353 ..... N90-11213 #
IC-88/383 ..... N90-11500 #
IC-88/384 ..... N90-11586 #
IC-88/392 ..... N90-11501 #
IC-88/404 ..... N90-11539 #
IC-88/410 ..... N90-11502 #
IC-88/420 ..... N90-11503 #
IC-88/421 ..... N90-11638 #
IC-88/428 ..... N90-11504 #
IC-88/429 ..... N90-11505 #
IC-89/2 ..... N90-11677 #
IC-89/11 ..... N90-11614 #

IC-89/36 ..... N90-11415 #
IC-89/38 ..... N90-11636 #
IC-89/44 ..... N90-11540 #
IC-89/47 ..... N90-11637 #

ICASE-89-16 ..... N90-11494* #
ICASE-89-60 ..... N90-11495* #
ICASE-89-66 ..... N90-10833* #
ICASE-89-76 ..... N90-11498* #

ICOMP-89-26 ..... N90-11250* #

IDA-P-2155 ..... N90-11491 #

IDA/HQ-88-33821 ..... N90-11491 #

IFSR-374 ..... N90-11583 #
IFSR-385 ..... N90-11582 #
IFSR-386 ..... N90-11584 #

IFT-P-28/88 ..... N90-11635 #

IFVE-OTF-88-110 ..... N90-11464 #

IGCAR-92 ..... N90-11104 #
IGCAR-95 ..... N90-11129 #
IGCAR-96 ..... N90-11130 #

INIS-BR-1530 ..... N90-11128 #

INPE-4766-PRE/1435 ..... N90-11447 #

IRF-PREPRINT-110 ..... N90-11641 #
IRF-PREPRINT-112 ..... N90-11599 #
IRF-PREPRINT-114 ..... N90-11600 #

ISBN-0-309-03842-1 ..... N90-11645 #
ISBN-0-309-03843-X ..... N90-11645 #
ISBN-3-923560-06-0 ..... N90-11292 #
ISBN-92-835-0500-X ..... N90-11361 #
ISBN-92-835-0509-3 ..... N90-10860 #
ISBN-92-835-0514-X ..... N90-10847 #

ISI/RR-89-199 ..... N90-11650 #

ISSN-0038-0911 ..... N90-11684 #
ISSN-0038-0911 ..... N90-11685
ISSN-0347-3694 ..... N90-11121 #
ISSN-0347-3694 ..... N90-11156 #
ISSN-0347-3694 ..... N90-11193 #
ISSN-0347-3694 ..... N90-11194 #
ISSN-0347-3694 ..... N90-11272 #
ISSN-0347-3708 ..... N90-11244 #
ISSN-0347-3708 ..... N90-11293 #
ISSN-0347-3708 ..... N90-11309 #
ISSN-0347-3708 ..... N90-11341 #
ISSN-0347-3708 ..... N90-11342 #
ISSN-0347-3708 ..... N90-11417 #
ISSN-0347-3708 ..... N90-11537 #
ISSN-0347-3708 ..... N90-11575 #
ISSN-0347-3708 ..... N90-11691 #
ISSN-0348-9329 ..... N90-11555 #
ISSN-0379-6546 ..... N90-10986 #
ISSN-0389-4010 ..... N90-11344 #
ISSN-0436-1199 ..... N90-11120 #
ISSN-0452-2982 ..... N90-10890 #
ISSN-0452-2982 ..... N90-10898 #
ISSN-0452-2982 ..... N90-10899 #
ISSN-0452-2982 ..... N90-11276 #
ISSN-0452-2982 ..... N90-11566 #
ISSN-0452-2982 ..... N90-11653 #
ISSN-0600-4412 ..... N90-11459 #
ISSN-0922-5641 ..... N90-11477 #
ISSN-0922-5641 ..... N90-11484 #
ISSN-0923-1714 ..... N90-11470 #
ISSN-0923-1714 ..... N90-11471 #
ISSN-0923-1714 ..... N90-11479 #
ISSN-0923-1714 ..... N90-11526 #
ISSN-0923-1714 ..... N90-11527 #
ISSN-0923-1714 ..... N90-11535 #

ISWS/BUL-70/89 ..... N90-11427 #

IYAF-88-34 ..... N90-11548 #

JAERI-M-89-015 ..... N90-11652 #

JECS-89-04-135 ..... N90-11113 #

JHU/APL/TG-1373 ..... N90-11115 #

JINR-E-5-88-456 ..... N90-11524 #

JINR-R-2-88-454 ..... N90-11541 #
JINR-R-4-88-587 ..... N90-11640 #
JINR-R-17-88-349 ..... N90-11525 #

JINR-9-88-533 ..... N90-11560 #
JINR-13-88-486 ..... N90-11308 #
JINR-13-88-589 ..... N90-11291 #

JPRS-USP-89-007 ..... N90-10900 #

JTN-88-80063 ..... N90-11276 #
JTN-88-80064 ..... N90-11653 #
JTN-88-80065 ..... N90-11566 #
JTN-88-80066 ..... N90-10890 #
JTN-88-80068 ..... N90-10898 #
JTN-88-80069 ..... N90-10899 #

KAPL-4701 ..... N90-11123 #

KIYI-88-9 ..... N90-11597 #

KURRI-TR-311 ..... N90-11631 #

L-16304 ..... N90-11454* #
L-16537 ..... N90-10830* #
L-16570 ..... N90-10829* #

LA-UR-89-602 ..... N90-11186 #
LA-UR-89-1833 ..... N90-11488 #
LA-UR-89-2170 ..... N90-10892 #
LA-UR-89-2246 ..... N90-11280* #
LA-UR-89-2324 ..... N90-11620 #
LA-UR-89-2403 ..... N90-11098 #
LA-UR-89-2429 ..... N90-10839 #
LA-UR-89-2456 ..... N90-11450 #
LA-UR-89-2489 ..... N90-11577 #
LA-UR-89-2564 ..... N90-11605 #
LA-UR-89-2656 ..... N90-11546 #
LA-UR-89-2657 ..... N90-11290 #
LA-UR-89-2660 ..... N90-11469 #
LA-UR-89-2680 ..... N90-11624 #
LA-UR-89-2687 ..... N90-11593 #
LA-UR-89-2691 ..... N90-11146 #
LA-UR-89-2701 ..... N90-11131 #
LA-UR-89-2706 ..... N90-11478 #
LA-UR-89-2710 ..... N90-11592 #
LA-UR-89-2716 ..... N90-11190 #
LA-UR-89-2717 ..... N90-11268 #
LA-UR-89-2723 ..... N90-11288 #
LA-UR-89-2740 ..... N90-11588 #
LA-UR-89-2746 ..... N90-11416 #
LA-UR-89-2773 ..... N90-11189 #
LA-UR-89-2782 ..... N90-11585 #
LA-UR-89-2791 ..... N90-11266 #
LA-UR-89-2795 ..... N90-11544 #
LA-UR-89-2798 ..... N90-11557 #
LA-UR-89-2818 ..... N90-11197 #
LA-UR-89-2825 ..... N90-11687 #
LA-UR-89-2840 ..... N90-11628 #
LA-UR-89-2864 ..... N90-11267 #
LA-UR-89-2867 ..... N90-11305 #
LA-UR-89-2869 ..... N90-11134 #
LA-UR-89-2877 ..... N90-11239 #
LA-UR-89-2899 ..... N90-11581 #
LA-UR-89-2915 ..... N90-11303 #
LA-UR-89-2929 ..... N90-11154 #
LA-UR-89-2962 ..... N90-11678 #

LAIC-IDA-89-B1 ..... N90-11537 #
LAIC-IDA-89-B2 ..... N90-11537 #

LBL-26513 ..... N90-11095 #

LC-79-640375 ..... N90-11684 #
LC-79-640375 ..... N90-11685
LC-88-12090 ..... N90-11645 #
LC-89-600728 ..... N90-11458 #
LC-89-600732 ..... N90-11274 #

LCDS-89-3 ..... N90-11510 #

LUIP-8903 ..... N90-11555 #

LUNFD6/(NFFK-7100)1-18(1989) ..... N90-11555 #

MCCI-TR-89-881002 ..... N90-10859 #

MEMO-INF-89-17 ..... N90-11470 #
MEMO-INF-89-18 ..... N90-11471 #
MEMO-INF-89-19 ..... N90-11526 #
MEMO-INF-89-22 ..... N90-11527 #
MEMO-INF-89-23 ..... N90-11535 #
MEMO-INF-89-25 ..... N90-11479 #

MIT/LCS/TM-395 ..... N90-11468 #

MLM-3603 ..... N90-11133 #

MPIS-18/1988 ..... N90-11120 #

MTI-87ASE555SA11 ..... N90-11654* #

MTL-TR-89-13 ..... N90-11573 #
MTL-TR-89-44 ..... N90-11088 #
MTL-TR-89-47 ..... N90-11087 #

MTR-10403 ..... N90-11221 #

N-2934-NASA ..... N90-11680* #

NADC-89004-60 ..... N90-11444 #

NAL-TM-568 ..... N90-11276 #
NAL-TM-569 ..... N90-11653 #
NAL-TM-570 ..... N90-11566 #
NAL-TM-571 ..... N90-10890 #
NAL-TM-573 ..... N90-10898 #
NAL-TM-577 ..... N90-10899 #

NAL-TR-945 ..... N90-11344 #

NAS 1.15:88329 ..... N90-11254* #
NAS 1.15:100034 ..... N90-10828* #
NAS 1.15:100376 ..... N90-10980* #
NAS 1.15:100378 ..... N90-11195* #
NAS 1.15:100381 ..... N90-10981* #
NAS 1.15:100450 ..... N90-11441* #
NAS 1.15:101266 ..... N90-11280* #
NAS 1.15:101472 ..... N90-11198* #
NAS 1.15:101625 ..... N90-11647* #
NAS 1.15:101642 ..... N90-10889* #
NAS 1.15:101789 ..... N90-10909* #
NAS 1.15:101888 ..... N90-10962* #
NAS 1.15:102156 ..... N90-11451* #
NAS 1.15:102229 ..... N90-10841* #
NAS 1.15:102336 ..... N90-11082* #
NAS 1.15:102341 ..... N90-10891* #
NAS 1.15:102346 ..... N90-11081* #
NAS 1.15:102354 ..... N90-11497* #
NAS 1.15:102357 ..... N90-11277* #
NAS 1.15:102362 ..... N90-11250* #
NAS 1.15:102382 ..... N90-11144* #
NAS 1.15:102394 ..... N90-10912* #
NAS 1.26:4254 ..... N90-11332* #
NAS 1.26:179442 ..... N90-11487* #
NAS 1.26:180839 ..... N90-11654* #
NAS 1.26:180844 ..... N90-11210* #
NAS 1.26:181708 ..... N90-10834* #
NAS 1.26:181890 ..... N90-11494* #
NAS 1.26:181911 ..... N90-10833* #
NAS 1.26:181912 ..... N90-11495* #
NAS 1.26:181935 ..... N90-11498* #
NAS 1.26:182178 ..... N90-10835* #
NAS 1.26:182179 ..... N90-10836* #
NAS 1.26:183289 ..... N90-11669* #
NAS 1.26:183398 ..... N90-11603* #
NAS 1.26:183782 ..... N90-11689* #
NAS 1.26:184594 ..... N90-11455* #
NAS 1.26:185078 ..... N90-11310* #
NAS 1.26:185135 ..... N90-11549* #
NAS 1.26:185136 ..... N90-11256* #
NAS 1.26:185137 ..... N90-10983* #
NAS 1.26:185139 ..... N90-11606* #
NAS 1.26:185408 ..... N90-11093* #
NAS 1.26:185485 ..... N90-11205* #
NAS 1.26:185492 ..... N90-11552* #
NAS 1.26:185524-VOL-1 ..... N90-10954* #
NAS 1.26:185524-VOL-2 ..... N90-10955* #
NAS 1.26:185524-VOL-3 ..... N90-10956* #
NAS 1.26:185525 ..... N90-10944* #
NAS 1.26:185526 ..... N90-10936* #
NAS 1.26:185527-VOL-1 ..... N90-10952* #
NAS 1.26:185527-VOL-2 ..... N90-10953* #
NAS 1.26:185529-VOL-1 ..... N90-10941* #
NAS 1.26:185529-VOL-2 ..... N90-10942* #
NAS 1.26:185530 ..... N90-10945* #
NAS 1.26:185531 ..... N90-10946* #
NAS 1.26:185532-VOL-1 ..... N90-10938* #
NAS 1.26:185532-VOL-2 ..... N90-10939* #
NAS 1.26:185532-VOL-3 ..... N90-10940* #
NAS 1.26:185533 ..... N90-10947* #
NAS 1.26:185534 ..... N90-10948* #
NAS 1.26:185535 ..... N90-10949* #
NAS 1.26:185536-VOL-1 ..... N90-10950* #
NAS 1.26:185536-VOL-2 ..... N90-10951* #
NAS 1.26:185538 ..... N90-10933* #
NAS 1.26:185540 ..... N90-10937* #
NAS 1.26:185541 ..... N90-10934* #
NAS 1.26:185545 ..... N90-10923* #
NAS 1.26:185546 ..... N90-10917* #
NAS 1.26:185547 ..... N90-10969* #
NAS 1.26:185548 ..... N90-10921* #
NAS 1.26:185549 ..... N90-10924* #
NAS 1.26:185551 ..... N90-10922* #
NAS 1.26:185554 ..... N90-10919* #
NAS 1.26:185555 ..... N90-10920* #

NAS 1.26:185556 ..... N90-10918* #
NAS 1.26:185558 ..... N90-10975* #
NAS 1.26:185560 ..... N90-10916* #
NAS 1.26:185561 ..... N90-10915* #
NAS 1.26:185562 ..... N90-10914* #
NAS 1.26:185564 ..... N90-10974* #
NAS 1.26:185565 ..... N90-10913* #
NAS 1.26:185566 ..... N90-10973* #
NAS 1.26:185567 ..... N90-10932* #
NAS 1.26:185568 ..... N90-10931* #
NAS 1.26:185569 ..... N90-10943* #
NAS 1.26:185570 ..... N90-10966* #
NAS 1.26:185571 ..... N90-10928* #
NAS 1.26:185572 ..... N90-10972* #
NAS 1.26:185573 ..... N90-10979* #
NAS 1.26:185574 ..... N90-10930* #
NAS 1.26:185575 ..... N90-10968* #
NAS 1.26:185576 ..... N90-10935* #
NAS 1.26:185577 ..... N90-10971* #
NAS 1.26:185578 ..... N90-10970* #
NAS 1.26:185579 ..... N90-10929* #
NAS 1.26:185580 ..... N90-10976* #
NAS 1.26:185581-VOL-1 ..... N90-10977* #
NAS 1.26:185581-VOL-2 ..... N90-10978* #
NAS 1.26:185582 ..... N90-10967* #
NAS 1.26:185583 ..... N90-10965* #
NAS 1.26:185584 ..... N90-10927* #
NAS 1.26:185585 ..... N90-10926* #
NAS 1.26:185586 ..... N90-10963* #
NAS 1.26:185587 ..... N90-10962* #
NAS 1.26:185588 ..... N90-10961* #
NAS 1.26:185589 ..... N90-10960* #
NAS 1.26:185590 ..... N90-10959* #
NAS 1.26:185591 ..... N90-10958* #
NAS 1.26:185592 ..... N90-10964* #
NAS 1.26:185593 ..... N90-10925* #
NAS 1.26:185594 ..... N90-10957* #
NAS 1.26:185716 ..... N90-11680* #
NAS 1.26:185831 ..... N90-11457* #
NAS 1.26:185838 ..... N90-11456* #
NAS 1.26:185885 ..... N90-11227* #
NAS 1.26:185925 ..... N90-11209* #
NAS 1.26:185927 ..... N90-11460* #
NAS 1.26:185959 ..... N90-11445* #
NAS 1.26:185962 ..... N90-11255* #
NAS 1.26:185975 ..... N90-11661* #
NAS 1.26:185976 ..... N90-11211* #
NAS 1.26:185998 ..... N90-10911* #
NAS 1.26:185999 ..... N90-11662* #
NAS 1.26:186003 ..... N90-10840* #
NAS 1.55:3042 ..... N90-11405* #
NAS 1.60:2760-REV ..... N90-11454* #
NAS 1.60:2879 ..... N90-11245* #
NAS 1.60:2939 ..... N90-10829* #
NAS 1.60:2945 ..... N90-10830* #
NAS 1.83:107/10-88 ..... N90-10907* #

NASA-CP-3042 ..... N90-11405* #

NASA-CR-4254 ..... N90-11332* #
NASA-CR-179442 ..... N90-11487* #
NASA-CR-180839 ..... N90-11654* #
NASA-CR-180844 ..... N90-11210* #
NASA-CR-181708 ..... N90-10834* #
NASA-CR-181890 ..... N90-11494* #
NASA-CR-181911 ..... N90-10833* #
NASA-CR-181912 ..... N90-11495* #
NASA-CR-181935 ..... N90-11498* #
NASA-CR-182178 ..... N90-10835* #
NASA-CR-182179 ..... N90-10836* #
NASA-CR-183289 ..... N90-11669* #
NASA-CR-183398 ..... N90-11603* #
NASA-CR-183782 ..... N90-11689* #
NASA-CR-184594 ..... N90-11455* #
NASA-CR-185078 ..... N90-11310* #
NASA-CR-185135 ..... N90-11549* #
NASA-CR-185136 ..... N90-11256* #
NASA-CR-185137 ..... N90-10983* #
NASA-CR-185139 ..... N90-11606* #
NASA-CR-185408 ..... N90-11093* #
NASA-CR-185485 ..... N90-11205* #
NASA-CR-185492 ..... N90-11552* #
NASA-CR-185524-VOL-1 ..... N90-10954* #
NASA-CR-185524-VOL-2 ..... N90-10955* #
NASA-CR-185524-VOL-3 ..... N90-10956* #
NASA-CR-185525 ..... N90-10944* #
NASA-CR-185526 ..... N90-10936* #
NASA-CR-185527-VOL-1 ..... N90-10952* #
NASA-CR-185527-VOL-2 ..... N90-10953* #
NASA-CR-185529-VOL-1 ..... N90-10941* #
NASA-CR-185529-VOL-2 ..... N90-10942* #
NASA-CR-185530 ..... N90-10945* #
NASA-CR-185531 ..... N90-10946* #
NASA-CR-185532-VOL-1 ..... N90-10938* #
NASA-CR-185532-VOL-2 ..... N90-10939* #
NASA-CR-185532-VOL-3 ..... N90-10940* #
NASA-CR-185533 ..... N90-10947* #
NASA-CR-185534 ..... N90-10948* #
NASA-CR-185535 ..... N90-10949* #
NASA-CR-185536-VOL-1 ..... N90-10950* #
NASA-CR-185536-VOL-2 ..... N90-10951* #
NASA-CR-185538 ..... N90-10933* #
NASA-CR-185540 ..... N90-10937* #
NASA-CR-185541 ..... N90-10934* #
NASA-CR-185545 ..... N90-10923* #
NASA-CR-185546 ..... N90-10917* #
NASA-CR-185547 ..... N90-10969* #
NASA-CR-185548 ..... N90-10921* #
NASA-CR-185549 ..... N90-10924* #
NASA-CR-185551 ..... N90-10922* #
NASA-CR-185554 ..... N90-10919* #
NASA-CR-185555 ..... N90-10920* #
NASA-CR-185556 ..... N90-10918* #
NASA-CR-185558 ..... N90-10975* #
NASA-CR-185560 ..... N90-10916* #
NASA-CR-185561 ..... N90-10915* #
NASA-CR-185562 ..... N90-10914* #
NASA-CR-185564 ..... N90-10974* #
NASA-CR-185565 ..... N90-10913* #
NASA-CR-185566 ..... N90-10973* #
NASA-CR-185567 ..... N90-10932* #
NASA-CR-185568 ..... N90-10931* #
NASA-CR-185569 ..... N90-10943* #
NASA-CR-185570 ..... N90-10966* #
NASA-CR-185571 ..... N90-10928* #
NASA-CR-185572 ..... N90-10972* #
NASA-CR-185573 ..... N90-10979* #
NASA-CR-185574 ..... N90-10930* #
NASA-CR-185575 ..... N90-10968* #
NASA-CR-185576 ..... N90-10935* #
NASA-CR-185577 ..... N90-10971* #
NASA-CR-185578 ..... N90-10970* #
NASA-CR-185579 ..... N90-10929* #
NASA-CR-185580 ..... N90-10976* #
NASA-CR-185581-VOL-1 ..... N90-10977* #
NASA-CR-185581-VOL-2 ..... N90-10978* #
NASA-CR-185582 ..... N90-10967* #
NASA-CR-185583 ..... N90-10965* #
NASA-CR-185584 ..... N90-10927* #
NASA-CR-185585 ..... N90-10926* #
NASA-CR-185586 ..... N90-10963* #
NASA-CR-185587 ..... N90-10962* #
NASA-CR-185588 ..... N90-10961* #
NASA-CR-185589 ..... N90-10960* #
NASA-CR-185590 ..... N90-10959* #
NASA-CR-185591 ..... N90-10958* #
NASA-CR-185592 ..... N90-10964* #
NASA-CR-185593 ..... N90-10925* #
NASA-CR-185594 ..... N90-10957* #
NASA-CR-185716 ..... N90-11680* #
NASA-CR-185831 ..... N90-11457* #
NASA-CR-185838 ..... N90-11456* #
NASA-CR-185885 ..... N90-11227* #
NASA-CR-185925 ..... N90-11209* #
NASA-CR-185927 ..... N90-11460* #
NASA-CR-185959 ..... N90-11445* #
NASA-CR-185962 ..... N90-11255* #
NASA-CR-185975 ..... N90-11661* #
NASA-CR-185976 ..... N90-11211* #
NASA-CR-185998 ..... N90-10911* #
NASA-CR-185999 ..... N90-11662* #
NASA-CR-186003 ..... N90-10840* #

NASA-NEWS-RELEASE-89-151 ..... N90-10982* #

NASA-NP-107/10-88 ..... N90-10907* #

NASA-TM-88329 ..... N90-11254* #
NASA-TM-100034 ..... N90-10828* #
NASA-TM-100376 ..... N90-10980* #
NASA-TM-100378 ..... N90-11195* #
NASA-TM-100381 ..... N90-10981* #
NASA-TM-100450 ..... N90-11441* #
NASA-TM-101266 ..... N90-11280* #
NASA-TM-101472 ..... N90-11196* #
NASA-TM-101625 ..... N90-11647* #
NASA-TM-101642 ..... N90-10889* #
NASA-TM-101789 ..... N90-10909* #
NASA-TM-101888 ..... N90-10982* #
NASA-TM-102156 ..... N90-11451* #
NASA-TM-102229 ..... N90-10841* #
NASA-TM-102336 ..... N90-11082* #
NASA-TM-102341 ..... N90-10891* #
NASA-TM-102346 ..... N90-11081* #
NASA-TM-102354 ..... N90-11497* #
NASA-TM-102357 ..... N90-11277* #
NASA-TM-102362 ..... N90-11250* #
NASA-TM-102382 ..... N90-11144* #
NASA-TM-102394 ..... N90-10912* #

NASA-TP-2760-REV ..... N90-11454* #
NASA-TP-2879 ..... N90-11245* #
NASA-TP-2939 ..... N90-10829* #
NASA-TP-2945 ..... N90-10830* #

NCAR/TN-333-STR ..... N90-11413 #

NCSU-5 ..... N90-11480* #

NDRE/PUBL-89/1001 ..... N90-11459 #

NEPRF-CR-89-04 ..... N90-11430 #

NHRC-89-6 ..... N90-11440 #

NIPER-200 ..... N90-11117 #

NIST/SP-250/35 ..... N90-11274 #
NIST/SP-500/161 ..... N90-11458 #
NIST/SP-500/164 ..... N90-11448 #

NIST/TN-1235-89 ..... N90-11310* #
NIST/TN-1259 ..... N90-11343 #

NISTIR-89/3908 ..... N90-11142 #

NMRI-88-23 ..... N90-11284 #

NOAA-TM-ERL-ARL-172 ..... N90-11412 #

NOAA-TM-ERL-PMEL-88 ..... N90-11436 #

NOAA-TM-ERL-SEL-79 ..... N90-11411 #

NOAA-TM-ERL-WPL-162 ..... N90-11425 #
NOAA-TM-ERL-WPL-163 ..... N90-10842 #

NOAA-TM-NMFS-SWFC-125 ..... N90-11434 #

NOAA-TM-NWS-ER-81 ..... N90-11424 #

NPS61-89-001 ..... N90-11286 #

NRL-MR-6510 ..... N90-11572 #

NRL-9188 ..... N90-11431 #

NSWC-TR-89-110 ..... N90-11237 #

NUSC-TR-8533 ..... N90-11533 #

OCS-TR-89-23 ..... N90-11564 #

ONR-89-1 ..... N90-11442 #

ORNL/CSD/TM-250 ..... N90-10844 #

ORNL/FTR-3092 ..... N90-11630 #
ORNL/FTR-3218 ..... N90-11306 #
ORNL/FTR-3288 ..... N90-11243 #
ORNL/FTR-3349 ..... N90-11622 #
ORNL/FTR-3351 ..... N90-11147 #

ORNL/M-772 ..... N90-11651 #

ORNL/SUB-86-SA578/1 ..... N90-11316 #
ORNL/SUB-87-00184/01 ..... N90-11092 #

ORNL/TM-11053 ..... N90-11607 #
ORNL/TM-11155 ..... N90-11655 #
ORNL/TM-11230 ..... N90-11319 #

OTA-BP-E-53 ..... N90-11439 #

OTA-BP-SET-52 ..... N90-11642 #

PB89-152268 ..... N90-11418 #
PB89-154884 ..... N90-11663 #
PB89-161046 ..... N90-11350 #
PB89-161053 ..... N90-11351 #
PB89-161061 ..... N90-11352 #
PB89-163075 ..... N90-10846 #
PB89-168769 ..... N90-11419 #
PB89-177877 ..... N90-11338 #
PB89-184360 ..... N90-11564 #
PB89-190227 ..... N90-11434 #
PB89-191290 ..... N90-11642 #
PB89-193833 ..... N90-11458 #
PB89-193940 ..... N90-11310* #
PB89-194617 ..... N90-11411 #
PB89-194716 ..... N90-11684 #
PB89-195036 ..... N90-11353 #
PB89-198709 ..... N90-11644 #
PB89-198840 ..... N90-11645 #
PB89-203871 ..... N90-11425 #
PB89-203988 ..... N90-11427 #
PB89-207369 ..... N90-11426 #
PB89-207393 ..... N90-11685

PB89-207476 ..... N90-11354 #
PB89-208102 ..... N90-10842 #
PB89-208326 ..... N90-11424 #
PB89-208375 ..... N90-11412 #
PB89-208979 ..... N90-11413 #
PB89-208987 ..... N90-11428 #
PB89-209340 ..... N90-11274 #
PB89-209357 ..... N90-11343 #
PB89-209985 ..... N90-11439 #
PB89-210256 ..... N90-11599 #
PB89-212328 ..... N90-11436 #
PB89-214753 ..... N90-11448 #
PB89-218325 ..... N90-11142 #

PNL-SA-16415 ..... N90-11265 #
PNL-SA-16974 ..... N90-11132 #
PNL-SA-17213 ..... N90-11125 #
PNL-SA-17221 ..... N90-11489 #

PNL-6279-VOL-10 ..... N90-11429 #
PNL-6887 ..... N90-11122 #
PNL-6935 ..... N90-11346 #

P89-10151 ..... N90-10982* #

R/D-5038-CH-01 ..... N90-11110 #
R/D-5390-CH-01 ..... N90-11116 #
R/D-6047-MS-02 ..... N90-11617 #

REPT-1.0-WP-VA86001-01 ..... N90-10922* #
REPT-1.0-WP-VA86001-02 ..... N90-10924* #
REPT-1.0-WP-VA86001-03 ..... N90-10921* #
REPT-1.0-WP-VA86001-04 ..... N90-10916* #
REPT-1.0-WP-VA86001-05 ..... N90-10930* #
REPT-1.0-WP-VA86001-06 ..... N90-10929* #
REPT-1.0-WP-VA86001-07 ..... N90-10935* #
REPT-1.0-WP-VA86001-08 ..... N90-10917* #
REPT-1.0-WP-VA86001-09 ..... N90-10913* #
REPT-1.0-WP-VA86001-10 ..... N90-10915* #
REPT-1.0-WP-VA86001-11 ..... N90-10918* #
REPT-1.0-WP-VA86001-12 ..... N90-10925* #
REPT-1.0-WP-VA86001-14 ..... N90-10931* #
REPT-1.0-WP-VA86001-15 ..... N90-10937* #
REPT-1.0-WP-VA86001-16 ..... N90-10920* #
REPT-1.0-WP-VA86001-17 ..... N90-10928* #
REPT-1.0-WP-VA86001-18 ..... N90-10932* #
REPT-1.0-WP-VA86001-19 ..... N90-10933* #
REPT-1.0-WP-VA86001-20 ..... N90-10934* #
REPT-1.0-WP-VA86001-21 ..... N90-10919* #
REPT-1.0-WP-VA86001-22 ..... N90-10927* #
REPT-1.0-WP-VA86001-23 ..... N90-10926* #
REPT-1.0-WP-VA86001-24 ..... N90-10914* #
REPT-1.0-WP-VA86001-25 ..... N90-10943* #
REPT-1.0-WP-VA86001-26 ..... N90-10936* #
REPT-1.0-WP-VA86001-27-VOL-1 ..... N90-10938* #
REPT-1.0-WP-VA86001-27-VOL-2 ..... N90-10939* #
REPT-1.0-WP-VA86001-27-VOL-3 ..... N90-10940* #
REPT-1.0-WP-VA86001-28-VOL-1 ..... N90-10941* #
REPT-1.0-WP-VA86001-28-VOL-2 ..... N90-10942* #
REPT-1.0-WP-VA87001-01 ..... N90-10958* #
REPT-1.0-WP-VA87001-03 ..... N90-10944* #
REPT-1.0-WP-VA87001-04 ..... N90-10969* #
REPT-1.0-WP-VA87001-07 ..... N90-10963* #
REPT-1.0-WP-VA87001-09 ..... N90-10967* #
REPT-1.0-WP-VA88003-01 ..... N90-10948* #
REPT-1.0-WP-VA88003-03 ..... N90-10959* #
REPT-1.0-WP-VA88003-04 ..... N90-10968* #
REPT-1.0-WP-VA88003-05 ..... N90-10970* #
REPT-1.0-WP-VA88003-07 ..... N90-10972* #
REPT-1.0-WP-VA88003-08 ..... N90-10975* #
REPT-1.0-WP-VA88003-09 ..... N90-10957* #
REPT-1.0-WP-VA88003-09-VOL-1 ..... N90-10952* #
REPT-1.0-WP-VA88003-09-VOL-2 ..... N90-10953* #
REPT-1.0-WP-VA88003-11 ..... N90-10974* #
REPT-1.0-WP-VA88003-15 ..... N90-10923* #
REPT-1.0-WP-VA88003-16 ..... N90-10964* #
REPT-1.0-WP-VA88003-17 ..... N90-10973* #
REPT-1.0-WP-VA88003-19-VOL-1 ..... N90-10977* #
REPT-1.0-WP-VA88003-19-VOL-2 ..... N90-10978* #
REPT-1.0-WP-VA88003-22 ..... N90-10947* #
REPT-1.0-WP-VA88003-35 ..... N90-10965* #
REPT-1.0-WP-VA88003-41-VOL-1 ..... N90-10950* #
REPT-1.0-WP-VA88003-41-VOL-2 ..... N90-10951* #
REPT-1.0-WP-VA88003-43 ..... N90-10966* #
REPT-1.0-WP-VA88003-47 ..... N90-10960* #
REPT-1.0-WP-VA88003-48-VOL-1 ..... N90-10954* #
REPT-1.0-WP-VA88003-010 ..... N90-10976* #
REPT-1.0-WP-VA88005-01 ..... N90-10945* #
REPT-1.0-WP-VA88005-02 ..... N90-10949* #
REPT-1.0-WP-VA88005-03 ..... N90-10962* #
REPT-1.0-WP-VA88005-04 ..... N90-10961* #
REPT-1.0-WP-VA88005-05 ..... N90-10946* #
REPT-1.0-WP-VA88005-06 ..... N90-10979* #
REPT-1.0-WP-VA88005-07 ..... N90-10971* #
REPT-88-88 ..... N90-11477 #
REPT-88-98 ..... N90-11484 #

REPT-88/32 ..... N90-11663 #
REPT-89B00192 ..... N90-11405* #

RIACS-M88.5 ..... N90-11455* #

RIACS-TR-88.23 ..... N90-11093* #

RRK-89-9 ..... N90-11679 #

RSI-0327 ..... N90-11649 #

R88-900064-F ..... N90-10835* #
R88-900064-F ..... N90-10836* #
R8906-3 ..... N90-11216 #

S-596 ..... N90-11451* #

SAND-88-1218 ..... N90-11520 #
SAND-88-1765 ..... N90-11240 #
SAND-88-2385C ..... N90-11185 #
SAND-88-2618C ..... N90-11101 #
SAND-88-2896 ..... N90-11499 #
SAND-88-3307C ..... N90-11594 #
SAND-88-3338C ..... N90-11287 #
SAND-88-3471C ..... N90-11231 #
SAND-88-3482 ..... N90-11543 #
SAND-89-0139C ..... N90-11242 #
SAND-89-0194C ..... N90-11233 #
SAND-89-0220C ..... N90-11568 #
SAND-89-0283C ..... N90-11596 #
SAND-89-0320C ..... N90-11187 #
SAND-89-0344C ..... N90-11191 #
SAND-89-0482C ..... N90-11188 #
SAND-89-0547 ..... N90-11322 #
SAND-89-0781C ..... N90-11289 #
SAND-89-0841C ..... N90-11232 #
SAND-89-0848C ..... N90-11414 #
SAND-89-0871C ..... N90-11097 #
SAND-89-0920C ..... N90-11103 #
SAND-89-0990C ..... N90-11100 #
SAND-89-0998C ..... N90-11124 #
SAND-89-1022C ..... N90-11145 #
SAND-89-1043C ..... N90-11282 #
SAND-89-1055 ..... N90-11649 #
SAND-89-1056C ..... N90-11569 #
SAND-89-1115C ..... N90-11629 #
SAND-89-1116C ..... N90-11627 #
SAND-89-1256 ..... N90-11324 #
SAND-89-1270C ..... N90-11595 #
SAND-89-1502 ..... N90-11449 #
SAND-89-1542C ..... N90-11461 #
SAND-89-1964C ..... N90-11337 #
SAND-89-7035 ..... N90-11347 #
SAND-89-8242 ..... N90-11315 #

SD-TR-89-37 ..... N90-11236 #
SD-TR-89-39 ..... N90-11300 #

SEI-89-03-15-WB ..... N90-10985 #

SERI/CP-211-3550 ..... N90-11348 #

SERI/STR-211-3529 ..... N90-11604 #
SERI/STR-211-3540 ..... N90-11345 #

SGD-536-PT-1 ..... N90-11684 #
SGD-537-PT-1 ..... N90-11685

SLCET-TR-89-3 ..... N90-11112 #

SR-1 ..... N90-11570 #

SSL-PREPRINT-88-136 ..... N90-11689* #

SU-SLAC-PUB-5022 ..... N90-11634 #
SU-SLAC-PUB-5031 ..... N90-11639 #

SWRI-12-6253 ..... N90-11438 #

TASC-TR-5547-1 ..... N90-11433 #

TGAL-88-06 ..... N90-11507 #

TR-1 ..... N90-11150 #
TR-1 ..... N90-11299 #
TR-2 ..... N90-11235 #
TR-9 ..... N90-11143 #
TR-16 ..... N90-11148 #
TR-31 ..... N90-11508 #
TR-37 ..... N90-11090 #
TR-38 ..... N90-11089 #
TR-56 ..... N90-11532 #
TR-165 ..... N90-11357 #
TR-293 ..... N90-11531 #
TR-419 ..... N90-11534 #
TR-0086A(2925-02)-5 ..... N90-11236 #

TR-0088(3930-04)-2 ..... N90-11300 #

UBUFFALO/DC/89/TR-107 ..... N90-11096 #

UC-TR-19 ..... N90-11113 #

UCB/CSD-88/476 ..... N90-11452 #

UCID-21519-REV-1 ..... N90-11589 #
UCID-21687 ..... N90-11241 #
UCID-21695 ..... N90-11519 #
UCID-21737 ..... N90-11590 #
UCID-21767 ..... N90-11223 #

UCLA/EE-ARO-1001 ..... N90-11571 #

UCLA/PPG-1247 ..... N90-11578 #

UCRL-53921-TH ..... N90-11463 #
UCRL-100283 ..... N90-11518 #
UCRL-100983 ..... N90-11683 #
UCRL-101190 ..... N90-11212 #
UCRL-101192 ..... N90-11238 #
UCRL-101228 ..... N90-11558 #
UCRL-101434 ..... N90-11099 #
UCRL-101506 ..... N90-11258 #
UCRL-101545 ..... N90-11608 #
UCRL-101562 ..... N90-11257 #
UCRL-101586 ..... N90-11633 #
UCRL-101617 ..... N90-11192 #

UILU-ENG-89-1744 ..... N90-11493 #
UILU-ENG-89-1753 ..... N90-11522 #

UIUCDCS-R-89-1525 ..... N90-11493 #
UIUCDCS-R-89-1534 ..... N90-11522 #

UMC-IE-4-0889 ..... N90-11456* #

USAAVSCOM-TR-87-A-6 ..... N90-10828* #

VTT-TUTK-576 ..... N90-11234 #

W-15/87 ..... N90-11204 #

WRDC-TR-89-3089 ..... N90-10985 #

Y/DX-833 ..... N90-11323 #

YALEU/DCS/RR-692 ..... N90-11516 #
YALEU/DCS/RR-718 ..... N90-11517 #

Appendix—About STAR

Scientific and Technical Aerospace Reports (STAR) is a major component of a comprehensive National Aeronautics and Space Administration information system covering aeronautics, space, and supporting disciplines. *STAR* is issued on the 8th and 23rd of each month and announces current publications of the following types:

- NASA, NASA contractor, and NASA grantee reports
- Reports issued by other U.S. Government agencies, domestic and foreign institutions, universities, and private firms
- Translations in report form
- NASA-owned patents and patent applications
- Other U.S. Government agency and foreign patents and patent applications
- Domestic and foreign dissertations and theses

Journal, book, and conference literature, cover-to-cover journal translations, and certain foreign dissertations are announced in a companion journal, *International Aerospace Abstracts (IAA),* available on subscription from the American Institute of Aeronautics and Astronautics, Technical Information Service, 555 West 57th Street, 12th Floor, New York, NY 10019.

SUBJECT SCOPE

The subject scope of *STAR* and *IAA* includes all aspects of aeronautics and space research and development, supporting basic and applied research, and applications. Aerospace aspects of earth resources, energy development, conservation, oceanography, environmental protection, urban transportation, and other topics of high national priority are also covered.

OTHER NASA PUBLICATIONS

Other NASA publications and information services are described in the publication, *The NASA Scientific and Technical Information System ... and How to Use It,* available without charge from the NASA Scientific and Technical Information Facility, P.O. Box 8757, BWI Airport, MD 21240.

HOW TO USE *STAR* SUBJECT CATEGORIES

STAR is categorized by 10 major subject divisions broken down further into 76 specific subject categories and one general division/category. The major subject divisions are listed on page ii in the Table of Contents, together with a note for each that defines its scope and provides any cross-references. For example:

AERONAUTICS

Includes aeronautics (general); aerodynamics; air transportation and safety; aircraft communications and navigation; aircraft design, testing and performance; aircraft instrumentation; aircraft propulsion and power; aircraft stability and control; and research and support facilities (air).

For related information see also *Astronautics.*

Each major division is further divided into as many as nine specific categories, which are identified by category numbers.

Abstracts in *STAR* are grouped by subject category, the categories appearing in sequential order. Category breaks in the abstract section are identified by the category number and title, and a scope note. Cross-references to other categories are provided as appropriate. For example:

02 AERODYNAMICS

Includes aerodynamics of bodies, combinations, wings, rotors, and control surfaces; and internal flow in ducts and turbomachinery.

For related information see also *34 Fluid Mechanics and Heat Transfer.*

CROSS-REFERENCES

Individual *STAR* abstracts are not ordinarily cross-referenced, except for certain conference reports or book translations that have had separate abstracts written for their component papers or chapters. Citations and abstracts of the components follow immediately after those of the parent document. When the subject content of a component differs sufficiently from the general content of the parent, a cross-reference citation also is printed at the end of the category to which it normally would have been assigned if it were independent.

DOCUMENTS ON MICROFICHE

Documents on microfiche(1) are designated by a pound sign (#) following the accession number. The pound sign is used without regard to the source or quality of the microfiche.

LIMITED REPRODUCIBILITY

A Note of Limited Reproducibility appears in the citation, if one or a combination of the following factors affect the reproducibility of more than 20% of the document. These factors include: faint or broken type, color photographs, black and white photographs, foldouts, dot matrix print, charts/graphs with script notation, non-Roman alphabet, or some other factor that limits the reproducibility of that document. This notation also appears on the microfiche header, with the specific causing factor checked off on a list visible in the second frame.

AVAILABILITIES

One or more sources from which a document announced in *STAR* is available to the public is given in each citation. The most commonly indicated sources and their acronyms or abbreviations are listed below. If the publication is available from a source other than those listed, the publisher and his address will be displayed on the availability line or in combination with the corporate source line.

Avail: NTIS. Sold by the National Technical Information Service. Prices for hard copy (HC) and microfiche (MF) are indicated by a price code following the letters HC or MF in the *STAR* citation. Current values for the price codes are given in the tables on page A-7.

Initially distributed microfiche under the NTIS SRIM (Selected Research in Microfiche) is available at greatly reduced unit prices. For this service and for information concerning subscription to NASA printed reports, consult the NTIS Subscription Section, Springfield, VA 22161.

NOTE ON ORDERING DOCUMENTS: When ordering NASA publications (those followed by the * symbol), use the N accession number. NASA patent applications (only the specifications are offered) should be ordered by the US-Patent-Appl-SN number. Non-NASA publications (no asterisk) should be ordered by the AD, PB, or other *report number* shown on the last line of the citation, not by the N accession number. It is also advisable to cite the title and other bibliographic identification.

(1) A microfiche is a transparent sheet of film, 105 by 148 mm in size, containing as many as 60 to 98 pages of information reduced to micro images (not to exceed 26:1 reduction).

Avail: SOD (or GPO). Sold by the Superintendent of Documents, U.S. Government Printing Office, in hard copy. The current price and order number are given following the availability line. (NTIS will fill microfiche requests, as indicated above, for those documents identified by a # symbol.)

Avail: BLL (formerly NLL): British Library Lending Division, Boston Spa, Wetherby, Yorkshire, England. Photocopies available from this organization at the price shown. (If none is given, inquiry should be addressed to the BLL.)

Avail: DOE Depository Libraries. Organizations in U.S. cities and abroad that maintain collections of Department of Energy reports, usually in microfiche form, are listed in *Energy Research Abstracts*. Services available from the DOE and its depositories are described in a booklet, *DOE Technical Information Center - Its Functions and Services* (TID-4660), which may be obtained without charge from the DOE Technical Information Center.

Avail: ESDU. Pricing information on specific data, computer programs, and details on Engineering Sciences Data Unit (ESDU) topic categories can be obtained from ESDU International Ltd. Requesters in North America should use the Virginia address while all other requesters should use the London address, both of which are on page A-6.

Avail: Fachinformationszentrum, Karlsruhe. Sold by the Fachinformationszentrum Energie, Physik, Mathematik GMBH, Eggenstein Leopoldshafen, Federal Republic of Germany, at the price shown in deutschmarks (DM).

Avail: HMSO. Publications of Her Majesty's Stationery Office are sold in the U.S. by Pendragon House, Inc. (PHI), Redwood City, CA. The U.S. price (including a service and mailing charge) is given, or a conversion table may be obtained from PHI.

Avail: NASA Public Document Rooms. Documents so indicated may be examined at or purchased from the National Aeronautics and Space Administration, Public Documents Room (Room 126), 600 Independence Ave., S.W., Washington, DC 20546, or public document rooms located at NASA installations, and the NASA Pasadena Office at the Jet Propulsion Laboratory.

Avail: Univ. Microfilms. Documents so indicated are dissertations selected from *Dissertation Abstracts* and are sold by University Microfilms as xerographic copy (HC) and microfilm. All requests should cite the author and the Order Number as they appear in the citation.

Avail: US Patent and Trademark Office. Sold by Commissioner of Patents and Trademarks, U.S. Patent and Trademark Office, at the standard price of $1.50 each, postage free. (See discussion of NASA patents and patent applications below.)

Avail: (US Sales Only). These foreign documents are available to users within the United States from the National Technical Information Service (NTIS). They are available to users outside the United States through the International Nuclear Information Service (INIS) representative in their country, or by applying directly to the issuing organization.

Avail: USGS. Originals of many reports from the U.S. Geological Survey, which may contain color illustrations, or otherwise may not have the quality of illustrations preserved in the microfiche or facsimile reproduction may be examined by the public at the libraries of the USGS field offices whose addresses are listed in this Introduction. The libraries may be queried

concerning the availability of specific documents and the possible utilization of local copying services, such as color reproduction.

Avail: Issuing Activity, or Corporate Author, or no indication of availability. Inquiries as to the availability of these documents should be addressed to the organization shown in the citation as the corporate author of the document.

NASA PATENTS AND PATENT APPLICATIONS

Patents and patent applications owned by NASA are announced in *STAR* under appropriate subject categories and are referenced in the *STAR* indexes. In the Report/Accession Number Index, patents are indexed by the NASA Case Number (which appears in lieu of the report number in other indexes), the U.S. Patent Number, the U.S. Patent Application Serial Number, and the U.S. Patent Class. Patent applications for which patents have not yet been issued are indexed by the NASA Case Number and the U.S. Patent Application Serial Number.

NASA *patent application specifications* are sold in paper copy and microfiche by the National Technical Information Service (NTIS). The US-Patent-Appl-SN- number should be used in ordering either paper copy or microfiche from NTIS. Printed copies of *patents* (which are not microfiched) are available for purchase from:

Commissioner of Patents and Trademarks
U.S. Patent and Trademark Office
Washington, DC 20231

When ordering patents, the U.S. Patent Number should be used, and payment must be remitted in advance, by money order or check payable to the Commissioner of Patents and Trademarks. Prepaid purchase coupons for ordering are also available from the Patent and Trademark Office. The patents and patent applications announced in *STAR* are owned by NASA and are available for royalty-free licensing. Requests for licensing terms and further information should be addressed to:

Associate General Counsel for Intellectual Property/Code GP
National Aeronautics and Space Administration
Washington, DC 20546

ELIGIBILITY AND REGISTRATION FOR NASA INFORMATION PRODUCTS AND SERVICES

A variety of services is available to organizations of the following types that have registered with NASA to receive specific services or products:

1. NASA offices and installations, contractors, subcontractors, grantees, and consultants;
2. Other U.S. Government agencies and their contractors;
3. Libraries in the United States that have arrangements with NASA to maintain collections of NASA documents for public reference;
4. Other organizations in the United States having a need for NASA documents in work related to aeronautics and space research;
5. Organizations abroad that have established reciprocal document exchange arrangements with NASA.

Only the central service points or central points of document acquisition and control within qualified organizations are eligible to register for NASA products and services. Domestic organizations that may be eligible to receive various classes of NASA publications and services should address their requests for registration or for further information to:

NASA Scientific and Technical Information Facility
ATTN: Registration Services
P.O. Box 8757
BWI Airport, MD 21240
301-621-0153

Organizations abroad should direct requests to Manager, International STI Activities, NTT, NASA Headquarters, Washington, DC 20546.

AVAILABILITY OF *STAR* ABSTRACTS ON MICROFICHE

Microfiche of the abstract sections of this issue and other issues of *STAR* are available on annual subscription from NTIS as PB90-911300, Attn: Subscriptions, 5285 Port Royal Road, Springfield, VA 22161. Annual subscription rates are $75.50 North America; $151.00 foreign. Abstract sections for previous years retroactive to 1964 are available at the current rates. Microfiche for individual *STAR* issue abstract sections are not available.

PUBLIC COLLECTIONS OF NASA DOCUMENTS

DOMESTIC: NASA and NASA-sponsored documents and a large number of aerospace publications are available to the public for reference purposes at the library maintained by the American Institute of Aeronautics and Astronautics, Technical Information Service, 555 West 57th Street, 12th Floor, New York, NY 10019

EUROPEAN: An extensive collection of NASA and NASA-sponsored publications is maintained by the British Library Lending Division, Boston Spa, Wetherby, Yorkshire, England, for public access. The British Library Lending Division also has available many of the non-NASA publications cited in *STAR*. European requesters may purchase facsimile copy or microfiche of NASA and NASA-sponsored documents, those identified by both the symbols # and * from ESA - Information Retrieval Service, European Space Agency, 8-10 rue Mario-Nikis, 75738 Paris CEDEX 15, France.

FEDERAL DEPOSITORY LIBRARY PROGRAM

In order to provide the general public with greater access to U.S. Government publications, Congress established the Federal Depository Library Program under the Government Printing Office (GPO), with 51 regional depositories responsible for permanent retention of material, inter-library loan, and reference services. At least one copy of nearly every NASA and NASA-sponsored publication, either in printed or microfiche format, is received and retained by the 51 regional depositories. A list of the regional GPO libraries, arranged alphabetically by state, appears on the inside back cover. These libraries are *not* sales outlets. A local library can contact a Regional Depository to help locate specific reports, or direct contact may be made by an individual.

ADDRESSES OF ORGANIZATIONS

American Institute of Aeronautics and Astronautics
Technical Information Service
555 West 57th Street, 12th Floor
New York, New York 10019

British Library Lending Division,
Boston Spa, Wetherby, Yorkshire,
England

Commissioner of Patents and Trademarks
U.S. Patent and Trademark Office
Washington, DC 20231

Department of Energy
Technical Information Center
P.O. Box 62
Oak Ridge, Tennessee 37830

European Space Agency-Information Retrieval Service
ESRIN
Via Galileo Galilei
00044 Frascati (Rome) Italy

Engineering Sciences Data Unit International
P.O. Box 1633
Manassas, Virginia 22110

Engineering Sciences Data Unit International, Ltd.
251-259 Regent Street
London, W1R 7AD, England

Fachinformationszentrum Energie, Physik, Mathematik
GMBH
7514 Eggenstein Leopoldshafen
Federal Republic of Germany

Her Majesty's Stationery Office
P.O. Box 569, S.E. 1
London, England

NASA Scientific and Technical Information Facility
P.O. Box 8757
BWI Airport, Maryland 21240

National Aeronautics and Space Administration
Scientific and Technical Information Division (NTT)
Washington, DC 20546

National Technical Information Service
5285 Port Royal Road
Springfield, Virginia 22161

Pendragon House, Inc.
899 Broadway Avenue
Redwood City, California 94063

Superintendent of Documents
U.S. Government Printing Office
Washington, DC 20402

University Microfilms
A Xerox Company
300 North Zeeb Road
Ann Arbor, Michigan 48106

University Microfilms, Ltd.
Tylers Green
London, England

U.S. Geological Survey Library National Center
MS 950
12201 Sunrise Valley Drive
Reston, Virginia 22092

U.S. Geological Survey Library
2255 North Gemini Drive
Flagstaff, Arizona 86001

U.S. Geological Survey
345 Middlefield Road
Menlo Park, California 94025

U.S. Geological Survey Library
Box 25046
Denver Federal Center, MS914
Denver, Colorado 80225

NTIS PRICE SCHEDULES

(Effective January 1, 1990)

Schedule A
STANDARD PRICE DOCUMENTS AND MICROFICHE

PRICE CODE	NORTH AMERICAN PRICE	FOREIGN PRICE
A01	$ 8.00	$ 16.00
A02	11.00	22.00
A03	15.00	30.00
A04-A05	17.00	34.00
A06-A09	23.00	46.00
A10-A13	31.00	62.00
A14-A17	39.00	78.00
A18-A21	45.00	90.00
A22-A25	53.00	106.00
A99	*	*
N01	60.00	120.00
N02	59.00	118.00
N03	20.00	40.00

Schedule E
EXCEPTION PRICE DOCUMENTS AND MICROFICHE

PRICE CODE	NORTH AMERICAN PRICE	FOREIGN PRICE
E01	$10.00	$ 20.00
E02	12.00	24.00
E03	14.00	28.00
E04	16.50	33.00
E05	18.50	37.00
E06	21.50	43.00
E07	24.00	48.00
E08	27.00	54.00
E09	29.50	59.00
E10	32.50	65.00
E11	35.00	70.00
E12	38.50	77.00
E13	41.00	82.00
E14	45.00	90.00
E15	48.50	97.00
E16	53.00	106.00
E17	57.50	115.00
E18	62.00	124.00
E19	69.00	138.00
E20	80.00	160.00
E99	*	*

* Contact NTIS for price quote.

IMPORTANT NOTICE

NTIS Shipping and Handling Charges

U.S., Canada, Mexico — ADD $3.00 per TOTAL ORDER

All Other Countries — ADD $4.00 per TOTAL ORDER

Exceptions — Does NOT apply to:

ORDERS REQUESTING NTIS RUSH HANDLING

ORDERS FOR SUBSCRIPTION OR STANDING ORDER PRODUCTS *ONLY*

NOTE: Each additional delivery address on an order requires a separate shipping and handling charge.

FEDERAL REGIONAL DEPOSITORY LIBRARIES

ALABAMA

AUBURN UNIV. AT MONTGOMERY LIBRARY
Documents Department
Montgomery, AL 36193
(205) 279-9110 ext.253

UNIV. OF ALABAMA LIBRARY
Reference Department/Documents
Box S
Tuscaloosa, AL 35486
(205) 348-6046

ARIZONA

DEPT. OF LIBRARY, ARCHIVES, AND PUBLIC RECORDS
Third Floor State Capitol
1700 West Washington
Phoenix, AZ 85007
(602) 255-4121

ARKANSAS

ARKANSAS STATE LIBRARY
Documents Service Section
One Capitol Mall
Little Rock, AR 72201
(501) 371-2090

CALIFORNIA

CALIFORNIA STATE LIBRARY
Govt. Publications Section
914 Capitol Mall
Sacramento, CA 95814
(916) 322-4572

COLORADO

UNIV. OF COLORADO
Norlin Library
Government Publications Division
Campus Box 184
Boulder, CO 80309
(303) 492-8834

DENVER PUBLIC LIBRARY
Govt. Pub. Department
1357 Broadway
Denver, CO 80203
(303) 571-2346

CONNECTICUT

CONNECTICUT STATE LIBRARY
231 Capitol Avenue
Hartford, CT 06106
(203) 566-4971

FLORIDA

UNIV. OF FLORIDA LIBRARIES
Documents Department
Library West
Gainesville, FL 32611
(904) 392-0367

GEORGIA

UNIV. OF GEORGIA LIBRARIES
Government Documents Dept.
Athens, GA 30602
(404) 542-8949

HAWAII

UNIV. OF HAWAII
Hamilton Library
Government Documents Collection
2550 The Mall
Honolulu, HI 96822
(808) 948-8230

IDAHO

UNIV. OF IDAHO LIBRARY
Documents Section
Moscow, ID 83843
(208) 885-6344

ILLINOIS

ILLINOIS STATE LIBRARY
Federal Documents
Centennial Building
Springfield, IL 62756
(217) 782-5012

INDIANA

INDIANA STATE LIBRARY
Serials Section
140 North Senate Avenue
Indianapolis, IN 46204
(317) 232-3686

IOWA

UNIV. OF IOWA LIBRARIES
Government Publications Dept.
Iowa City, IA 52242
(319) 335-5926

KANSAS

UNIVERSITY OF KANSAS
Spencer Research Library
Government Documents
Lawrence, KS 66045
(913) 864-4662

KENTUCKY

UNIV. OF KENTUCKY LIBRARIES
Government Publications/Maps Dept.
Lexington, KY 40506
(606) 257-8400

LOUISIANA

LOUISIANA STATE UNIVERSITY
Middleton Library
Government Documents Dept.
Baton Rouge, LA 70803
(504) 388-2570

LOUISIANA TECHNICAL UNIV.
Prescott Memorial Library
Government Documents Dept.
Ruston, LA 71272
(318) 257-4962

MAINE

UNIVERSITY OF MAINE
Raymond H. Fogler Library
Govt. Documents & Microforms Dept.
Orono, ME 04469
(207) 581-1680

MARYLAND

UNIVERSITY OF MARYLAND
McKeldin Library
Documents/Maps Room
College Park, MD 20742
(301) 454-3034

MASSACHUSETTS

BOSTON PUBLIC LIBRARY
Government Documents Dept.
666 Boylston Street
Boston, MA 02117
(617) 536-5400 ext.226

MICHIGAN

DETROIT PUBLIC LIBRARY
5201 Woodward Avenue
Detroit, MI 48202
(313) 833-1409

LIBRARY OF MICHIGAN
Government Documents
P.O. Box 30007
735 E. Michigan Avenue
Lansing, MI 48909
(517) 373-1593

MINNESOTA

UNIVERSITY OF MINNESOTA
Wilson Library
Government Publications
309 Nineteenth Avenue South
Minneapolis, MN 55455
(612) 373-7813

MISSISSIPPI

UNIV. OF MISSISSIPPI LIB.
Government Documents Dept.
106 Old Gym Bldg.
University, MS 38677
(601) 232-5857

MISSOURI

University of Missouri at Columbia Library
Government Documents
Columbia, MO 65201
(314) 882-6733

MONTANA

UNIV. OF MONTANA
Mansfield Library
Documents Division
Missoula, MT 59812
(406) 243-6700

NEBRASKA

UNIVERSITY OF NEBRASKA - LINCOLN
Love Memorial Library
Documents Department
Lincoln, NE 68588
(402) 472-2562

NEVADA

UNIV. OF NEVADA-RENO LIB.
Govt. Pub. Department
Reno, NV 89557
(702) 784-6579

NEW JERSEY

NEWARK PUBLIC LIBRARY
U.S. Documents Division
5 Washington Street
P.O. Box 630
Newark, NJ 07101
(201) 733-7812

NEW MEXICO

UNIVERSITY OF NEW MEXICO
General Library
Government Publications/Maps Dept.
Albuquerque, NM 87131
(505) 277-5441

NEW MEXICO STATE LIBRARY
325 Don Gaspar Avenue
Santa Fe, NM 87501
(505) 827-3826

NEW YORK

NEW YORK STATE LIBRARY
Documents Sect. Cultural Educ. Ctr.
Empire State Plaza
Albany, NY 12230
(518) 474-5563

NORTH CAROLINA

UNIVERSITY OF NORTH CAROLINA AT CHAPEL HILL
Davis Library 080A
BA/SS Department Documents
Chapel Hill, NC 27514
(919) 962-1151

NORTH DAKOTA

NORTH DAKOTA STATE UNIVERSITY LIBRARY
Government Documents Dept.
Fargo, ND 58105
(701) 237-8352
In cooperation with Univ. of North Dakota, Chester Fritz Library
Grand Forks

OHIO

STATE LIBRARY OF OHIO
Documents Section
65 South Front Street
Columbus, OH 43266
(614) 644-7051

OKLAHOMA

OKLAHOMA DEPT. OF LIBRARIES
Government Documents
200 NE 18th Street
Oklahoma City, OK 73105
(405) 521-2502, ext. 252

OKLAHOMA STATE UNIV. LIB.
Documents Department
Stillwater, OK 74078
(405) 624-0489

OREGON

PORTLAND STATE UNIV.
Millar Library
934 SW Harrison - P.O. Box 1151
Portland, OR 97207
(503) 229-3673

PENNSYLVANIA

STATE LIBRARY OF PENN.
Government Publications Section
Box 1601
Walnut St. & Commonwealth Ave.
Harrisburg, PA 17105
(717) 787-3752

SOUTH CAROLINA

CLEMSON UNIV. COOPER LIB.
Documents Department
Clemson, SC 29634
(803) 656-5174
In cooperation with Univ. of South Carolina, Thomas Cooper Library, Columbia

TEXAS

TEXAS STATE LIBRARY
Public Services Department
P.O. Box 12927 - 1201 Brazos
Austin, TX 78711
(512) 463-5455

TEXAS TECH. UNIV. LIBRARY
Documents Department
Lubbock, TX 79409
(806) 742-2268

UTAH

UTAH STATE UNIVERSITY
Merrill Library & Learning Resources Center, UMC-30
Documents Department
Logan, UT 84322
(801) 750-2682

VIRGINIA

UNIVERSITY OF VIRGINIA
Alderman Library
Government Documents
Charlottesville, VA 22903
(804) 924-3133

WASHINGTON

WASHINGTON STATE LIBRARY
Document Section
Olympia, WA 98504
(206) 753-4027

WEST VIRGINIA

WEST VIRGINIA UNIV. LIB.
Government Documents Section
P.O. Box 6069
Morgantown, WV 26506
(304) 293-3640

WISCONSIN

ST. HIST SOC. OF WISCONSIN LIB.
Government Pub. Section
816 State Street
Madison, WI 53706
(608) 262-2781
In cooperation with Univ. of Wisconsin-Madison, Memorial Library

MILWAUKEE PUBLIC LIBRARY
Documents Division
814 West Wisconsin Avenue
Milwaukee, WI 53233
(414) 278-3065

WYOMING

WYOMING STATE LIBRARY
Supreme Court & Library Bldg.
Cheyenne, WY 82002
(307) 777-5919

National Aeronautics and
Space Administration
Code NTT
Washington, D.C.
20546
Official Business
Penalty for Private Use, $300

SPECIAL FOURTH-CLASS RATE
POSTAGE & FEES PAID
NASA
PERMIT No. G27

POSTMASTER: If Undeliverable (Section 158
Postal Manual) Do Not Return